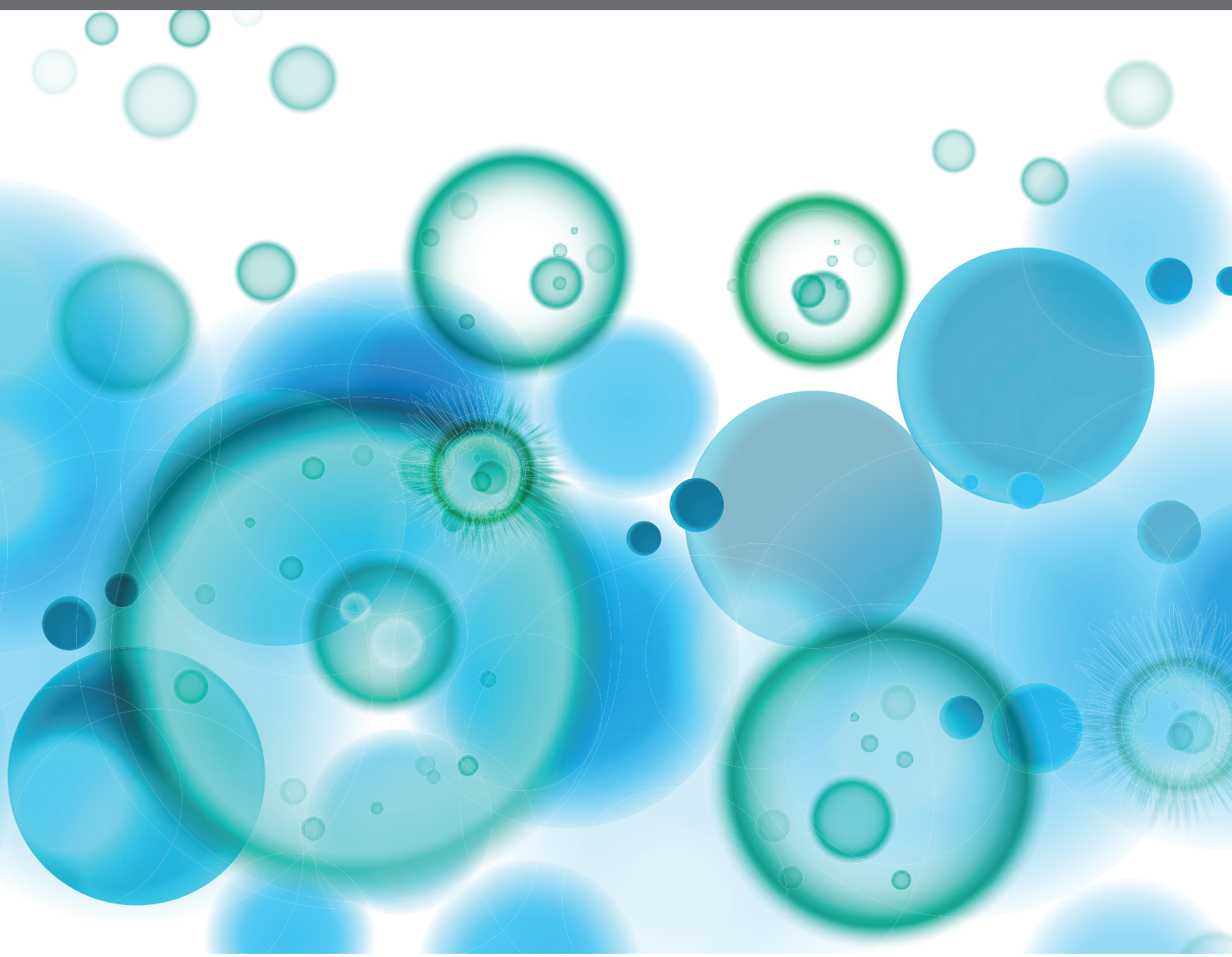
INNATE IMMUNITY IN KIDNEY INJURY, REPAIR AND FIBROSIS

EDITED BY: Bin Yang, Cheng Yang and Ying Wang
PUBLISHED IN: Frontiers in Immunology



frontiers Research Topics



frontiers

Frontiers eBook Copyright Statement

The copyright in the text of individual articles in this eBook is the property of their respective authors or their respective institutions or funders. The copyright in graphics and images within each article may be subject to copyright of other parties. In both cases this is subject to a license granted to Frontiers.

The compilation of articles constituting this eBook is the property of Frontiers.

Each article within this eBook, and the eBook itself, are published under the most recent version of the Creative Commons CC-BY licence. The version current at the date of publication of this eBook is CC-BY 4.0. If the CC-BY licence is updated, the licence granted by Frontiers is automatically updated to the new version.

When exercising any right under the CC-BY licence, Frontiers must be attributed as the original publisher of the article or eBook, as applicable.

Authors have the responsibility of ensuring that any graphics or other materials which are the property of others may be included in the CC-BY licence, but this should be checked before relying on the CC-BY licence to reproduce those materials. Any copyright notices relating to those materials must be complied with.

Copyright and source acknowledgement notices may not be removed and must be displayed in any copy, derivative work or partial copy which includes the elements in question.

All copyright, and all rights therein, are protected by national and international copyright laws. The above represents a summary only. For further information please read Frontiers' Conditions for Website Use and Copyright Statement, and the applicable CC-BY licence.

ISSN 1664-8714
ISBN 978-2-88974-979-9
DOI 10.3389/978-2-88974-979-9

About Frontiers

Frontiers is more than just an open-access publisher of scholarly articles: it is a pioneering approach to the world of academia, radically improving the way scholarly research is managed. The grand vision of Frontiers is a world where all people have an equal opportunity to seek, share and generate knowledge. Frontiers provides immediate and permanent online open access to all its publications, but this alone is not enough to realize our grand goals.

Frontiers Journal Series

The Frontiers Journal Series is a multi-tier and interdisciplinary set of open-access, online journals, promising a paradigm shift from the current review, selection and dissemination processes in academic publishing. All Frontiers journals are driven by researchers for researchers; therefore, they constitute a service to the scholarly community. At the same time, the Frontiers Journal Series operates on a revolutionary invention, the tiered publishing system, initially addressing specific communities of scholars, and gradually climbing up to broader public understanding, thus serving the interests of the lay society, too.

Dedication to Quality

Each Frontiers article is a landmark of the highest quality, thanks to genuinely collaborative interactions between authors and review editors, who include some of the world's best academicians. Research must be certified by peers before entering a stream of knowledge that may eventually reach the public - and shape society; therefore, Frontiers only applies the most rigorous and unbiased reviews.
Frontiers revolutionizes research publishing by freely delivering the most outstanding research, evaluated with no bias from both the academic and social point of view. By applying the most advanced information technologies, Frontiers is catapulting scholarly publishing into a new generation.

What are Frontiers Research Topics?

Frontiers Research Topics are very popular trademarks of the Frontiers Journals Series: they are collections of at least ten articles, all centered on a particular subject. With their unique mix of varied contributions from Original Research to Review Articles, Frontiers Research Topics unify the most influential researchers, the latest key findings and historical advances in a hot research area! Find out more on how to host your own Frontiers Research Topic or contribute to one as an author by contacting the Frontiers Editorial Office: frontiersin.org/about/contact

INNATE IMMUNITY IN KIDNEY INJURY, REPAIR AND FIBROSIS

Topic Editors:
Bin Yang, University of Leicester, United Kingdom
Cheng Yang, Fudan University, China
Ying Wang, Shanghai Institute of Nutrition and Health, Chinese Academy of Sciences (CAS), China

Citation: Yang, B., Yang, C., Wang, Y., eds. (2022). Innate Immunity in Kidney Injury, Repair and Fibrosis. Lausanne: Frontiers Media SA. doi: 10.3389/978-2-88974-979-9

Table of Contents

06 ***Editorial: Innate Immunity in Kidney Injury, Repair and Fibrosis***
Bin Yang, Cheng Yang and Ying Wang

11 ***Bone Marrow Mesenchymal Stem Cells Ameliorate Cisplatin-Induced Renal Fibrosis* via *miR-146a-5p/Tfdp2 Axis in Renal Tubular Epithelial Cells***
Lei Wu, Chao Rong, Qing Zhou, Xin Zhao, Xue-Mei Zhuansun, Shan Wan, Mao-Min Sun and Shou-Li Wang

21 ***The Role of Regulatory Myeloid Cell Therapy in Renal Allograft Rejection***
Jingming Zhuang and Jiangang Hou

29 ***TSC1 Affects the Process of Renal Ischemia-Reperfusion Injury by Controlling Macrophage Polarization***
Xiao Hu, Yanan Xu, Zhaoqi Zhang, Zuofu Tang, Jinhua Zhang, You Luo, Weiming Deng, Zhanwen Dong, Yong Zhao and Ning Na

41 ***Hydroxychloroquine Inhibits Macrophage Activation and Attenuates Renal Fibrosis After Ischemia-Reperfusion Injury***
Haofeng Zheng, Yannan Zhang, Jiannan He, Zhe Yang, Rui Zhang, Lei Li, Zihuan Luo, Yongrong Ye and Qiquan Sun

55 ***Cyclic Helix B Peptide Prolongs Skin Allograft Survival* via *Inhibition of B Cell Immune Responses in a Murine Model***
Long Zheng, Xuanchuan Wang, Linkun Hu, Wenjun Gao, Weitao Zhang, Xuepeng Zhang, Chao Hu, Ruiming Rong, Cheng Yang and Dong Zhu

64 ***Dendritic Cells: Versatile Players in Renal Transplantation***
Jinwen Lin, Hongyi Wang, Chenxi Liu, Ao Cheng, Qingwei Deng, Huijuan Zhu and Jianghua Chen

79 ***Macrophage Heterogeneity in Kidney Injury and Fibrosis***
Yi Wen, Hong-Ru Yan, Bin Wang and Bi-Cheng Liu

88 ***PARK7 Protects Against Chronic Kidney Injury and Renal Fibrosis by Inducing SOD2 to Reduce Oxidative Stress***
Lijun Yin, Honglin Li, Zhiwen Liu, Wenwen Wu, Juan Cai, Chengyuan Tang and Zheng Dong

104 ***The Role of Regulatory B cells in Kidney Diseases***
Wang Long, Hedong Zhang, Wenjia Yuan, Gongbin Lan, Zhi Lin, Longkai Peng and Helong Dai

115 ***Mesenchymal Stem Cell Protects Injured Renal Tubular Epithelial Cells by Regulating mTOR-Mediated Th17/Treg Axis***
Yongsheng Luo, Jingjing Guo, Pingbao Zhang, Yin Celeste Cheuk, Yamei Jiang, Jiyan Wang, Shihao Xu and Ruiming Rong

123 ***Mesenchymal Stem Cell-Derived Extracellular Vesicles: A Potential Therapeutic Strategy for Acute Kidney Injury***
Jia-Kun Li, Cheng Yang, Ying Su, Jing-Chao Luo, Ming-Hao Luo, Dan-Lei Huang, Guo-Wei Tu and Zhe Luo

136 ***Immunomodulatory Effects of Mesenchymal Stem Cells on Drug-Induced Acute Kidney Injury***
Qiuxia Han, Xiaochen Wang, Xiaonan Ding, Jun He, Guangyan Cai and Hanyu Zhu

146 ***Ischemia-Reperfusion Injury Reduces Kidney Folate Transporter Expression and Plasma Folate Levels***
Cheng Yang, Charith U. B. Wijerathne, Guo-wei Tu, Connie W. H. Woo, Yaw L. Siow, Susara Madduma Hewage, Kathy K. W. Au-Yeung, Tongyu Zhu and Karmin O

156 ***Fractalkine (CX3CL1) and Its Receptor CX3CR1: A Promising Therapeutic Target in Chronic Kidney Disease?***
Sarah Cormican and Matthew D. Griffin

170 ***Acute Kidney Injury Induced Lupus Exacerbation Through the Enhanced Neutrophil Extracellular Traps (and Apoptosis) in Fcgr2b Deficient Lupus Mice With Renal Ischemia Reperfusion Injury***
Wilasinee Saisorn, Supichcha Saithong, Pornpimol Phuengmaung, Kanyarat Udompornpitak, Thansita Bhunyakarnjanarat, Peerapat Visitchanakun, Awirut Chareonsappakit, Prapaporn Pisitkun, Direkrit Chiewchengchol and Asada Leelahavanichkul

192 ***Erythropoietin Receptor/β Common Receptor: A Shining Light on Acute Kidney Injury Induced by Ischemia-Reperfusion***
Yuanyuan Wu and Bin Yang

203 ***Approaches for Controlling Antibody-Mediated Allograft Rejection Through Targeting B Cells***
Yoshiko Matsuda, Takeshi Watanabe and Xiao-Kang Li

224 ***Identifying Biomarkers From Transcriptomic Signatures in Renal Allograft Biopsies Using Deceased and Living Donors***
Bin Yang, Nicolas Sylvius, Jinli Luo, Cheng Yang, Zhanyun Da, Charlottelrm Crotty and Michael L. Nicholson

241 ***Total Glucosides of Paeony Ameliorate Pristane-Induced Lupus Nephritis by Inducing PD-1 ligands^{+} Macrophages* via *Activating IL-4/STAT6/PD-L2 Signaling***
Chun-Ling Liang, Hongliang Jiang, Wenxuan Feng, Huazhen Liu, Ling Han, Yuchao Chen, Qunfang Zhang, Fang Zheng, Chuan-Jian Lu and Zhenhua Dai

253 ***NLRP3 Inflammasome in Metabolic-Associated Kidney Diseases: An Update***
Wei Xiong, Xian-Fang Meng and Chun Zhang

262 ***Long-Term Protection of CHBP Against Combinational Renal Injury Induced by Both Ischemia–Reperfusion and Cyclosporine A in Mice***
Yufang Zhang, Yuanyuan Wu, Wei Wang, Feng Liu, Yiwen Zhang, Cheng Yang, Aifen Liu, Jing Wu, Tongyu Zhu, Michael L. Nicholson, Yaping Fan and Bin Yang

275 ***Properdin Deficiency Impairs Phagocytosis and Enhances Injury at Kidney Repair Phase Post Ischemia–Reperfusion***
Yuanyuan Wu, Zinah D. Zwaini, Nigel J. Brunskill, Xinyue Zhang, Hui Wang, Ravinder Chana, Cordula M. Stover and Bin Yang

289 ***Myeloid-Derived Suppressor Cells Alleviate Renal Fibrosis Progression* via *Regulation of CCL5-CCR5 Axis***
Yue Qiu, Yirui Cao, Guowei Tu, Jiawei Li, Ying Su, Fang Fang, Xuepeng Zhang, Jing Cang, Ruiming Rong and Zhe Luo

302 ***Comprehensive Molecular and Cellular Characterization of Acute Kidney Injury Progression to Renal Fibrosis***

Renyan Wu, Jiawei Li, Guowei Tu, Ying Su, Xuepeng Zhang, Zhe Luo, Ruiming Rong and Yi Zhang

310 ***Hyperoside Suppresses Renal Inflammation by Regulating Macrophage Polarization in Mice With Type 2 Diabetes Mellitus***

Jialing Liu, Yanmei Zhang, Hongqin Sheng, Chunling Liang, Huazhen Liu, Jose Alberto Moran Guerrero, Zhaoyu Lu, Wei Mao, Zhenhua Dai, Xusheng Liu and Lei Zhang

327 ***Kidney-Draining Lymph Node Fibrosis Following Unilateral Ureteral Obstruction***

Xiaofei Li, Jing Zhao, Said Movahedi Naini, Gianmarco Sabiu, Stefan G. Tullius, Su Ryon Shin, Jonathan S. Bromberg, Paolo Fiorina, George C. Tsokos, Reza Abdi and Vivek Kasinath

336 ***Everolimus Alleviates Renal Allograft Interstitial Fibrosis by Inhibiting Epithelial-to-Mesenchymal Transition Not Only* via *Inducing Autophagy but Also* via *Stabilizing I*κ*B-*α**

Zeping Gui, Chuanjian Suo, Jun Tao, Zijie Wang, Ming Zheng, Shuang Fei, Hao Chen, Li Sun, Zhijian Han, Xiaobing Ju, Hengcheng Zhang, Min Gu and Ruoyun Tan

frontiers | Frontiers in Immunology

EDITORIAL
published: 05 May 2022
doi: 10.3389/fimmu.2022.909654

Editorial: Innate Immunity in Kidney Injury, Repair and Fibrosis

Bin Yang[1,2*], *Cheng Yang*[3,4,5] *and Ying Wang*[6]

[1] Department of Cardiovascular Sciences, College of Life Sciences, University of Leicester, University Hospitals of Leicester National Health Service (NHS) Trust, Leicester, United Kingdom, [2] Nantong-Leicester Joint Institute of Kidney Science, Department of Nephrology, Affiliated Hospital of Nantong University, Nantong, China, [3] Department of Urology, Zhongshan Hospital, Fudan University, Shanghai, China, [4] Shanghai Key Laboratory of Organ Transplantation, Shanghai, China, [5] Zhangjiang Institute of Fudan University, Shanghai, China, [6] Chinese Academy of Sciences (CAS) Key Laboratory of Tissue Microenvironment and Tumor, Shanghai Institute of Nutrition and Health, Chinese Academy of Sciences, Shanghai, China

Keywords: fibrosis, inflammation, innate immunity, kidney injury, macrophage, phagocytosis, repair and tubular epithelial cell

Editorial on the Research Topic

Innate Immunity in Kidney Injury, Repair and Fibrosis

OPEN ACCESS

Edited and reviewed by:
Francesca Granucci,
University of Milano-Bicocca, Italy

***Correspondence:**
Bin Yang
by5@le.ac.uk

Specialty section:
This article was submitted to Molecular Innate Immunity, a section of the journal Frontiers in Immunology

Received: *31 March 2022*
Accepted: *21 April 2022*
Published: *05 May 2022*

Citation:
Yang B, Yang C and Wang Y (2022) Editorial: Innate Immunity in Kidney Injury, Repair and Fibrosis. Front. Immunol. 13:909654. doi: 10.3389/fimmu.2022.909654

Innate immunity, a vital system in animals and humans, is precisely regulated, in which a balance between offensive and defensive actions maintains its homeostasis. The innate immunity is orchestrated by immune cells, cytokines and complement under physiological and pathological conditions. The activity of innate immune cells including dendritic cells (DC), neutrophils, macrophages, and tubular epithelial cells (TEC) and endothelial cells (EC) dominates innate immune responses. These innate immune cells not only participate in the occurrence of injury and inflammation, but also play beneficial roles in post-injury repair. Over-reactive and persistent immune-inflammatory responses result in further injury, mal-repair and fibrosis. On the other hand, the timely clearing damaged cells including apoptotic and necrotic cells, often executed by phagocytes including neutrophils, macrophages and TEC, is beneficial (1). Disclosing the complicated mechanisms of renal injury and repair, and the sophisticated actions of innate immunity will facilitate the strategy of limiting inflammation, promoting repair, and preventing fibrosis in both native and transplant kidneys.

Acute kidney injury (AKI) is a life-threatening disease, which affects 10%-15% hospitalized patients and 50% intensive care patients without effective early diagnosis and cause-specific treatment worldwide. AKI also predisposes to chronic kidney disease (CKD) that unavoidably develops to end stage renal disease, with 2 million patients dying each year worldwide due to a shortage of donor kidneys for transplant (2–4). Leading causes of AKI include ischemia-reperfusion (IR) and increased usage of nephrotoxic drugs, in which TEC and EC are the most vulnerable cells and important innate immune cells that regulate injury, repair and potential fibrosis (5). It is imperative to develop cause-specific interventions that will benefit patients clinically, healthcare

organizations financially and socioeconomic structures globally. Macrophages are central in the pathogenesis of kidney diseases, and also have therapeutic potential in limiting tissue injury and preventing fibrosis. The infiltration of macrophages, a major subset of innate immune cells, is a common feature after renal IR injury. The infiltrating macrophages can polarize into two distinct types: classically activated M1 macrophages, which not only inhibit infection, but also accelerate renal injury, while alternatively activated M2 macrophages, a repair phenotype, promote wound healing and subsequent fibrosis Xie et al. TSC1 is a negative regulator of the mammalian target of rapamycin (mTOR) signaling that regulates macrophage polarization in inflammation associated diseases. Hu et al. found that myeloid cell-specific TSC1 knockout mice had more severe functional and histological damage in the kidney than wild type (WT) mice during the early phase of IR injury with upregulated most M1 macrophage-related genes, but showed attenuated renal fibrosis during the repair phase with decreased M2 macrophage markers. These findings were confirmed in hypoxia-reoxygenation *in vitro* model. Therefore, TSC1 in macrophages contributes to the whole process of IR injury, serving as an inflammation suppressor during the early injury phase, but a fibrosis promoter over the repair. Liang et al. also reported that macrophages are main infiltrating cells in the kidney of lupus nephritis. PD-1 ligands (PD-Ls) are beneficial by contributing to M2 macrophage polarization and immunosuppression. Total glucosides of paeony (TGP) significantly decreased urinary protein and improved renal function, reducing serum anti-ds-DNA and ameliorating renal immunopathology in lupus nephritis murine model. TGP increased the frequency of splenic and peritoneal M2-like macrophages. TGP may be a potent drug to treat lupus nephritis by IL-4/STAT6/PD-L2 signaling pathway to induce M2-like macrophages. Liu et al. using C57BLKS/6J ^{Lep} *db/db* mice and a high glucose-induced bone marrow-derived macrophage polarization system showed that hyperoside (HPS), an active flavonoid glycoside in the Chinese herbal medicine Tu-Si-Zi, markedly reduced diabetes-induced albuminuria and glomerular mesangial matrix expansion, with a significant improvement of fasting blood glucose level, hyperlipidaemia and body weight. The pretreatment of HPS effectively regulated macrophage polarization by shifting M1 to M2 phenotype, resulting in the inhibition of M1 macrophage infiltration, reducing pre-inflammatory mediators including MCP-1, TNF-α and iNOS, and increasing anti-inflammatory cytokine Arg-1 and CD163/CD206. HPS also promoting $CD4^+$ T cell differentiation into Th2 and Treg populations. Wen et al. reviewed recent studies and highlighted that kidney macrophages are notably heterogeneous immune cells that fulfil opposing functions in terms of clearing deposited pathogens, maintaining immune tolerance, initiating and regulating inflammatory responses, and degrading the extracellular matrix, or promoting kidney fibrosis. Macrophage origins can partially explain macrophage heterogeneity in the kidneys. Circulating $Ly6C^+$ monocytes are recruited to inflammatory sites by chemokines, while self-renewed kidney resident macrophages contribute to kidney repair and fibrosis. Mechanisms underlying kidney macrophage heterogeneity may help develop macrophage-targeted therapies for kidney diseases. Saisorn et al. postulated that IR might be exacerbate lupus activity through neutrophil extracellular traps (NETs) and apoptosis. They performed renal IR injury in Fc gamma receptor 2b deficient (Fcgr2b-/-) lupus mice. At 24 h IR injury, NETs in peripheral blood neutrophils and in kidneys, and apoptosis in kidneys were more prominent in Fcgr2b-/- mice compared to WT. After 120 h renal IR injury, renal NETs were non-detectable, whereas glomerular immunoglobulin deposition and serum anti-dsDNA were increased in Fcgr2b-/- mice, implying that raised NETs at the early stage of IR injury have long-term impact on exacerbating lupus nephritis. Moreover, acute or chronic kidney diseases often cause micronutrient deficiency including reduced folate, an essential B vitamin, in which reabsorption of folate by TEC is important. Yang et al. reported that low plasma folate in rats subjected to kidney IR injury, which were inversely correlated to plasma creatinine, with decreased expression of folate transporters. Inhibiting folate transporter in human TEC reduced intracellular folate. These results suggest that IR injury downregulates folate transporters and folate uptake by TEC, and leads to low folate in the circulation.

Innate immunity plays multiple roles in kidney repair. Properdin, a positive regulator of complement alternative pathway, participates in renal IR injury, and also acts as a pattern-recognition molecule facilitating the phagocytic clearance of damaged cells. Wu et al. revealed that properdin knockout (P^{KO}) mice exhibited greater injury than WT mice post 72-h IR, with more apoptotic cells and macrophages in tubule luminal areas, and further raised EPOR. Properdin siRNA reduced properdin expression in H_2O_2 treated TEC, but raised apoptosis. The phagocytic ability of WT TEC was promoted by H_2O_2, but inhibited by P^{KO}, while only locally produced properdin plays crucial roles in opsonizing damaged cells and regulating TEC phagocytosis. Moreover, major causes of AKI including IR, not only induce injury, but also initiate self-defense system to limit injury and promote repair. One of these innate immune responses is to produce erythropoietin (EPO) that simultaneously triggers its homodimer receptor $(EPOR)_2$ and heterodimer EPOR/β common receptor (EPOR/βcR), also called innate repair receptor (6). EPOR/βcR is expressed in several cell types including TEC at low level, but is swiftly upregulated and also translocated to cellular membrane under stress such as IR injury. EPOR/βcR mediates anti-apoptosis, anti-inflammation, pro-regeneration, and remodeling in AKI *via* different signaling pathways including PI3K/Akt, STAT3 and MAPK. Wu and Yang also reviewed the biological functions and mechanistic signaling pathways of these receptors in AKI, and discuss its potential clinical applications as a biomarker for early diagnosis, predicting prognosis, and guiding cell target drug delivery. AKI requires more efficient and specific treatments, rather than just supportive therapy. Mesenchymal stem cells (MSCs) are promising for cellular therapy because of their low immunogenicity and ability to expand *in vitro*. The main

therapeutic effects of MSCs were mediated by MSC-derived extracellular vesicles (EVs) that even have more merits including lower immunogenicity, no tumorigenesis and artificially modifying potential. Li et al. reviewed the therapeutic efficacy and mechanism of MSCs and MSC-EVs in AKI and believe that MSC-EVs will become an effective approach to overcome the current limitations in AKI treatment, although it still face many challenges such as lack of clinical trials so far. Han et al. also reviewed recent studies that have provided a deeper understanding on the mechanisms of drug-induced AKI, among which acute tubular interstitial injury induced by the breakdown of innate immunity plays an important role. MSCs can inhibit kidney damage by regulating innate immunity, promote repair and prevent fibrosis. They addressed the immune pathogenesis of drug-induced AKI versus IR-induced AKI, and explored the immunomodulatory effects and therapeutic potential of MSCs for drug-induced AKI. Luo et al. further reviewed MSCs controlled the imbalance between T helper 17 cell (Th17)-mediated pro-inflammatory response and regulatory T cell (Treg)-mediated anti-inflammatory effect in renal TEC injury. Given that Th17 and Treg are derived from a common $CD4^+$ T cell precursor, MSC-mediated inhibition of mTOR to restrain $CD4^+$ T cell differentiation into Th17, but in turn promotes Treg generation. Therefore, MSC-mediated Th17-to-Treg polarization acts as a new immunotherapy for kidney injury. Furthermore, B cells, commonly regarded as proinflammatory antibody-producing cells, are detrimental to individuals with autoimmune diseases. However, it has been also revealed that regulatory B (Breg) cells, an immunosuppressive subset, may exert protective effects by producing immune-regulatory cytokines including IL-10, TGF-β, and IL-35. The functions of Breg cells vary according to their phenotype, but no specific marker or Breg cell-specific transcription factor has been identified. Long et al. reviewed the phenotypes and function of Breg cells and highlighted their potential therapeutic value in kidney diseases.

Renal fibrosis is the final common pathway of CKD regardless of etiology, in which innate immunity is crucial. Yin et al. demonstrated that parkinson disease protein 7 (PARK7) protects against unilateral ureteric obstruction (UUO)-induced CKD and renal fibrosis by inducing SOD2 to reduce transforming growth factor-b (TGFB1) associated oxidative stress in tubular cells. Innate immune cells, of course, are key contributors to kidney inflammation and fibrosis. *Cormican and Griffin.* reviewed the interactions of CX3CL1 and CX3CR1 in recruiting innate immune cells into the kidney, which that mediates the progression of CKD. They highlighted the therapeutic potential of targeting CX3CL1 or CX3CR1 to benefit CKD patients. In addition, metabolic syndrome refers to the pathological state of metabolism disorder of protein, fat, carbohydrate and other substances in human body. The kidney is an important organ of metabolism, in which various metabolic disorders can cause inflammatory response and kidney damage. Xiong et al. reviewed the function and specific regulatory mechanism of inflammasomes including NLRP3 in inflammatory infiltration, pyroptotic cell death and kidney damage caused by various metabolic disorders, and provide a new therapeutic perspective and targets for kidney diseases. Li et al. found for the first time that fibroblastic reticular cells (FRCs) increased production of extracellular matrix (ECM) fibers and remodeled the microarchitecture of the UUO kidney-draining lymph node (KLN) in mice, contributing to fibrosis that mirrored the changes in the kidney. The populations of $CD11b^+$ antigen-presenting cells, $CD11c^+$ DC, and activated $CD4^+$ and $CD8^+$ T cells were also significantly higher in the UUO KLN than that in the KLN draining the unaffected contralateral kidney, with upregulated TGFβ/TGFβR signaling pathway. Both release of ureteral ligation at 2 days following UUO and depletion of FRCs at the time of injury onset halted the progression of fibrosis in both the kidney and the KLN. Gui et al. found that everolimus (EVR) could attenuate the progression of epithelial-mesenchymal transition (EMT) and renal allograft interstitial fibrosis, and also activate autophagy in chronic allograft dysfunction rat model. EVR may retard impaired autophagic flux and block NF-κB pathway activation, and thereby prevent progression of TNF-α-induced EMT and renal allograft interstitial fibrosis. Zheng et al. reported hydroxychloroquine (HCQ) efficiently inhibited the activation of macrophages and MAPK signaling pathways, and attenuated renal fibrosis in a mouse model of IR-induced renal tubulointerstitial fibrosis. HCQ also inhibited macrophage activation *in vitro*, especially M2 macrophages, and promoted macrophage apoptosis. The effects of HCQ on renal fibrosis and macrophages were decreased after depletion of TLR-9. Therefore, HCQ could be a new anti-fibrotic drug and TLR-9 could be a potential therapeutic target for CKD following AKI. Wu et al. found microRNA (miR)-146a-5p was the most significant up-regulated miRNA in the TEC of renal fibrosis mouse model induced by repeated low-dose cisplatin, while Tfdp2 gene was one target gene of miR-146a-5p. Bone marrow MSCs attenuate cisplatin-induced renal fibrosis by regulating the miR-146a-5p/Tfdp2 axis in mouse renal TEC.

Innate immunity is also important in kidney transplantation. Renal IR injury and cyclosporine A (CsA) nephrotoxicity affect allograft function and survival. Zheng et al. showed that CHBP, only initiating EPOR/βcR, predominantly protects kidneys against IR injury at 2 weeks and/or CsA nephrotoxicity at 8 weeks in mouse kidneys, with different underlying mechanisms. Urinary albumin/creatinine is a good biomarker in monitoring the progression of transplant-related injuries. CsA divergently affects apoptosis in kidneys and cultured kidney epithelial cells, in which CHBP and/or CASP-3 siRNA reduces inflammation and apoptosis. Antibody-mediated rejection (AMR) represents a major cause of allograft dysfunction and results in allograft failure in solid organ transplantation. CHBP ameliorated renal allograft rejection in a renal transplantation model. Zheng et al. investigated the effect of CHBP on AMR using a secondary allogeneic skin transplantation model by transplanting skin from BALB/c mice to C57BL/6 mice. Skin allograft survival was significantly prolonged by CHBP, with reduced $CD19^+$ B cells, splenic plasma cells, germinal center B cells, and Tfh cells in skin

allografts, and ameliorated serum donor specific antibodies. CHBP inhibited AMR, which may be mediated by NF-κB signaling to suppress B cell immune responses. Acute and chronic AMR are directly mediated by B cells and difficult to treat. Long-lived plasma cells (LLPCs) in bone marrow play a crucial role in the production of the antibodies that induce AMR. LLPCs survive through a T cell-independent mechanism and resist conventional immunosuppressive therapy. Matsuda et al. reviewed the direct or indirect involvement of immunocompetent cells in the differentiation of naïve-B cells into LLPCs, the development and limitations of control methods for AMR, and their potential clinical applications. Wu et al. analyzed publicly available RNA-sequencing datasets from three mouse bulk kidney mRNA-sequencing including IR or cisplatin induced AKI and UUO induced fibrosis, and one human single-cell kidney RNA-sequencing. Regardless of causes of AKI, T cell activation was mainly related to renal fibrosis progression, while fatty acid metabolic process and arachidonic acid metabolism mainly occurred in tubule cells. The differences in the AKI-to-fibrosis process caused by different factors were connected to the different functions of immune cells and tubule cells in the kidney, which may pave the way for exploring novel potential therapeutic strategies. It is well known that the survival of transplant kidneys using deceased donor (DD) kidneys is inferior to living donor (LD) kidneys. Yang et al. conducted a microarray analysis of 24 human DD and LD kidney biopsies paired at 30 minutes and 3 months post-transplantation. 446 differentially expressed genes (DEGs) between DD and LD at 30 minutes reflected donor injury and acute immune responses, while 146 DEGs at 3 months represented adaptive immunity and immunosuppressive treatment. Some early expressed DEGs correlated with renal function and histology at 12 months were further validated by qPCR in additional 33 time point unpaired kidney biopsies. Divergent transcriptomic signatures between DD and LD might contribute to the allograft survival of two type donors. DEGs including SERPINA3 could be novel biomarkers for diagnosis and intervention over donor kidney preservation. The immune rejection is effectively controlled in the acute phase of kidney transplantation, but chronic rejection mediated by chronically activated antibodies ultimately lead to graft failure. At present, immunosuppressive agent fails to increase the long-term survival rate of allografts, and also has many adverse reactions. Zhuang et al. reviewed the latest prospects of immune cells focusing on regulatory myeloid cells to regulate the immune response in renal transplantation, and also introduce their respective progress from experimental research to clinical immunotherapy to control allograft rejection. Lin et al. also reviewed DC induce and regulate adaptive immunity in the kidney by discussing their origin, maturation, pathological effects, and interaction with effector T cells and Tregs. Divergent DCs play both positive and negative roles in IR-induced renal transplant injury, in terms of switching phenotypes to result in acute or chronic rejection, and orchestrating surface markers for allograft tolerance *via* alterations in metabolism. A multidimensional transcriptomic analysis of renal transplantation will facilitate the understanding DC ontogeny and subpopulations.

CONCLUSIONS

On the Research Topic of "Innate Immunity in Kidney Injury, Repair and Fibrosis", 16 research articles and 11 review papers were published, which addressed the involvement of macrophage polarization, neutrophils, TEC and DC, regulatory myeloid cells and B cells, and kidney-draining lymph node in a broad range of acute and chronic renal injury models induced by IR, UUO, cisplatin, lupus and diabetes, as well as immune response associated DEGs in biological samples from kidney transplant patients. In addition, a variety of relevant therapeutic interventions including erythropoietin derived peptide CHBP, everolimus and Chinese medicine hyperoside in limiting injury, promoting repair and preventing fibrosis were validated in different disease models *via* different mechanisms and signalling pathways associated with innate immunity cells and mediators. We believe this Research Topic provides new findings of innate immunity in both native and transplant kidney diseases. We much appreciate all contributions from authors, reviewers and editors alike.

AUTHOR CONTRIBUTIONS

BY, CY and YW wrote the editorial. All authors contributed to the editorial and approved the submitted version.

REFERENCES

1. Zwaini Z, Dai H, Stover C, Yang B. Role of Complement Properdin in Renal Ischemia-Reperfusion Injury. *Curr Gene Ther* (2018) 17:411–23. doi: 10.2174/1566523218666180214093043
2. Ronco C, Bellomo R, Kellum JA. Acute Kidney Injury. *Lancet* (2019) 394:1949–64. doi: 10.1016/S0140-6736(19)32563-2
3. Mehta RL, Cerda J, Burdmann EA, Tonelli M, Garcia-Garcia G, Jha V, et al. International Society of Nephrology's 0by25 Initiative for Acute Kidney Injury (Zero Preventable Deaths by 2025): A Human Rights Case for Nephrology. *Lancet* (2015) 385:2616–43. doi: 10.1016/S0140-6736(15)60126-X
4. De Chiara L, Conte C, Antonelli G, Lazzeri E. Tubular Cell Cycle Response Upon AKI: Revising Old and New Paradigms to Identify Novel Targets for CKD Prevention. *Int J Mol Sci* (2021) 22:11093–111. doi: 10.3390/ijms222011093
5. Wu Y, Chen W, Zhang Y, Liu A, Yang C, Wang H, et al. Potent Therapy and Transcriptional Profile of Combined Erythropoietin-Derived Peptide Cyclic Helix B Surface Peptide and Caspase-3 siRNA Against Kidney Ischemia/Reperfusion Injury in Mice. *J Pharmacol Exp Ther* (2020) 375:92–103. doi: 10.1124/jpet.120.000092
6. Yang C, Zhang Y, Wang J, Li L, Wang L, Hu M, et al. A Novel Cyclic Helix B Peptide Inhibits Dendritic Cell Maturation During Amelioration of Acute

Kidney Graft Rejection Through Jak-2/Stat3/Socs1. *Cell Death Dis* (2015) 6: e1993-2004. doi: 10.1038/cddis.2015.338

Conflict of Interest: The authors declare that the research was conducted in the absence of any commercial or financial relationships that could be construed as a potential conflict of interest.

Publisher's Note: All claims expressed in this article are solely those of the authors and do not necessarily represent those of their affiliated organizations, or those of the publisher, the editors and the reviewers. Any product that may be evaluated in this article, or claim that may be made by its manufacturer, is not guaranteed or endorsed by the publisher.

Copyright © 2022 Yang, Yang and Wang. This is an open-access article distributed under the terms of the Creative Commons Attribution License (CC BY). The use, distribution or reproduction in other forums is permitted, provided the original author(s) and the copyright owner(s) are credited and that the original publication in this journal is cited, in accordance with accepted academic practice. No use, distribution or reproduction is permitted which does not comply with these terms.

frontiers in Immunology

ORIGINAL RESEARCH
published: 16 February 2021
doi: 10.3389/fimmu.2020.623693

Bone Marrow Mesenchymal Stem Cells Ameliorate Cisplatin-Induced Renal Fibrosis *via* miR-146a-5p/Tfdp2 Axis in Renal Tubular Epithelial Cells

Lei Wu[1,2†], *Chao Rong*[1†], *Qing Zhou*[3], *Xin Zhao*[1], *Xue-Mei Zhuansun*[4], *Shan Wan*[1], *Mao-Min Sun*[4*] and *Shou-Li Wang*[1,2*]

[1] Department of Pathology, School of Biology & Basic Medical Sciences, Soochow University, Suzhou, China, [2] Collaborative Innovation Center of Clinical Immunology, Sihong People's Hospital, Soochow University, Suzhou, China, [3] Department of General Surgery, Affiliated Hospital of Jiangsu University, Zhenjiang, China, [4] Laboratory Animal Research Center, Medical College of Soochow University, Suzhou, China

OPEN ACCESS

Edited by:
Cheng Yang,
Fudan University, China

Reviewed by:
Helong Dai,
Central South University, China
Ruiming Rong,
Fudan University, China

***Correspondence:**
Mao-Min Sun
sunmaomin@suda.edu.cn
Shou-Li Wang
wangshouli@suda.edu.cn

[†]These authors have contributed equally to this work

Specialty section:
This article was submitted to Alloimmunity and Transplantation, a section of the journal Frontiers in Immunology

Received: 30 October 2020
Accepted: 24 December 2020
Published: 16 February 2021

Citation:
Wu L, Rong C, Zhou Q, Zhao X, Zhuansun X-M, Wan S, Sun M-M and Wang S-L (2021) Bone Marrow Mesenchymal Stem Cells Ameliorate Cisplatin-Induced Renal Fibrosis via miR-146a-5p/Tfdp2 Axis in Renal Tubular Epithelial Cells. Front. Immunol. 11:623693. doi: 10.3389/fimmu.2020.623693

Mesenchymal stem cells (MSCs) have regenerative properties in acute kidney injury (AKI). However, the potential function of MSCs in chronic kidney disease remains elusive. Renal fibrosis is the common endpoint of chronic progressive kidney diseases and causes a considerable health burden worldwide. In this study, the protective effects of bone marrow mesenchymal stem cells (BM-MSCs) were assessed in repeated administration of low-dose cisplatin-induced renal fibrosis mouse model *in vivo* as well as a TGF-β1-induced fibrotic model *in vitro*. Differentially expressed miRNAs in mouse renal tubular epithelial cells (mRTECs) regulated by BM-MSCs were screened by high-throughput sequencing. We found microRNA (miR)-146a-5p was the most significant up-regulated miRNA in mRTECs. In addition, the gene Tfdp2 was identified as one target gene of miR-146a-5p by bioinformatics analysis. The expression of Tfdp2 in the treatment of BM-MSCs on cisplatin-induced renal injury was evaluated by immunohistochemistry analysis. Our results indicate that BM-MSC attenuates cisplatin-induced renal fibrosis by regulating the miR-146a-5p/Tfdp2 axis in mRTECs.

Keywords: bone marrow mesenchymal stem cells, renal fibrosis, microRNA, TGF-β1, renal tubular epithelial cells

INTRODUCTION

Renal fibrosis is characterized by the activation of massive fibroblast and deposition of the fibrotic matrix in kidney tissue, which is considered as the common endpoint of chronic kidney disease (CKD) (1, 2). Renal fibrosis mainly affects over 70-years old adults who account for over 10% of the world population (3). In 2017, the global population of CKDs was about 6.97 million, and patients with CKD in China were approximately 1.32 million. Between 1990 and 2017, the global prevalence of CKD increased by 29.3%, and the global mortality rate increased by 41.5% (4). However, the therapeutic strategies for CKD, such as kidney transplantation or dialysis, are still limited. A shortage of donor organs impedes kidney transplantation, and the cost of dialysis becomes

unsustainable, especially in developing countries (5). Therefore, exploring novel and better therapeutic approaches are urgently needed.

Mesenchymal stem cells (MSCs) are multipotent cells with robust capacities of self-renewal, regeneration, proliferation, and differentiating into distinct functional cells (6, 7). MSCs can differentiate into various types of cells, such as osteoblasts, chondrocytes, or adipocytes under appropriate conditions *in vivo* or *in vitro*. Therefore, MSCs are widely used in tissue engineering, gene therapy, and immunotherapy (8, 9). The immunomodulatory and paracrine capabilities of MSCs may present the potential for therapeutic capacities in response to local environmental cues. Recent studies have reported that bone marrow MSCs (BM-MSCs) possess regenerative properties and immense plasticity to contribute to their therapeutic effects in organ injury, including acute kidney injury (AKI) and CKD (10–13). However, the mechanisms by which BM-MSCs protect renal tissues are complex, such as preventing renal tubular epithelial cell apoptosis, promoting renal tubular epithelial cell proliferation, and modulating the immune system by various cytokines and growth factors (14). MicroRNAs (miRNAs) are endogenous non-coding RNAs with a length of about 21–24 nucleotides, which regulate protein translation by combining with complementary sequences in the 3'non-coding region (3'UTR) various mRNAs (15). Recently, it has been widely accepted that miRNAs play vital roles in the progression of kidney disease (16). Specific miRNAs are associated with the initiation and development of renal fibrosis by anti- or pro-fibrogenic effects (17).

In the present study, we established a mouse model with renal fibrosis by repeated administration of low-dose cisplatin. The protective effects of BM-MSCs have been examined *in vivo* as well as in TGF-β1-treated mouse renal tubular epithelial cells (mRTECs) with an indirect co-culture environment. Next, we performed a high-throughput sequencing to identify significantly regulated miRNAs by mRTECs and probe further the underlying indirect molecular mechanism of miRNAs in the therapeutic process of BM-MSCs.

MATERIALS AND METHODS

Ethical Considerations

Experimental protocols were approved by the Animal Ethics Committee of Soochow University and were performed following the guidelines for use and care of laboratory animals of the Experimental Animal Committee of Soochow University (Approval No : ECSU-201800099).

Mouse Model of Renal Fibrosis

Eight-week-old male C57BL/6 mice were purchased from Zhao Yan Animals Co., Ltd. (Suzhou, China). On arrival, the mice were housed under antiviral and antibody-free micro-isolator conditions and fed a standard diet. Previous studies reported that multiple administrations of cisplatin cause renal fibrosis (18). We established and developed kidney injury and fibrosis C57BL/6 mice models using a low dose treatment of cisplatin once a week for 6 weeks. The mice were randomly divided into three groups as normal control (NC) group, cisplatin group, and cisplatin + BM-MSC group (n=6 for each group): 1) NC group: mice underwent intraperitoneal injection of 0.9% NaCl solution 10μl/g, once a week; from the 4th week underwent injection of 0.9% NaCl solution 0.4 ml through the tail vein, once per week. 2) Cisplatin group: intraperitoneal injection of 3.5mg/kg cisplatin solution according to the bodyweight of the mouse, once per week; from the 4th week, 0.9% NaCl solution 0.4 ml was injected through the tail vein once per week. 3) Cisplatin + BM-MSC group: intraperitoneal injection of 3.5mg/kg cisplatin solution according to the bodyweight of the mouse, once per week; from the 4th week, injection with normal saline containing 1.5×10^6/ml BM-MSCs, 0.4 ml per mouse, once a week. At 6th weeks post-injection, the mice were sacrificed, the kidneys and serum from all mice were collected for further investigation.

In Vitro Co-Culture Experiments

mRTECs were obtained from ScienCell Research Laboratories. BM-MSCs were gifted by Prof. Dr. Yufang Shi's Laboratory, Soochow University. mRTECs and BM-MSCs were cultured in DMEM, low glucose medium (HyClone) with 10% FBS (Gibco), 100 units/ml penicillin, and 100 μg/ml streptomycin. All cells were maintained at 37°C in a humidified atmosphere with 5% CO_2. mRTECs were seeded in 6-well plates at 1×10^5/well, and TGF-β1 (10 ng/ml) was added into the medium. After 48 h of stimulation, the medium of each group was changed to a complete medium without exogenous cytokine TGF-β1. A Transwell system was selected to establish the indirect co −culture environment. BM-MSCs were added to the transwell chamber at 1×10^5/well and indirectly co-cultured with mRTECs in a 37°C incubator for 24 h. A complete medium without BM-MSCs was added to the upper chamber for the control group.

Histological Analysis

C57BL/6 mouse kidney tissues were sectioned and fixed in formalin. Paraffin-embedded tissues were stained with Hematoxylin and eosin (H&E), Masson trichrome, and Sirius red. Sirius red staining was performed following the Sirius Red Stain Kit (Yuanye Bio-Technology, Shanghai, China). Interstitial fibrosis areas were assessed using microscopy (Olympus) by examining five randomly selected fields (×100) of the cortex. The staining figures were evaluated independently by two pathologists and quantified by histograms.

MiRNA High-Throughput Sequencing and Quantitative Real-Time Reverse-Transcription Polymerase Chain Reaction

High-throughput sequencing of miRNA was performed by Cloud-seq Biotechnology Co., Ltd (Shanghai, China). Isolation of miRNA from cultured cells and tissues was performed by using the Total RNA Miniprep Purification Kit (GeneMark). Grind fresh mouse kidney tissues with an electric grinder, total RNA was extracted from mRTECs, and grated kidney tissues by 1ml TRIzol and miRNA were isolated according to the manufacture's

instructions. Reverse transcription for specific miRNAs was performed using 2 μg miRNA and respective primers for reverse transcription (listed in **Supplementary Table 1**) according to the Stem-loop method. Quantitative real-time PCR was carried out using the ABsolute qPCR SYBR Green ROX Mix (Thermo Fisher Scientific) and the following cycling condition: 95°C for 10 min, 40 cycles of 95°C for 15 s, and 60°C for 60 s. StepOne Plus device (Thermo Fisher Scientific) was used for detection. The snRNA U6 was used for normalization.

Western Blotting Analysis

The protein was extracted from fresh tissues and mRTECs by using RIPA lysate. The total protein concentration was measured using a BCA protein quantitative kit and denatured by heating. The protein samples were assessed by 10% sodium dodecyl sulfate polyacrylamide gel electrophoresis (SDS-PAGE), semi-dry transferred to polyvinylidene fluoride (PVDF), and incubated with primary antibody against α-SMA (1:350, Affinity, USA) and Col1α1 (1:500, Abcam, USA) at 4°C overnight. Next, after being washed by TBST three times and incubated with a specific secondary antibody (1:3,000; Boster, China) for 2 h at room temperature. Immunoreactivity was visualized using an ECL detection system.

Cell Transfection

Cells were transfected with 50nM miR-146a-5p mimics/inhibitors or Tfdp2 siRNA (RiboBio Co, Guangzhou, China) when the cell density reached 80–90% prior. Lipofectamine 2000 reagent (Invitrogen, No. 1070962) was used for siRNA transfection. The cells were transferred to low glucose-DMEM with 10% FBS complete medium 6 h after transfection. Cells were harvested after 24 h.

Immunochemistry Staining

C57BL/6 mouse kidney tissues were sectioned and fixed in formalin. After the sections were dewaxed, antigen repaired, and serum sealed, Incubate membrane and Tfdp2 primary antibody (1:200, Abcam, ab235830) overnight at 4°C. PBS was used to wash the sections, and then the samples were incubated in biotinylated anti-rabbit secondary antibody (1:200, Beyotime, China).

Statistical Analysis

All data are expressed as the mean + standard error of the mean. Multiple comparisons were performed using Student's *t*-test and one-way ANOVA. Statistical analysis was processed by Prism 8 software (GraphPad Software, CA). Differences between mean values were considered statistically significant at $P < 0.05$.

RESULTS

Bone Marrow Mesenchymal Stem Cells Attenuate Renal Injury and Fibrosis *In Vitro* and *In Vivo*

We established and developed kidney injury and fibrosis C57BL/6 mice models using a low dose treatment of cisplatin once a week for 6 weeks (cisplatin group). To explore the effect of BM-MSCs on renal injury and fibrosis, mice were injected with the suspension of BM-MSCs *via* the tail vein (cisplatin +BM-MSCs group) (**Figure 1A**). All mice were euthanized at 6 weeks after the first cisplatin administration. Compared to the normal control group (NC), the volume and weight of kidneys in the cisplatin group and BM-MSCs-treated group were obviously reduced, which displayed granular or nodular surface. There was no significant difference in the appearance of the kidney between cisplatin group and cisplatin +BM-MSCs group (**Figure 1B**). To characterize this phenotype in more details, histologic and molecular tests were performed. H&E staining, Masson staining (collagen fibers marked blue), and Sirius red staining (collagen fibers marked red) showed that the fibrotic areas of the cisplatin group were significantly induced as compared to NC group kidneys. After injected the suspension of BM-MSCs *via* the tail vein, the fibrotic areas were reduced as compared with the cisplatin group (**Figure 1C**, **Supplementary Figures 1A, B**). Next, the biomarkers of kidney function and injury in serum were measured. The apparent elevation of serum creatinine (SCr) and blood urea nitrogen (BUN) levels was observed in the cisplatin group. Only the BUN level was significantly decreased by the treatment of BM-MSCs (**Figures 1D, E**). Analysis of fibrotic gene markers by RT-qPCR showed that the transcript levels of α-SMA and Col1α1 were significantly elevated in the cisplatin group compared to NC kidney tissues, while injection of BM-MSCs reduced the levels of α-SMA and Col1α1 (**Figures 1F, G**). The findings were confirmed by western blot analysis in protein level (**Figure 1H**). These results demonstrated that multiple administrations of cisplatin induced renal injury and fibrosis in mice, which could be attenuated by treatment with BM-MSCs through decreasing the expression of α-SMA and Col1α1.

To verify whether BM-MSCs had a therapeutic effect on renal fibrosis *in vitro*, we used exogenous cytokine TGF-β1 to stimulate mRTECs for 48h and to establish a fibrotic model *in vitro*. Subsequently, TGF-β1-treated mRTECs were divided into two groups: with or without BM-MSCs co-cultured treatment for 24 h. The expression of α-SMA and Col1α1 in mRTECs were detected by RT-qPCR analysis in transcript level (**Figures 2A, B**) and western blot analysis in protein level (**Figure 2C**). Our results revealed that both transcriptional and translational levels of α-SMA and Col1α1 in mRTECs were significantly reduced while co-cultured with BM-MSCs, which suggested that BM-MSCs could alleviate fibrosis in mRTECs.

Screening and Validation of Differentially Expressed miRNAs in Mouse Renal Tubular Epithelial Cells Regulated by Bone Marrow Mesenchymal Stem Cells

To screen the differentially expressed miRNAs in mRTECs regulated by BM-MSCs, we performed a miRNA high-throughput sequencing (series GSE148144) for TGF-β1-treated mRTECs with or without BM-MSCs co-culture. The heatmap of all the different expressed miRNAs was shown in **Figure 3A**. We

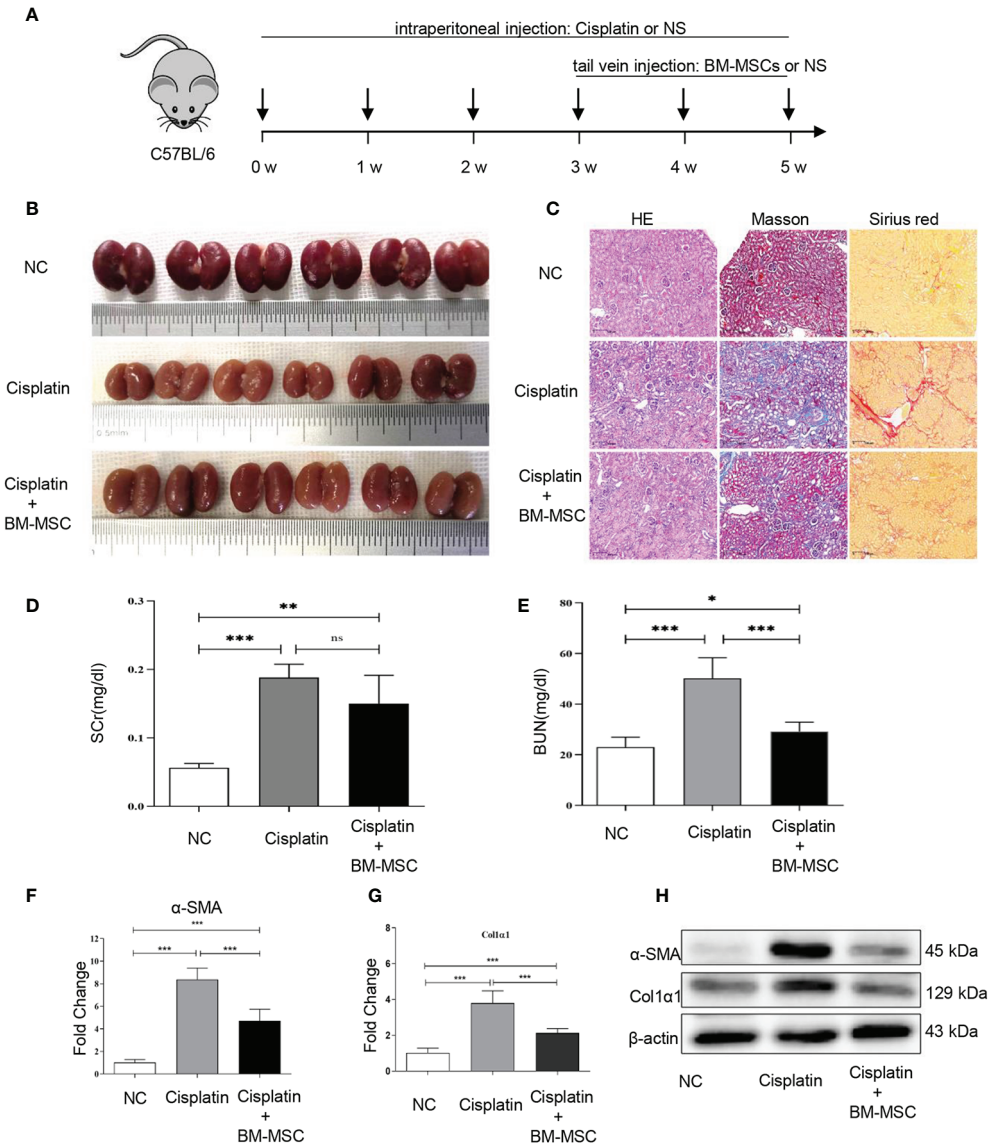


FIGURE 1 | The effect of bone marrow mesenchymal stem cells (BM-MSCs) on cisplatin-induced renal injury and fibrosis *in vivo*. **(A)** The schematic diagram of mice infected with cisplatin solution intraperitoneally and suspension of BM-MSCs *via* the tail vein. **(B)** Image of the morphology of kidney in mice infected cisplatin solution intraperitoneally and suspension of BM-MSCs *via* the tail vein. **(C)** H&E, Masson, and Sirius red staining. **(D, E)** serum creatinine (SCr) and blood urea nitrogen (BUN) levels of serum in mice were determined. The relative mRNA expression levels **(F, G)** and the protein levels **(H)** of α-SMA and Col1α1 in mice kidney tissues were evaluated by real-time PCR and Western blot, respectively. Data represent the mean ± SE from three independent experiments. *P < 0.05; **P < 0.01; ***P < 0.001; NS, not significant.

discovered a panel of miRNAs (miR-146a-5p, miR-12194-3p, miR-210-3p, miR-210-5p, let-7i-3p) with the top-five most significant changes in two groups, which were verified by RT-qPCR analysis and revealed that miR-146a-5p was the most significant up-regulated miRNA (**Figure 3B**). According to these results, we confirmed that BM-MSCs exert the anti-fibrosis function by regulating miR-146a-5p expression in mRTECs.

To investigate the function of miR-146a-5p regulated by BM-MSCs in the progression of renal fibrosis *in vitro*, we transiently transfected miR-146a-5p mimics into TGF-β1-treated mRTECs to significantly up-regulate the expression of miR-146a-5p (**Figure 3C**). In line with the previous results, both transcriptional and translational levels of α-SMA and Col1α1 in mRTECs were significantly reduced by the miR-146a-5p mimics treatment (**Figures 3D–F**). Next, we transiently transfected miR-146a-5p inhibitors into TGF-β1-treated mRTECs to down-regulate miR-146a-5p expression (**Figure 3G**). The RT-qPCR analysis and western blot analysis

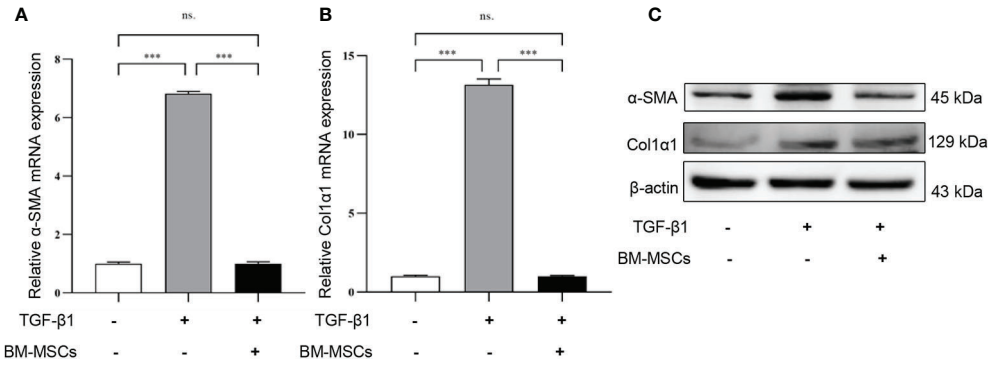


FIGURE 2 | The effect of bone marrow mesenchymal stem cells (BM-MSCs) on TGF-β1-induced a fibrotic model *in vitro*. The relative mRNA expression levels **(A, B)** and the protein levels **(C)** of α-SMA and Col1α1 in mRTECs were evaluated by real-time PCR and Western blot, respectively. Data represent the mean ± SE from three independent experiments. ***P < 0.001; NS, not significant.

showed that loss of miR-146a-5p significantly increased the expression of α-SMA and Col1α1 in mRTECs (**Figures 3H–J**). In summary, gain- or loss-function of miR-146a-5p studies by mimic and inhibitor revealed that BM-MSCs might exert its anti-fibrosis effect by increasing the expression of miR-146a-5p in mRTECs.

Prediction and Verification of miR-146a-5p Target Genes in Mouse Renal Tubular Epithelial Cells

We predicted the potential target genes of miR-146a-5p using multiple software programs (TargetScan, miRanda, miRDB, and DIANA-microT). Totally, 59 candidate genes were identified (**Figure 4A**). Next, gene ontology (GO) and Kyoto Encyclopedia of Genes and Genomes (KEGG) analysis were performed to evaluate mRNA enrichments in terms of biological process, cellular component, and molecular function. The top 10 enriched GO terms were involved in the regulation of cellular and metabolic processes (**Figure 4B**). KEGG analysis revealed two pathways, including the cell cycle and the pathways in cancer (**Figure 4C**), which are associated with cell activation and cell proliferation. Our results suggested that the differentially expressed miRNAs might be involved in the progression of renal fibrosis.

Next, six candidate target genes of miR-146a-5p were selected from the KEGG pathway analysis. Expression of one candidate gene Tfdp2 was increased by exogenous cytokine TGF-β1 stimulation and decreased after co-cultured with BM-MSCs in mRTECs (**Figure 5A**). Whereas the expression of the other five candidate target genes (Smad4, Traf6, Rbl1, Ar, Rarb) revealed no statistical significance (**Supplementary Figures 1A–E**). The experimental data confirmed Tfdp2 gene as a candidate target gene of miR-146a-5p. To explore the direct relationship between Tfdp2 and miR-146a-5p, the expression of Tfdp2 mRNA and protein in mRTECs transfected by miR-146a-5p mimics was detected by RT-qPCR and western blot analysis. Our data showed that both mRNA and protein levels of Tfdp2 were decreased significantly compared with control (**Figures 5B, C**). Moreover, the mRNA level of Tfdp2 was gradually decreased depending on the miR-146a-5p mimic transfection concentration (**Figure 5D**). In summary, our experimental data indicate that Tfdp2 is the target gene of miR-146a-5p.

Expression and Function of Tfdp2 in Renal Fibrosis

To evaluate the expression and function of Tfdp2 in renal fibrosis, we first transiently transfected Tfdp2 siRNA into mRTECs to down-regulate the expression of Tfdp2 in mRTECs (**Figure 6A**). Both transcriptional and translational levels of α-SMA and Col1α1 in mRTECs were significantly reduced by the knockdown of Tfdp2 (**Figures 6B–D**). These results suggested that inhibition of Tfdp2 expression can reduce the expression of fibrosis-related proteins. IHC analysis showed that a weak staining of Tfdp2 was predominantly localized to the cytoplasm in the normal tubulointerstitial compartment which was utilized as a reference. Stronger staining of Tfdp2 in renal tubular epithelial cells was observed in the renal tissues of the cisplatin group as compared with the control group, whereas the expression of Tfdp2 was obviously reduced in cisplatin + BM-MSCs group as compared to the cisplatin group. Taken together, these experimental data indicated that Tfdp2 exerts a significant function in the treatment of BM-MSCs on cisplatin -induced renal injury and fibrosis.

DISCUSSION

MSCs-based therapeutic approaches have been successfully applied to attenuate organ injury, including the kidney. Kidney fibrosis is a common endpoint outcome of CKD, which has a poor clinical outcome (19, 20). BM-MSCs are extracted from bone marrow and are defined as multipotent cells due to the robust capacities of differentiating into distinct functional cells.

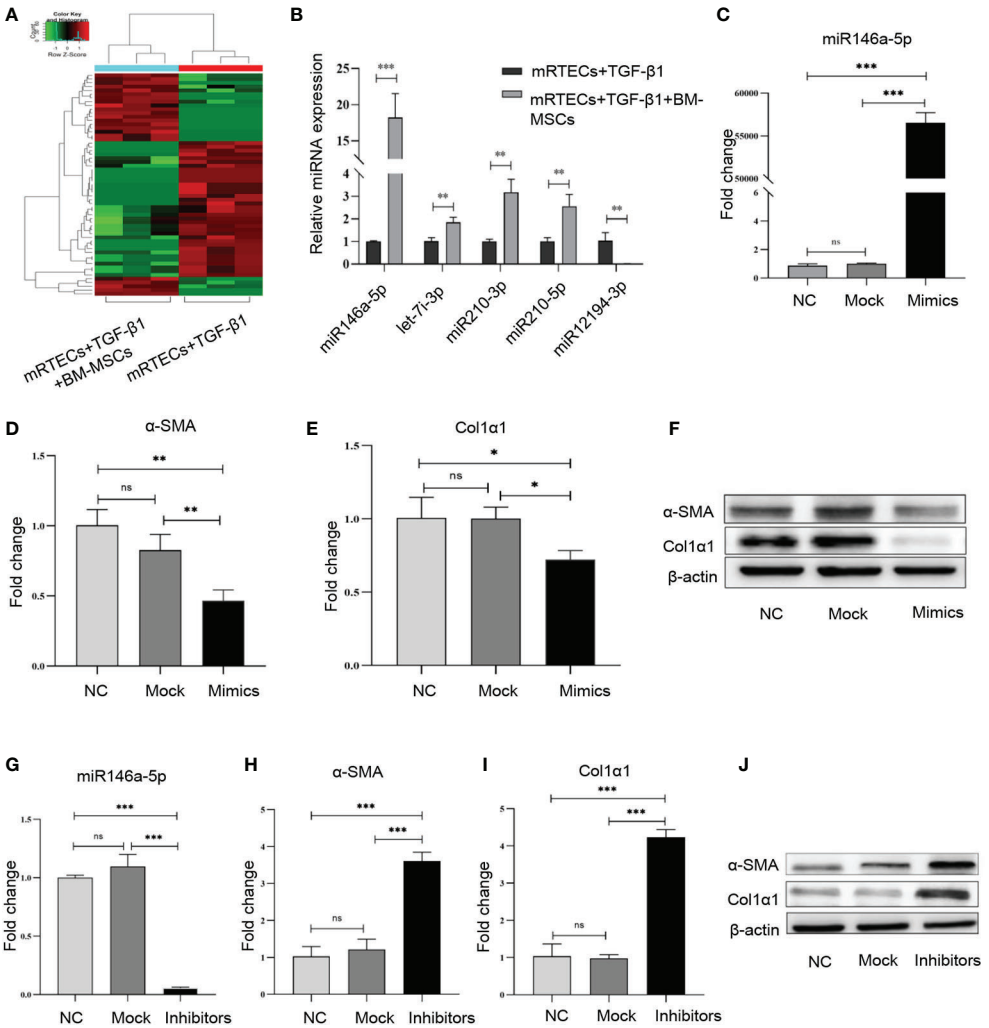


FIGURE 3 | miR-146a-5p was significantly up-regulated by bone marrow mesenchymal stem cells (BM-MSCs) in mouse renal tubular epithelial cells (mRTECs). **(A)** Heatmap of differential microRNA (miRNA) expression in TGF-β1-treated mRTECs with or without BM-MSCs. Gene expression data were obtained with miRNA sequence and the most obvious values are shown. Red indicates up-regulation, while green means down-regulation. **(B)** Top-five most significant changed miRNAs were verified by real-time PCR. **(C)** TGF-β1-treated mRTECs were transfected with miR-146a-5p mimics. The levels of miR-146a-5p were determined by real-time PCR. The relative mRNA expression levels **(D, E)** and the protein levels **(F)** of α-SMA and Col1α1 in mRTECs transfected with miR-146a-5p mimics were evaluated by real-time PCR and Western blot, respectively. **(G)** TGF-β1-treated mRTECs were transfected with miR-146a-5p inhibitor. The levels of miR-146a-5p were determined by real-time PCR. The relative mRNA expression levels **(H, I)** and the protein levels **(J)** of α-SMA and Col1α1 in mRTECs transfected with miR-146a-5p inhibitor were evaluated by real-time PCR and Western blot, respectively. Data represent the mean ± SE from three independent experiments. *P < 0.05; **P < 0.01; ***P < 0.001; NS, not significant.

Most data reveal that BM-MSCs repair renal injury processes by the means of indirect secreted biomaterial, including the extracellular vesicles and multiple miRNA particles (21). In the present study, we established a model of cisplatin-induced renal fibrosis in C57BL/6 mice and found that BM-MSCs have an anti-renal fibrosis effect and renoprotection *in vivo*. Moreover, we showed that BM-MSCs significantly reduced the levels of α-SMA and Col1α1 in mRTECs treated by TGF-β1 in an indirect co-culture environment. Mechanically, we have identified miR-146a-5p as the most significant up-regulated miRNA in mRTECs regulated by BM-MSCs and plays a significant role in renal fibrosis in a co-culture experimental model. The results also found the gene Tfdp2 is one target gene of miR-146a-5p and exerts a vital role in the treatment of BM-MSCs on cisplatin-induced renal injury and fibrosis. Our study indicates that BM-MSC attenuates cisplatin-induced renal fibrosis by regulating miR-146a-5p/Tfdp2 axis in mRTECs.

Renal tubulointerstitial fibrosis is generally characterized by an excessive accumulation of extracellular matrix (ECM) factors (predominantly collagen type I) that prevent the regeneration of kidney tissue (22, 23). The severity of fibrosis notably correlates with the degree of kidney dysfunction and the renal failure

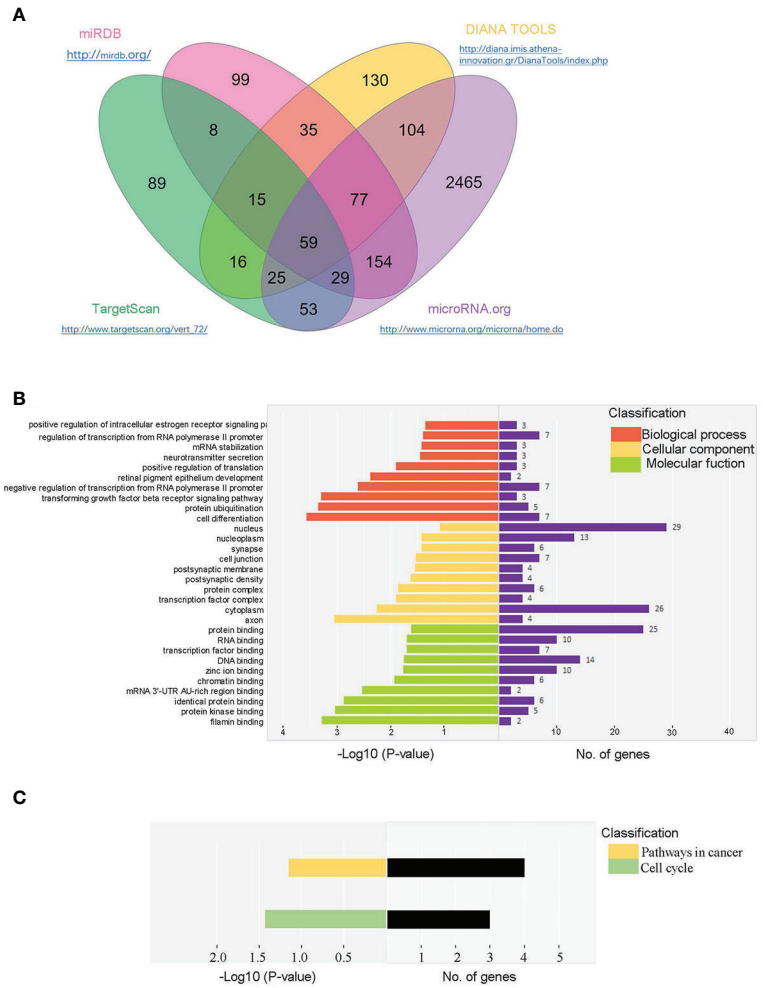


FIGURE 4 | Bioinformatic prediction of miR-146a-5p target genes in mRTECs. **(A)** Venn diagram of identified miR-146a-5p target genes using multiple software programs (TargetScan, miRanda, miRDB, and DIANA-microT). Gene ontology (GO) analysis **(B)** and Kyoto Encyclopedia of Genes and Genomes (KEGG) analysis **(C)** of candidate genes in terms of biological process, cellular component, and molecular function.

outcome (24). TGF-β is well accepted as a critical regulator in renal fibrosis. Growing evidence indicates that exogenous cytokine, such as TGF-β1, can induce renal tubular epithelial cells to undergo phenotypic transformation into matrix-producing myofibroblasts (25, 26). Our study successfully established a mouse model to investigate the multiple low-dose cisplatin-induced renal fibrosis, which could be determined by increased levels of α-SMA and Col1α1 in mRTECs. In line with previous studies (11), we found BM-MSCs alleviate the severity of kidney dysfunction and fibrosis. Asanuma et al. (27). found arterially delivered MSCs protect against obstruction induced epithelial-mesenchymal transition (EMT) and chronic renal fibrosis involving alterations in TNF-α production. MSCs-based therapy was also reported to attenuate renal fibrosis through immune response modulation (28). However, the specific mechanisms of MSCs renoprotection remain poorly elucidative.

As a post-transcriptional regulator, miRNAs play an important role in the development, physiology, and maintenance of kidney microstructure. Dysregulation of miRNAs disrupts early kidney development, differentiation of kidney progenitor cells, and mature nephrons' maintenance (29). Recent studies indicate that dysregulation of miRNAs is associated with the initiation and development of renal fibrosis in patients with diabetic nephropathy (DN) as well as in mouse models of DN (30, 31). Based on the function of BM-MSCs and miRNAs in renal fibrosis, we performed a high-throughput sequencing to identify the most significant regulated miRNAs by BM-MSCs in a co-culture experimental model. MiR-146a-5p was found as the most significant up-regulated miRNA, which was also verified by RT-PCR. Subsequently, we explored the function of miR-146a-5p in renal fibrosis *in vitro*. The gain- and loss-function of miR-146a-5p studies by mimic and inhibitor showed that the expression of α-SMA, Col1α1 mRNA, and

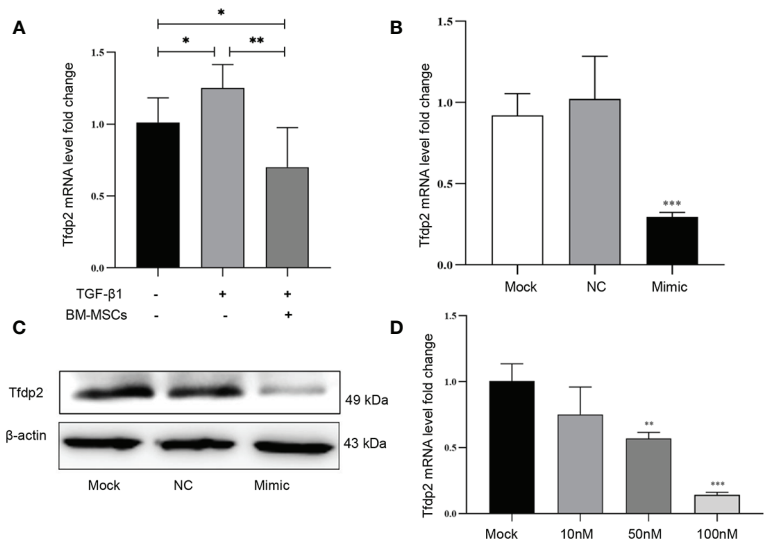


FIGURE 5 | Verification of one candidate gene Tfdp2 in mouse renal tubular epithelial cells (mRTECs). **(A)** The levels of Tfdp2 were determined by real-time PCR in TGF-β1-treated mRTECs with or without bone marrow mesenchymal stem cells (BM-MSCs). The relative mRNA expression levels **(B)** and the protein levels **(C)** of Tfdp2 in mRTECs transfected by miR-146a-5p mimics were evaluated by real-time PCR and Western blot, respectively. **(D)** The transcript levels of Tfdp2 in mRTECs transfected by miR-146a-5p mimics with different concentrations. Data represent the mean ± SE from three independent experiments. *P < 0.05; **P < 0.01; ***P < 0.001.

protein were significantly altered in mRTECs. Therefore, our results indicate that BM-MSCs could inhibit the progression of renal fibrosis by regulating the expression of miR-146a-5p in mRTECs. Interestingly, a previous study has reported that miR-146a-5p acts as a negative regulator of TGF-β signaling in skeletal muscle after acute contusion, which indicates that miR-146 might have a therapeutic potential to alleviate skeletal muscle fibrosis (32). In addition, miR-146a-5p was found to inhibit the activation and proliferation of hepatic stellate cells (HSCs) in the progress of non-alcoholic fibrosing steatohepatitis (33). Therefore, miR-146a-5p exerts a critical function in the renoprotection of BM-MSCs.

Six candidate genes from the KEGG pathway analyses were confirmed by RT-qPCR. We found the transcription factor DP2 (Tfdp2) gene was increased in mRTECs stimulated by exogenous cytokine TGF-β1 and reduced after co-cultured with BM-MSCs. Consistent with miR-146a-5p targeting mRNA of Tfdp2, expression of Tfdp2 in mRTECs was significantly altered by the mimic and inhibitor of miR-146a-5p. To further investigate the function of Tfdp2 in renal fibrosis, Tfdp2 expression was knockdown by siRNA transfection. Both transcriptional and translational levels of α-SMA and Col1α1 in mRTECs were significantly reduced by the knockdown of Tfdp2. In addition, the relevance of Tfdp2 in renal fibrosis was confirmed in cisplatin-treated mouse kidney tissues by the IHC staining. Tfdp2 is a significant cofactor for the cell cycle control and gene expression, which combines with E2F family members to drive the function of c-Myc gene (34). The whole-genome analysis report for chronic kidney disease shows that Tfdp2 is related to renal function and CKD (35, 36). In the present study, we provided the first experimental evidence that BM-MSCs attenuate cisplatin-induced renal injury and fibrosis by the regulation of miR-146a-5p and the targeting gene Tfdp2, indicating that BM-MSCs may be a promising approach for developing novel therapeutics to treat renal fibrosis.

Nevertheless, our findings are only confirmed in the mouse model. The value and significance of BM-MSCs for the clinical treatment of renal fibrosis require more preclinical data support. In addition, the contribution of miR-146a-5p/Tfdp2 axis in renal fibrosis is worth further investigating and verifying in human kidney tissues.

CONCLUSION

In conclusion, our findings demonstrate that BM-MSCs ameliorate renal injury and fibrosis *in vivo* and *in vitro*. Our study provides the first evidence that the protection of BM-MSCs on renal fibrosis *via* miR-146a-5p/Tfdp2 axis in renal tubular epithelial cells. These results offer novel mechanistic insights into the renoprotection of BM-MSCs, which highlights the promising clinical studies on MSCs-based therapy for kidney diseases in the near future. Additionally, the function of miR-146a-5p/Tfdp2 axis in renal fibrosis should be further investigated in preclinical and clinical studies, which might be a potential therapeutic target for renal fibrosis.

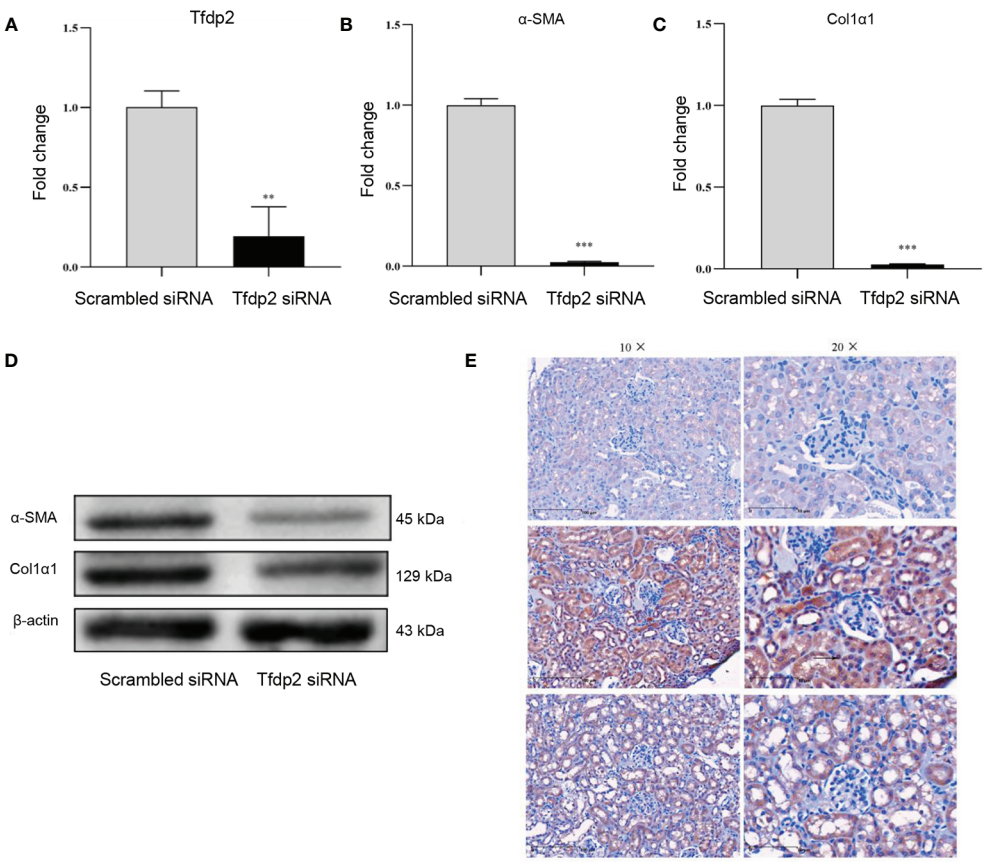


FIGURE 6 | Overexpression of Tfdp2 in cisplatin-induced renal fibrosis. **(A)** The transcript levels of Tfdp2 in mouse renal tubular epithelial cells (mRTECs) was down-regulated by siRNA. The relative mRNA expression levels **(B, C)** and the protein levels **(D)** of α-SMA and Col1α1 after knockdown of Tfdp2 were by real-time PCR and Western blot, respectively. **(E)** Representative images of Tfdp2 immunohistochemical staining in cisplatin (CP)-induced mice kidney with or without bone marrow mesenchymal stem cells (BM-MSCs) treatment. Data represent the mean ± SE from three independent experiments. **P < 0.01; ***P < 0.001.

DATA AVAILABILITY STATEMENT

The datasets presented in this study can be found in online repositories. The names of the repository/repositories and accession number(s) can be found below: https://www.ncbi.nlm.nih.gov/geo/, GSE148144.

ETHICS STATEMENT

The animal study was reviewed and approved by Experimental Animal Committee of Soochow University (Approval No: ECSU-201800099).

AUTHOR CONTRIBUTIONS

S-LW and M-MS conceived and guided the study. LW, QZ, XZ, and X-MZ performed the experiments. LW, CR, and SW analyzed and interpreted the data. LW and CR contributed to the writing and data presentation of the manuscript. All authors contributed to the article and approved the submitted version.

FUNDING

This study was supported by the grants from the National Key R&D Program of China (No. 2018YFA0107500), Natural Science Foundation of Jiangsu Province (No. BK20200878), and the Priority Academic Program Development of Jiangsu Higher Education Institutions (PAPD).

ACKNOWLEDGMENTS

We thank Prof. Dr. Yufang Shi for the establishment of BM-MSCs and technical assistance from his laboratory.

SUPPLEMENTARY MATERIAL

The Supplementary Material for this article can be found online at: https://www.frontiersin.org/articles/10.3389/fimmu.2020.623693/full#supplementary-material

REFERENCES

1. Boor P, Ostendorf T, Floege J. Renal fibrosis: novel insights into mechanisms and therapeutic targets. *Nat Rev Nephrol* (2010) 6(11):643–56. doi: 10.1038/nrneph.2010.120
2. O'Sullivan ED, Hughes J, Ferenbach DA. Renal Aging: Causes and Consequences. *J Am Soc Nephrol* (2017) 28(2):407–20. doi: 10.1681/ASN.2015121308
3. Webster AC, Nagler EV, Morton RL, Masson P. Chronic Kidney Disease. *Lancet* (2017) 389(10075):1238–52. doi: 10.1016/S0140-6736(16)32064-5
4. Collaboration GBDCKD. Global, regional, and national burden of chronic kidney disease, 1990-2017: a systematic analysis for the Global Burden of Disease Study 2017. *Lancet* (2020) 395(10225):709–33. doi: 10.1016/S0140-6736(20)30045-3
5. Alicic RZ, Rooney MT, Tuttle KR. Diabetic Kidney Disease: Challenges, Progress, and Possibilities. *Clin J Am Soc Nephrol* (2017) 12(12):2032–45. doi: 10.2215/CJN.11491116
6. Wei X, Yang X, Han ZP, Qu FF, Shao L, Shi YF. Mesenchymal stem cells: a new trend for cell therapy. *Acta Pharmacol Sin* (2013) 34(6):747–54. doi: 10.1038/aps.2013.50
7. Weiss ARR, Dahlke MH. Immunomodulation by Mesenchymal Stem Cells (MSCs): Mechanisms of Action of Living, Apoptotic, and Dead MSCs. *Front Immunol* (2019) 10:1191. doi: 10.3389/fimmu.2019.01191
8. Brown C, McKee C, Bakshi S, Walker K, Hakman E, Halassy S, et al. Mesenchymal stem cells: Cell therapy and regeneration potential. *J Tissue Eng Regener Med* (2019) 13(9):1738–55. doi: 10.1002/term.2914
9. Ridge SM, Sullivan FJ, Glynn SA. Mesenchymal stem cells: key players in cancer progression. *Mol Cancer* (2017) 16(1):31. doi: 10.1186/s12943-017-0597-8
10. Uccelli A, Moretta L, Pistoia V. Mesenchymal stem cells in health and disease. *Nat Rev Immunol* (2008) 8(9):726–36. doi: 10.1038/nri2395
11. El Agha E, Kramann R, Schneider RK, Li X, Seeger W, Humphreys BD, et al. Mesenchymal Stem Cells in Fibrotic Disease. *Cell Stem Cell* (2017) 21(2):166–77. doi: 10.1016/j.stem.2017.07.011
12. Herzog EL, Chai L, Krause DS. Plasticity of marrow-derived stem cells. *Blood* (2003) 102(10):3483–93. doi: 10.1182/blood-2003-05-1664
13. Zhang F, Wang C, Wen X, Chen Y, Mao R, Cui D, et al. Mesenchymal stem cells alleviate rat diabetic nephropathy by suppressing CD103(+) DCs-mediated CD8(+) T cell responses. *J Cell Mol Med* (2020) 24(10):5817–31. doi: 10.1111/jcmm.15250
14. Rabelink TJ, Little MH. Stromal cells in tissue homeostasis: balancing regeneration and fibrosis. *Nat Rev Nephrol* (2013) 9(12):747–53. doi: 10.1038/nrneph.2013.152
15. O'Reilly S. MicroRNAs in fibrosis: opportunities and challenges. *Arthritis Res Ther* (2016) 18:11. doi: 10.1186/s13075-016-0929-x
16. Chandrasekaran K, Karolina DS, Sepramaniam S, Armugam A, Wintour EM, Bertram JF, et al. Role of microRNAs in kidney homeostasis and disease. *Kidney Int* (2012) 81(7):617–27. doi: 10.1038/ki.2011.448
17. Chung AC, Lan HY. MicroRNAs in renal fibrosis. *Front Physiol* (2015) 6:50. doi: 10.3389/fphys.2015.00050
18. Sharp CN, Doll MA, Dupre TV, Shah PP, Subathra M, Siow D, et al. Repeated administration of low-dose cisplatin in mice induces fibrosis. *Am J Physiol Renal Physiol* (2016) 310(6):F560–8. doi: 10.1152/ajprenal.00512.2015
19. Zhao L, Han F, Wang J, Chen J. Current understanding of the administration of mesenchymal stem cells in acute kidney injury to chronic kidney disease transition: a review with a focus on preclinical models. *Stem Cell Res Ther* (2019) 10(1):385. doi: 10.1186/s13287-019-1507-3
20. Ruiz-Ortega M, Rayego-Mateos S, Lamas S, Ortiz A, Rodrigues-Diez RR. Targeting the progression of chronic kidney disease. *Nat Rev Nephrol* (2020) 16(5):269–88. doi: 10.1038/s41581-019-0248-y
21. Bochon B, Kozubska M, Surygala G, Witkowska A, Kuzniewicz R, Grzeszczak W, et al. Mesenchymal Stem Cells-Potential Applications in Kidney Diseases. *Int J Mol Sci* (2019) 20(10):2462. doi: 10.3390/ijms20102462
22. Liu Y. Cellular and molecular mechanisms of renal fibrosis. *Nat Rev Nephrol* (2011) 7(12):684–96. doi: 10.1038/nrneph.2011.149
23. Hong S, Healy H, Kassianos AJ. The Emerging Role of Renal Tubular Epithelial Cells in the Immunological Pathophysiology of Lupus Nephritis. *Front Immunol* (2020) 11:578952. doi: 10.3389/fimmu.2020.578952
24. Law BMP, Wilkinson R, Wang X, Kildey K, Giuliani K, Beagley KW, et al. Human Tissue-Resident Mucosal-Associated Invariant T (MAIT) Cells in Renal Fibrosis and CKD. *J Am Soc Nephrol* (2019) 30(7):1322–35. doi: 10.1681/ASN.2018101064
25. Meng XM, Nikolic-Paterson DJ, Lan HY. TGF-beta: the master regulator of fibrosis. *Nat Rev Nephrol* (2016) 12(6):325–38. doi: 10.1038/nrneph.2016.48
26. Tang PM, Zhang YY, Mak TS, Tang PC, Huang XR, Lan HY. Transforming growth factor-beta signalling in renal fibrosis: from Smads to non-coding RNAs. *J Physiol* (2018) 596(16):3493–503. doi: 10.1113/JP274492
27. Asanuma H, Vanderbrink BA, Campbell MT, Hile KL, Zhang H, Meldrum DR, et al. Arterially delivered mesenchymal stem cells prevent obstruction-induced renal fibrosis. *J Surg Res* (2011) 168(1):e51–9. doi: 10.1016/j.jss.2010.06.022
28. Semedo P, Correa-Costa M, Antonio Cenedeze M, Maria Avancini Costa Malheiros D, Antonia dos Reis M, Shimizu MH, et al. Mesenchymal stem cells attenuate renal fibrosis through immune modulation and remodeling properties in a rat remnant kidney model. *Stem Cells* (2009) 27(12):3063–73. doi: 10.1002/stem.214
29. Fan Y, Chen H, Huang Z, Zheng H, Zhou J. Emerging role of miRNAs in renal fibrosis. *RNA Biol* (2020) 17(1):1–12. doi: 10.1080/15476286.2019.1667215
30. Kato M, Zhang J, Wang M, Lanting L, Yuan H, Rossi JJ, et al. MicroRNA-192 in diabetic kidney glomeruli and its function in TGF-beta-induced collagen expression via inhibition of E-box repressors. *Proc Natl Acad Sci USA* (2007) 104(9):3432–7. doi: 10.1073/pnas.0611192104
31. Wang Q, Wang Y, Minto AW, Wang J, Shi Q, Li X, et al. MicroRNA-377 is up-regulated and can lead to increased fibronectin production in diabetic nephropathy. *FASEB J* (2008) 22(12):4126–35. doi: 10.1096/fj.08-112326
32. Sun Y, Li Y, Wang H, Li H, Liu S, Chen J, et al. miR-146a-5p acts as a negative regulator of TGF-beta signaling in skeletal muscle after acute contusion. *Acta Biochim Biophys Sin (Shanghai)* (2017) 49(7):628–34. doi: 10.1093/abbs/gmx052
33. Du J, Niu X, Wang Y, Kong L, Wang R, Zhang Y, et al. MiR-146a-5p suppresses activation and proliferation of hepatic stellate cells in nonalcoholic fibrosing steatohepatitis through directly targeting Wnt1 and Wnt5a. *Sci Rep* (2015) 5:16163. doi: 10.1038/srep16163
34. Chen C, Lodish HF. Global analysis of induced transcription factors and cofactors identifies Tfdp2 as an essential coregulator during terminal erythropoiesis. *Exp Hematol* (2014) 42(6):464–76.e5. doi: 10.1016/j.exphem.2014.03.001
35. Boger CA, Heid IM. Chronic kidney disease: novel insights from genome-wide association studies. *Kidney Blood Press Res* (2011) 34(4):225–34. doi: 10.1159/000326901
36. Wang B, Hsu SH, Wang X, Kutay H, Bid HK, Yu J, et al. Reciprocal regulation of microRNA-122 and c-Myc in hepatocellular cancer: role of E2F1 and transcription factor dimerization partner 2. *Hepatology* (2014) 59(2):555–66. doi: 10.1002/hep.26712

Conflict of Interest: The authors declare that the research was conducted in the absence of any commercial or financial relationships that could be construed as a potential conflict of interest.

Copyright © 2021 Wu, Rong, Zhou, Zhao, Zhuansun, Wan, Sun and Wang. This is an open-access article distributed under the terms of the Creative Commons Attribution License (CC BY). The use, distribution or reproduction in other forums is permitted, provided the original author(s) and the copyright owner(s) are credited and that the original publication in this journal is cited, in accordance with accepted academic practice. No use, distribution or reproduction is permitted which does not comply with these terms.

frontiers in Immunology

MINI REVIEW
published: 24 February 2021
doi: 10.3389/fimmu.2021.625998

The Role of Regulatory Myeloid Cell Therapy in Renal Allograft Rejection

*Jingming Zhuang and Jiangang Hou**

Department of Urology, Huashan Hospital, Fudan University, Shanghai, China

Kidney transplantation is a primary therapy for end-stage renal disease (ESRD) all the time. But it does not mean that we have fully unraveling the mystery of kidney transplantation and confer every patient favorable prognosis. Immune rejection has always been a stumbling block when we try to increase the success rate of kidney transplantation and improve long-term outcomes. Even if the immune rejection is effectively controlled in acute phase, there is a high possibility that the immune response mediated by chronically activated antibodies will trigger chronic rejection and ultimately lead to graft failure. At present, immunosuppressive agent prepared chemically is mainly used to prevent acute or chronic rejection, but it failed to increase the long-term survival rate of allografts or reduce the incidence of chronic rejection after acute rejection, and is accompanied by many adverse reactions. Therefore, many studies have begun to use immune cells to regulate the immune response in order to control allograft rejection. This article will focus on the latest study and prospects of more popular regulatory myeloid cells in the direction of renal transplantation immunotherapy and introduce their respective progress from experimental research to clinical research.

Keywords: kidney transplant, regulatory myeloid cell, allograft rejection, immunosuppression, prevention, end-stage renal disease

OPEN ACCESS

Edited by:
Bin Yang,
University of Leicester,
United Kingdom

Reviewed by:
Ruiming Rong,
Fudan University, China
Hu Linkun,
Soochow University, China

****Correspondence:***
Jiangang Hou
hou_jiangang@126.com

Specialty section:
This article was submitted to Alloimmunity and Transplantation, a section of the journal Frontiers in Immunology

Received: *04 November 2020*
Accepted: *03 February 2021*
Published: *24 February 2021*

Citation:
Zhuang J and Hou J (2021) The Role of Regulatory Myeloid Cell Therapy in Renal Allograft Rejection. Front. Immunol. 12:625998. doi: 10.3389/fimmu.2021.625998

INTRODUCTION

In 1954, Dr. Merril and Murray of Harvard University completed the first successful kidney transplant between a pair of twins in order to avoid allograft immunity. The patient did not take any immunosuppressive drugs, and the transplanted kidney achieved long-term survival (1). But this is a rare condition after all, and there are certain genetic differences between most donors and recipients, mainly referring to human leukocyte antigen (HLA), which greatly ascends the possibility of allograft rejection (2). Based on the onset time, the rejections that occur after kidney transplantation can be classified into hyperacute rejection reaction, accelerated rejection reaction, acute rejection reaction, and chronic rejection reaction. The most important ones are acute rejection and chronic active antibody-mediated rejection (AMR). We are going to discuss the prevention and treatment of them (3). Thanks to preoperative histocompatibility tests, more reasonable and standardized surgical procedures, improved tissue typing, and especially the advent of securer and more efficient immunosuppressive drugs, the incidence of rejection (mostly acute rejection) during the first year has gradually decreased over the years (4). Clinical kidney transplant has become the gold standard for ESRD, which improves patients' quality of life within a certain period compared with continuous dialysis (3, 5). At present, the main clinical method of chemical immunosuppressive treatment routinely after kidney transplantation is calcineurin inhibitor (CNI), and other drugs including mycophenolic acid and corticosteroids are usually used in combination (6, 7). Immunosuppressive agents seem to have reached their

limits, but many problems remain, such as leading to excessive suppression of immune system and increasing the rate of infectious diseases and the incidence of tumors (8). It can also cause side effects without an immunological relationship, including nephrotoxicity, making recipients susceptible to cardiovascular dysfunction, metabolic diseases, and complications of other organs (9). Unfortunately, due to the lack of immunological or antigen specificity, CNI based immunosuppressive can hinder alloresponses, but does not ultimately prevent late dysfunction or loss. And in fact, CNI treatment even causes inhibition of regulatory T-cell development, which leaves a major challenge (10). Therefore, although these drugs reduce the rate of acute rejection, they fail to significantly improve the long-term survival of transplanted kidney (11).

Given the concerns over chemical immunosuppressive agents and the disappointing long-term results of kidney transplants, it is clearly necessary to revisit our choice of immunomodulation methods. Although immune rejection is mainly mediated by effector T cells or antibodies secreted by B cells, some other types of white blood cells can promote a tolerant immune response and extend survival of the graft (12). In kidney transplant immunity, mechanisms of tolerance are crucial because whether an allograft is acceptable to the recipient depends largely on the balance between effector cells with alloantigen reactivity and regulatory immune cells (13). Regulatory immune cells are one such group of leukocyte populations that have the potential to specifically prevent acute rejection or graft-vs.-host disease (GVHD). They gradually acquire regulatory functions during development, and the immunosuppressive property is acquired in the local microenvironment of allografts or in lymphatic tissue drained by the graft. And this immunosuppressive property will cause the surrounding environment to change toward the long-term survival of the graft, thereby preventing the graft from being rejected or GVHD. Therefore, regulatory immune cells play a critical role in influencing long-term outcomes after kidney transplantation (14).

REGULATORY MYELOID CELLS

Currently, researchers working on organ transplantation are hoping to minimize the dependence of recipients on immunosuppressive drugs and increase donor-specific immune tolerance using immunomodulatory therapy. Many animal experiments and observations have shown that regulatory immune cells can promote transplant tolerance and reduce the infection rate after kidney transplantation (15). There are also considerable experiments confirming that they could prolong the survival of kidney allografts in non-human primate (NHP) models (16, 17). Most of these experiments focus on the role of regulatory T cells (Tregs). From basic experiments to clinical related research, Tregs have excellent immune regulation effect after transplantation of various organs, and they occupied an important position in transplantation immunity (13, 18, 19). There was some small-scale clinical trials which purify Tregs from patients' own blood and perform polyclonal expansion. Experimental results show that the project is safe and well-tolerated. The infused Tregs have a certain degree of durability and stability, proven to reduce the inflammation of the transplanted kidney through biopsy (20). Another group of cells with regulatory functions, regulatory myeloid cells, has excellent immunosuppressive effects in many transplant responses, in addition to being more diverse and complex. Some of these effects received widespread attention because they may be related to Tregs (**Figure 1**). The regulatory myeloid cells discussed in the previous articles generally include three types, which are regulatory macrophages, regulatory dendritic cells, and myeloid-derived suppressor cells (21). Due to the homology and excellent anti-rejection prospects, here we will broadly include bone marrow mesenchymal stromal cells. We will focus on the progress of kidney transplantation immunity of several regulatory myeloid cells, and their characteristics are shown (**Table 1**).

REGULATORY MACROPHAGES

Macrophages are derived from monocytes and they are an important part of innate immunity. When the body is injured, monocytes in the blood vessels are transported to the inflamed tissue and become macrophages. The accumulation of macrophages in organs has been considered a feature of allograft rejection for many years (26). Depending on the microenvironment, immunogenic monocytes will infiltrate into the allograft early after transplantation, and be renamed macrophages, which will respond to the transplanted organ and trigger organ rejection (27). The classically activated macrophages' (M1) inflammatory response is characterized by high levels of pro-inflammatory cytokines in the surrounding environment and the promotion of the Th1 response. However, in addition to the role of M1 in promoting immune responses, alternatively activated macrophages (M2) are believed to be associated with the alleviation of tissue inflammation. The latest research found that when macrophage colony-stimulating factor (M-CSF) and interferon-γ (IFN-γ) act on monocytes, they will transform into a new type of inhibitory cells called regulatory macrophages (Mregs). Mregs are another uniquely characterized group of cells that can produce interleukin 10 (IL-10) but do not generate arginase-1, which can reduce the proinflammatory immune response (28). Recent studies have shown that Mregs promote successful long-term transplantation and may be necessary for inducing transplant tolerance (29). Hutchinson et al. administered Mregs to two living donor kidney transplant recipients. After transplantation, two patients were treated with the smallest dose of tacrolimus monotherapy (aiming for trough serum levels between 4 and 8 ng/ml) in 24 weeks and maintained favorable transplant function later. No adverse effects were observed in 2 patients, with 3 years follow-up (30). It is inferred that this phenomenon may be caused by Mregs inhibiting the proliferation of effector T cells by producing IFN-γ. During cell experiments, it was found that mouse Mregs can produce induced nitric oxide synthase (iNOS) to inhibit the activity of T cells *in vitro* and can kill and engulf co-cultured

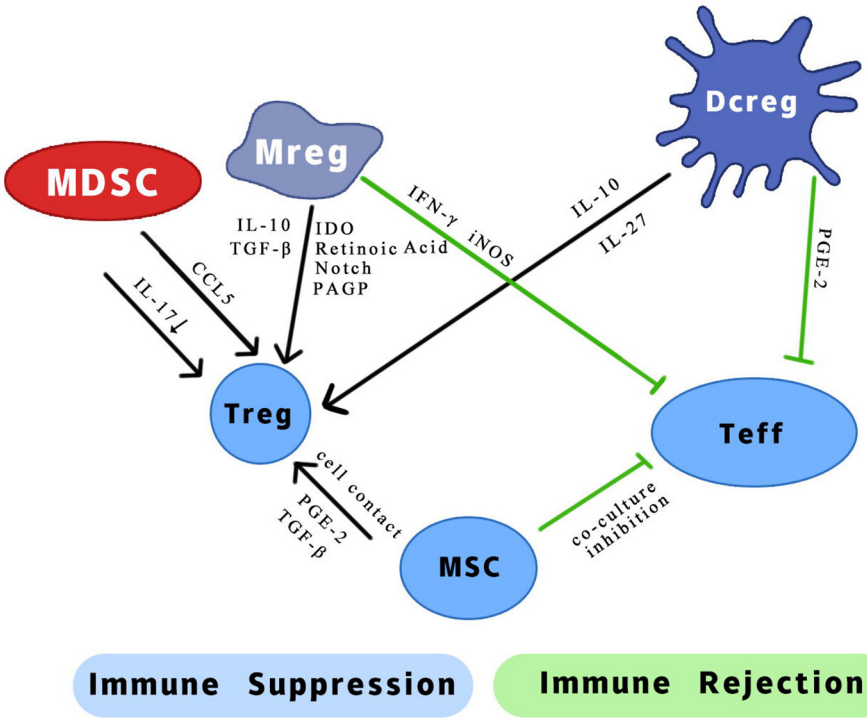


FIGURE 1 | Possible mechanism of different effects of regulatory myeloid cells on two types of T cells. IL, interleukin; CCL5, chemotactic C-C motif 5; IFN-γ, interferon-gamma; iNOS, inducible nitric oxide synthase; TGF-β, transforming growth factor-β; IDO, indoleamine 2,3-dioxygenase; PAGP, progestagen-associated endometrial protein; PGE-2, prostaglandin E2.

TABLE 1 | Feature of regulatory myeloid cell (22–25).

Regulatory myeloid cell	Source	Growth factor	Immunophenotypic markers
Regulatory macrophages	Rodent BM cells or human PBMC	M-CSF, IFN-γ	$CD14^{low}$ $CD16^{-/low}$ $CD80^{low}$ $CD83^{-/low}$ $CD86^{+/hi}$ $HLA\text{-}DR^{+/hi}$
Regulatory dendritic cells	Rodent BM cells or human PBMC	GM-CSF,IL-4 Tolerogenic Factor(s):IL-10, TGF-β, VitD3, Dexamethasone, rapamycin	MHC II^{low} $CD40^{low}$ $CD80^{low}$ $CD86^{low}$ $PDL1^{hi}$ $TGF\text{-}\beta^{hi}$ $IL\text{-}10^{hi}$
Myeloid-derived suppressor cells	Rodent BM cells or human PBMC	Activation:IL-1β, IL-6, IL-13, PGE-2, TNF-α, VEGF Expansion: G-CSF, GM-CSF	Three subpopulations (22)
Mesenchymal stromal cells	Extraction from BM	–	$CD117^{-}$ $CD31^{-}$ $CD44^{+}$ $CD29^{+}$ $Sca\text{-}1^{+}$

BM, bone marrow; PBMC, peripheral blood mononuclear cell; M-CSF, macrophage colony stimulating factor; IFN-γ, interferon-γ; GM-CSF, granulocyte-macrophage colony stimulating factor; TGF-β, transforming growth factor-β; PDL1, programmed cell death ligand-1; PGE-2, prostaglandin E2; TNF-α, tumor necrosis factor-α; G-CSF, granulocyte colony stimulating factor.

T cells subsequently (31). The latest research also shows that Mregs can convert allogeneic CD4 + T cells into regulatory T cells, thereby non-specifically inhibiting bystander T cells and the maturation of dendritic cells. Preoperative administration of donor-sourced Mreg to kidney transplant recipients can cause a sharp increase in circulating Treg, promoting the acceptance of allogeneic transplantation by rapidly inducing Tregs (32). In addition to conducting further clinical and *in vitro* experiments, some researchers have proposed the concept of macrophage isolation and characterization according to the tissue environment, and the function of macrophages according to different circumstances (33). Du et al. conducted *in vitro* and *in vivo* experiments and found that insulin-like growth factor 2 (IGF-2) can induce anti-inflammatory phenotype of mature macrophages by changing their mitochondrial metabolism, and transfer them to mice can alleviate their disease (34). Maybe using IGF-2 or other inducing factors can also actively induce macrophages to produce specific cells with Mreg function based on their phenotypes for application in immune regulation after kidney transplantation.

REGULATORY DENDRITIC CELLS

Dendritic cells (DCs) are another type of cells that are essential to elicit a specific T cell response to alloantigen, but they

can also enhance a tolerance response in some cases (35). DCs are functionally classified as myeloid DCs (mDCs) and plasmacytoid DCs (pDCs). Since most of them belong to mDCs, they are generally classified as myeloid immune cells. DCs belong to important antigen presenting cells (APCs), which play an essential role in the activation and adjustment of non-specific and specific immunity and induction of immune tolerance to maintain homeostasis in steady state under inflammatory conditions. Although the main function of DCs is to trigger the immune system, it seems that both mDCs and pDCs can enhance the tolerance to the same antigen (36). The two-way role of DCs in coordinating this delicate balance has attracted widespread attention. Increasing evidence indicates that the coordinate ability of DCs is dependent upon their immature state and can be regulated by many factors such as immunosuppressive molecules, genetic mechanism, certain pathogenic stimulation, signals from immune cells or apoptotic cells, and tissue or tumor microenvironment (37). Regulatory DCs (DCregs) retain the ability to present antigens to specific T cells. However, at the same time, they descend the expression of costimulatory molecules (CD80, CD86, and CD40) and pro-inflammatory cytokines (IL-12), and ascend the expression of inhibitory molecules (PDL1, CD95L, and IDO) and anti-inflammatory cytokines (TGF-β and IL-10), and is resistant to signals that induce maturation (38). The mechanisms of DCregs promoting immune tolerance include inducing T cell non-responsiveness, generating Tregs, inhibiting T cell response and inducing T cell apoptosis (39). The result published by Marin E et al. shows that DCregs regulate immune responses through lactate synthesis, inhibition of T cell proliferation and expansion of Tregs by secreting factors. The high level of lactate shifts T cell response to tolerance, delaying graft-vs.-host disease (40). At the University of Nantes, as part of the ONE Study, autologous DCreg infusion 1 day before transplant, is under examination in renal transplantation with SOC triple immunosuppressive (azathroprine, steroid, tacrolimus) (41). Therefore, researchers have begun to consider how to efficiently prepare DCregs to facilitate future large-scale use. Cai et al. produced enough high-quality functional DCregs from induced pluripotent stem cells (iPSCs) derived from murine, and named them iPS-DCregs. Even under strong stimuli, this kind of DCreg can still be in a "stable immature stage," and can induce permanent acceptance of mouse heart allografts (42). Some researchers have successfully used mouse DCregs to perform allogeneic transplantation of mouse skin and significantly prolonged graft survival (43). Pang et al. went a step further, purifying exosomes from DCregs and injecting them into allogeneic kidney transplantation model mice. After observation, it was determined that the exosomal group significantly improved survival, reduced the levels of (CD4+) T cell and cytokines related to rejection (IFN-γ, IL-2, and IL-17), and promoted the percentage of (Foxp3+) (CD4+)T cells in mice allograft, which indicates that exosomes of DCregs are involved in the induction of immune tolerance (44). Recently, Thomson et al. have produced Good Manufacturing Practice (GMP) grade DCregs for human organ transplantation. They briefly reviewed their experience in modulating immunotherapy in organ transplantation and the generation and characterization of human monocyte-derived DCregs. And they proposed a phase I/II safety study in which the effect of donor-derived DCregs combined with traditional immunosuppressive agent treatment on subclinical and clinical allograft rejection and adverse reactions will be observed in detail (45).

MYELOID-DERIVED SUPPRESSOR CELLS

Myeloid derived suppressor cells (MDSCs) are a heterogeneous population of bone marrow-derived myeloid progenitors that suppress immune responses in different kinds of inflammatory environments, such as organ transplantation, malignant tumors, infectious diseases, and autoimmune diseases (46). They are functionally defined as a class because of phenotypically expression with characteristics related to precursors of hematopoietic cells that can stably differentiate into mature macrophages, DCs and granulocytes at all stages (47). The pivotal position of MDSCs was initially established in the field of tumor immunity (48). Since then, many researchers have begun to explore the role of MDSCs in the host's immune response during organ transplantation. Dugast et al. first reported the important role of MDSCs in inducing tolerance in rat kidney transplant models. By increasing the number of MDSCs, the proliferation of allogenic T cells can be inhibited *in vivo*, and MDSCs may participate in the phase of NO-dependent tolerance maintenance (49). After this groundbreaking study determined the importance of MDSCs in transplant immunity, research on the therapeutic potential and immunoregulatory effects of MDSCs has been extensively conducted. Currently, MDSC are divided in three subpopulations: polymorphonuclear (PMN), monocytic (M) and early-stage (e) MDSC, and each one has different immunosuppressive mechanism (22). Dilek et al. focused on the connection between MDSCs and Tregs in transplant immunity and discovered the importance of a chemotactic C-C motif 5 (CCL5) between the two. The results show that the gradient of CCL5 around the graft contributes to MDSC's enhancement of tolerance in kidney allograft recipients. This gradient controls the recruitment of Tregs to the graft, which may help maintain tolerance (50). Studies performed by Luan et al. revealed blood derived M-MDSCs were able to expand Treg *in vitro* and correlated with increased Treg numbers *in vivo* (51). There are also many studies focusing on the effect of using MDSCs to extend the survival time of transplants after allogeneic transplantation of organs such as heart and skin in mice (52–55). These studies have discovered pathways and mechanisms such as carbon monoxide that may be related to the immune suppression of MDSCs through animal experiments, but more teams have begun to turn more to clinical trials. Meng et al. compared the allogeneic function, severity of tissue damage, and long-term survival of patients with high and low MDSCs *in vivo* after kidney transplantation. Compared with the low-dose MDSCs group, the allograft function of the

high-dose MDSCs group was significantly enhanced. In addition, his team also found that MDSCs isolated from transplant recipients can up-regulate Tregs and inhibit IL-17 production *in vitro* (56). Hock et al. found that the number of MDSCs in patients after kidney transplantation increased rapidly and reached a peak after the start of immunosuppression, but then fluctuated due to unknown reasons. Therefore, the purpose of establishing follow-up research is to explore the factors that regulate MDSC mobilization (57). Recent studies have shown that in patients with intestinal transplantation, MDSCs increase *in vivo* and restrain the response of effector T cells to the intestinal epithelium of the graft (58). This shows that due to the close relationship with T cells, MDSCs may have the prospect of immunosuppression for various organ transplants throughout the body. But some pessimistic points emerged, Lee et al. showed that adoptive MDSCs transfer after transplantation improves graft survival in mice, however their late depletion did not damage graft survival (59). Moreover, Utrero-Rico et al. found that higher maintained level of M-MDSC after transplantation in kidney recipients is associated with higher risk of cancer (60). These findings demonstrate together that MDSC could be beneficial early after transplantation to prolong graft survival, but, if maintained, it may promote tumoral development for patients due to excessive immunosuppression.

MESENCHYMAL STROMAL CELLS

Bone marrow-derived mesenchymal stromal cells (MSCs) are also a type of cells that have regulatory functions in transplantation immunity. Although MSCs are found in many tissues, most are derived from bone marrow, as we also include them in regulatory myeloid cells. MSCs are a kind of cells with multi-directional differentiation potential. They can induce differentiation into a variety of tissue cells under specific *in vivo* and *in vitro e*nvironments (61). MSCs could also migrate to sites of inflammation and to transplanted organs. So, many researchers have put it into testing for autoimmune diseases and post-transplant immunomodulatory therapies (62, 63). In experiments aimed at post-transplant immunity, MSCs have shown unique, effective, and undisputed immune-modulating properties. MSCs can act on a wide range of immune cells such as T cells, B cells, macrophages, natural killer cells, dendritic cells, and granulocytes (64). The much profound impact of MSC on adaptive immune response may be closely related to its innate source, so myeloid cells may be the earliest affected cells. MSCs interact with innate and acquired immune cells and immunomodulate them to make them develop more stable (and occasionally more intense) (65, 66). They impede the differentiation of dendritic cells and inhibit their maturation, thereby downregulating the ability of antigen presenting cells *in vivo* and *in vitro* (67–69). MSCs reduce the cytotoxicity of T lymphocytes that respond to foreign antigens and prevent effector T cells from replicating at the G0/G1 phase, thereby reducing their ability to produce IFN-γ and IL-2 (70). And they also promoted T cells to differentiate into Tregs and induce graft tolerance (71, 72). In addition, MSCs alter the proliferation of natural killer cells and γδT cells (73), reduce cytotoxicity and IFN-γ production, and inhibit B cell activation and antibody secretion (74).

Although there are many studies in various fields, the exact mechanism of action of MSCs has not been obtained. However, since MSCs can be easily isolated from different tissues including bone marrow, umbilical cord or connective tissue, and based on the current advanced technology, MSCs can be expanded *in vitro* to achieve an applicable cell dose in a relatively short time for clinic (75). Many studies on the use of MSCs cell therapy to modulate immunity after kidney transplantation have been performed worldwide. The goal of these studies is usually to induce inhibition through various forms of treatment with MSCs, so that patients can maintain the effect of immune tolerance based on minimal doses of immunosuppressive drug therapy to get the long-time survival of graft (76).

CONCLUSION

From the above analysis, it can be found that the immune system has a natural balance. This balance consists of the coordination of pro-inflammatory and regulatory cells, which involves a large series of regulatory factors. This is a very complicated and delicate process. As an important part of the regulatory cell side and possessing capability of promoting Treg proliferation, regulatory myeloid cells are expected to enhance success of early immunosuppressive drug withdrawal and become one of the anti-rejection options for patients after renal transplantation soon. An interesting matter to remark would be the need of prospective studies regarding the regulation of myeloid regulatory cells on the long term and which is the effect of immunosuppressive regiments on these cells, as well as their relationship with clinical outcomes, in order to develop strategies to promote tolerance. Most pilot studies were highly variable in design, did not incorporate a parallel trial arm of patients. This requires us all to further carry out more clinical-based experiments based on researches that has been reproduced in order to prove the advantages of its efficacy and higher safety and operability. In addition, whether it can be made into the very promising and available cell-based medicinal products (CBMP) also requires a unified standard. The existing data is still very ambiguous on this point.

AUTHOR CONTRIBUTIONS

JZ collected data, performed the analysis, and prepared the manuscript. JH conceived the article contents and endorsed the final draft submitted. Both authors contributed to the article and approved the submitted version.

FUNDING

Publication fees are covered by the National Natural Science Foundation of China (Grant No. 81771683).

REFERENCES

1. Murray JE. Reflections on the first successful kidney transplantation. *World J Surg.* (1982) 6:372–6. doi: 10.1007/BF01653562
2. Cornell LD, Smith RN, Colvin RB. Kidney transplantation: mechanisms of rejection and acceptance. *Annu Rev Pathol.* (2008) 3:189–220. doi: 10.1146/annurev.pathmechdis.3.121806.151508
3. Kidney Disease: Improving Global Outcomes Transplant Work G. KDIGO clinical practice guideline for the care of kidney transplant recipients. *Am J Transplant.* (2009) 9(Suppl. 3):S1–155. doi: 10.1111/j.1600-6143.2009.02834.x
4. Meier-Kriesche HU, Schold JD, Srinivas TR, Kaplan B. Lack of improvement in renal allograft survival despite a marked decrease in acute rejection rates over the most recent era. *Am J Transplant.* (2004) 4:378–83. doi: 10.1111/j.1600-6143.2004.00332.x
5. Fisher R, Gould D, Wainwright S, Fallon M. Quality of life after renal transplantation. *J Clin Nurs.* (1998) 7:553–63. doi: 10.1046/j.1365-2702.1998.00189.x
6. Tsipotis E, Gupta NR, Raman G, Zintzaras E, Jaber BL. Bioavailability, efficacy and safety of generic immunosuppressive drugs for kidney transplantation: a systematic review and meta-analysis. *Am J Nephrol.* (2016) 44:206–18. doi: 10.1159/000449020
7. Halloran PF. Immunosuppressive drugs for kidney transplantation. *N Engl J Med.* (2004) 351:2715–29. doi: 10.1056/NEJMra033540
8. Rizvi SMH, Aagnes B, Holdaas H, Gude E, Boberg KM, Bjortuft O, et al. Long-term change in the risk of skin cancer after organ transplantation: a population-based nationwide cohort study. *JAMA Dermatol.* (2017) 153:1270–7. doi: 10.1001/jamadermatol.2017.2984
9. Srinivas TR, Meier-Kriesche HU. Minimizing immunosuppression, an alternative approach to reducing side effects: objectives and interim result. *Clin J Am Soc Nephrol.* (2008) 3(Suppl. 2):S101–16. doi: 10.2215/CJN.03510807
10. Kirchhof J, Wilde B, Schmidt J, Mulling N, Petrakova L, Brinkhoff A, et al. Acute versus chronic administration of calcineurin-inhibitors differen-tially affect T-cell function. *Endocr Metab Immune Disord Drug Targets.* (2020). doi: 10.2174/1871530320999200831161710. [Epub ahead of print].
11. Xu QX, Qiu XY, Jiao Z, Zhang M, Zhong MK. FOXP3 rs3761549 polymorphism predicts long-term renal allograft function in patients receiving cyclosporine-based immunosuppressive regimen. *Gene.* (2018) 644:93–100. doi: 10.1016/j.gene.2017.10.081
12. Wood KJ, Goto R. Mechanisms of rejection: current perspectives. *Transplantation.* (2012) 93:1–10. doi: 10.1097/TP.0b013e31823cab44
13. Papp G, Boros P, Nakken B, Szodoray P, Zeher M. Regulatory immune cells and functions in autoimmunity and transplantation immunology. *Autoimmun Rev.* (2017) 16:435–44. doi: 10.1016/j.autrev.2017.03.011
14. Wood KJ, Bushell A, Hester J. Regulatory immune cells in transplantation. *Nat Rev Immunol.* (2012) 12:417–30. doi: 10.1038/nri3227
15. Sawitzki B, Harden PN, Reinke P, Moreau A, Hutchinson JA, Game DS, et al. Regulatory cell therapy in kidney transplantation (The ONE Study): a harmonised design and analysis of seven non-randomised, single-arm, phase 1/2A trials. *Lancet.* (2020) 395:1627–39. doi: 10.1016/S0140-6736(20)30167-7
16. Bashuda H, Kimikawa M, Seino K, Kato Y, Ono F, Shimizu A, et al. Renal allograft rejection is prevented by adoptive transfer of anergic T cells in nonhuman primates. *J Clin Invest.* (2005) 115:1896–902. doi: 10.1172/JCI23743
17. Ma A, Qi S, Song L, Hu Y, Dun H, Massicotte E, et al. Adoptive transfer of CD4+CD25+ regulatory cells combined with low-dose sirolimus and anti-thymocyte globulin delays acute rejection of renal allografts in Cynomolgus monkeys. *Int Immunopharmacol.* (2011) 11:618–29. doi: 10.1016/j.intimp.2010.11.001
18. Taylor PA, Lees CJ, Blazar BR. The infusion of ex vivo activated and expanded CD4(+)CD25(+) immune regulatory cells inhibits graft-versus-host disease lethality. *Blood.* (2002) 99:3493–9. doi: 10.1182/blood.V99.10.3493
19. Wood KJ, Sakaguchi S. Regulatory T cells in transplantation tolerance. *Nat Rev Immunol.* (2003) 3:199–210. doi: 10.1038/nri1027
20. Chandran S, Tang Q, Sarwal M, Laszik ZG, Putnam AL, Lee K, et al. Polyclonal Regulatory T Cell Therapy for Control of Inflammation in Kidney Transplants. *Am J Transplant.* (2017) 17:2945–54. doi: 10.1111/ajt.14415
21. Rosborough BR, Raich-Regue D, Turnquist HR, Thomson AW. Regulatory myeloid cells in transplantation. *Transplantation.* (2014) 97:367–79. doi: 10.1097/TP.0b013e3182a860de
22. Bronte V, Brandau S, Chen SH, Colombo MP, Frey AB, Greten TF, et al. Recommendations for myeloid-derived suppressor cell nomenclature and characterization standards. *Nat Commun.* (2016) 7:12150. doi: 10.1038/ncomms12150
23. Guo F, Hu M, Huang D, Zhao Y, Heng B, Guillemin G, et al. Human regulatory macrophages are potent in suppression of the xenoimmune response via indoleamine-2,3-dioxygenase-involved mechanism(s). *Xenotransplantation.* (2017) 24:e12326. doi: 10.1111/xen.12326
24. Moreau A, Varey E, Beriou G, Hill M, Bouchet-Delbos L, Segovia M, et al. Tolerogenic dendritic cells and negative vaccination in transplantation: from rodents to clinical trials. *Front Immunol.* (2012) 3:218. doi: 10.3389/fimmu.2012.00218
25. Pool M, Leuvenink H, Moers C. Reparative and regenerative effects of mesenchymal stromal cells-promising potential for kidney transplantation? *Int J Mol Sci.* (2019) 20:4614. doi: 10.3390/ijms20184614
26. Jose MD, Ikezumi Y, van Rooijen N, Atkins RC, Chadban SJ. Macrophages act as effectors of tissue damage in acute renal allograft rejection. *Transplantation.* (2003) 76:1015–22. doi: 10.1097/01.TP.0000083507.67995.13
27. Oberbarnscheidt MH, Zeng Q, Li Q, Dai H, Williams AL, Shlomchik WD, et al. Non-self recognition by monocytes initiates allograft rejection. *J Clin Invest.* (2014) 124:3579–89. doi: 10.1172/JCI74370
28. Fleming BD, Mosser DM. Regulatory macrophages: setting the threshold for therapy. *Eur J Immunol.* (2011) 41:2498–502. doi: 10.1002/eji.201141717
29. Conde P, Rodriguez M, van der Touw W, Jimenez A, Burns M, Miller J, et al. DC-SIGN(+) macrophages control the induction of transplantation tolerance. *Immunity.* (2015) 42:1143–58. doi: 10.1016/j.immuni.2015.05.009
30. Hutchinson JA, Riquelme P, Sawitzki B, Tomiuk S, Miqueu P, Zuhayra M, et al. Cutting edge: immunological consequences and trafficking of human regulatory macrophages administered to renal transplant recipients. *J Immunol.* (2011) 187:2072–8. doi: 10.4049/jimmunol.1100762
31. Riquelme P, Tomiuk S, Kammler A, Fandrich F, Schlitt HJ, Geissler EK, et al. IFN-gamma-induced iNOS expression in mouse regulatory macrophages prolongs allograft survival in fully immunocompetent recipients. *Mol Ther.* (2013) 21:409–22. doi: 10.1038/mt.2012.168
32. Riquelme P, Haarer J, Kammler A, Walter L, Tomiuk S, Ahrens N, et al. TIGIT(+) iTregs elicited by human regulatory macrophages control T cell immunity. *Nat Commun.* (2018) 9:2858. doi: 10.1038/s41467-018-05167-8
33. Ochando J, Conde P. Functional Characterization of Regulatory Macrophages That Inhibit Graft-reactive Immunity. *J Vis Exp.* (2017) (124). doi: 10.3791/54242
34. Du L, Lin L, Li Q, Liu K, Huang Y, Wang X, et al. IGF-2 preprograms maturing macrophages to acquire oxidative phosphorylation-dependent anti-inflammatory properties. *Cell Metab.* (2019) 29:1363–75 e8. doi: 10.1016/j.cmet.2019.01.006
35. Banchereau J, Steinman RM. Dendritic cells and the control of immunity. *Nature.* (1998) 392:245–52. doi: 10.1038/32588
36. van Kooten C, Lombardi G, Gelderman KA, Sagoo P, Buckland M, Lechler R, et al. Dendritic cells as a tool to induce transplantation tolerance: obstacles and opportunities. *Transplantation.* (2011) 91:2–7. doi: 10.1097/TP.0b013e31820263b3
37. Steinman RM, Banchereau J. Taking dendritic cells into medicine. *Nature.* (2007) 449:419–26. doi: 10.1038/nature06175
38. Morelli AE, Thomson AW. Tolerogenic dendritic cells and the quest for transplant tolerance. *Nat Rev Immunol.* (2007) 7:610–21. doi: 10.1038/nri2132
39. Manicassamy S, Pulendran B. Dendritic cell control of tolerogenic responses. *Immunol Rev.* (2011) 241:206–27. doi: 10.1111/j.1600-065X.2011.01015.x
40. Marin E, Bouchet-Delbos L, Renoult O, Louvet C, Nerriere-Daguin V, Managh AJ, et al. Human tolerogenic dendritic cells regulate immune responses through lactate synthesis. *Cell Metab.* (2019) 30:1075–90 e8. doi: 10.1016/j.cmet.2019.11.011
41. Thomson AW, Humar A, Lakkis FG, Metes DM. Regulatory dendritic cells for promotion of liver transplant operational tolerance: rationale for a clinical

trial and accompanying mechanistic studies. *Hum Immunol.* (2018) 79:314–21. doi: 10.1016/j.humimm.2017.10.017
42. Cai S, Hou J, Fujino M, Zhang Q, Ichimaru N, Takahara S, et al. iPSC-derived regulatory dendritic cells inhibit allograft rejection by generating alloantigen-specific regulatory T cells. *Stem Cell Reports.* (2017) 8:1174–89. doi: 10.1016/j.stemcr.2017.03.020
43. Segovia M, Louvet C, Charnet P, Savina A, Tilly G, Gautreau L, et al. Autologous dendritic cells prolong allograft survival through Tmem176b-dependent antigen cross-presentation. *Am J Transplant.* (2014) 14:1021–31. doi: 10.1111/ajt.12708
44. Pang XL, Wang ZG, Liu L, Feng YH, Wang JX, Xie HC, et al. Immature dendritic cells derived exosomes promotes immune tolerance by regulating T cell differentiation in renal transplantation. *Aging (Albany NY).* (2019) 11:8911–24. doi: 10.18632/aging.102346
45. Thomson AW, Zahorchak AF, Ezzelarab MB, Butterfield LH, Lakkis FG, Metes DM. Prospective clinical testing of regulatory dendritic cells in organ transplantation. *Front Immunol.* (2016) 7:15. doi: 10.3389/fimmu.2016.00015
46. Almand B, Clark JI, Nikitina E, van Beynen J, English NR, Knight SC, et al. Increased production of immature myeloid cells in cancer patients: a mechanism of immunosuppression in cancer. *J Immunol.* (2001) 166:678–89. doi: 10.4049/jimmunol.166.1.678
47. Dilek N, van Rompaey N, Le Moine A, Vanhove B. Myeloid-derived suppressor cells in transplantation. *Curr Opin Organ Transplant.* (2010) 15:765–8. doi: 10.1097/MOT.0b013e3283401742
48. Pak AS, Wright MA, Matthews JP, Collins SL, Petruzzelli GJ, Young MR. Mechanisms of immune suppression in patients with head and neck cancer: presence of CD34(+) cells which suppress immune functions within cancers that secrete granulocyte-macrophage colony-stimulating factor. *Clin Cancer Res.* (1995) 1:95–103.
49. Dugast AS, Haudebourg T, Coulon F, Heslan M, Haspot F, Poirier N, et al. Myeloid-derived suppressor cells accumulate in kidney allograft tolerance and specifically suppress effector T cell expansion. *J Immunol.* (2008) 180:7898–906. doi: 10.4049/jimmunol.180.12.7898
50. Dilek N, Poirier N, Usal C, Martinet B, Blancho G, Vanhove B. Control of transplant tolerance and intragraft regulatory T cell localization by myeloid-derived suppressor cells and CCL5. *J Immunol.* (2012) 188:4209–16. doi: 10.4049/jimmunol.1101512
51. Luan Y, Mosheir E, Menon MC, Wilson D, Woytovich C, Ochando J, et al. Monocytic myeloid-derived suppressor cells accumulate in renal transplant patients and mediate CD4(+) Foxp3(+) Treg expansion. *Am J Transplant.* (2013) 13:3123–31. doi: 10.1111/ajt.12461
52. Liao J, Wang X, Bi Y, Shen B, Shao K, Yang H, et al. Dexamethasone potentiates myeloid-derived suppressor cell function in prolonging allograft survival through nitric oxide. *J Leukoc Biol.* (2014) 96:675–84. doi: 10.1189/jlb.2HI1113-611RR
53. Nakamura T, Nakao T, Ashihara E, Yoshimura N. Myeloid-derived suppressor cells recruit CD4(+)/Foxp3(+) regulatory T cells in a murine cardiac allograft. *Transplant Proc.* (2016) 48:1275–8. doi: 10.1016/j.transproceed.2015.10.060
54. Zhao Y, Shen XF, Cao K, Ding J, Kang X, Guan WX, et al. Dexamethasone-induced myeloid-derived suppressor cells prolong allo cardiac graft survival through iNOS- and glucocorticoid receptor-dependent mechanism. *Front Immunol.* (2018) 9:282. doi: 10.3389/fimmu.2018.00282
55. Nakao T, Nakamura T, Masuda K, Matsuyama T, Ushigome H, Ashihara E, et al. Dexamethasone prolongs cardiac allograft survival in a murine model through myeloid-derived suppressor cells. *Transplant Proc.* (2018) 50:299–304. doi: 10.1016/j.transproceed.2017.11.014
56. Meng F, Chen S, Guo X, Chen Z, Huang X, Lai Y, et al. Clinical significance of myeloid-derived suppressor cells in human renal transplantation with acute T cell-mediated rejection. *Inflammation.* (2014) 37:1799–805. doi: 10.1007/s10753-014-9910-5
57. Hock BD, McKenzie JL, Cross NB, Currie MJ. Dynamic changes in myeloid derived suppressor cell subsets following renal transplant: a prospective study. *Transpl Immunol.* (2015) 32:164–71. doi: 10.1016/j.trim.2015.05.001
58. Okano S, Abu-Elmagd K, Kish DD, Keslar K, Baldwin WM, 3rd, Fairchild RL, et al. Myeloid-derived suppressor cells increase and inhibit donor-reactive T cell responses to graft intestinal epithelium in intestinal transplant patients. *Am J Transplant.* (2018) 18:2544–58. doi: 10.1111/ajt.14718
59. Lee YS, Zhang T, Saxena V, Li L, Piao W, Bromberg JS, et al. Myeloid-derived suppressor cells expand after transplantation and their augmentation increases graft survival. *Am J Transplant.* (2020) 20:2343–55. doi: 10.1111/ajt.15879
60. Utrero-Rico A, Laguna-Goya R, Cano-Romero F, Chivite-Lacaba M, Gonzalez-Cuadrado C, Rodriguez-Sanchez E, et al. Early posttransplant mobilization of monocytic myeloid-derived suppressor cell correlates with increase in soluble immunosuppressive factors and predicts cancer in kidney recipients. *Transplantation.* (2020) 104:2599–608. doi: 10.1097/TP.0000000000003179
61. Casiraghi F, Perico N, Remuzzi G. Mesenchymal stromal cells for tolerance induction in organ transplantation. *Hum Immunol.* (2018) 79:304–13. doi: 10.1016/j.humimm.2017.12.008
62. Hashmi S, Ahmed M, Murad MH, Litzow MR, Adams RH, Ball LM, et al. Survival after mesenchymal stromal cell therapy in steroid-refractory acute graft-versus-host disease: systematic review and meta-analysis. *Lancet Haematol.* (2016) 3:e45–52. doi: 10.1016/S2352-3026(15)00224-0
63. Pistoia V, Raffaghello L. Mesenchymal stromal cells and autoimmunity. *Int Immunol.* (2017) 29:49–58. doi: 10.1093/intimm/dxx008
64. Le Blanc K, Mougiakakos D. Multipotent mesenchymal stromal cells and the innate immune system. *Nat Rev Immunol.* (2012) 12:383–96. doi: 10.1038/nri3209
65. Bernardo ME, Fibbe WE. Mesenchymal stromal cells: sensors and switchers of inflammation. *Cell Stem Cell.* (2013) 13:392–402. doi: 10.1016/j.stem.2013.09.006
66. Spaggiari GM, Moretta L. Cellular and molecular interactions of mesenchymal stem cells in innate immunity. *Immunol Cell Biol.* (2013) 91:27–31. doi: 10.1038/icb.2012.62
67. Jiang XX, Zhang Y, Liu B, Zhang SX, Wu Y, Yu XD, et al. Human mesenchymal stem cells inhibit differentiation and function of monocyte-derived dendritic cells. *Blood.* (2005) 105:4120–6. doi: 10.1182/blood-2004-02-0586
68. Nauta AJ, Kruisselbrink AB, Lurvink E, Willemze R, Fibbe WE. Mesenchymal stem cells inhibit generation and function of both CD34+-derived and monocyte-derived dendritic cells. *J Immunol.* (2006) 177:2080–7. doi: 10.4049/jimmunol.177.4.2080
69. Chiesa S, Morbelli S, Morando S, Massollo M, Marini C, Bertoni A, et al. Mesenchymal stem cells impair *in vivo* T-cell priming by dendritic cells. *Proc Natl Acad Sci USA.* (2011) 108:17384–9. doi: 10.1073/pnas.1103650108
70. Karlsson H, Samarasinghe S, Ball LM, Sundberg B, Lankester AC, Dazzi F, et al. Mesenchymal stem cells exert differential effects on alloantigen and virus-specific T-cell responses. *Blood.* (2008) 112:532–41. doi: 10.1182/blood-2007-10-119370
71. Luz-Crawford P, Kurte M, Bravo-Alegria J, Contreras R, Nova-Lamperti E, Tejedor G, et al. Mesenchymal stem cells generate a CD4+CD25+Foxp3+ regulatory T cell population during the differentiation process of Th1 and Th17 cells. *Stem Cell Res Ther.* (2013) 4:65. doi: 10.1186/scrt216
72. Hall BM. CD4+CD25+ T regulatory cells in transplantation tolerance: 25 years on. *Transplantation.* (2016) 100:2533–47. doi: 10.1097/TP.0000000000001436
73. Najar M, Fayyad-Kazan M, Merimi M, Burny A, Bron D, Fayyad-Kazan H, et al. Mesenchymal stromal cells and natural killer cells: a complex story of love and hate. *Curr Stem Cell Res Ther.* (2019) 14:14–21. doi: 10.2174/1574888X13666180912125736
74. Rosado MM, Bernardo ME, Scarsella M, Conforti A, Giorda E, Biagini S, et al. Inhibition of B-cell proliferation and antibody production by mesenchymal stromal cells is mediated by T cells. *Stem Cells Dev.* (2015) 24:93–103. doi: 10.1089/scd.2014.0155
75. Perico N, Casiraghi F, Gotti E, Introna M, Todeschini M, Cavinato RA, et al. Mesenchymal stromal cells and kidney transplantation: pretransplant infusion protects from graft dysfunction while fostering immunoregulation. *Transpl Int.* (2013) 26:867–78. doi: 10.1111/tri.12132
76. Sun Q, Huang Z, Han F, Zhao M, Cao R, Zhao D, et al. Allogeneic mesenchymal stem cells as induction therapy are safe and feasible in renal allografts: pilot results of a multicenter randomized controlled trial. *J Transl Med.* (2018) 16:52. doi: 10.1186/s12967-018-1422-x

Conflict of Interest: The authors declare that the research was conducted in the absence of any commercial or financial relationships that could be construed as a potential conflict of interest.

The reviewer RR declared shared affiliation, with no collaboration, with the authors to the handling editor at the time of review.

Copyright © 2021 Zhuang and Hou. This is an open-access article distributed under the terms of the Creative Commons Attribution License (CC BY). The use, distribution or reproduction in other forums is permitted, provided the original author(s) and the copyright owner(s) are credited and that the original publication in this journal is cited, in accordance with accepted academic practice. No use, distribution or reproduction is permitted which does not comply with these terms.

frontiers in Immunology

ORIGINAL RESEARCH
published: 09 March 2021
doi: 10.3389/fimmu.2021.637335

TSC1 Affects the Process of Renal Ischemia-Reperfusion Injury by Controlling Macrophage Polarization

Xiao Hu[1,2†], Yanan Xu[2,3†], Zhaoqi Zhang[2,3†], Zuofu Tang[1†], Jinhua Zhang[1], You Luo[1], Weiming Deng[1], Zhanwen Dong[1], Yong Zhao[2,3,4] and Ning Na[1*]*

[1] Department of Kidney Transplantation, The Third Affiliated Hospital of Sun Yat-sen University, Guangzhou, China, [2] State Key Laboratory of Membrane Biology, Institute of Zoology, Chinese Academy of Sciences, Beijing, China, [3] Savaid Medical School, University of Chinese Academy of Sciences, Beijing, China, [4] Institute for Stem Cell and Regeneration, Chinese Academy of Sciences, Beijing, China

OPEN ACCESS

Edited by:
Cheng Yang,
Fudan University, China

Reviewed by:
Hu Linkun,
Soochow University, China
Yanlin Wang,
University of Connecticut,
United States

***Correspondence:**
Ning Na
naning@mail.sysu.edu.cn
Yong Zhao
zhaoy@ioz.ac.cn

[†]These authors have contributed equally to this work

Specialty section:
This article was submitted to Molecular Innate Immunity, a section of the journal Frontiers in Immunology

Received: 03 December 2020
Accepted: 15 January 2021
Published: 09 March 2021

Citation:
Hu X, Xu Y, Zhang Z, Tang Z, Zhang J, Luo Y, Deng W, Dong Z, Zhao Y and Na N (2021) TSC1 Affects the Process of Renal Ischemia-Reperfusion Injury by Controlling Macrophage Polarization. Front. Immunol. 12:637335. doi: 10.3389/fimmu.2021.637335

Renal ischemia-reperfusion injury (IRI) contributes to acute kidney injury (AKI), increases morbidity and mortality, and is a significant risk factor for chronic kidney disease (CKD). Macrophage infiltration is a common feature after renal IRI, and infiltrating macrophages can be polarized into the following two distinct types: M1 macrophages, i.e., classically activated macrophages, which can not only inhibit infection but also accelerate renal injury, and M2 macrophages, i.e., alternatively activated macrophages, which have a repair phenotype that can promote wound healing and subsequent fibrosis. The role of TSC1, which is a negative regulator of mTOR signaling that regulates macrophage polarization in inflammation-linked diseases, has been well documented, but whether TSC1 contributes to macrophage polarization in the process of IRI is still unknown. Here, by using a mouse model of renal ischemia-reperfusion, we found that myeloid cell-specific TSC1 knockout mice (termed Lyz-TSC1 cKO mice) had higher serum creatinine levels, more severe histological damage, and greater proinflammatory cytokine production than wild-type (WT) mice during the early phase after renal ischemia-reperfusion. Furthermore, the Lyz-TSC1 cKO mice showed attenuated renal fibrosis during the repair phase of IRI with decreased levels of M2 markers on macrophages in the operated kidneys, which was further confirmed in a cell model of hypoxia-reoxygenation (H/R) *in vitro*. Mechanistically, by using RNA sequencing of sorted renal macrophages, we found that the expression of most M1-related genes was upregulated in the Lyz-TSC1 cKO group (Supplemental Table 1) during the early phase. However, C/EBPβ and CD206 expression was decreased during the repair phase compared to in the WT group. Overall, our findings demonstrate that the expression of TSC1 in macrophages contributes to the whole process of IRI but serves as an inflammation suppressor during the early phase and a fibrosis promoter during the repair phase.

Keywords: kidney, ischemia-reperfusion (IR), macrophage polarization, fibrosis, tuberous sclerosis complex 1 (TSC1)

INTRODUCTION

Renal ischemia-reperfusion injury is a major risk factor affecting the prognosis of AKI and the functional recovery and long-term survival of grafts after renal transplantation (1). Innate and adaptive immune cells, such as macrophages, dendritic cells, neutrophils, and lymphocytes, are involved in the pathogenesis of renal injury after ischemia-reperfusion injury (IRI) (2). Specifically, macrophages, which are primary components of the phagocytic system, aggravate damage during the initial stage of reperfusion but promote tubular repair and long-term renal fibrosis during the late stage after IRI (3). During the early phase, monocytes adhere to the vasa recta 2 h after IRI, and most macrophage recruitment occurs surrounding postcapillary venules (4). Then, proinflammatory monocytes/macrophages are thought to mediate tubular injury by releasing several important cytokines (such as IL-6, TNF-α, and IL-12) and nitric oxide (NO) by iNOS (3). Among all cell types associated with renal fibrogenesis, macrophages can promote the progression of renal fibrosis as a driving force; $CD206^+$ M2 macrophages, especially those derived from bone marrow cells that can directly contribute to renal fibrosis, are strongly involved in renal fibrosis (5). In the injured kidney, macrophages from bone marrow cells can differentiate into α-SMA^+ myofibroblasts termed macrophage-to-myofibroblast transition (MMT), which contribute to pathogenic collagen production during tissue fibrosis (6–8). The CD206+ α-SMA+ cells co-expressing suggests that macrophages that undergo MMT are predominantly M2 (5, 9). Moreover, some cytokines and growth factors secreted by macrophages, such as TGF-β1, IL-10, and matrix metalloproteinase (MMP), can contribute to fibrosis (10). In addition, it has been confirmed in various disease models that transforming growth factor-β (TGF-β) is a main cause of fibrosis in most forms of chronic kidney disease (CKD) (11). IL-10 is considered an anti-inflammatory and antifibrotic cytokine, but paradoxically, IL-10 appears to affect profibrotic signaling pathways that are unique to the kidney (12). Barbarin et al. reported that IL-10 inhibits the infiltration of inflammatory cells during the early stage of fibrosis but promoted fibrosis during the later stage (13).

Macrophages can differentiate into distinct phenotypes when stimulated by certain cytokines or exposed to different microenvironments (14). M1 macrophages are induced by exposure to IFNγ, LPS, TNFα, or GM-CSF and express proinflammatory cytokines, such as IL-1β, TNFα, and IL-6, while M2 macrophages resulting from IL-4/IL-13 stimulation produce anti-inflammatory factors, including IL-10 and TGFβ (15, 16). Several studies have shown that renal tubular cells participate in the activation and polarization of macrophages by producing macrophage growth factors, such as macrophage colony-stimulating factor (M-CSF), granulocyte macrophage colony-stimulating factor (GM-CSF), and IL-34 (17–20). In coculture with tubular epithelial cells, macrophages activate and upregulate the expression of the alternative activation markers CD206 and Arginase-1 (Arg-1) (21). These conclusions imply that macrophages contribute to renal ischemia-reperfusion injury and subsequent recovery *via* different phenotypic polarizations.

The tuberous sclerosis complex (TSC) comprises TSC1, TSC2, and TBC1D7 (22). The mechanistic target of rapamycin (mTOR) is a serine/threonine protein kinase belonging to the PI3K-related kinase (PIKK) family that forms the catalytic subunit of two protein complexes, i.e., mTOR complex 1 (mTORC1) and mTOR complex 1 (mTORC2); the TSC1 and TSC2 proteins form a heterodimeric complex that acts as a functional unit that inhibits mTOR as the key negative regulator of mTORC1 signaling (23). Using an acute endotoxin shock model, our previous study revealed that TSC1 inhibits M1 polarization by suppressing the Ras GTPase–Raf1–MEK–ERK pathway in an mTOR-independent manner while promoting M2 properties by mTOR-dependent CCAAT/enhancer-binding protein-b (C/EBP-β) pathways (24).

This study demonstrates that *TSC1* deficiency in macrophages promotes M1 polarization to aggravate kidney dysfunction during the early phase of renal IRI and attenuates renal fibrosis during the repair stage resulting from reduced M2 polarization. Therefore, these findings demonstrate that TSC1 controls macrophage polarization to affect the whole process of renal ischemia-reperfusion injury.

METHODS

Mice

Myeloid cell-specific TSC1 conditional knockout mice (C57BL/6 background) were obtained by crossing $TSC1^{loxp/loxp}$ mice with mice expressing Cre recombinase under the control of the lysozyme promoter (LysMCre), and WT littermates were used as controls. The $TSC1^{loxp/loxp}$ mice were kindly provided by Dr. Hongbin Zhang (Institute of Basic Medical Sciences and School of Basic Medicine, Peking Union Medical College, and Chinese Academy of Medical Sciences, Beijing, China) (25, 26). The LysMCre mice were generous gifts from Dr. Lianfeng Zhang, Key Laboratory of Human Diseases Comparative Medicine, Ministry of Health, Institute of Laboratory Animal Science, CAMS & PUMC (27). All mice were maintained in the specific pathogen-free Laboratory Animal Centre of the Institute of Zoology, Beijing, China. All studies were performed according to the institutional guidelines and approved by the research ethics committee (IRB: [2020]02-166) of the Third Affiliated Hospital of Sun Yat-sen University.

IRI Model

Male C57BL/6 mice (aged 6–8 weeks; weight 18–22 g) were anesthetized using isoflurane (2% for induction and 1.5% for maintenance) on a 36°C warming pad using a rectal probe. Non-damaged microvascular clamps (AESCULAP YASARGIL, Cat: FT222T) were used to block the bilateral renal pedicles for 30 min. The peritoneum and skin were closed in turn with 5-0 silk threads. One milliliter of saline was injected *via* the intraperitoneal route to prevent dehydration. All mice were kept under 12-h light/dark cycles, and normal food was

provided *ad libitum*. The mice were euthanized, and the kidneys were collected on days 1, 4, 7, 14, and 21 after IRI. The kidney tissue was harvested for the histology, immunohistochemistry, and immunofluorescence analyses, RNA seq and RNA extraction after fluorescence-activated cell sorting (FACS).

BMDMs and Adoptive Transfer

After separating the tibia, femur, and ilium of the mice, the cells in the bone marrow were collected with a syringe filled with Dulbecco's modified Eagle medium (DMEM). The bone marrow cells were cultured in DMEM supplemented with 10% fetal bovine serum (FBS) and 10 ng/ml mouse macrophage colony-stimulating factor (M-CSF) for 7 days to acquire bone marrow-derived macrophages (BMDMs). Then, the harvested BMDMs were labeled by CFSE (MedChemExpress, Cat No.: HY-D0938) as previously reported (16). CFSE-labeled WT/Lyz-TSC1 cKO BMDMs (1 × 107) were intravenously injected into WT mice 2 h before kidney IRI.

Hypoxia-Reoxygenation (H/R) Injury in RTECs *In Vitro*

Renal tubular epithelial cells (RTECs, BeNa Culture, Cat: BNCC340198) were cultured in DMEM supplemented with 5% FBS, penicillin (100 U/ml), and streptomycin (100 μg/ml) until they reached 90% confluence. Then, the cells were exposed to serum-free medium and cultured in a hypoxic incubator (1% O2, 94% N2, and 5% CO2) for 4 h at 37°C to induce hypoxic injury. Then, the cells were returned to 5% CO2 and 95% air for reoxygenation. The supernatants were harvested at 24 h after centrifugation to remove cell impurities. The BMDMs from the WT and Lyz-TSC1 cKO mice were treated with CM supplemented with 5% FBS, penicillin (100 U/ml), and streptomycin (100 μg/ml) for 24–48 h and were collected for RNA extraction.

Kidney Histology and Immunohistochemical and Immunofluorescence Staining

The kidney samples were embedded in paraffin. Sections at a thickness of 4 μm were used for the hematoxylin and eosin (H&E), Masson staining, and Sirius Red staining following standard protocols. Renal tubular damage was graded on a five-level scale according to the extent of necrosis in the proximal tubules as described by Jablonski et al. (28). All assessments were performed by two investigators blinded to the experimental conditions. The positively stained tissue relative to the selected field was quantified by ImageJ (National Institutes of Health, Bethesda, MD, USA). For IHC experiments, α-SMA, Collagen III, fibronectin, and KIM-1 were detected by immunohistochemistry using primary monoclonal antibodies against α-SMA (Servicebio, Cat: GB13044), Collagen III (Servicebio, Cat: GB13023-2), fibronectin (Servicebio, Cat: GB13091), and primary polyclonal antibodies against KIM-1 (Sigma, Cat: SAB3500252-100ug). F4/80 and CD206 were detected by immunofluorescence using primary monoclonal antibodies against F4/80 (Abcam, Cat: ab6640) and primary polyclonal antibodies against CD206 (Abcam, Cat: Ab64693). CD206 and α-SMA were also detected by immunofluorescence using amCD206-FITC (Biolengend, Cat: 141703) and primary monoclonal antibodies against α-SMA (Abclonal, Cat: A17910). Fluorescent images were acquired using a Ti-E A1R+STORM confocal microscope.

Assessment of Renal Function

Serum creatinine was measured to assess renal function and analyzed by an AU5811 analyzer (Beckman Coulter) using the enzymatic assay method (DONGOU, Cat: 59400377071).

Flow Cytometry

The recipient mice were sacrificed and perfused with 20 ml 0.9% NaCl solution containing 125 U/ml heparin sodium *in situ*. The kidneys were acquired and grinded. A single-cell suspension was digested at 37°C for 30 min in 1640 medium containing 1 mg/ml type IV collagenase (Sigma, Cat: C5138-5 g) and 20 U/ml DNase I (Sigma, Cat: D5025-150 KU). Then, the cells were stained with antibodies (including CD45 [30-F11], F4/80 [BM8], CD11b [M1/70] [from eBioscience {San Diego, CA, USA}], and CD206 [C068C2] [from BD Biosciences {San Jose, CA, USA}]) against surface antigens for 30 min at 4℃. For FACS, the cells were stained with the following antibodies: anti-F4/80 (BM8) (eBioscience), anti-CD45.2 (clone 104), and anti-CD11b (M1/70) (from eBioscience). Then, the labeled cells were sorted by a MoFlo XDP sorter (Beckman). All flow cytometry data were obtained with an LSRFortessa™ X-20 instrument (BD Biosciences, CA, USA) and analyzed with FlowJo (Treestar, OR, USA).

RNA-Seq Analysis

The macrophages were sorted by $CD45^+F4/80^+CD11b^+$ in the kidneys from the WT and Lyz-TSC1 cKO mice at 24 h and 2 weeks after IRI using a MoFlo XDP cell sorter (BeckMan Coulter, Brea, CA, USA). All samples were collected in tubes containing lysis components and ribonuclease inhibitors. All RNA extraction, library preparation, and sequencing were performed by Annoroad Gene Tech. (Beijing) Co., Ltd. Then, amplification was carried out by the Smart-Seq2 method. An oligo-dT primer was introduced to the reverse transcription reaction for the first-strand cDNA synthesis, followed by PCR amplification to enrich the cDNA and magbead purification step to clean the production. Then, the cDNA production was checked by Qubit® 3.0 Fluorometer and Agilent 2100 Bioanalyzer to ensure the expected production with a length of approximately 1~2 kbp. Then, the cDNA was randomly sheared by ultrasonication for the Illumina library preparation protocol, including DNA fragmentation, end repair, 3' end A-tailing, adapter ligation, PCR amplification, and library validation. After the library preparation, a PerkinElmer LabChip® GX Touch and Step OnePlus™ Real-Time PCR System was used for the library quality inspection. Then, the qualified libraries were loaded onto the Illumina HiSeq platform for the PE150 sequencing. We downloaded macrophage polarization data from the NCBI GEO database (GSE107776).

For both the downloaded data and our data, we used the mapping software HISAT2 to map the reads to the mouse mm10 reference genome and StringTie to construct transcripts independently for each cell (29). DEseq2 was used to identify the differentially expressed genes between the WT and TSC1-deficient macrophages (30). We considered adjp < 0.05 and |log2 (fold change)| > 1 indicative of a significant difference in the two cell thresholds. Gene Ontology (GO) functional annotation and KEGG pathway analysis were performed to analyze all differential genes using the DAVID Bioinformatics Resources 6.8 online search tool (https://david.ncifcrf.gov/) and the Kobas online search tool (http://kobas.cbi.pku.edu.cn/). The functional protein network analysis was performed by String (https://string-db.org/) and shown by Cytoscape software (31).

Quantitative PCR Analysis

Kidney RNA, FACS-sorted cell RNA, or cultured cell RNA was extracted with TRIzol Reagent (Invitrogen, Carlsbad, CA, USA) or E.Z.N.A. Total RNA kit I (#R6834) and reverse transcribed (Bio-Rad). The RNA was quantified using a Take3 Gen5 spectrophotometer (BioTek, Winooski, VT). The gene expression analysis was determined by quantitative real-time PCR (iTaq Universal Sybr Green Supermix; Bio-Rad) using CFX96 (Bio-Rad) and normalized to the expression level of the housekeeping gene hypoxanthine phosphoribosyltransferase.

Statistical Analysis

All results are expressed as the mean ± SEM. GraphPad Prism software (GraphPad Inc., San Diego, CA, USA) was used to analyze the data. Unpaired t-tests and analysis of variance were performed, and $P < 0.05$ was considered indicative of statistical significance.

RESULTS

Elevated Injury Was Caused by Increased Proinflammatory Polarization of *TSC1* Knockout Macrophages in the Kidney During the Early Phase

To explore the role of TSC1 expression in macrophages during the process of renal IRI, a standardized model of renal IRI was established in this study by blocking the bilateral renal pedicles for 30 min. The kidneys were obtained on days 1, 4, 7, 14, and 21 after IRI (**Figure 1A**). During the early phase after reperfusion, the Lyz-TSC1 cKO mice showed aggravated kidney dysfunction, and significantly higher serum creatinine levels were observed in the Lyz-TSC1 cKO mice 1 and 3 days after injury (**Figure 1B**). In addition, the renal tubular injury scores were assessed 1 and 3 days after reperfusion by H&E staining (**Figure 1C**). The renal tubular injury scores of the Lyz-TSC1 cKO mice were

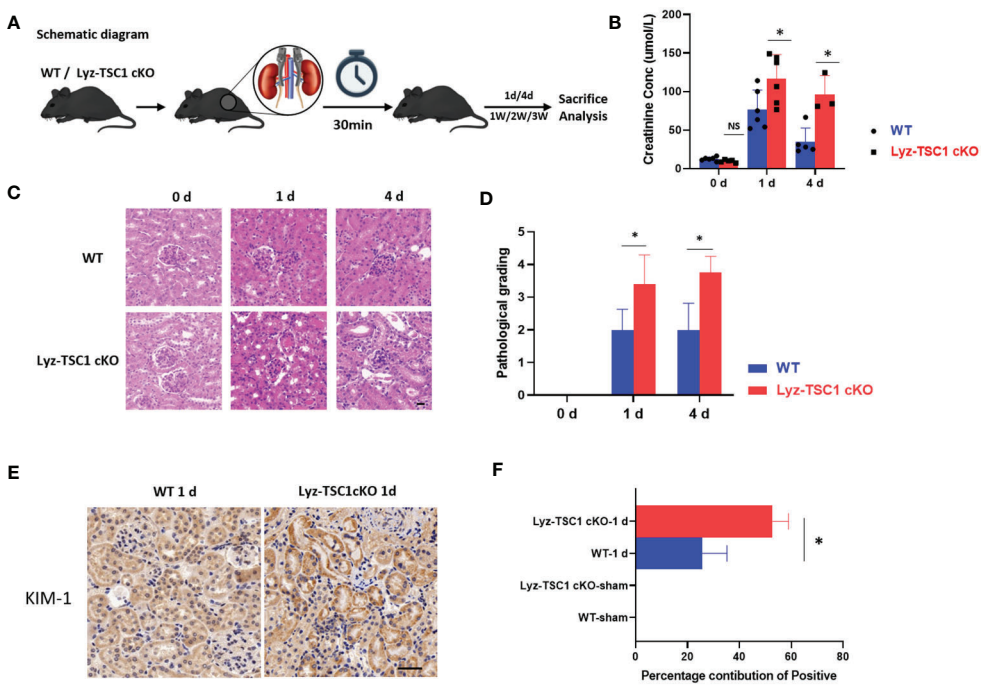


FIGURE 1 | *TSC1* depletion in macrophage aggravated mice IR-induced tubular injury. **(A)** Schematic diagram. **(B)** Serum creatinine levels in wild-type (WT) and Lyz-TSC1 cKO mice at baseline (0) and 1 and 4 days post-IRI. **(C)** Representative H&E-stained renal sections of WT and Lyz-TSC1 cKO mice. Scale bar: 20 μm. **(D)** Quantification of H&E staining corresponding to the WT and Lyz-TSC1 cKO mice shown in **(C)**. **(E)** Representative Kidney Injury Molecule 1 (KIM-1) immunohistochemistry in renal sections from WT and KO mice on day 1 post-IRI (×200). **(F)** Quantification of KIM-1 immunohistochemistry-stained murine renal cortical sections on day 0 and day 1 after IRI. In **(B**, **D**, **F)**, the data are shown as the mean ± SD and were analyzed by an unpaired two-tailed Student's t-test ($n \geq 3$). *$P < 0.05$; **$P < 0.01$; NS, not significant.

significantly higher than those of the wild-type mice, suggesting accentuation of tubular injury in the Lyz-TSC1 cKO mice (**Figure 1D**). Kidney injury molecule-1 (Kim-1) is an acute kidney injury (AKI) biomarker that is always upregulated during the early phase of IRI. In the sham-operated mice, the immunostaining of Kim-1 could not be detected in the kidney. However, the positively stained kidney area was significantly increased in the Lyz-TSC1 cKO mice compared to that in the WT kidneys (**Figures 1E, F**). These results indicate that the AKI induced by ischemia-reperfusion in the Lyz-TSC1 cKO mice is more severe than that in the control mice.

Renal interstitial cell infiltration after I/R mainly involves monocytes/macrophages and is a vital indicator of inflammation after IR injury (32). However, by conducting a flow cytometry analysis, we found that the levels of renal total leukocytes ($CD45^+$) in the WT and Lyz-TSC1 cKO mice were comparable before and 1 day after the ischemia-reperfusion operation (**Supplementary Figure 1A**, **Figure 2A**). Previous studies have shown that F4/$80^{low}CD11b^+$ cells are M1-like macrophages, while F4/$80^{high}CD11b^+$ cells are M2-like macrophages (33, 34). In our study, the ratios of F4/80^{high} macrophages and F4/80^{low} cells in the WT and Lyz-TSC1 cKO mice gated on $CD45^+$ were also comparable before and 1 day after reperfusion (**Supplementary Figure 1B**, **Figure 2B**). To evaluate the infiltration ability of TSC1 cKO macrophages, we labeled the WT and Lyz-TSC1 cKO mouse-derived BMDMs with CFSE and adoptively transferred them to WT recipients 2 h before kidney IRI (**Supplementary Figure 2A**). After 24 h of reperfusion, we obtained the kidneys to trail the transferred cells by flow cytometry. The data show that there was no statistically significant difference in the number of CFSE-labeled WT BMDMs and TSC1 cKO BMDMs that infiltrated the kidneys (**Supplementary Figures 2B, C**). These data indicate that the elevated renal IRI in the Lyz-TSC1 cKO mice was not caused by increased infiltration of inflammatory macrophages during the initial stage.

To ensure functional shifts of macrophages during the early stage of reperfusion, we sorted the kidney macrophages ($CD45^+F4/80^+CD11b^+$) in the WT and Lyz-TSC1 cKO mice 24 h after reperfusion and performed RNA sequencing. Although the pathways related to macrophage polarization were not obvious among the most enriched pathways of DEGs, most M1-related genes (*Tgfb1*, *Il6*, *Il1b*, *Il16*, *Il17c*, *Il18*, *Icam1*, *Ltb*, *Ccl2*, *Tnf*, *Tnfaip1*, *Tnfaip2*, *Tnfaip3*, *Tnfaip6*, and *Tnfaip8*) in the Lyz-TSC1 cKO group were upregulated compared to those in the WT group (**Figures 2C–E**) (35). To further verify these results, we performed a quantitative real-time PCR analysis of FACS-sorted macrophages from kidneys 24 h post-IRI. The results show that the macrophages sorted from the kidneys of the Lyz-TSC1 cKO

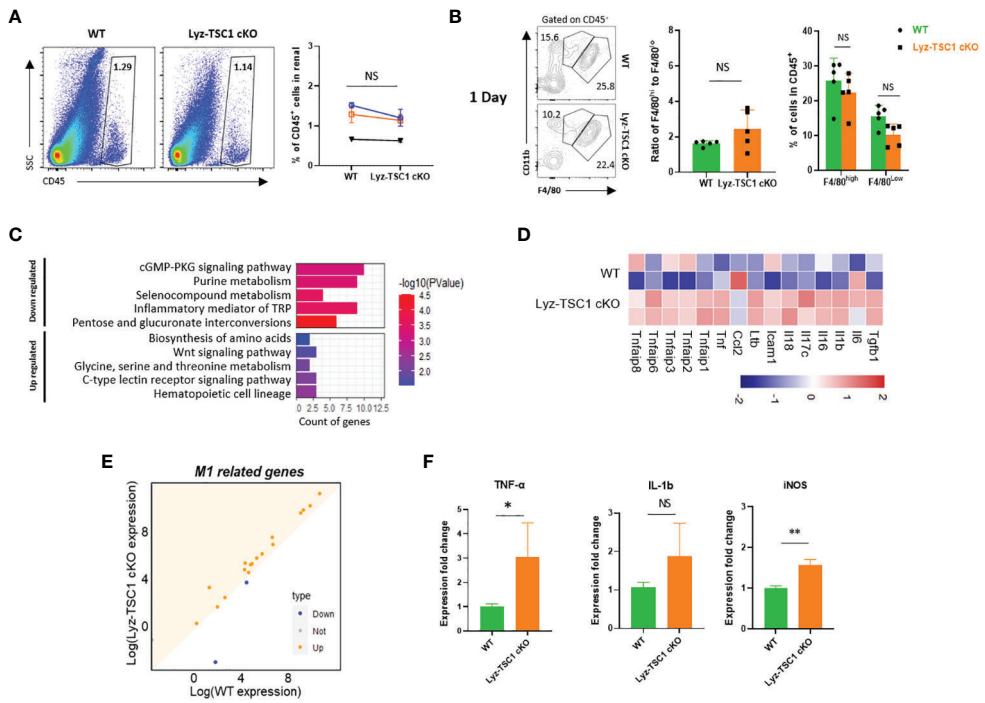


FIGURE 2 | Increased M1 polarization of *TSC1* knockout macrophages during the early phase. **(A)** Inflammatory cell infiltration and percentage of $CD45^+$ cells in WT and Lyz-TSC1 cKO kidneys on day 1 after reperfusion. **(B)** F4/80^{high} macrophages and F4/80^{low} macrophages from WT and Lyz-TSC1 cKO mice gated on $CD45^+$ cells. **(C)** Histogram of the top 10 most up- and downregulated KEGG pathways. **(D)** Dot plot of M1-related genes. The orange color represents the upregulated genes in the Lyz-TSC1 cKO macrophages. **(E)** Heatmap of up- and downregulated M1-related genes in the WT and Lyz-TSC1 cKO groups. **(F)** Relative mRNA expression of interleukin -1β (IL-1β), tumor necrosis factor-α (TNF-α), and iNOS in kidney macrophages sorted from WT and Lyz-TSC1 cKO mice 24 h after IRI. In **(A**, **B**, **F)**, the data are shown as the mean ± SD and were analyzed by an unpaired two-tailed Student's t-test (n ≥ 3). *P < 0.05; **P < 0.01; NS, not significant.

mice had increased expression of interleukin-1β (IL-1β), tumor necrosis factor-a (TNF-a), and iNOS, which are hallmarks of M1 polarization (**Figure 2F**) (34). These data demonstrate that *TSC1* deficiency promoted renal macrophage inflammatory M1 polarization to enhance inflammation and aggravate early tubular epithelial injury after ischemia-reperfusion during the early phase.

Conditional Depletion of *TSC1* in Macrophages Reduced Renal Fibrosis After IRI

We also explored the performance in the two groups during the late stage of renal ischemia-reperfusion. We performed Masson's trichrome staining to assess renal fibrosis 1, 2, and 3 weeks after reperfusion (**Figure 3A**). Interestingly, the Masson staining of the Lyz-TSC1 cKO group showed decreased collagen deposition compared to that in the WT group, especially at 2 weeks (**Figure 3B**). As fibrosis-related cytokines, we examined the transcription of transforming growth factor-β (TGF-β) and IL-10 in the kidneys 14 days after ischemia-reperfusion. Compared to the control littermates, much lower IL-10 levels were detected in the knockouts, while the level of TGF-β did not significantly differ between the two groups (**Figure 3C**). The positive area of Sirius Red was increased during this process, with a sharp increase at day 21 (**Figures 3D, E**). Collagens especially collagen III (COL 3), fibronectin (FN), alpha-SMA are metabolic balance-related genes and proteins of extracellular matrix (ECM) (36). Immunohistochemistry showed that Lyz-TSC1 CKO kidneys had a reduced deposition of collagen III, α-SMA, and fibronectin (FN), compared to WT kidneys (**Supplementary Figures 3A–F**). We also assessed the renal tubular injury scores of the two groups by H&E staining during the repair phase after IR (**Figure 3F**). The renal tubular damage score of the Lyz-TSC1 cKO mice tended to be slightly higher than that of

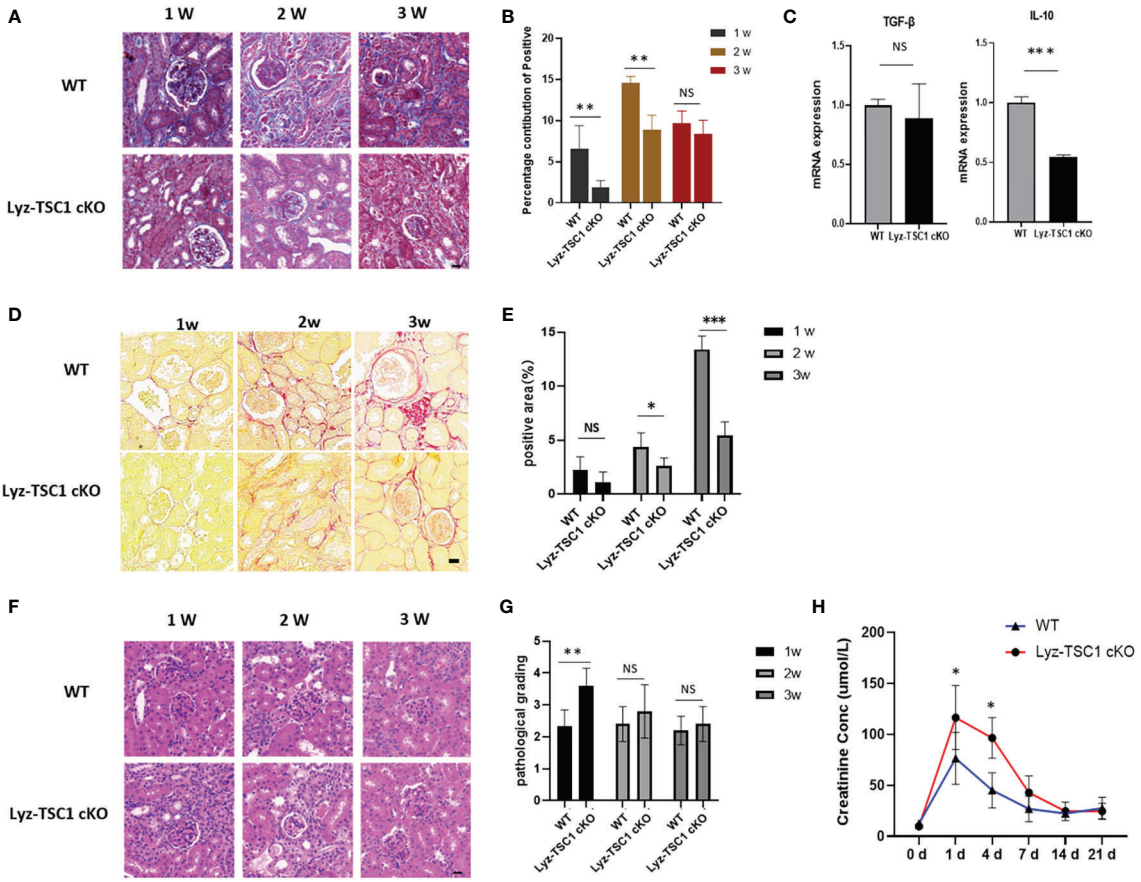


FIGURE 3 | Decreased renal fibrosis after IRI in Lyz-TSC1 cKO mice. **(A)** Representative images of Masson's trichrome staining of WT and Lyz-TSC1 cKO kidneys on days 7, 14, and 21 after reperfusion. Scale bar: 20 μm. **(B)** Quantification of Masson's trichrome staining corresponding to the WT and Lyz-TSC1 cKO mice shown in **(A)**. **(C)** Fibrosis-related cytokines (transforming growth factor-β [TGF-β] and IL-10) mRNA relative expression in kidneys from WT or Lyz-TSC1 cKO mice on day 14 after reperfusion. **(D)** Representative Sirius Red-stained renal sections of WT and Lyz-TSC1 cKO mice. Scale bar: 20 μm. **(E)** Quantification of Sirius Red staining corresponding to the WT and Lyz-TSC1 cKO mice shown in **(D)**. **(F)** Representative images of HE staining of WT and Lyz-TSC1 cKO kidneys on days 7, 14, and 21 after reperfusion. Scale bar: 20 μm. **(G)** Renal tubular injury scores of H&E staining corresponding to the WT and Lyz-TSC1 cKO mice shown in **(F)**. **(H)** Serum creatinine levels in WT and Lyz-TSC1 cKO mice on days 7, 14, and 21 after ischemia-reperfusion. In **(B**, **C**, **E**, **G**, **H)**, the data are shown as the mean ± SD and were analyzed by an unpaired two-tailed Student's t-test ($n \geq 3$). *$P < 0.05$; **$P < 0.01$; NS, not significant.

the wild-type mice during the initial stage of restoration, but the degree of damage between the two groups did not continue to deteriorate during the late phase (**Figure 3G**), and serum creatinine showed a similar trend (**Figure 3H**). The serum creatinine levels in the Lyz-TSC1 cKO mice were significantly higher 7 days post-IRI and then rapidly returned to levels comparable to those in the WT mice. These results suggest that the deletion of *TSC1* in macrophages reduces kidney fibrosis after IRI in mice and prevents further deterioration of tubular injury to a certain extent.

M2 Macrophages in the Kidneys of Lyz-TSC1 cKO Mice Are Significantly Reduced During the Ischemia-Reperfusion Repair Phase

Macrophages (especially the $CD206^+$ subset of M2 macrophages) are strongly associated with renal fibrosis and tubule repair in both human and experimental diseases (5, 21). Thus, we hypothesized that the depletion of *TSC1* in macrophages would reduce fibrosis because of the attenuated polarization to M2 after ischemia-reperfusion. To verify this hypothesis, we determined whether the $F4/80^{high}CD11b^+$ macrophages in the kidney from the Lyz-TSC1 cKO mice were decreased 7, 14, and 21 days after IRI. M2 macrophages (also termed alternatively activated) are anti-inflammatory and tend to promote injury repair and resolution of inflammation (3). The flow cytometry analysis showed that the Lyz-TSC1 cKO kidneys had significantly fewer $F4/80^{high}$ (M2-like macrophages) macrophages and a lower ratio of $F4/80^{high}$ to $F4/80^{low}$ gating on $CD45^+$ than the WT kidneys 7, 14, and 21 days after reperfusion (**Figures 4A–D**). Additionally, the levels of $F4/80^{high}$ macrophages and the ratio of $F4/80^{high}$ to $F4/80^{low}$ in the WT and Lyz-TSC1 cKO mice were comparable before ischemia-reperfusion injury (**Supplementary Figure 1B**). CD206 (also known as mannose receptor) is a marker of M2 macrophages that is expressed in not only monocyte-derived macrophages (MDMs) but also tissue macrophages (37). To further assess M2 macrophage expression in the kidneys, we stained the kidney tissues and performed immunofluorescence. We costained the kidney tissues with antibodies against F4/80 and CD206 to identify M2 macrophages 14 days after IR. The number of stained M2 macrophages in the kidneys from the knockout mice was significantly lower than that in the control littermates (**Figure 4E**). Immunohistochemistry further showed that Lyz-TSC1 cKO group had a reduced co-expressing of CD206 and α-SMA, compared to WT group 14 days after IR (**Figure 4F**). Also, we determined the difference in CD206 expression between the WT group and the Lyz-TSC1 cKO group by a flow cytometry analysis. The mean fluorescence intensity (MFI) of CD206 in the WT and Lyz-TSC1 cKO mice was comparable before ischemia-reperfusion injury (**Supplementary Figure 1C**). Notably, CD206 expression in the renal macrophages in the Lyz-TSC1 cKO groups 7, 14, and 21 days after reperfusion was significantly lower than that in the WT group (**Figures 4G, H**). These results indicate that the decreased renal fibrosis after IRI in the Lyz-TSC1 cKO mice may result from the attenuated M2 polarization of *TSC1* cKO renal macrophages.

The Defective Response of *TSC1* cKO Macrophages to CM Is Mediated by mTOR-C/EBPβ *In Vitro*

Tubular epithelial cells (TECs) play diverse roles in renal repair or progression to chronic kidney disease (CKD) by releasing bioactive mediators that drive fibrosis and are vulnerable to various injuries, especially hypoxia insult (38). We used an *in vitro* cell model that has been widely used to simulate renal IRI by harvesting the culture supernatant (termed conditioned medium, CM) from a mouse renal TEC cell line (mRTECs) after hypoxia-reoxygenation (H/R) injury (39–41). Bone marrow-derived macrophages (BMDMs) from WT and Lyz-TSC1 cKO mice were induced by M-CSF stimulation and then treated with CM for 48 h (**Figure 5A**). The treated BMDMs in each group were collected for a flow cytometry analysis. The data show that after the treatment with CM, the *TSC1* cKO BMDMs expressed significantly lower levels of CD206 than the WT BMDMs (**Figures 5B, C**). The transcriptional level of gene expression was also determined by real-time PCR. The hallmarks of M2 macrophages, including CD206 and Arginase-1 (Arg-1), showed significantly lower expression in the *TSC1* cKO macrophages. Moreover, the expression of C/EBPβ in the *TSC1* cKO BMDMs was significantly lower than that in the WT BMDMs (**Figure 5D**). The rapamycin treatment for 48 h markedly reversed the damaged C/EBPβ expression in the *TSC1* cKO macrophages (**Figure 5E**). These findings demonstrate that the decreased C/EBPβ expression in the *TSC1* cKO macrophages may also be induced by overactivated mTOR activity, which is consistent with our previous study (24).

The Decreased C/EBPβ Expression in the *TSC1* cKO Macrophages During the Repair Phase of IRI May Also Be Induced by Overactivated mTOR Activity

To further verify the conclusions drawn in the previous section, we sorted the WT and Lyz-TSC1 cKO mouse kidney macrophages ($CD45^+F4/80^+CD11b^+$) 2 weeks after reperfusion and performed RNA sequencing. According to previous reports, we summarized the previous enrichment of the KEGG pathway related to M2 polarization (**Figure 6A**). Accordingly, we enriched the related top 12 of the most up- and downregulated pathways by the differential mRNAs (**Figure 6B**). We further selected the gene set enrichment analysis (GSEA) results of the top M2 polarization-related items in **Supplementary Figure 4**, including the autophagy signaling pathway, NF-kb signaling pathway, PI3K-Akt signaling pathway, and Notch signaling pathway. However, regarding these pathways, the WT group showed a commonly lower enrichment score (ES) than the Lyz-TSC1 cKO group. By analyzing the data in the GEO database (GEO accession GSE107776), we found that during the M2 polarization process induced by IL-4, the expression of C/EBPβ was increased compared to that in the control group (**Figure 6C**), which is consistent with the results of the previous regulation of M2 polarization observed in our laboratory (24). Our sequencing data demonstrated that the expression of Raptor and Rictor, which are unique subunits in mTORC1 and mTORC2, respectively, was upregulated in the

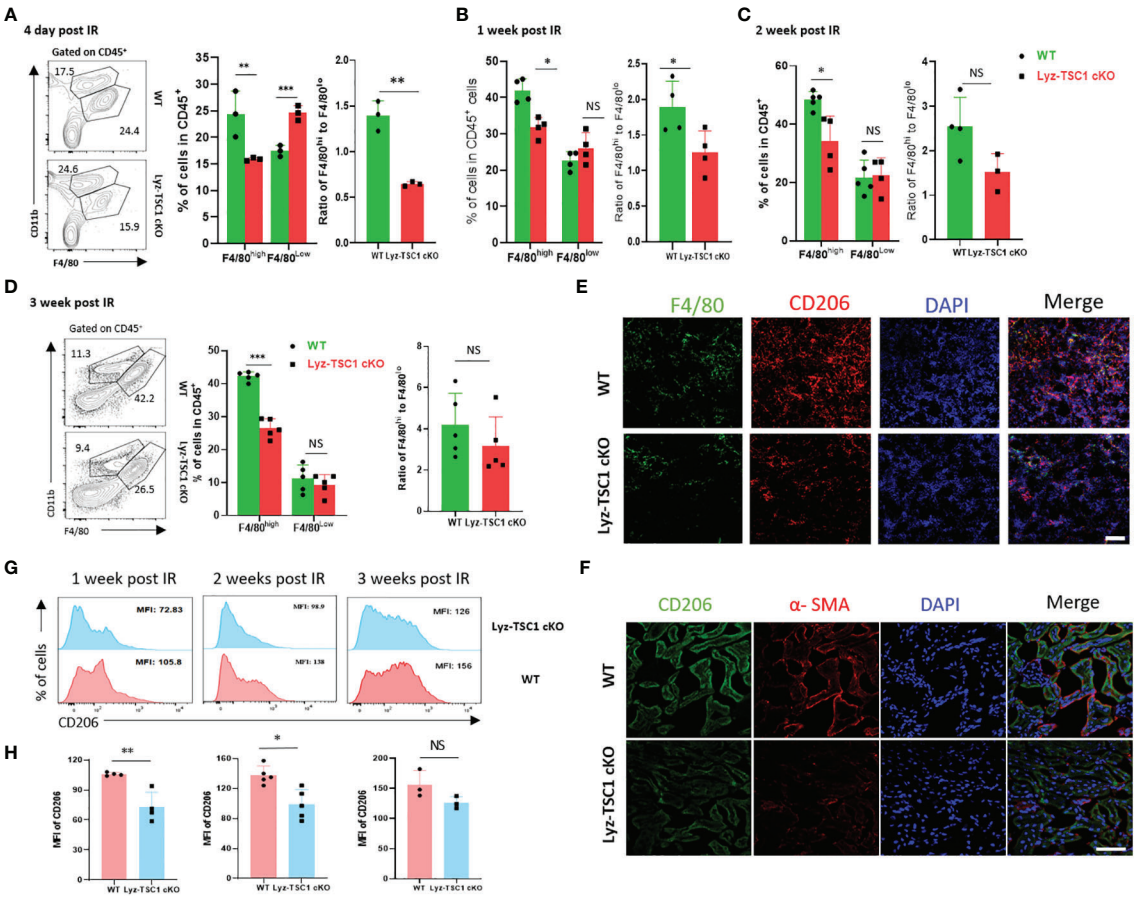


FIGURE 4 | Decreased M2 polarization in Lyz-TSC1 cKO macrophages during the repair process of renal ischemia-reperfusion. **(A–D)** Left panel: representative dot plots of the proportion of F4/80^{hi} and F4/80^{low} macrophage subsets in CD45^{+} cells in the WT and Lyz-TSC1 cKO kidneys. Middle panel: quantification of the proportion of F4/80^{hi} and F4/80^{low} macrophage subsets in CD45^{+} cells. Right panel: ratio of F4/80^{hi} and F4/80^{low} macrophage subsets. **(A)** Day 4 post-IRI. **(B)** Day 7 post-IRI. **(C)** Day 14 post-IRI. **(D)** Day 21 post-IRI. **(E)** M2 macrophages were double-positive for F4/80 (green) and CD206 (red) by immunofluorescence in the WT and Lyz-TSC1 cKO kidneys on day 14. Scale bar: 50 μm. **(F)** Kidney sections were subjected to immunofluorescence staining for CD206 and a-SMA. Scale bar: 50 μm. **(G, H)** CD206 mean fluorescence intensity (MFI) in macrophages in WT and Lyz-TSC1 cKO mice kidney were analyzed after ischemia-reperfusion injury on days 7, 14, and 21. Each dot represents an individual mouse. In **(A–D, G, H)**, the data are shown as the mean ± SD and were analyzed by an unpaired two-tailed Student's t-test (n ≥ 3). *P < 0.05; **P < 0.01; NS, not significant.

Lyz-TSC1 cKO group; The Lyz-TSC1 cKO group expressed lower levels of C/EBPβ than the WT group (**Figure 6D**). Larabee JL's study demonstrated that C/EBPβ binding was detected in the promoter of the IL-10 gene in macrophages, which is necessary for the induction of IL-10 (42). Our sequencing data confirmed that the expression of IL-10 was consistent with the expression of C/EBPβ in the two groups. Then, the WT and Lyz-TSC1 cKO mouse kidney macrophages (CD45^{+}F4/80^{+}CD11b^{+}) were sorted 2 weeks after reperfusion, and we performed real-time quantitative PCR. The macrophages from the Lyz-TSC1 cKO mouse group expressed decreased C/EBPβ, CD206, and IL-10, which is consistent with the sequencing data (**Figures 6D, E**). These data support our *in vitro* study and indicate that the M2 polarization deficiency of the TSC1KO renal macrophages after ischemia-reperfusion may also be mediated by the mTOR-C/EBPβ pathway.

DISCUSSION

We previously reported that TSC1 is an important regulator of M1 and M2 activation of macrophages (24). In this study, we found that during the early phase after renal ischemia-reperfusion, the elevated injury in the Lyz-TSC1 cKO mice was related to increased M1 polarization of *TSC1* cKO renal macrophages. We also demonstrated that during the repair process of renal IRI, the depletion of *TSC1* in macrophages decreased renal fibrosis by preventing M2 polarization. Collectively, TSC1 affects the overall process of ischemia-reperfusion by regulating the polarization of macrophages.

Our results show an aggravated trend of renal injury in Lyz-TSC1 cKO mice during the early stage after renal ischemia-reperfusion, including higher renal tubular injury scores, higher serum creatinine levels, and increased KIM-1 levels. We also

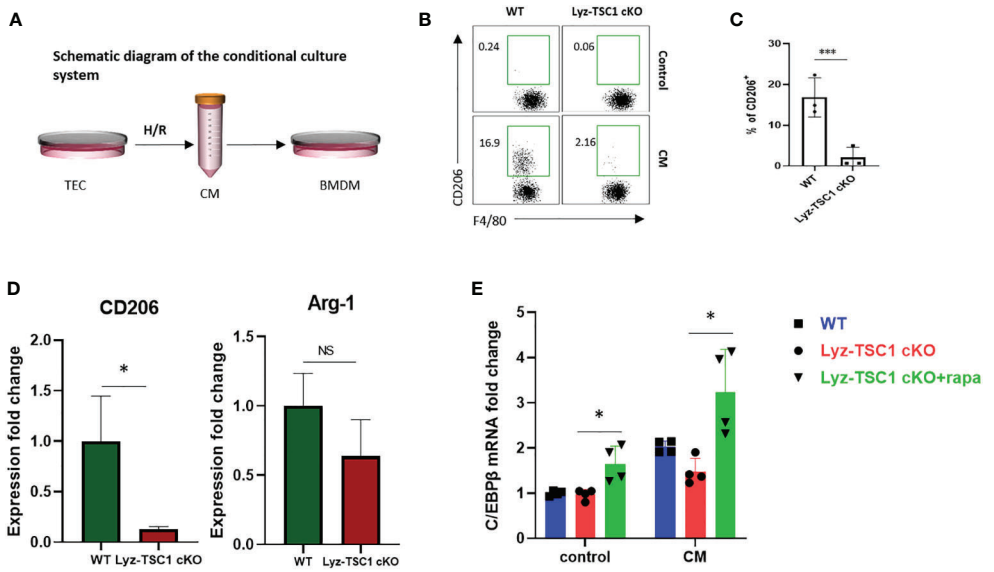


FIGURE 5 | Defective polarization to conditional medium of *TSC1* cKO macrophages is mediated by mTOR-C/EBPβ *in vitro*. **(A)** Experimental design of the BMDMs from the WT and Lyz-TSC1 cKO mice, which were treated with CM from mouse renal TECs (mRTECs) cell line after hypoxia-reoxygenation (H/R) injury. **(B)** Representative dot plots of the $CD206^+$ subset in the $F4/80^+$ compartment in the WT or *TSC1* cKO BMDMs treated with conditional medium. **(C)** Quantification of the proportion of the $CD206^+$ subset in $F4/80^+$ macrophages. **(D)** Relative expression of CD206 and Arginase-1 (Arg-1) in WT or *TSC1* cKO BMDMs treated with CM. **(E)** Lyz-tsc1 cKO BMDMs were pretreated with Rapa (100 nM) for 1 h and then stimulated with CM for an additional 48 h. C/EBPβ expression in WT, Lyz-TSC1 cKO, and Lyz-TSC1 cKO treated with Rapa as determined by quantitative PCR after treatment with or without CM. In **(C, D)**, the data are shown as the mean ± SD and were analyzed by an unpaired two-tailed Student's t-test ($n \geq 3$). *$P < 0.05$; **$P < 0.01$; NS, not significant.

found that elevated injury may be caused by increased M1 polarization in TSC1 knockout macrophages during the early phase rather than an increased number of infiltrated leukocytes or macrophages by RNA sequencing, flow cytometry analysis, adoptive transfer, and quantitative PCR. Our previous study and the work of others demonstrated that Lyz-TSC1 cKO mice exhibited an enhanced M1 response when treated with LPS *in vivo* or *in vitro* in an mTOR-independent or mTOR-dependent pathway (24, 43). LPS induces an acute endotoxin shock model, which is a type of septic shock (44). Therefore, we first proved that *TSC1* deficiency in macrophages may promote M1 polarization to enhance inflammation and aggravate early tubular epithelial injury after ischemia-reperfusion during the early phase of ischemia-reperfusion injury, i.e., sterile inflammation. However, whether mTOR is dependent in this study needs further exploration.

During the recovery and repair phase of postischemia/reperfusion injury, we found that the renal interstitial fibrotic and cellulosic area in the Lyz-TSC1 cKO mice was decreased compared with that in the WT group. M2 macrophages perform wound healing and play profibrotic roles during renal repair (21, 45). As mentioned above, macrophages (especially the $CD206^+$ subset of M2 macrophages) are strongly associated with renal fibrosis (5). Therefore, we hypothesized that the depletion of *TSC1* in macrophages would reduce fibrosis by blocking M2 polarization after ischemia-reperfusion. First, we verified that *TSC1* cKO macrophages are refractory to M2 polarization, which was confirmed by a flow cytometry analysis of M2-like macrophages (F4/80highCD11b+ cells) and CD206 expression 7, 14, and 21 days after reperfusion. The coimmunostaining of immunofluorescence with F4/80 and CD206 14 days after reperfusion also supported the above results. Reduced co-expressing of CD206 and α-SMA in Lyz-TSC1 cKO group suggests lower numbers of MMT cells and reduced fibrosis compared with WT group. Our previous study indicated that the reduced C/EBPβ expression in *TSC1* cKO macrophages is induced by overactivated mTOR activity and is involved in poor M2 polarization (24). Similar to the *in vivo* results, the *TSC1* cKO BMDMs demonstrated a decreased M2 polarization trend compared to the WT BMDMs after the treatment with CM *in vitro*, which is a cell model that has been widely used to study IRI (39–41). The expression of C/EBPβ in the *TSC1* cKO macrophages was significantly lower than that in the WT macrophages, while the Rapa treatment reversed the expression of C/EBPβ by *TSC1* cKO macrophages, which is consistent with previous reports. To verify this finding, kidney macrophages ($CD45^+F4/80^+CD11b^+$) from WT and Lyz-TSC1 cKO mice were sorted for RNA sequencing and real-time quantitative PCR 2 weeks after reperfusion. Both results demonstrated that the macrophages from the Lyz-TSC1 cKO mice also expressed decreased C/EBP-β.

A previous study found that the 38 kDa isoform of C/EBPβ is indispensable for the expression of IL-10 (42). Consistent with this observation, our study demonstrated that the expression of IL-10 in Lyz-TSC1 cKO kidney macrophages was reduced based on sequencing data and real-time quantitative PCR. As

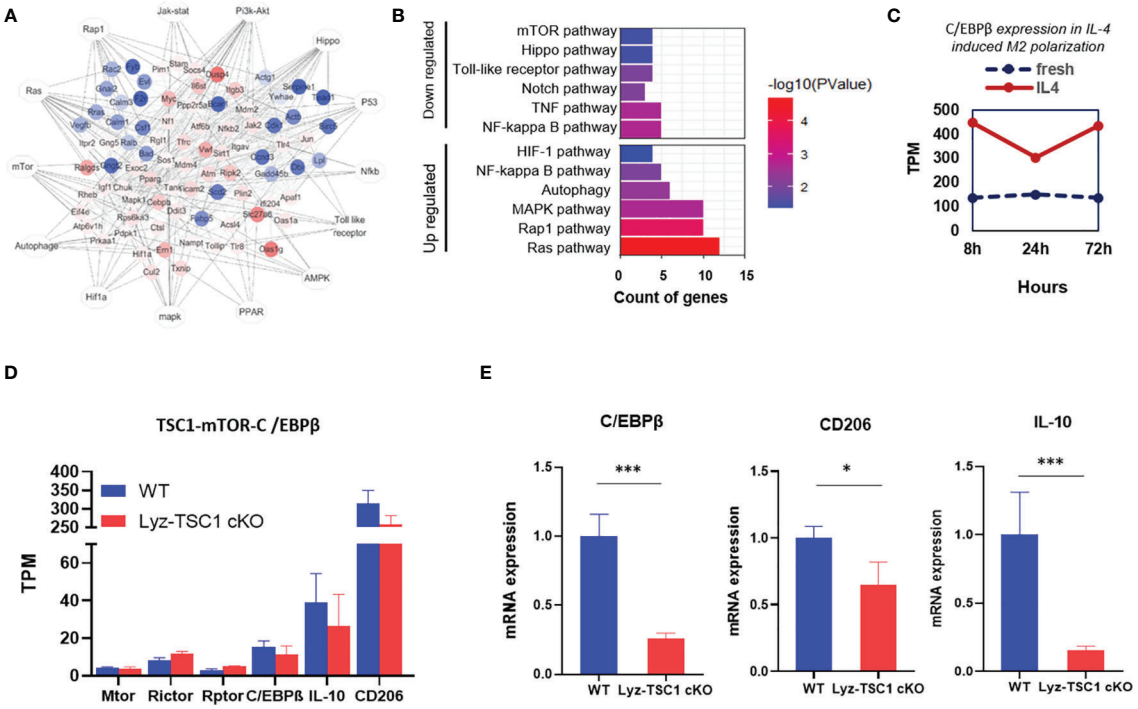


FIGURE 6 | Decreased C/EBPβ expression in *TSC1* cKO renal macrophages during the repair phase of IRI may also be induced by overactivated mTOR activity. **(A)** Network summary of previous enrichment of the KEGG pathway related to M2 polarization. **(B)** Top 12 most up- and downregulated pathways by differential mRNA. **(C)** C/EBPβ expression with or without IL-4 induced M2 polarization in the downloaded data. **(D)** TPM value of mTOR, Rictor, Raptor, C/EBPβ, and IL-10 in macrophages from WT or Lyz-TSC1 cKO mouse kidneys 2 weeks after ischemia-reperfusion. **(E)** Relative expression of C/EBPβ, CD206, and IL-10 in kidney macrophages sorted from WT and Lyz-TSC1 cKO mice on day 14 post-IRI. In **(E)**, the data are shown as the mean ± SD and were analyzed by an unpaired two-tailed Student's t-test (n ≥ 3). *P < 0.05; **P < 0.01; NS, not significant.

previously noted, long-term IL-10 exposure or IL-10 application to chronic disease processes may promote fibrotic results (12, 13, 46, 47). Therefore, these findings may indicate that C/EBPβ has multiple regulatory effects on renal fibrosis during the recovery and repair phases. On the one hand, decreased C/EBPβ expression in *TSC1* cKO macrophages is involved in poor M2 polarization, which is strongly associated with renal fibrosis. On the other hand, a decrease in IL-10 may lead to weakened subsequent tubule interstitial fibrosis by reducing C/EBPβ expression. In addition, studies have shown that the chronic fibrogenic process is detrimental to the nephron and surrounding vasculature (48–50), which might explain why the Lyz-TSC1 cKO mice showed aggravated kidney dysfunction (tubular damage and serum creatinine) after reperfusion during the early phase; however, surprisingly, during renal repair, kidney dysfunction did not continue to deteriorate, and no significant difference was observed between the groups. Besides, we did not conduct *in vivo* experiments using Rapa to reverse the fibrosis reduction because under pathological conditions, the mTOR activities of numerous fibroblasts in mouse kidneys are also upregulated (51, 52). Therefore, the combined effects of Rapa on overall fibrosis of the kidney are mostly considered to have an improved effect (53, 54). Guochun Chen's study demonstrated that Rapa ameliorates kidney fibrosis by inhibiting the activation of mTOR signaling in interstitial macrophages (55). However, this conclusion is based on a report suggesting that inflammatory cell infiltration is an early feature of renal fibrosis in almost all cases (56); thus, the role of macrophage subpopulations was not considered because macrophages exhibit completely different phenotypes during kidney injury and repair.

In summary, this study demonstrates that *TSC1* deficiency in macrophages may promote M1 polarization to aggravate kidney dysfunction after ischemia-reperfusion during the early phase, while during the repair process of ischemia-reperfusion, *TSC1* deficiency reduced M2 macrophage polarization, leading to decreased renal fibrosis. The findings presented in this study provide new insight into therapeutic targeting in sterile renal injury and kidney fibrosis during the transition from AKI to CKD.

DATA AVAILABILITY STATEMENT

The datasets presented in this study can be found in online repositories. The names of the repository/repositories and accession number(s) can be found below: http://www.ncbi.nlm.nih.gov, PRJNA679157.

ETHICS STATEMENT

The animal study was reviewed and approved by the research ethics committee (IRB: [2020]02-166) at the third affiliated Hospital of Sun Yat-sen University.

AUTHOR CONTRIBUTIONS

NN and YZ conceived the project. XH, YX, ZZ, ZT, JZ, YL, WD, and ZD designed the experiments. XH and YX conducted the experiments. ZZ performed the sequencing and statistical analyses. XH, YX, and ZZ wrote the manuscript. All authors contributed to the article and approved the submitted version.

FUNDING

This research was supported by the National Natural Science Foundation of China (No. 81970652 and No. 81470977), the Natural Science Foundation of Guangdong Province (No. 2019A1515011219), the Bioengineering Research Center Training Project of the Third Affiliated Hospital of Sun Yat-sen University (SW201904), and the Science and Technology Planning Project of Guangzhou (No. 201803010016).

ACKNOWLEDGMENTS

We gratefully acknowledge Qing Meng (State Key Laboratory of Membrane Biology, Institute of Zoology, Chinese Academy of Sciences, Beijing, China) for assistance with cell sorting. We thank Dr. Hongbin Zhang (Institute of Basic Medical Sciences and School of Basic Medicine, Peking Union Medical College and Chinese Academy of Medical Sciences, Beijing, China) for kindly providing the TSC1 loxp/loxp mice. The LysMCre mice were generous gifts from Dr. Lianfeng Zhang (Key Laboratory of Human Diseases Comparative Medicine, Ministry of Health).

SUPPLEMENTARY MATERIAL

The Supplementary Material for this article can be found online at: https://www.frontiersin.org/articles/10.3389/fimmu.2021.637335/full#supplementary-material

REFERENCES

1. Tammaro A, Kers J, Scantlebery AML, Florquin S. Metabolic flexibility and innate immunity in renal ischemia reperfusion injury: The fine balance between adaptive repair and tissue degeneration. *Front Immunol* (2020) 11:1346. doi: 10.3389/fimmu.2020.01346
2. Kezić A, Stajic N, Thaiss F. Innate immune response in kidney ischemia/reperfusion injury: Potential target for therapy. *J Immunol Res* (2017) 2017:6305439. doi: 10.1155/2017/6305439
3. Huen SC, Cantley LG. Macrophages in renal injury and repair. *Annu Rev Physiol* (2017) 79:449–69. doi: 10.1146/annurev-physiol-022516-034219
4. De Greef KE, Ysebaert DK, Dauwe S, Persy V, Vercauteren SR, Mey D, et al. Anti-b7-1 blocks mononuclear cell adherence in vasa recta after ischemia. *Kidney Int* (2001) 60:1415–27. doi: 10.1046/j.1523-1755.2001.00944.x
5. Tang PM-K, Nikolic-Paterson DJ, Lan H-Y. Macrophages: Versatile players in renal inflammation and fibrosis. *Nat Rev Nephrol* (2019) 15:144–58. doi: 10.1038/s41581-019-0110-2
6. Nikolic-Paterson DJ, Wang S, Lan HY. Macrophages promote renal fibrosis through direct and indirect mechanisms. *Kidney Int Suppl (2011)* (2014) 4:34–8. doi: 10.1038/kisup.2014.7
7. Wang S, Meng X-M, Ng Y-Y, Ma FY, Zhou S, Zhang Y, et al. Tgf-β/smad3 signalling regulates the transition of bone marrow-derived macrophages into myofibroblasts during tissue fibrosis. *Oncotarget* (2016) 7:8809–22. doi: 10.18632/oncotarget.6604
8. Klingberg F, Hinz B, White ES. The myofibroblast matrix: Implications for tissue repair and fibrosis. *J Pathol* (2013) 229:298–309. doi: 10.1002/path.4104
9. Meng XM, Wang S, Huang XR, Yang C, Xiao J, Zhang Y, et al. Inflammatory macrophages can transdifferentiate into myofibroblasts during renal fibrosis. *Cell Death Dis* (2016) 7:e2495. doi: 10.1038/cddis.2016.402
10. Wynn TA, Vannella KM. Macrophages in tissue repair, regeneration, and fibrosis. *Immunity* (2016) 44:450–62. doi: 10.1016/j.immuni.2016.02.015
11. Meng XM, Nikolic-Paterson DJ, Lan HY. Tgf-β: The master regulator of fibrosis. *Nat Rev Nephrol* (2016) 12:325–38. doi: 10.1038/nrneph.2016.48
12. Steen EH, Wang X, Balaji S, Butte MJ, Bollyky PL, Keswani SG. The role of the anti-inflammatory cytokine interleukin-10 in tissue fibrosis. *Adv Wound Care (New Rochelle)* (2020) 9:184–98. doi: 10.1089/wound.2019.1032
13. Barbarin V, Arras M, Misson P, Delos M, McGarry B, Phan SH, et al. Characterization of the effect of interleukin-10 on silica-induced lung fibrosis in mice. *Am J Respir Cell Mol Biol* (2004) 31:78–85. doi: 10.1165/rcmb.2003-0299OC
14. Murray PJ, Wynn TA. Protective and pathogenic functions of macrophage subsets. *Nat Rev Immunol* (2011) 11:723–37. doi: 10.1038/nri3073
15. Mosser DM, Edwards JP. Exploring the full spectrum of macrophage activation. *Nat Rev Immunol* (2008) 8:958–69. doi: 10.1038/nri2448
16. Van Dyken SJ, Locksley RM. Interleukin-4- and interleukin-13-mediated alternatively activated macrophages: Roles in homeostasis and disease. *Annu Rev Immunol* (2013) 31:317–43. doi: 10.1146/annurev-immunol-032712-095906
17. Zhang M-Z, Yao B, Yang S, Jiang L, Wang S, Fan X, et al. Csf-1 signaling mediates recovery from acute kidney injury. *J Clin Invest* (2012) 122:4519–32. doi: 10.1172/JCI60363
18. Wang Y, Chang J, Yao B, Niu A, Kelly E, Breeggemann MC, et al. Proximal tubule-derived colony stimulating factor-1 mediates polarization of renal macrophages and dendritic cells, and recovery in acute kidney injury. *Kidney Int* (2015) 88:1274–82. doi: 10.1038/ki.2015.295
19. Huen SC, Huynh L, Marlier A, Lee Y, Moeckel GW, Cantley LG. Gm-csf promotes macrophage alternative activation after renal ischemia/reperfusion injury. *J Am Soc Nephrol* (2015) 26:1334–45. doi: 10.1681/ASN.2014060612
20. Baek J-H, Zeng R, Weinmann-Menke J, Valerius MT, Wada Y, Ajay AK, et al. Il-34 mediates acute kidney injury and worsens subsequent chronic kidney disease. *J Clin Invest* (2015) 125:3198–214. doi: 10.1172/JCI81166
21. Lee S, Huen S, Nishio H, Nishio S, Lee HK, Choi B-S, et al. Distinct macrophage phenotypes contribute to kidney injury and repair. *J Am Soc Nephrol* (2011) 22:317–26. doi: 10.1681/ASN.2009060615
22. Dibble CC, Elis W, Menon S, Qin W, Klekota J, Asara JM, et al. Tbc1d7 is a third subunit of the tsc1-tsc2 complex upstream of mtorc1. *Mol Cell* (2012) 47:535–46. doi: 10.1016/j.molcel.2012.06.009
23. Saxton RA, Sabatini DM. Mtor signaling in growth, metabolism, and disease. *Cell* (2017) 168:960–76. doi: 10.1016/j.cell.2017.02.004
24. Zhu L, Yang T, Li L, Sun L, Hou Y, Hu X, et al. Tsc1 controls macrophage polarization to prevent inflammatory disease. *Nat Commun* (2014) 5:4696. doi: 10.1038/ncomms5696
25. Goto J, Talos DM, Klein P, Qin W, Chekaluk YI, Anderl S, et al. Regulable neural progenitor-specific tsc1 loss yields giant cells with organellar dysfunction in a model of tuberous sclerosis complex. *Proc Natl Acad Sci USA* (2011) 108:E1070–E79. doi: 10.1073/pnas.1106454108

26. Zhang H, Cicchetti G, Onda H, Koon HB, Asrican K, Bajraszewski N, et al. Loss of tsc1/tsc2 activates mtor and disrupts pi3k-akt signaling through downregulation of pdgfr. *J Clin Invest* (2003) 112:1223–33. doi: 10.1172/JCI17222
27. Clausen BE, Burkhardt C, Reith W, Renkawitz R, Förster I. Conditional gene targeting in macrophages and granulocytes using lysmcre mice. *Transgenic Res* (1999) 8:265–77. doi: 10.1023/a:1008942828960
28. Jablonski P, Howden BO, Rae DA, Birrell CS, Marshall VC, Tange J. An experimental model for assessment of renal recovery from warm ischemia. *Transplantation* (1983) 35:198–204. doi: 10.1097/00007890-198303000-00002
29. Pertea M, Kim D, Pertea GM, Leek JT, Salzberg SL. Transcript-level expression analysis of rna-seq experiments with hisat, stringtie and ballgown. *Nat Protoc* (2016) 11:1650–67. doi: 10.1038/nprot.2016.095
30. Love MI, Huber W, Anders S. Moderated estimation of fold change and dispersion for rna-seq data with deseq2. *Genome Biol* (2014) 15:550. doi: 10.1186/s13059-014-0550-8
31. Shannon P, Markiel A, Ozier O, Baliga NS, Wang JT, Ramage D, et al. Cytoscape: A software environment for integrated models of biomolecular interaction networks. *Genome Res* (2003) 13:2498–504. doi: 10.1101/gr.1239303
32. Ysebaert DK, De Greef KE, Vercauteren SR, Verhulst A, Kockx M, Verpooten GA, et al. Effect of immunosuppression on damage, leukocyte infiltration, and regeneration after severe warm ischemia/reperfusion renal injury. *Kidney Int* (2003) 64:864–73. doi: 10.1046/j.1523-1755.2003.00150.x
33. Peng Q, Wu W, Wu K-Y, Cao B, Qiang C, Li K, et al. The c5a/c5ar1 axis promotes progression of renal tubulointerstitial fibrosis in a mouse model of renal ischemia/reperfusion injury. *Kidney Int* (2019) 96:117–28. doi: 10.1016/j.kint.2019.01.039
34. Cieslewicz M, Tang J, Yu JL, Cao H, Zavaljevski M, Motoyama K, et al. Targeted delivery of proapoptotic peptides to tumor-associated macrophages improves survival. *Proc Natl Acad Sci USA* (2013) 110:15919–24. doi: 10.1073/pnas.1312197110
35. Murray PJ. Macrophage polarization. *Annu Rev Physiol* (2017) 79:541–66. doi: 10.1146/annurev-physiol-022516-034339
36. Xin Y, Xu P, Wang X, Chen Y, Zhang Z, Zhang Y. Human foreskin-derived dermal stem/progenitor cell-conditioned medium combined with hyaluronic acid promotes extracellular matrix regeneration in diabetic wounds. *Stem Cell Res Ther* (2021) 12:49. doi: 10.1186/s13287-020-02116-5
37. Arce-Mendoza A, Rodriguez-de Ita J, Salinas-Carmona MC, Rosas-Taraco AG. Expression of cd64, cd206, and rage in adherent cells of diabetic patients infected with mycobacterium tuberculosis. *Arch Med Res* (2008) 39:306–11. doi: 10.1016/j.arcmed.2007.11.013
38. Liu B-C, Tang T-T, Lv L-L, Lan H-Y. Renal tubule injury: A driving force toward chronic kidney disease. *Kidney Int* (2018) 93:568–79. doi: 10.1016/j.kint.2017.09.033
39. Kaul DK, Hebbel RP. Hypoxia/reoxygenation causes inflammatory response in transgenic sickle mice but not in normal mice. *J Clin Invest* (2000) 106:411–20. doi: 10.1172/JCI9225
40. Yeh C-H, Hsu S-P, Yang C-C, Chien C-T, Wang N-P. Hypoxic preconditioning reinforces hif-alpha-dependent hsp70 signaling to reduce ischemic renal failure-induced renal tubular apoptosis and autophagy. *Life Sci* (2010) 86:115–23. doi: 10.1016/j.lfs.2009.11.022
41. Yang J-R, Yao F-H, Zhang J-G, Ji Z-Y, Li K-L, Zhan J, et al. Ischemia-reperfusion induces renal tubule pyroptosis via the chop-caspase-11 pathway. *Am J Physiol Renal Physiol* (2014) 306:F75–84. doi: 10.1152/ajprenal.00117.2013
42. Larabee JL, Hauck G, Ballard JD. Unique, intersecting, and overlapping roles of c/ebp β and creb in cells of the innate immune system. *Sci Rep* (2018) 8:16931. doi: 10.1038/s41598-018-35184-y
43. Byles V, Covarrubias AJ, Ben-Sahra I, Lamming DW, Sabatini DM, Manning BD, et al. The tsc-mtor pathway regulates macrophage polarization. *Nat Commun* (2013) 4:2834. doi: 10.1038/ncomms3834
44. Hsiao H-B, Wu J-B, Lin H, Lin W-C. Kinsenoside isolated from anoectochilus formosanus suppresses lps-stimulated inflammatory reactions in macrophages and endotoxin shock in mice. *Shock* (2011) 35:184–90. doi: 10.1097/SHK.0b013e3181f0e7a3
45. Meng XM, Tang PM, Li J, Lan HY. Macrophage phenotype in kidney injury and repair. *Kidney Dis (Basel)* (2015) 1:138–46. doi: 10.1159/000431214
46. Kim M-G, Kim SC, Ko YS, Lee HY, Jo S-K, Cho W. The role of m2 macrophages in the progression of chronic kidney disease following acute kidney injury. *PloS One* (2015) 10:e0143961. doi: 10.1371/journal.pone.0143961
47. Sun L, Louie MC, Vannella KM, Wilke CA, LeVine AM, Moore BB, et al. New concepts of il-10-induced lung fibrosis: Fibrocyte recruitment and m2 activation in a ccl2/ccr2 axis. *Am J Physiol Lung Cell Mol Physiol* (2011) 300:L341–L53. doi: 10.1152/ajplung.00122.2010
48. Duffield JS. Cellular and molecular mechanisms in kidney fibrosis. *J Clin Invest* (2014) 124:2299–306. doi: 10.1172/JCI72267
49. Chen Y-T, Chang F-C, Wu C-F, Chou Y-H, Hsu H-L, Chiang W-C, et al. Platelet-derived growth factor receptor signaling activates pericyte-myofibroblast transition in obstructive and post-ischemic kidney fibrosis. *Kidney Int* (2011) 80:1170–81. doi: 10.1038/ki.2011.208
50. Lin S-L, Chang F-C, Schrimpf C, Chen Y-T, Wu C-F, Wu V-C, et al. Targeting endothelium-pericyte cross talk by inhibiting vegf receptor signaling attenuates kidney microvascular rarefaction and fibrosis. *Am J Pathol* (2011) 178:911–23. doi: 10.1016/j.ajpath.2010.10.012
51. Winbanks CE, Grimwood L, Gasser A, Darby IA, Hewitson TD, Becker GJ. Role of the phosphatidylinositol 3-kinase and mtor pathways in the regulation of renal fibroblast function and differentiation. *Int J Biochem Cell Biol* (2007) 39:206–19. doi: 10.1016/j.biocel.2006.08.004
52. Shegogue D, Trojanowska M. Mammalian target of rapamycin positively regulates collagen type i production via a phosphatidylinositol 3-kinase-independent pathway. *J Biol Chem* (2004) 279:23166–75. doi: 10.1074/jbc.M401238200
53. Huber TB, Walz G, Kuehn EW. Mtor and rapamycin in the kidney: Signaling and therapeutic implications beyond immunosuppression. *Kidney Int* (2011) 79:502–11. doi: 10.1038/ki.2010.457
54. Wu MJ, Wen MC, Chiu YT, Chiou YY, Shu KH, Tang MJ. Rapamycin attenuates unilateral ureteral obstruction-induced renal fibrosis. *Kidney Int* (2006) 69:2029–36. doi: 10.1038/sj.ki.5000161
55. Chen G, Chen H, Wang C, Peng Y, Sun L, Liu H, et al. Rapamycin ameliorates kidney fibrosis by inhibiting the activation of mtor signaling in interstitial macrophages and myofibroblasts. *PloS One* (2012) 7:e33626. doi: 10.1371/journal.pone.0033626
56. Strutz F, Zeisberg M. Renal fibroblasts and myofibroblasts in chronic kidney disease. *J Am Soc Nephrol* (2006) 17:2992–8. doi: 10.1681/asn.2006050420

Conflict of Interest: The authors declare that the research was conducted in the absence of any commercial or financial relationships that could be construed as potential conflicts of interest.

Copyright © 2021 Hu, Xu, Zhang, Tang, Zhang, Luo, Deng, Dong, Zhao and Na. This is an open-access article distributed under the terms of the Creative Commons Attribution License (CC BY). The use, distribution or reproduction in other forums is permitted, provided the original author(s) and the copyright owner(s) are credited and that the original publication in this journal is cited, in accordance with accepted academic practice. No use, distribution or reproduction is permitted which does not comply with these terms.

frontiers in Immunology

ORIGINAL RESEARCH
published: 14 April 2021
doi: 10.3389/fimmu.2021.645100

Hydroxychloroquine Inhibits Macrophage Activation and Attenuates Renal Fibrosis After Ischemia-Reperfusion Injury

*Haofeng Zheng†, Yannan Zhang†, Jiannan He†, Zhe Yang, Rui Zhang, Lei Li, Zihuan Luo, Yongrong Ye and Qiquan Sun**

Organ Transplantation Research Institute of Sun Yat-sen University, The Third Affiliated Hospital of Sun Yat-sen University, Guangzhou, China

Chronic kidney disease (CKD), which is associated with high morbidity, remains a worldwide health concern, while effective therapies remain limited. Hydroxychloroquine (HCQ), which mainly targets toll-like receptor-7 (TLR-7) and TLR-9, is associated with a lower risk of incident CKD. Taking into account that TLR-9 is involved in the development of renal fibrosis and serves as a potential therapy target for CKD, we investigated whether HCQ could attenuate CKD *via* TLR-9 signal pathway. The effects of HCQ on renal tubulointerstitial fibrosis were further explored using a mouse model of renal tubulointerstitial fibrosis after ischemia/reperfusion injury. Bone marrow-derived macrophages were isolated to explore the effects of HCQ *in vitro*. Judicious use of HCQ efficiently inhibited the activation of macrophages and MAPK signaling pathways, thereby attenuating renal fibrosis *in vivo*. In an *in vitro* model, results showed that HCQ promoted apoptosis of macrophages and inhibited activation of macrophages, especially M2 macrophages, in a dose-dependent manner. Because TLR-7 is not involved in the development of CKD post-injury, a TLR-9 knockout mouse was used to explore the mechanisms of HCQ. The effects of HCQ on renal fibrosis and macrophages decreased after depletion of TLR-9 *in vivo* and *in vitro*. Taken together, this study indicated that proper use of HCQ could be a new strategy for anti-fibrotic therapy and that TLR-9 could be a potential therapeutic target for CKD following acute kidney injury.

Keywords: hydroxychloroquine, chronic kidney disease, fibrosis, macrophage, inflammation

OPEN ACCESS

Edited by:
Cheng Yang,
Fudan University, China

Reviewed by:
Ruiming Rong,
Fudan University, China
Hu Linkun,
Soochow University, China

***Correspondence:**
Qiquan Sun
sunqiq@mail.sysu.edu.cn

†These authors have contributed equally to this work

Specialty section:
This article was submitted to Molecular Innate Immunity, a section of the journal Frontiers in Immunology

Received: *22 December 2020*
Accepted: *19 March 2021*
Published: *14 April 2021*

Citation:
Zheng H, Zhang Y, He J, Yang Z, Zhang R, Li L, Luo Z, Ye Y and Sun Q (2021) Hydroxychloroquine Inhibits Macrophage Activation and Attenuates Renal Fibrosis After Ischemia-Reperfusion Injury. Front. Immunol. 12:645100. doi: 10.3389/fimmu.2021.645100

INTRODUCTION

Acute kidney injury (AKI) is a worldwide health problem, and approximately two million deaths occur due to AKI. The incidence of AKI is rising, and patients with severe AKI have a mortality rate of >50% (1, 2). AKI is considered to represent not only acute injury, but also influences recovery from injury. Approximately 13% hospitalized patients experience AKI annually in the US; moreover, around 10% individuals worldwide develop chronic kidney disease (CKD) and end-stage renal disease consequent to AKI (3, 4). Till date, detailed mechanisms underlying the

progression of AKI to CKD are poorly understood, and effective treatments for renal tubulointerstitial fibrosis following AKI are limited. Hence, novel approaches that attenuate renal tubulointerstitial fibrosis are urgently needed (5).

Hydroxychloroquine (HCQ), which was used initially as an antimalarial drug, was found to have beneficial effects on several immune diseases (6). The effects of HCQ, which include inhibition of lysosomal activity, inhibition of toll-like pattern recognition receptors (TLRs), and inhibition of RIG-I–stimulated induction of interferons, are multifaceted. Recently, HCQ was confirmed to be associated with a lower risk of incident CKD in users compared to non-users in patients with rheumatoid arthritis; however, little is known about the role of HCQ in renal tubulointerstitial fibrosis (7, 8). Although it seems that the use of HCQ is associated with benefits in some renal diseases, the mechanisms of HCQ need to be further explored (9–11).

TLRs, which serve as targets of HCQ, are pivotal components of the innate immune response and are expressed by macrophages and other immune cells (12). Although the mechanisms of action of HCQ in diseases are complex, the most important molecular targets of HCQ are TLRs. HCQ can inhibit the expression of TLR-7 and TLR-9, thereby contributing to the regulation of inflammatory responses. Recently, we found that depletion of TLR-9 could attenuate renal tubulointerstitial fibrosis; however, whether HCQ could serve as a TLR-9 inhibitor and attenuate CKD still remains to be elucidated (13).

To resolve the unsolved puzzle regarding the role of HCQ in renal tubulointerstitial fibrosis, in this study we utilized a traditional rodent model of renal tubulointerstitial fibrosis to further explore the biological effects of HCQ, especially on macrophages. A series of *in vivo* and *in vitro* assays were performed to explore the relationships among HCQ, macrophages, and renal fibrosis. A TLR-9 knockout (KO) mouse was constructed to further elucidate the underlying mechanisms of HCQ in CKD development following ischemia-reperfusion injury (IRI). Our results suggest that HCQ inhibits macrophage activation and MAPKs *via* the TLR-9 pathway, thereby attenuating renal fibrosis after IRI.

MATERIALS AND METHODS

Animals and Ethics Statement

This study was performed in accordance with the animal welfare guidelines laid down in China (Laboratory Animal Guidelines for Ethical Review of Animal Welfare, GB/T 35892-2018) and approved by the Institutional Animal Care and Use Committee of Sun Yat-Sen University. Wildtype (WT) C57BL/6J mice were obtained from Charles River Laboratories (Beijing, China) and TLR-9 deficient (TLR-9$^{-/-}$) mice with a C57BL/6J congenic background were provided by S.G. Wan (Gannan Medical University). Only male mice aged 6 to 8 weeks were used in subsequent experiments. Sources and confirmation of TLR-9 KO mice are provided in Supplementary Materials (Detailed methods and **Figure S1**).

Induction of IRI in Mice

IRI was induced in male mice using an established method (13, 14). Mice were randomized placed either in an IRI or sham group (details of the number of mice per group can be found in the related paragraph). The bilateral IRI (bIRI) model was used for the IRI group. Mice were euthanized using isoflurane before surgery or on days 1, 7, 14, 21, or 28 post-surgery. Renal and blood samples were harvested for subsequent analyses. For HCQ (S4430, Selleck) treatment, HCQ was dissolved in carboxymethyl cellulose (CMC) and gavages were performed 30 min after induction of IRI for 7 days. The concentrations of HCQ used for treatment were 5, 10, and 20 mg/kg/day. The effects of 5 mg/kg/day HCQ were not significant, and no significant difference was found between 10 mg/kg/day HCQ and 20 mg/kg/day HCQ; hence, a final concentration of 10 mg/kg/day was used (data not shown).

Measurement of Renal Function

Blood samples were first centrifuged at 2,000 ×*g* for 10 min at 4°C and then at 8,000 × *g* for 10 min at 4°C. Serum was collected and frozen at −80°C until use. Creatine (Cr) and blood urea nitrogen (BUN) levels were measured using an automatic biochemistry analyzer (7020; Hitachi, Tokyo, Japan).

Renal Histology and Fibrosis Assessment

Renal tissues were retrieved without perfusion and fixed in 4% paraformaldehyde. Kidney paraffin sections (4 μm) were stained with Hematoxylin and Eosin (H&E) and Periodic Acid-Schiff (PAS) to assess renal injury. Sirius Red (SR) and Masson's trichome (MT) staining were used for assessment of fibrosis.

Immunohistochemistry and Immunofluorescence

Renal tissues were first perfused with cold saline (0.9%) followed by fixation with 4% paraformaldehyde. Paraffin-embedded slices (4 μm) were subjected to immunohistochemical staining as described in our previous study (15). Antibodies against fibronectin (FN; Ab2413; RRID: AB_2262874; Abcam), collagen I (COL I, Ab88147; RRID: AB_2081873; Abcam), α-smooth muscle actin (α-SMA; Ab32575; RRID: AB_722538; Abcam), and E-cadherin (E-Cad, Ab76319; RRID: AB_2076796; Abcam) were used to assess fibrosis and epithelial-to-mesenchymal transition (EMT). TLR-9 antibody (Ab53396; RRID: AB_883065; Abcam) was used to detect TLR-9, and cytokeratin 18 antibody (CK18; Ab668; RRID: AB_305647; Abcam) was used for verification of renal tubular epithelial cells (RTECs) (**Figure S2**).

Real-Time Quantitative PCR (RT qPCR)

The RNAeasy™ Animal RNA Isolation Kit with Spin Column (R0024; Beyotime, Shanghai, China) was used to obtain total RNA from fresh tissues according to the manufacturer's guidelines. Mean fold changes were calculated by averaging three duplicate measurements, and the gene expression results were normalized to *Gapdh*. Relative gene expressions in treated groups were compared with those in blank or sham groups.

The$2^{-\triangle\triangle CT}$ method was used for calculation. The sequences of the primer pairs are listed in **Table 1**. Transcript-specific primers were generated from GenBank and primer specificity was verified using the NCBI Primer Blast. For Real-Time qPCR, 2 μg RNA was used for reverse transcription using PrimeScript™ RT Master Mix (RR036A; Takara, Shiga, Japan); amplification was performed using SYBR Green Master Mix (Roche; Bruxelles, Belgium) and the LightCycler480 system (Roche).

Flow Cytometry

Flow cytometry was performed as previously described (16). Anti-mouse CD16/CD32 (553141; RRID: AB_394656, clone 2.4G2; BD Biosciences, San Jose, CA, USA) was used for blocking nonspecific Fc sites. The antibodies used in this assay were acquired from BioLegend (San Diego, CA, USA). BV421 anti-mouse CD45 (RRID: AB_2562559), APC anti-mouse F4/80 (RRID: AB_893481), PE anti-mouse CD206 (MMR) (RRID: AB_10895754), FITC anti-mouse CD86 (RRID: AB_313149), and PerCP/Cyanine5.5 anti-mouse/human CD11b (RRID: AB_893232) antibodies were employed for detection of immune cells. Annexin V-FITC Apoptosis Detection Kit was used for apoptosis detection (Thermo Fisher Scientific Cat# BMS500FI/100, RRID: AB_2575598). Data were acquired on a FACS Calibur cytometer (Becton Dickinson [BD], Bedford, MA, USA) and analyzed using FlowJo software (Tree Star, Ashland, OR, USA).

Isolation of Primary RTE Cells

RTE cells were extracted from adult male mice (6–8 weeks of age) following the method described by Ichimura et al. (17). Detailed methods can be found in the Supplementary Materials. For TGF-β culture, the second passage of RTE cells was used for subsequent assays. RTE cells isolated from WT and KO mice were exposed to TGF-β1 (10 ng/ml) (BioLegend, cat: 763102) for 72 h. Results were acquired from three independent assays.

Isolation of Bone Marrow–Derived Macrophages

Bone marrow–derived macrophages (BMDMs) were generated using an established method (18). Cells generated from mouse femur were cultured with macrophage colony-stimulating factor (M-CSF; 25 ng/ml; Novoprotein, China) for 7 days. To achieve polarization of BMDMs, BMDMs were stimulated with IL-4 (20 ng/ml, Novoprotein, China), IL-13 (20 ng/ml, Novoprotein, China) or Lipopolysaccharides (LPS) (250 ng/ml, Sigma), and IFN-γ (20 ng/ml, Sigma) for 24 h.

Cellular Immunofluorescence

For cellular immunofluorescence, cells were washed three times with phosphate-buffered saline (Sigma) to remove the culture medium. Fixation and permeability were performed for 15 min with 4% paraformaldehyde (P0099, Beyotime) for 20 min with 1% Triton X-100 (P0096, Beyotime). QuickBlock™ Blocking Buffer for Immunol Staining (P0260, Beyotime) was used to block non-specific antigens. Primary antibodies were used according to the objectives of each experiment, and the cells were incubated in appropriate antibodies overnight. Nuclear staining was performed using 4,6-diamidino-2-phenylindole (DAPI; P0131; Beyotime).

Western Blotting Assay

After perfusion with cold saline (0.9%), proteins from renal tissue were acquired using a tissue homogenizer (KZ-II; Servicebio). A total of 20 μg of protein was used for WB analysis, and 10% SDS-PAGE gels were used for WB. Polyvinylidene fluoride membranes (0.45 μm; IPVH00010; Millipore, Billerica, MA) were used for protein transfer. Primary antibodies used for WB were purchased from Cell Signaling Technology (CST). Antibodies, such as SAPK/JNK (9252; RRID: AB_2250373; CST), Phospho-SAPK/JNK (Thr183/Tyr185) (81E11) (4668; RRID: AB_823588; CST), p38 MAPK (D13E1) (8690; RRID: AB_10999090; CST), Phospho-p38 MAPK (Thr180/Tyr182) (4511; RRID: AB_2139682; CST), p44/42 MAPK (Erk1/2) (4695; RRID: AB_390779; CST), and

TABLE 1 | Primer sequences for Real-time quantitative PCR.

Transcript	Seq ID	Forward 5′ to 3′	Reverse 5′ to 3′
IL-1β	NM_008361	GAAATGCCACCTTTTGACAGTG	TGGATGCTCTCATCAGGACAG
IL-6	NM_031168	TAGTCCTTCCTACCCCAATTTCC	TTGGTCCTTAGCCACTCCTTC
TNF-α	NM_013693	CCCTCACACTCAGATCATCTTCT	GCTACGACGTGGGCTACAG
TGF-β1	NM_011577	CTCCCGTGGCTTCTAGTGC	GCCTTAGTTTGGACAGGATCTG
CD86	NM_019388	TGTTTCCGTGGAGACGCAAG	TTGAGCCTTTGTAAATGGGCA
CD206	NM_008625	CTCTGTTCAGCTATTGGACGC	CGGAATTTCTGGGATTCAGCTTC
IL-4	NM_021283	GGTCTCAACCCCCAGCTAGT	GCCGATGATCTCTCTCAAGTGAT
IL-10	NM_010548	GCTCTTACTGACTGGCATGAG	CGCAGCTCTAGGAGCATGTG
MIP-2	/	TTCCTGCTGTTTCTCTTACACCT	CTGTCTGCCTCTTTTGGTCAG
MCP-1	NM_011333	ACCTGCTGCTACTCATTCAC	TTGAGGTGGTTGTGGAAAAG
Arg-1	NM_007482	AGGAGCTGTCATTAGGGACATC	CTCCAAGCCAAAGTCCTTAGAG
Icam-1	NM_010493	TGTTTCCTGCCTCTGAAGC	CTTCGTTTGTGATCCTCCG
Vcam-1	NM_011693	AGTTGGGGATTCGGTTGTTCT	CCCCTCATTCCTTACCACCC
Smad 1	NM_008539	GCTTCGTGAAGGGTTGGGG	CGGATGAAATAGGATTGTGGGG
MyD88	NM_010851	TCATGTTCTCCATACCCTTGGT	AAACTGCGAGTGGGGTCAG
Snail 1	/	CACACGCTGCCTTGTGTCT	GGTCAGCAAAAGCACGGTT
TLR-9	NM_031178	CCAGTTTGTCAGAGGGAGCC	GGACAGGTGGACGAAGTCAG
Gapdh	NM_008085	AATGGATTTGGACGCATTGGT	TTTGCACTGGTACGTGTTGAT

phospho-p44/42 MAPK (Erk1/2) (Thr202/Tyr204) (4370; RRID: AB_2315112; CST) were used to detect MAPK signaling pathways. GAPDH (D16H11) XP® Rabbit mAb (HRP Conjugate) antibody was used for GAPDH detection (8884; RRID: AB_11129865; CST).

Histology, Immunohistochemistry, and Immunofluorescence Analysis

Quantification of fibrosis, immunohistochemistry, and immunofluorescence analysis was performed using ImageJ software (NIH Image, Bethesda, MD, USA). Five randomly chosen high-resolution images per mouse (original magnification ×100) captured using the Leica system were used for quantification. Two independent investigators, blinded to the experimental conditions, performed this process.

Statistics

The Kolmogorov-Smirnov (KS) normality test was first used to test whether the data were normally distributed; all the data met this criterion. Student's t-test (two groups) and one-way analysis of variance (for ≥3 groups) were used to analyze significant differences. All values are expressed as the mean ± standard deviation (SD). Data were analyzed using GraphPad Prism 8.0 (GraphPad Software Inc., La Jolla, CA, USA). A P-value<0.05 was considered statistically significant.

RESULTS

HCQ Reduces Renal Tubulointerstitial Fibrosis Following IRI *In Vivo*

To construct a renal tubulointerstitial fibrosis model, WT mice were first used to examine the development of AKI in CKD (19). Renal tissues of WT mice subjected to bilateral clamping of renal arteries and veins for 26 min were obtained. Picrosirius red (PSR) and Masson's trichrome (MT) were used to assess tubulointerstitial fibrosis on days 14, 21, and 28 post-injury. The degree of positive PSR- and MT-stained areas increased in a time-dependent manner, which indicated the successful construction of a renal tubulointerstitial fibrosis model after acute injury (**Figure 1A**). The effects of HCQ were further explored, and results suggested that renal fibrosis was attenuated in the HCQ-treated WT group than in CMC-treated WT group (**Figures 1A, B**) (P <0.01). Expression of FN and COL I was significantly inhibited in the HCQ-treated WT group compared to that in CMC-treated WT group (P <0.01) (**Figures 1B, C**). Renal function at days 7 and 14 was better preserved in HCQ-treated mice, whereas the difference was less apparent by day 21 post-IRI (**Figure 1C** and **Figure S3**).

HCQ Treatment Inhibits Leukocyte and Macrophage Infiltration in the Kidney Following IRI *In Vivo*

Leukocyte infiltration is an important hallmark of inflammation during tissue injury (20). Infiltration of leukocytes, especially macrophages, which substantially contribute to IRI, was observed. Results showed that HCQ-treated mice exhibited significantly fewer CD45+ (total leukocyte) cells at day 28 post-IRI (7.46% vs. 1.63%, p = 0.001) (**Figure 2A**). Fewer macrophages were observed in the HCQ-treated WT group than in CMC-treated WT group post-injury (P<0.01) (**Figure 2A**). Macrophage phenotypes that contribute to the processes of fibrosis and tissue repair were also observed. $CD11b^{+}F4/80^{high}$ cells are regarded as M2-like macrophages, whereas $CD11b^{+}F4/80^{low}$ cells are M1-like macrophages (21, 22). The results showed that HCQ treatment decreased the number of M2-like macrophages to a greater extent than that of M1-like macrophages (**Figures 2A, B**). Cytokine and chemokine production-related M1 and M2 macrophages were also explored using RT qPCR, and the results were consistent with flow cytometry results. M1 macrophage-related (CD86, IL-1β, and IL-6) and M2 macrophages-related (CD206 and Arg-1) cytokines were inhibited in the HCQ-treated WT group, as also cytokines associated with migration (MIP-2, MCP-1, Icam-1, and Vcam-1) in renal tissue post-injury (**Figure 2C**). HCQ is a TLR inhibitor that can inhibit TLR-7 and TLR-9; therefore, the expression of TLRs was also assessed. Results showed that the expression of TLR-9 increased post-injury and was inhibited after HCQ treatment; however, no significant difference was found regarding the expression of TLR-7 (**Figure 2C**).

HCQ Modulates Activation of Macrophages *In Vitro*

To further explore the effects of HCQ on macrophages, BMDMs were acquired from the mouse femur and identified using CD11b and F4/80 (**Figure 3A**). M1 or M2 macrophages were induced using an established method (**Figure 3B**) (18, 23). Results suggested that the purity of macrophages ($CD11b^{+}F4/80^{+}$) was over 90% after co-culture with M-CSF (25 ng/ml) for 7 days. BMDMs were cultured with different doses of HCQ for 24 h, and the results indicated that HCQ promoted the apoptosis of BMDMs, including early apoptosis and late apoptosis (**Figures 3C, D**). Considering that the difference in apoptotic effects between 25 and 100 μM of HCQ was not significant, 25, 50, and 100 μM were used for further studies. Taken together, these results demonstrated that HCQ could inhibit the induction of M1 and M2 macrophages *in vitro* (**Figure 3E**).

TLR-9 Knockout Limits the Inhibitory Effects of HCQ on BMDMs *In Vitro*

HCQ is a TLR inhibitor that mainly inhibits the TLR-7 and TLR-9 pathways (12). Previous results indicated that the effects of HCQ on renal fibrosis may have relied on the inhibition of TLR-9 (**Figure 2C**); therefore, a TLR-9 KO mouse was constructed (**Figure 4A**). TLR-9 KO BMDMs were obtained from KO mice, and macrophage differentiation was induced using the same methods mentioned above. Upon induction, the proportions of M1 and M2 macrophages were found to be lower in KO BMDMs than in WT BMDMs (**Figure 4B**). The inhibitory effects of HCQ on proportions of CD86+ cells (M1) and CD206 cells (M2) were also observed. Proportions of M1- and M2-like macrophages were significantly reduced in KO group than in WT group

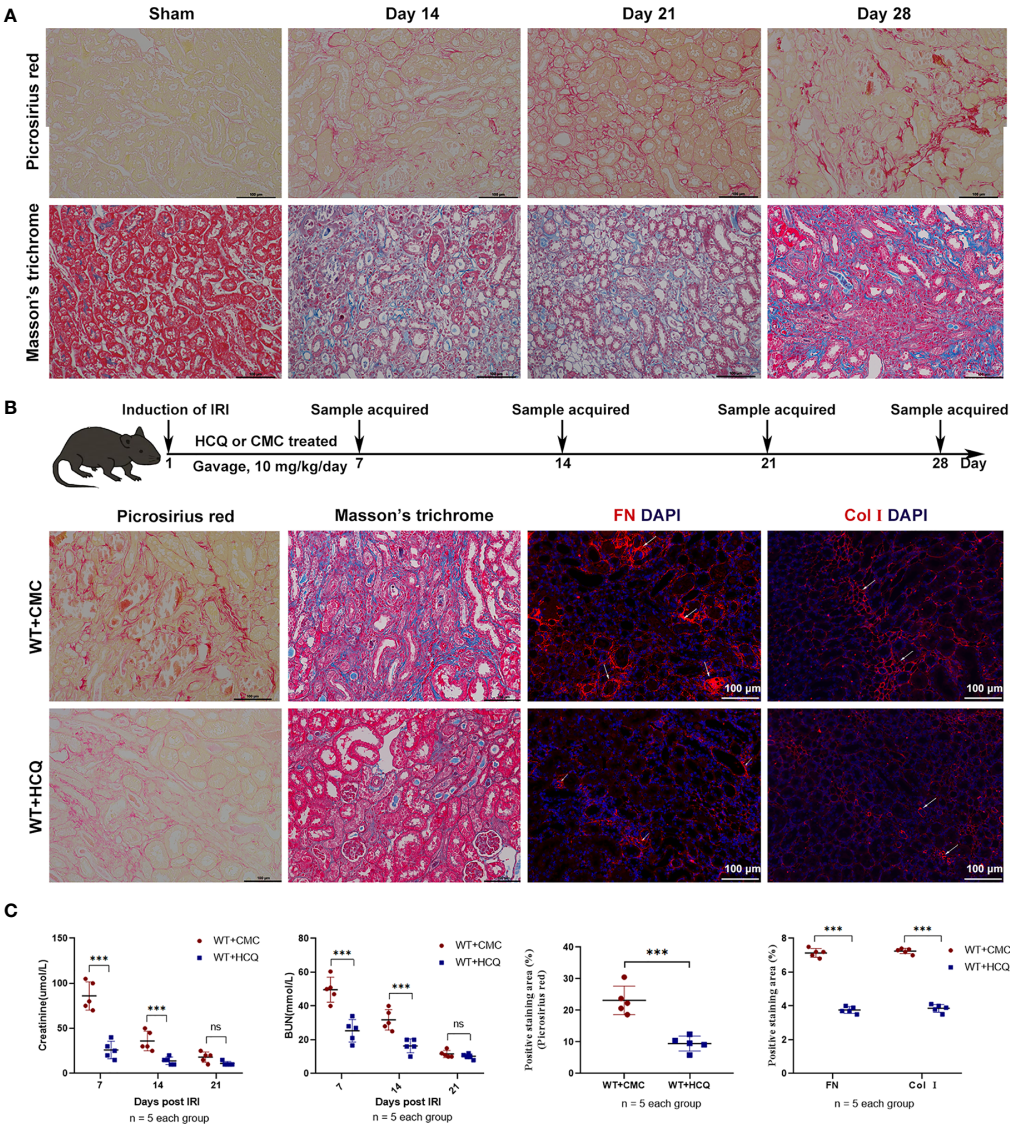


FIGURE 1 | HCQ treatment reduces renal tubulointerstitial fibrosis following IRI *in vivo*. Mice were subjected to IRI and treated with either CMC or HCQ (10 mg/kg/day for 7 days). Serum samples and kidneys were harvested at various days following reperfusion. Tissue sections are representative of five mice per group. **(A)** Representative images of Sirius red and Masson's trichrome stains on normal and injured kidneys of WT mice at various time points following reperfusion. The scale bars represent 100 μm. **(B)** Upper panel: Design of HCQ intervention and samples acquired; Down panel: Representative images of Picrosirius red - and Masson's trichrome-treated FN and Col I at day 28 following reperfusion in CMC-treated and HCQ-treated groups for WT mice; the scale bars represent 100 μm. **(C)** Left panel: levels of serum creatinine and BUN from CMC-treated and HCQ-treated WT mice at various time-points following reperfusion; right panel: quantification of Sirius red-stained areas in sections of murine renal cortical medullary junction and semiquantitative analysis of COL I and FN immunofluorescence staining. Data are represented as means ± SD and analyzed using the Student's t test. Magnification: 200×. NS, no significant difference, ***P < 0.001.

(P<0.01), and it seemed that the proportion of M2 macrophages was reduced to a greater extent when treated with HCQ at the concentration of 100 μM (**Figure 4C**). Assessment of cytokine and chemokine production also indicated that HCQ could decrease the expression of CD86, TNF-α, IL-6, and Vcam-1 when stimulated with LPS and IFN-γ (**Figure 4D**). The expression of CD206, TNF-α, IL-6, TGF-β1, and Vcam-1 was also inhibited by HCQ when stimulated with IL-4 and IL-13 (**Figure 4E**).

HCQ Attenuates Renal Tubulointerstitial Fibrosis Through TLR-9 Receptor *In Vivo*

KO mice were also used to further explore the effects of HCQ on CKD *in vivo*, and renal tissues were acquired 28 days post-IRI. Results showed that the improved effects of HCQ on the transition of AKI to CKD were eliminated in KO mice, and no significant difference in renal fibrosis or infiltration of leukocytes was found between HCQ- and CMC- treated KO groups (**Figure 5**).

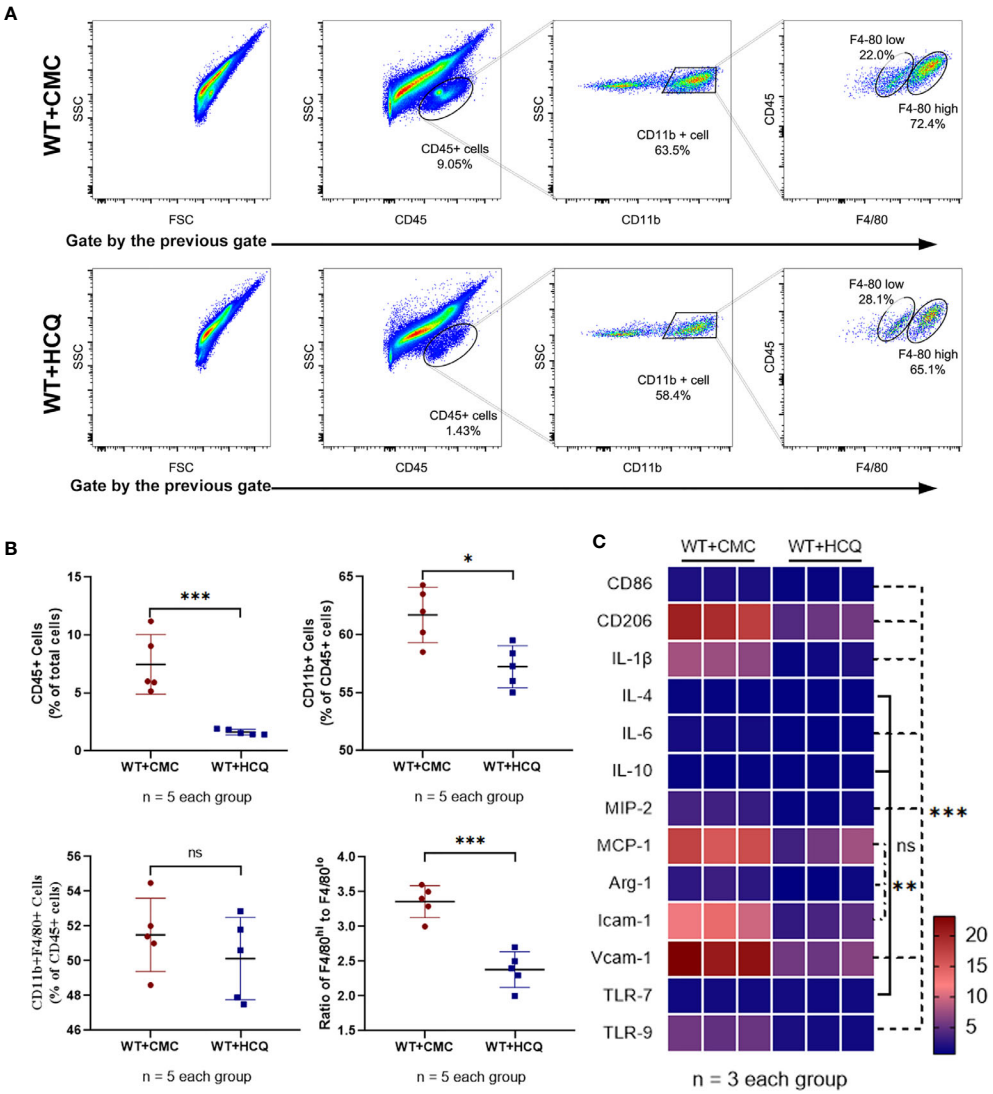


FIGURE 2 | HCQ treatment regulates leukocyte infiltration and phenotype of macrophage in the kidney following IRI *in vivo*. Inflammatory cell infiltration in CMC-treated and HCQ-treated kidneys at day 28 following IRI was determined using flow cytometry. **(A)** Representative dot plots of CD45+ cells and different types of macrophages ($CD11b^{+}F4/80^{high}$ and $CD11b^{+}F4/80^{low}$). **(B)** Quantification of related immune cell infiltration, including CD 45+ cells, $F4/80^{high}$, and $F4/80^{low}$ subsets in CD11b+. **(C)** Heatmap of mRNA expressions related to macrophages in renal tissue at day 28 post IRI. Data are represented as means and analyzed using the Student's t test. NS, no significant difference, *P < 0.05, **P < 0.01, ***P < 0.001.

HCQ Down-Regulates Mitogen-Activated Protein Kinase Inflammatory Signaling Pathways During Renal Tubulointerstitial Fibrosis Vial TLR-9 *In Vivo*

To further determine how HCQ might affect the inflammatory signaling pathways during renal fibrosis following IRI, kidneys were acquired at day 21 post-injury to evaluate the mitogen-activated protein kinase (MAPK) signaling pathway, a major contributor to fibrosis (24, 25). Phosphorylation of p38, Erk, and JNK decreased following HCQ treatment in the WT group, while no significant difference was found after HCQ treatment in the KO group (**Figures 6A, B**). Cytokines related to pro-fibrotic and TLR-9 signaling pathways were also explored. Levels of TGF-β1, Smad, Snail 1, and MyD88 were downregulated in the WT group when treated with HCQ, and no significant difference was found between HCQ- and CMC-treated KO groups (**Figure 6C**).

TLR-9 Signal Pathways Do Not Contribute to Improvement of Partial Epithelial-to-Mesenchymal Transition (EMT) *In Vitro*

Partial EMT, which leads to dedifferentiation of renal epithelial cells and promotes fibrosis, also plays a role in renal fibrosis (26, 27). Renal tissues were acquired at day 21 post-IRI, and the roles of TLR-9 signaling pathway in EMT were also explored.

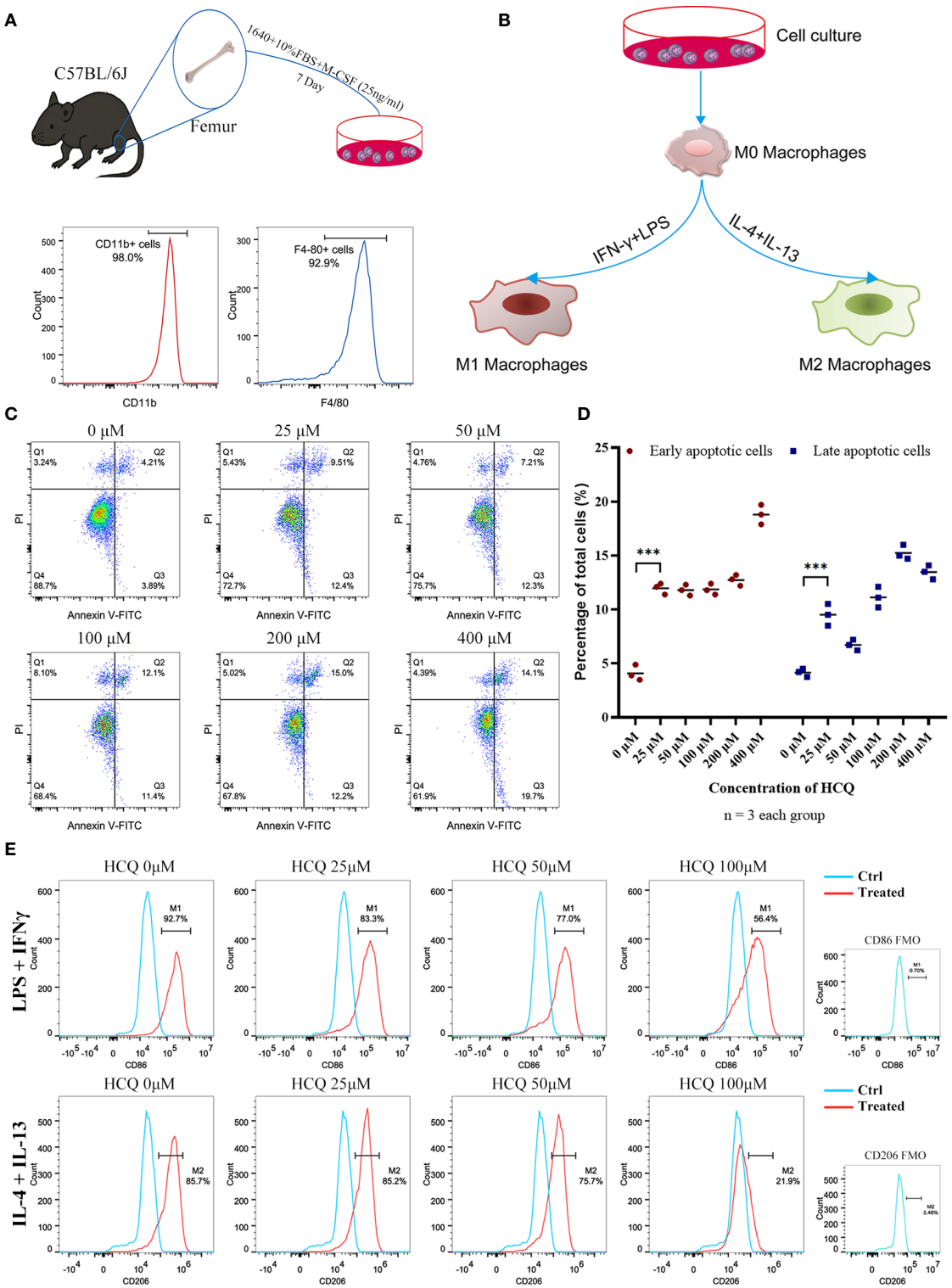


FIGURE 3 | HCQ affects differentiation of BMDMs *in vitro*. **(A)** Models of BMDM acquisition and results of purity identification. **(B)** Models of polarization of BMDMs. **(C)** Apoptosis of BMDMs was assessed using Annexin V-FITC/PI Kit. Annexin V+ PI– represents early apoptotic cells, and Annexin V+ PI+ represents late apoptotic cells. **(D)** Quantitative analysis of related apoptotic cells. **(E)** Effects of HCQ on macrophage polarization. BMDMs were polarized into M1 or M2 subsets, and various concentrations of HCQ were added for 24 h to assess the effects of HCQ on the differentiation of macrophages. Data are represented as means and analyzed using the Student's t test. ***P < 0.001.

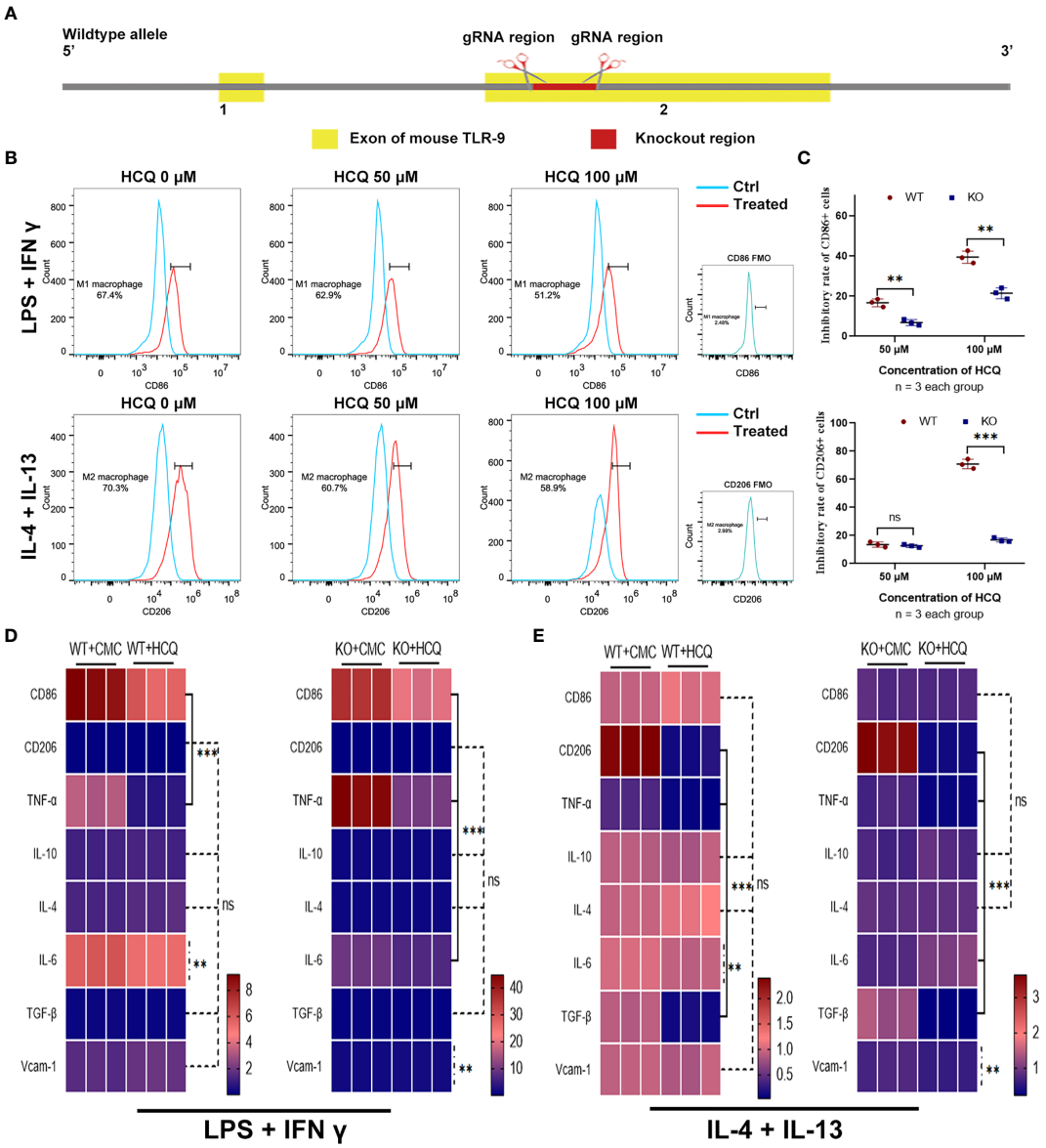


FIGURE 4 | Effects of HCQ on differentiation of BMDMs are reduced after depletion of TLR-9 *in vitro*. **(A)** Overview of the target strategy. **(B)** Effects of HCQ on polarization of TLR-9$^{-/-}$ macrophages. TLR-9$^{-/-}$ BMDMs were polarized into M1 or M2 subsets, and various concentrations of HCQ were added for 24 h to assess the effects of HCQ on differentiation of macrophages. **(C)** Quantification of the rate of inhibition. **(D)** Heatmap of mRNA expressions related to macrophage polarization when stimulated with LPS + IFN-γ. **(E)** Heatmap of mRNA expressions related to macrophage polarization when stimulated with IL-4 + IL-13. Data are represented as means or means ± SD and analyzed using the Student's t test. NS, no significant difference; **P < 0.01, ***P < 0.001.

Expression of E-Cad (an epithelial marker) was significantly higher in the HCQ-treated WT group than in CMC-treated WT group *in vivo* (P < 0.01), whereas the expression of α-SMA (indicating a subset of activated fibrogenic cells) was lower in the HCQ-treated WT group than in CMC-treated WT group *in vivo* (P < 0.01) (**Figures 7A, B**). To further determine the effects of TLR-9 on RTECs, RTECs were isolated. A traditional EMT model involving treatment with TGF-β (10 ng/ml) was used (28). In contrast to the *in vivo* results, depletion of TLR-9 aggravated fibrosis (defined as high levels of FN and Col I, P < 0.001) and EMT (defined as low levels of E-Cad and high levels of α-SMA, P < 0.001) of RTECs *in vitro* (**Figures 7C, D**).

DISCUSSION

IRI is a major cause of AKI that leads to CKD (5, 29). In the present study, we first identified that HCQ served as a TLR-9 inhibitor and inhibited the activation of macrophages, thereby attenuating renal fibrosis post-IRI. Treatment with HCQ

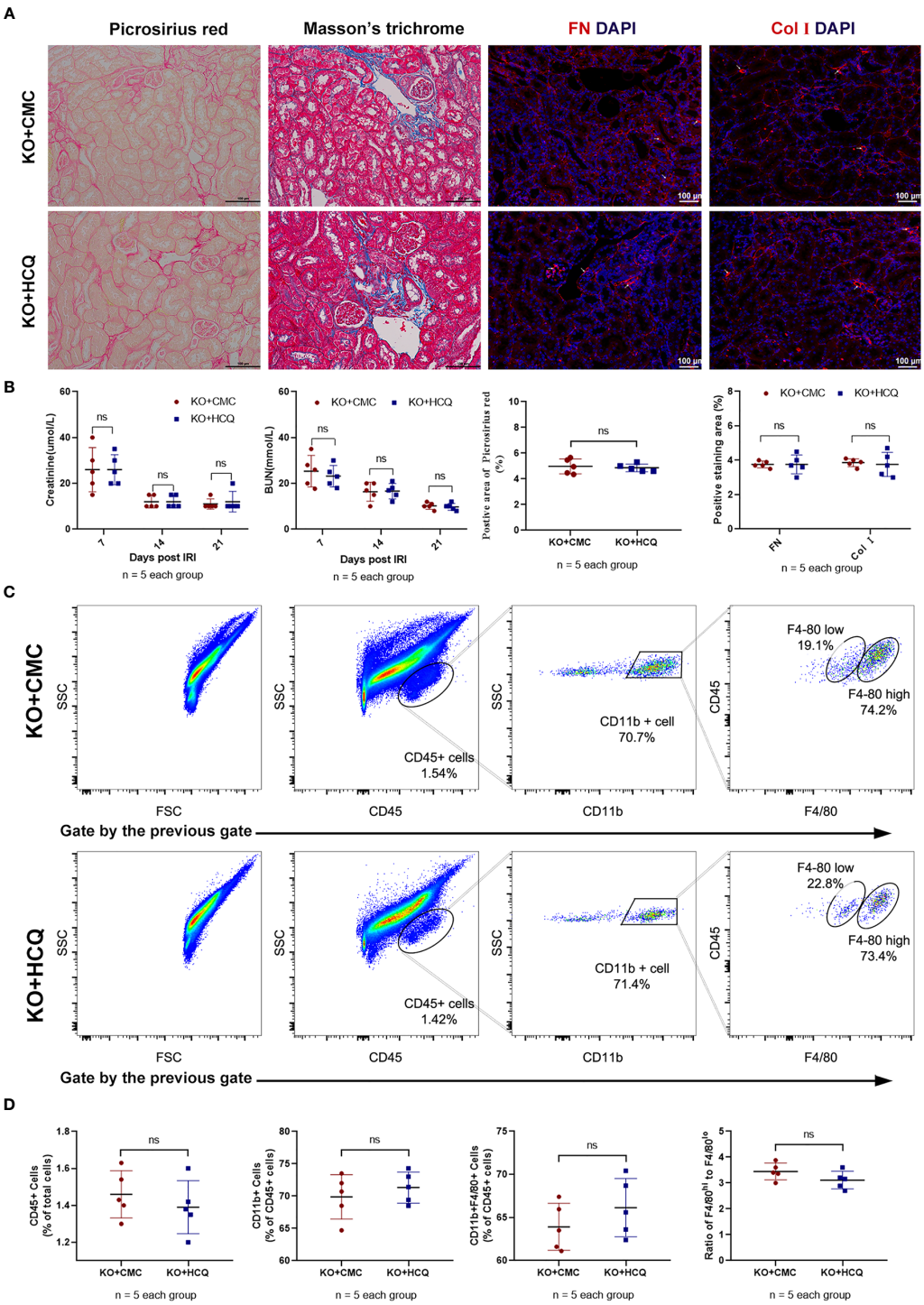


FIGURE 5 | Effects of HCQ on renal tubulointerstitial fibrosis following IRI mainly rely on the TLR-9 signal pathway *in vivo*. KO mice were subjected to IRI and treated with either CMC or HCQ (10 mg/kg/day for 7 days). Serum samples and kidneys were collected 28 days post- reperfusion. Tissue sections are representative of five mice per group. **(A)** Representative images of Sirius red- Masson's trichrome-staining of FN and Col I at day 28 following reperfusion in CMC-treated KO mice and HCQ treated-KO mice; the scale bars represent 100 μm. **(B)** Left panel: serum creatinine and urea from CMC-treated and HCQ-treated WT mice at various time-points following reperfusion; right panel: quantification of Sirius red-stained areas in murine renal cortical medullary junction sections and semiquantitative analysis of COL I and FN immunofluorescence staining; **(C)** Representative dot plots of CD45+ cells and different types of macrophage ($CD11b^{+}F4/80^{high}$ and $CD11b^{+}F4/80^{low}$). **(D)** Quantification of related immune cell infiltration, including CD 45+ cells, $F4/80^{high}$, and $F4/80^{low}$ subsets in CD11b+. Data are represented as means ± SD and analyzed using the Student's t test. Magnification: 200×. NS, no significant difference.

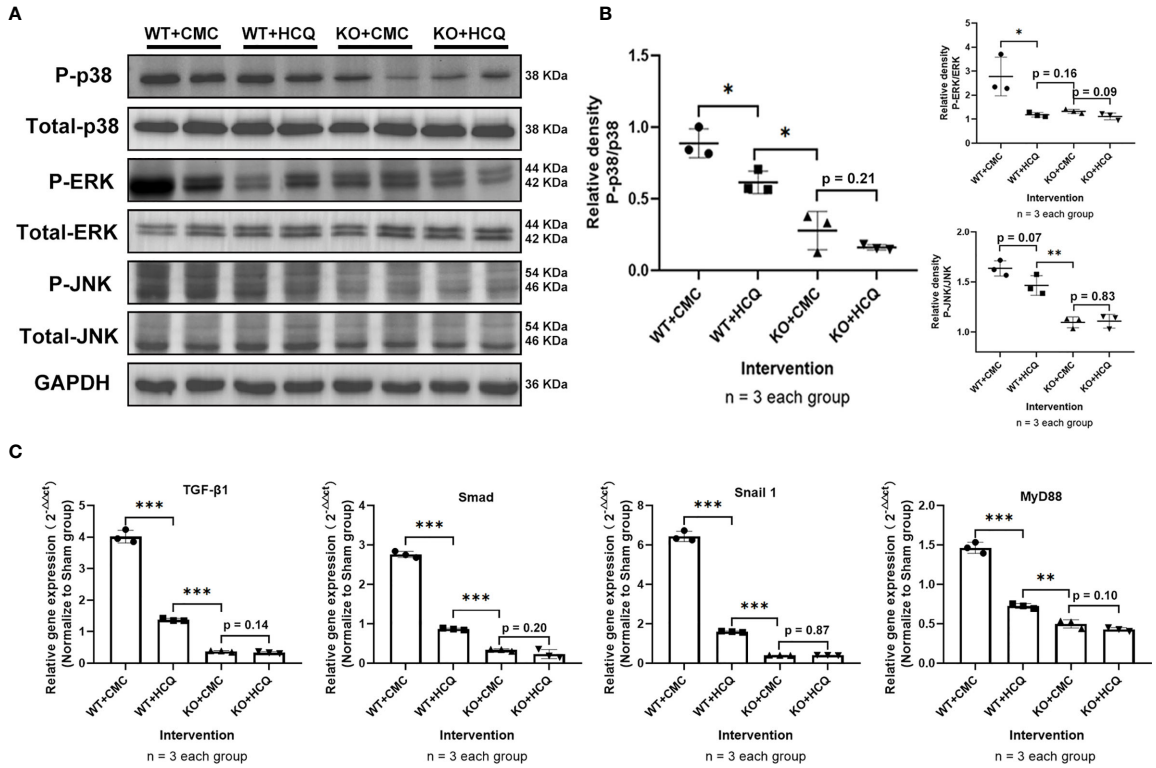


FIGURE 6 | Depletion of TLR-9 attenuates renal fibrosis following IRI through the inhibition of MAPKs and pro-inflammatory chemokine/cytokine induction *in vivo*. Renal tissues were acquired on day 21 following IRI. **(A)** Activations of MAPKs. **(B)** Semiquantitative analysis of the activation of MAPKs. **(C)** Expression of pro-inflammatory chemokines/cytokines. Data are shown as means ± SD and analyzed using one-way analysis of variance. Each dot represents an individual mouse. *P < 0.05, **P < 0.01, ***P < 0.001. IRI, ischemia-reperfusion injury; WT, wild-type; KO, knockout; MAPK, mitogen-activated protein kinase; HCQ, hydroxychloroquine; CMC, carboxymethyl cellulose.

decreased intrarenal infiltration of macrophages, especially M-2 macrophages, and reduced the severity of inflammation during renal tubulointerstitial fibrosis *in vivo*. However, the effects of HCQ on renal fibrosis or activation of macrophages decreased after TLR-9 depletion (**Figure 8**).

HCQ was first approved in the United States for the therapy and prevention of malaria in 1955. The effects of HCQ are complex, and it can not only serve as an immunomodulatory molecule, but also as an autophagy modulator (30). The functions of HCQ have been explored in some renal diseases, including IRI and IgAN (9, 11), but little is known about the effects of HCQ on renal tubulointerstitial fibrosis. In this study, we focused on the effects of HCQ on TLRs. Expression of TLR-9 but not TLR-7 in renal tissue post-IRI was inhibited by HCQ, and the results are consistent with our previous study showing that depletion of TLR-9 attenuated renal fibrosis. Previous results indicated that the use of HCQ was associated with a lower rate of incidence of CKD in rheumatoid arthritis patients (8). Our study demonstrated direct effects and mechanisms of HCQ on renal tubulointerstitial fibrosis.

TLRs are major sensors of the innate immune system and mediate inflammation and tissue regeneration (31). TLR-9, a member of the toll-like receptor family, also serves as a target of HCQ (32). Because HCQ attenuates renal fibrosis and inhibits activation of macrophages, we hypothesized that the effects of HCQ on renal tubulointerstitial fibrosis mainly rely on TLR-9. A TLR-9 KO mouse was constructed to further confirm our hypothesis. *In vivo* and *in vitro* results suggest that the effects of HCQ on macrophages and renal fibrosis decreased after depletion of TLR-9, and HCQ could not attenuate renal fibrosis post-IRI in the KO group. These results highlight that HCQ attenuates kidney fibrosis through the TLR-9 signaling pathway. Taking into account that it is difficult to distinguish between the effects of TLR-9 on CKD from those on AKI, effects of TLR-9 on AKI were also explored. The results revealed that TLR-9 was not required for the recovery of early renal function following IRI. Moreover, no significant difference was found in the levels of serum Cr or BUN between TLR-9 KO and WT mice or renal tubular injury scores at 24 and 48 h (Data not shown). These results also indicate TLR-9 could be an ideal therapeutic target for CKD.

TLR-9 is widely expressed in multiple cells, including macrophages, dendritic cells, B lymphocytes, and some interstitial tissues (33). It is primarily located in endosomes and recognizes viruses, endogenous nucleic acids, and bacteria. Following IRI injury, damage-associated molecular patterns are released and sensed by these TLR-9—expressed cells, especially macrophages (34, 35). In this study, we focused on the effects of HCQ on macrophages during

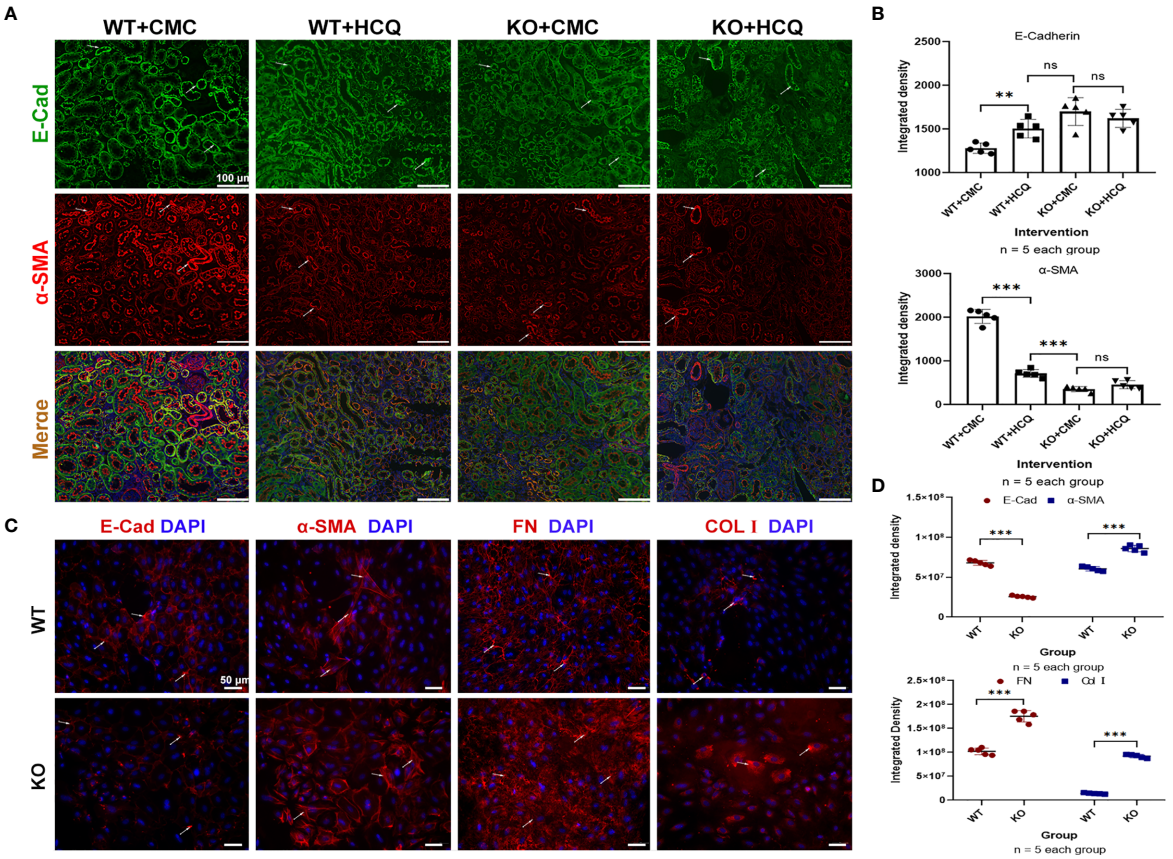


FIGURE 7 | TLR-9 signal pathway did not contribute to the improvement of EMT *in vitro*. **(A)** First row: representative fluorescence microscope images of E-Cad (Green), α-SMA (Red), and DAPI (Blue) staining of the kidneys of WT and KO mice that were treated with CMC or HCQ following reperfusion; the scale bars represent 100 μm.; **(B)** Semiquantitative analysis of E-Cad and α-SMA immunofluorescence staining. **(C)** Immunofluorescence of COL I, FN, E-Cad, and α-SMA was used to assess fibrosis and EMT of RTECs after being exposed to TGF-β (10 ng/ml) for 72 h; the scale bars represent 100 μm. **(D)** Semiquantitative analysis of E-Cad, α-SMA, FN, and COL I immunofluorescence staining of RTECs following TGF-β treatment. Data are shown as means ± SD and analyzed using one-way analysis of variance or Student's t test. Each dot represents an individual assay. Magnification: 200×. NS, no significant difference; $^{**}P < 0.01$, $^{***}P < 0.001$. EMT, epithelial-to-mesenchymal transition; RTECs, renal tubular epithelial cells; WT, wild-type; KO, knockout; E-Cad, E-cadherin; α-SMA, α-smooth muscle; COL I, collagen I; FN, fibronectin.

CKD to further determine the relationship between HCQ and macrophages and tubulointerstitial fibrosis. *In vivo* and *in vitro* results suggest that HCQ inhibits the activation and differentiation of macrophages. A low concentration (50 μM) of HCQ decreased the differentiation of macrophages into an M1-like phenotype, while a high concentration (100 μM) of HCQ reduced differentiation of M2-like macrophages to a greater extent. M1-like macrophages mainly participate in acute inflammatory response and mediate ROS-induced tissue damage, including IRI. These results are consistent with previous results, which indicate that HCQ can attenuate renal IRI injury (11). M2-like macrophages are recognized to be anti-inflammatory and may also lead to fibrosis post-injury. Hence, inhibition of M1-like and M2-like macrophages by HCQ not only attenuates the inflammatory response during AKI, but also inhibits renal fibrosis.

Proinflammatory and profibrotic cytokines can also accelerate the progression of fibrosis (36). Activation of TLR-9 can induce several signaling pathways, especially those involving MAPKs. Moreover, proinflammatory and profibrotic cytokines, including IL-1β, IL-6, TNF-α, and TGF-β, can also be released (37, 38). Previous studies have shown that activation of MAPKs could directly contribute to fibroblast activation and renal fibrosis (39); these results were also confirmed in the present study. Consistent with the histological and immunohistochemical results, we found that inflammation and fibrosis signaling pathways were inhibited by HCQ and terminated after depletion of TLR-9.

Recently, increasing attention has been paid to the effects of renal intrinsic cells, especially RTECs, on fibrosis and inflammation. RTECs have been shown not only to contribute to the aggravation of inflammation, but also to take part in EMT (26, 27). Notably, TLR-9 deficiency did not lead to better preservation of RTECs; rather, fibrosis and EMT in TLR-9 KO RTE cells were indicative of more severe injury. These results also provide evidence that the effects of HCQ on renal fibrosis do not rely on the improvement of EMT. Inhibition of infiltrating lymphocytes and reduced pro-inflammatory cytokines may account for the improvement in EMT *in vivo*.

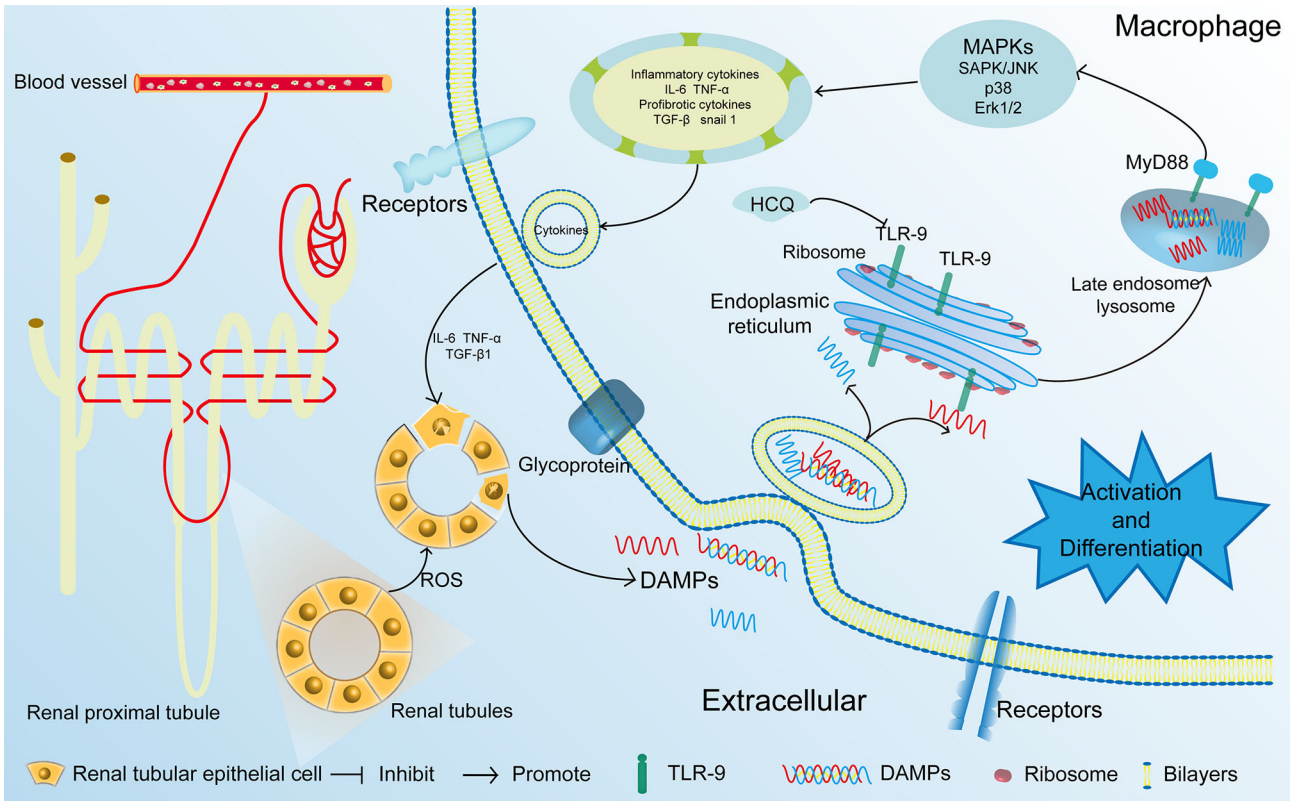


FIGURE 8 | Proposed mechanisms of HCQ function in renal fibrosis following IRI. After being exposed to ischemia and reperfusion, RTECs were damaged. DAMPs that were released from the damaged RTECs flowed into blood vessels and activated monocytes. DAMPs also activated the TLR-9/MyD88 signal pathway, thereby activating MAPKs. Inflammatory and profibrotic cytokines including IL-6, TNF α, TGF-β were synthesized and released, resulting in the aggravation damage and fibrosis of kidney. RTECs, renal tubular epithelial cells; TLR-9, toll-like receptor-9; IRI, ischemia-reperfusion injury; DAMP, damage-associated molecular pattern.

This study, nevertheless, has a few limitations. First, although the effects of HCQ on macrophages have been investigated *in vitro*, we focused only on the effects of HCQ on macrophages and inflammation. Other effects of HCQ on fibrosis should also be explored. Second, M2 macrophages can be divided into various subsets, including M2a, M2b, M2c, and M2d; detailed effects of HCQ on such macrophage subsets should be further explored. Finally, because the effects of HCQ were observed only in animal studies and HCQ has been used clinically, clinical trials should be performed to further confirm the effect of HCQ on patients with CKD.

Overall, the results of this study provide novel insights into the roles of HCQ in acute and chronic kidney injury. HCQ treatment attenuated renal fibrosis following renal injury *in vivo*, whereas the effects of HCQ could be terminated by depletion of TLR-9. Our results also provide new evidence that HCQ could be an ideal TLR-9 inhibitor for the treatment of renal tubulointerstitial fibrosis.

DATA AVAILABILITY STATEMENT

The original contributions presented in the study are included in the article/**Supplementary Material**. Further inquiries can be directed to the corresponding author.

ETHICS STATEMENT

The animal study was reviewed and approved by the Institutional Animal Care and Use Committee of Sun Yat-Sen University. Written informed consent was obtained from the owners for the participation of their animals in this study.

AUTHOR CONTRIBUTIONS

HZ and QS conceived and designed the experiments. HZ, YZ, and JH performed experiments with the help of ZY, RZ, LL, ZL, and YY, HZ, and YZ analyzed the data and drafted the manuscript. All authors contributed to the article and approved the submitted version.

FUNDING

This study was supported by the National Natural Science Foundation of China (grants 81970650, 81770753, 81800662), National Key R&D Program of China (grant numbers 2018YFA0108804), and The PhD Start-up Fund of Natural Science Foundation of Guangdong Province, China (grant 2018A030310324).

ACKNOWLEDGMENTS

We thank Shaogui, Wan (Gannan Medical University) for TLR9$^{-/-}$ mice. We would like to thank Editage (www.editage.com) for English language editing.

SUPPLEMENTARY MATERIAL

The Supplementary Material for this article can be found online at: https://www.frontiersin.org/articles/10.3389/fimmu.2021.645100/full#supplementary-material

REFERENCES

1. Li L, Kang H, Zhang Q, D'Agati VD, Al-Awqati Q, Lin F. FoxO3 activation in hypoxic tubules prevents chronic kidney disease. *J Clin Invest* (2019) 129 (6):2374–89. doi: 10.1172/JCI122256
2. Kishi S, Brooks CR, Taguchi K, Ichimura T, Mori Y, Akinfolarin A, et al. Proximal tubule ATR regulates DNA repair to prevent maladaptive renal injury responses. *J Clin Invest* (2019) 129(11):4797–816. doi: 10.1172/JCI122313
3. Bonventre JV, Yang L. Cellular pathophysiology of ischemic acute kidney injury. *J Clin Invest* (2011) 121(11):4210–21. doi: 10.1172/JCI45161
4. Palomba H, Castro I, Yu L, Burdmann EA. The duration of acute kidney injury after cardiac surgery increases the risk of long-term chronic kidney disease. *J Nephrol* (2017) 30(4):567–72. doi: 10.1007/s40620-016-0351-0
5. Forni LG, Darmon M, Ostermann M, Oudemans-van Straaten HM, Pettila V, Prowle JR, et al. Renal recovery after acute kidney injury. *Intensive Care Med* (2017) 43(6):855–66. doi: 10.1007/s00134-017-4809-x
6. Muller-Calleja N, Manukyan D, Canisius A, Strand D, Lackner KJ. Hydroxychloroquine inhibits proinflammatory signalling pathways by targeting endosomal NADPH oxidase. *Ann Rheum Dis* (2017) 76(5):891–7. doi: 10.1136/annrheumdis-2016-210012
7. Bethel M, Yang FM, Li S, Nahman NS, Oliver AM, Machua W, et al. Hydroxychloroquine in patients with systemic lupus erythematosus with end-stage renal disease. *J Investig Med* (2016) 64(4):908–10. doi: 10.1136/jim-2016-000065
8. Wu CL, Chang CC, Kor CT, Yang TH, Chiu PF, Tarng DC, et al. Hydroxychloroquine Use and Risk of CKD in Patients with Rheumatoid Arthritis. *Clin J Am Soc Nephrol* (2018) 13(5):702–9. doi: 10.2215/CJN.11781017
9. Liu LJ, Yang YZ, Shi SF, Bao YF, Yang C, Zhu SN, et al. Effects of Hydroxychloroquine on Proteinuria in IgA Nephropathy: A Randomized Controlled Trial. *Am J Kidney Dis* (2019) 74(1):15–22. doi: 10.1053/j.ajkd.2019.01.026
10. Bai L, Li J, Li H, Song J, Zhou Y, Lu R, et al. Renoprotective effects of artemisinin and hydroxychloroquine combination therapy on IgA nephropathy via suppressing NF-kappaB signaling and NLRP3 inflammasome activation by exosomes in rats. *Biochem Pharmacol* (2019) 169:113619. doi: 10.1016/j.bcp.2019.08.021
11. Tang TT, Lv LL, Pan MM, Wen Y, Wang B, Li ZL, et al. Hydroxychloroquine attenuates renal ischemia/reperfusion injury by inhibiting cathepsin mediated NLRP3 inflammasome activation. *Cell Death Dis* (2018) 9(3):351. doi: 10.1038/s41419-018-0378-3
12. Clancy RM, Markham AJ, Buyon JP. Endosomal Toll-like receptors in clinically overt and silent autoimmunity. *Immunol Rev* (2016) 269(1):76–84. doi: 10.1111/imr.12383
13. Zheng H, Zhang Y, Li L, Zhang R, Luo Z, Yang Z, et al. Depletion of Toll-Like Receptor-9 Attenuates Renal Tubulointerstitial Fibrosis After Ischemia-Reperfusion Injury. *Front Cell Dev Biol* (2021) 9:641527. doi: 10.3389/fcell.2021.641527
14. Kenwood BM, Weaver JL, Bajwa A, Poon IK, Byrne FL, Murrow BA, et al. Identification of a novel mitochondrial uncoupler that does not depolarize the plasma membrane. *Mol Metab* (2014) 3(2):114–23. doi: 10.1016/j.molmet.2013.11.005
15. Liao T, Zhang Y, Ren J, Zheng H, Zhang H, Li X, et al. Noninvasive quantification of intrarenal allograft C4d deposition with targeted ultrasound imaging. *Am J Transplant* (2019) 19(1):259–68. doi: 10.1111/ajt.15105
16. Zhao D, Li S, Liao T, Wei Y, Liu M, Han F, et al. Triptolide inhibits donor-specific antibody production and attenuates mixed antibody-mediated renal allograft injury. *Am J Transplant* (2018) 18(5):1083–95. doi: 10.1111/ajt.14602
17. Ichimura T, Asseldonk EJ, Humphreys BD, Gunaratnam L, Duffield JS, Bonventre JV. Kidney injury molecule-1 is a phosphatidylserine receptor that confers a phagocytic phenotype on epithelial cells. *J Clin Invest* (2008) 118 (5):1657–68. doi: 10.1172/JCI34487
18. Ma PF, Gao CC, Yi J, Zhao JL, Liang SQ, Zhao Y, et al. Cytotherapy with M1-polarized macrophages ameliorates liver fibrosis by modulating immune microenvironment in mice. *J Hepatol* (2017) 67(4):770–9. doi: 10.1016/j.jhep.2017.05.022
19. Fu Y, Tang C, Cai J, Chen G, Zhang D, Dong Z. Rodent models of AKI-CKD transition. *Am J Physiol Renal Physiol* (2018) 315(4):F1098–F106. doi: 10.1152/ajprenal.00199.2018
20. Ernandez T, Mayadas TN. The Changing Landscape of Renal Inflammation. *Trends Mol Med* (2016) 22(2):151–63. doi: 10.1016/j.molmed.2015.12.002
21. Satoh T, Takeuchi O, Vandenbon A, Yasuda K, Tanaka Y, Kumagai Y, et al. The Jmjd3-Irf4 axis regulates M2 macrophage polarization and host responses against helminth infection. *Nat Immunol* (2010) 11(10):936–44. doi: 10.1038/ni.1920
22. Peng Q, Wu W, Wu KY, Cao B, Qiang C, Li K, et al. The C5a/C5aR1 axis promotes progression of renal tubulointerstitial fibrosis in a mouse model of renal ischemia/reperfusion injury. *Kidney Int* (2019) 96(1):117–28. doi: 10.1016/j.kint.2019.01.039
23. Mao L, Kitani A, Hiejima E, Montgomery-Recht K, Zhou W, Fuss I, et al. Bruton tyrosine kinase deficiency augments NLRP3 inflammasome activation and causes IL-1beta-mediated colitis. *J Clin Invest* (2020) 130(4):1793–807. doi: 10.1172/JCI128322
24. Budas GR, Boehm M, Kojonazarov B, Viswanathan G, Tian X, Veeroju S, et al. ASK1 Inhibition Halts Disease Progression in Preclinical Models of Pulmonary Arterial Hypertension. *Am J Respir Crit Care Med* (2018) 197 (3):373–85. doi: 10.1164/rccm.201703-0502OC
25. Fan J, Zou L, Cui K, Woo K, Du H, Chen S, et al. Atrial overexpression of angiotensin-converting enzyme 2 improves the canine rapid atrial pacing-induced structural and electrical remodeling. Fan, ACE2 improves atrial substrate remodeling. *Basic Res Cardiol* (2015) 110(4):45. doi: 10.1007/s00395-015-0499-0
26. Lovisa S, LeBleu VS, Tampe B, Sugimoto H, Vadnagara K, Carstens JL, et al. Epithelial-to-mesenchymal transition induces cell cycle arrest and parenchymal damage in renal fibrosis. *Nat Med* (2015) 21(9):998–1009. doi: 10.1038/nm.3902
27. Grande MT, Sanchez-Laorden B, Lopez-Blau C, De Frutos CA, Boutet A, Arevalo M, et al. Snail1-induced partial epithelial-to-mesenchymal transition drives renal fibrosis in mice and can be targeted to reverse established disease. *Nat Med* (2015) 21(9):989–97. doi: 10.1038/nm.3901
28. Su J, Morgani SM, David CJ, Wang Q, Er EE, Huang YH, et al. TGF-beta orchestrates fibrogenic and developmental EMTs via the RAS effector RREB1. *Nature* (2020) 577(7791):566–71. doi: 10.1038/s41586-019-1897-5
29. Jang HR, Rabb H. Immune cells in experimental acute kidney injury. *Nat Rev Nephrol* (2015) 11(2):88–101. doi: 10.1038/nrneph.2014.180
30. Lei ZN, Wu ZX, Dong S, Yang DH, Zhang L, Ke Z, et al. Chloroquine and hydroxychloroquine in the treatment of malaria and repurposing in treating COVID-19. *Pharmacol Ther* (2020) 216:107672. doi: 10.1016/j.pharmthera.2020.107672
31. Fitzgerald KA, Kagan JC. Toll-like Receptors and the Control of Immunity. *Cell* (2020) 180(6):1044–66. doi: 10.1016/j.cell.2020.02.041
32. Gies V, Bekaddour N, Dieudonne Y, Guffroy A, Frenger Q, Gros F, et al. Beyond Anti-viral Effects of Chloroquine/Hydroxychloroquine. *Front Immunol* (2020) 11:1409. doi: 10.3389/fimmu.2020.01409
33. Leemans JC, Kors L, Anders HJ, Florquin S. Pattern recognition receptors and the inflammasome in kidney disease. *Nat Rev Nephrol* (2014) 10(7):398–414. doi: 10.1038/nrneph.2014.91
34. Huen SC, Cantley LG. Macrophages in Renal Injury and Repair. *Annu Rev Physiol* (2017) 79:449–69. doi: 10.1146/annurev-physiol-022516-034219

35. Ren Q, Cheng L, Yi J, Ma L, Pan J, Gou SJ, et al. Toll-like Receptors as Potential Therapeutic Targets in Kidney Diseases. *Curr Med Chem* (2020) 27 (34):5829–54. doi: 10.2174/0929867325666190603110907
36. Humphreys BD. Mechanisms of Renal Fibrosis. *Annu Rev Physiol* (2018) 80:309–26. doi: 10.1146/annurev-physiol-022516-034227
37. O'Keeffe M, Grumont RJ, Hochrein H, Fuchsberger M, Gugasyan R, Vremec D, et al. Distinct roles for the NF-kappaB1 and c-Rel transcription factors in the differentiation and survival of plasmacytoid and conventional dendritic cells activated by TLR-9 signals. *Blood* (2005) 106(10):3457–64. doi: 10.1182/blood-2004-12-4965
38. Kuo CH, Hsieh CC, Kuo HF, Huang MY, Yang SN, Chen LC, et al. Phthalates suppress type I interferon in human plasmacytoid dendritic cells via epigenetic regulation. *Allergy* (2013) 68(7):870–9. doi: 10.1111/all.12162
39. Inoue T, Takenaka T, Hayashi M, Monkawa T, Yoshino J, Shimoda K, et al. Fibroblast expression of an IkappaB dominant-negative transgene attenuates renal fibrosis. *J Am Soc Nephrol* (2010) 21(12):2047–52. doi: 10.1681/ASN.2010010003

Conflict of Interest: The authors declare that the research was conducted in the absence of any commercial or financial relationships that could be construed as a potential conflict of interest.

Copyright © 2021 Zheng, Zhang, He, Yang, Zhang, Li, Luo, Ye and Sun. This is an open-access article distributed under the terms of the Creative Commons Attribution License (CC BY). The use, distribution or reproduction in other forums is permitted, provided the original author(s) and the copyright owner(s) are credited and that the original publication in this journal is cited, in accordance with accepted academic practice. No use, distribution or reproduction is permitted which does not comply with these terms.

frontiers in Immunology

ORIGINAL RESEARCH
published: 12 May 2021
doi: 10.3389/fimmu.2021.682749

Cyclic Helix B Peptide Prolongs Skin Allograft Survival *via* Inhibition of B Cell Immune Responses in a Murine Model

Long Zheng[1,2†], *Xuanchuan Wang*[1,2†], *Linkun Hu*[3†], *Wenjun Gao*[1,2], *Weitao Zhang*[1,2], *Xuepeng Zhang*[4], *Chao Hu*[1,2], *Ruiming Rong*[1,5*], *Cheng Yang*[1,2,6*] *and Dong Zhu*[1,2*]

[1] *Department of Urology, Zhongshan Hospital, Fudan University, Shanghai, China,* [2] *Shanghai Key Laboratory of Organ Transplantation, Shanghai, China,* [3] *Department of Urology, The First Affiliated Hospital of Soochow University, Suzhou, China,* [4] *Department of Critical Care Medicine, Zhongshan Hospital, Fudan University, Shanghai, China,* [5] *Department of Blood Transfusion, Zhongshan Hospital, Fudan University, Shanghai, China,* [6] *Zhangjiang Institute of Fudan University, Shanghai, China*

OPEN ACCESS

Edited by:
Bin Yang,
University of Leicester,
United Kingdom

Reviewed by:
Helong Dai,
Central South University, China
Liping Li,
Johns Hopkins Medicine,
United States

***Correspondence:**
Ruiming Rong
rong.ruiming@zs-hospital.sh.cn
Cheng Yang
yang.cheng1@zs-hospital.sh.cn
Dong Zhu
wgzd82@163.com

†These authors have contributed equally to this work

Specialty section:
This article was submitted to Alloimmunity and Transplantation, a section of the journal Frontiers in Immunology

Received: *19 March 2021*
Accepted: *23 April 2021*
Published: *12 May 2021*

Citation:
Zheng L, Wang X, Hu L, Gao W, Zhang W, Zhang X, Hu C, Rong R, Yang C and Zhu D (2021) Cyclic Helix B Peptide Prolongs Skin Allograft Survival via Inhibition of B Cell Immune Responses in a Murine Model. Front. Immunol. 12:682749. doi: 10.3389/fimmu.2021.682749

Antibody-mediated rejection (AMR) represents a major cause of allograft dysfunction and results in allograft failure in solid organ transplantation. Cyclic helix B peptide (CHBP) is a novel erythropoietin-derived peptide that ameliorated renal allograft rejection in a renal transplantation model. However, its effect on AMR remains unknown. This study aimed to investigate the effect of CHBP on AMR using a secondary allogeneic skin transplantation model, which was created by transplanting skin from BALB/c mice to C57BL/6 mice with or without CHBP treatment. A secondary syngeneic skin transplantation model, involving transplantation from C57BL/6 mice to C57BL/6 mice, was also created to act as a control. Skin graft rejection, $CD19^+$ B cell infiltration in the skin allograft, the percentages of splenic plasma cells, germinal center (GC) B cells, and Tfh cells, the serum levels of donor specific antibodies (DSAs), and NF-κB signaling in splenocytes were analyzed. Skin allograft survival was significantly prolonged in the CHBP group compared to the allogeneic group. CHBP treatment also significantly reduced the $CD19^+$ B cell infiltration in the skin allograft, decreased the percentages of splenic plasma cells, GC B cells, and Tfh cells, and ameliorated the increase in the serum DSA level. At a molecular level, CHBP downregulated P100, RelB, and P52 in splenocytes. CHBP prolonged skin allograft survival by inhibiting AMR, which may be mediated by inhibition of NF-κB signaling to suppress B cell immune responses, thereby decreasing the DSA level.

Keywords: cyclic helix B peptide, antibody-mediated rejection, plasma cells, germinal center B cells, Tfh cells, donor specific antibodies

INTRODUCTION

Antibody-mediated rejection (AMR) represents a major cause of allograft dysfunction and results in allograft failure in solid organ transplantation (1, 2). It is driven by circulating donor-specific antibodies (DSAs), which are mainly secreted by plasma cells differentiated from B cells (2, 3). The differentiation of B cells into plasma cells involves an ordered cascade of cellular events. After

antigen stimulation, IgM^+IgD^+ naive B cells in secondary lymphoid follicles are activated and migrate to the T–B border, where B cells proliferate and interact with T follicular helper (Tfh) cells, completing the activation (4). Thereafter, some of the activated B cells enter the center of follicles to form germinal centers (GCs) (5). In GCs, Tfh cells instruct GC B cells to proliferate and undergo affinity maturation, class switching, and eventually, differentiation into long-lived plasma cells (6). As AMR, which is mediated by B cell immune responses, is an important contributor to allograft dysfunction and failure after organ transplantation and lacks effective therapies, there is an urgent need for novel therapies for AMR.

Cyclic helix B peptide (CHBP) is a novel erythropoietin (EPO)-derived peptide (7). It was synthesized by our group in 2014 and has a thioether-cyclized structure that is resistant to proteolytic degradation while exerting its tissue protective effects. CHBP achieves its effects by binding to tissue protective receptor (TPR) and does not induce the side effects or toxicity of EPO (7). Our previous studies revealed that CHBP restored renal function and/or attenuated pathological changes in a renal ischemia–reperfusion injury (IRI) model, an aristolochic acid-induced acute kidney injury model, a unilateral IRI-induced renal fibrosis model, and a unilateral ureter obstruction-induced renal fibrosis model (8–12). Additionally, the tissue protective effect has also been shown in an acute myocardial infarction model, in which CHBP ameliorated cardiac injury and improved cardiac function (13). Moreover, there has been a single study on the effect of CHBP on allograft rejection in a renal transplantation model, and it yielded positive results (14). Thus, CHBP may inhibit transplantation rejection. The effect of CHBP on AMR, as a type of transplantation rejection, was therefore investigated.

In this study, a secondary skin transplantation model was established to evaluate the effect of CHBP on skin allograft survival. We also investigated whether the mechanism of AMR inhibition involves inhibition of B cell immune responses.

MATERIALS AND METHODS

Experimental Animals

The donor mice were 8-week-old male BALB/c or C57BL/6 mice. The recipient mice were 8-week-old male C57BL/6 mice. The mice were purchased from Shanghai SLAC Laboratory Animal Co., Ltd. They were bred in a specific-pathogen-free experimental animal room with a 12/12-h light/dark cycle. Before the experiments, the mice were left to acclimatize for 1 week, with free access to food and water. All animal procedures were performed in accordance with bioethics guidelines and were approved by the Bioethics Committee of Zhongshan Hospital, Fudan University, Shanghai, China.

Skin Transplantation Model

Twenty-four recipient C57BL/6 mice were randomly assigned to four groups (n = 6 each): (1) syngeneic group (donors: C57BL/6 mice), (2) allogeneic group (donors: BALB/c mice), (3) low-dose CHBP (donors: BALB/c mice) group, and (4) high-dose CHBP (donors: BALB/c mice) group. The mice in the former two groups were injected with normal saline (NS) daily after the secondary transplantation. The mice in the latter two groups, *i.e.*, the low- and high-dose CHBP groups, were injected with 100 and 500 μg/kg CHBP daily, respectively, after the secondary transplantation.

To prepare the donor skin, both C57BL/6 and BALB/c mice were sacrificed by cervical dislocation. Skin was removed from the tails, placed in cold saline, and cut into 1.0×1.5 cm^2 pieces. To prepare the recipient mice, C57BL/6 mice were anesthetized with intraperitoneal pentobarbital (0.1 g/kg). After being shaved and disinfected, a 1.0×1.5 cm^2 graft bed was cut in the skin on the dorsal neck of each recipient mouse. Next, donor skin was placed into the graft bed and stitched with absorbable 6-0 sutures. The primary skin transplantation was performed on day −14, and a secondary transplantation was performed on day 0. Each graft site was wrapped with a bandage, and photographs were taken daily from day 5 after secondary transplantation with a digital camera for 19 days or until the graft was rejected completely.

After the secondary skin transplantation, hardened, sloughed off, or necrotic skin indicated immune rejection, while ruddy soft skin with hair indicated lack of immune rejection.

Hematoxylin and Eosin Staining

Skin grafts from the recipient mice were harvested on day 10, fixed in 4% paraformaldehyde, dehydrated in ethanol, and embedded in paraffin. The skin tissue was then cut into 5-μm sections, deparaffinized in xylene, and rehydrated using a graded ethanol series before H&E staining. The structure and inflammatory cell infiltration of skin allografts (0: absent; 1: discrete; 2: moderately discrete; 3: moderate; 4: moderately severe; 5: severe) were observed and photographed under light microscopy.

Immunohistochemical Staining

The paraffin-embedded skin sections were deparaffinized, rehydrated, and blocked with 3% hydrogen peroxide and then incubated at 37°C for 1 h with anti-CD19 antibody (1:1,600; Cell Signaling Technology, Inc., Danvers, MA, USA). Thereafter, the sections were washed with phosphate-buffered saline (PBS) and incubated at room temperature for 1 h with horseradish peroxidase (HRP)-conjugated secondary antibody (1:200; Abcam). The reaction was subsequently visualized with 3,3′-diaminobenzidine solution (Gene Tech Co., Ltd., Shanghai, China), and the sections were counterstained with hematoxylin. Semi-quantification of the IHC staining results was performed under a high-power field (400×).

Flow Cytometry Analysis

To obtain spleen cell suspensions, spleens were harvested from recipient mice on day 10, milled gently in PBS supplemented with 1% fetal bovine serum using a 10-ml syringe, and forced through a 200-μm nylon mesh. Lymphocytes were isolated from the spleen cell suspensions using lymphocyte separation solution (Dakewe Biotech Co., Ltd., Shenzhen, China) according to the

manufacturer's instructions. Thereafter, the isolated lymphocytes were washed with PBS and incubated with the following fluorochrome-conjugated antibodies (all from BD Biosciences, New York, USA): FITC-GL7 (1:100; #553666), APC-B220 (1:100; #553092), PE-Fas (1:100; #555293), FITC-CD4 (1:100; #553651), APC-CXCR5 (1:100; #560615), PE-ICOS (1:100; #552146), FITC-CD19 (1:100; #553666), and APC-CD138 (1:100; #561705), and then assessed using a BD FACS Aria II Cell Sorter (BD Biosciences). The percentages of $CD4^+CXCR5^+ICOS^+$ Tfh cells, $GL7^+B220^+Fas^+$ GC B cells, and $CD19^+CD138^+$ plasma cells were analyzed using FlowJo software 6.0 (Tree Star Inc., Ashland, OR, USA).

Circulating Donor-Specific Antibodies

The levels of circulating DSA-IgG and DA-IgM in recipient serum were assessed by flow cytometry on day 10 as previously described (15). Briefly, recipient serum was obtained by centrifugation at 2,000 g and 20°C for 10 min. Donor lymphocytes were isolated from spleen cell suspensions using lymphocyte separation solution (Dakewe Biotech Co., Ltd.). Thereafter, the recipient serum was incubated with the donor lymphocytes at 37°C for 30 min. After being washed with PBS, the lymphocytes were incubated with anti-mouse IgG (1:100; #405305; BD Biosciences) and anti-mouse IgM (1:100; #406509; BD Biosciences) at 4°C for 1 h. Subsequently, the cells were analyzed by flow cytometry, with the results represented as mean fluorescence intensity to reflect the individual serum DSA levels.

Western Blot Analysis

Recipient splenic lymphocytes were obtained using lymphocyte separation solution (Dakewe Biotech Co., Ltd.) according to the manufacturer's instructions. The lymphocytes were homogenized in ice-cold radioimmunoprecipitation assay lysis buffer containing phenylmethylsulfonyl fluoride (PMSF) and phosphatase inhibitor. Lysates were centrifuged at 12,000 g and 4°C for 25 min, and the supernatant was subsequently collected. Total proteins were quantified by bicinchoninic acid assay. Thereafter, 20 μg proteins were separated *via* 10% sodium dodecyl sulfate-polyacrylamide gel electrophoresis and transferred onto a polyvinylidene difluoride membrane. After being blocked with 5% milk for 1 h, the membrane was incubated at 4°C overnight with the following primary antibodies (all from Cell Signaling Technology, Inc.): anti-P100/P52 (1:1,000; #4882), anti-RelB (1:1,000; #10544), and anti-β-actin (1:1,000; #3700). The membranes were washed using Tris-buffered saline with Tween-20 and incubated with horseradish peroxidase-conjugated goat anti-rabbit secondary antibody (1:5,000; Abcam) at room temperature for 1 h. The proteins were visualized using an enhanced chemiluminescence system (Thermo Fisher Scientific, Rockford, IL, USA). Band intensity was analyzed using ImageJ software and normalized to the value of β-actin.

Statistical Analysis

Data are presented as mean ± standard deviation (SD). SPSS 19.0 software (IBM Corp., Armonk, NY, USA) was used for statistical analysis of data among the three groups, using one-way analysis of variance followed by Bonferroni's correction. Differences in animal survival were analyzed using the log-rank test (with Kaplan–Meier survival curves). $P < 0.05$ was considered statistically significant.

RESULTS

CHBP Prolonged Skin Allograft Survival

We first investigated the effect of CHBP on skin allograft survival. Daily treatment with NS or CHBP was started after completion of the secondary skin transplantation. As shown in **Figure 1A**, the syngeneic group showed normal skin growth without hardening, incrustation, necrosis, or rejection. In contrast, the allogeneic group exhibited obvious rejection, starting from day 5, after the bandage was removed (which occurred on day 5), including progressive loss of hair, hardening, dermal necrosis, and scab formation. The first rejection was observed in the low-dose CHBP group (100 μg/kg) on day 6 and in the high-dose CHBP group (500 μg/kg) on day 9.

Consistent with skin allograft observations, the survival analysis showed that the syngeneic group displayed no rejection of skin allografts. In contrast, rejection in the allogeneic group started on day 11, and all the skin allografts were rejected by day 13. Additionally, rejection in the low-dose CHBP group started on day 12 and was completed on day 15, while rejection in the high-dose CHBP group started on day 14 and was completed on day 17 (**Figure 1B**). These results suggested that CHBP prolonged skin allograft survival, which was especially obvious in the high-dose group.

CHBP Decreased Inflammatory Cell Infiltration in the Skin Allograft

Based on the previous result, we used a dose of 500 μg/kg CHBP for the subsequent experiments. Histological examination of skin allografts in the syngeneic group on day 10 after secondary transplantation showed that the skin structure had normal morphology and low inflammatory cell infiltration in the dermis and subcutaneous tissue (**Figure 2A**). In contrast, obvious skin peeling and severe inflammatory cell infiltration was observed in the allogeneic group. CHBP improved the skin structure and led to a significant moderate decrease in the inflammatory cell infiltration.

CHBP Decreased $CD19^+$ B Cell Infiltration in the Skin Allograft

To investigate whether the CHBP-induced decrease in inflammatory cell infiltration involved B cells, $CD19^+$ B cells in skin allografts were subjected to immunochemistry staining. As shown in **Figure 2B**, the $CD19^+$ B cell infiltration was significantly increased in the allogeneic group compared to the syngeneic group. CHBP significantly decreased $CD19^+$ B cell infiltration compared to the level in the allogeneic group, implying that the prolonged skin allograft survival may be due to decreased $CD19^+$ B cell infiltration.

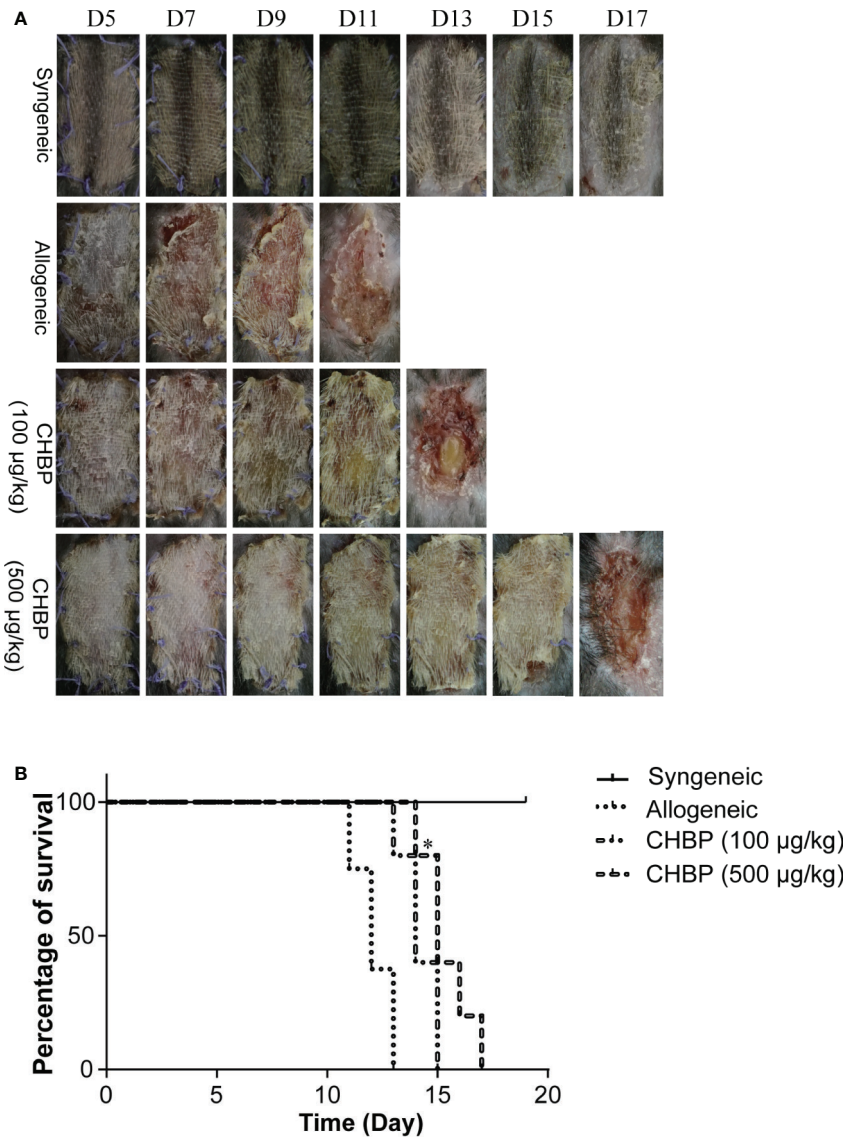


FIGURE 1 | CHBP prolonged skin allograft survival. **(A)** Photographs of skin allografts at various time points after secondary transplantation in each group. **(B)** Kaplan–Meier survival curves of mice in each group by day of post-transplantation. *P < 0.05: This P value is compared between the allogeneic group and the CHBP (500 μg/kg) group.

CHBP Decreased the Percentage of Plasma Cells in the Spleen

Plasma cells are important factors in organ rejection. To confirm whether plasma cells were altered (among the $CD19^+$ B cells), the percentage of plasma cells in the spleen of recipient mice was analyzed. As shown in **Figure 3A**, flow cytometry revealed that $CD19^+CD138^+$ plasma cells in the spleen 10 days after secondary transplantation were significantly increased in the allogeneic group compared to the syngeneic group. However, CHBP ameliorated the increase of plasma cells, with a significantly lower level compared to the level in the allogeneic group. This shows that CHBP decreased the percentage of plasma cells in recipient mice.

CHBP Decreased the Percentages of GC B Cells and Tfh Cells in the Spleen

Plasma cells are differentiated from GC B cells after being instructed by Tfh cells. The percentages of both $GL7^+B220^+Fas^+$ GC B cells and $CD4^+CXCR5^+ICOS^+$ Tfh cells were assessed by flow cytometry. The results revealed that the percentages of GC B cells and Tfh cells were significantly increased in the allogeneic group compared to the syngeneic group. CHBP significantly decreased the percentages of these cells compared to the levels in the allogeneic group (**Figures 3B, C**), suggesting that CHBP may reduce the differentiation of GC B cells into plasma cells by decreasing the percentages of Tfh cells and GC B cells.

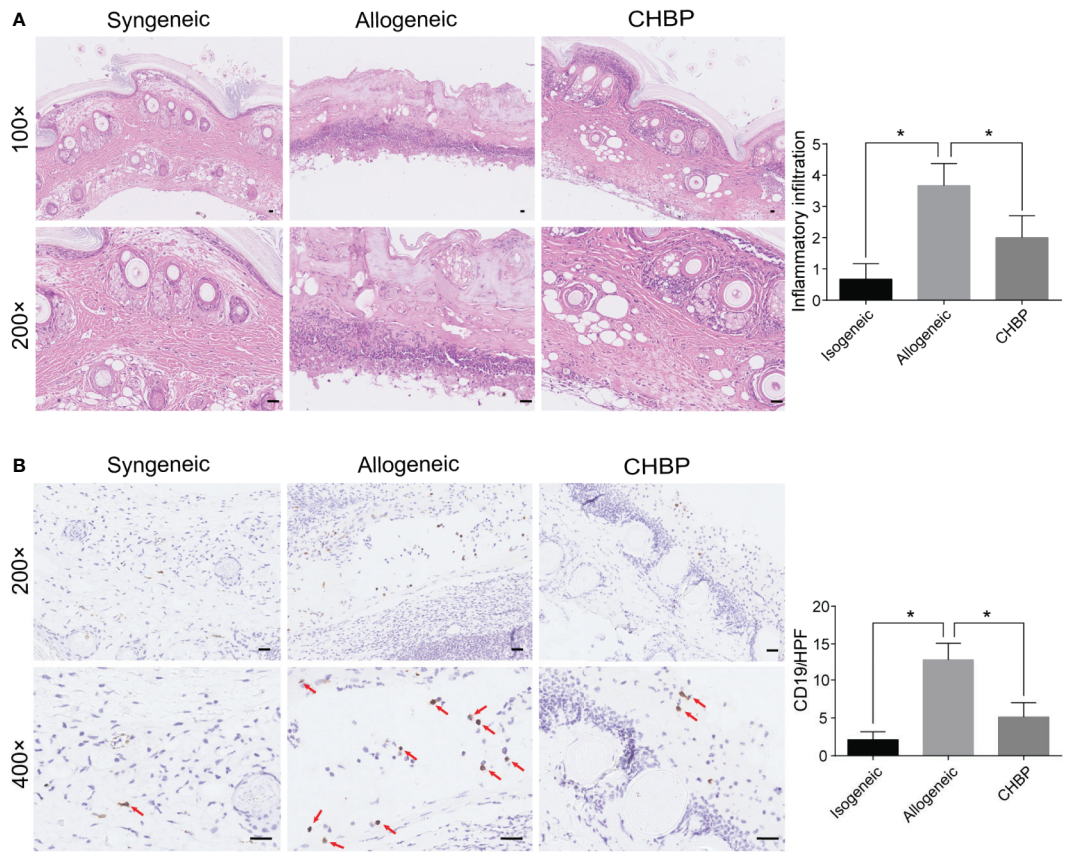


FIGURE 2 | CHBP decreased the inflammatory cell infiltration and CD19+ B cell infiltration in skin allografts. **(A)** Representative images of H&E staining in the syngeneic, allogeneic, and CHBP groups and semi-quantification of inflammatory cell infiltration in the three groups. **(B)** Representative images of immunohistochemical staining (IHC) for CD19 in the syngeneic, allogeneic, and CHBP groups and semi-quantification of IHC staining in the three groups. *P < 0.05.

CHBP Decreased the DSA Levels in Recipient Mice

DSAs are secreted by plasma cells. To assess whether CHBP affects the secretion of DSAs, the DSA-IgG and DSA-IgM levels in the serum of recipient mice were assessed 10 days after secondary skin transplantation. As shown in **Figure 4**, the levels of both DSA-IgG and DSA-IgM were significantly elevated in the allogeneic group compared to the syngeneic group. CHBP ameliorated these increases, with significantly lower levels compared to the levels in the allogeneic group, implying that CHBP may decrease the percentage of Tfh cells and GC B cells to reduce the differentiation of GC B cells into plasma cells, thereby decreasing the DSA levels.

CHBP Inhibited the NF-κB Signaling Pathway

The NF-κB signaling pathway is reported to be involved in B cell immune responses. To investigate whether the NF-κB pathway is involved in the inhibition of B cell immune responses by CHBP, we used western blotting to evaluate the protein expression of P100, RelB, and P52 in splenic lymphocytes. As shown in **Figure 5**, the NF-κB signaling pathway was activated in the splenic lymphocytes in the allogeneic group, as evidenced by significantly upregulated P100, RelB and P52 compared to the levels in the syngeneic group. CHBP obviously downregulated these proteins compared to the levels in the allogeneic group, suggesting that CHBP may inhibit the NF-κB signaling pathway and thereby inhibit B cell immune responses and decrease the DSA levels, thus reducing the occurrence of AMR.

DISCUSSION

CHBP is a newly synthesized peptide derived from EPO. Our previous studies indicated that CHBP protects against various conditions, including renal IRI, acute kidney injury, renal fibrosis, and acute myocardial infarction (8–13). Additionally, research has indicated that CHBP can ameliorate acute renal allograft rejection (14). Herein, the effect of CHBP on AMR was investigated. We found that treatment with CHBP prolonged skin allograft survival. The mechanism may involve inhibition of the NF-κB signaling pathway in order to inhibit B cell immune responses, thereby decreasing the DSA level and the occurrence of AMR.

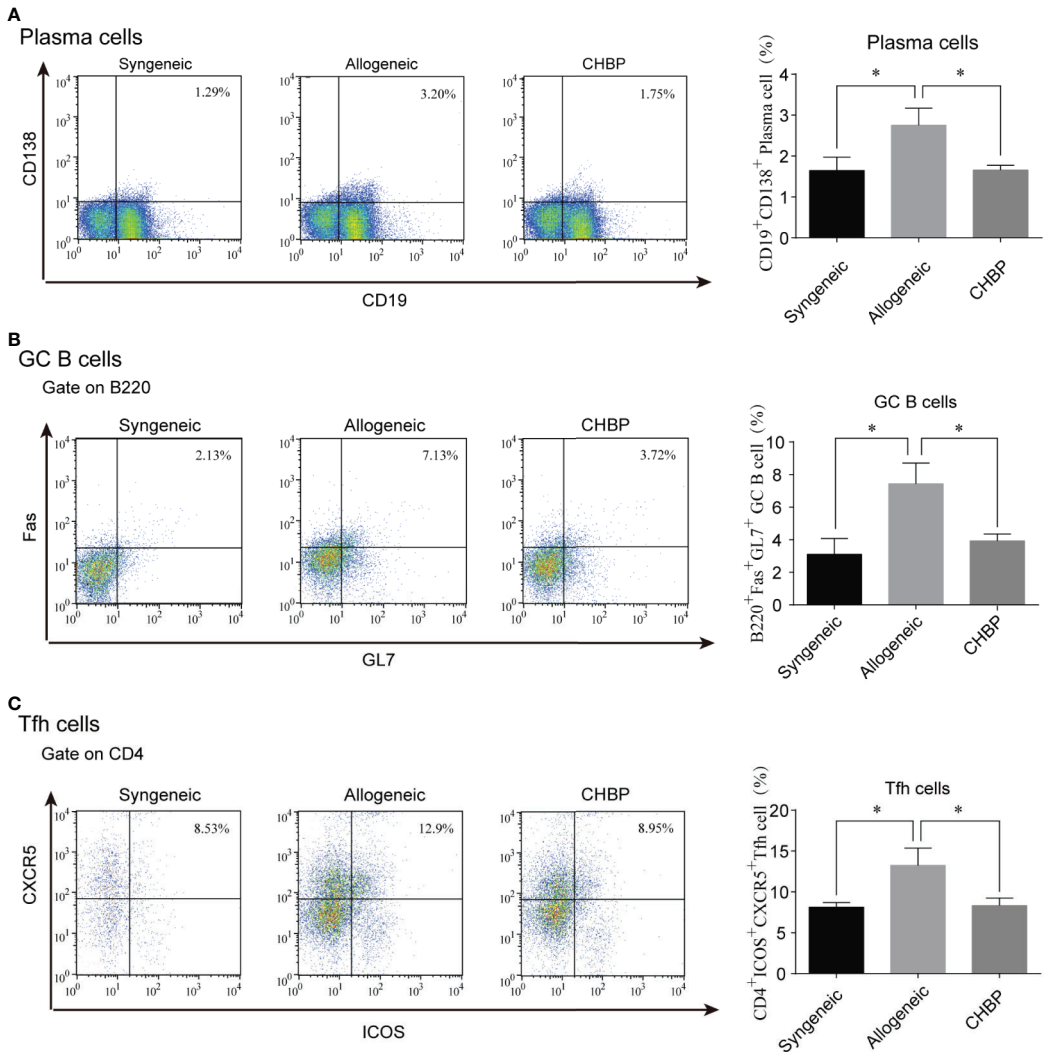


FIGURE 3 | CHBP decreased the percentages of plasma cells, GC B cells, and Tfh cells in the spleen. Percentages of **(A)** $CD19^+CD138^+$ plasma cells, **(B)** $GL7^+B220^+Fas^+$GC B cells, and **(C)** $CD4^+CXCR5^+ICOS^+$ Tfh cells in the spleen in each group. *P < 0.05.

AMR is mediated by immune responses involving B cells, which are one of the major cellular components that play vital roles in allograft rejection. AMR is the most vexing barrier to organ transplantation. The contributions of B cells during allograft rejection are reported to include serving as antigen-presenting cells to regulate the immune response, promoting $CD4^+$ T cell expansion and memory formation, and differentiating into plasma cells to secrete antibodies (16). GCs are specialized structures that conventionally form within secondary lymphoid organs, such as the spleen. In GCs, B cells undergo proliferation, hypermutation, selection, and differentiation, generating plasma cells (17, 18). The GC response arises from the interactions between B and Tfh cells. Tfh cells are a specialized subset of $CD4^+$ T helper cells, located in GCs to instruct GC B cells to proliferate and differentiate into plasma cells (19). Multiple studies have revealed that Tfh cells play an important role in B cell activation and antibody production. Chen et al. revealed that mice immunized with IL-7-overexpressing recombinant canine distemper virus (rCDV) exhibited significantly increased Tfh cell generation, GC formation, GC B and plasma cell generation, and antibody production (20). Furthermore, Elsner et al. reported that using IL-12 to block Tfh cell differentiation contributed to GC suppression, inhibiting humoral immunity (21), suggesting that inhibition of Tfh cell generation inhibits B cell immune responses and antibody production. In this study, we discovered that the percentages of Tfh cells and GC B cells were significantly elevated in the allogeneic group compared to the syngeneic group, while CHBP significantly decreased the percentages of these cells compared to the levels in the allogeneic group. Similar changes in the percentages of plasma cells were also observed, suggesting

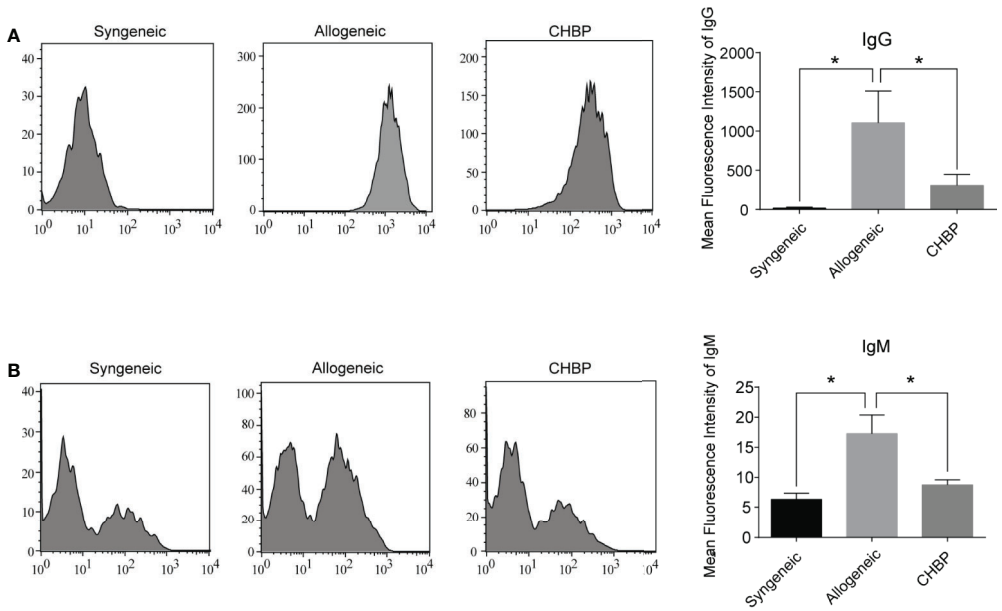


FIGURE 4 | CHBP decreased donor-specific antibodies (DSAs) in recipient mice. **(A)** DSA-IgG and **(B)** DSA-IgM level in recipient serum in each group were detected by flow cytometry and expressed as mean fluorescence intensity (MFI). *P < 0.05.

that the CHBP-induced prolonged skin allograft survival may be achieved by decreasing the percentages of Tfh cells and GC B cells, thus reducing the differentiation of GC B cells into plasma cells.

The differentiation of B cells into plasma cells to secrete DSAs is a critical component of the development of AMR and a major risk factor for allograft rejection (22–24). Given that the percentage of plasma cells decreased, the DSA levels were subsequently assessed. Consistent with the finding that CHBP significantly decreased the percentage of plasma cells compared to the level in the allogeneic group, corresponding significant decreases in the DSA-IgG and DSA-IgM levels were detected in the CHBP group compared to the allogeneic group. This implies that CHBP decreases the percentages of Tfh and GC B cells to reduce the differentiation of GC B cells into plasma cells; this, in turn, lowers the DSA levels, thus prolonging skin allograft survival.

The NF-κB signaling pathway is commonly regarded as being associated with cellular proliferation and plays an important role in the regulation of both innate and adaptive immunity (18, 25).

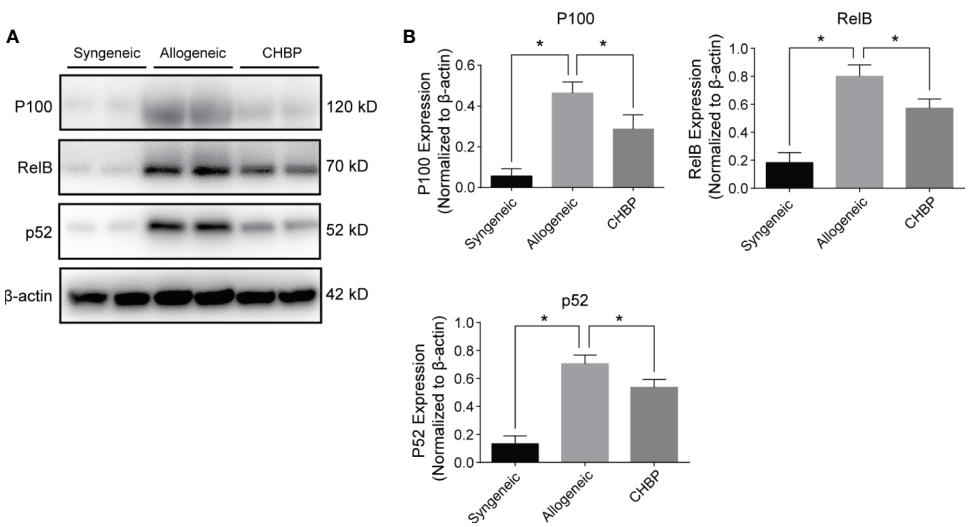


FIGURE 5 | CHBP inhibited NF-κB signaling pathway. **(A)** Representative western blot images of P100, RelB, P52, and β-actin in the syngeneic, allogeneic, and CHBP groups. **(B)** Ratios of P100, RelB, and P52 to β-actin. *P < 0.05.

B cells are one of the most critical components of innate and adaptive immunity, and B cell survival, apoptosis, proliferation, and class switch recombination are dependent on appropriate regulation of the NF-κB pathway (19, 25). Evidence from multiple studies has revealed that mice with constitutive activation of the NF-κB pathway exhibit autoimmunity, lymphomagenesis, and B cell hyperplasia (26–28), indicating the potential effects of NF-κB pathway activation on B cells. Another study indicated that conditional deletion of the transcription factor Relb in GC B cells led to the collapse of established GCs after day 7 of the GC response (29). In addition, knockout of the central component of the non-canonical NF-κB signaling pathway, NF-κB-inducing kinase (NIK), resulted in decreased Tfh cell generation (30), suggesting that the non-canonical NF-κB pathway may promote the development of Tfh cells and the GC response.

The NF-κB cascade is known to comprise two pathways, the canonical and non-canonical NF-κB pathways. The canonical NF-κB pathway results in the nuclear translocation of Rel, p65, and p50, and it is mainly involved in broad inflammatory responses in various cell types of the lymphoid system. The non-canonical NF-κB pathway leads to the nuclear translocation of RelB and P52, and it exhibits specific functions related to B cell biology (29, 31). In this study, non-canonical pathway signaling was assessed, and CHBP obviously downregulated P100, RelB, and P52, suggesting that CHBP may inhibit the NF-κB signaling pathway and thereby inhibit B cell immune responses, decrease the DSA levels, reduce the occurrence of AMR, and prolong skin allograft survival.

The main limitation of this study is that the NF-κB signaling pathway was assessed in splenic lymphocytes but not specifically in T and B cells. Compared to detection in splenic lymphocytes, specific detection in T and B cells would provide stronger evidence to explain the reduction in GC B and Tfh cells. Additionally, we only revealed that CHBP inhibited the occurrence of AMR in a secondary skin rejection model. The role of CHBP in AMR in other organ transplantation models, such as renal and lung transplantation, needs to be further explored.

In conclusion, this study revealed that CHBP prolonged skin allograft survival in mice. The mechanism may involve the inhibition of the NF-κB signaling pathway in order to inhibit B cell immune responses, thereby decreasing the DSA level and the occurrence of AMR.

DATA AVAILABILITY STATEMENT

The original contributions presented in the study are included in the article/supplementary material. Further inquiries can be directed to the corresponding authors.

ETHICS STATEMENT

The animal study was reviewed and approved by the Ethics Committee of Zhongshan Hospital, Fudan University.

AUTHOR CONTRIBUTIONS

DZ, CY, and RR conceived the study and participated in its design. LZ, XW, LH, WG, WZ, and XZ carried out the experiments. CH and LZ analyzed the data and drafted the manuscript. RR, CY, and DZ obtained the funding. All authors contributed to the article and approved the submitted version.

FUNDING

This study was supported by National Natural Science Foundation of China (81500569 to DZ, 81770747 to RR, 81770746 to CY, 81800659 to XW), National Key R&D Program of China (2018YFA0107501 to RR, 2018YFA0107502 to CY), Shanghai Rising-Star Program (19QA1406300 to CY), Medical and Health Talents Training Plan for the Excellent Youth of Shanghai Municipal (2018YQ50 to CY), 2019 Shanghai Youth Talent Development Program (to CY), and Fujian Provincial Health and Health Career Training Project for Young and Middle-aged Talents (2020GGB058 to DZ).

REFERENCES

1. Kenta I, Takaaki K. Molecular Mechanisms of Antibody-Mediated Rejection and Accommodation in Organ Transplantation. *Nephron* (2020) 144(Suppl 1):2–6. doi: 10.1159/000510747
2. Suchanek O, Clatworthy MR. Novel Strategies to Target the Humoral Alloimmune Response. *HLA* (2020) 96(6):667–80. doi: 10.1111/tan.14092
3. Dijke EI, Platt JL, Blair P, Clatworthy MR, Patel JK, Kfoury AG, et al. B Cells in Transplantation. *J Heart Lung Transplant* (2016) 35(6):704–10. doi: 10.1016/j.healun.2016.01.1232
4. Hao Y, Li Z, Wang Y, Liu X, Ye L. Analyzing Mouse B Cell Responses Specific to LCMV Infection. *Methods Mol Biol* (2018) 1707:15–38. doi: 10.1007/978-1-4939-7474-0_2
5. Kerfoot SM, Yaari G, Patel JR, Johnson KL, Gonzalez DG, Kleinstein SH, et al. Germinal Center B Cell and T Follicular Helper Cell Development Initiates in the Interfollicular Zone. *Immunity* (2011) 34(6):947–60. doi: 10.1016/j.immuni.2011.03.024
6. Pardi N, Hogan MJ, Naradikian MS, Parkhouse K, Cain DW, Jones L, et al. Nucleoside-Modified mRNA Vaccines Induce Potent T Follicular Helper and Germinal Center B Cell Responses. *J Exp Med* (2018) 215(6):1571–88. doi: 10.1084/jem.20171450
7. Zhang C, Yang C, Zhu T. From Erythropoietin to its Peptide Derivatives: Smaller But Stronger. *Curr Protein Pept Sci* (2017) 18(12):1191–4. doi: 10.2174/1389203717666160909130006
8. Yang C, Xu Z, Zhao Z, Li L, Zhao T, Peng D, et al. A Novel Proteolysis-Resistant Cyclic Helix B Peptide Ameliorates Kidney Ischemia Reperfusion Injury. *Biochim Biophys Acta* (2014) 1842(11):2306–17. doi: 10.1016/j.bbadis.2014.09.001
9. Liu A, Wu J, Yang C, Wu Y, Zhang Y, Zhao F, et al. TRPM7 in CHBP-induced Renoprotection Upon Ischemia Reperfusion-Related Injury. *Sci Rep* (2018) 8 (1):5510. doi: 10.1038/s41598-018-22852-2

10. Zeng Y, Zheng L, Yang Z, Yang C, Zhang Y, Li J, et al. Protective Effects of Cyclic Helix B Peptide on Aristolochic Acid Induced Acute Kidney Injury. *Biomed Pharmacother* (2017) 94:1167–75. doi: 10.1016/j.biopha.2017.07.131
11. Yang C, Cao Y, Zhang Y, Li L, Xu M, Long Y, et al. Cyclic Helix B Peptide Inhibits Ischemia Reperfusion-Induced Renal Fibrosis Via the PI3K/Akt/FoxO3a Pathway. *J Trans Med* (2015) 13:355. doi: 10.1186/s12967-015-0699-2
12. Qi R, Zhang W, Zheng L, Xu M, Rong R, Zhu T, et al. Cyclic Helix B Peptide Ameliorates Renal Tubulointerstitial Fibrosis Induced by Unilateral Ureter Obstruction Via Inhibiting NLRP3 Pathway. *Ann Trans Med* (2020) 8(5):167. doi: 10.21037/atm.2020.02.12
13. Yang C, Zhang C, Jia J, Wang L, Zhang W, Li J, et al. Cyclic Helix B Peptide Ameliorates Acute Myocardial Infarction in Mice by Inhibiting Apoptosis and Inflammatory Responses. *Cell Death Discov* (2019) 5:78. doi: 10.1038/s41420-019-0161-y
14. Yang C, Zhang Y, Wang J, Li L, Wang L, Hu M, et al. A Novel Cyclic Helix B Peptide Inhibits Dendritic Cell Maturation During Amelioration of Acute Kidney Graft Rejection Through Jak-2/STAT3/SOCS1. *Cell Death Dis* (2015) 6:e1993. doi: 10.1038/cddis.2015.338
15. Zhao D, Li S, Liao T, Wei Y, Liu M, Han F, et al. Triptolide Inhibits Donor-Specific Antibody Production and Attenuates Mixed Antibody-Mediated Renal Allograft Injury. *Am J Transplant* (2018) 18(5):1083–95. doi: 10.1111/ajt.14602
16. DiLillo DJ, Griffiths R, Seshan SV, Magro CM, Ruiz P, Coffman TM, et al. B Lymphocytes Differentially Influence Acute and Chronic Allograft Rejection in Mice. *J Immunol* (2011) 186(4):2643–54. doi: 10.4049/jimmunol.1002983
17. Silva-Cayetano A, Linterman MA. Stromal Cell Control of Conventional and Ectopic Germinal Centre Reactions. *Curr Opin Immunol* (2020) 64:26–33. doi: 10.1016/j.coi.2020.03.007
18. De Silva NS, Klein U. Dynamics of B Cells in Germinal Centres. *Nat Rev Immunol* (2015) 15(3):137–48. doi: 10.1038/nri3804
19. Walsh NC, Waters LR, Fowler JA, Lin M, Cunningham CR, Brooks DG, et al. LKB1 Inhibition of NF-kappaB in B Cells Prevents T Follicular Helper Cell Differentiation and Germinal Center Formation. *EMBO Rep* (2015) 16 (6):753–68. doi: 10.15252/embr.201439505
20. Chen C, Zhou M, Yan XG, Chen YX, Cui M, Chen HC, et al. A Recombinant Canine Distemper Virus Expressing Interleukin-7 Enhances Humoral Immunity. *J Gen Virol* (2019) 100(4):602–15. doi: 10.1099/jgv.0.001247
21. Elsner RA, Shlomchik MJ. IL-12 Blocks Tfh Cell Differentiation During Salmonella Infection, Thereby Contributing to Germinal Center Suppression. *Cell Rep* (2019) 29(9):2796–809.e5. doi: 10.1016/j.celrep.2019.10.069
22. Harrison DK, Waldrip ZJ, Burdine L, Shalin SC, Burdine MS. DNA-PKcs Inhibition Extends Allogeneic Skin Graft Survival. *Transplantation* (2021) 105 (3):540–9. doi: 10.1097/TP.0000000000003442
23. Imamura R, Matsuda Y, Tsutahara K, Nonomura N, Takahara S. Impact of Immunoglobulin M-type Donor-Specific Human Leukocyte Antigen-Antibody Levels in Supernatants From Cultured Peripheral Blood Mononuclear Cells as Predictors of Antibody-Mediated Rejection. *Pathogens* (2020) 9(9):733. doi: 10.3390/pathogens9090733
24. Bertrand D, Gatault P, Jaureguy M, Garrouste C, Sayegh J, Bouvier N, et al. Protocol Biopsies in Patients With Subclinical De Novo Donor-Specific Antibodies After Kidney Transplantation: A Multicentric Study. *Transplantation* (2020) 104(8):1726–37. doi: 10.1097/TP.0000000000003055
25. Goetz CA, Baldwin AS. NF-Kappab Pathways in the Immune System: Control of the Germinal Center Reaction. *Immunol Res* (2008) 41(3):233–47. doi: 10.1007/s12026-008-8033-1
26. Homig-Holzel C, Hojer C, Rastelli J, Casola S, Strobl LJ, Muller W, et al. Constitutive CD40 Signaling in B Cells Selectively Activates the Noncanonical NF-kappaB Pathway and Promotes Lymphomagenesis. *J Exp Med* (2008) 205 (6):1317–29. doi: 10.1084/jem.20080238
27. Tavares RM, Turer EE, Liu CL, Advincula R, Scapini P, Rhee L, et al. The Ubiquitin Modifying Enzyme A20 Restricts B Cell Survival and Prevents Autoimmunity. *Immunity* (2010) 33(2):181–91. doi: 10.1016/j.immuni.2010.07.017
28. Xie P, Stunz LL, Larison KD, Yang B, Bishop GA. Tumor Necrosis Factor Receptor-Associated Factor 3 is a Critical Regulator of B Cell Homeostasis in Secondary Lymphoid Organs. *Immunity* (2007) 27(2):253–67. doi: 10.1016/j.immuni.2007.07.012
29. De Silva NS, Anderson MM, Carette A, Silva K, Heise N, Bhagat G, et al. Transcription Factors of the Alternative NF-kappaB Pathway are Required for Germinal Center B-cell Development. *Proc Natl Acad Sci U S A* (2016) 113 (32):9063–8. doi: 10.1073/pnas.1602728113
30. Hu H, Wu X, Jin W, Chang M, Cheng X, Sun SC. Noncanonical NF-kappaB Regulates Inducible Costimulator (ICOS) Ligand Expression and T Follicular Helper Cell Development. *Proc Natl Acad Sci U S A* (2011) 108(31):12827–32. doi: 10.1073/pnas.1105774108
31. De Leo P, Gazzurelli L, Baronio M, Montin D, Di Cesare S, Giancotta C, et al. NFKB2 Regulates Human Tfh and Tfr Pool Formation and Germinal Center Potential. *Clin Immunol* (2020) 210:108309. doi: 10.1016/j.clim.2019.108309

Conflict of Interest: The authors declare that the research was conducted in the absence of any commercial or financial relationships that could be construed as a potential conflict of interest.

Copyright © 2021 Zheng, Wang, Hu, Gao, Zhang, Zhang, Hu, Rong, Yang and Zhu. This is an open-access article distributed under the terms of the Creative Commons Attribution License (CC BY). The use, distribution or reproduction in other forums is permitted, provided the original author(s) and the copyright owner(s) are credited and that the original publication in this journal is cited, in accordance with accepted academic practice. No use, distribution or reproduction is permitted which does not comply with these terms.

frontiers in Immunology

REVIEW
published: 19 May 2021
doi: 10.3389/fimmu.2021.654540

Dendritic Cells: Versatile Players in Renal Transplantation

Jinwen Lin[1,2,3†], *Hongyi Wang*[4†], *Chenxi Liu*[4†], *Ao Cheng*[4], *Qingwei Deng*[4], *Huijuan Zhu*[5] *and Jianghua Chen*[1,2,3*]

[1] Kidney Disease Center, The First Affiliated Hospital, College of Medicine, Zhejiang University, Hangzhou, China, [2] Key Laboratory of Kidney Disease Prevention and Control Technology, National Key Clinical Department of Kidney Disease, Institute of Nephrology, Zhejiang University, Hangzhou, China, [3] The Third Grade Laboratory under the National State, Administration of Traditional Chinese Medicine, Hangzhou, China, [4] Xiangya School of Medicine, Central South University, Changsha, China, [5] Department of Pathology, The First Affiliated Hospital, College of Medicine, Zhejiang University, Hangzhou, China

Dendritic cells (DCs) induce and regulate adaptive immunity through migrating and maturing in the kidney. In this procedure, they can adopt different phenotypes—rejection-associated DCs promote acute or chronic injury renal grafts while tolerogenic DCs suppress the overwhelmed inflammation preventing damage to renal functionality. All the subsets interact with effector T cells and regulatory T cells (Tregs) stimulated by the ischemia–reperfusion procedure, although the classification corresponding to different effects remains controversial. Thus, in this review, we discuss the origin, maturation, and pathological effects of DCs in the kidney. Then we summarize the roles of divergent DCs in renal transplantation: taking both positive and negative stages in ischemia–reperfusion injury (IRI), switching phenotypes to induce acute or chronic rejection, and orchestrating surface markers for allograft tolerance *via* alterations in metabolism. In conclusion, we prospect that multidimensional transcriptomic analysis will revolute researches on renal transplantation by addressing the elusive mononuclear phagocyte classification and providing a holistic view of DC ontogeny and subpopulations.

Keywords: dendritic cells, renal transplantation, rejection, tolerance, ischemic–reperfusion injury

OPEN ACCESS

Edited by:
Cheng Yang,
Fudan University, China

Reviewed by:
Helong Dai,
Central South University, China
Qi Cao,
Westmead Institute for Medical Research, Australia

****Correspondence:***
Jianghua Chen
chenjianghua@zju.edu.cn

†These authors have contributed equally to this work

Specialty section:
This article was submitted to Alloimmunity and Transplantation, a section of the journal Frontiers in Immunology

Received: *16 January 2021*
Accepted: *22 April 2021*
Published: *19 May 2021*

Citation:
Lin J, Wang H, Liu C, Cheng A, Deng Q, Zhu H and Chen J (2021) Dendritic Cells: Versatile Players in Renal Transplantation. Front. Immunol. 12:654540. doi: 10.3389/fimmu.2021.654540

INTRODUCTION

In all tissues, DCs function in a network of mononuclear phagocytes with many innate immune cells taking center stage (1). This network in the kidney is complex and heterogeneous, highly relying on macrophages and DCs (2). Discovered by Metchnikoff 150 years ago, macrophages can mediate fibrosis after renal transplantation, whereas DCs were first described in 1973 by Steinman and Cohn as even elongated or stellate cells to present antigens. Given that DCs and macrophages are both involved in innate immune networks, DCs should have overlapping functionalities as macrophages in tissue homeostasis, promoting pathogen defense and contributing to acute or chronic rejection (2, 3). But compared with macrophages, the unique roles of DCs in rejection or tolerance are still ambiguous and undefined partly because they often share similar surface markers (4–7). Equipped with increasingly available kidney biopsy data, the recent outbreak in the high-dimensional analysis of single-cell has sparked instructions for the classification of these immune cells (8–11). In this review, we first describe the consensus of DC ontogeny encompassing the origins, maturation, and pathological effects of DCs

in the kidney. We then summarize the major roles of kidney DCs in three major aspects of renal transplantation, including ischemic injury when grafts are removed from the donors, rejection including acute and chronic process, and tolerance including induced or natural genic tolerance. Finally, we point out certain obstacles and disadvantages to prospect the value of multidimensional transcriptomic analysis.

DC-LINKED PATHOLOGICAL PROCEDURE IN RENAL TRANSPLANTATION

The Origin and Migration of DCs in Kidney Allograft Rejection

Like other tissues, dendritic cells in the kidney are derived from bone hematopoietic stem cells (**Figure 1**). Traditionally, cell surface markers were used to subdivide cDCs into cDC1 and cDC2 (12). Human cDC1 mainly expressed CD11c, CD141, CLEC9A (C-type lectin domain family 9 member A) and highly expressed MHC (major histocompatibility complex) class II, while cDC2 mainly expressed CD11c, high- affinity Fc receptor for immunoglobin E, CD1c, CD1a and highly expressed CD11c and MHC class II. CD11c, MHC class II, CD26, and interferon-regulatory factor 8 (IRF8) are highly expressed in murine cDC1, and CLEC9A, XCR1, and CD103 are also expressed. In mice, cDC2 expresses high CD11c, MHC class II, CD11b, CD26, CX3CR1, interferon-regulatory factor 4, dendritic cell inhibitory receptor 2 but expresses low IRF8 and F4/80 (**Table 1**).

Moreover, traditional DC subsets are described by lineage-specific transcription factors including DNA binding inhibitor 2 and interferon regulatory factor 4. In mice, the conventional DC group 1 (cDC1) express neither SiglecH nor Ly6C, while the precursor of the conventional DC group 2 (cDC2) express no SiglecH but Ly6C (21). Based on these transcription factors, phagocytes expressing major histocompatibility complex (MHC) class II and integrin CD11c are named cDCs. Another independent subgroup, unconventional plasma-like dendritic cells, expressed transcription factor E2-2 and its myeloid antigen but did not express CD123. Whether they are related to traditional DC is still doubtable.

During circulation, the precursor dendritic cells develop and differentiate into kidney-specific dendritic cells (22). In the kidney, no more than 5% of dendritic cells are cDC1 expressing CD103; most DCs express CD11b and CX3CR1 and can be categorized into cDC2. Compared with dendritic cells in other parts of the body, kidney-specific dendritic cells can be

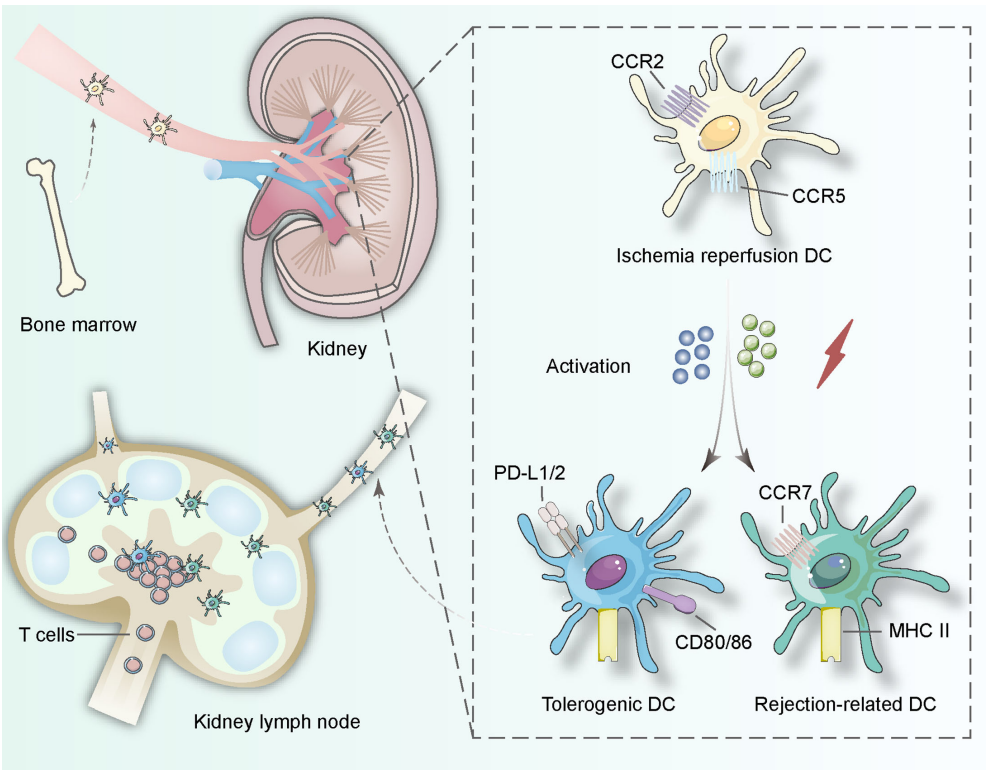


FIGURE 1 | DCs in the kidney originate from bone hematopoietic stem cells and involve in lymphatic recycling *in vivo*. When ischemia–reperfusion occurs, immature DCs start to search for interactions with T lymphocytes and change their surface proteins including CCR2, CCR5 to induce tolerance procedure (expressing PD-L1/2 and CD80/86) or rejection procedure (expressing CCR7 and MHC class II). The activation can be derived from pathogen-associated molecular patterns and danger-associated molecular patterns in the procedure of ischemia-reperfusion.

TABLE 1 | Remarkable features of three different types of DCs in renal transplantation.

Clinical subsets	General functions	Key markers	References
DCs in IRI	Promotion of both inflammation and anti-inflammation	CD45, CD11c, MHC-II, TNF-α, CD80, CD86, CD40, CD54, C1d, CD8 α, but not CD4 and CD205	(13, 14)
Rejection-related DCs	Promoting acute rejection and chronic rejection *via* different interaction with T cells	CD11c, MHC class II, CD1c, FcεRI	(15)
Tolerogenic DCs	Inducing anti-rejection effects *via* suppressing various types of T cells and activating Treg cells	poor expression of MHC, T cell co-stimulatory molecules like CD40, CD80/86, and T cell co-inhibitory ligands (*e.g.*, programmed death ligand-1 and death-inducing ligands)	(16–20)

FcεRI, high- affinity Fc receptor for IgE; MHC, major histocompatibility complex.

located in the lymph nodes around the kidney and the kidney itself, which is essential for the control of adaptive immunity (23) (**Figure 1**). In the kidney, most of these phagocytes with the ability to activate T cells are located in the cortex. It can be confirmed that cDC1 is located near the blood vessels, while most of these cells near the subcapsular and arterial connective tissue have the morphology of macrophages. The high osmotic pressure of transplanted medulla may inhibit the antigen presentation of DCS to $CD8^+$ T cells, but the specific type of DCs still needs to be further studied.

Chemokines and corresponding receptors induce the migration of kidney-specific DCs. Chemokines are detected by receptors on the surface of precursor DCs and precursor DCs can migrate along the inverse chemical gradient pathway to the source. Receptor expression determines the specificity of kidney DCs. CX3CR1 and CCR2 are incorporated into the action of leaving the bone marrow, and CXCR4 helps precursor DCs retention in the marrow (24–26). But the inflammatory conditions after transplantation possibly alter the migration mechanism to mediate both rejection and tolerance, which remain unidentified and might be potential intervention sites in the future (**Figure 1**).

The Maturation of DCs in Kidney Allograft Rejection

With no stimuli, immature kidney DCs inhibit T and B lymphocytes, which also can coordinate tolerance (25). Danger-associated molecular patterns occur when ischemia and reperfusion happen, activating TLR4 (toll-like receptor 4) and leading to the maturation of DCs (27–29). This maturation induces inflammation and provokes adaptive immunity to specific antigens, such as alloantigen and so on (30, 31). According to Sporri and Reis e Sousa's report, danger-associated molecular patterns (DAMPs) cannot make DCs promote T-helper responses, but exposure to pathogen-associated molecular patterns can (32). Taken together, DAMPs are not the most crucial pathway to activate DCs for allograft rejection (33–36). Furthermore, rejection can happen in T lymphocyte deficient conditions, implying that the maturation of DCs might be more than a complex mechanism triggered by DAMPs or pathogen-associated molecular patterns (37–40).

The Possible Downstream Effects of DCs in Kidney Allograft Rejection

Conventional hypothesis indicated donor DCs activate anti-donor rejection *via* migration to the host second lymphoid nodes providing alloantigen to recipient T cells (41). This hypothesis resulted from observations on mouse models: T lymphocytes respond to antigen-presenting cells with non-self-MHC (major histocompatibility complex) *in vivo* (42, 43). Moreover, depleting leukocytes in the allografts drives long-term survival, whereas injecting donor DCs into the host restores acute rejection (44–49). Later research established that donor and recipient DCs play equal roles in mediating the rejection process, and recipient DCs are even more stable to present antigens. Deleting recipient DCs prolonged allograft survival significantly but depleting donor DCs did not (50). Also, DCs lacking MHC or CD80/86 molecules are killed by recipient natural killer cells during migration to the lymphoid nodes (50–53). Recently, donor DCs are viewed as transporters of antigen rather than presenters of antigen (54). MHC molecules can be exchanged between the donor and recipient DCs (55, 56). Therefore, recipient DCs gain non-self MHC from donor DCs, capable to activate T lymphocytes originated from recipients through both non-self MHC and self MHC (57–62).

The basic function of mouse cDC1 is to use MHC class I molecules on its surface to extract antigens from $CD8^+$ cytotoxic T cells and induce them to kill target cells. This plays a decisive role in the process of renal transplantation and may be directly related to cellular immunity. Also, mouse cDC1 can induce regulatory T cells in lymphatic circulation (63, 64). The function of human cDC1, which is different from that of mice, needs further study. However, compared with cDC1, cDC2 generally does not have the aforementioned antigen targeted by cytotoxic T cells (65–67). Therefore, in renal transplantation, cDC2 will not be killed by cytotoxic T cells but can induce B cells to respond through helper T cells, which may be the mechanism of antibody-mediated immune rejection (68). Finally, it has been revealed that cDC2 cells induce T helper cells to stimulate the production of pro-inflammatory mediators in the chronic renal inflammation model, so in the same chronic rejection, cDC2 may also be the center of inflammation and participate in the pathogenesis of immune effectors including antibodies.

DCs IN IRI

IRI happens frequently following renal transplantation *via* recruitment of immune cells including DCs by pro-inflammatory cytokines like tumor necrosis factor derived from hypoxic endothelial cells (13, 69) (**Figure 2**). The DCs involved in IRI have not been completely defined. Current studies tend to

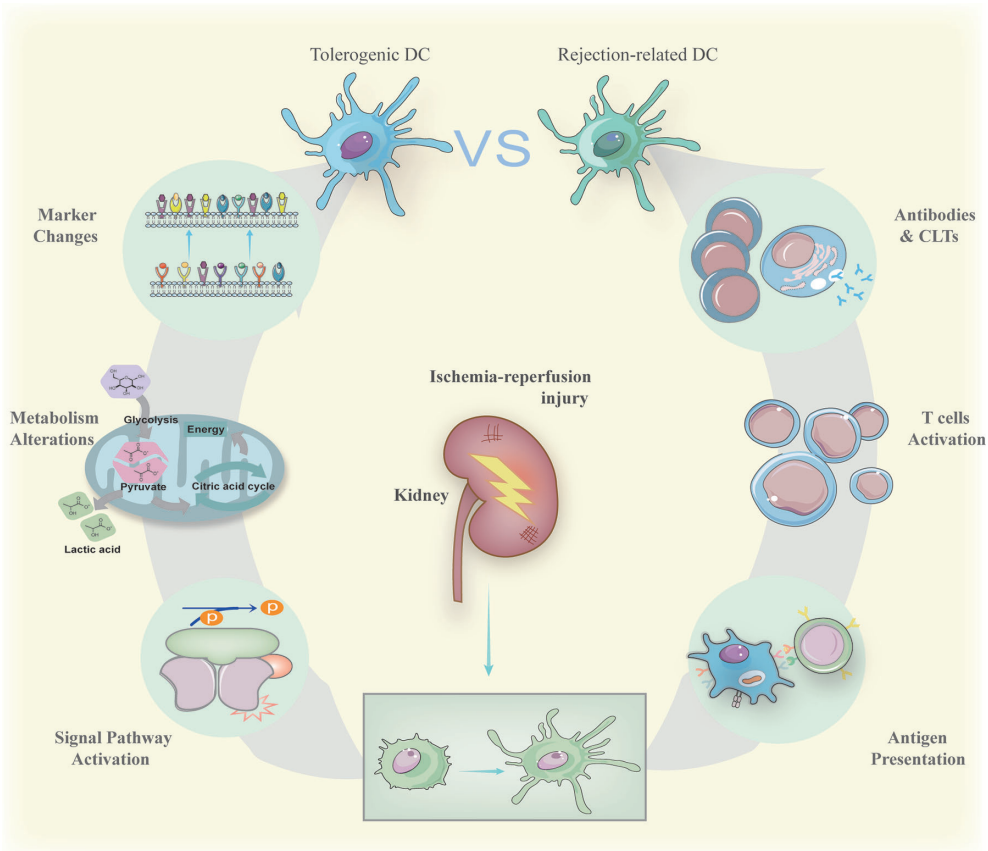


FIGURE 2 | Immature DCs can be activated by antigens derived from ischemia-reperfusion and act as the role of powerful antigen-presenting cells to trigger antibody-mediated rejection and cell-mediated rejection. The result of antibody-mediated rejection is activated B cell releasing harmful antibodies while active cytotoxic T cells kill donor cells forming cell-mediated rejection. On the contrary, when treated by specific drugs, immature DCs can also maintain their surface markers to suppress possible inflammation caused by transplantations *via* signal pathways activation regulating metabolism alterations. The signal pathways include NF-κB and mTOR summarized in the section *The Generation of Tolerogenic DCs*. The metabolism alterations involve glycometabolism and lipid metabolism with more details in the section *The Generation of Tolerogenic DCs*.

claim that DCs involved in IRI express CD45, CD11c, MHC-II, TNF-α, CD80, CD86, CD40, CD54 (ICAM), C1d, CD8 α, but not CD4 and CD205. All the markers might be useful in further investigations (**Table 1**). Then hypoxia-inducible factor 1α induces kidney DC maturation, damaging renal functionality (70–72). DCs can promote harmful activations of immune effects *in vivo*, but they are also associated with protecting renal function from IRI. Since immature DCs are less stimulatory than mature DCs, some researchers supposed that kidney DCs' role is to harm allograft (73–76). DCs feature in IL-10 as well as single Ig IL-1-related receptor, therefore, exhibiting the inhibiting effects on inflammation in IRI (77). On the contrary, immature kidney DCs can serve as an adverse player to mature DCs, preventing IRI (78, 79). Thrombin could release IL-12, IL-17, and C3a thus causing T helper-1 bias to influence kidney DCs' behaviors and determine the outcomes of IRI (80). High concentrations of tissue factors in the kidney may also contribute to IRI (81). Further studies are warranted to clarify the discrepancy about kidney DCs, especially the relationship between rejection-related DCs and tolerogenic DCs (**Figure 2**).

REJECTION-RELATED DCs IN ALLOGRAFTS

The traditional function of DCS is to mediate the rejection of harmful non-autogenous substances or abnormal autogenous materials, so the research on rejection-related DCs mostly employs traditional surface markers of cDCs. Although it is not recommended to judge the types of DCs based on only one surface marker, the comprehensive use of different surface markers can still accurately define rejection-related DCs (**Table 1** for specific markers).

Acute Rejection Based on the DC-Dependent Mechanism

The interaction between DCs and T lymphocytes triggers a so-called acute rejection through the conventional pathway—donor DCs present alloantigen to recipient T cells directly (82, 83) (**Figure 2**). At first, the ischemia–reperfusion condition drives donor DCs to induce acute rejection (14). Secondly, active DCs search for immature or memory T cells attracted by the chemical

gradient of CCR7 to present the allografts (84). Early studies usually located this process in second lymphoid organs (85), while later observation indicated that second lymphoid organs are not necessary for acute rejection: acute rejection occurs even when lacking secondary lymphoid organs (86, 87). The identical role of DCs in acute renal rejection could be separated into interaction with memory T cells and naive T cells, which happens in many different places including the second lymphoid organs. Taken different DCs into consideration, recipient DCs may be germane to the acute rejection as well as donor DCs (88).

Chronic Rejection Based on the DC-Dependent Mechanism

Owing to a longer lifespan, recipient DCs are more likely to mediate the chronic rejection rather than donor DCs. According to observations in mouse kidney grafts, the recipient DCs replace most of the donor DCs within 24 h after surgery, and over 90% DCs are derived from recipients on the 7th day after transplantation (57). Subsequently, these DCs originated from monocytes in the host, but a few donor DCs still survive to activate T cells (57). The interaction between DCs and T cells has been more stable and prolonged since DCs reach into the renal cortex to arrest antigen-specific T cells around the endothelium with no regard to the chemical gradient. Independent of the chemical gradient, interruption of the protracted connection with T cells induces tolerance (89, 90). Also, infiltrating DCs activate B cells to promote chronic allograft rejection with the assist of T helper cells. This procedure depends on recipient DCs presenting antigen to recipient T helper cells, but the molecular mechanism remains elucidated (91–94). A few clinical trials are targeting this approach, whereas more current studies are paying attention to mediate tolerance taking advantage of the tolerogenic DCs and Tregs (95).

TOLEROGENIC DCs IN RENAL TRANSPLANTATION

Remarkable Features of Tolerogenic DCs

As a pivotal part of innate immunity, tolerogenic DCs are usually defined as immature rejection-related DCs (96, 97). Tolerogenic DCs, also called DCregs, circulate in the body quiescently responding to endogenous or exogenous stimuli, for example, endogenous alarmins. These tolerogenic DCs exhibit poor expression of MHC, T cell co-stimulatory molecules like CD40, CD80/86, as well as T cell co-inhibitory ligands (*e.g.*, programmed death ligand-1 and death-inducing ligands), presenting non-phagocyte properties (16–20) (**Table 1**). Meanwhile, these DCs express a larger amount of the macrophage inhibitor cytokine than rejection-related DCs (98). Moreover, tolerogenic DCs can change the amount of C1q on its surface approaching the mature state with the assistance of globular C1q receptors (99, 100). C1q, a complement subunit, mediates IL-10 secretion involved in the interaction between DCs and myeloid or lymphoid cells (101–103). Besides, tolerogenic DCs confine promoting inflammatory factors including IL-12p70 into a low level while producing a high level of anti-inflammatory molecular-like transforming growth factor β as well as IL-10 (104) (**Figure 3**).

According to transcription analysis, the Wnt/β-catenin pathway programs tolerogenic DCs to maintain a series of unique molecular markers (105–108), and tolerogenic DCs specifically express some genes, including CNGA1, CCL18, C1QB, MUCL1, MAP7, C1QC, CYP7B1, and CYP24A1 (109). Compared to immunologic DC, tolerogenic DCs possess a steady oxidative phosphorylation program and favor fatty acid oxidation associated with decreased reactive oxygen species (110). Based on these features, tolerogenic DCs stimulate T cells weakly or even suppress the function of T cells *via* anergy or apoptosis for long-term immaturity (111). Additionally, tolerogenic DCs can spare, expand, and induce Tregs as shown in **Figure 3** (111–113). The interaction between tolerogenic DCs and divergent T cells results in conditions such as allograft rejection, hematopoietic stem cell transplantation, graft-*versus*-host diseases, and autoimmune disorders (111, 114–116). But the specific mechanism buried in these phenomena remains elusive. Therefore, an increasing number of studies incorporate tolerogenic DCs into clinical trials in organ transplantation and autoimmune diseases (117–119).

Tolerogenic DCs Possible Anti-Rejection Effects

DCs inducing tolerance was first discovered in 1995/1996 (120, 121). Tolerogenic DCs have the potential to suppress allograft rejection because DCs with $CD16^-$ markers exist in transplant recipients compared with healthy people using single-cell RNA sequence (122). Also, infusion of tolerogenic DCs appears to be reliable and acceptable with or without immunosuppressive agents, which probably provides anti-rejection therapy in the future (111, 123). Ezzelarab et al. infused donor-derived tolerogenic DCs processed by vitamin D3, IL-10 into rhesus macaque models, showing that graft survival prolonged with no evidence of host sensitization (124). Autologous tolerogenic DC infusion could also lengthen the survival time of grafts, and murine IL-10-induced DCs can function as rejection inhibitors *in vivo* and *in vitro* expressing lower levels of MHCII, CD40, CD86, CD205 (125–127).

Donor-derived tolerogenic DCs can interact with alloreactive memory T cells including $CD8^+$ and $CD4^+$ cells (128, 129) (**Figure 3**). In specific, tolerogenic DCs increase allograft survival time relying on co-inhibition of cytotoxic T lymphocyte antigen-4 (CTLA-4) downregulation (128) (**Figure 3**), and coinhibitory CTLA-4 blocker treatment has the potential to improve prognosis in renal allografts (130, 131). Moreover, DC-induced $CD95^+$ memory T cells could be an immunosuppressive phenotype with increased expression of programmed death-1 as well as coinhibitory CTLA-4 *via* Eomesodermin (an essential transcription factor maintenance) (124, 128, 132). Thereafter, the infusion of coinhibitory CTLA-4 immune globulin and tolerogenic DCs promotes transplant tolerance (129, 133). In this promotion, high expression of

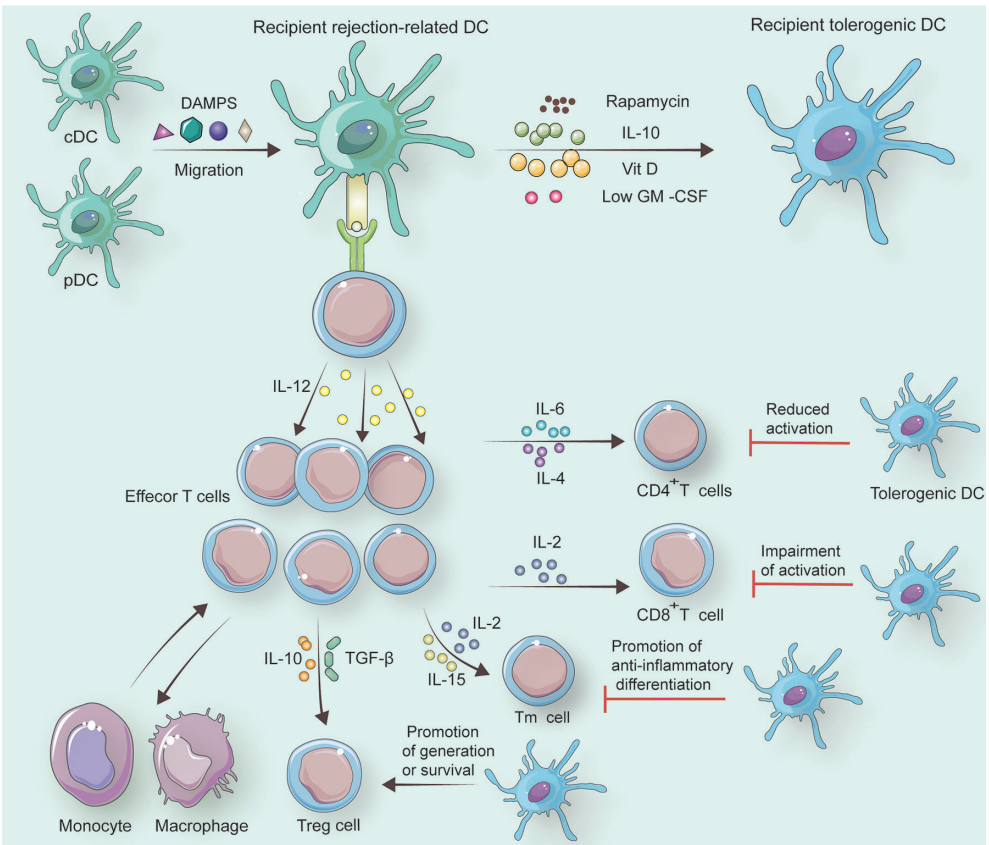


FIGURE 3 | In response to specific factors including DAMPs, recipient cDCs and pDCs change into recipient rejection-related DCs. If rapamycin, IL-10, Vit D, or a low dose of GM-CSF is employed to treat recipient rejection-related DCs, recipient tolerogenic DCs can be generated. Under the control of recipient rejection-related DCs, naive T cells differentiate to $CD8^+$ T cells with the help of IL-2 and differentiate to $CD4^+$ T cells assisted by IL-6 and IL-4. Memory T cells (Tm cells) also originate from naïve T cells, and this alteration is associated with IL-2 and IL-15. Treg cells can occur when IL-10 and TGF-β are secreted by recipient rejection-related DCs. Besides, tolerogenic DCs reduce $CD4^+$ T cell activation, and they can impair active $CD8^+$ T cells. Furthermore, Tm cells tend to be anti-inflammatory promoted by tolerogenic DCs. Treg cells survive for a longer period with tolerogenic DCs than with rejection-related DCs.

immune-globulin-like transcript 3 and immune-globulin-like transcript 4 causes $CD4^+CD45RO^+CD25^+$ T cells to become Tregs mediated by the enzyme indoleamine 2, 3-dioxygenase in allografts (134) (135). As a result, the identical indoleamine-2,3-dioxygenase and immunoglobulin-l like transcript 3 as well as high expressions of both MAP7 and MUCL1 genes occur in the mechanism of vitamin D3 inducted tolerogenic DCs (136–140) (**Figure 3**).

Donor-derived tolerogenic DCs can prolong graft survival time: treatment of these DCs ensures graft survival another 50 to 300 days (125). Donor tolerogenic DCs regulate $CD8^+$ as well as $CD4^+$ memory T cell responses, and this regulation prevents potential rejections (141–145). These DCs capture vesicles containing allograft antigens but choose an anti-inflammation phenotype: the number of donor-reactive IL-17^+ T cells remains low (125, 146). Further, donor-derived tolerogenic DCs induced by vitamin D3 and IL-10 moderate IL-17 associated inflammation and maintain stability even exposed to inflammatory molecules (124, 147). Most importantly, humans produce no specific antibody against injecting tolerogenic DCs (124). Moreover, without active recipient T cells, harmful antibodies derived from B cells will be reduced (148). Besides, multiple subsets of freshly isolated human DCs, including non-conventional plasmacytoid DCs, can regulate immune responses as well (107, 108, 149). **Table 2** summarizes the versatile roles of DCs targeting solving rejection problems in renal transplantation, implying future evaluable clinical advances (153).

The Generation of Tolerogenic DCs

Various cytokines and similar materials serve as triggers *in vivo*. Exposure to donor blood and immunosuppressive mediators, rapamycin, for example, might be a useful method in a non-human primate model (124, 129). Also, effective tolerogenic DCs can be endogenous. However, recipients' natural killer cells tend to kill donor-derived DCs that can mediate Tregs. Addressing this issue, Morelli and colleagues deleted host DCs to protect the donor-derived DCs from being killed (154). Through this method, recipient DCs acquired exosomes released by the donor tolerogenic DCs and amplified the effect of tolerance *via* the third mechanism mentioned in *The Possible Downstream*

TABLE 2 | Versatile roles of DCs in renal transplantation.

Animal Models	Interventions	Results	Functional roles or mechanisms	References
Rat	i.v. tolerogenic DCs derived from donors	increasing content of CD4+CD25 +Foxp3+Tregs and up-regulated secretion of Th2 cytokines	The enzyme indoleamine 2, 3-dioxygenase in tolerogenic DCs may induce allograft immunotolerance.	(135)
Monkey	i.v. CTLA-4 immunoglobulin and tapered rapamycin	Graft median survival time prolongation as well as IL-17 production attenuation combined with no circulating anti-donor antibody	The beneficial effect of donor Ag-pulsed autologous tolerogenic DC on nonhuman primate graft survival may be modest but not statistically significant.	(125)
Monkey	i.v. donor-derived regulatory dendritic cell	Tolerogenic DC-mediated tolerance with or without cytotoxic T-lymphocyte-associated antigen activation.	Pre-transplant DCreg infusion promotes tolerance after transplantation with no regard to CD28 blockade.	(129)
Mouse	Renal DCs were studied in collagenase-digested mouse kidneys	DCs migrate from the renal interstitial to renal lymph node within 48 h accompanied by increased DCs	Renal DCs respond to localized or systemic acute kidney injury by increasing the transport of protein antigens from the kidney to lymph nodes.	(74)
Mouse	Antigen coupled to an anti-CD205 antibody	Antigen-specific CD8 T-cell deletional tolerance	DEC-205 provides an effective receptor mechanism for DCs to deal with MHC class I presentation *in vivo*, which makes DCs produce stable immune tolerance and immune response after maturation.	(150)
Rhesus monkey	i.v. MD-3 anti- intercellular adhesion molecule antibody combined with low dose rapamycin and CD154	Long-term survival of pig xenoislets	The maturation of DCs relies on intercellular adhesion molecule-1 and anti-intercellular adhesion molecule-1-induced antigen-specific T cell tolerance.	(151)
Humanized mouse	i.v. MD-3 antibody before transplantation	Xenospecific T-cell tolerance; prevention of xenoislet rejection	The maturation of DCs relies on intercellular adhesion molecule-1 and anti-intercellular adhesion molecule-1 -induced antigen-specific T cell tolerance.	(151)
Cynomolgus monkey	i.d. immunization with antigen fused to anti-DC-asialoglycoprotein receptor antibody every 5–6 weeks after the flu virus	Ag-specific, IL-10 producing Tregs *in vivo*	human DCs can generate antigen-specific suppressive CD4 T cells that produce interleukin 10 *via* DC-asialoglycoprotein receptor but not Dectin-1 or DC-specific intercellular adhesion molecule-3-grabbing nonintegrin.	(152)
Rhesus macaques	i.v. DCreg + B7-CD28 costimulation blocking agent cytotoxic T-lymphocyte-associated antigen immunoglobin, 7 days before renal transplantation and for up to 8 weeks	Median graft survival time was 39.5 days in control monkeys and 113.5 days in tolerogenic DCs treated animals	Tolerogenic DCs generated from cytokine-mobilized donor blood monocytes in vitamin D3 and IL-10 moderate combined T cell- and antibody-mediated rejection.	(124)

Effects of DCs in Kidney Allograft Rejection (60). A few cytokines are able to induce tolerogenic DCs *in vitro*, for example, IL-10 and TGF-β (optimal inducible factors) (155) (**Figure 4**). IL-10 decreases MHC-II expression and costimulatory molecules in DC (156, 157). TGF-β increases the expression level of programmed death-ligand 1 and Fas-ligand on DC, inducing T cell apoptosis, and Treg differentiation (158, 159). Also, valuable methods can be used to produce tolerogenic DCs *in vitro* such as soluble Schistosoma Mansoni egg antigen, tumor necrosis factor α-induced protein 8 like-1, human soluble CD83, and prostaglandin E2 (PGE2). Soluble Schistosoma Mansoni egg antigen increases IL-10 level and suppresses Il-12p40 secretion, implying a novel method of tolerogenic DC generation (160). Except for IL-10 and TGF-β, tumor necrosis factor α-induced protein 8 like-1 could control the T cell activation procedure (161, 162). Human soluble CD83 alone achieves kidney allograft tolerance (>100 days) involving tolerogenic DC generation and indoleamine 2,3-dioxygenase activation (163). Mature DCs treated with PGE2 could inhibit inflammation *via* IL-10 secretion (164, 165). Traditional immunosuppressants can also serve as inducers of tolerogenic DCs, for instance, rapamycin and dexamethasone (166–170). Tolerogenic DCs generated from dexamethasone exhibit few costimulatory molecules or pro-inflammatory cytokines (171). Besides, metastasis-associated lung adenocarcinoma transcript 1, mesenchymal stem cells, nuclear paraspeckle assembly transcript 1, LF 15-0195, and pluripotent stem cells have a potential capacity to facilitate the tolerogenic DCs since they have been proven in other organ transplants (172–174).

Tolerogenic DC activation relies on adenosine triphosphate derived from glycolysis and tricarboxylic acid. Thus, control of glycolysis regulates DCs in renal transplantation especially in a few key active sites (175, 176). For instance, insufficient energy support causes morphological alteration and disorders in migration to lymph nodes (177). Lipopolysaccharide, complement component C1q subcomponent-binding protein, 2-deoxyglucose, and 1,25-dihydroxy vitamin D3 are associated with oxidative phosphorylation, fatty acid oxidation, and reactive oxygen species. In glycolysis, lipopolysaccharide mediates fatty acid synthesis forming adenosine triphosphate to trigger DC activation (178). C1q subcomponent-binding protein participates in the tricarboxylic acid cycle *via* regulating pyruvate dehydrogenase as a chaperone protein (179). 2-deoxyglucose plays an essential role in reducing CD40, CD86,

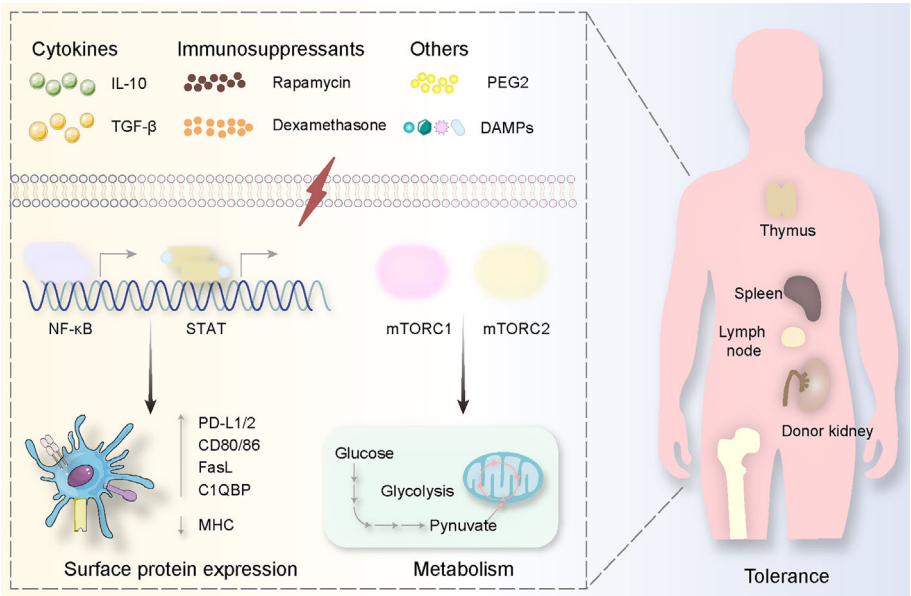


FIGURE 4 | Tolerogenic DCs are usually generated *via* specific substances. These stimulations derived from cytokines (IL-10, TGF-*β*), immunosuppressants (Rapamycin, Dexamethasone), and others (PEG2, DAMPs) mediate signal pathways involving NF-κB and mTOR activation, causing surface protein expression alterations (highly expressing PD-L1/2, CD80/86, FasL C1QBP while decreasing MHC expression) and metabolism changes (from glucose to pynuvate). All these procedures happen in the donor kidney and the immune organs including the thymus, spleen, lymph node, and bone marrow.

and MHC-II expression and secreting IL-6, IL-12p70, and TNF, which can be defined as features of tolerogenic DCs (178). Oxidative phosphorylation and fatty acid oxidation can be regulated by paracrine-derived Wnt5a protein linked tolerogenic DC generation, vitamin D3 or 1,25-dihydroxy vitamin D3 induction of tolerogenic DCs, and dexamethasone mediated tolerance (109, 180, 181). Specifically, these materials generate tolerogenic DCs through inducible nitric oxide synthase, nuclear factor E2-related factor 2: inducible nitric oxide synthase reduces oxidative phosphorylation and fatty acid oxidation, but nuclear factor E2-related factor 2 decreases the amount of inducible nitric oxide synthase expression (182, 183). As for the relationship between oxidative phosphorylation and fatty acid oxidation, miR-142 links to carnitine palmitoyltransferase-1a and induces more active fatty acid oxidation and further increases glycolysis promoting pro-inflammatory cytokines (184). Fatty acid inhibits oxidative phosphorylation and facilitates reactive oxygen species leading to more severe inflammation (185–187).

In addition to general metabolism, it is accurate and stable to induce tolerogenic DCs employing regulating signal pathways. The most well-known pathway that has been focused on is mTOR (mammalian target of rapamycin) involving mTOR complex 1 (mTORC1) as well as mTOR complex 2 (mTORC2) (**Figure 4**). The inhibition of mTOR produces tolerogenic DCs associated with glucose metabolism. GM-CSF, IL-4, rapamycin, alum, and graphene quantum dots have effects on mTOR mediating potential tolerance *via* lower adenosine triphosphate generation (167, 188–190). Specifically, mTORC2 decreases adenosine triphosphate generated from mTORC1 mediating glycolysis, and mTORC1 takes crucial tasks in DC maturation (191) (**Figure 4**). Also, the upstream and downstream molecules contribute to the generation of tolerogenic DCs (**Figure 2**). An upstream complex called adenosine monophosphate-activated protein kinase can be suppressed by polyphenol resveratrol causing poor expression of mTOR (192). A downstream complex named after the peroxisome proliferators-activated receptor plays a metabolic role in DC maturation through targeting at mTORC1 and hypoxia-inducible factor-1a as a downstream complex serves to reprogram glycolysis for DC maturation *via* mTOR activation (177, 193–195). Reprogramming glycolysis in DCs can be finished by another kinase known as spleen tyrosine kinase depending on the production of IL-1b through a different mechanism compared with infection (196, 197).

STAT and NF-κB have also been incorporated into the maturity of DC as a family containing STAT1, STAT2, STAT3, STAT4, STAT5a, STAT5b, STAT6 as well as inhibiting STAT1, STAT2, and STAT5, and activating STAT3 induces tolerogenic DCs (198, 199) (**Figures 2**, **4**). Targeting at STAT1, flavonoids decrease the expression of programmed death-ligand 1 to enable DCs more mature (200, 201). Silencing STAT1 with small interfering RNA in DCs causes low expression of CD83 and CD86, implying anti-inflammatory effects (202). STAT2 functions as a co-worker with STAT1 mediating cross-presentation of DC, and thus STAT2 should be suppressed when tolerogenic DCs are needed (203). STAT3 activation provides tolerogenic DCs because IFN-α-induced programmed death-ligand 1 expression is inhibited by suppressed STAT3, and STAT3-

deficient DC could increase pro-inflammatory cytokines, promote antigen-dependent T cell activation (204, 205). With STAT5 inhibited by JQ1 in lipopolysaccharide-mediated DCs, the level of IL-12p70 secretion is decreased (206). Moreover, materials preventing NF-κB like small interfering RNA and Bay11-7082 have the potential to generate tolerogenic DCs in that they can serve as immunosuppressive tools in other organ transplants (207, 208) (**Figure 4**).

CONCLUSIONS AND POSSIBLE THERAPEUTIC PROSPECTS

Compared with macrophages in kidney transplantation, renal DCs' roles in ischemia–reperfusion, rejection or tolerance still need to clarify. For further investigation, a unified standard to separate kidney DCs from macrophages must be established based on the current level, since macrophages and DCs are both essential parts of innate immunity and they often function together inducing rejection or tolerance. This objective can be promoted by high-dimensional analysis of single-cell because increasing kidney biopsy samples provide an opportunity for revealing the markers and transcription different from macrophages. Additionally, the comparison of normal kidney and rejected kidney engenders valuable hypothesis and remarkable conclusions analyzed by artificial intelligence. In some respects, researchers tend to establish mouse models in experiments and this choice produces numerous discoveries and hinders translational medicine. Kidney transplantation saves tens of thousands of patients' lives every year and costs millions of dollars handling rejection-associated problems meanwhile. Although donor DCs might mediate tolerance *in vivo*, patients still rely on traditional glucocorticoids and non-specific immunosuppress drugs. As a result, translational medicine should be emphasized immediately after the roles of DCs in renal transplantation being clarified. Finally, the relationship between rejection and tolerance and DCS is relatively clear, but the relationship between DCs and other complications of renal transplantation is still in a vague state. For example, infection related to renal transplantation may be related to intestinal flora, and the effect of intestinal flora on host immune status is likely to be achieved through DCs. In addition, the lifespan of donor DCS is not as long as that of recipient DCs, so the details of the interaction between the two DCS will also be the key to anti-rejection intervention at different time points after renal transplantation. On this basis, the understanding of the interaction between DCs and T cells of each transcript will also provide support for the development of anti-rejection drugs after transplantation.

AUTHOR CONTRIBUTIONS

All authors listed have made a substantial, direct, and intellectual contribution to the work and approved it for publication.

FUNDING

The research reported in this study was funded by the Natural Science Foundation of China (81770752).

REFERENCES

1. Van Furth R, Cohn ZA. The Origin and Kinetics of Mononuclear Phagocytes. *J Exp Med* (1968) 128(3):415–35. doi: 10.1084/jem.128.3.415
2. Nelson PJ, Rees AJ, Griffin MD, Hughes J, Kurts C, Duffield J. The Renal Mononuclear Phagocytic System. *J Am Soc Nephrol* (2012) 23(2):194–203. doi: 10.1681/asn.2011070680
3. Kurts C, Panzer U, Anders HJ, Rees AJ. The Immune System and Kidney Disease: Basic Concepts and Clinical Implications. *Nat Rev Immunol* (2013) 13(10):738–53. doi: 10.1038/nri3523
4. Steinman RM, Cohn ZA. Identification of a Novel Cell Type in Peripheral Lymphoid Organs of Mice. I. Morphology, Quantitation, Tissue Distribution. *J Exp Med* (1973) 137(5):1142–62. doi: 10.1084/jem.137.5.1142
5. Hume DA, Gordon S. Mononuclear Phagocyte System of the Mouse Defined by Immunohistochemical Localization of Antigen F4/80. Identification of Resident Macrophages in Renal Medullary and Cortical Interstitium and the Juxtaglomerular Complex. *J Exp Med* (1983) 157 (5):1704–9. doi: 10.1084/jem.157.5.1704
6. Krüger T, Benke D, Eitner F, Lang A, Wirtz M, Hamilton-Williams EE, et al. Identification and Functional Characterization of Dendritic Cells in the Healthy Murine Kidney and in Experimental Glomerulonephritis. *J Am Soc Nephrol* (2004) 15(3):613–21. doi: 10.1097/01.asn.0000114553.36258.91
7. Gottschalk C, Kurts C. The Debate About Dendritic Cells and Macrophages in the Kidney. *Front Immunol* (2015) 6:435. doi: 10.3389/fimmu.2015.00435
8. Regev A, Teichmann SA, Lander ES, Amit I, Benoist C, Birney E, et al. Science Forum: The Human Cell Atlas. *Elife* (2017) 6:e27041. doi: 10.7554/eLife.27041
9. Young MD, Mitchell TJ, Vieira Braga FA, Tran MGB, Stewart BJ, Ferdinand JR, et al. Single-Cell Transcriptomes From Human Kidneys Reveal the Cellular Identity of Renal Tumors. *Science* (2018) 361(6402):594–9. doi: 10.1126/science.aat1699
10. Segerer S, Heller F, Lindenmeyer MT, Schmid H, Cohen CD, Draganovici D, et al. Compartment Specific Expression of Dendritic Cell Markers in Human Glomerulonephritis. *Kidney Int* (2008) 74(1):37–46. doi: 10.1038/ki.2008.99
11. Mueller FB, Yang H, Lubetzky M, Verma A, Lee JR, Dadhania DM, et al. Landscape of Innate Immune System Transcriptome and Acute T Cell–Mediated Rejection of Human Kidney Allografts. *JCI Insight* (2019) 4(13): e128014. doi: 10.1172/jci.insight.128014
12. Guilliams M, Ginhoux F, Jakubzick C, Naik SH, Onai N, Schraml BU, et al. Dendritic Cells, Monocytes and Macrophages: A Unified Nomenclature Based on Ontogeny. *Nat Rev Immunol* (2014) 14(8):571–8. doi: 10.1038/nri3712
13. Dong X, Swaminathan S, Bachman LA, Croatt AJ, Nath KA, Griffin MD. Resident Dendritic Cells are the Predominant TNF-secreting Cell in Early Renal Ischemia-Reperfusion Injury. *Kidney Int* (2007) 71(7):619–28. doi: 10.1038/sj.ki.5002132
14. Dai H, Thomson AW, Rogers NM. Dendritic Cells as Sensors, Mediators, and Regulators of Ischemic Injury. *Front Immunol* (2019) 10:2418. doi: 10.3389/fimmu.2019.02418
15. Jongbloed SL, Kassianos AJ, McDonald KJ, Clark GJ, Ju X, Angel CE, et al. Human CD141+ (Bdca-3)+ Dendritic Cells (Dcs) Represent a Unique Myeloid DC Subset That Cross-Presents Necrotic Cell Antigens. *J Exp Med* (2010) 207(6):1247–60. doi: 10.1084/jem.20092140

16. Steinman RM, Adams JC, Cohn ZA. Identification of a Novel Cell Type in Peripheral Lymphoid Organs of Mice. IV. Identification and Distribution in Mouse Spleen. *J Exp Med* (1975) 141(4):804–20. doi: 10.1084/jem.141.4.804
17. Marín E, Cuturi MC, Moreau A. Tolerogenic Dendritic Cells in Solid Organ Transplantation: Where Do We Stand? *Front Immunol* (2018) 9:274. doi: 10.3389/fimmu.2018.00274
18. Zahorchak AF, Macedo C, Hamm DE, Butterfield LH, Metes DM, Thomson AW. High PD-L1/CD86 MFI Ratio and IL-10 Secretion Characterize Human Regulatory Dendritic Cells Generated for Clinical Testing in Organ Transplantation. *Cell Immunol* (2018) 323:9–18. doi: 10.1016/j.cellimm.2017.08.008
19. Lu L, Thomson AW. Manipulation of Dendritic Cells for Tolerance Induction in Transplantation and Autoimmune Disease. *Transplantation* (2002) 73(1 SUPPL.):S19–22. doi: 10.1097/00007890-200201151-00008
20. Lu L, Qian S, Hershberger PA, Rudert WA, Lynch DH, Thomson AW. Fas Ligand (CD95L) and B7 Expression on Dendritic Cells Provide Counter-Regulatory Signals for T Cell Survival and Proliferation. *J Immunol* (1997) 158(12):5676–84.
21. Schlitzer A, Sivakamasundari V, Chen J, Sumatoh HR, Schreuder J, Lum J, et al. Identification of cDC1- and Cdc2-Committed DC Progenitors Reveals Early Lineage Priming at the Common DC Progenitor Stage in the Bone Marrow. *Nat Immunol* (2015) 16(7):718–28. doi: 10.1038/ni.3200
22. Worbs T, Hammerschmidt SI, Förster R. Dendritic Cell Migration in Health and Disease. *Nat Rev Immunol* (2017) 17(1):30–48. doi: 10.1038/nri.2016.116
23. Alvarez D, Vollmann EH, von Andrian UH. Mechanisms and Consequences of Dendritic Cell Migration. *Immunity* (2008) 29(3):325–42. doi: 10.1016/j.immuni.2008.08.006
24. Nakano H, Lyons-Cohen MR, Whitehead GS, Nakano K, Cook DN. Distinct Functions of CXCR4, CCR2, and CX3CR1 Direct Dendritic Cell Precursors From the Bone Marrow to the Lung. *J Leukoc Biol* (2017) 101(5):1143–53. doi: 10.1189/jlb.1A0616-285R
25. Shi Q, Zhuang F, Liu JT, Li N, Chen YX, Su XB, et al. Single-Cell Analyses Reveal Functional Classification of Dendritic Cells and Their Potential Roles in Inflammatory Disease. *FASEB J* (2019) 33(3):3784–94. doi: 10.1096/fj.201801489R
26. Scott CL, Bain CC, Wright PB, Sichien D, Kotarsky K, Persson EK, et al. CCR2(+)CD103(-) Intestinal Dendritic Cells Develop From DC-committed Precursors and Induce interleukin-17 Production by T Cells. *Mucosal Immunol* (2015) 8(2):327–39. doi: 10.1038/mi.2014.70
27. Matzinger P. Tolerance, Danger, and the Extended Family. *Annu Rev Immunol* (1994) 12:991–1045. doi: 10.1146/annurev.iy.12.040194.005015
28. Krüger B, Krick S, Dhillon N, Lerner SM, Ames S, Bromberg JS, et al. Donor Toll-Like Receptor 4 Contributes to Ischemia and Reperfusion Injury Following Human Kidney Transplantation. *Proc Natl Acad Sci USA* (2009) 106(9):3390–5. doi: 10.1073/pnas.0810169106
29. LaRosa DF, Rahman AH, Turka LA. The Innate Immune System in Allograft Rejection and Tolerance. *J Immunol* (2007) 178(12):7503–9. doi: 10.4049/jimmunol.178.12.7503
30. Rao DA, Pober JS. Endothelial Injury, Alarmins, and Allog Raft Rejection. *Crit Rev Immunol* (2008) 28(3):229–48. doi: 10.1615/critrevimmunol.v28.i3.40
31. Kono H, Rock KL. How Dying Cells Alert the Immune System to Danger. *Nat Rev Immunol* (2008) 8(4):279–89. doi: 10.1038/nri2215
32. Spörri R, Reis e Sousa C. Inflammatory Mediators are Insufficient for Full Dendritic Cell Activation and Promote Expansion of CD4+ T Cell Populations Lacking Helper Function. *Nat Immunol* (2005) 6(2):163–70. doi: 10.1038/ni1162
33. Tesar BM, Zhang J, Li Q, Goldstein DR. TH1 Immune Responses to Fully MHC Mismatched Allografts are Diminished in the Absence of MyD88, a Toll-Like Receptor Signal Adaptor Protein. *Am J Transplant* (2004) 4(9):1429–39. doi: 10.1111/j.1600-6143.2004.00544.x
34. McKay D, Shigeoka A, Rubinstein M, Surh C, Sprent J. Simultaneous Deletion of MyD88 and Trif Delays Major Histocompatibility and Minor Antigen Mismatch Allograft Rejection. *Eur J Immunol* (2006) 36(8):1994–2002. doi: 10.1002/eji.200636249
35. Oberbarnscheidt MH, Obhrai JS, Williams AL, Rothstein DM, Shlomchik WD, Chalasani G, et al. Type I Interferons are Not Critical for Skin Allograft Rejection or the Generation of Donor-Specific CD8+ Memory T Cells: Brief Communication. *Am J Transplant* (2010) 10(1):162–7. doi: 10.1111/j.1600-6143.2009.02871.x
36. Li H, Matte-Martone C, Tan HS, Venkatesan S, McNiff J, Demetris AJ, et al. Graft-Versus-Host Disease is Independent of Innate Signaling Pathways Triggered by Pathogens in Host Hematopoietic Cells. *J Immunol* (2011) 186(1):230–41. doi: 10.4049/jimmunol.1002965
37. Bingaman AW, Ha J, Waitze SY, Durham MM, Cho HR, Tucker-Burden C, et al. Vigorous Allograft Rejection in the Absence of Danger. *J Immunol* (2000) 164(6):3065–71. doi: 10.4049/jimmunol.164.6.3065
38. Anderson CC, Carroll JM, Gallucci S, Ridge JP, Cheever AW, Matzinger P. Testing Time-, Ignorance-, and Danger-Based Models of Tolerance. *J Immunol* (2001) 166(6):3663–71. doi: 10.4049/jimmunol.166.6.3663
39. Anderson CC, Matzinger P. Immunity or Tolerance: Opposite Outcomes of Microchimerism From Skin Grafts. *Nat Med* (2001) 7(1):80–7. doi: 10.1038/83393
40. Zecher D, Li Q, Oberbarnscheidt MH, Demetris AJ, Shlomchik WD, Rothstein DM, et al. NK Cells Delay Allograft Rejection in Lymphopenic Hosts by Downregulating the Homeostatic Proliferation of CD8+ T Cells. *J Immunol* (2010) 184(12):6649–57. doi: 10.4049/jimmunol.0903729
41. Larsen CP, Morris PJ, Austyn JM. Migration of Dendritic Leukocytes From Cardiac Allografts Into Host Spleens. A Novel Pathway for Initiation of Rejection. *J Exp Med* (1990) 171(1):307–14. doi: 10.1084/jem.171.1.307
42. MacEdo C, Orkis EA, Popescu I, Elinoff BD, Zeevi A, Shapiro R, et al. Contribution of Naïve and Memory T-Cell Populations to the Human Alloimmune Response. *Am J Transplant* (2009) 9(9):2057–66. doi: 10.1111/j.1600-6143.2009.02742.x
43. Suchin EJ, Langmuir PB, Palmer E, Sayegh MH, Wells AD, Turka LA. Quantifying the Frequency of Alloreactive T Cells In Vivo: New Answers to an Old Question. *J Immunol* (2001) 166(2):973–81. doi: 10.4049/jimmunol.166.2.973
44. Lafferty KJ, Bootes A, Dart G, Talmage DW. Effect of Organ Culture on the Survival of Thyroid Allografts in Mice. *Transplantation* (1976) 22(2):138–49. doi: 10.1097/00007890-197608000-00009
45. Talmage DW, Dart G, Radovich J, Lafferty KJ. Activation of Transplant Immunity: Effect of Donor Leukocytes on Thyroid Allograft Rejection. *Science* (1976) 191(4225):385–8. doi: 10.1126/science.1082167
46. Bowen KM, Andrus L, Lafferty KJ. Successful Allotransplantation of Mouse Pancreatic Islets to Nonimmunosuppressed Recipients. *DIABETES* (1980) 29(SUPPL. 1):98–104. doi: 10.2337/diab.29.1.s98
47. Batchelor JR, Welsh KI, Maynard A, Burgos H. Failure of Long Surviving, Passively Enhanced Kidney Allografts to Provoke T-dependent Alloimmunity: I. Retransplantation of (as × AUG)F1 Kidneys Into Secondary AS Recipients. *J Exp Med* (1979) 150(3):455–64. doi: 10.1084/jem.150.3.455
48. Lechler RI, Batchelor JR. Restoration of Immunogenicity to Passenger Cell-Depleted Kidney Allografts by the Addition of Donor Strain Dendritic Cells. *J Exp Med* (1982) 155(1):31–41. doi: 10.1084/jem.155.1.31
49. Welsh KI, Batchelor JR, Maynard A, Burgos H. Failure of Long Surviving, Passively Enhanced Kidney Allografts to Provoke T-dependent Alloimmunity: II. Retransplantation of (as × AUG)F1 Kidneys From as Primary Recipients Into (as X WF)F1 Secondary Hosts. *J Exp Med* (1979) 150(3):465–70. doi: 10.1084/jem.150.3.465
50. Garrod KR, Liu FC, Forrest LE, Parker I, Kang SM, Cahalan MD. NK Cell Patrolling and Elimination of Donor-Derived Dendritic Cells Favor Indirect Alloreactivity. *J Immunol* (2010) 184(5):2329–36. doi: 10.4049/jimmunol.0902748
51. Mannon RB, Griffiths R, Ruiz P, Platt JL, Coffman TM. Absence of Donor MHC Antigen Expression Ameliorates Chronic Kidney Allograft Rejection. *Kidney Int* (2002) 62(1):290–300. doi: 10.1046/j.1523-1755.2002.00422.x
52. Grusby MJ, Auchincloss J, Lee R, Johnson RS, Spencer JP, Zijlstra M, et al. Mice Lacking Major Histocompatibility Complex Class I and Class II Molecules. *Proc Natl Acad Sci U.S.A.* (1993) 90(9):3913–7. doi: 10.1073/pnas.90.9.3913
53. Garrod KR, Wei SH, Parker I, Cahalan MD. Natural Killer Cells Actively Patrol Peripheral Lymph Nodes Forming Stable Conjugates to Eliminate MHC-mismatched Targets. *Proc Natl Acad Sci USA* (2007) 104(29):12081–6. doi: 10.1073/pnas.0702867104

54. Morelli AE. Dendritic Cells of Myeloid Lineage: The Masterminds Behind Acute Allograft Rejection. *Curr Opin Organ Transplant* (2014) 19(1):20–7. doi: 10.1097/MOT.0000000000000039
55. Herrera OB, Golshayan D, Tibbott R, Ochoa FS, James MJ, Marelli-Berg FM, et al. A Novel Pathway of Alloantigen Presentation by Dendritic Cells. *J Immunol* (2004) 173(8):4828–37. doi: 10.4049/jimmunol.173.8.4828
56. Sivaganesh S, Harper SJ, Conlon TM, Callaghan CJ, Saeb-Parsy K, Negus MC, et al. Copresentation of Intact and Processed MHC Alloantigen by Recipient Dendritic Cells Enables Delivery of Linked Help to Alloreactive CD8 T Cells by Indirect-Pathway CD4 T Cells. *J Immunol* (2013) 190 (11):5829–38. doi: 10.4049/jimmunol.1300458
57. Zhuang Q, Lakkis FG. Dendritic Cells and Innate Immunity in Kidney Transplantation. *Kidney Int* (2015) 87(4):712–8. doi: 10.1038/ki.2014.430
58. Liu Q, Rojas-Canales DM, Divito SJ, Shufesky WJ, Stolz DB, Erdos G, et al. Donor Dendritic Cell-Derived Exosomes Promote Allograft-Targeting Immune Response. *J Clin Invest* (2016) 126(8):2805–20. doi: 10.1172/JCI84577
59. Marino J, Babiker-Mohamed MH, Crosby-Bertorini P, Paster JT, LeGuern C, Germana S, et al. Donor Exosomes Rather Than Passenger Leukocytes Initiate Alloreactive T Cell Responses After Transplantation. *Sci Immunol* (2016) 1(1):aaf8759. doi: 10.1126/sciimmunol.aaf8759
60. Lindenbergh MFS, Stoorvogel W. Antigen Presentation by Extracellular Vesicles From Professional Antigen-Presenting Cells. *Annu Rev Immunol: Annu Rev Inc* (2018) 36:435–59. doi: 10.1146/annurev-immunol-041015-055700
61. Zhuang Q, Liu Q, Divito SJ, Zeng Q, Yatim KM, Hughes AD, et al. Graft-Infiltrating Host Dendritic Cells Play a Key Role in Organ Transplant Rejection. *Nat Commun* (2016) 7(1):1–12. doi: 10.1038/ncomms12623
62. Joffre OP, Segura E, Savina A, Amigorena S. Cross-Presentation by Dendritic Cells. *Nat Rev Immunol* (2012) 12(8):557–69. doi: 10.1038/nri3254
63. Yamazaki S, Dudziak D, Heidkamp GF, Fiorese C, Bonito AJ, Inaba K, et al. Cd8+ CD205+ Splenic Dendritic Cells are Specialized to Induce Foxp3+ Regulatory T Cells. *J Immunol* (2008) 181(10):6923–33. doi: 10.4049/jimmunol.181.10.6923
64. Gotot J, Dhana E, Yagita H, Kaiser R, Ludwig-Portugall I, Kurts C. Antigen-Specific Helios(-), Neuropilin-1(-) Tregs Induce Apoptosis of Autoreactive B Cells Via PD-L1. *Immunol Cell Biol* (2018) 96(8):852–62. doi: 10.1111/imcb.12053
65. den Haan JM, Lehar SM, Bevan MJ. CD8(+) But Not CD8(-) Dendritic Cells Cross-Prime Cytotoxic T Cells In Vivo. *J Exp Med* (2000) 192(12):1685–96. doi: 10.1084/jem.192.12.1685
66. Belz GT, Behrens GM, Smith CM, Miller JF, Jones C, Lejon K, et al. The CD8alpha(+) Dendritic Cell is Responsible for Inducing Peripheral Self-Tolerance to Tissue-Associated Antigens. *J Exp Med* (2002) 196(8):1099–104. doi: 10.1084/jem.20020861
67. Hildner K, Edelson BT, Purtha WE, Diamond M, Matsushita H, Kohyama M, et al. Batf3 Deficiency Reveals a Critical Role for CD8alpha+ Dendritic Cells in Cytotoxic T Cell Immunity. *Science* (2008) 322(5904):1097–100. doi: 10.1126/science.1164206
68. Kurts C, Robinson BW, Knolle PA. Cross-Priming in Health and Disease. *Nat Rev Immunol* (2010) 10(6):403–14. doi: 10.1038/nri2780
69. Schlichting CL, Schareck WD, Weis M. Renal Ischemia-Reperfusion Injury: New Implications of Dendritic Cell-Endothelial Cell Interactions. *Transplant Proc* (2006) 38(3):670–3. doi: 10.1016/j.transproceed.2006.01.059
70. Jantsch J, Chakravortty D, Turza N, Prechtel AT, Buchholz B, Gerlach RG, et al. Hypoxia and Hypoxia-Inducible Factor-1 Alpha Modulate Lipopolysaccharide-Induced Dendritic Cell Activation and Function. *J Immunol* (2008) 180(7):4697–705. doi: 10.4049/jimmunol.180.7.4697
71. Xu L, Sharkey D, Cantley LG. Tubular GM-CSF Promotes Late Mcp-1/Ccr2-Mediated Fibrosis and Inflammation After Ischemia/Reperfusion Injury. *J Am Soc Nephrol* (2019) 30(10):1825–40. doi: 10.1681/asn.2019010068
72. Ferhat M, Robin A, Giraud S, Sena S, Goujon JM, Touchard G, et al. Endogenous IL-33 Contributes to Kidney Ischemia-Reperfusion Injury as an Alarmin. *J Am Soc Nephrol* (2018) 29(4):1272–88. doi: 10.1681/asn.2017060650
73. Rogers NM, Matthews TJ, Kausman JY, Kitching AR, Coates PT. Review Article: Kidney Dendritic Cells: Their Role in Homeostasis, Inflammation and Transplantation. *Nephrol (Carlton)* (2009) 14(7):625–35. doi: 10.1111/j.1440-1797.2009.01200.x
74. Dong X, Swaminathan S, Bachman LA, Croatt AJ, Nath KA, Griffin MD. Antigen Presentation by Dendritic Cells in Renal Lymph Nodes is Linked to Systemic and Local Injury to the Kidney. *Kidney Int* (2005) 68(3):1096–108. doi: 10.1111/j.1523-1755.2005.00502.x
75. Burne-Taney MJ, Kofler J, Yokota N, Weisfeldt M, Traystman RJ, Rabb H. Acute Renal Failure After Whole Body Ischemia is Characterized by Inflammation and T Cell-Mediated Injury. *Am J Physiol Renal Physiol* (2003) 285(1):F87–94. doi: 10.1152/ajprenal.00026.2003
76. Ysebaert DK, De Greef KE, De Beuf A, Van Rompay AR, Vercauteren S, Persy VP, et al. T Cells as Mediators in Renal Ischemia/Reperfusion Injury. *Kidney Int* (2004) 66(2):491–6. doi: 10.1111/j.1523-1755.2004.761_4.x
77. Lech M, Avila-Ferrufino A, Allam R, Segerer S, Khandoga A, Krombach F, et al. Resident Dendritic Cells Prevent Postischemic Acute Renal Failure by Help of Single Ig IL-1 Receptor-Related Protein. *J Immunol* (2009) 183 (6):4109–18. doi: 10.4049/jimmunol.0900118
78. Kim H, Seed B. The Transcription Factor MafB Antagonizes Antiviral Responses by Blocking Recruitment of Coactivators to the Transcription Factor IRF3. *Nat Immunol* (2010) 11(8):743–50. doi: 10.1038/ni.1897
79. Cho WY, Choi HM, Lee SY, Kim MG, Kim HK, Jo SK. The Role of Tregs and CD11c(+) Macrophages/Dendritic Cells in Ischemic Preconditioning of the Kidney. *Kidney Int* (2010) 78(10):981–92. doi: 10.1038/ki.2010.266
80. Pontrelli P, Cariello M, Rascio F, Gigante M, Verrienti R, Tataranni T, et al. Thrombin may Modulate Dendritic Cell Activation in Kidney Transplant Recipients With Delayed Graft Function. *Nephrol Dial Transplant* (2015) 30 (9):1480–7. doi: 10.1093/ndt/gfv129
81. Stallone G, Pontrelli P, Rascio F, Castellano G, Gesualdo L, Grandaliano G. Coagulation and Fibrinolysis in Kidney Graft Rejection. *Front Immunol* (2020) 11:1807. doi: 10.3389/fimmu.2020.01807
82. Siu JHY, Surendrakumar V, Richards JA, Pettigrew GJ. T Cell Allorecognition Pathways in Solid Organ Transplantation. *Front Immunol* (2018) 9:2548. doi: 10.3389/fimmu.2018.02548
83. Merad M, Collin M, Bromberg J. Dendritic Cell Homeostasis and Trafficking in Transplantation. *Trends Immunol* (2007) 28(8):353–9. doi: 10.1016/j.it.2007.06.003
84. Sallusto F, Lenig D, Förster R, Lipp M, Lanzavecchia A. Two Subsets of Memory T Lymphocytes With Distinct Homing Potentials and Effector Functions. *Nature* (1999) 401(6754):708–12. doi: 10.1038/44385
85. Lakkis FG, Arakelov A, Konieczny BT, Inoue Y. Immunologic 'Ignorance' of Vascularized Organ Transplants in the Absence of Secondary Lymphoid Tissue. *Nat Med* (2000) 6(6):686–8. doi: 10.1038/76267
86. Chalasani G, Dai Z, Konieczny BT, Baddoura FK, Lakkis FG. Recall and Propagation of Allospecific Memory T Cells Independent of Secondary Lymphoid Organs. *Proc Natl Acad Sci USA* (2002) 99(9):6175–80. doi: 10.1073/pnas.092596999
87. Obhrai JS, Oberbarnscheidt MH, Hand TW, Diggs L, Chalasani G, Lakkis FG. Effector T Cell Differentiation and Memory T Cell Maintenance Outside Secondary Lymphoid Organs. *J Immunol* (2006) 176(7):4051–8. doi: 10.4049/jimmunol.176.7.4051
88. Heeger PS, Greenspan NS, Kuhlenschmidt S, Dejelo C, Hricik DE, Schulak JA, et al. Pretransplant Frequency of Donor-Specific, IFN-γ-Producing Lymphocytes is a Manifestation of Immunologic Memory and Correlates With the Risk of Posttransplant Rejection Episodes. *J Immunol* (1999) 163 (4):2267–75.
89. Wakim LM, Waithman J, Van Rooijen N, Heath WR, Carbone FR. Dendritic Cell-Induced Memory T Cell Activation in Nonlymphoid Tissues. *Science* (2008) 319(5860):198–202. doi: 10.1126/science.1151869
90. Walch JM, Zeng Q, Li Q, Oberbarnscheidt MH, Hoffman RA, Williams AL, et al. Cognate Antigen Directs CD8+ T Cell Migration to Vascularized Transplants. *J Clin Invest* (2013) 123(6):2663–71. doi: 10.1172/JCI66722
91. Dong VM, Womer KL, Sayegh MH. Transplantation Tolerance: The Concept and its Applicability. *Pediatr Transplant* (1999) 3(3):181–92. doi: 10.1034/j.1399-3046.1999.00042.x
92. Zhuang Q, Liu Q, Divito SJ, Zeng Q, Yatim KM, Hughes AD, et al. Graft-Infiltrating Host Dendritic Cells Play a Key Role in Organ Transplant Rejection. *Nat Commun* (2016) 7:12623. doi: 10.1038/ncomms12623

93. Snelgrove SL, Lo C, Hall P, Lo CY, Alikhan MA, Coates PT, et al. Activated Renal Dendritic Cells Cross Present Intrarenal Antigens After Ischemia-Reperfusion Injury. *Transplantation* (2017) 101(5):1013–24. doi: 10.1097/tp.0000000000001427
94. Ruben JM, García-Romo GS, Breman E, van der Kooij S, Redeker A, Arens R, et al. Human Plasmacytoid Dendritic Cells Acquire Phagocytic Capacity by TLR9 Ligation in the Presence of Soluble Factors Produced by Renal Epithelial Cells. *Kidney Int* (2018) 93(2):355–64. doi: 10.1016/j.kint.2017.08.006
95. Ochando J, Ordikhani F, Jordan S, Boros P, Thomson AW. Tolerogenic Dendritic Cells in Organ Transplantation. *Transpl Int* (2020) 33(2):113–27. doi: 10.1111/tri.13504
96. Banchereau J, Steinman RM. Dendritic Cells and the Control of Immunity. *Nature* (1998) 392(6673):245–52. doi: 10.1038/32588
97. Steinman RM. Decisions About Dendritic Cells: Past, Present, and Future. *Annu Rev Immunol* (2012) 30:1–22. doi: 10.1146/annurev-immunol-100311-102839
98. Zhou Z, Li W, Song Y, Wang L, Zhang K, Yang J, et al. Growth Differentiation factor-15 Suppresses Maturation and Function of Dendritic Cells and Inhibits Tumor-Specific Immune Response. *PloS One* (2013) 8(11):e78618. doi: 10.1371/journal.pone.0078618
99. Castellano G, Woltman AM, Nauta AJ, Roos A, Trouw LA, Seelen MA, et al. Maturation of Dendritic Cells Abrogates C1q Production In Vivo and In Vitro. *Blood* (2004) 103(10):3813–20. doi: 10.1182/blood-2003-09-3046
100. Son M, Santiago-Schwarz F, Al-Abed Y, Diamond B. C1q Limits Dendritic Cell Differentiation and Activation by Engaging LAIR-1. *Proc Natl Acad Sci U.S.A.* (2012) 109(46):E3160–7. doi: 10.1073/pnas.1212753109
101. Mascarell L, Airouche S, Berjont N, Gary C, Gueguen C, Fourcade G, et al. The Regulatory Dendritic Cell Marker C1q is a Potent Inhibitor of Allergic Inflammation. *Mucosal Immunol* (2017) 10(3):695–704. doi: 10.1038/mi.2016.87
102. Hosszu KK, Valentino A, Vinayagasundaram U, Vinayagasundaram R, Joyce MG, Ji Y, et al. Dc-Sign, C1q, and gC1qR Form a Trimolecular Receptor Complex on the Surface of Monocyte-Derived Immature Dendritic Cells. *Blood* (2012) 120(6):1228–36. doi: 10.1182/blood-2011-07-369728
103. Zimmer A, Bouley J, Le Mignon M, Pliquet E, Horiot S, Turfkruyer M, et al. A Regulatory Dendritic Cell Signature Correlates With the Clinical Efficacy of Allergen-Specific Sublingual Immunotherapy. *J Allergy Clin Immunol* (2012) 129(4):1020–30. doi: 10.1016/j.jaci.2012.02.014
104. Maldonado RA, von Andrian UH. How Tolerogenic Dendritic Cells Induce Regulatory T Cells. *Adv Immunol* (2010) 108:111–65. doi: 10.1016/b978-0-12-380995-7.00004-5
105. Vander Lugt B, Riddell J, Khan AA, Hackney JA, Lesch J, DeVoss J, et al. Transcriptional Determinants of Tolerogenic and Immunogenic States During Dendritic Cell Maturation. *J Cell Biol* (2017) 216(3):779–92. doi: 10.1083/jcb.201512012
106. Swafford D, Manicassamy S. Wnt Signaling in Dendritic Cells: Its Role in Regulation of Immunity and Tolerance. *Discovery Med* (2015) 19 (105):303–10.
107. Liu YJ. Dendritic Cell Subsets and Lineages, and Their Functions in Innate and Adaptive Immunity. *Cell* (2001) 106(3):259–62. doi: 10.1016/S0092-8674(01)00456-1
108. Ueno H, Klechevsky E, Morita R, Aspord C, Cao T, Matsui T, et al. Dendritic Cell Subsets in Health and Disease. *Immunol Rev* (2007) 219(1):118–42. doi: 10.1111/j.1600-065X.2007.00551.x
109. Navarro-Barriuso J, Mansilla MJ, Naranjo-Gómez M, Sánchez-Pla A, Quirant-Sánchez B, Teniente-Serra A, et al. Comparative Transcriptomic Profile of Tolerogenic Dendritic Cells Differentiated With Vitamin D3, Dexamethasone and Rapamycin. *Sci Rep* (2018) 8(1):14985. doi: 10.1038/s41598-018-33248-7
110. Sim WJ, Ahl PJ, Connolly JE. Metabolism Is Central to Tolerogenic Dendritic Cell Function. *Mediators Inflammation* (2016) 2016:2636701. doi: 10.1155/2016/2636701
111. Morelli AE, Thomson AW. Tolerogenic Dendritic Cells and the Quest for Transplant Tolerance. *Nat Rev Immunol* (2007) 7(8):610–21. doi: 10.1038/nri2132
112. Huang H, Dawicki W, Zhang X, Town J, Gordon JR. Tolerogenic Dendritic Cells Induce CD4+CD25 hiFoxp3+ Regulatory T Cell Differentiation From CD4 +Cd25-/loFoxp3- Effector T Cells. *J Immunol* (2010) 185(9):5003–10. doi: 10.4049/jimmunol.0903446
113. Raker VK, Domogalla MP, Steinbrink K. Tolerogenic Dendritic Cells for Regulatory T Cell Induction in Man. *Front Immunol* (2015) 6:569. doi: 10.3389/fimmu.2015.00569
114. Stenger EO, Turnquist HR, Mapara MY, Thomson AW. Dendritic Cells and Regulation of Graft-Versus-Host Disease and Graft-Versus-Leukemia Activity. *Blood* (2012) 119(22):5088–103. doi: 10.1182/blood-2011-11-364091
115. Hilkens CMU, Isaacs JD, Thomson AW. Development of Dendritic Cell-Based Immunotherapy for Autoimmunity. *Int Rev Immunol* (2010) 29 (2):156–83. doi: 10.3109/08830180903281193
116. Thomson AW, Robbins PD. Tolerogenic Dendritic Cells for Autoimmune Disease and Transplantation. *Ann Rheum Dis* (2008) 67(SUPPL. 3):iii90–iii6. doi: 10.1136/ard.2008.099176
117. Verhasselt V, Vosters O, Beuneu C, Nicaise C, Stordeur P, Goldman M. Induction of FOXP3-expressing Regulatory CD4pos T Cells by Human Mature Autologous Dendritic Cells. *Eur J Immunol* (2004) 34(3):762–72. doi: 10.1002/eji.200324552
118. Jonuleit H, Schmitt E, Schuler G, Knop J, Enk AH. Induction of Interleukin 10-Producing, Nonproliferating CD4(+) T Cells With Regulatory Properties by Repetitive Stimulation With Allogeneic Immature Human Dendritic Cells. *J Exp Med* (2000) 192(9):1213–22. doi: 10.1084/jem.192.9.1213
119. Dhodapkar MV, Steinman RM, Krasovsky J, Munz C, Bhardwaj N. Antigen-Specific Inhibition of Effector T Cell Function in Humans After Injection of Immature Dendritic Cells. *J Exp Med* (2001) 193(2):233–8. doi: 10.1084/jem.193.2.233
120. Rastellini C, Lu L, Ricorbi C, Starzl TE, Rao AS, Thomson AW. Granulocyte/Macrophage Colony-Stimulating Factor-Stimulated Hepatic Dendritic Cell Progenitors Prolong Pancreatic Islet Allograft Survival. *Transplantation* (1995) 60(11):1366–70.
121. Fu F, Li Y, Qian S, Lu L, Chambers F, Starzl TE, et al. Costimulatory Molecule-Deficient Dendritic Cell Progenitors (MHC Class II+, CD80(Dim), CD86-) Prolong Cardiac Allograft Survival in Nonimmunosuppressed Recipients. *Transplantation* (1996) 62(5):659–65. doi: 10.1097/00007890-199609150-00021
122. Wu H, Malone AF, Donnelly EL, Kirita Y, Uchimura K, Ramakrishnan SM, et al. Single-Cell Transcriptomics of a Human Kidney Allograft Biopsy Specimen Defines a Diverse Inflammatory Response. *J Am Soc Nephrol* (2018) 29(8):2069–80. doi: 10.1681/asn.2018020125
123. Beriou G, Moreau A, Cuturi MC. Tolerogenic Dendritic Cells: Applications for Solid Organ Transplantation. *Curr Opin Organ Transplant* (2012) 17 (1):42–7. doi: 10.1097/MOT.0b013e32834ee662
124. Ezzelarab MB, Zahorchak AF, Lu L, Morelli AE, Chalasani G, Demetris AJ, et al. Regulatory Dendritic Cell Infusion Prolongs Kidney Allograft Survival in Nonhuman Primates. *Am J Transplant* (2013) 13(8):1989–2005. doi: 10.1111/ajt.12310
125. Ezzelarab MB, Raich-Regue D, Lu L, Zahorchak AF, Perez-Gutierrez A, Humar A, et al. Renal Allograft Survival in Nonhuman Primates Infused With Donor Antigen-Pulsed Autologous Regulatory Dendritic Cells. *Am J Transplant* (2017) 17(6):1476–89. doi: 10.1111/ajt.14182
126. Madelon N, Montanari E, Gruaz L, Pimenta J, Muller YD, Bühler LH, et al. Prolongation of Rat-to-Mouse Islets Xenograft Survival by Co-Transplantation of Autologous IL-10 Differentiated Murine Tolerogenic Dendritic Cells. *Xenotransplantation* (2020) 27(4):e12584. doi: 10.1111/xen.12584
127. Marinelarena A, Bhattacharya P, Kumar P, Maker AV, Prabhakar BS. Identification of a Novel Ox40l(+) Dendritic Cell Subset That Selectively Expands Regulatory T Cells. *Sci Rep* (2018) 8(1):14940. doi: 10.1038/s41598-018-33307-z
128. Ezzelarab MB, Lu L, Guo H, Zahorchak AF, Shufesky WF, Cooper DKC, et al. Eomesoderminlo CTLA4hi Alloreactive CD8+ Memory T Cells Are Associated With Prolonged Renal Transplant Survival Induced by Regulatory Dendritic Cell Infusion in CTLA4 Immunoglobulin-Treated Nonhuman Primates. *Transplantation* (2016) 100(1):91–102. doi: 10.1097/TP.0000000000000871
129. Ezzelarab MB, Lu L, Shufesky WF, Morelli AE, Thomson AW. Donor-Derived Regulatory Dendritic Cell Infusion Maintains Donor-Reactive CD4

(+)CTLA4(Hi) T Cells in Non-Human Primate Renal Allograft Recipients Treated With CD28 Co-Stimulation Blockade. *Front Immunol* (2018) 9:250. doi: 10.3389/fimmu.2018.00250
130. Lin H, Rathmell JC, Gray GS, Thompson CB, Leiden JM, Alegre ML. Cytotoxic T Lymphocyte Antigen 4 (CTLA4) Blockade Accelerates the Acute Rejection of Cardiac Allografts in CD28-deficient Mice: CTLA4 can Function Independently of CD28. *J Exp Med* (1998) 188(1):199–204. doi: 10.1084/jem.188.1.199
131. Grimbert P, Audard V, Diet C, Matignon M, Plonquet A, Mansour H, et al. T-Cell Phenotype in Protocol Renal Biopsy From Transplant Recipients Treated With Belatacept-Mediated Co-Stimulatory Blockade. *Nephrol Dial Transplant* (2011) 26(3):1087–93. doi: 10.1093/ndt/gfq453
132. Intlekofer AM, Takemoto N, Wherry EJ, Longworth SA, Northrup JT, Palanivel VR, et al. Effector and Memory CD8+ T Cell Fate Coupled by T-bet and Eomesodermin. *Nat Immunol* (2005) 6(12):1236–44. doi: 10.1038/ni1268
133. Vincenti F, Charpentier B, Vanrenterghem Y, Rostaing L, Bresnahan B, Darji P, et al. A Phase III Study of Belatacept-Based Immunosuppression Regimens Versus Cyclosporine in Renal Transplant Recipients (BENEFIT Study). *Am J Transplant* (2010) 10(3):535–46. doi: 10.1111/j.1600-6143.2009.03005.x
134. Stallone G, Pontrelli P, Infante B, Gigante M, Netti GS, Ranieri E, et al. Rapamycin Induces ILT3(high)ILT4(high) Dendritic Cells Promoting a New Immunoregulatory Pathway. *Kidney Int* (2014) 85(4):888–97. doi: 10.1038/ki.2013.337
135. Na N, Luo Y, Zhao DQ, Yang SC, Hong LQ, Li H, et al. Prolongation of Kidney Allograft Survival Regulated by Indoleamine 2,3-Dioxygenase in Immature Dendritic Cells Generated From Recipient Type Bone Marrow Progenitors. *Mol Immunol* (2016) 79:22–31. doi: 10.1016/j.molimm.2016.09.005
136. Széles L, Keresztes G, Töröcsik D, Balajthy Z, Krenács L, Póliska S, et al. 1,25-Dihydroxyvitamin D3 is an Autonomous Regulator of the Transcriptional Changes Leading to a Tolerogenic Dendritic Cell Phenotype. *J Immunol* (2009) 182(4):2074–83. doi: 10.4049/jimmunol.0803345
137. Vanherwegen AS, Cook DP, Ferreira GB, Gysemans C, Mathieu C. Vitamin D-modulated Dendritic Cells Delay Lethal Graft-Versus-Host Disease Through Induction of Regulatory T Cells. *J Steroid Biochem Mol Biol* (2019) 188:103–10. doi: 10.1016/j.jsbmb.2018.12.013
138. Penna G, Roncari A, Amuchastegui S, Daniel KC, Berti E, Colonna M, et al. Expression of the Inhibitory Receptor ILT3 on Dendritic Cells is Dispensable for Induction of CD4+Foxp3+ Regulatory T Cells by 1,25-Dihydroxyvitamin D3. *Blood* (2005) 106(10):3490–7. doi: 10.1182/blood-2005-05-2044
139. Farias AS, Spagnol GS, Bordeaux-Rego P, Oliveira CO, Fontana AG, de Paula RF, et al. Vitamin D3 Induces IDO+ Tolerogenic DCs and Enhances Treg, Reducing the Severity of EAE. *CNS Neurosci Ther* (2013) 19(4):269–77. doi: 10.1111/cns.12071
140. Navarro-Barriuso J, Mansilla MJ, Quirant-Sánchez B, Ardiaca-Martínez A, Teniente-Serra A, Presas-Rodríguez S, et al. MAP7 and MUCL1 are Biomarkers of Vitamin D3-Induced Tolerogenic Dendritic Cells in Multiple Sclerosis Patients. *Front Immunol* (2019) 10:1251. doi: 10.3389/fimmu.2019.01251
141. Divito SJ, Wang Z, Shufesky WJ, Liu Q, Tkacheva OA, Montecalvo A, et al. Endogenous Dendritic Cells Mediate the Effects of Intravenously Injected Therapeutic Immunosuppressive Dendritic Cells in Transplantation. *Blood* (2010) 116(15):2694–705. doi: 10.1182/blood-2009-10-251058
142. Kenna TJ, Thomas R, Steptoe RJ. Steady-State Dendritic Cells Expressing Cognate Antigen Terminate Memory CD8+ T-Cell Responses. *Blood* (2008) 111(4):2091–100. doi: 10.1182/blood-2007-07-103200
143. Kenna TJ, Waldie T, McNally A, Thomson M, Yagita H, Thomas R, et al. Targeting Antigen to Diverse APCs Inactivates Memory CD8+ T Cells Without Eliciting Tissue-Destructive Effector Function. *J Immunol* (2010) 184(2):598–606. doi: 10.4049/jimmunol.0900032
144. Nasreen M, Waldie TM, Dixon CM, Steptoe RJ. Steady-State Antigen-Expressing Dendritic Cells Terminate CD4+ Memory T-cell Responses. *Eur J Immunol* (2010) 40(7):2016–25. doi: 10.1002/eji.200940085
145. Kleijwegt FS, Jansen DTSL, Teeler J, Joosten AM, Laban S, Nikolic T, et al. Tolerogenic Dendritic Cells Impede Priming of Naïve CD8+ T Cells and Deplete Memory CD8+ T Cells. *Eur J Immunol* (2013) 43(1):85–92. doi: 10.1002/eji.201242879
146. Kwan T, Chadban SJ, Ma J, Bao S, Alexander SI, Wu H. Il-17 Deficiency Attenuates Allograft Injury and Prolongs Survival in a Murine Model of Fully MHC-mismatched Renal Allograft Transplantation. *Am J Transplant* (2015) 15(6):1555–67. doi: 10.1111/ajt.13140
147. Zahorchak AF, Kean LS, Tokita D, Turnquist HR, Abe M, Finke J, et al. Infusion of Stably Immature Monocyte-Derived Dendritic Cells Plus CTLA4Ig Modulates Alloimmune Reactivity in Rhesus Macaques. *Transplantation* (2007) 84(2):196–206. doi: 10.1097/01.tp.0000268582.21168.f6
148. Morelli AE, Thomson AW. Orchestration of Transplantation Tolerance by Regulatory Dendritic Cell Therapy or in-Situ Targeting of Dendritic Cells. *Curr Opin Organ Transplant* (2014) 19(4):348–56. doi: 10.1097/MOT.0000000000000097
149. Rogers NM, Isenberg JS, Thomson AW. Plasmacytoid Dendritic Cells: No Longer an Enigma and Now Key to Transplant Tolerance? *Am J Transplant* (2013) 13(5):1125–33. doi: 10.1111/ajt.12229
150. Bonifaz L, Bonnyay D, Mahnke K, Rivera M, Nussenzweig MC, Steinman RM. Efficient Targeting of Protein Antigen to the Dendritic Cell Receptor DEC-205 in the Steady State Leads to Antigen Presentation on Major Histocompatibility Complex Class I Products and Peripheral CD8+ T Cell Tolerance. *J Exp Med* (2002) 196(12):1627–38. doi: 10.1084/jem.20021598
151. Jung KC, Park CG, Jeon YK, Park HJ, Ban YL, Min HS, et al. In Situ Induction of Dendritic Cell-Based T Cell Tolerance in Humanized Mice and Nonhuman Primates. *J Exp Med* (2011) 208(12):2477–88. doi: 10.1084/jem.20111242
152. Li D, Romain G, Flamar AL, Duluc D, Dullaers M, Li XH, et al. Targeting Self- and Foreign Antigens to Dendritic Cells Via DC-ASGPR Generates IL-10-producing Suppressive CD4+ T Cells. *J Exp Med* (2012) 209(1):109–21. doi: 10.1084/jem.20110399
153. Phillips BE, Garciafigueroa Y, Trucco M, Giannoukakis N. Clinical Tolerogenic Dendritic Cells: Exploring Therapeutic Impact on Human Autoimmune Disease. *Front Immunol* (2017) 8:1279. doi: 10.3389/fimmu.2017.01279
154. Wang Z, Divito SJ, Shufesky WJ, Sumpter T, Wang H, Tkacheva OA, et al. Dendritic Cell Therapies in Transplantation Revisited: Deletion of Recipient DCs Deters the Effect of Therapeutic Dcs. *Am J Transplant* (2012) 12(6):1398–408. doi: 10.1111/j.1600-6143.2012.04060.x
155. Boks MA, Kager-Groenland JR, Haasjes MS, Zwaginga JJ, van Ham SM, ten Brinke A. Il-10-generated Tolerogenic Dendritic Cells are Optimal for Functional Regulatory T Cell Induction–a Comparative Study of Human Clinical-Applicable DC. *Clin Immunol* (2012) 142(3):332–42. doi: 10.1016/j.clim.2011.11.011
156. Comi M, Amodio G, Gregori S. Interleukin-10-Producing DC-10 is a Unique Tool to Promote Tolerance Via Antigen-Specific T Regulatory Type 1 Cells. *Front Immunol* (2018) 9:682. doi: 10.3389/fimmu.2018.00682
157. Kryczanowsky F, Raker V, Graulich E, Domogalla MP, Steinbrink K. Il-10-Modulated Human Dendritic Cells for Clinical Use: Identification of a Stable and Migratory Subset With Improved Tolerogenic Activity. *J Immunol* (2016) 197(9):3607–17. doi: 10.4049/jimmunol.1501769
158. Song S, Yuan P, Wu H, Chen J, Fu J, Li P, et al. Dendritic Cells With an Increased PD-L1 by TGF-β Induce T Cell Anergy for the Cytotoxicity of Hepatocellular Carcinoma Cells. *Int Immunopharmacol* (2014) 20(1):117–23. doi: 10.1016/j.intimp.2014.02.027
159. Qian C, Qian L, Yu Y, An H, Guo Z, Han Y, et al. Fas Signal Promotes the Immunosuppressive Function of Regulatory Dendritic Cells Via the ERK/β-Catenin Pathway. *J Biol Chem* (2013) 288(39):27825–35. doi: 10.1074/jbc.M112.425751
160. Lopes DM, Oliveira SC, Page B, Carvalho LP, Carvalho EM, Cardoso LS. Schistosoma Mansoni Rsm29 Antigen Induces a Regulatory Phenotype on Dendritic Cells and Lymphocytes From Patients With Cutaneous Leishmaniasis. *Front Immunol* (2018) 9:3122. doi: 10.3389/fimmu.2018.03122
161. Luan YY, Zhang L, Zhu FJ, Dong N, Lu JY, Yao YM. Effect of TIPE1 on Immune Function of Dendritic Cells and Its Signaling Pathway in Septic Mice. *J Infect Dis* (2019) 220(4):699–709. doi: 10.1093/infdis/jiz158
162. Xu Y, Tang X, Yang M, Zhang S, Li S, Chen Y, et al. Interleukin 10 Gene-Modified Bone Marrow-Derived Dendritic Cells Attenuate Liver Fibrosis in Mice by Inducing Regulatory T Cells and Inhibiting the TGF-β/Smad

Signaling Pathway. *Mediators Inflammation* (2019) 2019:4652596. doi: 10.1155/2019/4652596
163. Lan Z, Ge W, Arp J, Jiang JF, Liu WH, Gordon D, et al. Induction of Kidney Allograft Tolerance by Soluble Cd83 Associated With Prevalence of Tolerogenic Dendritic Cells and Indoleamine 2,3-Dioxygenase. *Transplantation* (2010) 90(12):1286–93. doi: 10.1097/TP.0b013e3182007bbf
164. Trabanelli S, Lecciso M, Salvestrini V, Cavo M, Očadlíková D, Lemoli RM, et al. PGE2-Induced IDO1 Inhibits the Capacity of Fully Mature DCs to Elicit an In Vitro Antileukemic Immune Response. *J Immunol Res* (2015) 2015:253191. doi: 10.1155/2015/253191
165. Flórez-Grau G, Cabezón R, Borgman KJE, España C, Lozano JJ, Garcia-Parajo MF, et al. Up-Regulation of EP(2) and EP(3) Receptors in Human Tolerogenic Dendritic Cells Boosts the Immunosuppressive Activity of PGE (2). *J Leukoc Biol* (2017) 102(3):881–95. doi: 10.1189/jlb.2A1216-526R
166. Turnquist HR, Raimondi G, Zahorchak AF, Fischer RT, Wang Z, Thomson AW. Rapamycin-Conditioned Dendritic Cells are Poor Stimulators of Allogeneic CD4+ T Cells, But Enrich for Antigen-Specific Foxp3+ T Regulatory Cells and Promote Organ Transplant Tolerance. *J Immunol* (2007) 178(11):7018–31. doi: 10.4049/jimmunol.178.11.7018
167. Campos-Acuña J, Pérez F, Narváez E, Campos-Mora M, Gajardo T, Catalán D, et al. Rapamycin-Conditioned Dendritic Cells Activated With Monophosphoryl Lipid-a Promote Allograft Acceptance In Vivo. *Immunotherapy* (2015) 7(2):101–10. doi: 10.2217/imt.14.116
168. Kim SH, Moon JH, Jeong SU, Jung HH, Park CS, Hwang BY, et al. Induction of Antigen-Specific Immune Tolerance Using Biodegradable Nanoparticles Containing Antigen and Dexamethasone. *Int J Nanomed* (2019) 14:5229–42. doi: 10.2147/ijn.S210546
169. Jauregui-Amezaga A, Cabezón R, Ramírez-Morros A, España C, Rimola J, Bru C, et al. Intraperitoneal Administration of Autologous Tolerogenic Dendritic Cells for Refractory Crohn's Disease: A Phase I Study. *J Crohns Colitis* (2015) 9(12):1071–8. doi: 10.1093/ecco-jcc/jjv144
170. Bell GM, Anderson AE, Diboll J, Reece R, Eltherington O, Harry RA, et al. Autologous Tolerogenic Dendritic Cells for Rheumatoid and Inflammatory Arthritis. *Ann Rheum Dis* (2017) 76(1):227–34. doi: 10.1136/annrheumdis-2015-208456
171. Harry RA, Anderson AE, Isaacs JD, Hilkens CM. Generation and Characterisation of Therapeutic Tolerogenic Dendritic Cells for Rheumatoid Arthritis. *Ann Rheum Dis* (2010) 69(11):2042–50. doi: 10.1136/ard.2009.126383
172. Zhang M, Zheng Y, Sun Y, Li S, Chen L, Jin X, et al. Knockdown of NEAT1 Induces Tolerogenic Phenotype in Dendritic Cells by Inhibiting Activation of NLRP3 Inflammasome. *Theranostics* (2019) 9(12):3425–42. doi: 10.7150/thno.33178
173. Wu J, Zhang H, Zheng Y, Jin X, Liu M, Li S, et al. The Long Noncoding RNA Malat1 Induces Tolerogenic Dendritic Cells and Regulatory T Cells Via Mir155/Dendritic Cell-Specific Intercellular Adhesion Molecule-3 Grabbing Nonintegrin/Il10 Axis. *Front Immunol* (2018) 9:1847. doi: 10.3389/fimmu.2018.01847
174. Zhang X, Li M, Lian D, Zheng X, Zhang ZX, Ichim TE, et al. Generation of Therapeutic Dendritic Cells and Regulatory T Cells for Preventing Allogeneic Cardiac Graft Rejection. *Clin Immunol* (2008) 127(3):313–21. doi: 10.1016/j.clim.2008.01.013
175. Pearce EL, Pearce EJ. Metabolic Pathways in Immune Cell Activation and Quiescence. *Immunity* (2013) 38(4):633–43. doi: 10.1016/j.immuni.2013.04.005
176. Thwe PM, Pelgrom LR, Cooper R, Beauchamp S, Reisz JA, D'Alessandro A, et al. Cell-Intrinsic Glycogen Metabolism Supports Early Glycolytic Reprogramming Required for Dendritic Cell Immune Responses. *Cell Metab* (2017) 26(3):558–67.e5. doi: 10.1016/j.cmet.2017.08.012
177. Guak H, Al Habyan S, Ma EH, Aldossary H, Al-Masri M, Won SY, et al. Glycolytic Metabolism is Essential for CCR7 Oligomerization and Dendritic Cell Migration. *Nat Commun* (2018) 9(1):2463. doi: 10.1038/s41467-018-04804-6
178. Everts B, Amiel E, Huang SC, Smith AM, Chang CH, Lam WY, et al. TLR-Driven Early Glycolytic Reprogramming Via the Kinases TBK1-IKKε Supports the Anabolic Demands of Dendritic Cell Activation. *Nat Immunol* (2014) 15(4):323–32. doi: 10.1038/ni.2833
179. Gotoh K, Morisaki T, Setoyama D, Sasaki K, Yagi M, Igami K, et al. Mitochondrial P32/C1qbp Is a Critical Regulator of Dendritic Cell Metabolism and Maturation. *Cell Rep* (2018) 25(7):1800–15.e4. doi: 10.1016/j.celrep.2018.10.057
180. Holtzhausen A, Zhao F, Evans KS, Tsutsui M, Orabona C, Tyler DS, et al. Melanoma-Derived Wnt5a Promotes Local Dendritic-Cell Expression of IDO and Immunotolerance: Opportunities for Pharmacologic Enhancement of Immunotherapy. *Cancer Immunol Res* (2015) 3(9):1082–95. doi: 10.1158/2326-6066.Cir-14-0167
181. Ferreira GB, Vanherwegen AS, Eelen G, Gutiérrez ACF, Van Lommel L, Marchal K, et al. Vitamin D3 Induces Tolerance in Human Dendritic Cells by Activation of Intracellular Metabolic Pathways. *Cell Rep* (2015) 10(5):711–25. doi: 10.1016/j.celrep.2015.01.013
182. Everts B, Amiel E, van der Windt GJ, Freitas TC, Chott R, Yarasheski KE, et al. Commitment to Glycolysis Sustains Survival of NO-producing Inflammatory Dendritic Cells. *Blood* (2012) 120(7):1422–31. doi: 10.1182/blood-2012-03-419747
183. Wei HJ, Gupta A, Kao WM, Almudallal O, Letterio JJ, Pareek TK. Nrf2-mediated Metabolic Reprogramming of Tolerogenic Dendritic Cells is Protective Against Aplastic Anemia. *J Autoimmun* (2018) 94:33–44. doi: 10.1016/j.jaut.2018.07.005
184. Sun Y, Oravecz-Wilson K, Bridges S, McEachin R, Wu J, Kim SH, et al. miR-142 Controls Metabolic Reprogramming That Regulates Dendritic Cell Activation. *J Clin Invest* (2019) 129(5):2029–42. doi: 10.1172/jci123839
185. Mogilenko DA, Haas JT, L'Homme L, Fleury S, Quemener S, Levavasseur M, et al. Metabolic and Innate Immune Cues Merge Into a Specific Inflammatory Response Via the UPR. *Cell* (2019) 177(5):1201–16.e19. doi: 10.1016/j.cell.2019.03.018
186. Romero MM, Duarte A, Pastorini M, Alemán M. Role of α-Glucan-Induced Oxygen Species in Dendritic Cells and its Impact in Immune Response Against Tuberculosis. *Int J Med Microbiol* (2019) 309(6):151328. doi: 10.1016/j.ijmm.2019.07.002
187. Oberkampf M, Guillerey C, Mouriès J, Rosenbaum P, Fayolle C, Bobard A, et al. Mitochondrial Reactive Oxygen Species Regulate the Induction of CD8 (+) T Cells by Plasmacytoid Dendritic Cells. *Nat Commun* (2018) 9(1):2241. doi: 10.1038/s41467-018-04686-8
188. Woltman AM, van der Kooij SW, Coffer PJ, Offringa R, Daha MR, van Kooten C. Rapamycin Specifically Interferes With GM-CSF Signaling in Human Dendritic Cells, Leading to Apoptosis Via Increased p27KIP1 Expression. *Blood* (2003) 101(4):1439–45. doi: 10.1182/blood-2002-06-1688
189. Perl A. mTOR Activation is a Biomarker and a Central Pathway to Autoimmune Disorders, Cancer, Obesity, and Aging. *Ann N Y Acad Sci* (2015) 1346(1):33–44. doi: 10.1111/nyas.12756
190. Tomić S, Janjetović K, Mihajlović D, Milenković M, Kravić-Stevović T, Marković Z, et al. Graphene Quantum Dots Suppress Proinflammatory T Cell Responses Via Autophagy-Dependent Induction of Tolerogenic Dendritic Cells. *Biomaterials* (2017) 146:13–28. doi: 10.1016/j.biomaterials.2017.08.040
191. Watson AR, Dai H, Zheng Y, Nakano R, Giannou AD, Menk AV, et al. Mtorc2 Deficiency Alters the Metabolic Profile of Conventional Dendritic Cells. *Front Immunol* (2019) 10:1451. doi: 10.3389/fimmu.2019.01451
192. Liu Y, Tong L, Luo Y, Li X, Chen G, Wang Y. Resveratrol Inhibits the Proliferation and Induces the Apoptosis in Ovarian Cancer Cells Via Inhibiting Glycolysis and Targeting AMPK/mTOR Signaling Pathway. *J Cell Biochem* (2018) 119(7):6162–72. doi: 10.1002/jcb.26822
193. Wculek SK, Khouili SC, Priego E, Heras-Murillo I, Sancho D. Metabolic Control of Dendritic Cell Functions: Digesting Information. *Front Immunol* (2019) 10:775. doi: 10.3389/fimmu.2019.00775
194. Kelly B, O'Neill LA. Metabolic Reprogramming in Macrophages and Dendritic Cells in Innate Immunity. *Cell Res* (2015) 25(7):771–84. doi: 10.1038/cr.2015.68
195. Bhandari T, Olson J, Johnson RS, Nizet V. Hif-1α Influences Myeloid Cell Antigen Presentation and Response to Subcutaneous OVA Vaccination. *J Mol Med (Berl)* (2013) 91(10):1199–205. doi: 10.1007/s00109-013-1052-y
196. Thwe PM, Fritz DI, Snyder JP, Smith PR, Curtis KD, O'Donnell A, et al. Syk-Dependent Glycolytic Reprogramming in Dendritic Cells Regulates IL-1β Production to β-Glucan Ligands in a TLR-independent Manner. *J Leukoc Biol* (2019) 106(6):1325–35. doi: 10.1002/jlb.3a0819-207rr
197. Bode K, Bujupi F, Link C, Hein T, Zimmermann S, Peiris D, et al. Dectin-1 Binding to Annexins on Apoptotic Cells Induces Peripheral Immune Tolerance Via NADPH Oxidase-2. *Cell Rep* (2019) 29(13):4435–46.e9. doi: 10.1016/j.celrep.2019.11.086

198. Mitchell S, Vargas J, Hoffmann A. Signaling Via the Nfκb System. *Wiley Interdiscip Rev Syst Biol Med* (2016) 8(3):227–41. doi: 10.1002/wsbm.1331
199. Rescigno M, Martino M, Sutherland CL, Gold MR, Ricciardi-Castagnoli P. Dendritic Cell Survival and Maturation are Regulated by Different Signaling Pathways. *J Exp Med* (1998) 188(11):2175–80. doi: 10.1084/jem.188.11.2175
200. Jackson SH, Yu CR, Mahdi RM, Ebong S, Egwuagu CE. Dendritic Cell Maturation Requires STAT1 and is Under Feedback Regulation by Suppressors of Cytokine Signaling. *J Immunol* (2004) 172(4):2307–15. doi: 10.4049/jimmunol.172.4.2307
201. Xu L, Zhang Y, Tian K, Chen X, Zhang R, Mu X, et al. Apigenin Suppresses PD-L1 Expression in Melanoma and Host Dendritic Cells to Elicit Synergistic Therapeutic Effects. *J Exp Clin Cancer Res* (2018) 37(1):261. doi: 10.1186/s13046-018-0929-6
202. Zhu J, Yao K, Guo J, Shi H, Ma L, Wang Q, et al. miR-181a and miR-150 Regulate Dendritic Cell Immune Inflammatory Responses and Cardiomyocyte Apoptosis Via Targeting JAK1-STAT1/c-Fos Pathway. *J Cell Mol Med* (2017) 21(11):2884–95. doi: 10.1111/jcmm.13201
203. Xu J, Lee MH, Chakhtoura M, Green BL, Kotredes KP, Chain RW, et al. Stat2 Is Required for TLR-Induced Murine Dendritic Cell Activation and Cross-Presentation. *J Immunol* (2016) 197(1):326–36. doi: 10.4049/jimmunol.1500152
204. Melillo JA, Song L, Bhagat G, Blazquez AB, Plumlee CR, Lee C, et al. Dendritic Cell (DC)-Specific Targeting Reveals Stat3 as a Negative Regulator of DC Function. *J Immunol* (2010) 184(5):2638–45. doi: 10.4049/jimmunol.0902960
205. Bazhin AV, von Ahn K, Fritz J, Werner J, Karakhanova S. Interferon-α Up-Regulates the Expression of PD-L1 Molecules on Immune Cells Through STAT3 and p38 Signaling. *Front Immunol* (2018) 9:2129. doi: 10.3389/fimmu.2018.02129
206. Toniolo PA, Liu S, Yeh JE, Moraes-Vieira PM, Walker SR, Vafaizadeh V, et al. Inhibiting STAT5 by the BET Bromodomain Inhibitor JQ1 Disrupts Human Dendritic Cell Maturation. *J Immunol* (2015) 194(7):3180–90. doi: 10.4049/jimmunol.1401635
207. Zhu HC, Qiu T, Liu XH, Dong WC, Weng XD, Hu CH, et al. Tolerogenic Dendritic Cells Generated by RelB Silencing Using shRNA Prevent Acute Rejection. *Cell Immunol* (2012) 274(1-2):12–8. doi: 10.1016/j.cellimm.2012.02.012
208. Benham H, Nel HJ, Law SC, Mehdi AM, Street S, Ramnoruth N, et al. Citrullinated Peptide Dendritic Cell Immunotherapy in HLA Risk Genotype-Positive Rheumatoid Arthritis Patients. *Sci Transl Med* (2015) 7(290):290ra87. doi: 10.1126/scitranslmed.aaa9301

Conflict of Interest: The authors declare that the research was conducted in the absence of any commercial or financial relationships that could be construed as a potential conflict of interest.

Copyright © 2021 Lin, Wang, Liu, Cheng, Deng, Zhu and Chen. This is an open-access article distributed under the terms of the Creative Commons Attribution License (CC BY). The use, distribution or reproduction in other forums is permitted, provided the original author(s) and the copyright owner(s) are credited and that the original publication in this journal is cited, in accordance with accepted academic practice. No use, distribution or reproduction is permitted which does not comply with these terms.

frontiers in Immunology

REVIEW
published: 20 May 2021
doi: 10.3389/fimmu.2021.681748

Macrophage Heterogeneity in Kidney Injury and Fibrosis

Yi Wen[†], *Hong-Ru Yan*[†], *Bin Wang and Bi-Cheng Liu*[*]

Department of Nephrology, Zhongda Hospital, Southeast University School of Medicine, Nanjing, China

Kidney macrophages are central in kidney disease pathogenesis and have therapeutic potential in preventing tissue injury and fibrosis. Recent studies highlighted that kidney macrophages are notably heterogeneous immune cells that fulfill opposing functions such as clearing deposited pathogens, maintaining immune tolerance, initiating and regulating inflammatory responses, promoting kidney fibrosis, and degrading the extracellular matrix. Macrophage origins can partially explain macrophage heterogeneity in the kidneys. Circulating Ly6C^{+} monocytes are recruited to inflammatory sites by chemokines, while self-renewed kidney resident macrophages contribute to kidney repair and fibrosis. The proliferation of resident macrophages or infiltrating monocytes provides an alternative explanation of macrophage accumulation after kidney injury. In addition, dynamic Ly6C expression on infiltrating monocytes accompanies functional changes in handling kidney inflammation and fibrosis. Mechanisms underlying kidney macrophage heterogeneity, either by recruiting monocyte subpopulations, regulating macrophage polarization, or impacting distinctive macrophage functions, may help develop macrophage-targeted therapies for kidney diseases.

Keywords: macrophage heterogeneity, resident macrophage, kidney, inflammation, fibrosis

OPEN ACCESS

Edited by:
Cheng Yang,
Fudan University, China

Reviewed by:
Guillaume Hoeffel,
U1104 Centre d'immunologie de Marseille-Luminy (CIML) (INSERM), France
Yinghong Hu,
Emory University, United States

***Correspondence:**
Bi-Cheng Liu
liubc64@163.com

[†]*These authors have contributed equally to this work*

Specialty section:
This article was submitted to Molecular Innate Immunity, a section of the journal Frontiers in Immunology

Received: *17 March 2021*
Accepted: *07 May 2021*
Published: *20 May 2021*

Citation:
Wen Y, Yan H-R, Wang B and Liu B-C (2021) Macrophage Heterogeneity in Kidney Injury and Fibrosis. Front. Immunol. 12:681748. doi: 10.3389/fimmu.2021.681748

INTRODUCTION

Macrophage plays an important role in kidney disease pathogenesis and is a potential therapeutic target for kidney injury and fibrosis. Kidney macrophage subpopulations can either promote or prevent the extracellular matrix deposition in the kidney, drawing the possibility of reversing kidney fibrosis (1). However, the functionally opposing macrophage subpopulations rising ambivalence in understanding macrophage activities during kidney injury and fibrosis, disturbing the development of macrophage-targeted therapies (2). Studies have focused on macrophage functional diversities mechanisms and applied novel approaches in precisely identifying macrophage subpopulations. Therefore, intriguing questions have arisen, such as the macrophage origin (kidney-resident macrophages vs. circulating monocyte precursors), macrophage differentiation (oversimplified M1/M2 categorization vs. newly subsets defined by cell surface markers and single-cell RNA-sequence), and their effector functions in the pathogenesis of kidney diseases.

MACROPHAGE HETEROGENEITY

Macrophage heterogeneity attracts attention since the discovery of macrophages. Following studies expand macrophage heterogeneity definition depending on the origin, cell surface markers, and cytokines secretion (3). Macrophages obtain distinct phenotypes under physiological conditions and differentiate into functional phenotypes in response to pathological stimulation. According to their cooperation with distinct T cell subsets, macrophages have generally been classified either into classical M1 or alternative M2 macrophages. M1 macrophages are characterized by pro-inflammatory effects and engage with T helper 1 (Th1) cells, whereas M2 macrophages exhibit immunoregulatory efforts and intimately cooperate with T helper 2 (Th2) cells (4). M1 macrophage differentiation is initiated by pathogen-associated molecular patterns (PAMPs), danger-associated molecular patterns (DAMPs), and pro-inflammatory cytokines, especially under acute deleterious conditions (5). Representative functions of M1 macrophages are host defense and secretion of pro-inflammatory cytokines, such as tumor necrosis factor-α (TNF-α), interleukine-1β (IL-1β), interleukine-6 (IL-6), and interleukine-12 (IL-12). M2 macrophage is typically polarized by interleukine-4 (IL-4) and interleukine-13 (IL-13), suppressing inflammation and promoting wound repair. Recent studies further classify M2 macrophages into different subsets depending on their differentiation stimuli, markers, and functions (6). While classic M2 macrophages are classified into M2a macrophages, M2b macrophages are induced by immune complexes, toll-like receptors and/or interleukine-1 receptors (IL-1R), contributing to immunoregulation and Th2 cells activation. M2c macrophages are induced by interleukine-10 (IL-10) and glucocorticoids, participating in immunosuppression, tissue repair, and matrix deposition. The simplified paradigm of M1/M2 macrophages facilitates the studies of macrophage phenotypes and functions. However, typical M1/M2 macrophages are induced in carefully regulated circumstances *in vitro* and not uniformly observed under the dynamic and complex environment *in vivo*. In fact, macrophages appear to express M1/M2 markers simultaneously during kidney injury, and their origins largely determine the functions of renal macrophages. Lineage tracing studies demonstrated that postnatal kidney macrophages predominately originate from the yolk sac EMP and hematopoietic stem cells, and bone marrow-derived monocytes infiltrate the kidney under inflammatory conditions (7, 8).

RENAL MACROPHAGE DISTRIBUTION DURING DEVELOPMENT, HEALTH, AND DISEASE

Macrophages contribute to morphogenesis during organ development. In cultured kidney explants, colony-stimulating factor-1 (CSF-1) application stimulates ureteric bud branching and nephron formation (9). By binding to the membrane receptor CSF1R, CSF-1 accelerates macrophage proliferation and differentiation (10, 11). Macrophages infiltrate the nephrogenic zone and facilitate nephron progenitor proliferation after the transient loss of nephron progenitor cells (12). Munro et al. (13) demonstrated that macrophages directly interacted with endothelium in developing cortical nephrogenic caliber vessels. These F4/80$^+$CD206$^+$ macrophages are perivascular and enriched for mRNAs associated with organogenesis. Moreover, the subpopulation of Gal3^{high} myeloid cells are professional phagocytes and intermingle with pro-development F4/80$^+$CD206$^+$ macrophages in the developing mouse kidney. Therefore, fetal kidney macrophages possibly facilitate organogenesis by interacting with newly forming nephrogenic blood vessels. In addition, macrophages distribute around renal tubules during kidney development (9), but the underlying mechanisms are unclear. Experimental models of invertebrate species, such as *Drosophila melanogaster* (*D. melanogaster*), provide novel insights. In *D. melanogaster*, the Malpighian tubules are analogous to kidneys, while hemocytes are similar to macrophages. Hemocyte deposition around the developing Malpighian tubules is mediated by type IV collagen, necessary for the normal organogenesis of anterior Malpighian tubules (14). In mammalian kidneys, the renal tubular basement membrane is abundant in collagen IV and attracts macrophage recruitment (15, 16). However, it is difficult to extend these findings to mammalian kidneys due to the unique nephron structure.

In normal human kidneys, Marshall et al. (17) observed monocyte/macrophage distribution by immunoperoxidase staining of α-1-antitrypsin, muramidase, and serum 22. Most positive staining cells were scattered in glomerular capillaries and intertubular blood vessels. Macrophages rarely infiltrated into tubulointerstitium except in scarring tissues. However, the generality of these findings is limited by non-specific markers. Recently, Cao et al. (18) demonstrated that F4/80$^+$CD11c$^-$ macrophages distribute throughout the renal cortex and medulla in healthy kidneys. In contrast, F4/80$^+$CD11c$^+$ mononuclear phagocytes are distributed in the renal cortex rather than the medulla under normal and injured conditions. These double-positive mononuclear phagocytes performed M1-like macrophage phenotype and aggravated kidney injury during Adriamycin nephropathy. However, a large percentage of CD11c$^+$ dendritic cells co-express F4/80 marker in healthy kidneys, the preference to determine the nature of F4/80$^+$CD11c$^+$ cells should be circumspect.

Due to a double set of arterioles and capillaries, the kidney owns a unique vascular supply and receives about 25% of the cardiac output. The renal cortex exposed continuously to large amounts of blood-derived antigens and antibodies, resulting in a high sensitivity to renal glomerular diseases (19). Glomerular macrophage accumulation is an important feature in human glomerulonephritis. Macrophage clearance decreased glomerular damage in experimental glomerulonephritis (20). Further studies targeting monocyte chemotactic molecule-1 (MCP-1) or leukocyte adhesion molecules (ICAM) successfully attenuated macrophage accumulation and kidney injury in experimental

models (21, 22). Interestingly, the numbers of tubulointerstitial macrophages rather than glomerular macrophages predict renal dysfunction (23, 24). Our previous studies found that tubular epithelial exosomes contribute to macrophage infiltration and activation, providing a novel insight into tubulointerstitial macrophages (25–27). This review focus on macrophage heterogeneity in the kidney and excellent works have been done to card macrophage function and distribution during acute kidney injury (AKI) and chronic kidney disease (CKD) (1, 28).

KIDNEY RESIDENT MACROPHAGE ORIGIN AND SPECIFICITY

Kidney-resident macrophages are *in situ* self-renewed and characterized by their phagocytic activities, expression of pattern recognition receptors (PRRs), and immunological regulation capacity, thus, maintaining kidney homeostasis (29). Kidney-resident macrophages derive from 3 sources: (1) yolk sac erythro-myeloid progenitors (EMP)-derived macrophages, (2) fetal liver EMP-derived macrophages, and (3) hematopoietic stem cells (HSC)-derived macrophages. The relative proportion of each progenitor dramatically changes during the development, adulthood, and damaged kidney state.

At embryonic day 12.5, kidney macrophages are $CD45^+$ $CD11b^{lo}$ $F4/80^{hi}$ $Ly6C^-$ cells deriving from yolk sac EMP; in contrast, $CD45^+$ $CD11b^{hi}$ $F4/80^{lo}$ $Ly6C^+$ monocytes are undetectable at this stage (30). Using tamoxifen-inducible $Runx1^{Cre/EYFP}$ and $Csf1r^{Cre/EYFP}$ mice, fate tracing studies demonstrated that the relative proportion of yolk sac EMP-derived macrophages in the kidney decrease dramatically after embryonic day 13.5 (30). Consistently, *Csf1r-Cre* positive yolk sac-derived macrophages represent a minimal proportion of kidney macrophages after postnatal, possibly due to their dilution by the later arrival of fetal liver EMP-derived and HSC-derived macrophages (7). Sheng et al. (8) provided evidence of HSC-derived kidney macrophages using tamoxifen-inducible c-$Kit^{Cre/EYFP}$ mice. They further concluded that HSC precursors rather than EMPs are the source of kidney resident macrophages (8). However, the non-specific expression of *c-Kit-Cre* makes this conclusion debatable (31, 32). As HSCs transiently expressing *Flt3-cre* (33), Epelman et al. (7) distinguished the origin of HSC-derived monocytes and EMP-derived monocytes using $Flt3^{Cre/GFP}$ mice and found their equal contribution to the pool of resident macrophages. In contrast, Hoeffel et al. (30) demonstrated that fetal liver EMP-derived c-Myb^+ monocytes are the predominant source of kidney resident macrophages. Thus, further studies based on fate-mapping studies must concern the limitations of genetic models, and single-cell RNA-sequence classifies ability worth more attention. While the kidney exposes to circulating monocytes throughout the development and adulthood, the kidney resident macrophages are mainly EMP- and HSC-derived rather than bone marrow-derived (7, 8, 30, 32, 34), partially explained by the niche competition hypothesis (35). Recent studies found that under certain types of kidney disease, expanded macrophages derive from the subset of resident macrophages, especially yolk sac-derived macrophages (36, 37). Ide et al. (37) demonstrated that $CX3CR1^+$ yolk sac-derived macrophages have a higher proliferating capacity and progressively expand in number in older mice kidneys. Kidney resident macrophage proliferation contributes to the proangiogenic and pro-inflammatory environment after ischemic AKI and is confirmed by staining with Ki67 or BrdU (36, 38).

Kidney resident macrophages monitor trans-endothelial transport of circulating immune complexes and regulate the infiltration of lymphocytes and neutrophils (39). Using an unbiased flow cytometry approach, Kawakami et al. (40) classified kidney resident mononuclear phagocytes into five distinct subpopulations according to their cell surface markers, including $CD11b^{hi}$ $CD11c^{hi}$, $CD11b^{hi}$ $CD11c^{lo}$, $CD11b^{int}$ $CD11c^{int}$, $CD11b^{lo}$ $CD11c^{hi}$, and $CD11b^-$ $CD11c^{int}$. $CD11b^{int}$ $CD11c^{int}$ $F4/80^{high}$ monocytes perform anti-inflammation effects as endogenous defenders. Kidney resident macrophages are *in situ* self-renewal and minimally differentiated from circulating monocytes after ischemic AKI. However, bone marrow-derived monocytes can replenish the kidney resident macrophages when they are depleted using polyinosinic/polycytidylic acid (poly I:C), consistent with the niche competition hypothesis (38). Interestingly, kidney resident macrophages lack major histocompatibility complex class II (MHCII) expression in the repair phase after AKI, a phenotype occurring during the nephrogenesis, and enrich Wnt ligands production, such as Axin2, Tcf4, and Jun (38). In ischemic AKI, C-C chemokine receptor type 2 (CCR2) deficiency alleviates circulating $Ly6C^+$ macrophage recruitment and kidney injury and augments interstitial accumulation of $Ly6C^-$ embryonic yolk sac-derived resident macrophages and kidney fibrosis in late phases (41). Clodronate Liposome-induced macrophage depletion attenuates kidney injury and fibrosis, which can be restored by adoptive transfer of $Ly6C^-$ macrophages from injured wide type kidneys. While $Ly6C^-$ macrophage-derived cytokines facilitate the fibroblast-myofibroblast differentiation *in vivo* and *in vitro*, direct evidence targeting the trans-differentiation from $Ly6C^-$ macrophages to myofibroblasts remains missing (41). Similarly, $CX3CR1^+$ resident renal phagocytes amplify leukocyte infiltration in an NLRP3-dependent manner in contrast-induced acute kidney injury (42). Accumulation of infiltrating and resident macrophages augments in autosomal dominant polycystic kidneys. In unilateral nephrectomy accelerated *Pkd1* mice, lrf5 expression in resident macrophages aggravates cystic disease severity by producing pro-inflammatory cytokines (43). In ischemia-reperfusion injury (IRI) accelerated cystic mice, the phenotype of kidney resident macrophages transfers from $F4/80^{high}$ $CD11C^{low}$ to $F4/80^{high}$ $CD11C^{high}$, and reappearance of juvenile-like resident macrophages correlated with the accelerated cyst formation (44).

However, kidney resident macrophages also perform protective effects during acute and chronic kidney disease.

Park et al. (45) found renal repair after ischemic AKI in mice lacking kidney resident $CD45^+$ $Ly6G^-$ $F4/80^{high}$ $CD11b^{int}$ macrophages but containing infiltrating $CD45^+$ $Ly6G^-$ $F4/80^{int}$ $CD11b^{high}$ macrophages is delayed compared to the wide type mice. V-domain Ig suppressor of T cell activation (VISTA), an inhibitory immune checkpoint molecule, is mainly expressed by $CD45^+$ $Ly6G^-$ $F4/80^{high}$ $CD11b^{int}$ kidney resident macrophages and has the biomarker potential in distinguishing the renal macrophages (45). CX3CR1 mediated phagocytes by kidney resident macrophages initiate within the first hours during the innate host defense against *Candidiasis*, confirmed by CX3CR1-M280 associated susceptibility to systemic candidiasis in humans (46). $CD11b^{int}$ $F4/80^{bright}$ kidney resident macrophages protect renal artery stenosis-induced kidney injury by promoting the proangiogenic environments (36). Thus, kidney resident macrophages perform diverse effects depending on the phase and injury types. Based on a better understanding of cell surface markers and *Cre* specificity, further strategies should be explored to maintain protective resident macrophage phenotype during kidney disease. To advance these studies toward clinic interventions in patients, we must overcome two shortages of kidney resident macrophages. Firstly, minimal information is known about the anatomy and functions of resident macrophages in human kidney. Secondly, the similarities and differences of resident macrophages between rodent models and human kidneys remain unclear.

MONOCYTE AS PRECURSORS OF KIDNEY MACROPHAGES

While circulating monocytes minimally contribute to the renal macrophage pool under homeostasis, toxic or infectious damages result in augmented recruitment of monocyte-derived macrophages into the kidney. When renal macrophage niches are ablated, peripheral monocytes rapidly differentiate and replenish kidney macrophages (Munro et al. Nature Communications 11(1):2280 DOI:10.1038/s41467-020-16158-z). Bone marrow-derived monocyte precursors can reconstitute ischemic kidney macrophages in niches when kidney resident macrophages are depleted (38). Colony-stimulating factor-1 (CSF-1) stimulates macrophage proliferation at various time phases and tissues (47). Genetic deficiency or pharmacological blockade targeting CSF-1 inhibits macrophage proliferation, therefore prolonging the tissue repair phase after AKI (48). Rodent models revealed that $Ly6C^{high}$ pro-inflammatory monocytes infiltrate early in damaged kidneys (49, 50), depending on chemokines such as CCL2, CCL5, and CX3CR1 (26, 51–53). Initial infiltrating bone marrow-derived macrophages are characterized as Ly6C ^{high} $iNOS^+$ cells by flow cytometry in rodent kidneys, whereas late $Ly6C^{low}$ macrophages perform profibrotic M2-like effects (49, 50). CD11b diphtheria toxin receptor (DTR)-mediated depletion of monocyte/macrophages (50) or pharmacological blockade targeting chemokine pathways (54) attenuates kidney fibrosis, suggesting a profibrotic role of infiltrating macrophages in renal fibrogenesis. In severe IRI-induced AKI-CKD models, adoptive transplantation of $F4/80^{int}$ $B7\text{-}H4^{high}$ (M2c) macrophages rather than $F4/80^{high}$ B7-H4 ^{int} (M1) macrophages restore renal interstitial fibrosis in liposome clodronate-induced macrophage abrogated mice (55). Similarly, adoptive transfer of $F4/80^+$ $CD301^+$ (M2) macrophages rescue renal fibrosis in obstructed kidneys after macrophage depletion (56). Monocyte-derived kidney macrophages aggravate fibroblast activation and renal fibrosis by secreting cytokines (1, 57). Despite the direct and indirect profibrotic effects, bone marrow-derived macrophages can transdifferentiate into collagen-producing myofibroblasts *via* macrophage-myofibroblast transition (MMT) (58). Using Lyz2-Cre/Rosa26-Tomato mice, lineage tracing studies demonstrated that approximal 50% of the αSMA^+ $Collagen^+$ myofibroblasts derive from $F4/80^+$ $Tomato^+$ myeloid cells (59, 60). In contrast, a 2018 study challenges the MMT hypothesis as bone marrow-derived myofibroblasts make a limited contribution to the myofibroblasts in the obstructed kidney (61). The conflicting results come from the identification of myeloid cells by $CD45^+$ and myofibroblasts by $PDGFR\beta^+$, as unspecific markers amplify the miscalculation. Another limitation is the deficiency of markers to distinguish bone marrow-derived fibroblasts from macrophage-derived myofibroblasts.

Moreover, macrophages perform diversified roles in renal fibrogenesis *via* secreting matrix metalloproteinases. Matrix metalloproteinases, especially macrophage-derived matrix metalloproteinase-9 (MMP-9), promote kidney fibrosis through stimulating extracellular matrix deposition (62, 63). In contrast, Twist1 in infiltrating macrophages promotes extracellular matrix degradation by stimulating $CD11b^+$ $Ly6C^{low}$-derived matrix metalloproteinase-13 (MMP-13) production (64). As $CD11b^+$ $Ly6C^{high}$ monocytes freshly infiltrate after kidney injury and represent the onset of renal inflammation, $CD11b^+$ $Ly6C^{int}$ and $CD11b^+$ $Ly6C^{low}$ populations expand in the phases of repair and fibrosis (41). The evidence that terminally differentiated macrophages rather than freshly infiltrating monocyte progenitors are the major players in kidney fibrogenesis suggests that kidney macrophages function varies due to disease types and time phases.

The $Ly6C^{low}$ subpopulation of circulating monocytes is characterized by monitoring and phagocytosing circulating immune complexes (65). These $Ly6C^{low}$ monocytes present antigens and activate effector $CD4^+$ T lymphocytes in the glomerular capillaries (66). Circulating myeloid-derived suppressor cells (MDSCs) are immune suppressive populations and initially investigated in cancer (67). MDSCs were firstly reported to maintain cardiac transplant tolerance in rodent models (46), whereas renal MDSCs accumulation positively correlates with graft survival and kidney transplant recipients (68, 69). The effects of MDSCs further expand to immune-regulation and fibrogenesis during septic and metabolic kidney disease (70, 71), suggesting the therapeutic potential of MDSCs in acute and chronic kidney disease.

HETEROGENEITY OF HUMAN KIDNEY MACROPHAGES AND CLINICAL TRANSFORMATION

Human monocyte/macrophages are classified into three distinct populations, including classical $CD14^{++}$ $CD16^{-}$ subset, non-classical $CD14^{+}$ $CD16^{+}$ subset, and intermediate $CD14^{++}$ $CD16^{+}$ subset (72). In a 35 months cohort with 94 dialysis patients, the number of classical $CD14^{++}$ $CD16^{-}$ monocytes can independently predict cardiovascular events and death (73). Rogacev et al. (74) demonstrated $CD14^{++}$ $CD16^{-}$ monocytes numbers can also predict cardiovascular events in CKD patients. Non-classical $CD14^{+}$ $CD16^{+}$ monocytes from CKD patients express high levels of chemokines, facilitating their adhesion to vascular walls (75). Pro-inflammatory $CD14^{+}$ $CD16^{+}$ monocytes correlate with blood vessel stiffness in predialysis CKD patients, suggesting that non-classical $CD14^{+}$ $CD16^{+}$ subset damage endothelial cells (76). However, most clinical studies lack direct evidence of macrophage populations inside the kidney, and the predictive ability of human macrophage populations in kidney injury and fibrosis requires further investigations.

To expand experimental knowledge of macrophages to clinical applications, we still have to overcome several obstacles. Firstly, available data of human kidney macrophages is significantly insufficient, especially the dynamic changes of macrophage function and subpopulations. Secondly, $CD14^{++}CD16^{-}$ and $CD14^{++}CD16^{+}$ monocytes resemble mouse $Ly6C^{+}$ inflammatory monocytes, whereas $CD14^{+}CD16^{+}$ monocytes share phenotypic features with $Ly6C^{-}$ anti-inflammatory monocytes and adhering vascular endothelium (77). As classical $CD14^{++}$ $CD16^{-}$ subset is known for the phagocytic capability, the overlapping and sometimes conflicting features of human and murine monocytes require further investigation. Thirdly, the functionality of kidney macrophages is dynamically variable and affected by the nature of kidney diseases. Thus, clinic translation must address the characteristics of kidney macrophages in different types and phases of the disease (**Table 1**).

Nevertheless, characterized macrophage recruitment and maturation pathways are also appliable in patients with kidney diseases. Renoprotective effects of interventions targeting CCL2/CCR2 have been confirmed in rodent models of kidney inflammation and fibrosis (26, 41). Consistently, CCR2 inhibitor CCX140-B further attenuates albuminuria levels in patients with type 2 diabetes in addition to the standard renin-angiotensin system (RAS) blocking therapies (84). Although the definite effects of CSF1R in macrophage recruitment and proliferation, the role of CSF1R inhibitors and neutralizing antibodies have not been tested in clinical trials to treat kidney diseases. The JAK-STAT pathway regulates macrophage activation and renal function decline in patients with type 2 diabetic nephropathy (85). JAK1 and JAK2 inhibition by Bariticinib decreases albuminuria levels in patients with diabetic kidney diseases (DKD) (86). Our recent studies found that macrophage-derived extracellular vesicles are kidney-targeted drug carriers and worth further expansion into clinical trials (87).

SINGLE-CELL RNA-SEQUENCING REVOLUTION

After the qualitative leap from the oversimplified M1/M2 paradigm to individual subpopulations identified by cell surface markers, single-cell RNA-sequencing (scRNA-seq) categorizes macrophages by their function and phenotype, revealing the continuum and complexity of macrophages during the development and pathogenesis of kidney disease (88, 89). Zimmerman et al. (80) identified *C1q* expression as a novel marker of resident macrophage clusters in mouse kidneys, and *C1q* expressing clusters in other species were verified by the expression of *Cd74*, *Cd81*, and *Apoe*. In a rodent model of rhabdomyolysis-induced AKI, $F4/80^{low}$ $CD11b^{high}$ $Ly6b^{high}$ $CD206^{low}$ pro-inflammatory macrophages infiltrate early

TABLE 1 | Macrophage markers in human and mouse.

Markers	Gene	Species	Protein Type	Reference
B7-H4	VTCN1	Human, Mouse	Cell Membrane Receptor	(55)
B7-H5 (VISTA)	VSIR	Human, Mouse	Cell Membrane Cytokine	(45)
CD11b	ITGAM	Human, Mouse	Cell Membrane Receptor	(30, 36, 41, 45, 64)
CDIIc	ITGAX	Human, Mouse	Cell Membrane Receptor	(18, 44, 78)
CDI4	CD I4	Human, Mouse	Cell Membrane Receptor	(72–76)
CD16	FCGR3A	Human, Mouse	Cell Membrane Receptor	(72–77)
CD45	PTPRC	Human, Mouse	Cell Membrane Receptor	(30, 45)
CD115	CSF1R	Human, Mouse	Cell Membrane Receptor	(30)
CD192	CCR2	Human, Mouse	Cell Membrane Receptor	(79)
CD206	MRC1	Human, Mouse	Cell Membrane Receptor	(13, 80)
CCRL1	CX3CR1	Human, Mouse	Cell Membrane Receptor	(37, 42)
F4/80	ADGRE1	Human, Mouse	Cell Membrane Receptor	(13, 18, 30, 36, 40, 44, 45, 55, 56, 81, 82)
iNOS	NOS2	Human, Mouse	Cytoplasm Enzyme	(49, 50)
Ly6C	Ly6c1	Mouse	Cell Membrane Receptor	(30, 41, 49, 50, 77)
MHC class II	MHCII	Human Mouse	Cell Membrane Receptor	(38)
MCP-1	CCL2	Human Mouse	Secreted Cytokine	(26, 79)
SCARD1	CD68	Human Mouse	Cell Membrane Receptor	(83)
TNF-α	TFN	Human, Mouse	Cell Membrane Cytokine	(57)

after rhabdomyolysis, while F4/80^{high} CD11b^{+} Ly6b^{low} CD206^{high} reparative macrophages are dominant at late phase. However, the scRNA-seq analysis demonstrated that signal pathways do not precisely match macrophage phenotypes and the existence of individual subpopulations simultaneously expressing heterogeneous markers (81). At the late phase after ischemic AKI, macrophages expressing *Ccl2* and *Ccr2* infiltrate around the Vcam1^{+} damaged tubules (79). By evaluating the typical *C1qa*, *Cd74*, and *Adgre1* expression, macrophages are defined as the predominant immune cells in diabetic glomeruli and mainly M1-like macrophages (90). The scRNA-seq analysis revealed that both extent and levels of *Axl* expression increased in F4/80^{+} macrophages from rejecting allografts compared to tolerized kidneys; and *Axl* promotes the differentiation of intra-graft myeloid cells towards pro-inflammatory phenotypes after transplantation (82). Moreover, the combination of scRNA-seq and lineage tracing technique attracts particular attention. Lineage tracing can elucidate the clonal relationships during development and differentiation, enable lifecycle monitoring. In contrast, scRNA-seq can identify exact cell types but unable to determine the lineage relationships. Thus, integrating scRNA-seq and lineage tracing will provide extra information about cell types, development, and differentiation in a longstanding pattern.

Stewart et al. (78) demonstrated that human kidney monocyte phagocytes (MNPs) expressing *ITGAX* and *HLA-DRA* are categorized into four distinct clusters (MNPa to MNPd). MNPa subpopulation expressing *CD14* in mature kidney analogous classical monocytes, whereas MNPb expressing *CD16* is transcriptionally similar to non-classical monocytes. Consistently, CD14^{+} CD68^{+} monocyte/macrophages are the most abundant immune cells in urine and account for one-third of urinary clusters. These monocyte/macrophages are enriched in genes related to antigen presentation and macrophage activation and further classified into CD16^{+} and CD16^{-} subpopulations (83).

CONCLUSIONS AND PERSPECTIVES

Macrophages are recruited by chemokines and contribute to the pathogenesis of kidney injury, repair, and fibrosis. Despite the wide application of the oversimplified pro-inflammatory M1 and anti-inflammatory M2 macrophage paradigm, macrophage complexity in origin, phenotype, and function has attracted attention. Macrophage subpopulations were distinguished by combining cell surface markers and using novel single-cell RNA sequence technology to explore macrophage contribution in tissue injury,

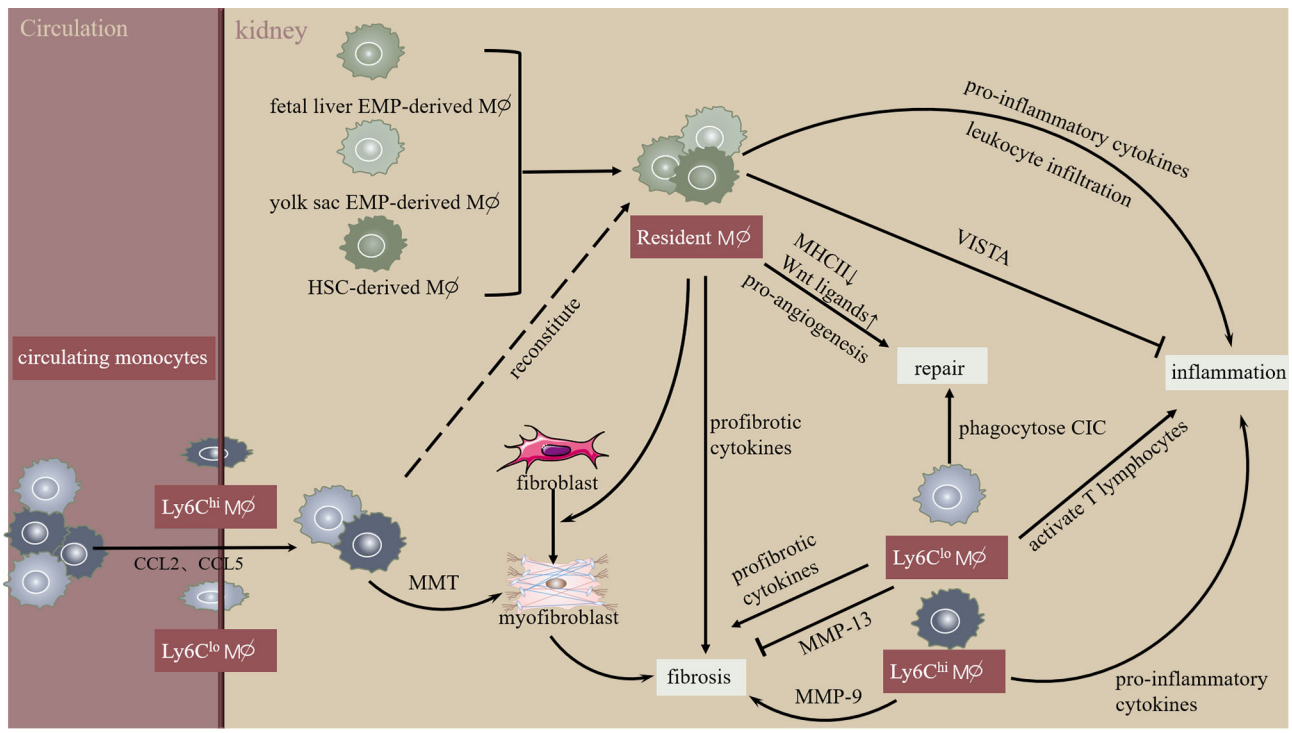


FIGURE 1 | Macrophage heterogeneity during initiation and progression of kidney injury and fibrosis. Kidney resident macrophages derive from multi-sources and monitor trans-endothelial transport of circulating immune complexes. In the initial phase of kidney injury, resident macrophages stimulate leukocyte infiltration and cytokine secretion. Interestingly, kidney resident macrophages express V-domain Ig suppressor of T cell activation (VISTA), an inhibitory immune checkpoint molecule. Increased chemokines (CCL2, CCL5) promote circulating monocyte chemotaxis into the kidney, developing into infiltrating Ly-6C^{hi} macrophages exhibiting pro-inflammatory phenotype or macrophage-myofibroblast transition (MMT). Similarly, infiltrating Ly6C^{low} macrophages promote kidney inflammation and fibrosis *via* activating T lymphocytes or pro-inflammatory cytokines. However, Ly6C^{hi} macrophages inhibit kidney fibrosis by producing MMP-13. Overall, these mechanisms lead to extracellular matrix dynamic homeostasis during the resolution of kidney injury and fibrosis.

regeneration, and fibrosis. Our data and others have confirmed the therapeutic potential of macrophage pathways in acute and chronic kidney diseases; however, the functionally opposing macrophage subpopulations require incisive and tissue-specific strategies (**Figure 1**). Moreover, an in-depth understanding of the specialty and commonality in scRNA-seq defined macrophage clusters requires further investigation.

AUTHOR CONTRIBUTIONS

YW and H-RY contributed equally to the writing of the manuscript. BW contributed to the figure of the manuscript. B-CL conceived the concept and contributed to the writing of the manuscript. All authors contributed to the article and approved the submitted version.

FUNDING

This work was supported by China National Natural Science Foundation (8203000544, 81720108007) and the key research project of the Ministry of China Science and Technology (2018YFC1314000) to B-CL as PI, and National Natural Science Foundation of China (81900623), and the Natural Science Foundation of Jiangsu Province (BK20190349) to YW as PI.

REFERENCES

1. Tang PM, Nikolic-Paterson DJ, Lan HY. Macrophages: Versatile Players in Renal Inflammation and Fibrosis. *Nat Rev Nephrol* (2019) 15(3):144–58. doi: 10.1038/s41581-019-0110-2
2. Wen Y, Crowley SD. The Varying Roles of Macrophages in Kidney Injury and Repair. *Curr Opin Nephrol Hypertens* (2020) 29(3):286–92. doi: 10.1097/MNH.0000000000000595
3. Cao Q, Wang Y, Harris DC. Macrophage Heterogeneity, Phenotypes, and Roles in Renal Fibrosis. *Kidney Int Suppl (2011)* (2014) 4(1):16–9. doi: 10.1038/kisup.2014.4
4. Lee S, Huen S, Nishio H, Nishio S, Lee HK, Choi BS, et al. Distinct Macrophage Phenotypes Contribute to Kidney Injury and Repair. *J Am Soc Nephrol* (2011) 22(2):317–26. doi: 10.1681/ASN.2009060615
5. Lv LL, Tang PM, Li CJ, You YK, Li J, Huang XR, et al. The Pattern Recognition Receptor, Mincle, is Essential for Maintaining the M1 Macrophage Phenotype in Acute Renal Inflammation. *Kidney Int* (2017) 91(3):587–602. doi: 10.1016/j.kint.2016.10.020
6. Chen T, Cao Q, Wang Y, Harris DCH. M2 Macrophages in Kidney Disease: Biology, Therapies, and Perspectives. *Kidney Int* (2019) 95(4):760–73. doi: 10.1016/j.kint.2018.10.041
7. Epelman S, Lavine KJ, Beaudin AE, Sojka DK, Carrero JA, Calderon B, et al. Embryonic and Adult-Derived Resident Cardiac Macrophages are Maintained Through Distinct Mechanisms at Steady State and During Inflammation. *Immunity* (2014) 40(1):91–104. doi: 10.1016/j.immuni.2013.11.019
8. Sheng J, Ruedl C, Karjalainen K. Most Tissue-Resident Macrophages Except Microglia Are Derived From Fetal Hematopoietic Stem Cells. *Immunity* (2015) 43(2):382–93. doi: 10.1016/j.immuni.2015.07.016
9. Rae F, Woods K, Sasmono T, Campanale N, Taylor D, Ovchinnikov DA, et al. Characterisation and Trophic Functions of Murine Embryonic Macrophages Based Upon the Use of a Csf1r-EGFP Transgene Reporter. *Dev Biol* (2007) 308(1):232–46. doi: 10.1016/j.ydbio.2007.05.027
10. Dai XM, Ryan GR, Hapel AJ, Dominguez MG, Russell RG, Kapp S, et al. Targeted Disruption of the Mouse Colony-Stimulating Factor 1 Receptor Gene Results in Osteopetrosis, Mononuclear Phagocyte Deficiency, Increased Primitive Progenitor Cell Frequencies, and Reproductive Defects. *Blood* (2002) 99(1):111–20. doi: 10.1182/blood.v99.1.111
11. Mouchemore KA, Pixley FJ. CSF-1 Signaling in Macrophages: Pleiotrophy Through Phosphotyrosine-Based Signaling Pathways. *Crit Rev Clin Lab Sci* (2012) 49(2):49–61. doi: 10.3109/10408363.2012.666845
12. Muthukrishnan SD, Ryzhov S, Karolak M, Mukherjee E, Sims-Lucas S, Oxburgh L. A Macrophage-Based Regenerative Response to Fetal Kidney Damage. *Mech Dev* (2017) 145:S50–0. doi: 10.1016/j.mod.2017.04.094
13. Munro DAD, Wineberg Y, Tarnick J, Vink CS, Li Z, Pridans C, et al. Macrophages Restrict the Nephrogenic Field and Promote Endothelial Connections During Kidney Development. *Elife* (2019) 8:e43271. doi: 10.7554/eLife.43271
14. Bunt S, Hooley C, Hu N, Scahill C, Weavers H, Skaer H. Hemocyte-Secreted Type IV Collagen Enhances BMP Signaling to Guide Renal Tubule Morphogenesis in Drosophila. *Dev Cell* (2010) 19(2):296–306. doi: 10.1016/j.devcel.2010.07.019
15. Schnoor M, Cullen P, Lorkowski J, Stolle K, Robenek H, Troyer D, et al. Production of Type VI Collagen by Human Macrophages: A New Dimension in Macrophage Functional Heterogeneity. *J Immunol* (2008) 180(8):5707–19. doi: 10.4049/jimmunol.180.8.5707
16. Abrahamson DR, Leardkamolkarn V. Development of Kidney Tubular Basement Membranes. *Kidney Int* (1991) 39(3):382–93. doi: 10.1038/ki.1991.50
17. Marshall RJ, MacIver AG. The Monocyte/Macrophage Population of the Normal Human Kidney. *J Pathol* (1984) 143(4):275–80. doi: 10.1002/path.1711430407
18. Cao Q, Wang Y, Wang XM, Lu J, Lee VW, Ye Q, et al. Renal F4/80+ CD11c+ Mononuclear Phagocytes Display Phenotypic and Functional Characteristics of Macrophages in Health and in Adriamycin Nephropathy. *J Am Soc Nephrol* (2015) 26(2):349–63. doi: 10.1681/ASN.2013121336
19. Couser WG. Basic and Translational Concepts of Immune-Mediated Glomerular Diseases. *J Am Soc Nephrol* (2012) 23(3):381–99. doi: 10.1681/ASN.2011030304
20. Duffield JS, Tipping PG, Kipari T, Cailhier JF, Clay S, Lang R, et al. Conditional Ablation of Macrophages Halts Progression of Crescentic Glomerulonephritis. *Am J Pathol* (2005) 167(5):1207–19. doi: 10.1016/S0002-9440(10)61209-6
21. Tesch GH, Schwarting A, Kinoshita K, Lan HY, Rollins BJ, Kelley VR. Monocyte Chemoattractant Protein-1 Promotes Macrophage-Mediated Tubular Injury, But Not Glomerular Injury, in Nephrotoxic Serum Nephritis. *J Clin Invest* (1999) 103(1):73–80. doi: 10.1172/JCI4876
22. Chow FY, Nikolic-Paterson DJ, Ozols E, Atkins RC, Tesch GH. Intercellular Adhesion Molecule-1 Deficiency is Protective Against Nephropathy in Type 2 Diabetic db/db Mice. *J Am Soc Nephrol* (2005) 16(6):1711–22. doi: 10.1681/ASN.2004070612
23. Silva GE, Costa RS, Ravinal RC, Ramalho LN, Reis MA, Moyses-Neto M, et al. Renal Macrophage Infiltration is Associated With a Poor Outcome in IgA Nephropathy. *Clinics (Sao Paulo)* (2012) 67(7):697–703. doi: 10.6061/clinics/2012(07)01
24. Liu D, Xu M, Ding LH, Lv LL, Liu H, Ma KL, et al. Activation of the Nlrp3 Inflammasome by Mitochondrial Reactive Oxygen Species: A Novel Mechanism of Albumin-Induced Tubulointerstitial Inflammation. *Int J Biochem Cell Biol* (2014) 57:7–19. doi: 10.1016/j.biocel.2014.09.018
25. Li ZL, Lv LL, Tang TT, Wang B, Feng Y, Zhou LT, et al. HIF-1alpha Inducing Exosomal microRNA-23a Expression Mediates the Cross-Talk Between Tubular Epithelial Cells and Macrophages in Tubulointerstitial Inflammation. *Kidney Int* (2019) 95(2):388–404. doi: 10.1016/j.kint.2018.09.013
26. Lv LL, Feng Y, Wen Y, Wu WJ, Ni HF, Li ZL, et al. Exosomal CCL2 From Tubular Epithelial Cells is Critical for Albumin-Induced Tubulointerstitial Inflammation. *J Am Soc Nephrol* (2018) 29(3):919–35. doi: 10.1681/ASN.2017050523

27. Lv LL, Feng Y, Wu M, Wang B, Li ZL, Zhong X, et al. Exosomal miRNA-19b-3p of Tubular Epithelial Cells Promotes M1 Macrophage Activation in Kidney Injury. *Cell Death Differ* (2020) 27(1):210–26. doi: 10.1038/s41418-019-0349-y
28. Cao Q, Harris DC, Wang Y. Macrophages in Kidney Injury, Inflammation, and Fibrosis. *Physiol (Bethesda)* (2015) 30(3):183–94. doi: 10.1152/physiol.00046.2014
29. Munro DAD, Hughes J. The Origins and Functions of Tissue-Resident Macrophages in Kidney Development. *Front Physiol* (2017) 8:837. doi: 10.3389/fphys.2017.00837
30. Hoeffel G, Chen J, Lavin Y, Low D, Almeida FF, See P, et al. C-Myb(+) Erythro-Myeloid Progenitor-Derived Fetal Monocytes Give Rise to Adult Tissue-Resident Macrophages. *Immunity* (2015) 42(4):665–78. doi: 10.1016/j.immuni.2015.03.011
31. Gomez Perdiguero E, Klapproth K, Schulz C, Busch K, Azzoni E, Crozet L, et al. Tissue-Resident Macrophages Originate From Yolk-Sac-Derived Erythro-Myeloid Progenitors. *Nature* (2015) 518(7540):547–51. doi: 10.1038/nature13989
32. Hoeffel G, Ginhoux F. Ontogeny of Tissue-Resident Macrophages. *Front Immunol* (2015) 6:486. doi: 10.3389/fimmu.2015.00486
33. Boyer SW, Schroeder AV, Smith-Berdan S, Forsberg EC. All Hematopoietic Cells Develop From Hematopoietic Stem Cells Through Flk2/Flt3-positive Progenitor Cells. *Cell Stem Cell* (2011) 9(1):64–73. doi: 10.1016/j.stem.2011.04.021
34. Epelman S, Lavine KJ, Randolph GJ. Origin and Functions of Tissue Macrophages. *Immunity* (2014) 41(1):21–35. doi: 10.1016/j.immuni.2014.06.013
35. Guilliams M, Scott CL. Does Niche Competition Determine the Origin of Tissue-Resident Macrophages? *Nat Rev Immunol* (2017) 17(7):451–60. doi: 10.1038/nri.2017.42
36. Puranik AS, Leaf IA, Jensen MA, Hedayat AF, Saad A, Kim KW, et al. Kidney-Resident Macrophages Promote a Proangiogenic Environment in the Normal and Chronically Ischemic Mouse Kidney. *Sci Rep* (2018) 8(1):13948. doi: 10.1038/s41598-018-31887-4
37. Ide S, Yahara Y, Kobayashi Y, Strausser SA, Ide K, Watwe A, et al. Yolk-Sac-Derived Macrophages Progressively Expand in the Mouse Kidney With Age. *Elife* (2020) 9:e51756. doi: 10.7554/eLife.51756
38. Lever JM, Hull TD, Boddu R, Pepin ME, Black LM, Adedoyin OO, et al. Resident Macrophages Reprogram Toward a Developmental State After Acute Kidney Injury. *JCI Insight* (2019) 4(2):e125503. doi: 10.1172/jci.insight.125503
39. Stamatiades EG, Tremblay ME, Bohm M, Crozet L, Bisht K, Kao D, et al. Immune Monitoring of Trans-endothelial Transport by Kidney-Resident Macrophages. *Cell* (2016) 166(4):991–1003. doi: 10.1016/j.cell.2016.06.058
40. Kawakami T, Lichtnekert J, Thompson LJ, Karna P, Bouabe H, Hohl TM, et al. Resident Renal Mononuclear Phagocytes Comprise Five Discrete Populations With Distinct Phenotypes and Functions. *J Immunol* (2013) 191(6):3358–72. doi: 10.4049/jimmunol.1300342
41. Yang Q, Wang Y, Pei G, Deng X, Jiang H, Wu J, et al. Bone Marrow-Derived Ly6C(-) Macrophages Promote Ischemia-Induced Chronic Kidney Disease. *Cell Death Dis* (2019) 10(4):291. doi: 10.1038/s41419-019-1531-3
42. Lau A, Chung H, Komada T, Platnich JM, Sandall CF, Choudhury SR, et al. Renal Immune Surveillance and Dipeptidase-1 Contribute to Contrast-Induced Acute Kidney Injury. *J Clin Invest* (2018) 128(7):2894–913. doi: 10.1172/JCI96640
43. Zimmerman KA, Huang J, He L, Revell DZ, Li Z, Hsu JS, et al. Interferon Regulatory Factor-5 in Resident Macrophage Promotes Polycystic Kidney Disease. *Kidney360* (2020) 1(3):179–90. doi: 10.34067/KID.0001052019
44. Zimmerman KA, Song CJ, Li Z, Lever JM, Crossman DK, Rains A, et al. Tissue-Resident Macrophages Promote Renal Cystic Disease. *J Am Soc Nephrol* (2019) 30(10):1841–56. doi: 10.1681/ASN.2018080810
45. Park JG, Lee CR, Kim MG, Kim G, Shin HM, Jeon YH, et al. Kidney Residency of VISTA-positive Macrophages Accelerates Repair From Ischemic Injury. *Kidney Int* (2020) 97(5):980–94. doi: 10.1016/j.kint.2019.11.025
46. Lionakis MS, Swamydas M, Fischer BG, Plantinga TS, Johnson MD, Jaeger M, et al. CX3CR1-Dependent Renal Macrophage Survival Promotes Candida Control and Host Survival. *J Clin Invest* (2013) 123(12):5035–51. doi: 10.1172/JCI71307
47. Menke J, Rabacal WA, Byrne KT, Iwata Y, Schwartz MM, Stanley ER, et al. Circulating CSF-1 Promotes Monocyte and Macrophage Phenotypes That Enhance Lupus Nephritis. *J Am Soc Nephrol* (2009) 20(12):2581–92. doi: 10.1681/ASN.2009050499
48. Zhang MZ, Yao B, Yang S, Jiang L, Wang S, Fan X, et al. CSF-1 Signaling Mediates Recovery From Acute Kidney Injury. *J Clin Invest* (2012) 122(12):4519–32. doi: 10.1172/JCI60363
49. Menezes S, Melandri D, Anselmi G, Perchet T, Loschko J, Dubrot J, et al. The Heterogeneity of Ly6C(hi) Monocytes Controls Their Differentiation Into iNOS(+) Macrophages or Monocyte-Derived Dendritic Cells. *Immunity* (2016) 45(6):1205–18. doi: 10.1016/j.immuni.2016.12.001
50. Lin SL, Castano AP, Nowlin BT, Lupher MLJr., Duffield JS. Bone Marrow Ly6Chigh Monocytes are Selectively Recruited to Injured Kidney and Differentiate Into Functionally Distinct Populations. *J Immunol* (2009) 183(10):6733–43. doi: 10.4049/jimmunol.0901473
51. Rudemiller NP, Patel MB, Zhang JD, Jeffs AD, Karlovich NS, Griffiths R, et al. C-C Motif Chemokine 5 Attenuates Angiotensin II-Dependent Kidney Injury by Limiting Renal Macrophage Infiltration. *Am J Pathol* (2016) 186(11):2846–56. doi: 10.1016/j.ajpath.2016.07.015
52. Cassini MF, Kakade VR, Kurtz E, Sulkowski P, Glazer P, Torres R, et al. Mcp1 Promotes Macrophage-Dependent Cyst Expansion in Autosomal Dominant Polycystic Kidney Disease. *J Am Soc Nephrol* (2018) 29(10):2471–81. doi: 10.1681/ASN.2018050518
53. Chousterman BG, Boissonnas A, Poupel L, Baudesson de Chanville C, Adam J, Tabibzadeh N, et al. Ly6Chigh Monocytes Protect Against Kidney Damage During Sepsis Via a CX3CR1-Dependent Adhesion Mechanism. *J Am Soc Nephrol* (2016) 27(3):792–803. doi: 10.1681/ASN.2015010009
54. McRae JL, Vikstrom IB, Bongoni AK, Salvaris EJ, Fisicaro N, Ng M, et al. Blockade of the G-CSF Receptor Is Protective in a Mouse Model of Renal Ischemia-Reperfusion Injury. *J Immunol* (2020) 205(5):1433–40. doi: 10.4049/jimmunol.2000390
55. Kim MG, Kim SC, Ko YS, Lee HY, Jo SK, Cho W. The Role of M2 Macrophages in the Progression of Chronic Kidney Disease Following Acute Kidney Injury. *PloS One* (2015) 10(12):e0143961. doi: 10.1371/journal.pone.0143961
56. Shen B, Liu X, Fan Y, Qiu J. Macrophages Regulate Renal Fibrosis Through Modulating TGFbeta Superfamily Signaling. *Inflammation* (2014) 37(6):2076–84. doi: 10.1007/s10753-014-9941-y
57. Wen Y, Lu X, Ren J, Privratsky JR, Yang B, Rudemiller NP, et al. KLF4 in Macrophages Attenuates TNFalpha-Mediated Kidney Injury and Fibrosis. *J Am Soc Nephrol* (2019) 30(10):1925–38. doi: 10.1681/ASN.2019020111
58. Phua YL, Martel N, Pennisi DJ, Little MH, Wilkinson L. Distinct Sites of Renal Fibrosis in Crim1 Mutant Mice Arise From Multiple Cellular Origins. *J Pathol* (2013) 229(5):685–96. doi: 10.1002/path.4155
59. Wang YY, Jiang H, Pan J, Huang XR, Wang YC, Huang HF, et al. Macrophage-to-Myofibroblast Transition Contributes to Interstitial Fibrosis in Chronic Renal Allograft Injury. *J Am Soc Nephrol* (2017) 28(7):2053–67. doi: 10.1681/ASN.2016050573
60. Meng XM, Wang S, Huang XR, Yang C, Xiao J, Zhang Y, et al. Inflammatory Macrophages can Transdifferentiate Into Myofibroblasts During Renal Fibrosis. *Cell Death Dis* (2016) 7(12):e2495. doi: 10.1038/cddis.2016.402
61. Kramann R, Machado F, Wu H, Kusaba T, Hoeft K, Schneider RK, et al. Parabiosis and Single-Cell RNA Sequencing Reveal a Limited Contribution of Monocytes to Myofibroblasts in Kidney Fibrosis. *JCI Insight* (2018) 3(9):e99561. doi: 10.1172/jci.insight.99561
62. Tan TK, Zheng G, Hsu TT, Lee SR, Zhang J, Zhao Y, et al. Matrix Metalloproteinase-9 of Tubular and Macrophage Origin Contributes to the Pathogenesis of Renal Fibrosis Via Macrophage Recruitment Through Osteopontin Cleavage. *Lab Invest* (2013) 93(4):434–49. doi: 10.1038/labinvest.2013.3
63. Wang X, Zhou Y, Tan R, Xiong M, He W, Fang L, et al. Mice Lacking the Matrix Metalloproteinase-9 Gene Reduce Renal Interstitial Fibrosis in Obstructive Nephropathy. *Am J Physiol Renal Physiol* (2010) 299(5):F973–982. doi: 10.1152/ajprenal.00216.2010
64. Ren J, Zhang J, Rudemiller NP, Griffiths R, Wen Y, Lu X, et al. Twist1 in Infiltrating Macrophages Attenuates Kidney Fibrosis Via Matrix Metallopeptidase 13-Mediated Matrix Degradation. *J Am Soc Nephrol* (2019) 30(9):1674–85. doi: 10.1681/ASN.2018121253

65. Carlin LM, Stamatiades EG, Auffray C, Hanna RN, Glover L, Vizcay-Barrena G, et al. Nr4a1-Dependent Ly6C(low) Monocytes Monitor Endothelial Cells and Orchestrate Their Disposal. *Cell* (2013) 153(2):362–75. doi: 10.1016/j.cell.2013.03.010
66. Westhorpe CLV, Norman MU, Hall P, Snelgrove SL, Finsterbusch M, Li A, et al. Effector CD4(+) T Cells Recognize Intravascular Antigen Presented by Patrolling Monocytes. *Nat Commun* (2018) 9(1):747. doi: 10.1038/s41467-018-03181-4
67. Iglesias-Escudero M, Sansegundo-Arribas D, Riquelme P, Merino-Fernandez D, Guiral-Foz S, Perez C, et al. Myeloid-Derived Suppressor Cells in Kidney Transplant Recipients and the Effect of Maintenance Immunotherapy. *Front Immunol* (2020) 11:643. doi: 10.3389/fimmu.2020.00643
68. Pengam S, Durand J, Usal C, Gauttier V, Dilek N, Martinet B, et al. SIRPalpha/CD47 Axis Controls the Maintenance of Transplant Tolerance Sustained by Myeloid-Derived Suppressor Cells. *Am J Transplant* (2019) 19(12):3263–75. doi: 10.1111/ajt.15497
69. Du XX, Guo YL, Zhao YP, Yang M, Chang S, Liu B, et al. Accumulation of High Levels of Monocytic Myeloid-Derived Suppressor Cells Enhances Graft Survival in Almost-Tolerant Kidney Transplant Recipients. *Transplant Proc* (2018) 50(10):3314–20. doi: 10.1016/j.transproceed.2018.04.043
70. Venet F, Monneret G. Advances in the Understanding and Treatment of Sepsis-Induced Immunosuppression. *Nat Rev Nephrol* (2018) 14(2):121–37. doi: 10.1038/nrneph.2017.165
71. Islam J, Lee HJ, Yang SH, Kim DK, Joo KW, Kim YS, et al. Expansion of Myeloid-Derived Suppressor Cells Correlates With Renal Progression in Type 2 Diabetic Nephropathy. *Immune Netw* (2020) 20(2):e18. doi: 10.4110/in.2020.20.e18
72. Kapellos TS, Bonaguro L, Gemund I, Reusch N, Saglam A, Hinkley ER, et al. Human Monocyte Subsets and Phenotypes in Major Chronic Inflammatory Diseases. *Front Immunol* (2019) 10:2035. doi: 10.3389/fimmu.2019.02035
73. Heine GH, Ulrich C, Seibert E, Seiler S, Marell J, Reichart B, et al. CD14(++) CD16+ Monocytes But Not Total Monocyte Numbers Predict Cardiovascular Events in Dialysis Patients. *Kidney Int* (2008) 73(5):622–9. doi: 10.1038/sj.ki.5002744
74. Rogacev KS, Seiler S, Zawada AM, Reichart B, Herath E, Roth D, et al. CD14++CD16+ Monocytes and Cardiovascular Outcome in Patients With Chronic Kidney Disease. *Eur Heart J* (2011) 32(1):84–92. doi: 10.1093/eurheartj/ehq371
75. Ramirez R, Carracedo J, Merino A, Soriano S, Ojeda R, Alvarez-Lara MA, et al. CD14+CD16+ Monocytes From Chronic Kidney Disease Patients Exhibit Increased Adhesion Ability to Endothelial Cells. *Contrib Nephrol* (2011) 171:57–61. doi: 10.1159/000327134
76. Lee JW, Cho E, Kim MG, Jo SK, Cho WY, Kim HK. Proinflammatory CD14(+)CD16(+) Monocytes are Associated With Vascular Stiffness in Predialysis Patients With Chronic Kidney Disease. *Kidney Res Clin Pract* (2013) 32(4):147–52. doi: 10.1016/j.krcp.2013.08.001
77. Geissmann F, Jung S, Littman DR. Blood Monocytes Consist of Two Principal Subsets With Distinct Migratory Properties. *Immunity* (2003) 19(1):71–82. doi: 10.1016/s1074-7613(03)00174-2
78. Stewart BJ, Ferdinand JR, Young MD, Mitchell TJ, Loudon KW, Riding AM, et al. Spatiotemporal Immune Zonation of the Human Kidney. *Science* (2019) 365(6460):1461–6. doi: 10.1126/science.aat5031
79. Kirita Y, Wu H, Uchimura K, Wilson PC, Humphreys BD. Cell Profiling of Mouse Acute Kidney Injury Reveals Conserved Cellular Responses to Injury. *Proc Natl Acad Sci USA* (2020) 117(27):15874–83. doi: 10.1073/pnas.2005477117
80. Zimmerman KA, Bentley MR, Lever JM, Li Z, Crossman DK, Song CJ, et al. Single-Cell RNA Sequencing Identifies Candidate Renal Resident Macrophage Gene Expression Signatures Across Species. *J Am Soc Nephrol* (2019) 30(5):767–81. doi: 10.1681/ASN.2018090931
81. Belliere J, Casemayou A, Ducasse L, Zakaroff-Girard A, Martins F, Iacovoni JS, et al. Specific Macrophage Subtypes Influence the Progression of Rhabdomyolysis-Induced Kidney Injury. *J Am Soc Nephrol* (2015) 26(6):1363–77. doi: 10.1681/ASN.2014040320
82. Dangi A, Natesh NR, Husain I, Ji Z, Barisoni L, Kwun J, et al. Single Cell Transcriptomics of Mouse Kidney Transplants Reveals a Myeloid Cell Pathway for Transplant Rejection. *JCI Insight* (2020) 5(20):e141321. doi: 10.1172/jci.insight.141321
83. Wang Y, Zhao Y, Zhao Z, Li D, Nie H, Sun Y, et al. Single-Cell RNA-Seq Analysis Identified Kidney Progenitor Cells From Human Urine. *Protein Cell* (2021) 12(4):305–12. doi: 10.1007/s13238-020-00816-5
84. de Zeeuw D, Bekker P, Henkel E, Hasslacher C, Gouni-Berthold I, Mehling H, et al. The Effect of CCR2 Inhibitor CCX140-B on Residual Albuminuria in Patients With Type 2 Diabetes and Nephropathy: A Randomised Trial. *Lancet Diabetes Endocrinol* (2015) 3(9):687–96. doi: 10.1016/S2213-8587(15)00261-2
85. Berthier CC, Zhang H, Schin M, Henger A, Nelson RG, Yee B, et al. Enhanced Expression of Janus Kinase-Signal Transducer and Activator of Transcription Pathway Members in Human Diabetic Nephropathy. *Diabetes* (2008) 58(2):469–77. doi: 10.2337/db08-1328
86. Tuttle KR, Brosius FC3rd, Adler SG, Kretzler M, Mehta RL, Tumlin JA, et al. JAK1/JAK2 Inhibition by Baricitinib in Diabetic Kidney Disease: Results From a Phase 2 Randomized Controlled Clinical Trial. *Nephrol Dial Transplant* (2018) 33(11):1950–9. doi: 10.1093/ndt/gfx377
87. Tang TT, Lv LL, Wang B, Cao JY, Feng Y, Li ZL, et al. Employing Macrophage-Derived Microvesicle for Kidney-Targeted Delivery of Dexamethasone: An Efficient Therapeutic Strategy Against Renal Inflammation and Fibrosis. *Theranostics* (2019) 9(16):4740–55. doi: 10.7150/thno.33520
88. Potter SS. Single-Cell RNA Sequencing for the Study of Development, Physiology and Disease. *Nat Rev Nephrol* (2018) 14(8):479–92. doi: 10.1038/s41581-018-0021-7
89. Clatworthy MR. How to Find a Resident Kidney Macrophage: The Single-Cell Sequencing Solution. *J Am Soc Nephrol* (2019) 30(5):715–6. doi: 10.1681/ASN.2019030245
90. Fu J, Akat KM, Sun Z, Zhang W, Schlondorff D, Liu Z, et al. Single-Cell RNA Profiling of Glomerular Cells Shows Dynamic Changes in Experimental Diabetic Kidney Disease. *J Am Soc Nephrol* (2019) 30(4):533–45. doi: 10.1681/ASN.2018090896

Conflict of Interest: The authors declare that the research was conducted in the absence of any commercial or financial relationships that could be construed as a potential conflict of interest.

Copyright © 2021 Wen, Yan, Wang and Liu. This is an open-access article distributed under the terms of the Creative Commons Attribution License (CC BY). The use, distribution or reproduction in other forums is permitted, provided the original author(s) and the copyright owner(s) are credited and that the original publication in this journal is cited, in accordance with accepted academic practice. No use, distribution or reproduction is permitted which does not comply with these terms.

frontiers in Immunology

ORIGINAL RESEARCH
published: 21 May 2021
doi: 10.3389/fimmu.2021.690697

PARK7 Protects Against Chronic Kidney Injury and Renal Fibrosis by Inducing SOD2 to Reduce Oxidative Stress

Lijun Yin[1], Honglin Li[1], Zhiwen Liu[1], Wenwen Wu[1], Juan Cai[1], Chengyuan Tang[1] and Zheng Dong[1,2]**

[1] Department of Nephrology, Hunan Key Laboratory of Kidney Disease and Blood Purification, The Second Xiangya Hospital at Central South University, Changsha, China, [2] Department of Cellular Biology and Anatomy, Medical College of Georgia at Augusta University and Charlie Norwood VA Medical Center, Augusta, GA, United States

Renal fibrosis is the final common pathway to chronic kidney diseases regardless of etiology. Parkinson disease protein 7 (PARK7) is a multifunctional protein involved in various cellular processes, but its pathophysiological role in kidneys remain largely unknown. Here, we have determined the role of PARK7 in renal fibrosis and have further elucidated the underlying mechanisms by using the *in vivo* mouse model of unilateral ureteric obstruction (UUO) and the *in vitro* model of transforming growth factor-b (TGFB1) treatment of cultured kidney proximal tubular cells. PARK7 decreased markedly in atrophic kidney tubules in UUO mice, and *Park7* deficiency aggravated UUO-induced renal fibrosis, tubular cell apoptosis, ROS production and inflammation. In *vitro*, TGFB1 treatment induced fibrotic changes in renal tubular cells, which was accompanied by alterations of PARK7. *Park7* knockdown exacerbated TGFB1-induced fibrotic changes, cell apoptosis and ROS production, whereas *Park7* overexpression or treatment with ND-13 (a PARK7-derived peptide) attenuated these TGFB1-induced changes. Mechanistically, PARK7 translocated into the nucleus of renal tubular cells following TGFB1 treatment or UUO, where it induced the expression of SOD2, an antioxidant enzyme. Taken together, these results indicate that PARK7 protects against chronic kidney injury and renal fibrosis by inducing SOD2 to reduce oxidative stress in tubular cells.

Keywords: renal fibrosis, tubular cells, PARK7, reactive oxygen species, antioxidant

OPEN ACCESS

Edited by:
Bin Yang,
University of Leicester,
United Kingdom

Reviewed by:
Rahul Sharma,
University of Virginia, United States
Bi-Cheng Liu,
Southeast University, China

****Correspondence:***
Chengyuan Tang
tangchengyuan@csu.edu.cn
Zheng Dong
zdong@augusta.edu

Specialty section:
This article was submitted to Molecular Innate Immunity, a section of the journal Frontiers in Immunology

Received: *03 April 2021*
Accepted: *06 May 2021*
Published: *21 May 2021*

Citation:
Yin L, Li H, Liu Z, Wu W, Cai J, Tang C and Dong Z (2021) PARK7 Protects Against Chronic Kidney Injury and Renal Fibrosis by Inducing SOD2 to Reduce Oxidative Stress. Front. Immunol. 12:690697. doi: 10.3389/fimmu.2021.690697

INTRODUCTION

Renal tubulointerstitial fibrosis (TIF) characterized by tubular atrophy, deposition of extracellular matrix and myofibroblast expansion represents the final common pathway to chronic or progressive kidney diseases (CKD) regardless of etiology (1–3). The pathogenesis of renal TIF involves major types of resident renal cells including tubular epithelial cells (TECs), endothelial cells, fibroblasts and pericytes, and also involves inflammatory cells. Accumulating evidence suggests that injury of renal TECs plays a

driving role in renal TIF[2,] (4). After kidney injury, survival TECs undergo proliferation and then redifferentiation to replace damaged or dead TECs to repair renal tubules. Under conditions of severe or repeated injury, renal TECs under phenotypic changes to synthesize and secrete varieties of bioactive molecules that drive interstitial inflammation and fibrosis (2). Thus, understanding the molecular mechanisms responsible for TEC injury is a key to the understanding of the pathogenic mechanism of renal TIF.

Experimental studies have demonstrated that epithelial-mesenchymal transition, cell-cycle arrest at G2/M check points, mitochondrial damage, autophagy, endoplasmic reticulum(ER) stress, and excessive reactive oxygen species (ROS) production contribute to renal tubular cell injury during renal TIF (1–8). Among them, overproduction of ROS appears to be an important pathological factor for renal TIF, which is supported by the findings of ROS accumulation in renal tubules and the beneficial effects of supplementation of exogenous antioxidants in renal TIF regardless of initial etiology (9). Excessive ROS causes oxidative damage to cellular components and organelles including mitochondria, which may lead to cell death. Besides the acute destructive effects of high levels of ROS, a moderate increase of ROS might regulate various signaling pathways that are involved in kidney injury and maladaptive kidney repair, such as the hypoxia-inducible factor 1α pathway, the NLRP3-inflammasome pathway, and the transforming growth factor-β (TGFB1/TGFβ) pathway (10). Investigation of the molecules involved in oxidative stress and the anti-oxidative response in renal tubular cells during renal TIF may provide novel therapeutic targets.

Parkinson disease protein 7 (PARK7/DJ-1) was initially identified as an activated ras-dependent oncoprotein (11), but later studies have implicated PARK7 in the pathogenesis of Parkinson`s disease, diabetes, and male infertility et al (12, 13). Evidence has recently emerged that PARK7 also plays a key role in immune and inflammatory disorders, such as sepsis, and atherosclerosis (14). As a multifunctional protein, PARK7 can act as an antioxidant, transcriptional co-activator, molecular chaperone, deglycase, and/or regulator of signaling pathways (15). PARK7 is abundant in kidneys, particularly in renal tubules (16). Emerging evidence suggests a role of PARK7 in the development of both AKI and CKD (17–20). However, the role of PARK7 in renal TIF and its underlying mechanism remain largely unclear.

In the present study, by using a unilateral ureteric obstruction (UUO)-induced mouse model of renal fibrosis, and culturing renal TECs exposed to TGFB1, we demonstrated that PARK7 protects against renal TIF and related kidney injury by inducing SOD2 and scavenging ROS.

MATERIALS AND METHODS

Antibodies and Reagents

The primary antibodies used in this study include anti-Fibronectin (ab19245) and anti-PARK7/DJ 1(ab18257) from Abcam, anti-cleaved caspase3 (9664), anti-α/β-Tubulin(2148) and anti-GAPDH (5174) from Cell Signaling Technology, anti-Lamin B1 (66095-1-Ig) and anti-Myc tag (6003-2-Ig) from Proteintech, anti-Collagen I (AF7001) from Affinity, anti-α-SMA(A5228) from Sigma-Aldrich, anti-SOD2(sc-137254) from Santa Cruz, and anti-F4/80 (GB11027) from Servicebio. All secondary antibodies were purchased from Thermo-Fisher Scientific. Special reagents were from the following sources: CM-H2DCFDA(C6827), Mito-SOX (M36008) and DHE (D11347) from Thermo Fisher Scientific, TUNEL assay kit (12156792910) from Roche Life Science, and recombinant human TGFB1 (GF111) from EMD Millipore. The PARK7-based peptide ND-13 (YGRKKRRKGAEEMETVIPVD) was synthesized by China Peptides (China).

Cells, Plasmids, Short Interfering RNA, and Transfection

The Boston University mouse proximal tubular cell line (BUMPT) was initially from Drs. William Lieberthal and John Shwartz at Boston University and maintained as previously described (21). BUMPT cells stably expressing *Park7* shRNA were generated by infecting cells with lentivirus encoding *Park7* shRNA followed by selection with puromycin. The shRNA target sequence of *Park7* was 5′-ATCTGGGTGCACAGAATTTAT-3′. The *Park7* shRNA was synthesized by Gene Pharma (Shanghai, China). The PARK7 overexpression plasmid was generated by inserting the coding sequence for C-terminal myc-tagged human *PARK7* into NheI and KpnI enzyme sites of into pcDNA3.1 (+) expression vector. Transfection was performed by using Lipofectamine 2000 reagents (Invitrogen, Carlsbad, MA, USA) under the manufacturer's instruction. TGFB1 treatment was performed as previously described (22). Briefly, cells were planted in 35mm cell culture dishes to reach >40% confluence by next day. After starving for 12 hours in serum-free high glucose DMEM medium, cells were cultured in DMEM medium containing 0.2% fetal bovine serum and 5 ng/ml of TGFB1. Cells cultured in medium containing 0.2% fetal bovine serum without TGFB1 were as controls. ND13 was dissolved in normal saline and administered at the same time with TGFB1 treatment.

Mouse Model of Unilateral Ureteral Obstruction

Animal studies were conducted under a protocol approved by the Animal Ethics Committee of the Second Xiangya Hospital of Central South University. Male C57BL/6 mice (8 ~10 weeks old) were from Hunan Slack King Experimental Animal Company (Changsha, China). *Park7*^{tm1Shn}/*Park7* knockout mice were purchased from the Jackson laboratory. Ureteral obstruction (UUO) surgery was performed as described in our recent studies (23). Briefly, mice were anaesthetized with pentobarbital (60 mg/kg) followed by a midline abdominal incision. The left ureter was exposed and separated, and then ligated by using 4/0 silk thread at two different sites in the middle of the ureter. Sham control mice underwent left ureter exposure, separation, but no ligations. For treatment, ND-13 (2 mg/kg of body weight) was administered *via* tail vein injection starting from the day after surgery, daily till the day before euthanasia.

Histological Analysis of Kidney Tissues

Hematoxylin and eosin (H&E) and Masson's trichrome staining in kidney sections were performed as previously described (24). Renal tubules with the following histopathological changes were considered as tubular atrophy: tubular epithelial thinning, pyknotic nuclei or tubular dilation, expansion of the interstitial space, with or without protein casts. Tubular atrophy was examined in a blinded manner and scored by the percentage of atrophic tubules: 0, no damage; 1, < 25%; 2, 25-50%; 3, 50-75%; 4, > 75%. For quantification, at least 10 randomly selected fields per mouse and four mice for each group were scored. Aniline blue staining was conducted to label collagen fibrils in kidney tissues. The ratio of positively (blue) stained area to the entire area (excluding the area of glomerular, small vena cava and blood vessels) was quantitated with Image Pro Plus software. At least 10 randomly selected areas with a magnification of 200 x were assessed.

Immunohistochemical Analysis

Deparaffinized kidney sections were sequentially incubated with 0.1 M sodium citrate for antigen retrieval, 3% H2O2 to block endogenous peroxidase activity and 5% normal goat serum in phosphate-buffered saline to reduce nonspecific binding. The kidney sections were them exposed to a specific primary antibody at 4°C overnight and then biotinylated goat anti-rabbit secondary antibody (Zhongshan Jinqiao Biotechnology, Beijing, China) for 2 hours at room temperature. The signals were detected with a DAB kit. Positive staining was observed by phase contrast microscopy. For quantification, the number of positively stained tubules or cells per mm2 in at least 10 randomly selected fields from each tissue section were evaluated.

TUNEL Assay

TUNEL assay in kidney tissues and cultured cells was performed as previously described (25). Kidney tissue sections were sequentially deparaffinized, permeabilized, and incubated with TUNEL reaction mixture for 1 h at 37°C in a humidified and dark cassette. Hoechst 33342 staining was conducted to label nucleus. For quantification, the number of TUNEL-positive tubular cells per mm2 in at least 10 randomly selected fields from each tissue section were counted. For TUNEL assay in cultured cells, cells were fixed, and then sequentially subjected to permeabilization, incubation with TUNEL reaction mixture and then Hoechst 33342. The percentage of TUNEL-positive cells in 10 randomly selected fields containing around 200 cells was quantified.

Isolation of Nuclear Proteins

Isolation of nuclear proteins in cells was conducted by using a kit from Beyotime (China). Briefly, cells were centrifuged at 1000g for 5 minutes, and cell pellets were resuspended in buffer A (10 mM HEPES pH 7.9, 1.5 mM MgCl2, 0.2 mM KCl 0.2 mM phenylmethylsulphonyl fluoride, 0.5 mM dithiothreitol). After incubation on ice for 15 minutes, the suspension was centrifuged at 14,000g for 5 minutes at 4°C to collect the nuclear pellets. The nuclear pellets were resuspended in cold buffer B(20 mmol/l N-2-hydroxyethylpiperazine-N-2-ethanesulfonic acid potassium hydroxide at pH 7.9, 420 mmol/l NaCl, 1.5 mmol/l MgCl2, 0.5 mmol/l dithiothreitol, 25% glycerol, 0.2 mmol/l dithiothreitol) and vortexed every 20 seconds for 30minutes. Finally, nuclear extracts were cleared by centrifugation at 14000g for 10 minutes to collect supernatants for immunoblotting.

Determination of Reactive Oxygen Species

Mitochondrial ROS and intracellular ROS in BUMPT cells were determined by using Mito-SOX Red (Thermo Fisher Scientific, M36008) and by CM-DCFDA (Invitrogen, C6827), respectively. ROS in kidney tissues was measured by dihydroethidium (Thermo Fisher Scientific, D11347) staining as previously described (26). Briefly, after harvesting, kidneys were snap frozen by liquid nitrogen. 20 mm sections of the kidneys were incubated with 10 mM DHE in a humidified and dark chamber at 37°C for 30 min and then counterstained with DAPI (Sigma-Aldrich, D9542). Images of the above staining were captured with fluorescence microscopy. For quantification, the fluorescence intensity in the nuclei of proximal tubular cells within 10 random optical sections was determined with ImageJ software. At least 10 randomly selected fields per mouse and four mice for each group were examined.

Immunofluorescence Staining

BUMPT cells were collected and washed once with phosphate-buffered saline (PBS), followed by fixation with 4% paraformaldehyde. After additional washing with PBS, fixed cells were sequentially underwent permeabilization with 0.1% Triton X-100, blocking with 5% bovine serum albumin hydration, and incubation with primary antibodies overnight at 4°C. And then cells were exposed to Alexa-conjugated secondary antibodies(Abcam, Cambridge, MA). Eventually, the sample were examined under fluorescence microscopy.

Immunoblotting Analysis and Real-Time PCR

Cells or renal cortical tissues were lysed with 2% SDS buffer (63 mM Tris-HCl, 10% glycerol, and 2% SDS) containing protease inhibitor cocktail (Sigma-Aldrich, P8340). Immunoblot analysis was conducted as previously described (27). RNA extraction and quantitative real-time PCR analysis were described in our recent studies (28). The sequences for the primers used in this study are listed below:

Park7 forward, 5′-AGTCGCCTATGGTGAAGGAGATCC-3′,
Park7 reverse, 5′-TGAGCCAACAGAGCCGTAGGAC-3′,
Tgfβ forward, 5′-GAGCCCGAAGCGGACTACTA-3′,
Tgfβ reverse, 5′-GTTGTTGCGGTCCACCATT-3′,
Tnfα forward, 5′-CAGGCGGTGCCTATGTCTC-3′,
Tnfα reverse, 5′-CGATCACCCCGAAGTTCAGTAG-3′,
Sod2 forward, 5′- AAGGGAGATGTTACAACTCAGG-3′,
Sod2 reverse, 5′- GCTCAGGTTTGTCCAGAAAATG-3′,
Gapdh forward, 5′- AGGTCGGTGTGAACGGATTTG -3′,
Gapdh reverse, 5′- GGGGTCGTTGATGGCAACA -3′.

Statistics

Statistical analysis was conducted by using GraphPad Prism software. Multiple comparisons with ANOVA and student's t-test were applied to determine statistical differences in multiple groups and two groups, respectively. Quantitative data in the present study are representatives of at least 3 independent experiments and are expressed as means ± SEM. $P < 0.05$ indicates significant differences.

RESULTS

PARK7 Is Reduced in Renal Proximal Tubules Following UUO

We first evaluated the levels of PARK7 during renal TIF in a mouse model of unilateral ureteral obstruction (UUO). Immunohistochemical analysis of kidney sections showed that in sham-operation mice, PARK7 was abundant in renal tubules, and mainly localizes in cell cytosol (**Figure 1A**). Compared to sham-operation mice, UUO mice had high levels of PARK7 in intact renal tubules, but atrophic tubules with dilation showed an obvious decrease of PARK7 (**Figure 1A**). In addition, the intact renal tubules appeared to have more PARK7 in cell nucleus (**Figure 1A**). Immunoblot analysis showed that UUO induced renal expression of fibrosis marker proteins like fibronectin and alpha-smooth muscle actin (α-SMA) in a time-dependent manner, while the expression of PARK7 was decreased (**Figures 1B–E**). Furthermore, We investigated the mRNA level of *Park7* and found that UUO did not alter its transcriptional process (**Figure 1F**). These results indicate an overall reduction of renal PARK7 during renal TIF.

UUO-Induced Renal Interstitial Fibrosis Is Aggravated in *Park7*-Knockout Mice

To determine the role of PARK7 in renal TIF, *Park7* knockout (KO) mice were applied. Day 7 after UUO surgery, the obstructed kidneys from wildtype (WT) or *Park7* ko mice were collected. Immunoblot analysis demonstrated that *Park7* ko mice had higher renal levels of fibronectin and α-SMA than WT mice after UUO (**Figures 2A–C**). Masson's trichrome staining was performed to detect collagen deposition, and the results revealed that *Park7* ko mice had an increase of renal collagen deposition compared to WT mice after UUO (**Figures 2D, E**). In addition, quantification of tubular atrophy in kidney sections stained with hematoxylin and eosin (H&E) demonstrated that following UUO, had tubular atrophy was more severe in *Park7* ko mice than in WT mice (**Figures 2D, F**). Collectively, these findings suggest that *Park7* deficiency aggravates UUO-induced renal TIF.

Park7 Deficiency Increases Tubular Cell Apoptosis and Inflammation In UUO

Tubular cell death and inflammation contribute critically to the development of renal fibrosis regardless of initial etiology (2, 4). The effect of *Park7* deficiency on UUO-induced tubular cell apoptosis was evaluated by TUNEL assay. As shown **Figure 3A**, both WT and *Park7* ko mice had very few TUNEL positive cells in kidney tissues after sham-operation, but they had an obvious increase of TUNEL positive cells following UUO. Moreover, quantification analysis by cell counting revealed that *Park7* ko mice had significantly more TUNEL positive cells than WT mice in response to UUO (**Figure 3B**). Consistent with the results of TUNEL assay, UUO-operated *Park7* ko mice had higher renal levels of activated/cleaved caspase 3 compared to UUO-operated WT mice (**Figures 3C, D**). Immunohistochemical analysis of macrophages in kidney tissue sections was performed to evaluate inflammatory cell infiltration into kidneys. As shown in **Figures 3E, F**, UUO induced infiltration of macrophage into the kidney tissues of both WT and *Park7* ko mice and induced significantly more infiltration of macrophage in *Park7* ko kidneys than in WT kidneys. Collectively, these findings indicate that PARK7 is protective against tubular cell apoptosis and inflammation during renal fibrosis.

Park7 Deficiency Leads to Excessive ROS in Renal Tubular Cells Following UUO

PARK7 can act as an antioxidant (29, 30). We thus determined the effect of *Park7* deficiency on the levels of ROS in renal tubules during UUO-induced renal fibrosis by dihydroethidium (DHE) staining. DHE exhibits red fluorescence in the nucleus when oxidized by ROS. WT and *Park7* ko mice showed comparable low DHE signal intensity in renal tubules after sham-operation, and both WT and mutant mice had a dramatic increase of DHE signal intensity after UUO. Importantly, following UUO, *Park7* ko mice exhibited significantly stronger DHE signal intensity in renal tubules compared to WT mice (**Figures 4A, B**). Taken together, these findings suggest that PARK7 suppresses ROS accumulation during renal TIF.

TGFB1 Treatment Alters PARK7 Expression in BUMPT cells

Transforming growth factor beta 1(TGFB1 or TGF-β1) is a critical profibrotic factor in renal fibrosis. (31) We determined the effect of TGFB1 treatment on PARK7 expression *in vitro*. BUMPT cells formed cobblestone monolayer with intact cell-cell connection under control condition, but, after TGFB1 treatment for 36 hours, the cells exhibited a spindle-shape, fibroblast like morphology (**Figure 5A**). Immunoblot analysis demonstrated that TGFB1 treatment increased the expression of fibrosis maker proteins, such as fibronectin and collagen 1, in a time-dependent manner during the observation period of 72 hours. Remarkably, TGFB1 induced a biphasic change in PARK7 expression. PARK7 increased in a time-dependent manner during 36 hours of TGFB1 treatment, but after that, it started to decrease (**Figures 5B–E**). In addition, We estimated the mRNA level of *Park7* and found that TGFB1 did not change its transcriptional process (**Figure 5F**).

Park7 Knockdown Sensitizes BUMPT Cells to TGFB1-Induced Fibrotic Changes, Apoptosis, and ROS Production

To determine the role of PARK7 in TGFB1-induced changes in renal tubular cells, we knocked down *Park7* with a short hairpin (sh) RNA specifically targeting *Park7*. Immunoblot analysis showed that *Park7*-shRNA significantly reduced PARK7 expression in BUMPT cells (**Figure 6A**). In response to TGFB1 treatment, cells

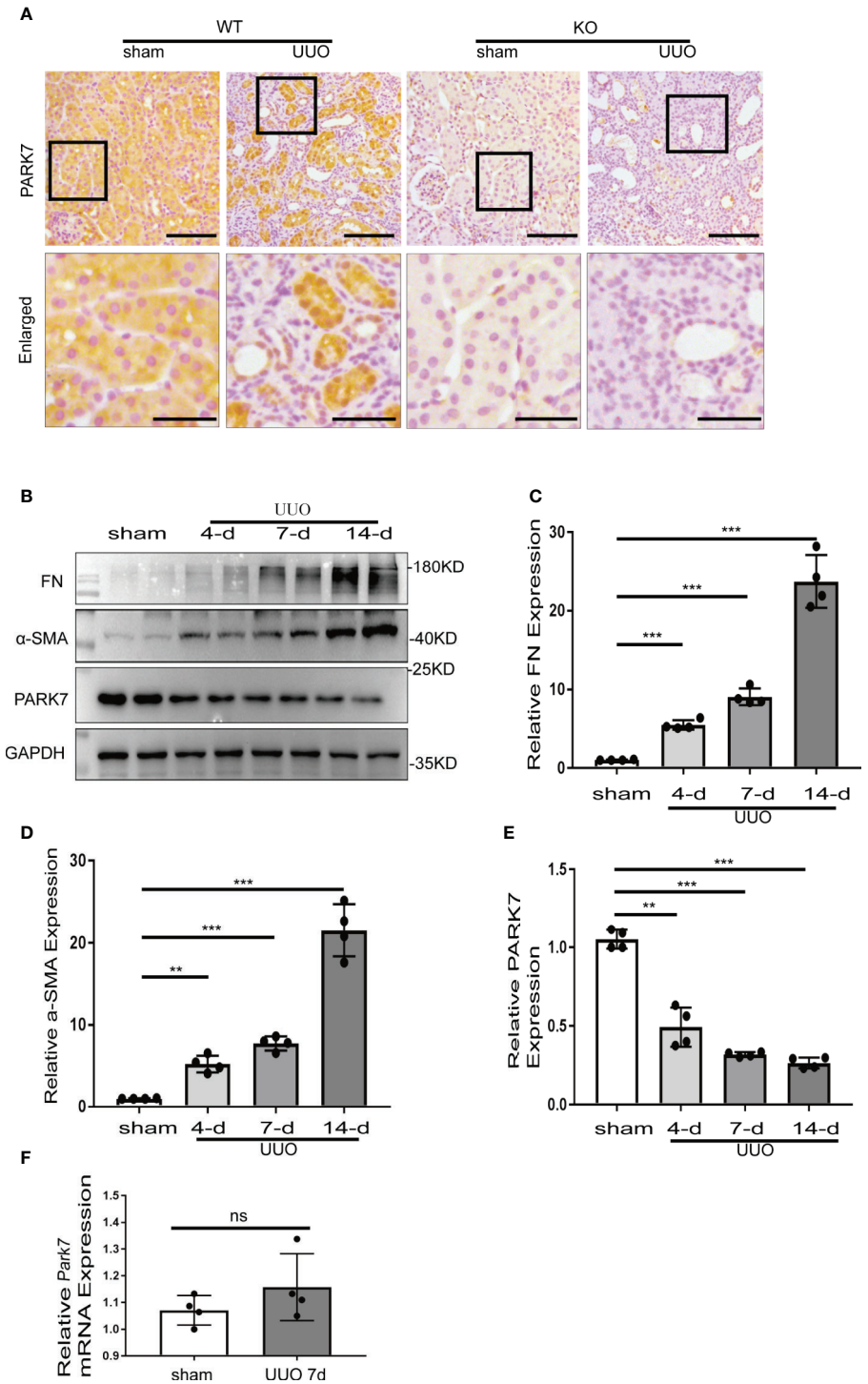


FIGURE 1 | PARK7 is reduced in renal proximal tubules during UUO. C57BL/6 mice (female, 8weeks old) were subjected to sham operation or UUO surgery. The mice were euthanized at 4 days, 7 days or 14 days after surgery, and the UUO-obstructed kidneys were collected. **(A)** Representative images of histochemical staining of PARK7 in kidney tissues. Bar: 100μm in the top images and 50μm in the bottom enlarged images. **(B)** Representative blots of Fibronectin (FN), α-SMA, PARK7 and GAPDH(as protein loading control). **(C–E)** Densitometry of FN, α-SMA, and PARK7 signals(n=4). The signal of FN, α-SMA, or PARK7 was normalized to the GAPDH signal of the same samples to determine the ratios. The values are expressed as fold change over sham control. Each symbol (circle) represents an individual mouse. **(F)** Quantification of Park7 mRNA levels. Error bars: SEM. $^{**}p < 0.01$, $^{***}p < 0.001$. ns, not significant.

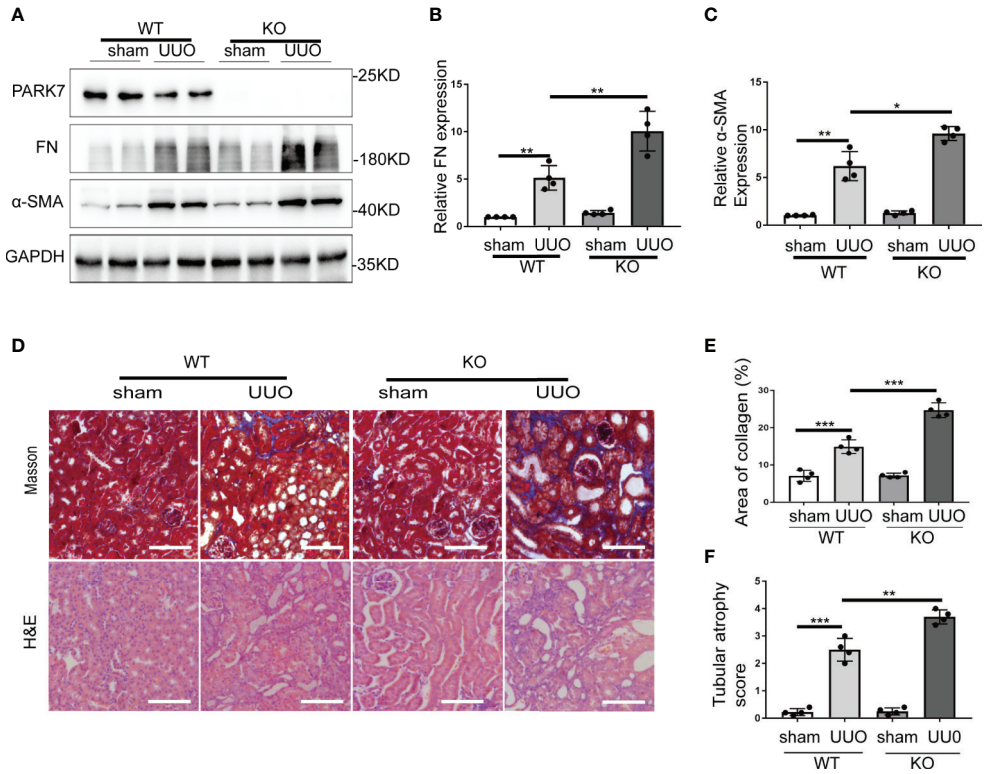


FIGURE 2 | PARK7 deficiency aggravates UUO-induced renal interstitial fibrosis. *Park7* knockout (KO) and wildtype (WT) mice were subjected to either sham operation or UUO surgery. The mice were euthanized at 7 days and UUO-obstructed kidneys were collected. **(A)** Representative blots of PARK7, Fibronectin (FN), α-SMA and GAPDH(as a loading control). **(B, C)** Densitometry of FN and α-SMA signals(n=4). The signal of FN, α-SMA was normalized to the GAPDH signal of the same samples to determine the ratios. The values are expressed as fold change over sham control in WT mice. **(D)** Representative images of Masson's trichrome staining and hematoxylin and eosin (H&E) staining. Bar: 100μm. **(E)** Quantitative analysis of Masson's trichrome staining. **(F)** Tubular atrophy score(n=4). Tubular atrophy was graded by 0, 1 (1%-25%), 2 (26%-50%), 3 (51%-75%), 4 (76%-100% tubules showing atrophy. Each symbol (circle) represents an individual mouse. Error bars: SEM. *p < 0.05, **p < 0.01, ***p < 0.001.

expressing *Park7*-shRNA had higher levels of fibronectin and active/cleaved caspase 3 than the cells transfected with a scrambled-shRNA(*Scr*-shRNA) (**Figures 6A–C**). *Park7* knockdown also increased the number of TUNEL-positive cells following TGFB1 treatment (**Figures 6D, E**). We further analyzed intracellular ROS and mitochondrial ROS by CM-H2DCFDA and Mito-SOX staining, respectively. Regardless of the status of *Park7*, BUMPT cells showed comparable low signal intensity of these ROS indicators under control conditions (**Figures 6F–H**). TGFB1 induced significant ROS, and totably, the *Park7*-knockdown cells had stronger signal intensity of CM-H2DCFDA and Mito-SOX than the cells transfected with scrambled-shRNA. Collectively, these findings suggest that PARK7 may protect against renal fibrosis by reducing ROS and suppressing cell death.

PARK7 Overexpression Attenuates TGFB1-Induced Profibrotic Changes, Apoptosis, and ROS Production

To further verify the role of PARK7, we evaluated the effect of PARK7 overexpression on TGFB1-induced cellular changes in renal tubular cells. To this end, BUMPT cells stably expressing human PARK7 conjugated with a C-terminal c-Myc epitope were generated. As shown in **Figure 7A**, TGFB1 induced a spindle-shape morphology in the cells stablely transfected with empty vectors, which was partially prevented in cells overexpressing PARK7. In addition, BUMPT cells overexpressing PARK7 had lower levels of fibronectin and cleaved caspase 3 compared to control cells (**Figures 7B–D**). In line with the results of cleaved caspase 3, cells overexpression PARK7 had fewer TUNEL-staining positive cells than control cells following TGFB1 treatment (**Figures 7E, F**). In addition, cells overexpressing PARK7 showed lower signal intensity of both CM-H2DCFDA and Mito-SOX staining than control cells in response to TGFB1 treatment(**Figures 7G–I**). Together, these findings provide further evidence that PARK7 protects against apoptosis, ROS production and fibrotic change in renal tubular cells.

ND-13 Attenuates TGFB1-Induced Fibrosis Changes in BUMPT Cells

ND-13 is a 20-amino acid peptide composed of a 13-amino acids sequence from PARK7 (KGAEEMETVIPVD) and a TAT-derived 7-amino acid sequence (YGRKKRR) at the N-

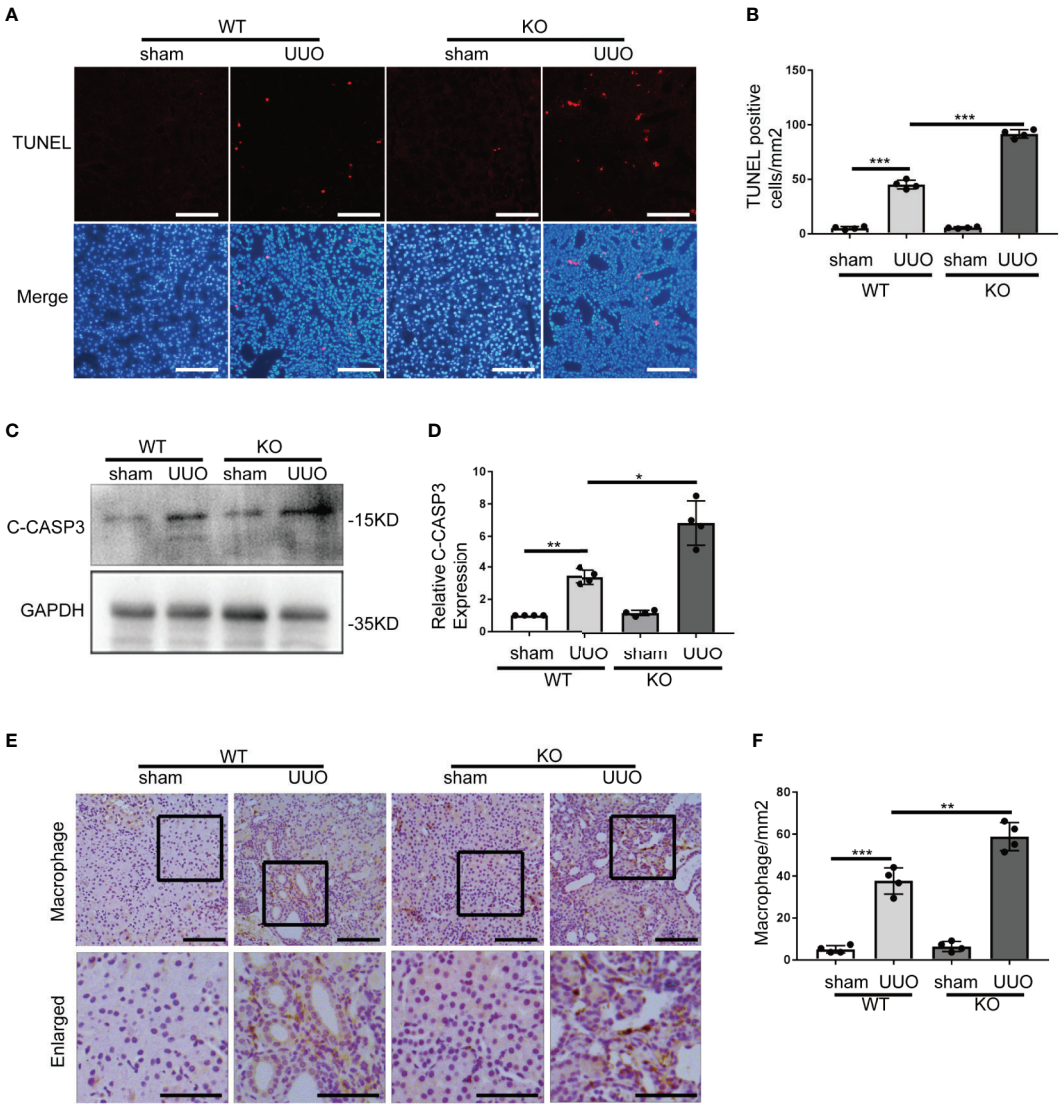


FIGURE 3 | *Park7* deficiency increases tubular cell apoptosis and inflammation in UUO. Animals and their treatment were the same as described in **Figure 2**. **(A)** Representative images of TUNEL analysis of kidney tissues. Bar:100μm. **(B)** Quantification of TUNEL-positive cells in kidney tissues(n=4). **(C)** Representative immunoblots of cleaved/activated caspase3 (C-CASP3) and GAPDH(as a loading control). **(D)** Densitometry of C-CASP3 signals(n=4). The signal of C-CASP3 was normalized to the GAPDH signal of the same samples to determine the ratios. The values are expressed as fold change over sham control in WT mice. **(E)** Representative images of macrophage staining. Bar: 100μm in the top images and 50μm in the bottom enlarged images. **(F)** Quantification of macrophage -positive cells(n=4). Each symbol (circle) represents an individual mouse. Error bars: SEM. *$p < 0.05$, **$p < 0.01$, ***$p < 0.001$.

terminus for cellular permeability (32). We first evaluated the effect of ND-13 on the TGFB1-induced cellular changes *in vitro*. To this end, BUMPT cells were exposed to TGFB1 with/without 5~20μM of ND-13 for 24 hours to examine cell morphology and the levels of fibronectin and ROS. As shown in **Figures 8A–F**, ND-13 treatment partially prevented TGFB1-induced morphological changes in BUMPT cell, attenuated TGFB1-induced expression of fibronectin, and also reduced the signal intensity of both CM-H2DCFDA and Mito-SOX staining. We further evaluated the effect of ND-13 treatment on UUO-induced renal fibrosis. Administration of ND-13 (2 mg/kg of body weight) *via* tail veil injection starting from the day of surgery, daily for 7 days partially reduced the renal levels of *Tgfβ* mRNA in UUO mice (**Figure 8G**). ND-13 treatment also significantly reduced the expression of tumor necrosis factor alpha (TNF-α), and also reduced infiltration of macrophages into kidney tissues (**Figures 8H–J**). Taken together, these findings indicate a renoprotective role ND-13 against oxidative stress, inflammation, and renal fibrosis.

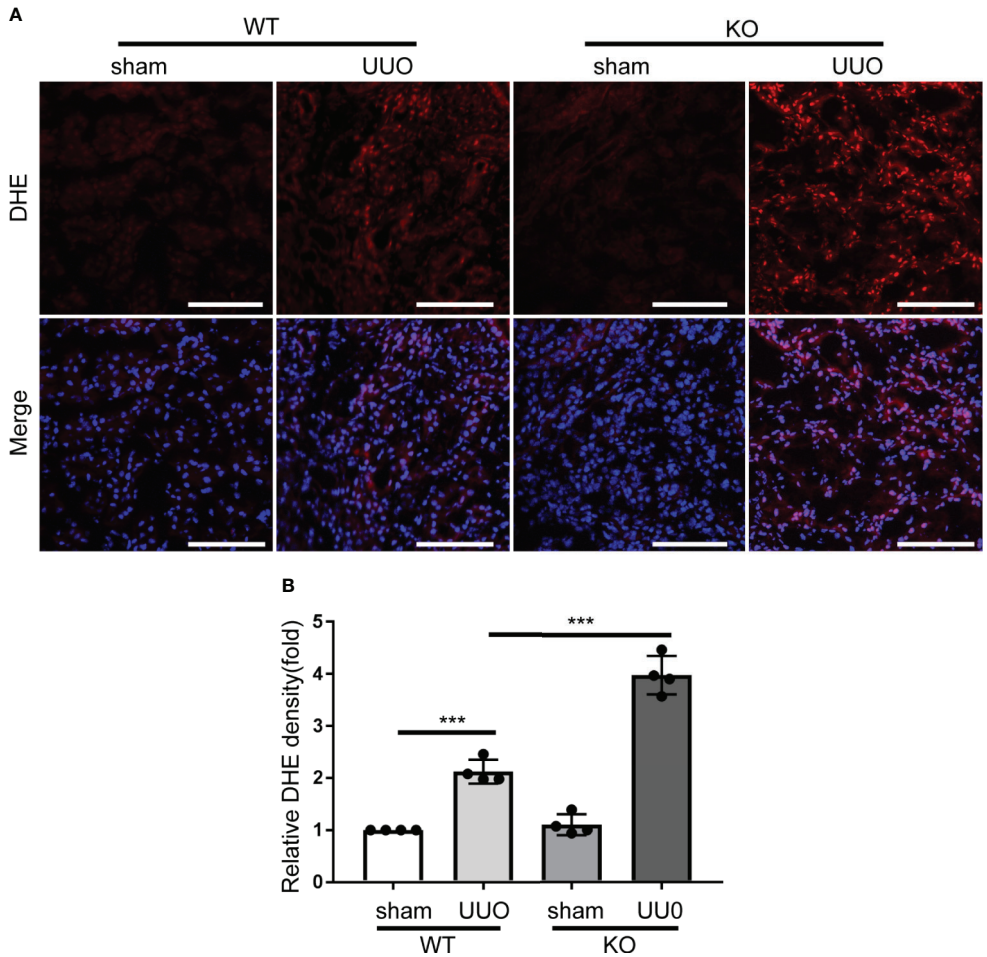


FIGURE 4 | *Park7* deficiency accumulates ROS accumulation in renal tubular cells in UUO. Animals and their treatment were the same as described in **Figure 2**. **(A)** Representative images of dihydroethidium (DHE) staining. DHE nuclear staining indicates the presence of reactive oxygen species(ROS). Bar:100μm. **(B)** Quantification of DHE fluorescence intensity (n=4). Each symbol (circle) represents an individual mouse. Error bars: SEM. ***p < 0.001.

PARK7 Translocates Into Nucleus and Positively Regulates SOD2 Expression During Renal Fibrosis

In UUO kidneys, PARK7 showed nuclear accumulation in intact renal tubules (**Figure 1A**). We thus examined the nuclear levels of PARK7 in BUMPT cell with or without TGFB1 treatment. Immunofluorescence staining showed that in cells without TGFB1 treatment, PARK7 existed mainly in cytosol, and to less extent in the nucleus (**Figure 9A**). Immunoblotting of PARK7 in the nuclear and cytoplasmic fractions verified that PARK7 localized predominantly in the cytosol in control cells and showed a dramatical increase in both cytosolic and nuclear fractions following TGFB1 treatment (**Figure 9B**). Emerging evidence indicates that nuclear PARK7 may regulate gene transcription by acting as a transcriptional cofactor (33). Because PARK7 regulated ROS production in mitochondria (**Figures 6F** and **7G**), we tested the possible regulation of SOD2 (mitochondrial superoxide dismutase 2, also known as manganese-dependent superoxide dismutase or MnSOD) by PARK7. As shown in **Figures 9C, D**, both WT and *Park7* ko mice showed high levels of SOD2 in kidney tissues, which decreased during UUO. Notably, the SOD2 decrease was obviously more in *Park7* ko mice than in WT mice. Consistently, TGFB1 treatment reduced SOD2 expression in both *Park7* knockdown cells and control cells, but the reduction was significantly higher in *Park7* knockdown cells. Moreover, *PARK7* overexpression could partially but significantly restore SOD2 levels in TGFB1-treated cells (**Figures 9E, F**). Furthermore, we analyzed *Sod2* mRNA, which showed the regulation by PARK7 both *in vitro* and *in vivo* (**Figures 9G, H**). Collectively, these findings suggest that PARK7 may protect against chronic kidney injury and renal fibrosis by inducing SOD2 and reducing ROS and oxidative stress.

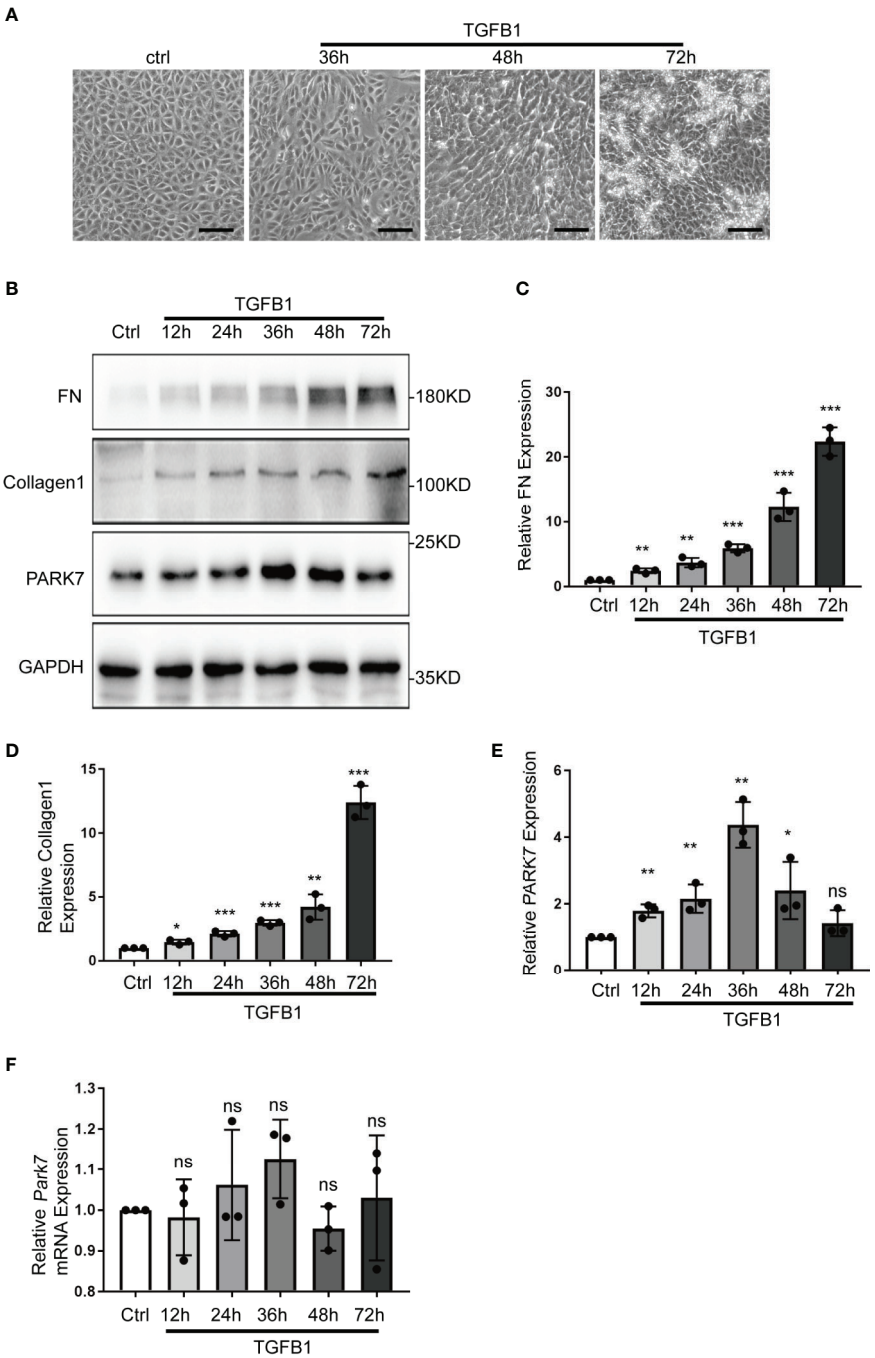


FIGURE 5 | TGFB1 treatment altered PARK7 expression in BUMPT cells. BUMPT cells were incubated with 5 ng/ml TGFB1 for 12h to 72h, and the cells treated without TGFB1 were as control (Ctrl). **(A)** Representative images of contrast microscopy to show cellular morphologic changes. Bar:100μm. **(B)** Representative immunoblot of Fibronectin (FN), Collagen 1, PARK7 and GAPDH (protein loading control) in whole cell lysates. **(C–E)** Densitometry of FN, Collagen 1 and PARK7 (n=3). The signal of FN, Collagen 1, or PARK7 was normalized to the GAPDH signal of the same samples to determine the ratios. The values are expressed as fold change over control cells. Each symbol (circle) represents an independent experiment. **(F)** Quantification of Park7 mRNA levels. Error bars: SEM. *p < 0.05, **p < 0.01, ***p < 0.001. ns, not significant.

DISCUSSION

In the present study, we have provided substantial evidence supporting a renoprotective role of renal tubular cell PARK7 in renal fibrosis. First, we showed that PARK7 expression was altered in renal tubules in UUO mice and in BUMPT cells exposed to TGFB1. Second, we demonstrated that *Park7* deficiency aggravated UUO-induced renal fibrosis in mice.

Park7 knockdown in BUMPT cells exacerbated TGFB1-induced fibrotic changes, while *PARK7* overexpression attenuated the fibrotic changes. Third, we provided further evidence that *Park7* deficiency or knockdown aggravated ROS accumulation, tubular cell apoptosis, and inflammation in renal fibrosis models. Mechanistically, we showed that during renal fibrosis, PARK7 accumulated in the nucleus in renal tubular cells, and positively regulated expression of the antioxidant enzyme SOD2. Together, these findings suggest a protective function of PARK7 in chronic kidney injury and renal fibrosis, and accordingly, enhancement of PARK7 expression and/or activity may represent a promising therapeutic approach.

Recent studies have suggested a role of PARK7 in the development of kidney diseases. For instance, Leeds et al. demonstrated that activation of PARK7 was renoprotective in lipopolysaccharides- or cecal ligation and puncture-induced septic AKI in mice (34). Shen et al. showed that increased expression of renal tubular PARK7 might represent a renoprotective response in a rat model of high glucose-induced diabetic kidney diseases (35). However, the pathophysiological role and mechanism of PARK7 in the pathogenesis of renal fibrosis remain largely unclear. Our present study has provided evidence supporting a beneficial role of renal tubular PARK7 in renal fibrosis. In *vitro*, TGFB1-induced fibrotic changes in BUMPT cells, including cell morphological changes and increases of extracellular matrix proteins were enhanced by *PARK7* knockdown (**Figures 6A, B**), but attenuated by *PARK7* overexpression (**Figures 7A–C**). In *vivo*, *Park7* deficiency aggravated UUO-induced renal fibrosis, as manifested by more severe tubular atrophy and kidney deposition of extracellular matrix proteins in *Park7* ko mice than in WT mice following UUO (**Figure 2**). Consistently, the latest work by Miguel et al. demonstrated the inhibitory effect of ND-13 (PARK7 peptide) on UUO-induced renal fibrosis (36). Collectively, these studies indicate that renal tubular cell PARK7 has an anti-fibrotic, protective function in kidney diseases.

PARK7 expression appears to be differently altered according to diseases conditions, and/or cell types (37, 38). For instance, PARK7 is highly expressed in lipopolysaccharides-induced acute lung injury (39), while decreased in heavy smoking-induced lung disease (40). Compared to control animals, altered PARK7 levels in kidney tissues have also demonstrated in experimental animal of kidney diseases. An increase of PARK7 levels in kidney tissues was detected in in mouse models of septic AKI, and a ischemia-reperfusion-induced rat model in diabetic kidney injury (34, 41). Eltoweissy et al. showed a disease grade dependent increase of PARK7 levels in the kidneys of a mouse model of COL4A3-deficiency-induced renal fibrosis (42). Consistently, Eltoweissy et al. also revealed that treatment of renal epithelial cells with the profibrogenic agonist ANG II or PDGF resulted in a significant up-regulation of PARK7 expression parallel to an increase in the expression of fibrosis markers (42). In a sharp contrast, in the present study, immunoblot analysis revealed that UUO mice had a dramatic reduction of PARK7 levels in kidney tissues compared to sham-operated mice (**Figures 1B, E**). Immunohistochemical staining further demonstrated that PARK7 decreased in atrophic renal tubules in UUO mice, but it increased in the intact renal tubules (**Figure 1A**). Further evaluation of *Park7* mRNA levels revealed no differences between UUO- and sham-operated mice (**Figure 1F**). In BUMPT cells, we showed an initial increase of PARK7 followed by a decrease during TGFB1 treatment (**Figures 5B, E**), but TGFB1 had no effect on the levels of *Park7* mRNA (**Figure 5F**). These results suggest an increased degradation of PARK7 in UUO, especially in those atrophic tubules. The different alteration of kidney expression of PARK7 between the present study and Eltoweissy et al. study may be attributed to the differences in the experimental models. Recent evidences have implicated that PARK7 oxidation facilitates its degradation (43, 44). In the present study, accumulation of ROS occurred in atrophic renal tubules in UUO mice as evaluated by DHE staining analysis (**Figure 4**). However, PARK7 oxidation and its contribution to PARK7 degradation during renal fibrosis remain to be determined. In addition, RNA modifications have been shown to affect the outcome of gene expression by modulating RNA processing, localization, translation, and eventual decay (45, 46). Whether modification in *Park7* mRNA contributes to the PARK7 reduction without changing the *Park7* mRNA levels in renal tubules of UUO mice remain to be explored.

PARK7 has multiple functions including antioxidant, transcriptional co-activator, molecular chaperone, deglycase, and/or regulator of signaling pathways (15). Among them, the antioxidant capacity has been demonstrated as an important cytoprotective mechanism in various disease conditions, such as PARK7 protection of rat retinal pericytes against high glucose-induced oxidative stress (47). Accumulation of ROS in renal tubules is a comment feature of chronic kidney disease, and contributes critically to the development to both AKI and CKD (48). High levels of ROS cause oxidative damage to cellular components, which may increase the tendency of cell injury and death (49). ROS are also an activator of inflammation (50). In the present study, we provided evidence that PARK7 has an important role in scavenging ROS and thereby reduces cell death and inflammation in kidneys during renal fibrosis. In *vivo*, *Park7* deficiency led to the excessive accumulation of ROS (**Figure 4**), increased renal tubular cell apoptosis and inflammation in UUO mice (**Figure 3**). Consistently, *Park7* knockdown increased the levels of ROS and apoptosis (**Figure 6**), while *PARK7* overexpression showed opposite effects (**Figure 7**). Thus, PARK7 plays an important role in scavenging ROS in renal tubules during renal fibrosis.

PARK7 can act as a transcription cofactor, a molecular chaperon, and can also modulate signaling pathway involving stress response, and also regulate protein degradation, all of which may contribute to its regulation of protein expression (51). For instance, PARK7 has been shown to disrupt KEAP1 interaction with transcriptional factors NRF2, leading to nuclear translocation of NRF2 to transactivate various antioxidative stress-related genes (52). PARK7 has also been demonstrated to regulate the 20S proteasome and thus protein degradation (53). In our experimental setting, nuclear accumulation of PARK7 was

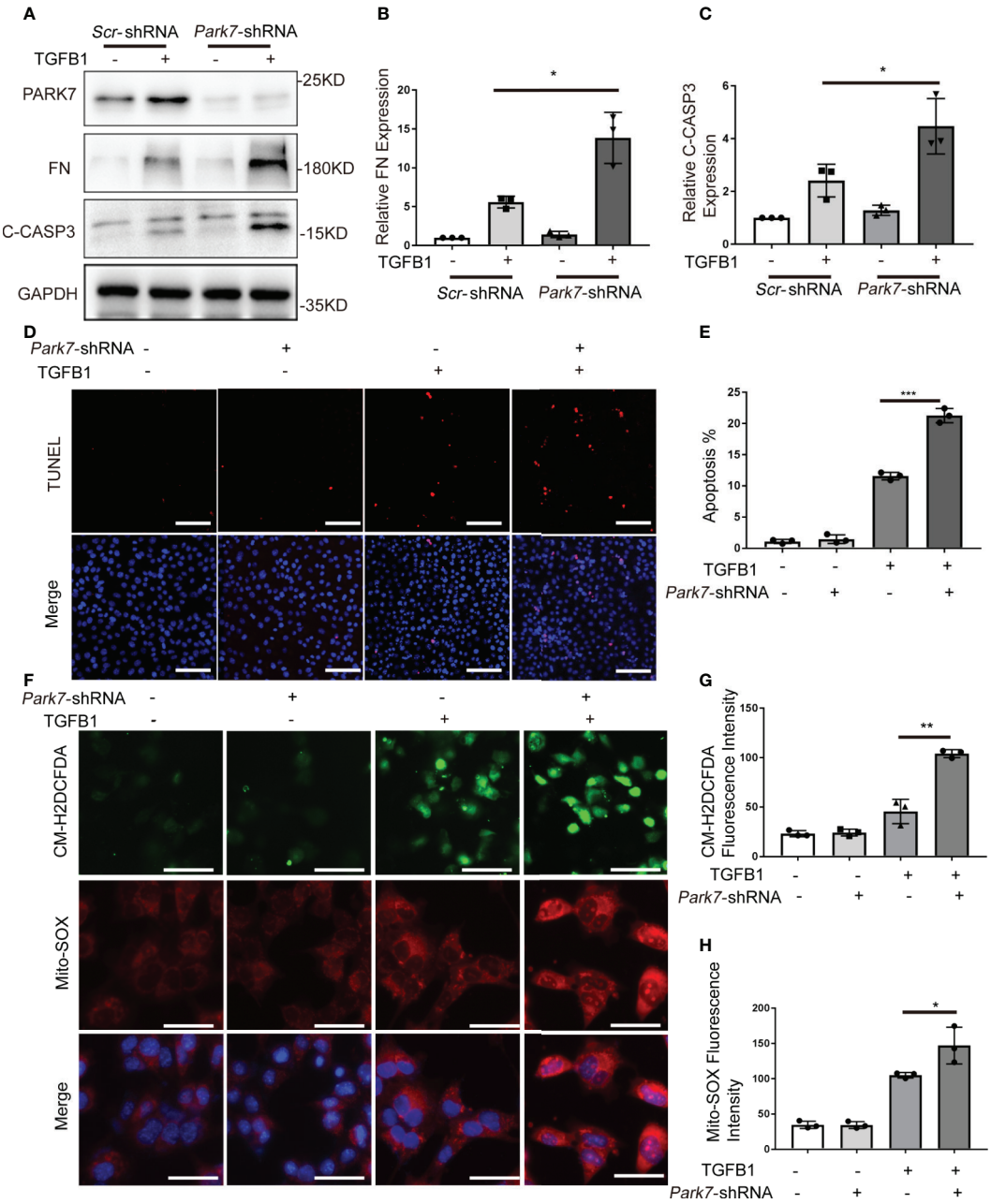


FIGURE 6 | *Park7* knockdown sensitizes BUMPT cells to TGFB1-induced fibrotic changes, apoptosis and ROS production. BUMPT cells were transfected with *Park7*-shRNA or scrambled-shRNA(*Scr*-shRNA), and at 24 hours after transfection, the cells were incubated with/without 5 ng/ml TGFB1 for another 24 hours. **(A)** Representative immunoblot of PARK7, Fibronectin (FN), cleaved/activated caspase 3(C-CASP3) and GAPDH (protein loading control). **(B, C)** Densitometry of FN and C-CASP3(n=3). The signal of FN, or C-CASP3 was normalized to the GAPDH signal of the same samples to determine the ratios. The values are expressed as fold change over control cells without *Park7* shRNA transfection. **(D)** Representative images of TUNEL assay and DAPI staining (X200). Bar:100μm. **(E)** Apoptosis percentage(n=3). **(F)** Representative images of CM-H2DCFDA and Mito-SOX staining. Bar: 100μm in the CM-H2DCFDA image, 50μm in the Mito-SOX and Merge images. CM-H2DCFDA and Mito-SOX staining was performed to evaluate intracellular and mitochondrial ROS, respectively. **(G, H)** Quantification of CM-H2DCFDA and Mito-SOX fluorescence intensity(n=3). Each symbol (circle, diamond and trigon) represents an independent experiment. Error bars: SEM. *p < 0.05, **p < 0.01, ***p < 0.001.

detected in the intact renal tubule of UUO mice and BUMPT cells exposed to TGFB1 (**Figures 1A** and **9A, B**). In addition, PARK7 seemed to positively regulate the protein levels of enzymatic antioxidant SOD2 (**Figures 9C–H**). However, the precise mechanism responsible for the regulatory role of PARK7 on SOD2 awaits future investigation.

ND-13 is PARK7-based peptide that has been shown be cytoprotective under stressful conditions, such as Cerebral

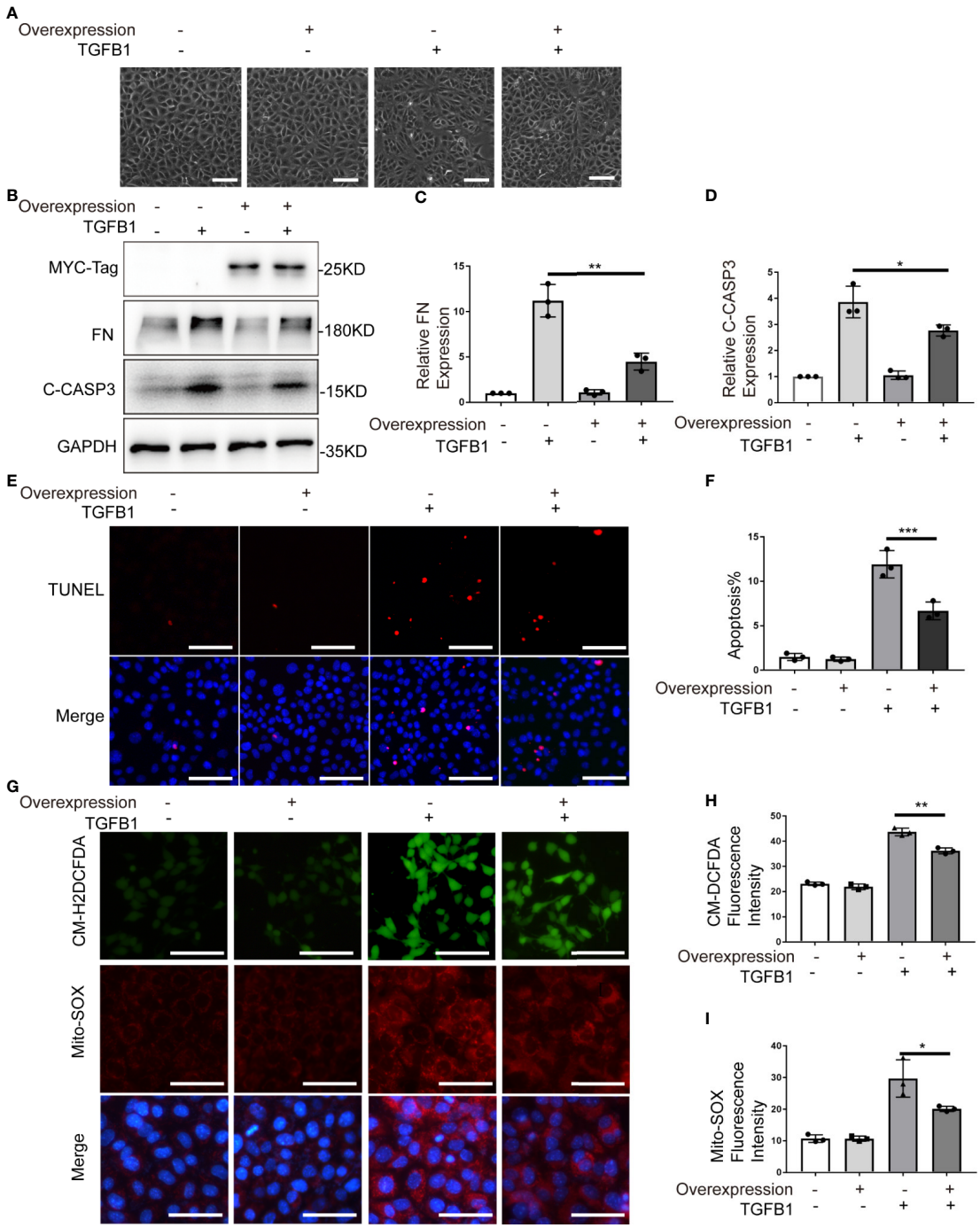


FIGURE 7 | PARK7 overexpression attenuates TGFB1-induced profibrotic changes, apoptosis and ROS production. BUMPT cells were transfected with PARK7 overexpression plasmid or empty vector, and 24 hours after transfection, the cells were cultured in medium with/without 5 ng/ml TGFB1 for another 24 hours. **(A)** Representative images of cell morphology. Bar: 100μm. **(B)** Representative immunoblot of Fibronectin (FN), cleaved/activated caspase 3(C-CASP3), MCY-Tag and GAPDH (protein loading control). **(C, D)** Densitometry of FN and C-CASP3 (n=3). The signal of FN, or C-CASP3 was normalized to the GAPDH signal of the same samples to determine the ratios. The values are expressed as fold change over control cells without *Park7* overexpression. **(E)** Representative images of TUNEL assay and DAPI staining (X200). Bar: 100μm. **(F)** Apoptosis percentage (n=3). Greater than 200 cells in each group were evaluated to determine the percentage of TUNEL-positive cells. **(G)** Representative images of CM-H2DCFDA and Mito-SOX staining. Bar: 100μm in the CM-H2DCFDA image, 50μm in the Mito-SOX and Merge images. CM-H2DCFDA and Mito-SOX staining was performed to evaluate intracellular and mitochondrial ROS, respectively. **(H, I)** Quantification of CM-H2DCFDA and Mito-SOX fluorescence intensity (n=3). Each symbol (circle, diamond and trigon) represents an independent experiment. Error bars: SEM. *p < 0.05, **p < 0.01, ***p < 0.001.

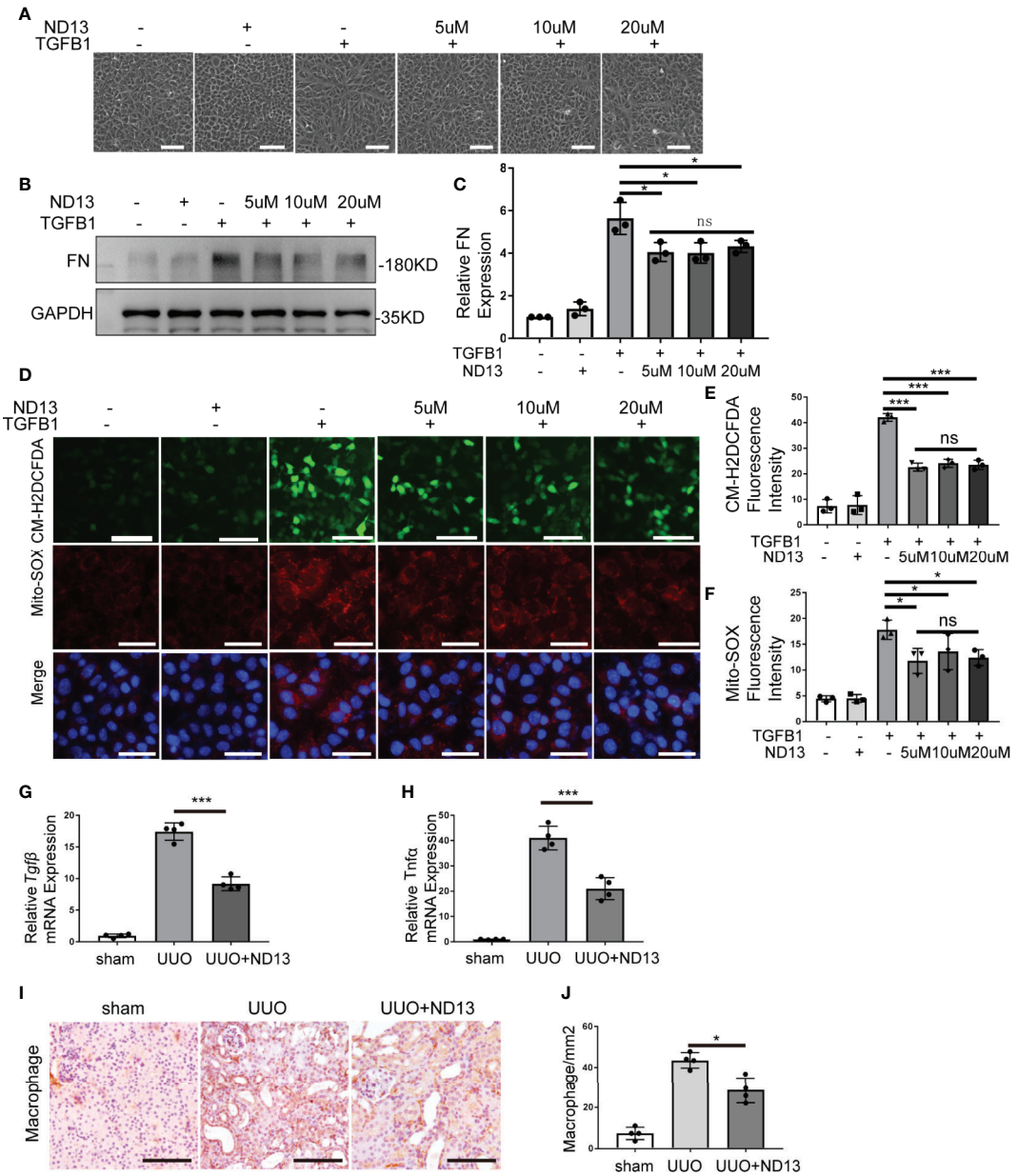


FIGURE 8 | ND-13 attenuates TGFB1-induced fibrosis changes in BUMPT cells. **(A–F)** BUMPT cells were cultured in medium with/without 5ng/ml TGFB1 in the presence/absence of ND13 for 24 hours. **(A)** Representative images of cell morphology. Bar: 100μm. **(B)** Representative immunoblot of Fibronectin (FN), GAPDH (protein loading control). **(C)** Densitometry of FN (n=3). The signal of FN was normalized to the GAPDH signal of the same samples to determine the ratios. The values are expressed as fold change over control cells. **(D)** Representative images of CM-H2DCFDA and Mito-SOX staining. Bar: 100μm in the CM-H2DCFDA image, 50μm in the Mito-SOX and Merge images. CM-H2DCFDA and Mito-SOX staining was performed to evaluate intracellular and mitochondrial ROS, respectively. **(E, F)** Quantification of CM-H2DCFDA and Mito-SOX fluorescence intensity (n=3). **(G–J)** C57BL/6 mice (female, 8weeks old) were subjected to sham operation or UUO surgery. Administration of ND-13 (2 mg/kg of body weight) *via* tail veil injection starting from the day of surgery and daily thereafter. The mice were euthanized at 7 days after surgery, and the UUO-obstructed kidneys were collected. **(G, H)** mRNA levels of transforming growth factor-β (*Tgfβ*) and tumor necrosis factor alpha (*Tnfα*) were measured by quantitative RT-PCR. **(I)** Representative images of macrophage staining. Bar: 100μm. **(J)** Quantification of macrophage -positive cells (n=4). Each symbol (circle, diamond and trigon) represents an independent experiment. Error bars: SEM. *p < 0.05, ***p < 0.001, ns not significant.

reperfusion injury (32). Miguel et al. showed that UUO mice received ND-13 (3 mg/kg of body weight) *via* subcutaneous injection starting from the day of surgery, daily for 14 days showed reduced expression of fibrotic and inflammatory markers compared to UUO mice received vehicle, suggesting a beneficial effect of ND-13 in renal fibrosis (36). In the present study, administration of ND-13 (2 mg/kg of body weight) *via* tail veil injection starting from the day after surgery, daily for 7 days reduced

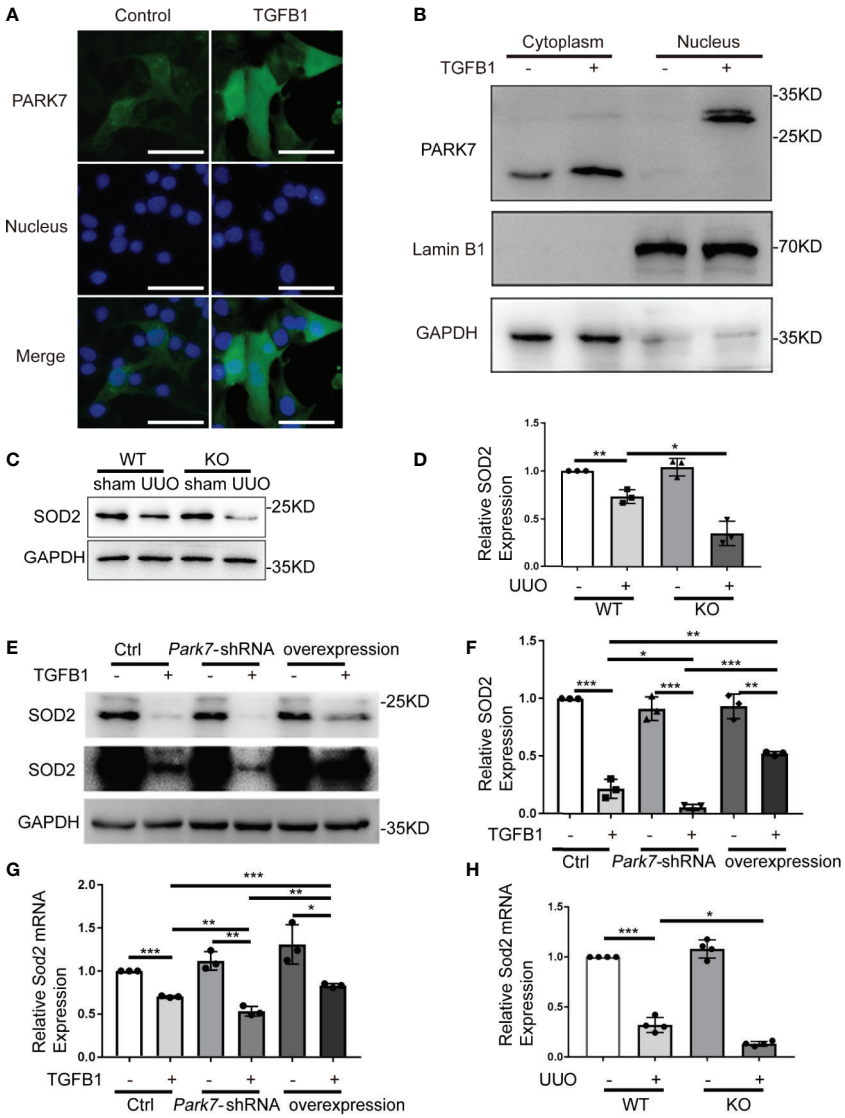


FIGURE 9 | PARK7 translocates into nucleus and positively regulates SOD2 expression during renal fibrosis. **(A, B)** BUMPT cells were cultured in medium with/without 5 ng/ml TGFB1 for 24 hours. **(A)** Representative images of immunofluorescence staining of PARK7 in BUMPT cells. Bar:50μm. **(B)** Representative immunoblot of PARK7, LaminB1 (nuclear marker), and GAPDH (cytosolic marker) in cytosolic and nuclear fractions. **(C, D)** Animals and their treatment were the same as described in **Figure 2**. **(C)** Representative immunoblot of SOD2 and GAPDH. **(D)** Densitometry of SOD2 signals (n=4). **(E, F)** BUMPT cells were transfected with *Park7* siRNA or PARK7 overexpression plasmid. 24 hours after transfection, the cells were cultured in medium with or without 5 ng/ml TGFB1 for another 24 hours. **(E)** Representative immunoblot of SOD2 and GAPDH. **(F)** Densitometry of SOD2 signals (n=3). The signal of SOD2 was normalized to the GAPDH signal of the same samples to determine the ratios. The values are expressed as fold change over control cells. **(G, H)** *Sod2* mRNA expression. Each symbol (circle, diamond and trigon) represents an independent experiment or an individual mouse. Error bars: SEM. *p < 0.05, **p < 0.01, ***p < 0.001.

the renal levels of *Tgfβ* mRNA, *Tnfα* mRNA and infiltration of macrophages into kidney tissues (**Figures 8G–J**). In addition, we showed that ND-13 treatment reduced TGFB1-induced fibrotic changes in BUMPT cells (**Figures 8A–C**). Thus, ND-13 may represent a potential drug for renal fibrosis.

In summary, this study provide evidence that PARK7 in renal tubular cells is renoprotective during renal fibrosis through suppressing ROS accumulation, cell apoptosis and inflammation. Thus, prevention of ROS accumulation *via* enhancing intracellular PARK7 levels and/or activity represents potential therapeutic strategies for renal fibrosis.

DATA AVAILABILITY STATEMENT

The original contributions presented in the study are included in the article/supplementary material. Further inquiries can be directed to the corresponding authors.

ETHICS STATEMENT

The animal study was reviewed and approved by The Animal Ethics Committee of the Second Xiangya Hospital of Central South University.

AUTHOR CONTRIBUTIONS

ZD, CT and LY conceived the study. LY performed the experiments. LY, HL, ZL, WW, JC, CT and ZD analyzed the results and approved the publication. LY drafted the manuscript. ZD and CT revised the paper. All authors contributed to the article and approved the submitted version.

FUNDING

This study was supported partly by the Natural Science Foundation of China (Grant Number 81870474), the National Key R&D Program of China (2018YFC1312700), and the Natural Science Foundation of Hunan Province (2019JJ40415).

REFERENCES

1. Liu Y. Cellular and Molecular Mechanisms of Renal Fibrosis. *Nat Rev Nephrol* (2011) 7(12):684–96. doi: 10.1038/nrneph.2011.149
2. Venkatachalam MA, Weinberg JM, Kriz W, Bidani AK. Failed Tubule Recovery, AKI-CKD Transition, and Kidney Disease Progression. *J Am Soc Nephrol* (2015) 26(8):1765–76. doi: 10.1681/asn.2015010006
3. Humphreys BD. Mechanisms of Renal Fibrosis. *Annu Rev Physiol* (2018) 80:309–26. doi: 10.1146/annurev-physiol-022516-034227
4. Liu BC, Tang TT, Lv LL, Lan HY. Renal Tubule Injury: A Driving Force Toward Chronic Kidney Disease. *Kidney Int* (2018) 93(3):568–79. doi: 10.1016/j.kint.2017.09.033
5. Yang L, Besschetnova TY, Brooks CR, Shah JV, Bonventre JV. Epithelial Cell Cycle Arrest in G2/M Mediates Kidney Fibrosis After Injury. *Nat Med* (2010) 16(5):535–43. doi: 10.1038/nm.2144. 531p following 143.
6. Shu S, Zhu J, Liu Z, Tang C, Cai J, Dong Z. Endoplasmic Reticulum Stress is Activated in Post-Ischemic Kidneys to Promote Chronic Kidney Disease. *EBioMedicine* (2018) 37:269–80. doi: 10.1016/j.ebiom.2018.10.006
7. Tang C, Cai J, Yin XM, Weinberg JM, Venkatachalam MA, Dong Z. Mitochondrial Quality Control in Kidney Injury and Repair. *Nat Rev Nephrol* (2020a) 17(5):299–318. doi: 10.1038/s41581-020-00369-0
8. Tang C, Livingston MJ, Liu Z, Dong Z. Autophagy in Kidney Homeostasis and Disease. *Nat Rev Nephrol* (2020b) 16(9):489–508. doi: 10.1038/s41581-020-0309-2
9. Basile DP, Leonard EC, Beal AG, Schleuter D, Friedrich J. Persistent Oxidative Stress Following Renal Ischemia-Reperfusion Injury Increases ANG II Hemodynamic and Fibrotic Activity. *Am J Physiol Renal Physiol* (2012) 302 (11):F1494–1502. doi: 10.1152/ajprenal.00691.2011
10. Finkel T. Signal Transduction by Reactive Oxygen Species. *J Cell Biol* (2011) 194(1):7–15. doi: 10.1083/jcb.201102095
11. Nagakubo D, Taira T, Kitaura H, Ikeda M, Tamai K, Iguchi-Ariga SM, et al. Dj-1, a Novel Oncogene Which Transforms Mouse NIH3T3 Cells in Cooperation With Ras. *Biochem Biophys Res Commun* (1997) 231(2):509–13. doi: 10.1006/bbrc.1997.6132
12. Honbou K, Suzuki NN, Horiuchi M, Niki T, Taira T, Ariga H, et al. The Crystal Structure of DJ-1, a Protein Related to Male Fertility and Parkinson's Disease. *J Biol Chem* (2003) 278(33):31380–4. doi: 10.1074/jbc.M305878200
13. Zhou B, Lei S, Xue R, Leng Y, Xia Z, Xia ZY. DJ-1 Overexpression Restores Ischaemic Post-Conditioning-Mediated Cardioprotection in Diabetic Rats: Role of Autophagy. *Clin Sci (Lond)* (2017) 131(11):1161–78. doi: 10.1042/cs20170052
14. Zhang L, Wang J, Wang J, Yang B, He Q, Weng Q. Role of DJ-1 in Immune and Inflammatory Diseases. *Front Immunol* (2020) 11:994. doi: 10.3389/fimmu.2020.00994
15. Ariga H, Takahashi-Niki K, Kato I, Maita H, Niki T, Iguchi-Ariga SM. Neuroprotective Function of DJ-1 in Parkinson's Disease. *Oxid Med Cell Longev* (2013) 2013:683920. doi: 10.1155/2013/683920
16. Cuevas S, Yang Y, Konkalmatt P, Asico LD, Feranil J, Jones J, et al. Role of Nuclear Factor Erythroid 2-Related Factor 2 in the Oxidative Stress-Dependent Hypertension Associated With the Depletion of DJ-1. *Hypertension* (2015) 65(6):1251–7. doi: 10.1161/hypertensionaha.114.04525
17. Sun Q, Shen ZY, Duan WN, Meng QT, Xia ZY. Mechanism of Myocardial Ischemia/Reperfusion-Induced Acute Kidney Injury Through DJ-1/Nrf2 Pathway in Diabetic Rats. *Exp Ther Med* (2017) 14(5):4201–7. doi: 10.3892/etm.2017.5095
18. Qu XH, Zhang K. MiR-122 Regulates Cell Apoptosis and ROS by Targeting DJ-1 in Renal Ischemic Reperfusion Injury Rat Models. *Eur Rev Med Pharmacol Sci* (2018) 22(24):8830–8. doi: 10.26355/eurrev_201812_16651
19. Yin J, Xu R, Wei J, Zhang S. The Protective Effect of Glutaredoxin 1/DJ-1/HSP70 Signaling in Renal Tubular Epithelial Cells Injury Induced by Ischemia. *Life Sci* (2019) 223:88–94. doi: 10.1016/j.lfs.2019.03.015
20. Tsai BC, Hsieh DJ, Lin WT, Tamilselvi S, Day CH, Ho TJ, et al. Functional Potato Bioactive Peptide Intensifies Nrf2-dependent Antioxidant Defense Against Renal Damage in Hypertensive Rats. *Food Res Int* (2020) 129:108862. doi: 10.1016/j.foodres.2019.108862
21. Sinha D, Wang Z, Price VR, Schwartz JH, Lieberthal W. Chemical Anoxia of Tubular Cells Induces Activation of c-Src and its Translocation to the Zonula Adherens. *Am J Physiol Renal Physiol* (2003) 284(3):F488–97. doi: 10.1152/ajprenal.00172.2002
22. Livingston MJ, Ding HF, Huang S, Hill JA, Yin XM, Dong Z. Persistent Activation of Autophagy in Kidney Tubular Cells Promotes Renal Interstitial Fibrosis During Unilateral Ureteral Obstruction. *Autophagy* (2016) 12 (6):976–98. doi: 10.1080/15548627.2016.1166317
23. Cai J, Liu Z, Huang X, Shu S, Hu X, Zheng M, et al. The Deacetylase Sirtuin 6 Protects Against Kidney Fibrosis by Epigenetically Blocking β-Catenin Target Gene Expression. *Kidney Int* (2020) 97(1):106–18. doi: 10.1016/j.kint.2019.08.028
24. Zheng M, Cai J, Liu Z, Shu S, Wang Y, Tang C, et al. Nicotinamide Reduces Renal Interstitial Fibrosis by Suppressing Tubular Injury and Inflammation. *J Cell Mol Med* (2019) 23(6):3995–4004. doi: 10.1111/jcmm.14285
25. Tang C, Han H, Yan M, Zhu S, Liu J, Liu Z, et al. Pink1-PRKN/PARK2 Pathway of Mitophagy is Activated to Protect Against Renal Ischemia-Reperfusion Injury. *Autophagy* (2018) 14(5):880–97. doi: 10.1080/15548627.2017.1405880
26. Tang C, Han H, Liu Z, Liu Y, Yin L, Cai J, et al. Activation of BNIP3-mediated Mitophagy Protects Against Renal Ischemia-Reperfusion Injury. *Cell Death Dis* (2019) 10(9):677. doi: 10.1038/s41419-019-1899-0
27. Wang Y, Tang C, Cai J, Chen G, Zhang D, Zhang Z, et al. PINK1/Parkin-Mediated Mitophagy is Activated in Cisplatin Nephrotoxicity to Protect Against Kidney Injury. *Cell Death Dis* (2018) 9(11):1113. doi: 10.1038/s41419-018-1152-2
28. Fu Y, Cai J, Li F, Liu Z, Shu S, Wang Y, et al. Chronic Effects of Repeated Low-Dose Cisplatin Treatment in Mouse Kidneys and Renal Tubular Cells. *Am J Physiol Renal Physiol* (2019) 317(6):F1582–92. doi: 10.1152/ajprenal.00385.2019
29. Yanagida T, Tsushima J, Kitamura Y, Yanagisawa D, Takata K, Shibaike T, et al. Oxidative Stress Induction of DJ-1 Protein in Reactive Astrocytes Scavenges Free Radicals and Reduces Cell Injury. *Oxid Med Cell Longev* (2009) 2(1):36–42. doi: 10.4161/oxim.2.1.7985
30. Eltoweissy M, Müller GA, Bibi A, Nguye PV, Dihazi GH, Müller CA, et al. Proteomics Analysis Identifies PARK7 as an Important Player for Renal Cell Resistance and Survival Under Oxidative Stress. *Mol Biosyst* (2011) 7(4):1277–88. doi: 10.1039/c0mb00116c

31. Meng XM, Nikolic-Paterson DJ, Lan HY. TGF-Beta: The Master Regulator of Fibrosis. *Nat Rev Nephrol* (2016) 12(6):325–38. doi: 10.1038/nrneph.2016.48
32. Molcho L, Ben-Zur T, Barhum Y, Offen D. DJ-1 Based Peptide, ND-13, Promote Functional Recovery in Mouse Model of Focal Ischemic Injury. *PloS One* (2018) 13(2):e0192954. doi: 10.1371/journal.pone.0192954
33. Lu L, Zhao S, Gao G, Sun X, Zhao H, Yang H. Dj-1/Park7, But Not Its L166p Mutant Linked to Autosomal Recessive Parkinsonism, Modulates the Transcriptional Activity of the Orphan Nuclear Receptor Nurr1 In Vitro and In Vivo. *Mol Neurobiol* (2016) 53(10):7363–74. doi: 10.1007/s12035-016-9772-y
34. Leeds J, Scindia Y, Loi V, Wlazlo E, Ghias E, Cechova S, et al. Protective Role of DJ-1 in Endotoxin-Induced Acute Kidney Injury. *Am J Physiol Renal Physiol* (2020) 319(4):F654–f663. doi: 10.1152/ajprenal.00064.2020
35. Shen ZY, Sun Q, Xia ZY, Meng QT, Lei SQ, Zhao B, et al. Overexpression of DJ-1 Reduces Oxidative Stress and Attenuates Hypoxia/Reoxygenation Injury in NRK-52E Cells Exposed to High Glucose. *Int J Mol Med* (2016) 38(3):729–36. doi: 10.3892/ijmm.2016.2680
36. De Miguel C, Kraus AC, Saludes MA, Konkalmatt P, Ruiz Domínguez A, Asico LD, et al. Nd-13, a DJ-1-Derived Peptide, Attenuates the Renal Expression of Fibrotic and Inflammatory Markers Associated With Unilateral Ureter Obstruction. *Int J Mol Sci* (2020) 21(19):7048. doi: 10.3390/ijms21197048
37. Neumann M, Müller V, Görner K, Kretzschmar HA, Haass C, Kahle PJ. Pathological Properties of the Parkinson's Disease-Associated Protein DJ-1 in Alpha-Synucleinopathies and Tauopathies: Relevance for Multiple System Atrophy and Pick's Disease. *Acta Neuropathol* (2004) 107(6):489–96. doi: 10.1007/s00401-004-0834-2
38. Abd El Atti RM, Abou Gabal HH, Osman WM, Saad AS. Insights Into the Prognostic Value of DJ-1 and MIB-1 in Astrocytic Tumors. *Diagn Pathol* (2013) 8:126. doi: 10.1186/1746-1596-8-126
39. Amatullah H, Maron-Gutierrez T, Shan Y, Gupta S, Tsoporis JN, Varkouhi AK, et al. Protective Function of DJ-1/PARK7 in Lipopolysaccharide and Ventilator-Induced Acute Lung Injury. *Redox Biol* (2021) 38:101796. doi: 10.1016/j.redox.2020.101796
40. Bahmed K, Messier EM, Zhou W, Tuder RM, Freed CR, Chu HW, et al. Dj-1 Modulates Nuclear Erythroid 2-Related Factor-2-Mediated Protection in Human Primary Alveolar Type II Cells in Smokers. *Am J Respir Cell Mol Biol* (2016) 55(3):439–49. doi: 10.1165/rcmb.2015-0304OC
41. Cheng Z, Qian S, Qingtao M, Zhongyuan X, Yeda X. Effects of ATRA on Diabetic Rats With Renal Ischemia-Reperfusion Injury. *Acta Cir Bras* (2020) 35(1):e202000106. doi: 10.1590/s0102-865020200010000006
42. Eltoweissy M, Dihazi GH, Müller GA, Asif AR, Dihazi H. Protein DJ-1 and its Anti-Oxidative Stress Function Play an Important Role in Renal Cell Mediated Response to Profibrotic Agents. *Mol Biosyst* (2016) 12(6):1842–59. doi: 10.1039/c5mb00887e
43. Meulener MC, Xu K, Thomson L, Ischiropoulos H, Bonini NM. Mutational Analysis of DJ-1 in Drosophila Implicates Functional Inactivation by Oxidative Damage and Aging. *Proc Natl Acad Sci USA* (2006) 103 (33):12517–22. doi: 10.1073/pnas.0601891103
44. Ooe H, Maita C, Maita H, Iguchi-Ariga SM, Ariga H. Specific Cleavage of DJ-1 Under an Oxidative Condition. *Neurosci Lett* (2006) 406(3):165–8. doi: 10.1016/j.neulet.2006.06.067
45. Meyer KD, Jaffrey SR. The Dynamic Epitranscriptome: N6-methyladenosine and Gene Expression Control. *Nat Rev Mol Cell Biol* (2014) 15(5):313–26. doi: 10.1038/nrm3785
46. Zaccara S, Ries RJ, Jaffrey SR. Reading, Writing and Erasing mRNA Methylation. *Nat Rev Mol Cell Biol* (2019) 20(10):608–24. doi: 10.1038/s41580-019-0168-5
47. Wang W, Zhao H, Chen B. DJ-1 Protects Retinal Pericytes Against High Glucose-Induced Oxidative Stress Through the Nrf2 Signaling Pathway. *Sci Rep* (2020) 10(1):2477. doi: 10.1038/s41598-020-59408-2
48. Podkowińska A, Formanowicz D. Chronic Kidney Disease as Oxidative Stress- and Inflammatory-Mediated Cardiovascular Disease. *Antioxidants (Basel)* (2020) 9(8):752. doi: 10.3390/antiox9080752
49. Circu ML, Aw TY. Reactive Oxygen Species, Cellular Redox Systems, and Apoptosis. *Free Radic Biol Med* (2010) 48(6):749–62. doi: 10.1016/j.freeradbiomed.2009.12.022
50. Morgan MJ, Liu ZG. Crosstalk of Reactive Oxygen Species and NF-κb Signaling. *Cell Res* (2011) 21(1):103–15. doi: 10.1038/cr.2010.178
51. Biosa A, Sandrelli F, Beltramini M, Greggio E, Bubacco L, Bisaglia M. Recent Findings on the Physiological Function of DJ-1: Beyond Parkinson's Disease. *Neurobiol Dis* (2017) 108:65–72. doi: 10.1016/j.nbd.2017.08.005
52. Clements CM, McNally RS, Conti BJ, Mak TW, Ting JP. Dj-1, a Cancer- and Parkinson's Disease-Associated Protein, Stabilizes the Antioxidant Transcriptional Master Regulator Nrf2. *Proc Natl Acad Sci USA* (2006) 103 (41):15091–6. doi: 10.1073/pnas.0607260103
53. Moscovitz O, Ben-Nissan G, Fainer I, Pollack D, Mizrachi L, Sharon M. The Parkinson's-Associated Protein DJ-1 Regulates the 20S Proteasome. *Nat Commun* (2015) 6:6609. doi: 10.1038/ncomms7609

Conflict of Interest: The authors declare that the research was conducted in the absence of any commercial or financial relationships that could be construed as a potential conflict of interest.

Copyright © 2021 Yin, Li, Liu, Wu, Cai, Tang and Dong. This is an open-access article distributed under the terms of the Creative Commons Attribution License (CC BY). The use, distribution or reproduction in other forums is permitted, provided the original author(s) and the copyright owner(s) are credited and that the original publication in this journal is cited, in accordance with accepted academic practice. No use, distribution or reproduction is permitted which does not comply with these terms.

frontiers in Immunology

REVIEW
published: 24 May 2021
doi: 10.3389/fimmu.2021.683926

The Role of Regulatory B cells in Kidney Diseases

Wang Long[1,2†], *Hedong Zhang*[1,3†], *Wenjia Yuan*[1,3], *Gongbin Lan*[1,3], *Zhi Lin*[1,3], *Longkai Peng*[1,3,4*] and *Helong Dai*[1,3,4*]

[1] Department of Kidney Transplantation, The Second Xiangya Hospital of Central South University, Changsha, China, [2] Graduate School of Medical and Dental Science, Department of Pathological Cell Biology, Tokyo Medical and Dental University, Tokyo, Japan, [3] Clinical Research Center for Organ Transplantation in Hunan Province, Changsha, China, [4] Clinical Immunology Center, Central South University, Changsha, China

OPEN ACCESS

Edited by:
Cheng Yang,
Fudan University, China

Reviewed by:
Jinfeng Li,
First Affiliated Hospital of Zhengzhou University, China
Cheng Yu,
National Eye Institute (NEI), United States
Keishi Fujio,
The University of Tokyo, Japan

***Correspondence:**
Helong Dai
helong68888@csu.edu.cn
Longkai Peng
penglongkai@csu.edu.cn

[†]These authors have contributed equally to this work and share first authorship

Specialty section:
This article was submitted to Molecular Innate Immunity, a section of the journal Frontiers in Immunology

Received: 22 March 2021
Accepted: 04 May 2021
Published: 24 May 2021

Citation:
Long W, Zhang H, Yuan W, Lan G, Lin Z, Peng L and Dai H (2021) The Role of Regulatory B cells in Kidney Diseases. Front. Immunol. 12:683926. doi: 10.3389/fimmu.2021.683926

B cells, commonly regarded as proinflammatory antibody-producing cells, are detrimental to individuals with autoimmune diseases. However, in recent years, several studies have shown that regulatory B (Breg) cells, an immunosuppressive subset of B cells, may exert protective effects against autoimmune diseases by secretion of inhibitory cytokines such as IL-10. In practice, Breg cells are identified by their production of immune-regulatory cytokines, such as IL-10, TGF-β, and IL-35, however, no specific marker or Breg cell-specific transcription factor has been identified. Multiple phenotypes of Breg cells have been found, whose functions vary according to their phenotype. This review summarizes the discovery, phenotypes, development, and function of Breg cells and highlights their potential therapeutic value in kidney diseases.

Keywords: regulatory B cells, Breg, kidney disease, IL-10, transplantation

INTRODUCTION

B lymphocytes play a critical role in adaptive immune system by secreting antibodies. They also present antigens for the activation of T cells and produce several essential cytokines. A small population of B cells known as regulatory B (Breg) cells demonstrates the ability of regulating immune responses. Breg cells are a subtype of B cells that were first discovered in 1974 when two studies described the suppressive function of B cells that could delay hypersensitivity independently (1, 2). However, few studies have focused on suppressive B cells till 1996. Wolf et al. found that in the development of experimental autoimmune encephalomyelitis (EAE), commonly considered as an animal model of multiple sclerosis (MS) mediated by $CD4^+$ T cells, EAE is inducible without the exhibition of differences in disease onset or severity between wild-type and B cell-deficient mice. However, B cell-depleted mice recovered with increased difficulty, highlighting the modulation function of B cells in acute EAE (3). Subsequently, an increasing number of studies have found that B cells with regulatory functions are involved in the development of not only EAE but also in other inflammatory diseases (4, 5). To date, these regulatory B cell-induced immune response suppression has been observed in autoimmune diseases, HIV, pregnancy, inflammatory diseases, and transplant immunity, among others. In this review, we have described the different phenotypes and functions of Breg cells and focused on their role in several types of kidney-related diseases, as well as potential challenges in the study of these cells in the future.

WHAT IS THE PHENOTYPE OF BREG CELLS?

With gradual advances in the existing knowledge since their discovery, Breg cells have not been restricted to a single phenotype, but rather displaying several phenotypes, in both humans and mice.

Phenotypes of Breg Cells Identified in Humans

B cells that regulate immune responses were initially found to exert their suppressive function in some specific diseases by producing interleukin-10 (IL-10). Subsequently, several studies have shown Breg cells exert suppressive functions mainly by secretion of IL-10 which also is the most important cytokine in Breg cells (6–10). It should also be noted that in certain circumstances IL-10 can serve as an enhancing role in the immune responses of B cells (11, 12) and CD8 T cells (13, 14). The most frequently observed phenotype for IL-10-producing B cells in peripheral blood is transitional $CD19^+CD24^{hi}CD38^{hi}$ B cells (9, 15–20), since IL-10^+ B cells are abundant in this phenotype. Other phenotypes include plasmablasts ($CD19^+CD27^{int}CD38^+$) (21) and regulatory B1 cells (Br1: $CD19^+CD25^+CD71^+CD73^-$) (22). Depending on the expression of CD27, IL-10^+ B cells can be divided into naïve IL-10^+ B cells ($CD19^+CD27^-$IL-10^+) and memory IL-10^+ B cells ($CD19^+CD27^+$IL-10^+), wherein the ratio of naïve/memory IL-10^+ B cells may hint at its function (7).

Additionally, Breg cells exhibit other markers. While transcription factor Forkhead Box P3 (Foxp3) is known to be expressed on several immune cells and is commonly regarded as a marker for Tregs, it has also been identified as a transcription factor of Breg cells, namely $CD19^+CD5^+$ B cells; in contrast, $CD5^-$ B cells do not express Foxp3 (17, 23–25). Another transcription factor should be noticed is T cell immunoglobulin and mucin domain 1 (Tim-1), a member of Tim family. It is first discovered on the cell surface of T cells and dendritic cells (DCs) and plays a crucial role in immune response regulation (26–28). More recently, B cells have also been found to express Tim-1 (29–31). Human IL-10^+ B cells also express Tim-1, Tim-1^+IL-10^+ B cells are reported to suppress certain autoimmune diseases in human (32). Moreover, Tim-1 may prove to be a better marker for the identification of IL-10-producing B cells than $CD5^+CD1d^+$, since Tim-1 is predominantly expressed on IL-10^+ B cells in humans (32). While not all of the Breg cells play a protective role in diseases, tumor-evoked Breg cells (tBreg cells), which are functionally different from conventional Breg cells, play negative roles in the occurrence of lung metastasis. The phenotype of tBreg cells is $CD19^+CD25^+CD81^{hi}$ (33). tBreg cells reportedly dampen the immune system in breast cancer and the mechanism relies not on the secretion of IL-10, IL-35, or activation of other suppressive pathways, but on the secretion of transforming growth factor-β (TGF-β) to facilitate $Foxp3^+$ Treg cells (34).

Phenotypes of Breg Cells in Mice

The phenotypes of Breg cells vary considerably between humans and mice. In a murine study, Breg cells were mainly defined as IL-10-producing B cells, which varied from the IL-10^+ B cell population in the peripheral blood and spleen. Interestingly, according to the analysis of tiger mice, a type of IL-10 reporter mouse, the majority of IL-10-producing cells in the spleen of WT mice comprise B cells, and not T cells (6). The majority of IL-10-producing T cells comprise $CD4^+$ T cells ($TCR\beta^+CD4^+$) (83% ± 2%), and most IL-10^+ B cells include follicular (FO) B cells ($CD19^+CD23^+CD21^{int}$) (41% ± 3%), while other IL-10-producing cells include neutrophils, monocytes/macrophages, and myeloid DCs. IL-10-producing B cells in the spleen include FO B cells ($CD19^+CD23^+CD21^{int}$), marginal zone (MZ) B cells ($CD19^+CD23^-CD21^{hi}$), transitional T1+T2 B cells ($CD19^+$AA4/$CD93^+$), plasma/plasmablast cells ($CD19^+/B220^{lo/-}CD138^+$), and B1 a/b cells ($CD19^+CD138^-CD21^-CD23^-CD43^+CD5^{+/-}$) (6). In murine studies, the commonly observed IL-10^+ B cells in the spleen are $CD19^+/B220^{lo/-}CD1d^+CD5^+$ cells (B10 cells) (35–40), since IL-10^+ B cells are enriched in B10 cells.

Except for B10 cells, other markers or cytokines related to B cells may also play a regulatory role in immune responses. IL-35 secreted by B cells can inhibit inflammation in certain diseases, including inflammatory bowel disease, and such cells are referred to as IL-35-producing B cells (41–43). IL-35-treated mice showed increased abundance of $CD4^+CD25^+Foxp3^+$ Tregs and IL-10^+ Breg cells, indicating that IL-35 secreted by Breg cells might exert positive feedback on Breg cells (44, 45). CD9 is a cell surface glycoprotein that is encoded by a gene belonging to the tetraspanin family and is considered a key marker expressed on the cell surface of IL-10-producing B cells. Furthermore, most IL-10^+ B cells (87.5% ± 1.69%) express CD9 on their cell surface. $CD9^+$ B cells have been found to exert a stronger suppressive function than $CD9^-$ B cells, while a small proportion of $CD9^-$ B cells are known to also secrete IL-10. When CD9 expressed on B cells is subjected to blockade by anti-CD9 antibody, the suppression of T cell proliferation is inhibited, which is related to the ratio of T/B cells in a co-culture system, indicating that the suppressive function of CD9 is related to the establishment of T-B cell crosstalk in an IL-10-dependent manner (38). Tim-1 is not only expressed on human IL-10^+ B cells, but also a marker for mouse IL-10^+ B cells. Interestingly, the expression of Tim-1 in B cells is higher than that in T cells. B cells express Tim-1, including transitional B cells, MZ B cells, FO B cells, and B10 cells, and most IL-10^+ B cells express Tim-1 on their cell surface. IL-4 and IL-10 secretion from Breg cells can be induced with the use of anti-Tim-1 antibody, demonstrating that Tim-1 ligation can induce B10 cell expansion (**Table 1**) (37).

DEVELOPMENT AND FUNCTION OF BREG CELLS

Breg cells induction *in vitro* under different stimuli may associate to Breg cells development *in vivo*. Breg cells constitute several phenotypes of B cells, including transitional B cells, FO B cells, plasmablasts and so forth. They are enriched in the spleen and peritoneal cavity, while few Breg cells exist in the blood, peripheral lymph nodes, mesenteric lymph nodes, and Peyer's

TABLE 1 | Subsets of Breg cells.

Subsets	Mouse	Human	Reference
Transitional 2 marginal zone precursor B cells (T2-MZP cells)	$CD19^+CD21^{hi}$ $CD23^+CD24^{hi}$ $IgM^{hi}IgD^+$	$CD23^+sIgM^{hi}$ $sIgD^+CD35^{hi}$	(46–49)
Marginal zone B cells	$CD19^+CD23^-CD21^+$	–	(50–52)
B10 cells	$CD5^+CD1d^{hi}$	$CD5^+CD1d^{hi}$/ $CD24^{hi}CD27^+$	(51, 53–57)
$CD1d^{hi}$ B cells	$CD19^+CD1d^{hi}$	$CD19^+CD1d^{hi}$	(58, 59)
Plasma cells/plasmablasts	$CD138^+CD22^-$	$CD27^{int}CD38^+$	(21, 60, 61)
Peritoneal B1a B cells	$CD19^+CD5^+$ $CD11b^+$	–	(50, 62)
Tim-1^+ B cells	$CD19^+$Tim-1^+	$CD19^+$Tim-1^+	(37, 63–66)
Immature B cells	–	$CD19^+CD24^{hi}$ $CD38^{hi}$	(67–73)
Circulating B cells	–	$CD19^+CD25^{hi}$ $CD27^{hi}CD1d^{hi}CD86^{hi}$	(74)

patches (53). *In vitro*, Breg cells can be expanded when stimulated with LPS (75), thereby inducing IL-10^+ B cell differentiation into plasma/plasmablast cells after transient IL-10 production. After subjection to LPS stimulation for a period of 3 days, B10 cells gradually express CD43 and GL7 activation markers for antibody-secreting cells. Furthermore, the proportion of plasma/plasmablasts in IL-10^+ B cells increased with an increase in the expression of the plasma/plasmablast-associated transcription factors, namely *blimp1*, *xbp1*, and *irf4*, which are related to plasma/plasmablast cell expansion (76). IL-10^+ B cells can also be induced by anti-CD40 antibody (75, 77), anti-Tim-1 antibody (37), PMA/ionomycin (78), IL-21 (77, 79) and IL-35 (43, 44, 80). For example, IL-10^+ B cells that mature into functional IL-10^+ B cells rely on IL-21 and CD40 signaling activation, whereas IL-10 is not necessary for IL-10^+ B cell development (75, 77, 79), IL-21 secreted from follicular helper T cells (Tfh) mediates the expansion of B10 cells *via* the phosphorylation of STAT3 (39, 40). Interestingly, IL-21-induced Breg cells exhibit a phenotype that expresses granzyme B, which is a serine protease that is expressed in the granules of NK cells and cytotoxic T cells. Granzyme B secreted by Breg cells inhibits T cell proliferation and the degradation of TCR ζ-chain (81, 82). Furthermore, IL-35 is also involved in the development and function of Breg cells. Breg cell-secreted IL-35 is a cytokine that exerts an inhibitory on the immune response. IL-35 induces the production of Treg cells, IL-10-producing Breg cells, and IL-35-producing Breg cells, indicating that Breg cell development is dependent on IL-35 signaling (43, 44, 80).

Breg cells regulate immune responses by many ways, such as anti-inflammatory cytokines IL-10, IL-35, IL-12 (83), or TGF-β (84, 85) secretion, or *via* the Fas-FasL (86) and PD-1/PD-L1 (86, 87) pathways. Through all these pathways, Breg cells regulate the immune system by controlling immune cell differentiation and proliferation. As the major functional cytokine secreted by Breg cells, IL-10 production is related to the B-cell linker protein (BLNK) expression, which is involved in the regulation of the immune response in allergic and autoimmune diseases (88), it regulates the differentiation of Th1 cells and Th17 cells and inhibits T cell cytokine secretion resultantly (47). IL-10^+ B cells also modulate the function of Foxp3^+ Tregs and $CD8^+$ T cells. For example, the levels of IL-10 in the serum are elevated in patients with chronic hepatitis B virus (HBV) infection, and the blockade of IL-10 supports the function of virus-specific $CD8^+$ T cells. Both the frequency of IL-10^+ B cells and the secretion of IL-10 from IL-10^+ B cells are facilitated in these patients, suggesting that Breg cells inhibit $CD8^+$ T cell function in an IL-10-dependent manner (9). Additionally, IL-10^+ B cells promote $CD4^+$Foxp3^+ T cell proliferation both *in vivo* and *in vitro* (89, 90) (91, 92). Evidence also indicates that IL-10 produced by Breg cells induces $CD4^+$ T cell apoptosis (93). IL-10^+ B cells function is also different among naïve IL-10^+ B cells and memory IL-10^+ B cells. Naïve IL-10^+ B cells are involved in the prevention of immune responses in autoimmune diseases, while memory IL-10^+ B cells prevent disease exacerbation (94). The ratio of naïve/memory IL-10^+ B cells may be an indicator of the major function of IL-10^+ B cells in specific diseases (7). Breg cells also regulate IgG production, with B10 cell depletion enhancing IgG production in WT mice (35). In a human study, Breg cells were found to impair the function of IgG4-producing B cells (22). Moreover, Breg cells inhibit the differentiation of $CD4^+$ T cells into Tfh cells and suppress the antibody production mediated by Tfh cells (91, 92). Breg cells not only participate in the suppression of peripheral immune response but also perform inhibitory functions in the brain. They are capable of inhibiting inflammation and central nervous system damage resulting from infiltrating pro-inflammatory cells (95). Collectively, even though only 1%–2% of splenic B cells are IL-10^+ B cells, they play a critical role in the regulation of immune responses (53) by suppressing immune responses and by ameliorating autoimmune diseases.

Regarding tBreg cells, which play a negative role in immune responses, anti-CD20 antibody treatment facilitates tumor escape from the immune system *via* the enrichment of tBreg cells that express low levels of CD20. Thus, using anti-CD20 antibody may enrich tBreg cells, which impairs the immune system and promotes breast cancer development (33).

However, the role of Breg cells in mice and human are somehow not always the same. It is also reported that $CD19^+CD24^{hi}CD38^{hi}$

Breg cells are enriched in some SLE patients, together with elevated serum IL-10 level from Breg cells and reduced IL-10R in circulating lymphocytes, demonstrating that IL-10 secreted from Breg cells in human is not necessarily protective in autoimmune diseases, and can be targeted in some cases (96).

WHAT IS THE ROLE OF BREG CELLS IN KIDNEY DISEASE?

Breg cells exert protective effects in systemic diseases that affect the kidney, including allograft rejection (46, 97), systemic lupus erythematosus (SLE) (98), type 1 diabetes (T1D) (99, 100), anti-neutrophil cytoplasmic antibody-associated vasculitis (AAV) (101), Sjogren's syndrome (SS) (102), Immunoglobin G4-related disease (IgG4-RD) (103), and IgA vasculitis with nephritis (IgAVN) (104), among others. Breg cell populations tend to be reduced in the above-mentioned kidney-targeting diseases. The transfer or increase of Breg cell numbers and the increased secretion of inhibitory cytokines from Breg cells alleviates disease, leading to improved kidney function. Several diseases, including AAV, T1D, and SLE, result from the generation of autoantibodies and inflammatory cytokine secretion, with or without T cell infiltration. An increased number of Breg cells reduces antibody production and $CD4^+$ and $CD8^+$ T cell infiltration, and promotes the infiltration of Treg cells, thereby leading to disease remission.

Kidney Transplantation

B cells play an important role in graft rejection by producing donor-specific antibodies, while increasing evidence support the role of B cells in the induction of tolerance. Long-term acceptance was more likely to be induced in kidney-transplanted rats administered with donor-derived B cells compared to donor-derived T cells (105). The importance of B cells in tolerance induction has also been demonstrated in human studies (67, 106). Based on the studies conducted using B cells collected from operational tolerant (OT) recipients, B cells were found to produce higher levels of IL-10 (107). Furthermore, the frequency of naïve B cells, memory B cells, and Breg cells increased and tended to be normal (15, 108). Breg cells may inhibit T cell function *via* the direct interaction of T:B cells (109). Different from most settings, IL-10 shows counter-regulatory effects in the setting of anti-CD45RB-induced tolerance. In anti-CD45RB-induced heart allograft mice model, IL-10 deficiency or IL-10 neutralization was found to improve chronic allograft vasculopathy and reduce allograft reactive antibody production. However the underlying mechanism behind this abnormality is not yet known in this specific setting (110). Breg cells in patients with tolerance were found to be similar to those in healthy individuals, while patients who experienced chronic rejection showed impaired Breg cell population (15). The immunologic injury targeting allografts is markedly related to the IL-10/TNF-α expression ratio on Breg cells (111). Therefore, elevated circulating $IL\text{-}10^+$ Breg cells could be a marker for relatively lower risk of antibody-mediated rejection (20). More convincing evidence indicates that Breg cells are protective in inducing the tolerance or preventing the rejection of allografts in cases with $IL10^{-/-}$ on B cells or B cell depletion, which are more likely to be rejected; furthermore, evidence also indicates that the adoptive transfer of $IL10^{+/+}$ marginal zone precursor regulatory B cells in recipients prevents rejection (46, 97). The main mechanisms involved in the induction of tolerance by Breg cells are as follows: (1) the regulation of $IL\text{-}10^+$ Breg cells promote $Foxp3^+$ T cell proliferation (90, 112), inhibit the proliferation (113) and induce the apoptosis (93) of $CD4^+$ T cells, and dampen the function of $CD8^+$ T cells (9); (2) activation of other cytokines and pathways.

Lupus Nephritis (LN)

Kidney function is commonly investigated in the prognosis of patients with SLE. As autoantibodies are the key factors in the pathogenesis of SLE and LN, increasing evidence shows the significant role of Breg cells in LN (98). Early studies have reported that the number of IL-10-producing B cells is increased in patients with SLE (114, 115). However, in patients with new-onset SLE (116) and LN patients (117), the $IL\text{-}10^+$ B cell population is decreased. The percentages of $CD19^+CD24^{hi}CD38^{hi}$ subsets, including putative Breg cells in PBMCs, between SLE patients and healthy controls are similar (68, 117). However, Breg cells in the PBMCs of SLE patients secrete fewer amounts of IL-10 with an impaired $CD4^+$ T cell suppressive capacity (118). Consistent with this finding, $CD19^+CD24^{hi}CD38^{hi}$ Breg cells in SLE patients produced fewer amounts of IL-10 with an impaired suppressive capacity. The suppressive effect of Breg cells on $CD4^+$ T helper 1 cells is dependent on IL-10, CD80, and CD86, but is not TGF-β-dependent. This suppression impairment of SLE-derived Breg cells may be related to its inability to upregulate STAT3 phosphorylation upon CD40 engagement (68). Early immature B cells can produce a substantial number of self-reactive antibodies, including ssDNA-reactive antibodies (119, 120). Interestingly, IL-10-producing $CD27^-CD38^{int}IgD^+$ pre-naïve B cells in SLE patients secrete fewer amounts of IL-10 with enhanced CD80 and CD86 expression, and this occurrence leads to the loss of self-regulation (120).

The reason for the reduced population of $IL\text{-}10^+$ Breg cells in SLE patients may be related to the regulatory circuit between plasmacytoid dendritic cells (pDCs) and $CD24^+CD38^{hi}$ Breg cells (69). In healthy individuals, pDCs can promote the differentiation of both Breg cells and plasmablasts by moderating IFN-α secretion and CD40 signaling. On the other hand, IL-10 produced by Breg cells can restrain the release of IFN-α by pDCs. However, in SLE patients, increased IFN-α production by hyperactive pDCs drives immature B cell differentiation with an inclination toward plasmablast generation. As a result, SLE Breg cells with reduced IL-10 production fail to restrain pDC-derived IFN-α, thus creating a vicious circle. This study also found that in SLE patients responding to rituximab, repopulated B cells contained a normal frequency of $CD24^+CD38^{hi}$ Breg cells, and this

mitigated pDC activation and restored the balance (69). Epratuzumab, which targets CD22, can reportedly inhibit B cell-derived pro-inflammatory IL-6 and TNF-α secretion while maintaining the production of IL-10 (121). This represents a potential therapeutic strategy to disrupt the vicious cycle between pDCs and Breg cells.

Another immunosuppressive agent, prednisolone, is also commonly used in SLE patients. However, the percentage of IL-10$^+$ B cells in LN patients is negatively correlated with the daily dose of prednisolone (117) which indicates that the currently available immunosuppressive agents can affect both the effector and regulatory aspects of B cells. This might indicate that the current immunosuppressive treatment strategy failed to treat SLE/LN because of its inability to restore the natural immune balance.

Efforts have been engaged to consider and utilize Breg cells as therapeutic targets for treating LN. Human adipose-derived mesenchymal stem cells (MSCs) can trigger the expansion of IL-10-producing Breg cells *in vitro* and *in vivo* in a mouse model. After MSC treatment in the SLE mouse model, both renal histopathology improvement and autoantibody mitigation have been achieved (122). A similar effect has also been reported with the application of MDSCs, which can be subjected to blockade using an inhibitor of iNOS (89).

Type 1 Diabetes (T1D)

T1D is an autoimmune disease characterized by the destruction of cells of the islets of Langerhans, particularly beta cells. Autoantibodies, such as an anti-insulin antibody, anti-islet cell antibody, and anti-glutamic acid decarboxylase (GAD) antibody, can be detected in most T1D patients, accompanied by lymphocyte infiltration in the pancreas. Several immunosuppressive therapies have been tested, including those involving the use of cyclosporine A (CsA) and anti-CD3 monoclonal antibodies (123). Although CsA is an effective initial therapeutic strategy to confer protection to the pancreas, it is not appropriate for long-term use due to side effects (123). Although anti-CD3 antibody showed long-term effects in NOD mice, a mouse model for T1D, treatment strategies using the antibody did not achieve success in phase III clinical studies (124).

Despite considerable efforts to develop immunotherapies that target Treg or T cells for the treatment of T1D, thus far, there is a lack of effective immunotherapies. Interestingly, accumulating evidence indicates that Breg cells play an important role in the suppression of the pathology of T1D. B cell depletion by anti-CD20 antibody leads to the long-term remission of T1D in NOD mice, possibly due to the removal of autoreactive B cells and the reduction in autoantibody generation, which is critical for the development of disease in NOD mice. Another critical mechanism is the increase in the number of Foxp3$^+$ Treg cells, which may be caused by an altered proportion of regenerated B cells (100, 125–127); however, the anti-CD20 antibody is effective only in the early stage of T1D, since pancreas-infiltrating B cells lose the ability to express CD20 (126). A similar result was obtained when B cells were subjected to depletion with the use of anti-CD22 antibody in NOD mice. When conducting the transfer of the regenerated B cells into NOD mice, Treg cells underwent expansion, anti-inflammatory cytokine secretion from Treg cells increased, and infiltrated T cell populations reduced, indicating that these regenerated B cells were regulatory and might exert a protective effect in T1D (128). Additionally, several studies have shown that Breg cells alleviate T1D pathophysiology in an IL-10-dependent manner in both mice and humans (99, 129). In a study using NOD mice of different ages, long-term normoglycemic NOD mice (average age, 30 weeks) exhibited reduced lymphoid infiltration with an increase in pancreas-infiltrating IL-10-producing B cells compared with glycemic NOD mice. To elucidate the role of IL-10$^+$ B cells in NOD mice, a reduction in IFN-γ production by CD4$^+$ T cells was observed when the cells were co-cultured with IL-10$^+$ B cells and DCs. Additionally, milder disease pathology was observed when IL-10$^+$ B cells were transferred with diabetogenic CD4$^+$ T cells into NOD mice compared to the mice subjected to transfer with IL-10-producing B cells, demonstrating that IL-10$^+$ B cells played a protective role in the development of T1D in NOD mice (99, 130). In a study conducted in humans, the proportion of CD5$^+$CD1d$^+$ B cells was positively correlated with blood C-peptide levels, a test performed to analyze insulin secretion, indicating that B10 cell reduction was related to islet destruction (129). Taken together, Breg cells seem to play a protective role in the development of type 1 diabetes in an IL-10-dependent manner, suggesting that Breg cells may be a potential target for the treatment of type 1 diabetes.

Anti-Neutrophil Cytoplasmic Antibody (ANCA)-Associated Vasculitis (AAV)

ANCAs are autoantibodies that target neutrophil cytoplasmic antigens, such as proteinase 3 (PR3) and myeloperoxidase (MPO). Over 75% of the patients with AAV present with rapidly progressive glomerulonephritis, which is an important predictor of mortality (131). Studies have shown that CD19$^+$CD24^{hi}CD38^{hi} cell populations are decreased in active AAV patients, while its suppressive functions and the ability to produce IL-10 are not altered (101, 132). However, during remission in AAV patients, one study found that this subset was subjected to continuous reduction (101) while another study found that the frequency of this subset did not vary from that of healthy controls. The CD19$^+$CD24^{hi}CD27$^+$ subset, supposedly comprising B10 memory Breg cells, is reportedly reduced during an active disease state and restored during remission (132). Human CD5$^+$ B cells are considered to produce IL-10 and TGF-β (133, 134). This CD5$^+$ B cell population decreases in active AAV patients and rebounds after remission, highlighting its potential role as an indicator of disease activity, remission, and relapse (135, 136). Following B cell depletion with rituximab, a lower CD5$^+$ percentage in B cells was correlated with a shorter time of relapse (137). However, whether CD5 alone is a practicable putative surrogate marker for Breg cells and whether its status can be considered as an indicator of AAV disease activity warrant investigation. Another study found that CD5$^+$ B cells were inversely correlated with disease activity during relapse after treatment with rituximab; however, they

were could not be used to predict the time to subsequent relapse (138).

Sjogren's Syndrome (SS)

Sjogren's syndrome is one of the most common autoimmune diseases, characterized by impaired exocrine function due to lymphocyte infiltration (139). The clinically overt implication of the kidney has been reported in approximately 5% of SS patients, with a low incidence of progression to end-stage disease (140, 141). Most cases of renal involvement comprise tubulointerstitial nephritis (TIN). Biopsies have shown the infiltration of T cells, B cells, and plasma cells (142). SS patients have been reported to present with a higher frequency of $CD19^+CD24^{hi}CD38^{hi}$ Breg cells, whose suppression ability is compromised (102, 143). However, IL-10^+ B cell populations are substantially lower in both primary SS patients and SS mice models, and such a phenomenon is caused by a decreased production of IL-10 by $CD19^+CD24^{hi}CD38^{hi}$ cells. The adoptive transfer of IL-10-producing Breg cells can be used to ameliorate SS progression in a mouse model, thereby revealing the potential therapeutic effect of Breg cells (144). Another study found no significant difference in the percentage of $CD5^+$ B cells compared to that observed in healthy controls; however, IL-21 receptor and Granzyme B expression in $CD5^+$ B cells in primary SS patients were markedly enhanced, indicating the elicitation of an increased counter-regulatory reaction (145).

Immunoglobin G4-Related Disease (IgG4-RD)

IgG4-RD is a rare fibroinflammatory disease histologically characterized by lymphoplasmacytic infiltration enriched with $IgG4^+$ plasma cells and with the occurrence of storiform fibrosis. Approximately 15% of the IgG4-RD patients exhibit clinical implications in the kidney (146). In type 1 AIP (pancreatic manifestation of IgG4-RD), $CD19^+CD24^{hi}CD38^{hi}$ Breg cell populations were found to be significantly increased, while the $CD19^+CD24^{hi}CD27^+$ subset was decreased. IL-10-producing B cells were found to be similar between type 1 AIP and healthy controls (103). However, in another study involving 48 newly diagnosed IgG4-RD patients, $CD19^+CD24^{hi}CD38^{hi}$ Breg cells showed a marked reduction (143). This may be attributed to the heterogeneity of IgG4-RD.

IgA Vasculitis With Nephritis (IgAVN)

IgA vasculitis, formally known as Henoch-Schönlein purpura, is a type of IgA-mediated small-vessel vasculitis (147). Studies have reported that, compared with healthy controls, all $CD19^+CD24^{hi}CD38^{hi}$, $CD19^+CD5^+$, and $CD19^+IL\text{-}10^+$ subsets are decreased in patients with IgAVN (54, 104). Moreover, even the concentration of IL-10 in the serum has been found to be considerably lower. After treatment, mainly with the glucocorticoid prednisolone, an increase was observed among $CD5^+CD1d^+$, $CD5^+CD1d^+IL\text{-}10^+$, and IL-$10^+$ B cell subsets, accompanied by an increase in the serum IL-10 concentration (54).

Breg Cells in Other Kidney Diseases

Numerical changes or functional alterations of Breg cells have also been observed in other immune-related kidney diseases. IgA nephropathy (IgAN) patients tend to have a lower frequency of $CD5^+CD1d^+CD19^+$ Breg cells with a reduced IL-10 expression. $CD5^+CD1d^+CD19^+$ Breg cells and Breg-derived IL-10 concentrations are negatively correlated with serum IgA and Gd-IgA1 levels, respectively (148). Similar findings have been reported in diabetic nephropathy (DN) patients in terms of the $CD19^+CD24^{hi}CD38^{hi}$ Breg subtype (149). However, among patients with hepatitis B virus-associated membranous nephropathy (HBV-MN), higher proportions of $CD5^+CD19^+$ and IL-10^+CD19^+ B cells and serum IL-10 levels have been reported (150). These differences could be attributed to various distinct Breg cell phenotypes or Breg cell changes that occur depending on the immunological environment. However, whether these numerical or functional changes in Breg cells are a cause or an effect of immune-related kidney diseases should be elucidated in future studies.

In addition carious studies have shown that renal fibrosis, as an inevitable outcome of nearly every kind of chronic kidney diseases, can be driven by TGF- β (151). On the other hand, IL-10 was found as a protective factor in animal studies (152–154). Presumably Breg cells might play a role in renal fibrosis through cytokine production or interactions with other immune cells such as macrophage, T cells etc. However, currently few works has been done regarding the effects of Breg cells on renal fibrosis which calls for further study.

DISCUSSION

Breg cells regulates immune responses through the secretion of several inhibitory cytokines such as IL-10, IL-35 and TGF-β or PD1/PDL1, Fas/FasL pathways, thus facilitate Treg cells, impair $CD4^+$ T cells, $CD8^+$ T cells, DCs, Th1/Th17 and IgG production. These aspects are crucial to achieve successful treatment of autoimmune diseases, inflammation disease regulation, tumor growth prevention, and transplant tolerance induction. Breg cells exhibit several phenotypes, including transitional B cells, MZ B cells, and plasma/plasmablasts, among others. As a result, there is no single specific marker that can be considered for identifying effective Breg cells. Therefore, Breg cells are generally identified *via* their secretion of suppressive cytokines such as IL-10. Since Breg cells secrete several cytokines, including IL-10, IL-35, and TGF-β, to regulate immune responses, IL-10^+ B cells may constitute a considerable population of Breg cells, but cannot represent all Breg cells.

Breg cells exert protective effects against many inflammatory diseases and tolerance induction, While IL10 KO in B cells result in deterioration of inflammatory disease conditions. The transfer of IL-10^+ B cells ameliorates autoimmune responses and induces tolerance. Although Breg cells possess properties that are beneficial in the immune response, they cannot be easily utilized in clinical trials. Unlike Treg cells, Breg cell development is not well understood due to its variation in phenotypes. Thus, the identification of a surface marker pattern or lineage-specific transcription factor involved in Breg cell development remains a challenge.

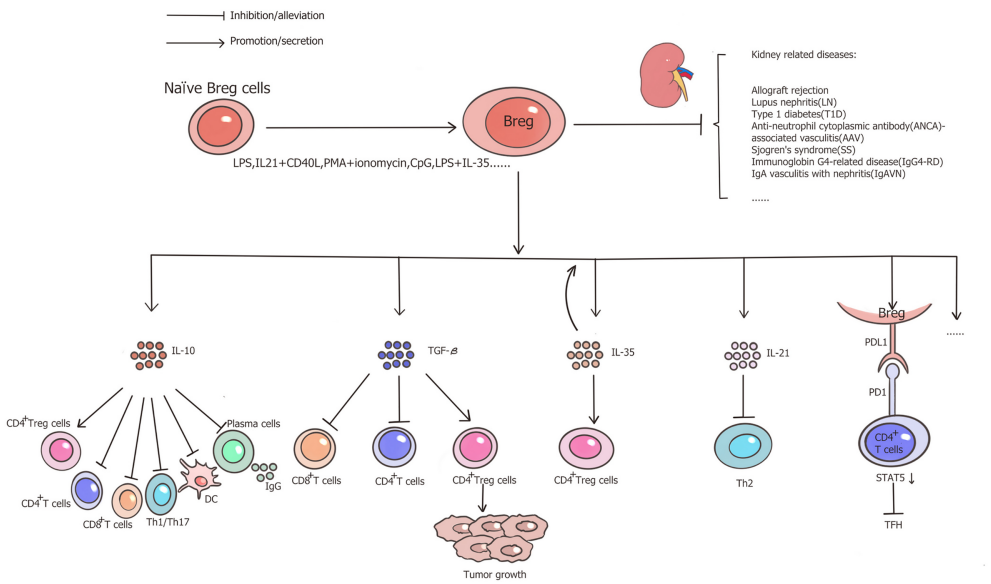


FIGURE 1 | Functional properties of Breg cells and role in kidney-related diseases. Through the secretion of IL-10, IL-35, TGF-β, or the PD1/PDL1 pathways, Breg cells facilitate Treg cells, impair $CD4^+$ T cells, $CD8^+$ T cells, Th1/Th17, DC and IgG production from plasma cells, therefore, Breg cells play a protective role in allograft rejection and several kidney-related inflammatory diseases.

In summary, Breg cells are a robust inhibitory phenotype of B cells that secrete several suppressive cytokines, such as IL-10, TGF-β, and IL-35. Among these, IL-10-producing B cells are the most extensively studied cells in research. These cells have been proven to exhibit inhibitory functions in autoimmune diseases, inflammation, and transplantation. Its role in transplantation is a topic of immense interest, with Breg cells being comprehensively studied for their crucial role in countering graft rejection and inducing tolerance. The activation of tBreg cells has also attracted attentions of many researchers in cancer immunology field. The protective role of Breg cells have been well studied in many kidney-affecting diseases such as SLE, T1D, AAV and other inflammatory diseases, also including kidney transplantation (**Figure 1**). Cell therapy with *in vitro* induction of effective Breg cells to alleviate immune responses and to induce tolerance in clinical settings could be a major focus for future studies in kidney.

AUTHOR CONTRIBUTIONS

WL and HZ drafted the manuscript. ZL generated the figure. GL, WY, and LP revised the manuscript. HD designed the outline of the manuscript and revised the manuscript. All authors contributed to the article and approved the submitted version.

FUNDING

This work is supported by the National Science Foundation of China (81900370, 81800664, 81970655, 82070776), Natural Science Foundation of Hunan Province of China (2019JJ50842), and Huxiang Young Talents of Hunan Province (2019RS2013).

REFERENCES

1. Katz SI, Parker D, Turk JL. B-Cell Suppression of Delayed-Hypersensitivity Reactions. *Nature* (1974) 251(5475):550–1. doi: 10.1038/251550a0
2. Neta R, Salvin SB. Specific Suppression of Delayed Hypersensitivity: The Possible Presence of a Suppressor B Cell in the Regulation of Delayed Hypersensitivity. *J Immunol* (1974) 113(6):1716–25.
3. Wolf SD, Dittel BN, Hardardottir F, Janeway CAJr. Experimental Autoimmune Encephalomyelitis Induction in Genetically B Cell-Deficient Mice. *J Exp Med* (1996) 184(6):2271–8. doi: 10.1084/jem.184.6.2271
4. Goetz M, Atreya R, Ghalibafian M, Galle PR, Neurath MF. Exacerbation of Ulcerative Colitis After Rituximab Salvage Therapy. *Inflammation Bowel Dis* (2007) 13(11):1365–8. doi: 10.1002/ibd.20215
5. Dass S, Vital EM, Emery P. Development of Psoriasis After B Cell Depletion With Rituximab. *Arthritis Rheum* (2007) 56(8):2715–8. doi: 10.1002/art.22811
6. Scapini P, Lamagna C, Hu YM, Lee K, Tang QZ, DeFranco AL, et al. B Cell-Derived IL-10 Suppresses Inflammatory Disease in Lyn-deficient Mice. *Proc Natl Acad Sci USA* (2011) 108(41):E823–E32. doi: 10.1073/pnas.1107913108
7. Knippenberg S, Peelen E, Smolders J, Thewissen M, Menheere P, Cohen Tervaert JW, et al. Reduction in IL-10 Producing B Cells (Breg) in Multiple Sclerosis Is Accompanied by a Reduced Naive/Memory Breg Ratio During a Relapse But Not in Remission. *J Neuroimmunol* (2011) 239(1-2):80–6. doi: 10.1016/j.jneuroim.2011.08.019
8. Saussine A, Tazi A, Feuillet S, Rybojad M, Juillard C, Bergeron A, et al. Active Chronic Sarcoidosis Is Characterized by Increased Transitional Blood B Cells, Increased IL-10-producing Regulatory B Cells and High BAFF Levels. *PloS One* (2012) 7(8):e43588. doi: 10.1371/journal.pone.0043588
9. Das A, Ellis G, Pallant C, Lopes AR, Khanna P, Peppa D, et al. IL-10-producing Regulatory B Cells in the Pathogenesis of Chronic Hepatitis B

Virus Infection. *J Immunol* (2012) 189(8):3925–35. doi: 10.4049/jimmunol.1103139
10. Liu F, Dai W, Li C, Lu X, Chen Y, Weng D, et al. Role of IL-10-Producing Regulatory B Cells in Modulating T-helper Cell Immune Responses During Silica-Induced Lung Inflammation and Fibrosis. *Sci Rep* (2016) 6:28911. doi: 10.1038/srep28911
11. Rousset F, Garcia E, Defrance T, Péronne C, Vezzio N, Hsu DH, et al. Interleukin 10 Is a Potent Growth and Differentiation Factor for Activated Human B Lymphocytes. *Proc Natl Acad Sci USA* (1992) 89(5):1890–3. doi: 10.1073/pnas.89.5.1890
12. Itoh K, Hirohata S. The Role of IL-10 in Human B Cell Activation, Proliferation, and Differentiation. *J Immunol* (1995) 154(9):4341–50.
13. Groux H, Bigler M, de Vries JE, Roncarolo MG. Inhibitory and Stimulatory Effects of IL-10 on Human CD8+ T Cells. *J Immunol* (1998) 160(7):3188–93.
14. Naing A, Infante JR, Papadopoulos KP, Chan IH, Shen C, Ratti NP, et al. Pegylated IL-10 (Pegilodecakin) Induces Systemic Immune Activation, Cd8. *Cancer Cell* (2018) 34(5):775–91.e3. doi: 10.1016/j.ccell.2018.10.007
15. Silva HM, Takenaka MC, Moraes-Vieira PM, Monteiro SM, Hernandez MO, Chaara W, et al. Preserving the B-cell Compartment Favors Operational Tolerance in Human Renal Transplantation. *Mol Med* (2012) 18:733–43. doi: 10.2119/molmed.2011.00281
16. Noh J, Noh G, Lee SJ, Lee JH, Kim A, Kim HS, et al. Tolerogenic Effects of Interferon-Gamma With Induction of Allergen-Specific Interleukin-10-producing Regulatory B Cell (Br1) Changes in Non-IgE-Mediated Food Allergy. *Cell Immunol* (2012) 273(2):140–9. doi: 10.1016/j.cellimm.2011.12.006
17. Noh J, Noh G, Kim HS, Kim AR, Choi WS. Allergen-Specific Responses of CD19(+)CD5(+)Foxp3(+) Regulatory B Cells (Bregs) and CD4(+)Foxp3(+) Regulatory T Cell (Tregs) in Immune Tolerance of Cow Milk Allergy of Late Eczematous Reactions. *Cell Immunol* (2012) 274(1-2):109–14. doi: 10.1016/j.cellimm.2012.01.005
18. Li X, Zhong H, Bao W, Boulad N, Evangelista J, Haider MA, et al. Defective Regulatory B-cell Compartment in Patients With Immune Thrombocytopenia. *Blood* (2012) 120(16):3318–25. doi: 10.1182/blood-2012-05-432575
19. Li J, Luo Y, Wang X, Feng G. Regulatory B Cells and Advances in Transplantation. *J Leukoc Biol* (2019) 105(4):657–68. doi: 10.1002/JLB.5RU0518-199R
20. Luo Y, Luo F, Zhang K, Wang S, Zhang H, Yang X, et al. Elevated Circulating IL-10 Producing Breg, But Not Regulatory B Cell Levels, Restrain Antibody-Mediated Rejection After Kidney Transplantation. *Front Immunol* (2020) 11:627496. doi: 10.3389/fimmu.2020.627496
21. Matsumoto M, Baba A, Yokota T, Nishikawa H, Ohkawa Y, Kayama H, et al. Interleukin-10-Producing Plasmablasts Exert Regulatory Function in Autoimmune Inflammation. *Immunity* (2014) 41(6):1040–51. doi: 10.1016/j.immuni.2014.10.016
22. van de Veen W, Stanic B, Yaman G, Wawrzyniak M, Sollner S, Akdis DG, et al. IgG4 Production is Confined to Human IL-10-producing Regulatory B Cells That Suppress Antigen-Specific Immune Responses. *J Allergy Clin Immunol* (2013) 131(4):1204–12. doi: 10.1016/j.jaci.2013.01.014
23. Vadasz Z, Peri R, Eiza N, Slobodin G, Balbir-Gurman A, Toubi E. The Expansion of CD25 High IL-10 High FoxP3 High B Regulatory Cells Is in Association With SLE Disease Activity. *J Immunol Res* (2015) 2015:254245. doi: 10.1155/2015/254245
24. Park MK, Jung YO, Lee SY, Lee SH, Heo YJ, Kim EK, et al. Amelioration of Autoimmune Arthritis by Adoptive Transfer of Foxp3-Expressing Regulatory B Cells Is Associated With the Treg/Th17 Cell Balance. *J Transl Med* (2016) 14 (1):191. doi: 10.1186/s12967-016-0940-7
25. Noh J, Choi WS, Noh G, Lee JH. Presence of Foxp3-expressing CD19(+) CD5(+) B Cells in Human Peripheral Blood Mononuclear Cells: Human CD19(+)CD5(+)Foxp3(+) Regulatory B Cell (Breg). *Immune Network* (2010) 10(6):247–9. doi: 10.4110/in.2010.10.6.247
26. Rennert PD. Novel Roles for TIM-1 in Immunity and Infection. *Immunol Lett* (2011) 141(1):28–35. doi: 10.1016/j.imlet.2011.08.003
27. Xiao S, Zhu B, Jin H, Zhu C, Umetsu DT, DeKruyff RH, et al. Tim-1 Stimulation of Dendritic Cells Regulates the Balance Between Effector and Regulatory T Cells. *Eur J Immunol* (2011) 41(6):1539–49. doi: 10.1002/eji.201040993
28. Curtiss M, Colgan J. The Role of the T-cell Costimulatory Molecule Tim-1 in the Immune Response. *Immunologic Res* (2007) 39(1-3):52–61. doi: 10.1007/s12026-007-0063-6
29. Xiao S, Brooks CR, Zhu C, Wu C, Sweere JM, Petecka S, et al. Defect in Regulatory B-cell Function and Development of Systemic Autoimmunity in T-cell Ig Mucin 1 (Tim-1) Mucin Domain-Mutant Mice. *Proc Natl Acad Sci USA* (2012) 109(30):12105–10. doi: 10.1073/pnas.1120914109
30. Wong SH, Barlow JL, Nabarro S, Fallon PG, McKenzie AN. Tim-1 is Induced on Germinal Centre B Cells Through B-cell Receptor Signalling But Is Not Essential for the Germinal Centre Response. *Immunology* (2010) 131(1):77–88. doi: 10.1111/j.1365-2567.2010.03276.x
31. Gielen AW, Lobell A, Lidman O, Khademi M, Olsson T, Piehl F. Expression of T Cell Immunoglobulin- and Mucin-Domain-Containing Molecules-1 and -3 (TIM-1 and -3) in the Rat Nervous and Immune Systems. *J Neuroimmunol* (2005) 164(1-2):93–104. doi: 10.1016/j.jneuroim.2005.04.004
32. Ma L, Liu B, Jiang Z, Jiang Y. Reduced Numbers of Regulatory B Cells are Negatively Correlated With Disease Activity in Patients With New-Onset Rheumatoid Arthritis. *Clin Rheumatol* (2014) 33(2):187–95. doi: 10.1007/s10067-013-2359-3
33. Bodogai M, Lee Chang C, Wejksza K, Lai J, Merino M, Wersto RP, et al. Anti-CD20 Antibody Promotes Cancer Escape Via Enrichment of Tumor-Evoked Regulatory B Cells Expressing Low Levels of CD20 and CD137L. *Cancer Res* (2013) 73(7):2127–38. doi: 10.1158/0008-5472.CAN-12-4184
34. Olkhanud PB, Damdinsuren B, Bodogai M, Gress RE, Sen R, Wejksza K, et al. Tumor-Evoked Regulatory B Cells Promote Breast Cancer Metastasis by Converting Resting CD4(+) T Cells to T-regulatory Cells. *Cancer Res* (2011) 71(10):3505–15. doi: 10.1158/0008-5472.CAN-10-4316
35. Poe JC, Smith SH, Haas KM, Yanaba K, Tsubata T, Matsushita T, et al. Amplified B Lymphocyte CD40 Signaling Drives Regulatory B10 Cell Expansion in Mice. *PloS One* (2011) 6(7):e22464. doi: 10.1371/journal.pone.0022464
36. Fang D, Kuan Y-C, Wu Y-J, Hung C-L, Sheu F. Trametes Versicolor Protein Yzp Activates Regulatory B Lymphocytes – Gene Identification Through De Novo Assembly and Function Analysis in a Murine Acute Colitis Model. *PloS One* (2013) 8(9):e72422. doi: 10.1371/journal.pone.0072422
37. Ding Q, Yeung M, Camirand G, Zeng Q, Akiba H, Yagita H, et al. Regulatory B Cells are Identified by Expression of TIM-1 and can be Induced Through TIM-1 Ligation to Promote Tolerance in Mice. *J Clin Invest* (2011) 121 (9):3645–56. doi: 10.1172/JCI46274
38. Sun J, Wang J, Pefanis E, Chao J, Rothschild G, Tachibana I, et al. Transcriptomics Identify CD9 as a Marker of Murine Il-10-Competent Regulatory B Cells. *Cell Rep* (2015) 13(6):1110–7. doi: 10.1016/j.celrep.2015.09.070
39. Yang X, Yang J, Chu Y, Wang J, Guan M, Zhu X, et al. T Follicular Helper Cells Mediate Expansion of Regulatory B Cells Via IL-21 in Lupus-prone MRL/lpr Mice. *PloS One* (2013) 8(4):e62855. doi: 10.1371/journal.pone.0062855
40. Margry B, Kersemakers SC, Hoek A, Arkesteijn GJ, Wieland WH, van Eden W, et al. Activated Peritoneal Cavity B-1a Cells Possess Regulatory B Cell Properties. *PloS One* (2014) 9(2):e88869. doi: 10.1371/journal.pone.0088869
41. Wang K, Gong H, Chai R, Yuan H, Chen Y, Liu J. Aberrant Frequency of IL-35 Producing B Cells in Colorectal Cancer Patients. *Cytokine* (2018) 102:206–10. doi: 10.1016/j.cyto.2017.10.011
42. Yu CR, Choi JK, Uche AN, Egwuagu CE. Production of IL-35 by Bregs is Mediated Through Binding of BATF-IRF-4-IRF-8 Complex to il12a and Ebi3 Promoter Elements. *J Leukoc Biol* (2018) 104(6):1147–57. doi: 10.1002/JLB.3A0218-071RRR
43. Dambuza IM, He C, Choi JK, Yu CR, Wang R, Mattapallil MJ, et al. IL-12p35 Induces Expansion of IL-10 and IL-35-expressing Regulatory B Cells and Ameliorates Autoimmune Disease. *Nat Commun* (2017) 8(1):719. doi: 10.1038/s41467-017-00838-4
44. Cai Z, Wong CK, Dong J, Chu M, Jiao D, Kam NW, et al. Remission of Systemic Lupus Erythematosus Disease Activity With Regulatory Cytokine Interleukin (IL)-35 in Murphy Roths Large (MRL)/Lpr Mice. *Clin Exp Immunol* (2015) 181(2):253–66. doi: 10.1111/cei.12639
45. Fonseca-Camarillo G, Furuzawa-Carballeda J, Yamamoto-Furusho JK. Interleukin 35 (IL-35) and IL-37: Intestinal and Peripheral Expression by T and B Regulatory Cells in Patients With Inflammatory Bowel Disease. *Cytokine* (2015) 75(2):389–402. doi: 10.1016/j.cyto.2015.04.009
46. Lal G, Nakayama Y, Sethi A, Singh AK, Burrell BE, Kulkarni N, et al. Interleukin-10 From Marginal Zone Precursor B-Cell Subset Is Required for Costimulatory Blockade-Induced Transplantation Tolerance. *Transplantation* (2015) 99(9):1817–28. doi: 10.1097/TP.0000000000000718

47. Carter NA, Vasconcellos R, Rosser EC, Tulone C, Munoz-Suano A, Kamanaka M, et al. Mice Lacking Endogenous IL-10-producing Regulatory B Cells Develop Exacerbated Disease and Present With an Increased Frequency of Th1/Th17 But a Decrease in Regulatory T Cells. *J Immunol* (2011) 186(10):5569–79. doi: 10.4049/jimmunol.1100284
48. Evans JG, Chavez-Rueda KA, Eddaoudi A, Meyer-Bahlburg A, Rawlings DJ, Ehrenstein MR, et al. Novel Suppressive Function of Transitional 2 B Cells in Experimental Arthritis. *J Immunol* (2007) 178(12):7868–78. doi: 10.4049/jimmunol.178.12.7868
49. Blair PA, Chavez-Rueda KA, Evans JG, Shlomchik MJ, Eddaoudi A, Isenberg DA, et al. Selective Targeting of B Cells With Agonistic anti-CD40 is an Efficacious Strategy for the Generation of Induced Regulatory T2-Like B Cells and for the Suppression of Lupus in MRL/lpr Mice. *J Immunol* (2009) 182(6):3492–502. doi: 10.4049/jimmunol.0803052
50. Miles K, Heaney J, Sibinska Z, Salter D, Savill J, Gray D, et al. A Tolerogenic Role for Toll-like Receptor 9 is Revealed by B-cell Interaction With DNA Complexes Expressed on Apoptotic Cells. *Proc Natl Acad Sci USA* (2012) 109(3):887–92. doi: 10.1073/pnas.1109173109
51. Bankoti R, Gupta K, Levchenko A, Stäger S. Marginal Zone B Cells Regulate Antigen-Specific T Cell Responses During Infection. *J Immunol* (2012) 188 (8):3961–71. doi: 10.4049/jimmunol.1102880
52. Gray M, Miles K, Salter D, Gray D, Savill J. Apoptotic Cells Protect Mice From Autoimmune Inflammation by the Induction of Regulatory B Cells. *Proc Natl Acad Sci USA* (2007) 104(35):14080–5. doi: 10.1073/pnas.0700326104
53. Yanaba K, Bouaziz JD, Haas KM, Poe JC, Fujimoto M, Tedder TF. A Regulatory B Cell Subset With a Unique CD1dhiCD5+ Phenotype Controls T Cell-Dependent Inflammatory Responses. *Immunity* (2008) 28(5):639–50. doi: 10.1016/j.immuni.2008.03.017
54. Hu X, Tai J, Qu Z, Zhao S, Zhang L, Li M, et al. A Lower Proportion of Regulatory B Cells in Patients With Henoch-Schoenlein Purpura Nephritis. *PloS One* (2016) 11(3):e0152368. doi: 10.1371/journal.pone.0152368
55. Matsushita T, Tedder TF. Identifying Regulatory B Cells (B10 Cells) That Produce IL-10 in Mice. *Methods Mol Biol* (2011) 677:99–111. doi: 10.1007/978-1-60761-869-0_7
56. Matsushita T, Horikawa M, Iwata Y, Tedder TF. Regulatory B Cells (B10 Cells) and Regulatory T Cells Have Independent Roles in Controlling Experimental Autoimmune Encephalomyelitis Initiation and Late-Phase Immunopathogenesis. *J Immunol* (2010) 185(4):2240–52. doi: 10.4049/jimmunol.1001307
57. Iwata Y, Matsushita T, Horikawa M, Dilillo DJ, Yanaba K, Venturi GM, et al. Characterization of a Rare IL-10-Competent B-Cell Subset in Humans That Parallels Mouse Regulatory B10 Cells. *Blood* (2011) 117(2):530–41. doi: 10.1182/blood-2010-07-294249
58. Khan AR, Amu S, Saunders SP, Hams E, Blackshields G, Leonard MO, et al. Ligation of TLR7 on CD19(+) CD1d(Hi) B Cells Suppresses Allergic Lung Inflammation Via Regulatory T Cells. *Eur J Immunol* (2015) 45(6):1842–54. doi: 10.1002/eji.201445211
59. van der Vlugt LE, Zinsou JF, Ozir-Fazalalikhan A, Kremsner PG, Yazdanbakhsh M, Adegnika AA, et al. Interleukin 10 (IL-10)-Producing CD1dhi Regulatory B Cells From Schistosoma Haematobium-Infected Individuals Induce IL-10-Positive T Cells and Suppress Effector T-cell Cytokines. *J Infect Dis* (2014) 210(8):1207–16. doi: 10.1093/infdis/jiu257
60. Shen P, Roch T, Lampropoulou V, O'Connor RA, Stervbo U, Hilgenberg E, et al. IL-35-Producing B Cells are Critical Regulators of Immunity During Autoimmune and Infectious Diseases. *Nature* (2014) 507(7492):366–70. doi: 10.1038/nature12979
61. Neves P, Lampropoulou V, Calderon-Gomez E, Roch T, Stervbo U, Shen P, et al. Signaling Via the MyD88 Adaptor Protein in B Cells Suppresses Protective Immunity During Salmonella Typhimurium Infection. *Immunity* (2010) 33(5):777–90. doi: 10.1016/j.immuni.2010.10.016
62. Maseda D, Candando KM, Smith SH, Kalampokis I, Weaver CT, Plevy SE, et al. Peritoneal Cavity Regulatory B Cells (B10 Cells) Modulate IFN-Gamma+CD4+ T Cell Numbers During Colitis Development in Mice. *J Immunol* (2013) 191(5):2780–95. doi: 10.4049/jimmunol.1300649
63. Liu J, Zhan W, Kim CJ, Clayton K, Zhao H, Lee E, et al. IL-10-Producing B Cells are Induced Early in HIV-1 Infection and Suppress HIV-1-Specific T Cell Responses. *PloS One* (2014) 9(2):e89236. doi: 10.1371/journal.pone.0089236
64. Aravena O, Ferrier A, Menon M, Mauri C, Aguillón JC, Soto L, et al. TIM-1 Defines a Human Regulatory B Cell Population That is Altered in Frequency and Function in Systemic Sclerosis Patients. *Arthritis Res Ther* (2017) 19 (1):8. doi: 10.1186/s13075-016-1213-9
65. Zhang Y, Zhang X, Xia Y, Jia X, Li H, Shao Z, et al. CD19+ Tim-1+ B Cells are Decreased and Negatively Correlated With Disease Severity in Myasthenia Gravis Patients. *Immunol Res* (2016) 64(5-6):1216–24. doi: 10.1007/s12026-016-8872-0
66. Yeung MY, Ding Q, Brooks CR, Xiao S, Workman CJ, Vignali DA, et al. TIM-1 Signaling is Required for Maintenance and Induction of Regulatory B Cells. *Am J Transplant* (2015) 15(4):942–53. doi: 10.1111/ajt.13087
67. Newell KA, Asare A, Kirk AD, Gisler TD, Bourcier K, Suthanthiran M, et al. Identification of a B Cell Signature Associated With Renal Transplant Tolerance in Humans. *J Clin Invest* (2010) 120(6):1836–47. doi: 10.1172/JCI39933
68. Blair PA, Noreña LY, Flores-Borja F, Rawlings DJ, Isenberg DA, Ehrenstein MR, et al. CD19(+)CD24(Hi)CD38(Hi) B Cells Exhibit Regulatory Capacity in Healthy Individuals But Are Functionally Impaired in Systemic Lupus Erythematosus Patients. *Immunity* (2010) 32(1):129–40. doi: 10.1016/j.immuni.2009.11.009
69. Menon M, Blair PA, Isenberg DA, Mauri C. A Regulatory Feedback Between Plasmacytoid Dendritic Cells and Regulatory B Cells Is Aberrant in Systemic Lupus Erythematosus. *Immunity* (2016) 44(3):683–97. doi: 10.1016/j.immuni.2016.02.012
70. Lemoine S, Morva A, Youinou P, Jamin C. Human T Cells Induce Their Own Regulation Through Activation of B Cells. *J Autoimmun* (2011) 36(3-4):228–38. doi: 10.1016/j.jaut.2011.01.005
71. Flores-Borja F, Bosma A, Ng D, Reddy V, Ehrenstein MR, Isenberg DA, et al. CD19+CD24HICD38HI B Cells Maintain Regulatory T Cells While Limiting TH1 and TH17 Differentiation. *Sci Transl Med* (2013) 5 (173):173ra23. doi: 10.1126/scitranslmed.3005407
72. Sagoo P, Perucha E, Sawitzki B, Tomiuk S, Stephens DA, Miqueu P, et al. Development of a Cross-Platform Biomarker Signature to Detect Renal Transplant Tolerance in Humans. *J Clin Invest* (2010) 120(6):1848–61. doi: 10.1172/JCI39922
73. Liu Y, Cheng LS, Wu SD, Wang SQ, Li L, She WM, et al. IL-10-Producing Regulatory B-Cells Suppressed Effector T-Cells But Enhanced Regulatory T-Cells in Chronic HBV Infection. *Clin Sci (Lond)* (2016) 130(11):907–19. doi: 10.1042/CS20160069
74. Kessel A, Haj T, Peri R, Snir A, Melamed D, Sabo E, et al. Human CD19(+) CD25(High) B Regulatory Cells Suppress Proliferation of CD4(+) T Cells and Enhance Foxp3 and CTLA-4 Expression in T-Regulatory Cells. *Autoimmun Rev* (2012) 11(9):670–7. doi: 10.1016/j.autrev.2011.11.018
75. Kim HS, Lee JH, Han HD, Kim AR, Nam ST, Kim HW, et al. Autocrine Stimulation of IL-10 Is Critical to the Enrichment of IL-10-Producing CD40 (Hi)CD5(+) Regulatory B Cells In Vitro and In Vivo. *BMB Rep* (2015) 48 (1):54–9. doi: 10.5483/bmbrep.2015.48.1.213
76. Maseda D, Smith SH, DiLillo DJ, Bryant JM, Candando KM, Weaver CT, et al. Regulatory B10 Cells Differentiate Into Antibody-Secreting Cells After Transient IL-10 Production In Vivo. *J Immunol* (2012) 188(3):1036–48. doi: 10.4049/jimmunol.1102500
77. Yoshizaki A, Miyagaki T, DiLillo DJ, Matsushita T, Horikawa M, Kountikov EI, et al. Regulatory B Cells Control T-Cell Autoimmunity Through IL-21-dependent Cognate Interactions. *Nature* (2012) 491(7423):264–8. doi: 10.1038/nature11501
78. Lighaam LC, Unger PA, Vredevoogd DW, Verhoeven D, Vermeulen E, Turksma AW, et al. In Vitro-Induced Human Il-10(+) B Cells Do Not Show a Subset-Defining Marker Signature and Plastically Co-Express IL-10 With Pro-Inflammatory Cytokines. *Front Immunol* (2018) 9:1913. doi: 10.3389/fimmu.2018.01913
79. Ma L, Qin J, Ji H, Zhao P, Jiang Y. Tfh and Plasma Cells are Correlated With Hypergammaglobulinaemia in Patients With Autoimmune Hepatitis. *Liver Int* (2014) 34(3):405–15. doi: 10.1111/liv.12245
80. Wang RX, Yu CR, Dambuza IM, Mahdi RM, Dolinska MB, Sergeev YV, et al. Interleukin-35 Induces Regulatory B Cells That Suppress Autoimmune Disease. *Nat Med* (2014) 20(6):633–41. doi: 10.1038/nm.3554
81. Lindner S, Dahlke K, Sontheimer K, Hagn M, Kaltenmeier C, Barth TF, et al. Interleukin 21-Induced Granzyme B-Expressing B Cells Infiltrate Tumors and Regulate T Cells. *Cancer Res* (2013) 73(8):2468–79. doi: 10.1158/0008-5472.CAN-12-3450

82. Durand J, Huchet V, Merieau E, Usal C, Chesneau M, Remy S, et al. Regulatory B Cells With a Partial Defect in CD40 Signaling and Overexpressing Granzyme B Transfer Allograft Tolerance in Rodents. *J Immunol* (2015) 195(10):5035–44. doi: 10.4049/jimmunol.1500429
83. Sugimoto K, Ogawa A, Shimomura Y, Nagahama K, Mizoguchi A, Bhan AK. Inducible IL-12-Producing B Cells Regulate Th2-mediated Intestinal Inflammation. *Gastroenterology* (2007) 133(1):124–36. doi: 10.1053/j.gastro.2007.03.112
84. Tian J, Zekzer D, Hanssen L, Lu Y, Olcott A, Kaufman DL. Lipopolysaccharide-Activated B Cells Down-Regulate Th1 Immunity and Prevent Autoimmune Diabetes in Nonobese Diabetic Mice. *J Immunol* (2001) 167(2):1081–9. doi: 10.4049/jimmunol.167.2.1081
85. Parekh VV, Prasad DV, Banerjee PP, Joshi BN, Kumar A, Mishra GC. B Cells Activated by Lipopolysaccharide, But Not by Anti-Ig and Anti-CD40 Antibody, Induce Anergy in CD8+ T Cells: Role of TGF-beta 1. *J Immunol* (2003) 170(12):5897–911. doi: 10.4049/jimmunol.170.12.5897
86. Tang Y, Jiang Q, Ou Y, Zhang F, Qing K, Sun Y, et al. BIP Induces Mice CD19(hi) Regulatory B Cells Producing IL-10 and Highly Expressing PD-L1, Fasl. *Mol Immunol* (2016) 69:44–51. doi: 10.1016/j.molimm.2015.10.017
87. Khan AR, Hams E, Floudas A, Sparwasser T, Weaver CT, Fallon PG. PD-L1hi B Cells Are Critical Regulators of Humoral Immunity. *Nat Commun* (2015) 6:5997. doi: 10.1038/ncomms6997
88. Jin G, Hamaguchi Y, Matsushita T, Hasegawa M, Le Huu D, Ishiura N, et al. B-Cell Linker Protein Expression Contributes to Controlling Allergic and Autoimmune Diseases by Mediating IL-10 Production in Regulatory B Cells. *J Allergy Clin Immunol* (2013) 131(6):1674–82. doi: 10.1016/j.jaci.2013.01.044
89. Park MJ, Lee SH, Kim EK, Lee EJ, Park SH, Kwok SK, et al. Myeloid-Derived Suppressor Cells Induce the Expansion of Regulatory B Cells and Ameliorate Autoimmunity in the Sanroque Mouse Model of Systemic Lupus Erythematosus. *Arthritis Rheumatol* (2016) 68(11):2717–27. doi: 10.1002/art.39767
90. Mutnal MB, Hu S, Schachtele SJ, Lokensgard JR. Infiltrating Regulatory B Cells Control Neuroinflammation Following Viral Brain Infection. *J Immunol* (2014) 193(12):6070–80. doi: 10.4049/jimmunol.1400654
91. Achour A, Simon Q, Mohr A, Seite JF, Youinou P, Bendaoud B, et al. Human Regulatory B Cells Control the TFH Cell Response. *J Allergy Clin Immunol* (2017) 140(1):215–22. doi: 10.1016/j.jaci.2016.09.042
92. Zhan J, Huang L, Ma H, Chen H, Yang Y, Tan S, et al. Reduced Inflammatory Responses of Follicular Helper T Cell Promote the Development of Regulatory B Cells After Roux-en-Y Gastric Bypass. *Clin Exp Pharmacol Physiol* (2017) 44(5):556–65. doi: 10.1111/1440-1681.12740
93. Brosseau C, Durand M, Colas L, Durand E, Foureau A, Cheminant MA, et al. CD9(+) Regulatory B Cells Induce T Cell Apoptosis Via IL-10 and Are Reduced in Severe Asthmatic Patients. *Front Immunol* (2018) 9:3034. doi: 10.3389/fimmu.2018.03034
94. Rieger A, Bar-Or A. B-Cell-Derived Interleukin-10 in Autoimmune Disease: Regulating the Regulators. *Nat Rev Immunol* (2008) 8(6):486–7. doi: 10.1038/nri2315-c1
95. Chen Y, Bodhankar S, Murphy SJ, Vandenbark AA, Alkayed NJ, Offner H. Intrastriatal B-Cell Administration Limits Infarct Size After Stroke in B-cell Deficient Mice. *Metab Brain Dis* (2012) 27(4):487–93. doi: 10.1007/s11011-012-9317-7
96. Wang T, Li Z, Li X, Chen L, Zhao H, Jiang C, et al. Expression of CD19 +CD24highCD38high B Cells, IL−10 and IL−10R in Peripheral Blood From Patients With Systemic Lupus Erythematosus. *Mol Med Rep* (2017) 16 (5):6326–33. doi: 10.3892/mmr.2017.7381
97. Lal G, Kulkarni N, Nakayama Y, Singh AK, Sethi A, Burrell BE, et al. IL-10 From Marginal Zone Precursor B Cells Controls the Differentiation of Th17, Tfh and Tfr Cells in Transplantation Tolerance. *Immunol Lett* (2016) 170:52–63. doi: 10.1016/j.imlet.2016.01.002
98. Yap DYH, Chan TM. B Cell Abnormalities in Systemic Lupus Erythematosus and Lupus Nephritis-Role in Pathogenesis and Effect of Immunosuppressive Treatments. *Int J Mol Sci* (2019) 20(24):6231. doi: 10.3390/ijms20246231
99. Kleffel S, Vergani A, Tezza S, Ben Nasr M, Niewczas MA, Wong S, et al. Interleukin-10+ Regulatory B Cells Arise Within Antigen-Experienced CD40+ B Cells to Maintain Tolerance to Islet Autoantigens. *Diabetes* (2015) 64(1):158–71. doi: 10.2337/db13-1639
100. Boldison J, Da Rosa LC, Davies J, Wen L, Wong FS. Dendritic Cells License Regulatory B Cells to Produce IL-10 and Mediate Suppression of Antigen-Specific CD8 T Cells. *Cell Mol Immunol* (2020) 17(8):843–55. doi: 10.1038/s41423-019-0324-z
101. Todd SK, Pepper RJ, Draibe J, Tanna A, Pusey CD, Mauri C, et al. Regulatory B Cells are Numerically But Not Functionally Deficient in Anti-Neutrophil Cytoplasm Antibody-Associated Vasculitis. *Rheumatol (Oxford)* (2014) 53 (9):1693–703. doi: 10.1093/rheumatology/keu136
102. Furuzawa-Carballeda J, Hernández-Molina G, Lima G, Rivera-Vicencio Y, Férez-Blando K, Llorente L. Peripheral Regulatory Cells Immunophenotyping in Primary Sjögren's Syndrome: A Cross-Sectional Study. *Arthritis Res Ther* (2013) 15(3):R68. doi: 10.1186/ar4245
103. Sumimoto K, Uchida K, Kusuda T, Mitsuyama T, Sakaguchi Y, Fukui T, et al. The Role of CD19+ Cd24high CD38high and CD19+ Cd24high CD27+ Regulatory B Cells in Patients With Type 1 Autoimmune Pancreatitis. *Pancreatology* (2014) 14(3):193–200. doi: 10.1016/j.pan.2014.02.004
104. Yang B, Tan X, Xiong X, Wu D, Zhang G, Wang M, et al. Effect of CD40/CD40L Signaling on IL-10-producing Regulatory B Cells in Chinese Children With Henoch-Schönlein Purpura Nephritis. *Immunol Res* (2017) 65(3):592–604. doi: 10.1007/s12026-016-8877-8
105. Yan Y, van der Putten K, Bowen DG, Painter DM, Kohar J, Sharland AF, et al. Postoperative Administration of Donor B Cells Induces Rat Kidney Allograft Acceptance: Lack of Association With Th2 Cytokine Expression in Long-Term Accepted Grafts. *Transplantation* (2002) 73(7):1123–30. doi: 10.1097/00007890-200204150-00020
106. Newell KA, Asare A, Sanz I, Wei C, Rosenberg A, Gao Z, et al. Longitudinal Studies of a B Cell-Derived Signature of Tolerance in Renal Transplant Recipients. *Am J Transplant* (2015) 15(11):2908–20. doi: 10.1111/ajt.13480
107. Chesneau M, Pallier A, Braza F, Lacombe G, Le Gallou S, Baron D, et al. Unique B Cell Differentiation Profile in Tolerant Kidney Transplant Patients. *Am J Transplant* (2014) 14(1):144–55. doi: 10.1111/ajt.12508
108. Pallier A, Hillion S, Danger R, Giral M, Racape M, Degauque N, et al. Patients With Drug-Free Long-Term Graft Function Display Increased Numbers of Peripheral B Cells With a Memory and Inhibitory Phenotype. *Kidney Int* (2010) 78(5):503–13. doi: 10.1038/ki.2010.162
109. Mohib K, Cherukuri A, Zhou Y, Ding Q, Watkins SC, Rothstein DM. Antigen-Dependent Interactions Between Regulatory B Cells and T Cells at the T:B Border Inhibit Subsequent T Cell Interactions With DCs. *Am J Transplant* (2020) 20(1):52–63. doi: 10.1111/ajt.15546
110. Zhao G, Moore DJ, Lee KM, Kim JI, Duff PE, O'Connor MR, et al. An Unexpected Counter-Regulatory Role of IL-10 in B-Lymphocyte-Mediated Transplantation Tolerance. *Am J Transplant* (2010) 10(4):796–801. doi: 10.1111/j.1600-6143.2010.03027.x
111. Cherukuri A, Rothstein DM, Clark B, Carter CR, Davison A, Hernandez-Fuentes M, et al. Immunologic Human Renal Allograft Injury Associates With an Altered IL-10/TNF-Alpha Expression Ratio in Regulatory B Cells. *J Am Soc Nephrol* (2014) 25(7):1575–85. doi: 10.1681/Asn.2013080837
112. Mielle J, Audo R, Hahne M, Macia L, Combe B, Morel J, et al. IL-10 Producing B Cells Ability to Induce Regulatory T Cells Is Maintained in Rheumatoid Arthritis. *Front Immunol* (2018) 9:961. doi: 10.3389/fimmu.2018.00961
113. Qin Y, Zhang M, Jiang RM, Wu Q, Xu XY, Chen H, et al. B10 Cells Play a Role in the Immune Modulation of Pro- and Anti-Inflammatory Immune Responses in Mouse Islet Allograft Rejection. *Cell Immunol* (2016) 310:184–92. doi: 10.1016/j.cellimm.2016.09.010
114. Díaz-Alderete A, Crispin JC, Vargas-Rojas MI, Alcocer-Varela J. IL-10 Production in B Cells Is Confined to CD154+ Cells in Patients With Systemic Lupus Erythematosus. *J Autoimmun* (2004) 23(4):379–83. doi: 10.1016/j.jaut.2004.10.001
115. Amel Kashipaz MR, Huggins ML, Lanyon P, Robins A, Powell RJ, Todd I. Assessment of Be1 and Be2 Cells in Systemic Lupus Erythematosus Indicates Elevated interleukin-10 Producing CD5+ B Cells. *Lupus* (2003) 12(5):356–63. doi: 10.1191/0961203303lu338oa
116. Wang L, Zhao P, Ma L, Shan Y, Jiang Z, Wang J, et al. Increased Interleukin 21 and Follicular Helper T-like Cells and Reduced Interleukin 10+ B Cells in Patients With New-Onset Systemic Lupus Erythematosus. *J Rheumatol* (2014) 41(9):1781–92. doi: 10.3899/jrheum.131025
117. Heinemann K, Wilde B, Hoerning A, Tebbe B, Kribben A, Witzke O, et al. Decreased IL-10(+) Regulatory B Cells (Bregs) in Lupus Nephritis Patients. *Scand J Rheumatol* (2016) 45(4):312–6. doi: 10.3109/03009742.2015.1126346

118. Rosser EC, Mauri C. Regulatory B Cells: Origin, Phenotype, and Function. *Immunity* (2015) 42(4):607–12. doi: 10.1016/j.immuni.2015.04.005
119. Ochsenbein AF, Fehr T, Lutz C, Suter M, Brombacher F, Hengartner H, et al. Control of Early Viral and Bacterial Distribution and Disease by Natural Antibodies. *Science* (1999) 286(5447):2156–9. doi: 10.1126/science.286.5447.2156
120. Sim JH, Kim HR, Chang SH, Kim IJ, Lipsky PE, Lee J. Autoregulatory Function of Interleukin-10-producing Pre-Naïve B Cells is Defective in Systemic Lupus Erythematosus. *Arthritis Res Ther* (2015) 17:190. doi: 10.1186/s13075-015-0687-1
121. Fleischer V, Sieber J, Fleischer SJ, Shock A, Heine G, Daridon C, et al. Epratuzumab Inhibits the Production of the Proinflammatory Cytokines IL-6 and TNF-α, But Not the Regulatory Cytokine IL-10, by B Cells From Healthy Donors and SLE Patients. *Arthritis Res Ther* (2015) 17:185. doi: 10.1186/s13075-015-0686-2
122. Park MJ, Kwok SK, Lee SH, Kim EK, Park SH, Cho ML. Adipose Tissue-Derived Mesenchymal Stem Cells Induce Expansion of Interleukin-10-producing Regulatory B Cells and Ameliorate Autoimmunity in a Murine Model of Systemic Lupus Erythematosus. *Cell Transplant* (2015) 24 (11):2367–77. doi: 10.3727/096368914X685645
123. Bluestone JA, Herold K, Eisenbarth G. Genetics, Pathogenesis and Clinical Interventions in Type 1 Diabetes. *Nature* (2010) 464(7293):1293–300. doi: 10.1038/nature08933
124. Barnett R. Type 1 Diabetes. *Lancet* (2018) 391(10117):195. doi: 10.1016/S0140-6736(18)30024-2
125. Hu CY, Rodriguez-Pinto D, Du W, Ahuja A, Henegariu O, Wong FS, et al. Treatment With CD20-specific Antibody Prevents and Reverses Autoimmune Diabetes in Mice. *J Clin Invest* (2007) 117(12):3857–67. doi: 10.1172/JCI32405
126. Serreze DV, Chapman HD, Niens M, Dunn R, Kehry MR, Driver JP, et al. Loss of Intra-Islet CD20 Expression may Complicate Efficacy of B-cell-directed Type 1 Diabetes Therapies. *Diabetes* (2011) 60(11):2914–21. doi: 10.2337/db11-0705
127. Da Rosa LC, Boldison J, De Leenheer E, Davies J, Wen L, Wong FS. B Cell Depletion Reduces T Cell Activation in Pancreatic Islets in a Murine Autoimmune Diabetes Model. *Diabetologia* (2018) 61(6):1397–410. doi: 10.1007/s00125-018-4597-z
128. Fiorina P, Vergani A, Dada S, Jurewicz M, Wong M, Law K, et al. Targeting CD22 Reprograms B-cells and Reverses Autoimmune Diabetes. *Diabetes* (2008) 57(11):3013–24. doi: 10.2337/db08-0420
129. Deng C, Xiang Y, Tan T, Ren Z, Cao C, Huang G, et al. Altered Peripheral B-Lymphocyte Subsets in Type 1 Diabetes and Latent Autoimmune Diabetes in Adults. *Diabetes Care* (2016) 39(3):434–40. doi: 10.2337/dc15-1765
130. Hussain S, Delovitch TL. Intravenous Transfusion of BCR-Activated B Cells Protects NOD Mice From Type 1 Diabetes in an IL-10-dependent Manner. *J Immunol* (2007) 179(11):7225–32. doi: 10.4049/jimmunol.179.11.7225
131. Geetha D, Jefferson JA. ANCA-Associated Vasculitis: Core Curriculum 2020. *Am J Kidney Dis* (2020) 75(1):124–37. doi: 10.1053/j.ajkd.2019.04.031
132. Lepse N, Abdulahad WH, Rutgers A, Kallenberg CG, Stegeman CA, Heeringa P. Altered B Cell Balance, But Unaffected B Cell Capacity to Limit Monocyte Activation in Anti-Neutrophil Cytoplasmic Antibody-Associated Vasculitis in Remission. *Rheumatol (Oxford)* (2014) 53 (9):1683–92. doi: 10.1093/rheumatology/keu149
133. Karim MR, Wang YF. Phenotypic Identification of CD19. *Arch Med Sci* (2019) 15(5):1176–83. doi: 10.5114/aoms.2018.77772
134. Gary-Gouy H, Harriague J, Bismuth G, Platzer C, Schmitt C, Dalloul AH. Human CD5 Promotes B-cell Survival Through Stimulation of Autocrine IL-10 Production. *Blood* (2002) 100(13):4537–43. doi: 10.1182/blood-2002-05-1525
135. Bunch DO, McGregor JG, Khandoobhai NB, Aybar LT, Burkart ME, Hu Y, et al. Decreased $CD5^+$ B Cells in Active ANCA Vasculitis and Relapse After Rituximab. *Clin J Am Soc Nephrol* (2013) 8(3):382–91. doi: 10.2215/CJN.03950412
136. Aybar LT, McGregor JG, Hogan SL, Hu Y, Mendoza CE, Brant EJ, et al. Reduced CD5(+) CD24(Hi) CD38(hi) and Interleukin-10(+) Regulatory B Cells in Active Anti-Neutrophil Cytoplasmic Autoantibody-Associated Vasculitis Permit Increased Circulating Autoantibodies. *Clin Exp Immunol* (2015) 180(2):178–88. doi: 10.1111/cei.12483
137. Bunch DO, Mendoza CE, Aybar LT, Kotzen ES, Colby KR, Hu Y, et al. Gleaning Relapse Risk From B Cell Phenotype: Decreased CD5+ B Cells Portend a Shorter Time to Relapse After B Cell Depletion in Patients With ANCA-associated Vasculitis. *Ann Rheum Dis* (2015) 74(9):1784–6. doi: 10.1136/annrheumdis-2014-206756
138. Unizony S, Lim N, Phippard DJ, Carey VJ, Miloslavsky EM, Tchao NK, et al. Peripheral CD5+ B Cells in Antineutrophil Cytoplasmic Antibody-Associated Vasculitis. *Arthritis Rheumatol* (2015) 67(2):535–44. doi: 10.1002/art.38916
139. Vivino FB, Bunya VY, Massaro-Giordano G, Johr CR, Giattino SL, Schorpion A, et al. Sjogren's Syndrome: An Update on Disease Pathogenesis, Clinical Manifestations and Treatment. *Clin Immunol* (2019) 203:81–121. doi: 10.1016/j.clim.2019.04.009
140. Goules AV, Tatouli IP, Moutsopoulos HM, Tzioufas AG. Clinically Significant Renal Involvement in Primary Sjögren's Syndrome: Clinical Presentation and Outcome. *Arthritis Rheum* (2013) 65(11):2945–53. doi: 10.1002/art.38100
141. Ramos-Casals M, Solans R, Rosas J, Camps MT, Gil A, Del Pino-Montes J, et al. Primary Sjögren Syndrome in Spain: Clinical and Immunologic Expression in 1010 Patients. *Med (Baltimore)* (2008) 87(4):210–9. doi: 10.1097/MD.0b013e318181e6af
142. Jasiek M, Karras A, Le Guern V, Krastinova E, Mesbah R, Faguer S, et al. A Multicentre Study of 95 Biopsy-Proven Cases of Renal Disease in Primary Sjögren's Syndrome. *Rheumatol (Oxford)* (2017) 56(3):362–70. doi: 10.1093/rheumatology/kew376
143. Lin W, Jin L, Chen H, Wu Q, Fei Y, Zheng W, et al. B Cell Subsets and Dysfunction of Regulatory B Cells in IgG4-related Diseases and Primary Sjögren's Syndrome: The Similarities and Differences. *Arthritis Res Ther* (2014) 16(3):R118. doi: 10.1186/ar4571
144. Lin X, Wang X, Xiao F, Ma K, Liu L, Xu D, et al. IL-10-producing Regulatory B Cells Restrain the T Follicular Helper Cell Response in Primary Sjögren's Syndrome. *Cell Mol Immunol* (2019) 16(12):921–31. doi: 10.1038/s41423-019-0227-z
145. Papp G, Gyimesi E, Szabó K, Zöld É, Zeher M. Increased IL-21 Expression Induces Granzyme B in Peripheral CD5(+) B Cells as a Potential Counter-Regulatory Effect in Primary Sjögren's Syndrome. *Mediators Inflammation* (2016) 2016:4328372. doi: 10.1155/2016/4328372
146. Cortazar FB, Stone JH. IgG4-related Disease and the Kidney. *Nat Rev Nephrol* (2015) 11(10):599–609. doi: 10.1038/nrneph.2015.95
147. Piram M, Mahr A. Epidemiology of Immunoglobulin A Vasculitis (Henoch-Schönlein): Current State of Knowledge. *Curr Opin Rheumatol* (2013) 25 (2):171–8. doi: 10.1097/BOR.0b013e32835d8e2a
148. Wang YY, Zhang L, Zhao PW, Ma L, Li C, Zou HB, et al. Functional Implications of Regulatory B Cells in Human IgA Nephropathy. *Scand J Immunol* (2014) 79(1):51–60. doi: 10.1111/sji.12128
149. Li T, Yu Z, Qu Z, Zhang N, Crew R, Jiang Y. Decreased Number of CD19. *Mol Immunol* (2019) 112:233–9. doi: 10.1016/j.molimm.2019.05.014
150. Liu Y, Wang H, Hu X, Qu Z, Zhang H, Crew R, et al. A Higher Frequency of IL-10-Producing B Cells in Hepatitis B Virus-Associated Membranous Nephropathy. *Clin Exp Pharmacol Physiol* (2016) 43(4):417–27. doi: 10.1111/1440-1681.12552
151. Meng XM, Nikolic-Paterson DJ, Lan HY. TGF-β: The Master Regulator of Fibrosis. *Nat Rev Nephrol* (2016) 12(6):325–38. doi: 10.1038/nrneph.2016.48
152. Jin Y, Liu R, Xie J, Xiong H, He JC, Chen N. Interleukin-10 Deficiency Aggravates Kidney Inflammation and Fibrosis in the Unilateral Ureteral Obstruction Mouse Model. *Lab Invest* (2013) 93(7):801–11. doi: 10.1038/labinvest.2013.64
153. Mu W, Ouyang X, Agarwal A, Zhang L, Long DA, Cruz PE, et al. Il-10 Suppresses Chemokines, Inflammation, and Fibrosis in a Model of Chronic Renal Disease. *J Am Soc Nephrol* (2005) 16(12):3651–60. doi: 10.1681/ASN.2005030297
154. Kim DH, Chun SY, Lee E, Kim B, Yoon B, Gil H, et al. Il-10 Deficiency Aggravates Renal Inflammation, Fibrosis and Functional Failure in High-Fat Dieted Obese Mice. *Tissue Eng Regener Med* (2021). doi: 10.1007/s13770-020-00328-7

Conflict of Interest: The authors declare that the research was conducted in the absence of any commercial or financial relationships that could be construed as a potential conflict of interest.

Copyright © 2021 Long, Zhang, Yuan, Lan, Lin, Peng and Dai. This is an open-access article distributed under the terms of the Creative Commons Attribution License (CC BY). The use, distribution or reproduction in other forums is permitted, provided the original author(s) and the copyright owner(s) are credited and that the original publication in this journal is cited, in accordance with accepted academic practice. No use, distribution or reproduction is permitted which does not comply with these terms.

frontiers in Immunology

MINI REVIEW
published: 28 May 2021
doi: 10.3389/fimmu.2021.684197

Mesenchymal Stem Cell Protects Injured Renal Tubular Epithelial Cells by Regulating mTOR-Mediated Th17/Treg Axis

Yongsheng Luo[1,2†], *Jingjing Guo*[1,2†], *Pingbao Zhang*[12†], *Yin Celeste Cheuk*[1,2], *Yamei Jiang*[1,2], *Jiyan Wang*[2,3], *Shihao Xu*[1,2] *and Ruiming Rong*[1,2*]

[1] Department of Urology, Zhongshan Hospital, Fudan University, Shanghai, China, [2] Shanghai Key Laboratory of Organ Transplantation, Shanghai, China, [3] Shanghai Medical College, Fudan University, Shanghai, China

OPEN ACCESS

Edited by:
Ying Wang,
Shanghai Institute of Nutrition and Health (CAS), China

Reviewed by:
Yu Wang,
Shanghai Institute of Nutrition and Health (CAS), China
Menghui Jiang,
Qingdao University, China

***Correspondence:**
Ruiming Rong
rong.ruiming@zs-hospital.sh.cn

[†]*These authors have contributed equally to this work*

Specialty section:
This article was submitted to Molecular Innate Immunity, a section of the journal Frontiers in Immunology

Received: *22 March 2021*
Accepted: *10 May 2021*
Published: *28 May 2021*

Citation:
Luo Y, Guo J, Zhang P, Cheuk YC, Jiang Y, Wang J, Xu S and Rong R (2021) Mesenchymal Stem Cell Protects Injured Renal Tubular Epithelial Cells by Regulating mTOR-Mediated Th17/Treg Axis. Front. Immunol. 12:684197. doi: 10.3389/fimmu.2021.684197

The increase in T helper 17 cell (Th17)-mediated pro-inflammatory response and decrease in regulatory T cell (Treg)-mediated anti-inflammatory effect aggravate renal tubular epithelial cell (RTEC) injury. However, increasing evidence indicated that mesenchymal stem cell (MSC) possessed the ability to control the imbalance between Th17 and Treg. Given that Th17 and Treg are derived from a common $CD4^+$ T cell precursor, we summarize the current knowledge of MSC-mediated inhibition of the mammalian target of rapamycin (mTOR), which is a master regulator of $CD4^+$ T cell polarization. During $CD4^+$ T cell differentiation, mTOR signaling mediates Th17 and Treg differentiation *via* hypoxia-inducible factor-1α (HIF-1α)-dependent metabolic regulation and signaling pathway, as well as mTOR-mediated phosphorylation of signal transducer and activator of transcription (STAT) 3 and 5. Through interfering with mTOR signaling, MSC restrains $CD4^+$ T cell differentiation into Th17, but in turn promotes Treg generation. Thus, this review indicates that MSC-mediated Th17-to-Treg polarization is expected to act as new immunotherapy for kidney injury.

Keywords: mesenchymal stem cell, kidney injury, regulatory T cell, T helper 17 cell, mTOR

INTRODUCTION

Renal tubular epithelial cell (RTEC) injury due to ischemia–reperfusion injury (IRI), nephrotoxicity and other causes lead to a rapid decline in renal function and over-activated inflammatory immune response. If the inflammatory damage to RTEC was not controlled timely, a continuous renal injury would result in renal fibrosis and failure (1–3). Unfortunately, current pharmacological interventions have failed to prevent intrarenal inflammatory cascade. However, increasing studies showed that a diverse mesenchymal stem cell (MSC) population could form a balanced inflammatory microenvironment and protect injured RTEC by regulating mammalian target of

rapamycin (mTOR)-mediated balance between pro-inflammatory T helper 17 cell (Th17) and anti-inflammatory regulatory T cell (Treg) (4–7).

In this review, we will introduce the imbalance between Th17 and Treg in RTEC injury, subsequently discuss MSC control for Th17 and Treg balance, and ultimately integrate current major mechanisms of MSC regulation on mTOR-mediated Th17 and Treg differentiation.

THE IMBALANCE AND FUNCTIONS OF TH17 AND TREG IN RTEC INJURY

Th17 characterized by the expression of specific transcription factor RAR-related receptor γ thymus isoform (RORγt) plays a vital role in RTEC damage by producing IL-17 and other pro-inflammatory cytokines (8, 9). However, through the specific immunoregulatory functions, Treg that express the transcription factor forkhead box protein P3 (Foxp3) can inhibit Th17-mediated inflammatory response, promote inhibitory cytokine secretion, and ultimately protect renal injury (5, 6, 10).

Th17-Dominant Kidney Damage

Numerous studies indicated that Th17 participated as the main kidney infiltrating inflammatory mediator in RTEC injury due to ureteral obstruction, acute kidney injury, chronic kidney disease, etc (11–14). Moreover, some studies reported that the Th17 number and Th17/Treg ratio were positively associated with the level of renal injury. Meanwhile, Th17 deficient mice due to IL-17 or RORγt null significantly alleviated RTEC injury (15).

The predominant Th17 exerted a robust pro-inflammatory response in renal injury *via* the expressions of IL-17 and C–C–motif chemokine receptor (CCR) 6 (9, 16–18). For example, Kaneko et al. reported that Th17-secreting IL-17 bound to the corresponding receptor and promoted the expression of C-C motif chemokine ligand (CCL) 20, which attracted pro-inflammatory lymphocytes, dendritic cells, monocytes, and neutrophils to RTEC and ultimately led to immune-mediated damage to the kidney (9). Moreover, IL–17 was also found to increase CCL2 and IL–8 expressions in human proximal RTEC (19). Meanwhile, in obstructive renal injury, Th17 may contribute to the fibrotic transition from acute kidney injury to chronic kidney disease due to IL-17A expression (11, 12). In addition, some studies indicated that Th17 exerted distinct effector functions by necessarily migrating to target organs, which was mediated by chemokines [such as CCL20] and corresponding receptors [such as CCR6] (16, 19, 20). Moreover, Th17 was reported to induce CCL20 expression in RTEC, promoting the recruitment of other leukocytes to the kidney (19).

Treg-Weak Renoprotection

A recent study of single-cell RNA-seq of renal immune cells showed that Treg in regenerating renal existed the high expression of tissue repair- and pro-angiogenesis-related genes. This finding suggested that Treg provided potential kidney protection from kidney damage (21). Indeed, Treg was reported to exert a key role in preventing kidney injury and facilitating renal repair (22–24). For instance, Treg can prevent inflammatory cell accumulation and promote anti-inflammatory M2-macrophage generation, which exerted a renoprotective function during acute or chronic renal injury (5, 10). In addition, some studies reported that Treg depletion in mice enhanced inflammatory response and aggravated kidney injury (25–28). Moreover, the deficiency of Foxp3 in *Rag1*$^{-/-}$ mice also caused severe kidney damage (28). These studies indicated Treg renoprotection.

Unfortunately, Cao et al. reported that low percentages of Treg in intrarenal leucocytes existed in mice renal at 24 h after IRI (25). Moreover, Dong et al. also found decreased Treg number in patients with acute kidney injury (29). Meanwhile, increasing studies indicated that lower Treg infiltration, compared with Th17, existed in the injured kidney (30–32). Some studies also found that the adoptive transfer of Treg reduced pro-inflammatory IFN-γ and TNF-α generation, improved kidney function, and relieved acute tubular necrosis after migration to the postischemic kidney (33–35). These transferred cells were also able to inhibit innate immune-related renal injury *via* switching ATP into adenosine mediated by CD73 on the surface of Treg. Subsequently, the adenosine bound to the A_{2a} receptor and then enhanced the expression of PD-1, which exerted a vital renoprotective effect during IRI (34, 36).

THE BALANCE BETWEEN TH17 AND TREG CONTROLLED BY MSC

MSC is a fibroblast-like cell population extracted from fat, bone marrow, umbilical cord, and other tissues, with an immune privilege due to low immunogenicity (8). Recent studies showed that the most intriguing role of MSC was the immunomodulatory effect on the $CD4^+$ T cell polarization, with induction of Treg and suppression of Th17 differentiation (9, 37). For example, in an arthritis model, human MSC infusion could reduce Th17 number, promote Treg generation and enhance IL-10 production (38). Ghannam et al. reported that MSC induced a regulatory Th17 generation with RORγt downregulation and FOXP3 upregulation, which suppressed T cell proliferation and alleviated inflammation (39). Therefore, MSC-mediated Th17-to-Treg polarization creates anti-inflammatory processes and then protects injured RTEC.

The Enhancement of Treg Effect

Hu et al. reported that MSC infusion increased Treg proportion in the renal and spleen, protecting the injured kidney (40, 41). Moreover, Casiraghi et al. found that transfer of MSC expanded Treg proportion in lymphoid organs and further prolonged kidney allograft survival (42). Similarly, autologous transfer of MSC to patients after kidney transplantation possessed the ability to generate Treg (43). Indeed, it was demonstrated that Treg depletion eliminated MSC protection for organ injury (44).

It is well established that Treg and Th17 derive from a common $CD4^+$ T cell precursor, which offers the potential for MSC-mediated $CD4^+$ T cells differentiating into Treg but not Th17 (45). For instance, English et al. reported that $CD4^+$ T cells and MSC coculture suppressed lymphocyte proliferation due to an increased Treg differentiation (46). Meanwhile, Liu et al.

reported that the coculture of T cells and mice MSC showed a significant increase in Foxp3 expression and Treg proportion (47), which was similar to the human MSC coculture experiment (48). Moreover, both *in vivo* and *in vitro*, MSC favored Treg generation and their immunosuppressive function (49).

The Attenuation of Th17 Effect

Numerous studies indicated that the inhibition of Th17 and corresponding function could act as effective methods of protecting renal injury (12, 50–52). In vitro experiments from rat and human indicated that MSC possessed the ability to decrease Th17 generation from naive T cells and inhibit IL-17 and IL-22 secretion from Th17 (39, 53). Meanwhile, *in vivo*, the application of MSC suppressed EAE progress by reducing the secretion of IL-17 and IL-23 (54).

Furthermore, Th17 was reported to possess the ability to transdifferentiate into $Foxp3^{-}IL{-}10^{+}$ type 1 Treg (Tr1) with suppressive properties (55, 56). Moreover, MSC also was found to promote Foxp3 expression with increased IL-10 secretion, but suppress RORC expression with reduced IL-17 and IL-22 in differentiated Th17. Meanwhile, MSC stimulated by inflammatory cytokine showed a high CD54 expression, which contributed to the adhesion of Th17 to MSC and the induction of T cell with regulatory features (39). These findings suggest a new approach of treating injured RTEC by intervening pathogenic Th17 into suppressive Th17.

In addition, some studies indicated that Treg also possessed the ability to inhibit Th17-mediated kidney injury (12, 45, 57, 58). Particularly, recent studies reported a specialized Treg type 17 that colocalized with Th17 and exclusively inhibited Th17-mediated effect *via* spatial interaction, IL-10 production, and CCR6 expression (19, 59).

MSC-MEDIATED MTOR INHIBITION REGULATING TH17/TREG AXIS

Mechanistically, MSC regulates the balance between Th17 and Treg predominantly *via* indoleamine 2, 3-dioxgenase (IDO) and TGF-β secretions as well as other mechanisms, which mimic the rapamycin effect of inhibiting mTOR, including mTOR complex 1 (mTORC1) and 2 (mTORC2) (8, 9, 60–65). Accumulating evidence indicates that mTOR, a serine/threonine kinase, acts as a key regulator of metabolic programmers and signaling pathways in $CD4^{+}$ T cell differentiation (62, 66, 67). For example, stimulating mTOR activation in $CD4^{+}$ T cell drove glycolytic metabolism and promoted RORγt expression. However, MSC-mediated mTOR downregulation during $CD4^{+}$ T cell differentiation induced Treg generation by fostering oxidative metabolism and Foxp3 transcription. Thus, MSC-mediated mTOR inhibition in $CD4^{+}$ T cell promotes Th17-to-Treg polarization, conducive to protecting injured RTEC (5, 6, 8, 62–64) (**Figure 1**).

MSC Inhibition on mTOR Signaling

Several studies showed that MSC-producing IDO could inhibit Th17 differentiation, induce Treg generation, and subsequently prevent renal injury (9, 61, 64). IDO is the main enzyme for promoting tryptophan catabolism into kynurenine. However, tryptophan was reported to possess the ability to activate the Rag complex, which recruited and linked mTORC1 to Rheb on the lysosomes. Subsequently, mTORC1 was activated due to the spatial regulation of Rheb and Rag (68–70). These findings may explain the phenomenon that IDO-mediated tryptophan exhaustion caused mTORC1 (as a nutrient sensor) inhibition, which further suppressed Th17 number and function but promoted Treg generation. Moreover, IDO depletion or tryptophan supplement reversed the effects (9, 61, 62, 64).

In addition to IDO, TGF-β secreted by MSC plays a role for inducing Treg generation due to mTOR inhibition (8, 61, 63). Priyadharshini et al. found that exposure of Treg to TGF-β repressed S6 and Akt phosphorylation targeting mTORC1 and mTORC2, respectively. Moreover, TGF-β reprogrammed Treg metabolism by inhibiting PI3K-mediated mTOR signaling (63). These results are in line with the report that Smad3 phosphorylation mediated by the interaction between TGF-β/TGF-β receptor limited $CD4^{+}$ T cell proliferation and inhibited classic PI3K/Akt/mTOR pathway, which resembled rapamycin inhibition of mTOR signaling (65). Moreover, *in vitro*, the stimulation of TGF-β altogether with all-trans retinoic acid promoted the expression of a set of microRNAs such as microRNA-15b/16, which inhibited Akt/mTOR signaling and further induced Treg generation (71, 72).

Additionally, Yoo et al. demonstrated that MSC suppressed CD25 expression on the surface of T cells *via* increased liver kinase B1 and AMP-activated protein kinase phosphorylation induced by low adenosine triphosphate (ATP) concentration (66). Liver kinase B1, a serine/threonine kinase, can increase phosphorylation of AMP-activated protein kinase and then inhibit mTORC1 signaling, which ultimately reduces inflammatory cytokine secretion in T cells (60, 66).

mTOR-Mediated Th17/Treg Axis

Increasing studies showed that mTOR-low populations of $CD4^{+}$ T cells with increased oxidative phosphorylation were likely to become Treg with high signal transducer and activator of transcription (STAT) 5 and Foxp3 expression, while mTOR-high populations with enhanced hypoxia-inducible factor-1α (HIF-1α)-mediated glycolysis were enriched for Th17 with high STAT3 and RORγt expression (22, 73, 74). Moreover, the transfer of Treg pretreated by pharmacological mTOR inhibition to kidney injury mice following by IRI can improve the renal function recovery and reduce kidney fibrosis due to enhanced immunoregulatory effect of Treg (75). These studies indicated that mTOR inhibition played a vital role in renal protection by promoting Treg but not Th17 differentiation, which involved mTOR-dependent energy metabolism and protein translation networks.

mTOR/HIF-1α-Mediated Metabolic Reprogramming

With $CD4^{+}$ T cell activation, some glycolytic molecules, such as glyceraldehyde-3-phosphate dehydrogenase, lactate dehydrogenase and glucose transporters were upregulated to promote glucose uptake due to the increased bioenergetic demands (66). The process can be regulated by mTOR-mediated signaling, such as the transcription

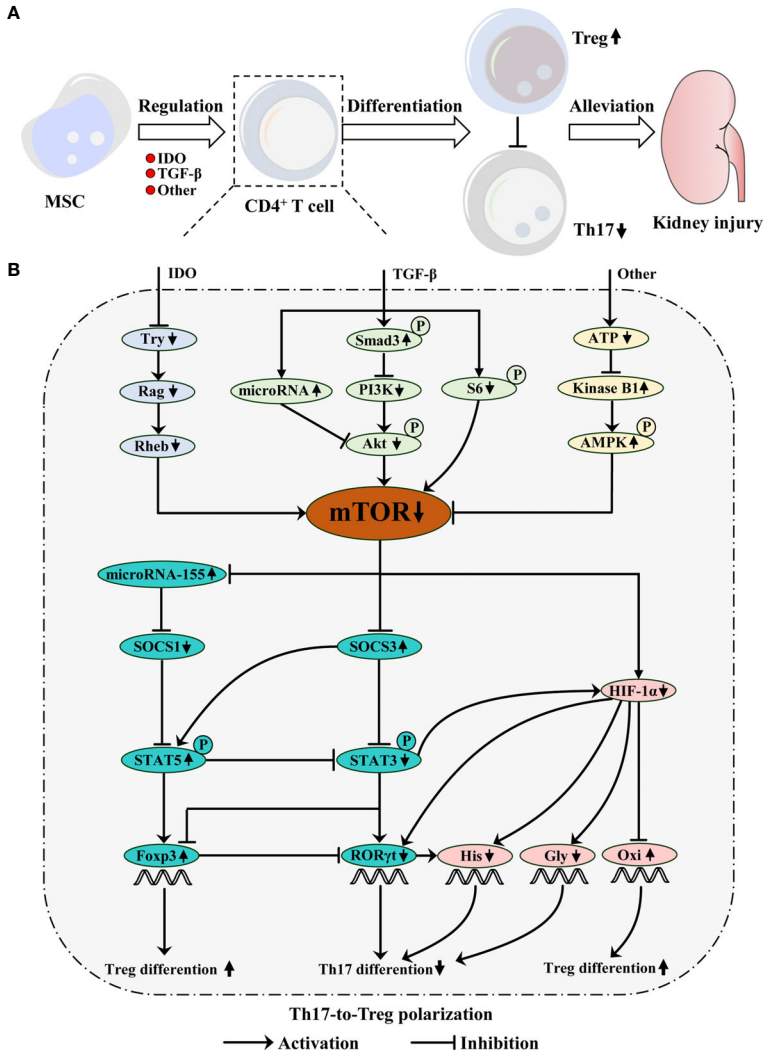


FIGURE 1 | Mesenchymal stem cell (MSC) protects kidney injury *via* mTOR-mediated Th17-to-Treg polarization. **(A)** MSC inhibits mTOR signaling during $CD4^+$ T cell differentiation *via* IDO and TGF-β secretions as well as other mechanisms, which restrains Th17 differentiation, but promotes Treg generation. Consequently, MSC-mediated Th17-to-Treg polarization alleviates kidney injury. **(B)** TGF-β phosphorylates Smad3, which inhibits PI3K/Akt/mTOR pathway. TGF-β also inhibits S6-mediated mTOR signaling. Moreover, TGF-β promotes microRNA expression, which can inhibit Akt/mTOR pathway. IDO can deplete tryptophan (Try), which results in mTOR inhibition mediated by the Rag and following Rheb. Additionally, MSC-mediated low ATP concentration increases kinase B1, subsequently phosphorylates AMPK, ultimately inhibits mTOR signaling. However, mTOR signaling can inhibit microRNA-155 and SOCS3 expression, but promote HIF-1α generation. Briefly, microRNA-155 inhibits SOCS1 expression, which can restrain STAT5 phosphorylation. The phosphorylation of STAT5 not only restrains STAT3 phosphorylation, but also upregulates Foxp3 expression, which promotes Treg differentiation. SOCS3 can promote STAT5 phosphorylation, but inhibit STAT3-mediated HIF-1α and RORγt expression, which ultimately reduces Th17 differentiation. Moreover, STAT3 possesses the ability to inhibit Foxp3 expression. HIF-1α can promote RORγt expression and increase histone acetylation (His) with RORγt collaboration, which possesses the ability to induce Th17 differentiation. Meanwhile, HIF-1α inhibition can promote Treg but not Th17 differentiation by mediating glycolysis (Gly) switching into the oxidative phosphorylation (Oxi).

factor HIF-1α expression (76). For example, mTOR was reported to promote STAT3 activation, which increased HIF-1α expression *via* direct binding of STAT3 to the HIF-1α gene promoter region (45, 62). Subsequently, increased HIF-1α can mediate oxidative phosphorylation switching into aerobic glycolysis by targeting glycolytic genes such as glycolytic enzymes hexokinase 2, monocarboxylic acid transporter member 4, and glucose transporter 1, which are vital for Th17 differentiation and IL-17 expression (22, 62). Consequently, HIF-1α-mediated glycolytic molecules act as main metabolic checkpoints to regulate $CD4^+$ T cell polarization. For instance, HIF-1α deficiency in $CD4^+$ T cells resulted in less Th17 and IL-17 generations by diminishing glycolytic molecule expression (22, 45, 62). In addition, the glucose analogue 2-deoxyglucose was also reported to promote Treg differentiation but dampen the generation of Th17 during $CD4^+$ T cell polarization by inhibiting key glycolytic molecules (22). Therefore, HIF-1α-dependent metabolic reprogramming mediated by mTOR signaling distinguishes the lineage decisions between Treg and Th17.

mTOR/HIF-1α-Mediated Signaling Pathway

In addition to metabolic regulation, mTOR-mediated HIF-1α also directly binds to RORγt gene promoter region and subsequently promotes RORγt transcription. Moreover, HIF-1α with RORγt collaboration activates p300-mediated histone acetyltransferase, which increases histone acetylation, opens up the chromatin structure, and ultimately facilitates Th17 differentiation (45, 77). Additionally, HIF-1α was reported to activate the process that promoted the degradation of Foxp3, which inhibited the differentiation of Treg. Foxp3 degradation may explain that $Foxp3^+ROR\gamma t^+$ Treg/TH17 precursors committed to the differentiation of Th17 by diminishing Foxp3 transcription (45). Moreover, HIF-1α could drive the IL-23 receptor upregulation, vital for IL-17 and Th17 generation (22, 78). These results were in line with the report that HIF-1α has high expression during the differentiation of Th17, while Treg showed a low level of HIF-1α (26). Correspondingly, HIF-1α absence mediated by mTOR inhibition impaired Th17 differentiation as well as IL-17 and IL-23 receptor expressions, but upregulated Foxp3 expression (22, 79). Meanwhile, Foxp3 upregulation antagonizes RORγt expression and Th17 generation. Furthermore, Shi et al. also indicated that Ctla4 and Gpr83 molecules on the surface of Treg were upregulated due to HIF-1α absence (22). Therefore, mTOR-mediated HIF-1α signaling would be expected to act as a key regulator of $CD4^+$ T cell polarization.

mTOR/STATs-Mediated Signaling Pathway

Several studies showed that mTORC1 could activate STAT3 by inhibiting the suppressor of cytokine signaling (SOCS) 3 expression, which could repress STAT3 phosphorylation or induce proteasomal degradation of STAT3 (76, 80, 81). Moreover, mTORC1 inhibited STAT5 activation by downregulating microRNA-155, an inhibitor of the SOCS1 (82–84). Similarly, mTORC1 inhibition was reported to increase the phosphorylation of STAT5 by inhibiting SOCS3 expression (76, 85).

Accumulating studies showed that STAT3 induced RORγt and IL-17 expressions, while the deficiency of STAT3 impaired the expressions of RORγt and IL-17, but increased Foxp3 expression (62, 76, 86, 87). However, through competition with STAT3, STAT5 could bind to IL-17a gene sites, subsequently modifying the IL-17 gene locus due to a decrease in histone-3 lysine-4 trimethylation (IL-17 expression promoter) and increase in histone 3 lysine 27 trimethylation (IL-17 expression inhibition) (62, 87). Moreover, STAT5 activation was reported to promote the differentiation of Treg by upregulating the expression of Foxp3 (76, 88, 89). Interestingly, several studies indicated that $Foxp3^+ROR\gamma t^+$ Treg/TH17 precursors under an anti-inflammatory environment (such as high TGF-β levels without IL-6) showed a high Foxp3 expression that antagonized the binding of RORγt to DNA *via* an exon 2-encoded sequence interaction, which inhibited IL-17 expression and further pushed T cell differentiation towards the Treg. Reversely, given that STAT3 activation stimulated by pro-inflammatory cytokines (such as IL-21 or IL-6 with low TGF-β levels) overcame Foxp3 antagonism of RORγt, the precursors tended to IL-23 receptor upregulation and subsequently pushed T cell differentiation into Th17 (45, 90). Therefore, the activation of STAT3 or STAT5 mediated Th17 or Treg differentiation.

CONCLUSIONS AND PERSPECTIVES

Currently, MSC has been extensively reported as a promising therapy for renal injury due to its renoprotection for injured RTEC (91–93). However, the therapeutic effect of MSC was greatly weakened in the light of the fact that a majority of MSC were stuck in the lungs after adoptive transfer, with a small part reaching to the spleen, liver, renal, and other organs (1, 94). In view of a similar mechanism of mTOR inhibition, the transfer of MSC combination with rapamycin was also reported to exert immunosuppressive effect and protect injured RTEC to a higher degree (66). Although MSC-mediated Th17-to-Treg polarization mainly depended on mTOR inhibition, the immunoregulatory mechanism was complex and not fully understood. Therefore, a successful application would rely on deep exploration and further resolution of the unanswered question.

AUTHOR CONTRIBUTIONS

YL, JG, and PZ conceived the conception, performed the literature search and wrote the manuscript. YC, YJ, JW, and SX performed the literature search and participated in the writing. RR conceived the conception and revised the manuscript. All authors contributed to the article and approved the submitted version.

FUNDING

This work was supported by the National Key R&D Program of China (2018YFA0107501) and National Natural Science Foundation of China (81770747 and 81970646).

REFERENCES

1. Fazekas B, Griffin MD. Mesenchymal Stromal Cell-Based Therapies for Acute Kidney Injury: Progress in the Last Decade. *Kidney Int* (2020) 97(6):1130–40. doi: 10.1016/j.kint.2019.12.019
2. Zilberman-Itskovich S, Efrati S. Mesenchymal Stromal Cell Uses for Acute Kidney Injury-Current Available Data and Future Perspectives: A Mini-Review. *Front Immunol* (2020) 11:1369. doi: 10.3389/fimmu.2020.01369
3. Liu Y, Fang J. Mesenchymal Stem Cells as Therapeutic Agents and Novel Carriers for the Delivery of Candidate Genes in Acute Kidney Injury. *Stem Cells Int* (2020) 2020:8875554. doi: 10.1155/2020/8875554
4. Savio-Silva C, Soinski-Sousa PE, Balby-Rocha M, Lira AO, Rangel EB. Mesenchymal Stem Cell Therapy in Acute Kidney Injury (AKI): Review and Perspectives. *Rev Assoc Med Bras* (20201992) 66Suppl 1(Suppl 1):s45–54. doi: 10.1590/1806-9282.66.S1.45
5. Song T, Eirin A, Zhu X, Zhao Y, Krier JD, Tang H, et al. Mesenchymal Stem Cell-Derived Extracellular Vesicles Induce Regulatory T Cells to Ameliorate

Chronic Kidney Injury. *Hypertension* (2020) 75(5):1223–32. doi: 10.1161/HYPERTENSIONAHA.119.14546
6. Zhu Z, Han C, Xian S, Zhuang F, Ding F, Zhang W, et al. Placental Mesenchymal Stromal Cells (PMSCs) and PMSC-Derived Extracellular Vesicles (PMSC-EVs) Attenuated Renal Fibrosis in Rats With Unilateral Ureteral Obstruction (UUO) by Regulating CD4(+) T Cell Polarization. *Stem Cells Int* (2020) 2020:2685820. doi: 10.1155/2020/2685820
7. Shi Y, Wang Y, Li Q, Liu K, Hou J, Shao C, et al. Immunoregulatory Mechanisms of Mesenchymal Stem and Stromal Cells in Inflammatory Diseases. *Nat Rev Nephrol* (2018) 14(8):493–507. doi: 10.1038/s41581-018-0023-5
8. Duffy MM, Ritter T, Ceredig R, Griffin MD. Mesenchymal Stem Cell Effects on T-Cell Effector Pathways. *Stem Cell Res Ther* (2011) 2(4):34. doi: 10.1186/scrt75
9. Yang Y, Liu K, Chen Y, Gong Y, Liang Y. Indoleamine 2,3-Dioxygenase (IDO) Regulates Th17/Treg Immunity in Experimental Iga Nephropathy. *Folia Biol (Praha)* (2019) 65(2):101–8.
10. Sharma R, Kinsey GR. Regulatory T Cells in Acute and Chronic Kidney Diseases. *Am J Physiol Renal Physiol* (2018) 314(5):F679–98. doi: 10.1152/ajprenal.00236.2017
11. Peng X, Xiao Z, Zhang J, Li Y, Dong Y, Du J, et al. IL-17A Produced by Both Gammadelta T and Th17 Cells Promotes Renal Fibrosis Via RANTES-Mediated Leukocyte Infiltration After Renal Obstruction. *J Pathol* (2015) 235(1):79–89. doi: 10.1002/path.4430
12. Mehrotra P, Patel JB, Ivancic CM, Collett JA, Basile DP. Th-17 Cell Activation in Response to High Salt Following Acute Kidney Injury Is Associated With Progressive Fibrosis and Attenuated by AT-1R Antagonism. *Kidney Int* (2015) 88(4):776–84. doi: 10.1038/ki.2015.200
13. Mehrotra P, Sturek M, Neyra JA, Basile DP. Calcium Channel Orai1 Promotes Lymphocyte IL-17 Expression and Progressive Kidney Injury. *J Clin Invest* (2019) 129(11):4951–61. doi: 10.1172/JCI126108
14. Pindjakova J, Hanley SA, Duffy MM, Sutton CE, Weidhofer GA, Miller MN, et al. Interleukin-1 Accounts for Intrarenal Th17 Cell Activation During Ureteral Obstruction. *Kidney Int* (2012) 81(4):379–90. doi: 10.1038/ki.2011.348
15. Chan AJ, Alikhan MA, Odobasic D, Gan PY, Khouri MB, Steinmetz OM, et al. Innate IL-17A-Producing Leukocytes Promote Acute Kidney Injury Via Inflammasome and Toll-Like Receptor Activation. *Am J Pathol* (2014) 184(5):1411–8. doi: 10.1016/j.ajpath.2014.01.023
16. Zhang YM, Liu XZ, Zhou XJ, Liu LJ, Shi SF, Hou P, et al. A Functional Variant rs3093023 in CCR6 is Associated With IgA Nephropathy by Regulating Th17 Cells in a North Han Chinese Population. *Front Immunol* (2021) 12:600598. doi: 10.3389/fimmu.2021.600598
17. Jang SG, Lee J, Hong SM, Kwok SK, Cho ML, Park SH, et al. Metformin Enhances the Immunomodulatory Potential of Adipose-Derived Mesenchymal Stem Cells Through STAT1 in an Animal Model of Lupus. *Rheumatology (Oxford)* (2020) 59(6):1426–38. doi: 10.1093/rheumatology/kez631
18. Shanmugasundaram U, Bucsan AN, Ganatra SR, Ibegbu C, Quezada M, Blair RV, et al. Pulmonary Mycobacterium Tuberculosis Control Associates With CXCR3- and CCR6-expressing Antigen-Specific Th1 and Th17 Cell Recruitment. *JCI Insight* (2020) 5(14):e137858. doi: 10.1172/jci.insight.137858
19. Krebs CF, Schmidt T, Riedel JH, Panzer U. T Helper Type 17 Cells in Immune-Mediated Glomerular Disease. *Nat Rev Nephrol* (2017) 13(10):647–59. doi: 10.1038/nrneph.2017.112
20. Koga T, Otomo K, Mizui M, Yoshida N, Umeda M, Ichinose K, et al. Calcium/Calmodulin-Dependent Kinase IV Facilitates the Recruitment of Interleukin-17-Producing Cells to Target Organs Through the CCR6/CCL20 Axis in Th17 Cell-Driven Inflammatory Diseases. *Arthritis Rheumatol* (2016) 68(8):1981–8. doi: 10.1002/art.39665
21. Do VDF, Lafont A, Beibel M, Martin K, Darribat K, Cuttat R, et al. Immune Cell Landscaping Reveals a Protective Role for Regulatory T Cells During Kidney Injury and Fibrosis. *JCI Insight* (2020) 5(3):e130651. doi: 10.1172/jci.insight.130651
22. Shi LZ, Wang R, Huang G, Vogel P, Neale G, Green DR, et al. HIF1alpha-Dependent Glycolytic Pathway Orchestrates a Metabolic Checkpoint for the Differentiation of TH17 and Treg Cells. *J Exp Med* (2011) 208(7):1367–76. doi: 10.1084/jem.20110278
23. Ali R, Patel SN, Hussain T. Angiotensin Type 2 Receptor Activation Limits Kidney Injury During Early Phase and Induces Treg Cells During Late Phase of Renal Ischemia. *Am J Physiol Renal Physiol* (2021) 320(5):F814–25. doi: 10.1152/ajprenal.00507.2020
24. Sakai R, Ito M, Komai K, Iizuka-Koga M, Matsuo K, Nakayama T, et al. Kidney GATA3(+) Regulatory T Cells Play Roles in the Convalescence Stage After Antibody-Mediated Renal Injury. *Cell Mol Immunol* (2020) 18(5):1249–61. doi: 10.1038/s41423-020-00547-x
25. Jun C, Qingshu L, Ke W, Ping L, Jun D, Jie L, et al. Protective Effect of CXCR3(+)CD4(+)CD25(+)Foxp3(+) Regulatory T Cells in Renal Ischemia-Reperfusion Injury. *Mediators Inflamm* (2015) 2015:360973. doi: 10.1155/2015/360973
26. Kinsey GR, Sharma R, Huang L, Li L, Vergis AL, Ye H, et al. Regulatory T Cells Suppress Innate Immunity in Kidney Ischemia-Reperfusion Injury. *J Am Soc Nephrol* (2009) 20(8):1744–53. doi: 10.1681/ASN.2008111160
27. Jun C, Ke W, Qingshu L, Ping L, Jun D, Jie L, et al. Protective Effect of CD4(+)CD25(high)CD127(low) Regulatory T Cells in Renal Ischemia-Reperfusion Injury. *Cell Immunol* (2014) 289(1-2):106–11. doi: 10.1016/j.cellimm.2014.04.002
28. Kinsey GR, Sharma R, Huang L, Li L, Vergis AL, Ye H, et al. Regulatory T Cells Suppress Innate Immunity in Kidney Ischemia-Reperfusion Injury. *J Am Soc Nephrol* (2009b) 20(8):1744–53. doi: 10.1681/ASN.2008111160
29. Dong Q, Cai C, Gao F, Chen P, Gong W, Shen M, et al. Defective Treg Response in Acute Kidney Injury was Caused by a Reduction in TIM-3(+) Treg Cells. *Immunol Invest* (2019) 48(1):27–38. doi: 10.1080/08820139.2018.1493497
30. Wang Y, Zhang S, Zhang N, Feng M, Liang Z, Zhao X, et al. Reduced Activated Regulatory T Cells and Imbalance of Th17/activated Treg Cells Marks Renal Involvement in ANCA-Associated Vasculitis. *Mol Immunol* (2020) 118:19–29. doi: 10.1016/j.molimm.2019.11.010
31. Li Y, Shi Y, Huang Z, Bai Y, Niu Q, Cai B, et al. CNI Induced Th17/Treg Imbalance and Susceptibility to Renal Dysfunction in Renal Transplantation. *Int Immunopharmacol* (2011) 11(12):2033–8. doi: 10.1016/j.intimp.2011.08.015
32. Wang D, Zhang Z, Si Z, Yang Y, Li S, Xue Y, et al. Dapagliflozin Reverses the Imbalance of T Helper 17 and T Regulatory Cells by Inhibiting SGK1 in a Mouse Model of Diabetic Kidney Disease. *FEBS Open Bio* (2021) 11(5):1395–405. doi: 10.1002/2211-5463.13147
33. Gandolfo MT, Jang HR, Bagnasco SM, Ko GJ, Agreda P, Satpute SR, et al. Foxp3+ Regulatory T Cells Participate in Repair of Ischemic Acute Kidney Injury. *Kidney Int* (2009) 76(7):717–29. doi: 10.1038/ki.2009.259
34. Kinsey GR, Sharma R, Okusa MD. Regulatory T Cells in AKI. *J Am Soc Nephrol* (2013) 24(11):1720–6. doi: 10.1681/ASN.2013050502
35. Heidari N, Abbasi-Kenarsari H, Namaki S, Baghaei K, Zali MR, Ghaffari KS, et al. Adipose-Derived Mesenchymal Stem Cell-Secreted Exosome Alleviates Dextran Sulfate Sodium-Induced Acute Colitis by Treg Cell Induction and Inflammatory Cytokine Reduction. *J Cell Physiol* (2021) 236(8):5906–20. doi: 10.1002/jcp.30275
36. Alikhan MA, Huynh M, Kitching AR, Ooi JD. Regulatory T Cells in Renal Disease. *Clin Transl Immunol* (2018) 7(1):e1004. doi: 10.1002/cti2.1004
37. Lee DK, Song SU. Immunomodulatory Mechanisms of Mesenchymal Stem Cells and Their Therapeutic Applications. *Cell Immunol* (2018) 326:68–76. doi: 10.1016/j.cellimm.2017.08.009
38. Gonzalez MA, Gonzalez-Rey E, Rico L, Buscher D, Delgado M. Treatment of Experimental Arthritis by Inducing Immune Tolerance With Human Adipose-Derived Mesenchymal Stem Cells. *Arthritis Rheum* (2009) 60(4):1006–19. doi: 10.1002/art.24405
39. Ghannam S, Pene J, Moquet-Torcy G, Jorgensen C, Yssel H. Mesenchymal Stem Cells Inhibit Human Th17 Cell Differentiation and Function and Induce a T Regulatory Cell Phenotype. *J Immunol* (2010) 185(1):302–12. doi: 10.4049/jimmunol.0902007
40. Jang HR, Park JH, Kwon GY, Lee JE, Huh W, Jin HJ, et al. Effect of Preemptive Treatment With Human Umbilical Cord Blood-Derived Mesenchymal Stem Cells on the Development of Renal Ischemia-Reperfusion Injury in Mice. *Am J Physiol Renal Physiol* (2014) 307(10):F1149–61. doi: 10.1152/ajprenal.00555.2013
41. Hu J, Zhang L, Wang N, Ding R, Cui S, Zhu F, et al. Mesenchymal Stem Cells Attenuate Ischemic Acute Kidney Injury by Inducing Regulatory T Cells Through Splenocyte Interactions. *Kidney Int* (2013) 84(3):521–31. doi: 10.1038/ki.2013.114

42. Casiraghi F, Azzollini N, Todeschini M, Cavinato RA, Cassis P, Solini S, et al. Localization of Mesenchymal Stromal Cells Dictates Their Immune or Proinflammatory Effects in Kidney Transplantation. *Am J Transplant* (2012) 12(9):2373–83. doi: 10.1111/j.1600-6143.2012.04115.x
43. Perico N, Casiraghi F, Introna M, Gotti E, Todeschini M, Cavinato RA, et al. Autologous Mesenchymal Stromal Cells and Kidney Transplantation: A Pilot Study of Safety and Clinical Feasibility. *Clin J Am Soc Nephrol* (2011) 6 (2):412–22. doi: 10.2215/CJN.04950610
44. Gazdic M, Markovic BS, Arsenijevic A, Jovicic N, Acovic A, Harrell CR, et al. Crosstalk Between Mesenchymal Stem Cells and T Regulatory Cells Is Crucially Important for the Attenuation of Acute Liver Injury. *Liver Transpl* (2018) 24(5):687–702. doi: 10.1002/lt.25049
45. Dang EV, Barbi J, Yang HY, Jinasena D, Yu H, Zheng Y, et al. Control of T(H) 17/T(reg) Balance by Hypoxia-Inducible Factor 1. *Cell* (2011) 146(5):772–84. doi: 10.1016/j.cell.2011.07.033
46. English K, Ryan JM, Tobin L, Murphy MJ, Barry FP, Mahon BP, et al. Cell Contact, Prostaglandin E(2) and Transforming Growth Factor Beta 1 Play Non-Redundant Roles in Human Mesenchymal Stem Cell Induction of CD4+ CD25(High) Forkhead Box P3+ Regulatory T Cells. *Clin Exp Immunol* (2009) 156(1):149–60. doi: 10.1111/j.1365-2249.2009.03874.x
47. Liu X, Ren S, Qu X, Ge C, Cheng K, Zhao RC, et al. Mesenchymal Stem Cells Inhibit Th17 Cells Differentiation Via IFN-Gamma-Mediated SOCS3 Activation. *Immunol Res* (2015) 61(3):219–29. doi: 10.1007/s12026-014-8612-2
48. Casiraghi F, Perico N, Cortinovis M, Remuzzi G. Mesenchymal Stromal Cells in Renal Transplantation: Opportunities and Challenges. *Nat Rev Nephrol* (2016) 12(4):241–53. doi: 10.1038/nrneph.2016.7
49. Prevosto C, Zancolli M, Canevali P, Zocchi MR, Poggi A. Generation of CD4+ or CD8+ Regulatory T Cells Upon Mesenchymal Stem Cell-Lymphocyte Interaction. *Haematologica* (2007) 92(7):881–8. doi: 10.3324/haematol.11240
50. Motavalli R, Etemadi J, Soltani-Zangbar MS, Ardalan MR, Kahroba H, Roshangar L, et al. Altered Th17/Treg Ratio as a Possible Mechanism in Pathogenesis of Idiopathic Membranous Nephropathy. *Cytokine* (2021) 141:155452. doi: 10.1016/j.cyto.2021.155452
51. Marquez-Exposito L, Rodrigues-Diez RR, Rayego-Mateos S, Fierro-Fernandez M, Rodrigues-Diez R, Orejudo M, et al. Deletion of Delta-Like 1 Homologue Accelerates Renal Inflammation by Modulating the Th17 Immune Response. *FASEB J* (2021) 35(1):e21213. doi: 10.1096/fj.201903131R
52. Chen Y, Tao T, Wang W, Yang B, Cha X. Dihydroartemisinin Attenuated the Symptoms of Mice Model of Systemic Lupus Erythematosus by Restoring the Treg/Th17 Balance. *Clin Exp Pharmacol Physiol* (2021) 48(4):626–33. doi: 10.1111/1440-1681.13461
53. Tang J, Yang R, Lv L, Yao A, Pu L, Yin A, et al. Transforming Growth Factor-Beta-Expressing Mesenchymal Stem Cells Induce Local Tolerance in a Rat Liver Transplantation Model of Acute Rejection. *Stem Cells* (2016) 34 (11):2681–92. doi: 10.1002/stem.2437
54. Wang J, Wang G, Sun B, Li H, Mu L, Wang Q, et al. Interleukin-27 Suppresses Experimental Autoimmune Encephalomyelitis During Bone Marrow Stromal Cell Treatment. *J Autoimmun* (2008) 30(4):222–9. doi: 10.1016/j.jaut.2007.10.001
55. Gagliani N, Amezcua VM, Iseppon A, Brockmann L, Xu H, Palm NW, et al. Th17 Cells Transdifferentiate Into Regulatory T Cells During Resolution of Inflammation. *Nature* (2015) 523(7559):221–5. doi: 10.1038/nature14452
56. Brockmann L, Gagliani N, Steglich B, Giannou AD, Kempski J, Pelczar P, et al. IL-10 Receptor Signaling Is Essential for TR1 Cell Function In Vivo. *J Immunol* (2017) 198(3):1130–41. doi: 10.4049/jimmunol.1601045
57. Dellepiane S, Leventhal JS, Cravedi P. T Cells and Acute Kidney Injury: A Two-Way Relationship. *Front Immunol* (2020) 11:1546. doi: 10.3389/fimmu.2020.01546
58. Yang XY, Song J, Hou SK, Fan HJ, Lv Q, Liu ZQ, et al. Ulinastatin Ameliorates Acute Kidney Injury Induced by Crush Syndrome Inflammation by Modulating Th17/Treg Cells. *Int Immunopharmacol* (2020) 81:106265. doi: 10.1016/j.intimp.2020.106265
59. Kluger MA, Melderis S, Nosko A, Goerke B, Luig M, Meyer MC, et al. Treg17 Cells Are Programmed by Stat3 to Suppress Th17 Responses in Systemic Lupus. *Kidney Int* (2016) 89(1):158–66. doi: 10.1038/ki.2015.296
60. Gu Z, Tan W, Ji J, Feng G, Meng Y, Da Z, et al. Rapamycin Reverses the Senescent Phenotype and Improves Immunoregulation of Mesenchymal Stem Cells From MRL/lpr Mice and Systemic Lupus Erythematosus Patients Through Inhibition of the mTOR Signaling Pathway. *Aging (Albany NY)* (2016) 8(5):1102–14. doi: 10.18632/aging.100925
61. He Y, Zhou S, Liu H, Shen B, Zhao H, Peng K, et al. Indoleamine 2, 3-Dioxgenase Transfected Mesenchymal Stem Cells Induce Kidney Allograft Tolerance by Increasing the Production and Function of Regulatory T Cells. *Transplantation* (2015) 99(9):1829–38. doi: 10.1097/TP.0000000000000856
62. Ren W, Yin J, Duan J, Liu G, Tan B, Yang G, et al. mTORC1 Signaling and IL-17 Expression: Defining Pathways and Possible Therapeutic Targets. *Eur J Immunol* (2016) 46(2):291–9. doi: 10.1002/eji.201545886
63. Priyadharshini B, Loschi M, Newton RH, Zhang JW, Finn KK, Gerriets VA, et al. Cutting Edge: TGF-Beta and Phosphatidylinositol 3-Kinase Signals Modulate Distinct Metabolism of Regulatory T Cell Subsets. *J Immunol* (2018) 201(8):2215–9. doi: 10.4049/jimmunol.1800311
64. Terraza-Aguirre C, Campos-Mora M, Elizondo-Vega R, Contreras-Lopez RA, Luz-Crawford P, Jorgensen C, et al. Mechanisms Behind the Immunoregulatory Dialogue Between Mesenchymal Stem Cells and Th17 Cells. *Cells* (2020) 9(7):1660–80. doi: 10.3390/cells9071660
65. Delisle JS, Giroux M, Boucher G, Landry JR, Hardy MP, Lemieux S, et al. The TGF-Beta-Smad3 Pathway Inhibits CD28-Dependent Cell Growth and Proliferation of CD4 T Cells. *Genes Immun* (2013) 14(2):115–26. doi: 10.1038/gene.2012.63
66. Bottcher M, Hofmann AD, Bruns H, Haibach M, Loschinski R, Saul D, et al. Mesenchymal Stromal Cells Disrupt mTOR-Signaling and Aerobic Glycolysis During T-Cell Activation. *Stem Cells* (2016) 34(2):516–21. doi: 10.1002/stem.2234
67. Chi H. Regulation and Function of mTOR Signalling in T Cell Fate Decisions. *Nat Rev Immunol* (2012) 12(5):325–38. doi: 10.1038/nri3198
68. Inoki K, Kim J, Guan KL. AMPK and mTOR in Cellular Energy Homeostasis and Drug Targets. *Annu Rev Pharmacol Toxicol* (2012) 52:381–400. doi: 10.1146/annurev-pharmtox-010611-134537
69. Hellsten Y, Richter EA, Kiens B, Bangsbo J. AMP Deamination and Purine Exchange in Human Skeletal Muscle During and After Intense Exercise. *J Physiol* (1999) 520 Pt 3:909–20. doi: 10.1111/j.1469-7793.1999.00909.x
70. Sancak Y, Peterson TR, Shaul YD, Lindquist RA, Thoreen CC, Bar-Peled L, et al. The Rag GTPases Bind Raptor and Mediate Amino Acid Signaling to mTORC1. *Science* (2008) 320(5882):1496–501. doi: 10.1126/science.1157535
71. Schiavinato J, Haddad R, Saldanha-Araujo F, Baiochi J, Araujo AG, Santos SP, et al. TGF-Beta/atRA-Induced Tregs Express a Selected Set of microRNAs Involved in the Repression of Transcripts Related to Th17 Differentiation. *Sci Rep* (2017) 7(1):3627. doi: 10.1038/s41598-017-03456-8
72. Singh Y, Garden OA, Lang F, Cobb BS. MicroRNA-15b/16 Enhances the Induction of Regulatory T Cells by Regulating the Expression of Rictor and mTOR. *J Immunol* (2015) 195(12):5667–77. doi: 10.4049/jimmunol.1401875
73. Pollizzi KN, Waickman AT, Patel CH, Sun IH, Powell JD. Cellular Size as a Means of Tracking mTOR Activity and Cell Fate of CD4+ T Cells Upon Antigen Recognition. *PloS One* (2015) 10(4):e121710. doi: 10.1371/journal.pone.0121710
74. Pollizzi KN, Sun IH, Patel CH, Lo YC, Oh MH, Waickman AT, et al. Asymmetric Inheritance of mTORC1 Kinase Activity During Division Dictates CD8(+) T Cell Differentiation. *Nat Immunol* (2016) 17(6):704–11. doi: 10.1038/ni.3438
75. Chen G, Dong Z, Liu H, Liu Y, Duan S, Liu Y, et al. mTOR Signaling Regulates Protective Activity of Transferred CD4+Foxp3+ T Cells in Repair of Acute Kidney Injury. *J Immunol* (2016) 197(10):3917–26. doi: 10.4049/jimmunol.1601251
76. Saleiro D, Platanias LC. Intersection of mTOR and STAT Signaling in Immunity. *Trends Immunol* (2015) 36(1):21–9. doi: 10.1016/j.it.2014.10.006
77. Thompson PR, Wang D, Wang L, Fulco M, Pediconi N, Zhang D, et al. Regulation of the P300 HAT Domain Via a Novel Activation Loop. *Nat Struct Mol Biol* (2004) 11(4):308–15. doi: 10.1038/nsmb740
78. McGeachy MJ, Chen Y, Tato CM, Laurence A, Joyce-Shaikh B, Blumenschein WM, et al. The Interleukin 23 Receptor Is Essential for the Terminal Differentiation of Interleukin 17-Producing Effector T Helper Cells In Vivo. *Nat Immunol* (2009) 10(3):314–24. doi: 10.1038/ni.1698
79. Chapman NM, Chi H. mTOR Links Environmental Signals to T Cell Fate Decisions. *Front Immunol* (2014) 5:686. doi: 10.3389/fimmu.2014.00686

80. Yoshimura A, Naka T, Kubo M. SOCS Proteins, Cytokine Signalling and Immune Regulation. *Nat Rev Immunol* (2007) 7(6):454–65. doi: 10.1038/nri2093
81. Linossi EM, Babon JJ, Hilton DJ, Nicholson SE. Suppression of Cytokine Signaling: The SOCS Perspective. *Cytokine Growth Factor Rev* (2013) 24 (3):241–8. doi: 10.1016/j.cytogfr.2013.03.005
82. Shan J, Feng L, Sun G, Chen P, Zhou Y, Xia M, et al. Interplay Between mTOR and STAT5 Signaling Modulates the Balance Between Regulatory and Effective T Cells. *Immunobiology* (2015) 220(4):510–7. doi: 10.1016/j.imbio.2014.10.020
83. Lu LF, Thai TH, Calado DP, Chaudhry A, Kubo M, Tanaka K, et al. Foxp3-Dependent microRNA155 Confers Competitive Fitness to Regulatory T Cells by Targeting SOCS1 Protein. *Immunity* (2009) 30(1):80–91. doi: 10.1016/j.immuni.2008.11.010
84. Yao R, Ma YL, Liang W, Li HH, Ma ZJ, Yu X, et al. MicroRNA-155 Modulates Treg and Th17 Cells Differentiation and Th17 Cell Function by Targeting SOCS1. *PloS One* (2012) 7(10):e46082. doi: 10.1371/journal.pone.0046082
85. Delgoffe GM, Pollizzi KN, Waickman AT, Heikamp E, Meyers DJ, Horton MR, et al. The Kinase mTOR Regulates the Differentiation of Helper T Cells Through the Selective Activation of Signaling by mTORC1 and Mtorc2. *Nat Immunol* (2011) 12(4):295–303. doi: 10.1038/ni.2005
86. Milner JD, Brenchley JM, Laurence A, Freeman AF, Hill BJ, Elias KM, et al. Impaired T(H)17 Cell Differentiation in Subjects With Autosomal Dominant Hyper-IgE Syndrome. *Nature* (2008) 452(7188):773–6. doi: 10.1038/nature06764
87. Yang XP, Ghoreschi K, Steward-Tharp SM, Rodriguez-Canales J, Zhu J, Grainger JR, et al. Opposing Regulation of the Locus Encoding IL-17 Through Direct, Reciprocal Actions of STAT3 and STAT5. *Nat Immunol* (2011) 12(3):247–54. doi: 10.1038/ni.1995
88. Zhang S, Gan X, Qiu J, Ju Z, Gao J, Zhou J, et al. IL-10 Derived From Hepatocarcinoma Cells Improves Human Induced Regulatory T Cells Function Via JAK1/STAT5 Pathway in Tumor Microenvironment. *Mol Immunol* (2021) 133:163–72. doi: 10.1016/j.molimm.2021.02.014
89. Mendu SK, Stremska ME, Schappe MS, Moser EK, Krupa JK, Rogers JS, et al. Targeting the Ion Channel TRPM7 Promotes the Thymic Development of Regulatory T Cells by Promoting IL-2 Signaling. *Sci Signal* (2020) 13(661): eabb0619. doi: 10.1126/scisignal.abb0619
90. Zhou L, Lopes JE, Chong MM, Ivanov II, Min R, Victora GD, et al. TGF-Beta-Induced Foxp3 Inhibits T(H)17 Cell Differentiation by Antagonizing RORgammat Function. *Nature* (2008) 453(7192):236–40. doi: 10.1038/nature06878
91. Lohmann S, Eijken M, Moldrup U, Moller BK, Hunter J, Moers C, et al. Ex Vivo Administration of Mesenchymal Stromal Cells in Kidney Grafts Against Ischemia-Reperfusion Injury-Effective Delivery Without Kidney Function Improvement Posttransplant. *Transplantation* (2021) 105(3):517–28. doi: 10.1097/TP.0000000000003429
92. Zhao Y, Zhu XY, Song T, Zhang L, Eirin A, Conley S, et al. Mesenchymal Stem Cells Protect Renal Tubular Cells Via TSG-6 Regulating Macrophage Function and Phenotype Switching. *Am J Physiol Renal Physiol* (2021) 320 (3):F454–63. doi: 10.1152/ajprenal.00426.2020
93. Lohmann S, Pool M, Rozenberg KM, Keller AK, Moers C, Moldrup U, et al. Mesenchymal Stromal Cell Treatment of Donor Kidneys During Ex Vivo Normothermic Machine Perfusion: A Porcine Renal Autotransplantation Study. *Am J Transplant* (2020). doi: 10.1111/ajt.16473
94. Luk F, de Witte SF, Korevaar SS, Roemeling-van RM, Franquesa M, Strini T, et al. Inactivated Mesenchymal Stem Cells Maintain Immunomodulatory Capacity. *Stem Cells Dev* (2016) 25(18):1342–54. doi: 10.1089/scd.2016.0068

Conflict of Interest: The authors declare that the research was conducted in the absence of any commercial or financial relationships that could be construed as a potential conflict of interest.

Copyright © 2021 Luo, Guo, Zhang, Cheuk, Jiang, Wang, Xu and Rong. This is an open-access article distributed under the terms of the Creative Commons Attribution License (CC BY). The use, distribution or reproduction in other forums is permitted, provided the original author(s) and the copyright owner(s) are credited and that the original publication in this journal is cited, in accordance with accepted academic practice. No use, distribution or reproduction is permitted which does not comply with these terms.

frontiers in Immunology

REVIEW
published: 03 June 2021
doi: 10.3389/fimmu.2021.684496

Mesenchymal Stem Cell-Derived Extracellular Vesicles: A Potential Therapeutic Strategy for Acute Kidney Injury

Jia-Kun Li[1†], Cheng Yang[2†], Ying Su[1], Jing-Chao Luo[1], Ming-Hao Luo[3], Dan-Lei Huang[3], Guo-Wei Tu[1] and Zhe Luo[1,4*]*

[1] Department of Critical Care Medicine, Zhongshan Hospital, Fudan University, Shanghai, China, [2] Department of Urology, Zhongshan Hospital, Fudan University, Shanghai, China, [3] Shanghai Medical College, Fudan University, Shanghai, China, [4] Department of Critical Care Medicine, Xiamen Branch, Zhongshan Hospital, Fudan University, Xiamen, China

OPEN ACCESS

Edited by:
Bin Yang,
University of Leicester,
United Kingdom

Reviewed by:
Min Shi,
Sichuan University, China
Xiangchun Liu,
The Second Hospital of Shandong University, China

***Correspondence:**
Zhe Luo
luo.zhe@zs-hospital.sh.cn
Guo-Wei Tu
tu.guowei@zs-hospital.sh.cn

[†]These authors have contributed equally to this work

Specialty section:
This article was submitted to Molecular Innate Immunity, a section of the journal Frontiers in Immunology

Received: 23 March 2021
Accepted: 18 May 2021
Published: 03 June 2021

Citation:
Li J-K, Yang C, Su Y, Luo J-C, Luo M-H, Huang D-L, Tu G-W and Luo Z (2021) Mesenchymal Stem Cell-Derived Extracellular Vesicles: A Potential Therapeutic Strategy for Acute Kidney Injury. Front. Immunol. 12:684496. doi: 10.3389/fimmu.2021.684496

Acute kidney injury (AKI) is a common and potential life-threatening disease in patients admitted to hospital, affecting 10%–15% of all hospitalizations and around 50% of patients in the intensive care unit. Severe, recurrent, and uncontrolled AKI may progress to chronic kidney disease or end-stage renal disease. AKI thus requires more efficient, specific therapies, rather than just supportive therapy. Mesenchymal stem cells (MSCs) are considered to be promising cells for cellular therapy because of their ease of harvesting, low immunogenicity, and ability to expand *in vitro*. Recent research indicated that the main therapeutic effects of MSCs were mediated by MSC-derived extracellular vesicles (MSC-EVs). Furthermore, compared with MSCs, MSC-EVs have lower immunogenicity, easier storage, no tumorigenesis, and the potential to be artificially modified. We reviewed the therapeutic mechanism of MSCs and MSC-EVs in AKI, and considered recent research on how to improve the efficacy of MSC-EVs in AKI. We also summarized and analyzed the potential and limitations of EVs for the treatment of AKI to provide ideas for future clinical trials and the clinical application of MSC-EVs in AKI.

Keywords: acute kidney injury, mesenchymal stem cell, extracellular vesicle, cytokine, tubular epithelial cell

INTRODUCTION

Acute kidney injury (AKI) is a common and sometimes life-threatening disease in patients admitted to hospital, affecting 10%–15% of all hospitalizations and around 50% of patients in the intensive care unit (1). AKI is mainly caused by ischemia reperfusion injury (IRI), medication toxicity, and sepsis (1). Severe, recurrent, and uncontrolled AKI progresses to chronic kidney disease (CKD) or end-stage renal disease (2, 3). Treatments are currently limited to dialysis and kidney transplantation; however, these are restricted by the shortage of donor organs and high costs (4, 5), and there is thus a need to develop new and effective ways of treating AKI. The common pathological features of AKI include renal tubular epithelial cell (TEC) damage (6). TECs are injured as a result of an excessive inflammatory response, and undergo apoptosis *via* Bax/Bcl pathway activation (7, 8). In addition, the mechanistic target of rapamycin/mitogen-activated protein kinase (MAPK) signaling is consistently

activated in TECs and the mitochondria are damaged, leading to maladaptive repair of the injured TECs, interstitial fibrosis, and the progression of AKI into CKD (9–12). Meanwhile, expression changes in various cytokines can be detected in AKI, including vascular endothelial growth factor (VEGF), hepatocyte growth factor (HGF), and insulin-like growth factor-1 (IGF-1) (13, 14). These mechanisms involving TECs are regarded as potential therapeutic targets in AKI.

Different types of stem cells have recently been transplanted to prevent kidney damage. Among these, mesenchymal stem cells (MSCs) are considered to be one of the most promising types of cells for cellular therapy because of their ease of harvesting, low immunogenicity, and ability to be stored and expanded *in vitro* (15, 16). Notably, numerous preclinical and clinical studies have confirmed the potential role of MSCs in kidney protection and repair (17–22). However, the mechanisms by which MSCs exert their therapeutic effects remain controversial. Researchers previously believed that MSCs replaced injured cells through differentiation after introduction into the body, but this view was challenged by the fact that MSCs disappeared from the injured kidney and other organs within 72 h after administration, suggesting that differentiation and replacement of damaged cells by stem cells is probably a rare and late event in AKI *in vivo* (22, 23).

Several studies have also demonstrated that MSCs depend on complex and powerful endocrine and paracrine functions, and secrete extracellular vesicles to promote the recovery of renal function in AKI (24, 25). Secretion of growth factors, regulation of the inflammatory response, promotion of mitosis and cell proliferation, anti-apoptosis and anti-inflammatory effects, the reduction of fibrosis, and the promotion of angiogenesis have been reported in multiple studies (17). However, the main therapeutic effects of MSCs appear to be mediated by MSC-EVs, rather than by the MSCs themselves (26). Compared with MSCs, MSC-EVs have lower immunogenicity, easier storage, no tumorigenesis, and the ability to be artificially modified (24, 27–29). Increasing numbers of researchers have accordingly recognized the curative potential of MSC-EVs for AKI, and extensive preclinical research has proven their effectiveness and safety in AKI (30).

In this paper, we review the possible therapeutic mechanisms of MSCs and MSC-EVs in AKI, and consider recent research aimed at improving the therapeutic efficacy of MSC-EVs in AKI. Finally, we summarize and analyze the potential and limitations of EVs for the treatment of AKI, to provide ideas for future clinical trials and clinical applications of MSC-EV-based therapy.

MECHANISMS OF MSC THERAPY IN AKI

MSCs are the most widely used cells for AKI treatment and allograft protocols because they can be obtained from bone marrow and expanded in culture (17). MSCs originate from the mesoderm and have the ability to differentiate into mesenchymal and non-mesenchymal cell lines, including bone and cartilage (17).

Although MSCs are mainly obtained from bone marrow, they can also be isolated from other tissues such as liver, muscle, adipose tissue, and cord blood. Such cells are distinguished by their adherent growth in culture, expression of CD90, CD73, and CD105, and lack of expression of CD34, CD45, CD19, CD11a, and human leukocyte antigen-DR (18).

Previous studies indicated that the therapeutic effect of MSCs was largely dependent on their homing ability to injured organs (31). MSCs rely on their homing ability to localize in damaged tissues. In addition to their anti-inflammatory and vascular-support effects, the homing ability of MSCs supplements their paracrine function, and is involved in protecting microvessel density (32). Transplanted MSCs detect signals from injured kidney cells and are chemoattracted to the damaged site (33). During AKI, endothelial cells express high levels of tumor necrosis factor (TNF) and interleukins (ILs), which can up-regulate the β subunit of very late antigen-4 and vascular adhesion molecule 1 to mediate the effect of bone marrow MSCs on endothelial cell adhesion (33). CXC motif chemokine receptor 4 (CXCR4) is a specific receptor for chemokine stromal cell-derived factor-1 (CXCL12), and CXCR4 cells are responsible for the renal repair function in AKI (34). Location of the damaged tissue by MSCs can be mediated by stromal cell-derived factor-1, which is robustly up-regulated during AKI and mobilizes CXCR4 cell homing to the injured kidney tissue (35).

MSCs can exert significant therapeutic effects in terms of repairing the injured kidney and improving renal function after AKI, and are distributed to the spleen, lung, lymph nodes, and kidney following intravenous administration (36). However, intravenously administered MSCs disappear within 72 h, although some MSCs can remain around the glomerulus and perirenal capillaries following renal artery injection (37), suggesting that MSCs are unlikely to treat AKI through differentiation and the replacement of damaged cells. Meanwhile, MSCs located in the lung were also shown to affect AKI through a secretory function (38), and the hypothesis that the therapeutic effects of MSCs are mainly caused by a secretory mechanism appears to be more credible. Indeed, MSCs are involved in immune regulation, anti-inflammation, anti-apoptosis, and angiogenesis promotion in the local microenvironment in injured tissue, unrelated to their differentiation ability (39). Animal models of AKI are accompanied by significant changes in cytokines, including VEGF, HGF, epidermal growth factor (EGF), IGF-1, and transforming growth factor-β (TGF-β), which participate in endothelial cell apoptosis during AKI (40). These growth factors are also widely recognized as essential components in cell regeneration and kidney repair (41). MSCs secrete molecules directly or secrete EVs that carry molecules such as VEGF, HGF, IGF-1, IL-10, fibroblast growth factor (FGF), and TGF-α, and down-regulate the inducibility of related proinflammatory molecules (such as IL-1b and TNF-α), thus, having anti-inflammatory and anti-apoptosis effects and promoting kidney repair (42). Expression levels of related cytokines have been shown to be up-regulated during the treatment of AKI with

MSCs, while kidney tissue inflammation was reduced, indicating the relationship between cytokines and kidney repair in MSC-based therapy; however, more studies are needed to identify the specific mechanism involved (43).

MSC-EVS MEDIATE THE THERAPEUTIC EFFECTS OF MSCS IN AKI

Further research into MSC therapy of AKI has shown the presence of MSC-EVs in AKI models treated with MSCs (44). MSCs can also release proteins (43), RNA (45), and mitochondria (46) into injured kidney tissue *via* EVs, in addition to their secretory function (30) (**Figure 1**). Various cytokines and their mRNAs are found in MSC-EVs, and there is gradual recognition that the therapeutic effects of MSCs are mainly mediated by MSC-EVs (43, 47). The effects exerted by MSC-EVs are similar to those reported following MSC administration in previous studies (48). EVs derived from cells such as MSCs act as messengers mediating cell-to-cell communication by carrying a train of biologically active molecules, which is regarded as a critical mechanism in AKI (24, 45). As intercellular messengers, EVs implement the therapeutic effects of MSCs, including regulating the damaged local microenvironment, regulating gene expression in injured kidney cells, improving the survival of damaged cells, resisting apoptosis, regulating inflammation, and reducing mitochondrial damage (49). In MSC-EV-based therapy of AKI, EVs can locate to the injured kidney tissue spontaneously after administration (50). Importantly, this effect is specific to MSC-EVs, involving the EV adhesion molecules CD44 and CD29, while EVs obtained from fibroblasts are ineffective (51). EVs, as endocytic vesicles, are bound to the membrane and are released by eukaryotic cells in an evolutionarily conserved manner, enabling cell-to-cell communication (52). MSC-EVs are generated by the paracrine and secretory functions of MSCs, carrying proteins, lipids, and nucleic acids into injured tissues (53). EVs can also deliver mRNAs and microRNAs (miRNAs) *via* endocytosis to regulate target cells at the transcriptional level (**Figure 2**) (45). As an intercellular messenger, EVs are responsible for regulating the damaged local microenvironment, regulating gene expression in AKI cells, improving the survival of damaged cells, resisting apoptosis and inflammation, and reducing mitochondrial damage (11, 12, 54).

To identify the candidate therapeutic factors in EVs, Eirin et al. used proteomics to characterize the protein content of MSC-EVs derived from porcine MSCs from abdominal fat (42). The expression characteristics of MSC and EV markers detected by liquid chromatography-tandem mass spectrometry proteomics analysis showed that proteins enriched in MSC-EVs were related to a wide range of biological functions, including angiogenesis, blood coagulation, apoptosis, extracellular matrix remodeling, and inflammation regulation (43). Thus, EVs include selectively enriched protein cargo with specific biological characteristics, and these proteins are used for cell-to-cell communication to promote tissue repair. For example, MSC-derived EVs directly transferred IGF-1 receptors to renal tubular cells (13), accelerating kidney repair after AKI and reducing AKI by enhancing the activation of the

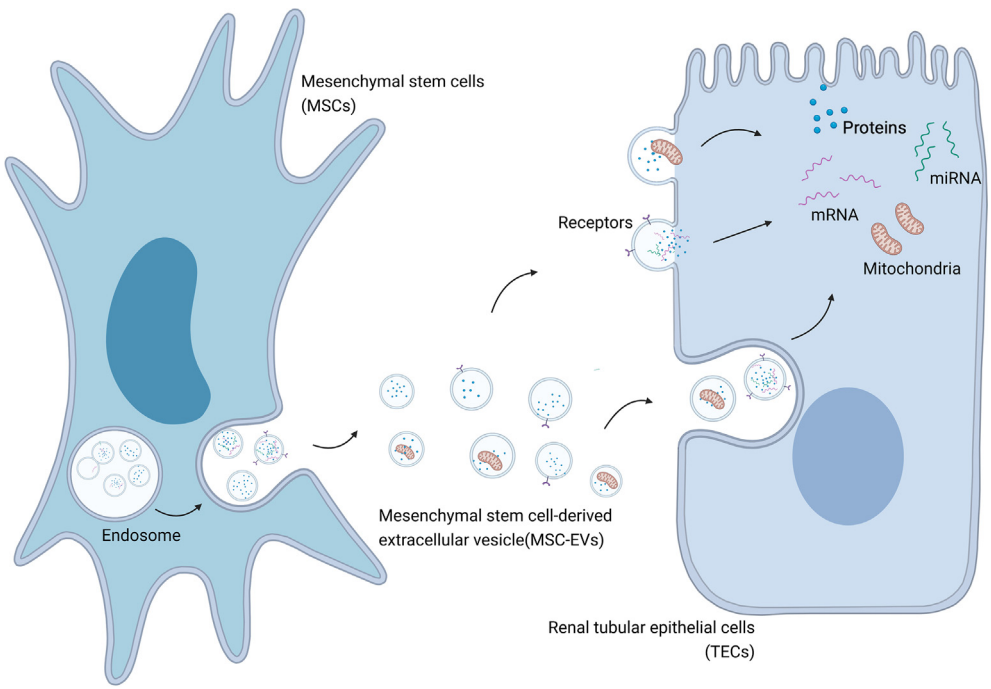


FIGURE 1 | MSC-EVs mediate transportation of biological modules to injured cells in AKI. Created with BioRender.com.

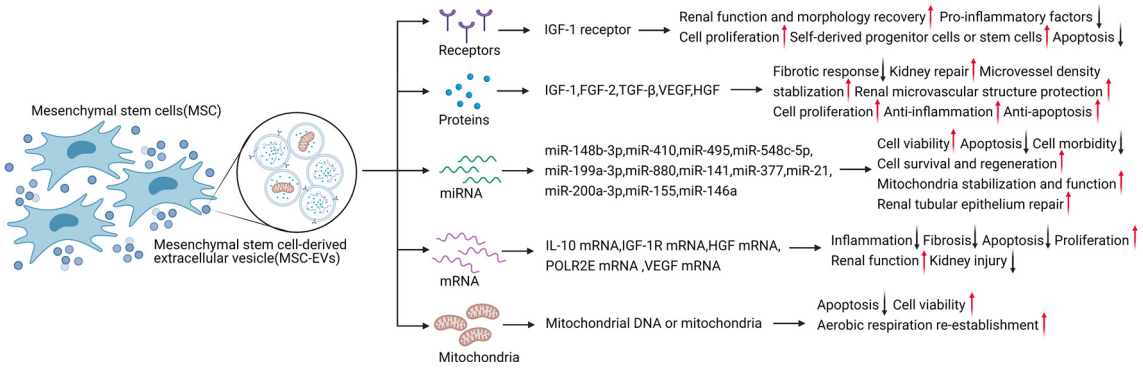


FIGURE 2 | MSC-EVs carry various contents to exert therapeutic effects in AKI. Created with BioRender.com.

Nrf2/ARE pathway to exert antioxidant effects (46, 55). Human adipose-derived MSCs (AD-MSCs) activated SOX9 in renal tubules and prevented the transformation of TGF-β1 into the pro-fibrotic phenotype induced by EV shuttling, resulting in anti-fibrotic effects (35, 56, 57).

Cytokines delivered by MSC-EVs and paracrine factors such as HGF, TGF, IGF-1, VEGF, and FGF-2 can regulate inflammation, resist apoptosis, promote damaged cell repair, and prevent fibrosis in AKI (36).

MSC-EV-based treatment of AKI involves the transport of various cytokines, including IGF-1. MSC-EVs secrete IGF-1 receptor mRNA directly to renal TECs, as well as directly secreting IGF-1 and carrying IGF-1 receptors to promote kidney repair in AKI (13). Several studies have indicated that this occurs *via* IGF-1-induced activation of the Akt survival pathway (38). AKI is associated with increased expression of the pro-apoptotic protein Bcl-2-associated X protein (Bax) and decreased expression of anti-apoptotic Bcl-2 (58). EVs can be integrated into injured renal TECs to promote the recovery of renal function and morphology. The beneficial effect of MSCs on renal tissue was related to the inhibition of renal tubular oxidative damage in a cisplatin-induced AKI model, manifested by the expression of nitrotyrosine and induction of Akt phosphorylation (59). IGF-1 activates Akt, as a kinase located on the phosphoinositide-3 kinase (PI3K) signaling pathway with an important regulatory role, through phosphorylation modification to inhibit Bax to resist apoptosis and up-regulate the Bcl-2 survival pathway, and to block mitochondrial caspase-9 to reduce inflammation and resist apoptosis (60). At the same time, IGF-1 activates the MAPK pathway to promote cell proliferation (13, 61). Morigi et al. confirmed that MSC treatment significantly increased phospho-Akt and activated downstream targets for cell proliferation and cell survival in a cisplatin-induced AKI model (56). In an *in vitro* model, proinflammatory factors such as TNF-α and IL-1b significantly reduced proximal tubular cell injury following treatment with MSCs and cisplatin (56). IGF-1 has demonstrated several biological effects in mouse kidney tissues treated with bone marrow MSCs, including promoting cell proliferation, changing the hemodynamics, and reducing apoptosis (13). In the same experimental model, Imberti et al. tested the effects of cord blood MSCs, which can improve kidney function and enhance the protective effect in AKI animal models. As a mitogenic and pro-survival factor, IGF-1 helps recruit self-derived progenitor cells or stem cells, thus, promoting the regeneration process in the kidney (62).

In addition to IGF-1, other growth factors transported by MSC-EVs also protect the microenvironment of the injured site and damaged cells. FGF-2 affects AKI *via* its anti-fibrotic effect, and knockout of FGF-2 blocked the repair process and induced a fibrotic response (63). TGF-β binds to the TGF receptor and activates downstream Smad and non-Smad pathways to perform a variety of biological effects in AKI (64). Acting *via* TGF-β-dependent macrophages, it can prevent ischemic kidney injury and tubular interstitial fibrosis (56, 60, 65). Up-regulation of VEGF receptor-2 can also be observed in kidney tissue during the ischemic AKI response, suggesting that VEGF may also be a potential therapeutic target (66–68). VEGF stabilized microvessel density to protect the renal microvascular structure and promote renal recovery through mitogenic and anti-apoptotic mechanisms (32). HGF can reduce kidney damage by promoting cell proliferation, anti-inflammation, and anti-apoptosis. HGF also promoted kidney repair and the proliferation of kidney cells *via* tyrosine phosphorylation of the c-met receptor in kidney injury induced by IRI and glycerol (13). Moreover, HGF gene therapy and HGF-modified MSCs had a significant therapeutic effect in AKI in an anti-apoptotic manner (13, 69, 70).

MSC-EVs can be internalized into renal TECs to treat AKI at the translational level. Recent studies showed that mRNAs for factors such as IL-10, IGF-1R, HGF, DNA-directed RNA polymerases I, II, and III subunit RPABC1, and VEGF could be loaded into EVs and transported to the target cells to exert translational effects, including anti-inflammation, anti-fibrosis, and anti-apoptosis effects, promoting proliferation, improving renal function, and reducing kidney injury (43, 71). Notably, the efficacy of MSC-EVs was partly mediated by miRNAs loaded in EVs, which directly regulated transcription and translation (50).

EV-mediated miRNAs have also been shown to play a significant role in AKI (72). For example, miR-148b-3p and miR-548c-5p promoted cell viability (73, 74), miR-199a-3p reduced AKI *via* anti-apoptotic effects (75), miR-30 stabilized mitochondria, improved renal function, and exerted anti-apoptotic effects (76), and miRNA let-7a-5p reduced cell morbidity and improved cell survival (77, 78). Other miRNAs are regulated and actively participate in the regeneration process involving miR-21 in MSC-EV therapy of AKI, possibly related to renal tubular epithelium repair and internal cell reprogramming (79). EVs can also stabilize mitochondria through miRNAs, especially miRNA-200a-3p, which shuttles to TECs *via* MSC-EVs and targets the Keap1-Nrf2 signaling pathway to normalize mitochondrial membrane potential by reducing mitochondrial fragmentation, increasing the number of mitochondrial DNA copies, and protecting mitochondrial function in TECs during kidney repair (55, 71).

Mitochondria are considered to play an integral role in AKI development (80), suggesting the possibility that mitochondria might be transferred horizontally into kidney cells to reprogram cell metabolism and promote kidney recovery. Mitochondrial DNA or mitochondria can be transported directly into the damaged site by EVs, thus reducing kidney damage (81). Spees et al. first showed in 2006 that MSCs could serve as mitochondrial donors in cell survival (82). Actively transferring healthy mitochondria from MSCs can restore aerobic metabolism and protect cells from being eliminated (83). Plotnikov et al. subsequently confirmed the transport of mitochondria from MSCs to renal tubular cells in normal *in vitro* culture medium (84). In addition to renal tubular cells, vascular endothelial cells are also damaged during AKI. The delivery of mitochondria from MSC-EVs reduced apoptosis and increased cell viability, and restored the normal balance between aerobic respiration and glycolysis, indicating the re-establishment of aerobic respiration (12, 81). EVs derived from MSCs have previously demonstrated huge therapeutic potential in AKI *via* transporting proteins and RNAs with biological activity, and by conveying mitochondria and their DNA directly, suggesting that modifying the contents of MSC-EVs to affect specific signaling pathways may represent a promising therapeutic approach (28, 85).

EVS PARTICIPATE IN THE IMMUNE REGULATION OF MSCS IN AKI

MSCs-EVs have shown strong immune regulation in AKI treatment (**Figure 3**) and have demonstrated significant regulatory effects in a variety of immune cells, including inhibiting the transendothelial migration and chemotaxis of neutrophils, promoting macrophage M2 type polarization, inhibiting T cell activation, and inhibiting IFN-γ secretion (86–90). These processes were mainly mediated by TNF-α-stimulated gene 6 (TSG-6), which regulates inflammation with multiple functions (91–93). Apart from TSG-6, MSC-EVs also depend on IL-6, IL-10, prostaglandin E2, HGF, and indoleamine2,3-dioxygenase to regulate the immune microenvironment (94, 95), secreting miRNAs involving miR-155 regulate inflammation on the extracellular environment interact with dendritic cells to regulate endotoxin-induced inflammation (96–99). In addition, MSC-derived signals mediated by EVs can inhibit the proliferation of natural killer cells, reduce the activity of B lymphocytes, and secrete IL-17 to promote T cell transformation into Treg cells (86, 100).

As noted above, AKI is usually associated with disorders and abnormal activation of the immune system, which can in turn be affected by treatment with MSCs and their EVs, suggesting that utilizing and modifying EVs to regulate the immunomicroenvironment might be an efficient and effective therapeutic approach for AKI (100–106). Although some researchers have reported that MSCs and MSC-EVs can affect the immune function and immune microenvironment in AKI both *in vitro* and *in vivo*, the findings have been inconsistent (107). Unfortunately, the specific mechanism by which MSC-EVs act as immune mediators remains elusive, and further research into the therapeutic mechanisms of EVs in AKI is warranted.

MSC-EVS ARE SUPERIOR TO MSCS AND CAN BE MODIFIED ARTIFICIALLY AS MEDICATION CARRIERS, WITH RARE ADVERSE REACTIONS

Although many preclinical studies have shown the effectiveness of MSCs and MSC-EVs in AKI, few clinical trials have utilized MSC-EVs for the clinical treatment of patients (49, 108, 109). Compared with MSCs, MSC-EVs generate a reduced inflammatory response with lower immunogenicity after administration, with beneficial effects in terms of administration dose and frequency, as well as reducing stem cell-associated risks such as cytokine release syndrome, ectopic tissue caused by poor differentiation, and tumorigenesis (31, 48, 110–113). In a comparative study, MSC-EVs were at least as effective as MSCs, indicating that many of the therapeutic effects of MSCs could be attributed to EVs (114, 115). In addition, MSCs may have more efficient homing ability than EVs (116, 117).

Preclinical studies *in vitro* and *in vivo* showed that EVs may have advantages over MSCs and may thus have great potential for future stem cell therapies (118, 119). First, MSC-EVs are highly stable and suitable for long-term storage without the need to add potentially toxic cryopreservatives (120, 121). Second, MSC-EVs can transfer functional proteins and miRNAs directly to recipient cells, inducing stronger signal transmission *via* cell-to-cell communication (45). Third, MSC-EVs have a lower risk of a rejection reaction, and an immune response after allogeneic application is rare (72). In addition, MSC-EVs avoid the potential tumorigenicity of MSCs, with no evidence of carcinogenic potential to date and no signs of unwanted differentiation (24, 28, 110). In contrast, MSCs have the possibility of tumorigenesis and poor differentiation (122). One study reported that MSC-EVs with anti-tumor activity inhibited tumor growth both *in vivo* and *in vitro* (123).

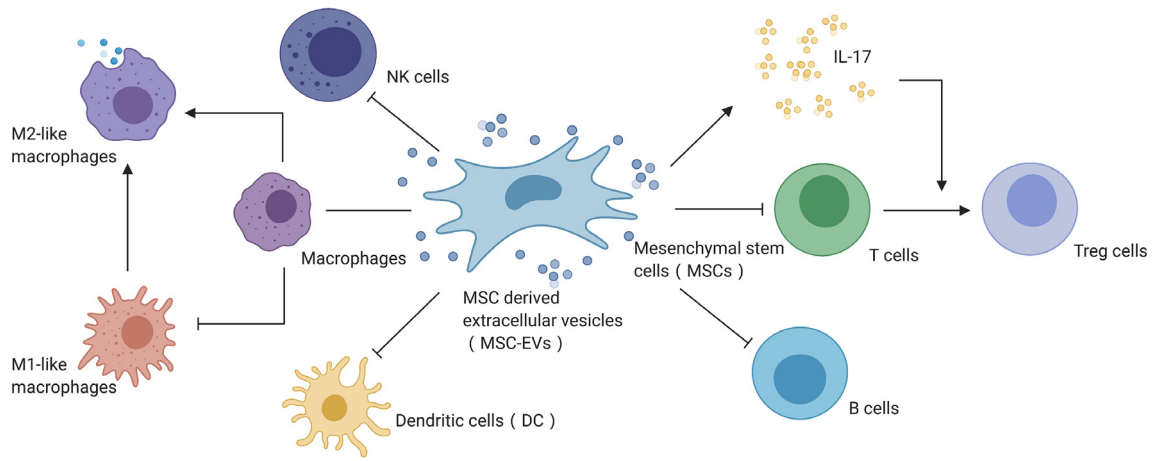


FIGURE 3 | MSC-EVs mediate immune regulation in AKI. Created with BioRender.com.

EVs have important unique characteristics. MSC-EVs may have a weaker homing ability than MSCs, which could partly reduce the accuracy of EV-based therapy; however, EVs are safe, with few adverse reactions (24, 28). EVs also show plasticity, and their contents can be modified artificially to improve and enhance not only their homing ability, but also their therapeutic effects (28, 29, 85). However, robust evidence is still lacking, and more research involving animal models and clinical studies is needed.

HOW TO ADMINISTER MSC-EVS

When administered *via* peripheral intravenous injection, most MSCs or MSC-EVs distribute to the lung, spleen, or celiac lymph nodes, thus, reducing their therapeutic efficacy (36). Moreover, the homing ability of EVs is lower than that of MSCs. However, a recent study showed that renal artery administration could transport more EVs and generate better therapeutic effects to injured kidney tissue with greater precision compared with other administration routes (30, 50, 124). Renal artery puncture in clinical patients may be performed under ultrasound image guidance (124). However, although EV injection *via* the renal artery provides a possible approach, this administration route is more difficult and is associated with ethical concerns in clinical practice (49, 114).

Bruno et al. utilized MSC-derived microvesicles, a kind of EVs, in lethal cisplatin-induced AKI and showed that increased administration times improved the therapeutic effects due to anti-apoptosis in AKI. The single administration of EVs ameliorated renal function and morphology and improved survival, but had no effect on chronic tubular injury and persistent increases in blood urea nitrogen (BUN) and creatinine. They also found that using multiple injections of EVs significantly reduced the mortality of mice, and mice surviving at day 21 showed normal histology and renal function (125).

Recent meta-analyses investigating the effects of administration and cell source on the therapeutic effects of EVs have indicated the importance of these factors in clinical research and applications. A meta-analysis using serum creatinine (Scr) as an indicator of efficacy compared the timing of administration in various studies (between 1 h and 3 days after the occurrence of AKI), and showed a better treatment effect following administration of MSC-EVs within 1 h after the occurrence of AKI, suggesting that they should be administered as early as possible (114). Current research mainly focuses on EVs secreted by MSCs derived from adipose tissue, bone marrow, and cord blood. However, the source tissue also has an impact on MSC-EVs (47, 126). For example, compared with cord blood-derived MSCs, signals mediated by EVs derived from bone marrow MSCs had greater effects on bone growth and differentiation (49, 114). In addition, adipose-derived MSCs had similar immune regulation effects to bone marrow-derived MSCs (17). The EV source should be selected flexibly according to the type of kidney injury and treatment needs. Meanwhile, because MSC from different sources have different characteristics, the EVs secreted by them will also differ. The therapeutic effects of EVs from other sources of MSCs in AKI are still unclear, and there is much need for further research. Bone marrow-derived MSCs may be more likely to express specific proteins *via* lentiviral expression vector transduction, such as angiogenin-1, IGF-1, and Akt, thus, influencing the restructuring and repair of injured tissue (13). This research could indicate the ability to utilize lentiviral vectors to modify MSCs to produce EVs with specific efficacies (127).

HOW TO IMPROVE THE THERAPEUTIC EFFECT OF MSC-EVS

Several studies have focused on improving MSC-EVs in a variety of areas (128) (**Table 1**). These studies have mainly involved

TABLE 1 | Recent research into the therapeutic effects of MSC-EVs.

Authors	Title	Year	EVs source	AKI model	Intervention	Effects
Lee, JH et al. (128)	Reproducible large-scale isolation of exosomes from adipose tissue-derived mesenchymal stem/stromal cells and their application in acute kidney injury	2020	Adipose tissue-derived MSCs	Cisplatin-induced AKI	Produce ASC-EVs with tangential flow filtration	EV yield↑; EV quality↑
Cao, J et al. (127)	Three-dimensional culture of MSCs produces exosomes with improved yield and enhanced therapeutic efficacy for cisplatin-induced acute kidney injury	2020	Fresh human umbilical cord-derived MSCs	Cisplatin-induced AKI	Produce MSC-EVs with a hollow fiber bioreactor-based three-dimensional culture system	EV yield↑; EV quality↑; therapeutic efficacy↑; collection efficiency↑; efficiency of TECs uptake↑
Ullah, M et al. (129)	Reversing acute kidney injury using pulsed focused ultrasound and MSC therapy: a role for HSP-mediated PI3K/AKT signaling	2020	Bone marrow-derived MSCs	Cisplatin-induced AKI	Combine pFUS pretreatment of the kidney with MSC-derived EVs	No significant improvement in homing ability of EVs; kidney injury markers↓; renal function↓; inflammation↓; apoptosis↓; cell proliferation↑
Ullah, M et al. (130)	HSP70-mediated NLRP3 inflammasome suppression underlies reversal of acute kidney injury following extracellular vesicle and focused ultrasound combination therapy	2020	Bone marrow-derived MSCs	Cisplatin-induced AKI	Combine pFUS pretreatment of the kidney with MSC-derived EVs	HSP70↓; NLRP3 inflammasome↓;IL-1↓; IL-18↓; therapeutic effects of MSC-EVs↑; anti-inflammation↑; cell regeneration↑
Ullah, M et al. (131)	Pulsed focused ultrasound enhances the therapeutic effect of mesenchymal stromal cell-derived extracellular vesicles in acute kidney injury	2020	Bone marrow-derived MSCs	Cisplatin-induced AKI	Combine pFUS pretreatment of the kidney with MSC-derived EVs	MAPK/ERK↑; PI3K/Akt↑; eNOS↑; SIRT3↑; kidney injury markers↓; renal function↓; inflammation↓; apoptosis↓; cell proliferation↑; survival↑
Zhang, C et al. (77)	Supramolecular nanofibers containing arginine-glycine-aspartate (RGD) peptides boost therapeutic efficacy of extracellular vesicles in kidney repair	2020	Human placenta-derived MSCs	Ischemic reperfusion injury-induced AKI	Precondition EVs with RGD peptides	Stability and retention of MSC-EVs↑; anti-fibrosis in the chronic phase↑; kidney injury↓; cell proliferation↑; EV integrin-mediated loading↑
Liu, Y et al. (132)	Enhanced therapeutic effects of MSC-derived extracellular vesicles with an injectable collagen matrix for experimental acute kidney injury treatment	2020	Human placenta-derived MSCs	Ischemic reperfusion injury-induced AKI	Precondition EVs with collagen matrix	Angiogenesis↑; apoptosis↓; stability and retention of MSC-EVs↑; therapeutic efficacy↑
Alzahrani, FA et al. (133)	Melatonin improves therapeutic potential of mesenchymal stem cells-derived exosomes against renal ischemia-reperfusion injury in rats	2019	Bone marrow-derived MSCs	Ischemic reperfusion injury-induced AKI	Precondition EVs with melatonin	Kidney damage↓; inflammation; renal regeneration↑; angiogenesis↑; anti-oxidation↑; oxidative stress↓
Zhang, ZY et al. (134)	Oct-4 enhanced the therapeutic effects of mesenchymal stem cell-derived extracellular vesicles in acute kidney injury	2020	Human umbilical cord-derived MSCs	Ischemic reperfusion injury-induced AKI	Overexpress Oct-4 by lentiviral vector transduction	Apoptosis↓; Scr↓; BUN↓; renal fibrosis↓; renal tubular epithelial cell proliferation↑

EV, extracellular vesicle; MSC, mesenchymal stem cell; AKI, acute kidney injury; pFUS, pulsed focused ultrasound; HSP70, heat shock protein 70; NLRP3, NLR Family, Pyrin Domain Containing Protein 3; IL, interleukin; TEC, tubular epithelial cell; RGD, arginine-glycine-aspartate; MAPK, mitogen-activated protein kinase; ERK, extracellular regulated protein kinase; Scr, serum creatinine; BUN, blood urea nitrogen; eNOS, endothelial nitric oxide synthase.

improving the technology for the isolation of EVs, investigating potential administration routes, the use of pulsed focused ultrasound (pFUS), preconditioning EVs, and inducing the overexpression of EVs by lentiviral vector transduction.

EVs are traditionally separated by ultracentrifugation, but this method has major limitations, including the co-precipitation of EVs with contaminants including protein aggregates, loss of EV function due to aggregation or distortion during the isolation process, and functional inhibition of EVs by the media used for density gradient ultracentrifugation (129). AKI is common in clinical practice, and improved large-scale production of EVs would be needed to satisfy the requirements if EVs were applied for the clinical treatment of these patients (1). Large-scale isolation of single-batch EVs by ultracentrifugation is also restricted by the limited instrument capacity (130). Lee et al. showed that it was possible to isolate adipose tissue-derived MSC-EVs stably and reproducibly on a large scale without loss of function using tangential flow filtration (131), with successful life-preserving effects in a cisplatin-induced lethal rat model of AKI. Other studies have indicated that the production of EVs by three-dimensional (3D) culture of MSCs could improve the efficacy and increase yield. Cao et al. produced EVs in 3D culture and showed that, compared with conventional 2D culture, the 3D culture system increased the total yield of EVs 19.4-fold, thus, indicating that the 3D culture system had a higher EV-collection efficiency. Surprisingly, EVs obtained by 3D culture were taken up more efficiently by renal TECs, showing better anti-inflammatory effects and increasing the survival rate of TECs *in vitro* (130).

pFUS was shown to alter the kidney microenvironment to enhance homing of subsequently infused MSCs. Mujib et al. investigated if the combined use of pFUS with MSC-EVs could improve the therapeutic effect by improving the homing ability of EVs in AKI (132). Surprisingly, although pFUS did not up-regulate local cytokine expression or improve bone marrow MSC homing, it did enhance the therapeutic efficacy of MSC-EVs in AKI. Further analysis showed that this effect was related to the up-regulation of heat shock protein (HSP) 20/HSP40 and subsequent PI3K/Akt signaling. This indicated that pFUS had independent as well as synergistic therapeutic effects in the context of AKI, and is thus, a promising affiliated method for MSC-EV therapy (132). Further studies of the combined use of MSC-EVs and pFUS showed that pFUS affected HSP70-mediated NLRP3 inflammasome suppression to improve the anti-inflammatory and regenerative effects (133). In addition, Mujib et al. also showed that pFUS upregulated the proliferative signaling (MAPK/extracellular signal-regulated kinase, PI3K/Akt) and regenerative pathways (endothelial nitric oxide synthase, sirtuin 3) to suppress inflammation in AKI (134).

The low stability and retention of MSC-EVs have partly limited their therapeutic efficacy, and methods involving novel biological materials such as arginine-glycine-aspartate (RGD) peptides and collagen matrix have been investigated with the aim of improving these features. Zhang et al. developed an RGD peptide scaffold to increase EV integrin-mediated loading, and found that RGD hydrogels facilitated MSC-EVs containing miRNA let-7a-5p, which improved their repair potential in AKI (78). Liu et al. isolated EVs from human placental mesenchymal stem cells and wrapped them in a collagen matrix, and *Gaussia* luciferase imaging confirmed that the collagen matrix effectively encapsulated the EVs and augmented their efficacy in AKI by improving the stability and promoting the sustained release of EVs (135). Biological modules can be used to cover EVs and interact with the microenvironment in AKI to improve the positive effects of MSC-EV-based therapy (78, 135, 136). However, few studies have investigated the mechanisms involved in the interaction between the injured tissue microenvironment and biological modules covering EVs. This warrants further investigation to guide clinical trials aimed at identifying the most efficient artificial biological modules to improve the therapeutic effects of MSC-EVs.

Scientists have also tried to improve the effects of MSC-EVs in AKI by preconditioning them with medications to prevent further damage deterioration and help renal recovery. Alzahrani et al. tested MSC-EVs preconditioned with melatonin in AKI induced by IRI with bilateral renal artery clipping, and showed that melatonin-preconditioned MSC-EVs performed better than untreated EVs in terms of alleviating kidney damage and inflammation, promoting regeneration, angiogenesis, and anti-oxidation, and inhibiting oxidative stress (136). EVs can also be artificially modified to overexpress specific modules. Zhang et al. transduced MSCs with Oct-4 *via* a lentiviral vector to produce Oct-4-overexpressing MSCs, which significantly reduced attenuated apoptosis, Scr and BUN levels, promoted renal TEC proliferation, and rescued renal fibrosis in IRI-induced AKI (137).

Recent studies concentrating on improving the limitations of MSC-EV-based therapy showed that it was possible to safely modify MSC-EVs and enhance their therapeutic effects. As noted above, their homing ability and tissue stability limit the therapeutic effects of EVs, but these issues can be overcome by the use of collagen matrix and RGD peptides (78, 135). In addition to enhancing the effects of EVs, 3D culture and tangential flow filtration may also allow the large-scale clinical application of EVs (130, 131). However, MSC-EVs still face numerous challenges and limitations before they can be clinically applied in patients.

LIMITATIONS AND FUTURE PERSPECTIVES OF MSC-EVS

Various challenges still need to be overcome before MSC-EVs can be utilized in clinical treatments. First, there is significant heterogeneity between MSC-EVs in terms of size, leading to variations in the secreted components and functional characteristics of the EVs (15). Further studies are therefore needed to choose the specific size of EVs according to their cargo (138). Second, the isolation and storage methods of EVs

may affect their therapeutic efficacy (139). Ensuring the quality of EVs is an important problem, and producers are supposed to confirm that the EVs are derived from cellular matrix, rather than being components from cells damaged during cryopreservation and mechanical failure (130, 131, 135). It is advisable to optimize and confirm the preservation conditions to maintain the efficacy of the EVs after defrosting (128). Importantly, the follow-up time in previous studies was only between 1 day and 2 weeks, which is inadequate for evaluating the long-term outcome and prognosis (114), and more clinical trials with long-term follow-up are therefore needed to provide more robust evidence. Catering for the demands of large-scale clinical applications and producing enough high-quality MSCs then become critical issues (99). In addition, even though EVs have demonstrated similar effects to MSCs, their homing ability is much weaker than that of MSCs, representing a limitation of MSC-EV-based therapy that needs improving. Zhang et al. recently used monocyte mimics to enhance the homing ability of MSC-EVs to the injured site in a myocardial IRI model, suggesting a possible approach for improving the homing ability of MSC-EVs for the therapy of AKI (140). Regarding monitoring the distribution of EVs, their physicochemical properties may be affected by some lipophilic markers, which could affect the observations (13), and new tracing markers will be needed to detect the distribution and effects of EVs in clinical practice. Increasing research is currently focused on investigating ways of modifying the cargo of MSC-EVs to improve their therapeutic efficiency (28, 141). Clinical trials are currently required to verify and approve the use of customized EVs and to assess the safety and tolerance of modified MSC-EVs.

CONCLUSION

MSC-EVs are responsible for the main therapeutic effects of MSCs in AKI, and demonstrate specific therapeutic effects and improve the efficacy of regenerative stem cell therapies. However, the lack of clinical trials means that MSC-EVs still face many challenges before they can be used for clinical treatment. Nonetheless, we believe that MSC-EVs will become an effective approach to overcome the current limitations of AKI treatment.

AUTHOR CONTRIBUTIONS

J-KL and CY drafted the manuscript. ZL, G-WT and YS conceived the proposal, revised the manuscript and provided funding support. J-CL, M-HL and D-LH collected literatures and revised the manuscript. ZL and G-WT helped the language editing and provided funding support. All authors contributed to the article and approved the submitted version.

FUNDING

This article was supported by grants from the Research Funds of Shanghai Municipal Health Commission (2019ZB0105), Natural Science Foundation of Shanghai (20ZR1411100), Program of Shanghai Academic/Technology Research Leader (20XD1421000), National Natural Science Foundation of China (82070085), Clinical Research Funds of Zhongshan Hospital (2020ZSLC38 and 2020ZSLC27), and Smart Medical Care of Zhongshan Hospital (2020ZHZS01).

REFERENCES

1. Ronco C, Bellomo R, Kellum JA. Acute Kidney Injury. *Lancet* (2019) 394:1949–64. doi: 10.1016/s0140-6736(19)32563-2
2. Hsu CY. Yes, Aki Truly Leads to Ckd. *J Am Soc Nephrol* (2012) 23:967–9. doi: 10.1681/asn.2012030222
3. Zhao L, Han F, Wang J, Chen J. Current Understanding of the Administration of Mesenchymal Stem Cells in Acute Kidney Injury to Chronic Kidney Disease Transition: A Review With a Focus on Preclinical Models. *Stem Cell Res Ther* (2019) 10:3855. doi: 10.1186/s13287-019-1507-3
4. Pickkers P, Mehta RL, Murray PT, Joannidis M, Molitoris BA, Kellum JA, et al. Effect of Human Recombinant Alkaline Phosphatase on 7-Day Creatinine Clearance in Patients With Sepsis-Associated Acute Kidney Injury: A Randomized Clinical Trial. *Jama* (2018) 320:1998–2009. doi: 10.1001/jama.2018.14283
5. Forni LG, Darmon M, Ostermann M, Oudemans-van Straaten HM, Pettilä V, Prowle JR, et al. Renal Recovery After Acute Kidney Injury. *Intensive Care Med* (2017) 43:855–66. doi: 10.1007/s00134-017-4809-x
6. Hu L, Yang C, Zhao T, Xu M, Tang Q, Yang B, et al. Erythropoietin Ameliorates Renal Ischemia and Reperfusion Injury Via Inhibiting Tubulointerstitial Inflammation. *J Surg Res* (2012) 176:260–6. doi: 10.1016/j.jss.2011.06.035
7. Xu Y, Li D, Wu J, Zhang M, Shao X, Xu L, et al. Farnesoid X Receptor Promotes Renal Ischaemia-Reperfusion Injury by Inducing Tubular Epithelial Cell Apoptosis. *Cell Proliferation* (2021), 54(4):e13005. doi: 10.1111/cpr.13005
8. Wang J, Zhu P, Li R, Ren J, Zhang Y, Zhou H. Bax Inhibitor 1 Preserves Mitochondrial Homeostasis in Acute Kidney Injury Through Promoting Mitochondrial Retention of Phb2. *Theranostics* (2020) 10:384–97. doi: 10.7150/thno.40098
9. Liu G, Sabatini D. Mtor at the Nexus of Nutrition, Growth, Ageing and Disease. Nature Reviews. *Mol Cell Biol* (2020) 21:183–203. doi: 10.1038/s41580-019-0199-y
10. Rostamzadeh D, Yousefi M, Haghshenas M, Ahmadi M, Dolati S, Babaloo Z. Mtor Signaling Pathway as a Master Regulator of Memory Cd8 T-Cells, th17, and Nk Cells Development and Their Functional Properties. *J Cell Physiol* (2019) 234:12353–68. doi: 10.1002/jcp.28042
11. Tang C, Livingston M, Liu Z, Dong Z. Autophagy in Kidney Homeostasis and Disease. Nature Reviews. *Nephrology* (2020) 16:489–508. doi: 10.1038/s41581-020-0309-2
12. Emma F, Montini G, Parikh SM, Salviati L. Mitochondrial Dysfunction in Inherited Renal Disease and Acute Kidney Injury. *Nat Rev Nephrol* (2016) 12:267–80. doi: 10.1038/nrneph.2015.214
13. Gao L, Zhong X, Jin J, Li J, Meng X. Potential Targeted Therapy and Diagnosis Based on Novel Insight Into Growth Factors, Receptors, and Downstream Effectors in Acute Kidney Injury and Acute Kidney Injury-Chronic Kidney Disease Progression. *Signal Transduct Targeted Ther* (2020) 5:95. doi: 10.1038/s41392-020-0106-1
14. Yang C, Liu J, Li L, Hu M, Long Y, Liu X, et al. Proteome Analysis of Renoprotection Mediated by a Novel Cyclic Helix B Peptide in Acute Kidney Injury. *Sci Rep* (2015) 5:180455. doi: 10.1038/srep18045
15. Yun C, Lee S. Potential and Therapeutic Efficacy of Cell-Based Therapy Using Mesenchymal Stem Cells for Acute/Chronic Kidney Disease. *Int J Mol Sci* (2019) 20(7):1619. doi: 10.3390/ijms20071619
16. Rota C, Morigi M, Cerullo D, Introna M, Colpani O, Corna D, et al. Therapeutic Potential of Stromal Cells of Non-Renal or Renal Origin in

Experimental Chronic Kidney Disease. *Stem Cell Res Ther* (2018) 9:220. doi: 10.1186/s13287-018-0960-8
17. Gwam C, Mohammed N, Ma X. Stem Cell Secretome, Regeneration, and Clinical Translation: A Narrative Review. *Ann Transl Med* (2021) 9:70. doi: 10.21037/atm-20-5030
18. Tögel FE, Westenfelder C. Kidney Protection and Regeneration Following Acute Injury: Progress Through Stem Cell Therapy. *Am J Kidney Dis* (2012) 60:1012–22. doi: 10.1053/j.ajkd.2012.08.034
19. Abumaree MH, Abomaray FM, Alshabibi MA, AlAskar AS, Kalionis B. Immunomodulatory Properties of Human Placental Mesenchymal Stem/Stromal Cells. *Placenta* (2017) 59:87–95. doi: 10.1016/j.placenta.2017.04.003
20. Bochon B, Kozubska M, Surygała G, Witkowska A, Kuźniewicz R, Grzeszczak W, et al. Mesenchymal Stem Cells-Potential Applications in Kidney Diseases. *Int J Mol Sci* (2019) 20(10):2462. doi: 10.3390/ijms20102462
21. De Miguel MP, Fuentes-Julián S, Blázquez-Martínez A, Pascual CY, Aller MA, Arias J, et al. Immunosuppressive Properties of Mesenchymal Stem Cells: Advances and Applications. *Curr Mol Med* (2012) 12:574–915. doi: 10.2174/156652412800619950
22. Wang X, Yang C, Hu L, Wei Z, Tang Q, Chen B, et al. Tolerance Induction With Donor Hematopoietic Stem Cell Infusion in Kidney Transplantation: A Single-Center Experience in China With a 10-Year Follow-Up. *Ann Transl Med* (2020) 8:13785. doi: 10.21037/atm-20-2502a
23. Bianco P, Robey PG, Simmons PJ. Mesenchymal Stem Cells: Revisiting History, Concepts, and Assays. *Cell Stem Cell* (2008) 2:313–9. doi: 10.1016/j.stem.2008.03.002
24. Aghajani Nargesi A, Lerman L, Eirin A. Mesenchymal Stem Cell-Derived Extracellular Vesicles for Kidney Repair: Current Status and Looming Challenges. *Stem Cell Res Ther* (2017) 8:2735. doi: 10.1186/s13287-017-0727-7
25. Keating A. Mesenchymal Stromal Cells: New Directions. *Cell Stem Cell* (2012) 10:709–16. doi: 10.1016/j.stem.2012.05.015
26. Zhao Y, Zhu X, Zhang L, Ferguson CM, Song T, Jiang K, et al. Mesenchymal Stem/Stromal Cells and Their Extracellular Vesicle Progeny Decrease Injury in Poststenotic Swine Kidney Through Different Mechanisms. *Stem Cells Dev* (2020) 29:1190–200. doi: 10.1089/scd.2020.0030
27. Bei Y, Das S, Rodosthenous RS, Holvoet P, Vanhaverbeke M, Monteiro MC, et al. Extracellular Vesicles in Cardiovascular Theranostics. *Theranostics* (2017) 7:4168–82. doi: 10.7150/thno.21274
28. Lai R, Yeo R, Tan K, Lim S. Exosomes for Drug Delivery - a Novel Application for the Mesenchymal Stem Cell. *Biotechnol Adv* (2013) 31:543–1. doi: 10.1016/j.biotechadv.2012.08.008
29. Du W, Zhang K, Zhang S, Wang R, Nie Y, Tao H, et al. Enhanced Proangiogenic Potential of Mesenchymal Stem Cell-Derived Exosomes Stimulated by a Nitric Oxide Releasing Polymer. *Biomaterials* (2017) 133:70–81. doi: 10.1016/j.biomaterials.2017.04.030
30. Grange C, Tapparo M, Bruno S, Chatterjee D, Quesenberry PJ, Tetta C, et al. Biodistribution of Mesenchymal Stem Cell-Derived Extracellular Vesicles in a Model of Acute Kidney Injury Monitored by Optical Imaging. *Int J Mol Med* (2014) 33:1055–63. doi: 10.3892/ijmm.2014.1663
31. Zheng X, He X, Zhang L, Qin H, Lin X, Liu X, et al. Bone Marrow-Derived Excr4-Overexpressing MSCs Display Increased Homing to Intestine and Ameliorate Colitis-Associated Tumorigenesis in Mice. *Gastroenterol Rep* (2019) 7:127–38. doi: 10.1093/gastro/goy017
32. Yuan L, Wu MJ, Sun HY, Xiong J, Zhang Y, Liu CY, et al. Vegf-Modified Human Embryonic Mesenchymal Stem Cell Implantation Enhances Protection Against Cisplatin-Induced Acute Kidney Injury. *Am J Physiol Renal Physiol* (2011) 300:F207–18. doi: 10.1152/ajprenal.00073.2010
33. Hervás-Salcedo R, Fernández-García M, Hernando-Rodríguez M, Quintana-Bustamante O, Segovia J, Alvarez-Silva M, et al. Enhanced Anti-Inflammatory Effects of Mesenchymal Stromal Cells Mediated by the Transient Ectopic Expression of Cxcr4 and Il10. *Stem Cell Res Ther* (2021) 12:124. doi: 10.1186/s13287-021-02193-0
34. Singh P, Mohammad K, Pelus L. Cxcr4 Expression in the Bone Marrow Microenvironment Is Required for Hematopoietic Stem and Progenitor Cell Maintenance and Early Hematopoietic Regeneration After Myeloablation. *Stem Cells (Dayton Ohio)* (2020) 38(7):849–59. doi: 10.1002/stem.3174
35. Togel F, Westenfelder C. Role of SDF-1 as a Regulatory Chemokine in Renal Regeneration After Acute Kidney Injury. *Kidney Int Suppl* (2011) 1:87–9. doi: 10.1038/kisup.2011.20
36. Luo C, Zhang F, Zhang L, Geng Y, Li Q, Hong Q, et al. Mesenchymal Stem Cells Ameliorate Sepsis-Associated Acute Kidney Injury in Mice. *Shock (Augusta Ga)* (2014) 41:123–9. doi: 10.1097/shk.0000000000000080
37. Westenfelder C, Togel F. Protective Actions of Administered Mesenchymal Stem Cells in Acute Kidney Injury: Relevance to Clinical Trials. *Kidney Int Suppl* (2011) 1:103–6. doi: 10.1038/kisup.2011.24
38. Ullah I, Subbarao RB, Rho GJ. Human Mesenchymal Stem Cells - Current Trends and Future Prospective. *Biosci Rep* (2015) 35(2):e00191. doi: 10.1042/BSR20150025.
39. Morigi M, Imberti B, Zoja C, Corna D, Tomasoni S, Abbate M, et al. Mesenchymal Stem Cells are Renotropic, Helping to Repair the Kidney and Improve Function in Acute Renal Failure. *J Am Soc Nephrol* (2004) 15:1794–804. doi: 10.1097/01.asn.0000128974.07460.34
40. Little MH, Rae FK. Review Article: Potential Cellular Therapies for Renal Disease: Can We Translate Results From Animal Studies to the Human Condition? *Nephrol (Carlton)* (2009) 14:544–53. doi: 10.1111/j.1440-1797.2009.01144.x
41. Yang C, Zhao T, Lin M, Zhao Z, Hu L, Jia Y, et al. Helix B Surface Peptide Administered After Insult of Ischemia Reperfusion Improved Renal Function, Structure and Apoptosis Through Beta Common Receptor/Erythropoietin Receptor and pi3k/akt Pathway in a Murine Model. *Exp Biol Med (Maywood)* (2013) 238:111–9. doi: 10.1258/ebm.2012.012185
42. Magnasco A, Corselli M, Bertelli R, Ibatici A, Peresi M, Gaggero G, et al. Mesenchymal Stem Cells Protective Effect in Adriamycin Model of Nephropathy. *Cell Transplant* (2008) 17:1157–67. doi: 10.3727/096368908787236567
43. Eirin A, Zhu X, Puranik A, Woollard J, Tang H, Dasari S, et al. Comparative Proteomic Analysis of Extracellular Vesicles Isolated From Porcine Adipose Tissue-Derived Mesenchymal Stem/Stromal Cells. *Sci Rep* (2016) 6:36120. doi: 10.1038/srep36120
44. Phan J, Kumar P, Hao D, Gao K, Farmer D, Wang A. Engineering Mesenchymal Stem Cells to Improve Their Exosome Efficacy and Yield for Cell-Free Therapy. *J Extracell Vesicles* (2018) 7:1522236. doi: 10.1080/20013078.2018.1522236
45. O'Brien K, Breyne K, Ughetto S, Laurent L, Breakefield X. RNA Delivery by Extracellular Vesicles in Mammalian Cells and Its Applications. Nature Reviews. *Mol Cell Biol* (2020) 21:585–606. doi: 10.1038/s41580-020-0251-y
46. Cao H, Cheng Y, Gao H, Zhuang J, Zhang W, Bian Q, et al. *In Vivo* Tracking of Mesenchymal Stem Cell-Derived Extracellular Vesicles Improving Mitochondrial Function in Renal Ischemia-Reperfusion Injury. *ACS Nano* (2020) 14:4014–26. doi: 10.1021/acsnano.9b08207
47. Heo JS, Choi Y, Kim HS, Kim HO. Comparison of Molecular Profiles of Human Mesenchymal Stem Cells Derived From Bone Marrow, Umbilical Cord Blood, Placenta and Adipose Tissue. *Int J Mol Med* (2016) 37:115–25. doi: 10.3892/ijmm.2015.2413
48. Anjos-Afonso F, Siapati EK, Bonnet D. In Vivo Contribution of Murine Mesenchymal Stem Cells Into Multiple Cell-Types Under Minimal Damage Conditions. *J Cell Sci* (2004) 117:5655–64. doi: 10.1242/jcs.01488
49. Liu C, Wang J, Hu J, Fu B, Mao Z, Zhang H, et al. Extracellular Vesicles for Acute Kidney Injury in Preclinical Rodent Models: A Meta-Analysis. *Stem Cell Res Ther* (2020) 11:115. doi: 10.1186/s13287-019-1530-4
50. Yin K, Wang S, Zhao RC. Exosomes From Mesenchymal Stem/Stromal Cells: A New Therapeutic Paradigm. *Biomark Res* (2019) 7:85. doi: 10.1186/s40364-019-0159-x
51. Munshi A, Mehic J, Creskey M, Gobin J, Gao J, Rigg E, et al. A Comprehensive Proteomics Profiling Identifies Nrp1 as a Novel Identity Marker of Human Bone Marrow Mesenchymal Stromal Cell-Derived Small Extracellular Vesicles. *Stem Cell Res Ther* (2019) 10:401. doi: 10.1186/s13287-019-1516-2
52. Baer PC, Geiger H. Mesenchymal Stem Cell Interactions With Growth Factors on Kidney Repair. *Curr Opin Nephrol Hypertens* (2010) 19:1–6. doi: 10.1097/MNH.0b013e328333062c
53. van Niel G, D'Angelo G, Raposo G. Shedding Light on the Cell Biology of Extracellular Vesicles. *Nat Rev Mol Cell Biol* (2018) 19:213–8. doi: 10.1038/nrm.2017.125
54. Bellomo R. Acute Kidney Injury—A Decade of Progress. *Nat Rev Nephrol* (2015) 11:636–37. doi: 10.1038/nrneph.2015.147
55. Nezu M, Souma T, Yu L, Suzuki T, Saigusa D, Ito S, et al. Transcription Factor Nrf2 Hyperactivation in Early-Phase Renal Ischemia-Reperfusion

Injury Prevents Tubular Damage Progression. *Kidney Int* (2017) 91:387–401. doi: 10.1016/j.kint.2016.08.023
56. Morigi M, Rota C, Montemurro T, Montelatici E, Lo Cicero V, Imberti B, et al. Life-Sparing Effect of Human Cord Blood-Mesenchymal Stem Cells in Experimental Acute Kidney Injury. *Stem Cells* (2010) 28:513–22. doi: 10.1002/stem.293
57. Zhang K, Chen S, Sun H, Wang L, Li H, Zhao J, et al. In Vivo Two-Photon Microscopy Reveals the Contribution of sox9(+) Cell to Kidney Regeneration in a Mouse Model With Extracellular Vesicle Treatment. *J Biol Chem* (2020) 295:12203–13. doi: 10.1074/jbc.RA120.012732
58. Villanueva S, Céspedes C, Vio CP. Ischemic Acute Renal Failure Induces the Expression of a Wide Range of Nephrogenic Proteins. *Am J Physiol Regul Integr Comp Physiol* (2006) 290:R861–70. doi: 10.1152/ajpregu.00384.2005
59. Gnecchi M, He H, Liang OD, Melo LG, Morello F, Mu H, et al. Paracrine Action Accounts for Marked Protection of Ischemic Heart by Akt-Modified Mesenchymal Stem Cells. *Nat Med* (2005) 11:367–8. doi: 10.1038/nm0405-367
60. Gobé G, Zhang XJ, Willgoss DA, Schoch E, Hogg NA, Endre ZH. Relationship Between Expression of Bcl-2 Genes and Growth Factors in Ischemic Acute Renal Failure in the Rat. *J Am Soc Nephrol* (2000) 11:454–67. doi: 10.1681/ASN.V113454
61. Xinaris C, Morigi M, Benedetti V, Imberti B, Fabricio AS, Squarcina E, et al. A Novel Strategy to Enhance Mesenchymal Stem Cell Migration Capacity and Promote Tissue Repair in an Injury Specific Fashion. *Cell Transplant* (2013) 22:423–36. doi: 10.3727/096368912x653246
62. Imberti B, Morigi M, Benigni A. Potential of Mesenchymal Stem Cells in the Repair of Tubular Injury. *Kidney Int Suppl* (2011) 1:90–3. doi: 10.1038/kisup.2011.21
63. Iwasaki M, Adachi Y, Minamino K, Suzuki Y, Zhang Y, Okigaki M, et al. Mobilization of Bone Marrow Cells by G-Csf Rescues Mice From Cisplatin-Induced Renal Failure, and M-Csf Enhances the Effects of G-Csf. *J Am Soc Nephrol JASN* (2005) 16:658–65. doi: 10.1681/asn.2004010067
64. Chen H, Lin K, Wallace C, Chen Y, Yang C, Leu S, et al. Additional Benefit of Combined Therapy With Melatonin and Apoptotic Adipose-Derived Mesenchymal Stem Cell Against Sepsis-Induced Kidney Injury. *J Pineal Res* (2014) 57:16–32. doi: 10.1111/jpi.12140
65. Tögel F, Hu Z, Weiss K, Isaac J, Lange C, Westenfelder C. Administered Mesenchymal Stem Cells Protect Against Ischemic Acute Renal Failure Through Differentiation-Independent Mechanisms. *Am J Physiol Renal Physiol* (2005) 289:F31–42. doi: 10.1152/ajprenal.00007.2005
66. Mori da Cunha MG, Zia S, Beckmann DV, Carlon MS, Arcolino FO, Albersen M, et al. Vascular Endothelial Growth Factor Up-Regulation in Human Amniotic Fluid Stem Cell Enhances Nephroprotection After Ischemia-Reperfusion Injury in the Rat. *Crit Care Med* (2017) 45:e86–e96. doi: 10.1097/ccm.0000000000002020
67. Jiang M, Li G, Liu J, Liu L, Wu B, Huang W, et al. Nestin(+) Kidney Resident Mesenchymal Stem Cells for the Treatment of Acute Kidney Ischemia Injury. *Biomaterials* (2015) 50:56–66. doi: 10.1016/j.biomaterials.2015.01.029
68. Kinnaird T, Stabile E, Burnett MS, Lee CW, Barr S, Fuchs S, et al. Marrow-Derived Stromal Cells Express Genes Encoding a Broad Spectrum of Arteriogenic Cytokines and Promote In Vitro and In Vivo Arteriogenesis Through Paracrine Mechanisms. *Circ Res* (2004) 94:678–85. doi: 10.1161/01.Res.0000118601.37875.Ac
69. Du T, Zou X, Cheng J, Wu S, Zhong L, Ju G, et al. Human Wharton's Jelly-Derived Mesenchymal Stromal Cells Reduce Renal Fibrosis Through Induction of Native and Foreign Hepatocyte Growth Factor Synthesis in Injured Tubular Epithelial Cells. *Stem Cell Res Ther* (2013) 4:59. doi: 10.1186/scrt215
70. Xing L, Cui R, Peng L, Ma J, Chen X, Xie R, et al. Mesenchymal Stem Cells, Not Conditioned Medium, Contribute to Kidney Repair After Ischemia-Reperfusion Injury. *Stem Cell Res Ther* (2014) 5:1015. doi: 10.1186/scrt489
71. Toh W, Lai R, Hui J, Lim S. MSC Exosome as a Cell-Free Msc Therapy for Cartilage Regeneration: Implications for Osteoarthritis Treatment. *Semin Cell Dev Biol* (2017) 67:56–64. doi: 10.1016/j.semcdb.2016.11.008
72. Sun X, Meng H, Wan W, Xie M, Wen C. Application Potential of Stem/Progenitor Cell-Derived Extracellular Vesicles in Renal Diseases. *Stem Cell Res Ther* (2019) 10:8. doi: 10.1186/s13287-018-1097-5
73. Zhang H, Ye Q, Du Z, Huang M, Zhang M, Tan H. Mir-148b-3p Inhibits Renal Carcinoma Cell Growth and Pro-Angiogenic Phenotype of Endothelial Cell Potentially by Modulating Fgf2. *Biomed Pharmacother* (2018) 107:359–67. doi: 10.1016/j.biopha.2018.07.054
74. Christofides A, Papagregoriou G, Dweep H, Makrides N, Gretz N, Felekkis K, et al. Evidence for mir-548c-5p Regulation of Foxc2 Transcription Through a Distal Genomic Target Site in Human Podocytes. *Cell Mol Life Sci CMLS* (2020) 77:2441–59. doi: 10.1007/s00018-019-03294-z
75. Zhu G, Pei L, Lin F, Yin H, Li X, He W, et al. Exosomes From Human-Bone-Marrow-Derived Mesenchymal Stem Cells Protect Against Renal Ischemia/Reperfusion Injury Via Transferring Mir-199a-3p. *J Cell Physiol* (2019) 234:23736–49. doi: 10.1002/jcp.28941
76. Cao G, Li S, Shi H, Yin P, Chen J, Li H, et al. Schisandrin B Attenuates Renal Fibrosis Via mir-30e-Mediated Inhibition of EMT. *Toxicol Appl Pharmacol* (2019) 385:114769. doi: 10.1016/j.taap.2019.114769
77. Ragni E, De Luca P, Perucca Orfei C, Colombini A, Viganò M, Lugano G, et al. Insights Into Inflammatory Priming of Adipose-Derived Mesenchymal Stem Cells: Validation of Extracellular Vesicles-Embedded MiRNA Reference Genes as a Crucial Step for Donor Selection. *Cells* (2019) 8 (4):369. doi: 10.3390/cells8040369
78. Zhang C, Shang Y, Chen X, Midgley A, Wang Z, Zhu D, et al. Supramolecular Nanofibers Containing Arginine-Glycine-Aspartate (Rgd) Peptides Boost Therapeutic Efficacy of Extracellular Vesicles in Kidney Repair. *ACS Nano* (2020) 14:12133–47. doi: 10.1021/acsnano.0c05681
79. Baglio S, Rooijers K, Koppers-Lalic D, Verweij F, Pérez Lanzón M, Zini N, et al. Human Bone Marrow- and Adipose-Mesenchymal Stem Cells Secrete Exosomes Enriched in Distinctive Mirna and Trna Species. *Stem Cell Res Ther* (2015) 6:127. doi: 10.1186/s13287-015-0116-z
80. Li B, Liu J, Gu G, Han X, Zhang Q, Zhang W. Impact of Neural Stem Cell-Derived Extracellular Vesicles on Mitochondrial Dysfunction, Sirtuin 1 Level, and Synaptic Deficits in Alzheimer's Disease. *J Neurochem* (2020) 154:502–18. doi: 10.1111/jnc.15001
81. Zhao M, Liu S, Wang C, Wang Y, Wan M, Liu F, et al. Mesenchymal Stem Cell-Derived Extracellular Vesicles Attenuate Mitochondrial Damage and Inflammation by Stabilizing Mitochondrial DNA. *ACS Nano* (2021) 15:1519–38. doi: 10.1021/acsnano.0c08947
82. Spees JL, Olson SD, Whitney MJ, Prockop DJ. Mitochondrial Transfer Between Cells Can Rescue Aerobic Respiration. *Proc Natl Acad Sci USA* (2006) 103:1283–8. doi: 10.1073/pnas.0510511103
83. Spees J, Lee R, Gregory C. Mechanisms of Mesenchymal Stem/Stromal Cell Function. *Stem Cell Res Ther* (2016) 7:1255. doi: 10.1186/s13287-016-0363-7
84. Plotnikov EY, Khryapenkova TG, Vasileva AK, Marey MV, Galkina SI, Isaev NK, et al. Cell-to-Cell Cross-Talk Between Mesenchymal Stem Cells and Cardiomyocytes in Co-Culture. *J Cell Mol Med* (2008) 12:1622–31. doi: 10.1111/j.1582-4934.2007.00205.x
85. Ingato D, Lee J, Sim S, Kwon Y. Good Things Come in Small Packages: Overcoming Challenges to Harness Extracellular Vesicles for Therapeutic Delivery. *J Controlled Release Off J Controlled Release Soc* (2016) 241:174–85. doi: 10.1016/j.jconrel.2016.09.016
86. Song T, Eirin A, Zhu X, Zhao Y, Krier J, Tang H, et al. Mesenchymal Stem Cell-Derived Extracellular Vesicles Induce Regulatory T Cells to Ameliorate Chronic Kidney Injury. *Hypertension (Dallas Tex 1979)* (2020) 75:1223–32. doi: 10.1161/hypertensionaha.119.14546
87. Gao F, Chiu SM, Motan DA, Zhang Z, Chen L, Ji HL, et al. Mesenchymal Stem Cells and Immunomodulation: Current Status and Future Prospects. *Cell Death Dis* (2016) 7:e20625. doi: 10.1038/cddis.2015.327
88. Robbins PD, Morelli AE. Regulation of Immune Responses by Extracellular Vesicles. *Nat Rev Immunol* (2014) 14:195–208. doi: 10.1038/nri3622
89. Martin-Rufino J, Espinosa-Lara N, Osugui L, Sanchez-Guijo F. Targeting the Immune System With Mesenchymal Stromal Cell-Derived Extracellular Vesicles: What is the Cargo's Mechanism of Action? *Front Bioeng Biotechnol* (2019) 7:308. doi: 10.3389/fbioe.2019.00308
90. Wang S, Zhang C, Li J, Niyazi S, Zheng L, Xu M, et al. Erythropoietin Protects Against Rhabdomyolysis-Induced Acute Kidney Injury by Modulating Macrophage Polarization. *Cell Death Dis* (2017) 8:e27255. doi: 10.1038/cddis.2017.104
91. Roura S, Monguió-Tortajada M, Munizaga-Larroudé M, Clos-Sansalvador M, Franquesa M, Rosell A, et al. Potential of Extracellular Vesicle-Associated Tsg-6 From Adipose Mesenchymal Stromal Cells in Traumatic Brain Injury. *Int J Mol Sci* (2020) 21(18):6761. doi: 10.3390/ijms21186761.

92. Cheng A, Choi D, Lora M, Shum-Tim D, Rak J, Colmegna I. Human Multipotent Mesenchymal Stromal Cells Cytokine Priming Promotes rab27b-Regulated Secretion of Small Extracellular Vesicles With Immunomodulatory Cargo. *Stem Cell Res Ther* (2020) 11:539. doi: 10.1186/s13287-020-02050-6
93. Zhang R, Liu Y, Yan K, Chen L, Chen X, Li P, et al. Anti-Inflammatory and Immunomodulatory Mechanisms of Mesenchymal Stem Cell Transplantation in Experimental Traumatic Brain Injury. *J Neuroinflamm* (2013) 10:1065. doi: 10.1186/1742-2094-10-106
94. An J, Li Q, Ryu M, Nam A, Bhang D, Jung Y, et al. Tsg-6 in Extracellular Vesicles From Canine Mesenchymal Stem/Stromal Is a Major Factor in Relieving Dss-Induced Colitis. *PloS One* (2020) 15:e0220756. doi: 10.1371/journal.pone.0220756
95. Wang S, Cai S, Zhang W, Liu X, Li Y, Zhang C, et al. High-Mobility Group Box 1 Protein Antagonizes the Immunosuppressive Capacity and Therapeutic Effect of Mesenchymal Stem Cells in Acute Kidney Injury. *J Trans Med* (2020) 18:1755. doi: 10.1186/s12967-020-02334-8
96. Karachi A, Fazeli M, Karimi MH, Geramizadeh B, Moravej A, Ebrahimnezhad S, et al. Evaluation of Immunomodulatory Effects of Mesenchymal Stem Cells Soluble Factors on mir-155 and mir-23b Expression in Mice Dendritic Cells. *Immunol Invest* (2015) 44:427–37. doi: 10.3109/08820139.2015.1017046
97. Reis M, Mavin E, Nicholson L, Green K, Dickinson A, Wang X. Mesenchymal Stromal Cell-Derived Extracellular Vesicles Attenuate Dendritic Cell Maturation and Function. *Front Immunol* (2018) 9:2538. doi: 10.3389/fimmu.2018.02538
98. Favaro E, Carpanetto A, Caorsi C, Giovarelli M, Angelini C, Cavallo-Perin P, et al. Human Mesenchymal Stem Cells and Derived Extracellular Vesicles Induce Regulatory Dendritic Cells in Type 1 Diabetic Patients. *Diabetologia* (2016) 59:325–3. doi: 10.1007/s00125-015-3808-0
99. Mihajlovic M, Wever KE, van der Made TK, de Vries RBM, Hilbrands LB, Masereeuw R. Are Cell-Based Therapies for Kidney Disease Safe? A Systematic Review of Preclinical Evidence. *Pharmacol Ther* (2019) 197:191–211. doi: 10.1016/j.pharmthera.2019.01.004
100. Bai M, Zhang L, Fu B, Bai J, Zhang Y, Cai G, et al. Il-17a Improves the Efficacy of Mesenchymal Stem Cells in Ischemic-Reperfusion Renal Injury By Increasing Treg Percentages by The Cox-2/Pge2 Pathway. *Kidney Int* (2018) 93:814–25. doi: 10.1016/j.kint.2017.08.030
101. Zheng L, Gao W, Hu C, Yang C, Rong R. Immune Cells in Ischemic Acute Kidney Injury. *Curr Protein Pept Sci* (2019) 20:770–6. doi: 10.2174/1389203720666190507102529
102. Karbian N, Abutbul A, El-Amore R, Eliaz R, Beeri R, Reicher B, et al. Apoptotic Cell Therapy for Cytokine Storm Associated With Acute Severe Sepsis. *Cell Death Dis* (2020) 11:5355. doi: 10.1038/s41419-020-02748-8
103. Venkatachalam M, Weinberg J, Kriz W, Bidani A. Failed Tubule Recovery, Aki-Ckd Transition, and Kidney Disease Progression. *J Am Soc Nephrol JASN* (2015) 26:1765–76. doi: 10.1681/asn.2015010006
104. Messerer D, Halbgebauer R, Nilsson B, Pavenstädt H, Radermacher P, Huber-Lang M. Immunopathophysiology of Trauma-Related Acute Kidney Injury. *Nat Rev Nephrol* (2020) 17(2):91–111. doi: 10.1038/s41581-020-00344-9
105. Zilberman-Itskovich S, Efrati S. Mesenchymal Stromal Cell Uses for Acute Kidney Injury-Current Available Data and Future Perspectives: A Mini-Review. *Front Immunol* (2020) 11:1369. doi: 10.3389/fimmu.2020.01369
106. Grivei A, Giuliani K, Wang X, Ungerer J, Francis L, Hepburn K, et al. Oxidative Stress and Inflammasome Activation in Human Rhabdomyolysis-Induced Acute Kidney Injury. *Free Radical Biol Med* (2020) 160:690–95. doi: 10.1016/j.freeradbiomed.2020.09.011
107. Miura Y. [Current Basic Understanding and Clinical Application of Mesenchymal Stromal/Stem Cells]. *Rinsho Ketsueki* (2018) 59:1935–41. doi: 10.11406/rinketsu.59.1935
108. Witwer KW, Van Balkom BWM, Bruno S, Choo A, Dominici M, Gimona M, et al. Defining Mesenchymal Stromal Cell (MSC)-Derived Small Extracellular Vesicles for Therapeutic Applications. *J Extracell Vesicles* (2019) 8:16092065. doi: 10.1080/20013078.2019.1609206
109. Zhang K, Zhao X, Chen X, Wei Y, Du W, Wang Y, et al. Enhanced Therapeutic Effects of Mesenchymal Stem Cell-Derived Exosomes With an Injectable Hydrogel for Hindlimb Ischemia Treatment. *ACS Appl Mater Interfaces* (2018) 10:30081–91. doi: 10.1021/acsami.8b08449
110. Tolar J, Nauta AJ, Osborn MJ, Panoskaltsis Mortari A, McElmurry RT, Bell S, et al. Sarcoma Derived From Cultured Mesenchymal Stem Cells. *Stem Cells* (2007) 25:371–9. doi: 10.1634/stemcells.2005-0620
111. Zhang ZX, Guan LX, Zhang K, Wang S, Cao PC, Wang YH, et al. Cytogenetic Analysis of Human Bone Marrow-Derived Mesenchymal Stem Cells Passaged *In Vitro*. *Cell Biol Int* (2007) 31:645–8. doi: 10.1016/j.cellbi.2006.11.025
112. Xu S, De Becker A, De Raeve H, Van Camp B, Vanderkerken K, Van Riet I. In Vitro Expanded Bone Marrow-Derived Murine (c57bl/kalwrij) Mesenchymal Stem Cells can Acquire cd34 Expression and Induce Sarcoma Formation *In Vivo*. *Biochem Biophys Res Commun* (2012) 424:391–7. doi: 10.1016/j.bbrc.2012.06.118
113. Binato R, de Souza Fernandez T, Lazzarotto-Silva C, Du Rocher B, Mencalha A, Pizzatti L, et al. Stability of Human Mesenchymal Stem Cells During In Vitro Culture: Considerations for Cell Therapy. *Cell Prolif* (2013) 46:10–22. doi: 10.1111/cpr.12002
114. Zhang G, Wang D, Miao S, Zou X, Liu G, Zhu Y. Extracellular Vesicles Derived From Mesenchymal Stromal Cells may Possess Increased Therapeutic Potential for Acute Kidney Injury Compared With Conditioned Medium in Rodent Models: A Meta-Analysis. *Exp Ther Med* (2016) 11:1519–25. doi: 10.3892/etm.2016.3076
115. Kunter U, Rong S, Moeller M, Floege J. Mesenchymal Stem Cells as a Therapeutic Approach to Glomerular Diseases: Benefits and Risks. *Kidney Int Suppl* (2011) 1:68–73. doi: 10.1038/kisup.2011.16
116. Zhang M, Methot D, Poppa V, Fujio Y, Walsh K, Murry CE. Cardiomyocyte Grafting for Cardiac Repair: Graft Cell Death and Anti-Death Strategies. *J Mol Cell Cardiol* (2001) 33:907–21. doi: 10.1006/jmcc.2001.1367
117. Ashour R, Saad M, Sobh M, Al-Husseiny F, Abouelkheir M, Awad A, et al. Comparative Study of Allogenic and Xenogeneic Mesenchymal Stem Cells on Cisplatin-Induced Acute Kidney Injury in Sprague-Dawley Rats. *Stem Cell Res Ther* (2016) 7:1265. doi: 10.1186/s13287-016-0386-0
118. An X, Liao G, Chen Y, Luo A, Liu J, Yuan Y, et al. Intervention for Early Diabetic Nephropathy by Mesenchymal Stem Cells in a Preclinical Nonhuman Primate Model. *Stem Cell Res Ther* (2019) 10:3635. doi: 10.1186/s13287-019-1401-z
119. Cheng Y, Cao X, Qin L. Mesenchymal Stem Cell-Derived Extracellular Vesicles: A Novel Cell-Free Therapy for Sepsis. *Front Immunol* (2020) 11:647. doi: 10.3389/fimmu.2020.00647
120. Gholami L, Nooshabadi V, Shahabi S, Jazayeri M, Tarzemany R, Afsartala Z, et al. Extracellular Vesicles in Bone and Periodontal Regeneration: Current and Potential Therapeutic Applications. *Cell Biosci* (2021) 11:165. doi: 10.1186/s13578-020-00527-8
121. Bæk R, Søndergaard E, Varming K, Jørgensen M. The Impact of Various Preanalytical Treatments on the Phenotype of Small Extracellular Vesicles in Blood Analyzed by Protein Microarray. *J Immunol Methods* (2016) 438:11–20. doi: 10.1016/j.jim.2016.08.007
122. Caldas HC, Lojudice FH, Dias C, Fernandes-Charpiot IMM, Baptista M, Kawasaki-Oyama RS, et al. Induced Pluripotent Stem Cells Reduce Progression of Experimental Chronic Kidney Disease But Develop Wilms' Tumors. *Stem Cells Int* (2017) 2017:7428316. doi: 10.1155/2017/7428316
123. Lopatina T, Grange C, Fonsato V, Tapparo M, Brossa A, Fallo S, et al. Extracellular Vesicles From Human Liver Stem Cells Inhibit Tumor Angiogenesis. *Int J Cancer* (2019) 144:322–3. doi: 10.1002/ijc.31796
124. Ullah M, Liu D, Rai S, Razavi M, Choi J, Wang J, et al. A Novel Approach to Deliver Therapeutic Extracellular Vesicles Directly Into the Mouse Kidney Via its Arterial Blood Supply. *Cells* (2020) 9(4):937. doi: 10.3390/cells9040937.
125. Bruno S, Grange C, Collino F, Deregibus M, Cantaluppi V, Biancone L, et al. Microvesicles Derived From Mesenchymal Stem Cells Enhance Survival in a Lethal Model of Acute Kidney Injury. *PloS One* (2012) 7:e331155. doi: 10.1371/journal.pone.0033115
126. Nancarrow-Lei R, Mafi P, Mafi R, Khan W. A Systemic Review of Adult Mesenchymal Stem Cell Sources and Their Multilineage Differentiation Potential Relevant to Musculoskeletal Tissue Repair and Regeneration. *Curr Stem Cell Res Ther* (2017) 12:601–10. doi: 10.2174/1574888x12666170608124303
127. Allan D, Tieu A, Lalu M, Burger D. Mesenchymal Stromal Cell-Derived Extracellular Vesicles for Regenerative Therapy and Immune Modulation:

Progress and Challenges Toward Clinical Application. *Stem Cells Transl Med* (2020) 9:39–46. doi: 10.1002/sctm.19-0114

128. Cardoso R, Rodrigues S, Gomes C, Duarte F, Romao M, Leal E, et al. Development of an Optimized and Scalable Method for Isolation of Umbilical Cord Blood-Derived Small Extracellular Vesicles for Future Clinical Use. *Stem Cells Trans Med* (2021) 10(6):910–21. doi: 10.1002/sctm.20-0376
129. Tsiapalis D, O'Driscoll L. Mesenchymal Stem Cell Derived Extracellular Vesicles for Tissue Engineering and Regenerative Medicine Applications. *Cells* (2020) 9(4):991. doi: 10.3390/cells9040991
130. Cao J, Wang B, Tang T, Lv L, Ding Z, Li Z, et al. Three-Dimensional Culture of MSCs Produces Exosomes With Improved Yield and Enhanced Therapeutic Efficacy for Cisplatin-Induced Acute Kidney Injury. *Stem Cell Res Ther* (2020) 11:2065. doi: 10.1186/s13287-020-01719-2
131. Lee J, Ha D, Go H, Youn J, Kim H, Jin R, et al. Reproducible Large-Scale Isolation of Exosomes From Adipose Tissue-Derived Mesenchymal Stem/Stromal Cells and Their Application in Acute Kidney Injury. *Int J Mol Sci* (2020) 21(13):4774. doi: 10.3390/ijms21134774
132. Ullah M, Liu D, Rai S, Dadhania A, Jonnakuti S, Concepcion W, et al. Reversing Acute Kidney Injury Using Pulsed Focused Ultrasound and Msc Therapy: A Role for Hsp-Mediated pi3k/akt Signaling. Molecular Therapy. *Methods Clin Dev* (2020) 17:683–94. doi: 10.1016/j.omtm.2020.03.023
133. Ullah M, Liu D, Rai S, Concepcion W, Thakor A. Hsp70-mediated Nlrp3 Inflammasome Suppression Underlies Reversal of Acute Kidney Injury Following Extracellular Vesicle and Focused Ultrasound Combination Therapy. *Int J Mol Sci* (2020) 21(11):4085. doi: 10.3390/ijms21114085.
134. Ullah M, Liu D, Rai S, Razavi M, Concepcion W, Thakor A. Pulsed Focused Ultrasound Enhances the Therapeutic Effect of Mesenchymal Stromal Cell-Derived Extracellular Vesicles in Acute Kidney Injury. *Stem Cell Res Ther* (2020) 11:3985. doi: 10.1186/s13287-020-01922-1
135. Liu Y, Cui J, Wang H, Hezam K, Zhao X, Huang H, et al. Enhanced Therapeutic Effects of MSC-Derived Extracellular Vesicles With an Injectable Collagen Matrix for Experimental Acute Kidney Injury Treatment. *Stem Cell Res Ther* (2020) 11:1615. doi: 10.1186/s13287-020-01668-w
136. Alzahrani F. Melatonin Improves Therapeutic Potential of Mesenchymal Stem Cells-Derived Exosomes Against Renal Ischemia-Reperfusion Injury in Rats. *Am J Trans Res* (2019) 11(5):2887–907.
137. Zhang Z, Hou Y, Zou X, Xing X, Ju G, Zhong L, et al. Oct-4 Enhanced the Therapeutic Effects of Mesenchymal Stem Cell-Derived Extracellular Vesicles in Acute Kidney Injury. *Kidney Blood Pressure Res* (2020) 45:95–108. doi: 10.1159/000504368
138. Shekari F, Nazari A, Assar Kashani S, Hajizadeh-Saffar E, Lim R, Baharvand H. Pre-Clinical Investigation of Mesenchymal Stromal Cell-Derived Extracellular Vesicles: A Systematic Review. *Cytotherapy* (2021) 23(4):277–84. doi: 10.1016/j.jcyt.2020.12.009
139. Théry C, Witwer K, Aikawa E, Alcaraz M, Anderson J, Andriantsitohaina R, et al. Minimal Information for Studies of Extracellular Vesicles 2018 (Misev2018): A Position Statement of the International Society for Extracellular Vesicles and Update of the Misev2014 Guidelines. *J Extracell Vesicles* (2018) 7:1535750. doi: 10.1080/20013078.2018.1535750
140. Zhang N, Song Y, Huang Z, Chen J, Tan H, Yang H, et al. Monocyte Mimics Improve Mesenchymal Stem Cell-Derived Extracellular Vesicle Homing in a Mouse Mi/Ri Model. *Biomaterials* (2020) 255:1201685. doi: 10.1016/j.biomaterials.2020.120168
141. Armstrong JP, Holme MN, Stevens MM. Re-Engineering Extracellular Vesicles as Smart Nanoscale Therapeutics. *ACS Nano* (2017) 11:69–83. doi: 10.1021/acsnano.6b07607

Conflict of Interest: The authors declare that the research was conducted in the absence of any commercial or financial relationships that could be construed as a potential conflict of interest.

The handling editor has declared past co-authorships with one of the authors (CY) in the time of review.

Copyright © 2021 Li, Yang, Su, Luo, Luo, Huang, Tu and Luo. This is an open-access article distributed under the terms of the Creative Commons Attribution License (CC BY). The use, distribution or reproduction in other forums is permitted, provided the original author(s) and the copyright owner(s) are credited and that the original publication in this journal is cited, in accordance with accepted academic practice. No use, distribution or reproduction is permitted which does not comply with these terms.

frontiers in Immunology

REVIEW
published: 04 June 2021
doi: 10.3389/fimmu.2021.683003

Immunomodulatory Effects of Mesenchymal Stem Cells on Drug-Induced Acute Kidney Injury

Qiuxia Han[1,2†], Xiaochen Wang[1†], Xiaonan Ding[1], Jun He[3], Guangyan Cai[1,2*] and Hanyu Zhu[1*]*

[1] Department of Nephrology, First Medical Center of Chinese People's Liberation Army (PLA) General Hospital, Nephrology Institute of the Chinese People's Liberation Army, State Key Laboratory of Kidney Diseases, National Clinical Research Center for Kidney Diseases, Beijing Key Laboratory of Kidney Disease Research, Beijing, China, [2] School of Medicine, Nankai University, Tianjin, China, [3] Department of Genetics, Changsha Hospital for Maternal and Child Health Care, Hunan, China

OPEN ACCESS

Edited by:
Ying Wang, Shanghai Institute of Nutrition and Health (CAS), China

Reviewed by:
Liming Du, University of Texas Southwestern Medical Center, United States
Bing Yu, Second Military Medical University, China

***Correspondence:**
Hanyu Zhu
Hanyuzhu301@126.com
Jun He
19252702@qq.com
Guangyan Cai
caiguangyan@sina.com

[†]These authors have contributed equally to this work

Specialty section:
This article was submitted to Molecular Innate Immunity, a section of the journal Frontiers in Immunology

Received: *19 March 2021*
Accepted: *10 May 2021*
Published: *04 June 2021*

Citation:
Han Q, Wang X, Ding X, He J, Cai G and Zhu H (2021) Immunomodulatory Effects of Mesenchymal Stem Cells on Drug-Induced Acute Kidney Injury. Front. Immunol. 12:683003. doi: 10.3389/fimmu.2021.683003

Drug-induced nephrotoxicity is an important and increasing cause of acute kidney injury (AKI), which accounts for approximately 20% of hospitalized patients. Previous reviews studies on immunity and AKI focused mainly on ischemia-reperfusion (IR), whereas no systematic review addressing drug-induced AKI and its related immune mechanisms is available. Recent studies have provided a deeper understanding on the mechanisms of drug-induced AKI, among which acute tubular interstitial injury induced by the breakdown of innate immunity was reported to play an important role. Emerging research on mesenchymal stem cell (MSC) therapy has revealed its potential as treatment for drug-induced AKI. MSCs can inhibit kidney damage by regulating the innate immune balance, promoting kidney repair, and preventing kidney fibrosis. However, it is important to note that there are various sources of MSCs, which impacts on the immunomodulatory ability of the cells. This review aims to address the immune pathogenesis of drug-induced AKI versus that of IR-induced AKI, and to explore the immunomodulatory effects and therapeutic potential of MSCs for drug-induced AKI.

Keywords: acute kidney injury, mesenchymal stem cell, immunomodulation, cell therapy, kidney repair, drug-induced AKI, ischemia-reperfusion

INTRODUCTION

In the past decade, pharmaceutical companies have developed many life-saving drugs for patients with cancer. Unfortunately, some of these drugs are associated with nephrotoxicity, which remains an important and more frequent cause of acute kidney injury (AKI). Currently, AKI represents a serious global public health challenge, with significant adverse economic and medical burden, that affects approximately 13.3 million people annually (1, 2). Drug-induced AKI is a particularly important category, accounting for 19–26% of AKI cases (2). The use of nephrotoxic drugs is the main cause of severe AKI in critically ill patients. Moreover, drug-induced nephrotoxicity is one of the main factors leading to unsuccessful drug development, leading to loss of money and time in the pharmaceutical industry (3). Notably, approximately 19% of phase 3 clinical trial failures are caused by nephrotoxicity (3).

Recent studies have provided a deeper understanding of the mechanisms underlying drug-induced AKI. In particular, oxidative stress was shown to activate inflammatory responses, by promoting the release of pro-inflammatory cytokines and the accumulation of inflammatory cells in tissues, which supports the progression of AKI (4). Mesenchymal stem cell (MSC) therapy has been considered to hold great potential for the treatment of drug-induced AKI given its powerful immune regulatory effects (5). Previous studies on the immune pathogenesis of AKI and MSC therapy mostly focused on ischemia-reperfusion (IR), but drug-induced AKI is also important and needs more attention. The immune pathogenesis of IR and drug-induced AKI were reported to be different, which may also impact on the efficiency of MSC treatment on drug-induced AKI. Therefore, the differences between these two types of AKI could provide a good reference for scientists to explore MSC-based treatment strategies for drug-induced AKI in the future. In addition, it is very important to notice that MSCs can be derived from various sources and their immunomodulatory ability may differ based on their origin. When using MSCs for clinical treatment of patients, it should be considered the difficulty of obtaining these cells, as well as the number of cells and ethical limitations. Therefore, understanding the immunomodulatory ability, proliferative potential, and clinical application characteristics of MSCs from different sources can aid to choose the most appropriate MSC population for clinical use in AKI treatment.

In this review, we provide an in-depth, comprehensive summary of the immune pathogenesis of drug-induced AKI and subsequent molecular mechanisms, including the different types of immune cells, cytokines, and related signaling pathways. The immunomodulatory effects of MSCs for the treatment of drug-induced AKI were also explored based on the latest research progress. In particular, we compared the different immune pathogenesis of drug-induced and IR-induced AKI, as well as the different immune regulatory abilities of MSCs from different sources.

DRUG-INDUCED AKI AND COMMON NEPHROTOXIC DRUGS: THE CISPLATIN EXAMPLE

Several recent, large-scale epidemiological studies have shown that nephrotoxic drugs cause severe acute renal failure in many critically ill patients (2), for whom the use of potentially nephrotoxic drugs is, in most cases, unavoidable (6). Drug-induced AKI usually presents as one of two types: acute tubular necrosis, which is directly related to nephrotoxicity to the renal tubular epithelial cells, or immune-mediated acute interstitial nephritis, which develops from drugs that cause allergic reactions. Approximately 60% of patients with hospital-acquired AKI experience nephrotoxic induced by medications (7). Among the various cellular mechanisms of drug-induced AKI, the most important is the accumulation of inflammatory cells in the tissue, which in turn activates the inflammatory response and oxidative stress that triggers the release of pro-inflammatory factors. Nephrotoxic injuries often occur in the proximal renal tubules due to the administration of cisplatin, aminoglycosides (gentamycin, kanamycin, streptomycin, or tobramycin), amphotericin B, antiviral agents (adefovir, cidofovir, or tenofovir), radiocontrast, bisphosphonate, among other drugs (4).

Cisplatin is a chemotherapy drug, and is the most classic and commonly used model for basic research on drug-induced AKI, with a reported frequency of cisplatin-induced AKI ranging from 20% to 30% due to dose-limiting side effects in the treatment of various solid cancers, including testicular, ovarian, cervical, breast, lung, head and neck, bladder, and gastric cancer (8). Although there are other less common cisplatin-induced toxicities (such as ototoxicity, gastrotoxicity, and myelosuppression), nephrotoxicity has a major impact on the patient health and should be the first side effect to be monitored and evaluated in patients undergoing cancer chemotherapy. Notably, the accumulation of toxic intermediates in the kidney limits the use of cisplatin, which leads to incomplete chemotherapy. Therefore, the mechanism reviewed hereafter is mainly based on basic research conducted with the cisplatin-induced AKI model.

The typical histological features of drug-induced AKI are severe tubule damage comprising lumen dilation, significant cytoplasmic simplification, increased cytoplasmic eosinophilia, and disappearance of brush borders and of the tubule epithelium. First, several events, such as loss of polarity and cytoskeletal integrity, and cell necrosis and apoptosis, occur in the proximal tubular epithelial cells of the kidney over time (9, 10). Subsequently, necrosis induces inflammation, and damage-associated molecular patterns (DAMPs) and other pro-inflammatory molecules are released, resulting in the activation of the innate immune system *via* membrane surface receptors. Inflammatory cells, such as white blood cells, are recruited into the peritubular interstitium. Furthermore, inflammation accelerates the damage to the renal tubular tissues and causes necroptosis and the release of tumor necrosis factor alpha (TNF-α) and other inflammatory factors that continue to drive cell necrosis. This leads to tubular necrosis and renal insufficiency, forming an inflammation-necrosis amplification loop (11, 12). Another mechanism of drug-induced AKI is oxidative stress. Drug nephrotoxicity directly acts on the proximal renal tubules and causes cell damage, such as mitochondrial dysfunction, lysosomal hydrolase inhibition, phospholipid damage, and increased intracellular calcium concentrations, thereby leading to the formation of reactive oxygen species (ROS) (13). The pathogenic mechanisms of ROS have three main aspects: first, nephrotoxic drugs react with cellular antioxidants (such as glutathione) when they are in a highly reactive form (14, 15), thus, depleting or inactivating them, leading to the accumulation of endogenous ROS in cells. ROS activates the intracellular mitogen-activated protein kinases, p53, p21, and other pathways, leading to the death of renal tubular cells. Second, ROS directly or indirectly promotes fibrosis by promoting tissue inflammation. Fibrosis and

inflammation will, in turn, promote positive feedback pathways, further increasing ROS production and stimulating the secretion of inflammatory factors. Third, nephrotoxic drugs affect the normal respiration of mitochondria, making them dysfunctional and increasing the production of ROS (16).

DIFFERENT IMMUNE MECHANISMS OF DRUG-INDUCED AND IR-INDUCED AKI

AKI is mainly triggered by IR injury, which causes high morbidity and mortality in both adults and children (17). IR-induced AKI results from acute hypoxia caused by reduced blood perfusion in the renal tissue, which is prone to occur in the renal tubule region. Reperfusion leads to the production of metabolites, such as nitric oxide and ROS, which can damage the cell membranes and lead to cell apoptosis. However, drug-induced AKI is more common in infants and older people with underlying cardiovascular diseases and renal dysfunction, such as intravascular volume depletion, diabetes, congestive heart failure, chronic kidney disease, and sepsis (18, 19). Drug-induced renal injury, which results from the direct damage to the renal tubular epithelial cells, occurs when the increasing concentration of nephrotoxic drugs in the renal tubule reaches a toxic level. Therefore, the degree of damage is related to the drug dose administrated. Noteworthy, there are several differences in the pathogenesis of IR-induced and drug-induced AKI; however, there are very limited systematic reviews comparing the differences in the pathogenesis between these two models. Understanding the differences in their immune pathogenesis may be helpful for the management of AKI. A summary of these differences is provided in **Table 1**.

T cells play an important role in AKI. In IR-induced AKI, $CD8^+$ cells have no obvious pathogenic effects. However, in the cisplatin-induced AKI model, CD8-deficient mice had significantly less damage than wild-type mice, indicating that $CD8^+$ cells have an important pathogenic role in this model (20). No obvious differences in other subpopulations of T cells were found between the two models. During the inflammatory response to IR injury, the main role of renal dendritic cells (DCs) is to serve as antigen-presenting cells to T cells, release TNF-α, upregulate adhesion molecules, and promote leukocyte extravasation (21, 22). However, renal DCs play a protective role in drug-induced AKI. In one study, infiltration of DCs in damaged tissues resulted in secretion of cytokines such as interleukin (IL)-10 to prevent AKI progression (23). In the IR model, inhibition of neutrophil recruitment can significantly reduce kidney damage, which suggests that neutrophil infiltration is one of the pathogenic mechanisms of renal IR injury (24). In contrast, inhibition of neutrophil infiltration has no effect on cisplatin-induced kidney injury, indicating that neutrophil infiltration is not necessary for cisplatin-induced kidney damage (25). Importantly, macrophages have pro-inflammatory (M1) and anti-inflammatory (M2) cell phenotypes and their roles in the two AKI models are similar (26), with M1 cells being dominant in the damage stage, whereas M2 cells playing an important role in the repair stage. In addition, the relationship between the complement system and AKI has been studied more in the IR injury model than in the drug-induced AKI model. However, the mechanism of action of the complement system in both models is mainly mediated by the activation of the complement component 5a and its receptor (C5a/C5aR)–nuclear factor kappa B (NF-κB) pathway (27).

Cytokines and chemokines are differently expressed in drug-induced and IR-induced AKI, which may be due to the different cellular origins and actions of the molecules. IL-11 is upregulated in IR-induced (but not in cisplatin-induced) AKI (28). In addition, inhibition of IL-18 can significantly reduce IR-induced renal injury but not cisplatin-induced nephrotoxicity (29), which suggests that IL-18 may be an important factor in IR-induced AKI. Moreover, the expression of the C-C motif chemokine ligand (CCL) 5 and IL-1α is significantly increased in cisplatin-induced AKI, but only slightly increased in the IR injury model (28). Furthermore, TNF-α-deficient mice are resistant to cisplatin nephrotoxicity, thereby suggesting that TNF-α plays an important role in the pathogenesis of

TABLE 1 | Comparison of the immune mechanisms between drug-induced and ischemia reperfusion-induced AKI.

Immune system component	Mechanism of IR-induced AKI (e.g., organ grafting)	Mechanism of drug-induced AKI (e.g., cisplatin)
T cells	$CD8^+$ cells have no obvious pathogenic effect in IR injury (20).	Inhibition of $CD8^+$ can significantly improve kidney damage (20).
Dendritic cells	Higher proportion of mature dendritic cells, antigen presentation effect and pro-inflammatory response (21, 22).	Higher proportion of immature dendritic cells, promote kidney repair (23).
Neutrophils	Infiltration at the injury site, but inhibition of neutrophils can significantly reduce kidney damage (24).	Infiltration at the injury site, but inhibition of neutrophils cannot significantly reduce kidney damage (25).
Macrophages	Macrophages have similar actions in drug-induced and IR-induced AKI. M1 cells are the dominant cells in damage stage; M2 cells play a role in tissue repair (26).	
Complement system	The mechanism of action of the complement system in drug-induced and IR-induced AKI involves the activation of C5a/C5aR–NF-κB pathway (27).	
Cytokines/pathway	The levels of IL-11 increase (28). Inhibition of IL-18 can significantly prevent kidney damage (29). CCL5 and IL-1α slightly increase (28). Inhibition of TNF-α cannot significantly reduce kidney damage (28). NLRP3 pathway is the key pathogenesis of inflammation (30).	The levels of IL-11 do not increase (28). Inhibition of IL-18 cannot significantly prevent kidney damage (29). CCL5 and IL-1α significantly increase (28). Inhibition of TNF-α can significantly reduce kidney damage (28). NLRP3 pathway is less important (30).

AKI, acute kidney injury; C5a, complement component 5a; C5aR, complement component 5a receptor; CCL5, C-C motif chemokine ligand 5; IL, interleukin; IR, ischemia-reperfusion; M1, pro-inflammatory macrophages; M2, anti-inflammatory macrophages; NF-κB, nuclear factor kappa B; NLRP3, NLR family pyrin domain containing 3; TNF, tumor necrosis factor.

cisplatin-induced renal injury. Accordingly, TNF-α inhibitors can ameliorate renal dysfunction and reduce the structural damage caused by cisplatin, and inhibition of TNF-α more effectively reduce cisplatin-induced than IR-induced kidney damage (28). In addition, the nucleotide-binding oligomerization domain-like receptors (NLR) family pyrin domain containing 3 (NLRP3) pathway is critical in the pathogenesis of IR-induced AKI, but is less important in cisplatin-induced AKI (30).

DIFFERENT IMMUNOREGULATION CAPABILITY OF MSCS FROM VARIOUS ORIGINS

MSCs are pluripotent stem cells with anti-inflammatory and immune tolerance potential (31), which were first identified in the bone marrow stroma where supported the development and differentiation of hematopoietic stem cells. In recent years, with research advances, MSCs have been increasingly used in clinical practice given their immunosuppressive functions and tissue repair ability (32). Hence, stem cell therapy is another medical revolution that may be considered after drug therapy and surgical treatment. MSCs can easily expand *in vitro* into high numbers in a short period of time. This is an important prerequisite for MSCs that are widely used in experimental research and clinical practice, including AKI treatment (33). Moreover, MSCs can be cultured from adipose tissue, cord blood, umbilical cord, placenta, and fetal lungs. However, the biological characteristics of the MSCs originating from these various tissues are different, especially concerning their immune regulation capacity (34). The immunological activity of MSCs from different tissues may differ because of the different original activation states of these cells in the source tissues (35–37). The differences in the immunomodulatory ability, proliferation potential, and clinical application characteristics of MSCs from different sources is summarized in **Table 2**.

Current studies have shown that the immunological activity of MSCs originating from different tissues is "strong" or "weak" rather than "present" or "absent" (38). Yoo et al. compared the immune regulatory functions of adipose-derived MSCs (AD-MSCs), umbilical cord blood-derived MSCs, umbilical cord-derived MSCs (UC-MSCs), and bone marrow-derived MSCs (BM-MSCs) on T lymphocytes (34), and found that all four types of MSCs inhibited the proliferation of activated T cells and the secretion of interferon-γ and TNF-α. Moreover, Bochev et al. found that both BM-MSCs and AD-MSCs could inhibit the secretion of immunoglobulins by activating B lymphocytes (39). However, the inhibitory effects of AD-MSCs on immunoglobulin secretion were stronger than those of BM-MSCs. Some study also reported that AD-MSCs have higher indoleamine 2,3-dioxygenase (IDO) activity and secret more IL-6, IL-10, and transforming growth factor (TGF)-β than BM-MSCs (35, 40). Moreover, Barcia et al. found that compared with BM-MSCs, UC-MSCs have stronger immunomodulatory abilities, can more efficiently inhibit CD3- and CD28-induced lymphocyte proliferation, and can more efficiently induce the production of $CD3^+CD4^+CD25^+Foxp3^+$ regulatory T cells (Tregs) (41).

Nevertheless, some studies have shown that the *in vitro* expansion capabilities of MSCs from different tissues are not completely the same. Different microenvironments may be the reason for these differences. Li et al. compared the proliferative capacity of BM-MSCs and AD-MSCs, and found that AD-MSCs have stronger proliferation potential (42). However, as the age of the donor increases, the number and proliferation capacity of BM-MSCs and AD-MSCs significantly decreases. MSCs derived from perinatal tissues (such as umbilical cord, placental chorion, and amniotic membrane) have much stronger proliferation potential than BM-MSCs. Comparing MSCs isolated from umbilical cord tissue and bone marrow, more MSCs can be obtained from umbilical cord tissues, and with greater proliferation ability than BM-MSCs (43). After 30 generations, the proliferative capacity of UC-MSCs did not change significantly, whereas BM-MS showed weakened proliferation ability and prolonged doubling time after six passages.

In summary, perinatal MSCs (MSCs derived from the umbilical cord and placenta) generally have higher immunomodulatory capabilities, while BM-MSCs show higher potential to support the regeneration process, such as neuronal differentiation and development (43). These differences between perinatal and bone marrow-derived MSCs may impact on their clinical application. In addition, when MSCs are used in the clinical treatment of diseases, the feasibility of its acquisition, the number of cells, and ethical limitations must be considered. For example, BM-MSCs and AD-MSCs have several limitations. They are generally obtained from adults and the number of

TABLE 2 | Immunomodulatory ability, proliferation potential, and clinical application characteristics of MSCs from different sources.

Source	Immunomodulatory ability[1]	Proliferation potential[1]	Clinical application characteristics
Bone marrow	+	+	The related research started earlier and is more thorough. The number of cells that can be extracted is relatively small. The passage ability that can maintain the characteristics is weak.
Umbilical cord	+++	+++	The number of extractable cells is obviously more than that of bone marrow. Strong ability of passage. No ethical limit.
Placenta	+++	+++	The number of extractable cells is more than that of umbilical cord and bone marrow. No ethical limit.
Adipose tissue	++	++	Easy to get relatively large number of cells from rich resource of adipose tissue. Whether the cells can adapt to the environment *in vivo* remains to be further studied.

[1]*Higher number of + represents a stronger degree.*

cells available is limited. Moreover, there are restrictions regarding the age of the donor. However, MSCs in the perinatal period have stronger expansion capacity and have no ethical restrictions. After expansion, the basic properties and morphology of MSCs have no obvious changes, so that a large number of MSCs can be obtained from the same sample to meet the needs of the clinical cell therapy (43). Therefore, compared with adult-derived stem cells that proliferate slowly, perinatal MSCs have unique advantages. From this perspective, MSCs derived from umbilical cord and placenta are an ideal choice.

IMMUNOMODULATORY EFFECTS OF MSCS ON DRUG-INDUCED AKI

The strong ability of MSCs to differentiate is one of the main mechanisms contributing for tissue damage repair. Although the initial focus on MSCs was on their regenerative ability to differentiate into various tissue cell types (33), more attention is currently addressed onto their ability to regulate immune responses (44). *In vivo* and *in vitro* studies have shown that MSCs can directly inhibit the proliferation, differentiation, and effector mechanisms of T cells by preventing the externalization and maturation of DCs. In addition to T cells and DCs, the target cells of MSCs include many other types of immune cells, including natural killer cells, B cells, neutrophils, and macrophages (45). MSCs regulate the function of these cells, including the secretion of cytokines and their subsequent cytotoxic effects, eventually exerting anti-inflammatory effects and/or inducing an immune tolerance state. To date, the immune regulation mechanisms of MSCs remain poorly understood, but it is generally believed that MSCs have an immunosuppressive function mainly through cell-to-cell contact with a variety of immune cells and secretion of soluble factors, such as prostaglandin E2 (PGE2) and IDO, thereby reducing tissue damage caused by inflammation (46). MSCs have low immunogenicity, that is, MSCs do not express major histocompatibility complex class II molecules or costimulatory molecules, and do not cause the activation and proliferation of allogeneic lymphocytes, which provides the possibility for the clinical application of allogeneic MSCs transplantation (47). These cells inhibit the proliferation of activated T lymphocytes and the secretion of interferon-γ, the proliferation of B lymphocytes and the secretion of immunoglobulins, the killing activity of natural killer cells, the differentiation of M1 macrophages, the secretion of pro-inflammatory factors, and the differentiation of monocytes into DCs (48).

There is a very close connection between the immune system and the kidney system (49). Pro-inflammatory DAMPs, pathogen-associated molecular patterns (PAMPs), toll-like receptors (TLRs), oxidative stress, complement system, resident DCs, neutrophils, T lymphocytes, macrophages, and secreted cytokines and chemokines, all participate in the immunopathological mechanism of drug-induced AKI and promote disease progression (20, 28, 50–53). Therefore, imbalance of the immune system has a direct or indirect impact on the progression of kidney disease. If the immunopathological process of AKI continues, this may lead to renal fibrosis and/or chronic kidney disease. The immunomodulatory mechanism of MSCs in AKI treatment is shown in **Figure 1**.

THE IMMUNE MICROENVIRONMENT OF DRUG-INDUCED AKI

T Cells

Approximately 30% of the circulating white blood cells in healthy adults are T cells from the thymus (51). T cells are important immune regulators of drug-induced AKI, as T cell infiltration was observed in damaged renal tissues within 1 h after cisplatin administration, which reached a peak at 12 h and decreased after 24 h (54). Compared with wild-type mice, T cell knockout significantly improved renal function and prolonged survival in cisplatin-induced AKI mice. Furthermore, infiltration of neutrophils and macrophages into the kidney was reduced in T cell knockout mice, suggesting that T cells play a critical role in the recruitment of immune cells to the site of injury. $CD4^+$ T cells are activated and quickly infiltrate the damaged kidneys, mediating further renal tissue damage (54, 55). Depending on the regulation of the immune microenvironment, naive $CD4^+$ cells can differentiate into helper T cells (Th) or Tregs, and play different roles. Cisplatin nephrotoxicity causes naïve $CD4^+$ T cells to differentiate into Th, resulting in a strong immune response and kidney damage. Tregs are believed to play a protective role against cisplatin-induced AKI. They enter the kidney tissue and directly modulate the response of cells to inhibit the pro-inflammatory signals promoted by cisplatin toxicity, reduce renal macrophage infiltration, as well as the levels of TNF-α and IL-1β, thereby reducing renal dysfunction. $CD4^+$ T cells complete the immune response to cisplatin through the paracrine pathway (secreting TNF-α, IL-17, IL-33, and IL-10), whereas cytotoxic $CD8^+$ T cells induce renal cell injury in a contact-dependent manner (54). Cisplatin can upregulate the expression of Fas receptors on damaged renal tubular epithelial cells, allowing it to interact with Fas ligands on $CD8^+$ T cells infiltrating the kidney, and then trigger the apoptosis of damaged cells (49). MSCs can inhibit the production and activation of Th and $CD8^+$ T cells, and reduce inflammation in cisplatin-induced AKI. Furthermore, MSCs promote the differentiation of naïve $CD4^+$ T cells into Tregs by secreting hepatocyte growth factor, TGF-β, PGE2, and IDO, which in turn secrete IL-10. Moreover, PGE2 and IDO secreted by MSCs can promote the differentiation of macrophages into the anti-inflammatory M2 phenotype (56). Therefore, the anti-inflammatory effects of MSCs can be further improved, and the kidney damage caused by cisplatin can be reduced.

Dendritic Cells

DCs are the most common immune cells that maintain renal homeostasis. Renal DCs are located between the renal tubules and the peritubular capillaries. They act as effector cells and

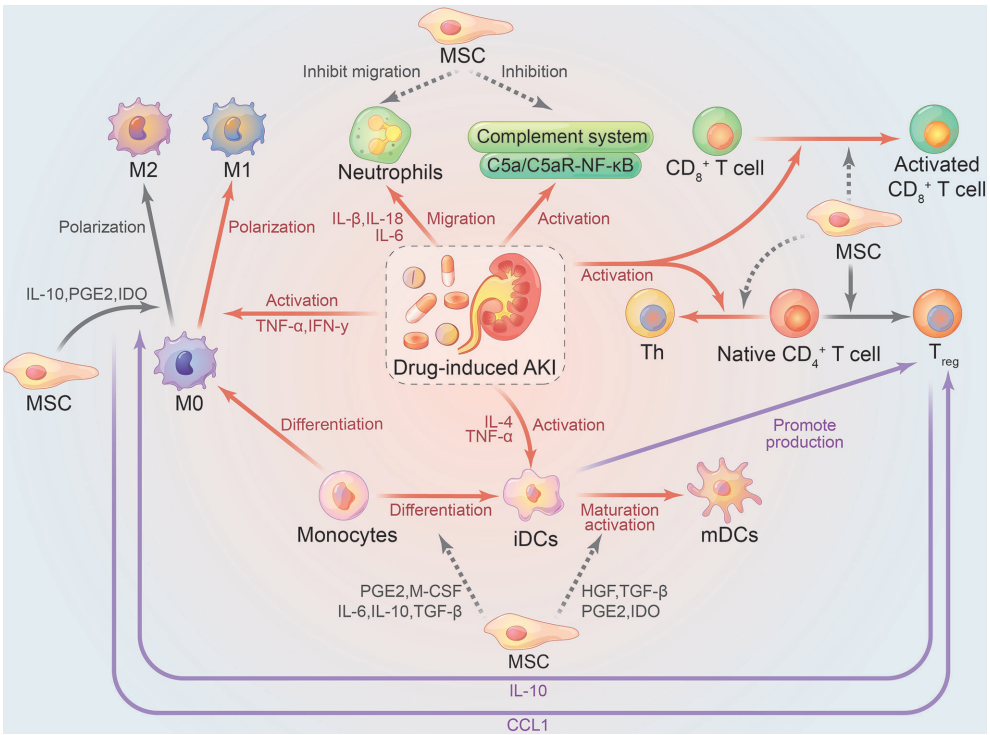


FIGURE 1 | Immunomodulatory effects of mesenchymal stem cells on drug-induced AKI. Gray, therapeutic effect of mesenchymal stem cells on the kidney; Red, damage effect of AKI on the kidney; Purple, interaction between immune cells; Solid line, promoting effect; dashed line, inhibiting effect. AKI, acute kidney injury; iDCs, immature dendritic cells; mDCs, mature dendritic cells; Th, helper T cells; Treg, $CD3^+CD4^+CD25^+Foxp3^+$ regulatory T cells; HGF, hepatocyte growth factor; IDO, indoleamine 2,3-dioxygenase; PGE2, prostaglandin E2; TGF-β, transforming growth factor β.

intermediates between endothelial and epithelial cells (21). In the injured state, renal DCs express specific cytokines through toll-like receptors, nod-like receptors, cell fragments, or other DAMPs, and present antigens to T cells to complete the transition from innate to adaptive immunity (57, 58). Similar to macrophages, DCs have two types: a pro-inflammatory phenotype (mature DCs; mDCs) and an anti-inflammatory phenotype (immature DCs; iDCs). Renal DCs are capable of immune induction and/or immune tolerance; thus, imbalanced immune regulation leads to the occurrence and progression of AKI. In cisplatin-induced AKI, IL-4 and TNF-α activate iDCs into mature phenotypes at the initial stage, causing kidney damage. IL-10, which is mainly derived from renal iDCs and plays an important role in immune regulation, has a nephroprotective effect and can reduce the nephrotoxicity of cisplatin in an inducible nitric oxide synthase-dependent manner (59). Hence, inhibition of nitric oxide synthase activity leads to a reduced number of IL-10-secreting DCs and loss of the renal protective effect of BM-MSCs (60). Furthermore, clearance of IL-10-secreting DCs can aggravate cisplatin-induced nephrotoxicity (52, 59). MSCs can inhibit the maturation of DCs and promote their transition to a tolerant immunosuppressive phenotype. They can also inhibit the differentiation of monocytes into iDCs by secreting PGE2, monocyte colony-stimulating factor, IL-6, IL-10, and TGF-β. Furthermore, MSCs can inhibit the maturation of iDCs into mDCs by secreting hepatocyte growth factor, TGF-β, PGE2, and IDO (56). PGE2 can inhibit the production and secretion of osteopontin, a cytokine released from DCs, which contributes to tissue inflammation (61). In the inflammatory microenvironment, iDCs stimulated by IL-10 (produced by MSCs) fail to express markers of mDCs (62). These iDCs do not produce TNF-α and, thus, can inhibit the progression of inflammation at the site of injury (63, 64). In addition, iDCs can promote the production of Tregs and exert anti-inflammatory effects. Some studies have shown that MSCs reduce the expression of major histocompatibility complex class II, CD40, and CD86 costimulatory molecules by mDCs, which is the cause of the decrease in T cell proliferation and weaker immune responses (65). MSCs also inhibit the antigen-presenting effects of DCs on $CD4^+$ and $CD8^+$ T cells in inflammatory lymph nodes (66), and reduce the production of pro-inflammatory factors, such as interferon-γ and IL-17 (67). These immunomodulatory effects help to reduce cisplatin-induced kidney damage.

Neutrophilic Granulocytes

When AKI occurs, many neutrophils are transported and accumulate in the blood vessels of the kidney, leading to blockage of the microvascular network. With the help of endothelial chemokines and adhesion molecules, neutrophils are attracted to the damaged site, mediate inflammation, and assist in the elimination of damaged cells in preparation for the

repair of the kidney (68). However, this effect is a double-edged sword. If the inflammatory response is insufficient, damaged or dead cells cannot be cleared in a timely manner, resulting in delayed tissue healing and AKI may eventually develop into chronic kidney disease. However, if the inflammatory response is excessive, cytotoxic compounds (ROS, proteases, and inflammatory cytokines) secreted by neutrophils will adhere to the kidney endothelial cells in large quantities, which triggers inflammatory factor infiltration and impairs the cell repair processes. A study reported that neutrophil infiltration increased in a group of cisplatin-treated mice compared to the control group (25). Interestingly, when caspase-11 was inhibited, neutrophil infiltration decreased, suggesting that cisplatin can induce neutrophil infiltration *via* caspase-11 activation (69). Other ways to significantly reduce neutrophil infiltration after administration of cisplatin include the use of TNF-α inhibitors, TLR-4 antagonists, or anti-intercellular adhesion molecule-1 antibodies (53), thereby partially improving cisplatin-induced AKI. Studies have shown that when MSCs are used to treat AKI, the migration and infiltration of neutrophils in the kidneys, as well as the serum creatinine and blood urea nitrogen levels, are significantly reduced, and renal function and kidney pathological damage is ameliorated (31, 70).

Macrophages

The mononuclear-macrophage system plays a crucial role in the immune response. According to changes in the microenvironment at the injury site, macrophages can differentiate into pro-inflammatory (M1) or anti-inflammatory (M2) cell phenotypes, which play an important role in the stage of damage and repair, respectively (26). After acute renal tissue destruction, monocytes are immediately recruited to the damaged site and are stimulated by DAMPs and PAMPs (TNF-α, interferon-γ, saturated fatty acids, and IL-6) to differentiate into the M1 phenotype and participate in the innate immune response (71, 72). Additionally, through the production and secretion of various cytotoxic substances, such as chemokines, pro-inflammatory cytokines, and inducible nitric oxide synthase, M1 cells amplify the renal inflammatory response in AKI and exacerbate disease progression (50). However, blockage of macrophage recruitment does not completely prevent cisplatin-induced AKI (73). Some studies have shown that the M2 phenotype inhibits excessive inflammatory reactions by secreting anti-inflammatory mediators (such as IL-10 and TGF-β), and promotes renal cell repair (74, 75). MSCs therapy can significantly reduce cisplatin-mediated immune cell infiltration in damaged kidney tissues, such as macrophages, DCs, neutrophils, and $CD4^+$ and $CD8^+$ T cells. As a result, it inhibits the production of inflammatory factors, but stimulates the secretion of the anti-inflammatory factors IL-10, IL-6, nitric oxide, and kynurenine (60). In addition, MSCs can promote the differentiation of macrophages into the anti-inflammatory M2 phenotype by secreting various factors including PGE2, IL-10, and IDO (67). Furthermore, the M2 phenotype can secrete CCL1 to promote Treg production. Therefore, the anti-inflammatory effects of MSCs can be further improved, and the kidney damage caused by cisplatin can be ameliorated.

Complement System

The complement system plays an important role in innate immunity and is activated by either of three pathways: classical, alternative, or lectin pathways (76), which eventually lead to the cleavage of C5 into C5a and C5b. These two allergenic proteins later form the complement membrane in the first step of forming the attack complex. Studies have shown that N-acetylcysteine can reduce the nephrotoxic effect of cisplatin by inhibiting the binding of C5a to C5aR. In addition, inhibiting C5aR can reduce neutrophil infiltration and the effects of inflammatory factors (77). When MSCs were used to treat AKI, serum C5a levels and C5aR expression in renal tissues were significantly reduced, and NF-κB translocation was also reduced. Hence, MSCs can reduce AKI by inhibiting the activation of the C5a/C5aR–NF-κB pathway (27).

CONCLUSION AND PERSPECTIVE

To date, the safest route of administration of MSCs in clinical applications is through vascular injection; thus, the number of MSCs that can reach the kidney is very small (47). Several scientists have attempted to improve the efficacy of MSCs through various methods. Improving the immunomodulatory ability of MSCs is key to improving their therapeutic effect. Studies have been conducted to regulate the relevant immune responses by innovative pretreatment methods, thereby enhancing the kidney repairing effect (78, 79). Currently, most reviews focus on AKI due to ischemia-reperfusion. However, there are relatively few studies on drug-induced AKI, especially on the role of the complement system. Drugs-induced kidney injury is also one of the biggest causes of AKI (4). Future research in this area will help deepen our understanding of the immune regulation mechanism of MSCs therapy for AKI, and discover more potential therapeutic targets.

AUTHOR CONTRIBUTIONS

QH and XW had the original idea and wrote the first draft. HZ, JH, and GC reviewed the manuscript. HZ and XD provided critical input. All authors contributed to the article and approved the submitted version.

FUNDING

This research was funded by The National Natural Science Foundation of China (No. 61971441) and the National Key R&D Program of China (No. 2016YFC1305500, 2018YFA0108803).

ACKNOWLEDGMENTS

QH thanks Mr. Xu for his love and support.

REFERENCES

1. Hoste EAJ, Kellum JA, Selby NM, Zarbock A, Palevsky PM, Bagshaw SM, et al. Global Epidemiology and Outcomes of Acute Kidney Injury. *Nat Rev Nephrol* (2018) 14(10):607–25. doi: 10.1038/s41581-018-0052-0
2. Izzedine H, Perazella MA. Anticancer Drug-Induced Acute Kidney Injury. *Kidney Int Rep* (2017) 2(4):504–14. doi: 10.1016/j.ekir.2017.02.008
3. Rolland AL, Garnier AS, Meunier K, Drablier G, Briet M. Drug-Induced Acute Kidney Injury: A Study From the French Medical Administrative and the French National Pharmacovigilance Databases Using Capture-Recapture Method. *J Clin Med* (2021) 10(2):168. doi: 10.3390/jcm10020168
4. Perazella MA. Drug-Induced Acute Kidney Injury: Diverse Mechanisms of Tubular Injury. *Curr Opin Crit Care* (2019) 25(6):550–7. doi: 10.1097/MCC.0000000000000653
5. Liu Y, Fang J. Mesenchymal Stem Cells as Therapeutic Agents and Novel Carriers for the Delivery of Candidate Genes in Acute Kidney Injury. *Stem Cells Int* (2020) 2020:8875554. doi: 10.1155/2020/8875554
6. Brown JR, Rezaee ME, Marshall EJ, Matheny ME. Hospital Mortality in the United States Following Acute Kidney Injury. *BioMed Res Int* (2016) 2016:4278579. doi: 10.1155/2016/4278579
7. Oh GS, Kim HJ, Shen A, Lee SB, Khadka D, Pandit A, et al. Cisplatin-Induced Kidney Dysfunction and Perspectives on Improving Treatment Strategies. *Electrolyte Blood Press* (2014) 12(2):55–65. doi: 10.5049/ebp.2014.12.2.55
8. Volarevic V, Djokovic B, Jankovic MG, Harrell CR, Fellabaum C, Djonov V, et al. Molecular Mechanisms of Cisplatin-Induced Nephrotoxicity: A Balance on the Knife Edge Between Renoprotection and Tumor Toxicity. *J BioMed Sci* (2019) 26(1):25. doi: 10.1186/s12929-019-0518-9
9. Zhou J, An C, Jin X, Hu Z, Safirstein RL, Wang Y. TAK1 Deficiency Attenuates Cisplatin-Induced Acute Kidney Injury. *Am J Physiol Renal Physiol* (2020) 318(1):F209–15. doi: 10.1152/ajprenal.00516.2019
10. Ozkok A, Edelstein CL. Pathophysiology of Cisplatin-Induced Acute Kidney Injury. *BioMed Res Int* (2014) 2014:967826. doi: 10.1155/2014/967826
11. Xu Y, Ma H, Shao J, Wu J, Zhou L, Zhang Z, et al. A Role for Tubular Necroptosis in Cisplatin-Induced Aki. *J Am Soc Nephrol* (2015) 26(11):2647–58. doi: 10.1681/asn.2014080741
12. Mulay SR, Linkermann A, Anders HJ. Necroinflammation in Kidney Disease. *J Am Soc Nephrol* (2016) 27(1):27–39. doi: 10.1681/asn.2015040405
13. Wu L, Rong C, Zhou Q, Zhao X, Zhuansun XM, Wan S, et al. Bone Marrow Mesenchymal Stem Cells Ameliorate Cisplatin-Induced Renal Fibrosis Via Mir-146a-5p/Tfdp2 Axis in Renal Tubular Epithelial Cells. *Front Immunol* (2020) 11:623693. doi: 10.3389/fimmu.2020.623693
14. Qi J, Xue Q, Kuang L, Xie L, Luo R, Nie X. Berberine Alleviates Cisplatin-Induced Acute Kidney Injury by Regulating Mitophagy Via PINK 1/Parkin Pathway. *Transl Androl Urol* (2020) 9(4):1712–24. doi: 10.21037/tau-20-1129
15. Yang SK, Han YC, He JR, Yang M, Zhang W, Zhan M, et al. Mitochondria Targeted Peptide SS-31 Prevent on Cisplatin-Induced Acute Kidney Injury Via Regulating Mitochondrial ROS-NLRP3 Pathway. *BioMed Pharmacother* (2020) 130:110521. doi: 10.1016/j.biopha.2020.110521
16. Huang J, Bao D, Lei CT, Tang H, Zhang CY, Su H, et al. Selenoprotein T Protects Against Cisplatin-Induced Acute Kidney Injury Through Suppression of Oxidative Stress and Apoptosis. *FASEB J* (2020) 34 (9):11983–96. doi: 10.1096/fj.202000180RR
17. Han SJ, Lee HT. Mechanisms and Therapeutic Targets of Ischemic Acute Kidney Injury. *Kidney Res Clin Pract* (2019) 38(4):427–40. doi: 10.23876/j.krcp.19.062
18. Ghane Shahrbaf F, Assadi F. Drug-Induced Renal Disorders. *J Renal Inj Prev* (2015) 4(3):57–60. doi: 10.12861/jrip.2015.12
19. Robert L, Ficheur G, Gautier S, Servais A, Luyckx M, Soula J, et al. Community-Acquired Acute Kidney Injury Induced By Drugs In Older Patients: A Multifactorial Event. *Clin Interv Aging* (2019) 14:2105–13. doi: 10.2147/CIA.S217567
20. Dellepiane S, Leventhal JS, Cravedi P. T Cells and Acute Kidney Injury: A Two-Way Relationship. *Front Immunol* (2020) 11:1546. doi: 10.3389/fimmu.2020.01546
21. Lemley KV, Kriz W. Anatomy of the Renal Interstitium. *Kidney Int* (1991) 39 (3):370–81. doi: 10.1038/ki.1991.49
22. Aggarwal BB. Signalling Pathways of the TNF Superfamily: A Double-Edged Sword. *Nat Rev Immunol* (2003) 3(9):745–56. doi: 10.1038/nri1184
23. Wang WW, Wang Y, Li K, Tadagavadi R, Friedrichs WE, Budatha M, et al. Il-10 From Dendritic Cells But Not From T Regulatory Cells Protects Against Cisplatin-Induced Nephrotoxicity. *PloS One* (2020) 15(9):e0238816. doi: 10.1371/journal.pone.0238816
24. Zhang J, Li Q, Zou YR, Wu SK, Lu XH, Li GS, et al. Hmgb1-TLR4-IL-23-IL-17A Axis Accelerates Renal Ischemia-Reperfusion Injury Via the Recruitment and Migration of Neutrophils. *Int Immunopharmacol* (2021) 94:107433. doi: 10.1016/j.intimp.2021.107433
25. Faubel S, Lewis EC, Reznikov L, Ljubanovic D, Hoke TS, Somerset H, et al. Cisplatin-Induced Acute Renal Failure Is Associated With an Increase in the Cytokines Interleukin (IL)-1beta, IL-18, Il-6, and Neutrophil Infiltration in the Kidney. *J Pharmacol Exp Ther* (2007) 322(1):8–15. doi: 10.1124/jpet.107.119792
26. Fan Y, Hao Y, Gao D, Gao L, Li G, Zhang Z. Phenotype and Function of Macrophage Polarization in Monocrotaline-Induced Pulmonary Arterial Hypertension Rat Model. *Physiol Res* (2021) 70(2):213–226. doi: 10.33549/physiolres.934456
27. Tang M, Zhang K, Li Y, He QH, Li GQ, Zheng QY, et al. Mesenchymal Stem Cells Alleviate Acute Kidney Injury by Down-Regulating C5a/C5aR Pathway Activation. *Int Urol Nephrol* (2018) 50(8):1545–53. doi: 10.1007/s11255-018-1844-7
28. Ramesh G, Reeves WB. TNF-Alpha Mediates Chemokine and Cytokine Expression and Renal Injury in Cisplatin Nephrotoxicity. *J Clin Invest* (2002) 110(6):835–42. doi: 10.1172/jci15606
29. Liu P, Li X, Lv W, Xu Z. Inhibition of CXCL1-CXCR2 Axis Ameliorates Cisplatin-Induced Acute Kidney Injury by Mediating Inflammatory Response. *BioMed Pharmacother* (2020) 122:109693. doi: 10.1016/j.biopha.2019.109693
30. Andrade-Oliveira V, Foresto-Neto O, Watanabe IKM, Zatz R, Camara NOS. Inflammation in Renal Diseases: New and Old Players. *Front Pharmacol* (2019) 10:1192. doi: 10.3389/fphar.2019.01192
31. Hu J, Zhang L, Cui S, Zhu F, Li D, Feng Z, et al. [Mesenchymal Stem Cells Attenuate Acute Kidney Injury Via Regulation of Natural Immune System]. *Zhonghua Wei Zhong Bing Ji Jiu Yi Xue* (2016) 28(3):235–40.
32. Ceruso A, Gonzalez-Pujana A, Igartua M, Santos-Vizcaino E, Hernandez RM. Latest Advances to Enhance the Therapeutic Potential of Mesenchymal Stromal Cells for the Treatment of Immune-Mediated Diseases. *Drug Delivery Transl Res* (2021) 11(2):498–514. doi: 10.1007/s13346-021-00934-5
33. Wright A, Arthaud-Day ML, Weiss ML. Therapeutic Use of Mesenchymal Stromal Cells: The Need for Inclusive Characterization Guidelines to Accommodate All Tissue Sources and Species. *Front Cell Dev Biol* (2021) 9:632717. doi: 10.3389/fcell.2021.632717
34. Yoo KH, Jang IK, Lee MW, Kim HE, Yang MS, Eom Y, et al. Comparison of Immunomodulatory Properties of Mesenchymal Stem Cells Derived From Adult Human Tissues. *Cell Immunol* (2009) 259(2):150–6. doi: 10.1016/j.cellimm.2009.06.010
35. El-Sayed M, El-Feky MA, El-Amir MI, Hasan AS, Tag-Adeen M, Urata Y, et al. Immunomodulatory Effect of Mesenchymal Stem Cells: Cell Origin and Cell Quality Variations. *Mol Biol Rep* (2019) 46(1):1157–65. doi: 10.1007/s11033-018-04582-w
36. Ribeiro A, Laranjeira P, Mendes S, Velada I, Leite C, Andrade P, et al. Mesenchymal Stem Cells From Umbilical Cord Matrix, Adipose Tissue and Bone Marrow Exhibit Different Capability to Suppress Peripheral Blood B, Natural Killer and T Cells. *Stem Cell Res Ther* (2013) 4(5):125. doi: 10.1186/scrt336
37. Wegmeyer H, Broske AM, Leddin M, Kuentzer K, Nisslbeck AK, Hupfeld J, et al. Mesenchymal Stromal Cell Characteristics Vary Depending on Their Origin. *Stem Cells Dev* (2013) 22(19):2606–18. doi: 10.1089/scd.2013.0016
38. Heo JS, Choi Y, Kim HS, Kim HO. Comparison of Molecular Profiles of Human Mesenchymal Stem Cells Derived From Bone Marrow, Umbilical Cord Blood, Placenta and Adipose Tissue. *Int J Mol Med* (2016) 37(1):115–25. doi: 10.3892/ijmm.2015.2413
39. Bochev I, Elmadjian G, Kyurkchiev D, Tzvetanov L, Altankova I, Tivchev P, et al. Mesenchymal Stem Cells From Human Bone Marrow or Adipose Tissue Differently Modulate Mitogen-Stimulated B-cell Immunoglobulin Production In Vitro. *Cell Biol Int* (2008) 32(4):384–93. doi: 10.1016/j.cellbi.2007.12.007

40. Li G, Zhang XA, Wang H, Wang X, Meng CL, Chan CY, et al. Comparative Proteomic Analysis of Mesenchymal Stem Cells Derived From Human Bone Marrow, Umbilical Cord, and Placenta: Implication in the Migration. *Proteomics* (2009) 9(1):20–30. doi: 10.1002/pmic.200701195
41. Barcia RN, Santos JM, Filipe M, Teixeira M, Martins JP, Almeida J, et al. What Makes Umbilical Cord Tissue-Derived Mesenchymal Stromal Cells Superior Immunomodulators When Compared to Bone Marrow Derived Mesenchymal Stromal Cells? *Stem Cells Int* (2015) 2015:583984. doi: 10.1155/2015/583984
42. Li CY, Wu XY, Tong JB, Yang XX, Zhao JL, Zheng QF, et al. Comparative Analysis of Human Mesenchymal Stem Cells From Bone Marrow and Adipose Tissue Under Xeno-Free Conditions for Cell Therapy. *Stem Cell Res Ther* (2015) 6:55. doi: 10.1186/s13287-015-0066-5
43. Baksh D, Yao R, Tuan RS. Comparison of Proliferative and Multilineage Differentiation Potential of Human Mesenchymal Stem Cells Derived From Umbilical Cord and Bone Marrow. *Stem Cells* (2007) 25(6):1384–92. doi: 10.1634/stemcells.2006-0709
44. Cantaluppi V, Biancone L, Quercia A, Deregibus MC, Segoloni G, Camussi G. Rationale of Mesenchymal Stem Cell Therapy in Kidney Injury. *Am J Kidney Dis* (2013) 61(2):300–9. doi: 10.1053/j.ajkd.2012.05.027
45. Fontaine MJ, Shih H, Schäfer R, Pittenger MF. Unraveling the Mesenchymal Stromal Cells' Paracrine Immunomodulatory Effects. *Transfus Med Rev* (2016) 30(1):37–43. doi: 10.1016/j.tmrv.2015.11.004
46. Muller L, Tunger A, Wobus M, von Bonin M, Towers R, Bornhauser M, et al. Immunomodulatory Properties of Mesenchymal Stromal Cells: An Update. *Front Cell Dev Biol* (2021) 9:637725. doi: 10.3389/fcell.2021.637725
47. Peired AJ, Sisti A, Romagnani P. Mesenchymal Stem Cell-Based Therapy for Kidney Disease: A Review of Clinical Evidence. *Stem Cells Int* (2016) 2016:4798639. doi: 10.1155/2016/4798639
48. Najar M, Raicevic G, Fayyad-Kazan H, Bron D, Toungouz M, Lagneaux L. Mesenchymal Stromal Cells and Immunomodulation: A Gathering of Regulatory Immune Cells. *Cytotherapy* (2016) 18(2):160–71. doi: 10.1016/j.jcyt.2015.10.011
49. Jang HR, Rabb H. Immune Cells in Experimental Acute Kidney Injury. *Nat Rev Nephrol* (2015) 11(2):88–101. doi: 10.1038/nrneph.2014.180
50. Huen SC, Cantley LG. Macrophage-Mediated Injury and Repair After Ischemic Kidney Injury. *Pediatr Nephrol* (2015) 30(2):199–209. doi: 10.1007/s00467-013-2726-y
51. Holditch SJ, Brown CN, Lombardi AM, Nguyen KN, Edelstein CL. Recent Advances in Models, Mechanisms, Biomarkers, and Interventions in Cisplatin-Induced Acute Kidney Injury. *Int J Mol Sci* (2019) 20(12):3011. doi: 10.3390/ijms20123011
52. Tadagavadi RK, Reeves WB. Renal Dendritic Cells Ameliorate Nephrotoxic Acute Kidney Injury. *J Am Soc Nephrol* (2010) 21(1):53–63. doi: 10.1681/asn.2009040407
53. Zhang B, Ramesh G, Uematsu S, Akira S, Reeves WB. TLR4 Signaling Mediates Inflammation and Tissue Injury in Nephrotoxicity. *J Am Soc Nephrol* (2008) 19(5):923–32. doi: 10.1681/asn.2007090982
54. Liu M, Chien CC, Burne-Taney M, Molls RR, Racusen LC, Colvin RB, et al. A Pathophysiologic Role for T Lymphocytes in Murine Acute Cisplatin Nephrotoxicity. *J Am Soc Nephrol* (2006) 17(3):765–74. doi: 10.1681/asn.2005010102
55. Zhang J, Rudemiller NP, Patel MB, Wei Q, Karlovich NS, Jeffs AD, et al. Competing Actions of Type 1 Angiotensin Ii Receptors Expressed on T Lymphocytes and Kidney Epithelium During Cisplatin-Induced Aki. *J Am Soc Nephrol* (2016) 27(8):2257–64. doi: 10.1681/asn.2015060683
56. Abumaree MH, Abomaray FM, Alshabibi MA, AlAskar AS, Kalionis B. Immunomodulatory Properties of Human Placental Mesenchymal Stem/Stromal Cells. *Placenta* (2017) 59:87–95. doi: 10.1016/j.placenta.2017.04.003
57. Snelgrove SL, Lo C, Hall P, Lo CY, Alikhan MA, Coates PT, et al. Activated Renal Dendritic Cells Cross Present Intrarenal Antigens After Ischemia-Reperfusion Injury. *Transplantation* (2017) 101(5):1013–24. doi: 10.1097/tp.0000000000001427
58. Dong X, Swaminathan S, Bachman LA, Croatt AJ, Nath KA, Griffin MD. Resident Dendritic Cells Are the Predominant TNF-secreting Cell in Early Renal Ischemia-Reperfusion Injury. *Kidney Int* (2007) 71(7):619–28. doi: 10.1038/sj.ki.5002132
59. Tadagavadi RK, Reeves WB. Endogenous IL-10 Attenuates Cisplatin Nephrotoxicity: Role of Dendritic Cells. *J Immunol* (2010) 185(8):4904–11. doi: 10.4049/jimmunol.1000383
60. Simovic Markovic B, Gazdic M, Arsenijevic A, Jovicic N, Jeremic J, Djonov V, et al. Mesenchymal Stem Cells Attenuate Cisplatin-Induced Nephrotoxicity in iNOS-Dependent Manner. *Stem Cells Int* (2017) 2017:1315378. doi: 10.1155/2017/1315378
61. Scutera S, Salvi V, Lorenzi L, Piersigilli G, Lonardi S, Alotto D, et al. Adaptive Regulation of Osteopontin Production by Dendritic Cells Through the Bidirectional Interaction With Mesenchymal Stromal Cells. *Front Immunol* (2018) 9:1207. doi: 10.3389/fimmu.2018.01207
62. Jiang XX, Zhang Y, Liu B, Zhang SX, Wu Y, Yu XD, et al. Human Mesenchymal Stem Cells Inhibit Differentiation and Function of Monocyte-Derived Dendritic Cells. *Blood* (2005) 105(10):4120–6. doi: 10.1182/blood-2004-02-0586
63. Nauta AJ, Kruisselbrink AB, Lurvink E, Willemze R, Fibbe WE. Mesenchymal Stem Cells Inhibit Generation and Function of Both CD34+-derived and Monocyte-Derived Dendritic Cells. *J Immunol* (2006) 177(4):2080–7. doi: 10.4049/jimmunol.177.4.2080
64. English K, Barry FP, Mahon BP. Murine Mesenchymal Stem Cells Suppress Dendritic Cell Migration, Maturation and Antigen Presentation. *Immunol Lett* (2008) 115(1):50–8. doi: 10.1016/j.imlet.2007.10.002
65. Djouad F, Charbonnier LM, Bouffi C, Louis-Plence P, Bony C, Apparailly F, et al. Mesenchymal Stem Cells Inhibit the Differentiation of Dendritic Cells Through an interleukin-6-dependent Mechanism. *Stem Cells* (2007) 25(8):2025–32. doi: 10.1634/stemcells.2006-0548
66. Chiesa S, Morbelli S, Morando S, Massollo M, Marini C, Bertoni A, et al. Mesenchymal Stem Cells Impair In Vivo T-cell Priming by Dendritic Cells. *Proc Natl Acad Sci USA* (2011) 108(42):17384–9. doi: 10.1073/pnas.1103650108
67. Gazdic M, Volarevic V, Arsenijevic N, Stojkovic M. Mesenchymal Stem Cells: A Friend or Foe in Immune-Mediated Diseases. *Stem Cell Rev Rep* (2015) 11(2):280–7. doi: 10.1007/s12015-014-9583-3
68. Bolisetty S, Agarwal A. Neutrophils in Acute Kidney Injury: Not Neutral Any More. *Kidney Int* (2009) 75(7):674–6. doi: 10.1038/ki.2008.689
69. Miao N, Yin F, Xie H, Wang Y, Xu Y, Shen Y, et al. The Cleavage of Gasdermin D by caspase-11 Promotes Tubular Epithelial Cell Pyroptosis and Urinary IL-18 Excretion in Acute Kidney Injury. *Kidney Int* (2019) 96(5):1105–20. doi: 10.1016/j.kint.2019.04.035
70. Luo CJ, Zhang FJ, Zhang L, Geng YQ, Li QG, Hong Q, et al. Mesenchymal Stem Cells Ameliorate Sepsis-Associated Acute Kidney Injury in Mice. *Shock* (2014) 41(2):123–9. doi: 10.1097/shk.0000000000000080
71. Matsumoto M, Tanaka T, Kaisho T, Sanjo H, Copeland NG, Gilbert DJ, et al. A Novel LPS-inducible C-Type Lectin is a Transcriptional Target of NF-IL6 in Macrophages. *J Immunol* (1999) 163(9):5039–48.
72. Ichioka M, Suganami T, Tsuda N, Shirakawa I, Hirata Y, Satoh-Asahara N, et al. Increased Expression of Macrophage-Inducible C-type Lectin in Adipose Tissue of Obese Mice and Humans. *Diabetes* (2011) 60(3):819–26. doi: 10.2337/db10-0864
73. Lu LH, Oh DJ, Dursun B, He Z, Hoke TS, Faubel S, et al. Increased Macrophage Infiltration and Fractalkine Expression in Cisplatin-Induced Acute Renal Failure in Mice. *J Pharmacol Exp Ther* (2008) 324(1):111–7. doi: 10.1124/jpet.107.130161
74. Rogers NM, Ferenbach DA, Isenberg JS, Thomson AW, Hughes J. Dendritic Cells and Macrophages in the Kidney: A Spectrum of Good and Evil. *Nat Rev Nephrol* (2014) 10(11):625–43. doi: 10.1038/nrneph.2014.170
75. Cao Q, Wang Y, Harris DC. Pathogenic and Protective Role of Macrophages in Kidney Disease. *Am J Physiol Renal Physiol* (2013) 305(1):F3–11. doi: 10.1152/ajprenal.00122.2013
76. Recknagel S, Bindl R, Kurz J, Wehner T, Schoengraf P, Ehrnthaller C, et al. C5aR-antagonist Significantly Reduces the Deleterious Effect of a Blunt Chest Trauma on Fracture Healing. *J Orthop Res* (2012) 30(4):581–6. doi: 10.1002/jor.21561
77. Huang S, You J, Wang K, Li Y, Zhang Y, Wei H, et al. N-Acetylcysteine Attenuates Cisplatin-Induced Acute Kidney Injury by Inhibiting the C5a Receptor. *BioMed Res Int* (2019) 2019:4805853. doi: 10.1155/2019/4805853
78. Ullah M, Liu D, Rai S, Concepcion W, Thakor A. Hsp70-Mediated NLRP3 Inflammasome Suppression Underlies Reversal of Acute Kidney Injury Following Extracellular Vesicle and Focused Ultrasound Combination Therapy. *Int J Mol Sci* (2020) 21(11):4085. doi: 10.3390/ijms21114085
79. Ullah M, Liu D, Rai S, Dadhania A, Jonnakuti S, Concepcion W, et al. Reversing Acute Kidney Injury Using Pulsed Focused Ultrasound and MSC

Therapy: A Role for HSP-Mediated Pi3k/Akt Signaling. *Mol Ther Methods Clin Dev* (2020) 17:683–94. doi: 10.1016/j.omtm.2020.03.023

Conflict of Interest: The authors declare that the research was conducted in the absence of any commercial or financial relationships that could be construed as a potential conflict of interest.

Copyright © 2021 Han, Wang, Ding, He, Cai and Zhu. This is an open-access article distributed under the terms of the Creative Commons Attribution License (CC BY). The use, distribution or reproduction in other forums is permitted, provided the original author(s) and the copyright owner(s) are credited and that the original publication in this journal is cited, in accordance with accepted academic practice. No use, distribution or reproduction is permitted which does not comply with these terms.

frontiers in Immunology

ORIGINAL RESEARCH
published: 04 June 2021
doi: 10.3389/fimmu.2021.678914

Ischemia-Reperfusion Injury Reduces Kidney Folate Transporter Expression and Plasma Folate Levels

Cheng Yang[1,2†], Charith U. B. Wijerathne[3,4†], Guo-wei Tu[5†], Connie W. H. Woo[6], Yaw L. Siow[3,7,8], Susara Madduma Hewage[3,8], Kathy K. W. Au-Yeung[3,4], Tongyu Zhu[1,2] and Karmin O[3,4,8*]*

[1] Department of Urology, Zhongshan Hospital, Fudan University, Shanghai, China, [2] Key Laboratory of Organ Transplantation, Shanghai, China, [3] St. Boniface Hospital Research Centre, Winnipeg, MB, Canada, [4] Department of Animal Science, University of Manitoba, Winnipeg, MB, Canada, [5] Department of Critical Care Medicine, Zhongshan Hospital, Fudan University, Shanghai, China, [6] Department of Pharmacology and Pharmacy, University of Hong Kong, Hong Kong, China, [7] Agriculture and Agri Food Canada, Winnipeg, MB, Canada, [8] Department of Physiology and Pathophysiology, University of Manitoba, Winnipeg, MB, Canada

OPEN ACCESS

Edited by:
Bin Yang,
University of Leicester,
United Kingdom

Reviewed by:
Guangdong Yang,
Laurentian University, Canada
Haipeng Guo,
Shandong University, China

***Correspondence:**
Tongyu Zhu
tyzhu@fudan.edu.cn
Karmin O
karmino@sbrc.ca

†These authors have contributed equally to the work

Specialty section:
This article was submitted to Molecular Innate Immunity, a section of the journal Frontiers in Immunology

Received: 10 March 2021
Accepted: 04 May 2021
Published: 04 June 2021

Citation:
Yang C, Wijerathne CUB, Tu G-w, Woo CWH, Siow YL, Madduma Hewage S, Au-Yeung KKW, Zhu T and O K (2021) Ischemia-Reperfusion Injury Reduces Kidney Folate Transporter Expression and Plasma Folate Levels. Front. Immunol. 12:678914. doi: 10.3389/fimmu.2021.678914

Acute or chronic kidney disease can cause micronutrient deficiency. Patients with end-stage renal disease, kidney transplantation or on dialysis have reduced circulating levels of folate, an essential B vitamin. However, the molecular mechanism is not well understood. Reabsorption of folate in renal proximal tubules through folate transporters is an important process to prevent urinary loss of folate. The present study investigated the impact of acute kidney injury (AKI) on folate transporter expression and the underlying mechanism. AKI was induced in Sprague-Dawley rats that were subjected to kidney ischemia (45 min)-reperfusion (24 h). Both male and female rats displayed kidney injury and low plasma folate levels compared with sham-operated rats. The plasma folate levels were inversely correlated to plasma creatinine levels. There was a significant increase in neutrophil gelatinase-associated lipocalin (NGAL) and IL-6 mRNA expression in the kidneys of rats with ischemia-reperfusion, indicating kidney injury and increased inflammatory cytokine expression. Ischemia-reperfusion decreased mRNA and protein expression of folate transporters including folate receptor 1 (FOLR1) and reduced folate carrier (RFC); and inhibited transcription factor Sp1/DNA binding activity in the kidneys. Simulated ischemia-reperfusion through hypoxia-reoxygenation or Sp1 siRNA transfection in human proximal tubular cells inhibited folate transporter expression and reduced intracellular folate levels. These results suggest that ischemia-reperfusion injury downregulates renal folate transporter expression and decreases folate uptake by tubular cells, which may contribute to low folate status in AKI. In conclusion, ischemia-reperfusion injury can downregulate Sp1 mediated-folate transporter expression in tubular cells, which may reduce folate reabsorption and lead to low folate status.

Keywords: acute kidney injury, ischemia, folate, folate transporters, tubular cells

INTRODUCTION

Acute kidney injury (AKI) is characterized by a rapid decline of kidney function over a short period of time and often progresses to chronic kidney disease (CKD). Despite improvements in renal replacement therapy, AKI is associated with a high morbidity and mortality (1). AKI occurs in patients with kidney transplantation, cardiac surgery, sepsis or critical illness (2–4). The principal function of the kidneys is to maintain body fluid volume, electrolyte and acid-base balance as well as regulating the excretion of wastes and reabsorption of nutrients or metabolic products (5, 6). Micronutrient deficiency is common in patients with kidney disease and malnutrition is an independent predictor of AKI mortality (7). Patients with CKD or end-stage renal disease have reduced circulating folate levels despite adequate dietary intake or receiving renal replacement therapy (8–13). A recent study reported a decreased circulating folate level with an elevated homocysteine level in adolescents and young adults undergoing kidney transplantation (14).

Folate is an essential micronutrient (vitamin B9) that participates in methylation reactions, nucleic acid synthesis and sulfur-containing amino acid metabolism. Folic acid, a synthetic form of folate, is used as a supplement or in fortified foods (15, 16). General populations in countries with mandatory fortification policies have achieved adequate intake of folate (15). The kidneys play an important role in maintaining folate homeostasis in the body through glomerular filtration and tubular reabsorption process. Folate in the circulation, mainly in the form of 5-methyltetrahydrofolate (5-MTHF), is freely filtered in glomeruli. Much of the filtered folate is reabsorbed in the proximal tubules. This reabsorption process is an important mechanism to prevent urinary loss of folate (17). Folate receptor alpha or folate receptor 1 (FOLR1) is the major transporter for folate reabsorption in the kidneys. FOLR1 is located on the apical surface of proximal tubular cells. Folate is transported by FOLR1 from the lumen of tubules into tubular cells *via* receptor-mediated endocytosis (17–19). The promoter region of FOLR1 gene contains transcription factor Sp1 binding sites (20–22). Tubular cells also express other folate transporters. The reduced folate carrier (RFC) is located in the basolateral membrane of proximal tubular cells. RFC transports folate into the peritubular capillaries through a bidirectional anion-exchange mechanism (23). Proton-coupled folate transporter (PCFT), mainly responsible for dietary folate absorption in the intestine, is also present in the kidneys (24).

Ischemia-reperfusion is one of the most common causes for AKI (6). Proximal tubular cells are more susceptible to ischemia-reperfusion injury (25, 26). We have observed tubular damage and declining kidney function in animal models with ischemia-reperfusion induced AKI (27–34). The expression of folate transporters is closely linked to folate status and its biological function. Although low serum folate levels have been reported in patients with CKD, kidney transplant recipients or on dialysis, limited information is available regarding the impact of AKI on folate transporter expression and folate status. In the present study, we investigated (1) the impact of ischemia-reperfusion on renal folate transporter expression and folate status in rats; and (2) the potential mechanism of altered folate transporter expression in human proximal tubular cells.

MATERIALS AND METHODS

Induction of Kidney Ischemia-Reperfusion in Rats

Sprague-Dawley rats (270-300 g, male and female) were randomly divided into two groups that were subjected to kidney ischemia-reperfusion or sham-operation. Kidney ischemia was induced by clamping the left renal pedicle with a non-traumatic vascular clamp for 45 min. At the end of ischemia, the clamp was removed to allow blood flow to the left kidney (reperfusion) and right nephrectomy was performed as described in our previous studies (27–31). Rats were sacrificed 24 h after reperfusion. In the sham-operated group (control), rats were subjected to the same surgical procedure but without inducing kidney ischemia and were sacrificed at the corresponding time point. All procedures were performed in accordance with the Guide to the Care and Use of Experimental Animals published by the Canadian Council on Animal Care and approved by the University of Manitoba Protocol Management and Review Committee. Plasma creatinine was measured using the Cobas C111 analyzer (Roche, Laval, Canada). Total folate in the plasma and proximal tubular cells was measured by using the *L. rhamnosus* coated microtitre plates according to the manufacturer's instructions provided in the Folic acid Vitamin B9 Microbiological Test Kit (ALPCO, Salem, NH).

Histological and Immunohistochemical Staining

Kidneys were excised and immersion-fixed in 10% neutral-buffered formalin, embedded in paraffin and sectioned at 5 μm. Sections were stained with hematoxylin and eosin (H&E) to examine histological changes in the kidney (28, 35). For immunohistochemical staining, sequential sections (10 μm) were prepared from cryofixed kidney. Sections were incubated with primary antibodies, rabbit anti-FOLR1 monoclonal antibody (1:100 Abcam, Cambridge, MA) or rabbit anti-SLC19A1 (RFC) (1:100, Abcam) monoclonal antibody and then with biotinylated goat anti-rabbit IgG (1:200, Dako, Glostrup, Denmark) secondary antibody followed by incubation with streptavidin-horse radish peroxidase (HRP) conjugate (Zymed Laboratories, Inc., San Francisco, CA). For a negative control, non-specific rabbit IgG was used as primary antibodies. The images from H&E and immunohistochemical staining were captured by using Olympus BX43 light microscope equipped with an Olympus Q-Color3 camera.

Induction of Hypoxia-Reoxygenation in Tubular Cells

Human kidney proximal tubular cell line (HK-2) was purchased from the American Type Culture Collection (ATCC, Manassas, VA). Cells were cultured at 37°C in a normal atmosphere of 95% air and 5% CO_2 in keratinocyte-serum free medium supplemented

with human recombinant epidermal growth factor and bovine pituitary extract (Life Technologies, Carlsbad, CA). Hypoxia-reoxygenation was induced in tubular cells to simulate ischemia-reperfusion injury as described in previous studies (30, 31, 36). In brief, hypoxia was induced in tubular cells by incubation for 2 h in a modified Krebs buffer (137 mM NaCl sodium chloride, 15.8 mM KCl potassium chloride, 0.49 mM $MgCl_2$ magnesium chloride, 0.9 mM $CaCl_2$ calcium chloride, 4 mM HEPES) supplemented with 10 mM 2-deoxyglucose, 20 mM sodium lactate, 12 mM KCl potassium chloride and 1 mM sodium dithionite (pH 6.4) in a hypoxia chamber (Billups-Rothenberg, Inc., Del Mar, CA) containing 95% N_2/5% CO_2 at 37°C. After 2 h hypoxia, the modified Krebs buffer was replaced with keratinocyte-serum free medium and cells were cultured for 48 h to 72 h in 95% air and 5% CO_2. Cells without induction of hypoxia were used as a control.

Measurement of mRNA Expression

Total RNA was isolated from kidneys or proximal tubular cells by using TRIzol reagent (Thermo Fisher Scientific, Waltham, MA) and 1-2 μg was converted to cDNA through reverse transcription. The real-time PCR reaction mixture consisted of 2 μL of cDNA product, 0.4 μM of 5' and 3' primers and iQ-SYBR green supermix reagent (Bio-Rad, Mississauga, Canada). The mRNA expression of folate receptor-1 (FOLR1), reduced folate carrier (RFC), proton-coupled folate transporter (PCFT), specificity protein-1 (Sp1), neutrophil gelatinase-associated lipocalin (NGAL) and interleukin-6 (IL-6) was determined by using a StepOnePlus™ Real-Time PCR System (Life Technologies). The mRNA expression was calculated using the threshold cycle (2−ΔΔCT) method with β-actin as an internal reference. The primer sequences used in this study are listed in **Table 1**.

Western Immunoblotting Analysis

The folate receptor proteins (FOLR1, RFC and PCFT) were determined by Western immunoblotting analysis. Proteins (10-50 μg) isolated from kidneys or proximal tubular cells were separated in SDS-PAGE (10-12%) and subsequently transferred to a nitrocellulose membrane. The membrane was probed with primary antibodies, rabbit anti-FOLR1 monoclonal antibody (1:1000, Abcam), rabbit anti-SLC19A1 monoclonal antibody (RFC, 1:1000, Abcam) or rabbit anti-HCP1 (PCFT) monoclonal antibody (1:1000, Abcam) followed by HRP conjugated anti-rabbit IgG secondary antibody (1:2000, Cell Signaling Technology, Danvers, MA). For Sp1 protein, the membrane was probed by goat anti-Sp1 polyclonal antibody (1:1000, Santa Cruz Biotechnology, CA, USA) followed by HRP conjugated anti-goat IgG secondary antibody (1:1000, Thermo Fisher Scientific). Equal protein loading of each sample was confirmed by probing the nitrocellulose membrane with rabbit anti-β-actin monoclonal antibody (1:1000, Cell Signaling Technology). The protein bands were visualized by using Luminata Crescendo chemiluminescent HRP detection reagent (Millipore Ltd, Etobicoke, Canada).

Electrophoretic Mobility Shift Assay

Nuclear proteins were isolated from kidney tissue and the Sp1/DNA binding activity was measured by electrophoretic mobility shift assay (EMSA). In brief, oligonucleotides were biotin-labelled by using the Biotin 3' End DNA labelling kit (Thermo Fisher Scientific). The sequence of the Sp1 oligonucleotide probe was 5′-CTGGGCTGGGC-3′. The EMSA was performed by using the LightShift Chemiluminescent EMSA Kit (Thermo Fisher Scientific).

Cell transfection With Sp1 Small Interfering RNAs (siRNAs)

Proximal tubular cells were transfected with human Sp1 siRNA duplex oligoribonucleotides (25 pmol, Stealth RNAi™, Invitrogen, Carlsbad, CA) by using Lipofectamine 2000 transfection reagent (Invitrogen) according to the manufacturer's instructions. As a control, cells were transfected with Stealth™ RNA negative control (Invitrogen) consisting of a scrambled sequence that was unable to inhibit gene expression. At 72 h after transfection, cells were harvested and total mRNAs were prepared. The Sp1 mRNA and FOLR1 mRNA were determined. In another set of experiments, intracellular folate content was measured 72 h after transfection.

Statistical Analysis

The results were analyzed by using two-tailed Student's t-test or Pearson correlation test. The data were presented as mean ± standard error (SE). A p value less than 0.05 was considered as statistically significant.

RESULTS

Ischemia-Reperfusion Impaired Kidney Function and Reduced Circulating Folate Levels in Rats

Kidney ischemia-reperfusion caused a significant elevation of plasma creatinine levels in male and female rats (**Figures 1A, B**), indicating that kidney function was impaired. There was a significant decrease in plasma folate levels in rats subjected to kidney ischemia-reperfusion (**Figures 1A, B**). The plasma folate levels were inversely correlated with plasma creatinine levels in both male and female rats (**Figures 1A, B**). The histological analysis of the kidney tissue revealed irregular glomerular structure, red blood cell accumulation and tubular cell necrosis in rats subjected to ischemia-reperfusion (**Figure 2A**). There was a significant increase in the expression of NGAL and IL-6 mRNA in the kidneys of rats with ischemia-reperfusion (**Figures 2B, C**), indicating kidney injury and increased inflammatory cytokine expression.

Ischemia-Reperfusion Decreased Folate Transporter Expression in the Rat Kidneys

The expression of folate transporters in the rat kidneys was examined. Ischemia-reperfusion caused a significant decrease in FOLR1 mRNA and protein levels in the kidney tissue of male and female rats (**Figure 3A**). Ischemia-reperfusion also reduced RFC mRNA and protein levels in the kidney tissue (**Figure 3B**). There was no significant change in PCFT expression upon ischemia-reperfusion (**Figure 3C**). Immunohistochemical staining of the kidneys detected FOLR1 and RFC proteins that were mainly localized in kidney tubules (**Figures 4A, B**).

TABLE 1 | Gene primer sequences of human and rat used for real-time PCR.

Target gene	Forward Primer (5'-3')	Reverse Primer (5'-3')	Size (bp)
Human			
FOLR1	ACTGGACTTCAGGGTTTAACAAG	GTAGGAGTGAGTCCAGATTTCATT	110
RFC	ATGGTGCCCTCCAGCCCAGCGGTG	TCACTGGTTCACATTCTGAACACC	1780
PCFT	ATGCAGCTTTCTGCTTTGGT	GGAGCCACATAGAGCTGGAC	100
Sp1	GCCTCCAGACCATTAACCTCAG	TCATGTATTCCATCACCACCAG	148
IL-6	AGGAGACTTGCCTGGTGAAA	GTCAGGGGTGGTTATTGCAT	182
β-actin	AGATCAAGATCATTGCTCCTCCT	GATCCACATCTGCTGGAAGG	95
Rat			
FOLR1	CGGAGACAAGGGTAGGTGTG	TTGAGAAGTTCGGTCCTGGC	166
RFC	CATGCTAAGCGAACTGGTGA	TTTTCCACAGGACATGGACA	122
PCFT	AAGCCAGTTATGGGCAACAC	GGATAGGCTGTGGTCAAGGA	300
Sp1	GGCTACCCCTACCTCAAAGG	CACAACATACTGCCCACCAG	103
NGAL	GATCAGAACATTCGTTCCAA	TTGCACATCGTAGCTCTGTA	91
IL-6	CCGGAGAGGAGACTTCACAG	ACAGTGCATCATCGCTGTTC	161
β-actin	ACAACCTTCTTGCAGCTCCTC	GACCCATACCCACCATCACA	198

FOLR1, folate receptor 1; RFC, reduced folate carrier; PCFT, Proton-coupled folate transporter; Sp1, Specificity protein-1; NGAL, neutrophil gelatinase-associated lipocalin; IL-6, interleukin-6.

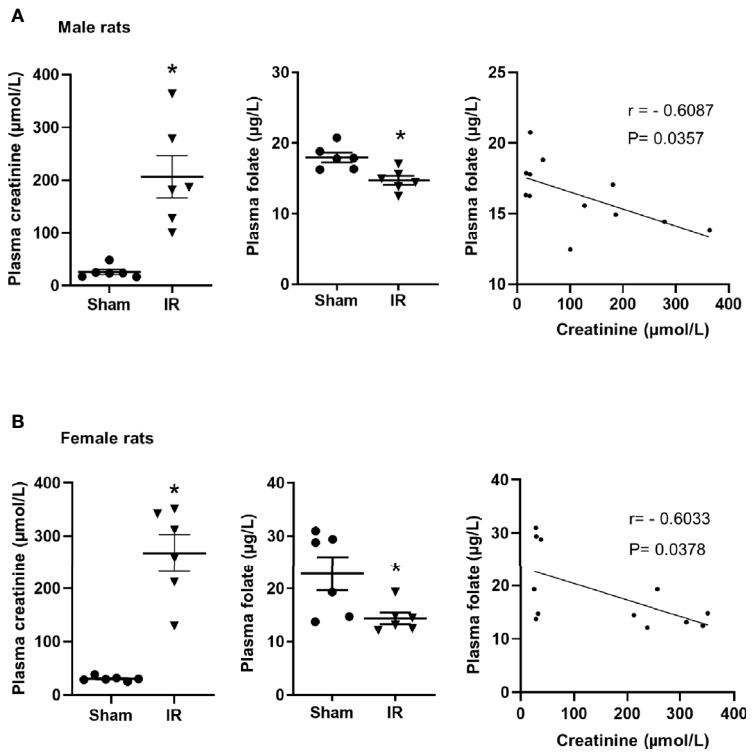


FIGURE 1 | Plasma creatinine and folate measurement in rats. Rats were subjected to kidney ischemia-reperfusion (IR) or sham operation (sham). Plasma creatinine and folate were measured in **(A)** male and **(B)** female rats. Pearson's correlation between plasma folate levels and plasma creatinine levels was analyzed. Results are expressed as mean ± SE (n = 6). *$P < 0.05$ when compared with the value obtained from the sham-operated group.

Hypoxia-Reoxygenation Decreased Folate Transporter Expression in Human Proximal Tubular Cells

Folate reabsorption in the kidneys mainly occurs in the proximal tubules where folate transporters are abundantly expressed in tubular cells. Experiments were performed in human proximal tubular cells with hypoxia-reoxygenation that simulated ischemia-reperfusion. Hypoxia-reoxygenation caused a significant decrease in FOLR1 mRNA and protein levels in tubular cells (**Figure 5A**). Hypoxia-reoxygenation also reduced RFC expression in tubular cells (**Figure 5B**) but did not change PCFT expression (data not shown). There was a significant decrease in intracellular folate levels

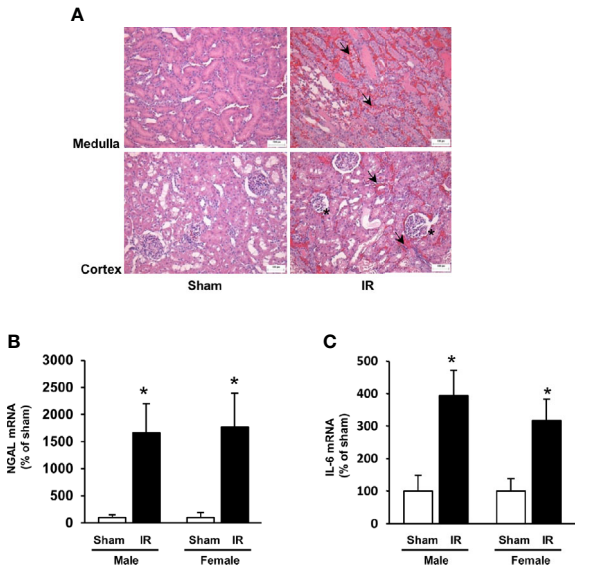


FIGURE 2 | Kidney histology and expression of NGAL and IL-6. Rats were subjected to kidney ischemia-reperfusion (IR) or sham operation (sham). **(A)** Representative hematoxylin and eosin (H&E) staining images of kidney sections are shown (magnification x200). Arrows and stars point the area having red blood cell accumulation and irregular glomerular structures, respectively. The bar on the images represents 100 μm. The mRNA of NGAL **(B)** and IL-6 **(C)** was measured by real-time PCR analysis. Results are expressed as mean ± SE (n = 6). *$P < 0.05$ when compared with the value obtained from the sham-operated group.

after hypoxia-reoxygenation (**Figure 5C**). Hypoxia-reoxygenation significantly increased IL-6 mRNA in tubular cells (**Figure 5D**).

Reduced Sp1 Activity Might Contribute To Decreased Folate Transporter Expression During Ischemia-Reperfusion

To investigate the mechanism by which ischemia-reperfusion decreased folate transporter expression, siRNA transfection was conducted in tubular cells. Cells were transiently transfected with Sp1 siRNA or a scrambled siRNA control. Inhibition of Sp1 expression by Sp1 siRNA transfection resulted in a significant reduction of Sp1 mRNA (**Figure 6A**) and FOLR1 mRNA expression in tubular cells (**Figure 6B**). Furthermore, silencing Sp1 caused a significant decrease in intracellular folate levels (**Figure 6C**) and a significant increase in IL-6 mRNA (**Figure 6D**). Sp1 is a transcription factor that regulates FOLR1 expression. The nuclear proteins in the kidney tissue were prepared and the EMSA was performed. Compared to the sham-operated group, there was a significant decrease in the Sp1/DNA binding activity in the kidneys collected from rats subjected to ischemia-reperfusion (**Figure 7A**). The super-shift assay was also performed to confirm the presence of Sp1 in the EMSA complex (**Figure 7B**). These results suggested that Sp1 might contribute to the down-regulation of FOLR1 expression in the kidney, which in turn, decreased folate reabsorption in tubular cells during ischemia-reperfusion injury. However, there was no significant change in Sp1 mRNA

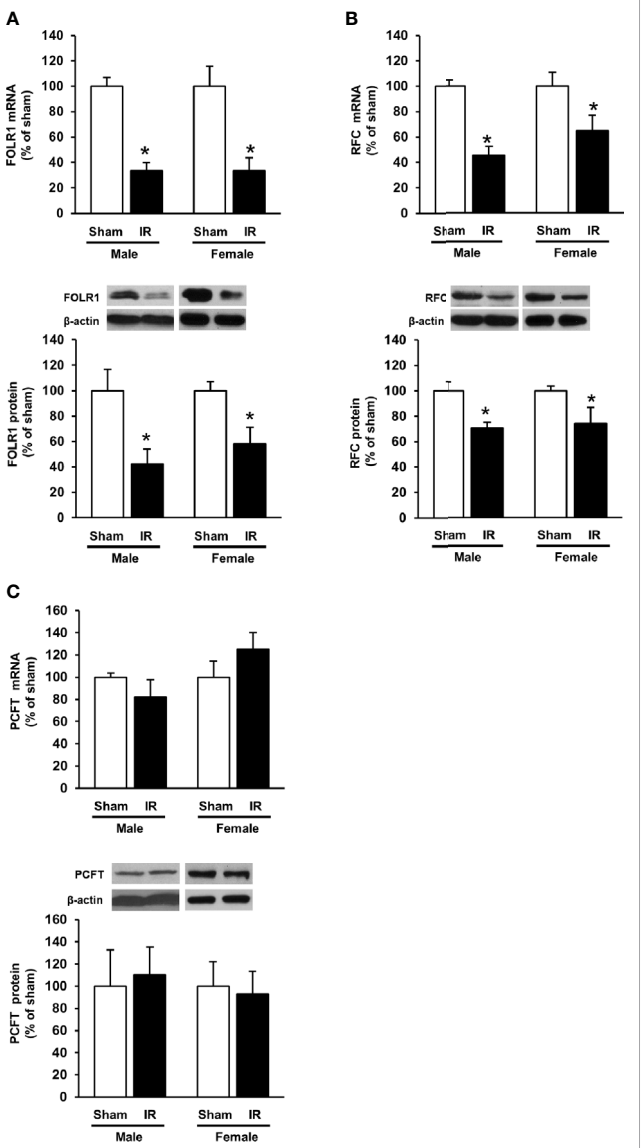


FIGURE 3 | Expression of folate transporters in rat kidneys. Rats were subjected to kidney ischemia-reperfusion (IR) or sham operation (sham). The mRNA and protein of **(A)** folate receptor 1 (FOLR1), **(B)** reduced folate carrier (RFC) and **(C)** proton-coupled folate transporter (PCFT) in the kidneys of male and female rats were determined by real-time PCR and Western immunoblotting analysis, respectively. Results are expressed as mean ± SE (n = 6). *$P < 0.05$ when compared with the value obtained from the sham-operated group.

(**Figure 7C**) and protein (**Figure 7D**) levels in the kidneys upon ischemia-reperfusion. Furthermore, there was no change in Sp1 mRNA in proximal tubular cells that were subjected to hypoxia-reoxygenation (**Figure 7E**).

DISCUSSION

The kidneys play an important role in folate homeostasis through transporter-mediated reabsorption in proximal tubules. In the

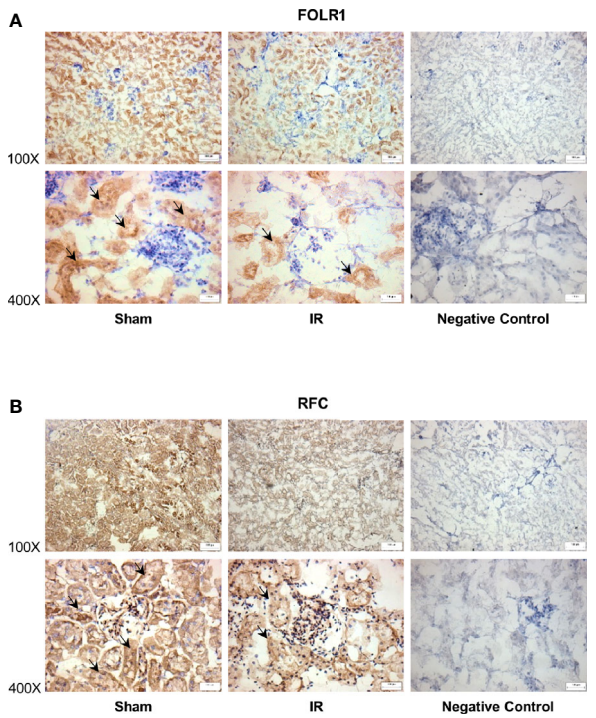


FIGURE 4 | Immunohistochemical staining of folate transporters in rat kidneys. Rats were subjected to kidney ischemia-reperfusion (IR) or sham operation (sham). Immunohistochemical staining for **(A)** folate receptor 1 (FOLR1) and **(B)** reduced folate carrier (RFC) in the kidney tissue was carried out with anti-FOLR1 antibodies and anti-RFC antibodies, respectively (magnification x100 and x400). As a negative control, immunohistochemical staining was performed by using non-specific rabbit IgG as primary antibodies. Arrows point to the areas stained with FOLR1 or RFC antibodies (brown color). All staining analyses were performed in kidneys isolated from 6 rats of each group. Representative photos were shown. The bar on the image represents 100 μm.

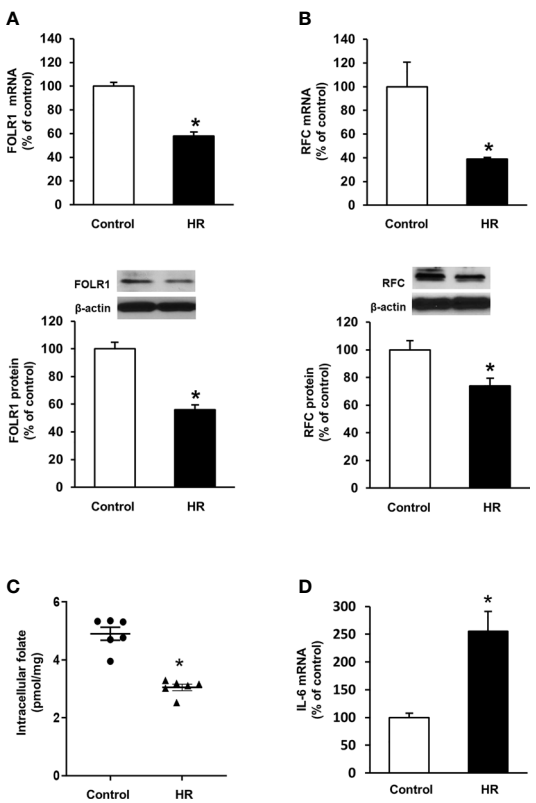


FIGURE 5 | Effect of hypoxia-reoxygenation on folate transporter expression and folate levels in proximal tubular cells. Cells were subjected to 2 h hypoxia followed by reoxygenation (HR) for 48 h or 72 h. The mRNA and protein expression of **(A)** folate receptor-1 (FOLR-1) and **(B)** reduced folate carrier (RFC) were determined by real-time PCR analysis 48 h after hypoxia-reoxygenation and by Western immunoblotting analysis 72 h after hypoxia-reoxygenation, respectively. **(C)** Intracellular folate was measured 72 h after hypoxia-reoxygenation. **(D)** IL-6 mRNA was determined. Cells cultured under normal condition were used as control. Results are expressed as mean ± SE (n = 5-6). *$P < 0.05$ when compared with the value obtained from the control cells.

present study, ischemia-reperfusion caused severe kidney injury and a decrease in plasma folate levels in rats. Our results, for the first time, demonstrated that kidney ischemia-reperfusion significantly reduced the expression of folate transporters (FOLR1, RFC) in the kidneys of both male and female rats. Such an inhibitory effect might be mediated, in part, *via* down-regulation of transcription factor Sp1. The plasma folate levels were inversely correlated to plasma creatinine levels, suggesting that low circulating folate levels were associated with impaired kidney function.

Patients with end-stage renal disease or kidney transplantation often develop nutrient deficiency. A recent prospective study indicates that altered micronutrient status is common in patients with severe AKI regardless of receiving continuous renal replacement therapy (37). It has been reported that kidney transplant recipients have reduced blood folate levels and elevated homocysteine levels (hyperhomocysteinemia) (14), the latter is a risk factor for cardiovascular disease. Reduced serum folate and elevated homocysteine levels have also been observed in patients with chronic renal failure (11, 12). However, the mechanism of low circulating folate levels associated with kidney disease is not fully understood. In the present study, we examined the effect of AKI on plasma folate levels in a rodent model. Rats with kidney ischemia-reperfusion injury had significantly low levels of plasma folate. Further analysis revealed that the plasma folate levels inversely correlated to creatinine levels. These results suggested that as kidney function deteriorated, the peripheral circulating folate level decreased. Folate is an essential micronutrient that is required for many biochemical reactions in the body. Nutritional support is a key element for AKI patients to ensure adequate nutrient balance. According to the Kidney Disease Improving Global Outcomes (KDIGO) Clinical Practice Guideline for AKI, improving nutritional status in AKI patients is critical for better clinical outcomes (7). Our results suggest that patients with AKI may be at a higher risk of developing folate deficiency.

The 5-MTHF is the predominant form of folate in the circulation. It is estimated that 20% of circulating 5-MTHF in rats is protein-bound (17, 38). The non-protein bound folate (5-MTHF) is freely filtered in the glomeruli. Reabsorption of folate in renal proximal tubules through folate transporters is

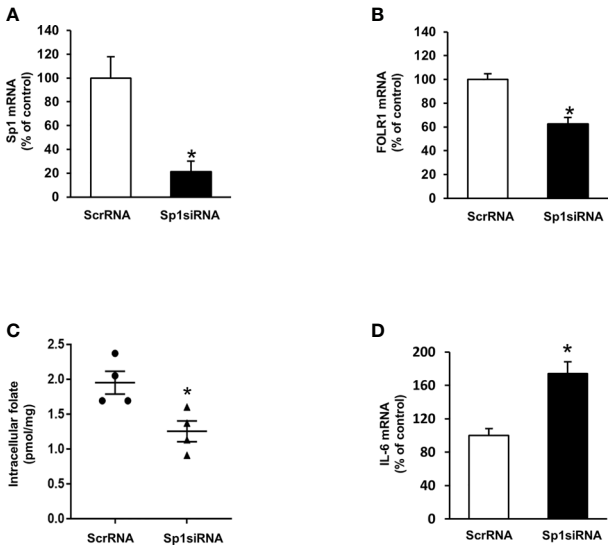


FIGURE 6 | Effect of Sp1 siRNA transfection on folate receptor expression, folate content and IL-6 expression in proximal tubular cells. Cells were transfected with Sp1 siRNA or scrambled RNA (ScrRNA) as a control. **(A)** Sp1 mRNA, **(B)** folate receptor (FOLR-1) mRNA, **(C)** intracellular folate and **(D)** IL-6 mRNA was determined by real-time PCR analysis. Results are expressed as means ± SE (n = 4-6). *$P < 0.05$ when compared with the value obtained from cells transfected with ScrRNA.

an important process to prevent urinary loss of folate. In healthy individuals, folate is reabsorbed from the lumen into tubular cells, a process primarily mediated by FOLR1 (17, 19, 39). Such a reabsorption of folate in renal proximal tubules is an important process to prevent urinary loss of folate. Diminished folate transporter expression in tubular cells might contribute to impaired folate reabsorption in the kidneys, which, in turn, led to reduced plasma (circulating) folate levels. Several lines of evidence from the present study suggested that impaired FOLR1 expression might be one of the mechanisms contributing to low circulating folate levels in AKI. Ischemia-reperfusion significantly reduced FOLR1 mRNA and protein in the kidneys. Simulation of ischemia-reperfusion in proximal tubular cells by hypoxia-reoxygenation decreased FOLR1 expression and significantly reduced intracellular folate levels. The expression of folate receptor can be regulated by a transcription factor Sp1. The human and rat folate receptor gene contains Sp1 binding sites in its promoter region (20–22). There are three Sp1 binding sites identified in human folate receptor and the binding of Sp1 to all these sites are necessary for optimal transcriptional regulation (21, 22). In the present study, ischemia-reperfusion decreased Sp1/DNA binding activity and the expression of FOLR1 in the kidney. Silencing Sp1 by siRNA transfection caused a reduction of FOLR1 expression and low folate levels in human proximal tubular cells. In a previous study, we observed that ischemia-reperfusion could reduce the phosphorylation of Sp1, which, in turn, decreased its transcriptional regulation of cystathionine-beta-synthase expression in the kidneys (30). However, it remains to be investigated whether ischemia-reperfusion alters the binding of Sp1 to the promoter region of FOLR1 in the kidneys. Aside from FOLR1-mediated folate reabsorption in the kidney, RFC is involved in transporting folate from tubular cells into the peritubular capillaries (23). Ischemia-reperfusion also inhibited RFC expression in the kidneys, which might cause less folate being transported into the circulation. Taken together, our results demonstrated that ischemia-reperfusion injury could inhibit folate transporter expression in the kidneys and reduce folate levels in the circulation.

The present study included both male and female rats. To the best of our knowledge, this is the first study reporting a downregulation of renal folate transporter expression and low plasma folate levels in a rodent model with ischemia-reperfusion induced AKI. However, the present study also had some limitations. First, down-regulation of renal folate transporter expression and low plasma folate levels were observed in rats 24 h after ischemia-reperfusion injury. It remains to be investigated whether such an injury has a long-term impact on folate homeostasis. Second, ischemia-reperfusion elicited inflammatory response in the kidneys. Folate deficiency is associated with increased oxidative stress, inflammatory response and/or hepatic steatosis in metabolic disease (40–44). Folic acid supplementation can attenuate high fat diet/fatty acid induced inflammatory cytokines including IL-6 in the liver and hepatocytes (42, 45). Our previous studies have shown that folic acid supplementation can also attenuate hyperhomocysteinemia-induced inflammatory response in the aorta (46) as well as reduce oxidative stress in rat liver and kidneys (47, 48). However, there is no direct evidence of a causal relationship between a decreased folate transporter expression/low folate levels and an increased inflammatory response in the kidneys upon ischemia-reperfusion injury. Future studies are warranted to investigate (1) whether folic acid supplementation can attenuate ischemia-reperfusion induced inflammatory cytokine expression in the kidneys; and (2) the impact of inflammation on folate transporter expression and folate status in patients with kidney injury. Third, cautions should be taken to interpret results obtained from an animal model. Results obtained from the present study need to be corroborated with clinical investigation in patients with AKI to confirm an inverse correlation between kidney function parameters and folate levels in the circulation as well as its impact on clinical outcomes. It remains to be investigated if folate supplementation can improve AKI associated biochemical and pathological changes such as inflammatory cytokine expression, oxidative stress and kidney injury. Furthermore, the present study focused on the impact of AKI on folate status and the mechanism involved. The impact of AKI on the status of other micronutrients and clinical outcomes remains to be investigated in future studies.

In conclusion, the present study has identified a significant association between kidney function and plasma folate levels. Our results, for the first time, demonstrate that kidney ischemia-reperfusion injury decreases renal folate transporter expression, in part, mediated *via* Sp1 transcriptional downregulation and causes a significant reduction of plasma folate levels in a rat model. Future studies are warranted to confirm if circulating

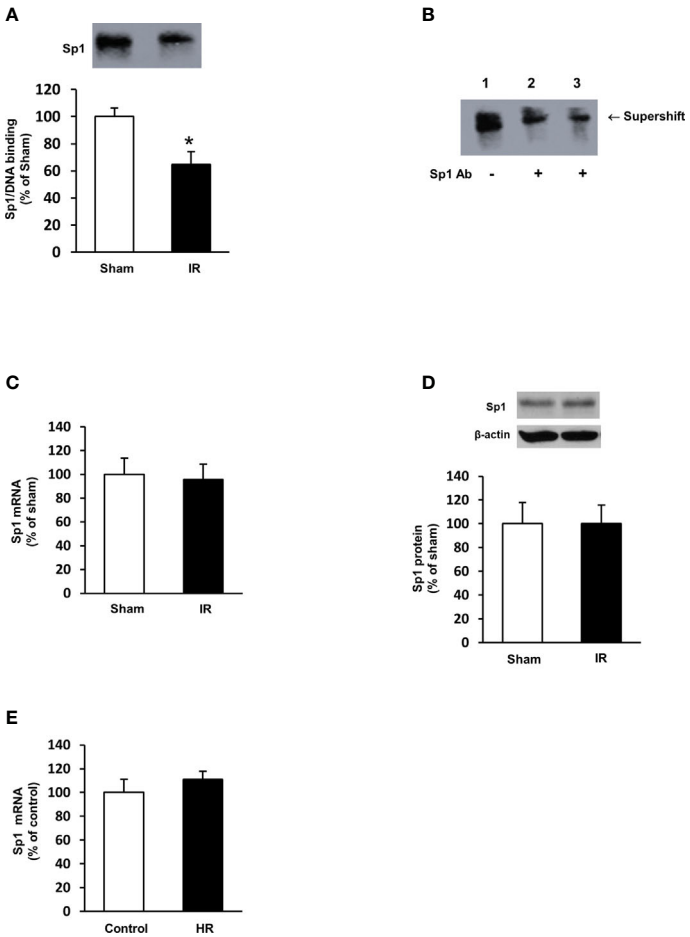


FIGURE 7 | Sp1/DNA binding activity and expression in rat kidneys and proximal tubular cells. Rats were subjected to kidney ischemia-reperfusion (IR) or sham operation (sham). Nuclear proteins were isolated from the kidneys. **(A)** The DNA binding activity of Sp1 was determined by EMSA. The binding activity in the sham-operated group was expressed at 100%. **(B)** In the supershift assay, the nuclear protein and DNA oligonucleotides were incubated in the absence (lane 1) or presence of anti-Sp1 antibody (Abcam, 2 μL in lane 2 and 4 μL in lane 3) for supershift assay. The shift of the Sp1/DNA complex is indicated by an arrow. **(C)** The mRNA of Sp1 in the kidneys was determined by real-time PCR analysis. **(D)** The Sp1 protein in the kidneys was determined by Western immunoblotting analysis. **(E)** Proximal tubular cells were subjected to 2 h hypoxia followed by reoxygenation (HR) for 48 h. Cells cultured under normal condition were used as control. The mRNA of Sp1 was measured. Results are expressed as mean ± SE (n = 5-6). *$P < 0.05$ when compared with the value obtained from the sham-operated group or the control cells.

folate level is inversely correlated with kidney function in AKI patients. Improvement of folate status in patients with kidney disease may be critical for better clinical outcomes.

DATA AVAILABILITY STATEMENT

The raw data supporting the conclusions of this article will be made available by the authors, without undue reservation.

ETHICS STATEMENT

The animal study was reviewed and approved by University of Manitoba Protocol Management and Review Committee.

AUTHOR CONTRIBUTIONS

KO, YS, and TZ conceived and designed research. CW, SH, and KA-Y performed experiments and data analysis. CY, GT, and CW performed data analysis and interpretation. CY and CW prepared figures and table. CY, CW, YS, and KO drafted the manuscript. All authors edited and approved submission of the manuscript. All authors contributed to the article and approved the submitted version.

FUNDING

This work was supported, in part, by grants from St. Boniface Hospital Foundation, and Natural Sciences and Engineering Research Council of Canada.

REFERENCES

1. Chawla LS, Bellomo R, Bihorac A, Goldstein SL, Siew ED, Bagshaw SM, et al. Acute Kidney Disease and Renal Recovery: Consensus Report of the Acute Disease Quality Initiative (ADQI) 16 Workgroup. *Nat Rev Nephrol* (2017) 13 (4):241–57. doi: 10.1038/nrneph.2017.2
2. Hertzberg D, Ryden L, Pickering JW, Sartipy U, Holzmann MJ. Acute Kidney Injury-an Overview of Diagnostic Methods and Clinical Management. *Clin Kidney J* (2017) 10(3):323–31. doi: 10.1093/ckj/sfx003
3. Fortrie G, Stads S, Aarnoudse AJ, Zietse R, Betjes MG. Long-Term Sequelae of Severe Acute Kidney Injury in the Critically Ill Patient Without Comorbidity: A Retrospective Cohort Study. *PloS One* (2015) 10(3):e0121482. doi: 10.1371/journal.pone.0121482
4. Koeze J, Keus F, Dieperink W, van der Horst IC, Zijlstra JG, van Meurs M. Incidence, Timing and Outcome of AKI in Critically Ill Patients Varies With the Definition Used and the Addition of Urine Output Criteria. *BMC Nephrol* (2017) 18(1):70. doi: 10.1186/s12882-017-0487-8
5. Scott RP, Quaggin SE. Review Series: The Cell Biology of Renal Filtration. *J Cell Biol* (2015) 209(2):199–210. doi: 10.1083/jcb.201410017
6. Basile DP, Anderson MD, Sutton TA. Pathophysiology of Acute Kidney Injury. *Compr Physiol* (2012) 2(2):1303–53. doi: 10.1002/cphy.c110041
7. Palevsky PM, Liu KD, Brophy PD, Chawla LS, Parikh CR, Thakar CV, et al. KDOQI US Commentary on the 2012 KDIGO Clinical Practice Guideline for Acute Kidney Injury. *Am J Kidney Dis* (2013) 61(5):649–72. doi: 10.1053/j.ajkd.2013.02.349
8. Fortin MC, Amyot SL, Geadah D, Leblanc M. Serum Concentrations and Clearances of Folic Acid and Pyridoxal-5-Phosphate During Venovenous Continuous Renal Replacement Therapy. *Intensive Care Med* (1999) 25 (6):594–8. doi: 10.1007/s001340050908
9. Teschner M, Kosch M, Schaefer RM. Folate Metabolism in Renal Failure. *Nephrol Dial Transplant* (2002) 17(Suppl 5):24–7. doi: 10.1093/ndt/17.suppl_5.24
10. Steiber AL, Kopple JD. Vitamin Status and Needs for People With Stages 3-5 Chronic Kidney Disease. *J Ren Nutr* (2011) 21(5):355–68. doi: 10.1053/j.jrn.2010.12.004
11. Canepa A, Carrea A, Caridi G, Dertenois L, Minniti G, Cerone R, et al. Homocysteine, Folate, Vitamin B12 Levels, and C677T MTHFR Mutation in Children With Renal Failure. *Pediatr Nephrol* (2003) 18(3):225–9. doi: 10.1007/s00467-002-1058-0
12. Sevitt LH, Hoffbrand AV. Serum Folate and Vitamin B12 Levels in Acute and Chronic Renal Disease. Effect of Peritoneal Dialysis. *Br Med J* (1969) 2 (5648):18–21. doi: 10.1136/bmj.2.5648.18
13. Capelli I, Cianciolo G, Gasperoni L, Zappulo F, Tondolo F, Cappuccilli M, et al. Folic Acid and Vitamin B12 Administration in CKD, Why Not? *Nutrients* (2019) 11(2):383. doi: 10.3390/nu11020383
14. Hamatani R, Otsu M, Chikamoto H, Akioka Y, Hattori M. Plasma Homocysteine and Folate Levels and Dietary Folate Intake in Adolescents and Young Adults Who Underwent Kidney Transplantation During Childhood. *Clin Exp Nephrol* (2014) 18(1):151–6. doi: 10.1007/s10157-013-0819-3
15. Crider KS, Bailey LB, Berry RJ. Folic Acid Food Fortification-Its History, Effect, Concerns, and Future Directions. *Nutrients* (2011) 3(3):370–84. doi: 10.3390/nu3030370
16. Stover PJ. Physiology of Folate and Vitamin B12 in Health and Disease. *Nutr Rev* (2004) 62(6 Pt 2):S3–12. doi: 10.1111/j.1753-4887.2004.tb00070.x
17. Birn H. The Kidney in Vitamin B12 and Folate Homeostasis: Characterization of Receptors for Tubular Uptake of Vitamins and Carrier Proteins. *Am J Physiol Renal Physiol* (2006) 291(1):F22–36. doi: 10.1152/ajprenal.00385.2005
18. Damaraju VL, Cass CE, Sawyer MB. Renal Conservation of Folates Role of Folate Transport Proteins. *Vitam Horm* (2008) 79:185–202. doi: 10.1016/S0083-6729(08)00406-8
19. Birn H, Spiegelstein O, Christensen EI, Finnell RH. Renal Tubular Reabsorption of Folate Mediated by Folate Binding Protein 1. *J Am Soc Nephrol* (2005) 16(3):608–15. doi: 10.1681/ASN.2004080711
20. Sadasivan E, Meng Y, Rothenberg SP. Coding Sequence, Genomic Organization and Expression of a Folate Binding Protein Gene in the Rat. *Gene* (2000) 254(1-2):219–28. doi: 10.1016/S0378-1119(00)00262-6
21. Saikawa Y, Price K, Hance KW, Chen TY, Elwood PC. Structural and Functional Analysis of the Human KB Cell Folate Receptor Gene P4 Promoter: Cooperation of Three Clustered Sp1-Binding Sites With Initiator Region for Basal Promoter Activity. *Biochemistry* (1995) 34(31):9951–61. doi: 10.1021/bi00031a018
22. Tran T, Shatnawi A, Zheng X, Kelley KM, Ratnam M. Enhancement of Folate Receptor Alpha Expression in Tumor Cells Through the Glucocorticoid Receptor: A Promising Means to Improved Tumor Detection and Targeting. *Cancer Res* (2005) 65(10):4431–41. doi: 10.1158/0008-5472.CAN-04-2890
23. Wang Y, Zhao R, Russel RG, Goldmen ID. Localization of the Murine Reduced Folate Carrier as Assessed by Immunohistochemical Analysis. *Biochim Biophys Acta* (2001) 1513:49–54. doi: 10.1016/S0005-2736(01)00340-6
24. Zhao R, Matherly LH, Goldman ID. Membrane Transporters and Folate Homeostasis: Intestinal Absorption and Transport Into Systemic Compartments and Tissues. *Expert Rev Mol Med* (2009) 11:e4. doi: 10.1017/S1462399409000969
25. Venkatachalam MA, Bernard DB, Donohoe JF, Levinsky NG. Ischemic Damage and Repair in the Rat Proximal Tubule: Differences Among the S1, S2, and S3 Segments. *Kidney Int* (1978) 14(1):31–49. doi: 10.1038/ki.1978.87
26. Vallon V. Tubular Transport in Acute Kidney Injury: Relevance for Diagnosis, Prognosis and Intervention. *Nephron* (2016) 134(3):160–6. doi: 10.1159/000446448
27. Sung FL, Zhu TY, Au-Yeung KK, Siow YL, O K. Enhanced MCP-1 Expression During Ischemia/Reperfusion Injury is Mediated by Oxidative Stress and NF-kappaB. *Kidney Int* (2002) 62(4):1160–70. doi: 10.1111/j.1523-1755.2002.kid577.x
28. Prathapasinghe GA, Siow YL, O K. Detrimental Role of Homocysteine in Renal Ischemia-Reperfusion Injury. *Am J Physiol Renal Physiol* (2007) 292(5): F1354–63. doi: 10.1152/ajprenal.00301.2006
29. Xu Z, Prathapasinghe G, Wu N, Hwang SY, Siow YL, O K. Ischemia-Reperfusion Reduces Cystathionine-Beta-Synthase-Mediated Hydrogen Sulfide Generation in the Kidney. *Am J Physiol Renal Physiol* (2009) 297(1): F27–35. doi: 10.1152/ajprenal.00096.2009
30. Wu N, Siow YL, O K. Ischemia/Reperfusion Reduces Transcription Factor Sp1-mediated Cystathionine Beta-Synthase Expression in the Kidney. *J Biol Chem* (2010) 285(24):18225–33. doi: 10.1074/jbc.M110.132142
31. Wang P, Isaak CK, Siow YL, O K. Downregulation of Cystathionine Beta-Synthase and Cystathionine Gamma-Lyase Expression Stimulates Inflammation in Kidney Ischemia-Reperfusion Injury. *Physiol Rep* (2014) 2 (12):e12251. doi: 10.14814/phy2.12251
32. Yang C, Zhao T, Lin M, Zhao Z, Hu L, Jia Y, et al. Helix B Surface Peptide Administered After Insult of Ischemia Reperfusion Improved Renal Function, Structure and Apoptosis Through Beta Common Receptor/Erythropoietin Receptor and PI3K/Akt Pathway in a Murine Model. *Exp Biol Med (Maywood)* (2013) 238(1):111–9. doi: 10.1258/ebm.2012.012185
33. Yang C, Zhao T, Zhao Z, Jia Y, Li L, Zhang Y, et al. Serum-Stabilized Naked Caspase-3 siRNA Protects Autotransplant Kidneys in a Porcine Model. *Mol Ther* (2014) 22(10):1817–28. doi: 10.1038/mt.2014.111
34. Wu S, Yang C, Xu N, Wang L, Liu Y, Wang J, et al. The Protective Effects of Helix B Surface Peptide on Experimental Acute Liver Injury Induced by Carbon Tetrachloride. *Dig Dis Sci* (2017) 62(6):1537–49. doi: 10.1007/s10620-017-4553-7
35. Wang P, Zhu Q, Wu N, Siow YL, Aukema H, O K. Tyrosol Attenuates Ischemia-Reperfusion-Induced Kidney Injury *Via* Inhibition of Inducible Nitric Oxide Synthase. *J Agric Food Chem* (2013) 61(15):3669–75. doi: 10.1021/jf400227u
36. Isaak CK, Petkau JC, O K, Debnath SC, Siow YL. Manitoba Lingonberry (Vaccinium Vitis-Idaea) Bioactivities in Ischemia-Reperfusion Injury. *J Agric Food Chem* (2015) 63(23):5660–9. doi: 10.1021/acs.jafc.5b00797
37. Ostermann M, Summers J, Lei K, Card D, Harrington DJ, Sherwood R, et al. Micronutrients in Critically Ill Patients With Severe Acute Kidney Injury - A Prospective Study. *Sci Rep* (2020) 10(1):1505. doi: 10.1038/s41598-020-58115-2
38. Selhub J, Emmanouel D, Stavropoulos T, Arnold R. Renal Folate Absorption and the Kidney Folate Binding Protein. I. Urinary Clearance Studies. *Am J Physiol* (1987) 252(4 Pt 2):F750–6. doi: 10.1152/ajprenal.1987.252.4.F750

39. Sikka PK, McMartin KE. Determination of Folate Transport Pathways in Cultured Rat Proximal Tubule Cells. *Chem Biol Interact* (1998) 114(1-2):15–31. doi: 10.1016/S0009-2797(98)00038-6
40. Sid V, Siow YL, O K. Role of Folate in Nonalcoholic Fatty Liver Disease. *Can J Physiol Pharmacol* (2017) 95(10):1141–8. doi: 10.1139/cjpp-2016-0681
41. O K, Woo CW, Sid V, Siow YL. Nonalcoholic Fatty Liver Disease and Use of Folate. In: VB Patel, editor. *Molecular Nutrition: Vitamins*. London: Academic Press (2020). p. 323–43.
42. Sid V, Shang Y, Siow YL, Hewage SM, House JD, O K. Folic Acid Supplementation Attenuates Chronic Hepatic Inflammation in High-Fat Diet Fed Mice. *Lipids* (2018) 53(7):709–16. doi: 10.1002/lipd.12084
43. Sid V, Siow YL, Shang Y, Woo CW, O K. High-Fat Diet Consumption Reduces Hepatic Folate Transporter Expression *Via* Nuclear Respiratory Factor-1. *J Mol Med (Berl)* (2018) 96(11):1203–13. doi: 10.1007/s00109-018-1688-8
44. Leclerc D, Christensen KE, Cauvi O, Yang E, Fournelle F, Bahous RH, et al. Mild Methylenetetrahydrofolate Reductase Deficiency Alters Inflammatory and Lipid Pathways in Liver. *Mol Nutr Food Res* (2019) 63(3):e1801001. doi: 10.1002/mnfr.201801001
45. Bagherieh M, Kheirollahi A, Zamani-Garmsiri F, Emamgholipour S, Meshkani R. Folic Acid Ameliorates Palmitate-Induced Inflammation Through Decreasing Homocysteine and Inhibiting NF-kappaB Pathway in HepG2 Cells. *Arch Physiol Biochem* (Forthcoming 2021). doi: 10.1080/13813455.2021.1878539
46. Wang G, Woo CW, Sung FL, Siow YL, O K. Increased Monocyte Adhesion to Aortic Endothelium in Rats With Hyperhomocysteinemia: Role of Chemokine and Adhesion Molecules. *Arterioscler Thromb Vasc Biol* (2002) 22(11):1777–83. doi: 10.1161/01.atv.0000035404.18281.37
47. Woo CW, Prathapasinghe GA, Siow YL, O K. Hyperhomocysteinemia Induces Liver Injury in Rat: Protective Effect of Folic Acid Supplementation. *Biochim Biophys Acta* (2006) 1762(7):656–65. doi: 10.1016/j.bbadis.2006.05.012
48. Hwang SY, Siow YL, Au-Yeung KK, House J, O K. Folic Acid Supplementation Inhibits NADPH Oxidase-Mediated Superoxide Anion Production in the Kidney. *Am J Physiol Renal Physiol* (2011) 300(1):F189–98. doi: 10.1152/ajprenal.00272.2010

Conflict of Interest: The authors declare that the research was conducted in the absence of any commercial or financial relationships that could be construed as a potential conflict of interest.

The handling editor declared a past co-authorship with the authors (CY and TZ).

Copyright © 2021 Yang, Wijerathne, Tu, Woo, Siow, Madduma Hewage, Au-Yeung, Zhu and O. This is an open-access article distributed under the terms of the Creative Commons Attribution License (CC BY). The use, distribution or reproduction in other forums is permitted, provided the original author(s) and the copyright owner(s) are credited and that the original publication in this journal is cited, in accordance with accepted academic practice. No use, distribution or reproduction is permitted which does not comply with these terms.

frontiers in Immunology

REVIEW
published: 07 June 2021
doi: 10.3389/fimmu.2021.664202

Fractalkine (CX3CL1) and Its Receptor CX3CR1: A Promising Therapeutic Target in Chronic Kidney Disease?

Sarah Cormican [1,2] *and Matthew D. Griffin* [1,2*]

[1] Regenerative Medical Institute (REMEDI) at CÚRAM Centre for Research in Medical Devices, School of Medicine, College of Medicine, Nursing and Health Sciences, National University of Ireland, Galway, Ireland, [2] Nephrology Services, Galway University Hospitals, Saolta University Health Group, Galway, Ireland

Innate immune cells are key contributors to kidney inflammation and fibrosis. Infiltration of the renal parenchyma by innate immune cells is governed by multiple signalling pathways. Since the discovery of the chemokine fractalkine (CX3CL1) and its receptor, CX3CR1 over twenty years ago, a wealth of evidence has emerged linking CX3CL1-CX3CR1 signalling to renal pathologies in both acute and chronic kidney diseases (CKD). However, despite the extent of data indicating a pathogenic role for this pathway in kidney disease and its complications, no human trials of targeted therapeutic agents have been reported. Although acute autoimmune kidney disease is often successfully treated with immunomodulatory medications, there is a notable lack of treatment options for patients with progressive fibrotic CKD. In this article we revisit the CX3CL1-CX3CR1 axis and its functional roles. Furthermore we review the accumulating evidence that CX3CL1-CX3CR1 interactions mediate important events in the intra-renal pathophysiology of CKD progression, particularly *via* recruitment of innate immune cells into the kidney. We also consider the role that systemic activation of the CX3CL1-CX3CR1 axis in renal disease contributes to CKD-associated cardiovascular disease. Based on this evidence, we highlight the potential for therapies targeting CX3CL1 or CX3CR1 to benefit people living with CKD.

Keywords: CX3CL1 (fractalkine), CX3CR1, chronic kidney disease, fibrosis, macrophage, innate immunity, renal fibrosis, renal inflammation and fibrosis

OPEN ACCESS

Edited by:
Bin Yang,
University of Leicester,
United Kingdom

Reviewed by:
Helen Grania Healy,
Royal Brisbane and Women's Hospital, Australia
Yuanyuan Wu,
Nantong University, China

***Correspondence:**
Matthew D. Griffin
matthew.griffin@nuigalway.ie

Specialty section:
This article was submitted to Molecular Innate Immunity, a section of the journal Frontiers in Immunology

Received: *04 February 2021*
Accepted: *11 May 2021*
Published: *07 June 2021*

Citation:
Cormican S and Griffin MD (2021) Fractalkine (CX3CL1) and Its Receptor CX3CR1: A Promising Therapeutic Target in Chronic Kidney Disease? Front. Immunol. 12:664202. doi: 10.3389/fimmu.2021.664202

INTRODUCTION

Innate immune cells are key contributors to kidney inflammation and fibrosis. Infiltration of the renal parenchyma by innate immune cells is governed by multiple signalling pathways. Since the discovery of the chemokine fractalkine (CX3CL1) and its receptor, CX3CR1 over twenty years ago, a wealth of evidence has emerged linking CX3CL1-CX3CR1 signalling to renal pathologies in both acute and chronic kidney diseases (CKD). However, despite the extent of data indicating a pathogenic role for this pathway in kidney disease and its complications, no human trials of targeted therapeutic agents have been reported. Although acute autoimmune kidney disease is often

successfully treated with immunomodulatory medications, there is a notable lack of treatment options for patients with progressive fibrotic CKD. In this article we revisit the CX3CL1-CX3CR1 axis and its functional roles. Furthermore we review the accumulating evidence that CX3CL1-CX3CR1 interactions mediate important events in the intra-renal pathophysiology of CKD progression, particularly *via* recruitment of innate immune cells into the kidney. We also consider the role that systemic activation of the CX3CL1-CX3CR1 axis in renal disease contributes to CKD-associated cardiovascular disease. Based on this evidence, we highlight the potential for therapies targeting CX3CL1 or CX3CR1 to benefit people living with CKD.

DISCOVERY OF THE CX3CL1-CX3CR1 AXIS AS A REGULATOR OF CHEMOTAXIS AND ADHESION

CX3CL1 was identified independently by two separate research groups in 1997 and termed neurotactin and fractalkine by the respective authors (1, 2). Neurotactin may also refer to a surface glycoprotein first identified in *Drosophilia melanogaster* and this term has therefore not remained in extensive use (3, 4). Throughout this article we will refer to this unique chemokine as CX3CL1.

Pan et al. identified CX3CL1 following sequencing of the murine choroid plexus while Bazan et al. identified it by searching for chemokine-like sequences in an expressed sequence tag database in the National Centre for Biotechnology Information (NCBI). Both groups identified a cDNA clone which corresponded to a large protein containing a sequence of hydrophobic residues suggestive of a transmembrane domain. Pan et al. reported that messenger RNA for CX3CL1 was identified in most human tissues with the notable exception of peripheral blood cells but corresponding analyses of protein expression were not reported in this paper. Human endothelial and epithelial cell lines transfected with the coding region of CX3CL1 were found to express CX3CL1 on the cell surface, consistent the hypothesis that the newly discovered protein was membrane-bound. Bazan et al. showed that CX3CL1 could also be released into cell culture supernatants. The authors described disparate results for chemotactic assays with CX3CL1 which was reported to induce *in vitro* neutrophil chemotaxis by Pan et al. and *in vitro* monocyte and lymphocyte chemotaxis by Bazan et al. The latter also reported that surface CX3CL1 triggered adhesion of monocytes or T-cells. Notably, Pan et al. observed that CX3CL1 was upregulated in the brains of mice treated with lipopolysaccharide or in mice with experimental autoimmune encephalitis, suggesting a pro-inflammatory role. Thus, CX3CL1 was demonstrated to be a new and structurally unique chemokine which was comprised of CX3C domain and a mucin stalk. The CX3C domain may be shed from the mucin stalk to act as a soluble chemokine or may be expressed on the cell surface *via* this transmembrane mucin stalk.

In the same year, Imai et al. identified that the orphan receptor V28 was a high-affinity receptor for CX3CL1 and that this receptor mediated *in vitro* CX3CL1-induced chemotaxis (5). This G protein coupled receptor (GPCR) was previously reported by Raport et al. who used degenerate PCR to identify GPCRs related to the IL-8 receptor with potential relevance to immune function. Notably V28 had been identified as highly expressed in neural and lymphoid tissue but no known chemokines were found to trigger Ca^{2+} influx in V28 transfected cell lines (6). In contrast, CX3CL1 ligation of the V28 receptor induced calcium influx which was inhibited by pertussis toxin, indicating that CX3CL1 signal transduction is mediated by a Gαi class G-protein. This work further demonstrated that V28 is capable of inducing cellular adhesion through a mechanism independent of G-protein signalling. V28 surface expression was identified on natural killer cells, T-cells and monocytes but not on granulocytes and was capable of triggering trans-endothelial migration of both lymphocytes and monocytes. Finally, endothelial expression of the fractalkine protein was shown to induce adhesion of V28 transfected cells or natural killer cells to the endothelium (5). The mechanism of adhesion was shown to require both the CX3C and mucin stalk domains of the CX3CL1 protein. Overall, these initial studies demonstrated that CX3CL1 functions as both a chemokine and an adhesion molecule *via* binding of the V28 receptor. The V28 receptor was subsequently re-named CX3CR1 and remains the only receptor through which CX3CL1 has been shown to function (5). Combadiere et al. reached similar conclusions and also reported that CX3CR1 may function as a fusion co-receptor in HIV infection (7).

In the years following these discoveries, the role of the CX3CL1-CX3CR1 axis in inducing chemotaxis and adhesion of leucocyte populations was pursued in detail by several groups. Al-Aoukaty et al. further confirmed that engagement of CX3CR1 results in G-protein activation in the cellular membrane, specifically G_i or G_z proteins (8). Al Aoukaty et al. postulated that the mucin stalk contained within CX3CL1 was key to the mechanism of CX3CL1-CX3CR1 mediated adhesion. CX3CL1-CX3CR1 interactions were shown by Fong et al. to be capable of inducing monocyte, $CD8^+$ lymphocyte and NK-cell arrest and firm binding under physiologic flow conditions, including when CX3CL1 was expressed on the surface of endothelial cells (9). Work by Goda et al. indicated that exposure to CX3CL1 also enhances the ability of both THP-1 cells and *ex vivo* monocytes to bind to integrins and fibronectin (10). With regards to the effect of inflammation on regulation of CX3CL1-CX3CR1 signalling, Harrison et al. demonstrated that CX3CL1 is expressed at a low level by rat endothelial cells in steady state but that both mRNA and protein expression are increased after *in vivo* treatment with lipopolysaccharide (LPS) or the pro-inflammatory cytokines tumour necrosis factor-alpha (TNF-α) and interleukin-1 (IL-1) (11). It was subsequently demonstrated that CX3CL1 induction by pro-inflammatory stimuli is mediated by nuclear factor kappa-light-chain-enhancer of activated B cells (NF-κB) signalling (12).

In relation to the kidney, the signalling pathways involved in TNF-α–mediated CX3CL1 expression within mesangial cells were first dissected by Chen et al. (13). Mesangial cells stimulated with TNF-α upregulate CX3CL1 expression at the mRNA and protein levels. The protein produced is cleaved by matrix metalloproteinases (MMPs) and can then induce transmigration of a monocytic cell line. Intracellular signalling cascades triggered by TNF-α were investigated using protein kinase inhibitors and inhibitors of NF-κB. Inhibitors of protein kinase C (PKC) or of p42/44 (ERK1/2) mitogen activated protein kinase (MAPK) reduced CX3CL1 expression after TNF-α stimulation, as did inhibition of NF-κB or activation protein-1 (AP-1). Overall, these data indicate that TNF-α induces CX3CL1 through multiple intracellular signalling including PKC, ERK1/2 MAPK, NF-κB and AP-1.

PHYSIOLOGICAL ROLES OF CX3CL1-CX3CR1 BEYOND CHEMOTAXIS

A further physiological role for CX3CR1 was reported by Auffray et al. (14). This work used real-time intra-vital microscopy and $CX3CR1^{gfp/+}$ mice to demonstrate that $Ly6C^{lo}$ monocytes crawl on the luminal surface of blood vessels and extensively patrol the endothelial surface (14). This patrolling process, which is dependent on both the integrin LFA-1 (CD11a/CD18) and CX3CR1, plays a role in immune surveillance and allows early response to tissue damage or infection. Subsequently, Cros et al. demonstrated, using adoptive transfer of human nonclassical monocytes into *Rag*$^{-/-}$ mice, that human nonclassical monocytes, the equivalent of murine $Ly6C^{lo}$ monocytes, also patrol the vasculature (15).

CX3CL1-CX3CR1 signalling has also been reported to play an anti-apoptotic role in myeloid cell development and survival during steady-state conditions (16). Lyszkiewcz et al. demonstrated that, in steady-state, CX3CR1 deficiency results in accelerated turnover of myeloid precursors in the bone marrow. In a competitive adoptive transfer model, CX3CR1-deficient dendritic cells, monocytes, macrophages and granulocytes have a survival disadvantage. These effects are not seen in animals subjected to sub-lethal whole body irradiation suggesting that the survival disadvantage conferred by CX3CR1 deficiency is overcome in inflammatory conditions (17). This indicates a role for the CX3CL1-CX3CR1 pathway in homeostatic but not inflammation-driven generation of myeloid cells. It has also been demonstrated, however, that anti-apoptotic signalling through the CX3CL1-CX3CR1 pathway is important for monocyte survival within atherosclerotic plaques (18). This elegant work demonstrated less severe atherosclerosis with reduced monocyte survival and increased apoptotic monocytes within atherosclerotic plaques of CX3CR1-deficient mice - effects that were reversed by enforced expression of the anti-apoptotic protein Bcl-2. Furthermore, cultured human monocytes are rescued from cell death by treatment with recombinant CX3CL1. The anti-apoptotic effects of CX3CL1 appear to be G-protein mediated as they are abolished by exposure to pertussis toxin. Interestingly, monocytes isolated from individuals carrying the M280 mutation in the CX3CR1 gene are not rescued from apoptosis by exposure to CX3CL1 (19) and homozygotes for this mutation are protected from atherosclerotic cardiovascular disease (20) while being at increased risk of systemic candidiasis (21) – suggesting important, non-redundant, biological roles for this pathway in human atherogenesis and immunity. CX3CL1-CX3CR1 anti-apoptotic signalling may also enable T-cell survival during inflammation (22). Furthermore, CX3CL1 mediates survival and proliferation of vascular smooth muscle cells through ERK- and Akt-dependent signalling - with Akt phosphorylation mediated by transactivation of the epidermal growth factor receptor (EGFR) (23).

It is evident that the CX3CL1-CX3CR1 axis is key in leucocyte trafficking throughout the body and immune cell survival in certain circumstances. CX3CR1 is also expressed by microglia in the brain and CX3CL1-CX3CR1 is of importance in neurodevelopment and inflammatory disease of the central nervous system (24, 25). Certain cells of mesenchymal origin including smooth muscle cells and mesangial cells also express CX3CR1, as discussed later in this review. Within the central nervous system it has been shown that CX3CL1 signalling may stimulate increased pro-inflammatory cytokine production through in a p38-MAPK dependent fashion (26). Whether such a role exists in other organs or circulating immune cells remains to be seen. CX3CL1- CX3CR1 signalling may be of broader importance in embryonic development, including nephrogenesis, as both CX3CL1 and CX3CR1 are expressed by various structures and cells within the developing kidney (27). **Table 1** summarises the expression of CX3CR1 by different immune cells and its functional roles in these cells. These data present a breakdown of CX3CR1 expression and responses to CX3CL1 by cell type based on data published early in the twenty first century. It should be noted that each leucocyte population referred to in this table is comprised of multiple, functionally distinct, subpopulations. Further work examining lymphocyte and monocyte subtype-specific expression and functional responses would be of value in elucidating the precise role of this pathway in immune cell function. Multiple signalling pathways mediate various cellular responses to CX3CL1 binding to CX3CR1 including intracellular calcium release and the MAP/ERK, PI3K/Akt, JAK/STAT pathways, as illustrated in **Figure 1**.

THE CX3CL1-CX3CR1 AXIS IN KIDNEY DISEASE: EARLY DISCOVERIES (1998–2002)

Shortly after the discovery of CX3CL1 and its cognate receptor CX3CR1, studies examining the role of the CX3CL1-CX3CR1 axis in multiple disease states and the potential for therapeutic blockade emerged. The first such study of relevance to kidney disease examined the potential for chemokine receptor blockade by viral macrophage inflammatory protein-II (vMIP-II),

TABLE 1 | Summary of expression of CX3CR1 and chemotactic, adhesive and other physiological responses to CX3CL1 in major immune cell subtypes.

Cell Type	CX3CR1 Expression	Chemotactic Response to CX3CL1	Adhesion Response to CX3CL1	Other Responses to CX3CL1
Monocytes	Yes (higher on non-classical monocytes)	Yes (variable data regarding subset-specific response)	Yes	Crawling on vasculature (nonclassical subset) Survival *via* anti-apoptotic signalling in both steady state and atherosclerosis
Macrophages	Yes	Yes	Not reported	Maturation and survival
Dendritic Cells	High expression by cDC, low or absent expression on pDC	Yes (cDC)	Not reported	Maturation and survival
T-cells	Some subtypes	Some subtypes	Some subtypes	Cell survival in inflammatory lung disease
B-cells	No	No	No	N/A
NK-cells	Yes	Yes	Yes (after activation)	None reported
Neutrophils	No (mRNA expression reported)	Varying Reports*	No	Possible cell survival role in steady-state

*cDC, conventional dendritic cells; pDC, plasmacytoid dendritic cells; *Pan et al. reported an effect on neutrophil chemotaxis but this was not shown in subsequent studies, Becker et al. suggested a possible role in in vivo recruitment (28).*

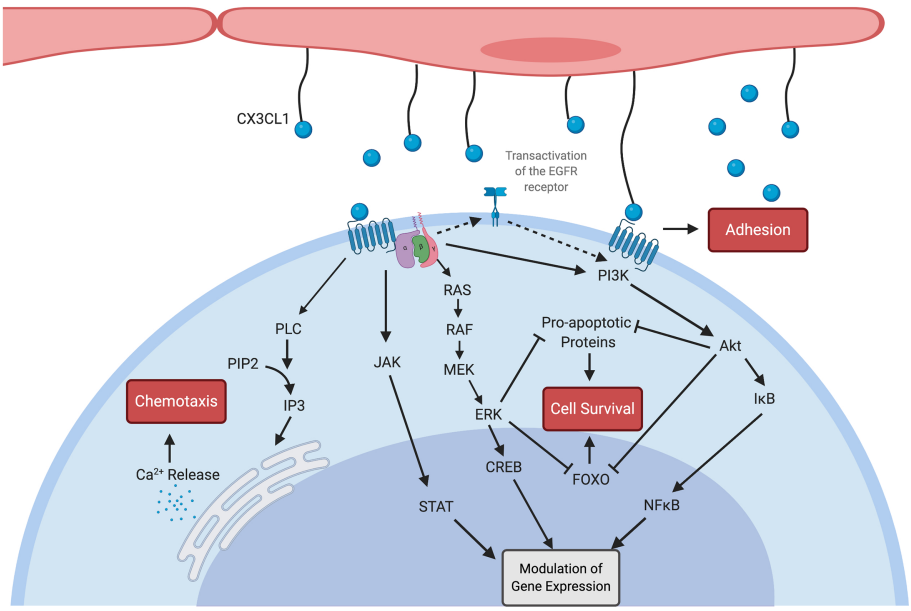


FIGURE 1 | Multiple signalling pathways are activated by both soluble and membrane-bound CX3CL1 (blue spheres) as outlined here. CX3CR1 is a G-protein coupled receptor linked to Gi and Gz proteins (8). Calcium release resulting in chemotaxis was demonstrated by Harrison et al. (29). CX3CL1 also contributes to intercellular adhesion through mechanisms which do not appear to be G-protein sensitive (5). Enhanced cellular survival is mediated by both the Akt and ERK pathways, including *via* transactivation of the EGFR receptor (16). CX3CL1 ligation of the CX3CR1 receptor also leads to nuclear translocation of transcription factors (30) including NFκB (31), CREB (32) and STAT (33) with resulting modulation of gene expression. Created with BioRender.com.

a chemokine analogue produced by human herpes virus-8, in experimental anti-GBM glomerulonephritis in Wistar-Kyoto rats (34). This study confirmed that v-MIP-II competitively inhibits CX3CL1 binding to immune cells and showed that administration of v-MIP-II in this rat model of glomerulonephritis attenuated disease severity. However, v-MIP-II is an antagonist of multiple chemokine receptors and there results could not be definitively ascribed to blockade of CX3CL1/CX3CR1 interaction (34). A subsequent study looked more specifically at the effects of CX3CR1 blockade in the same model of acute glomerular inflammation. Expression of both CX3CL1 and CX3CR1 were increased after the induction of anti-GBM glomerulonephritis. CX3CL1 expression was induced on the glomerular endothelium while CX3CR1 expression was identified on infiltrating T-cells and macrophages. Notably, these cells, once isolated from inflamed kidneys, were capable of undergoing chemotaxis towards a CX3CL1 gradient. In keeping with the proposed pathological relevance of CX3CL1 in kidney inflammation, daily treatment with an anti-CX3CR1 antibody resulted in attenuated disease severity (35). In a study of human renal biopsy samples from 23 patients with crescentic glomerulonephritis, CX3CL1 expression was shown to be increased in acute disease and decreased after steroid treatment (36). These findings provoked interest in the therapeutic use of chemokine blockade in renal disease (37, 38).

In 2002, Cockwell et al. examined the expression of CX3CL1 in renal biopsies from patients with acute glomerulonephritis due to ANCA-associated vasculitis (AAV) or with acute transplant rejection, using either normal tissue obtained at the time of tumour nephrectomy or biopsies showing minimal change disease as negative controls. At gene expression level, mRNA for CX3CL1 was increased in the glomeruli of patients with acute AAV and increased to a lesser extent in patients with acute transplant rejection. In the tubulointerstitium, mRNA for CX3CL1 was increased in both groups compared to control tissue but to a greater degree in transplant rejection. At protein level, CX3CL1 expression, determined by immunohistochemistry, was higher in biopsies with renal inflammation. Serial section analysis demonstrated that CX3CL1 positivity was localised to areas of T-cell or macrophage infiltrates (39). Related *in vitro* work demonstrated that proximal tubular epithelial cells (PTEC) upregulate CX3CL1 expression after TNF-α stimulation and that this upregulation is capable of supporting adhesion of either THP-1 cells or *ex vivo* natural killer (NK) cells (40).

Segerer et al. further studied the expression of CX3CR1 by infiltrating cells in human kidney disease using similar control samples (41). Serial section analysis was used to correlate the location of CX3CR1 positivity with the presence of T-cell or monocyte/macrophage infiltrates, identified by anti-CD3 and anti-CD68 staining, respectively. The negative control or uninflamed tissue showed occasional CX3CR1 positive cells and minimal cellular infiltration. By comparison, kidney biopsies of membranous nephropathy, focal segmental glomerulosclerosis or collapsing glomerulopathy had more CX3CR1 positive cells, corresponding to the locations of T-cell or monocyte/macrophage infiltration. In crescentic glomerulonephritis, cellular infiltration was much more pronounced with a preponderance of $CD68^+$ monocyte/macrophages. CX3CR1 was highly expressed and, similarly, corresponded to the location of monocyte/macrophage or T-cell infiltration. Of note, these and other early studies in animal models and human kidney samples focused primarily on expression patterns and associations of the CX3CL1-CX3CR1 axis in acute settings. Although clearly of potential mechanistic importance in the intense inflammation associated with acute kidney diseases, insights into the expression and functional significance of CX3CL1/CX3CR1 signalling in CKD was lacking. For the remainder of this article, we focus on subsequent evidence that CX3CL1 interaction with CX3CR1 is of distinct pathophysiological importance to the progression of fibrosis and impaired renal function in CKD.

THE ROLE OF THE CX3CL1-CX3CR1 AXIS IN CHRONIC KIDNEY DISEASE: EVIDENCE FROM ANIMAL STUDIES

Animal models have indicated that the CX3CL1-CX3CR1 axis is important in the progression of chronic renal diseases such as diabetic nephropathy (DN). Kikuchi et al. (42) showed, in rats with streptozocin-induced DN, that mRNA expression of CX3CL1 and CX3CR1 was increased four and eight weeks after induction of diabetes. Immunohistochemistry demonstrated that endothelial expression of CX3CL1 and number of CX3CR1 positive cells within the glomeruli were increased. Treatment with the ACE-inhibitor temocapril reduced intra-renal mRNA and protein levels of CX3CL1 and CX3CR1 eight weeks after induction of diabetes. Subsequently, micro-dissected glomeruli from normal rat kidneys were shown to upregulate CX3CL1 expression following *in-vitro* exposure to high concentrations of glucose, TNF-α or advanced glycation end-products (AGEs). These data demonstrate that CX3CL1 expression is induced in DN and may be modulated by therapeutic strategies already in use (43). The streptozocin-induced DN model was used in CX3CR1 knockout mice by Song et al. to further elucidate the role of CX3CL1 signalling in the development of DN (44). Renal fibrosis was induced in wild-type diabetic mice but was attenuated in CX3CR1-deficient animals. The streptozocin-treated knockout mice also had reduced mRNA expression of TGF-β, fibronectin and collagen-related genes and reduced macrophage accumulation within kidney tissue compared to their wild-type counterparts. *In vitro* work examined the role of CX3CL1 signalling in mesangial cells under diabetic conditions. In response to high glucose concentrations, mesangial cells increased expression of mRNA and protein for CX3CL1 and CX3CR1 and released greater amounts of CX3CL1 into the culture medium. Treatment of mesangial cells with CX3CL1 or with other diabetes-related stimuli also induced higher expression of the pro-fibrotic molecules TGF-β, collagen 4α1 and fibronectin at both mRNA and protein levels. Furthermore, small interfering (si)-RNA-mediated reduction of CX3CL1 expression attenuated these changes. These data highlight that CX3CL1 signalling *via* CX3CR1 contributes to macrophage infiltration and renal fibrosis in mouse models of DN and that mesangial cells both produce and respond to CX3CL1. Such findings related to mesangial cells in DN are consistent with reports in an acute glomerulonephritis model, indicating that CX3CL1, produced by mesangial cells plays a role in monocyte recruitment to the kidney (45) and in *in vitro* culture systems demonstrating that murine monocytes adhere to mesangial cells in a CX3CL1-CX3CR1 dependent fashion (46).

The importance of the CX3CL1-CX3CR1 axis in renal fibrosis following acute kidney injury has been studied by Furuichi et al. using an ischemia reperfusion injury (IRI) model. In this study, IRI resulted in increased expression of CX3CL1 protein in the kidney but did not demonstrate a corresponding change in mRNA levels. Furthermore, the location of CX3CL1 expression within the kidneys changed, being limited to endothelial cells in sham-operated animals while also detected on tubular epithelial cells and in association with infiltrating cells following IRI. Renal expression of CX3CR1 was increased at both protein and mRNA levels following IRI with protein expression mostly observed in association with infiltrating cells. The lack of correlation between mRNA and protein expression may simply reflect a technical limitation given the correlation between mRNA and protein level expression described by other authors. The severity of acute tubular necrosis following IRI did not differ between wild type (WT) and $CX3CR1^{-/-}$ mice. However, collagen deposition was reduced in the $CX3CR1^{-/-}$ animals, as was intra-renal macrophage infiltration while lymphocyte and neutrophil

numbers were unaffected. Overall, this work was consistent with a role for CX3CR1-dependent macrophage-mediated fibrosis following IRI. To account for the possibility of developmental differences in macrophage lineages in $CX3CR1^{-/-}$ mice, Furuichi et al. also used pharmacological blockade by administering a CX3CR1-neutralising antibody following IRI. Animals treated with the blocking antibody had significantly reduced post-IRI renal fibrosis compared to controls (47). Overall these data suggested that the CX3CL1-CX3CR1 axis was of mechanistic importance in the development of renal fibrosis and a potential for it to be targeted therapeutically.

Oh et al. also demonstrated increased CX3CL1 expression after IRI, using immunoblotting and immunohistochemistry. In this study, blockade of CX3CR1 was associated with protection against acute renal impairment, as assessed by histology and blood urea and creatinine levels, and with reduced macrophage infiltration (48). Another mouse model of IRI demonstrated that CX3CR1 deficiency is associated with protection against renal impairment after IRI and reduced infiltration of the renal parenchyma with monocyte-derived macrophages. Macrophage infiltration of the kidney was restored and protection from renal impairment attenuated after adoptive transfer of CX3CR1-competent blood monocytes (49). These results supported the conclusion that CX3CR1-signalling is required for monocyte/macrophage migration into the kidney and that CX3CR1-dependent migration has deleterious effects on renal function following IRI (49). Overall, these data from animal model studies are consistent with a mechanism by which intra-renal induction of CX3CL1 expression following IRI plays a key role in monocyte-derived macrophage infiltration of the renal parenchyma and in the subsequent severity of renal fibrosis. Whether this pathway is also an important, targetable mechanism of AKI progression to CKD in humans remains less well understood and merits more detailed investigation.

Other animal models of pro-fibrotic kidney injury have also provided compelling evidence of a role for CX3CL1 in mediating renal leucocyte infiltration and renal functional impairment. For example, in a mouse model of radiation-induced renal injury, increased CX3CL1 expression within glomeruli was observed at 30 and 40 weeks after irradiation (50) and correlated with areas of leucocyte infiltration on serial section analysis. Similarly, in a mouse model of hypertension, the combination of deoxycorticosterone and high salt diet following unilateral nephrectomy resulted in elevated mRNA for both CX3CL1 and CX3CR1 within the kidneys. In this study, CX3CL1 was chiefly expressed by PTEC, peritubular capillaries and vascular endothelial cells. Treated animals exhibited $F4/80^{+}$ macrophage infiltration of the kidneys with interstitial fibrosis and these changes, along with intra-renal TGFβ1 level, were ameliorated in CX3CR1-deficient mice (51). Mice with cisplatin-induced renal impairment have also been reported to have increased CX3CL1 expression within the kidneys. However, in this model of acute kidney injury, neither treatment with an anti-CX3CR1 neutralising antibody nor genetic CX3CR1 deficiency reduced the peak creatinine level, peak blood urea nitrogen level or macrophage infiltration of the kidney after injury (52). In a rat model of renovascular hypertension, serum CX3CL1 levels are increased in hypertensive rats, with or without concomitant *Trypanosoma cruzi* infection (53). High fructose diet-induced kidney injury is also ameliorated in CX3CR1-deficient mice *via* a reduction in NF-kB signalling (54).

Utilising the mouse unilateral ureteric obstruction (UUO) model, Peng et al. investigated the role of CX3CL1 in recruitment of different monocyte subsets into the obstructed kidney (55). This model demonstrated that both $Ly6C^{hi}/CX3CR1^{lo}$ (classical) and $Ly6C^{lo}/CX3CR1^{hi}$ (nonclassical) monocytes are recruited to the kidney after obstruction, albeit within different time-frames. The authors reported that, while $Ly6C^{hi}$ monocytes are the major producers of the proinflammatory cytokines TNF-α and IL-1β, $Ly6C^{lo}$ monocytes produce more of the pro-fibrotic cytokines TGF-β and platelet-derived growth factor (PDGF). Similar to other reported models, renal fibrosis was attenuated in CX3CR1-deficient mice after UUO. Further analyses demonstrated a specific lack of nonclassical monocyte accumulation within the obstructed kidneys of CX3CR1-deficient mice. Interestingly, this deficit was due to increased apoptosis rather than impaired recruitment, in keeping with the role of CX3CR1 signalling in cell survival outlined (18). Several of the studies described heretofore have indicated that macrophage accumulation is promoted *via* the CX3CR1-CX3CL1 axis. Of relevance to this literature, recent work has shown that the CX3CL1-CX3CR1 axis mediates blood monocyte infiltration of the colon and, thus, contributes to macrophage accumulation and tissue damage (56). More specifically, it was shown that CX3CL1 mediates crawling of monocytes on the colonic veins and that blockade of CX3CR1 prevents monocyte crawling and macrophage accumulation within the colon. Similar mechanisms may be responsible for macrophage accumulation in kidney injury.

To better address the potential relevance of CX3CL1-mediated signalling in CKD, Koziolek et al. (57) used a mouse folic acid nephropathy (FAN) model. Animals treated with a single high-dose intraperitoneal injection of folic acid consistently developed progressive tubulointerstitial fibrosis with renal functional impairment and proteinuria. Subsequent analyses of FAN kidneys demonstrated upregulation of CX3CL1 and CX3CR1 mRNA and protein for more than a hundred days after treatment. Compared to control kidneys, the location of CX3CL1 expression changed from limited expression on endothelial cells to expression on glomerular and peritubular capillaries, mesangial cells, tubular cells and cells within the interstitium. Immunohistochemistry also demonstrated increased expression of collagen-1, $CD3^{+}$ (T-cell) infiltrates and S100A4, a protein expressed by fibroblasts and associated with epithelial-to-mesenchymal transition (57). The intensity of CX3CL1 expression correlated with the degree of tubulointerstitial fibrosis. Further work utilised *in vitro* analyses of murine renal tubular epithelial cell lines and demonstrated that these cells were capable of upregulating CX3CL1 expression and demonstrated increased chemotactic potency for peripheral blood mononuclear cells after stimulation with cytokines such as TNF-α, IL-1β or TGF-β (57). This animal study indicated that many of the functional effects of CX3CL1 demonstrated in more acute models of renal disease are also relevant to CKD. Finally, treatment of human renal fibroblast

cell lines with CX3CL1 was shown to further upregulate CX3CL1 expression and to result in increased cell numbers, due to both increased proliferation and increased survival (57).

In contrast to the studies summarized above, work by Engel et al. has raised questions about the role of CX3CR1-CX3CL1 signalling in promoting renal fibrosis, instead providing experimental evidence that CX3CR1 deficiency can result in accelerated renal fibrosis under some circumstances (58). In this study, renal fibrosis following UUO was increased in CX3CR1-deficient mice compared to their wild type counterparts. CX3CR- deficient mice had a slightly decreased total number of mononuclear phagocytes after UUO but further analyses demonstrated a relative increase in blood monocyte-derived macrophages with a decrease in resident macrophages and dendritic cells. TGF-β producing macrophages were also increased in the CX3CR1-deficient mice, suggesting a mechanism for increased fibrogenesis. Finally, this work indicated that increased macrophage proliferation within the kidney occurred in CX3CR1-deficient mice. Overall, the authors proposed that lack of the CX3CR1 receptor allows macrophage proliferation within the renal parenchyma after injury, thus driving renal fibrosis (58). More recently, Ahadazadeh et al. examined the role of CX3CR1 in angiotensin-induced hypertension in mice. Greater albuminuria, more severe glomerular injury and increased renal fibrosis were seen in the CX3CR1-deficient mice, although blood urea nitrogen did not differ from that of wild type mice. Alongside these differences, increased neutrophil and F4/80$^+$ macrophage infiltration of the kidneys and reduced dendritic cell numbers were seen in the CX3CR1-deficient mice. Cardiac injury was also assessed and was not reduced by CX_3CR1 deficiency. In a different disease scenario, it has also been demonstrated that CX3CR1-dependent mechanisms protect against acute kidney injury in sepsis (59). These studies, which indicate that there may be counter-regulatory roles for CX3CR1-expressing myeloid cells during pro-fibrotic renal inflammation, must be taken into consideration when evaluating the clinical potential of CX3CR1 blockade in human CKD from diverse causes. It should be noted, however, that they depend on unconditional, whole-animal knockout of CX3CR1. Thus, differences in embryonic development, such as altered seeding of the renal tissue yolk sac-derived macrophages, may have impacted on the study findings. In order to better determine the potential for CX3CR1 targeting studies, incorporating a pharmacological blockade strategy at the time of renal injury or an inducible CX3CR1 knockout model should be utilised wherever possible.

THE ROLE OF THE CX3CL1-CX3CR1 AXIS IN CHRONIC KIDNEY DISEASE: EVIDENCE FROM STUDIES OF HUMAN TISSUE AND CELLS

In 2007, Koziolek et al. studied CX3CR1 expression within the renal parenchyma of patients with >40% interstitial fibrosis associated with only minor cellular infiltration compared to normal renal parenchyma obtained at the time of tumour nephrectomy. In normal kidneys, CX3CR1 expression was absent or minimal but, in fibrotic kidneys CX3CR1$^+$ cells were identified within both scarred glomeruli and the tubulointerstitial compartment. Serial sectioning indicated that some of the CX3CR1$^+$ cells were CD68$^+$ monocyte/macrophages or CD3$^+$ T-cells but not all cells co-stained with these markers and double immunofluorescence studies indicated that, in advanced renal fibrosis, tubular epithelial cells, myofibroblasts (α-SMA$^+$) and dendritic cells (CD11c$^+$) also express CX3CR1. In keeping with this, human renal fibroblast cell lines also express CX3CR1 and migrate towards a CX3CL1 gradient suggesting a functional role for the CX3CL1- CX3CR1 in promoting renal fibrogenesis through fibroblast recruitment (60). Wang et al. demonstrated that exposure to AGEs increases human renal mesangial cell expression of CX3CL1. Production of matrix metalloproteinase two (MMP-2), an enzyme required for extracellular matrix degradation is inhibited in mesangial cells by AGEs and in a monocytic cell line by CX3CL1. Thus, extracellular matrix degradation may be reduced in diabetes due, in part, to increased CX3CL1 expression and this may contribute to renal extracellular matrix deposition and progression of renal impairment in DN (61).

In a different clinical setting, Yoshimoto et al. reported glomerular CX3CL1 expression and CD16$^+$ monocyte infiltration in biopsies from people with acute lupus nephritis (62). Similar observations were subsequently reported in a mouse model of lupus nephritis. Of note, human CD16$^+$ monocytes are now conventionally subdivided on the basis of CD14 expression into intermediate and nonclassical subsets (63) and have been shown to circulate in higher numbers in CKD, atherosclerosis and multiple other pro-inflammatory conditions (64, 65). Despite the demonstrated expansion of these populations in CKD and their association with CKD progression (64), the extent to which they infiltrate the renal parenchyma and contribute to renal inflammation and fibrosis during CKD is incompletely understood (66). Further investigation of the role of CX3CL1 in mediating inflammatory monocyte subset activities in human CKD will be of value in elucidating these issues.

In addition to its reported role in renal monocyte/macrophage recruitment and activation, data also exist to indicate that CX3CL1-CX3CR1 signalling is important for the recruitment and retention of dendritic cells (DCs) and for their pro-fibrotic effects in human kidneys. For example, Kassianos et al. used flow cytometric analysis of leukocytes within human fibrotic and non-fibrotic kidneys to demonstrate that CD1c$^+$ DCs express CX3CR1 and are important producers of TGF-β within fibrotic kidneys. Immunohistochemical analyses of the same kidneys demonstrated upregulation of CX3CL1 on PTEC and co-localisation of CD1c$^+$ DCs with the CX3CL1-expressing tubular cells (67). In vitro analyses confirmed that PTEC-derived CX3CL1 is capable of mediating chemotaxis and adhesion of DCs. Overall, this study provides strong evidence that upregulation of CX3CL1 by PTEC is a mechanism by which pro-fibrogenic DCs are recruited and retained in the renal parenchyma in CKD.

Of potential relevance to these tissue-based observations, a number of groups have investigated the association between single nucleotide polymorphisms (SNPs) within the CX3CR1 gene and the presence of CKD or end stage kidney failure (ESKF). One such polymorphism is V249I. The frequency of the I allele and the II genotype were found to be increased in ESKF by two groups (68, 69). In contrast, Yadav et al. reported that the II genotype was more common in controls (70) without significantly different allelic frequency of the I allele. Variations in the frequency of T280M CX3CR1 polymorphisms have also been observed in CKD. Interestingly, these same polymorphisms may influence the risk of cancer (71) and of delayed graft function (72) after renal transplantation.

ATHEROSCLEROSIS IN CHRONIC KIDNEY DISEASE: CONTRIBUTION OF SYSTEMIC DYSREGULATION OF THE CX3CL1- CX3CR1 AXIS

It is well established that atherosclerosis is accelerated and cardiovascular morbidity and mortality increased among people with CKD (73, 74). One contributing factor to the burden of cardiovascular disease in CKD is a chronic micro-inflammatory state which may include systemic activation of the CX3CL1- CX3CR1 axis. Leucocyte recruitment into the blood vessel wall is required for the development of atherosclerotic plaques and CX3CL1-CX3CR1-mediated signalling has been shown to be an important mechanism in this process (75–77). This has prompted several groups to address the role of the CX3CL1-CX3CR1 axis in atherosclerosis acceleration in CKD.

In the first place, it has been reported that serum CX3CL1 concentrations are higher in people with CKD compared to age-matched controls (70, 78, 79) and correlate with eGFR (80). Additionally, serum CX3CL1 concentration been shown to be predictive of all-cause mortality and myocardial infarction in CKD cohorts (80, 81). Such observations have also been made in non-CKD populations (82, 83). Expression of CX3CR1 by circulating leukocytes may also be altered in CKD or ESKF. Blood monocytes were reported to have higher CX3CR1 expression in dialysis patients (84), although it is unclear from the data reported whether this was caused by upregulation of CX3CR1 expression by the whole monocyte population or by an increase in the proportion of $CX3CR1^{hi}$ intermediate and nonclassical monocytes. Increased CX3CR1 expression has been found in the arterial walls of people with CKD undergoing renal transplantation (80). The proportion of CX3CR1 expressing T-cells also increases in ESKF and CKD, largely due to an expansion of $CX3CR1^{hi}/CD4^{+}/CD28^{-}$ T-cells, the proportion of which is associated with intima-media thickness of the common carotid artery (79). Overall, these data favour a conclusion that CX3CL1-CX3CR1 signalling is increased in CKD. From a mechanistic perspective, one study indicated that *in vitro* exposure to the uremic toxin p-cresol (85), reduced trans-endothelial leukocyte migration and endothelial cell production of CX3CL1. However, high p-cresol concentrations were used in this study with potential implications for physiological relevance.

Importantly, animal and human data have also suggested a specific role for CX3CR1 expression by T-cells in CKD-associated acceleration of atherosclerosis (86). In a mouse model of CKD, atherosclerosis was attenuated in CX3CR1-deficient animals. Although macrophage infiltration of atherosclerotic lesions was reduced, reconstitution with $CX3CR1^{+}$ monocytes did not restore the deficit. Instead, the authors observed that CX3CR1 deficiency resulted in reduced T helper 17 (T_H17) cell polarization within atherosclerotic plaques and that this was necessary for the development of CKD-driven atherosclerosis. Adoptive transfer of $CX3CR1^{+}$ T-cells restored atherosclerosis progression in mice with renal impairment, suggesting a specific contribution of $CX3CR1^{+}$ T-cells to atherosclerosis in setting. This is in keeping with the study of Yadav et al. which an association between intima-medial thickening of the carotid artery and $CX3CR1^{+}/CD4^{+}$ T-cells in patients with CKD (79). Kim et al. examined upregulation of CX3CL1 by endothelial cells and the interactions between blood monocytes, endothelial cells and $CD4^{+}/CD28^{-}$ T-cells under ESKF-like *in vitro* conditions (87). Exposure of cultured endothelial cells to conditioned medium from monocytes treated with the uremic toxin indoxyl sulfate or directly to recombinant TNF-α resulted in upregulation of cell surface CX3CL1. In contrast, exposure to indoxyl sulphate itself did not increase endothelial CX3CL1. Treatment of $CD4^{+}$ T-cells with TNF–α increased the proportion of $CD4^{+}CD28^{-}CX3CR1^{+}$ T-cells – a subpopulation that is increased in ESKF – and co-culture of endothelial cells with $CD4^{+}CD28^{-}CX3CR1^{+}$ T-cells resulted in increased endothelial apoptosis. The authors propose that chronic uraemia leads to increased monocyte production of TNF-α which induces endothelial CX3CL1 expression and accumulation of $CD4^{+}$ $CD28^{-}$ $CX3CR1^{+}$ T-cells. This T-cell population may then bind to CX3CL1-expressing endothelial cells expressing CX3CL1 and compromise endothelial integrity (87).

Activation of the renin-angiotensin system and systemic angiotensinaemia may also contribute to CX3CL1-CX3CR1 dysregulation in CKD. Li et al. recently reported that mice with renal impairment have elevated expression of CX3CL1 and CX3CR1 in the aortic wall and that these levels were reduced by treatment with losartan. *In vitro* work using vascular smooth muscle (MOVAS) cells also showed that treatment with angiotensin increased CX3CR1 expression and that this was reduced by concomitant treatment with losartan. The induced CX3CR1 was functional, leading to increased migration of angiotensin-treated MOVAS cells compared to untreated cells and to cells treated with angiotensin + losartan (88).

PROGRESS TOWARD THERAPEUTIC MODULATION OF CX3CL1/CX3CR1 AXIS IN CKD

Modulation of fractalkine expression by existing medications or investigational medical products (IMP) has been reported and

may be a mechanism by which they contribute to renal protection in CKD. This was highlighted in the animal studies above regarding RAS blockade (42). Mesenchymal stromal cells (MSCs) and MSC-derived microcellular vesicles (MSC-MVs) are recently developed advanced medical therapies with ongoing clinical trials for multiple medical conditions, including chronic kidney disease (89). A pre-clinical study investigated the effect of human umbilical cord-derived MSC-MVs on renal inflammation and impairment in a rat renal IRI model. Rats treated with MSC-MVs following IRI were protected from renal fibrosis and renal functional impairment two weeks after injury. Macrophage infiltration of the renal tissue and CX3CL1 expression within the kidney were also reduced in the MSC-MV treated group. *In vitro*, endothelial cells subjected to hypoxia also demonstrated increased CX3CL1 expression, which was reduced by MSC-MV treatment. MSC-MVs were also found to contain six micro-RNAs matched to CX3CL1 mRNA. Although not conclusive, this study suggests that modulation of CX3CL1 expression may be a mechanism by which MSCs or MSC-MVs exert therapeutic effects (90). Studies of MSCs in animal models of other diseases, including myocarditis and amyotrophic lateral sclerosis have pointed to an increase in CX3CL1 in MSC treated animals, although with an overall beneficial effect of MSC treatment (91, 92). These discrepancies could be the result of tissue specific effects, particularly in the central nervous system where the pro-survival effects of CX3CL1 may be neuroprotective under certain circumstances (93). Another investigational medical product M4PTB, a histone de-acetylase inhibitor, has been shown to decrease CX3CL1 expression and fibrosis in a mouse model of ischemia renal IRI (94)

One of the first reports of a strategy to develop a therapeutic antagonist of CX3CR1 was made in 2009 by Dorgham et al. (95). A CX3CR1 antagonist was developed using PCR mutagenesis and phage selection. The resulting antagonist, termed 'F1', was capable of inhibiting CX3CL1-induced calcium signalling and chemotaxis of both a HEK293 cell line and primary human leukocytes. The antagonist also inhibited adhesion of $CX3CR1^+$ cell lines to CX3CL1 *in vitro*. Furthermore, the authors demonstrated that *in vivo* CX3CR1 antagonism with F1 led to reduced leukocyte recruitment in a mouse model of thioglycolate induced peritonitis. Neutralising antibodies are commonly used *in vitro* or *in vivo* to establish the pathogenic significance of a biological pathway and several experimental studies described in previous sections have utilized anti-CX3CR1 antibodies (35, 47, 48, 52). In the last two decades, monoclonal antibodies targeting pro-inflammatory chemokines or receptors have been a significant advance in treatment of numerous medical conditions, including malignancies and autoimmune disease. The potential for therapeutic targeting of the CX3CL1-CX3CR1 axis in inflammatory or fibrogenic diseases has been noted (96, 97). Toward this goal, the development of a variable domain of camelid, heavy chain only (VHH) antibody targeting CX3CR1 has recently been described in detail (98). A 30mg/kg dose of this "nanobody", named BI665088, which was developed by Ablynx™ in collaboration with Boehringer Ingelheim™ was shown to inhibit atherosclerosis development in mice with knock-in human CX3CR1 expression. A press release in 2016 reported planned initiation of a Phase I trial of an anti-CX3CR1 nanonbody in patients with CKD but further details have not been published to date (99). An anti-CX3CL1 monoclonal antibody has also been developed (100) and data from early stage clinical trials suggests possible benefit in patients with rheumatoid arthritis (101).

Small molecule inhibitors of CX3CR1 also have therapeutic potential. The pharmaceutical company, Astra Zeneca, reported the development of orally available small molecule inhibitors of CX3CR1. These were developed by systematically varying compounds capable of binding other chemokine receptors and selecting those with high CX3CR1 binding capacity (102). One of the identified proteins, named AZD8797, was shown by Cederblad et al. to function as a non-competitive allosteric modulator of CX3CR1, capable of preventing both CX3CL1-CX3CR1-mediated adhesion and downstream G-protein mediated signalling pathways (103). Animal studies indicated that AZD8797 may be effective in treating multiple sclerosis (104, 105). E6130, a pyrrolidin-3-ylacetic acid derivative with CX3CR1 modulating capacity was patented by Eisai Co. in 2013 and subsequently published data demonstrated that this compound downregulates CX3CR1 expression on NK cells and prevents CX3CL1-mediated chemotaxis (106). Moreover, this compound reduces the severity of a murine model of inflammatory bowel disease. A further small molecule inhibitor of CX3CR1, termed JMS 17-2 has been developed and used in animal studies regarding the potential for therapeutic targeting of this axis to prevent cancer metastasis (107). Most of the therapies developed to date, summarised in **Table 2**, focus on blockade of the CX3CR1 receptor, either through direct binding of the active site or through allosteric modulation. Targeting of the downstream signalling pathways, as illustrated in **Figure 1**, may also be of therapeutic value, albeit with less specificity.

CONCLUSIONS

More than 10% of the global population live with CKD (108). It is estimated that two million people worldwide have ESKF (109) and that more than one million deaths occur each year as a direct result of CKD (110). Despite this high burden, disease-modifying treatments for progressive CKD are lacking and new therapeutic strategies are needed. In this article we have highlighted a wealth of research from the past two decades that indicates a predominantly pathogenic role for the CX3CL1- CX3CR1 axis during both acute and chronic renal diseases. The CX3CL1-CX3CR1 axis is an attractive therapeutic target because it consists of a unique ligand/receptor pair which do not interact with other partners, limiting the potential for off-target effects. Multiple animal models have demonstrated that renal injury is associated with upregulation of CX3CL1 expression by multiple cell types

TABLE 2 | Pharmacological agents targeting the CX3CL1-CX3CR1 axis currently reported to be in development or clinical trials and disease of interest.

Product Name	Company/Institution	Class	Animal Models Reported	Human Trials In Progress/ Planned
F1	INSERM	Modified CX3CR1 Ligand	Periodontitis	N/A
BI665088	Boehringer-Ingelheim/ Ablynx	VHH Antibody to CX3CR1	Atherosclerosis	Chronic Kidney Disease
E6011	Eisai Co	Humanised monoclonal Antibody	Pharmacokinetics in cynomolgus monkeys reported	Rheumatoid Arthritis Inflammatory Bowel Disease
AZD8797	Astra Zeneca	Small molecule inhibitor	Spinal Cord Injury Multiple Sclerosis	N/A
E6130	Eisai Co	Small Molecule Inhibitor	Inflammatory Bowel Disease	N/A
JMS 17-2	Drexel University College of Medicine	Small Molecule Inhibitor	Breast Cancer Metastasis	N/A

IMP, Investigational Medical Product; N/A, Not applicable; VHH, Variable Domain of Camelid, Heavy Chain Only.

within the kidney. This pathway is of particular importance in the recruitment of innate immune cells into the kidney tissue and to their subsequent pro-inflammatory and pro-fibrotic activities as illustrated by the role of CX3CL1-CX3CR1 in macrophage accumulation in the kidney. Furthermore, although not universally reported, several studies have indicated that either genetic or pharmacological targeting of the CX3CL1-CX3CR1 pathway attenuated renal fibrosis after injury. *In vitro* experiments have also demonstrated that exposure of renal tubular epithelial cells to CKD-related

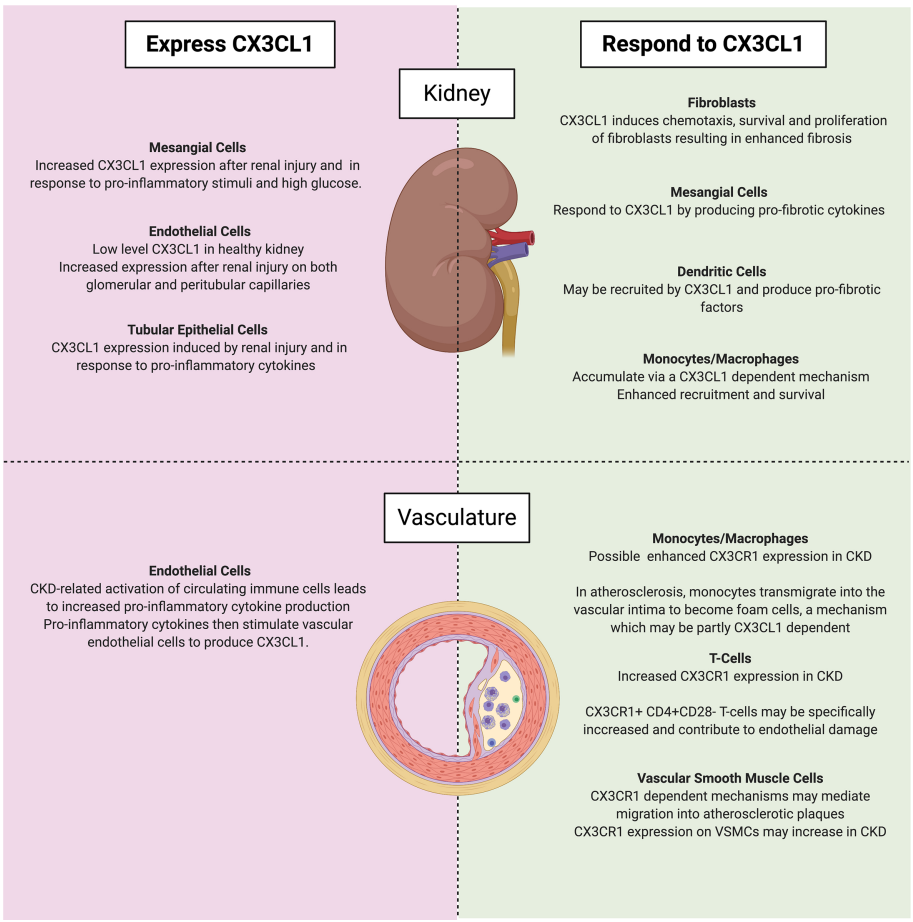


FIGURE 2 | Cell types which either express (left) or respond to (right) CX3CL1 in CKD within the kidney (top) and vasculature (bottom). Of note, mesangial cells may both express and respond to CX3CL1. Created with BioRender.com.

injurious stimuli such as high glucose, uremic toxins and pro-inflammatory cytokines may directly or indirectly induce increased CX3CL1 expression. In keeping with these observations, immunohistochemical studies of fibrotic human kidney specimens have demonstrated increased CX3CL1 expression and serial section analyses suggest an association between CX3CL1 expression and monocyte or T-cell recruitment. Interestingly, genetic polymorphisms in CX3CR1, may influence the risk of ESKF development, further suggesting a key role for this pathway in influencing progression of CKD in humans. Several studies suggest that dysregulation of the CX3CL1-CX3CR1 axis also occurs within the blood stream and vasculature of individuals with CKD and that this may contribute to the accelerated atherosclerosis typically seen in CKD. In **Figure 2**, we have summarised the cell types both within and outside of the kidney which produce or respond to CX3CL1. Finally, we have reviewed a number of recently developed small molecule inhibitors and monoclonal antibodies targeting the CX3CL1-CX3CR1 axis. We suggest that the time is ripe for further study of these agents in individuals with progressive fibrotic CKD.

AUTHOR CONTRIBUTIONS

SC wrote the first draft of the manuscript and revised subsequent drafts. MG reviewed and revised the manuscript. All authors contributed to the article and approved the submitted version.

FUNDING

SC was supported by the Irish Clinical Academic Training (ICAT) Programme, supported by the Wellcome Trust and the Health Research Board (Grant Number 203930/B/16/Z), the Health Service Executive National Doctors Training and Planning and the Health and Social Care, Research and Development Division, Northern Ireland. MG was supported by grants from the European Commission [Horizon 2020 Collaborative Health Project NEPHSTROM (grant number 634086) and FP7 Collaborative Health Project VISICORT (grant number 602470)] and from Science Foundation Ireland [CÚRAM Research Centre (grant number 13/RC/2073)] and by the European Regional Development Fund.

REFERENCES

1. Pan Y, Lloyd C, Zhou H, Dolich S, Deeds J, Gonzalo JA, et al. Neurotactin, a Membrane-Anchored Chemokine Upregulated in Brain Inflammation. *Nature* (1997) 387:611–7. doi: 10.1038/42491
2. Bazan JF, Bacon KB, Hardiman G, Wang W, Soo K, Rossi D, et al. A New Class of Membrane-Bound Chemokine With a CX3C Motif. *Nature* (1997) 385:640–4. doi: 10.1038/385640a0
3. Hortsch M. Duplications in Nomenclature. *Nature* (1997) 389:539–9. doi: 10.1038/39172
4. Pan Y, Lloyd C, Zhou H, Dolich S, Deeds J, Gonzalo JA, et al. Erratum: Neurotactin, a Membrane-Anchored Chemokine Upregulated in Brain Inflammation. *Nature* (1997) 389:100–0. doi: 10.1038/38048
5. Imai T, Hieshima K, Haskell C, Baba M, Nagira M, Nishimura M, et al. Identification and Molecular Characterization of Fractalkine Receptor CX3CR1, Which Mediates Both Leukocyte Migration and Adhesion. *Cell* (1997) 91:521–30. doi: 10.1016/S0092-8674(00)80438-9
6. Raport CJ, Schweickart VL, Eddy RL, Shows TB, Gray PW. The Orphan G-Protein-Coupled Receptor-Encoding Gene V28 Is Closely Related to Genes for Chemokine Receptors and Is Expressed in Lymphoid and Neural Tissues. *Gene* (1995) 163:295–9. doi: 10.1016/0378-1119(95)00336-5
7. Combadiere C, Salzwedel K, Smith ED, Tiffany HL, Berger EA, Murphy PM. Identification of CX3CR1. A Chemotactic Receptor for the Human CX3C Chemokine Fractalkine and a Fusion Coreceptor for HIV-1. *J Biol Chem* (1998) 273:23799–804. doi: 10.1074/jbc.273.37.23799
8. Al-Aoukaty A, Rolstad B, Giaid A, Maghazachi AA. MIP-3alpha, MIP-3beta and Fractalkine Induce the Locomotion and the Mobilization of Intracellular Calcium, and Activate the Heterotrimeric G Proteins in Human Natural Killer Cells. *Immunology* (1998) 95:618–24. doi: 10.1046/j.1365-2567.1998.00603.x
9. Fong AM, Robinson LA, Steeber DA, Tedder TF, Yoshie O, Imai T, et al. Fractalkine and CX3CR1 Mediate a Novel Mechanism of Leukocyte Capture, Firm Adhesion, and Activation Under Physiologic Flow. *J Exp Med* (1998) 188:1413–9. doi: 10.1084/jem.188.8.1413
10. Goda S, Imai T, Yoshie O, Yoneda O, Inoue H, Nagano Y, et al. CX3C-Chemokine, Fractalkine-Enhanced Adhesion of THP-1 Cells to Endothelial Cells Through Integrin-Dependent and -Independent Mechanisms. *J Immunol* (2000) 164:4313–20. doi: 10.4049/jimmunol.164.8.4313
11. Harrison JK, Jiang Y, Wees EA, Salafranca MN, Liang HX, Feng L. Belardinelli Inflammatory Agents Regulate In Vivo Expression of Fractalkine in Endothelial Cells of the Rat Heart. *J Leukoc Biol* (1999) 66:937–44. doi: 10.1002/jlb.66.6.937
12. Garcia GE, Xia Y, Chen S, Wang Y, Ye RD, Harrison JK, et al. NF-κB-Dependent Fractalkine Induction in Rat Aortic Endothelial Cells Stimulated by IL-1β, TNF-α, and LPS. *J Leukoc Biol* (2000) 67:577–84. doi: 10.1002/jlb.67.4.577
13. Chen Y-M, Lin S-L, Chen C-W, Chiang W-C, Tsai T-J, Hsieh B-S. Tumor Necrosis Factor-α Stimulates Fractalkine Production by Mesangial Cells and Regulates Monocyte Transmigration: Down-Regulation by Camp. *Kidney Int* (2003) 63:474–86. doi: 10.1046/j.1523-1755.2003.00766.x
14. Auffray C, Fogg D, Garfa M, Elain G, Join-Lambert O, Kayal S, et al. Monitoring of Blood Vessels and Tissues by a Population of Monocytes With Patrolling Behavior. *Science* (2007) 317:666. doi: 10.1126/science.1142883
15. Cros J, Cagnard N, Woollard K, Patey N, Zhang SY, Senechal B. Human CD14dim Monocytes Patrol and Sense Nucleic Acids and Viruses Via TLR7 and TLR8 Receptors. *Immunity* (2010) 33:375–86. doi: 10.1016/j.immuni.2010.08.012
16. White GE, Greaves DR. Fractalkine: A Survivor's Guide: Chemokines as Antiapoptotic Mediators. *Arterioscler Thromb Vasc Biol* (2012) 32:589–94. doi: 10.1161/ATVBAHA.111.237412
17. Łyszkiewicz M, Witzlau K, Pommerencke J, Krueger A. Chemokine Receptor CX3CR1 Promotes Dendritic Cell Development Under Steady-State Conditions. *Eur J Immunol* (2011) 41:1256–65. doi: 10.1002/eji.201040977
18. Landsman L, Bar-On L, Zernecke A, Krauthgamer R, Shagdarsuren E, Lira SA, et al. CX3CR1 Is Required for Monocyte Homeostasis and Atherogenesis by Promoting Cell Survival. *Blood* (2009) 113:963–72. doi: 10.1182/blood-2008-07-170787
19. Collar AL, Swamydas M, O'Hayre M, Sajib MS, Hoffman KW, Singh SP, et al. The Homozygous CX3CR1-M280 Mutation Impairs Human Monocyte Survival. *JCI Insight* (2018) 3:e95417. doi: 10.1172/jci.insight.95417
20. McDermott DH, Fong AM, Yang Q, Sechler JM, Cupples LA, Merrell MN, et al. Chemokine Receptor Mutant CX3CR1-M280 has Impaired Adhesive Function and Correlates With Protection From Cardiovascular Disease in Humans. *J Clin Invest* (2003) 111:1241–50. doi: 10.1172/JCI16790
21. Lionakis MS, Swamydas M, Fischer BG, Plantinga TS, Johnson MD, Jaeger M, et al. CX3CR1-Dependent Renal Macrophage Survival Promotes Candida Control and Host Survival. *J Clin Invest* (2013) 123:5035–51. doi: 10.1172/JCI71307

22. Mionnet C, Buatois V, Kanda A, Milcent V, Fleury S, Lair D, et al. CX3CR1 is Required for Airway Inflammation by Promoting T Helper Cell Survival and Maintenance in Inflamed Lung. *Nat Med* (2010) 16:1305–12. doi: 10.1038/nm.2253
23. White GE, Tan TCC, John AE, Whatling C, McPheat WL, Greaves DR. Fractalkine Has Anti-Apoptotic and Proliferative Effects on Human Vascular Smooth Muscle Cells Via Epidermal Growth Factor Receptor Signalling. *Cardiovasc Res* (2010) 85:825–35. doi: 10.1093/cvr/cvp341
24. Arnoux I, Audinat E. Fractalkine Signaling and Microglia Functions in the Developing Brain. *Neural Plast* (2015) 2015:689404. doi: 10.1155/2015/689404
25. Luo P, S-f C, Zhang Z, Xia C-y, Chen N-h. Fractalkine/CX3CR1 is Involved in the Cross-Talk Between Neuron and Glia in Neurological Diseases. *Brain Res Bull* (2019) 146:12–21. doi: 10.1016/j.brainresbull.2018.11.017
26. Liu Y, Reynolds LM, Ding J, Hou L, Lohman K, Young T, et al. Blood Monocyte Transcriptome and Epigenome Analyses Reveal Loci Associated With Human Atherosclerosis. *Nat Commun* (2017) 8:393. doi: 10.1038/s41467-017-00517-4
27. Gröne HJ, Cohen CD, Gröne E, Schmidt C, Kretzler M, Schlöndorff D, et al. Spatial and Temporally Restricted Expression of Chemokines and Chemokine Receptors in the Developing Human Kidney. *J Am Soc Nephrol* (2002) 13:957–67. doi: 10.1681/ASN.V134957
28. Becker F, Holthoff C, Anthoni C, Rijcken E, Alexander JS, Gavins FN, et al. Downregulation of CX3CR1 Ameliorates Experimental Colitis: Evidence for CX3CL1-CX3CR1-Mediated Immune Cell Recruitment. *Int J Colorectal Dis* (2017) 32:315–24. doi: 10.1007/s00384-016-2735-y
29. Harrison JK, Jiang Y, Chen S, Xia Y, Maciejewski D, McNamara RK, et al. Role for Neuronally Derived Fractalkine in Mediating Interactions Between Neurons and CX3CR1-Expressing Microglia. *Proc Natl Acad Sci USA* (1998) 95:10896–901. doi: 10.1073/pnas.95.18.10896
30. Poniatowski ŁA, Wojdasiewicz P, Krawczyk M, Szukiewicz D, Gasik R, Kubaszewski Ł, et al. Analysis of the Role of CX3CL1 (Fractalkine) and Its Receptor CX3CR1 in Traumatic Brain and Spinal Cord Injury: Insight Into Recent Advances in Actions of Neurochemokine Agents. *Mol Neurobiol* (2017) 54:2167–88. doi: 10.1007/s12035-016-9787-4
31. Hou S-M, Hou C-H, Liu J-F. CX3CL1 Promotes MMP-3 Production Via the CX3CR1, c-Raf, MEK, ERK, and NF-κB Signaling Pathway in Osteoarthritis Synovial Fibroblasts. *Arthritis Res Ther* (2017) 19:282. doi: 10.1186/s13075-017-1487-6
32. Lauro C, Catalano M, Di Paolo E, Chece G, de Costanzo I, Trettel F, et al. Fractalkine/CX3CL1 Engages Different Neuroprotective Responses Upon Selective Glutamate Receptor Overactivation. *Front Cell Neurosci* (2015) 8:472. doi: 10.3389/fncel.2014.00472
33. Huang LY, Chen P, Xu LX, Zhou YF, Zhang YP, Yuan YZ. Fractalkine Upregulates Inflammation Through CX3CR1 and the Jak-Stat Pathway in Severe Acute Pancreatitis Rat Model. *Inflammation* (2012) 35:1023–30. doi: 10.1007/s10753-011-9406-5
34. Chen S, Bacon KB, Li L, Garcia GE, Xia Y, Lo D, et al. In Vivo Inhibition of CC and CX3C Chemokine–Induced Leukocyte Infiltration and Attenuation of Glomerulonephritis in Wistar-Kyoto (WKY) Rats by vMIP-II. *J Exp Med* (1998) 188:193–8. doi: 10.1084/jem.188.1.193
35. Feng L, Chen S, Garcia GE, Xia Y, Siani MA, Botti P, et al. Prevention of Crescentic Glomerulonephritis by Immunoneutralization of the Fractalkine Receptor CX3CR1: Rapid Communication. *Kidney Int* (1999) 56:612–20. doi: 10.1046/j.1523-1755.1999.00604.x
36. Furuichi K, Wada T, Iwata Y, Sakai N, Yoshimoto K, Shimizu M, et al. Upregulation of Fractalkine in Human Crescentic Glomerulonephritis. *Nephron* (2001) 87:314–20. doi: 10.1159/000045936
37. Rovin BH. Chemokine Blockade as a Therapy for Renal Disease. *Curr Opin Nephrol Hypertens* (2000) 9:225–32. doi: 10.1097/00041552-200005000-00004
38. Holdsworth SR, Kitching AR, Tipping PG. Chemokines as Therapeutic Targets in Renal Disease. *Curr Opin Nephrol Hypertens* (2000) 9:505–11. doi: 10.1097/00041552-200009000-00008
39. Cockwell P, Chakravorty SJ, Girdlestone J, Savage COS. Fractalkine Expression in Human Renal Inflammation. *J Pathol* (2002) 196:85–90. doi: 10.1002/path.1010
40. Chakravorty SJ, Cockwell P, Girdlestone J, Brooks CJ, Savage COS. Fractalkine Expression on Human Renal Tubular Epithelial Cells: Potential Role in Mononuclear Cell Adhesion. *Clin Exp Immunol* (2002) 129:150–9. doi: 10.1046/j.1365-2249.2002.01906.x
41. Segerer S, Hughes E, Hudkins KL, Mack M, Goodpaster T, Alpers CE. Expression of the Fractalkine Receptor (CX3CR1) in Human Kidney Diseases. *Kidney Int* (2002) 62:488–95. doi: 10.1046/j.1523-1755.2002.00480.x
42. Kikuchi Y, Ikee R, Hemmi N, Hyodo N, Saigusa T, Namikoshi T, et al. Fractalkine and Its Receptor, CX3CR1, Upregulation in Streptozotocin-Induced Diabetic Kidneys. *Nephron Exp Nephrol* (2004) 97:e17–25. doi: 10.1159/000077594
43. Kikuchi Y, Imakiire T, Hyodo T, Kushiyama T, Higashi K, Hyodo N, et al. Advanced Glycation End-Product Induces Fractalkine Gene Upregulation in Normal Rat Glomeruli. *Nephrol Dialysis Transplant* (2005) 20:2690–6. doi: 10.1093/ndt/gfi232
44. Song KH, Park J, Park JH, Natarajan R, Ha H. Fractalkine and its Receptor Mediate Extracellular Matrix Accumulation in Diabetic Nephropathy in Mice. *Diabetologia* (2013) 56:1661–9. doi: 10.1007/s00125-013-2907-z
45. Ito Y, Kawachi H, Morioka Y, Nakatsue T, Koike H, Ikezumi Y, et al. Fractalkine Expression and the Recruitment of $CX3CR1^+$ Cells in the Prolonged Mesangial Proliferative Glomerulonephritis. *Kidney Int* (2002) 61:2044–57. doi: 10.1046/j.1523-1755.2002.00369.x
46. Park J, Song KH, Ha H. Lipopolysaccharide Increases Monocyte Binding to Mesangial Cells Through Fractalkine and Its Receptor. *Transplant Proc* (2012) 44:1029–31. doi: 10.1016/j.transproceed.2012.03.046
47. Furuichi K, Gao J-L, Murphy PM. Chemokine Receptor CX3CR1 Regulates Renal Interstitial Fibrosis After Ischemia-Reperfusion Injury. *Am J Pathol* (2006) 169:372–87. doi: 10.2353/ajpath.2006.060043
48. Oh D-J, Dursun B, He Z, Lu L, Hoke TS, Ljubanovic D, et al. Fractalkine Receptor (CX3CR1) Inhibition is Protective Against Ischemic Acute Renal Failure in Mice. *Am J Physiol Renal Physiol* (2008) 294:F264–71. doi: 10.1152/ajprenal.00204.2007
49. Li L, Huang L, Sung S-SJ, Vergis AL, Rosin DL, Rose CE Jr, et al. The Chemokine Receptors CCR2 and CX3CR1 Mediate Monocyte/Macrophage Trafficking in Kidney Ischemia–Reperfusion Injury. *Kidney Int* (2008) 74:1526–37. doi: 10.1038/ki.2008.500
50. Kruse JJCM, Bomhoff-Wijdenes IFM, Poele JAMT, Stewart FA. Fractalkine: An Important Candidate for Directing Periglomerular Leukocyte Accumulation in Irradiated Mouse Kidneys. *Acta Oncol* (2007) 46:945–50. doi: 10.1080/02841860701218618
51. Shimizu K, Furuichi K, Sakai N, Kitagawa K, Matsushima K, Mukaida N, et al. Fractalkine and its Receptor, CX3CR1, Promote Hypertensive Interstitial Fibrosis in the Kidney. *Hypertens Res* (2011) 34:747–52. doi: 10.1038/hr.2011.23
52. Lu LH, Oh DJ, Dursun B, He Z, Hoke TS, Faubel S, et al. Increased Macrophage Infiltration and Fractalkine Expression in Cisplatin-Induced Acute Renal Failure in Mice. *J Pharmacol Exp Ther* (2008) 324:111–7. doi: 10.1124/jpet.107.130161
53. Silva MC, Azevedo MA, Figueiredo VP, Moura Junior MR, Coelho Junior D, Martinelli PM, et al. Renovascular Hypertension Increases Serum TNF and CX3CL1 in Experimental Trypanosoma Cruzi Infection. *Braz J Med Biol Res* (2018) 51(5):e6690. . doi: 10.1590/1414-431x20186690
54. Yu YW, Li MX, Zhang ZY, Yu H. The Deficiency of CX3CL1/CX3CR1 System Ameliorates High Fructose Diet-Induced Kidney Injury by Regulating NF-κB Pathways in CX3CR1-knock Out Mice. *Int J Mol Med* (2018) 41:3577–85. doi: 10.3892/ijmm.2018.3573
55. Peng X, Zhang J, Xiao Z, Dong Y, Du J. CX3CL1–CX3CR1 Interaction Increases the Population of $Ly6C^-CX3CR1^{hi}$ Macrophages Contributing to Unilateral Ureteral Obstruction–Induced Fibrosis. *J Immunol* (2015) 195:2797. doi: 10.4049/jimmunol.1403209
56. Kuboi Y, Nishimura M, Ikeda W, Nakatani T, Seki Y, Yamaura Y, et al. Blockade of the Fractalkine–CX3CR1 Axis Ameliorates Experimental Colitis by Dislodging Venous Crawling Monocytes. *Int Immunol* (2019) 31:287–302. doi: 10.1093/intimm/dxz006
57. Koziolek MJ, Müller G-A, Zapf A, Patschan D, Schmid H, Cohen CD, et al. Role of CX3C-Chemokine CX3C-L/fractalkine Expression in a Model of

Slowly Progressive Renal Failure. *Nephrol Dialysis Transplant* (2010) 25:684–98. doi: 10.1093/ndt/gfp602
58. Engel DR, Krause TA, Snelgrove SL, Thiebes S, Hickey MJ, Boor P, et al. CX3CR1 Reduces Kidney Fibrosis by Inhibiting Local Proliferation of Profibrotic Macrophages. *J Immunol* (2015) 194:1628. doi: 10.4049/jimmunol.1402149
59. Chousterman BG, Boissonnas A, Poupel L, Baudesson de Chanville C, Tabibzadeh N, Licata F, et al. Ly6Chigh Monocytes Protect Against Kidney Damage During Sepsis Via a CX3CR1-Dependent Adhesion Mechanism. *J Am Soc Nephrol* (2016) 27:792–803. doi: 10.1681/ASN.2015010009
60. Koziolek MJ, Schmid H, Cohen CD, Blaschke S, Hemmerlein B, Zapf A, et al. Potential Role of Fractalkine Receptor Expression in Human Renal Fibrogenesis. *Kidney Int* (2007) 72:599–607. doi: 10.1038/sj.ki.5002368
61. Wang Y, Wei Q, Liu Q, Li Z, Zhou L, Zou F, et al. Crosstalk Between Monocytes and Renal Mesangial Cells Via Interaction of Metalloproteinases and Fractalkine in Diabetic Nephropathy. *Mol Med Rep* (2013) 8:1817–23. doi: 10.3892/mmr.2013.1703
62. Yoshimoto S, Nakatani K, Iwano M, Asai O, Samejima K, Sakan H, et al. Elevated Levels of Fractalkine Expression and Accumulation of CD16+ Monocytes in Glomeruli of Active Lupus Nephritis. *Am J Kidney Dis* (2007) 50:47–58. doi: 10.1053/j.ajkd.2007.04.012
63. Ziegler-Heitbrock L, Ancuta P, Crowe S, Dalod M, Grau V, Hart DN, et al. Nomenclature of Monocytes and Dendritic Cells in Blood. *Blood* (2010) 116: e74–80. doi: 10.1182/blood-2010-02-258558
64. Naicker SD, Cormican S, Griffin TP, Maretto S, Martin WP, Ferguson JP, et al. Chronic Kidney Disease Severity Is Associated With Selective Expansion of a Distinctive Intermediate Monocyte Subpopulation. *Front Immunol* (2018) 9:2845. doi: 10.3389/fimmu.2018.02845
65. Wong KL, Yeap WH, Tai JJY, Ong SM, Dang TM, Wong SC. The Three Human Monocyte Subsets: Implications for Health and Disease. *Immunol Res* (2012) 53:41–57. doi: 10.1007/s12026-012-8297-3
66. Leone DA, Kozakowski N, Kornauth C, Waidacher T, Neudert B, Loeffler AG, et al. The Phenotypic Characterization of the Human Renal Mononuclear Phagocytes Reveal a Co-Ordinated Response to Injury. *PloS One* (2016) 11:e0151674. doi: 10.1371/journal.pone.0151674
67. Kassianos AJ, Wang X, Sampangi S, Afrin S, Wilkinson R, Healy H. Fractalkine–CX3CR1-Dependent Recruitment and Retention of Human CD1c+ Myeloid Dendritic Cells by In Vitro–Activated Proximal Tubular Epithelial Cells. *Kidney Int* (2015) 87:1153–63. doi: 10.1038/ki.2014.407
68. Bagci B, Bagci G, Huzmeli C, Sezgin I, Ozdemir O. Associations of Fractalkine Receptor (CX3CR1) and CCR5 Gene Variants With Hypertension, Diabetes and Atherosclerosis in Chronic Renal Failure Patients Undergoing Hemodialysis. *Int Urol Nephrol* (2016) 48:1163–70. doi: 10.1007/s11255-016-1293-0
69. Borkar M, Tripathi G, Sharma RK, Sankhwar SN, Agrawal S. Chemokine (CCR) and Fractalkine (CX3CR) Receptors and End Stage Renal Disease. *Inflamm Res* (2011) 60:399–407. doi: 10.1007/s00011-010-0284-3
70. Yadav AK, Kumar V, Jha V. Association of Chemokine Receptor CX3CR1 V249I and T280M Polymorphisms With Chronic Kidney Disease. *Indian J Nephrol* (2016) 26:275–9. doi: 10.4103/0971-4065.163426
71. Courivaud C, Bamoulid J, Loupy A, Deschamps M, Ferrand C, Simula-Faivre D, et al. Influence of Fractalkine Receptor Gene Polymorphisms V249I-T280M on Cancer Occurrence After Renal Transplantation. *Transplantation* (2013) 95:728–32. doi: 10.1097/TP.0b013e31827d61cb
72. Dabrowska-Zamojcin E, Dziedziejko V, Safranow K, Kurzawski M, Domanski L, Pawlik A. Association Between the CX3CR1 Gene V249I Polymorphism and Delayed Kidney Allograft Function. *Transplant Immunol* (2015) 32:172–4. doi: 10.1016/j.trim.2015.04.002
73. Foley RN, Parfrey PS, Sarnak MJ. Clinical Epidemiology of Cardiovascular Disease in Chronic Renal Disease. *Am J Kidney Dis* (1998) 32:S112–9. doi: 10.1053/ajkd.1998.v32.pm9820470
74. Manjunath G, Tighiouart H, Ibrahim H, Macleod B, Salem DN, Griffith JL, et al. Level of Kidney Function as a Risk Factor for Atherosclerotic Cardiovascular Outcomes in the Community. *J Am Coll Cardiol* (2003) 41:47–55. doi: 10.1016/S0735-1097(02)02663-3
75. Tacke F, Alvarez D, Kaplan TJ, Jakubzick C, Spranbroek R, Llodra J, et al. Monocyte Subsets Differentially Employ CCR2, CCR5, and CX3CR1 to Accumulate Within Atherosclerotic Plaques. *J Clin Invest* (2007) 117:185–94. doi: 10.1172/JCI28549
76. Lesnik P, Haskell CA, Charo IF. Decreased Atherosclerosis in CX3CR1–/– Mice Reveals a Role for Fractalkine in Atherogenesis. *J Clin Invest* (2003) 111:333–40. doi: 10.1172/JCI15555
77. Combadière C, Potteaux S, Rodero M, Simon T, Pezard A, Esposito B, et al. Combined Inhibition of CCL2, CX3CR1, and CCR5 Abrogates Ly6Chi and Ly6Clo Monocytosis and Almost Abolishes Atherosclerosis in Hypercholesterolemic Mice. *Circulation* (2008) 117:1649–57. doi: 10.1161/CIRCULATIONAHA.107.745091
78. Wallquist C, Paulson JM, Hylander B, Lundahl J, Jacobson SH. Increased Accumulation of CD16+ Monocytes at Local Sites of Inflammation in Patients With Chronic Kidney Disease. *Scand J Immunol* (2013) 78:538–44. doi: 10.1111/sji.12115
79. Yadav AK, Lal A, Jha V. Association of Circulating Fractalkine (CX3CL1) and CX3CR1+CD4+ T Cells With Common Carotid Artery Intima-Media Thickness in Patients With Chronic Kidney Disease. *J Atheroscl Thromb* (2011) 18:958–65. doi: 10.5551/jat.8722
80. Claro LM, Moreno-Amaral AN, Gadotti AC, Dolenga JC, Nakao LS, Azevedo MLV, et al. The Impact of Uremic Toxicity Induced Inflammatory Response on the Cardiovascular Burden in Chronic Kidney Disease. *Toxins (Basel)* (2018) 10:384. doi: 10.3390/toxins10100384
81. Shah R, Matthews GJ, Shah RY, McLaughlin C, Chen J, Wolman M, et al. Serum Fractalkine (CX3CL1) and Cardiovascular Outcomes and Diabetes: Findings From the Chronic Renal Insufficiency Cohort (CRIC) Study. *Am J Kidney Dis* (2015) 66:266–73. doi: 10.1053/j.ajkd.2015.01.021
82. Guo Y, Apostalakis S, Blann AD, Lip GYH. Plasma CX3CL1 Levels and Long Term Outcomes of Patients With Atrial Fibrillation: The West Birmingham Atrial Fibrillation Project. *Cerebrovasc Dis* (2014) 38:204–11. doi: 10.1159/000365841
83. Ji CL, Nomi A, Li B, Shen C, Song BC, Zhang JG. Increased Plasma Soluble Fractalkine in Patients With Chronic Heart Failure and its Clinical Significance. *Int Heart J* (2019) 60:701–7. doi: 10.1536/ihj.18-422
84. Schepers E, Houthuys E, Dhondt A, De Meyer G, Neirynck N, Bernaert P, et al. Transcriptome Analysis in Patients With Chronic Kidney Disease on Hemodialysis Disclosing a Key Role for CD16+CX3CR1+ Monocytes. *PloS One* (2015) 10(4):e0121750. doi: 10.1371/journal.pone.0121750
85. Faure V, Cerini C, Paul P, Berland Y, Dignat-George F, Brunet P. The Uremic Solute P-Cresol Decreases Leukocyte Transendothelial Migration In Vitro. *Int Immunol* (2006) 18:1453–9. doi: 10.1093/intimm/dxl077
86. Dong L, Nordlohne J, Ge S, Hertel B, Melk A, Rong S, et al. T Cell CX3CR1 Mediates Excess Atherosclerotic Inflammation in Renal Impairment. *J Am Soc Nephrol* (2016) 27:1753. doi: 10.1681/ASN.2015050540
87. Kim HY, Yoo TH, Hwang Y, Lee GH, Kim B, Jang J, et al. Indoxyl Sulfate (IS)-Mediated Immune Dysfunction Provokes Endothelial Damage in Patients With End-Stage Renal Disease (ESRD). *Sci Rep* (2017) 7:3057. doi: 10.1038/s41598-017-03130-z
88. Li C, Zhong X, Xia W, He J, Gan H, Zhao HF, et al. The CX3CL1/CX3CR1 Axis is Upregulated in Chronic Kidney Disease and Contributes to Angiotensin II-Induced Migration of Vascular Smooth Muscle Cells. *Microvasc Res* (2020) 132:104037. doi: 10.1016/j.mvr.2020.104037
89. Griffin TP, Martin WP, Islam N, O'Brien T, Griffin MD. The Promise of Mesenchymal Stem Cell Therapy for Diabetic Kidney Disease. *Curr Diabetes Rep* (2016) 16:42. doi: 10.1007/s11892-016-0734-6
90. Zou X, Zhang G, Cheng Z, Yin D, Du T, Ju G, et al. Microvesicles Derived From Human Wharton's Jelly Mesenchymal Stromal Cells Ameliorate Renal Ischemia-Reperfusion Injury in Rats by Suppressing CX3CL1. *Stem Cell Res Ther* (2014) 5(2):40. doi: 10.1186/scrt428
91. Sun H, Bénardais K, Stanslowsky N, Thau-Habermann N, Hensel N, Huang D, et al. Therapeutic Potential of Mesenchymal Stromal Cells and MSC Conditioned Medium in Amyotrophic Lateral Sclerosis (ALS) - In Vitro Evidence From Primary Motor Neuron Cultures, NSC-34 Cells, Astrocytes and Microglia. *PloS One* (2013) 8(9):72926. doi: 10.1371/journal.pone.0072926
92. Miteva K, Pappritz K, El-Shafeey M, Dong F, Ringe J, Tschöpe C, et al. Mesenchymal Stromal Cells Modulate Monocytes Trafficking in Coxsackievirus B3-Induced Myocarditis. *Stem Cells Trans Med* (2017) 6:1249–61. doi: 10.1002/sctm.16-0353

93. Lauro C, Catalano M, Trettel F, Limatola C. Fractalkine in the Nervous System: Neuroprotective or Neurotoxic Molecule? *Ann N Y Acad Sci* (2015) 1351:141–8. doi: 10.1111/nyas.12805
94. Novitskaya T, McDermott L, Zhang KX, Chiba T, Paueksakon P, Hukriede NA, et al. A PTBA Small Molecule Enhances Recovery and Reduces Postinjury Fibrosis After Aristolochic Acid-Induced Kidney Injury. *Am J Physiol Renal Physiol* (2014) 306:F496–504. doi: 10.1152/ajprenal.00534.2013
95. Dorgham K, Ghadiri A, Hermand P, Rodero M, Poupel L, Iga M, et al. An Engineered CX3CR1 Antagonist Endowed With Anti-Inflammatory Activity. *J Leukoc Biol* (2009) 86:903–11. doi: 10.1189/jlb.0308158
96. D'Haese JG, Friess H, Ceyhan GO. Therapeutic Potential of the Chemokine-Receptor Duo Fractalkine/CX3CR1: An Update. *Expert Opin Ther Targets* (2012) 16:613–8. doi: 10.1517/14728222.2012.682574
97. Muraoka S, Nishio J, Kuboi Y, Imai T, Nanki T. Rationale for and Clinical Development of Anti-Fractalkine Antibody in Rheumatic Diseases. *Expert Opin Biol Ther* (2020) (11):1309–19. doi: 10.1080/14712598.2020.1764931
98. Low S, Wu H, Jerath K, Tibolla A, Fogal B, Conrad R, et al. VHH Antibody Targeting the Chemokine Receptor CX3CR1 Inhibits Progression of Atherosclerosis. *mAbs* (2020) 12:1709322. doi: 10.1080/19420862.2019.1709322
99. Ablynx. *Ablynx TO Receive an Eu8 Million Milestone as Boehringer Ingelheim Starts a Phase I Study with an Anti-CX3CR1 Nanobody*. Ablynx (2016). Available at: globalnewswire.com (Accessed May 24, 2021)
100. Tabuchi H, Katsurabara T, Mori M, Aoyama M, Obara T, Yasuda N, et al. Pharmacokinetics, Pharmacodynamics, and Safety of E6011, a Novel Humanized Antifractalkine (CX3CL1) Monoclonal Antibody: A Randomized, Double-Blind, Placebo-Controlled Single-Ascending-Dose Study. *J Clin Pharmacol* (2019) 59:688–701. doi: 10.1002/jcph.1361
101. Tanaka Y, Takeuchi T, Umehara H, Nanki T, Yasuda N, Tago F, et al. Safety, Pharmacokinetics, and Efficacy of E6011, an Antifractalkine Monoclonal Antibody, in a First-in-Patient Phase 1/2 Study on Rheumatoid Arthritis. *Mod Rheumatol* (2018) 28:58–65. doi: 10.1080/14397595.2017.1337056
102. Karlström S, Nordvall G, Sohn D, Hettman A, Turek D, Åhlin K, et al. Substituted 7-Amino-5-thio-thiazolo[4,5-d]pyrimidines as Potent and Selective Antagonists of the Fractalkine Receptor (CX3CR1). *J Med Chem* (2013) 56:3177–90. doi: 10.1021/jm3012273
103. Cederblad L, Rosengren B, Ryberg E, Hermansson N-O. AZD8797 Is an Allosteric Non-Competitive Modulator of the Human CX3CR1 Receptor. *Biochem J* (2016) 473:641–9. doi: 10.1042/BJ20150520
104. Ridderstad Wollberg A, Ericsson-Dahlstrand A, Juréus A, Ekerot P, Simon S, Nilsson M, et al. Pharmacological Inhibition of the Chemokine Receptor CX3CR1 Attenuates Disease in a Chronic-Relapsing Rat Model for Multiple Sclerosis. *Proc Natl Acad Sci* (2014) 111:5409. doi: 10.1073/pnas.1316510111
105. Chen G, Zhou Z, Sha W, Wang L, Yan F, Yang X, et al. A Novel CX3CR1 Inhibitor AZD8797 Facilitates Early Recovery of Rat Acute Spinal Cord Injury by Inhibiting Inflammation and Apoptosis. *Int J Mol Med* (2020) 45:1373–84. doi: 10.3892/ijmm.2020.4509
106. Wakita H, Yanagawa T, Kuboi Y, Imai T. E6130, A Novel CX3C Chemokine Receptor 1 (CX3CR1) Modulator, Attenuates Mucosal Inflammation and Reduces CX3CR1(+) Leukocyte Trafficking in Mice With Colitis. *Mol Pharmacol* (2017) 92:502–9. doi: 10.1124/mol.117.108381
107. Shen F, Zhang Y, Jernigan DL, Feng X, Yan J, Garcia FU, et al. Novel Small-Molecule CX3CR1 Antagonist Impairs Metastatic Seeding and Colonization of Breast Cancer Cells. *Mol Cancer Res* (2016) 14:518. doi: 10.1158/1541-7786.MCR-16-0013
108. Hill NR, Fatoba ST, Oke JL, Hirst JA, O'Callaghan CA, Lasserson DS, et al. Global Prevalence of Chronic Kidney Disease - A Systematic Review and Meta-Analysis. *PloS One* (2016) 11(7):e0158765. doi: 10.1371/journal.pone.0158765
109. Couser WG, Remuzzi G, Mendis S, Tonelli M. The Contribution of Chronic Kidney Disease to the Global Burden of Major Noncommunicable Diseases. *Kidney Int* (2011) 80:1258–70. doi: 10.1038/ki.2011.368
110. GBD Chronic Kidney Disease Collaboration. Global, Regional, and National Burden of Chronic Kidney Disease, 1990–2017: A Systematic Analysis for the Global Burden of Disease Study 2017. *Lancet* (2020) 395:709–33. doi: 10.1016/S0140-6736(20)30045-3

Conflict of Interest: The authors declare that the research was conducted in the absence of any commercial or financial relationships that could be construed as a potential conflict of interest.

Copyright © 2021 Cormican and Griffin. This is an open-access article distributed under the terms of the Creative Commons Attribution License (CC BY). The use, distribution or reproduction in other forums is permitted, provided the original author(s) and the copyright owner(s) are credited and that the original publication in this journal is cited, in accordance with accepted academic practice. No use, distribution or reproduction is permitted which does not comply with these terms.

frontiers in Immunology

ORIGINAL RESEARCH
published: 24 June 2021
doi: 10.3389/fimmu.2021.669162

Acute Kidney Injury Induced Lupus Exacerbation Through the Enhanced Neutrophil Extracellular Traps (and Apoptosis) in Fcgr2b Deficient Lupus Mice With Renal Ischemia Reperfusion Injury

*Wilasinee Saisorn[1,2], Supichcha Saithong[3], Pornpimol Phuengmaung[2,3], Kanyarat Udompornpitak[3], Thansita Bhunyakarnjanarat[3], Peerapat Visitchanakun[3], Awirut Chareonsappakit[3], Prapaporn Pisitkun[4], Direkrit Chiewchengchol[2,3] and Asada Leelahavanichkul[2,3]**

[1] Medical Microbiology, Interdisciplinary and International Program, Graduate School, Chulalongkorn University, Bangkok, Thailand, [2] Department of Microbiology, Faculty of Medicine, Chulalongkorn University, Bangkok, Thailand, [3] Translational Research in Inflammation and Immunology Research Unit (TRIRU), Department of Microbiology, Chulalongkorn University, Bangkok, Thailand, [4] Division of Allergy, Immunology, and Rheumatology, Department of Medicine, Faculty of Medicine, Ramathibodi Hospital, Mahidol University, Bangkok, Thailand

Renal ischemia is the most common cause of acute kidney injury (AKI) that might be exacerbate lupus activity through neutrophil extracellular traps (NETs) and apoptosis. Here, the renal ischemia reperfusion injury (I/R) was performed in Fc gamma receptor 2b deficient (Fcgr2b-/-) lupus mice and the *in vitro* experiments. At 24 h post-renal I/R injury, NETs in peripheral blood neutrophils and in kidneys were detected using myeloperoxidase (MPO), neutrophil elastase (NE) and citrullinated histone H3 (CitH3), as well as kidney apoptosis (activating caspase-3), which were prominent in Fcgr2b-/- mice more compared to wild-type (WT). After 120 h renal-I/R injury, renal NETs (using MPO and NE) were non-detectable, whereas glomerular immunoglobulin (Ig) deposition and serum anti-dsDNA were increased in Fcgr2b-/- mice. These results imply that renal NETs at 24 h post-renal I/R exacerbated the lupus nephritis at 120 h post-renal I/R injury in Fcgr2b-/- lupus mice. Furthermore, a Syk inhibitor attenuated NETs, that activated by phorbol myristate acetate (PMA; a NETs activator) or lipopolysaccharide (LPS; a potent inflammatory stimulator), more prominently in Fcgr2b-/- neutrophils than the WT cells as determined by dsDNA, *PAD4* and MPO. In addition, the inhibitors against Syk and PAD4 attenuated lupus characteristics (serum creatinine, proteinuria, and anti-dsDNA) in Fcgr2b-/- mice at 120 h post-renal I/R injury. In conclusion, renal I/R in Fcgr2b-/- mice induced lupus exacerbation at 120 h post-I/R injury partly because Syk-enhanced renal NETs led to apoptosis-induced anti-dsDNA, which was attenuated by a Syk inhibitor.

Keywords: Fcgr2b deficient mice, systemic lupus erythematosus, neutrophil extracellular traps, renal ischemia reperfusion injury, acute kidney injury

OPEN ACCESS

Edited by:
Bin Yang,
University of Leicester,
United Kingdom

Reviewed by:
Federico Pratesi,
University of Pisa, Italy
Szu Ting Jessica Chen,
National Yang-Ming University, Taiwan

***Correspondence:**
Asada Leelahavanichkul
aleelahavanit@gmail.com

Specialty section:
This article was submitted to Molecular Innate Immunity, a section of the journal Frontiers in Immunology

Received: *18 February 2021*
Accepted: *31 May 2021*
Published: *24 June 2021*

Citation:
Saisorn W, Saithong S, Phuengmaung P, Udompornpitak K, Bhunyakarnjanarat T, Visitchanakun P, Chareonsappakit A, Pisitkun P, Chiewchengchol D and Leelahavanichkul A (2021) Acute Kidney Injury Induced Lupus Exacerbation Through the Enhanced Neutrophil Extracellular Traps (and Apoptosis) in Fcgr2b Deficient Lupus Mice With Renal Ischemia Reperfusion Injury. Front. Immunol. 12:669162. doi: 10.3389/fimmu.2021.669162

INTRODUCTION

Prevalence of the dysfunction polymorphism in Fc gamma receptor 2b (Fcgr2b), which is the only one inhibitory receptor in Fc gamma receptor (FcgR) family (1–3), is usually found in Asian population. Fcgr2b is associated with systemic lupus erythematosus (SLE), a common autoimmune disease mostly associated with anti-dsDNA (4). Deficiency of the inhibitory Fcgr2b signaling causes SLE through the increased antibody production by hyper-reactive B cells (5), whereas Fcgr2b deficiency enhances the protection against malarial infection. Indeed, Fcgr2b is detectable in several immune cells (except for T cells and NK cells) (6) and the loss of Fcgr2b could induce macrophage hyper-responsiveness as demonstrated in Fcgr2b knockout (Fcgr2b-/-) macrophages (7). Additionally, Fcgr2b-/- mice develop age-dependent lupus characteristics, including asymptomatic lupus prone (less than 16 weeks old), asymptomatic lupus with anti-dsDNA (16-24 weeks old) and full-blown lupus (40 weeks old), which have been used as a representative model of lupus (8). Although the hyper-responsiveness of Fcgr2b-/- mice against several pathogen molecules, including pneumococcal antigens and lipopolysaccharide (LPS), has been demonstrated (2, 7, 8), studies on Fcgr2b-/- neutrophils are still very limited. However, lupus exacerbation is well-known for neutrophil apoptosis and neutrophil extracellular traps (NETs)-induced cell death (NETosis) (9, 10).

As such, apoptosis (cellular shrinkage, membrane blebbing and chromatin condensation) is triggered by intrinsic pathway containing the caspase 3 activation through cell damage and reactive oxygen species (ROS), and extrinsic pathway through several external death factors (11). The profound apoptosis (with an insufficient clearance) causes secondary necrosis that enhances the exposure to nuclear autoantigens (12) and accelerates anti-dsDNA production in lupus (13). Likewise, NETosis is a release of extracellular DNA networks by neutrophils in either infectious or non-infectious condition (14) through peptidylarginine deiminase 4 (PAD4)-induced citrullinated histone H3 (CitH3) (15). Extracellular DNA networks from NETosis, both of NADPH oxidase 2 (NOX2)-dependent and NOX2-independent pathways, enhance exposure of nuclear contents (16), including dsDNA that is normally contained in nuclei (17), and increased anti-dsDNA which is a specific auto-antibody in lupus (18, 19). With profound cell death, the free dsDNA is recognized as a damage associated molecular patterns (DAMPs) by innate immune cells (17) and processed by adaptive immune cells supporting the lupus exacerbation from inflammatory responses (20, 21). Not only cell death of the immune cells, but also the dying process of other cell types, exacerbate lupus as the avoidance of ultraviolet light, that induces keratinocyte cell death (22–24), is a current mandatory recommendation for lupus (17). Due to the abundance of neutrophils, cell death of neutrophils in the host with lupus-prone condition (loss of tolerance) (25), but not the normal host, might profoundly enhance the exposure of dsDNA that increases anti-dsDNA production. Besides, the susceptibility to program cell death of Fcgr2b-/- neutrophils might be higher than WT cells that have been triggered the lupus activity.

In parallel, acute kidney injury (AKI) is the common health care problem worldwide, which is mainly caused by ischemia (26) that was often represented by renal ischemia reperfusion injury (I/R) animal model (27, 28). As such, renal ischemia induces accumulation of immune cells, including neutrophils, as a response to the injury (29–31) and the injury also causes apoptosis (and necrosis) in renal parenchymal cells and neutrophils (32, 33). Consequently, the ischemic injury directly induces program cell deaths of neutrophils, including NETosis, in several organs after renal injury (34). After the renal ischemia, cell apoptosis and NETosis might be exacerbated the lupus disease activity due to the lupus exacerbation from the program cell deaths (35). Because of the prominent responses against several stimulators of the Fcgr2b-/- mice (2, 7, 8), apoptosis and NETosis derived from renal I/R might be more profound than the responses in the normal mice. TLR-4 is the significant pathway that induces both apoptosis and NETosis (36), while spleen tyrosine kinase (Syk) is the shared downstream signaling pathway of TLR-4 and FcgR (20, 21, 37, 38). Therefore, the Syk inhibitor may be an interesting drug to manipulate cell death in renal-I/R mediated cell death in lupus (39). Indeed, the Syk inhibitor (fostamatinib, previously known as R788) is a US FDA (the United States Food and Drug Administration) approved drug for autoimmune diseases (40–43). Here, we reported the *in vitro* and *in vivo* experiments to determine the effect of renal-I/R on lupus and evaluated the Syk inhibitor on Fcgr2b-/- lupus mice.

MATERIALS AND METHODS

Animals

The animal study protocol was approved from the Institutional Animal Care and Use Committee of the Faculty of Medicine, Chulalongkorn University, Bangkok, Thailand, under approval number 009/2564, following the animal care and use protocol of the National Institutes of Health (NIH), USA. Fcgr2b-/- mice on a C57BL/6 background were provided by Dr. Silvia Bolland (NIAID, NIH, Maryland, USA). The wild-type (WT) mice were purchased from the Nomura Siam International (Pathumwan, Bangkok, Thailand). Due to the age-dependent lupus characteristic (44, 45), 8-week-old Fcgr2b-/- female mice represented asymptomatic lupus prone mouse model and age-matched female WT mice were used in all experiments.

Renal Ischemia Reperfusion Injury Model and NETs Inhibitors

Renal I/R was performed following a previous publication (27). In brief, bilateral renal arteries were clamped for 35 min through the abdominal incision under ketamine anesthesia on a 37°C heated operation table. In sham surgery, renal arteries were only identified before closing the abdominal wall. Tramadol, 20 mg/kg diluted in 0.5 mL normal saline (NSS) was administered subcutaneously after surgery and at 24 h post-I/R. Mice were

sacrificed in several time-points after I/R under isoflurane anesthesia for sample collection. Serum was kept at −80°C until analysis and organs were processed in 10% formalin or Tissue-Tek O.C.T Compound (Sakura Finetek, CA, USA) for histological analysis or snap frozen and stored separately at -80°C. The Syk inhibitor was used for testing the anti-inflammatory effect (42) and a possible association between activating-FcgRs and Syk signaling (46). As such, a Syk inhibitor (R788 disodium, Selleckchem, Houston, USA) in 0.1 M citrate buffer (pH 6.8) at 25 mg/kg/dose was orally administered daily for 2 days, at 6 h prior to surgery, and at 6 h after renal-I/R. In parallel, a Cl-amidine (PAD4 inhibitor; Sigma-Aldrich, St. Louis, MO, USA) was dissolved in dimethyl sulfoxide (DMSO; Sigma-Aldrich). The stock solution was dissolved in normal saline at 10 mg/kg/dose and injected intraperitoneal 3 h prior to renal-I/R at once daily after following a previous publication (47) to test the influence of NETs in lupus model with renal-I/R. Mice were sacrificed with sample collection under isoflurane anesthesia.

Blood and Urine Analysis

Parameters of lupus characteristics, serum cytokines, liver injury, and NETosis were evaluated from blood samples. Lupus characteristics including serum creatinine (QuantiChrom Creatinine-Assay, DICT-500, BioAssay, Hayward, CA, USA), serum anti-dsDNA, and proteinuria were determined. Symptomatic lupus was defined as increased serum anti-dsDNA, high serum creatinine, and increased proteinuria when compared with the WT mice. The anti-dsDNA was evaluated using a protocol with coated-calf thymus DNA (Invitrogen, Carlsbad, CA, USA) with a minor modification (48). Briefly, each analyzed plate was coated with calf thymus DNA (for dsDNA) and ssDNA that was prepared using the thermal denaturation of calf thymus DNA (49). Briefly, the plates were incubated overnight at 4°C, filled with blocking solution at room temperature, and washed with 1X TBS 0.05% Tween 20, respectively. Subsequently, mouse serum samples were added into the plates and incubated overnight at 4°C. Then, HRP-conjugated goat anti-mouse antibodies and TMB peroxidase substrate (TMB Substrate Set; BioLegend, San Diego, CA, USA) were added to analyze the plates, and 2 N H_2SO_4 was added to stop the reaction. The measurement at a wavelength of 450 nm was determined using a Varioskan Flash spectrophotometer (Thermo Scientific, Waltham, MA, USA). The reported anti-dsDNA was represented from the values of calf-DNA coated plates subtracted by ssDNA-coated plates.

Proteinuria was calculated using spot urine protein creatinine index (UPCI) with the equation; UPCI = urine protein (mg)/urine creatinine (mg/dL). Urine protein and creatinine were measured by Bradford Bio-Rad Protein Assay (Bio-Rad, Hercules, CA, USA) and QuantiChrom Creatinine-Assay (DICT-500) (BioAssay), respectively. Serum pro-inflammatory cytokines (TNF-α and IL-6) and IL-1β, a NETs associated cytokine (50), were measured using enzyme-linked immunosorbent assay (ELISA) (Invitrogen). Liver injury was determined by alanine transaminase (ALT) using EnzyChrom ALT assay (EALT-100, BioAssay). For the evaluation of NETs in peripheral blood neutrophils, neutrophils were isolated using Polymorphprep (Alere Technologies AS, Norway) according to the manufacturer's instructions (51, 52), and hypotonic lysis buffer was used for red blood cell de-contamination. Blood neutrophils were resuspended in RPMI (Roswell Park Memorial Institute media)-1640 media and the purity was assessed by Wright's stains. The samples with >95% neutrophils were further used to determine the NETs formation as mentioned in the section of *in vitro* experiments. Additionally, NETs formation in serum was also determined using Quant-iT^{TM} PicoGreen dsDNA Assay Kit (Thermo Scientific), and serum MPO was measured by ELISA (Sigma Aldrich, St. Louis, MO, USA).

Polymerase Chain Reaction

Several molecules associated with inflammation (cytokines), neutrophil extracellular traps (NETs), and the possible downstream signals from mouse organs and the cell culture were evaluated by real time polymerase chain reaction (RT-PCR). Gene expression of several molecules, including inflammatory cytokines; *TNF-α*, *IL-6*, and *IL-10*, genes of NETs formation; peptidyl arginine deiminase 4 (*PAD4*) and *IL-1β*, genes of the downstream signals; spleen tyrosine kinase (*Syk*) and nuclear factor kappa B (*NFκB*), were evaluated. Total RNA was prepared from the samples with an RNA-easy mini kit (Qiagen, Hilden, Germany) and was quantified by Nanodrop 100 Spectrophotometer (Thermo Scientific) before the determination of gene expression. Total RNA reverse transcription was processed with a High-Capacity cDNA Reverse Transcription (Thermo Scientific). Samples were performed using SYBR Green PCR Master Mix for quantitative RT-PCR with QuantStudio6 Flex Real-time PCR System (Thermo Scientific), respectively. The results were demonstrated in terms of relative quantitation of the comparative threshold (delta-delta Ct) method (2-ΔΔCt) as normalized by *β-actin* (an endogenous housekeeping gene). The list of primers is shown in **Supplementary Table 1**.

Histological Analysis and Immunofluorescent Imaging

The semi-quantitative evaluation of renal and lung histology on paraffin-embedded slides was performed after 10% neutral buffered formalin fixation, followed by Hematoxylin and Eosin (H&E) staining at 200× magnification in 10 randomly selected fields for each animal (53–55). Renal injury was defined as tubular epithelial swelling, loss of brush border, vacuolar degeneration, necrotic tubules, cast formation, and desquamation using the scoring method as follows: 0, area of damage <5%; 1, area of damage 5%–10%; 2, area of damage 10%–25%; 3, area of damage 25%–50%; and 4, area of damage >50%. Lung injury was determined by alveolar hemorrhage, alveolar congestion, neutrophil infiltration, and alveolar wall thickness with the following score: 0, no injury in the observed field;1, injury up to 25%; 2, injury up to 50%; 3, injury up to 75%; and 4, injury in the entire field.

In parallel, immunofluorescent histological analysis was performed following previous publications (8, 13, 56). In brief, the internal organs were prepared in Tissue-Tek O.C.T Compound (Sakura Finetek, CA, USA) and three sections of each organ were stained as follows; i) NETs were detected with antibody against neutrophil elastase (NE; ab68672), myeloperoxidase (MPO; ab25989), and citrullinated histone H3 (citrulline R2 + R8 + R17;

ab5103) (Abcam, Cambridge, MA, USA) with DAPI (4′,6-diamidino-2-phenylindole), a blue-fluorescent DNA stain (Sigma Aldrich), ii) cell apoptosis was visualized by anti-Cleaved Caspase 3 (Asp175, 9661S) (Cell Signaling Technology, Boston, MA, USA) with the secondary antibodies; goat anti-rabbit IgG (ab150077) (green color), goat anti-mouse IgG (ab150115), and donkey anti-rabbit IgG (ab150075) (red color) and iii) immunoglobulin deposition was performed using goat anti-mouse IgG (green color) (ab150113; Abcam, Cambridge, MA, USA). The images were analyzed with ZEISS LSM 800 (Carl Zeiss, Germany).

Flow Cytometry Analysis of Spleen

Spleen lymphocytes were explored to compared between Fcgr2b-/- and WT mice after 120 h post renal-I/R (or sham), were following a previous published protocol (41). In short, spleens were dispersed through a cell strainer to generate a single-cell suspension in supplemented RPMI-1640 prior to centrifuged at 300 × *g* for 5 min at 4°C. Red blood cells were eliminated using an osmotic agent (ACK buffer; NH4Cl, KHCO3, and EDTA). Then, the cells were resuspended in staining buffer (0.5% bovine serum albumin and 10% fetal bovine serum in PBS), and were stained with fluorochrome-conjugated antibodies against different mouse immune cells, including anti-B220 (leukocyte common antigen) together with anti-CD138 (plasma cells), anti-major histocompatibility complex (MHC) class II (active immune cells), CXCR5 (follicular B cells), and anti-CD19 along with anti-GL-7 (germinal center B cells) (BioLegend, San Diego, CA, USA). All stained cells were examined by flow cytometry using BD LSR-II (BD Biosciences) and the data were analyzed by FlowJo software (Tree Star Inc., Ashland, OR, USA).

The *In Vitro* Experiments on Neutrophils

The apoptosis and NETosis susceptibility between Fcgr2b-/- and WT neutrophils, and the attenuation by inhibitors were tested using the *in vitro* experiment. Accordingly, neutrophils were derived from peritoneum using a published protocol (57). Briefly, 1 mL of 3% thioglycolate was intraperitoneal administered in 8-week-old mice. At 3 h after administration, mice were sacrificed and peritoneal cavity was thoroughly collected and washed with ice-cold phosphate buffer solution (PBS) before centrifugation at 1,800 × *g*, 4°C for 5 min to separate the cells and evaluated by Wright's-stains (55). Only the preparation with more than 90% neutrophils was further used for the experiments. Then, neutrophils at 2×10^5 cells/well in 24-well-plates containing RPMI media were incubated with phorbol myristate acetate (PMA), a NETs stimulator, (Sigma-Aldrich) at a final concentration of 25 ng/mL or lipopolysaccharide (LPS) (Escherichia coli 026: B6; Sigma-Aldrich) at 100 ng/mL under 5% CO_2 at 37°C for 4 h. Supernatants were used for cytokine measurement by ELISA (Invitrogen) and were quantified for dsDNA using PicoGreen assay kit (Invitrogen, Canada) following the manufacturer's protocol. Nuclei morphology has been identified with DAPI nuclear staining (58), which was presented by the percentage of cells with NETs formation, and *PAD4* expression was determined using RT-PCR as the previously mentioned. Additionally, neutrophils were suspended in PBS at a concentration of 5×10^5 cells/mL, stained for apoptosis/necrosis by annexin V-FITC and propidium iodide (PI) (5 μL/well) (BD Biosciences), respectively. Then, the samples were washed with FACS flow buffer, PBS supplemented with 1% (v/v) FBS, and 0.05% NaN_3 and processed by the BD LSR II Flow Cytometry (BD Biosciences) using the FlowJo software (Tree Star Inc.). Reactive oxygen species (ROS) was determined by DHE (Dihydroethidium) assay (ab236206; Abcam, Cambridge, MA, USA), according to the manufacturer's instructions. In addition, the active metabolites Syk inhibitor (R406; Selleckchem) at a final concentration of 5 μg/mL or nuclear factor kappa B (NFκB) inhibitor (BAY11-7082; Sigma–Aldrich) at a final concentration of 2 μg/mL were used in the experiments. RPMI 1640 supplemented with 10% FBS was used as the control.

Western Blot Analysis

Western blot analysis was performed as previously described (59) to determine the abundance of Syk and NFκB in activated neutrophils. In brief, cell lysate (in 1X SDS lysis buffer) was supplemented with the inhibitors against protease and phosphatase enzymes (Thermo-Scientific) and incubated on ice for 30 min before centrifugation at 10,000 rpm at 4°C. Protein quantification was performed by BCA assay (Pierce BCA Protein Assay) before administration in the 10% SDS-PAGE (Sodium Dodecyl Sulfate-Polyacrylamide Gel Electrophoresis) and transferred onto a nitrocellulose membrane, respectively. Then, the membranes were blocked with Intercept blocking buffer (Lincoln, NE, USA) and incubated with primary antibodies against Syk (D3Z1E), phospho-Zap-70 (Tyr319)/Syk (Tyr352) (65E4) (Cell Signaling Technology, Boston, MA, USA), NFκB p65 (NFκB; D14E12) and phospho-NFκB p-65 (p-NFκB (Ser536) (93H1); Cell Signaling Technology), and Beta-actin (β-actin, a house-keeping protein) (D6A8; Cell Signaling Technology). Subsequently, the secondary antibody is anti-rabbit IgG (DyLight 680 conjugate) was used and visualized by Odyssey CLx imaging system (Lincoln, NE, USA). The target bands were determined using Image Studio Lite version 5.2.

Statistical Analysis

Statistical differences among groups were examined using the unpaired Student's t-test or one-way analysis of variance (ANOVA) with Tukey's comparison test for the analysis of experiments with two groups or more than two groups, respectively, all of which are presented as the mean ± standard error (SE). Statistical comparisons of data were conducted by paired Student's t-test in the experiment condition of before and after treatment. SPSS 11.5 software (SPSS, Chicago, IL, USA) was used for all statistical analysis.

RESULTS

Although the renal I/R induced the renal excretory dysfunction (serum creatinine) at 24 h post-renal I/R of Fcgr2b-/- mice was similar to those of wild type (WT) mice, there was higher NETs and apoptosis in glomeruli which led to lupus nephritis possibly through Syk signaling after 120 h post-I/R.

Similar Organ Injury but More Prominent Neutrophil Extracellular Traps (NETs) and Glomerular Apoptosis at 24 h Post-Renal I/R in Fcgr2b-/- Lupus Mice Compared With WT

Fcgr2b-/- mice spontaneously developed full-blown lupus nephritis (impaired renal function, proteinuria, and increased anti-dsDNA) at 40 weeks old (**Supplementary Figures 1A–C**) without polyarthritis and serositis (data not shown). The renal I/R was performed in 8-week-old Fcgr2b-/- mice, asymptomatic lupus prone condition, and age-matched WT mice demonstrated that there was a similar kidney injury between Fcgr2b-/- and WT mice at 24 h post-renal I/R. Consequently, blood urea nitrogen (BUN), serum creatinine (Scr), proteinuria (UPCI), renal histology (**Figures 1A–E**), and gene expression of cytokines (*TNF-α*, *IL-6* and *IL-10*) in renal tissue (**Supplementary Figures 1D–F**) have no the difference between Fcgr2b-/- and WT mice. Notably, the highest renal injury occurred at 24 h post-renal I/R of both mouse strains supporting a previous publication (28). The remote organ injury at 24 h post-renal I/R has the similarity between both mouse strains, including liver enzyme (serum alanine transaminase), lung injury score, and serum cytokines (**Figures 1F–J**), except for gene expression of cytokines in liver, heart, and lung (**Supplementary Figures 1G–O**). However, prominent NETosis in Fcgr2b-/- mice was demonstrated as follows, i) peripheral blood neutrophils were detected using nuclear morphology (DAPI), which were co-stained with MPO and NE, as well as CitH3 staining, and gene expression of *PAD4* and *IL-1β* (**Figures 2A–H**), ii) serum (serum IL-1β and serum dsDNA) (**Figures 2I, J**), iii) glomeruli were visualized using co-staining of MPO and NE with *PAD4* and *IL-1β* expression (**Figures 3A–D**), CitH3 staining and IL-1β in renal tissue (**Figures 4A–C**), iv) lungs were performed using co-staining of MPO and NE, *PAD4* and *IL-1β* expression (**Supplementary Figures 2A–D**), except liver and heart (**Supplementary Figures 2E–J**).

The negative results of NETosis in liver and heart at 24 h post-renal I/R (**Supplementary Figures 1G–L**) suggested that the NETs inflammatory pathways in the remote organ injury post-renal I/R have not occurred. In parallel, apoptosis in glomeruli and lungs, excluding the immunoglobulin (Ig) deposition, was more prominent in Fcgr2b-/- mice compared with WT at 24 h post-renal I/R (**Figures 5A–C** and **Supplementary Figures 3A–C**). These data imply a prominent cell injury (apoptosis and NETosis) in Fcgr2b-/- mice than WT at 24 h post-renal I/R, whereas the functional renal damage was not different.

Recovery of Neutrophil Extracellular Traps (NETs) and Apoptosis at 120 h Post-Renal I/R With Enhanced Anti-dsDNA and Immunoglobulin Deposition in Fcgr2b-/- Lupus Mice

At 120 h post-renal I/R, renal function (BUN and Scr), non-renal organ damage, and serum cytokines, excepting proteinuria (UPCI), were returned to the baseline level in WT mice (**Figures 1A–I**). Notably, the sustained proteinuria that has a normal renal excretory function (BUN and Scr) supports the renal ischemia-induced podocyte injury (60, 61). In contrast, all the organ injury and serum cytokines in Fcgr2b-/- mice highly increased at 120 h post I/R (**Figures 1A–I** and **Supplementary Figures 1D–P**) with elevated anti-dsDNA (**Figure 1J**), suggesting an exacerbation of lupus disease activity. The rapid elevation of anti-dsDNA in 8-week-old Fcgr2b-/- lupus prone mice after 120 h post-I/R suggesting the non-specific activation of autoreactive B cells in Fcgr2b-/- mice post-renal I/R that was similar to a previous publication (62). Indeed, plasma cells (CD138 and B220 positive cells) and activated B cells (MHC class II and B220 positive cells), except germinal center B cells (CD19 and GL7 positive cells) and follicular B cells (CXCR5 and B220 positive cells), in Fcgr2b-/- mice spleen increased rapidly when compared with WT at 120 h post-renal I/R injury (**Supplementary Figures 4A–E**) that might be responsible for the rapid elevation of anti-dsDNA at 5 days post-renal I/R. Notably, the plasma cells and activated B cells in spleen of Fcgr2b-/- mice and WT were not different from sham control groups (**Supplementary Figures 4A, B**), implied that B cell activation in Fcgr2b-/- mice more rapid than WT, despite a similar B cells baseline state. In addition, NETs of both mouse strains were undetectable at 120 h post-renal I/R (**Figures 2A–J**, **3A–D**, **4A–C** and **Supplementary Figures 2A–J**) with glomerular apoptosis in Fcgr2b-/- mice, in contrast to WT (**Figures 5A–C**). Meanwhile, glomerular IgG deposition was detectable in both mouse strains with more prominent in Fcgr2b-/- mice at 120 h post-renal I/R (**Figures 5B, C**). The IgG deposition at 120 h post I/R, which was a part of the wound healing process (63), was more profound in Fcgr2b-/- mice than WT, partly indicated an increased antibody production from ischemia induced inflammation (64) in lupus mice. These data suggested that prominent NETs and apoptosis (16) at 24 h post-renal I/R enhanced lupus disease exacerbation (12), and increased the auto-antibody production at 120 h post-renal I/R.

Prominent Apoptosis and Neutrophil Extracellular Traps (NETs) in Fcgr2b-/- Neutrophils, Compared With WT Cells, at 2 h and 4 h of the Stimulation, Respectively, and an Impact of Spleen Tyrosine Kinase (Syk) Signaling

Because i) both apoptosis and NETosis exacerbate lupus disease activity (35), ii) both PMA and LPS could activate apoptosis and NETs (65–67), and iii) Fcgr2b-/- neutrophils might be more susceptible to apoptosis and NETosis than WT cells (the loss of inhibitory signaling) (20, 21), PMA and LPS are used as the representative stimulators. After the 2 h stimulation by PMA or LPS, Fcgr2b-/- neutrophils demonstrated more prominent apoptosis (and necrosis) than WT cells (**Figures 6A, B**), accompanying with the increased production of ROS (Dihydroethidium; DHE) (**Figure 6C**). Furthermore, LPS induced more severe necrosis with lower ROS in Fcgr2b-/- neutrophils when compared with PMA (**Figures 6B, C**). At 4 h of the stimulation, NETosis occurred in neutrophils from both mouse strains as indicated using dsDNA, *PAD4* expression, DAPI nucleus morphology, and co-staining of MPO and NE

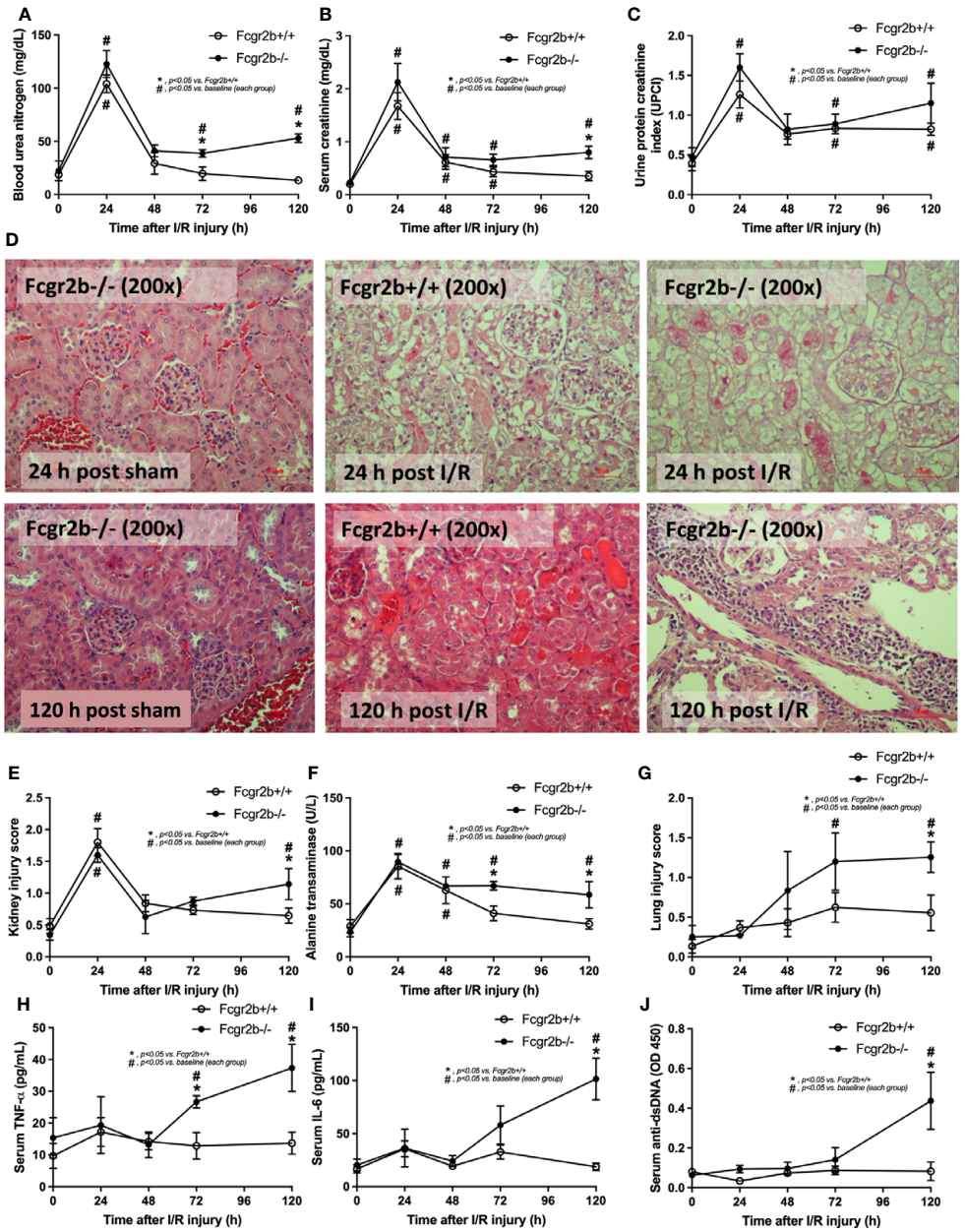


FIGURE 1 | Renal ischemia reperfusion injury (I/R) at 24 h induced lupus disease exacerbation at 120 h. The time-point characteristics of Fcgr2b-/- or wild-type (Fcgr2b+/+) mice after I/R as determined by i) renal injury; blood urea nitrogen (BUN), serum creatinine, and proteinuria (protein creatinine index; UPCI) along with the histological score of the representative images in Hematoxylin and Eosin (H&E) staining (original magnification 200x) **(A–E)**, ii) liver injury (serum alanine transaminase) **(F)**, iii) lung injury score **(G)**, and iv) the parameters in serum; serum pro-inflammatory cytokines (TNF-α and IL-6) **(H, I)** and serum anti-dsDNA, a major auto-antibody in lupus **(J)** are demonstrated (n = 6–7/time-point). Notably, the renal histological pictures at 24 h post sham of Fcgr2b+/+ mice and at 120 h post sham (both mouse strains) are not demonstrated due to the similarity to Fcgr2b-/- mice at 24 h post sham (normal histology).

(**Figures 6D–H**). However, PMA similarly induced NETs in neutrophils of both mouse strains at 4 h post-stimulation, while LPS inducing higher NETs (**Figures 6G, H**, **7**) with the prominent pro-inflammatory cytokine production (TNF-α and IL-6) (**Figures 8A–C**) in Fcgr2b-/- than WT cells. Because spleen tyrosine kinase (Syk) and nuclear factor kappa B (NFκB), a downstream signaling of Syk (68), are the possible shared downstream signaling of PMA and LPS (20, 21, 69, 70), these molecules are explored. At 4 h post-stimulation, PMA upregulated *Syk* only in Fcgr2b-/- neutrophils, while LPS upregulated *Syk* in neutrophils of both mouse strains (**Figures 8D, E**). In parallel, both PMA and LPS similarly upregulated *NFκB* in neutrophils of both mouse strains (**Figures 8D, E**). Meanwhile, both stimulators (PMA and LPS)

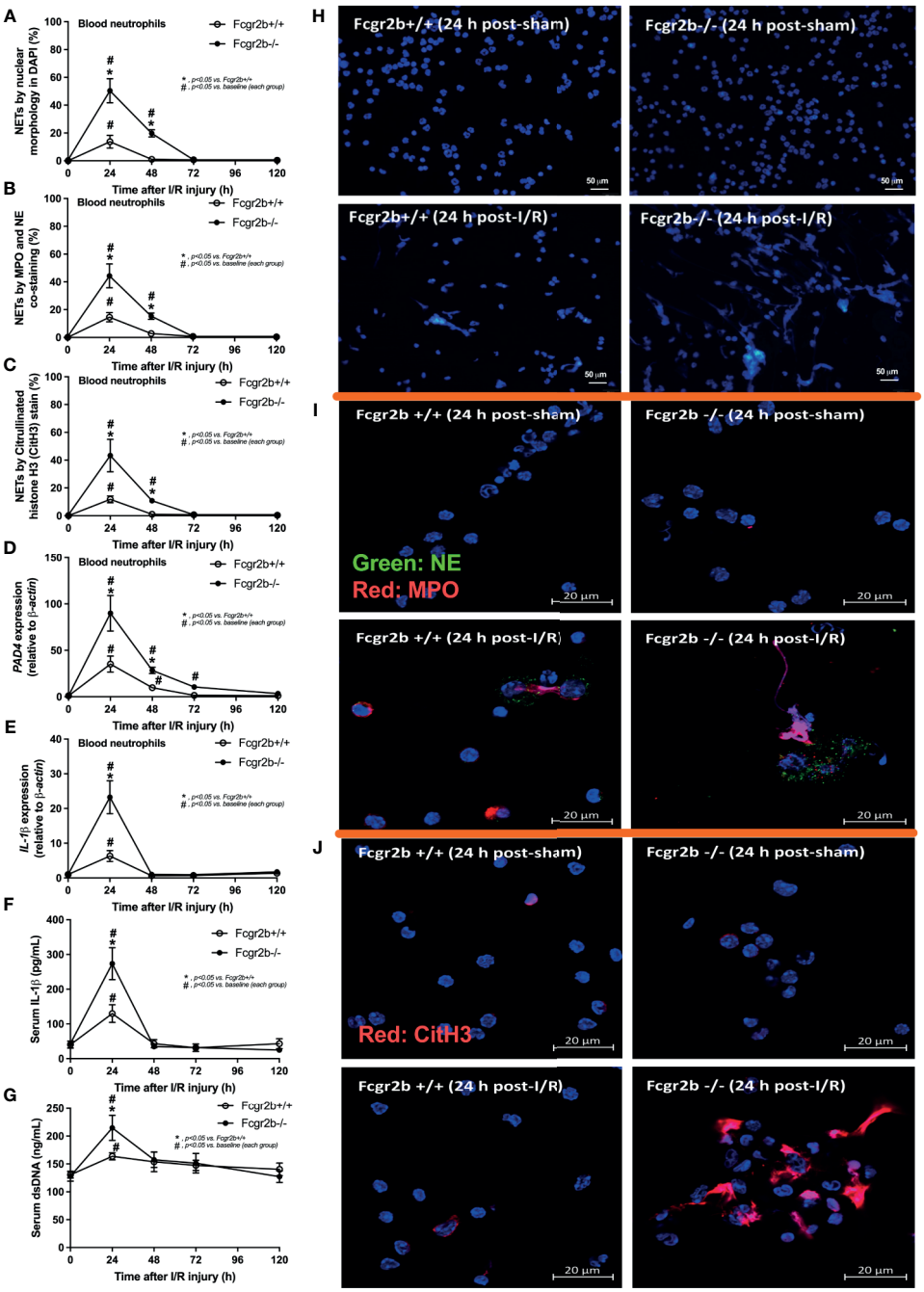


FIGURE 2 | Renal ischemia reperfusion injury (I/R) at 24 h induced more prominent neutrophil extracellular traps (NETs) in blood of lupus prone mice. Characteristics of NETs in peripheral blood neutrophils from Fcgr2b-/- or wild-type (Fcgr2b+/+) mice after renal ischemia reperfusion injury (I/R) as determined by the nuclear morphology by 4',6-diamidino-2-phenylindole (DAPI) staining (blue color) **(A)**, co-staining of myeloperoxidases (MPO) and neutrophil elastase (NE) **(B)**, citrullinated histone H3 (CitH3) staining **(C)** with the representative pictures from peripheral blood neutrophils at 24 h post-I/R (or sham) from both mouse strains with DAPI staining (original magnification 200x) **(D)**, and immunofluorescence of MPO/NE and CitH3 (original magnification 630x) **(E, F)** are demonstrated. Additionally, the gene expression of *PAD4* and *IL-1β* **(G, H)** together with serum IL-1β **(I)** and serum ds-DNA **(J)** are also demonstrated (n = 6–7/time-point).

induced the higher abundance of phosphorylated-Syk and phosphorylated-NFκB in Fcgr2b-/- neutrophils when compared with WT cells (**Figures 8F, G**). As such, detection of NETs (**Figures 6D–H**, **7**) along with Syk and NFκB (gene expression and protein abundance) (**Figures 8A–G**) at 4 h post-stimulation by PMA and LPS implied the association between NETosis and Syk or NFκB, especially in Fcgr2b-/- neutrophils.

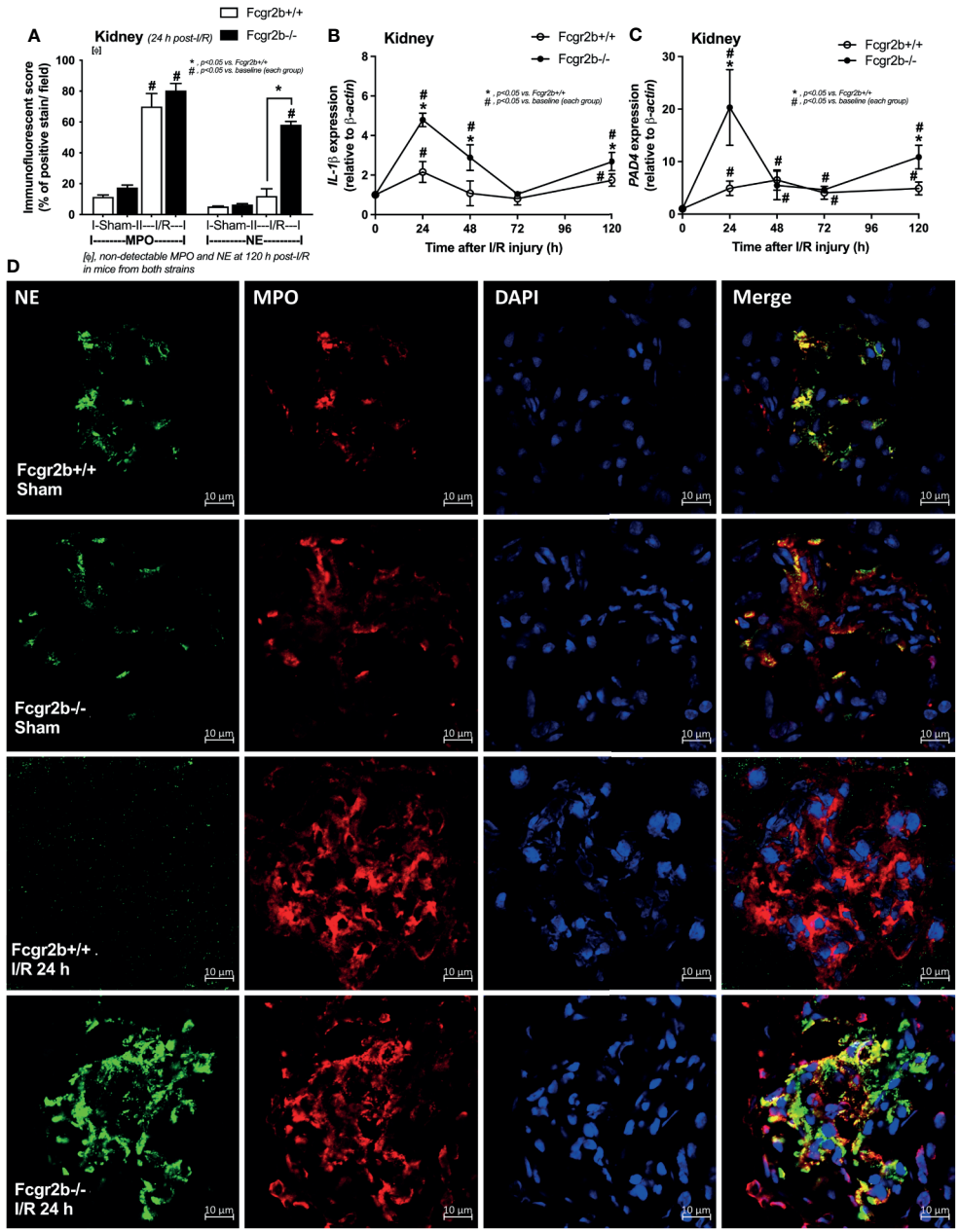


FIGURE 3 | Renal ischemia reperfusion injury (I/R) at 24 h induced more prominent neutrophil extracellular traps (NETs) in renal glomeruli of lupus prone mice. Characteristics of NETs in kidneys from Fcgr2b-/- or wild-type (Fcgr2b+/+) mice after renal ischemia reperfusion injury (I/R) as determined using co-detection of myeloperoxidases (MPO) and neutrophil elastase (NE) at 24 h post-I/R **(A)** (n = 5–8/group) and gene expression in the time-point of *IL-1β* and *PAD4* **(B, C)** (n = 6–7/time-point) with the representative immunofluorescent pictures of NE (green), MPO (red) and 4',6-diamidino-2-phenylindole (DAPI, blue nuclear staining) at 24 h post-I/R (or sham) (original magnification 630x) **(D)** are demonstrated.

Inhibition of Neutrophil Extracellular Traps (NETs) by Inhibitors Attenuated Renal I/R-Induced Lupus Exacerbation

Due to the possible Syk and NFκB mediated NETs after PMA and LPS stimulation, inhibitors against Syk and NFκB were tested using the *in vitro* experiments. As such, both inhibitors attenuated i) NETosis by PMA or LPS, which was evaluated by dsDNA, *PAD4* expression and co-detection of MPO with NE (**Figures 9A–H**) and ii) cytokine production (TNF-α, IL-6 and IL-10) (**Supplementary Figures 5A–F**) in neutrophils of both mouse strains (more prominent response to Fcgr2b-/- neutrophils than WT). Because of the NETosis attenuation of Syk inhibitor (39, 71) and the clinically availability of this drug (42) different from other NETs inhibitors, Syk inhibitor was further tested in mice. As such, Syk inhibitor attenuated

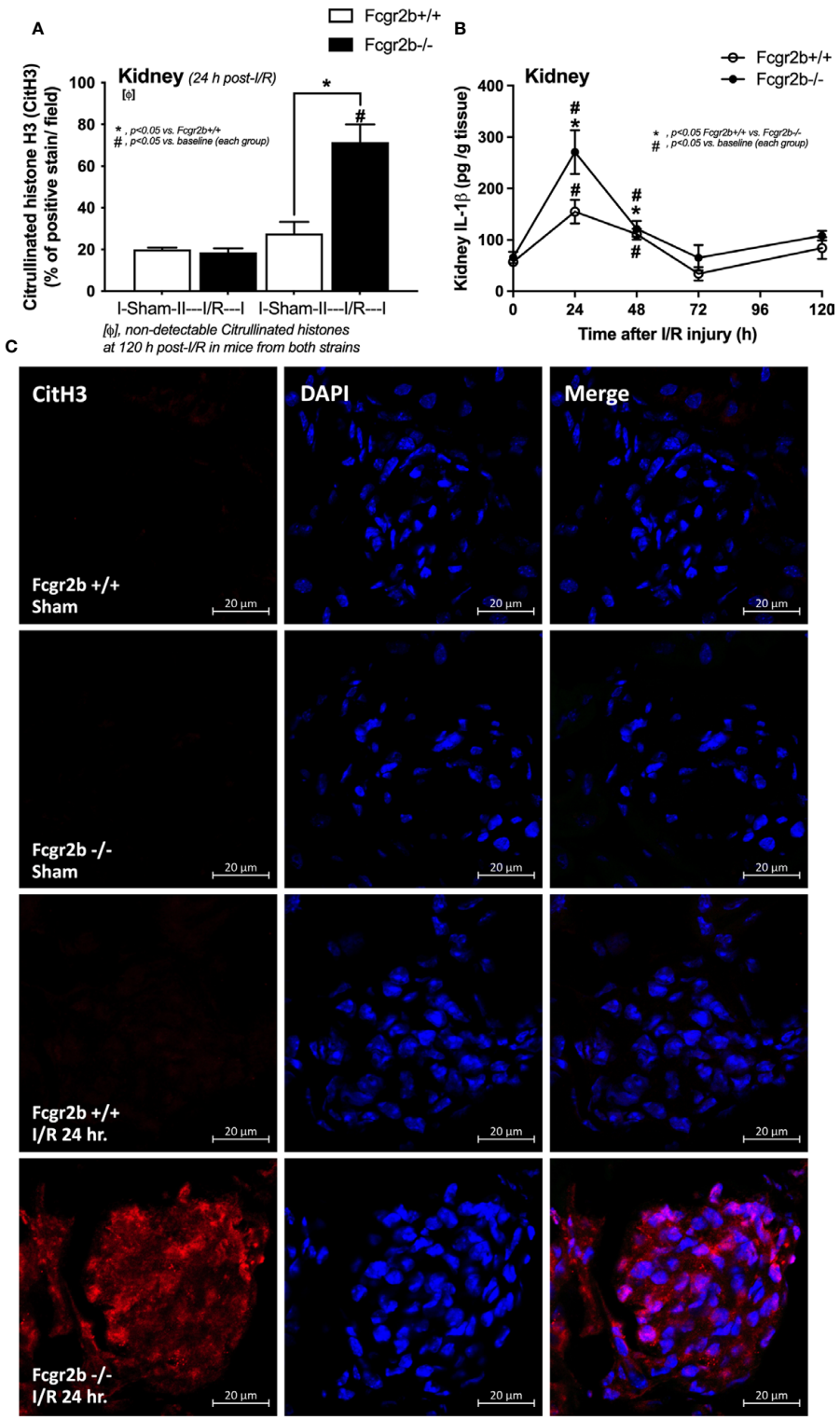


FIGURE 4 | Renal ischemia reperfusion injury (I/R) at 24 h induced more prominent neutrophil extracellular traps (NETs) in renal glomeruli of lupus prone mice. Characteristics of NETs in kidneys from Fcgr2b-/- mice or wild-type (Fcgr2b+/+) mice after renal ischemia reperfusion injury (I/R) as determined by immunofluorescent staining of citrullinated histone H3 (CitH3) at 24 h post-I/R **(A)** (n = 5–6/group) and IL-1β from renal tissue **(B)** (n = 5–6/time-point) with the representative immunofluorescent pictures of CitH3 (red) and 4',6-diamidino-2-phenylindole (DAPI, blue nuclear staining) at 24 h post-I/R (or sham) (original magnification 630x) **(C)** are demonstrated.

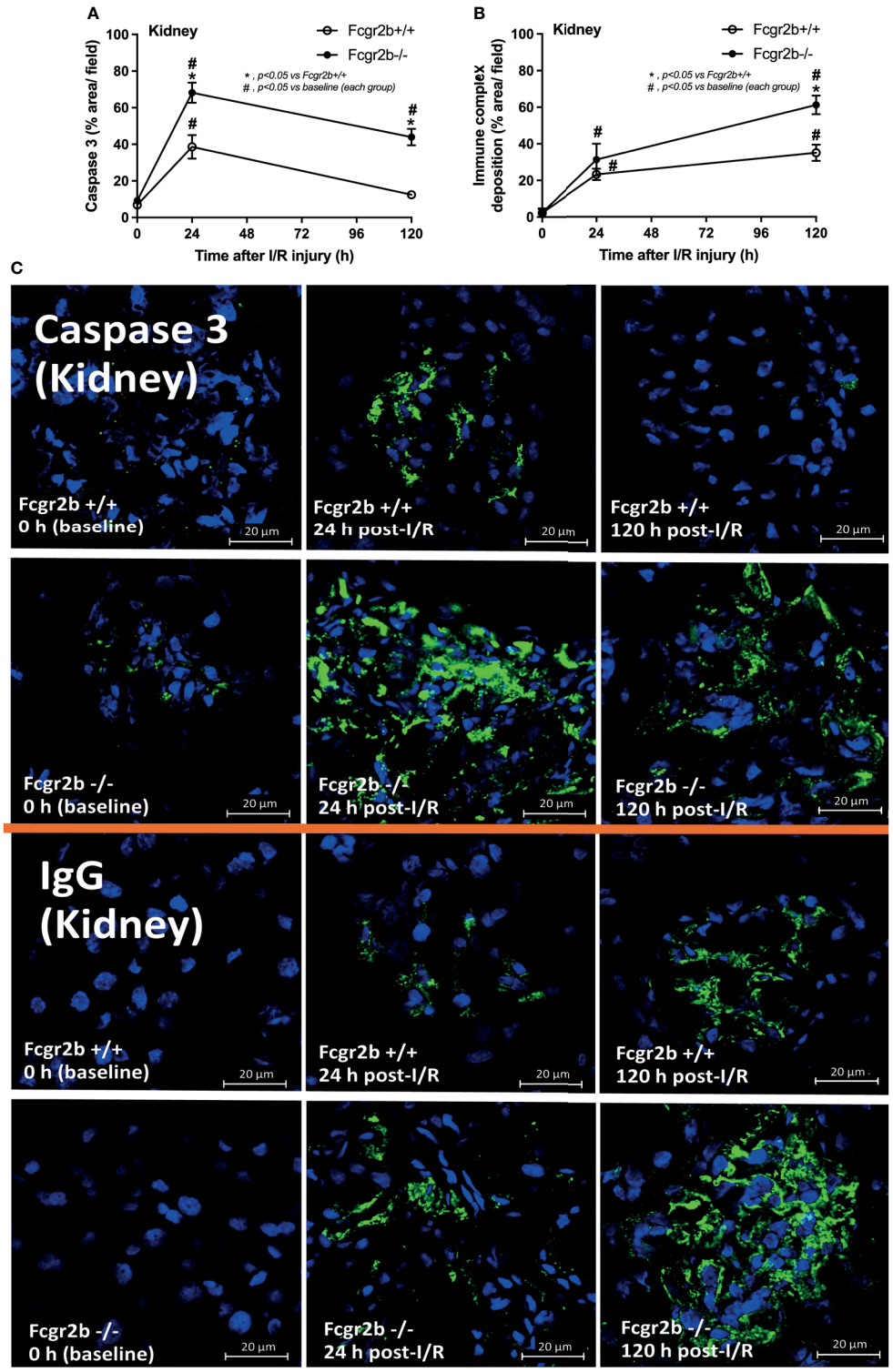


FIGURE 5 | Renal ischemia reperfusion injury (I/R) induced more prominent apoptosis at 24 h post-I/R and immunoglobulin G (IgG) deposition at120 h post-I/R in renal glomeruli of lupus prone mice. Characteristics of renal injury from Fcgr2b-/- or wild-type (Fcgr2b+/+) mice after renal ischemia reperfusion injury (I/R) as evaluated by glomerular apoptosis (activated caspase 3) **(A)**, glomerular IgG deposition **(B)** (n = 6–7/time-point) with the representative immunofluorescent glomerular pictures (activated caspase 3 and IgG deposition) from mice at 0, 24, and 120 h post-I/R (original magnification 630x) **(C)** are demonstrated.

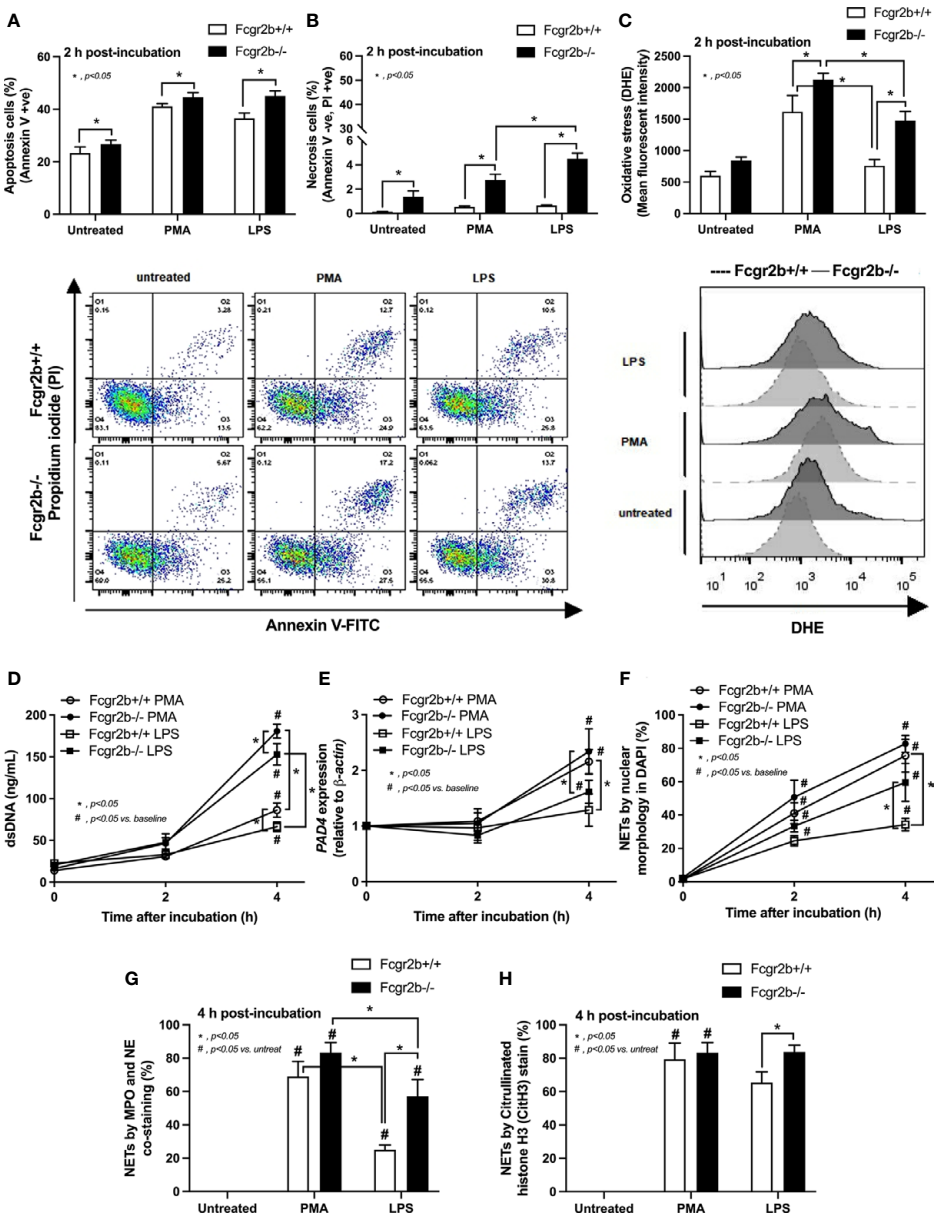


FIGURE 6 | Prominent apoptosis (with oxidative stress) and neutrophil extracellular traps (NETs) at 2 h and 4 h of the stimulation in neutrophils of lupus prone mice. Responses of Fcgr2b-/- and wild-type (Fcgr2b+/+) neutrophils after 2 h activation by phorbol myristate acetate (PMA), which is a NETs activator, or lipopolysaccharide (LPS), which is a TLR-4 stimulator, as evaluated using i) cell apoptosis, positive (+ve) Annexin V with negative (-ve) Propidium iodide (PI) or necrosis, -ve Annexin V negative with +ve PI, with the representative flow cytometry patterns **(A, B)** and ii) reactive oxygen species (ROS) using dihydroethidium (DHE) with the representative flow cytometry patterns **(C)** are demonstrated. Additionally, NETs were determined in time-points by supernatant dsDNA **(D)**, *PAD4* expression **(E)**, nuclear morphology by 4',6-diamidino-2-phenylindole (DAPI), a blue nuclear staining **(F)** and the co-staining of myeloperoxidases (MPO), and neutrophil elastase (NE) **(G)** or citrullinated histone H3 (CitH3) **(H)** at the 4 h of stimulation using immunofluorescence are demonstrated (independent triplicated experiments were performed).

NETosis (serum dsDNA, MPO, and glomerular NETs) and glomerular apoptosis (**Figures 10A–E**) in Fcgr2b-/- mice at 24 h post renal-I/R affected to decreased glomerular Ig deposition and attenuated lupus activity (anti-dsDNA, proteinuria and Scr) after 120 h post renal-I/R (**Figures 10F–I**). These data indicated that the attenuation of program cell death (apoptosis and NETosis) in renal injury by the Syk inhibitor could prevent lupus disease exacerbation.

Although the reduced NETs along with the decreased anti-dsDNA by Syk inhibitor implied an association between NETs and auto-antibody production of post-renal I/R, Syk inhibitor might directly block the antibody production through FcgR signaling (20, 21), except for NETs attenuation. To further support the association between NETs formation and auto-antibody production, a PAD4 inhibitor, a direct NETs inhibitor, was administered in Fcgr2b-/- mice

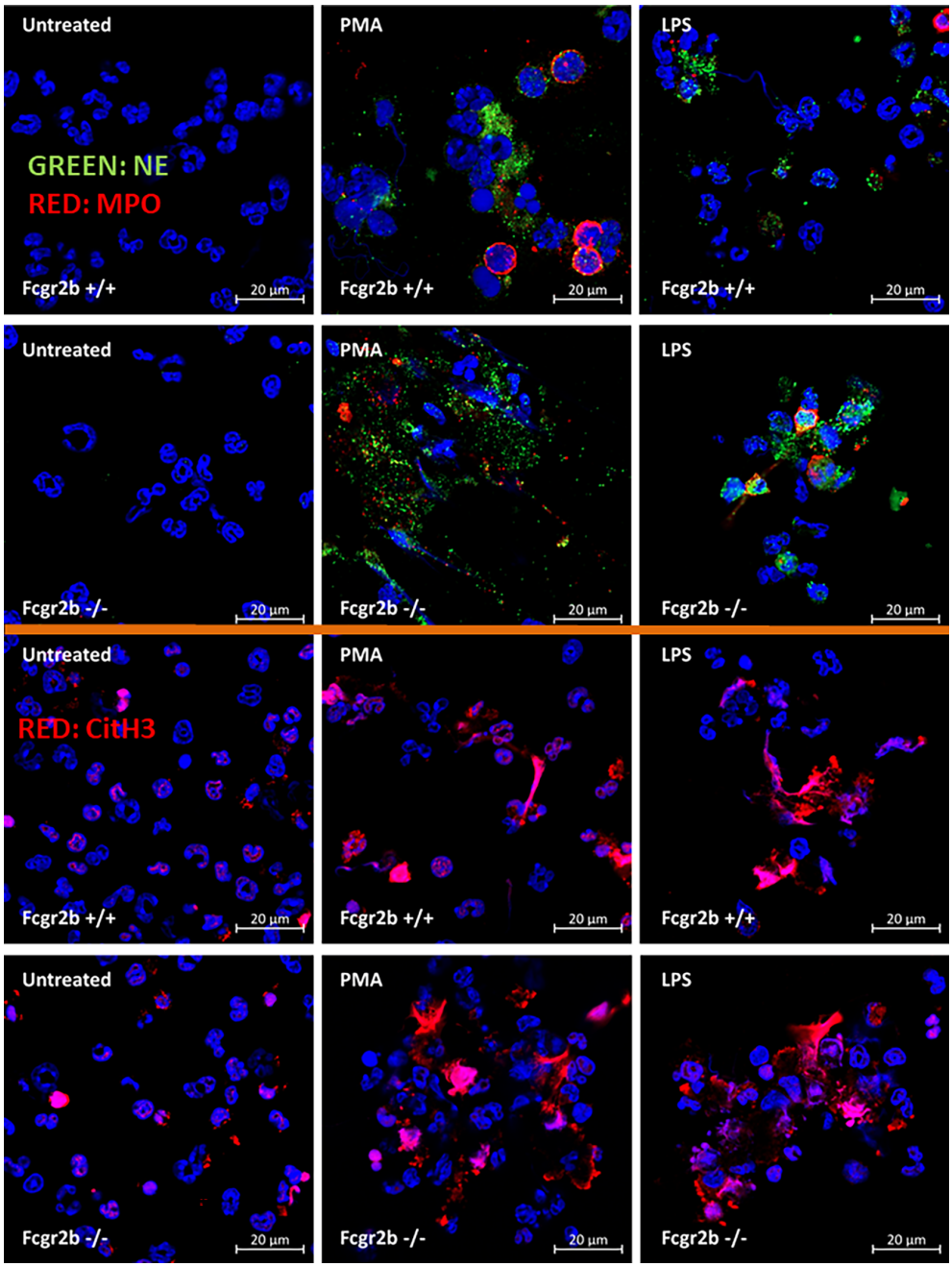


FIGURE 7 | Prominent neutrophil extracellular traps (NETs) at 4 h of the stimulation in neutrophils of lupus prone mice. The representative immunofluorescent pictures of NETs formation in Fcgr2b-/- and wild-type (Fcgr2b+/+) neutrophils after 4 h activation by phorbol myristate acetate (PMA), a NETs activator, or lipopolysaccharide (LPS), a TLR-4 stimulator, as evaluated by the co-staining of myeloperoxidases (MPO) and neutrophil elastase (NE) (upper part) or citrullinated histone H3 (CitH3) (lower part) are demonstrated.

with renal I/R. Indeed, PAD4 inhibitor decreased NETs (serum dsDNA, serum MPO, and glomerular NETs) at 24 h post-renal I/R and attenuated lupus characteristics (anti-dsDNA, proteinuria and Scr) at 120 h post-renal I/R (**Figures 11A–G**) supporting an impact of NETs formation on anti-dsDNA production and lupus exacerbation.

DISCUSSION

Renal injury at 24 h post renal-I/R prominently induced neutrophil extracellular traps (NETs) and apoptosis in kidneys of Fcgr2b-/- lupus mice that exacerbated the lupus activity at

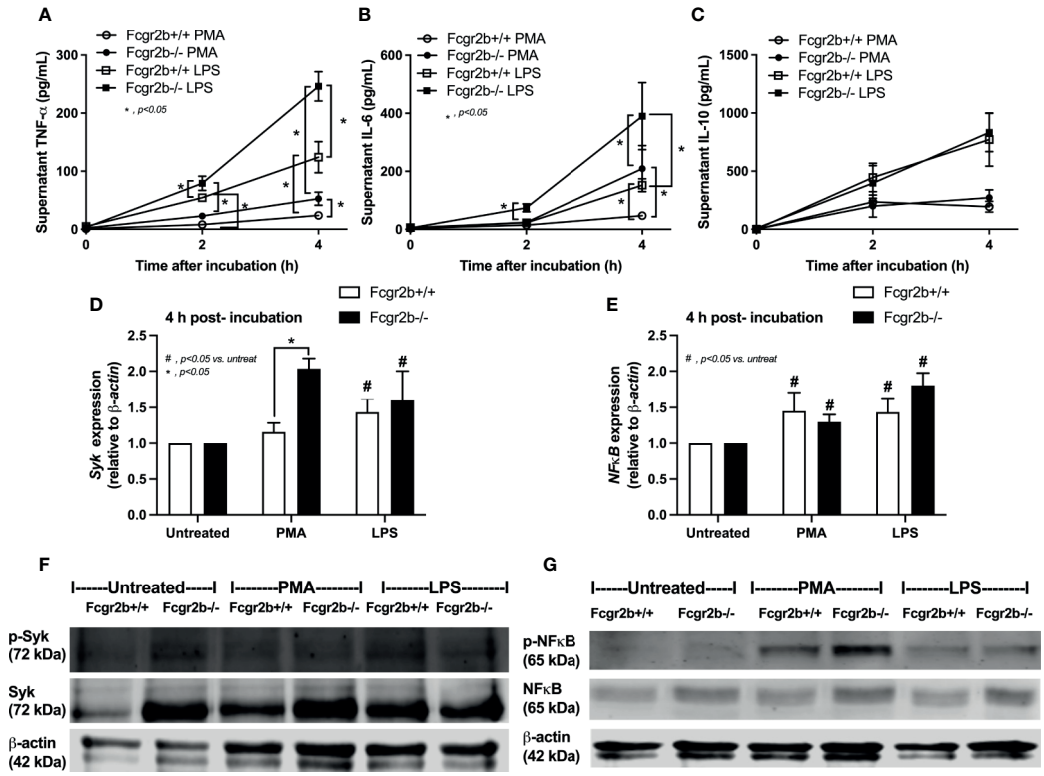


FIGURE 8 | Prominent cytokine production at 4 h through Spleen tyrosine kinase (*Syk*) and nuclear factor kappa B (*NFκB*) in neutrophils of lupus prone mice. Responses of Fcgr2b-/- and wild-type (Fcgr2b+/+) neutrophils after activation by phorbol myristate acetate (PMA), a NETs activator, or lipopolysaccharide (LPS), a TLR-4 stimulator, as evaluated in time-points by supernatant cytokines (TNF-α, IL-6 and IL-10) **(A–C)** and the downstream signals (at 4 h of the stimulation) in gene expression (*Syk* and *NFκB*) **(D, E)** and protein abundances (Syk/phosphorylated-Syk and NFκB/phosphorylated NFκB) with the representative pictures of Western blot analysis **(F, G)** are demonstrated (independent triplicated experiments were performed).

120 h post renal-I/R. However, the inhibitors against Syk and PAD4 attenuated the NETs at 24 h post-renal I/R and prevented lupus exacerbation at 120 h post-renal I/R.

Program Cell Death Exacerbates Lupus Disease Activity

To avoid an influence of lupus-induced renal impairment on the renal-I/R model, 8-week-old Fcgr2b-/- mice (asymptomatic lupus prone mice) were used in all experiments and lupus disease activity parameters (anti-dsDNA, proteinuria and Scr) were observed (72). They are well-known for apoptosis (with secondary necrosis), NETosis, and apoNETosis, the pathways of program cell death that cause exposure of auto-antigens from nuclei, which could exacerbate lupus activity (35). Indeed, both of NOX2-dependent NETosis and caspase 3-associated apoptosis after renal-I/R (34, 73) as well as apoNETosis (NOX2-independent NETosis together with caspase 3 activation in the same neutrophils) were activated by high intensity of ultra-violet light (16) might enhance lupus disease activity. Although a simultaneous detection of apoptosis and NETosis at 24 h post renal-I/R was demonstrated, these characteristics was not the apoNETosis (apoptosis and NETosis in the same neutrophils). Perhaps, glomerular apoptosis at 24 h post renal-I/R might be consisted of apoptosis in both renal parenchymal cells and neutrophils. The exploration in this topic is outside the scope of this study. Nevertheless, the enhanced exposure of self-antigens through any cell death pathways possibly exacerbates lupus disease activity (35).

Prominent NETs and Apoptosis in Fcgr2b-/- Lupus Mice at 24 h Post-Renal I/R

Both NETosis and apoptosis in several cells after renal I/R have been previously mentioned (34, 73, 74), which might be associated with lupus disease exacerbation. Here, there was a similar kidney damage at 24 h post-renal I/R between Fcgr2b-/- and WT mice, but NETs formation (in peripheral blood neutrophils and the internal organs) and apoptosis (in kidneys and lungs) were more prominent in Fcgr2b-/- mice. These data supported the more susceptibility to NETs and apoptosis of Fcgr2b-/- mice than the WT. For the renal I/R-induced NETs, NETs in neutrophils locally accumulated in the injured kidneys and remotely deposited in the lungs through the induction of damage, which was associated with the Damage Associated Molecular Patterns (DAMPs) from renal tubular necrosis as previously published (75). However, the effect of renal I/R on Fcgr2b-/- mice was more prominent than WT mice

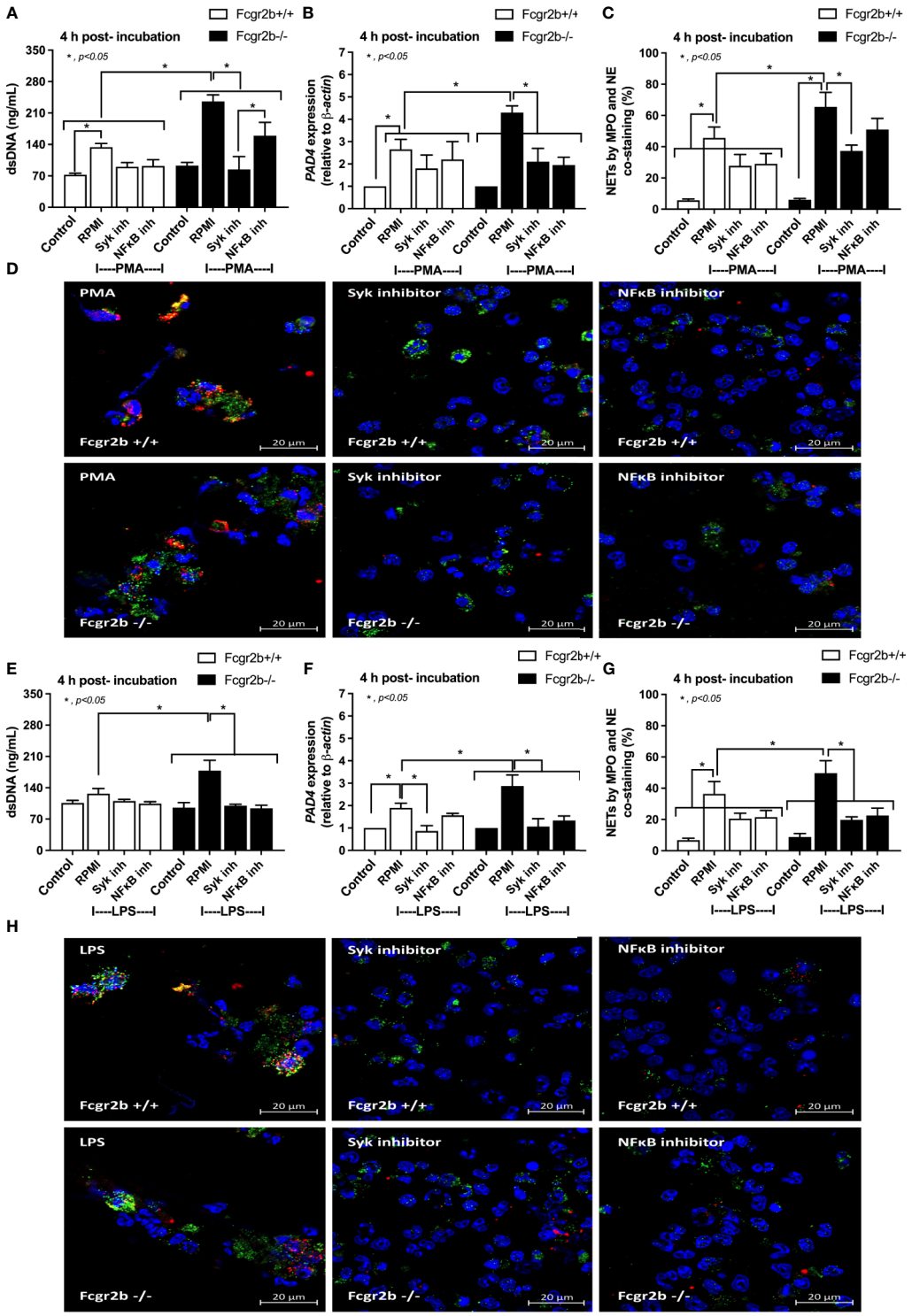


FIGURE 9 | The inhibitors against Spleen tyrosine kinase (Syk) or Nuclear factor kappa B (NFκB) attenuated neutrophil extracellular traps (NETs). NETs formation in Fcgr2b-/- and wild-type (Fcgr2b+/+) neutrophils after 4 h activation by phorbol myristate acetate (PMA), a NETs activator, with or without inhibitors against Syk (Syk inhibitor) or NFκB (NFκB inhibitor) as determined by supernatant dsDNA **(A)**, *PAD4* expression **(B)** and co-staining of myeloperoxidase (MPO) and neutrophil elastase (NE) with the representative immunofluorescent pictures **(C, D)** are demonstrated. In parallel, NETs formation after activation by lipopolysaccharide (LPS), a TLR-4 stimulator, with or without the inhibitors as determined by the same parameters **(E–H)** are also demonstrated (independent triplicated experiments were performed). RPMI, Roswell Park Memorial Institute media (for neutrophils); Control group using only RPMI without the stimulation.

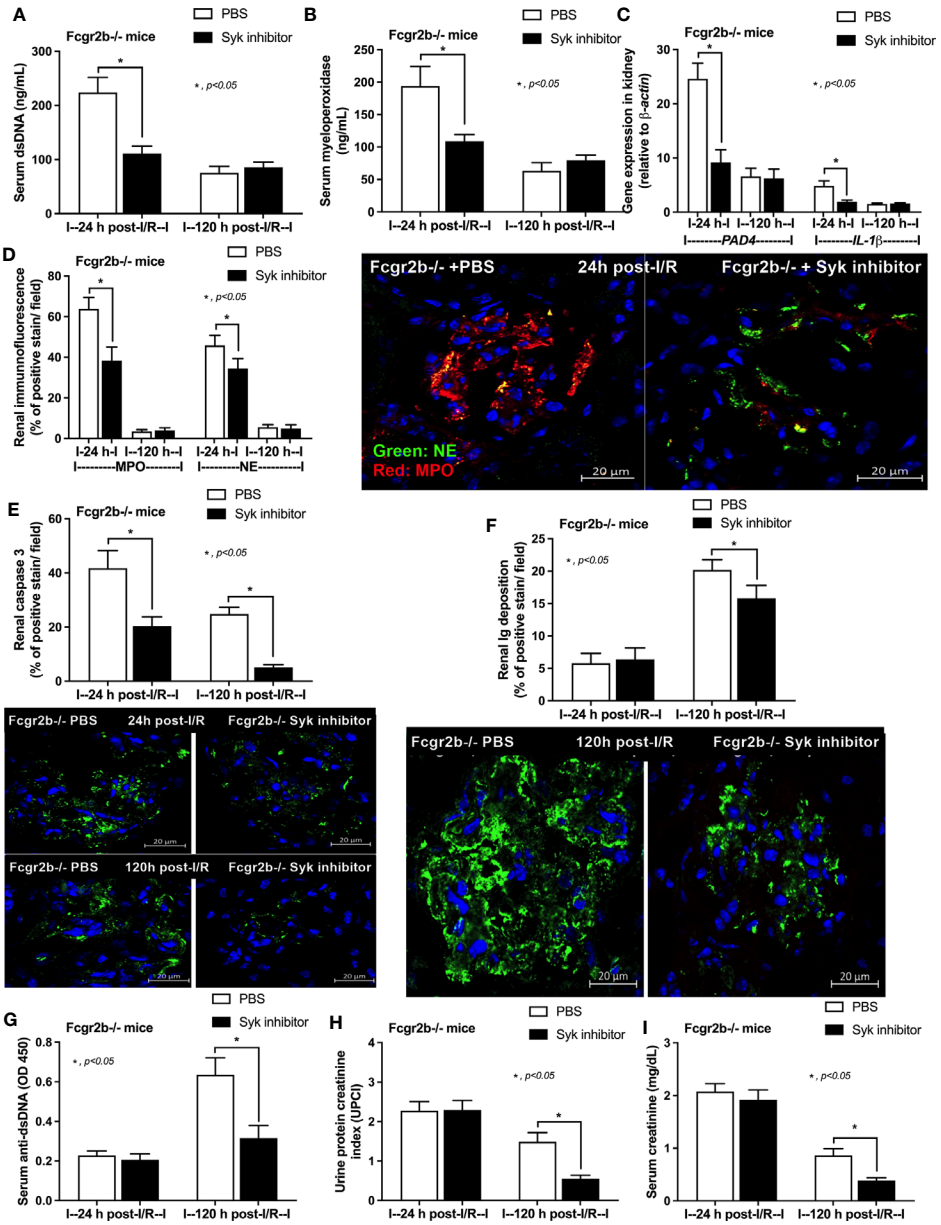


FIGURE 10 | Spleen tyrosine kinase (Syk) inhibitor decreased neutrophil extracellular traps (NETs) at 24 h after renal ischemia reperfusion injury (I/R) and attenuated lupus characteristics (anti-dsDNA, glomerular immunoglobulin deposition and lupus nephritis) at 120 h post-I/R in lupus prone mice. Characteristics of Fcgr2b-/- mice after renal I/R with Syk inhibitor or phosphate buffer solution (PBS) as determined by i) indicators of NETs in serum; serum dsDNA and serum myeloperoxidase (MPO) **(A, B)**, ii) NETs in kidneys; expression of *PAD4* and *IL-1β* **(C)** and co-staining of MPO and neutrophil elastase (NE) with the representative pictures **(D)**, iii) glomerular apoptosis (active caspase 3 staining) and immunoglobulin deposition with the representative pictures **(E, F)**, and iv) lupus nephritis characteristics; serum dsDNA, proteinuria (urine protein creatinine index; UPCI), and serum creatinine **(G–I)** are demonstrated (n = 5–7/group).

perhaps through the hyper-responsiveness from inhibitory Fc gamma receptor (FcgR) deficiency (76). The upregulation of activating-FcgRs without Fcgr2b inhibitory signaling partly generated the increased responses of Fcgr2b-/- macrophages (8, 77). Because i) NETosis from activation on TLR-4, one of the receptors for DAMPs (78, 79), is well-known (80), ii) the crosstalk between TLR-4 and activating-FcgRs (20, 21, 59), which is the profound reaction against DAMPs of Fcgr2b-/- mice, is possible, and iii) both TLR-4 and FcgRs are presented on neutrophils (78, 81). Therefore, the more severe NETosis at 24 h post-renal I/R in Fcgr2b-/- mice is probably resulted from the TLR-4/activating-FcgRs cross-talk on neutrophils, which is similar to the Fcgr2b-/- macrophages (20, 21). However, renal ischemia induced liver and cardiac injury (27, 28) was not associated with NETs that would be consistent with the non-detectable NETs in these organs. Notably, the upregulated *PAD4* and *IL-1β* without the positive detection of

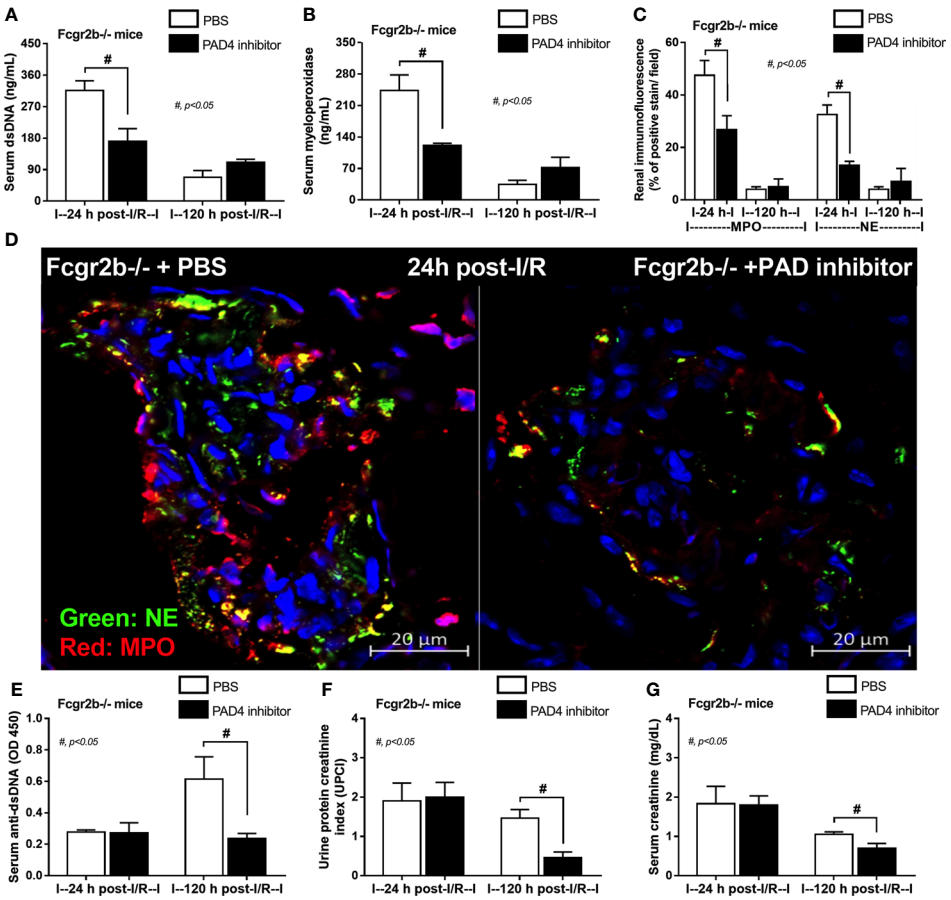


FIGURE 11 | Peptidylarginine deiminase 4 (PAD4) inhibitor decreased neutrophil extracellular traps (NETs) at 24 h after renal ischemia reperfusion injury (I/R) and attenuated lupus characteristics (anti-dsDNA, glomerular immunoglobulin deposition and lupus nephritis) at 120 h post-I/R in lupus prone mice. Characteristics of Fcgr2b-/- mice after renal I/R with PAD4 inhibitor or phosphate buffer solution (PBS) as determined by indicators of NETs in serum; serum dsDNA and serum myeloperoxidase (MPO) **(A, B)**, NETs in kidneys; co-staining of MPO and neutrophil elastase (NE) with the representative pictures **(C, D)** and characteristics of lupus nephritis; serum dsDNA, proteinuria (urine protein creatinine index; UPCI), and serum creatinine **(E–G)** are demonstrated (n = 4–5/group).

MPO and NE in livers and hearts supported pro-inflammatory activation (27, 28) in these organs without NETosis.

On the other hand, the renal I/R induces apoptosis of the renal parenchymal cells and the accumulated immune cells (32, 33), especially neutrophils (29–31). At 24 h post-renal I/R, apoptosis in kidneys and lungs of Fcgr2b-/- mice was more prominent than WT mice, possibly due to the hyper-inflammation induced apoptosis. Accordingly, DAMPs-activated TLR-4 induces massive apoptosis in parenchymal cells (kidneys and lungs) and immune cells (macrophages and neutrophils) after renal-I/R is well-known (82–85). Furthermore, the enhanced TLR-4 activation in Fcgr2b-/- mice through TLR-4/activating-FcgRs cross-talk (20, 21), might also be responsible to immune hyper-responsiveness and profound apoptosis. Nevertheless, both NETs and apoptosis were more prominent in Fcgr2b-/- mice than WT at 24 h post-I/R, which possibly enhanced self-antigens presentation and increased auto-antibody production (12, 16).

Prominent Anti-dsDNA and Immune Complex Deposition, but Not NETs, in Fcgr2b-/- Lupus Mice at 120 h Post-Renal I/R Exacerbates the Lupus Activity

The association between the program cell death pathways and the lupus exacerbation through the enhanced auto-antibody production is well-established (35). Here, the program cell deaths (NETosis and apoptosis) at 24 h post-renal I/R enhanced the production of anti-dsDNA in Fcgr2b-/- mice at 120 h post-renal I/R were demonstrated. The prominent anti-dsDNA, which is a major lupus auto-antibody, in Fcgr2b-/- mice at 120 h post-renal I/R suggests an impact of the loss of immune tolerance in these lupus mice (25). Interestingly, anti-dsDNA is inducible very shortly after I/R (5 days) in 8-week-old Fcgr2b-/- mice (asymptomatic lupus prone mice), despite the low-level of anti-dsDNA at baseline which is similar to the level in WT mice, indicating the existence of auto-reactive B cells in Fcgr2b-/- mice. Indeed, the clonal expansion of self-reactive B cells in germinal center is one of the main

pathogenesis of autoimmune diseases (86). In this study, plasma cells and activated B cells in spleen of Fcgr2b-/- mice were higher than WT at 120 h post-renal I/R, supporting that a prominent activity of these immune cells in lupus that might be responsible for the rapid induction of anti-dsDNA. Therefore, the loss of inhibitory FcgRs in autoreactive B cells of Fcgr2b-/- mice might be more susceptible to the non-specific inflammatory activation from renal-I/R, which led to a rapid clonal expansion and an acceleration of the auto-antibody production (62).

Additionally, the prominent immune complex (IC) deposition at 120 h post-renal I/R in Fcgr2b-/- mice possibly resulted in mononuclear cell infiltrations and inflammatory responses in several organs. In contrast, the only abnormality in WT mice at 120 h post-renal I/R was proteinuria (with normal Scr) due to the incomplete recovery of proximal renal tubules (87). At 120 h post-renal I/R, Fcgr2b-/- mice demonstrated the lupus characteristics as indicated by Scr, anti dsDNA, proteinuria, and glomerular IC deposition. Due to the non-detectable renal MPO and NE in lupus mice at 120 h post-I/R, renal injury was not directly caused by NETs but perhaps the enhanced glomerular IC deposition. Hence, profound NETs and apoptosis at 24 h post renal-I/R in Fcgr2b-/- mice further caused the lupus exacerbation at 120 h post-I/R which might be due to i) accelerated auto-antibody production from the enhanced self-antigen presentation by NETosis and apoptosis (88–90) and ii) IC deposition induced inflammation (91). These results indicated that acute kidney injury in lupus acted as an exacerbating factor through the program cell death pathways.

The Increased Susceptibility to Apoptosis and NETosis of Fcgr2b-/- Neutrophils and the Syk Inhibition: A Potential Clinical Translation

Although the activation of inhibitory-Fcgr2b in T cells could induce the T cell apoptosis (92), the hyper-inflammatory responses of Fcgr2b-/- macrophages (due to the inhibitory loss) cause the profound LPS-induced apoptosis (13). Because the inhibitory Fcgr2b presents in all myeloid cells (93) (not only macrophages but also neutrophils), Fcgr2b-/- neutrophils might be more susceptible to the cell death pathways. Although, PMA (94) and LPS (95) are a well-known NETs stimulator and a potent apoptosis inducer, respectively, both agents could induce both apoptosis and NETosis (65–67, 96, 97). Indeed, PMA and LPS induced the more prominent apoptosis and NETosis through Syk and NFκB in Fcgr2b-/- neutrophils compared with WT at 2 h and 4 h, respectively, supported the previous publications (69, 98). Because the data of NETosis were less compared to apoptosis in Fcgr2b-/- immune cells, NETosis was further explored. As such, both gene

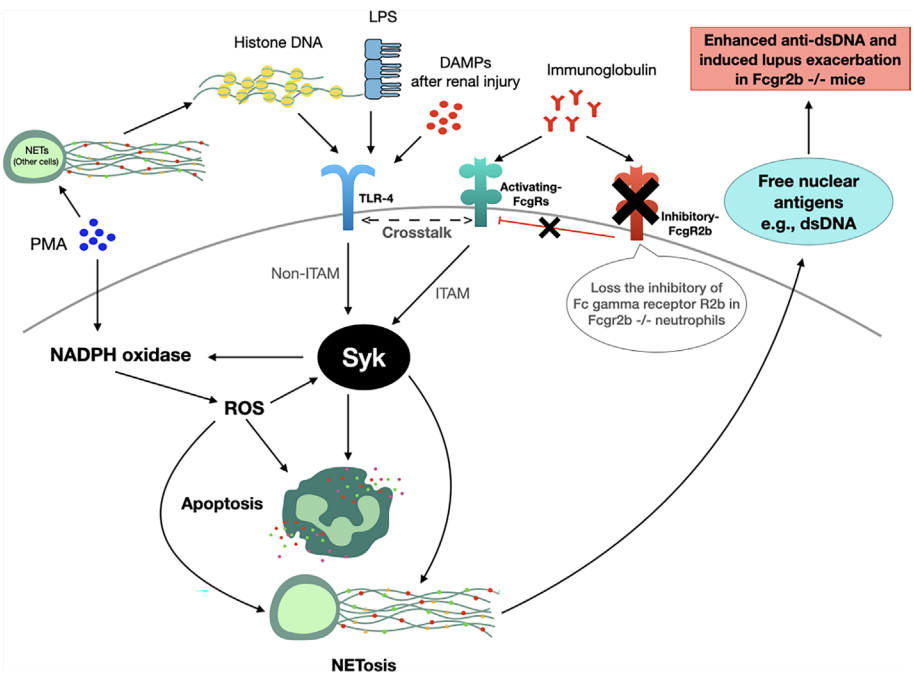


FIGURE 12 | The working hypothesis. Spleen tyrosine kinase (Syk) is a possible shared-downstream signaling of i) reactive oxygen species (ROS) derived from NADPH oxidase 2 (NOX2)-dependent PMA stimulation (100), ii) direct TLR-4 activation through DAMPs (damage associated molecular patterns) from renal ischemia (in mice) or lipopolysaccharide (LPS) (*in vitro*), iii) indirect TLR-4 activation from DNA histone released from PMA-induced NETosis (99) and iv) Fc gamma receptors (FcgRs) (98). Indeed, Syk, activated through immunoreceptor tyrosine-based activation motif (ITAM) and non-ITAM dependent signals from FcgRs and TLR-4, respectively (37), could enhance both apoptosis (2 h post-stimulation) and NETosis (4 h post-stimulation) (100, 101). Hence, prominent Syk activation in Fcgr2b-/- neutrophils compared with wild-type (WT) might be due to the crosslink between TLR-4 and activating-FcgRs (20, 21, 58) without the inhibitory receptor (blue cross line). After that, the profound free nuclear antigens, including dsDNA, from apoptosis and NETosis exacerbates lupus activity from the prominent anti-dsDNA production in Fcgr2b-/- mice but not in WT (+ve, positive signal; -ve, negative signal).

expression and protein quantification of Syk and NFκB in Fcgr2b-/- neutrophils were higher than WT cells and the inhibition of both Syk and NFκB attenuated the NETosis, indicating a possible association between Syk and Fc gamma receptors (46, 99). In addition, the association between NETs and lupus exacerbation was demonstrated in renal I/R Fcgr2b-/- mice along with the inhibitors against NETs (Syk and PAD4 inhibitors). Both inhibitors effectively attenuated NETs at 24 h post-renal I/R and decreased anti-dsDNA at 120 h of the model, supporting that NETs blockade could prevent the renal I/R-induced lupus exacerbation.

The working hypothesis of the *in vivo* and *in vitro* experiments is presented in **Figure 12**. Accordingly, TLR-4 is an important pathway for apoptosis and NETosis (36), which could be induced by LPS, DAMPs (from renal-I/R), and DNA histones (from NETosis of PMA and renal-I/R) (100) possibly through the NADPH oxidase 2 (NOX2) dependent pathway (66, 102, 103). Likewise, Fc gamma receptors are the initiation of NETosis through Syk activation (37). Because i) Syk is a downstream of Fc gamma receptors and TLR-4 through immunoreceptor tyrosine-based activation motif (ITAM) and non-ITAM dependent pathways, respectively (37), ii) Syk is a possible shared downstream signaling from TLR-4, Fc gamma receptors and PMA (**Figure 10**), which activated the Syk through ROS from NOX2-dependent PMA stimulation (102), and iii) Syk also enhances ROS production (104, 105) that could accelerate both apoptosis and NETosis (102), and this inhibitor is an interesting drug for use in lupus. Thus, a possible mechanism that is responsible for prominent apoptosis and NETosis in Fcgr2b-/- neutrophils over WT might be an enhanced TLR-4 activity due to the crosstalk between TLR-4 and activating Fc gamma receptors (106) through Syk (and NFκB) without the inhibitory Fcgr2b (**Figure 12**). Despite an incomplete data on the association between Syk and Fc gamma receptors, the attenuation of NETosis and apoptosis with the prevention on lupus exacerbation by Syk inhibitor in Fcgr2b-/- mice with renal-I/R is interesting. Since Syk inhibitors are clinically available (107–110) for either lupus (42) or non-lupus conditions (20, 21, 101, 111), Syk inhibitor might be useful for the prevention of renal injury-induced lupus exacerbation. Future studies are of interest.

In conclusion, the prominent NETs and the Syk activation were observed in Fcgr2b-/- mice after renal I/R injury that induced lupus exacerbation. The attenuation of NETs using Syk inhibitor, possibly through reduction of the downstream signaling of TLR-4 and Fc gamma receptors, was proposed as an interesting strategy for the treatment in lupus. Further studies are warranted.

DATA AVAILABILITY STATEMENT

The datasets presented in this study can be found in online repositories. The names of the repository/repositories and accession number(s) can be found in the article/**Supplementary Material**.

ETHICS STATEMENT

The animal study was reviewed and approved by Institutional Animal Care and Use Committee of the Faculty of Medicine, Chulalongkorn University, Bangkok, Thailand. Written informed consent was obtained from the owners for the participation of their animals in this study.

AUTHOR CONTRIBUTIONS

WS designed and coordinated all the experiments, performed *in vitro* and *in vivo* experiments, and wrote and approved the manuscript. SS performed *in vitro* experiments, and approved the manuscript. PPh performed *in vitro* and *in vivo* experiments, and approved the manuscript. KU performed *in vitro* experiments, and approved the manuscript. TB performed *in vitro* experiments, and approved the manuscript. PV performed *in vivo* experiments, and approved the manuscript. AC performed *in vitro* experiments, and approved the manuscript. PPi supervised *in vitro* experiments, and approved the manuscript. DC supervised *in vitro* experiments, and approved the manuscript. AL designed and coordinated all the experiments, analyzed all of these experiment, and wrote and approved the manuscript. All authors contributed to the article and approved the submitted version.

FUNDING

This research is supported by the Program Management Unit for Human Resources & Institutional Development Research and Innovation-CU [Global Partnership B16F630071 and Flagship B05F630073], and the TSRI Fund (CU_FRB640001_01_23_1) and National Research Council of Thailand. WS is funded by the 90th Anniversary of Chulalongkorn University Fund (Ratchadapisek Sompote Endowment Fund).

ACKNOWLEDGMENTS

The authors would like to thank Jiradej Makjaroen, Ph.D. and Dang Phi Cong, M.D., Faculty of Medicine, Chulalongkorn University, as well as Arthid Thim-uam, Ph.D., School of Medical Sciences, University of Phayao for helping with the Western Blot and flow cytometry analysis.

SUPPLEMENTARY MATERIAL

The Supplementary Material for this article can be found online at: https://www.frontiersin.org/articles/10.3389/fimmu.2021.669162/full#supplementary-material

Supplementary Figure 1 | The age-dependent lupus characteristics of Fcgr2b-/- mice and the injury from renal ischemia reperfusion injury (I/R). Age-dependent lupus nephritis of Fcgr2b-/- mice compared with wild-type (Fcgr2b+/+) mice; serum creatinine, urine protein creatinine index (UPCI) and serum anti-dsDNA, **(A–C)** and the characteristics in time-point of Fcgr2b-/- or Fcgr2b+/+ mice after renal ischemia reperfusion injury (I/R) as determined by gene expression of cytokines (*TNF-α*, *IL-6* and *IL-10*) in kidneys **(D–F)**, liver **(G–I)**, heart **(J–L)**, lung **(M–O)** and the

representative Hematoxylin and Eosin (H&E) staining (original magnification 200x) of liver and lung at 120 h post renal I/R **(P)** are demonstrated (n = 6–7/time-point). Notably, the renal histological pictures at other time-points of both mouse strains are not demonstrated due to the similarity to Fcgr2b-/- mice at 120 h post I/R (normal histology).

Supplementary Figure 2 | Renal ischemia reperfusion injury (I/R) induced more prominent neutrophil extracellular traps (NETs) in lungs of lupus prone mice. Characteristics of NETs in lungs from Fcgr2b-/- or wild-type (Fcgr2b+/+) mice after renal ischemia reperfusion injury (I/R) as determined by co-staining of myeloperoxidases (MPO) and neutrophil elastase (NE) at 24 h post-I/R **(A)** (n = 5–8/group) and gene expression in the time-point of *IL-1β* and *PAD4* **(B, C)** (n = 6–7/time-point) with the representative immunofluorescent pictures of NE (green), MPO (red) and 4',6-diamidino-2-phenylindole (DAPI, blue nuclear staining) at 24 h post-I/R (or sham) (original magnification 630x) **(D)** are demonstrated. Additionally, the score of MPO and NE co-staining at 24 h post-I/R **(E)** with *IL-1β* and *PAD4* in liver **(F, G)** and in hearts **(H–J)** (n = 6–7/group or time-point) are also demonstrated.

Supplementary Figure 3 | Renal ischemia reperfusion injury (I/R) induced more prominent apoptosis and immunoglobulin G (IgG) deposition in lungs of lupus prone mice. Characteristics of lung injury from Fcgr2b-/- or wild-type (Fcgr2b+/+) mice after renal ischemia reperfusion injury (I/R) as evaluated by apoptosis (activated caspase 3) **(A)**, IgG deposition **(B)** (n = 6–7/time-point for **A–D)** with the representative immunofluorescent pictures (activated caspase 3 and IgG deposition) from mice at 0, 24 and 120 h post-I/R (original magnification 630x) **(E)** are demonstrated.

Supplementary Figure 4 | Prominent activation of plasma cells and activated B cells in spleen of lupus mice at 120 h post-renal I/R. Characteristics of immune cells in spleen at 120 h after sham or renal ischemia reperfusion injury (I/R) from Fcgr2b-/- and wild-type (Fcgr2b+/+) mice as indicated by the abundance in spleen of plasma cell (CD138 and B220 positive cells) **(A)**, activated B cells (MHC II and B220 positive cells) **(B)**, germinal center B cells (CD19 and GL7 positive cells) **(C)**, follicular B cells (CXCR5 and B220 positive cells) **(D)** and the representative flow cytometry analysis of plasma cells and activated B cells **(E)** are demonstrated (n = 4-5/group).

Supplementary Figure 5 | Inhibitors against Spleen tyrosine kinase (Syk) or Nuclear factor kappa B (NFκB) attenuated neutrophil cytokine production. Supernatant cytokines (TNF-α, IL-6 and IL-10) in Fcgr2b-/- and wild-type (Fcgr2b+/+) neutrophils after 4 h activation by phorbol myristate acetate (PMA), a NETs activator, with or without inhibitors against Syk (Syk inh) or NFκB (NFκB inh) **(A–C)** or activation by lipopolysaccharide (LPS), a TLR-4 stimulator, **(D–F)** are demonstrated (independent triplicated experiments were performed). RPMI, Roswell Park Memorial Institute media (for neutrophils); Control group using only RPMI without the stimulation.

REFERENCES

1. Bolland S, Ravetch JV. Spontaneous Autoimmune Disease in Fcγriib-Deficient Mice Results From Strain-Specific Epistasis. *Immunity* (2000) 13 (2):277–85. doi: 10.1016/s1074-7613(00)00027-3
2. Clatworthy MR, Willcocks L, Urban B, Langhorne J, Williams TN, Peshu N, et al. Systemic Lupus Erythematosus-Associated Defects in the Inhibitory Receptor Fcγriib Reduce Susceptibility to Malaria. *Proc Natl Acad Sci* (2007) 104(17):7169–74. doi: 10.1073/pnas.0608889104
3. Crispín JC, Hedrich CM, Tsokos GC. Gene-Function Studies in Systemic Lupus Erythematosus. *Nat Rev Rheumatol* (2013) 9(8):476–84. doi: 10.1038/nrrheum.2013.78
4. Chu Z, Tsuchiya N, Kyogoku C, Ohashi J, Qian Y, Xu S, et al. Association of Fcγ Receptor IIb Polymorphism With Susceptibility to Systemic Lupus Erythematosus in Chinese: A Common Susceptibility Gene in the Asian Populations. *Tissue Antigens* (2004) 63(1):21–7. doi: 10.1111/j.1399-0039.2004.00142.x
5. Willcocks LC, Carr EJ, Niederer HA, Rayner TF, Williams TN, Yang W, et al. A Defunctioning Polymorphism in FCGR2B Is Associated With Protection Against Malaria But Susceptibility to Systemic Lupus Erythematosus. *Proc Natl Acad Sci USA* (2010) 107(17):7881–5. doi: 10.1073/pnas.0915133107
6. Smith KG, Clatworthy MR. FcgammaRIIB in Autoimmunity and Infection: Evolutionary and Therapeutic Implications. *Nat Rev Immunol* (2010) 10 (5):328–43. doi: 10.1038/nri2762
7. Ondee T, Surawut S, Taratummarat S, Hirankarn N, Palaga T, Pisitkun P, et al. Fc Gamma Receptor IIB Deficient Mice: A Lupus Model With Increased Endotoxin Tolerance-Related Sepsis Susceptibility. *Shock* (2017) 47(6):743–52. doi: 10.1097/SHK.0000000000000796
8. Issara-Amphorn J, Surawut S, Worasilchai N, Thim-Uam A, Finkelman M, Chindamporn A, et al. The Synergy of Endotoxin and (1→ 3)-β-D-glucan, From Gut Translocation, Worsens Sepsis Severity in a Lupus Model of Fc Gamma Receptor IIb-Deficient Mice. *J Innate Immun* (2018) 10(3):189–201. doi: 10.1159/000486321
9. Rosales C. Neutrophil: A Cell With Many Roles in Inflammation or Several Cell Types? *Front Physiol* (2018) 9:113. doi: 10.3389/fphys.2018.00113
10. Kaplan MJ. Role of Neutrophils in Systemic Autoimmune Diseases. *Arthritis Res Ther* (2013) 15(5):219. doi: 10.1186/ar4325
11. Mistry P, Kaplan MJ. Cell Death in the Pathogenesis of Systemic Lupus Erythematosus and Lupus Nephritis. *Clin Immunol* (2017) 185:59–73. doi: 10.1016/j.clim.2016.08.010
12. Mahajan A, Herrmann M, Muñoz LE. Clearance Deficiency and Cell Death Pathways: A Model for the Pathogenesis of SLE. *Front Immunol* (2016) 7:35. doi: 10.3389/fimmu.2016.00035
13. Thim-Uam A, Surawut S, Issara-Amphorn J, Jaroonwitchawan T, Hiengrach P, Chatthanathon P, et al. Leaky-Gut Enhanced Lupus Progression in the Fc Gamma Receptor-IIb Deficient and Pristane-Induced Mouse Models of Lupus. *Sci Rep* (2020) 10(1):777. doi: 10.1038/s41598-019-57275-0
14. Jorch SK, Kubes P. An Emerging Role for Neutrophil Extracellular Traps in Noninfectious Disease. *Nat Med* (2017) 23(3):279–87. doi: 10.1038/nm.4294
15. Rohrbach AS, Slade DJ, Thompson PR, Mowen KA. Activation of PAD4 in NET Formation. *Front Immunol* (2012) 3:360. doi: 10.3389/fimmu.2012.00360
16. Azzouz D, Palaniyar N. ApoNETosis: Discovery of a Novel Form of Neutrophil Death With Concomitant Apoptosis and Netosis. *Cell Death Dis* (2018) 9(8):839. doi: 10.1038/s41419-018-0846-9
17. Bai Y, Tong Y, Liu Y, Hu H. Self-dsDNA in the Pathogenesis of Systemic Lupus Erythematosus. *Clin Exp Immunol* (2018) 191(1):1–10. doi: 10.1111/cei.13041
18. Jin B, Sun T, Yu X-H, Liu C-Q, Yang Y-X, Lu P, et al. Immunomodulatory Effects of dsRNA and Its Potential as Vaccine Adjuvant. *J BioMed Biotechnol* (2010) 2010:690438. doi: 10.1155/2010/690438
19. Kobiyama K, Jounai N, Aoshi T, Tozuka M, Takeshita F, Coban C, et al. Innate Immune Signaling by, and Genetic Adjuvants for DNA Vaccination. *Vaccines (Basel)* (2013) 1(3):278–92. doi: 10.3390/vaccines1030278
20. Issara-Amphorn J, Chancharoenthana W, Visitchanakun P, Leelahavanichkul A. Syk Inhibitor Attenuates Polymicrobial Sepsis in FcgRIIb-Deficient Lupus Mouse Model, the Impact of Lupus Characteristics in Sepsis. *J Innate Immun* (2020) 12(6):461–79. doi: 10.1159/000509111
21. Issara-Amphorn J, Somboonna N, Pisitkun P, Hirankarn N, Leelahavanichkul A. Syk Inhibitor Attenuates Inflammation in Lupus Mice From FcgRIIb Deficiency But Not in Pristane Induction: The Influence of Lupus Pathogenesis on the Therapeutic Effect. *Lupus* (2020) 29(10):1248–62. doi: 10.1177/0961203320941106
22. Yu Y, Su K. Neutrophil Extracellular Traps and Systemic Lupus Erythematosus. *J Clin Cell Immunol* (2013) 4:139. doi: 10.4172/2155-9899.1000139
23. Kuechle MK, Elkon KB. Shining Light on Lupus and UV. *Arthritis Res Ther* (2007) 9(1):101. doi: 10.1186/ar2100
24. Caricchio R, McPhie L, Cohen PL. Ultraviolet B Radiation-Induced Cell Death: Critical Role of Ultraviolet Dose in Inflammation and Lupus Autoantigen Redistribution. *J Immunol* (2003) 171(11):5778–86. doi: 10.4049/jimminol.171.11.5778
25. Pieterse E, van der Vlag J. Breaking Immunological Tolerance in Systemic Lupus Erythematosus. *Front Immunol* (2014) 5:164. doi: 10.3389/fimmu.2014.00164
26. Srisawat N, Kulvichit W, Mahamitra N, Hurst C, Praditpornsilpa K, Lumlertgul N, et al. The Epidemiology and Characteristics of Acute

Kidney Injury in the Southeast Asia Intensive Care Unit: A Prospective Multicentre Study. *Nephrol Dial Transplant* (2020) 35(10):1729–38. doi: 10.1093/ndt/gfz087
27. Sukkummee W, Jittisak P, Wonganan P, Wittayalertpanya S, Chariyavilaskul P, Leelahavanichkul A. The Prominent Impairment of Liver/Intestinal Cytochrome P450 and Intestinal Drug Transporters in Sepsis-Induced Acute Kidney Injury Over Acute and Chronic Renal Ischemia, a Mouse Model Comparison. *Ren Fail* (2019) 41(1):314–25. doi: 10.1080/0886022X.2019.1602054
28. Leelahavanichkul A, Somparn P, Panich T, Chancharoenthana W, Wongphom J, Pisitkun T, et al. Serum miRNA-122 in Acute Liver Injury Induced by Kidney Injury and Sepsis in CD-1 Mouse Models. *Hepatol Res* (2015) 45(13):1341–52. doi: 10.1111/hepr.12501
29. Bolisetty S, Agarwal A. Neutrophils in Acute Kidney Injury: Not Neutral Any More. *Kidney Int* (2009) 75(7):674–6. doi: 10.1038/ki.2008.689
30. Bonventre JV, Yang L. Cellular Pathophysiology of Ischemic Acute Kidney Injury. *J Clin Invest* (2011) 121(11):4210–21. doi: 10.1172/JCI45161
31. Cho W, Song JY, Oh SW, Kim MG, Ko YS, Lee HY, et al. Fate of Neutrophils During the Recovery Phase of Ischemia/Reperfusion Induced Acute Kidney Injury. *J Korean Med Sci* (2017) 32(10):1616–25. doi: 10.3346/jkms.2017.32.10.1616
32. Bonegio R, Lieberthal W. Role of Apoptosis in the Pathogenesis of Acute Renal Failure. *Curr Opin Nephrol Hypertens* (2002) 11(3):301–8. doi: 10.1097/00041552-200205000-00006
33. Price PM, Hodeify R. A Possible Mechanism of Renal Cell Death After Ischemia/Reperfusion. *Kidney Int* (2012) 81(8):720–1. doi: 10.1038/ki.2011.495
34. Nakazawa D, Kumar SV, Marschner J, Desai J, Holderied A, Rath L, et al. Histones and Neutrophil Extracellular Traps Enhance Tubular Necrosis and Remote Organ Injury in Ischemic AKI. *J Am Soc Nephrol* (2017) 28(6):1753–68. doi: 10.1681/ASN.2016080925
35. Yang F, He Y, Zhai Z, Sun E. Programmed Cell Death Pathways in the Pathogenesis of Systemic Lupus Erythematosus. *J Immunol Res* (2019) 2019:3638562. doi: 10.1155/2019/3638562
36. Dong Y, Jin C, Ding Z, Zhu Y, He Q, Zhang X, et al. TLR4 Regulates ROS and Autophagy to Control Neutrophil Extracellular Traps Formation Against *Streptococcus Pneumoniae* in Acute Otitis Media. *Pediatr Res* (2020) 89(4):785–94. doi: 10.1038/s41390-020-0964-9
37. Mócsai A, Ruland J, Tybulewicz VL. The SYK Tyrosine Kinase: A Crucial Player in Diverse Biological Functions. *Nat Rev Immunol* (2010) 10(6):387–402. doi: 10.1038/nri2765
38. Lin Y-C, Huang D-Y, Chu C-L, Lin Y-L, Lin W-W. The Tyrosine Kinase Syk Differentially Regulates Toll-Like Receptor Signaling Downstream of the Adaptor Molecules TRAF6 and TRAF3. *Sci Signal* (2013) 6(289):ra71. doi: 10.1126/scisignal.2003973
39. Nanì S, Fumagalli L, Sinha U, Kamen L, Scapini P, Berton G. Src Family Kinases and Syk Are Required for Neutrophil Extracellular Trap Formation in Response to β-Glucan Particles. *J Innate Immun* (2015) 7(1):59–73. doi: 10.1159/000365249
40. McKeage K, Lyseng-Williamson KA. Fostamatinib in Chronic Immune Thrombocytopenia: A Profile of Its Use in the USA. *Drugs Ther Perspect* (2018) 34(10):451–6. doi: 10.1007/s40267-018-0551-x
41. Smith J, McDaid JP, Bhangal G, Chawanasuntorapoj R, Masuda ES, Cook HT, et al. A Spleen Tyrosine Kinase Inhibitor Reduces the Severity of Established Glomerulonephritis. *J Am Soc Nephrol* (2010) 21(2):231–6. doi: 10.1681/ASN.2009030263
42. Kitai M, Fukuda N, Ueno T, Endo M, Maruyama T, Abe M, et al. Effects of a Spleen Tyrosine Kinase Inhibitor on Progression of the Lupus Nephritis in Mice. *J Pharmacol Sci* (2017) 134(1):29–36. doi: 10.1016/j.jphs.2017.02.015
43. McAdoo SP, Reynolds J, Bhangal G, Smith J, McDaid JP, Tanna A, et al. Spleen Tyrosine Kinase Inhibition Attenuates Autoantibody Production and Reverses Experimental Autoimmune GN. *J Am Soc Nephrol* (2014) 25 (10):2291–302. doi: 10.1681/ASN.2013090978
44. Surawut S, Ondee T, Taratummarat S, Palaga T, Pisitkun P, Chindamporn A, et al. The Role of Macrophages in the Susceptibility of Fc Gamma Receptor IIb Deficient Mice to *Cryptococcus neoformans*. *Sci Rep* (2017) 7:40006. doi: 10.1038/srep40006
45. Surawut S, Makjaroen J, Thim-Uam A, Wongphoom J, Palaga T, Pisitkun P, et al. Increased Susceptibility Against *Cryptococcus Neoformans* of Lupus Mouse Models (Pristane-Induction and FcGRIIb Deficiency) Is Associated With Activated Macrophage, Regardless of Genetic Background. *J Microbiol* (2019) 57(1):45–53. doi: 10.1007/s12275-019-8311-8
46. Kiefer F, Brumell J, Al-Alawi N, Latour S, Cheng A, Veillette A, et al. The Syk Protein Tyrosine Kinase Is Essential for Fcgamma Receptor Signaling in Macrophages and Neutrophils. *Mol Cell Biol* (1998) 18(7):4209–20. doi: 10.1128/mcb.18.7.4209
47. Kang L, Yu H, Yang X, Zhu Y, Bai X, Wang R, et al. Neutrophil Extracellular Traps Released by Neutrophils Impair Revascularization and Vascular Remodeling After Stroke. *Nat Commun* (2020) 11(1):2488. doi: 10.1038/s41467-020-16191-y
48. Mihara M, Tan I, Chuzhin Y, Reddy B, Budhai L, Holzer A, et al. CTLA4Ig Inhibits T Cell-Dependent B-Cell Maturation in Murine Systemic Lupus Erythematosus. *J Clin Invest* (2000) 106(1):91–101. doi: 10.1172/JCI9244
49. Li HJ, Brand B, Rotter A. Thermal Denaturation of Calf Thymus DNA: Existence of a GC-Richer Fraction. *Nucleic Acids Res* (1974) 1(2):257–65. doi: 10.1093/nar/1.2.257
50. Meher AK, Spinosa M, Davis JP, Pope N, Laubach VE, Su G, et al. Novel Role of IL (Interleukin)-1β in Neutrophil Extracellular Trap Formation and Abdominal Aortic Aneurysms. *Arterioscler Thromb Vasc Biol* (2018) 38 (4):843–53. doi: 10.1161/ATVBAHA.117.309897
51. Chiewchengchol D, Midgley A, Sodsai P, Deekajorndech T, Hirankarn N, Beresford MW, et al. The Protective Effect of GM-CSF on Serum-Induced Neutrophil Apoptosis in Juvenile Systemic Lupus Erythematosus Patients. *Clin Rheumatol* (2015) 34(1):85–91. doi: 10.1007/s10067-014-2800-2
52. Chiewchengchol D, Wright HL, Thomas HB, Lam CW, Roberts KJ, Hirankarn N, et al. Differential Changes in Gene Expression in Human Neutrophils Following TNF-α Stimulation: Up-Regulation of Anti-Apoptotic Proteins and Down-Regulation of Proteins Involved in Death Receptor Signaling. *Immun Inflammation Dis* (2015) 4(1):35–44. doi: 10.1002/iid3.90
53. Leelahavanichkul A, Yan Q, Hu X, Eisner C, Huang Y, Chen R, et al. Angiotensin II Overcomes Strain-Dependent Resistance of Rapid CKD Progression in a New Remnant Kidney Mouse Model. *Kidney Int* (2010) 78(11):1136–53. doi: 10.1038/ki.2010.287
54. Leelahavanichkul A, Huang Y, Hu X, Zhou H, Tsuji T, Chen R, et al. Chronic Kidney Disease Worsens Sepsis and Sepsis-Induced Acute Kidney Injury by Releasing High Mobility Group Box Protein-1. *Kidney Int* (2011) 80 (11):1198–211. doi: 10.1038/ki.2011.261
55. Dang CP, Leelahavanichkul A. Over-Expression of miR-223 Induces M2 Macrophage Through Glycolysis Alteration and Attenuates LPS-Induced Sepsis Mouse Model, the Cell-Based Therapy in Sepsis. *PloS One* (2020) 15 (7):e0236038. doi: 10.1371/journal.pone.0236038
56. Visitchanakun P, Saisorn W, Wongphoom J, Chatthanathon P, Somboonna N, Svasti S, et al. Gut Leakage Enhances Sepsis Susceptibility in Iron-Overloaded β-Thalassemia Mice Through Macrophage Hyperinflammatory Responses. *Am J Physiol Gastrointest Liver Physiol* (2020) 318(5):G966–79. doi: 10.1152/ajpgi.00337.2019
57. Baron EJ, Proctor RA. Elicitation of Peritoneal Polymorphonuclear Neutrophils From Mice. *J Immunol Methods* (1982) 49(3):305–13. doi: 10.1016/0022-1759(82)90130-2
58. Sae-Khow K, Tachaboon S, Wright HL, Edwards SW, Srisawat N, Leelahavanichkul A, et al. Defective Neutrophil Function in Patients With Sepsis Is Mostly Restored by *Ex Vivo* Ascorbate Incubation. *J Inflammation Res* (2020) 13:263–74. doi: 10.2147/JIR.S252433
59. Ondee T, Jaroonwitchawan T, Pisitkun T, Gillen J, Nita-Lazar A, Leelahavanichkul A, et al. Decreased Protein Kinase C-β Type II Associated With the Prominent Endotoxin Exhaustion in the Macrophage of FcGRIIb-/- Lupus Prone Mice Is Revealed by Phosphoproteomic Analysis. *Int J Mol Sci* (2019) 20(6):1354. doi: 10.3390/ijms20061354
60. Wagner MC, Rhodes G, Wang E, Pruthi V, Arif E, Saleem MA, et al. Ischemic Injury to Kidney Induces Glomerular Podocyte Effacement and Dissociation of Slit Diaphragm Proteins Neph1 and ZO-1. *J Biol Chem* (2008) 283(51):35579–89. doi: 10.1074/jbc.M805507200
61. Chen Y, Lin L, Tao X, Song Y, Cui J, Wan J. The Role of Podocyte Damage in the Etiology of Ischemia-Reperfusion Acute Kidney Injury and Post-Injury Fibrosis. *BMC Nephrol* (2019) 20(1):106. doi: 10.1186/s12882-019-1298-x

62. Suurmond J, Diamond B. Autoantibodies in Systemic Autoimmune Diseases: Specificity and Pathogenicity. *J Clin Invest* (2015) 125(6):2194–202. doi: 10.1172/JCI78084
63. Nishio N, Ito S, Suzuki H, Isobe K. Antibodies to Wounded Tissue Enhance Cutaneous Wound Healing. *Immunology* (2009) 128(3):369–80. doi: 10.1111/j.1365-2567.2009.03119.x
64. Thurman JM. Triggers of Inflammation After Renal Ischemia/Reperfusion. *Clin Immunol* (2007) 123(1):7–13. doi: 10.1016/j.clim.2006.09.008
65. Lai JM, Hsieh CL, Chang ZF. Caspase Activation During Phorbol Ester-Induced Apoptosis Requires ROCK-Dependent Myosin-Mediated Contraction. *J Cell Sci* (2003) 116(Pt 17):3491–501. doi: 10.1242/jcs.00660
66. Li RHL, Ng G, Tablin F. Lipopolysaccharide-Induced Neutrophil Extracellular Trap Formation in Canine Neutrophils Is Dependent on Histone H3 Citrullination by Peptidylarginine Deiminase. *Vet Immunol Immunopathol* (2017) 193-194:29–37. doi: 10.1016/j.vetimm.2017.10.002
67. Petretto A, Bruschi M, Pratesi F, Croia C, Candiano G, Ghiggeri G, et al. Neutrophil Extracellular Traps (NET) Induced by Different Stimuli: A Comparative Proteomic Analysis. *PloS One* (2019) 14(7):e0218946. doi: 10.1371/journal.pone.0218946
68. Kawai T, Akira S. Signaling to NF-kappaB by Toll-Like Receptors. *Trends Mol Med* (2007) 13(11):460–9. doi: 10.1016/j.molmed.2007.09.002
69. Chang MY, Huang DY, Ho FM, Huang KC, Lin WW. PKC-Dependent Human Monocyte Adhesion Requires AMPK and Syk Activation. *PloS One* (2012) 7(7):e40999. doi: 10.1371/journal.pone.0040999
70. Wen HC, Huo YN, Chou CM, Lee WS. PMA Inhibits Endothelial Cell Migration Through Activating the PKC-δ/Syk/Nfκb-Mediated Up-Regulation of Thy-1. *Sci Rep* (2018) 8(1):16247. doi: 10.1038/s41598-018-34548-8
71. Strich JR, Ramos-Benitez MJ, Randazzo D, Stein SR, Babyak A, Davey RT, et al. Fostamatinib Inhibits Neutrophils Extracellular Traps Induced by COVID-19 Patient Plasma: A Potential Therapeutic. *J Infect Dis* (2021) 223 (6):981–4. doi: 10.1093/infdis/jiaa789
72. Mahler M, Bentow C, O'Malley T, Ibarra C, Conklin J, Aure MAR, et al. Performance Characteristics of Different Anti-Double-Stranded DNA Antibody Assays in the Monitoring of Systemic Lupus Erythematosus. *J Immunol Res* (2017) 2017:1720902. doi: 10.1155/2017/1720902
73. Havasi A, Borkan SC. Apoptosis and Acute Kidney Injury. *Kidney Int* (2011) 80(1):29–40. doi: 10.1038/ki.2011.120
74. Dépret F, Prud'homme M, Legrand M. A Role of Remote Organs Effect in Acute Kidney Injury Outcome. *Nephron* (2017) 137(4):273–6. doi: 10.1159/000476077
75. Liu J, Dong Z. Neutrophil Extracellular Traps in Ischemic AKI: New Way to Kill. *Kidney Int* (2018) 93(2):303–5. doi: 10.1016/j.kint.2017.09.031
76. Underhill DM, Iliev ID. The Mycobiota: Interactions Between Commensal Fungi and the Host Immune System. *Nat Rev Immunol* (2014) 14(6):405–16. doi: 10.1038/nri3684
77. Bhunyakarnjanarat T, Udompornpitak K, Saisorn W, Chantraprapawat B, Visitchanakun P, Dang CP, et al. Prominent Indomethacin-Induced Enteropathy in Fcgriib Deficient Lupus Mice: An Impact of Macrophage Responses and Immune Deposition in Gut. *Int J Mol Sci* (2021) 22(3):1377. doi: 10.3390/ijms22031377
78. Akira S. Toll Receptor Families: Structure and Function. *Semin Immunol* (2004) 16(1):1–2. doi: 10.1016/j.smim.2003.10.001
79. Piccinini AM, Midwood KS. Dampening Inflammation by Modulating TLR Signalling. *Mediators Inflammation* (2010) 2010:672395. doi: 10.1155/2010/672395
80. Clark SR, Ma AC, Tavener SA, McDonald B, Goodarzi Z, Kelly MM, et al. Platelet TLR4 Activates Neutrophil Extracellular Traps to Ensnare Bacteria in Septic Blood. *Nat Med* (2007) 13(4):463–9. doi: 10.1038/nm1565
81. Sabroe I, Prince LR, Jones EC, Horsburgh MJ, Foster SJ, Vogel SN, et al. Selective Roles for Toll-Like Receptor (TLR)2 and TLR4 in the Regulation of Neutrophil Activation and Life Span. *J Immunol* (2003) 170(10):5268–75. doi: 10.4049/jimmunol.170.10.5268
82. Zhao H, Perez JS, Lu K, George AJ, Ma D. Role of Toll-Like Receptor-4 in Renal Graft Ischemia-Reperfusion Injury. *Am J Physiol Renal Physiol* (2014) 306(8):F801–11. doi: 10.1152/ajprenal.00469.2013
83. Pulskens WP, Teske GJ, Butter LM, Roelofs JJ, van der Poll T, Florquin S, et al. Toll-Like Receptor-4 Coordinates the Innate Immune Response of the Kidney to Renal Ischemia/Reperfusion Injury. *PloS One* (2008) 3(10):e3596. doi: 10.1371/journal.pone.0003596
84. Choi Y, Sim S, Park HS. Is TLR4 Critical for Neutrophil Apoptosis in Occupational Asthma? *Allergy Asthma Immunol Res* (2020) 12(4):560–2. doi: 10.4168/aair.2020.12.4.560
85. Haase R, Kirschning CJ, Sing A, Schröttner P, Fukase K, Kusumoto S, et al. A Dominant Role of Toll-Like Receptor 4 in the Signaling of Apoptosis in Bacteria-Faced Macrophages. *J Immunol* (2003) 171(8):4294–303. doi: 10.4049/jimmunol.171.8.4294
86. Degn SE, van der Poel CE, Firl DJ, Ayoglu B, Al Qureshah FA, Bajic G, et al. Clonal Evolution of Autoreactive Germinal Centers. *Cell* (2017) 170(5):913–26.e19. doi: 10.1016/j.cell.2017.07.026
87. Hsu CY, Chinchilli VM, Coca S, Devarajan P, Ghahramani N, Go AS, et al. Post-Acute Kidney Injury Proteinuria and Subsequent Kidney Disease Progression: The Assessment, Serial Evaluation, and Subsequent Sequelae in Acute Kidney Injury (ASSESS-AKI) Study. *JAMA Intern Med* (2020) 180 (3):402–10. doi: 10.1001/jamainternmed.2019.6390
88. Bouts YM, Wolthuis DF, Dirkx MF, Pieterse E, Simons EM, van Boekel AM, et al. Apoptosis and NET Formation in the Pathogenesis of SLE. *Autoimmunity* (2012) 45(8):597–601. doi: 10.3109/08916934.2012.719953
89. van der Vlag J, Berden JH. Lupus Nephritis: Role of Antinucleosome Autoantibodies. *Semin Nephrol* (2011) 31(4):376–89. doi: 10.1016/j.semnephrol.2011.06.009
90. Muñoz LE, Lauber K, Schiller M, Manfredi AA, Herrmann M. The Role of Defective Clearance of Apoptotic Cells in Systemic Autoimmunity. *Nat Rev Rheumatol* (2010) 6(5):280–9. doi: 10.1038/nrrheum.2010.46
91. Gottschalk TA, Tsantikos E, Hibbs ML. Pathogenic Inflammation and Its Therapeutic Targeting in Systemic Lupus Erythematosus. *Front Immunol* (2015) 6:550. doi: 10.3389/fimmu.2015.00550
92. Morris AB, Farley CR, Pinelli DF, Adams LE, Cragg MS, Boss JM, et al. Signaling Through the Inhibitory Fc Receptor Fcγriib Induces CD8(+) T Cell Apoptosis to Limit T Cell Immunity. *Immunity* (2020) 52(1):136–50.e6. doi: 10.1016/j.immuni.2019.12.006
93. Nimmerjahn F, Ravetch JV. Fcgamma Receptors: Old Friends and New Family Members. *Immunity* (2006) 24(1):19–28. doi: 10.1016/j.immuni.2005.11.010
94. Vorobjeva NV, Chernyak BV. Netosis: Molecular Mechanisms, Role in Physiology and Pathology. *Biochem (Mosc)* (2020) 85(10):1178–90. doi: 10.1134/S0006297920100065
95. Liu S, Su X, Pan P, Zhang L, Hu Y, Tan H, et al. Neutrophil Extracellular Traps Are Indirectly Triggered by Lipopolysaccharide and Contribute to Acute Lung Injury. *Sci Rep* (2016) 6:37252. doi: 10.1038/srep37252
96. Farley K, Stolley JM, Zhao P, Cooley J, Remold-O'Donnell E. A serpinB1 Regulatory Mechanism Is Essential for Restricting Neutrophil Extracellular Trap Generation. *J Immunol* (2012) 189(9):4574–81. doi: 10.4049/jimmunol.1201167
97. Kuwabara T, Imajoh-Ohmi S. LPS-Induced Apoptosis Is Dependent Upon Mitochondrial Dysfunction. *Apoptosis* (2004) 9(4):467–74. doi: 10.1023/B:APPT.0000031453.90821.6a
98. Yi YS, Son YJ, Ryou C, Sung GH, Kim JH, Cho JY. Functional Roles of Syk in Macrophage-Mediated Inflammatory Responses. *Mediators Inflammation* (2014) 2014:270302. doi: 10.1155/2014/270302
99. Behnen M, Leschczyk C, Möller S, Batel T, Klinger M, Solbach W, et al. Immobilized Immune Complexes Induce Neutrophil Extracellular Trap Release by Human Neutrophil Granulocytes Via Fcγriiib and Mac-1. *J Immunol* (2014) 193(4):1954–65. doi: 10.4049/jimmunol.1400478
100. Tsourouktsoglou TD, Warnatsch A, Ioannou M, Hoving D, Wang Q, Papayannopoulos V. Histones, DNA, and Citrullination Promote Neutrophil Extracellular Trap Inflammation by Regulating the Localization and Activation of TLR4. *Cell Rep* (2020) 31(5):107602. doi: 10.1016/j.celrep.2020.107602
101. Al-Harbi NO, Nadeem A, Ahmad SF, Alanazi MM, Aldossari AA, Alasmari F. Amelioration of Sepsis-Induced Acute Kidney Injury Through Inhibition of Inflammatory Cytokines and Oxidative Stress in Dendritic Cells and Neutrophils Respectively in Mice: Role of Spleen Tyrosine Kinase Signaling. *Biochimie* (2019) 158:102–10. doi: 10.1016/j.biochi.2018.12.014
102. Uckun FM, Qazi S. SYK as a New Therapeutic Target in B-Cell Precursor Acute Lymphoblastic Leukemia. *J Cancer Ther* (2014) 5(1):124–31. doi: 10.4236/jct.2014.51015
103. Hamam HJ, Khan MA, Palaniyar N. Histone Acetylation Promotes Neutrophil Extracellular Trap Formation. *Biomolecules* (2019) 9(1):32. doi: 10.3390/biom9010032

104. Nguyen GT, Green ER, Mecsas J. Neutrophils to the ROScue: Mechanisms of NADPH Oxidase Activation and Bacterial Resistance. *Front Cell Infect Microbiol* (2017) 7:373. doi: 10.3389/fcimb.2017.00373
105. Elsori DH, Yakubenko VP, Roome T, Thiagarajan PS, Bhattacharjee A, Yadav SP, et al. Protein Kinase Cδ Is a Critical Component of Dectin-1 Signaling in Primary Human Monocytes. *J Leukoc Biol* (2011) 90(3):599–611. doi: 10.1189/jib.0610376
106. Rittirsch D, Flierl MA, Day DE, Nadeau BA, Zetoune FS, Sarma JV, et al. Cross-Talk Between TLR4 and FcgammaReceptorIII (CD16) Pathways. *PloS Pathog* (2009) 5(6):e1000464. doi: 10.1371/journal.ppat.1000464
107. Bahjat FR, Pine PR, Reitsma A, Cassafer G, Baluom M, Grillo S, et al. An Orally Bioavailable Spleen Tyrosine Kinase Inhibitor Delays Disease Progression and Prolongs Survival in Murine Lupus. *Arthritis Rheum* (2008) 58(5):1433–44. doi: 10.1002/art.23428
108. Weinblatt ME, Kavanaugh A, Burgos-Vargas R, Dikranian AH, Medrano-Ramirez G, Morales-Torres JL, et al. Treatment of Rheumatoid Arthritis With a Syk Kinase Inhibitor: A Twelve-Week, Randomized, Placebo-Controlled Trial. *Arthritis Rheum* (2008) 58(11):3309–18. doi: 10.1002/art.23992
109. Deng GM, Liu L, Bahjat FR, Pine PR, Tsokos GC. Suppression of Skin and Kidney Disease by Inhibition of Spleen Tyrosine Kinase in Lupus-Prone Mice. *Arthritis Rheum* (2010) 62(7):2086–92. doi: 10.1002/art.27452
110. Ozaki N, Suzuki S, Ishida M, Harada Y, Tanaka K, Sato Y, et al. Syk-Dependent Signaling Pathways in Neutrophils and Macrophages Are Indispensable in the Pathogenesis of Anti-Collagen Antibody-Induced Arthritis. *Int Immunol* (2012) 24(9):539–50. doi: 10.1093/intimm/dxs078
111. Drummond RA, Saijo S, Iwakura Y, Brown GD. The Role of Syk/CARD9 Coupled C-Type Lectins in Antifungal Immunity. *Eur J Immunol* (2011) 41 (2):276–81. doi: 10.1002/eji.201041252

Conflict of Interest: The authors declare that the research was conducted in the absence of any commercial or financial relationships that could be construed as a potential conflict of interest.

Copyright © 2021 Saisorn, Saithong, Phuengmaung, Udompornpitak, Bhunyakarnjanarat, Visitchanakun, Chareonsappakit, Pisitkun, Chiewchengchol and Leelahavanichkul. This is an open-access article distributed under the terms of the Creative Commons Attribution License (CC BY). The use, distribution or reproduction in other forums is permitted, provided the original author(s) and the copyright owner(s) are credited and that the original publication in this journal is cited, in accordance with accepted academic practice. No use, distribution or reproduction is permitted which does not comply with these terms.

frontiers in Immunology

REVIEW
published: 30 June 2021
doi: 10.3389/fimmu.2021.697796

Erythropoietin Receptor/β Common Receptor: A Shining Light on Acute Kidney Injury Induced by Ischemia-Reperfusion

Yuanyuan Wu[1,2] *and Bin Yang*[2,3]*

[1] Basic Medical Research Centre, Medical School, Nantong University, Nantong, China, [2] Nantong-Leicester Joint Institute of Kidney Science, Nephrology, Affiliated Hospital of Nantong University, Nantong, China, [3] Department of Cardiovascular Sciences, College of Life Sciences, University of Leicester, Leicester, United Kingdom

Acute kidney injury (AKI) is a health problem worldwide, but there is a lack of early diagnostic biomarkers and target-specific treatments. Ischemia-reperfusion (IR), a major cause of AKI, not only induces kidney injury, but also stimulates the self-defense system including innate immune responses to limit injury. One of these responses is the production of erythropoietin (EPO) by adjacent normal tissue, which is simultaneously triggered, but behind the action of its receptors, either by the homodimer EPO receptor $(EPOR)_2$ mainly involved in erythropoiesis or the heterodimer EPOR/β common receptor (EPOR/βcR) which has a broad range of biological protections. EPOR/βcR is expressed in several cell types including tubular epithelial cells at low levels or absent in normal kidneys, but is swiftly upregulated by hypoxia and inflammation and also translocated to cellular membrane post IR. EPOR/βcR mediates anti-apoptosis, anti-inflammation, pro-regeneration, and remodeling *via* the PI3K/Akt, STAT3, and MAPK signaling pathways in AKI. However, the precise roles of EPOR/βcR in the pathogenesis and progression of AKI have not been well defined, and its potential as an earlier biomarker for AKI diagnosis and monitoring repair or chronic progression requires further investigation. Here, we review biological functions and mechanistic signaling pathways of EPOR/βcR in AKI, and discuss its potential clinical applications as a biomarker for effective diagnosis and predicting prognosis, as well as directing cell target drug delivery.

Keywords: acute kidney injury, apoptosis, EPOR/βcR, fibrosis, inflammation, ischemia-reperfusion

OPEN ACCESS

Edited by:
Cheng Yang,
Fudan University, China

Reviewed by:
Dong Zhu,
Fudan University, China
Cordula M. Stover,
University of Leicester,
United Kingdom

***Correspondence:**
Bin Yang
by5@le.ac.uk

Specialty section:
This article was submitted to Molecular Innate Immunity, a section of the journal Frontiers in Immunology

Received: *20 April 2021*
Accepted: *17 May 2021*
Published: *30 June 2021*

Citation:
Wu Y and Yang B (2021) Erythropoietin Receptor/β Common Receptor: A Shining Light on Acute Kidney Injury Induced by Ischemia-Reperfusion. Front. Immunol. 12:697796. doi: 10.3389/fimmu.2021.697796

INTRODUCTION

Acute kidney injury (AKI) is a critical syndrome characterized by a sudden decline of renal function, with high morbidity and mortality (1–3). The poor prognosis of AKI is also evidenced by the high risk of progression to chronic kidney disease and end-stage renal disease over time, characterized by tubulointerstitial fibrosis (4, 5). Effective management of AKI is urgently needed including early diagnosis as well as target-specific treatment.

Renal ischemia-reperfusion (IR) injury is a common contributor to AKI, which could result from various clinical settings such as kidney transplantation, cardiac surgery, shock, vomiting, diarrhea, and burns (6). Parallel to injury, the kidney also develops defensive responses to restrict cellular damage and promote repair, one of which is associated with the classical hormone erythropoietin (EPO). Recombinant EPO, 5000 U/L in hemoperfusate, markedly decreased apoptotic cells in tubular areas, but increased the apoptotic cell death of inflammatory cells and their clearance in isolated porcine kidneys (n = 6) (7). *In vivo*, EPO at 1000 U/kg significantly improved renal function and structure at the acute stage (24 h) of IR-induced AKI in rats (n = 6) (8). These observations suggest a therapeutic opportunity of using EPO to improve the outcome of AKI. However, a large dose of EPO is needed for tissue protection, so it often results in side effects such as hypertension and thrombosis due to its high affinity to the classical homodimer $(EPOR)_2$. The renoprotective receptor of EPO was a complex composed of the EPO receptor and β common receptor (EPOR/βcR), also known as innate repair receptor (9), but EPO has a low affinity to EPOR/βcR. Therefore, EPO-derived helix B surface peptide (HBSP) or its cyclic form CHBP was designed, which recognizes only EPOR/βcR, but not $(EPOR)_2$, thus dissociating tissue protection and erythropoiesis (10).

Our previous work demonstrated the renoprotective effects of HBSP and CHBP in a series study using both animal and cellular models. It was shown that the expression of EPOR/βcR was greatly triggered by IR injury in kidneys, and in particular located in tubular epithelial cells (TECs) (11), while its ligand HBSP or CHBP protected the kidney against IR-induced AKI, as well as cyclosporine A-induced fibrotic damage in kidneys (12). Mechanically, HBSP or CHBP was found to regulate the activation of transient receptor potential melastatin 7 ion channels and endoplasmic reticulum stress in tubular epithelia (13, 14). Exploring the role of EPOR/βcR in renal IR-induced AKI could help researchers to better understand its self-defense mechanisms, its signaling pathways and associated outcomes, as well as assessing its role as a potential biomarker to facilitate timely diagnosis, monitor the progression of kidney injury, and direct cell target drug delivery.

EPO AND ITS DERIVATIVES

EPO is a highly-glycosylated protein with a molecular weight of around 30.4 kDa (15). In adults, interstitial fibroblasts in the kidneys are the major cells of EPO production, which maintain the level of EPO in the circulation by feedback signals (16). The main function of EPO is enabling the terminal differentiation of erythroid progenitor cells by inhibiting apoptosis and activating pro-survival signaling pathways (17–19). However, the action of EPO is not restricted to the hematopoietic system. Initial research observed a neuroprotective effect of recombinant EPO against ischemia-induced neuron damage in the brain (20). A similar effect was also described in other organs including the kidney, heart, and liver against ischemia-related injuries, by improving autophagy, anti-apoptosis, and anti-inflammation (21–23). It indicates that these organs have a receptor of EPO, which mediates the protection of tissues. Accumulated evidence suggests that heterodimer EPOR/βcR is responsible for the tissue protective effects (24–26). Upon injury, the expression of EPOR/βcR is instantly elevated, but EPO production in the site of injury is usually postponed, for example in astrocytes of the brain (27). Thus, there is a therapeutic window for exogenous supplement of EPO and its derivatives (9). Due to the much lower binding affinity of EPO to (1-20 nM) EPOR/βcR than to classic homodimer $(EPOR)_2$ (100-200 pM) (28), a significantly higher dose of EPO is required to induce cytoprotection compared to erythropoiesis. Nevertheless, a high dose of EPO showed no significant tissue-protective effect in clinical trials, including four trails of renal transplantation (29–32) and one trail of AKI (33). Additionally, a number of studies indicated a high risk of mortality and adverse events related to the cardiovascular system by raising hematocrit and enhancing the activation of platelets and endothelia after EPO administration (34–37). Therefore, the application of EPO is restricted due to significant risk compromising its benefit. Looking into the 3D structure of EPO, helices A, C, and D binding with $(EPOR)_2$ are associated with erythropoiesis, but only aqueous helix B binding with EPOR/βcR is related to tissue protection. Therefore, EPO was modified in a variety of ways to generate molecules retaining tissue protection and avoiding hematopoiesis, which included desialated EPO, carbamylated EPO (CEPO), and glutaraldehyde EPO. However, these EPO derivatives have different pitfalls including either short half-life, immune stimulation, or tissue permeability and compatibility (38–42).

Nevertheless, a small peptide derived from EPO, helix B surface peptide (HBSP), was designed and synthesized. It is a linear peptide formed by 11 amino acids, derived from the exterior aqueous surface of helix B, also known as ARA290 (10). HBSP possesses specific and powerful roles in tissue protection but without the side effect of erythropoiesis (43). Unfortunately, the plasma half-life of HBSP is short, around 2 min, which might affect its function *in vivo*. Scientists from the Chinese Academy of Sciences optimized the metabolic stabilization of HBSP in plasma by the conformational constraining of the head-to-tail connection that forms cyclic HBSP (CHBP) *via* thioether. CHBP gained proteolytic resistance significantly and prolonged its half-life time to at least 300 min *in vivo* (44). Preclinical studies proved that CHBP was renoprotective against IR injury in rodents (45) and large animal porcine models (3). The clinical application of CHBP, in particular HBSP, is promising as it is easily obtained, is an ambient dry powder for transportation, has low cost, and potential high efficacy for organ protection (45). However, metabolic characteristics such as serum stability, safety, tissue permeability, and cytoprotective efficacy in humans still need to be further investigated.

The effectiveness of a ligand drug is not only dependent on its specificity and tissue permeability, but also relies on the responsiveness of the receptor type. EPOR was reported to be associated with chronic fibrosis of the kidney by receiving persistent signals from EPO or excessive expression (46, 47).

It was also reported that recombinant EPO provided renoprotection against fibrosis in adenine-induced CKD (48). However, EPO protected the IR kidney at the acute stage but promoted renal fibrosis in the long term. It is necessary to note that recombinant human EPO greatly increased myofibroblast numbers and collagen deposition in kidneys at 28 days post IR (46). The same study revealed that EPO stimulated profibrotic transforming growth factor β, oxidative stress and phosphorylation of ERK in IR kidneys, and also promoted epithelial-to-mesenchymal transition and activated fibroblasts under oxidative stress *in vitro*. Through overexpression of EPOR in tubules, evidence also demonstrated that higher EPO/EPOR signaling caused fibrosis in the IR-injured kidney at 14 days post IR by suppressing basal autophagy activity and upregulating apoptotic events through modifying microtubule-associated protein 1A/1B-light chain 3 and active caspase-3 expression, respectively (47). This evidence indicates that the homodimer $(EPOR)_2$ could contribute to the fibrotic development of IR kidneys, as the heterodimer EPOR/βcR was demonstrated to have an anti-fibrotic role in the kidney after IR through its specific ligands such as CHBP (45). Thus, an advantage of EPO derivatives is that they only specifically bind to EPOR/βcR, avoiding the side effects of EPO caused by not only erythropoiesis but also pro-fibrosis. Understanding the expression, regulation, and function of $(EPOR)_2$ and EPOR/βcR under different diseases would be beneficial to increase the effectiveness of their respective ligand drugs, reduce side effects, and avoid invalid use.

PHYSICAL INTERACTION BETWEEN EPOR AND βCR

The protective role of EPO revealed in different organs indicates that a variety of non-hematopoietic tissues have the receptor of EPO. EPOR, a member of the type I cytokine receptor family, is present on the surface of erythroid progenitor cells at a high level, and assembly of the homodimer $(EPOR)_2$ mediates erythropoiesis upon receiving signals from EPO (49). During the developmental stages of embryos, EPOR was found broadly expressed in many organs and cells, such as the kidney, brain, and heart (50–52). It appeared predominantly in the kidney after the first two trimesters. Knockout of EPOR in a mouse fetus resulted in death of the mouse, which may be partially due to erythropoiesis and the development of organs including the kidney (53). Thus, the signaling of EPO/EPOR is crucial in the normal development of mouse fetuses, showing its potentially broader roles apart from erythropoiesis. However, EPOR expression was gradually decreased in the kidney cortex and became stable until the maturation of the kidney postnatally (54). In adult rats, EPOR expression in kidneys remains very low or absent under normal conditions, mainly in TECs (55). This expressional change of EPOR indicates its multiple functions that may be involved in the different periods of life.

Alike EPOR, βcR also belongs to the type I cytokine receptor family. βcR is a shared common β chain with a receptor of interleukin (IL)-3, IL-5, and granulocyte-macrophage colony stimulating factor (GMCSF), which binds to a corresponding α chain (56–58). βcR mainly locates on the surface of hematopoietic cells and exerts immune regulation (59). In 1995, βcR was found to be responsive to EPO as the tyrosine phosphorylation of βcR was observed upon EPO treatment to cultured cells (60). Paul and his colleagues (61) transfected B lymphocytes with vectors expressing both EPOR and βcR genes and then obtained their heterologous expression in these cells. The two receptors associated with each other as EPOR/βcR were demonstrated in transfected cells by the detection of co-immunoprecipitation. In 2004, Brines and his colleagues demonstrated that EPOR and βcR were physically linked *via* cysteine residues (24), which might be already assembled in the absence of the EPO molecule (61). Co-expression of EPOR and βcR has been detected in various organs, such as the kidney, heart, and nervous system (62, 63).

SIGNALING PATHWAYS MEDIATED BY EPOR/βCR

EPOR and βcR do not contain an intrinsic kinase domain for downstream signaling but could induce Janus kinase 2 (JAK2) auto-phosphorylation by spatial conformational change upon receptor occupancy (60, 64, 65). As EPO signals go through both homodimer and heteromer receptors, molecular pathways specifically associated with EPOR/βcR were demonstrated by non-erythropoietic tissue-protective compounds, primarily HBSP and CEPO (42). Three dominant pathways followed by JAK2 phosphorylation have been identified, which were similar to those used in the hematopoietic system followed by homodimer receptor $(EPOR)_2$ binding (**Figure 1**).

Firstly, the phosphatidylinositol 3-kinase (PI3K)/Akt (also known as protein kinase B) pathway was involved through EPOR/βcR in the kidney, liver, and heart (66–70). In a mouse renal IR model, autophagy was induced by CHBP *via* inhibition of mammalian target of rapamycin complex 1 (mTORC1), but activation of mTORC2 led to renoprotective effects (44). Forkhead box O 3α (FoxO3α), a downstream effector of Akt, was activated by CHBP and linked to anti-fibrotic effect in a kidney IR model (45). Nevertheless, upon CEPO treatment, FoxO3α was dephosphorylated and consequently stimulated p27 expression, which was a key factor responsible for the negative regulation of cell cycle and cell proliferation demonstrated in human acute myeloid leukemia cell line UT-7 (71).

The second major molecular pathway involves signal transducer and activator of transcription 3 (STAT3) signaling. Phosphorylation of STAT3 in murine kidneys was found upregulated by IR insult, along with decreased apoptotic events (44). The activation of the STAT3 pathway was reported to occur in a cardiovascular system insulted by IR by the blockade of apoptosis and inflammation (68, 69, 72). In addition, in a rat renal allograft model, JAK2/STAT3 signaling induced the downstream pathway of the suppressor of cytokine signaling 1 expression for inhibiting toll-like receptor-induced dendritic cell maturation, as well as pro-inflammatory cytokine production of these cells (73). Most recently, the same group discovered that the JAK2/STAT3

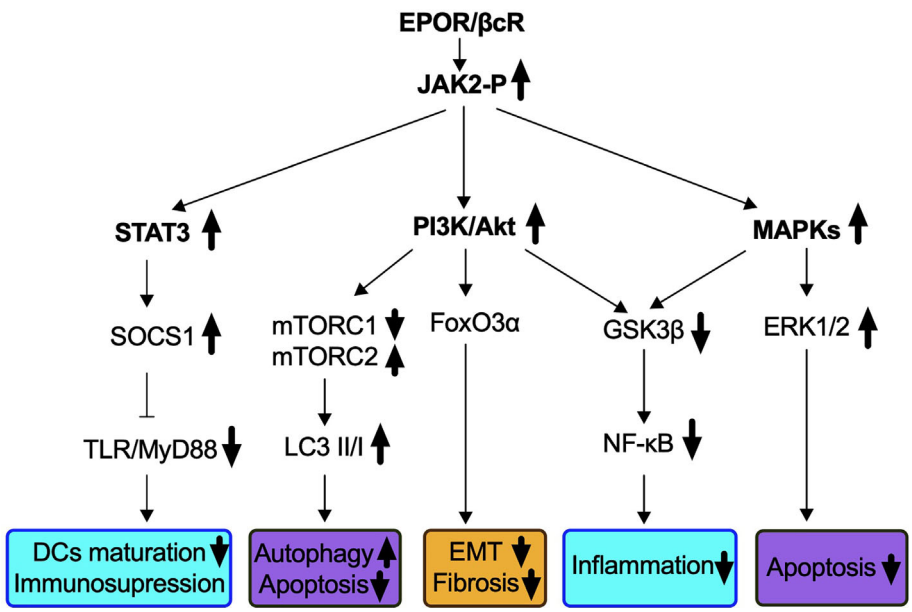


FIGURE 1 | Signaling pathways identified in IR-induced AKI *via* EPOR/βcR activation. EPO-derived tissue protective components such as CEPO, HBSP, and CHBP lead to the phosphorylation of EPOR/βcR-linked JAK2, and subsequently activates several downstream cascades. Biological processes that were influenced through EPOR/βcR signaling included immune response (blue box), cell death (purple box), and kidney repair/preventing renal fibrosis (yellow box).

pathway was also essential to enhance the immunosuppressive capability of myeloid-derived suppressor cells (74).

A third pathway refers to mitogen-activated protein kinases (MAPKs) identified in the heart, liver as well as the kidney *via* EPOR/βcR signaling (67–69). Extracellular signal-regulated kinase (ERK)1/2, a downstream pathway of MAPK, plays an important role in the protection of EPO from IR-induced renal apoptosis (75). Activation of ERK signals also accelerates repair of TECs and inhibits progression of interstitial fibrosis, and its correlation with EPOR/βcR needs investigation (76).

Additionally, both the PI3K and MAPK pathways inhibit glycogen synthase kinase 3β (GSK3β), which leads to stabilization of the mitochondrion, reduces oxidative stress damage, and subsequently inhibits death signals (72, 77). HBSP enhanced the phosphorylation of GSK3β in the rat kidney post IR and ultimately reduced inflammation by inhibiting nuclear factor-κB (NF-κB) (39). Moreover, an oxidative pathway including NADH-ubiquinone oxidoreductase Fe-S protein 6, alpha-aminoadipic semialdehyde synthase, and ATP-binding cassette subfamily D member 3 was also elicited by EPOR/βcR, leading to the renoprotective effect of CHBP (78).

RENOPROTECTION MEDIATED BY EPOR/βCR

The signaling pathways of EPOR/βcR bring multiple favorable effects on IR-injured kidney, not only against the injury, but also promotes repair. Upon IR insult, kidney cells were stressed with energy exploitation, waste retention, and accumulation of reactive oxygen species, then underwent sublethal, lethal damage, resulting in the release of alarm signals and evoking a sterile inflammatory reaction (7). Although the kidney has the capability to self-renew, maladaptive repair characterized as the deposition of collagen in tubulointerstitial areas cannot be avoided completely (79). As expected, the instant injury at an early stage of IR injury was greatly reversed by EPO and its derivatives through ameliorating kidney apoptosis and inflammatory response. Moreover, early intervention of EPO derivatives seems to turn on the switch of long-lasting biological actions as it can also inhibit chronic renal fibrosis. It was thought that EPOR/βcR mediated the balance of the microenvironment at injury sites, which benefited the recovery of the injured organ. However, the exact mechanism is still not very clear. The cell types in the kidney possessing EPOR/βcR were summarized (**Figure 2**), with detailed discussion below.

Ameliorating Apoptotic Cell Death

Injury of renal TECs was the most predominant pathological change of renal IR injury. These cells demand a high amount of oxygen and ATP, and thus are susceptible to ischemic insult. Severe stress to TECs could lead the cells to a variety of cell death modes including apoptosis (80). In both rodent and large animal experiments, inhibiting apoptotic pathways demonstrated substantial benefits to the recovery of IR kidneys (81, 82). Anti-apoptotic effect through EPOR/βcR in IR-induced AKI was also evidenced in animal models (3, 39, 83). The underlying mechanism could be manifested by the instant expression of EPOR/βcR on kidney TECs, which helps to construct an image that HBSP directly binds to EPOR/βcR on

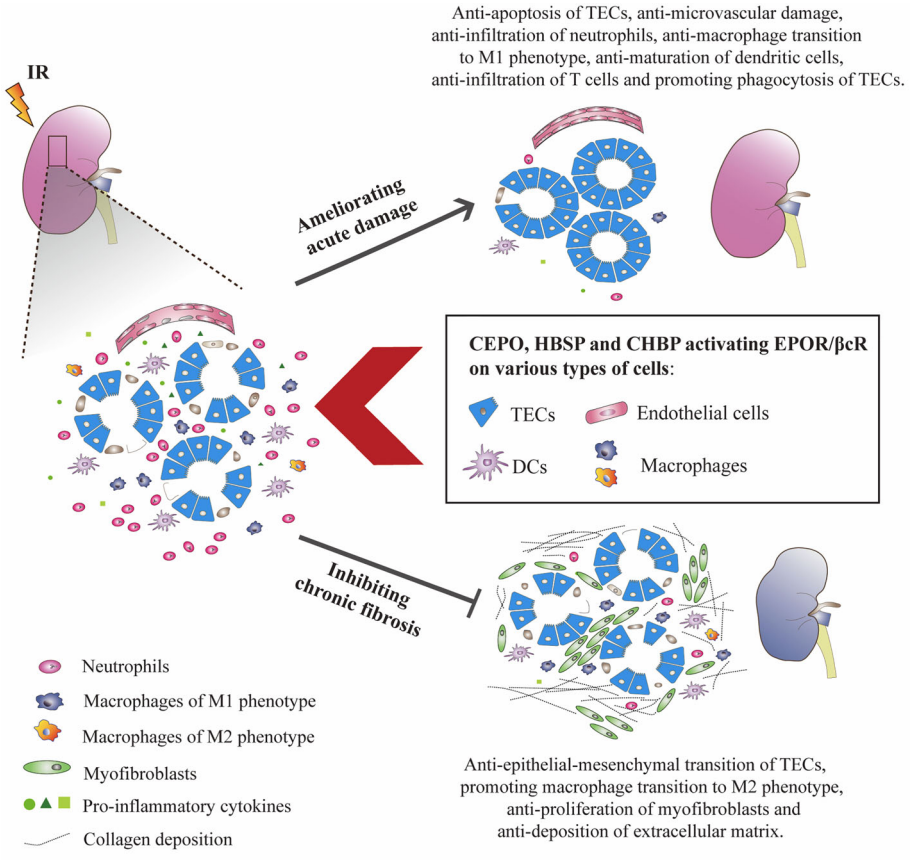


FIGURE 2 | EPO derivatives with tissue protective features benefited IR-injured kidneys at both acute and chronic stages. CEPO, HBSP and CHBP occupied EPOR/βcR on identified cells, reduced the apoptotic death of TECs, and the infiltration, pro-inflammatory transformation and maturation of inflammatory cells at the acute injury stage. The potential role of EPOR/βcR on the phagocytic function of TECs needs further study. These EPO derivatives also promoted the proliferation of TECs and transformation of macrophages to the M2 phenotype (anti-inflammatory) and reversed the proliferation of myofibroblasts and deposition of extracellular matrix proteins including collagen in interstitial areas at the chronic repair stage.

these cells and transmits protective signals inhibiting apoptosis (11). Evidence also suggested that the anti-apoptotic effect of EPOR/βcR activation would also contribute to the reduced level of oxidative (78) and enhanced autophagy *via* inhibition of mTORC1 and activation of mTORC2 (44), which rescues the TECs from apoptotic cell death. In addition, sustained dysfunction of the endothelium post reperfusion results in the obstruction of capillaries and a local 'no-reflow' phenomenon, which could lead to continuous hypoxia and cumulative apoptosis (84). Sautina et al. defined the association of vascular endothelial growth factor receptor 2 with EPOR/βcR to elicit downstream signals in the endothelium and attenuated microvascular damage (85, 86). It is indicated that EPOR/βcR would also mediate the maintenance of microvasculature and reduce further damage to tubules.

Regulating Immune Response

Neutrophils, Macrophages, Dendritic Cells, and T Cells

Inflammatory cells accumulated at the site of damage are usually a double-edged sword. These cells cause further damage at the early stage of AKI, and also initiate the clearance of injured cells and inflammation to limit damage and promote tissue repair. However, sustained inflammatory cell infiltration leads to uncontrolled inflammation in the kidney, further tissue injury, and maladaptive repair (87). Others and our previous work demonstrated that HBSP reduced infiltration of neutrophils and production of pro-inflammatory cytokines such as IL-1, IL-6, and tumor necrosis factor α by inhibiting the NF-κB pathway in rodent renal IR injury models (39, 44). Furthermore, in a large animal model, CHBP protected isolated porcine kidney and restored renal function by reducing interstitial neutrophils and decreasing pro-inflammatory cytokine transcripts 3 h after reperfusion (3). It has been found that EPOR/βcR presented or functioned in several types of immune cells, such as macrophages and dendritic cells (25). HBSP inhibited the transformation of macrophages to the pro-inflammatory M1 phenotype (88) but markedly increased the ratio of the anti-inflammatory M2 phenotype (89), of which the latter supports the transition from tubule injury to tubule repair in IR kidneys (90). In addition, CHBP also inhibited the maturation of dendritic cells through the

JAK2/STAT3 signaling pathway (73), suggesting the expression of EPOR/βcR on dendritic cells. This effect of CHBP also suppressed the infiltration of T cells, which would reduce tissue damage caused by excessive immune activation (91). The expressional and functional profile of EPOR/βcR on dendritic cells, antigen-presenting cells, and T cells should be further defined, which may influence the outcome of diseases.

Phagocytosis of TECs

Additionally, timely clearance of damaged cells also benefits the injured kidney from secondary inflammatory injury (92). Bangwei Luo et al. reported that apoptotic cell-released sphingosine 1-phosphate activated EPO/EPOR signaling in macrophages, which enhanced dying cell clearance (93). However, whether the phagocytic function of macrophages was enhanced through EPOR homodimer or hetero-receptor EPOR/βcR upon EPO binding remains unclear. Nevertheless, surviving TECs are the main (semi-professional) phagocytes to uptake dead cells in the kidneys subjected to IR injury by expressing kidney injury molecule-1 (KIM-1) (94). KIM-1, a specific molecule expressed by TECs upon injury, recognizes phosphatidylserine on apoptotic cells and transforms TECs to phagocytes (94). The mechanism of EPOR/βcR ameliorating IR injury in kidneys may also relate to the phagocytic function of TECs and facilitate clearance of apoptotic cells. Using a bioinformatics method, STAT3 was identified as an upstream regulator of KIM-1 expression (95), which could also be activated *via* EPOR/βcR. It is suggesting that ligands to EPOR/βcR might trigger signals for TECs turning into phagocytes.

Promoting Regeneration/Remodeling

The kidney could recover from IR injury that resulted in substantial loss of TECs (96). Nevertheless, kidney repair is often maladaptive when the injury is severe or mild but frequent (97). The sources of cells that contribute to the replenishment of the population of TECs after injury mainly originate from endogenous surviving TECs (98). Many injury factors, especially long-term hypoxia resulted from sustained loss of peritubular microvessels (99), and disturbance of immune-respondent components such as chronic activation of macrophages of the M1 phenotype (100, 101) have been suggested to contribute to post-ischemic fibrosis. These factors may then induce epigenetic changes in resident myofibroblasts, which result in prolonged fibroblast activation and fibrogenesis (102). Imbalanced regeneration of renal parenchymal cells and repair were characterized by interstitial fibrosis that might be the key determiner for the fate of the injured kidney in terms of its long-term outcome.

The activation of EPOR/βcR was observed to decrease the expression of α-smooth muscle actin (α-SMA), a specific marker for myofibroblasts, and deposition of the extracellular matrix in rodent IR injury and unilateral ureteral obstruction models (44, 83). EPOR/βcR signaling also compromised the pro-fibrotic effect of transforming growth factor-β in cultured TECs by maintaining the level of E-cadherin and lowering vimentin, attenuating their epithelial-mesenchymal transition *in vitro* (3, 45). This action would contribute to the reduced expression of pro-fibrotic FoxO3α on TECs through EPOR/βcR signaling. In addition, CEPO, which specifically recognizes EPOR/βcR, decreased α-SMA expression, a marker of myofibroblasts, in a 14-day rat AKI model induced by unilateral ureteral obstruction (103). These findings suggest that signals after EPOR/βcR activation would block the way of fibrogenesis by modifying the behavior of both parenchymal cells and interstitial cells, however, the exact mechanism needs further investigation. Evidence has shown that EPOR/βcR mediated the proliferation of endothelial cells and neural progenitor cells (26, 104). However, whether EPOR/βcR mediates the dedifferentiation and proliferation of surviving TECs is unknown. Moreover, communication among cells is critical to kidney repair, such as crosstalk between TECs and myofibroblasts, pericytes, or macrophages, which would lead to regeneration of kidney parenchymal cells or the bulk production of the extracellular matrix. Investigation of EPOR/βcR on cell-to-cell communication would not only lead to further understanding of its pro-repair and anti-fibrotic action but also benefit the determination of the pathogenesis of renal IR injury.

EPOR/βCR AS POTENTIAL BIOMARKER

Regulation and Modulation of EPOR/βcR

On a genomic level, the upstream regulation of EPOR expression has been studied in various studies involving the kidney. Hypoxia inducible factor-1α (HIF-α) is a major transcription factor mediating the cellular response to hypoxia and plays a pivotal role in the resolution of AKI (105). Exogenous HIF-α improved the survival of rat AKI induced by IR insult, as well as increased the downstream effector EPOR, indicating the association between EPOR and HIF-α (106). In addition, overexpression of transmembrane Klotho or administration of secreted Klotho exerted protective effects against IR-induced AKI (107, 108). Hu and colleagues reported that EPOR was a downstream effector of Klotho (55, 109). It was also suggested that tumor necrotic factor α and its receptor were required for the upregulation of EPOR and the therapeutic effects of EPO (110, 111). Furthermore, Youn-Soo Lee et al. found that deficiency of the Von Hippel-Lindau gene resulted in the development of tumors in the kidney, characterized by consistent upregulation of EPO and EPOR in renal carcinoma (112). Thus, it indicated that Von Hippel-Lindau might be an upstream inhibitor of EPO or EPOR, of which the latter genes are responsible for the proliferation of immature mesenchymal cells (113). Besides, EPO induces the ubiquitination and internalization of EPOR *via* clathrin-mediated endocytosis, following by the degradation of its intracellular part by the proteasome, preventing further signal transduction (114, 115). Nevertheless, the regulation of βcR expression in kidney parenchymal cells at the genomic level remains unreported, for which studies might be limited by the lack of specific ligands for $(\beta cR)_2$. The potential effect of upstream genes on EPOR regulation and EPOR/βcR formation for enhancing protection needs to be further explored.

Both EPOR and βcR belong to the type I cytokine superfamily, of which one family member usually creates a complex with the other in the same family as stimulated by the ligand. In addition, EPOR could be translocated from the nucleus

to the cytoplasm and cellular membrane under hypoxia (116). In addition, it was claimed that EPOR could be recruited into membrane lipid raft fractions within 1 min post the exposure of the growth factor, reaching a peak at 10 min (117). There is also evidence regarding the βcR migration to lipid rafts under stimulation of the ligand GMCSF in hematopoietic cells (118). Similarly, the altered cell surface expression of βcR in fibroblasts and macrophages that immediately occurred under stress indicated the swift translocation of the receptor (119). It was assumed that homodimer $(EPOR)_2$ and $(\beta cR)_2$ translocated from the cytoplasm to the plasma membrane quickly upon stimulation and assembled a heteroreceptor at the molecular level. Additionally, the regulation of heteroreceptor EPOR/βcR expression has been also shown by its ligand treatment in different disease models. CEPO promoted the complex association of EPOR and βcR on myocardium at 4 h post-reperfusion in a mouse myocardial IR injury model (70). However, the level of EPOR/βcR was decreased by HBSP in a 48-h mouse renal IR model, which may contribute to the decreased degree of kidney injury (11). These regulatory observations indicated potential differences in the underlying mechanisms of EPOR/βcR expression.

Potential Diagnostic Biomarker

Up to date, the diagnosis for AKI in the clinic mainly relies on the change of serum creatinine level and/or urine output (120). However, the functional alteration of the kidney always results from massive structural disorder, so the supreme timing for targeted therapeutics is often missed, which is crucial for the long-term outcome. Minor damage in the kidney might result in the poor prognosis without timely diagnosis and intervention (97). An ideal biomarker is one that can diagnose AKI at the early stage, monitor the development of the injury, direct the therapeutic interventions, and predict the prognosis of disease (33). The instant expression of EPOR/βcR in the kidney upon renal stress or insult suggested that EPOR, βcR, and/or EPOR/βcR might be a potential early biomarker(s) for IR-induced AKI. However, kidney biopsy is not a routine examination for AKI patients. Dropped off damage parenchymal cells and/or apoptotic inflammatory cells to the tubular lumen provided an opportunity for detecting these receptors in the urine, which might also reflect the level of these receptors in the kidney and the occurrence of renal injury. However, there is no available report regarding EPOR/βcR in plasma and urine so far, which may be due to the challenge of EPOR/βcR detection. Nevertheless, EPOR was found as a soluble protein in plasma that corresponds to the extracellular domain of EPOR on the cellular membrane. Biologically, the soluble EPOR exists in human plasma to bind excessive EPO and maintains the latter at a constant level (121). It has been reported that the level of soluble EPOR may contribute to erythropoietin resistance in end stage renal disease, and that its production may be mediated by pro-inflammatory cytokines such as TNF-α and IL-6 (122), indicating soluble EPOR as a potential biomarker of cell injury. However, the regulation of soluble EPOR in the plasma of animals or humans with IR-injured kidneys remains unclear. Understanding the expression and regulation of EPOR in different forms, as well as EPOR/βcR could benefit its potential application in AKI diagnosis and progression.

Therefore, exploration of the dynamic expressional profile of EPOR and potentially EPOR/βcR in the serum and urine post renal IR at different stages of injury would provide essential evidence to assess the diagnostic potential of these receptors. The association between the expression of these receptors and the development of renal IR injury might give information on the monitoring of disease. Early intervention using EPO derivatives that specifically activate EPOR/βcR will be beneficial for not only the short-term but also long-term outcome of IR-induced AKI. The dynamic change of EPOR/βcR in the kidney post insults such as IR at the initiation and the development of injury, as well as repair stage, might direct the application of specific ligand drugs.

CHALLENGES AND OPPORTUNITIES

Apart from the availability of the clinical specimens, the sensitivity and specificity of detection for the level of EPO and its receptors including EPOR, βcR, and EPOR/βcR in liquid specimens should be optimized. Especially for the heterocomplex, a co-immunoprecipitation assay needs a large sample with adequate expression. Whether EPOR or βcR protein, as well as the mRNA level of these receptors, could represent the level of heteroreceptor remains unclear and requires further study. Additionally, the complexity of disease may compromise the sensitivity of detection as various diseases may increase the expression of this protective receptor especially in patients with problems in other organs except the kidney or possessing complex kidney problems. Besides, there is also crosstalk between the kidney and other organs such as the brain, liver, and lung post renal IR (123). The level of EPOR, βcR, or EPOR/βcR in urine might not reflect the exact injury in the kidney, making the assessment of renal injury difficult. However, the functions, underlining mechanisms, and diagnostic potential regarding EPOR/βcR in AKI would also be applicable to other organs with acute injury. There are clinical trials using HBSP (also named ARA290) on neural systems (NCT02070783, NCT02039687) and the endocrine system (NCT01933529) indicating that HBSP possesses a wide range and great potential for clinical applications in different organ systems. EPOR/βcR has been found widely expressed in many kinds of cells including progenitor cells. The potential side effect of *in vivo* administration of EPOR/βcR ligands such as HBSP/CHBP in the clinic shall consider the potential that the repair signal of the receptor might lead to excessive proliferation of progenitor cells, resulting in tumorigenesis or fibrosis. In addition, EPOR/βcR might also be a natural guider for specific cell target drug delivery such as small interfering RNA conjugated with its ligand HBSP or CHBP, as TECs are most vulnerable to IR injury and highly expressed EPOR/βcR.

CONCLUSION

The timely and spatial expression of EPOR/βcR in the injured kidney upon IR suggests its potential for early diagnosis and

monitoring progression, as well as cell target drug delivering such as siRNA conjugated to its ligand. The key facts and messages are summarized as follows:

1. Hypoxia and inflammatory cytokines stimulate the swift translocation of EPOR and βcR to the cellular membrane and assemble the heterodimer.
2. EPO-derived peptide HBSP or CHBP only activates EPOR/βcR, possessing great renoprotection against IR injury. The metabolic profile and potential side effect of EPO derivatives should be further investigated before their clinical applications.
3. The signaling pathways of PI3K/Akt, STAT3, and MAPK were involved in the renoprotective effects of EPOR/βcR such as anti-apoptosis of TECs and endothelial cells and anti-inflammation at the acute stage, promoting proliferation of parenchymal cells and anti-fibrosis at the chronic stage.
4. Highly expressed EPOR/βcR in damaged cells provides a great opportunity for cell target delivery of drugs that was conjugated with its ligand such as siRNA conjugated with HBSP to precisely treat IR-induced AKI, promote repair/remodeling, and prevent its chronic progression to fibrosis.

AUTHOR CONTRIBUTIONS

BY and YW contributed to the conception and design of the article. The review was written by YW and revised by BY. Both authors approved the final version of the manuscript.

FUNDING

This work was supported by the grants from the National Natural Science Foundation of China (81873622) and the Leicester Kidney Care Appeal (2018); the Research and Innovation Department, the University Hospitals of Leicester NHS Trust, and the University of Leicester.

REFERENCES

1. Yang L, Xing G, Wang L, Wu Y, Li S, Xu G, et al. Acute Kidney Injury in China: A Cross-Sectional Survey. *Lancet* (2015) 386(10002):1465–71. doi: 10.1016/S0140-6736(15)00344-X
2. Coca SG, Yusuf B, Shlipak MG, Garg AX, Parikh CR. Long-Term Risk of Mortality and Other Adverse Outcomes After Acute Kidney Injury: A Systematic Review and Meta-Analysis. *Am J Kidney Dis* (2009) 53(6):961–73. doi: 10.1053/j.ajkd.2008.11.034
3. Yang C, Hosgood SA, Meeta P, Long Y, Zhu T, Nicholson ML, et al. Cyclic Helix B Peptide in Preservation Solution and Autologous Blood Perfusate Ameliorates Ischemia-Reperfusion Injury in Isolated Porcine Kidneys. *Transplant Direct* (2015) 1(2):e6. doi: 10.1097/TXD.0000000000000515
4. Hsu CY, Chertow GM, McCulloch CE, Fan D, Ordonez JD, Go AS. Nonrecovery of Kidney Function and Death After Acute on Chronic Renal Failure. *Clin J Am Soc Nephrol* (2009) 4(5):891–98. doi: 10.2215/CJN.05571008
5. Ishani A, Xue JL, Himmelfarb J, Eggers PW, Kimmel PL, Molitoris BA, et al. Acute Kidney Injury Increases Risk of ESRD Among Elderly. *J Am Soc Nephrol* (2009) 20(1):223–28. doi: 10.1681/ASN.2007080837
6. Mehta RL, Burdmann EA, Cerda J, Feehally J, Finkelstein F, Garcia-Garcia G, et al. Recognition and Management of Acute Kidney Injury in the International Society of Nephrology 0by25 Global Snapshot: A Multinational Cross-Sectional Study. *Lancet* (2016) 387(10032):2017–25. doi: 10.1016/S0140-6736(16)30240-9
7. Yang B, Hosgood SA, Bagul A, Waller HL, Nicholson ML. Erythropoietin Regulates Apoptosis, Inflammation and Tissue Remodelling *Via* Caspase-3 and IL-1β in Isolated Hemoperfused Kidneys. *Eur J Pharmacol* (2011) 660 (2-3):420–30. doi: 10.1016/j.ejphar.2011.03.044
8. Golmohammadi MG, Banaei S, Nejati K, Chinifroush-Asl MM. Vitamin D3 and Erythropoietin Protect Against Renal Ischemia-Reperfusion Injury *Via* Heat Shock Protein 70 and microRNA-21 Expression. *Sci Rep* (2020) 10 (1):20906. doi: 10.1038/s41598-020-78045-3
9. Brines M, Cerami A. The Receptor That Tames the Innate Immune Response. *Mol Med* (2012) 18:486–96. doi: 10.2119/molmed.2011.00414
10. Brines M, Patel NS, Villa P, Brines C, Mennini T, De Paola M, et al. Nonerythropoietic, Tissue-Protective Peptides Derived From the Tertiary Structure of Erythropoietin. *Proc Natl Acad Sci USA* (2008) 105(31):10925–30. doi: 10.1073/pnas.0805594105
11. Yang C, Zhao T, Lin M, Zhao Z, Hu L, Jia Y, et al. Helix B Surface Peptide Administered After Insult of Ischemia Reperfusion Improved Renal Function, Structure and Apoptosis Through Beta Common Receptor/Erythropoietin Receptor and PI3K/Akt Pathway in a Murine Model. *Exp Biol Med (Maywood)* (2013) 238(1):111–19. doi: 10.1258/ebm.2012.012185
12. Wu Y, Zhang J, Liu F, Yang C, Zhang Y, Liu A, et al. Protective Effects of HBSP on Ischemia Reperfusion and Cyclosporine a Induced Renal Injury. *Clin Dev Immunol* (2013) 2013(758159). doi: 10.1155/2013/758159
13. Liu A, Wu J, Yang C, Wu Y, Zhang Y, Zhao F, et al. TRPM7 in CHBP-Induced Renoprotection Upon Ischemia Reperfusion-Related Injury. *Sci Rep* (2018) 8(1):5510. doi: 10.1038/s41598-018-22852-2
14. Zhang Y, Wang Q, Liu A, Wu Y, Liu F, Wang H, et al. Erythropoietin Derived Peptide Improved Endoplasmic Reticulum Stress and Ischemia-Reperfusion Related Cellular and Renal Injury. *Front Med (Lausanne)* (2020) 7:5(5). doi: 10.3389/fmed.2020.00005
15. Jelkmann W. Molecular Biology of Erythropoietin. *Intern Med* (2004) 43 (8):649–59. doi: 10.1038/ki.1993.327
16. Bondurant MC, Koury MJ. Anemia Induces Accumulation of Erythropoietin mRNA in the Kidney and Liver. *Mol Cell Biol* (1986) 6(7):2731–33. doi: 10.1128/mcb.6.7.2731
17. Lin CS, Lim SK, D'Agati V, Costantini F. Differential Effects of an Erythropoietin Receptor Gene Disruption on Primitive and Definitive Erythropoiesis. *Genes Dev* (1996) 10(2):154–64. doi: 10.1101/gad.10.2.154
18. Wu H, Liu X, Jaenisch R, Lodish HF. Generation of Committed Erythroid BFU-E and CFU-E Progenitors Does Not Require Erythropoietin or the Erythropoietin Receptor. *Cell* (1995) 83(1):59–67. doi: 10.1016/0092-8674(95)90234-1
19. Nairz M, Sonnweber T, Schroll A, Theurl I, Weiss G. The Pleiotropic Effects of Erythropoietin in Infection and Inflammation. *Microbes Infect* (2012) 14 (3):238–46. doi: 10.1016/j.micinf.2011.10.005
20. Byts N, Sirén AL. Erythropoietin: A Multimodal Neuroprotective Agent. *Exp Transl Stroke Med* (2009) 1(4). doi: 10.1186/2040-7378-1-4
21. Kwak J, Kim JH, Jang HN, Jung MH, Cho HS, Chang SH, et al. Erythropoietin Ameliorates Ischemia/Reperfusion-Induced Acute Kidney Injury *Via* Inflammasome Suppression in Mice. *Int J Mol Sci* (2020) 21(10). doi: 10.3390/ijms21103453
22. Li GQ, Chen M. Cardioprotective Effect of Erythropoietin in Rats With Acute Myocardial Infarction Through JNK Pathway. *Eur Rev Med Pharmacol Sci* (2019) 23(3 Suppl):153–60. doi: 10.26355/eurrev_201901_18642
23. Tan R, Tian H, Yang B, Zhang B, Dai C, Han Z, et al. Autophagy and Akt in the Protective Effect of Erythropoietin Helix B Surface Peptide Against Hepatic Ischaemia/Reperfusion Injury in Mice. *Sci Rep* (2018) 8(1):14703. doi: 10.1038/s41598-018-33028-3
24. Brines M, Grasso G, Fiordaliso F, Sfacteria A, Ghezzi P, Fratelli M, et al. Erythropoietin Mediates Tissue Protection Through an Erythropoietin and

Common Beta-Subunit Heteroreceptor. *Proc Natl Acad Sci USA* (2004) 101 (41):14907–12. doi: 10.1073/pnas.0406491101
25. Lee TS, Lu KY, Yu YB, Lee HT, Tsai FC. Beta Common Receptor Mediates Erythropoietin-Conferred Protection on OxLDL-Induced Lipid Accumulation and Inflammation in Macrophages. *Mediators Inflamm* (2015) 2015(439759). doi: 10.1155/2015/439759
26. Su KH, Shyue SK, Kou YR, Ching LC, Chiang AN, Yu YB, et al. β Common Receptor Integrates the Erythropoietin Signaling in Activation of Endothelial Nitric Oxide Synthase. *J Cell Physiol* (2011) 226(12):3330–39. doi: 10.1002/jcp.22678
27. Masuda S, Okano M, Yamagishi K, Nagao M, Ueda M, Sasaki R. A Novel Site of Erythropoietin Production. Oxygen-Dependent Production in Cultured Rat Astrocytes. *J Biol Chem* (1994) 269(30):19488–93. doi: 10.1016/S0021-9258(17)32195-6
28. Brines M, Cerami A. Erythropoietin-Mediated Tissue Protection: Reducing Collateral Damage From the Primary Injury Response. *J Intern Med* (2008) 264(5):405–32. doi: 10.1111/j.1365-2796.2008.02024.x
29. Aydin Z, Mallat MJ, Schaapherder AF, van Zonneveld AJ, van Kooten C, Rabelink TJ, et al. Randomized Trial of Short-Course High-Dose Erythropoietin in Donation After Cardiac Death Kidney Transplant Recipients. *Am J Transplant* (2012) 12(7):1793–800. doi: 10.1111/j.1600-6143.2012.04019.x
30. Hafer C, Becker T, Kielstein JT, Bahlmann E, Schwarz A, Grinzoff N, et al. High-Dose Erythropoietin has No Effect on Short- or Long-Term Graft Function Following Deceased Donor Kidney Transplantation. *Kidney Int* (2012) 81(3):314–20. doi: 10.1038/ki.2011.349
31. Martinez F, Kamar N, Pallet N, Lang P, Durrbach A, Lebranchu Y, et al. High Dose Epoetin Beta in the First Weeks Following Renal Transplantation and Delayed Graft Function: Results of the Neo-PDGF Study. *Am J Transplant* (2010) 10(7):1695–700. doi: 10.1111/j.1600-6143.2010.03142.x
32. Sureshkumar KK, Hussain SM, Ko TY, Thai NL, Marcus RJ. Effect of High-Dose Erythropoietin on Graft Function After Kidney Transplantation: A Randomized, Double-Blind Clinical Trial. *Clin J Am Soc Nephrol* (2012) 7 (9):1498–506. doi: 10.2215/CJN.01360212
33. Endre ZH, Walker RJ, Pickering JW, Shaw GM, Frampton CM, Henderson SJ, et al. Early Intervention With Erythropoietin Does Not Affect the Outcome of Acute Kidney Injury (the EARLYARF Trial). *Kidney Int* (2010) 77(11):1020–30. doi: 10.1038/ki.2010.25
34. Lund A, Lundby C, Olsen NV. High-Dose Erythropoietin for Tissue Protection. *Eur J Clin Invest* (2014) 44(12):1230–8. doi: 10.1111/eci.12357
35. Ludman AJ, Yellon DM, Hasleton J, Ariti C, Babu GG, Boston-Griffiths E, et al. Effect of Erythropoietin as an Adjunct to Primary Percutaneous Coronary Intervention: A Randomised Controlled Clinical Trial. *Heart* (2011) 97(19):1560–65. doi: 10.1136/hrt.2011.223867
36. Najjar SS, Rao SV, Melloni C, Raman SV, Povsic TJ, Melton L, et al. Intravenous Erythropoietin in Patients With ST-Segment Elevation Myocardial Infarction: REVEAL: A Randomized Controlled Trial. *JAMA* (2011) 305(18):1863–72. doi: 10.1001/jama.2011.592
37. Ott I, Schulz S, Mehilli J, Fichtner S, Hadamitzky M, Hoppe K, et al. Erythropoietin in Patients With Acute ST-Segment Elevation Myocardial Infarction Undergoing Primary Percutaneous Coronary Intervention: A Randomized, Double-Blind Trial. *Circ Cardiovasc Interv* (2010) 3(5):408–13. doi: 10.1161/CIRCINTERVENTIONS.109.904425
38. Okada T, Sawada T, Kubota K. Asialoerythropoietin has Strong Renoprotective Effects Against Ischemia-Reperfusion Injury in a Murine Model. *Transplantation* (2007) 84(4):504–10. doi: 10.1097/01.tp.0000277672.02783.33
39. Patel NS, Kerr-Peterson HL, Brines M, Collino M, Rogazzo M, Fantozzi R, et al. Delayed Administration of Pyroglutamate Helix B Surface Peptide (pHBSP), a Novel Nonerythropoietic Analog of Erythropoietin, Attenuates Acute Kidney Injury. *Mol Med* (2012) 18(1):719–27. doi: 10.2119/molmed.2012.00093
40. Cassis P, Azzollini N, Solini S, Mister M, Aiello S, Cugini D, et al. Both Darbepoetin Alfa and Carbamylated Erythropoietin Prevent Kidney Graft Dysfunction Due to Ischemia/Reperfusion in Rats. *Transplantation* (2011) 92(3):271–9. doi: 10.1097/TP.0b013e3182241106
41. Chattong S, Tanamai J, Kiatsomchai P, Nakatsu M, Sereemaspun A, Pimpha N, et al. Glutaraldehyde Erythropoietin Protects Kidney in Ischaemia/Reperfusion Injury Without Increasing Red Blood Cell Production. *Br J Pharmacol* (2013) 168(1):189–99. doi: 10.1111/j.1476-5381.2012.02123.x
42. Leist M, Ghezzi P, Grasso G, Bianchi R, Villa P, Fratelli M, et al. Derivatives of Erythropoietin That Are Tissue Protective But Not Erythropoietic. *Science* (2004) 305(5681):239–42. doi: 10.1126/science.1098313
43. Zhang C, Yang C, Zhu T. From Erythropoietin to Its Peptide Derivatives: Smaller But Stronger. *Curr Protein Pept Sci* (2017) 18(12):1191–4. doi: 10.2174/1389203717666160909130006
44. Yang C, Xu Z, Zhao Z, Li L, Zhao T, Peng D, et al. A Novel Proteolysis-Resistant Cyclic Helix B Peptide Ameliorates Kidney Ischemia Reperfusion Injury. *Biochim Biophys Acta* (2014) 1842(11):2306–17. doi: 10.1016/j.bbadis.2014.09.001
45. Yang C, Cao Y, Zhang Y, Li L, Xu M, Long Y, et al. Cyclic Helix B Peptide Inhibits Ischemia Reperfusion-Induced Renal Fibrosis *Via* the PI3K/Akt/FoxO3a Pathway. *J Transl Med* (2015) 13(355). doi: 10.1186/s12967-015-0699-2
46. Gobe GC, Bennett NC, West M, Colditz P, Brown L, Vesey DA, et al. Increased Progression to Kidney Fibrosis After Erythropoietin Is Used as a Treatment for Acute Kidney Injury. *Am J Physiol Renal Physiol* (2014) 306 (6):F681–92. doi: 10.1152/ajprenal.00241.2013
47. Shi M, Flores B, Li P, Gillings N, McMillan KL, Ye J, et al. Effects of Erythropoietin Receptor Activity on Angiogenesis, Tubular Injury, and Fibrosis in Acute Kidney Injury: A "U-Shaped" Relationship. *Am J Physiol Renal Physiol* (2018) 314(4):F501–16. doi: 10.1152/ajprenal.00306.2017
48. Vázquez-Méndez E, Gutiérrez-Mercado Y, Mendieta-Condado E, Gálvez-Gastélum FJ, Esquivel-Solís H, Sánchez-Toscano Y, et al. Recombinant Erythropoietin Provides Protection Against Renal Fibrosis in Adenine-Induced Chronic Kidney Disease. *Mediators Inflamm* (2020) 2020 (8937657). doi: 10.1155/2020/8937657
49. Jelkmann W, Bohlius J, Hallek M, Sytkowski AJ. The Erythropoietin Receptor in Normal and Cancer Tissues. *Crit Rev Oncol Hematol* (2008) 67(1):39–61. doi: 10.1016/j.critrevonc.2008.03.006
50. Echigoya MH, Obikane K, Nakashima T, Sasaki S. Glomerular Localization of Erythropoietin Receptor mRNA and Protein in Neonatal and Mature Mouse Kidney. *Nephron Exp Nephrol* (2005) 100(1):e21–9. doi: 10.1159/000084109
51. Juul SE, Yachnis AT, Rojiani AM, Christensen RD. Immunohistochemical Localization of Erythropoietin and Its Receptor in the Developing Human Brain. *Pediatr Dev Pathol* (1999) 2(2):148–58. doi: 10.1007/s100249900103
52. Zafiriou MP, Noack C, Unsold B, Didie M, Pavlova E, Fischer HJ, et al. Erythropoietin Responsive Cardiomyogenic Cells Contribute to Heart Repair Post Myocardial Infarction. *Stem Cells* (2014) 32(9):2480–91. doi: 10.1002/stem.1741
53. Suzuki N, Ohneda O, Takahashi S, Higuchi M, Mukai HY, Nakahata T, et al. Erythroid-Specific Expression of the Erythropoietin Receptor Rescued Its Null Mutant Mice From Lethality. *Blood* (2002) 100(7):2279–88. doi: 10.1182/blood-2002-01-0124
54. Xiao L, Li Z, Xu P, Li Z, Xu J, Yang Z. The Expression of EPOR in Renal Cortex During Postnatal Development. *PloS One* (2012) 7(7):e41993. doi: 10.1371/journal.pone.0041993
55. Hu MC, Shi M, Cho HJ, Zhang J, Pavlenco A, Liu S, et al. The Erythropoietin Receptor Is a Downstream Effector of Klotho-Induced Cytoprotection. *Kidney Int* (2013) 84(3):468–81. doi: 10.1038/ki.2013.149
56. Brines M. The Therapeutic Potential of Erythropoiesis-Stimulating Agents for Tissue Protection: A Tale of Two Receptors. *Blood Purif* (2010) 29(2):86–92. doi: 10.1159/000245630
57. D'Andrea RJ, Gonda TJ. A Model for Assembly and Activation of the GM-CSF, IL-3 and IL-5 Receptors: Insights From Activated Mutants of the Common Beta Subunit. *Exp Hematol* (2000) 28(3):231–43. doi: 10.1016/S0301-472X(99)00159-9
58. Murphy JM, Young IG. IL-3, IL-5, and GM-CSF Signaling: Crystal Structure of the Human Beta-Common Receptor. *Vitam Horm* (2006) 74:1–30. doi: 10.1016/S0083-6729(06)74001-8
59. Metcalf D. Hematopoietic Regulators: Redundancy or Subtlety? *Blood* (1993) 82(12):3515–23. doi: 10.1182/blood.V82.12.3515.3515
60. Hanazono Y, Sasaki K, Nitta H, Yazaki Y, Hirai H. Erythropoietin Induces Tyrosine Phosphorylation of the Beta Chain of the GM-CSF Receptor. *Biochem Biophys Res Commun* (1995) 208(3):1060–6. doi: 10.1006/bbrc.1995.1442
61. Jubinsky PT, Krijanovski OI, Nathan DG, Tavernier J, Sieff CA. The Beta Chain of the Interleukin-3 Receptor Functionally Associates With the

Erythropoietin Receptor. *Blood* (1997) 90(5):1867–73. doi: 10.1182/blood.V90.5.1867
62. Uversky VN, Redwan EM. Erythropoietin and Co.: Intrinsic Structure and Functional Disorder. *Mol Biosyst* (2016) 13(1):56–72. doi: 10.1039/c6mb00657d
63. Collino M, Thiemermann C, Cerami A, Brines M. Flipping the Molecular Switch for Innate Protection and Repair of Tissues: Long-Lasting Effects of a Non-Erythropoietic Small Peptide Engineered From Erythropoietin. *Pharmacol Ther* (2015) 151:32–40. doi: 10.1016/j.pharmthera.2015.02.005
64. Funakoshi-Tago M, Pelletier S, Moritake H, Parganas E, Ihle JN. Jak2 FERM Domain Interaction With the Erythropoietin Receptor Regulates Jak2 Kinase Activity. *Mol Cell Biol* (2008) 28(5):1792–801. doi: 10.1128/MCB.01447-07
65. Chin H, Wakao H, Miyajima A, Kamiyama R, Miyasaka N, Miura O. Erythropoietin Induces Tyrosine Phosphorylation of the Interleukin-3 Receptor Beta Subunit (betaIL3) and Recruitment of Stat5 to Possible Stat5-docking Sites in Betail3. *Blood* (1997) 89(12):4327–36. doi: 10.1182/blood.V89.12.4327
66. Zhang J, Zou YR, Zhong X, Deng HD, Pu L, Peng K, et al. Erythropoietin Pretreatment Ameliorates Renal Ischaemia-Reperfusion Injury by Activating PI3K/Akt Signalling. *Nephrology (Carlton)* (2015) 20(4):266–72. doi: 10.1111/nep.12384
67. Patel NS, Nandra KK, Brines M, Collino M, Wong WF, Kapoor A, et al. A Nonerythropoietic Peptide That Mimics the 3D Structure of Erythropoietin Reduces Organ Injury/Dysfunction and Inflammation in Experimental Hemorrhagic Shock. *Mol Med* (2011) 17(9-10):883–92. doi: 10.2119/molmed.2011.00053
68. Ahmet I, Tae HJ, Juhaszova M, Riordon DR, Boheler KR, Sollott SJ, et al. A Small Nonerythropoietic Helix B Surface Peptide Based Upon Erythropoietin Structure Is Cardioprotective Against Ischemic Myocardial Damage. *Mol Med* (2011) 17(3-4):194–200. doi: 10.2119/molmed.2010.00235
69. Ueba H, Brines M, Yamin M, Umemoto T, Ako J, Momomura S, et al. Cardioprotection by a Nonerythropoietic, Tissue-Protective Peptide Mimicking the 3D Structure of Erythropoietin. *Proc Natl Acad Sci USA* (2010) 107(32):14357–62. doi: 10.1073/pnas.1003019107
70. Xu X, Cao Z, Cao B, Li J, Guo L, Que L, et al. Carbamylated Erythropoietin Protects the Myocardium From Acute Ischemia/Reperfusion Injury Through a PI3K/Akt-Dependent Mechanism. *Surgery* (2009) 146(3):506–14. doi: 10.1016/j.surg.2009.03.022
71. Chamorro ME, Maltaneri RE, Vittori DC, Nesse AB. Protein Tyrosine Phosphatase 1B (PTP1B) Is Involved in the Defective Erythropoietic Function of Carbamylated Erythropoietin. *Int J Biochem Cell Biol* (2015) 61:63–71. doi: 10.1016/j.biocel.2015.01.019
72. Liu P, You W, Lin L, Lin Y, Tang X, Liu Y, et al. Helix B Surface Peptide Protects Against Acute Myocardial Ischemia-Reperfusion Injury *Via* the RISK and SAFE Pathways in a Mouse Model. *Cardiology* (2016) 134(2):109–17. doi: 10.1159/000443680
73. Yang C, Zhang Y, Wang J, Li L, Wang L, Hu M, et al. A Novel Cyclic Helix B Peptide Inhibits Dendritic Cell Maturation During Amelioration of Acute Kidney Graft Rejection Through Jak-2/STAT3/SOCS1. *Cell Death Dis* (2015) 6:e1993. doi: 10.1038/cddis.2015.338
74. Li J, Zhang G, Zhang W, Zhang Y, Zhang X, Qiu Y, et al. CHBP Induces Stronger ImmunosuppressiveCD127 + M-^{M}DSC *Via* Erythropoietin Receptor. *Cell Death Dis* (2021) 12(2):177. doi: 10.1038/s41419-021-03448-7
75. Zou YR, Zhang J, Wang J, Peng L, Li GS, Wang L. Erythropoietin Receptor Activation Protects the Kidney From Ischemia/Reperfusion-Induced Apoptosis by Activating ERK/P53 Signal Pathway. *Transplant Proc* (2016) 48(1):217–21. doi: 10.1016/j.transproceed.2016.01.009
76. Jang HS, Han SJ, Kim JI, Lee S, Lipschutz JH, Park KM. Activation of ERK Accelerates Repair of Renal Tubular Epithelial Cells, Whereas it Inhibits Progression of Fibrosis Following Ischemia/Reperfusion Injury. *Biochim Biophys Acta* (2013) 1832(12):1998–2008. doi: 10.1016/j.bbadis.2013.07.001
77. Moon C, Krawczyk M, Paik D, Coleman T, Brines M, Juhaszova M, et al. Erythropoietin, Modified to Not Stimulate Red Blood Cell Production, Retains Its Cardioprotective Properties. *J Pharmacol Exp Ther* (2006) 316(3):999–1005. doi: 10.1124/jpet.105.094854
78. Yang C, Liu J, Li L, Hu M, Long Y, Liu X, et al. Proteome Analysis of Renoprotection Mediated by a Novel Cyclic Helix B Peptide in Acute Kidney Injury. *Sci Rep* (2015) 5:18045. doi: 10.1038/srep18045
79. Kumar S. Cellular and Molecular Pathways of Renal Repair After Acute Kidney Injury. *Kidney Int* (2018) 93(1):27–40. doi: 10.1016/j.kint.2017.07.030
80. Bonventre JV, Weinberg JM. Recent Advances in the Pathophysiology of Ischemic Acute Renal Failure. *J Am Soc Nephrol* (2003) 14(8):2199–210. doi: 10.1097/01.asn.0000079785.13922.f6
81. Yang C, Zhao T, Zhao Z, Jia Y, Li L, Zhang Y, et al. Serum-Stabilized Naked Caspase-3 siRNA Protects Autotransplant Kidneys in a Porcine Model. *Mol Ther* (2014) 22(10):1817–28. doi: 10.1038/mt.2014.111
82. Wu Y, Chen W, Zhang Y, Liu A, Yang C, Wang H, et al. Potent Therapy and Transcriptional Profile of Combined Erythropoietin-Derived Peptide Cyclic Helix B Surface Peptide and Caspase-3 siRNA Against Kidney Ischemia/Reperfusion Injury in Mice. *J Pharmacol Exp Ther* (2020) 375(1):92–103. doi: 10.1124/jpet.120.000092
83. Kitamura H, Isaka Y, Takabatake Y, Imamura R, Suzuki C, Takahara S, et al. Nonerythropoietic Derivative of Erythropoietin Protects Against Tubulointerstitial Injury in a Unilateral Ureteral Obstruction Model. *Nephrol Dial Transplant* (2008) 23(5):1521–8. doi: 10.1093/ndt/gfm842
84. Linkermann A, Chen G, Dong G, Kunzendorf U, Krautwald S, Dong Z. Regulated Cell Death in AKI. *J Am Soc Nephrol* (2014) 25(12):2689–701. doi: 10.1681/ASN.2014030262
85. Sautina L, Sautin Y, Beem E, Zhou Z, Schuler A, Brennan J, et al. Induction of Nitric Oxide by Erythropoietin Is Mediated by the {Beta} Common Receptor and Requires Interaction With VEGF Receptor 2. *Blood* (2010) 115(4):896–905. doi: 10.1182/blood-2009-04-216432
86. Stoyanoff TR, Rodriguez JP, Todaro JS, Colavita JPM, Torres AM, Aguirre MV. Erythropoietin Attenuates LPS-Induced Microvascular Damage in a Murine Model of Septic Acute Kidney Injury. *BioMed Pharmacother* (2018) 107:1046–55. doi: 10.1016/j.biopha.2018.08.087
87. Kreisel D, Sugimoto S, Tietjens J, Zhu J, Yamamoto S, Krupnick AS, et al. Bcl3 Prevents Acute Inflammatory Lung Injury in Mice by Restraining Emergency Granulopoiesis. *J Clin Invest* (2011) 121(1):265–76. doi: 10.1172/JCI42596
88. Watanabe M, Lundgren T, Saito Y, Cerami A, Brines M, Ostenson CG, et al. A Nonhematopoietic Erythropoietin Analogue, ARA 290, Inhibits Macrophage Activation and Prevents Damage to Transplanted Islets. *Transplantation* (2016) 100(3):554–62. doi: 10.1097/TP.0000000000001026
89. Ueba H, Shiomi M, Brines M, Yamin M, Kobayashi T, Ako J, et al. Suppression of Coronary Atherosclerosis by Helix B Surface Peptide, a Nonerythropoietic, Tissue-Protective Compound Derived From Erythropoietin. *Mol Med* (2013) 19:195–202. doi: 10.2119/molmed.2013.00037
90. Lee S, Huen S, Nishio H, Nishio S, Lee HK, Choi BS, et al. Distinct Macrophage Phenotypes Contribute to Kidney Injury and Repair. *J Am Soc Nephrol* (2011) 22(2):317–26. doi: 10.1681/ASN.2009060615
91. Purroy C, Fairchild RL, Tanaka T, Baldwin WM3rd, Manrique J, Madsen JC, et al. Erythropoietin Receptor-Mediated Molecular Crosstalk Promotes T Cell Immunoregulation and Transplant Survival. *J Am Soc Nephrol* (2017) 28(8):2377–92. doi: 10.1681/ASN.2016101100
92. Henson PM, Bratton DL, Fadok VA. Apoptotic Cell Removal. *Curr Biol* (2001) 11(19):R795–805. doi: 10.1016/s0960-9822(01)00474-2
93. Luo B, Gan W, Liu Z, Shen Z, Wang J, Shi R, et al. Erythropoeitin Signaling in Macrophages Promotes Dying Cell Clearance and Immune Tolerance. *Immunity* (2016) 44(2):287–302. doi: 10.1016/j.immuni.2016.01.002
94. Yang L, Brooks CR, Xiao S, Sabbisetti V, Yeung MY, Hsiao LL, et al. KIM-1-Mediated Phagocytosis Reduces Acute Injury to the Kidney. *J Clin Invest* (2015) 125(4):1620–36. doi: 10.1172/JCI75417
95. Ajay AK, Kim TM, Ramirez-Gonzalez V, Park PJ, Frank DA, Vaidya VS. A Bioinformatics Approach Identifies Signal Transducer and Activator of Transcription-3 and Checkpoint Kinase 1 as Upstream Regulators of Kidney Injury Molecule-1 After Kidney Injury. *J Am Soc Nephrol* (2014) 25(1):105–18. doi: 10.1681/ASN.2013020161
96. Witzgall R, Brown D, Schwarz C, Bonventre JV. Localization of Proliferating Cell Nuclear Antigen, Vimentin, c-Fos, and Clusterin in the Postischemic Kidney. Evidence for a Heterogenous Genetic Response Among Nephron Segments, and a Large Pool of Mitotically Active and Dedifferentiated Cells. *J Clin Invest* (1994) 93(5):2175–88. doi: 10.1172/JCI117214
97. Takaori K, Nakamura J, Yamamoto S, Nakata H, Sato Y, Takase M, et al. Severity and Frequency of Proximal Tubule Injury Determines Renal Prognosis. *J Am Soc Nephrol* (2016) 27(8):2393–406. doi: 10.1681/ASN.2015060647

98. Humphreys BD, Valerius MT, Kobayashi A, Mugford JW, Soeung S, Duffield JS, et al. Intrinsic Epithelial Cells Repair the Kidney After Injury. *Cell Stem Cell* (2008) 2(3):284–91. doi: 10.1016/j.stem.2008.01.014
99. Basile DP. The Endothelial Cell in Ischemic Acute Kidney Injury: Implications for Acute and Chronic Function. *Kidney Int* (2007) 72 (2):151–56. doi: 10.1038/sj.ki.5002312
100. Duffield JS. Macrophages and Immunologic Inflammation of the Kidney. *Semin Nephrol* (2010) 30(3):234–54. doi: 10.1016/j.semnephrol.2010.03.003
101. Ko GJ, Boo CS, Jo SK, Cho WY, Kim HK. Macrophages Contribute to the Development of Renal Fibrosis Following Ischaemia/Reperfusion-Induced Acute Kidney Injury. *Nephrol Dial Transplant* (2008) 23(3):842–52. doi: 10.1093/ndt/gfm694
102. Bechtel W, McGoohan S, Zeisberg EM, Müller GA, Kalbacher H, Salant DJ, et al. Methylation Determines Fibroblast Activation and Fibrogenesis in the Kidney. *Nat Med* (2010) 16(5):544–50. doi: 10.1038/nm.2135
103. Srisawat N, Manotham K, Eiam-Ong S, Katavetin P, Praditpornsilpa K. Erythropoietin and Its Non-Erythropoietic Derivative: Do They Ameliorate Renal Tubulointerstitial Injury in Ureteral Obstruction? *Int J Urol* (2008) 15 (11):1011–17. doi: 10.1111/j.1442-2042.2008.02149.x
104. Wang L, Zhang ZG, Gregg SR, Zhang RL, Jiao Z, LeTourneau Y, et al. The Sonic Hedgehog Pathway Mediates Carbamylated Erythropoietin-Enhanced Proliferation and Differentiation of Adult Neural Progenitor Cells. *J Biol Chem* (2007) 282(44):32462–70. doi: 10.1074/jbc.M706880200
105. Kolyada AY, Tighiouart H, Perianayagam MC, Liangos O, Madias NE, Jaber BL. A Genetic Variant of Hypoxia-Inducible Factor-1alpha Is Associated With Adverse Outcomes in Acute Kidney Injury. *Kidney Int* (2009) 75 (12):1322–9. doi: 10.1038/ki.2009.68
106. Wang H, Liu N, Li R, Tian J, Hu W, Zhang J. Nephropreventing Effect of Hypoxia-Inducible Factor 1alpha in a Rat Model of Ischaemic/Reperfusion Acute Kidney Injury. *Clin Exp Pharmacol Physiol* (2018) 45(10):1076–82. doi: 10.1111/1440-1681.12947
107. Hu MC, Shi M, Zhang J, Quiñones H, Kuro-o M, Moe OW. Klotho Deficiency Is an Early Biomarker of Renal Ischemia-Reperfusion Injury and Its Replacement Is Protective. *Kidney Int* (2010) 78(12):1240–51. doi: 10.1038/ki.2010.328
108. Sugiura H, Yoshida T, Mitobe M, Yoshida S, Shiohira S, Nitta K, et al. Klotho Reduces Apoptosis in Experimental Ischaemic Acute Kidney Injury *via* HSP-70. *Nephrol Dial Transplant* (2010) 25(1):60–8. doi: 10.1093/ndt/gfp451
109. Nangaku M. Tissue Protection by Erythropoietin: New Findings in a Moving Field. *Kidney Int* (2013) 84(3):427–9. doi: 10.1038/ki.2013.140
110. Taoufik E, Petit E, Divoux D, Tseveleki V, Mengozzi M, Roberts ML, et al. TNF Receptor I Sensitizes Neurons to Erythropoietin- and VEGF-Mediated Neuroprotection After Ischemic and Excitotoxic Injury. *Proc Natl Acad Sci USA* (2008) 105(16):6185–90. doi: 10.1073/pnas.0801447105
111. Wang L, Chopp M, Teng H, Bolz M, Francisco MA, Aluigi DM, et al. Tumor Necrosis Factor Alpha Primes Cerebral Endothelial Cells for Erythropoietin-Induced Angiogenesis. *J Cereb Blood Flow Metab* (2011) 31(2):640–7. doi: 10.1038/jcbfm.2010.138
112. Lee YS, Vortmeyer AO, Lubensky IA, Vogel TW, Ikejiri B, Ferlicot S, et al. Coexpression of Erythropoietin and Erythropoietin Receptor in Von Hippel-Lindau Disease-Associated Renal Cysts and Renal Cell Carcinoma. *Clin Cancer Res* (2005) 11(3):1059–64. doi: 10.1182/blood.V92.9.3388
113. Liu N, Tian J, Wang W, Cheng J, Hu D, Zhang J. Effect and Mechanism of Erythropoietin on Mesenchymal Stem Cell Proliferation *In Vitro* Under the Acute Kidney Injury Microenvironment. *Exp Biol Med (Maywood)* (2011) 236(9):1093–99. doi: 10.1258/ebm.2011.011001
114. Meyer L, Deau B, Forejtníková H, Duménil D, Margottin-Goguet F, Lacombe C, et al. beta-Trcp Mediates Ubiquitination and Degradation of the Erythropoietin Receptor and Controls Cell Proliferation. *Blood* (2007) 109(12):5215–22. doi: 10.1182/blood-2006-10-055350
115. Bulut GB, Sulahian R, Ma Y, Chi NW, Huang LJ. Ubiquitination Regulates the Internalization, Endolysosomal Sorting, and Signaling of the Erythropoietin Receptor. *J Biol Chem* (2011) 286(8):6449–57. doi: 10.1074/jbc.M110.186890
116. Miao S, Wang SM, Cheng X, Li YF, Zhang QS, Li G, et al. Erythropoietin Promoted the Proliferation of Hepatocellular Carcinoma Through Hypoxia Induced Translocation of Its Specific Receptor. *Cancer Cell Int* (2017) 17 (119). doi: 10.1186/s12935-017-0494-7
117. McGraw KL, Fuhler GM, Johnson JO, Clark JA, Caceres GC, Sokol L, et al. Erythropoietin Receptor Signaling Is Membrane Raft Dependent. *PloS One* (2012) 7(4):e34477. doi: 10.1371/journal.pone.0034477
118. Saulle E, Riccioni R, Coppola S, Parolini I, Diverio D, Riti V, et al. Colocalization of the VEGF-R2 and the Common IL-3/GM-CSF Receptor Beta Chain to Lipid Rafts Leads to Enhanced p38 Activation. *Br J Haematol* (2009) 145(3):399–411. doi: 10.1111/j.1365-2141.2009.07627.x
119. Bohr S, Patel SJ, Vasko R, Shen K, Iracheta-Vellve A, Lee J, et al. Modulation of Cellular Stress Response *Via* the Erythropoietin/CD131 Heteroreceptor Complex in Mouse Mesenchymal-Derived Cells. *J Mol Med (Berl)* (2015) 93 (2):199–210. doi: 10.1007/s00109-014-1218-2
120. Khwaja A. KDIGO Clinical Practice Guidelines for Acute Kidney Injury. *Nephron Clin Pract* (2012) 120(4):c179–84. doi: 10.1159/000339789
121. Yet MG, Jones SS. The Extracytoplasmic Domain of the Erythropoietin Receptor Forms a Monomeric Complex With Erythropoietin. *Blood* (1993) 82(6):1713–19. doi: 10.1182/blood.V82.6.1713.1713
122. Khankin EV, Mutter WP, Tamez H, Yuan HT, Karumanchi SA, Thadhani R. Soluble Erythropoietin Receptor Contributes to Erythropoietin Resistance in End-Stage Renal Disease. *PloS One* (2010) 5(2):e9246. doi: 10.1371/journal.pone.0009246
123. Grams ME, Rabb H. The Distant Organ Effects of Acute Kidney Injury. *Kidney Int* (2012) 81(10):942–48. doi: 10.1038/ki.2011.241

Conflict of Interest: The authors declare that the research was conducted in the absence of any commercial or financial relationships that could be construed as a potential conflict of interest.

The reviewer CS declared a shared affiliation with one of the authors BY to the handling editor at the time of review.

Copyright © 2021 Wu and Yang. This is an open-access article distributed under the terms of the Creative Commons Attribution License (CC BY). The use, distribution or reproduction in other forums is permitted, provided the original author(s) and the copyright owner(s) are credited and that the original publication in this journal is cited, in accordance with accepted academic practice. No use, distribution or reproduction is permitted which does not comply with these terms.

frontiers in Immunology

REVIEW
published: 01 July 2021
doi: 10.3389/fimmu.2021.682334

Approaches for Controlling Antibody-Mediated Allograft Rejection Through Targeting B Cells

Yoshiko Matsuda[1]*, *Takeshi Watanabe*[2] *and Xiao-Kang Li*[1]

[1] Division of Transplantation Immunology, National Research Institute for Child Health and Development, Tokyo, Japan,
[2] Laboratory of Immunology, Institute for Frontier Life and Medical Sciences, Kyoto University, Kyoto, Japan

Both acute and chronic antibody-mediated allograft rejection (AMR), which are directly mediated by B cells, remain difficult to treat. Long-lived plasma cells (LLPCs) in bone marrow (BM) play a crucial role in the production of the antibodies that induce AMR. However, LLPCs survive through a T cell-independent mechanism and resist conventional immunosuppressive therapy. Desensitization therapy is therefore performed, although it is accompanied by severe side effects and the pathological condition may be at an irreversible stage when these antibodies, which induce AMR development, are detected in the serum. In other words, AMR control requires the development of a diagnostic method that predicts its onset before LLPC differentiation and enables therapeutic intervention and the establishment of humoral immune monitoring methods providing more detailed information, including individual differences in the susceptibility to immunosuppressive agents and the pathological conditions. In this study, we reviewed recent studies related to the direct or indirect involvement of immunocompetent cells in the differentiation of naïve-B cells into LLPCs, the limitations of conventional methods, and the possible development of novel control methods in the context of AMR. This information will significantly contribute to the development of clinical applications for AMR and improve the prognosis of patients who undergo organ transplantation.

Keywords: antibody-mediated allograft rejection, naïve-B cell, memory-B cell, germinal center B cell, long-lived plasma cell, B cell biology

OPEN ACCESS

Edited by:
Cheng Yang,
Fudan University, China

Reviewed by:
Chao Hu,
Fudan University, China
Songjie Cai,
Brigham and Women's Hospital and Harvard Medical School, United States

***Correspondence:**
Yoshiko Matsuda
Yoshikomatsuday@gmail.com

Specialty section:
This article was submitted to Molecular Innate Immunity, a section of the journal Frontiers in Immunology

Received: *18 March 2021*
Accepted: *17 June 2021*
Published: *01 July 2021*

Citation:
Matsuda Y, Watanabe T and Li X-K (2021) Approaches for Controlling Antibody-Mediated Allograft Rejection Through Targeting B Cells. Front. Immunol. 12:682334. doi: 10.3389/fimmu.2021.682334

INTRODUCTION

Experiments by using thymectomized mice or chickens conducted during the mid-1960s show that T cell mediated immunity in tissue and organ allografts. Consequently, most immunosuppressive therapies for preventing allograft rejection were targeted on T cells, and the studies of the *in vitro* effects of immunosuppressive agents against the proliferating T cells significantly contributed to controlling T cell-mediated rejection (TCMR) (1). Although T cells mediate the activation of the humoral immune response to transplanted grafts through activating B cells, efforts to control antibody-mediated allograft rejection (AMR) using conventional immunosuppressive therapy have been still challenging until now (2–16).

Therefore, further understanding of B cell biology related to the differentiation of long-lived plasma cells (LLPCs) and the regulation of the production of antibodies that induce the development of AMR are required to improve disease prognosis.

During AMR development, naïve-B cells recognize donor-specific human leukocyte antigen (HLA) and differentiate into activated B cells. These activated B cells undergo negative selection in germinal centers (GCs), and only cells with high affinity for donor-specific HLA survive, subsequently differentiate into memory B cells (MBCs) or migrate into the bone marrow (BM), and differentiate into LLPCs. LLPCs maintain long-term donor-specific HLA antibodies (DSAs) production (17–19) and conventional immunosuppressive therapy is ineffective for removing these PCs, because their survival is independent on the activities of T cells and expression of CD20 is reduced on these PCs (19, 20). Moreover, the intramedullary environment may prevent these PCs from undergoing apoptosis induced by desensitization therapy (21). Therefore, the development of accurate and rapid techniques to evaluate humoral immune activation targeting transplanted grafts, independent of antibodies, are urgently required to control AMR.

Identifying of the antigen specificity of MBCs circulating in the peripheral blood, as measured using an ELISpot assay or *in vitro* assay system, will be useful to evaluate the activation of the humoral immune response to donor-specific HLA antigens (22–27). Furthermore, microarray techniques and next-generation sequencing (NGS) may provide detailed information that will contribute to therapeutic control of AMR, including the identification of antibodies that injure transplants and individual differences in patients' susceptibilities to immunosuppressive agents (28–36).

In addition, the components of humoral immunity involved in immune tolerance as well as in the repair of injured tissues are attracting attention, particularly in the fields of autoimmune diseases, severe infectious diseases, and others (37–42). Here, we discuss the possibility of AMR control by referring to the involvement mechanism of these components in the humoral immunity-associated pathology and the possibilities of these components as well as novel humoral immune monitoring in solving the problems associated with conventional AMR control.

MOLECULAR PATHOPHYSIOLOGY IN AMR

In the pathways or events leading to the development AMR, molecules such as donor-specific HLA antigens, non-HLA antigens, and self-antigens are recognized by antigen-presenting cells (APCs) that express the major histocompatibility complex (MHC) II on their surface. These latter molecules are presented to follicular helper T cells (Tfhs) through the interaction of MHC II with the T cell receptor (TCR), resulting in the activation of Tfhs (17). The B cell receptor (BCR), which is expressed on the surface of naïve-B cells, is activated through cross-linking to the aforementioned antigens in a T cell-dependent manner, and B cells monoclonally proliferate after stimulation by activated Tfhs in secondary lymphoid tissues. These activated B cells form GCs. After immunoglobulin class switching, they undergo affinity maturation and the cells with low affinity for foreign antigens or high affinity for self-antigens undergo apoptosis as a negative selection mechanism, followed by differentiation into MBCs or LLPCs that bind these antigens with high affinity. MBCs migrate to secondary lymphoid tissue to counter the ensuing invasion by foreign antigens, and LLPCs persist and continue to produce antibodies that induce AMR (17, 18, 43–45) (**Figure 1**).

Regarding the involvement of T cell in AMR development, Tfhs reside in the peripheral secondary lymphoid tissues and strongly promote the production of antigen-specific antibodies through the support of the GC reactions. The B7 (CD80/86) family of costimulatory molecules B7-1 and B7-2 binds to CD28 and cytotoxic T-lymphocyte associated antigen 4 (CTLA-4) on the surface of T cells binds more strongly to CD80/86 than to CD28 to release control over the generation of Tfhs (2). Human B7 homolog 1 (B7H-1) binds programmed death-ligand 1 (PD-L1) expressed by activated T cells and inhibits T cell activation through the interaction between PD-L1 and programmed cell death1 (PD-1). Human B7 homolog 2 (B7H-2) binds inducible T cell costimulator (ICOS) expressed by CD4/CD8 T cells to increase the secretion of interferon (IFN)-γ and interleukin (IL)-10. ICOS-ligand is expressed on the surface of B cells and supports their migration into B follicles (3, 4). In addition, Thfs support the formation of the GC through the interaction between CD40 and CD40-ligand (CD40-L) (5–9); and the G-protein-coupled receptor sphingosine-1-phosphate receptor 2 (S1PR2) cooperates with CXCR5 to retain Thfs in the GC (10). Members of the signaling lymphocyte activation molecule (SLAM) family act to maintain stable contacts between Tfhs and GC B cells to maintain the differentiation of Thfs, formation of the GC, and proliferation and survival of LLPCs and MBCs (11–16). In contrast, follicular regulatory T cells (Tfrs) inhibit the production of IL-21 by Thfs, and the CTLA-4-mediated signals cooperate with IL-10 and transforming growth factor (TGF)-beta to support the inhibitory effect on humoral immunity (48).

Macrophages (MPs) and natural killer (NK) cells also play an important role in the development of AMR (49). MPs present antigens to Tfhs *via* MHC class II, serve as a source of co-stimulatory signaling and cytokines required for activation of T cells, and subsequently activate B cells (50). Moreover, IgG DSAs have been revealed to bind to Fc gamma receptor (FcγR) such as FcγRIIIa on the cell membrane of MPs and NK cells, and subsequently, these cells are activated. These activated cells produce proinflammatory cytokines such as IFN-γ, Tumor Necrosis Factor (TNF), and granzyme B, which induce coagulation, inflammation, vascular permeability, and leukocyte trafficking on the vascular endothelium (51).

Regarding the involvement of the complement pathway in AMR development, the humoral immune response to thymus-dependent (TD) antigens requires complementary activation, which is required for the localization of the antigen and C3 ligand to follicular dendritic cells (FDCs). These events maintain the long-term memory function of B cells (52).

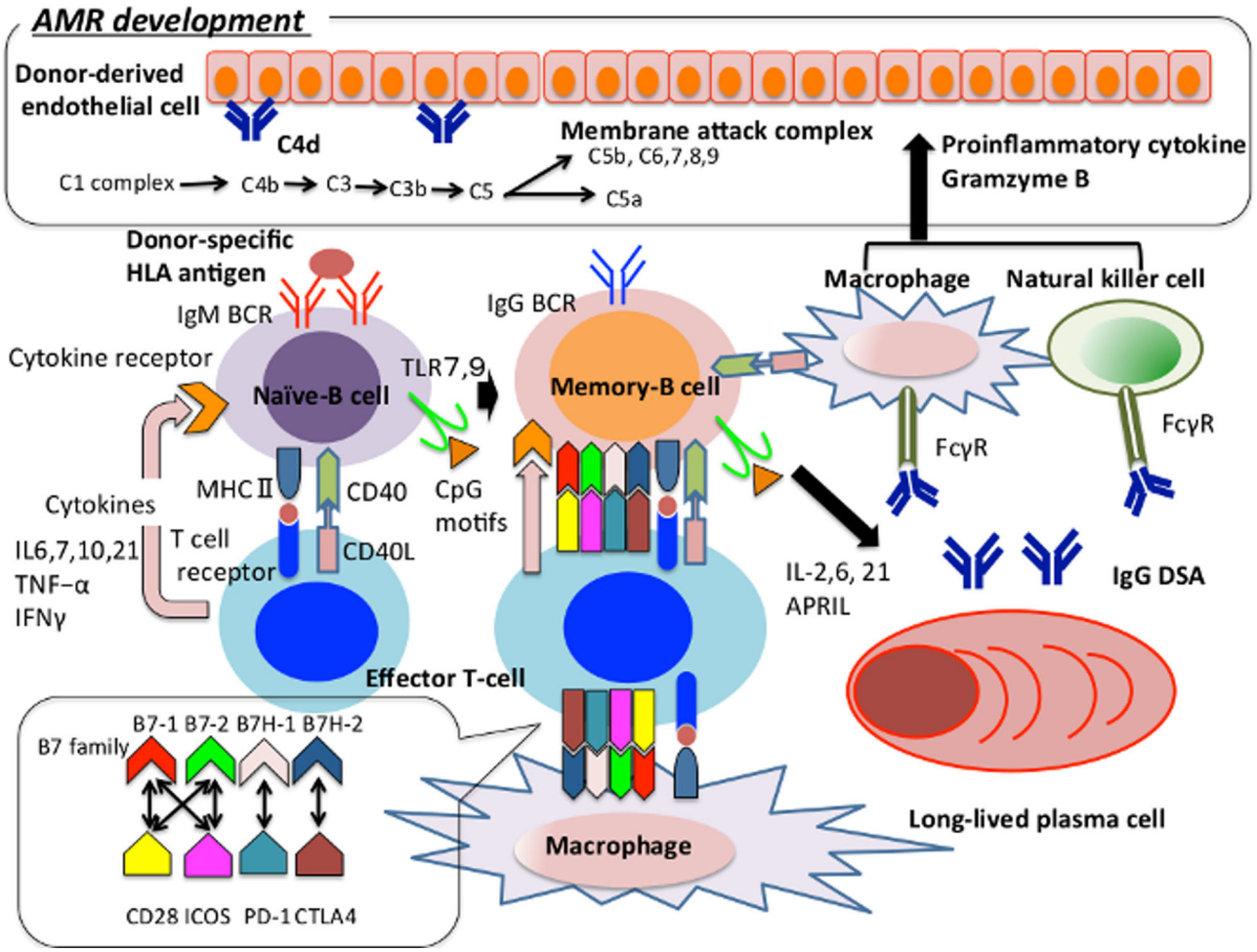


FIGURE 1 | The pathway of naïve-B cell differentiation into plasma cell in the context of AMR development. We show how immunocompetent cells are involved in the onset of AMR, focusing on B cells. Naïve-B cell recognises donor-specific HLA antigen and present the antigen peptides from MHCII to T cell receptor and activate T cells. The activated T cells regulate the growth and survival of B cells through the production of IL4, 6, 7, 10, 21, TNF-α, IFNγ, etc (46). Activated B cell migrates to secondary lymphoid tissue, class-switches to IgG and then undergoes gene conversion and hypersomatic mutation in the germinal center to have a high affinity for donor-specific HLA antigen. These cells migrate into the bone marrow and differentiate into long-lived plasma cells, and keep producing IgG DSAs for a long term. Furthermore, TLR 7/9 is expressed on the surface of naïve-B cells. TLR7 plays an important role in T cell activation and germinal center B-cell development (24). TLR9 recognizes the CpG motif and supports the survival and proliferation of B cells through IL-6 production and T cell activation (47). T cells regulate B cells' activation and sustain the interaction between follicular helper T cells and germinal center B cells through the association between the B7 family and CD28, ICOS, PD-1, CTLA-4 expressed by B cells, and CD 40 ligand and CD40 expressed by B cells. Regarding macrophages and natural killer cells function as antigen-presenting cells and induce B cells and T cells activation. IgG-type DSA binds to Fcγ on the macrophages and natural killer cells' surface and activates them. Complement activates adaptive immunity against thymus dependent antigen, or it activates the membrane attack complex and induces inflammation and tissue damage on vascular endothelial cells, thereby supporting the onset of AMR. AMR, Antibody-mediated allograft rejection; APRIL, A proliferation-inducing ligand; BCR, B cell receptor; CD40L, CD40 ligand; CTLA-4, Cytotoxic T-lymphocyte associated antigen 4; DSA, Donor-specific HLA antibody; FcγR, Fc gamma receptor; IFN, Interferon; ICOS, Inducible T-cell co-stimulator; MHC, Major histocompatibility complex; PD-1, Programmed cell death – 1; TNF, Tumor Necrosis Factor; TLR, Tool-like receptor.

As the detailed involvement mechanism in B cell activation and proliferation, the interaction of C3 fragments with CD21 is required for the internalization of antigens by B cell and their presentation. CD21 is a receptor that binds to complement C3d and Epstein–Barr virus and is expressed by mature B cells and FDCs. CD-21 plays a crucial role in B cell activation (53). The internalized antigen is presented to T cells by MHCs II and I, and it then activates T cells (54–57). Therefore, complement activation is required for the uptake of antigen by B cell and inhibiting CD21-mediated signal with polyclonal antibodies significantly inhibits antigen uptake and presentation. Furthermore, B cell uptake of C3d-coated antigen and engagement of the BCR and CD21 by C3d-opsonized antigen is required for the formation and maintenance of the GC and differentiation of MBCs into PCs (57, 58). CD35, an antagonist of CD21, inhibits B cell activation (59), and the CD21/CD19/Target of the Antiproliferative Antibody-1 (Tapa-1) receptor reduces the threshold of survival of follicular B cells and serves as a

unique signal that promotes their survival in the GCs, which, in turn, contributes to adaptive immunity (52).

Therefore, complement activation indirectly induces the development of AMR through B cell activation or directly induces inflammation and damage in vascular endothelial cells through formation of the membrane attack complex (60).

CHALLENGES OF CONVENTIONAL AMR CONTROL

Although the pathway described in "MOLECULAR PATHOPHYSIOLOGY IN AMR" is inhibited by immunosuppressive therapy, AMR control remains challenging.

The cause is that signals from immunocompetent cells, including T cells, to B cells are not well regulated, and humoral immune responses to transplanted graft have not been accurately detailed.

Furthermore, B cell subsets include IL-10-producing regulatory B cells (Bregs) ($CD19^{+}CD24^{high}CD38^{high}$ transitional immature B cells), whose reduction is associated with the incidence of posttransplant rejection (61, 62). Regulatory T cells (Tregs) induce tolerance to transplanted grafts through suppression of the humoral immune response. Calcineurin inhibitor (CNI) and mammalian Target of Rapamycin (mTOR) reduce the levels of Bregs, whereas mTOR expands and CNI reduces the levels of Tregs (63). Under pathological conditions, common variable immunodeficiency (CVID) is a pathology characterized by the loss of resistance to bacterial and viral infections due to decreased antibody production. This disease is associated with decreased expression of a proliferation-inducing ligand (APRIL), which supports the growth and survival of MBCs and PCs. An anti-APRIL antibody may serve as a therapeutic agent for SLE (64, 65). In contrast, APRIL supports the growth and survival of naïve-B cells *in vitro*, and administration of an anti-APRIL antibody may therefore suppress immune tolerance mediated by naïve-B cells (66).

In the other words, some immunosuppressive agents may inhibit the normal functions of these regulatory cells and the identification of the mechanisms through which the populations of these regulatory cells are reduced by immunosuppressive therapy and the differences of drug susceptibilities in subset-specific lymphocyte may help development of more appropriated immunosuppressive agents that maintain the functions of these regulatory cells. For example, IL-2 lengthens the survival and enhances the suppressive effects of Tregs, which increases the survival rates of transplanted grafts, because the decrease in the number of Tregs by CNI is the result of limiting the activity of IL-2 (67).

In addition, desensitization therapies such as plasmapheresis and low-dose intravenous immunoglobulin (IVig), alone or combined with recombinant antithymocyte globulin (rATG), do not significantly influence the number of $CD138^{+}$ antibody-secreting cells (ASCs), alloantibody production, and the frequency of HLA-producing ASCs in the BM before and after treatment (68). The resistance of ASCs to IVig and rATG may be explained by the inhibition of apoptosis mediated by the microenvironment of the BM and soluble and factors produced from the BM niche (21). Alternatively, the interaction of some receptors expressed on LLPC and their ligands expressed on niche play a critical role in the migration of LLPCs to the BM and their longevity in the BM (20, 69, 70). In the other words, the removal of antibody from the serum using desensitization therapy may not be mediated by the reduction of the numbers and functions of ASCs, but by antibody adsorption to the transplanted graft (68). Thus, further elucidation of the mechanisms of drug resistance in LLPCs and blockade of the signals supporting the migration of LLPCs into the BM and their longevity in the BM may contribute to the development of more effective immunosuppressive therapy.

As a diagnostic method, it is necessary for AMR control to establish a humoral immune monitoring method to evaluate AMR pathology in more detail and predict the development of AMR before antibodies, which induce AMR development, are detected in the serum (71, 72). In addition, it has been reported that the antigen specificity of the progenitor cells of LLPCs can be determined using an *in vitro* assay system (22–27), but there are no unambiguous criteria for predicting whether antibodies against donor-specific HLA antigens cause humoral immunity-mediated injury in transplanted grafts (73–75). It is therefore necessary to develop a method that evaluates the reactivity of the antibody to transplanted grafts.

DEVELOPMENT IN AMR CONTROL

Agents Targeting Complement System

The involvement of the complement system in the development of AMR has been reported. In the field of transplantation, the effects of C1-q–positive DSAs on the development of AMR and the incidence of glomerulopathy, as well as the prognosis of transplantation outcomes, have been reported administration of the humanized anti-C5 monoclonal antibody eculizumab, a C5 inhibitor, inhibits the cleavage of C5 to C5a and C5b and the formation of the membrane attack complex C5b-9, and this drug is effective against acute AMR, as indicated by its effective improvement of histopathology in lung transplantation (76–79). In immunologically high-risk cases, the incidence of biopsy-proven AMR following heart or kidney transplantation was significantly lower than that achieved using conventional antibody reduction therapy (80–83).

In addition, C1 esterase inhibitor (C1 INHs) effectively prevents ischemia reperfusion injury (IRI)/delayed graft function (DGF), which has been reported to be involved in the development of AMR through B cell activation, DSA development, and C1q-positive DSA production (84–86). Thus, C1 INHs can be expected to be effective in the maintenance of transplanted graft function by suppressing the aforementioned processes (87, 88). In contrast, no significant inhibitory effects on DSA production and the development of chronic AMR were observed in long-term DSA-positive patients, and no therapeutic effect on AMR was observed in patients with

complement-negative DSA (86). Thus, this complement inhibitor should be considered in combination with antibody reduction therapy for AMR control, and it has been reported that transplanted renal graft function and pathological findings are improved by treatment with the standard AMR treatments such as plasmapheresis, IVig, and human plasma-derived C1 INHs (88, 89).

The classic complement pathway inhibitor anti-C1s inhibits C4d deposition, but it does not affect DSA levels and graft function or significantly improve the pathological findings associated with AMR control and clinical prognosis (90, 91). Therefore, it is necessary to elucidate the mechanism by which these complement inhibitors participate in the development of AMR in more detail and improve treatment outcomes in consideration of the administration time and method.

Agents Targeting Costimulatory Signaling

As a clinical potential of agents targeting costimulatory signaling, the fusion protein belatacept comprises the Fc fragment of human IgG1 linked to the extracellular domain of CTLA-4 and inactivates T cells selectively (92).

In immunosuppressed patients who received of administration of belatacept, their survival and function of their grafts are significantly higher after 7 years of kidney transplantation (93). Compared with cyclosporine-based immunosuppression, this therapy is efficacious for maintaining the function of the transplanted grafts, reduces cardiovascular complications, improves the metabolic profile, and mitigates posttransplant lymphoproliferative disease associated with Epstein-Barr virus infection 1–2 years after transplantation (94). In mice model, an example of an immunosuppressive therapy that may effectively treat DSA-specific MBCs is provided using findings collapsing the GC in a mouse model 7 and 14 days after allo-sensitization directly involves B cells, independent of intervention by graft-specific $CD4^+$ Tfhs. Therefore, administration of CTLA- 4 Ig may exert a therapeutic effect on antigen-challenged B cells (95). In contrast, belatacept inhibits the expansion of the Tregs population, which is mediated through the methylation of CpG islands within the Treg-specific demethylation region of the gene encoding FoxP3 (96, 97).

The CTLA-4 Ig fusion protein abatacept, which inhibits CD28-mediated costimulatory signals by binding to CD80/CD86 on the surface of APCs, effectively suppresses T cell activation and cytokine production, which are associated with the development of rheumatoid arthritis (98–100). In the field of transplantation, the function of the transplanted graft persists, and no obvious immunological consequences are observed through the conversion from treatment of a CNI early after transplantation (100).

Action of conventional immunosuppressive therapies and these novel therapies targeting the complement system and co-stimulatory signaling in immune system and their clinical potential for AMR control, their clinical potential for AMR control, are presented in **Table 1** and the pathways of differentiation of naïve-B cells into LLPCs and the immunosuppressive agents that influence these processes are shown in **Figure 2**. In addition, the involvement mechanism and clinical potential of cytokines involved in the differentiation of naïve-B cells into LLPCs in the context of AMR are summarized in **Table 2A**, and the clinical applicability of these molecules and possible use in AMR control are summarized in **Table 2B**.

Agents Targeting Molecules Expressed in B Cell

In addition to these listed molecules, CD19-mediated signaling reduces the threshold for BCR-mediated signal and promotion of B cell development (190). Under pathological conditions, inebilizumab (humanised anti-CD19 monoclonal antibody) significantly reduced autoantibodies and relapse rates in patients with neuromyelitis optica (191).

Although antibodies targeting CD20 are used for the treatment of AMR, CD19 is expressed at all B cell differentiation stages, is more widely expressed than CD20 and is expressed in PCs. Therefore, CD19-targeting therapy may be more useful than CD20-targeting therapy in AMR treatment (19, 20) and the safety and tolerability of inebilizumab alone or in combination with VIB4920 (Fc-deficient CD40 Ligand antagonist) are currently being investigated in highly sensitised patients on the waiting list for kidney transplantation at clinicalTrials.gov (study identifier NCT04174677) (192).

CD138, a member of the integral membrane family of heparan sulfate proteoglycans, is highly expressed on PCs (193). CD138 increases heparan sulfate levels in ASCs, and APRIL and IL-6 support the growth and survival of ASCs by binding to heparan sulfate (194).

In other words, CD138 plays an important role in the maintenance of long-term humoral immunity (195).

In the field of transplantation, the relative abundance of CD138-positive cells is closely related to AMR development, the degree of humoral immunity-associated injury progression, and DSA production (196), and a higher frequency of CD138-positive cells and the co-existence of CD20-positive cells are associated with poor allograft function and poor response to treatment after acute rejection including TCMR and AMR (197). In addition, pathological findings indicate that the CD138-positive PCs infiltrates are associated with AMR development (196). Therefore, CD138-targeting therapy may be applicable for AMR control and the maintenance of graft function after further elucidation of the involvement mechanism of CD138-mediated signaling in the activation of humoral immunity to transplanted grafts (43). However, as described in B–cell based therapy, B cells contain a subset that has an immune regulatory function. Therefore, any clinical application for AMR control needs to be fully examined for the susceptibility of these agents for each of the B cell subsets, and the effect it will have upon their function.

B-Cell Based Therapy

In this section, we will discuss B cell subsets with immunoregulatory function because the expansion of regulatory cells that induces immune tolerance that may lead to the reduction of immunosuppressants.

Bregs mediate immune tolerance through mechanisms that involve the production of cytokines such as IL-10, IL-35, and

TABLE 1 | Effects of immunosuppressive therapy on the immune system and its clinical role in AMR control.

	Involvement mechanism in Immune system	Clinical role for AMR control	Reference
	Effects on The Cell Cycle		
Everolimus	Inhibition of cell division, cell proliferation, and angiogenesis through inhibition of the phosphorylation of mammalian targets of rapamycin and formation of a complex with the FK506-binding protein (FKBp)-12	Increased risk for the development of DSA and AMR by evelolimus-based immunosuppression Increased risk for the development of *de novo* DSA by early conversion of CNIs to everolimus No effect on the risk of *de novo* DSA development by late conversion of CNIs to evelolimus Induction of Tregs	(101–105)
Mycophenolic acid	Inhibition of DNA synthesis in lymphocytes through inhibition of the activity of IMPDH 2 and reduction of the sizes of intracellular pools of guanosine nucleotide	Reduction of anti-HLA class I and II antibody production Improvement of patient and graft survival and reduction of rejection episode while using with CsA and steroids	(106–108)
	Effects on Molecules Expressed By B Cells		
Alemtuzumab: A humanized anti-CD52 antibody	Induction of B cell apoptosis through binding to CD52, which is frequently expressed by B cells	Reduction of incidence of *de novo* DSAs and AMR development by Alemtuzumab induction therapy Reduction of the risk of AMR by using Alemtuzumab induction therapy combined with belatacept and rapamycin	(109–111)
Rituximab: Anti-CD20 monoclonal antibody	Induction of CD20 (+) B cell apoptosis through its binding to CD20, which is found on mature B cell	Improvement of survival in cardiac allograft AMR Reduction of DSA levels and microcirculation inflammation after late AMR by using with sterorid/Ivig	(112–117)
	Effects on Antibody-producing Cells and Antibody		
Bortezomib	Induction of apoptosis of antibody-producing cell through inhibiting the proteasome	Maintenance of renal graft survival after late occurrence of AMR with high probability using combined with rituximab and methylprednisolone, and plasmapheresis Reduction of DSA levels and prevention of AMR in sensitized patients with crossmatch-positive and elevated DSA in cardiac transplant	(118–120)
IdeS	Removal of anti-HLA antibodies through the cleavage of IgG at a specific amino acid sequence within the hinge region and reduction of antibody-producing cells	Reduction of anti-HLA antibodies level	(121, 122)
	Effects on Antibody-Receptor		
IVig	Induction of mature B cell apoptosis Suppression of proinflammatory cytokine production such as that of TNF-a through the inactivation of macrophages mediated by FCγR blocking	Reduction of DSA level and C4d deposition intensity after acute AMR using plasmapheresis and repeated infusions of IVig	(71, 123, 124)
	Effects on T Cells		
CNIs	Inactivation of the calcineurin-dependent NFAT pathway and T cells through the formation of a complex with cyclopherin or FK506	Prevention of *de novo* DSA formation	(102, 125–128)
rATG	Induction of T cells depletion	Depletion of DSAs No effect on the vascular AMR outcome and transplant prognosis improvement	(129–131)
Basiliximab: mouse-human chimeric monoclonal antibody	Induction of T cells depletion through reaction with the α-chain (CD25) of the IL-2 receptor expressed by T cells	Prevention of the rejection development, especially in kidney transplantation	(132)
	Effects on The Costimulatory Signaling		
Belatacept; CTLA-4 Ig	Reduction of antigen-challenged B cell Inactivation of T cell. Inhibition of Treg expansion	Depletion of plasma cells producing DSA and reduction of DSA levels in active AMR	(92–107)
Abatacept: CTLA- 4 Ig	Inactivation of T cell through inhibition of CD28-mediated costimulatory signals by binding to CD80/CD86 on the surface of APCs	Extension of graft survival with combined bortezomib use in a sensitized animal kidney transplant model	(98–100)
	Effects on The Complement System		
Eculizumab: humanized anti-C5 monoclonal antibody	Blocking membrane attack complex formation and its function	Improvement of histopathology and transplanted graft function and prevention of early active or chronic AMR development in positive crossmatch HLA incompatible patients	(76–79, 133, 134)
C1 INH: human plasma-derived C1 esterase inhibitor	Inactivation of C1r and C1s proteases in the C1 complex of classical pathway of complement.	Improvement of histopathology and graft survival with the combined use of plasmapheresis and IVig Prevention of AMR development through IRI/DGF prevention	(84–89)

(Continued)

TABLE 1 | Continued

	Involvement mechanism in Immune system	Clinical role for AMR control	Reference
	Effects on The Cell Cycle		
Anti-C1s: Classic complement pathway inhibitor	Inhibition of complement pathway	No significant effect on graft outcome and histological findings Reduction of C4d deposition	(90, 91)
	Anti-inflammatory Effects		
Glucocorticoids	Downregulation of the expression of AP-1 and NF-κB	Maintenance of renal allograft survival after combination of bortemizob, corticosteroids, rituximab, and plasma pheresis for late onset AMR	(135, 136)

AP-1, Activator protein1; AMR, Antibody-mediated allograft rejection; APC, Antibody producing cell; CNI, Calcineurin inhibitors; CsA, Cyclosporine; CTLA-4, Cytotoxic T-lymphocyte (associated)antigen 4; DGF, Delayed graft function; DSA, Donor-specific HLA antibody; FcγR, Fc gamma receptor; HLA, Human Leukocyte Antigen; Ides, IgG-degrading enzyme of streptococcus pyogenes; IMPDH2, Inosine-5'-monophosphate dehydrogenase 2; IRI, ischemia reperfusion injury; IVig, Intravenous immunoglobulin; MMF, Mycophenolate mofetil; NFAT, Nuclear factor of activated T-cells; NF-κB; Nuclear factor κB; rATG, Recombinant Anti-thymocyte globulin; SRL, Sirolimus; TNF, Tumor Necrosis Factor; Treg, Regulatory T cell.

TGF-beta as well as through cell–cell contact (154–161). Although IL-10 has been the focus of attention, IL-10 and IL-35 produced from Breg play important roles as negative regulators of immunity, which are involved in the antigen-presenting function and cytokine secretion of macrophages, dendritic cells, and B cells and activation of inflammatory T cells (156). B-1 cells and marginal zone (MZ) B cells exhibit innate-like immune functions (198). MZ-autoreactive B cells are required to maintain tolerance to self-antigens and the rapid acquisition of immunoregulatory function through the maintenance of the levels of natural IgM antibody and IL-10 (199, 200). Furthermore, ILBs serve as important sources of Bregs that play crucial roles in autoimmunity, inflammation, and infection in the models of autoimmune disease (201, 202).

As other B cell subsets that have been reported to be involved in the induction of immune tolerance, naïve-B cells function as APCs and induce the conversion of $CD4^+$ $CD25^-$ T cells into $CD25^+$ $Foxp3^-$ Tregs, which express lymphocyte activation gene 3 (LAG3), ICOS, glucocorticoid-induced TNF receptor family-regulated gene (GITR), OX40, PD1, and CTLA-4, to sustain immune tolerance through the production of anti-inflammatory cytokines such as IL-10. These findings indicate that naïve-B cells cooperate with Tregs to induce T cell tolerance, maintain the homeostasis of Tregs, and suppress inflammation by functioning as APCs (203, 204). In addition, $IgM^+CD138^{hi}TACI^+$ $CXCR4^+CD1d^{int}Tim1^{int}$ PCs expressing the transcription factor Blimp1 produce IL-10, IL-35 during infections with *Salmonella* species. Furthermore, $CD138^+$ PCs provide the major source of IL-35 and IL-10 in patients with experimental autoimmune encephalomyelitis (EAE) (156).

In the field of transplantation, IL-10 produced by Bregs is associated with drug resistance in AMR, and higher frequencies of transitional B cells and naïve-B cells and high production of IL-10 are related to the induction of immune tolerance following kidney transplantation. In contrast, the results are opposite in cases of chronic AMR (205), and $CD138^+$ PCs may be involved the induction of immune tolerance and the expansion of these B cells may mitigate the adverse effects of immunosuppressants and thereby improve the prognosis of patients who undergo transplantation.

DEVELOPMENT OF DIAGNOSTIC METHODS

Monitoring Humoral Immunity Using Memory-B Cell

The MBC pool has recently attracted more attention than humoral antibodies as a potential diagnostic tool to monitor the humoral immune response to donor-specific HLA antigens, which is evaluated according to the frequency of DSA-specific MBCs circulating in peripheral blood. For example, to determine the antigen specificities of MBCs circulating in the periphery, B cells or peripheral blood mononuclear cells (PBMCs) are induced to differentiate into ASCs with mitogens and cytokines suitable for the proliferation of MBCs and survival in a polyclonal activation-dependent manner. These findings were acquired through analysis of culture supernatants using a solid-phase assay platform with HLA-coated multiplex beads (23–29).

In the field of transplantation, current studies focus on the diagnostic value of IgG antibodies against HLA expressed in donor-derived vascular endothelial cells. On the other hands, there is currently no consensus on the clinical role of IgM antibodies (206).

We examined the clinical potential of DSA-specific IgM-MBCs as early diagnosis and humoral immune monitoring in the context of AMR; DSA-specific IgM-MBCs may achieve higher sensitivity when employed for conventional immunosuppressive therapy compared with IgG-MBCs (207). Therefore, the detection of DSA-specific IgM-MBCs contributes to the inhibition of AMR development by enabling early intervention using less invasive immunosuppression after elucidation of the optimal conditions for inducing DSA-specific IgM-MBC differentiation into IgG-PCs, the process that leads to AMR. In addition, the availability of an *in vitro* assay system capable of inducing the differentiation of MBCs into ASCs may lead to the introduction of more effective immunosuppressive therapy that recognizes differences in pathology or in patients' drug sensitivities (208).

However, it is unclear whether *in vitro* drug susceptibility data can be applied to patients because conventional two-dimensional culture may not reproduce the three-dimensional structure or function such as lymphoid tissue or organs in the living body.

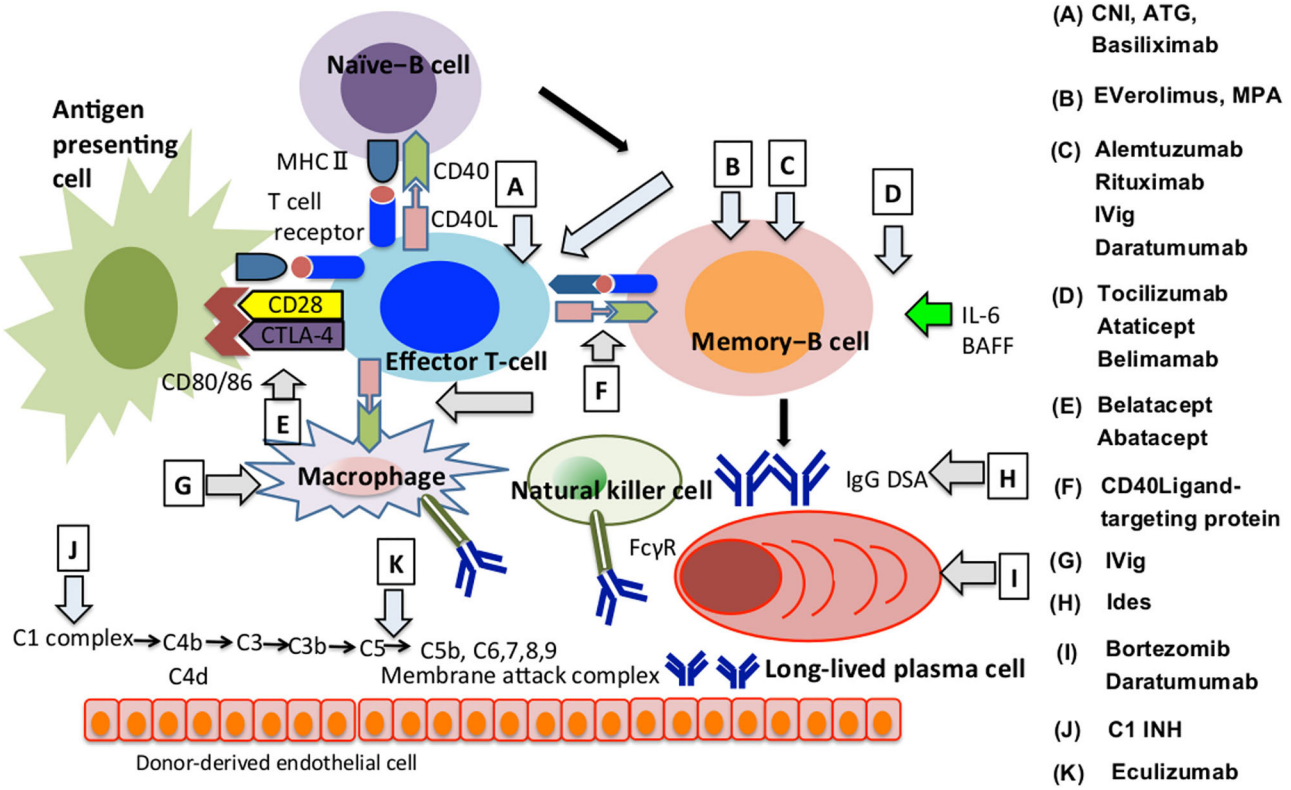


FIGURE 2 | How immunosuppressive agents influence the AMR development. We summarised how immunosuppressants are involved in regulating AMR onset at each B cell differentiation stage, direct or indirect involvement of T cells, macrophages or natural killer cells and the complement system. The alphabet represents immunosuppressants that are effective in the differentiation process indicated by arrows. AMR, Antibody-mediated allograft rejection; ATG, Antithymocyte globulin; BAFF, B Cell Activating Factor; CD40L, CD40 ligand; CTLA-4, Cytotoxic T-lymphocyte associated antigen 4; DSA, Donor-specific HLA antibody; FcγR, Fc gamma receptor; C1 INH, Human plasma-derived C1 esterase inhibitor; CNI, Calcineurin inhibitor; Ides, IgG-degrading enzyme of *streptococcus pyogenes*; IVig, Intravenous Immunoglobulin; MHC, Major histocompatibility complex; MPA, mycophenolic acid.

Organ-on-a-chip technology is attracting attention because it reproduces organs in functional units while maintaining the *in vivo* three-dimensional organ structure and physiological function. Thus, pharmacokinetic analysis using this model may be useful for resolving the aforementioned problem (209–212).

Microarray Technique

Attempts are being made to apply microarray technology or NGS to the field of transplantation. Microarrays simultaneously analyze the expression of tens of thousands of genes and obtain information about the transcriptional profiles. Furthermore, pathological changes in gene expression can be obtained, which will provide information to increase the accuracies of classification, diagnosis, and prognosis of diseases (28, 29). Errors frequently occur in analyses of single genes when small data sets are employed. Recently, Chen et al. focused on transcripts that are known to be associated with disease. Microarray evaluation of pathogenesis-based transcript sets, corresponding to events that mainly occur during allograft rejection, is useful for the diagnosis of AMR as well as identification of pathology and prediction of clinical course. For example, biopsy-based microarrays identified 45 genes upregulated in pediatric kidney transplants as well as in pediatric and adult heart transplants undergoing acute rejection. Among them, serum PECAM1 shows the greatest promise as a biomarker (89% sensitivity and 75% specificity) for analyzing renal transplant rejection, suggesting that microarray analysis will be useful for discovering new serum protein biomarkers by mining publicly available data sets (30). Thus, it is possible to identify the gene group associated with graft rejection and pathological condition by enabling comprehensive gene analysis; early diagnosis of the development of rejection is possible and genes related to immune status or drug resistance has also been identified (213).

Next-Generation Sequencing

NGS determines several million base pairs per run and provides the ability to distinguish different isoforms and allelic expression, which is an advantage over microarray analysis and detects somatic mutations with high accuracy and high specificity, which enables identification of candidate genes that cause disease. As an example of the application of NGS to transplantation, comparison of the complementary determining region 3 (CDR3) of the TCR beta

TABLE 2A | Involvement of cytokines in the immune system and clinical applicability for AMR.

Cytokine	Involvement of cytokines in the immune system	Clinical applicability for AMR control	Reference
IL-2	Plasma cell generation	Extension of heart allograft survival by IL-2 gene expression inhibition in a mouse model	(137–139)
IL-6	Support of B cell growth and survival including isotype switching, spontaneous germinal center formation, and IgG production Induction of IL-10-producing B cells Induction of Th 17 cell differentiation	Tocilizumab (anti-IL -6 receptor monoclonal antibody) showed significant improvement in graft survival, function, and DSA reduction 6 months after the treatment in chronic active AMR Clazakizumab (anti-IL-6) showed significant reduction of DSA levels and the suppression of AMR activity, progression	(140–149)
IL-7	Support of B cell development, immunoglobulin gene rearrangement Induction of Th17 cells Extension of the function of FoxP3 (+) natural regulatory T cells	Anti-IL-7 monoclonal antibody targeting IL-7 receptor α showed extension of allograft survival and induction of allograft tolerance in heart transplants and promotion of long-term allograft survival by IL-7 inhibition in combination with T cell depletion synergized with either CTLA-4 Ig administration or tacrolimus in pancreatic islet allografts	(150–153)
IL-10	Down-regulation of antigen-specific T cell response	Circulating IL-10 (+) Breg levels indicate the AMR resistance after kidney transplantation	(154–161)
Il-15	Support of B cell proliferation and antibody production Induction of regulatory CD8 (+) CD122 (+) T cell and NK cell-derived IFN-gamma Inhibition of pathogenic Th17-cell differentiation,	Antagonistic mutant IL-15/Fc fusion protein (mIL-15/Fc) is effective in the prevention of allograft rejection induce antigen-specific tolerance in minor histocompatibility complex-mismatched recipients and extend cardiac allograft survival in fully MHC-mismatched recipients IL-15 is a biomarker of acute and chronic allograft rejection Anti-IL-15 therapy is effective in the prevention of acute and chronic allograft rejection using classic immunosuppression	(162–164)
IL-21	Support of plasma cell differentiation, Support of IL-10-producing regulatory B cells differentiation	The administration of IL-21 receptor fusion protein (R-Fc) prevents chronic cardiac allograft vasculopathy in a heart allograft transplant mouse model Frequency of donor-specific IL-21 producing cells is effective as a biomarker for the prediction of rejection	(165–167)
IL-35	Induction of IL-10 producing B cell Expansion of regulatory B cell and regulatory T cell Antagonizing Th1/Th17 responses	IL-35 gene therapy prolonged graft survival in a mouse heterotopic abdominal heart transplantation model combined with a methyltransferase inhibitor treatment	(154–161)
TNF-α	Augmentation of B-cell proliferation, polyclonal B-cell, B cell malignancies Development of germinal center B cell Generation of extra follicular T-bet (+) B cell	Serum level of TNF-α is associated with histologically findings and is effective as a biomarker for AMR development	(168–170)
TGF-beta	Induction of immune tolerance Inhibition of antibody production Enhancement of FoxP3 and CTLA-4 expression in Tregs	Anti-TGF-beta antibody treatment significantly reduces chronic rejection and prevent dysfunction of renal allografts in rats	(48, 154–161)
BAFF	Promotion of B cell growth and survival, and antibody production Maintenance of survival of high-affinity B cell clones	Belimumab, a human monoclonal antibody that inhibits BAFF, removes complement-binding anti-HLA class I and class II antibody in pre-HLA sensitized patients Elevation of perioperative BAFF level predicts the risk of acute AMR development The BAFF mRNA expression level significantly unregulated in chronic AMR compared with graft function stable and healthy donors in renal transplants	(171–174)

AMR, Antibody-mediated allograft rejection; BAFF, B Cell Activating Factor; CTLA-4, cytotoxic T-lymphocyte(associated)antigen 4; DSA, Donor-specific HLA antibody; HLA, human leukocyte antigen; IFN, Interferon; IL, Interleukin; MHC, major histocompatibility complex; NK cell, Natural killer cell; TGF-beta, Transforming Growth Factor-beta; Th, T helper; TNF, Tumor Necrosis Factor.

chains expressed in AMR (+) and AMR (–), may lead to the prediction of the development of rejection before patients undergo transplantation (31). In addition, this technique can be applied to increase our understanding of the diversity of the variable regions of heavy and light chains of BCRs. Thus, detailed characterization of this repertoire, including reactivity with antigen, becomes possible and may be applied to predict the production of donor-specific antigen-reactive antibodies (32–34) and both specific sequences and the full length of genes including introns and untranslated regions are analyzed by NGS, and thus, HLA alleles can be analyzed in transplantation, ensuring better histocompatibility between donors and recipients (214, 215).

In addition, gene polymorphisms affect the distribution and drug metabolism. For example, Single Nucleotide Polymorphism (SNP) of CYP3A4/3A5, ABCB1 in CNI, CYP3A5 in sirolimus, TPMT in azathioprine, UGT1A9, ABCC2 in Mycophenolic acid (MPA), and MDR1 in tacrolimus affects their pharmacokinetics. Thus, NGS analysis of these SNP will likely provide useful information for developing more effective immunosuppressive therapy, which considers differences in pathology and drug susceptibility (35, 36).

In the other words, these techniques have potential application in developing strategies for controlling AMR and improving the prognosis of transplanted grafts.

TABLE 2B | Molecules expressed by B cells and clinical applicability for AMR control.

Molecules	Involvement mechanism in Immune system	Clinical applicability for AMR control	Reference
CD38	Support of B cell activation and proliferation as co-receptors for cytokine receptors and inhibit apoptosis of GC B cell through phosphorylation of CD19 Reduction of plasma cells in the BM	Daratumumab (humanized, CD38-targeting antibody) reduce DSA level rapidly and extent graft survival	(175–179)
CD40	Support of proliferation and survival B cell through CD40/CD40 ligand interaction	Inhibiting signaling through the CD40/CD40 L pathway inhibits B cell activation, suppresses plasma cells differentiation, and suppresses TD antigen-specific IgG production Blocking the CD28/B7 and CD40/CD40L interaction at the same time delay or prevent allograft rejection	(180, 181)
TACI	Inhibition of B cell expansion. Regulation of serum BAFF level Promotion of GC B cells apoptosis Promotion of plasma cells survival and differentiation, and antibody production	Atacicept is effective in the reduction of DSA levels and extension of graft survival TACI mRNA expression level significantly unregulated in chronic AMR compared with graft function stable and healthy donors in renal transplants	(172, 182–185)
BCMA	Induction of the antigen presentation response Support the survival of late memory-B cell and all plasma cells by binding APRIL	Elevation of BCMA level is an effective biomarker for the development of *de novo* alloantibody responses in a mouse skin allograft transplant mouse model BCMA mRNA expression level significantly unregulated in chronic AMR compared with graft function stable and healthy donors in renal transplants	(66, 172, 186–189)

APRIL, A proliferation inducing ligand; AMR, Antibody-mediated allograft rejection; BAFF, B Cell Activating Factor; BCMA, B-cell maturation antigen; BM, Bone marrow; CD40L, CD40 ligand; DSA, Donor-specific HLA antibody; GC, Germinal center; TACI, Transmembrane activator and calcium-modulating cyclophilin ligand interactor; TD, Thymus-dependent.

NOVEL APPLIABLE COMPONENTS IN AMR

As mentioned above, we are closely evaluating the possibility of using an IgM antibody in AMR control (207). Therefore, we evaluate its possible use not only as an early diagnosis tool but also as a treatment method. Here, we discuss the involvement, as well as their clinical applicability of humoral immunity-associated components involved in IgM antibody in AMR control whilst referring to reports on the involvement mechanisms in pathological conditions in fields outside of transplants.

Role of IgM Receptors

IgM is the first immunoglobulin produced in response to antigen challenge, and B cell activation is enhanced by stimulatory IgM Fc receptor (FcμR)-mediated signals during the early stage of the immune response. The levels of IgG exceed those of IgM during the late stage of the adaptive immune response, during which the activation of B cells is inhibited by FcγRIIB-mediated inhibitory signals, indicating that stimulatory or inhibitory signals transduced by IgM or IgG may regulate B cell activation and antibody production (216).

FcμR is mainly expressed by B, T, and NK cells in humans and by B cells of mice (216–219). The expression levels of mouse FcμR differ depending on the B cell subset, and FcμR expressed in the trans-Golgi network restricts the transport of IgM-BCR to the B cell surface. FcμR expression is downregulated during GC reactions and at a higher level in plasma blast cells compared with those expressed by PCs and expressed in class-switched B cells (187). In contrast, FcμR-deficient MZBs are significantly mitigated in a mouse knockout model, in which the number of B cell subsets is altered or tonic signaling through the reduction of BCR expression (216, 219, 220). The FcμR-mediated signal contributes further to the maturation of B cell subsets and enhances B cell survival in response to treatment with anti-IgM antibodies (216, 221). These findings indicate that signals transmitted by the FcμR and BCR may cooperate to activate B cells and maintain their survival. In addition, this signal regulates the expression of IgM-BCR in immature B cells, which regulates the signal emitted when antigen activates the BCR through their cross-linking by antigen binding (220). In FcμR KO mice, the levels of natural IgM antibodies in the peripheral blood circulation are increased, and the formation of the GC, MBCs, differentiation of PCs, and production of antigen-specific IgG1 antibodies are reduced. These findings support the conclusion that the FcμR is required for the maintenance of the adaptive immune response and the control of the homeostasis of B-1/B-2 cells (216, 219).

Under pathological conditions, FcμR-mediated signaling controls the production of harmful autoreactive IgG antibodies and is involved in the development of autoimmune and inflammatory diseases, chronic lymphocytic leukemia, and others (37). In a model of severe human multiple sclerosis, the development of EAE is suppressed through the regulation of the functions of dendritic cell and Tregs (222). FcμR-mediated signal transduction increases self-Ag-triggered BCR signaling in immature B cells and contributes to the deletion, anergy, or both of autoreactive immature B cells in the BM, which induces immune tolerance (38).

Soluble IgM is a ligand for CD22 and forms a complex with an antigen. This complex suppresses the CD22-mediated BCR signaling *via* its binding to CD22 expressed on the B cell surface. CD22, which is expressed on the surface of mature B cells, is an inhibitory receptor. Specifically, phosphorylated CD22 signals through the BCR to downregulate B cell activation that prevents the overactivation of the immune system and development of autoimmune disease (223, 224).

In CD22-deficient mice, BCR ligation promotes the mobilization of intracellular calcium and inhibits BCR

signaling. Furthermore, CD22 signaling contributes to the differentiation of B cells and is required for the expansion of B1-b cells after BCR ligation (225, 226). The response to the TD antigen is normal during adaptive immunity; however, Thfs do not support B cells in CD22-deficient mice, because the CD22-CD22-ligand (CD22L) interaction is required for the activation of T cells (224, 226). In CD22-deficient mice, naïve-B cells differentiate into GCB cells but cannot differentiate into MBCs or PCs (221, 222). CD22-mediated inhibition of the BCR signal is associated with B cell tolerance, and CD22-CD22L interactions are required to maintain self-tolerance (227, 228).

Under pathological conditions, CD22 is involved in the control of autoimmune diseases and genetic variants of CD22 are related to the susceptibility of individuals to autoimmune diseases through a defect in B cell tolerance (39, 40). In patients with autoimmune diseases such as rheumatism, T1-diabetes, and SLE, inactivating mutations are frequently found in the CD22-ligand (229–231). Although CD22 is not a major cause of susceptibility to SLE in humans, CD22 deficiency may exert additive or synergistic effects on susceptibility to disease. Moreover, CD22 regulates the B cell response in autoimmune disease through regulation of BCRs and Tool-like receptors (TLRs) (224, 232).

Role of Scavenger Protein

Accumulation of foreign pathogens, apoptotic or necrotic dead cells, and their debris causes chronic inflammation and induces an autoimmune response, which must be eliminated to prevent their onset.

Apoptosis inhibitor of macrophage (AIM, also called CD5L) is a circulating protein that is a member of the scavenger receptor cysteine-rich superfamily. Normally, high levels of AIM bind to IgM pentamers and circulate in the peripheral blood in the inactivated state (233).

In B cells, AIM cooperates with TGF–beta1 to suppress B cell proliferation strongly and persistently and inhibit antibody production. TGF-beta1-mediated increased expression of AIM receptors on the surface of B cells is required for AIM to exert an effect on these cells (234). In addition, it has been reported that IL-10 protects transplanted grafts from recipient immunity and exert anti-inflammatory effects by inhibiting NLRP3 inflammasome activation or MPs with proinflammatory phenotypes by increasing AIM expression. Therefore, regulation of AIM expression may be related to the induction of immune tolerance (35).

Under pathological conditions, IgM dissociates from AIM during the recovery from renal injury through the enhanced clearance of a luminal obstruction during acute renal injury (234–236). Specifically, free AIM bound to debris interacts with kidney injury molecule 1 (KIM-1) that is expressed by injured tubular epithelial cells, resulting in enhanced phagocytic clearance of AIM-bound debris by epithelial cells (234, 237–239). Thus, free AIM is involved in the repair of acute kidney injury, because delayed or deficient removal of dead cells, or both, may cause secondary inflammation and fibrosis in tissues and may impair the repair of tissue damage and the regeneration of such tissues (237). Alternatively, macrophages produce AIM (236), which is involved in the pathophysiology of inflammatory colitis through the maintenance of the survival of macrophages, and the elimination of dead cells and toxic substances in hepatitis by supporting the phagocytic activity of macrophages (239–241). In the field of transplantation, it has been reported that the blood concentration of free AIM increases during acute cellular rejection in cardiac allograft rejection (242).

Role of IgM Antibody

Natural IgMs exert anti-inflammatory effects through clearing pathogens, scavenging toxins, inhibiting the production of inflammatory mediators, neutralizing cytokines, and scavenging complement to directly protect antigens from humoral immune attack (207, 243–248). These antibodies suppress inflammation and injury of target tissues caused by IgG autoantibodies through anti-idiotype activity, competitive inhibition of binding of IgG autoantibody to antigens, and suppression of IgG autoantibody production *via* signals from the FcμR expressed on the surface of B cells (249). Furthermore, these antibodies significantly inhibit T cell proliferation in lectin-stimulated PBMCs *in vitro* through the suppression of IL-2 production that enhances the functions of immunocompetent cells, bacterial aggregation, and opsonic activity (37). A polyclonal antibody preparation designated trimodulin, which contains IgM (~23%), IgA (~21%), and IgG (~56%), decreases the levels of TLR2, 4 as well as those of coagulation receptors (CD11b and CD64) in monocytes and inhibits lymphocyte proliferation and regulate of the production of pro- and anti-inflammatory cytokines, including TNF-α and IL-10. Therefore, these antibodies achieve a protective effect to alleviate the inflammatory reaction to target organs through these extents of involvement in immune system (243, 246, 247, 250–252).

In a model of renal ischemia-reperfusion-induced injury, the tissue-protective effects of IgM antibodies that recognize and inhibit the activities of danger-associated molecular patterns reflect human pathology. These mechanisms support the regeneration of damaged hepatocytes in a model of liver ischemia (42). In patients with sepsis, IgM-enriched IVig ameliorates pathology and reduces mortality through the improvement of the peripheral circulation, such that the numbers of circulating B cells and levels of IgM are significantly reduced in nonsurvivors compared with survivors, indicating that IgM is required to achieve successful therapy (253–256).

In an *in vitro* model of xenotransplantation, compared with IVig, IgM-enriched IVig more strongly inhibits the classical complement pathway and complement-dependent cytotoxicity caused by the deposition of C4 and C3 on the cell surface of pig cells treated with human serum and suppresses the development of hyperacute rejection of a xenotransplanted graft (257).

In allograft transplantation, IgM inhibits complement activity 10-times more than IgG (258). In the case of *de novo* DSA production after lung transplant recipients; treatment with IgM-enriched IVig is associated with the DSA-clearance effect, which improves the prognosis of transplantation. In early DSA-positive cases, treatment with IgM-enriched IVig and rituximab was superior to that with plasma exchange and rituximab, and the patients were comparable to the DSA-negative group in 1-year

survival after transplantation; treatment with IgM-enriched IVig was superior to treatment with plasma exchange and rituximab in DSA clearance (259). In addition, a tissue biopsy confirms no AMR after treatment only by IgM-enriched IVig injection, when AMR develops after heart transplantation (258).

Clinical Potential of Humoral Immunity–Associated Components in AMR

Further elucidation of the involvement of AIM in the humoral immune response to transplanted grafts will be applicable for AMR control. Newly discovered cytokines, antibodies, and receptors involved in antibody production may be expected to be translated to the clinical application in early diagnosis, management, and prognosis prediction. These efforts require the identification of the roles of these components in the underlying mechanisms of AMR.

In the field of transplantation, FcμR-mediated signaling maintains the homeostasis of B1/B2 cells (216, 219) and potentially alleviates the pathology of AMR (38), and elucidation of the involvement of this signaling in AMR development will likely contribute to the development of therapies designed to protect target grafts from humoral immune responses mounted by recipients.

CD22-mediated signaling may be expected to be useful as B cell depletion therapy in AMR control, because IVig is administered as a treatment for AMR, and one of the mechanisms is the induction of mature B cell apoptosis *via* binding between sialylated IVig and CD22 (71). It is therefore important to evaluate the involvement of CD22-targeting agents in the activation of humoral immunity against transplanted grafts in the same manner as they are applied to the treatment of autoimmune diseases to effectively manage AMR (231, 232).

As a diagnostic method, clinical application of these receptors to new diagnostic methods will be achieved if the functions and structural properties of these receptors can be shown to be involved in humoral immunity to transplanted grafts.

As scavenger protein, it has also been reported that an increase in AIM blood concentrations is associated with the development of acute rejection following heart transplantation, indicating that the blood concentration of free AIM may increase in the early stage of humoral immunity activation in transplanted grafts, and it is expected to be useful as an early diagnostic method for AMR (242). Therefore, the utility of AIM as a diagnostic modality can be ascertained after elucidating its AIM in the development of AMR. In addition, AIM controls inflammation and repairs damaged tissues *via* phagocytosis of apoptotic cells.

Although IVig has been commonly used for AMR control, the significance of IgM-enriched IVig has been reported in the field of severe infection and organ ischemia (42, 253–258). IgM-enriched IVig may exert more strongly inhibits complement activation as compared with IVig (258, 259). Therefore, identifying the detailed mechanism of IgM involvement in humoral immune activation to transplanted grafts and the significance of IgM-enriched IVig compared with that of IVig will likely lead to further clinical application of IgM-enriched IVig to manage AMR.

Significantly, in addition to the potential induction of immune tolerance of humoral immunity-associated components to transplanted grafts (35, 243, 247, 248, 250–252), AIM and IgM-enriched IVig have a tissue repair and regeneration effect through the clearance of injured tissue (42, 224, 233–235). Therefore, humoral immunity associated injury after the onset of AMR, which was considered irreversible, could be recovered by clinical application of these humoral immunity-associated components.

We summarized clinical potential of these components in the context of AMR control (**Figure 3**).

CONCLUDING REMARKS

In this study, we discussed the pathways by which naïve-B cells are sensitized to donor-specific HLA antigens and differentiate into LLPCs, which produce DSAs. This study also presented evidence regarding the mechanism by which immunocompetent cells participate in the signal transduction pathways that contribute to AMR and the mechanisms of immunosuppressive therapy designed to suppress the development of AMR (17–19).

Although immunosuppressive therapies that may be useful for suppressing each process during AMR development have been developed, AMR control remains challenging. The main cause of poor AMR control is that positivity for antibodies to donor-specific HLA is used as a reference as one of the diagnostic methods for AMR (17); however, LLPCs, which produce antibodies inducing AMR, may be difficult to remove by applying conventional immunosuppressive therapy and the pathological condition progresses irreversibly when these antibodies are present in serum (20, 71, 72, 260). In addition, the information needed to improve management after transplantation including individual differences in pathological conditions and drug susceptibility has not been discovered.

It has been reported that humoral monitoring methods for better evaluating the humoral immune response to the transplanted graft might contribute to resolving this problem by analyzing the antigenic specificity of MBCs circulating in peripheral blood using *in vitro* assay systems (22–27) and further possibility of gene-based control method in the context of AMR as following; Microarray techniques can be used to elucidate the molecular mechanisms that induce the migration of LLPCs to BM and promote their longevity (259). Thus, these techniques may permit inhibition of the differentiation of LLPCs. Further; NGS analysis of antibody reactivity to transplanted grafts can be applied to predict the antibodies that cause AMR (28–36). This knowledge, combined with the identification of genetic polymorphisms associated with drug sensitivity, will undoubtedly contribute to the development of optimal management strategies.

In addition to the development of these diagnostic methods, recent studies revealed relevant factors, such as anti-inflammatory effects, reduction of harmful IgG autoantibodies production, tissue regeneration, and their clinical applicability in the fields of autoimmune diseases and inflammatory disease and severe infection disease, and the others (37–42). Therefore, in the field of transplantation, by further clarifying the mechanism of their involvement in AMR, methods for improving the control of AMR

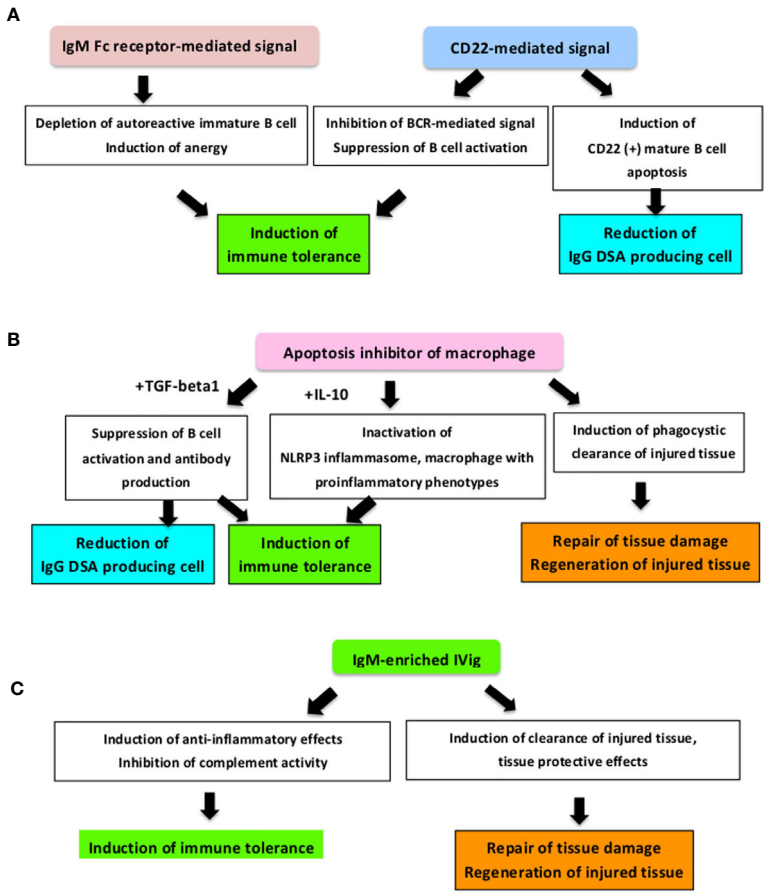


FIGURE 3 | How these novel applicable components improve the prognosis of AMR. We summarised the clinical potential of novel humoral immunity-associated components in AMR control and AMR development mechanisms. **(A)** As an IgM receptor, the FCu receptor-mediated signal controls harmful autoreactive IgG antibodies production and controls autoimmunity and inflammation through regulating immunoregulatory cells (37, 38, 216, 219, 222). In addition, this signal is associated with immune tolerance induction by promoting deletion and energy of immature B cells (38). CD22-mediated signaling also induces immune tolerance *via* CD22-CD22L interaction and CD22-mediated inhibition of the BCR-mediated signal (227, 228) and CD22 (+) mature B cell apoptosis (71). **(B)** As a scavenger protein, it has been reported that free Apoptosis inhibitor of macrophage (AIM) works to suppress inflammation, tissue injury and tissue regeneration through phagocytic activity during acute kidney injury (233–241) and AIM mediates immune tolerance induction by IL-10 and suppresses the immune response by inducing macrophages with immunosuppressive phenotype activation (35) and cooperates with TGF-beta to suppress B cell proliferation and antibody production (233). **(C)** As a polyclonal IgM antibody, IgM-enriched IVig strongly suppresses cell proliferation, has a inhibitory effect in complement activity (257, 258), and alleviates the humoral immunity-associated pathological condition in severe infection, organ ischemia, and transplants (42, 253–256, 258, 259). BCR, B cell receptor; DSA, Donor-specific HLA antibody; IVig, Intravenous immunoglobulin; TGF, Transforming Growth Factor.

including early diagnosis, suppression of AMR development, and alleviation of pathology may be developed.

Although IgG antibody has been the main focus in the field of transplants, we focused on the clinical potential of detecting DSA-specific IgM and IgG-MBC differentiation using *in vitro* assay systems as an early diagnostic method and biomarkers that enable the inhibition of AMR development with less invasive therapeutic intervention (207). The findings supported the clinical applicability of the detection of DSA-specific IgM-MBC differentiation after elucidating the optimal conditions for inducing the differentiation of DSA-specific IgM-MBC differentiation into IgG-PCs, the detailed mechanism leading to AMR.

Alternatively, IVig has been administered for AMR control mainly, but IgM-enriched IVig has been reported to improve the pathological condition and prognosis in severe infectious diseases and organ ischemia (42, 253–256). Therefore, further elucidation of how signal mediated by IgM-enriched-IVig are involved in the AMR development may contribute to the establishment of AMR control.

Therefore, focusing on the involvement mechanism of humoral immunity-associated components in the pathological conditions

regardless of the difference in fields and conventional knowledge and elucidating the mechanism by which these humoral immunity-associated components participate in AMR development will likely be applicable to the development of new diagnostic and therapeutic methods for improving AMR management.

AUTHOR CONTRIBUTIONS

YM designed and wrote the paper. TW revised the paper. TW and X-KL provided excellent advice. All authors contributed to the article and approved the submitted version.

REFERENCES

1. Bunjes D, Hardt C, Roöllinghoff M, Wagner H. Cyclosporin A Mediates Immu- Nosuppression of Primary Cytotoxic T Cell Responses by Impairing the Release of Interleukin 1 and Interleukin 2. *Eur J Immunol* (1981) 11 (8):657–61. doi: 10.1002/eji.1830110812
2. Wang CJ, Heuts F, Ovcinnikovs V, Wardzinski L, Bowers C, Schmidt EM, et al. CTLA-4 Controls Follicular Helper T-Cell Differentiation by Regulating the Strength of CD28 Engagement. *Proc Natl Acad Sci USA* (2015) 112:524–9. doi: 10.1073/pnas.1414576112
3. Xu H, Li X, Liu D, Li J, Zhang X, Chen X, et al. Follicular T-Helper Cell Recruitment Governed by Bystander B Cells and ICOS-Driven Motility. *Nature* (2013) 496:523–7. doi: 10.1038/nature12058
4. Lu D, Ni Z, Liu X, Feng S, Dong X, Shi X, et al. Beyond T Cells: Understanding the Role of PD-1/PD-L1 in Tumor-Associated Macrophages. *J Immunol Res* (2019) 2019:1919082. doi: 10.1155/2019/1919082
5. Crotty S. A Brief History of T Cell Help to B Cells. *Nat Rev Immunol* (2015) 15:185–9. doi: 10.1038/nri3803
6. McAdam AJ, Greenwald RJ, Levin MA, Chernova T, Malenkovich N, Ling V, et al. Icos Is Critical for CD40-Mediated Antibody Class Switching. *Nature* (2001) 409:102–5. doi: 10.1038/35051107
7. Tafuri A, Shahinian A, Bladt F, Yoshinaga SK, Jordana M, Wakeham A, et al. ICOS Is Essential for Effective T-Helper-Cell Responses. *Nature* (2001) 409:105–9. doi: 10.1038/35051113
8. Dong C, Juedes AE, Temann UA, Shresta S, Allison JP, Ruddle NH, et al. ICOS Co-Stimulatory Receptor Is Essential for T-Cell Activation and Function. *Nature* (2001) 409:97–101. doi: 10.1038/35051100
9. Dong C, Temann UA, Flavell RA. Cutting Edge: Critical Role of Inducible Costimulator in Germinal Center Reactions. *J Immunol* (2001) 166:3659–62. doi: 10.4049/jimmunol.166.6.3659
10. Moriyama S, Takahashi N, Green JA, Hori S, Kubo M, Cyster JG, et al. Sphingosine-1-Phosphate Receptor 2 Is Critical for Follicular Helper T Cell Retention in Germinal Centers. *J Exp Med* (2014) 211:1297–305. doi: 10.1084/jem.20131666
11. Qi H, Cannons JL, Klauschen F, Schwartzberg PL, Germain RN. SAP-Controlled T-B Cell Interactions Underlie Germinal Centre Formation. *Nature* (2008) 455:764–9. doi: 10.1038/nature07345
12. Cannons JL, Qi H, Lu KT, Dutta M, Gomez-Rodriguez J, Cheng J, et al. Optimal Germinal Center Responses Require a Multistage T Cell:B Cell Adhesion Process Involving Integrins, SLAM-Associated Protein, and CD84. *Immunity* (2010) 32:253–65. doi: 10.1016/j.immuni.2010.01.010
13. Czar MJ, Kersh EN, Mijares LA, Lanier G, Lewis J, Yap G, et al. Altered Lymphocyte Responses and Cytokine Production in Mice Deficient in the X-Linked Lymphoproliferative Disease Gene SH2D1A/DSHP/SAP. *Proc Natl Acad Sci USA* (2001) 98:7449–54. doi: 10.1073/pnas.131193098
14. Crotty S, Kersh EN, Cannons J, Schwartzberg PL, Ahmed R. SAP Is Required for Generating Long Term Humoral Immunity. *Nature* (2003) 421:282–7. doi: 10.1038/nature01318
15. Cannons JL, Yu LJ, Jankovic D, Crotty S, Horai R, Kirby M, et al. SAP Regulates T Cell-Mediated Help for Humoral Immunity by a Mechanism Distinct From Cytokine Regulation. *J Exp Med* (2006) 203:1551–65. doi: 10.1084/jem.20052097
16. Yusuf I, Kageyama R, Monticelli L, Johnston RJ, Ditoro D, Hansen K, et al. Germinal Center T Follicular Helper Cell IL-4 Production Is Dependent on Signaling Lymphocytic Activation Molecule Receptor (CD150). *J Immunol* (2010) 185:190–202. doi: 10.4049/jimmunol.0903505
17. Matsuda Y, Sarwal MM. Unraveling the Role of Allo-Antibodies and Transplant Injury. *Front Immunol* (2016) 7:432. doi: 10.1159/000501460
18. Perera J, Huang H. The Development and Function of Thymic B Cells. *Cell Mol Life Sci* (2015) 72(14):2657–63. doi: 10.1007/s00018-015-1895-1
19. Mei HE, Wirries I, Frölich D, Brisslert M, Giesecke C, Grün JR, et al. A Unique Population of IgG-Expressing Plasma Cells Lacking CD19 Is Enriched in Human Bone Marrow. *Blood* (2015) 125:1739–48. doi: 10.1182/blood-2014-02-555169
20. Brynjolfsson SF, Persson Berg L, Olsen Ekerhult T, Rimkute I, Wick MJ, Mårtensson IL, et al. Long-Lived Plasma Cells in Mice and Men. *Front Immunol* (2018) 16:2673. doi: 10.3389/fimmu.2018.02673
21. Lynch RJ, Silva IA, Chen BJ, Punch JD, Cascalho M, Platt JL. Cryptic B Cell Response to Renal Transplantation. *Am J Transpl* (2013) 13:1713–23. doi: 10.1111/ajt.12308
22. Jahnmatz M, Kesa G, Netterlid E, Buisman AM, Thorstensson R, Ahlborg N. Optimization of a Human IgG B-Cell ELISpot Assay for the Analysis of Vaccine-Induced B-Cell Responses. *J Immunol Methods* (2013) 391:50. doi: 10.1016/j.jim.2013.02.009
23. Pinna D, Corti D, Jarrossay D, Sallusto F, Lanzavecchia A. Clonal Dissection of the Human Memory B-Cell Repertoire Following Infection and Vaccination. *Eur J Immunol* (2009) 39:1260. doi: 10.1002/eji.200839129
24. Lúcia M, Luque S, Crespo E, Melilli E, Cruzado JM, Martorell J. Preformed Circulating HLA-Specific Memory B Cells Predict High Risk of Humoral Rejection in Kidney Transplantation. *Kidney Int* (2015) 88:874. doi: 10.1038/ki.2015.205
25. Han M, Rogers JA, Lavingia B. Stastny P.Peripheral Blood B Cells Producing Donor-Specific HLA Antibodies *In Vitro*. *Hum Immunol* (2009) 70:29. doi: 10.1016/j.humimm.2008.10.013
26. Snanoudj R, Claas FHJ, Heidt S, Legendre C, Chatenoud L, Candon S. Restricted Specificity of Peripheral Alloreactive Memory B Cells in HLA-Sensitized Patients Awaiting a Kidntransplant. *Kidney Int* (2015) 87:1230. doi: 10.1038/ki.2014.390
27. Heidt S, Roelen DL, de Vaal YJ, Kester MG, Eijsink C. Thomas, sA Novel ELISPOT Assay to Quantify HLA-Specific B Cells in HLA-Immunized Individuals. al *Am J Transpl* (2012) 12:1469–78. doi: 10.1111/j.1600-6143.2011.03982.x
28. Butte AJ, Sigdel TK, Wadia PP, Miklos DB, Sarwal MM. Protein Microarrays Discover Angiotensinogen and PRKRIP1 as Novel Targets for Autoantibodies in Chronic Renal Disease. *Mol Cell Proteomics* (2011) 10 (3):M110.000497. doi: 10.1074/mcp.M110.000497
29. Yang JY, Sigdel TK, Sarwal MM. Self-Antigens and Rejection: A Proteomic Analysis. *Curr Opin Organ Transpl* (2016) 21(4):362–7. doi: 10.1097/MOT.0000000000000328
30. Chen R, Sigdel TK, Li L, Kambham N, Dudley JT, Hsieh SC, et al. Differentially Expressed RNA From Public Microarray Data Identifies Serum Protein Biomarkers for Cross-Organ Transplant Rejection and Other Conditions. *PloS Comput Biol* (2010) 6(9):e1000940. doi: 10.1371/journal.pcbi.1000940
31. Aschauer C, Jelencsics K, Hu K, Heinzel A, Vetter J, Fraunhofer T, et al. Next Generation Sequencing Based Assessment of the Alloreactive T Cell Receptor Repertoire in Kidney Transplant Patients During Rejection: A Prospective Cohort Study. *BMC Nephrol* (2019) 20(1):346. doi: 10.1186/s12882-019-1541-5
32. Goldstein LD, Chen YJ, Wu J, Chaudhuri S, Hsiao YC, Schneider K. Single-Cell B-Cell Receptor Sequencing Enables Rapid Discovery of Diverse Antigen-Reactive Antibodies. *Commun Biol* (2019) 2:304. doi: 10.1038/s42003-019-0551-y
33. Kim D, Park D. Deep Sequencing of B Cell Receptor Repertoire. *BMB Rep* (2019) 52(9):540–7. doi: 10.5483/BMBRep.2019.52.9.192
34. Luque S,M, Bestard O. Refinement of Humoral Immune Monitoring in Kidney Transplantation: The Role of "Hidden" Alloreactive Memory B Cells. *Transpl Int* (2017) 30(10):955–68. doi: 10.1111/tri.13014

35. Su L, Yin L, Yang J, Sun L. Correlation Between Gene Polymorphism and Blood Concentration of Calcineurin Inhibitors in Renal Transplant Recipients: An Overview of Systematic Reviews. *Med (Baltimore)* (2019) 98(26):e16113. doi: 10.1097/MD.0000000000016113
36. Anglicheau D, Verstuyft C, Laurent-Puig P, Becquemont L, Schlageter MH, Cassinat B, et al. Association of the Multidrug Resistance-1 Gene Single-Nucleotide Polymorphisms With the Tacrolimus Dose Requirements in Renal Transplant Recipients. *J Am Soc Nephrol* (2003) 14(7):1889–96. doi: 10.1097/01.asn.0000073901.94759.36
37. Nguyen TT, Baumgarth N. Natural IgM and the Development of B Cell-Mediated Autoimmune Diseases. *Crit Rev Immunol* (2016) 36:163–77. doi: 10.1615/CritRevImmunol.2016018175
38. Honjo K, Kubagawa Y, Jones DM, Dizon B, Zhu Z, Ohno H, et al. Altered Ig Levels and Antibody Responses in Mice Deficient for the Fc Receptor for IgM (FcmuR). *Proc Natl Acad Sci USA* (2012) 109:15882–7. doi: 10.1073/pnas.1206567109
39. Angata T. Associations of Genetic Polymorphisms of Siglecs With Human Diseases. *Glycobiology* (2014) 24:785–93. doi: 10.1093/glycob/cwu043
40. Cariappa A, Takematsu H, Liu H, Diaz S, Haider K, Boboila C, et al. B Cell Antigen Receptor Signal Strength and Peripheral B Cell Development Are Regulated by a 9-O-Acetyl Sialic Acid Esterase. *J Exp Med* (2009) 206:125–38. doi: 10.1084/jem.20081399
41. Haruta I, Kato Y, Hashimoto E, Minjares C, Kennedy S, Uto H. Association of AIM, a Novel Apoptosis Inhibitory Factor, With Hepatitis *via* Supporting Macrophage Survival and Enhancing Phagocytotic Function of Macrophages. *J Biol Chem* (2001) 276:22910–4. doi: 10.1074/jbc.M100324200
42. Krautz C, Maier SL, Brunner M, Langheinrich M, Giamarellos-Bourboulis EJ, Gogos C, et al. Reduced Circulating B Cells and Plasma IgM Levels Are Associated With Decreased Survival in Sepsis—A Meta-Analysis. *J Crit Care* (2018) 45:71–5. doi: 10.1016/j.jcrc.2018.01.013
43. Woodle ES, Tremblay S, Rossi A, Rojas CC, Alloway R, Roskin K, et al. Plasma Cell Targeting to Prevent Antibody-Mediated Rejection. *Am J Transplant* (2020) 20 Suppl 4:33–41. doi: 10.1111/ajt.15889
44. Roco JA, Mesin L, Binder SC, Nefzger C, Gonzalez-Figueroa P, Canete PF, et al. Class-Switch Recombination Occurs Infrequently in Germinal Centers. *Immunity* (2016) 51:337–50. doi: 10.1016/j.immuni.2019.07.001
45. Su H, Zhang CY, Lin JH, Hammes HP, Zhang C. The Role of Long-Lived Plasma Cells in Antibody-Mediated Rejection of Kidney Transplantation: An Update. *Kidney Dis (Basel)* (2019) 5(4):211–9. doi: 10.1159/000501460.Epub 2019 Aug 20
46. de Goër de Herve MG, Durali D, Dembele B, Giuliani M, Tran TA, Azzarone B, et al. Interferon-Alpha Triggers B Cell Effector 1 (Be1) Commitment. *PloS One* (2011) 6(4):e19366. doi: 10.1371/journal.pone.0019366
47. Rookhuizen DC, DeFranco AL. Toll-Like Receptor 9 Signaling Acts on Multiple Elements of the Germinal Center to Enhance Antibody Responses. *Proc Natl Acad Sci USA* (2014) 111:E3224–33. doi: 10.1073/pnas.1323985111
48. Chen W, Bai J, Huang H, Bi L, Kong X, Gao Y, et al. Low Proportion of Follicular Regulatory T Cell in Renal Transplant Patients With Chronic Antibody-Mediated Rejection. *Sci Rep* (2017) 2. 7(1):1322. doi: 10.1038/s41598-017-01625-3
49. Yazdani S, Callemeyn J, Gazut S, Lerut E, de Loor H, Wevers M. Natural Killer Cell Infiltration Is Discriminative for Antibody-Mediated Rejection and Predicts Outcome After Kidney Transplantation. *Kidney Int* (2019) 95(1):188–98. doi: 10.1016/j.kint.2018.08.027
50. Guerriero JL. Macrophages: Their Untold Story in T Cell Activation and Function. *Int Rev Cell Mol Biol* (2019) 342:73–93. doi: 10.1016/bs.ircmb.2018.07.001
51. Charreau B. Cellular and Molecular Crosstalk of Graft Endothelial Cells During AMR: Effector Functions and Mechanisms. *Transplantation* (preprint). doi: 10.1097/TP.0000000000003741
52. Carroll MC. The Role of Complement in B Cell Activation and Tolerance. *Adv Immunol* (2000) 74:61–88. doi: 10.1016/s0065-2776(08)60908-6
53. Smith NA, Coleman CB, Gewurz BE, Rochford R. CD21 (Complement Receptor 2) Is the Receptor for Epstein-Barr Virus Entry Into T Cells. *J Virol* (2020) 94(11):e00428–20. doi: 10.1128/JVI.00428-20
54. Dempsey PW, Allison ME, Akkaraju S, Goodnow CC, Fearon DT. C3d of Complement as a Molecular Adjuvant: Bridging Innate and Acquired Immunity. *Science* (1996) 271:348–50. doi: 10.1126/science.271.5247.348
55. Lanzavecchia A. Receptor-Mediated Antigen Uptake and Its Effect on Antigen Presentation to Class II-Restricted T Lymphocytes. *Annu Rev Immunol* (1990) 8:773–93. doi: 10.1146/annurev.iy.08.040190.004013
56. Brimnes MK, Hansen BE, Nielsen LK, Dziegiel MH, Nielsen CH. Uptake and Presentation of Myelin Basic Protein by Normal Human B Cells. *PloS One* (2014) 9(11):e113388. doi: 10.1371/journal.pone.0113388
57. Heesters BA, Chatterjee P, Kim YA, Gonzalez SF, Kuligowski MP, Kirchhausen T, et al. Endocytosis and Recycling of Immune Complexes by Follicular Dendritic Cells Enhances B Cell Antigen Binding and Activation. *Immunity* (2013) 38(6):1164–75. doi: 10.1016/j.immuni.2013.02.023
58. Suzuki K, Grigorova I, Phan TG, Kelly LM, Cyster JG. Visualizing B Cell Capture of Cognate Antigen From Follicular Dendritic Cells. *J Exp Med* (2009) 206(7):1485–93. doi: 10.1084/jem.20090209
59. Jozsi M, Prechl J, Bajtay Z, Erdei A. Complement Receptor Type 1 (CD35) Mediates Inhibitory Signals in Human B Lymphocytes. *J Immunol* (2002) 168(6):2782–2788.42. doi: 10.1097/01.asn.0000073901.94759.36
60. Barnett AN, Asgari E, Chowdhury P, Sacks SH, Dorling A, Mamode N. The Use of Eculizumab in Renal Transplantation. *Clin Transplant* (2013) 27(3):E216–29. doi: 10.1111/ctr.12102
61. van de Veen W, Stanic B, Yaman G, Wawrzyniak M, Söllner S, Akdis DG, et al. IgG4 Production Is Confined to Human IL-10-Producing Regulatory B Cells That Suppress Antigen-Specific Immune Responses. *J Allergy Clin Immunol* (2013) 131(4):1204–12. doi: 10.1016/j.jaci.2013.01.014
62. Tebbe B, Wilde B, Ye Z, Wang J, Wang X, Jian F, et al. Renal Transplant Recipients Treated With Calcineurin-Inhibitors Lack Circulating Immature Transitional CD19+CD24hiCD38hi Regulatory B-Lymphocytes. *PloS One* (2016) 11(4):e0153170. doi: 10.1371/journal.pone.0153170
63. Latorre I, Esteve-Sole A, Redondo D, Giest S, Argilaguet J, Alvarez S, et al. Calcineurin and mTOR Inhibitors Have Opposing Effects on Regulatory T Cells While Reducing Regulatory B Cell Populations in Kidney Transplant Recipients. *Transpl Immunol* (2016) 35:1–6. doi: 10.1016/j.trim.2016.01.004
64. Knight AK, Radigan L, Marron T, Langs A, Zhang L, Cunningham-Rundles C. High Serum of BAFF, APRIL, and TACI in Common Variable Immunodeficiency. *Clin Immunol* (2007) 124(2):182–9. doi: 10.1016/j.clim.2007.04.012
65. Nakayamada S, Tanaka Y. BAFF- and APRIL-Targeted Therapy in Systemic Autoimmune Diseases. *Inflammation Regen* (2016) 36:6. doi: 10.1186/s41232-016-0015-4
66. Matsuda Y, Haneda M, Kadomatsu K, Kobayashi T. A Proliferation-Inducing Ligand Sustains the Proliferation of Human Naïve ($CD27^-$) B Cells and Mediates Their Differentiation Into Long-Lived Plasma Cells *In Vitro via* Transmembrane Activator and Calcium Modulator and Cyclophilin Ligand Interactor and B-Cell Mature Antigen. *Cell Immunol* (2015) 295(2):127–36. doi: 10.1016/j.cellimm.2015.02.011
67. Whitehouse G, Gray E, Mastoridis S, Merritt E, Kodela E, Yang JHM, et al. IL-2 Therapy Restores Regulatory T-Cell Dysfunction Induced by Calcineurin Inhibitors. *Proc Natl Acad Sci USA* (2017) 114(27):7083–8. doi: 10.1073/pnas.1620835114
68. Perry DK, Pollinger HS, Burns JM, Rea D, Ramos E, Platt JL. Alloantibody-Secreting Cells Demonstrating Resistance to Desensitization With IVIG and rATG. *Am J Transpl* (2008) 8(1):133–43. doi: 10.1111/j.1600-6143.2007.02039.x
69. Lightman SM, Utley A, Lee KP. Survival of Long-Lived Plasma Cells (LLPC): Piecing Together the Puzzle. *Front Immunol* (2019) 10:965. doi: 10.3389/fimmu.2019.00965
70. Nguyen DC, Garimalla S, Xiao H, Kyu S, Albizua I, Galipeau J. Factors of the Bone Marrow Microniche That Support Human Plasma Cell Survival and Immunoglobulin Secretion. *Nat Commun* (2018) 9(1):3698. doi: 10.1038/s41467-018-05853-7
71. Fehr T, Gaspert A. Antibody-Mediated Kidney Allograft Rejection: Therapeutic Options and Their Experimental Rationale. *Transpl Int* (2012) 25:623–32. doi: 10.1111/j.1432-2277.2012.01453.x
72. Marrari M, Duquesnoy RJ. Detection of Donor-Specific HLA Antibodies Before and After Removal of a Rejected Kidney Transplant. *Transpl Immunol* (2010) 22.3–4:105–9. doi: 10.1016/j.trim.2009.12.005

73. Cooper JE, Gralla J, Chan L, Wiseman AC. Clinical Significance of Post Kidney Transplant *De Novo* DSA in Otherwise Stable Grafts. *Clin Transpl* (2011) 359–64.
74. Knight R, Eagar T, Nguyen D, Graviss E, Kuten S, Patel S. Stable Renal Allograft Function Is a Benign Finding. *Transplantation* (2018) 102:S39. doi: 10.1097/01.tp.0000542596.39174.b7
75. Lee DR, Kim BC, Kim JP, Kim IG, Jeon MY. C3d-Binding Donor-Specific HLA Antibody Is Associated With a High Risk of Antibody-Mediated Rejection and Graft Loss in Stable Kidney Transplant Recipients: A Single-Center Cohort Study. *Transplant Proc* (2018) 50(10):3452–9. doi: 10.1016/j.transproceed.2018.06.037
76. Viglietti D, Bouatou Y, Kheav VD, et al. Complement-Binding Anti-HLAantibodies Are Independent Predictors of Response to Treatment in Kidney Recipients With Antibody-Mediated Rejection. *Kidney Int* (2018) 94 (4):773–87. doi: 10.1016/j.kint.2018.03.015
77. Shiina Y, Suzuki H, Kaiho T, Matsumoto H, Hata A, Yamamoto, et al. Complement Inhibition as Potential Novel Therapy for Antibody-Mediated Rejection After Lung Transplantation in Murine Antibody-Mediated Rejection Model. *J Heart Lung Transplant* 2020 (2020) .39:4. doi: 10.1097/01.asn.0000073901.94759.36
78. Stegall MD, Diwan T, Raghavaiah S, Cornell LD, Burns J, Dean PG, et al. Terminal Complement Inhibition Decreases Antibody-Mediated Rejection in Sensitized Renal Transplant Recipients. *Am J Transplant* (2011) 11 (11):2405–13. doi: 10.1111/j.1600-6143.2011.03757.x
79. Stegall MD, Chedid MF, Cornell LD. The Role of Complement in Anti-Body-Mediated Rejection in Kidney Transplantation. *Nat Rev Nephrol* (2012) 8(11):670–8. doi: 10.1038/nrneph.2012.212
80. Patel JK, Coutance G, Loupy A, Dilibero D, Hamilton M, Kittleson M, et al. Complement Inhibition for Prevention of Antibody Mediated Rejection in Immunologically High-Risk Heart Allograft Recipients, Terminal Complement Inhibition Decreases Antibody-Mediated Rejection in Sensitized Renal Transplant Recipients. *Am J Transplant* preprint. doi: 10.1111/ajt.16420
81. Locke JE, M ro CM, Singer AL, Segev DL, Haas M, Hillel AT, et al. The Use of Antibody to Complement Protein C5 for Salvage Treatment of Severe Antibody-Mediated Rejection. *Am J Transplant* (2009) 9(1):231–5. doi: 10.1111/j.1600-6143.2008.02451
82. Lefaucheur C, Viglietti D, Hidalgo LG, Ratner LE, Bagnasco SM, Batal I, et al. Complement-Activating Anti-HLA Antibodies in Kidney Transplantation: Allograft Gene Expression Profiling and Response to Treatment. *J Am Soc Nephrol* (2018) 29(2):620–35. doi: 10.1681/ASN.2017050589
83. Böhmig GA, Wahrmann M, Eskandary F, Rostaing L. Novel Approaches to Block Complement. *Transplantation* (2018) 102(11):1837–43. doi: 10.1097/TP.0000000000002267
84. Cippà PE, Liu J, Sun B, Kumar S, Naesens M, McMahon AP. A Late B Lymphocyte Action in Dysfunctional Tissue Repair Following Kidney Injury and Transplantation. *Nat Commun* (2019) 10(1):1157. doi: 10.1038/s41467-019-09092-2
85. Huang E, Vo A, Choi J, Ammerman N, Lim K, Sethi S, et al. Three-Year Outcomes of a Randomized, Double-Blind, Placebo-Controlled Study Assessing Safety and Efficacy of C1 Esterase Inhibitor for Prevention of Delayed Graft Function in Deceased Donor Kidney Transplant Recipients. *Clin J Am Soc Nephrol* (2020) 15(1):109–16. doi: 10.2215/CJN.04840419
86. Viglietti D, Gosset C, Loupy A, Deville L, Verine J, Zeevi A, et al. C1 Inhibitor in Acute Antibody-Mediated Rejection Nonresponsive to Conventional Therapy in Kidney Transplant Recipients: A Pilot Study. *Am J Transpl* (2016) 16(5):1596–603. doi: 10.1111/ajt.13663
87. Chun N, Fairchild RL, Li Y, Liu J, Zhang M, Baldwin WM, et al. Complement Dependence of Murine Costimulatory Blockade-Resistant Cellular Cardiac Allograft Rejection. *Am J Transpl* (2017) 17(11):2810–9. doi: 10.1111/ajt.14328
88. Jordan SC, Choi J, Aubert O, Haas M, Loupy A, Huang E, et al. A Phase I/II, Double-Blind, Placebo-Controlled Study Assessing Safety and Efficacy of C1 Esterase Inhibitor for Prevention of Delayed Graft Function in Deceased Donor Kidney Transplant Recipients. *Am J Transpl* (2018) 18(12):2955–64. doi: 10.1111/ajt.14767
89. Berger M, Lefaucheur C, Jordan SC. Update on C1 Esterase Inhibitor in Human Solid Organ Transplantation. *Transplantation* (2019) 103(9):1763–75. doi: 10.1097/TP.0000000000002717
90. Eskandary F, Jilma B, Mühlbacher J, Wahrmann M, Regele H, Kozakowski N, et al. Anti-C1s Monoclonal Antibody BIVV009 in Late Antibody-Mediated Kidney Allograft Rejection-Results From a First-in-Patient Phase 1 Trial. *Am J Transpl* (2018) 18(4):916–26. doi: 10.1111/ajt.14528
91. Freire PC, Muñoz CH, Derhaschnig U, Schoergenhofer C, Firbas C, Parry GC, et al. Specific Inhibition of the Classical Complement Pathway Prevents C3 Deposition Along the Dermal-Epidermal Junction in Bullous Pemphigoid. *Heil J Invest Dermatol* (2019) 139(12):2417–2424.e2. doi: 10.1016/j.jid.2019.04.025
92. Schwarz C, Mahr B, Muckenhuber M, Wekerle T. Belatacept/CTLA4Ig: An Update and Critical Appraisal of Preclinical and Clinical Results. *Expert Rev Clin Immunol* (2019) 14(7):583–92. doi: 10.1080/1744666X.2018.1485489
93. Vincenti F, Rostaing L, Grinyo J, Rice K, Steinberg S, Gaite L, et al. Belatacept and Long-Term Outcomes in Kidney Transplantation. *N Engl J Med* (2016) 374(4):333–43. doi: 10.1056/NEJMoa1506027
94. Jain D, Rajab A, Young JS, Yin D, Nadasdy T, Chong AS, et al. Reversing Donor-Specific Antibody Responses and Antibody-Mediated Rejection With Bortezomib and Belatacept in Mice and Kidney Transplant Recipients. *Am J Transplant* (2020) 20(10):2675–85. doi: 10.1111/ajt.15881
95. Young JS, Chen J, Miller ML, Vu V, Tian C, Moon JJ, et al. Delayed Cytotoxic T Lymphocyte-Associated Protein 4-Immunoglobulin Treatment Reverses Ongoing Alloantibody Responses and Rescues Allografts From Acute Rejection. *Am J Transplant* (2016) 16(8):2312–23. doi: 10.1111/ajt.13761
96. Levitsky J, Miller J, Huang X, Chandrasekaran D, Chen L, Mathew JM. Inhibitory Effects of Belatacept on Allospecific Regulatory T-Cell Generation in Humans. *Transplantation* (2013) 96(8):689–96. doi: 10.1097/TP.0b013e31829f1607
97. Alvarez, Salazar EK, Cortés-Hernández A, Alemán-Muench GR, Alberú J, Rodríguez-Aguilera JR, Recillas-Targa F, et al. Methylation of FOXP3 TSDR Underlies the Impaired Suppressive Function of Tregs From Long-Term Belatacept-Treated Kidney Transplant Patients. *Front Immunol* (2017) 8:219. doi: 10.3389/fimmu.2017.00219
98. Cagnotto G, Willim M, Nilsson JÅ, Compagno M, Jacobsson LTH, Saevarsdottir S, et al. Abatacept in Rheumatoid Arthritis: Survival on Drug, Clinical Outcomes, and Their Predictors-Data From a Large National Quality Register. *Turesson C Arthritis Res Ther* (2020) 22(1):15. doi: 10.1186/s13075-020-2100-y
99. Burghuber CK, Manook M, Ezekian B, Gibby AC, Leopardi FV, Song M, et al. Dual Targeting: Combining Costimulation Blockade and Bortezomib to Permit Kidney Transplantation in Sensitized Recipients. *Am J Transpl* (2019) 19(3):724–36. doi: 10.1111/ajt.15067
100. Badell IR, Karadkhele GM, Vasanth P, Farris AB3rd, Robertson JM, Larsen CP. Abatacept as Rescue Immunosuppression After Calcineurin Inhibitor Treatment Failure in Renal Transplantation. *Am J Transpl* (2019) 19 (8):2342–9. doi: 10.1111/ajt.15319
101. Edwards SR, Wandless TJ. The Rapamycin-Binding Domain of the Protein Kinase Mammalian Target of Rapamycin Is a Destabilizing Domain. *J Biol Chem* (2007) 282(18):13395–401. doi: 10.1074/jbc.M700498200.Epub 2007 Mar 9
102. Liefeldt L, Brakemeier S, Glander P, Waiser J, Lachmann N, Schönemann C, et al. Donor-Specific HLA Antibodies in a Cohort Comparing Everolimus With Cyclosporine After Kidney Transplantation. *Am J Transpl* (2012) 12 (5):1192–8. doi: 10.1111/j.1600-6143.2011.03961
103. Hay N, Sonenberg N. Upstream and Downstream of mTOR. *Genes Dev* (2004) 18(16):1926–45. doi: 10.1101/gad.1212704
104. Grimbert P, Thaunat O. mTOR Inhibitors and Risk of Chronic Antibody-Mediated Rejection After Kidney Transplantation: Where Are We Now? *Transpl Int* (2017) 30(7):647–57. doi: 10.1111/tri.12975
105. Chapman NM, Zeng H, Nguyen TM, Wang Y, Vogel P, Dhungana Y, et al. mTOR Coordinates Transcriptional Programs and Mitochondrial Metabolism of Activated Treg Subsets to Protect Tissue Homeostasis. *Nat Commun* (2018) 9(1):2095. doi: 10.1038/s41467-018-04392-5
106. Mele TS, Halloran PF. The Use of Mycophenolate Mofetil in Transplant Recipients. *Immunopharmacology* (2000) 47(2-3):215–45. doi: 10.1016/s0162-3109(00)00190-9
107. Lederer SR, Friedrich N, Banas B, Welser G, Albert ED, Sitter T. Effects of Mycophenolate Mofetil on Donor-Specific Antibody Formation in Renal

Transplantation. *Clin Transpl* (2005) 19(2):168–74. doi: 10.1111/j.1399-0012.2005.00261.x
108. Ransom JT. Mechanism of Action of Mycophenolate Mofetil. *Ther Drug Monit* (1995) 17(6):681–4. doi: 10.1097/00007691-199512000-00023
109. Moniodis A, Townsend K, Rabin A, Aloum O, Stempel J, Burkett P, et al. Comparison of Extracorporeal Photopheresis and Alemtuzumab for the Treatment of Chronic Lung Allograft Dysfunction. *J Heart Lung Transpl* (2018) 37:340–8. doi: 10.1016/j.healun.2017.03.017
110. Xu H, Mehta AK, Gao Q, Lee HJ, Ghali A, Guasch A, et al. B Cell Reconstitution Following Alemtuzumab Induction Under a Belatacept-Based Maintenance Regimen. *Am J Transplant* (2020) 20(3):653–62. doi: 10.1111/ajt.15639
111. Nückel H, Frey UH, Röth A, Dührsen U, Siffert W. Alemtuzumab Induces Enhanced Apoptosis *In Vitro* in B-Cells From Patients With Chronic Lymphocytic Leukemia by Antibody-Dependent Cellular Cytotoxicity. *Eur J Pharmacol* (2005) 514(2-3):217–24. doi: 10.1016/j.ejphar.2005.03.024
112. Ravichandran AK, Schilling JD, Novak E, Pfeifer J, Ewald GA, Joseph SM. Rituximab Is Associated With Improved Survival in Cardiac Allograft Patients With Antibody-Mediated Rejection: A Single Center Review. *Clin Transpl* (2013) 27(6):961–7. doi: 10.1111/ctr.12277
113. Benazzo A, Schwarz S, Geleff S, Weber D, Murakozy G, Lambers C, et al. Donor-Specific Antibodies and Antibody-Mediated Rejection After Alemtuzumab Induction Therapy: A Retrospective Analysis of a High-Volume Lung Transplant Center. *J Heart Lung Transplant* (2019) 38(4): S166–167. doi: 10.1016/j.healun.2019.01.399
114. Roberts DM, Jiang SH, Chadban SJ. The Treatment of Acute Antibody-Mediated Rejection in Kidney Transplant Recipients-A Systematic Review. *Transplantation* (2012) 27.94(8):775–83. doi: 10.1097/TP.0b013e31825d1587
115. Velidedeoglu E, Cavaillé-Coll MW, Bala S, Belen OA, Wang Y, Albrecht R. Summary of 2017 FDA Public Workshop: Antibody-Mediated Rejection in Kidney Transplantation. *Transplantation* (2018) 102(4):557–68. doi: 10.1097/TP.0000000000002049
116. Moreso F, Crespo M, Ruiz JC, Torres A, Gutierrez-Dalmau A, Osun A, et al. Treatment of Chronic Antibody Mediated Rejection With Intravenous Immunoglobulins and Rituximab: A Multicenter, Prospective, Randomized, Double-Blind Clinical Trial. *Am J Transpl* (2018) 18(4):927–35. doi: 10.1111/ajt.14520
117. Lefaucheur C, Loupy A, Vernerey D, Duong-Van-Huyen JP, Suberbielle C, Anglicheau D, et al. Antibody-Mediated Vascular Rejection of Kidney Allografts: A Population-Based Study. *Lancet* (2013) 381(9863):313–9. doi: 10.1016/S0140-6736(12)61265-3
118. Ding Y, Francis J, Gautam A, Pelletier L, Sanchorawala V, Quillen K. Durable Renal Response After Combination of Bortezomib, Corticosteroids, Rituximab, and Plasmapheresis for Late Antibody-Mediated Renal Transplant Rejection. *Clin Nephrol* (2018) 89(4):252–9. doi: 10.5414/CN109278
119. Tajima T, Hata K, Okajima H, Nishikori M, Yasuchika K, Kusakabe J, et al. Bortezomib Against Refractory Antibody-Mediated Rejection After ABO-Incompatible Living-Donor Liver Transplantation: Dramatic Effect in Acute-Phase? *Transplant Direct* (2019) 19: 5(10):e491. doi: 10.1097/TXD.0000000000000932
120. Moreno Gonzales MA, Gandhi MJ, Schinstock CA, Moore NA, Smith BH, Braaten NY, et al. 32 Doses of Bortezomib for Desensitization Is Not Well Tolerated and Is Associated With Only Modest Reductions in Anti-HLA Antibody. *Transplantation* (2017) 101(6):1222–7. doi: 10.1097/TP.0000000000001330
121. Lonze BE, Tatapudi VS, Weldon EP, Min ES, Ali NM, Deterville CL, et al. IdeS (Imlifidase): A Novel Agent That Cleaves Human IgG and Permits Successful Kidney Transplantation Across High-Strength Donor-Specific Antibody. *Ann Surg* (2018) 268(3):488–96. doi: 10.1097/SLA.0000000000002924
122. Jordan SC, Lorant T, Choi J, Kjellman C, Winstedt L, Bengtsson M, et al. IgG Endopeptidase in Highly Sensitized Patients Undergoing Transplantation. *N Engl J Med* (2017) 377(5):442–53. doi: 10.1056/NEJMoa1612567
123. Bujnowska A, Michon M, Konopelski P, Hryniewiecka E, Jalbrzykowska A, Perkowska-Ptasinska A, et al. Outcomes of Prolonged Treatment With Intravenous Immunoglobulin Infusions for Acute Antibody-Mediated Rejection in Kidney Transplant Recipients. *Transplant Proc* (2018) 50 (6):1720–5. doi: 10.1016/j.transproceed.2018.02.110
124. de Sousa MV, Gonçalez AC, de Lima Zollner R, Mazzali M. Treatment of Antibody-Mediated Rejection After Kidney Transplantation: Immunological Effects, Clinical Response, and Histological Findings. *Ann Transplant* (2020) 25:e925488. doi: 10.12659/AOT.925488
125. Liu J, Farmer JD Jr, Lane WS, Friedman J, Weissman I, Schreiber SL. Calcineurin Is a Common Target of Cyclophilin-Cyclosporin A and FKBP-FK506 Complexes. *Cell* (1991) 66(4):807–15. doi: 10.1016/0092-8674(91)90124-H
126. Nankivell BJ, Shingde M, Keung KL, Fung CL, Borrows RJ, O'Connell PJ, et al. The Causes, Significance and Consequences of Inflammatory Fibrosis in Kidney Transplantation: The Banff I-IFTA Lesion. *Am J Transpl* (2018) 18 (2):364–76. doi: 10.1111/ajt.14609
127. Sommerer C, Meuer S, Zeier M, Giese T. Calcineurin Inhibitors and NFAT-Regulated Gene Expression. *Clin Chim Acta* (2012) 413(17-18):1379–86. doi: 10.1016/j.cca.2011.09.041
128. Wiebe C, Rush DN, Nevins TE, Birk PE, Blydt-Hansen T, Gibson IW, et al. Class II Eplet Mismatch Modulates Tacrolimus Trough Levels Required to Prevent Donor-Specific Antibody Development. *J Am Soc Nephrol* (2017) 28 (11):3353–62. doi: 10.1681/ASN.2017030287
129. Kidney Disease: Improving Global Outcomes (KDIGO) Transplant Work Group. KDIGO Clinical Practice Guideline for the Care of Kidney Transplant Recipients. *Am J Transpl* (2009) 9 Suppl 3:S1–155. doi: 10.1111/j.1600-6143.2009.02834.x
130. Bamoulid J, Staeck O, Crépin T, Halleck F, Saas P, Brakemeier S, et al. Anti-Thymocyte Globulins in Kidney Transplantation: Focus on Current Indications and Long-Term Immunological Side Effects. *Nephrol Dial Transpl* (2017) 32(10):1601–8. doi: 10.1093/ndt/gfw368
131. Burton SA, Amir N, Asbury A, Lange A, Hardinger KL. Treatment of Antibody-Mediated Rejection in Renal Transplant Patients: A Clinical Practice Survey. *Clin Transpl* (2015) 29(2):118–23. doi: 10.1111/ctr.12491
132. Chapman TM, Keating GM. Basiliximab: A Review of Its Use as Induction Therapy in Renal Transplantation. *Drugs* (2003) 63(24):2803–35. doi: 10.2165/00003495-200363240-00009
133. Cornell LD, Schinstock CA, Gandhi MJ, Kremers WK, Stegall MD. Positive Crossmatch Kidney Transplant Recipients Treated With Eculizumab: Outcomes Beyond 1 Year. *Am J Transplant* (2015) 15(5):1293–302. doi: 10.1111/ajt.13168
134. Schinstock CA, Bentall AJ, Smith BH, Cornell LD, Everly M, Gandhi MJ, et al. Long-Term Outcomes of Eculizumab-Treated Positive Crossmatch Recipients: Allograft Survival, Histologic Findings, and Natural History of the Donor-Specific Antibodies. *Am J Transpl* (2019) 19(6):1671–83. doi: 10.1111/ajt.15175
135. Ding Y, Francis J, Gautam A, Pelletier L, Sanchorawala V, Quillen K. Durable Renal Response After Combination of Bortezomib, Corticosteroids, Rituximab, and Plasmapheresis for Late Antibody-Mediated Renal Transplant Rejection. *Clin Nephrol* (2018) 89(4):252–9. doi: 10.5414/CN109278
136. Sakurai H, Shigemori N, Hisada Y, Ishizuka T, Kawashima K, Sugita T. Suppression of NF-Kappa B and AP-1 Activation by Glucocorticoids in Experimental Glomerulonephritis in Rats: Molecular Mechanisms of Anti-Nephritic Action. *Biochim Biophys Acta* (1997) 1362(2-3):252–62. doi: 10.1016/s0925-4439(97)00068-9
137. Hipp N, Symington H, Pastoret C, Caron G, Monvoisin C, Tarte K, et al. IL-2 Imprints Human Naive B Cell Fate Towards Plasma Cell Through ERK/ELK1-Mediated BACH2 Repression. *Nat Commun* (2017) 8(1):1443. doi: 10.1038/s41467-017-01475-7
138. Le Gallou S, Caron G, Delaloy C, Rossille D, Tarte K, Fest T. IL-2 Requirement for Human Plasma Cell Generation: Coupling Differentiation and Proliferation by Enhancing MAPK-ERK Signaling. *J Immunol* (2012) 189(1):161–73. doi: 10.4049/jimmunol.1200301
139. Qu X, Kirken RA, Tian L, Wang M, Bennett CF, Stepkowski SM. Selective Inhibition of IL-2 Gene Expression by IL-2 Antisense Oligonucleotides Blocks Heart Allograft Rejection. *Transplantation* (2001) 72(5):915–23. doi: 10.1097/00007890-200109150-00029

140. McHugh J. Systemic Lupus Erythematosus: B Cell-Derived IL-6 Promotes Disease. *Nat Rev Rheumatol* (2017) 13(11):633. doi: 10.1038/nrrheum.2017.163
141. Maeda K, Mehta H, Drevets DA, Coggeshall KM. IL-6 Increases B-Cell IgG Production in a Feed-Forward Proinflammatory Mechanism to Skew Hematopoiesis and Elevate Myeloid Production. *Blood* (2010) 115 (23):4699–706. doi: 10.1182/blood-2009-07-230631
142. Rosser EC, Oleinika K, Tonon S, Doyle R, Bosma A, Carter NA, et al. Regulatory B Cells Are Induced by Gut Microbiota-Driven Interleukin-1beta and Interleukin-6 Production. *Nat Med* (2014) 20(11):1334–9. doi: 10.1038/nm.3680
143. Mauer J, Chaurasia B, Goldau J, Vogt MC, Ruud J, Nguyen KD, et al. Signaling by IL-6 Promotes Alternative Activation of Macrophages to Limit Endotoxemia and Obesity-Associated Resistance to Insulin. *Nat Immunol* (2014) 15(5):423–30. doi: 10.1038/ni.2865
144. Bettelli E, Carrier Y, Gao W, Korn T, Strom TB, Oukka M, et al. Reciprocal Developmental Pathways for the Generation of Pathogenic Effector TH17 and Regulatory T Cells. *Nature* (2006) 441(7090):235–8. doi: 10.1038/nature04753
145. Kimura A, Kishimoto T. IL-6: Regulator of Treg/Th17 Balance. *Eur J Immunol* (2010) 40(7):1830–5. doi: 10.1002/eji.201040391
146. Korn T, Mitsdoerffer M, Croxford AL, Awasthi A, Dardalhon VA, Galileos G, et al. IL-6 Controls Th17 Immunity *In Vivo* by Inhibiting the Conversion of Conventional T Cells Into Foxp3+ Regulatory T Cells. *Proc Natl Acad Sci USA* (2008) 105(47):18460–5. doi: 10.1073/pnas.0809850105
147. Schneider A, Long SA, Cerosaletti K, Ni CT, Samuels P, Kita M, et al. In Active Relapsing-Remitting Multiple Sclerosis, Effector T Cell Resistance to Adaptive T(regs) Involves IL-6-Mediated Signaling. *Sci Transl Med* (2013) 5 (170):170ra15. doi: 10.1126/scitranslmed.3004970
148. Doberer K, Duerr M, Halloran PF, Eskandary F, Budde K, Regele H, et al. A Randomized Clinical Trial of Anti-IL-6 Antibody Clazakizumab in Late Antibody-Mediated Kidney Transplant Rejection. *J Am Soc Nephrol* (2021) 32(3):708–22. doi: 10.1681/ASN.2020071106
149. Choi J, Aubert O, Vo A, Loupy A, Haas M, Puliyanda D, et al. Assessment of Tocilizumab (Anti-Interleukin-6 Receptor Monoclonal) as a Potential Treatment for Chronic Antibody-Mediated Rejection and Transplant Glomerulopathy in HLA-Sensitized Renal Allograft Recipients. *Am J Transpl* (2017) 17(9):2381–9. doi: 10.1111/ajt.14228
150. Vazquez MI, Catalan-Dibene J, Zlotnik. A. B Cells Responses and Cytokine Production Are Regulated by Their Immune Microenvironment. *Cytokine* (2015) 74(2):318–26. doi: 10.1016/j.cyto.2015.02.007
151. Corfe SA, Paige CJ. The Many Roles of IL-7 in B Cell Development; Mediator of Survival, Proliferation and Differentiation. *Semin Immunol* (2012) 24 (3):198–208. doi: 10.1016/j.smim.2012.02.001
152. Milne CD, Paige CJ. IL-7: A Key Regulator of B Lymphopoiesis. *Semin Immunol* (2006) 18(1):20– 30. doi: 10.1016/j.smim.2005.10.003
153. Mai HL, Boeffard F, Longis J, Danger R, Martinet B, Haspot F, et al. IL-7 Receptor Blockade Following T Cell Depletion Promotes Long-Term Allograft Survival. *J Clin Invest* (2014) 124(4):1723–33. doi: 10.1172/JCI66287
154. Luo Y, Luo F, Zhang K, Wang S, Zhang H, Yang X, et al. Elevated Circulating IL-10 Producing Breg, But Not Regulatory B Cell Levels, Restrain Antibody-Mediated Rejection After Kidney Transplantation. *Front Immunol* (2021) 11:627496. doi: 10.3389/fimmu.2020.627496
155. Lin X, Wang X, Xiao F, Ma K, Liu L, Wang X, et al. IL-10-Producing Regulatory B Cells Restrain the T Follicular Helper Cell Response in Primary Sjögren's Syndrome. *Cell Mol Immunol* (2019) 16(12):921–31. doi: 10.1038/s41423-019-0227-z
156. Shen P, Roch T, Lampropoulou V, O'Connor RA, Stervbo U, Hilgenberg E, et al. IL-35-Producing B Cells Are Critical Regulators of Immunity During Autoimmune and Infectious Diseases. *Nature* (2014) 507(7492):366–70. doi: 10.1038/nature12979
157. Guo H, Wang W, Zhao N, He X, Zhu L, Jiang X. Inhibiting Cardiac Allograft Rejection With Interleukin-35 Therapy Combined With Decitabine Treatment in Mice. *Transpl Immunol* (2013) 29(1-4):99–104. doi: 10.1016/j.trim.2013.10.001
158. Choi JK, Egwuagu CE. Interleukin 35 Regulatory B Cells. *J Mol Biol* (2021) 433(1):166607. doi: 10.1016/j.jmb.2020.07.019
159. Tsuchida Y, Sumitomo S, Ishigaki K, Suzuki A, Kochi Y, Tsuchiya H, et al. Antibody Production by Human B Cells. *PloS One* (2017) 12(1):e0169646. doi: 10.1371/journal.pone.0169646
160. Guan Q, Li S, Gao S, Chen H, Nguan CY, Du C. Reduction of Chronic Rejection of Renal Allografts by Anti-Transforming Growth Factor-β Antibody Therapy in a Rat Model. *Am J Physiol Renal Physiol* (2013) 305 (2):F199–207. doi: 10.1152/ajprenal.00665.2012
161. Rosser EC. Regulatory B Cells: Origin, Phenotype, and Function. *Immunity* (2015) 42(4):607–12. doi: 10.1016/j.immuni.2015.04.005
162. Pandiyan P, Yang XP, Saravanamuthu SS, Zheng L, Ishihara S, O'Shea JJ, et al. The Role of IL-15 in Activating STAT5 and Fine-Tuning IL-17A Production in CD4 T Lymphocytes. *J Immunol* (2012) 189(9):4237–46. doi: 10.4049/jimmunol.1201476
163. Zheng XX, Gao W, Donskoy E, Neuberg M, Ruediger M, Strom TB, et al. An Antagonist Mutant IL-15/Fc Promotes Transplant Tolerance. *Transplantation* (2006) 81(1):109–16. doi: 10.1097/01.tp.0000188139.11931.98
164. Conti F, Frappier J, Dharancy S, Chereau C, Houssin D, Weill B, et al. Interleukin-15 Production During Liver Allograft Rejection in Humans. *Calmus Y Transpl* (2003) 76(1):210–6. doi: 10.1097/01.TP.0000067530.95852.67
165. Wang S, Wang J, Kumar V, Karnell JL, Naiman B, Gross PS, et al. IL-21 Drives Expansion and Plasma Cell Differentiation of Autoreactive CD11chiT-Bet+ B Cells in SLE. *Nat Commun* (2018) 9(1):1758. doi: 10.1038/s41467-018-03750-7
166. Khattar M, Baum CE, Schroder P, Breidenbach JD, Haller ST, Chen W, et al. Interleukin 21 (IL-21) Regulates Chronic Allograft Vasculopathy (CAV) in Murine Heart Allograft Rejection. Stepkowski s. *PloS One* (2019) 14(11): e0225624. doi: 10.1371/journal.pone.0225624
167. van Besouw NM, Yan L, de Kuiper R, Klepper M, Reijerkerk D, Dieterich M, et al. The Number of Donor-Specific IL-21 Producing Cells Before and After Transplantation Predicts Kidney Graft Rejection. *Front Immunol* (2019) 10:748. doi: 10.3389/fimmu.2019.00748
168. Popescu M, Cabrera-Martinez B, Winslow GM. TNF-α Contributes to Lymphoid Tissue Disorganization and Germinal Center B Cell Suppression During Intracellular Bacterial Infection. *J Immunol* (2019) 203 (9):2415–24. doi: 10.4049/jimmunol.1900484
169. Tay C, Liu YH, Hosseini H, Kanellakis P, Cao A, Peter K, et al. B-Cell-Specific Depletion of Tumour Necrosis Factor Alpha Inhibits Atherosclerosis Development and Plaque Vulnerability to Rupture by Reducing Cell Death and Inflammation. *Cardiovasc Res* (2016) 111(4):385–97. doi: 10.1093/cvr/cvw186
170. Sonkar GK, Usha Singh RG. Evaluation of Serum Tumor Necrosis Factor Alpha and Its Correlation With Histology in Chronic Kidney Disease, Stable Renal Transplant and Rejection Cases. *Saudi J Kidney Dis Transpl* (2009) 20 (6):1000–4.
171. Furie R, Rovin BH, Houssiau F, Malvar A, Teng YKO, Contreras G, et al. Two-Year, Randomized, Controlled Trial of Belimumab in Lupus Nephritis. *N Engl J Med* (2020) 383(12):1117–28. doi: 10.1056/NEJMoa2001180
172. Afzali S, Salehi S, Shahi A, Esmaeili M, Farashi Bonab S, Peykari A, et al. Investigating the Role of BAFF and Its Receptors in Renal Transplant Recipients With Chronic Antibody-Mediated Rejection. *J Immunol Res* (2021) 2021:6654992. doi: 10.1155/2021/6654992
173. Wang XZ, Wan Z, Xue WJ, Zheng J, Li Y, Ding CG, et al. B-Cell Activating Factor Predicts Acute Rejection Risk in Kidney Transplant Recipients: A 6-Month Follow-Up Study. *Front Immunol* (2019) 10:1046. doi: 10.3389/fimmu.2019.01046
174. Pongpirul W, Chancharoenthana W, Pongpirul K, Leelahavanichkul A, Kittikowit W, Jutivorakool K, et al. B-Cell Activating Factor, a Predictor of Antibody Mediated Rejection in Kidney Transplantation Recipients. *Nephrol (Carlton)* (2018) 23(2):169–74. doi: 10.1111/nep.12972
175. Krejcik J, Casneuf T, Nijhof IS, Verbist B, Bald J, Plesner T, et al. Daratumumab Depletes CD38+ Immune Regulatory Cells, Promotes T-Cell Expansion, and Skews T-Cell Repertoire in Multiple Myeloma. *Blood* (2016) 128(3):384–94. doi: 10.1182/blood-2015-12-687749
176. Casneuf T, Xu XS, Adams HC3rd, Axel AE, Chiu C, Khan I, et al. Effects of Daratumumab on Natural Killer Cells and Impact on Clinical Outcomes in

Relapsed or Refractory Multiple Myeloma. *Blood Adv* (2017) 1(23):2105–14. doi: 10.1182/bloodadvances.2017006866
177. van de Donk N. Immunomodulatory Effects of CD38-Targeting Antibodies. *Immunol Lett* (2018) 199:16–22. doi: 10.1016/j.imlet.2018.04.005
178. Kwun J, Matignon M, Manook M, Guendouz S, Audard V, Kheav D, et al. Daratumumab in Sensitized Kidney Transplantation: Potentials and Limitations of Experimental and Clinical Use. *J Am Soc Nephrol* (2019) 30 (7):1206–19. doi: 10.1681/ASN.2018121254
179. Feng X, Zhang LI, Acharya C, An G, Wen K, Qiu L, et al. Targeting CD38 Suppresses Induction and Function of T Regulatory Cells to Mitigate Immunosuppression in Multiple Myeloma. *Clin Cancer Res* (2017) 23 (15):4290–300. doi: 10.1158/1078-0432.CCR-16-3192
180. Daoussis D, Andonopoulos AP, Liossis SN. Targeting CD40L: A Promising Therapeutic Approach. *Clin Diagn Lab Immunol* (2004) 11(4):635–41. doi: 10.1128/CDLI.11.4.635-641.2004
181. Karnell JL, Albulescu M, Drabic S, Wang L, Moate R, Baca M, et al. Protein Reduces Autoantibodies and Improves Disease Activity in Patients With Autoimmunity. *Sci Transl Med* (2019) 11(489):eaar6584. doi: 10.1126/scitranslmed.aar6584
182. Kreuzaler M, Rauch M, Salzer U, Birmelin J, Rizzi M, Grimbacher B, et al. Soluble BAFF Levels Inversely Correlate With Peripheral B Cell Numbers and the Expression of BAFF Receptors. *J Immunol* (2012) 188(1):497–503. doi: 10.4049/jimmunol.1102321
183. Tsuji S, Stein L, Kamada N, Nuñez G, Bram R, Vallance BA, et al. TACI Deficiency Enhances Antibody Avidity and Clearance of an Intestinal Pathogen. *J Clin Invest* (2014) 124(11):4857–66. doi: 10.1172/JCI74428
184. Ou X, Xu S, Lam KP. Deficiency in TNFRSF13B (TACI) Expands T-Follicular Helper and Germinal Center B Cells *via* Increased ICOS-Ligand Expression But Impairs Plasma Cell Survival. *Proc Natl Acad Sci USA* (2012) 109(38):15401–6. doi: 10.1073/pnas.1200386109
185. Salazar-Camarena DC, Ortiz-Lazareno PC, Cruz A, Oregon-Romero E, Machado-Contreras JR, Muñoz-Valle JF, et al. Association of BAFF, APRIL Serum Levels, BAFF-R, TACI and BCMA Expression on Peripheral B-Cell Subsets With Clinical Manifestations in Systemic Lupus Erythematosus. *Lupus* (2016) 25(6):582–92. doi: 10.1177/0961203315608254
186. Yang M, Hase H, Legarda-Addison D, Varughese L, Seed B, Ting AT. B Cell Maturation Antigen, the Receptor for a Proliferation-Inducing Ligand and B Cell-Activating Factor of the TNF Family, Induces Antigen Presentation in B Cells. *J Immunol* (2005) 175(5):2814–24. doi: 10.4049/jimmunol.175.5.2814
187. Huang HW, Chen CH, Lin CH, Wong CH, Lin KI. B-Cell Maturation Antigen Is Modified by a Single N-Glycan Chain That Modulates Ligand Binding and Surface Retention. *Proc Natl Acad Sci USA* (2013) 110 (27):10928–33. doi: 10.1073/pnas.1309417110
188. O'Connor BP, Raman VS, Erickson LD, Cook WJ, Weaver LK, Ahonen C, et al. BCMA Is Essential for the Survival of Long-Lived Bone Marrow Plasma Cells. *J Exp Med* (2004) 199(1):91–8. doi: 10.1084/jem.20031330
189. Jordan SC, Ammerman N, Choi J, Huang E, Peng A, Sethi S, et al. The Role of Novel Therapeutic Approaches for Prevention of Allosensitization and Antibody-Mediated Rejection. *Am J Transpl* (2020) 20 Suppl 4:42–56. doi: 10.1111/ajt.15913
190. Xu Y, Fairfax K, Light A, Huntington ND, Tarlinton DM. CD19 Differentially Regulates BCR Signalling Through the Recruitment of PI3K. *Autoimmunity* (2014) 47(7):430–7. doi: 10.3109/08916934.2014.921810
191. Cree BAC, Bennett JL, Kim HJ, Weinshenker BG, Pittock SJ, Wingerchuk DM, et al. Inebilizumab for the Treatment of Neuromyelitis Optica Spectrum Disorder (N-MOmentum): A Double-Blind, Randomised Placebo-Controlled Phase 2/3 Trial. *Lancet* (2019) 394(10206):1352–63. doi: 10.1016/S0140-6736(19)31817-3
192. Frampton JE. Inebilizumab: First Approval. *Drugs* (2020) 80(12):1259–64. doi: 10.1007/s40265-020-01370-4
193. Kharabi Masouleh B, Ten Dam GB, Wild MK, Seelige R, van der Vlag J, Rops AL, et al. Role of the Heparan Sulfate Proteoglycan Syndecan-1 (CD138) in Delayed-Type Hypersensitivity. *J Immunol* (2009) 182(8):4985–93. doi: 10.4049/jimmunol.0800574
194. McCarron MJ, Park PW, Fooksman DR. CD138 Mediates Selection of Mature Plasma Cells by Regulating Their Survival. *Blood* (2017) 129 (20):2749–59. doi: 10.1182/blood-2017-01-761643
195. Khodadadi L, Cheng Q, Radbruch A, Hiepe F. The Maintenance of Memory Plasma Cells. *Front Immunol* (2019) 10:721. doi: 10.3389/fimmu.2019.00721
196. Carpio VN, Noronha Ide L, Martins HL, Jobim LF, Gil BC, Külzer AS, et al. Expression Patterns of B Cells in Acute Kidney Transplant Rejection. *Exp Clin Transpl* (2014) 12(5):405–14.
197. Bhat ZY, Bostwick DG, Hossain D, Zeng X. Participation of Functionally Active Plasma Cells in Acute Rejection and Response to Therapy in Renal Allografts. *DNA Cell Biol* (2014) 33(7):448–54. doi: 10.1089/dna.2014.2371
198. Viau M, Zouali M. B-Lymphocytes, Innate Immunity, and Autoimmunity. *Clin Immunol* (2005) 114(1):17–26. doi: 10.1016/j.clim.2004.08.019
199. Lenert P, Brummel R, Field EH, Ashman RF. TLR-9 Activation of Marginal Zone B Cells in Lupus Mice Regulates Immunity Through Increased IL-10 Production. *J Clin Immunol* (2005) 25(1):29–40. doi: 10.1007/s10875-005-0355-6
200. Zhang X. Regulatory Functions of Innate-Like B Cells. *Cell Mol Immunol* (2013) 10(2):113–21. doi: 10.1038/cmi.2012.63
201. Ran Z, Yue-Bei L, Qiu-Ming Z, Huan Y. Regulatory B Cells and Its Role in Central Nervous System Inflammatory Demyelinating Diseases. *Front Immunol* (2020) 11:1884. doi: 10.3389/fimmu.2020.01884
202. Tsay GJ, Zouali M. The Interplay Between Innate-Like B Cells and Other Cell Types in Autoimmunity. *Front Immunol* (2018) 16:1064. doi: 10.3389/fimmu.2018.01064
203. Wang L, Ray A, Jiang X, Wang JY, Basu S, Liu X, et al. T Regulatory Cells and B Cells Cooperate to Form a Regulatory Loop That Maintains Gut Homeostasis and Suppresses Dextran Sulfate Sodium-Induced Colitis. *Mucosal Immunol* (2015) 8(6):1297–312. doi: 10.1038/mi.2015.20
204. Chien CH, Chiang BL. Regulatory T Cells Induced by B Cells: A Novel Subpopulation of Regulatory T Cells. *J BioMed Sci 18;* (2017) 24(1):86. doi: 10.1186/s12929-017-0391-3
205. Chesneau M, Pallier A, Braza F, Lacombe G, Le Gallou S, Baron D, et al. Unique B Cell Differentiation Profile in Tolerant Kidney Transplant Patients. *Am J Transpl* (2014) 14(1):144–55. doi: 10.1111/ajt.12508
206. Lefaucheur C, Viglietti D, Bentlejewski C, van Huyen JP D, Vernerey D, Aubert O, et al. IgG Donor-Specific Anti-Human HLA Antibody Subclasses and Kidney Allograft Antibody-Mediated Injury. *J Am Soc Nephrol* (2016) 27 (1):293–304. doi: 10.1681/ASN.2014111120
207. Imamura R, Matsuda Y, Tsutahara K, Nonomura N, Takahara S. Impact of Immunoglobulin M-Type Donor-Specific Human Leukocyte Antigen-Antibody Levels in Supernatants From Cultured Peripheral Blood Mononuclear Cells as Predictors of Antibody-Mediated Rejection. *Pathogens* (2020) 9(9):733. doi: 10.3390/pathogens9090733
208. Haneda M, Owaki M, Kuzuya T, Iwasaki K, Miwa Y, Kobayashi T. Comparative Analysis of Drug Action on B-Cell Proliferation and Differentiation for Mycophenolic Acid, Everolimus, and Prednisolone. *Transplantation* (2014) 97(4):405–12. doi: 10.1097/01.TP.0000441826.70687.f6
209. Kim J, Koo BK, Knoblich JA. Human Organoids: Model Systems for Human Biology and Medicine. *Nat Rev Mol Cell Biol* (2020) 21(10):571–84. doi: 10.1038/s41580-020-0259-3
210. Broutier L, Mastrogiovanni G, Verstegen MM, Francies HE, Gavarró LM, Bradshaw CR, et al. Human Primary Liver Cancer-Derived Organoid Cultures for Disease Modeling and Drug Screening. *Nat Med* (2017) 23 (12):1424–35. doi: 10.1038/nm.4438
211. Nanki Y, Chiyoda T, Hirasawa A, Ookubo A, Itoh M, Ueno M, et al. Patient-Derived Ovarian Cancer Organoids Capture the Genomic Profiles of Primary Tumours Applicable for Drug Sensitivity and Resistance Testing. *Sci Rep* (2020) 10(1):12581. doi: 10.1038/s41598-020-69488-9
212. Peelen DM, Hoogduijn MJ, Hesselink DA, Baan CC. Advanced *In Vitro* Research Models to Study the Role of Endothelial Cells in Solid Organ Transplantation. *Front Immunol* (2021) 12:607953. doi: 10.3389/fimmu.2021.607953
213. Sivozhelezov V, Braud C, Giacomelli L, Pechkova E, Giral M, Soulillou JP, et al. Immunosuppressive Drug-Free Operational Immune Tolerance in Human Kidney Transplants Recipients. Part II. Non-statistical gene microarray analysis. *J Cell Biochem* (2008) 103(6):1693–706. doi: 10.1002/jcb.21557

214. Wittig M, Anmarkrud JA, Kässens JC, Koch S, Forster M, Ellinghaus E, et al. Development of a High-Resolution NGS-Based HLA-Typing and Analysis Pipeline. *Nucleic Acids Res* (2015) 43(11):e70. doi: 10.1093/nar/gkv184
215. Liu C. A Long Road/Read to Rapid High-Resolution HLA Typing: The Nanopore Perspective. *Hum Immunol* (2020) S0198-8859(20):30189–0. doi: 10.1016/j.humimm.2020.04.009
216. Ouchida R, Mori H, Hase K, Takatsu H, Kurosaki T, Tokuhisa T, et al. Critical Role of the IgM Fc Receptor in IgM Homeostasis, B-Cell Survival, and Humoral Immune Responses. *Proc Natl Acad Sci USA* (2012) 109: E2699–706. doi: 10.1073/pnas.1210706109
217. Kubagawa H, Oka S, Kubagawa Y, Torii I, Takayama E, Kang DW, et al. Identity of the Elusive IgM Fc Receptor (FcmuR) in Humans. *J Exp Med* (2009) 206:2779–93. doi: 10.1084/jem.20091107
218. Shima H, Takatsu H, Fukuda S, Ohmae M, Hase K, Kubagawa H, et al. Identification of TOSO/FAIM3 as an Fc Receptor for IgM. *Int Immunol* (2010) 22:149–56. doi: 10.1093/intimm/dxp121
219. Liu J, Zhu H, Qian J, Xiong E, Zhang L, Wang YQ, et al. Fcmicro Receptor Promotes the Survival and Activation of Marginal Zone B Cells and Protects Mice Against Bacterial Sepsis. *Front Immunol* (2018) 9:160. doi: 10.3389/fimmu.2018.00160
220. Nguyen TT, Klasener K, Zurn C, Castillo PA , Brust-Mascher I , Imai DM, et al. The IgM Receptor FcmuR Limits Tonic BCR Signaling by Regulating Expression of the IgM BCR. *Nat Immunol* (2017) 18:321–33. doi: 10.1038/ni.3677
221. Choi SC, Wang H, Tian L, Murakami Y, Shin DM, Borrego F, et al. Mouse IgM Fc Receptor, FCMR, Promotes B Cell Development and Modulates Antigen-Driven Immune Responses. *J Immunol* (2013) 190:987–96. doi: 10.4049/jimmunol.1202227
222. Brenner D, Brustle A, Lin GH, Lang PA, Duncan GS, Knobbe-Thomsen CB, et al. Toso Controls Encephalitogenic Immune Responses by Dendritic Cells and Regulatory T Cells. *Proc Natl Acad Sci USA* (2014) 111:1060–5. doi: 10.1073/pnas.1323166111
223. Adachi T, Harumiya S, Takematsu H, Kozutsumi Y, Wabl M, Fujimoto M, et al. CD22 Serves as a Receptor for Soluble IgM. *Eur J Immunol* (2012) 42 (1):241–7. doi: 10.1002/eji.201141899
224. Clark EA, Giltiay NV. CD22: A Regulator of Innate and Adaptive B Cell Responses and Autoimmunity. *Front Immunol* (2018) 9:2235. doi: 10.3389/fimmu.2018.02235
225. Haas KM, Johnson KL, Phipps JP, Do C. CD22 Promotes B-1b Cell Responses to T Cell-Independent Type 2 Antigens. *J Immunol* (2018) 200 (5):1671–81. doi: 10.4049/jimmunol.1701578
226. Collins BE, Blixt O, DeSieno AR, Bovin N, Marth JD, Paulson JC. Masking of CD22 by Cis Ligands Does Not Prevent Redistribution of CD22 to Sites of Cell Contact. *Proc Natl Acad Sci USA* (2004) 101:6104–9. doi: 10.1073/pnas.0400851101
227. Macauley MS, Pfrengle F, Rademacher C, Nycholat CM, Gale AJ, von Drygalski A, et al. Antigenic Liposomes Displaying CD22 Ligands Induce Antigen-Specific B Cell Apoptosis. *J Clin Invest* (2013) 123:3074–83. doi: 10.1172/JCI69187
228. Chappell CP, Clark EA. STALing B Cell Responses With CD22. *J Clin Invest* (2013) 123:2778–80. doi: 10.1172/JCI69670
229. Pillai S, Cariappa A, Pirnie SP. Esterases and Autoimmunity: The Sialic Acid Acetylesterase Pathway and the Regulation of Peripheral B Cell Tolerance. *Trends Immunol* (2009) 30:488–93. doi: 10.1016/j.it.2009.07.006
230. Surolia I, Pirnie SP, Chellappa V, Taylor KN, Cariappa A, Moya J, et al. Functionally Defective Germline Variants of Sialic Acid Acetylesterase in Autoimmunity. *Nature* (2010) 466:243–7. doi: 10.1038/nature09115
231. Chellappa V, Taylor KN, Pedrick K, Donado C, Netravali IA, Haider K, et al. M89V Sialic Acid Acetyl Esterase (SIAE) and All Other Non-Synonymous Common Variants of This Gene Are Catalytically Normal. *PloS One* (2013) 8:e53453. doi: 10.1371/journal.pone.0053453
232. Dawidowicz K, Dieudé P, Avouac J, Wipff J, Hachulla E, Diot E, et al. Association Study of B-Cell Marker Gene Polymorphisms in European Caucasian Patients With Systemic Sclerosis. *Clin Exp Rheumatol* (2011) 29:839–42.
233. Kim TH, Yang K, Kim M, Kim HS, Kang JL. Apoptosis Inhibitor of Macrophage (AIM) Contributes to IL-10-Induced Anti-Inflammatory Response Through Inhibition of Inflammasome Activation. *Cell Death Dis* (2021) 12(1):19. doi: 10.1038/s41419-020-03332-w
234. Sugisawa R, Komatsu G, Hiramoto E, Takeda N, Yamamura KI, Arai S, et al. Independent Modes of Disease Repair by AIM Protein Distinguished in AIM-Felinized Mice. *Sci Rep* (2018) 8(1):13157. doi: 10.1038/s41598-018-31580-6
235. Yusa S, Ohnishi S, Onodera T, Miyazaki T. AIM, a Murine Apoptosis Inhibitory Factor, Induces Strong and Sustained Growth Inhibition of B Lymphocytes in Combination With TGF-Beta1. *Eur J Immunol* (1999) 29 (4):1086–93. doi: 10.1002/(SICI)1521-4141(199904)29:04<1086:AID-IMMU1086>3.0.CO;2-X
236. Arai S, Miyazaki T. A Scavenging System Against Internal Pathogens Promoted by the Circulating Protein Apoptosis Inhibitor of Macrophage (AIM). *Semin Immunopathol* (2018) 40(6):567–75. doi: 10.1007/s00281-018-0717-6
237. Sugisawa R, Hiramoto E, Matsuoka S, Iwai S, Takai R, Yamazaki T. AIM on the Susceptibility of Cats to Renal Disease. *Sci Rep* 2016 (2016) 6:35251. doi: 10.1038/srep35251
238. Arai S, Kitada K, Yamazaki T, Takai R, Zhang X, Tsugawa Y, et al. Macrophage Protein Enhances Intraluminal Debris Clearance and Ameliorates Acute Kidney Injury in Mice. *Nat Med* (2016) 22(2):183–93. doi: 10.1038/nm.4012
239. Ichimura T, Asseldonk EJ, Humphreys BD, Gunaratnam L, Duffield JS, Bonventre JV. Kidney Injury Molecule-1 Is a Phosphatidylserine Receptor That Confers a Phagocytic Phenotype on Epithelial Cells. *J Clin Invest* (2008) 118(5):1657–68. doi: 10.1172/JCI34487
240. Yang L, Brooks CR, Xiao S, Sabbisetti V, Yeung MY, Hsiao LL, et al. KIM-1-Mediated Phagocytosis Reduces Acute Injury to the Kidney. *J Clin Invest* (2015) 125(4):1620–36. doi: 10.1172/JCI75417
241. Ono Y, Kanmura S, Morinaga Y, Oda K, Kawabata K, Arima S, et al. Inhibitor of Macrophages as a Possible Diagnostic Marker in Patients With Crohn's Disease. *BMC Gastroenterol* (2017) 17(1):40. doi: 10.1186/s12876-017-0591-z
242. Tarazón E, Corbacho-Alonso N, Barderas MG, Gil-Cayuela C, García-Manzanares M, Feijóo-Bandín S, et al. Plasma CD5L and Non-Invasive Diagnosis of Acute Heart Rejection. *J Heart Lung Transplant* (2020) 39 (3):257–66. doi: 10.1016/j.healun.2019.11.004
243. Rodriguez-Zhurbenko N, Quach TD, Hopkins TJ, Rothstein TL, Hernandez AM. Human B-1 Cells and B-1 Cell Antibodies Change With Advancing Age. *Front Immunol* (2019) 10:483. doi: 10.3389/fimmu.2019.00483
244. Iyer SS, Cheng G. Role of Interleukin 10 Transcriptional Regulation in Inflammation and Autoimmune Disease. *Crit Rev Immunol* (2012) 32(1):23–63. doi: 10.1615/critrevimmunol.v32.i1.30
245. Shankar-Hari M, Spencer J, Sewell WA, Rowan KM, Singer M. Bench-To-Bedside Review: Immunoglobulin Therapy for Sepsis - Biological Plausibility From a Critical Care Perspective. *Crit Care* (2012) 16(2):206. doi: 10.1186/cc10597
246. Matsuda Y, Hiramitsu T, Li XK, Watanabe T. Characteristics of Immunoglobulin M Type Antibodies of Different Origins from the Immunologic and Clinical Viewpoints and Their Application in Controlling Antibody-Mediated Allograft Rejection. *Pathogens* (2020) 10 (1):4. doi: 10.3390/pathogens10010004
247. Morbach HO, Eichhorn EM, Liese JG, Girschick HJ. Reference Values for B Cell Subpopulations From Infancy to Adulthood. *Clin Exp Immunol* (2010) 162:271–9. doi: 10.1111/j.1365-2249.2010.04206.x
248. Notley CA, Brown MA, Wright GP, Ehrenstein MR. Natural IgM Is Required for Suppression of Inflammatory Arthritis by Apoptotic Cells. *J Immunol* (2011) 186(8):4967–72. doi: 10.4049/jimmunol.1003021
249. Aschetto R, Clemente N, Pagni A, Esposito T, Longhini F, Mercalli F, et al. A Double Blind Randomized Experimental Study on the Use of IgM-Enriched Polyclonal Immunoglobulins in an Animal Model of Pneumonia Developing Shock. *Immunobiology* (2017) 222(12):1074–80. doi: 10.1016/j.imbio.2017.09.002
250. Barratt-Due A, Sokolov A, Gustavsen A, Hellerud BC, Egge K, Pischke SE, et al. Polyvalent Immunoglobulin Significantly Attenuated the Formation of IL-1β in Escherichia Coli-Induced Sepsis in Pigs. *Immunobiology* (2013) 218 (5):683–9. doi: 10.1016/j.imbio.2012.08.268

251. Duerr C, Bacher A, de Martin A, Sachet M, Sadeghi K, Baumann S, et al. The Novel Polyclonal Ab Preparation Trimodulin Attenuates Ex Vivo Endotoxin-Induced Immune Reactions in Early Hyperinflammation. *Innate Immunity* (2019) 25(6):374–88. doi: 10.1177/1753425919853333
252. Marshall K, Jin J, Atkinson C, Alawieh A, Qiao F, Lei B, et al. Natural Immunoglobulin M Initiates an Inflammatory Response Important for Both Hepatic Ischemia Reperfusion Injury and Regeneration in Mice. *Hepatology* (2018) 67(2):721–35. doi: 10.1002/hep.29512
253. Alejandria MM, Lansang MA, Dans LF, Mantaring JBV. Intravenous Immunoglobulin for Treating Sepsis and Septic Shock. *Cochrane Database Syst Rev* (2002) 1:CD001090. doi: 10.1002/14651858
254. Toyoda M, Shin BH, Ge S, Mirocha J, Thomas D, Chu M, et al. Impact of Desensitization on Antiviral Immunity in HLA-Sensitized Kidney Transplant Recipients. *J Immunol Res* (2017) 2017:5672523. doi: 10.1155/2017/5672523
255. Morath C, Opelz G, Zeier M, Süsal CJ. Clinical Relevance of HLAantibody Monitoring After Kidney Transplantation. *Immunol Res* (2014) 2014:845040. doi: 10.1155/2014/845040
256. Roos A, Rieben R, Faber-Krol MC, Daha MR. IgM-Enriched Human Intravenous Immunoglobulin Strongly Inhibits Complement-Dependent Porcine Cell Cytotoxicity Mediated by Human Xenoreactive Antibodies. *Xenotransplantation* (2003) 10(6):596–605. doi: 10.1034/j.1399-3089.2003.00063.x
257. Barten Markus J, Buchholz C, Bernhardt A, Rybczynski M, Grahn H, Reichenspurner H. IgM-Enriched Human Intravenous Immunoglobulin for Treatment of Early Antibody Mediated Rejection After Heart Transplantation. *Transplantation* (2018) 102:S828. doi: 10.1097/01.tp.0000543877.96384.6e
258. Ius F, Sommer W, Kieneke D, Tudorache I, Kühn C, Avsar M. IgM-Enriched Human Intravenous Immunoglobulin-Based Treatment of Patients With Early Donor Specific Anti-HLA Antibodies After Lung Transplantation. *Transplantation* (2016) 100(12):2682–92. doi: 10.1097/TP.0000000000001027
259. De Vos J, Hose D, Rème T, Tarte K, Moreaux J, Mahtouk K, et al. Microarray-Based Understanding of Normal and Malignant Plasma Cells. *Immunol Rev* 2006 (2006) 210:86–104. doi: 10.1111/j.0105-2896.2006.00362.x
260. Vo AA, Choi J, Cisneros K, Reinsmoen N, Haas M, Ge S, et al. Benefits of Rituximab Combined With Intravenous Immunoglobulin for Desensitization in Kidney Transplant Recipients. *Transplantation* (2014) 98:312–9. doi: 10.1097/TP.0000000000000064

Conflict of Interest: The authors declare that the research was conducted in the absence of any commercial or financial relationships that could be construed as a potential conflict of interest.

Copyright © 2021 Matsuda, Watanabe and Li. This is an open-access article distributed under the terms of the Creative Commons Attribution License (CC BY). The use, distribution or reproduction in other forums is permitted, provided the original author(s) and the copyright owner(s) are credited and that the original publication in this journal is cited, in accordance with accepted academic practice. No use, distribution or reproduction is permitted which does not comply with these terms.

frontiers in Immunology

ORIGINAL RESEARCH
published: 01 July 2021
doi: 10.3389/fimmu.2021.657860

Identifying Biomarkers from Transcriptomic Signatures in Renal Allograft Biopsies Using Deceased and Living Donors

Bin Yang[1,2,3†], Nicolas Sylvius[4†], Jinli Luo[5], Cheng Yang[6,7], Zhanyun Da[8], Charlottelrm Crotty[1,2] and Michael L. Nicholson[1,2,9]*

[1] Department of Cardiovascular Sciences, University of Leicester, Leicester, United Kingdom, [2] Research and Innovation, University Hospitals of Leicester, Leicester, United Kingdom, [3] Nantong-Leicester Joint Institute of Kidney Science, Department of Nephrology, Affiliated Hospital of Nantong University, Nantong, China, [4] Genomics Core Facility, University of Leicester, Leicester, United Kingdom, [5] Bioinformatics and Biostatistics Support Hub Leicester, University of Leicester, Leicester, United Kingdom, [6] Department of Urology, Zhongshan Hospital, Fudan University, Shanghai, China, [7] Shanghai Key Laboratory of Organ Transplantation, Shanghai, China, [8] Department of Rheumatology and Immunology, Affiliated Hospital of Nantong University, Nantong, China, [9] Department of Surgery, Addenbrooke's Hospital, University of Cambridge, Cambridge, United Kingdom

OPEN ACCESS

Edited by:
Brian Duncan Tait, Australian Red Cross Blood Service, Australia

Reviewed by:
Nicole Andrea Mifsud, Monash University, Australia
Feifei Qiu, Guangdong Provincial Academy of Chinese Medical Sciences, China

***Correspondence:**
Bin Yang
by5@le.ac.uk

†These authors have contributed equally to this work

Specialty section:
This article was submitted to Alloimmunity and Transplantation, a section of the journal Frontiers in Immunology

Received: *24 January 2021*
Accepted: *07 June 2021*
Published: *01 July 2021*

Citation:
Yang B, Sylvius N, Luo J, Yang C, Da Z, Crotty C and Nicholson ML (2021) Identifying Biomarkers from Transcriptomic Signatures in Renal Allograft Biopsies Using Deceased and Living Donors. Front. Immunol. 12:657860. doi: 10.3389/fimmu.2021.657860

The survival of transplant kidneys using deceased donors (DD) is inferior to living donors (LD). In this study, we conducted a whole-transcriptome expression analysis of 24 human kidney biopsies paired at 30 minutes and 3 months post-transplantation using DD and LD. The transcriptome profile was found significantly different between two time points regardless of donor types. There were 446 differentially expressed genes (DEGs) between DD and LD at 30 minutes and 146 DEGs at 3 months, with 25 genes common to both time points. These DEGs reflected donor injury and acute immune responses associated with inflammation and cell death as early as at 30 minutes, which could be a precious window of potential intervention. DEGs at 3 months mainly represented the changes of adaptive immunity, immunosuppressive treatment, remodeling or fibrosis via different networks and signaling pathways. The expression levels of 20 highly DEGs involved in kidney diseases and 10 genes dysregulated at 30 minutes were found correlated with renal function and histology at 12 months, suggesting they could be potential biomarkers. These genes were further validated by quantitative polymerase chain reaction (qPCR) in 24 samples analysed by microarray, as well as in a validation cohort of 33 time point unpaired allograft biopsies. This analysis revealed that SERPINA3, SLPI and CBF were up-regulated at 30 minutes in DD compared to LD, while FTCD and TASPN7 were up-regulated at both time points. At 3 months, SERPINA3 was up-regulated in LD, but down-regulated in DD, with increased VCAN and TIMP1, and decreased FOS, in both donors. Taken together, divergent transcriptomic signatures between DD and LD, and changed by the time post-transplantation, might contribute to different allograft survival of two type kidney donors. Some DEGs including FTCD and TASPN7 could be novel biomarkers not only for timely diagnosis, but also for early precise genetic intervention at donor preservation, implantation and post-transplantation, in particular to effectively improve the quality and survival of DD.

Keywords: biomarkers, differentially expressed genes, fibrosis, immunity, inflammation, transplant kidney injury

INTRODUCTION

Kidney transplantation is a life-change treatment for end-stage renal failure patients. It has been reported that 1-year allograft survival increased to around 90% in deceased donors (DD) and 95% in living donors (LD), but 10-year survival fell to 51% and 68% respectively (1, 2). Immunological and non-immunological factors affect chronic allograft injury (CAI) and allograft survival *via* different mechanistic signaling pathways (3, 4), which need to be explored. Serum creatinine (SCr) or estimated glomerular filtration rate and histopathological score have been widely used, but clinical limitations also appeared in predicting early CAI (5). Virtually no conventional methods or available biomarkers well fit clinical requirements in timely diagnosis and personalized therapy (6).

High throughput genomic technologies, such as microarray, enable investigating hundreds of thousands of genes in one sample at one time, and identifying differentially expressed genes (DEGs) involved in allograft/recipient survival. The microarray analysis has been used to disclose the mechanism of CAI (7), delayed graft function (DGF) (8), rejection (9) and the nephrotoxicity of calcineurin inhibitors (10). A meta-analysis using 150 microarray samples from ischemia-reperfusion (IR) kidneys identified DEGs, corrected the bias in models and species. 26 DEGs including LCN2, CCL2, HMOX1, ICAM1 and TIMP1 were associated with kidney transplantation injury (11). The enrichment of hypoxia and complement-and-coagulation pathways were found in DD kidneys, which might be targeted in donors to improve allograft survival (12). An additional multicenter prospective study reported that 13 genes from 159 renal biopsies at 3 months post-transplantation with stable renal function could discriminate allografts at high or low risk of CAI before irreversible histological damage occurred at 12 months (13). Candidate genes and/or their proteins such as HAVCR1 (KIM-1) and LCN2 (NGAL) in body fluids were also associated with kidney injury (14). The ultimate goal of these studies is to identify and validate DEGs as potential biomarkers to predict and diagnose CAI and improve post-transplantation care.

In this study, genomic analyses were performed in surveillance renal biopsies at 3 months post-transplantation, as well as in paired biopsies obtained at 30 minutes, using DD and LD, for two purposes. Purpose 1 was to identify DEGs between two types of donors (DD *vs* LD) or two time points (3 months *vs* 30 minutes) in the first cohort (discovery cohort) of 24 renal biopsies by microarray analysis. The hypothesis was that the difference between DD and LD in terms of survival might be ascribed to the panel of DEGs and maladjusted signaling pathways, and changed by time post-transplantation. Purpose 2 was to validate the DEGs previously identified and involved in kidney diseases and explore the correlation between their expression and functional and histological readouts at prolonged time points in 24 microarray samples and in a second cohort (validation cohort) of 33 renal allograft biopsies (unpaired time points) by reverse transcription quantitative polymerase chain reaction (qPCR). The hypothesis was that selected DEGs at the early time point might be potential biomarkers for early diagnosis and specific intervention of CAI to offering effective personalized post-transplantation care.

This study revealed divergent transcriptomic signatures between DD and LD, changed by time post-transplantation, might contribute to the different survival of two type kidney allografts. Some of identified and validated DEGs, such as SERPINA3, SLPI, CBF, FTCD, TASPN7, VCAN, TIMP1 and FOS, could be novel biomarkers, which reflected initial donor injury, acute immune responses and adaptive immunity, and associated with inflammation, cell death, remodeling or potential fibrosis in transplant renal biopsies.

MATERIALS AND METHODS

Study Design and Sample Collection

In Leicester, United Kingdom, 80-100 patients per year are transplanted with kidneys: comprising 61% LD including living related and unrelated donors; and 39% DD including donation after brain death and donation after cardiac death. This study was approved by the Ethics Committee, the University Hospitals of Leicester (EDGE34225/UHL10587). From November 2008 to October 2010, 24 renal biopsies were collected from LD and DD paired at 30 minutes (a 30-minute biopsy missed replaced with one collected at day 7 of involved patient) and 3 months post-transplantation for microarray analysis, while additional 33 biopsies time point unpaired were also collected for qPCR validation (**Figure 1**). With the consent of patients, surveillance

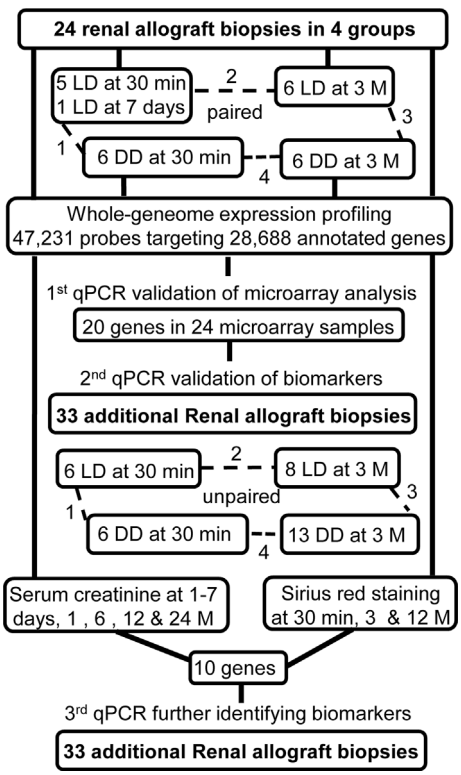


FIGURE 1 | Schematic picture illustrated the study design.

renal biopsies were obtained under ultrasound guidance. Routine biopsy samples were fixed in 10% neutral buffered formalin for histopathological diagnosis, while an additional core of renal tissue was snap-frozen in liquid nitrogen until further research analysis.

Total RNA Extraction

Total RNAs were extracted from renal biopsies using an RNeasy® Plus Mini Kit (Qiagen, West Sussex, UK) with gDNAs eliminated columns. Briefly, 10-15 mg tissues were homogenized in 350 µl of RLT Plus buffer containing guanidine thiocyanate, 1% 2-mercaptoethanol, garnet matrix and a ceramic sphere using a FastPrep®-24 homogenizer (MP Biomedicals, Cambridge, UK). Total RNA integrity and quantity were assessed by Bioanalyzer 2100 (Agilent Technologies, Cheshire, UK). Samples with RNA integrity number exceeding 6.5 were qualified for downstream processing (7, 15).

Microarray Analysis

Whole-transcriptome profiling was performed using Illumina HumanHT-12 v4 Expression BeadChips (Illumina, Essex, UK), which interrogate 47,231 transcripts targeting 28,688 well-established annotated genes. Raw microarray data were normalized by quantile normalization using the control panel in the GenomeStudio Software v2010.3 (Illumina). The quality and intensity of average background were determined in the samples of compared groups. The probes with signal intensity below the average background signal of 120 were excluded.

Reverse Transcription qPCR Validation

Total RNA was reverse-transcribed into cDNA using a Thermo Scientific RevertAid H minus First Strand cDNA Synthesis Kit (Fisher Scientific, Loughborough, UK). The primers were designed to target the same transcripts of the Illumina microarray Beadchips (**Table 1**). For each target gene, qPCR was performed using 1× Maxima SYBR Green qPCR master mix (Fisher Scientific) and 3.3 µM of forward and reverse primers. Expression values were normalized using the geometric mean of UBC, PGK1 and HPRT1, which were identified as stable housekeeping genes from microarray data. To identify potential biomarkers, 20 DEGs selected from microarray analysis, $P < 0.05$, fold change (FC) > 1.5, and involved in renal injury, plus 2 previously interested genes CASP1 and CASP3, were further validated by qPCR in 24 microarray samples and 33 biopsies (**Supplemental Table 1**). FC > 1.5 was chosen after balancing a number of DEGs between compared groups that could best describe the nature of available data, and disclose their association with biological events referring previous publications, as well as further qPCR validation (7, 16).

Identifying Networks, Pathways, and Biological Functions

The Ingenuity Pathway Analysis Software v4.0 (Ingenuity® Systems, Redwood City, CA) was used to map each DEG to its corresponding gene object in the Ingenuity Pathways Knowledge Base (17). P-values were calculated using a Right-Tailed Fisher's Exact Test, which reflected the likelihood and association between a set of DEGs in the input dataset and a given

TABLE 1 | 20 highly DEGs selected from microarray analysis for qPCR validation.

	Name	Forward sequence	Reverse sequence
1	**SERPINA3**	CTGACCTGTCAGGGATCACA	TGCAGAAAGGAGGGTGATTT
2	**SLPI**	AATGCCTGGATCCTGTTGAC	AAAGGACCTGGACCACACAG
3	**VCAN**	CAAGCATCCTGTCTCACGAA	CAACGGAAGTCATGCTCAAA
4	**TIMP1**	CTTCTGGCATCCTGTTGTTG	AGAAGGCCGTCTGTGGGT
5	**GSTM1**	TCGTGTGGACATTTTGGAGA	GGGCTCAAATATACGGTGGA
6	**CFB**	AAGCTGACTCGGAAGGAGGT	TCCACTACTCCCCAGCTGAT
7	**FGA**	AGCCGATCATGAAGGAACAC	AAAAGCCATCCTCCCAAACT
8	**FOS**	GAGAGCTGGTAGTTAGTAGCATGTTGA	AATTCCAATAATGAACCCAATAGATTAGTTA
9	**CCND1**	CCTGTCCTACTACCGCCTCA	CCAGGTCCACCTCCTCCT
10	**DUSP1**	GTACATCAAGTCCATCTGAC	GGTTCTTCTAGGAGTAGACA
11	**CX3CL1**	TCTGCCATCTGACTGTCCTG	CTGTGCTGTCTCGTCTCCAA
12	**VHL**	AGGTCACCTTTGGCTCTTCA	TGACGATGTCCAGTCTCCTG
13	**CD14**	CGACCATGGAGCGCGCGTCCTG	GGCATGGATCTCCACCTCTA
14	**ACTRT1**	GCGTGGACTGGTAACAGGAT	TGACACAGGCAGAGGCATAG
15	**ARRDC4**	TCCCACCTGTTACTCCATCC	CCACATCTGCATAATTTGGTG
16	**TMEM149**	GAGGTGCTGGAAGAGCTGAT	CTTGCCACCACCATCTCAAT
17	**DBI**	TGGCCACTACAAACAAGCAA	TGGCACAGTAACCAAATCCA
18	**UNCSCL**	AGCTGCGGATGTTATTGGAG	TGACGGTCATGAGGTAGTGC
19	**DARC**	CTGATGGCCCTCATTAGTCC	CTCCATCTGGGAAGGAATCA
20	**SOST**	TGCTGGTACACACAGCCTTC	GTCACGTAGCGGGTGAAGTG
21	***CASP3***	AGAACTGGACTGTGGCATTGAG	GCTTGTCGGCATACTGTTTCAG
22	***CASP1***	GCTTTCTGCTCTTCCACACC	CATCTGGCTGCTCAAATGAA
23	**UBC**	ATTTGGGTCGCGGTTCTTG	TGCCTTGACATTCTCGATGGT
24	**PGK1**	AAGTGAAGCTCGGAAAGCTTCTAT	AGGGAAAAGATGCTTCTGGG
25	**HPRT1**	GCCAGACTTTGTTGGATTTGA	ATTTTGCTTTTCCAGTTTCACT

2 previously validated genes (CASP3 and CASP1) and 3 unchanged genes (UBC, PGK1 and HPRT1) were also included.

process/pathway/transcription neighborhood is due to random chance. Gene networks were algorithmically generated based on their connectivity and assigned score to identify biological functions and/or diseases.

Relevant Clinical End-Points

Clinical data including the age of donors and recipients, warm and cold ischemic time, anastomosis time, DGF and rejection were collected (18). As chosen clinical end-points SCr and Sirius red (SR) staining were also followed up either at 1-7 days, 1, 3, 6, 12 and 24 months, or 30 minutes, 3 and 12 months. SR staining representing extracellular matrix collagens I and III deposition (19–21), were performed in paraffin sections using 0.1% SR in saturated aqueous picric acid overnight. Slides were rapidly dehydrated by consequential washing in 0.01 N HCl, 70, 80, 90, 100% ethanol and xylene, and then mounted by DPX mountant. The field of entire renal cortex in each biopsy was semi-quantitatively analyzed at 400 magnification using Image Pro Software (Media Cybernetics, Bethesda, USA).

Statistical Analysis

Non-parametric Man Whitney-U test was performed using Illumina GenomeStudio Software v2010.3. Unsupervised hierarchical clustering analysis (HCA, Manhattan average distance) and principal component analysis (PCA, autoscale) were also performed using Array Track (22). Correlation analyses between the expression level of DEGs and SCr or SR were performed with Microsoft Excel 2007 and SPSS v20 using the Pearson correlation coefficient. Clinical data such as SCr and SR staining score were expressed as means ± SEMs. Significance was assigned to $P \leq 0.05$.

RESULTS

Demographics of Patients and Clinical Data

Warm ischemic time was shorter, but cold ischemic time was longer in DD *vs* LD for 12 microarray analysis and 33 qPCR validation patients (**Tables 2A**, **B**). In addition, anastomosis time was also longer in DD at 30-minute qPCR validation patients. There were no significant differences in other parameters such as DGF and rejection episodes. The immunosuppression of all patients was consisted of tacrolimus, mycophenolate modetil and prednisolone.

Gene Expression Analysis

All confidently detected genes were analyzed by PCA and unsupervised HCA. Distinct separate clusters were revealed at 30 minutes and 3 months regardless of donor types (**Figure 2**). Interestingly, the DD biopsy collected at day 7 clearly fell into the gene cluster of 3 months.

The transcriptomic profile was then assessed in 5 DD *vs* 6 LD biopsies at 30 minutes. 1735 probes corresponding to 1517 annotated DEGs ($P < 0.05$) were identified, with 446 DEGs at FC > 1.5 (**Figure 3**). With a view to assessing whether different DEGs were restored later, similar analyses were performed in 6 DD *vs* 6 LD biopsies at 3 months, with 11 biopsies matched to 30 minutes. 1610 probes corresponding to 1444 annotated DEGs ($P < 0.05$) were identified, with 149 DEGs at FC > 1.5 (**Figure 3**). The Venn diagram showed 190 commonly DEGs (DD *vs* LD, $P < 0.05$) between two time points, which was reduced to 25 DEGs at FC > 1.5 (**Figure 3**), including GSTM1, SOD2, CCND1 and SLPI (**Supplemental Table 2**).

TABLE 2 |

(A) Demographic and clinical characteristics of 12 patients for microarray analysis.

Recipient	LD 30 min & 3 M (n = 6)	DD 30 min & 3 M (n = 6)	P value
Age at transplant (yr)	41.5±7.1	49.3±4.0	NS
Sex (% male)	3 (50%)	4 (67%)	
Donor age (yr)	48.7±5.6	51.7±4.7	NS
HLA mismatch	2.8±0.9	2.5±0.4	NS
Warm ischemia time (h)	0.08±0.01	0.00±0.00	P < 0.001
Cold ischemia time (h)	3.7±0.5	8.8±1.4	P < 0.01
Anastomasis time (h)	0.49±0.09	0.53±0.09	NS
Delayed graft function	0/6 (0%)	2/6 (33%)	NS
Rejection episode	2/6 (33%)	2/6 (33%)	NS

(B) Demographic and clinical characteristics of 33 patients for qPCR validation.

Recipient	LD 30 min (n = 6)	DD 30 min (n = 6)	P value	LD 3 M (n = 8)	DD 3 M (n = 13)	P value
Age at transplant (yr)	39.5±3.2	49.7±7.0	NS	51.6±2.6	47.0±4.7	NS
Sex (% male)	5 (83%)	4 (67%)		7 (89%)	9 (69%)	
Donor age (yr)	45.3±5.6	50.7±6.9	NS	47.0±5.8	50.0±3.6	NS
HLA mismatch	2.3±0.8	3.3±1.0	NS	2.8±0.5	2.7±0.6	NS
Warm ischemia time (h)	0.08±0.01	0.02±0.02	P < 0.01	0.07±0.01	0.02 ± 0.02	P < 0.05
Cold ischemia time (h)	5.2±1.7	12.0±1.2	P < 0.01	5.1±1.3	12.5±0.9	P < 0.001
Anastomasis time (h)	0.38±0.01	0.50±0.03	P < 0.01	0.47±0.05	0.52±0.04	NS
Delayed graft function	1/6 (17%)	2/6 (33%)	NS	0/8 (0%)	2/13 (15%)	NS
Rejection episode	1/6 (17%)	2/6 (33%)	NS	0/8 (0%)	0/13 (0%)	NS

The data were expressed as means ± SEMs or % of change.

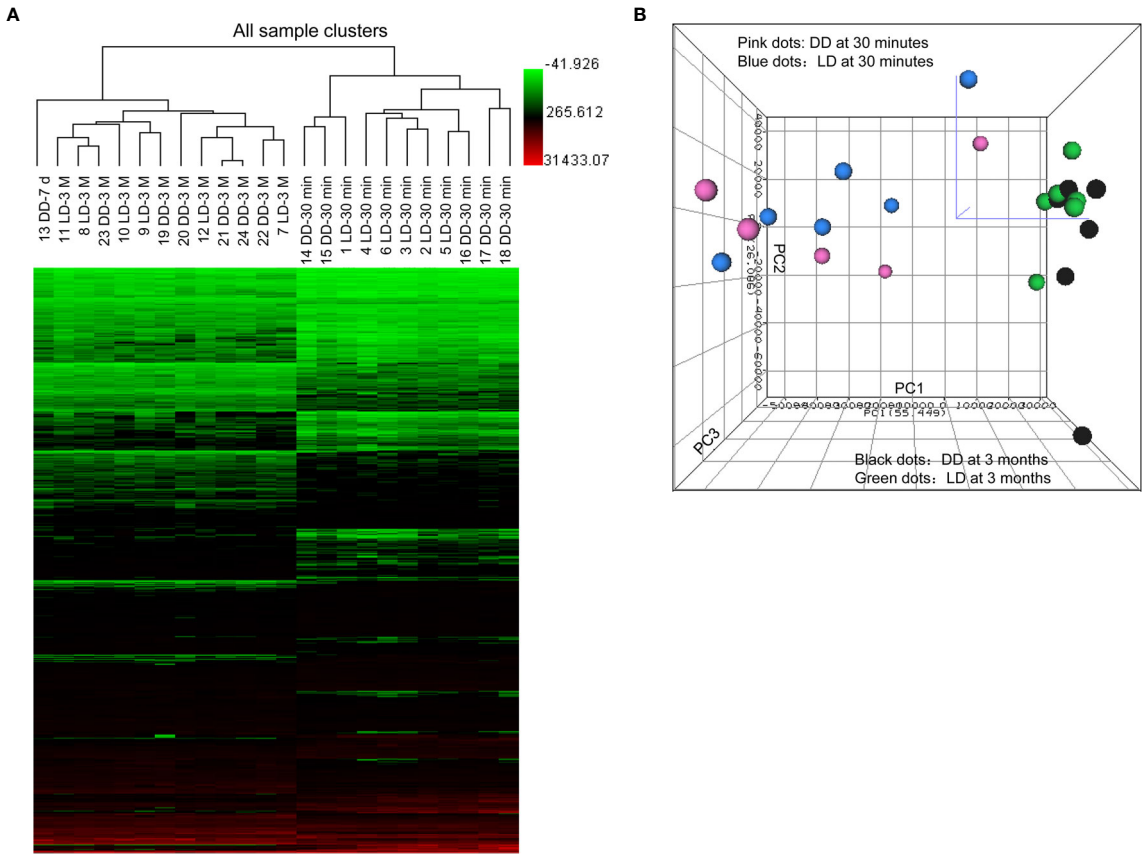


FIGURE 2 | Heat map of raw data analysis of microarray, unsupervised hierarchical clustering and principal component analysis. **(A)** 899 significant DEGs ($P < 0.05$ and $FC > 1.5$) in 24 microarray analyzed samples were included in the heat map for unsupervised hierarchical clustering analysis illustrated as Euclidean + Average of non-normalized data. **(B)** Samples from biopsies at 30 minutes (dots in pink for DD and blue for LD) and 3 months (dots in black for DD and green for LD) were located into two clearly separated areas demonstrating clear differences in the overall gene profile between two different time points post-transplantation, rather than two donor types, expect one day 7 sample. The bigger was the dot size, the closer was the dot to the reader.

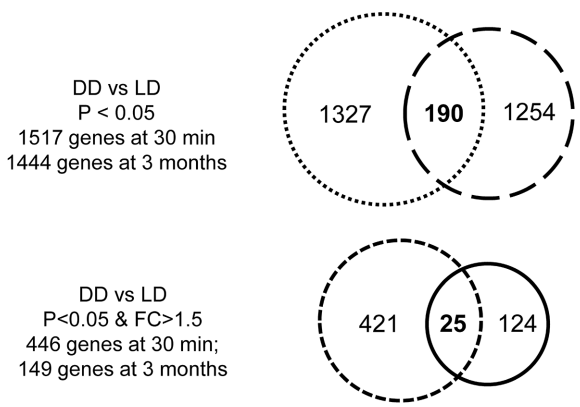


FIGURE 3 | Venn diagrams of DEGs. There were 1517 DEGs (DD *vs* LD) at 30 minutes and 1444 genes at 3 months when $P < 0.05$, with 190 genes in common over two time point, while the number of genes was reduced 446 or 149 at each respective time points when $P < 0.05$ and $FC > 1.5$, with only 25 genes in common.

The top 10 up and down-regulated DEGs (DD *vs* LD and 3 months *vs* 30 minutes) is presented (**Figure 4**). DEGs changed by time post-transplantation, with up-regulation of SERPINA3, FGA, SLPI and SOD2 at 30 minutes (27, 8, 6 and 4 fold-difference between DD *vs* LD respectively, **Figure 4A**), and 2-3 folds up-regulation of SLPI, GSTM1, GSTM2 and VCAN at 3 months in DD *vs* LD (**Figure 4B**). Interestingly, at 3 months, the two types of donors exhibited different DEGs, with up-regulation of COL3A1, MMM9 and VCAN (9, 6 and 6 fold-difference respectively) and 10-fold down-regulation of FGA in DD (**Figure 4D**). Also, at 30 minutes *vs* 3 months, SERPINA3 was found up-regulated by 8 folds in LD *vs* DD, whereas COL1A1 and COL1A2 were found upregulated by 8 to 10 folds, and FOSB, FOS, ATF3, EGR1, DUSP1, JUN and ZFP36 were downregulated by 8 to 74 folds in both donors (**Figures 4C, D**).

Functional Annotation, Network, and Pathway Analysis

Functional annotation analysis revealed many up-regulated acute phase response genes at 30 minutes (DD *vs* LD)

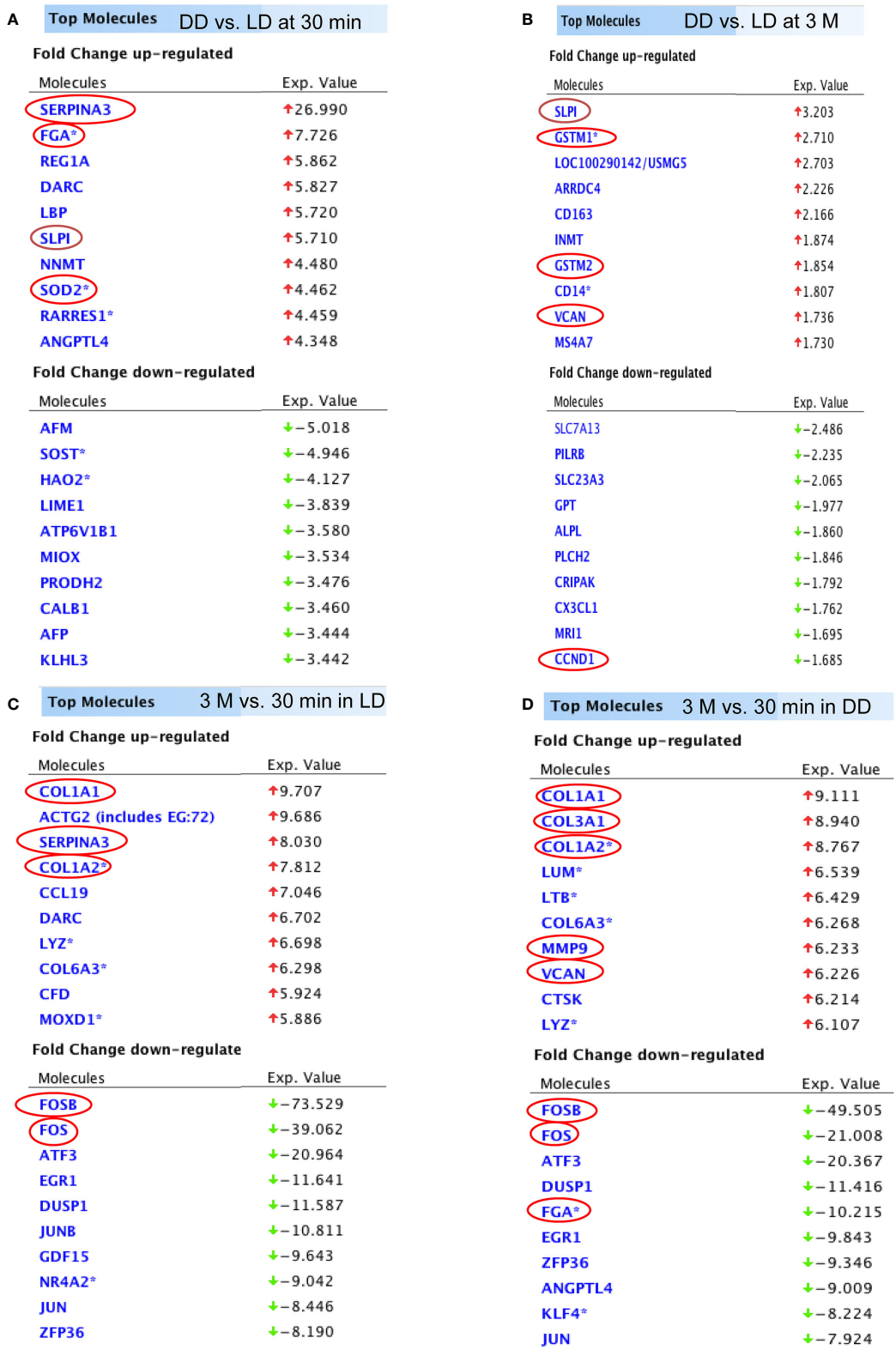


FIGURE 4 | The list of DEGs. Top 10 up and down-regulated genes (DD *vs* LD, P < 0.05, FC > 1.5) at 30 minutes and 3 months were shown **(A, B)**. In addition, top 10 up and down-regulated genes (3 months *vs* 30 minutes, P < 0.05 and FC > 1.5) in LD and DD **(C, D)** respectively were also demonstrated.

including AGT, CFB, TIMP1 and TNFSF10, except SERPINA3, SLPI, SOD2, GSTM1 and FGA described above, were found associated with the cell death including kidney cell apoptosis, proximal tubular toxicity and renal tubule injury (**Figure 5A**). Some of these dysregulated genes including SLPI, TIMP1 and GSTM1 also seen at 3 months are involved in oxidative stress, inflammation, tubular injury and cell proliferation (**Table 3**). In addition, adaptive immune response genes in DD or LD kidneys (3 months *vs* 30 minutes) were also revealed, for instance up-regulated CASP1, CCL5, CX3CR1, VWF, TIMP1 and LCN2 apart from COL3A1 and VCAN; and down-regulated AGT, EGF, CDKN1A and PLG apart from FGA, FOS, FOSB and DUSP1 described above, are associated with immune responses, cell death including apoptosis and necrosis, cell proliferation and tissue remodeling (**Figure 5B**).

The example network of DEGs was illustrated including SLPI, GSTM1, GSTM2, CD14, CD163, VCAN and CCND1 at 3 months (DD *vs* LD, **Figure 6**), as well as the signaling pathway of GSTM1/GSTM2/SLPI-JNK-AKT-ERK-NF-κB-VCAN. An additional schematic picture demonstrated signaling pathways of acute phase response DEGs at 30 minutes, such as TNF-α/IL-1-JNK1/2-P38/MARK-NF-κB/c-FOS-SOD2/CFB, IL-6-PI3K/AKT-mTOR/STAT3-FGA/SERPINA3, and RAS-MEK1/2-ERK1/2-NF-IL6-SERPINA1 in the nucleus, cytoplasm and extracellular space including plasma (**Figure 7**).

qPCR Validation

To validate microarray analysis, 25 genes (**Table 1**) were quantified by qPCR in the discovery cohort of samples analyzed by microarray. Excellent correlations were shown

A Acute phase response genes (DD vs LD at 30 minutes)

Process	Process
1 Process	1 Process
cell death of kidney cell lines	apoptosis of kidney cells
affects cell death of kidney cell lines (3/13)	decreases apoptosis of kidney cells (2/4)
↑AGT, ↑CDC42, ↑TNFSF10	↓NPHS1, ↑SOD2*
decreases cell death of kidney cell lines (6/13)	increases apoptosis of kidney cells (2/4)
↓CALB1, ↓GSTA5, ↑NAMPT*, ↑SOD2*, ↑SPP1*, ↑SRXN1	↑AGT, ↑GFPT1*
increases cell death of kidney cell lines (5/13)	
↓NRGN, ↑PMP22, ↑RASSF4*, ↑S100A9, ↑TNFSF10	

Process	
1 Process	injury of renal tubule
proximal tubular toxicity	affects injury of renal tubule (1/1)
affects proximal tubular toxicity (12/12)	↑CFB
↑CD24, ↑FGA*, ↓GSTA5, ↑GSTM1*, ↓HAGH, ↓PRKCZ, ↑PSMA3*, ↓SLC27A1, ↑SPP1*, ↑TIMP1, ↑TMSB10/TMSB4X, ↑TXNRD1	increases injury of renal tubule (1/1)
	↑CFB

B Adaptive immune response genes (in DD or LD at 3 months vs 30 minutes)

Functions Annotation	p-Value	Molecules
immune response	1.11E-31	↓ADM, ↓AGT, ↑ARHGDIB, ↑BTK, ↓C6, ↑C1QB, ↑CASP1, ↑CCL5*, ↑CCL21, ↑CCR7, ↑CD2, ↑CD27, ↑CD44, ↑CD48, ↑CD74*, ↑CD96*, ↑CD247*, ↑CD79A, ↑CD8A, ↓CDKN1A, ↓CEBPB, ↑CFH*, ↓CISH, ↑COL3A1, ↑CORO1A, ↑CSF1R, ↑CTSS, ↑CX3CR1, ↑CXCL6*, ↑CXCL9, ↑CXCL10, ↑CXCL12*, ↑CYBB, ↓DNASE1, ↑DOCK2, ↓DUSP1, ↓EGR2, ↑FCER1A, ↑FCER1G, ↑FERMT3, ↓FOS, ↑FYB, ↑GNLY, ↑GPSM3, ↑GZMA, ↑GZMB, ↑HLA-B, ↑HLA-DQA1, ↑HLA-DQB1, ↑HLA-DRA*, ↑HLA-DRB1, ↑HLA-DRB4, ↓IER3, ↑IGF1, ↓IL8, ↑IL10RA, ↓IL1RL1*, ↑IRF8, ↑ITGB2*, ↓KLF2, ↑LAT, ↓LBP, ↑LCN2, ↓LDLR, ↑LTB*, ↑LTF, ↑MDK, ↑MMP7*, ↑MX1, ↑NCF4, ↓NFIL3, ↑PTPRCAP, ↑PYCARD, ↓RGS1, ↓RGS2, ↑RNASE6, ↓SELE, ↑SERPING1, ↑SLAMF6, ↓ST6GAL1, ↑TLR7, ↑TNC*, ↑TNFRSF11B, ↑TNFSF13B*, ↑TPSAB1, ↑TYROBP, ↑VCAN, ↑VTCN1, ↑VWF, ↑WAS

Immune response in DD

Functions Annotation	p-Value	Molecules
proliferation of kidney cells	3.24E-09	↓AGT, ↑CCL21, ↑CCR7, ↑CXCL9, ↑CXCL10, ↓DUSP1, ↓EGF, ↑FCER1G, ↑IGF1, ↑LCN2, ↓PLAUR
proliferation of glomerular cells	7.46E-09	↓AGT, ↑CCL21, ↑CCR7, ↑CXCL9, ↑CXCL10, ↓DUSP1, ↓EGF, ↑FCER1G, ↑IGF1, ↓PLAUR
proliferation of mesangial cells	3.92E-08	↓AGT, ↑CCL21, ↑CCR7, ↑CXCL9, ↑CXCL10, ↓EGF, ↑FCER1G, ↑IGF1, ↓PLAUR
proliferation of tubular cells	1.75E-03	↓AGT, ↓EGF, ↑LCN2
proliferation of renal tubular epithelial cells	3.08E-03	↓EGF, ↑LCN2
proliferation of podocytes	4.56E-02	↓DUSP1

Cell proliferation in DD

Functions Annotation	p-Value	Molecules
cell death of kidney cells	6.37E-06	↑BGN, ↑CASP1, ↓CDKN1A, ↑DCN*, ↓DDIT3, ↓DUSP1, ↓EGF, ↑LCN2, ↑TNFRSF1B
apoptosis of kidney cells	1.59E-05	↑BGN, ↓CDKN1A, ↑DCN*, ↓DDIT3, ↓DUSP1, ↓EGF, ↑LCN2, ↑TNFRSF1B
necrosis of kidney cells	4.39E-04	↑CASP1, ↓CDKN1A, ↑TNFRSF1B
cell death of tubular cells	4.69E-04	↑CASP1, ↓CDKN1A, ↑DCN*, ↓EGF, ↑LCN2
apoptosis of tubular cells	1.66E-03	↓CDKN1A, ↑DCN*, ↓EGF, ↑LCN2
apoptosis of renal tubular epithelial cells	1.93E-03	↑DCN*, ↓EGF, ↑LCN2
necrosis of tubular cells	5.41E-03	↑CASP1, ↓CDKN1A
apoptosis of mesangial cells	3.72E-02	↑BGN, ↓DUSP1
necrosis of proximal tubule cells	4.71E-02	↓CDKN1A
necrosis of renal glomerulus	6.99E-02	↓PLG

Cell death in LD

FIGURE 5 | Functional annotation of DEGs in acute phase response and adaptive immunity by Ingenuity Pathway Analysis. **(A, B)** P-values were calculated using a Right-Tailed Fisher's Exact Test to reflect the association between DEGs and a given process.

TABLE 3 | Significantly dysregulated genes in 33 additional biopsies validated by qPCR among 20 DEGs relevant to renal diseases.

Genes	Change	Comparison	P value
SERPINA3	up	CAD *vs* LD at 30 minutes	0.041*
SERPINA3	down	3 months *vs* 30 minutes in CAD	0.022*
VCAN	up	3 months *vs* 30 minutes in LD	0.028*
VCAN	up	3 months *vs* 30 minutes in CAD	0.081#
TIMP1	up	3 months *vs* 30 minutes in LD	0.031**
TIMP1	up	3 months *vs* 30 minutes in CAD	0.092#
VHL	up	3 months *vs* 30 minutes in LD	0.052#
CD14	up	3 months *vs* 30 minutes in LD	0.058#
CFB	up	3 months *vs* 30 minutes in LD	0.075#
UNCSCL	up	3 months *vs* 30 minutes in LD	0.079#
CCND1	down	CAD *vs* LD at 30 minutes	0.088#
UBC	down	3 months *vs* 30 minutes in LD	0.062#
GSTM1	down	3 months *vs* 30 minutes in LD	0.097#
FOS	down	3 months *vs* 30 minutes in LD	0.001**
FOS	down	3 months *vs* 30 minutes in CAD	0.002**

***P < 0.01; *P < 0.05; #0.05 < P < 0.1.*

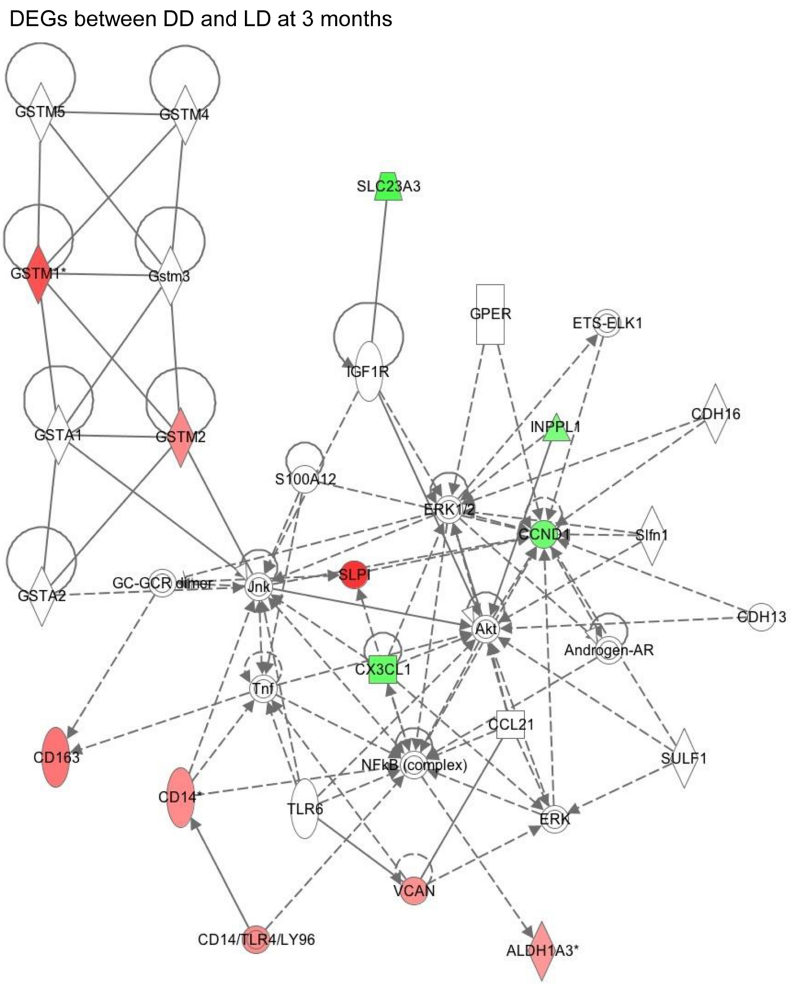


FIGURE 6 | This schematic figure demonstrated an example of complicated key network links in DEGs between DD and LD at 3 months generated by function annotation using Ingenuity Pathway Analysis, as well as certain signaling pathways, with red or green color highlighted up or down-regulated genes.

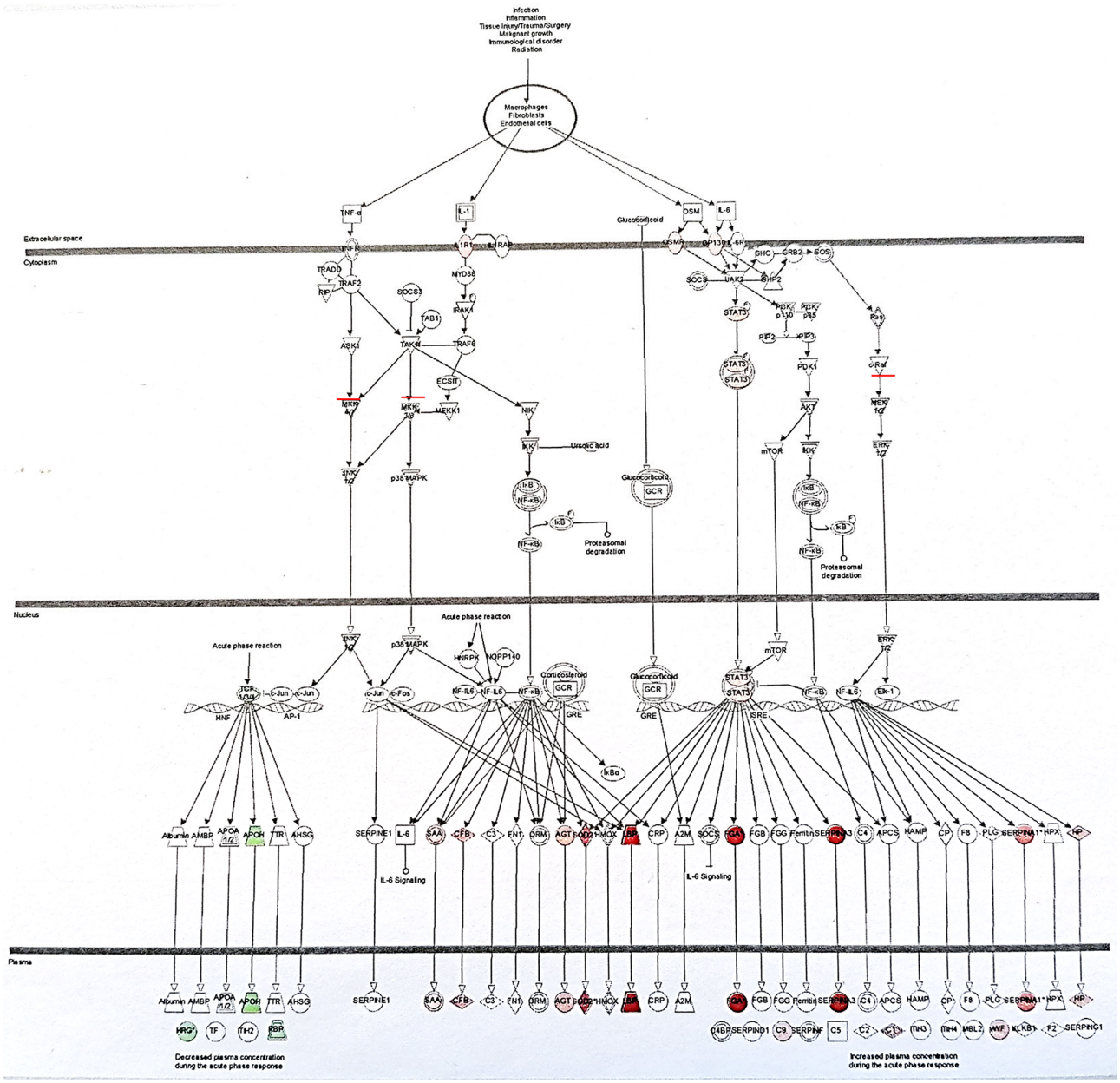


FIGURE 7 | This schematic picture illustrated an example of acute phase response signaling pathways in the different compartment of cells such as the nucleus, cytoplasm and extra cellular space produced by Ingenuity Pathway Analysis, with red or green color highlighted up or down-regulated genes.

between both detection platforms with correlation coefficient R^2 range from 0.70 to 0.94 for most DEGs, for example $R^2 = 0.974$, 0.885 and 0.780 for SERPINA3, TIMP1 and CCND1 respectively at 30 minutes, $R^2 = 0.938$, 0.775 and 0.832 for SLPI, VCAN, VHL respectively at 3 months, and $R^2 = 0.748$ for CASP1 at both time points. The most P-values were significant, except a few genes at borderlines or not confidently detected.

These 25 genes were also quantified by qPCR in a validation cohort of 33 additional biopsies to identify potential biomarkers. In DD, up-regulated SERPINA3 and SLPI, and marginally down-regulated CCND1 were shown at 30 minutes (**Table 3**), with up-regulated TIMP1, down-regulated SERPINA3 and FOS, marginally up-regulated VCAN at 3 months. At 3 months, up-regulated TIMP1 and VCAN, and down-regulated

FOS were revealed in LD, with marginally increased SLPI, CD14, CFB, VHL and UNC5CL (**Table 3**).

Renal Function and Histological Changes

The patients enrolled in microarray-based gene expression analysis were followed up for 24 months, with relatively stable renal function (**Figure 8A**), no graft loss, although one patient who had received a DD kidney died due to sepsis-cardiac arrest. No significant differences in SCr (obtained from the clinical database of the University Hospitals of Leicester NHS Trust) between two types of donors were shown at any time points, with a consistent better trend in LD (*vs* DD) at 2-7 days, 1, 6, 12 and 24 months, except pre-transplantation, 1 day and 3 months. Renal fibrosis assessed by SR staining in 24 microarray and additional 33 biopsies, mainly located in tubulointerstitial areas and scattered in glomerular areas, was increased in DD at 3 and 12 months compared with 30 min, without significant difference in LD (**Figure 8B**).

Correlation Between DEGs and Clinical Outcomes

To assess whether DEGs at 30 minutes or 3 months could be potential biomarkers to predict allograft survival, the correlations between the expression level of these DEGs, SCr and SR staining were analyzed at the same and extended time points. Using the microarray signal intensity of DD and LD at 30 minutes, a list of top 120 genes was identified significantly correlated with SCr and/or SR staining. For instance, SERPINA3 was found negatively correlated with SCr at 1-7 days, and TNFSF10 was found positively correlated with SCr at 1, 3, 6 and 12 months (**Figures 9A, B**). The expression levels of 10 DEGs (highly expressed and involved in renal physiopathology based on GO terms or previous publications)

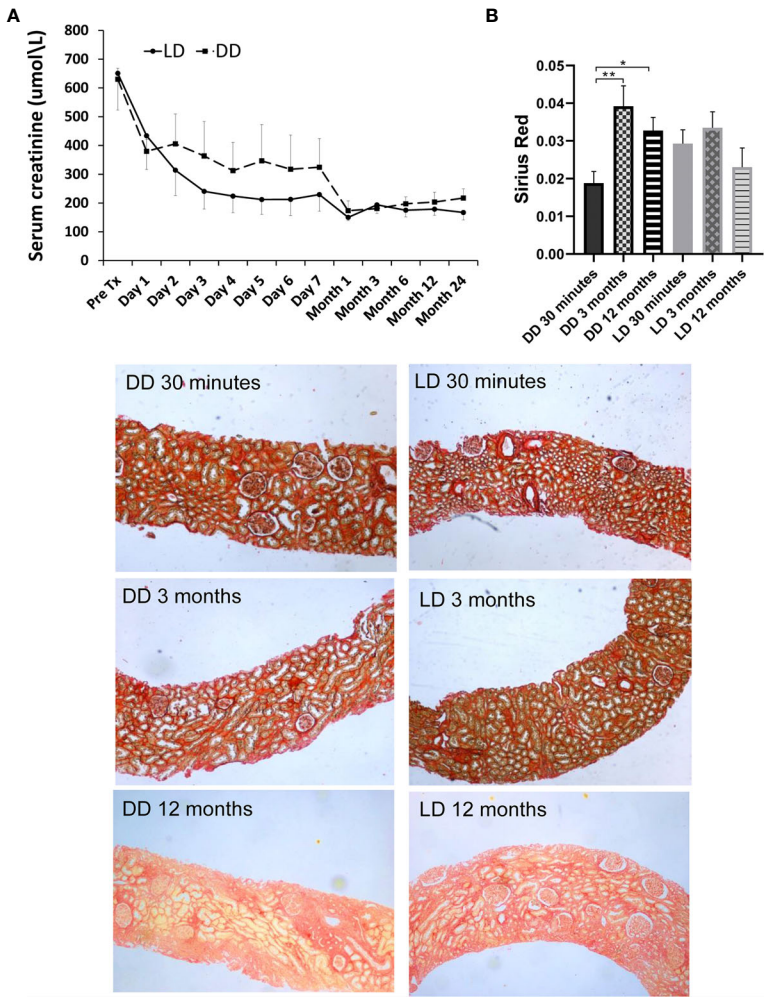


FIGURE 8 | Dynamic change of renal function and Sirius Red staining in 12 patients (6 LD and 6 DD) over a prolonged period up to 2-year post-transplant. **(A)** The data of SCr were collected at pre-transplantation, day1-7 daily, 1, 3, 6, 9, 12 and 24 months post-transplantation. **(B)** The change of Sirius Red staining at 30 minutes, 3 and 12 months. The staining was mainly located in tubulointerstitial areas, which was significantly increased at 3 and 12 months compared with 30 minutes in DD, without significant difference between time points in LD. *P < 0.05; **P < 0.01.

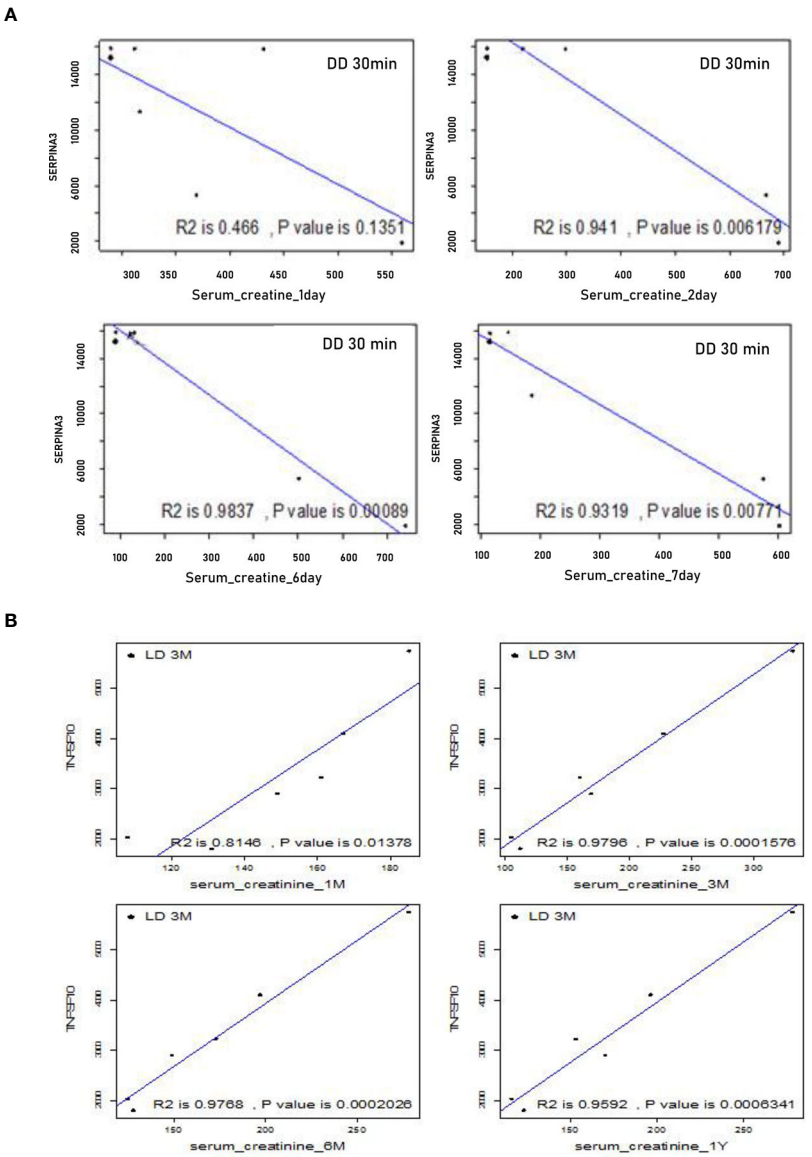


FIGURE 9 | Correlations between microarray analysis detected DEGs and renal function in the first cohort of 24 biopsies. **(A)** Negative correlations between SERPINA 3 and SCr at early time points from day 1 to 7; **(B)** Positive correlations between TNFSF10 and SCr at later time points from 1, 3, 6 to 12 months.

GSTM1, COQ2, CCND1, CFB, FTCD, UNC5CL, SERPINA3, RAI14, TSPAN7 and SOD2 were correlated with both SCr and SR staining at 12 months (**Supplemental Table 2**). Moreover, at 3 months TSPAN7, BTG3 or COQ2 expression was correlated with SCr, while FAU, UMOD, TSPO, IMPDH2, ADSS, RAF1, ARG2, AGTR1 or PDE6D expression was correlated with SR staining. In addition, other DEGs PTPN6, CNNM3, CSTF3, CHURC1, UCRC, COX7B, FXYD5, CD74, MRPL42P5, SENP2, TMEM129, EIF2AK1, FAM165B, C6ORF66 and ATP5J were also found in four patients with a rejection compared to those without.

Above 10 DEGs correlated with both SCr and SR staining were further validated by qPCR in the second cohort of 33 biopsies. In DD (*vs* LD), there were four up-regulated genes FTCD, SERPINA3, TASPN7 and CFB ($P < 0.05$) at 30 minutes, with a trend of increased SOD2 and decreased CCND1, while raised FTCD and TSPAN7 ($P < 0.001$) were also seen at 3 months, with marginally up-regulated CCND1 and SOD2.

The correlation between the 10 DEGs and SCr or SR at 12 months in the second cohort of 33 biopsies was further analyzed respectively using Pearson correlation coefficient. CFB (R=-0.669, P=0.034) and COQ2 (R=-0.649, P=0.042) at 30 minutes were significantly correlated with SR at 12 months, while UNC5CL (R=0.553, P=0.098) at 30 minutes was marginally correlated with SCr at 12 months. Other genes at 3 months such as

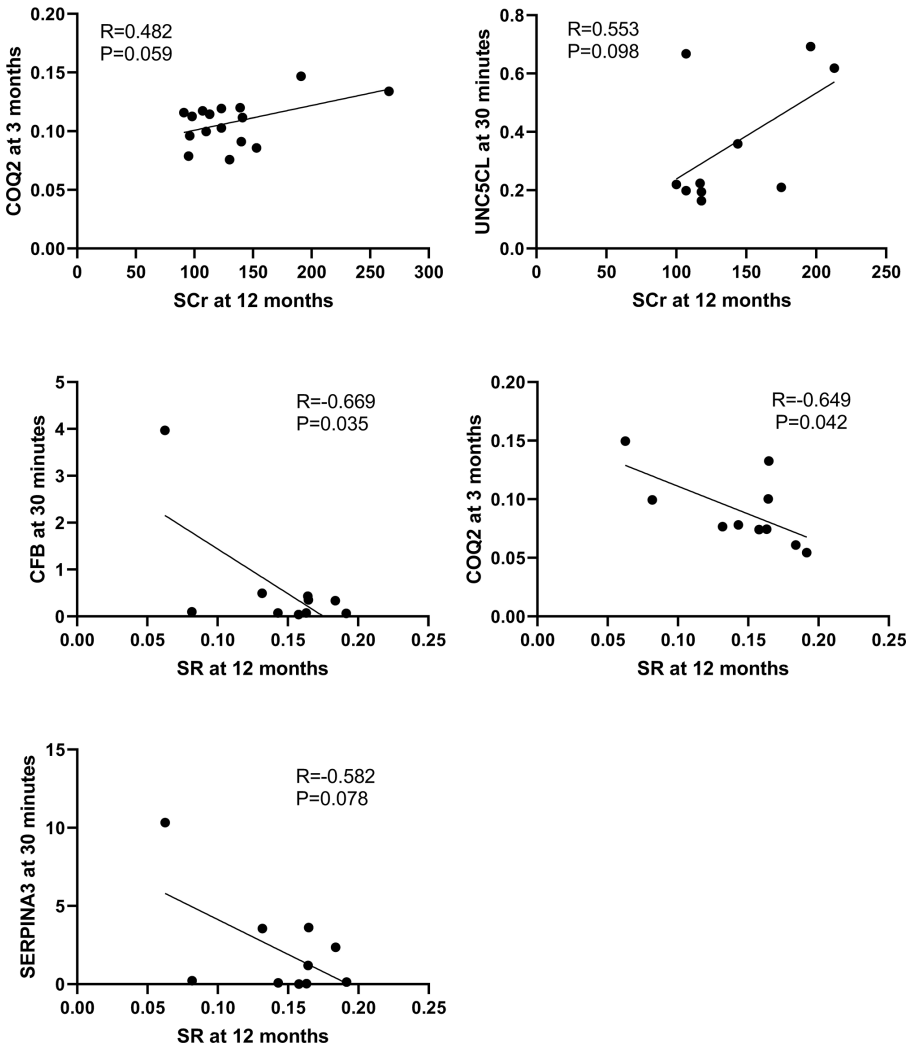


FIGURE 10 | Correlations between qPCR validated DEGs at 30 minutes or 3 months and SCr or SR at 12 months in the second cohort of 33 renal biopsies. The significant positive or marginal negative correlations were shown between COQ at 3 months or UNC5CL at 3 minutes and SCr at 12 months, as well as COQ, CFB or SERPINA3 at 30 minutes and SR at 12 months, respectively.

COQ2 (R=0.482, P=0.059) or SERPINA3 (R=0.405, P=0.095) were also marginally correlated with SCr or SR at 12 months respectively (**Figure 10**).

In addition, some DEGs such as SERPINA3, SLPI, VCAN, FOS and SOD2 revealed in this study by microarray analysis, validated by qPCR and associated with kidney injury, were also reported by a previous publication (14) (**Supplemental Table 3**).

DISCUSSION

An increasingly severe shortage of kidney donors leads to the expansion of donor pools by including DD for transplantation. However, the survival of transplant kidneys using DD is not as good as LD. In this study, the microarray analysis of renal allograft biopsies showed divergent transcriptomic signatures between LD and DD, which shifted from acute immune responses at 30 minutes to tissue injury/repair and remodeling/fibrosis at 3 months and might contribute to different long-term survival. DEGs might be attributed to initial donor conditions, innate and adaptive immune responses, persistent inflammation associated with immunosuppressants. Some DEGs including SERPINA3, SLPI, CBF, FTCD, TASPN7, VCAN, TIMP1 and FOS might be novel biomarkers to facilitate timely diagnosis and early therapeutic intervention in donor kidney preservation, implantation or post-transplantation, in particular, effectively improve the donor quality and allograft survival of DD.

Clearly different gene clusters revealed in allograft biopsies between two time points regardless of donor types indicates time post-transplantation playing crucial roles. DEGs affected by time

post-transplantation might mask initial differences of cold or warm ischemic time in donors, as donation trauma and acute immune responses were overwhelming in implantation. The dramatic changes were eased off, which was reflected by 3 times more DEGs at 30 minutes than 3 months.

We then prioritized to analyze how DEGs (DD *vs* LD) associated with allograft survival. The functional annotation revealed up-regulated acute response genes SERPINA3, FGA and SLPI, together with inflammation and nephrotoxicity associated genes SOD2, GSTM1, VCAN and TIMP1, but down-regulated repair related genes FGA, CCND1 and FOS in DD at 30 minutes. More fibrotic genes COL3A1, TIMP4 and MMP9 were raised in DD, with increased TIMP1, VCAN, COL1A1 and COL1A2 in both donors at 3 months. The dynamic change of these DEGs well reflected donor initial injury and recipient adaptive immunity *via* different networks and signaling pathways such as TNF-α/IL-1-JNK1/2-P38/MARK-NF-κB/c-FOS-SOD2/CFB and GSTM1/GSTM2/SLPI-JNK-AKT-ERK-NF-κB-VCAN. These results were consistent with a study using 59 protocol kidney biopsies that showed immune pathway activation, fibrotic gene expression and cell proliferation-repair-remodeling at 1, 3 and 12 months respectively (7). 40% DEGs and 50% pathways initially activated were persisted to 3 months, while pro-fibrotic genes were expressed before observed microscopic interstitial fibrosis, suggesting that DEGs might be early biomarkers.

FGA protein is crucial in coagulation, inflammation and tissue regeneration. Soluble fibrinogen-like protein 2 (sFGL2) increased in the circulation of allograft rejection patients, contributed to the apoptosis of cultured tubular epithelial cells (TECs), which is detrimental in early injury, but also initiates remodeling (23, 24). Increased sFGL2 in the recovery stage of auto-transplanted porcine kidneys was associated with inflammatory cell apoptosis and decreased inflammation (25). However, reduced FGA in the plasma of $FGA^{+/-}$ mice protected IR kidneys against TEC death and inflammation, with increased CCND1 and proliferation (26). Taken together, down-regulated FGA and CCND1 in DD at 3 months might affect allograft recovery.

SOD2 encoding mitochondrial enzyme protects against IR injury and inflammation (27). SOD2 was found decreased in the urine of aged-mice with increased oxidative stress, apoptosis tubulointerstitial fibrosis and proteinuria (28). GSTM1 protects against xenobiotic compounds and toxicity caused by immunosuppressants in renal transplant recipients. Up-regulated GSTM1 was protective to increased oxidative stress in chronic kidney disease (29). However, GSTM1 was also linked to high rejection risks and unfavorable to long-term allograft outcomes (30, 31). In this study, highly expressed SOD2 and GSTM1 in DD at 30 minutes and 3 months might reflect initial donor injury, as well as self-defense.

Strong positive correlations between two detection methods were shown for most detected DEGs, and potential biomarkers were also identified and validated by qPCR. Up-regulated SERPINA3 and SLPI were shown in DD at 30 minutes with SLPI remained high at 3 months, and raised both in LD at 3 months. SERPINA3 is a secreted acute phase protein associated with inflammatory diseases, a potential pharmacological target (32, 33). Elevated serum SERPINA3 in mice increased the transendothelial permeability of retina associated with diabetic retinopathy (34). Urine SERPINA3 was positively correlated with the activity of lupus nephritis, with SERPINA3 located in endothelial cells and TECs (35), and predicted renal inflammation and fibrosis, especially early transition of AKI to CKD (36). SLPI protein, an inhibiting proteolytic enzyme, participates in mucosa anti-microbial defense by mediating the production of anti-inflammatory cytokines, IL-10 and TGF-β (37). Up-regulated SLPI in epithelial cells plays active roles in defending airways upon inflammation (38). SLPI expressed in TECs of heathy renal biopsies and elevated in serum of uremic patients (39) to regulate proteolytic activity in inflammatory sites (40). SLPI in plasma and urine were increased in AKI post-transplantation, aortic aneurysm repair and cardiac surgery (41–43). SERPINA3 and SLPI, therefore, might be ideal biomarkers of kidney injury.

TIMP1 and VCAN were up-regulated in both DD and LD at 3 months, with reduced FOS. TIMP1 associated with renal IR injury (11), together with matrix metalloproteinases (MMPs), plays important roles in the progression of CAI (44). Urinary/serum TIMP1/MMPs was/were active in acute tubulointerstitial injury/inflammation (45). VCAN, an indicator of AKI post-transplantation and ongoing parenchymal injury, predicts allograft loss (14). FOS, a transcription factor, involves in MAPK signaling pathway (46). FOS protein has been described as stimulating central opioid receptors, activated renal sympathetic nerves and enhanced IR-induced AKI in mice (47). c-FOS and VEGF play synergistic roles in inflammation and angiogenesis in the peritoneal membrane upon inflammation and lead to ultrafiltration failure (48). The selective inhibitor of c-FOS/activator protein-1 (AP-1, a redox-sensitive transcription factor) inhibited proinflammatory cytokines and improved the survival of lipopolysaccharide-induced AKI (49).

Of note, in the top 10 down-regulated gene list, 7 genes FOSB, FOS, ATF3, EGR1, DUSP1, JUN and ZFP36 were down-regulated in both LD and DD at 3 months. All of them are transcription factors, and immediate early genes in the mouse mononuclear phagocyte system, while they co-expressed with cytokines and chemokines indicates disaggregated cells (50). Hydrogen peroxide-induced apoptosis in mesangial cells *via* JNK/c-FOS/c-JUN/AP-1 pathway (51). ATF3, a rapidly induced transcription factor by IR, strongly represses the transcription of inflammatory cytokines, plays essential roles in anti-apoptosis, anti-migration and anti-inflammation (52). EGR-1 is urea-inducible early gene transcription factor in renal inner medullary collecting ducts (53). Biological effects of these genes on CAI are worthy to explore.

Finally, the expression level of 10 DEGs at 30 minutes were found positively corrected with both renal function and histology at 12 months and were validated in 33 additional biopsies to identify more biomarkers. Up-regulated SERPINA3, FTCD, TSPAN7 and CFB were confirmed in both DD and LD at 30 minutes. FTCD, a liver-specific enzyme integrating Golgi complex with vimentin filament cytoskeleton, is linked to autoimmune hepatitis and glutamate formiminotransferase

deficiency (54, 55). FTCD appears to be the molecular "glue" crosslinking vimentin filaments into fibers (56). TSPAN7 plays a role in cell and membrane compartmentalization and regulates the trafficking and function of its partner proteins (57), associated with cancer metastasis-suppressive interactions (58–60). It has been hard to find a direct link between FTCD or TSPAN7 and kidney diseases so far. CFB is involved in the complement alternative pathway and atypical hemolytic uremic syndrome (aHUS) (61). Recurrence risk and kidney allograft outcome in recipients with aHUS were associated with thrombotic microangiopathy and *de novo* CFB mutation (62, 63). CBF was highly expressed in DD at 30 minutes and fell at 3 months, but increased in LD, implying that CBF, similar to SERPINA3, might be adjusted at different stages to limit damage and encourage remodeling.

Nevertheless, there are certain limitations in this study. A small size of 24 biopsies were used for microarray analysis, but DEGs were revealed between DD and LD at as early as 30 minutes after implantation (a precious therapeutic window), and some of these DEGs were persistent at 3 month. In addition, selected DEGs were also further validated by qPCR in the 24 microarray analyzed samples and additional 33 time point unpaired renal biopsies, and were correlated with renal function and renal fibrosis at extended time points up to 24 months. CASP1 and CASP3, intensively investigated in our previous studies, were not on the list of DEGs, but their importance in transplant-related injuries cannot be excluded as $FC > 1.5$ and $P < 0.05$ were selected.

The preliminary data from this study need to be cross-validated in large clinic cohorts with long-term follow-up, or in subgroups with/without DGF and/or rejection. There was no clinical difference in terms of DGF and rejection between LD and DD, but DEGs such as PTPN6, CNNM3, CSTF3, CHURC1 and UCRC were revealed in four patients with a rejection compared to without rejection. To validate these DEGs as biomarkers, analyzing samples collected from a large cohort of patients who received either LD or DD kidneys and showed clear allograft dysfunction, rejection or loss would be ideal dataset to explore associations between DEGs measured before 3 months post-transplantation and adverse outcomes or long-term survival. It has been reported that other DEGs detected by microarray such as HuMig and MIP-3β were abundant in patients with acute rejection (64), CD20 was associated with B cell infiltration and acute rejection (9), and KRT15 and HOXB7 at 6 months were linked to chronic rejection at 12 months (**Supplemental Table 3**) (65).

The microarray analysis used cDNA synthesized based on total RNA extracted from kidney homogenates might average DEGs in different cells/cell types due to their heterogeneity in kidneys (66). Laser captured microdissection and single cell sequence may be solutions. The relations between DEGs, upstream regulating miRNAs, corresponding proteins and downstream biological events were difficult to fully dissect. Current translational human studies require concurrent genomic, proteomic and metabolomic analysis in small tissues (67). The real time central molecular assessment of kidney transplant biopsies based on Molecular Microscope Diagnostic System classifier algorithms offers a useful new dimension in biopsy interpretation (68), although mining DEGs in bioinformatics data and transferring to clinical applications are still challenging.

Moreover, a great potential of gene therapy using RNAi has been demonstrated in translational medicine. Registered clinical trials of siRNAs (www.ClinicalTrials.gov) rapidly increased, only I5NP targeting p53 has been validated in kidney injury. siRNA target caspase-3 was renoprotective in our previous studies used a serial of biological models including TECs and mouse IR kidneys (69, 70). In particular, local and systemic administrating serum stabilized caspase-3 siRNA effectively silenced caspase-3, favorably changed serum cytokines, reduced apoptosis and inflammation, and protected cold static or normothermic machine preserved and auto-transplant porcine kidneys (71, 72). Therefore, siRNA therapy is promising in preservation/resuscitation donors and reducing declined rate of DD (73), and in implantation and post-transplantation to effectively prolong allograft survival.

In conclusion, the transcriptional profile of allograft biopsies is different between 30 minutes and 3 months, with more DEGs between DD and LD at 30 minutes reflected donor injury and recipient innate immunity. Consistent DEGs at 3 months mainly represented adaptive immunity, remodeling or fibrosis. Some DEGs such as SERPINA3, SLPI, CBF, FTCD, TSPAN7, VCAN, TIMP1 and FOS might be novel biomarkers for not only timely diagnosis, but also facilitating precise genetic intervention in donor preservation, implantation and the early stage of post-transplantation, monitoring CAI progression and therapeutic responses, and effectively improving the donor quality and allograft survival of DD.

DATA AVAILABILITY STATEMENT

The datasets presented in this study can be found in an online repository of Gene Expression Omnibus (GEO): https://www.ncbi.nlm.nih.gov/geo, and the accession number of the GEO: GSE178689.

ETHICS STATEMENT

The studies involving human participants were reviewed and approved by the Ethics Committee, the University Hospitals of Leicester (EDGE34225/UHL10587). The patients/participants provided their written informed consent to participate in this study.

AUTHOR CONTRIBUTIONS

BY, NS, and MN conceived and designed the study. BY, NS, CY, ZD, JL, and CC acquired, analyzed, and interpreted the data. BY and NS wrote the paper. BY approved the final submission of the

manuscript. All authors contributed to the article and approved the submitted version.

FUNDING

This study was supported the UK-China Fellowship for Excellence, Department for Business Innovation and Skills (2010/2011) and the National Nature Science Foundation of China (81170689, 81570677 and 81873622).

ACKNOWLEDGMENTS

This study was supported by the Research and Innovation, University Hospitals of Leicester NHS Trust, UK.

REFERENCES

1. Ibrahim M, Vece G, Mehew J, Johnson R, Forsythe J, Klassen D, et al. An International Comparison of Deceased Donor Kidney Utilization: What can the United States and the United Kingdom Learn From Each Other? *Am J Transplant* (2020) 20:1309–22. doi: 10.1111/ajt.15719
2. Cecka JM. The UNOS Renal Transplant Registry. *Clin Transplants* (2002), 1–20.
3. Akalin E, O'Connell PJ. Genomics of Chronic Allograft Injury. *Kidney Int Suppl* (2010) 119:S33–7. doi: 10.1038/ki.2010.420
4. Kezic A, Stajic N, Thaiss F. Innate Immune Response in Kidney Ischemia/Reperfusion Injury: Potential Target for Therapy. *J Immunol Res* (2017) 2017:6305439. doi: 10.1155/2017/6305439
5. Yilmaz S, Isik I, Afrouzian M, Monroy M, Sar A, Benediktsson H, et al. Evaluating the Accuracy of Functional Biomarkers for Detecting Histological Changes in Chronic Allograft Nephropathy. *Transplant Int: Off J Eur Soc Organ Transplant* (2007) 20:608–15. doi: 10.1111/j.1432-2277.2007.00494.x
6. Muhlberger I, Perco P, Fechete R, Mayer B, Oberbauer R. Biomarkers in Renal Transplantation Ischemia Reperfusion Injury. *Transplantation* (2009) 88: S14–9. doi: 10.1097/TP.0b013e3181af65b5
7. Vitalone MJ, O'Connell PJ, Wavamunno M, Fung CL, Chapman JR, Nankivell BJ. Transcriptome Changes of Chronic Tubulointerstitial Damage in Early Kidney Transplantation. *Transplantation* (2010) 89:537–47. doi: 10.1097/TP.0b013e3181ca7389
8. Guerrieri D, Re L, Petroni J, Ambrosi N, Pilotti RE, Chuluyan HE, et al. Gene Expression Profile in Delay Graft Function: Inflammatory Markers are Associated With Recipient and Donor Risk Factors. *Mediators Inflamm* (2014) 2014:167361. doi: 10.1155/2014/167361
9. Sarwal M, Chua MS, Kambham N, Hsieh SC, Satterwhite T, Masek M, et al. Molecular Heterogeneity in Acute Renal Allograft Rejection Identified by DNA Microarray Profiling. *N Engl J Med* (2003) 349:125–38. doi: 10.1056/NEJMoa035588
10. Vitalone MJ, Ganguly B, Hsieh S, Latek R, Kulbokas EJ, Townsend R, et al. Transcriptional Profiling of Belatacept and Calcineurin Inhibitor Therapy in Renal Allograft Recipients. *Am J Transplant* (2014) 14:1912–21. doi: 10.1111/ajt.12746
11. Grigoryev DN, Cheranova DI, Heruth DP, Huang P, Zhang LQ, Rabb H, et al. Meta-Analysis of Molecular Response of Kidney to Ischemia Reperfusion Injury for the Identification of New Candidate Genes. *BMC Nephrol* (2013) 14:231. doi: 10.1186/1471-2369-14-231
12. Damman J, Bloks VW, Daha MR, van der Most PJ, Sanjabi B, van der Vlies P, et al. Hypoxia and Complement-and-Coagulation Pathways in the Deceased Organ Donor as the Major Target for Intervention to Improve Renal Allograft Outcome. *Transplantation* (2015) 99:1293–300. doi: 10.1097/TP.0000000000000500
13. O'Connell PJ, Zhang W, Menon MC, Yi Z, Schroppel B, Gallon L, et al. Biopsy Transcriptome Expression Profiling to Identify Kidney Transplants at Risk of Chronic Injury: A Multicentre, Prospective Study. *Lancet* (2016) 388:983–93. doi: 10.1016/S0140-6736(16)30826-1
14. Famulski KS, Reeve J, de Freitas DG, Kreepala C, Chang J, Halloran PF. Kidney Transplants With Progressing Chronic Diseases Express High Levels of Acute Kidney Injury Transcripts. *Am J Transplant* (2013) 13:634–44. doi: 10.1111/ajt.12080
15. Fleige S, Pfaffl MW. RNA Integrity and the Effect on the Real-Time qRT-PCR Performance. *Mol Aspects Med* (2006) 27:126–39. doi: 10.1016/j.mam.2005.12.003
16. Mutch DM, Berger A, Mansourian R, Rytz A, Roberts MA. The Limit Fold Change Model: A Practical Approach for Selecting Differentially Expressed Genes From Microarray Data. *BMC Bioinf* (2002) 3:17. doi: 10.1186/1471-2105-3-17
17. Duncan WC, Shaw JL, Burgess S, McDonald SE, Critchley HO, Horne AW. Ectopic Pregnancy as a Model to Identify Endometrial Genes and Signaling Pathways Important in Decidualization and Regulated by Local Trophoblast. *PloS One* (2011) 6:e23595. doi: 10.1371/journal.pone.0023595
18. Summers DM, Johnson RJ, Allen J, Fuggle SV, Collett D, Watson CJ, et al. Analysis of Factors That Affect Outcome After Transplantation of Kidneys Donated After Cardiac Death in the UK: A Cohort Study. *Lancet* (2010) 376:1303–11. doi: 10.1016/S0140-6736(10)60827-6
19. Waller JR, Murphy GJ, Bicknell GR, Toomey D, Nicholson ML. Effects of the Combination of Rapamycin With Tacrolimus or Cyclosporin on Experimental Intimal Hyperplasia. *Br J Surg* (2002) 89:1390–5. doi: 10.1046/j.1365-2168.2002.02271.x
20. Grimm PC, Nickerson P, Gough J, McKenna R, Stern E, Jeffery J, et al. Computerized Image Analysis of Sirius Red-Stained Renal Allograft Biopsies as a Surrogate Marker to Predict Long-Term Allograft Function. *J Am Soc Nephrol* (2003) 14:1662–8. doi: 10.1097/01.asn.0000066143.02832.5e
21. Saunders RN, Bicknell GR, Nicholson ML. The Impact of Cyclosporine Dose Reduction With or Without the Addition of Rapamycin on Functional, Molecular, and Histological Markers of Chronic Allograft Nephropathy. *Transplantation* (2003) 75:772–80. doi: 10.1097/00007890-200303270-00008
22. Fang H, Harris SC, Su Z, Chen M, Qian F, Shi L, et al. Arraytrack: An FDA and Public Genomic Tool. *Methods Mol Biol* (2017) 1613:333–53. doi: 10.1007/978-1-4939-7027-8_13
23. Zhao Z, Yang C, Wang L, Li L, Zhao T, Hu L, et al. The Regulatory T Cell Effector Soluble Fibrinogen-Like Protein 2 Induces Tubular Epithelial Cell Apoptosis in Renal Transplantation. *Exp Biol Med (Maywood)* (2014) 239:193–201. doi: 10.1177/1535370213514921
24. Oberbauer R, Rohrmoser M, Regele H, Muhlbacher F, Mayer G. Apoptosis of Tubular Epithelial Cells in Donor Kidney Biopsies Predicts Early Renal Allograft Function. *J Am Soc Nephrol* (1999) 10:2006–13. doi: 10.1681/ASN.V1092006
25. Zhao Z, Yang C, Li L, Zhao T, Wang L, Rong R, et al. Increased Peripheral and Local Soluble FGL2 in the Recovery of Renal Ischemia Reperfusion Injury in a Porcine Kidney Auto-Transplantation Model. *J Trans Med* (2014) 12:53. doi: 10.1186/1479-5876-12-53
26. Ajay AK, Saikumar J, Bijol V, Vaidya VS. Heterozygosity for Fibrinogen Results in Efficient Resolution of Kidney Ischemia Reperfusion Injury. *PloS One* (2012) 7:e45628. doi: 10.1371/journal.pone.0045628

SUPPLEMENTARY MATERIAL

The Supplementary Material for this article can be found online at: https://www.frontiersin.org/articles/10.3389/fimmu.2021.657860/full#supplementary-material

Supplementary Table 1 | Details of 20 selected DEGs ($P < 0.05$, $FC > 1.5$) relevant to kidney diseases. FC, fold change. Grey color highlighted DEGs either commonly expressed in two time points or correlated with both SCr and SR staining.

Supplementary Table 2 | 25 DEGs (No.1-25) between DD & LD in common at 30 min and 3 months, and 10 DEGs (No.2, 3, 19 and 26-32) at 30 minutes correlated with both SCr and SR staining for further qPCR detection to identify biomarkers. SCr, serum creatinine; SR, Sirius red staining.

Supplementary Table 3 | DEGs revealed by microarray analysis and associated with kidney injury or allograft rejection from this study and previous publications. There were some commonly DEGs (underline) between studies.

27. Hernandez-Saavedra D, Zhou H, McCord JM. Anti-Inflammatory Properties of a Chimeric Recombinant Superoxide Dismutase: SOD2/3. *BioMed Pharmacother* (2005) 59:204–8. doi: 10.1016/j.biopha.2005.03.001
28. Lim JH, Kim EN, Kim MY, Chung S, Shin SJ, Kim HW, et al. Age-Associated Molecular Changes in the Kidney in Aged Mice. *Oxid Med Cell Longev* (2012) 2012:171383. doi: 10.1155/2012/171383
29. Chang J, Ma JZ, Zeng Q, Cechova S, Gantz A, Nievergelt C, et al. Loss of GSTM1, A NRF2 Target, Is Associated With Accelerated Progression of Hypertensive Kidney Disease in the African American Study of Kidney Disease (Aask). *Am J Physiol Renal Physiol* (2013) 304:F348–55. doi: 10.1152/ajprenal.00568.2012
30. Singh R, Manchanda PK, Kesarwani P, Srivastava A, Mittal RD. Influence of Genetic Polymorphisms in GSTM1, Gstm3, GSTT1 and GSTP1 on Allograft Outcome in Renal Transplant Recipients. *Clin Transplant* (2009) 23:490–8. doi: 10.1111/j.1399-0012.2009.00985.x
31. Chang HR, Tsai JP, Yang SF, Lin CK, Lian JD. Glutathione S-transferase M1 Gene Polymorphism Is Associated With Susceptibility to Impaired Long-Term Allograft Outcomes in Renal Transplant Recipients. *World J Surg* (2013) 37:466–72. doi: 10.1007/s00268-012-1815-6
32. Lannan EA, Galliher-Beckley AJ, Scoltock AB, Cidlowski JA. Proinflammatory Actions of Glucocorticoids: Glucocorticoids and TNFalpha Coregulate Gene Expression *In Vitro* and *In Vivo*. *Endocrinology* (2012) 153:3701–12. doi: 10.1210/en.2012-1020
33. Asakura M, Kitakaze M. Global Gene Expression Profiling in the Failing Myocardium. *Circ J* (2009) 73:1568–76. doi: 10.1253/circj.cj-09-0465
34. Takahashi E, Okumura A, Unoki-Kubota H, Hirano H, Kasuga M, Kaburagi Y. Differential Proteome Analysis of Serum Proteins Associated With the Development of Type 2 Diabetes Mellitus in the KK-A(y) Mouse Model Using the iTRAQ Technique. *J Proteomics* (2013) 84:40–51. doi: 10.1016/j.jprot.2013.03.014
35. Turnier JL, Brunner HI, Bennett M, Aleed A, Gulati G, Haffey WD, et al. Discovery of SERPINA3 as a Candidate Urinary Biomarker of Lupus Nephritis Activity. *Rheumatol (Oxf)* (2019) 58:321–30. doi: 10.1093/rheumatology/key301
36. Sanchez-Navarro A, Mejia-Vilet JM, Perez-Villalva R, Carrillo-Perez DL, Marquina-Castillo B, Gamba G, et al. SerpinA3 in the Early Recognition of Acute Kidney Injury to Chronic Kidney Disease (CKD) Transition in the Rat and its Potentiality in the Recognition of Patients With CKD. *Sci Rep* (2019) 9:10350. doi: 10.1038/s41598-019-46601-1
37. Sano C, Shimizu T, Sato K, Kawauchi H, Tomioka H. Effects of Secretory Leucocyte Protease Inhibitor on the Production of the Anti-Inflammatory Cytokines, IL-10 and Transforming Growth Factor-Beta (TGF-Beta), by Lipopolysaccharide-Stimulated Macrophages. *Clin Exp Immunol* (2000) 121:77–85. doi: 10.1046/j.1365-2249.2000.01269.x
38. Maruyama M, Hay JG, Yoshimura K, Chu CS, Crystal RG. Modulation of Secretory Leukoprotease Inhibitor Gene Expression in Human Bronchial Epithelial Cells by Phorbol Ester. *J Clin Invest* (1994) 94:368–75. doi: 10.1172/JCI117331
39. Bergenfeldt M, Bjork P, Ohlsson K. The Elimination of Secretory Leukocyte Protease Inhibitor (SLPI) After Intravenous Injection in Dog and Man. *Scand J Clin Lab Invest* (1990) 50:729–37. doi: 10.1080/00365519009091066
40. Ohlsson S, Ljungkrantz I, Ohlsson K, Segelmark M, Wieslander J. Novel Distribution of the Secretory Leucocyte Proteinase Inhibitor in Kidney. *Mediators Inflamm* (2001) 10:347–50. doi: 10.1080/09629350120102389
41. Wilflingseder J, Sunzenauer J, Toronyi E, Heinzel A, Kainz A, Mayer B, et al. Molecular Pathogenesis of Post-Transplant Acute Kidney Injury: Assessment of Whole-Genome mRNA and miRNA Profiles. *PloS One* (2014) 9:e104164. doi: 10.1371/journal.pone.0104164
42. Averdunk L, Ruckbeil MV, Zarbock A, Martin L, Marx G, Jalaie H, et al. SLPI - A Biomarker of Acute Kidney Injury After Open and Endovascular Thoracoabdominal Aortic Aneurysm (Taaa) Repair. *Sci Rep* (2020) 10:3453. doi: 10.1038/s41598-020-60482-9
43. Averdunk L, Fitzner C, Levkovich T, Leaf DE, Sobotta M, Vieten J, et al. Secretory Leukocyte Protease Inhibitor (Slpi)-A Novel Predictive Biomarker of Acute Kidney Injury After Cardiac Surgery: A Prospective Observational Study. *J Clin Med* (2019) 8:1931. doi: 10.3390/jcm8111931
44. Yan Q, Sui W, Wang B, Zou H, Zou G, Luo H. Expression of MMP-2 and TIMP-1 in Renal Tissue of Patients With Chronic Active Antibody-Mediated Renal Graft Rejection. *Diagn Pathol* (2012) 7:141. doi: 10.1186/1746-1596-7-141
45. Hirt-Minkowski P, Marti HP, Honger G, Grandgirard D, Leib SL, Amico P, et al. Correlation of Serum and Urinary Matrix Metalloproteases/Tissue Inhibitors of Metalloproteases With Subclinical Allograft Fibrosis in Renal Transplantation. *Transpl Immunol* (2014) 30:1–6. doi: 10.1016/j.trim.2013.11.004
46. Zawada AM, Rogacev KS, Muller S, Rotter B, Winter P, Fliser D, et al. Massive Analysis of Cdna Ends (MACE) and miRNA Expression Profiling Identifies Proatherogenic Pathways in Chronic Kidney Disease. *Epigenetics* (2014) 9:161–72. doi: 10.4161/epi.26931
47. Mutoh J, Ohsawa M, Hisa H. Effect of Naloxone on Ischemic Acute Kidney Injury in the Mouse. *Neuropharmacology* (2013) 71:10–8. doi: 10.1016/j.neuropharm.2013.03.001
48. Catar R, Witowski J, Wagner P, Annett Schramm I, Kawka E, Philippe A, et al. The Proto-Oncogene c-Fos Transcriptionally Regulates VEGF Production During Peritoneal Inflammation. *Kidney Int* (2013) 84:1119–28. doi: 10.1038/ki.2013.217
49. Ishida M, Ueki M, Morishita J, Ueno M, Shiozawa S. Maekawa N. T-5224, a Selective Inhibitor of c-Fos/activator Protein-1, Improves Survival by Inhibiting Serum High Mobility Group Box-1 in Lethal Lipopolysaccharide-Induced Acute Kidney Injury Model. *J Intensive Care* (2015) 3:49. doi: 10.1186/s40560-015-0115-2
50. Summers KM, Bush SJ, Hume DA. Network Analysis of Transcriptomic Diversity Amongst Resident Tissue Macrophages and Dendritic Cells in the Mouse Mononuclear Phagocyte System. *PloS Biol* (2020) 18:e3000859. doi: 10.1371/journal.pbio.3000859
51. Kitamura M, Ishikawa Y, Moreno-Manzano V, Xu Q, Konta T, Lucio-Cazana J, et al. Intervention by Retinoic Acid in Oxidative Stress-Induced Apoptosis. *Nephrol Dialysis Transplant: Off Publ Eur Dialysis Transplant Assoc - Eur Renal Assoc* (2002) 17(Suppl 9):84–7. doi: 10.1093/ndt/17.suppl_9.84
52. Lin H, Cheng CF. Activating Transcription Factor 3, an Early Cellular Adaptive Responder in Ischemia/Reperfusion-Induced Injury. *Ci Ji Yi Xue Za Zhi* (2018) 30:61–5. doi: 10.4103/tcmj.tcmj_37_18
53. Cohen DM. Urea-Inducible Egr-1 Transcription in Renal Inner Medullary Collecting Duct (mIMCD3) Cells is Mediated by Extracellular Signal-Regulated Kinase Activation. *Proc Natl Acad Sci USA* (1996) 93:11242–7. doi: 10.1073/pnas.93.20.11242
54. Mao Y, Vyas NK, Vyas MN, Chen DH, Ludtke SJ, Chiu W, et al. Structure of the Bifunctional and Golgi-Associated Formiminotransferase Cyclodeaminase Octamer. *EMBO J* (2004) 23:2963–71. doi: 10.1038/sj.emboj.7600327
55. Hennig D, Scales SJ, Moreau A, Murley LL, De Mey J, Kreis TE. A Formiminotransferase Cyclodeaminase Isoform Is Localized to the Golgi Complex and Can Mediate Interaction of Trans-Golgi Network-Derived Vesicles With Microtubules. *J Biol Chem* (1998) 273:19602–11. doi: 10.1074/jbc.273.31.19602
56. Gao YS, Vrielink A, MacKenzie R, Sztul E. A Novel Type of Regulation of the Vimentin Intermediate Filament Cytoskeleton by a Golgi Protein. *Eur J Cell Biol* (2002) 81:391–401. doi: 10.1078/0171-9335-00260
57. Charrin S, Jouannet S, Boucheix C, Rubinstein E. Tetraspanins at a Glance. *J Cell science* (2014) 127:3641–8. doi: 10.1242/jcs.154906
58. Arcaroli JJ, Touban BM, Tan AC, Varella-Garcia M, Powell RW, Eckhardt SG, et al. Gene Array and Fluorescence *In Situ* Hybridization Biomarkers of Activity of Saracatinib (AZD0530), A Src Inhibitor, in a Preclinical Model of Colorectal Cancer. *Clin Cancer Res* (2010) 16:4165–77. doi: 10.1158/1078-0432.CCR-10-0066
59. Cheong CM, Chow AW, Fitter S, Hewett DR, Martin SK, Williams SA, et al. Tetraspanin 7 (TSPAN7) Expression Is Upregulated in Multiple Myeloma Patients and Inhibits Myeloma Tumour Development *In Vivo*. *Exp Cell Res* (2015) 332:24–38. doi: 10.1016/j.yexcr.2015.01.006
60. Wuttig D, Zastrow S, Fussel S, Toma MI, Meinhardt M, Kalman K, et al. Cd31, EDNRB and TSPAN7 Are Promising Prognostic Markers in Clear-Cell Renal Cell Carcinoma Revealed by Genome-Wide Expression Analyses of Primary Tumors and Metastases. *Int J Cancer* (2012) 131:E693–704. doi: 10.1002/ijc.27419
61. Waters AM, Licht C. aHUS Caused by Complement Dysregulation: New Therapies on the Horizon. *Pediatr Nephrol* (2011) 26:41–57. doi: 10.1007/s00467-010-1556-4
62. Le Quintrec M, Lionet A, Kamar N, Karras A, Barbier S, Buchler M, et al. Complement Mutation-Associated *De Novo* Thrombotic Microangiopathy

Following Kidney Transplantation. *Am J Transplant* (2008) 8:1694–701. doi: 10.1111/j.1600-6143.2008.02297.x
63. Le Quintrec M, Zuber J, Moulin B, Kamar N, Jablonski M, Lionet A, et al. Complement Genes Strongly Predict Recurrence and Graft Outcome in Adult Renal Transplant Recipients With Atypical Hemolytic and Uremic Syndrome. *Am J Transplant* (2013) 13:663–75. doi: 10.1111/ajt.12077
64. Akalin E, Hendrix RC, Polavarapu RG, Pearson TC, Neylan JF, Larsen CP, et al. Gene Expression Analysis in Human Renal Allograft Biopsy Samples Using High-Density Oligoarray Technology. *Transplantation* (2001) 72:948–53. doi: 10.1097/00007890-200109150-00034
65. Scherer A, Krause A, Walker JR, Korn A, Niese D, Raulf F. Early Prognosis of the Development of Renal Chronic Allograft Rejection by Gene Expression Profiling of Human Protocol Biopsies. *Transplantation* (2003) 75:1323–30. doi: 10.1097/01.TP.0000068481.98801.10
66. Yuen PS, Jo SK, Holly MK, Hu X, Star RA. Ischemic and Nephrotoxic Acute Renal Failure are Distinguished by Their Broad Transcriptomic Responses. *Physiol Genomics* (2006) 25:375–86. doi: 10.1152/physiolgenomics.00223.2005
67. Berglund SR, Schwietert CW, Jones AA, Stern RL, Lehmann J, Goldberg Z. Optimized Methodology for Sequential Extraction of RNA and Protein From Small Human Skin Biopsies. *J Invest Dermatol* (2007) 127:349–53. doi: 10.1038/sj.jid.5700557
68. Halloran PF, Reeve J, Akalin E, Aubert O, Bohmig GA, Brennan D, et al. Real Time Central Assessment of Kidney Transplant Indication Biopsies by Microarrays: The INTERCOMEX Study. *Am J Transplant* (2017) 17:2851–62. doi: 10.1111/ajt.14329
69. Yang B, Elias JE, Bloxham M, Nicholson ML. Synthetic Small Interfering RNA Down-Regulates Caspase-3 and Affects Apoptosis, IL-1 Beta, and Viability of Porcine Proximal Tubular Cells. *J Cell Biochem* (2011) 112:1337–47. doi: 10.1002/jcb.23050
70. Wu Y, Chen W, Zhang Y, Liu A, Yang C, Wang H, et al. Potent Therapy and Transcriptional Profile of Combined Erythropoietin-Derived Peptide Cyclic Helix B Surface Peptide and Caspase-3 siRNA Against Kidney Ischemia/Reperfusion Injury in Mice. *J Pharmacol Exp Ther* (2020) 375:92–103. doi: 10.1124/jpet.120.000092
71. Yang B, Hosgood SA, Nicholson ML. Naked Small Interfering RNA of Caspase-3 in Preservation Solution and Autologous Blood Perfusate Protects Isolated Ischemic Porcine Kidneys. *Transplantation* (2011) 91:501–7. doi: 10.1097/TP.0b013e318207949f
72. Yang C, Zhao T, Zhao Z, Jia Y, Li L, Zhang Y, et al. Serum-Stabilized Naked Caspase-3 siRNA Protects Autotransplant Kidneys in a Porcine Model. *Mol Ther* (2014) 22:1817–28. doi: 10.1038/mt.2014.111
73. Zwaini Z, Patel M, Stover C, Dormer J, Nicholson ML, Hosgood SA, et al. Comparative Analysis of Risk Factors in Declined Kidneys From Donation After Brain Death and Circulatory Death. *Medicina (Kaunas)* (2020) 56:313–25. doi: 10.3390/medicina56060317

Conflict of Interest: The authors declare that the research was conducted in the absence of any commercial or financial relationships that could be construed as a potential conflict of interest.

Copyright © 2021 Yang, Sylvius, Luo, Yang, Da, Crotty and Nicholson. This is an open-access article distributed under the terms of the Creative Commons Attribution License (CC BY). The use, distribution or reproduction in other forums is permitted, provided the original author(s) and the copyright owner(s) are credited and that the original publication in this journal is cited, in accordance with accepted academic practice. No use, distribution or reproduction is permitted which does not comply with these terms.

frontiers in Immunology

ORIGINAL RESEARCH
published: 05 July 2021
doi: 10.3389/fimmu.2021.683249

Total Glucosides of Paeony Ameliorate Pristane-Induced Lupus Nephritis by Inducing PD-1 ligands^{+} Macrophages *via* Activating IL-4/STAT6/PD-L2 Signaling

Chun-Ling Liang[1,2†], *Hongliang Jiang*[3†], *Wenxuan Feng*[2†], *Huazhen Liu*[1,2], *Ling Han*[2*], *Yuchao Chen*[1,2], *Qunfang Zhang*[1,2], *Fang Zheng*[1,2], *Chuan-Jian Lu*[1,2,4*] *and Zhenhua Dai*[1,2,4*]

[1] Section of Immunology & Joint Immunology Program, Guangdong Provincial Academy of Chinese Medical Sciences, Guangzhou, China, [2] The Second Affiliated Hospital of Guangzhou University of Chinese Medicine, Guangzhou, China, [3] Gaozhou Hospital of Traditional Chinese Medicine Affiliated to Guangzhou University of Chinese Medicine, Maoming, China, [4] Guangdong Provincial Key Laboratory of Clinical Research on Traditional Chinese Medicine Syndrome, Guangzhou, China

OPEN ACCESS

Edited by:
Bin Yang,
University of Leicester,
United Kingdom

Reviewed by:
Cheng Yang,
Fudan University, China
Yuqun Zeng,
Zhejiang Provincial People's Hospital,
China

***Correspondence:**
Chuan-Jian Lu
lcj@gzucm.edu.cn
Ling Han
linghan36@163.com
Zhenhua Dai
zdai2009@outlook.com

[†]These authors have contributed equally to this work

Specialty section:
This article was submitted to Molecular Innate Immunity, a section of the journal Frontiers in Immunology

Received: 20 March 2021
Accepted: 24 May 2021
Published: 05 July 2021

Citation:
Liang C-L, Jiang H, Feng W, Liu H, Han L, Chen Y, Zhang Q, Zheng F, Lu C-J and Dai Z (2021) Total Glucosides of Paeony Ameliorate Pristane-Induced Lupus Nephritis by Inducing PD-1 ligands^{+} Macrophages via Activating IL-4/STAT6/PD-L2 Signaling. Front. Immunol. 12:683249. doi: 10.3389/fimmu.2021.683249

Macrophages, a major subset of innate immune cells, are main infiltrating cells in the kidney in lupus nephritis. Macrophages with different phenotypes exert diverse or even opposite effects on the development of lupus nephritis. Substantial evidence has shown that macrophage M2 polarization is beneficial to individuals with chronic kidney disease. Further, it has been reported that PD-1 ligands (PD-Ls) contribute to M2 polarization of macrophages and their immunosuppressive effects. Total glucosides of paeony (TGP), originally extracted from Radix Paeoniae Alba, has been approved in China to treat some autoimmune diseases. Here, we investigated the potentially therapeutic effects of TGP on lupus nephritis in a pristane-induced murine model and explored the molecular mechanisms regulating macrophage phenotypes. We found that TGP treatment significantly improved renal function by decreasing the urinary protein and serum creatinine, reducing serum anti-ds-DNA level and ameliorating renal immunopathology. TGP increased the frequency of splenic and peritoneal F4/80^{+}CD11b^{+}CD206^{+} M2-like macrophages with no any significant effect on F4/80^{+}CD11b^{+}CD86^{+} M1-like macrophages. Immunofluorescence double-stainings of the renal tissue showed that TGP treatment increased the frequency of F4/80^{+}Arg1^{+} subset while decreasing the percentage of F4/80^{+}iNOS^{+} subset. Importantly, TGP treatment increased the percentage of both F4/80^{+}CD11b^{+}PD-L1^{+} and F4/80^{+}CD11b^{+}PD-L2^{+} subsets in spleen and peritoneal lavage fluid as well as the kidney. Furthermore, TGP augmented the expressions of CD206, PD-L2 and phosphorylated STAT6 in IL-4-treated Raw264.7 macrophages *in vitro* while its effects on PD-L2 were abolished by pretreatment of the cells with an inhibitor of STAT6, AS1517499. However, TGP treatment did not affect the expressions of STAT1 and PD-L1 in Raw264.7 macrophages treated with LPS/IFN-γ *in vitro*, indicating a possibly indirect effect of TGP on PD-L1 expression on

macrophages *in vivo*. Thus, for the first time, we demonstrated that TGP may be a potent drug to treat lupus nephritis by inducing F4/80$^+$CD11b$^+$CD206$^+$ and F4/80$^+$CD11b$^+$PD-L2$^+$ macrophages through IL-4/STAT6/PD-L2 signaling pathway.

Keywords: lupus nephritis, total glueosides of paeony (TGP), macrophage polarization, PD-1 ligand, PD-L1, PD-L2

INTRODUCTION

Lupus nephritis (LN) is one of the most common complications in patients with systemic lupus erythematosus and represents a leading cause of end-stage renal failure (1). LN is a complex autoimmune and inflammatory disease resulting from sustained imbalance between pro- and anti-inflammatory immune responses. The substantial infiltration of inflammatory cells in the kidney is a morphologic hallmark of human and experimental lupus nephritis. It is generally accepted that macrophages are the main infiltrating immune cells and play a unique role in the immune-based pathogenesis of lupus nephritis. Infiltrating macrophages can alter the renal microenvironment by interacting with other immune cells, renal stromal cells or propria cells, which then determine the outcome of renal diseases (2, 3). Macrophages with different phenotypes exert diverse or even opposite effects on the development of lupus nephritis (4). A number of studies have demonstrated that inhibiting macrophage infiltration or promoting macrophage M2 polarization is beneficial in the context of chronic kidney disease (5–7). M2 macrophage is capable of inducing Tregs, suppressing the activation of T cells, phagocytosing apoptotic cells and inducing anti-inflammatory factors (8). Further, it has been reported that PD-1 ligands (PD-Ls) contribute to the M2 polarization and immunosuppressive effects of macrophages (9–11). In parallel with effects of PD-Ls on macrophages, adoptive transfer of PD-L2$^+$ M2 macrophages delayed the progression of murine experimental autoimmune encephalomyelitis (EAE) (12). In view of the crucial roles for macrophages in the pathogenesis of LN, it is necessary to explore the mechanisms underlying macrophage activation and to seek an efficient therapeutic strategy of treating LN *via* rebalancing macrophage activation.

Total glueosides of paeony (TGPs) are the total glucosides originally extracted from Radix Paeoniae Alba, and TGPs have been approved in China for the treatment of some autoimmune diseases. Indeed, TGP treatment suppressed joint destruction and histological changes in experimental rheumatoid arthritis (13, 14), attenuated skin inflammation in psoriatic patients (15) and animal models (16, 17) and improved renal function in diabetic rats. Mechanistically, TGP treatment suppressed macrophage activation in both gouty arthritis (18) and diabetes in experimental rats (19). In addition, TGP reportedly increased the PD-L1 expression on CD14$^+$ monocytes in PBMCs from patients with primary Sjögren's syndrome (20). Therefore, we hypothesized that TGP could be effective in treating lupus nephritis by inducing PD-Ls$^+$ M2 macrophages.

In the present study, we determined whether TGP treatment would suppress lupus nephritis using a pristane-induced murine model of lupus nephritis. We demonstrated that TGP treatment for eight weeks significantly improved renal injury and function in pristane-induced LN mice by inducing PD-L2$^+$ macrophages through acting on IL4/STAT6/PD-L2 signaling pathway.

MATERIALS AND METHODS

Mice and Reagents

Female wild-type C57BL/6 mice were obtained from Guangdong Medical Laboratory Animal Center (Fushan, Guangdong, China). All mice were housed in a SPF facility, and all animal experiments were approved by the Animal Ethics Committee of Guangdong Provincial Academy of Chinese Medical Sciences. Pristane and lipopolysaccharide (LPS, L2637, from Escherichia coli O55:B5) was purchased from Sigma-Aldrich (St. Louis, MO, USA). Recombinant mouse IL-4 and IFN-γ were purchased from PeproTech (Rocky Hill, NJ).

Total glucosides of paeony (TGP) were bought from Daosifu Bio-Technique Inc (Nanjing, China). STAT6 inhibitor AS1517499 were obtained from MCE (NJ, USA) and dissolved in dimethylsulfoxide (DMSO). Anti-CD45-BV605 (Clone 30-F11), anti-F4/80-APC (Clone BM8), anti-CD11b-V450 (Clone M1/70), anti-CD206-PE-cy7 (Clone MR6F3), anti-CD86-FITC (Clone GL-1) and anti-CD16/CD32 Abs were bought from BD Biosciences (CA, USA). Anti-PD-L1-Percyp-efluor710 (Clone B7-H1) and anti-PD-L2 (Clone B7-DC) monoclonal antibodies were purchased from eBioscience (San Diego, CA), while rabbit iNOS (Clone D6B6S), Arg1 (Clone D4E3M^{TM}), STAT6 (Clone D3H4), p-STAT6 (Clone Tyr641), STAT1 (Clone D1K9Y), p-STAT1 (Clone Tyr701) and PD-L1 Abs (Clone E1J2J^{TM}) were purchased from Cell Signaling Technology (Danvers, MA). Mouse F4/80 (Clone C-7) and PD-L2 (Clone TY25) Abs were from Santa Cruz Biotechnology (Santa Cruz, CA). Mouse anti-ds-DNA Ab ELISA kit was purchased from Wuhan Huamei Biotech Co., Ltd (Wuhan, China). Creatinine sarcosine oxidase creatinine assay kits were from Nanjing Jian Cheng Bioengineering Institute (Nanjing, China).

Animal Treatment

Female C57BL/6 mice (6-8 weeks old) were acclimatized for 2 weeks before experiments and then received a single intraperitoneal injection of 0.5 ml pristane in phosphate-buffered saline (PBS) to induce murine lupus nephritis. About six months (24 weeks) after pristane injection, 24-h urinary protein was measured, and mice with more than 0.4 mg/24 h urinary protein were included in the subsequent experiments. The included mice were randomized into different groups and treated orally without or with TGP (200 mg/kg or 100 mg/kg, prepared with distilled water containing 0.4% CMC-Na) daily for another two months. Serum creatinine (Scr)

levels were measured 24 hours after the last drug treatment. Blood, spleen, peritoneal lavage fluids and kidney were also collected 24 hours after the last drug administration.

Measurement of Renal Function

Proteinuria was measured by collecting 24-h urine every 2 weeks before and during TGP treatment. All mice were prohibited from getting food but allowed for free access to water during the collection of urine samples. The urine samples were centrifuged at 400g for 5 min and tested with Cobas-8000 automatic biochemical analyzer (Roche). Serum creatinine (Scr) and serum anti-dsDNA Ab levels were detected using sarcosine oxidase creatinine assay kits and murine anti-dsDNA standard enzyme-linked immunosorbent assay (ELISA) kits, respectively.

HE Staining of Renal Tissue

Kidneys were fixed in 4% paraformaldehyde for 24h and then embedded in paraffin. Tissues were then cut into 3μm sections for hematoxylin and eosin (H&E) staining. Glomerular pathology and renal interstitial infiltration were examined under light microscope fields.

Flow Cytometric Analysis

Spleens and kidneys were harvested while single-cell suspensions were prepared by passing the tissues through a 70-μm cell strainer. For analysis of peritoneal macrophages, peritoneal lavage fluid was obtained after flushing the peritoneal cavity with 4 ml of cold PBS. Cells were blocked with anti-CD16/CD32 Abs and then stained for surface makers, including anti-CD45-BV605, anti-F4/80-APC, anti-CD11b-V450, anti-CD206-PE-cy7, anti-CD86-FITC, Anti-PD-L1-Percyp-efluor and anti-PD-L2-PE Abs. The populations of $CD206^+$, $CD86^+$, $PD\text{-}L1^+$ and $PD\text{-}L2^+$ cells in spleen/peritoneal $F4/80^+CD11b^+$macrophages or *in vitro* treated Raw264.7 cells were also analyzed. The $CD86^+PD\text{-}L1^+$ and $CD206^+PD\text{-}L2^+$ macrophages in the kidney finally were calculated.

Immunofluorescence

For immunofluorescence stainings of renal macrophages, kidney tissues were embedded in OTC and cut into 3μm-thick sections. Sections then were fixed in precooled acetone for 10 min and blocked with 0.5% BSA containing 0.1% Tween 20 for 1h. For double-stainings of immunofluorescence, tissues were incubated with mixed primary antibodies (mouse F4/80 with rabbit iNOS, or mouse F4/80 with rabbit Arg1) that were diluted with blocking buffer at 4°C overnight. The next day, the slides were incubated with a mixture of fluorescence- labeled goat anti-rabbit and anti-mouse secondary antibodies for 1h. Pictures were acquired using an inverted fluorescence microscope or confocal laser microscopy (400×).

Cell Culture

Raw264.7 cell lines were purchased from Cell Resource Center of Shanghai Institute of Life Sciences, Chinese Academy of Sciences (Shanghai, China). Cells were seeded in 12-well or 24-well plates at a concentration of 2×10^5 or 3×10^5 per well, respectively. 12 hours after incubation, cells were pretreated with IL-4 (20 ng ml−1) or LPS (50 ng·ml−1) plus IFN-γ (20 ng·ml−1) for 12h to generate M1 and M2 macrophages and maintained for another 48h with or without TGP (20 ug/ml, or 40 ug/ml, dissolved in DMSO), and with or without 100nM STAT6 inhibitor, AS1717499, which was dissolved in DMSO. The final concentration of DMSO in all wells was 0.1%. Cells finally were harvested for whole cell lysates or for flow cytometric analysis.

Western Blot

Whole protein was obtained using RAPA buffer and protein concentrations were measured using BCA Kit. Samples were run on 10% SDS-PAGE gels and transferred onto a PVDF membrane. After blocking with 5% milk prepared in TBST buffer, membranes were incubated at 4°C overnight with the primary anti-p-STAT6, anti-p-STAT1, anti-PD-L1 and anti-PD-L2 Abs. The next day, membranes were washed and incubated with HRP-labeled secondary antibody for 1 h at room temperature. For detecting of STAT6 and STAT1 and GAPDH, membranes were stripped and reblotted with anti-STAT6, anti-STAT1 and GAPDH Abs. Signals were revealed by ECL system and analyzed using Image J Program software.

Statistical Analyses

Data were presented as the mean ± SD and comparisons of the means were analyzed by one-way ANOVA using GraphPad Prism 6 (GraphPad Software, La Jolla, CA, USA). A value of $P < 0.05$ was considered statistically significant.

RESULTS

TGP Treatment Improves Renal Function and Pathology in Mice With Pristane-Induced Lupus Nephritis (LN)

It's well known that one-time injection of pristane can induce multiple pathological manifestations resembling human lupus nephritis, including autoantibodies, progressive proteinuria and renal injury. Here, we established a lupus nephritis animal model in C57BL/6 mice *via* intraperitoneal injection of pristane. 24 weeks after injection, almost all mice had an increase in autoantibodies to a high level of around 100 ug/L (data not shown). Almost 80% mice developed mild proteinuria of around 0.45 mg/24h 24 weeks after the injection and progressed to a level of 0.6 mg/24h at the point of 26 weeks with a statistical significance compared with that of normal control mice (**Figure 1A**). However, although mice treated with TGP also showed an increase of proteinuria compared to normal control group. TGP treatment at 200 mg/kg significantly decreased the pristine-induced proteinuria 6 or 8 weeks after TGP treatment (30 and 32 weeks after pristane injection, respectively), while TGP treatment at 100 mg/kg reduced the proteinuria only 8 weeks after TGP treatment (32 weeks after pristane injection) (**Figure 1A**). Meanwhile, TGP treatment for 8 weeks also decreased the serum levels of creatinine (Scr, **Figure 1B**) and anti-dsDNA Ab (**Figure 1C**). Moreover, we performed HE staining of renal tissue and found that mice injected with pristane exhibited obvious interstitial and glomerular cellular

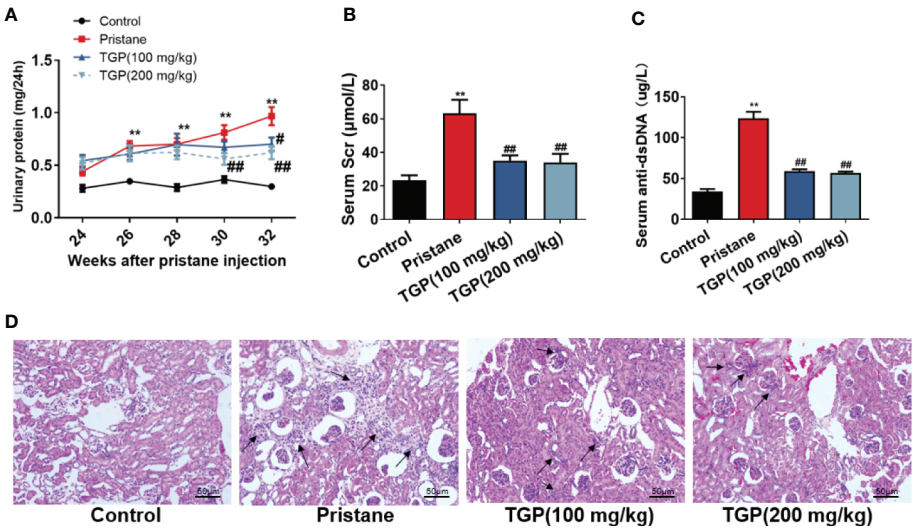


FIGURE 1 | TGP treatment improves renal pathology and function in mice with pristane-induced lupus nephritis. **(A)** 24 weeks after pristane injection, 24-h urinary protein was determined every two weeks and mice with >0.4 mg/24 h urinary protein were also treated with total glucosides of paeony (TGP) in subsequent experiments starting at the same 24-week point. The effects of TGP on kinetics of 24-h urinary protein in pristane-induced lupus mice were observed. In addition, eight weeks after TGP treatment, the serum creatinine (Scr) **(B)** and serum anti-ds-DNA **(C)** were measured using sarcosine oxidase creatinine assay kits and murine anti-dsDNA standard enzyme-linked immunosorbent assay (ELISA) kits, respectively. Data are presented as means ± SD (n=5-6, ** $p < 0.01$ compared with control, and $^{\#\#}p < 0.01$ or $^{\#}p < 0.05$ compared with pristane-treated mice). **(D)** HE staining of the kidney in the pristane-induced lupus mice 8 weeks after TGP treatment (200×, with black arrows pointing to infiltrating immune cells).

infiltration with proliferative glomerular basilar membrane and mesangium (**Figure 1D**). TGP treatment at both 100 mg/kg and 200 mg/kg significantly attenuated the cellular infiltration and improved glomerular injury induced by the pristane.

TGP Promotes Macrophage M2 Polarization in Mice With Pristane-Induced LN

In general, macrophages are divided into the "classically" activated macrophages (M1) and "alternatively" activated macrophages (M2). An important approach to inhibiting the immune responsiveness in autoimmune diseases includes an induction of M2 macrophage polarization. To determine whether TGP affects macrophage polarization in LN mice, M1 and M2 macrophages in spleen and peritoneal lavage fluid were detected *via* FACS analysis. As shown in **Figure 2**, pristane induced a marked decrease in the subset of F4/80$^+$CD11b$^+$CD206$^+$ M2 but not F4/80$^+$CD11b$^+$CD86$^+$ M1 macrophages. While TGP did not alter the frequency of F4/80$^+$CD11b$^+$CD86$^+$ M1 macrophages in spleen and peritoneal lavage fluid of LN mice (**Figures 2A, C, D**), it (either 100 or 200 mg/kg) significantly increased the percentage of F4/80$^+$CD11b$^+$CD206$^+$ cells in both spleen and peritoneal lavage fluid compared to that of pristane alone group (**Figures 2B, E, F**). These data suggest that TGP promotes macrophage M2 polarization.

TGP Upregulates Expression of PD-Ls on Macrophages in Pristane-Induced LN Mice

The role of PD1/PD-L1/PD-L2 pathway in regulating immunological tolerance and immune-mediated tissue damage has been highlighted previously. PD-L1 and PD-L2 are expressed on macrophages, monocytes, endothelial cells and cancer cells, and they influence both macrophage polarization and macrophage function. Here, we asked whether TGP would affect the PD-Ls expression on macrophages. As displayed in **Figure 3**, pristane alone upregulated PD-L1, but not PD-L2, expression on F4/80$^+$CD11b$^+$ macrophages in spleen and peritoneal lavage fluid of LN mice. TGP treatment at high, but not low, doses significantly increased the frequency of F4/80$^+$CD11b$^+$PD-L1$^+$ and F4/80$^+$CD11b$^+$PD-L2$^+$ macrophages in both spleen and peritoneal lavage fluid. These data suggest that an increase in PD-L1/PD-L2 expression on macrophages may contribute to one of the mechanisms responsible for the effects of TGP on lupus nephritis.

TGP Promotes Renal PD-Ls$^+$ Macrophage Infiltration in Pristane-Induced LN Mice

Macrophages are a predominant population of immune cells that infiltrate the kidney during lupus nephritis. Thus, infiltration of macrophages into the kidney was analyzed in pristane-induced LN mice. Immunofluorescence staining showed that there were very few F4/80$^+$ macrophages in normal control mice. In contrast, extensive F4/80$^+$ macrophage infiltration was seen in the tubular and glomeruli of pristane-treated mice, indicating the likely participation of macrophages in the renal pathology of lupus nephritis. TGP treatment did not appear to alter F4/80$^+$ macrophage infiltration compared with the pristane group. However, as shown in **Figure 4**, TGP treatment at doses of 200 mg/kg decreased the F4/80$^+$iNOS$^+$ macrophages (**Figure 4A**),

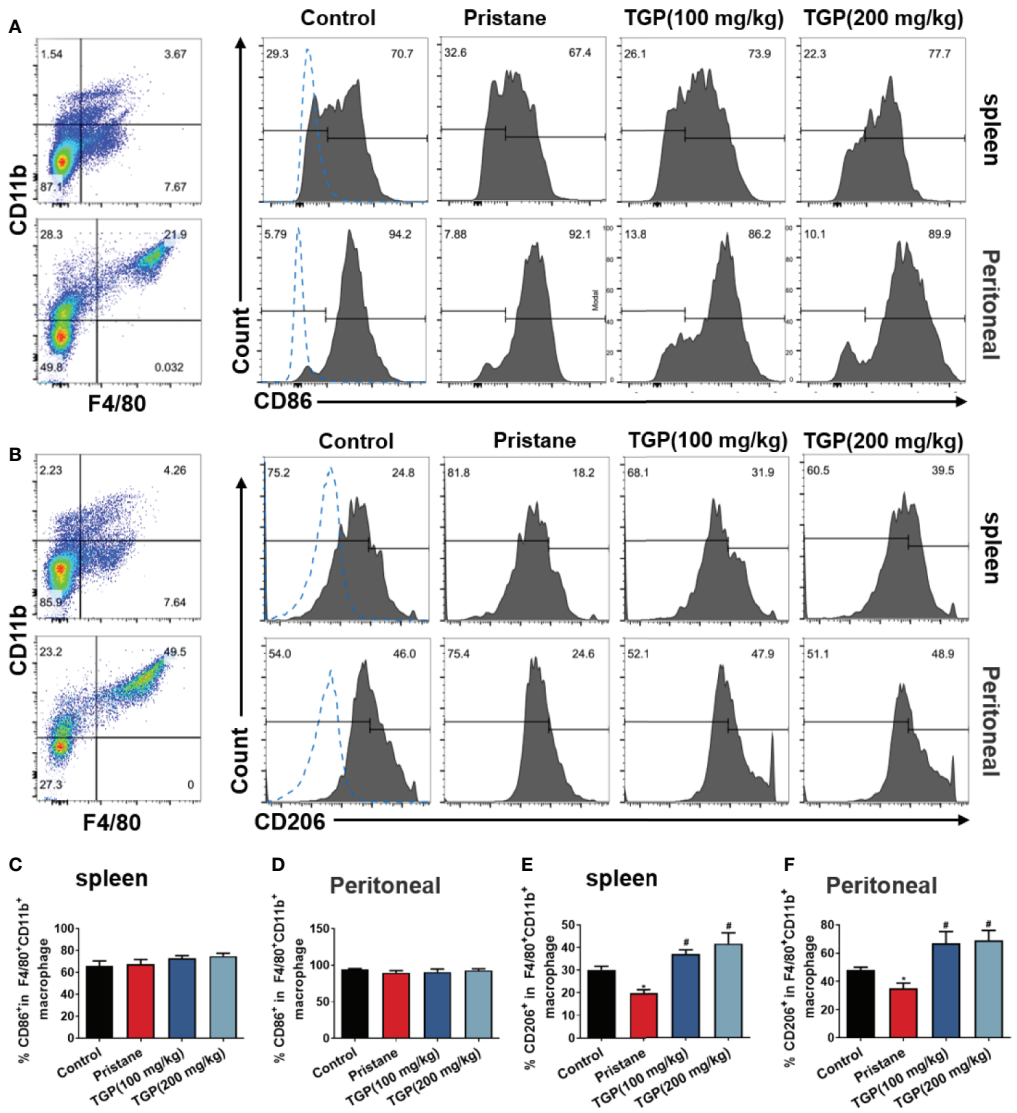


FIGURE 2 | TGP treatment promotes macrophage M2 polarization in pristane-induced lupus mice. Single-cell suspensions from spleens and peritoneal lavage fluids were collected 8 weeks after TGP treatment following pristane injection 24 weeks ago. The effects of TGP on the frequency of $CD86^+$ **(A)** and $CD206^+$ **(B)** subsets in the splenic and peritoneal $F4/80^+CD11b^+$ macrophages were analyzed *via* flow cytometry. **(C, D)** The percentages of $CD86^+$ subset in splenic and peritoneal $F4/80^+CD11b^+$ macrophages are shown as means ± SD. **(E, F)** Shown also are the means ± SD of the percentages of $CD206^+$ subset in splenic and peritoneal $F4/80^+CD11b^+$ macrophages. (n=6, $^*p < 0.05$ compared with control, and $^\#p<0.05$ compared with pristane-treated mice).

but increased $F4/80^+Arg1^+$ macrophage infiltration in the kidney (**Figure 4B**), when compared to the pristane-alone group. Further, the percentages of $CD86^+/CD206^+$ and $PD\text{-}L1^+/PD\text{-}L2^+$ macrophages in the kidney were evaluated by flow cytometry. As shown in **Figures 4C–G**, among the total $F4/80^+CD11b^+$ macrophages, $CD206^+$, $PD\text{-}L1^+$ and $PD\text{-}L2^+$ macrophage subsets were decreased in pristane-treated group, compared with normal control group, while TGP treatment significantly increased the percentages of $CD206^+$, $PD\text{-}L1^+$ and $PD\text{-}L2^+$ macrophages in the kidney compared to pristane-alone group. However, neither pristane nor TGP treatment had a significant effect on the frequency of $CD86^+$ macrophage subset. Therefore, TGP preferentially promoted infiltration of macrophages expressing PD-L1/PD-L2 in the kidney of pristane-treated LN mice.

TGP Enhances M2 Polarization of PD-Ls$^+$ Macrophages *In Vitro*

We then determined the effects of TGP on macrophage polarization *in vitro*. Raw264.7 cells were pretreated with LPS/INF-γ or IL-4 to mimic the *in vivo* polarization. Expression of PD-L1/PD-L2 was determined *via* flow cytometry and represented as mean fluorescence intensity (MFI). As shown in **Figures 5A, B**, at basal state, expression of PD-L2 on Raw264.7 cells was significantly lower than that of PD-L1. Although LPS/

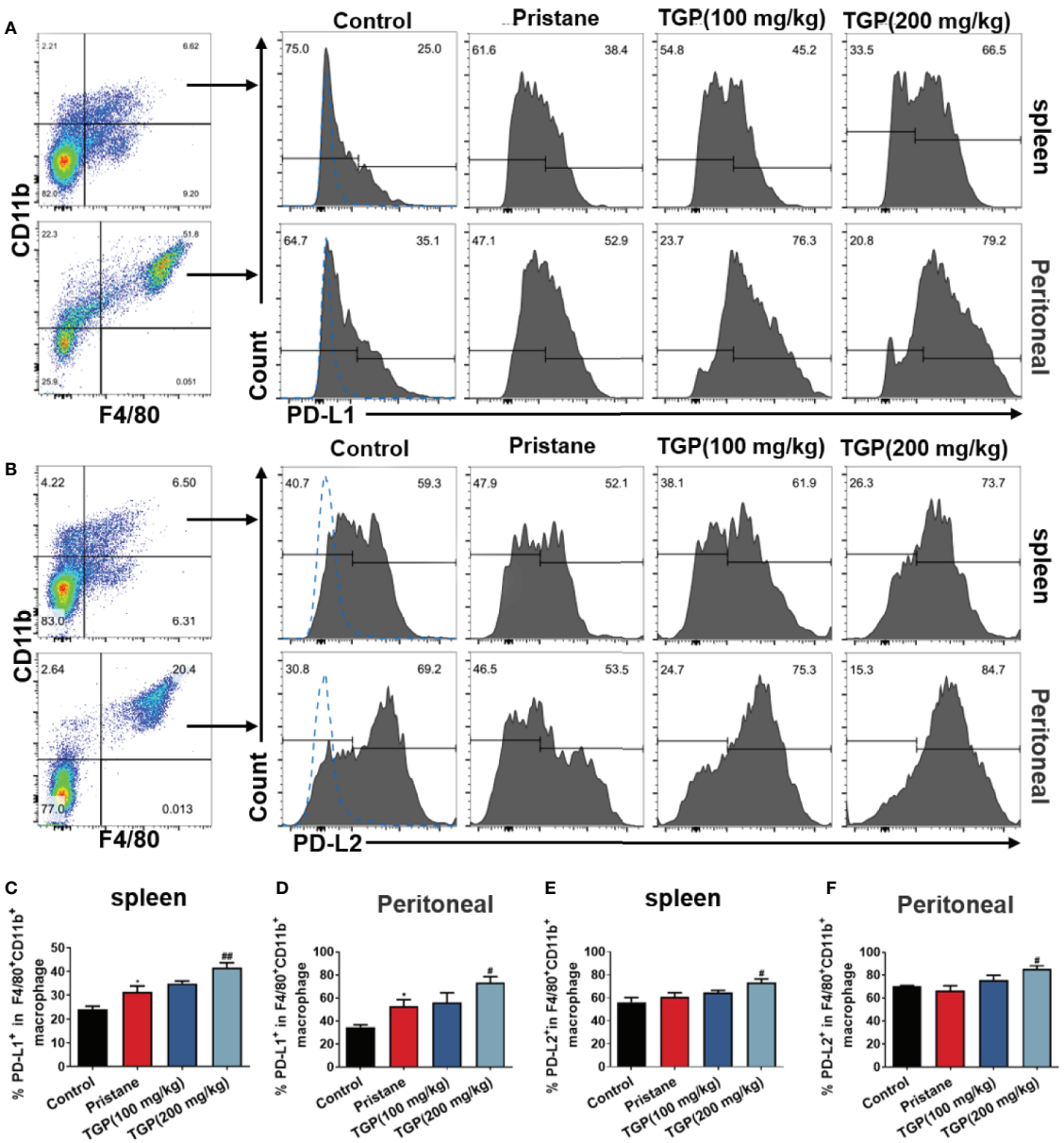


FIGURE 3 | TGP treatment upregulates macrophage expression of PD-Ls in pristane-induced lupus mice. Single-cell suspensions from spleens and peritoneal lavage fluids were collected 8 weeks after TGP treatment following pristane injection 24 weeks ago. The effects of TGP on the frequency of PD-L1$^+$ **(A)** or PD-L2$^+$ **(B)** subsets in splenic and peritoneal F4/80$^+$CD11b$^+$ macrophages were determined *via* FACS. **(C, D)** The percentages of PD-L1$^+$ subset in splenic and peritoneal F4/80$^+$CD11b$^+$ macrophages are shown as means ± SD. **(E, F)** Shown are the means ± SD of the percentages of PD-L2$^+$ subset in splenic and peritoneal F4/80$^+$CD11b$^+$ macrophages. (n=5-6, $^*p < 0.05$ compared with control, and $^{\#\#}p < 0.01$ or $^{\#}p < 0.05$ compared with pristane treated mice).

INF-γ treatment increased expression of CD86 and PD-L1 on macrophages, addition of TGP did not further alter their expression compared to LPS/INF-γ group (**Figures 5C, E, F**). However, macrophages alternatively activated by IL-4 exhibited an increase in PD-L2, while addition of TGP further augmented their expression of both CD206 and PD-L2 compared with IL-4 alone group (**Figures 5D, G, H**). Thus, TGP significantly increases CD206 and PD-L2 expressions in IL-4 treated macrophages but not CD86 and PD-L1 expressions in LPS/INF-γ-treated ones.

TGP Increases PD-L2 Expression on Macrophages *via* Phosphorylating STAT6

It has been reported that STAT6 is involved in IL-4-mediated macrophage M2 polarization and PD-L2 expression, while STAT1 is involved in LPS/IFN-γ mediated macrophage M1

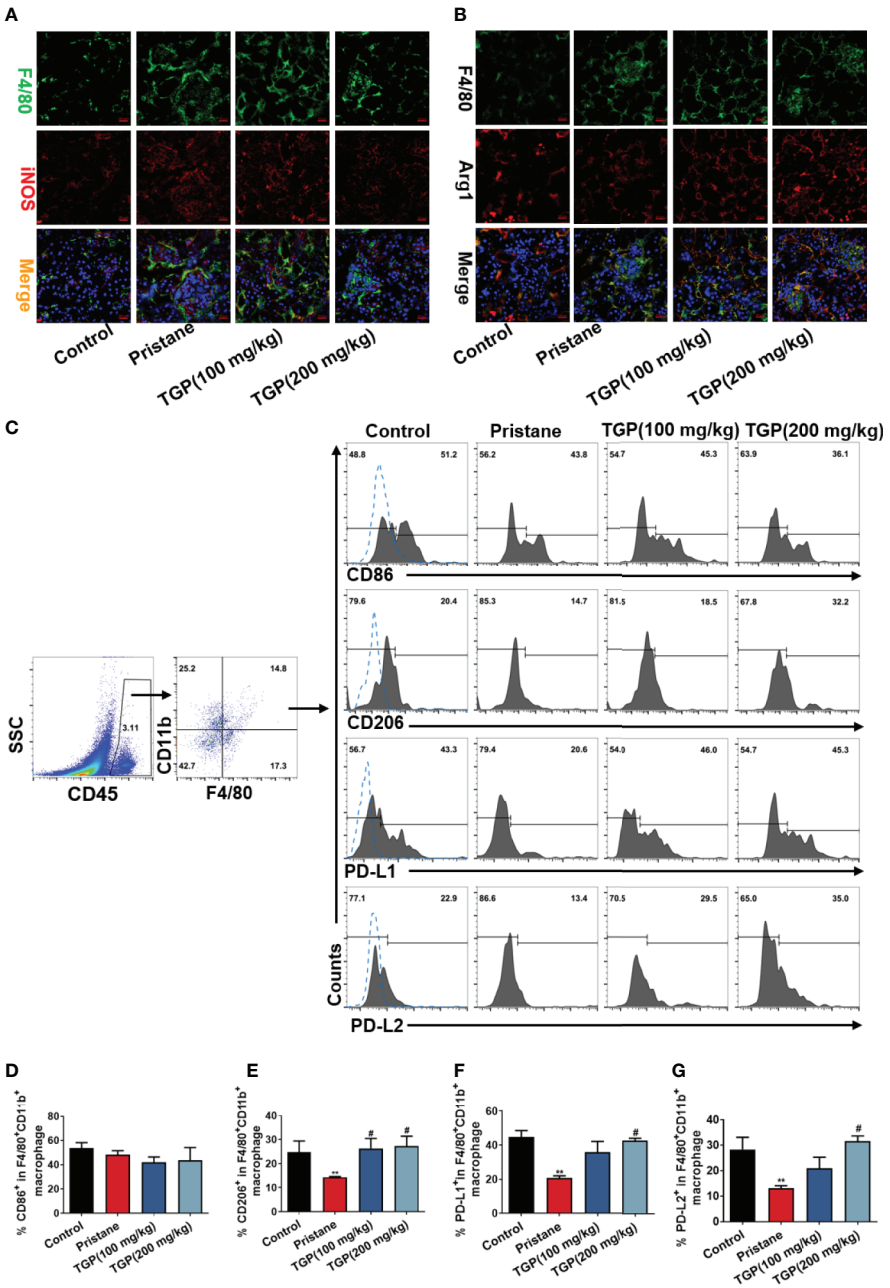


FIGURE 4 | TGP treatment increases renal PD-Ls$^+$ macrophage infiltration in pristane-induced lupus mice. **(A)** Immunofluorescence double-stainings for F4/80 and iNOS or **(B)** for F4/80 and Arg1 in the kidney of pristane-induced LN mice 8 weeks after TGP treatment (400×). **(C)** Kidney infiltrating cells were isolated 8 weeks after TGP treatment following pristane injection 24 weeks ago and the total infiltrating macrophages were gated on CD45$^+$F4/80$^+$CD11b$^+$ population. The percentages of kidney infiltrating CD86$^+$ **(D)**, CD206$^+$ **(E)**, PD-L1$^+$ **(F)** or PD-L2$^+$ **(G)** macrophages were determined *via* flow cytometer, as shown by the bar graphs, in which data are presented as means ± SD (n=5-6, $^{**}p < 0.01$ compared with control, and $^{\#}p < 0.05$ compared with pristane-treated mice).

polarization and PD-L1 expression. Therefore, we adopted an *in vitro* model of macrophage polarization to see how the polarization of macrophages alters PD-Ls expression and whether TGP induces PD-L2 expression on macrophages by activating STAT6 signaling pathway. As shown in **Figure 6**, LPS/IFN-γ induced phosphorylation of STAT1 and upregulated PD-L1 expression. TGP only slightly reduced p-STAT1 and PD-L1 expression but with no statistical significance (**Figure 6A**). IL-4 upregulated both p-STAT6 and PD-L2 expression in macrophages, while TGP treatment further enhanced IL-4-induced phosphorylation of STAT6 and PD-L2 expression compared to IL-4 alone group (**Figure 6B**). More importantly,

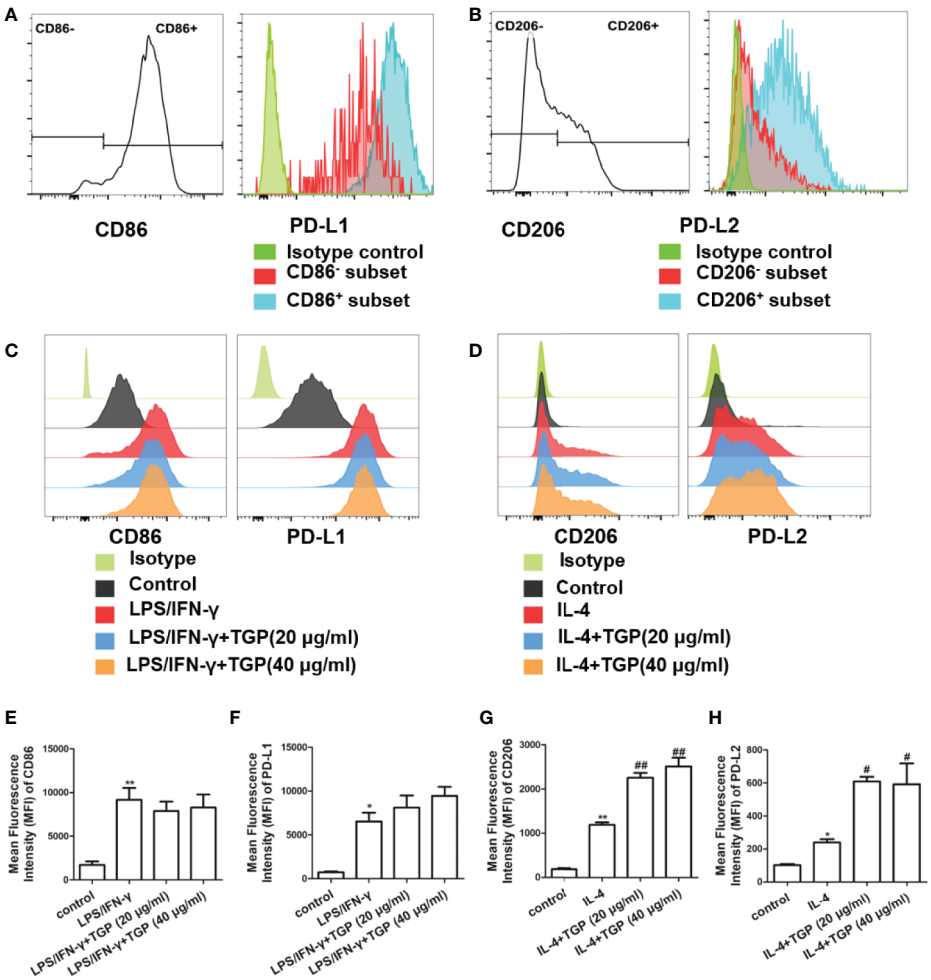


FIGURE 5 | TGP promotes PD-Ls-expressing macrophage polarization *in vitro*. **(A)** Representative FACS plots show the expression of PD-L1 in CD86$^-$ and CD86$^+$ Raw264.7 macrophages stimulated with LPS/IFN-γ. **(B)** Representative FACS plots display the expression of PD-L2 in CD206$^-$ and CD206$^+$ Raw264.7 macrophages stimulated with IL-4. **(C)** The expression of CD86 or PD-L1 in LPS/IFN-γ-treated Raw264.7 cells was determined *via* FACS. **(D)** The expression of CD206 or PD-L2 in IL-4-treated Raw264.7 cells was determined *via* FACS. **(E–H)** Data are shown as the mean percentages of CD86 **(E)** and PD-L1 **(F)** expression in LPS/IFN-γ-treated Raw264.7 cells or CD206 **(G)** and PD-L2 **(H)** expression in IL-4-treated Raw264.7 cells. Data are presented as means ± SD (n=3-4, $^{**}p<0.01$ or $^{*}p < 0.05$ compared with control, and $^{\#\#}p < 0.01$ or $^{\#}p < 0.05$ compared with LPS/IF-γ or IL-4 group without TGP).

the induction of PD-L2 expression by TGP was abolished by a STAT6 inhibitor, AS1517499 (**Figure 6C**), indicating that TGP exerts its effects on macrophage polarization and PD-L2 expression mainly through activating STAT6/PD-L2 signaling pathway.

DISCUSSION

Renal macrophage infiltration represents a prominent feature of inflammation and immunopathology for lupus nephritis. Macrophage phenotypes and functions directly impact the progression and prognosis of lupus nephritis. This present study demonstrated that few PD-L1$^+$ and PD-L2$^+$ macrophages infiltrated in the kidney of mice with pristane-induced lupus nephritis. However, TGP treatment induced both PD-L1$^+$ and PD-L2$^+$ macrophages with less renal infiltration of iNOS$^+$ macrophages, thereby ameliorating lupus nephritis in pristane-treated mice. Furthermore, using an *in vitro* macrophage polarization model, our study revealed that STAT6 signaling contributed to the expression of PD-L2 on macrophages. These results suggest that induction of PD-Ls$^+$ macrophages represents a strategy for treating lupus nephritis or even other autoimmune kidney diseases.

TGP is a group of glycosides extracted from the dried root of *Paeonia lactiflora Pallas*, and it has been approved for marketing in China to treat rheumatoid arthritis. TGP have been widely used in clinic for the treatment of inflammatory diseases and autoimmune diseases, including rheumatoid arthritis, SLE, psoriasis and Sjögren's syndrome (21, 22). Moreover, previous

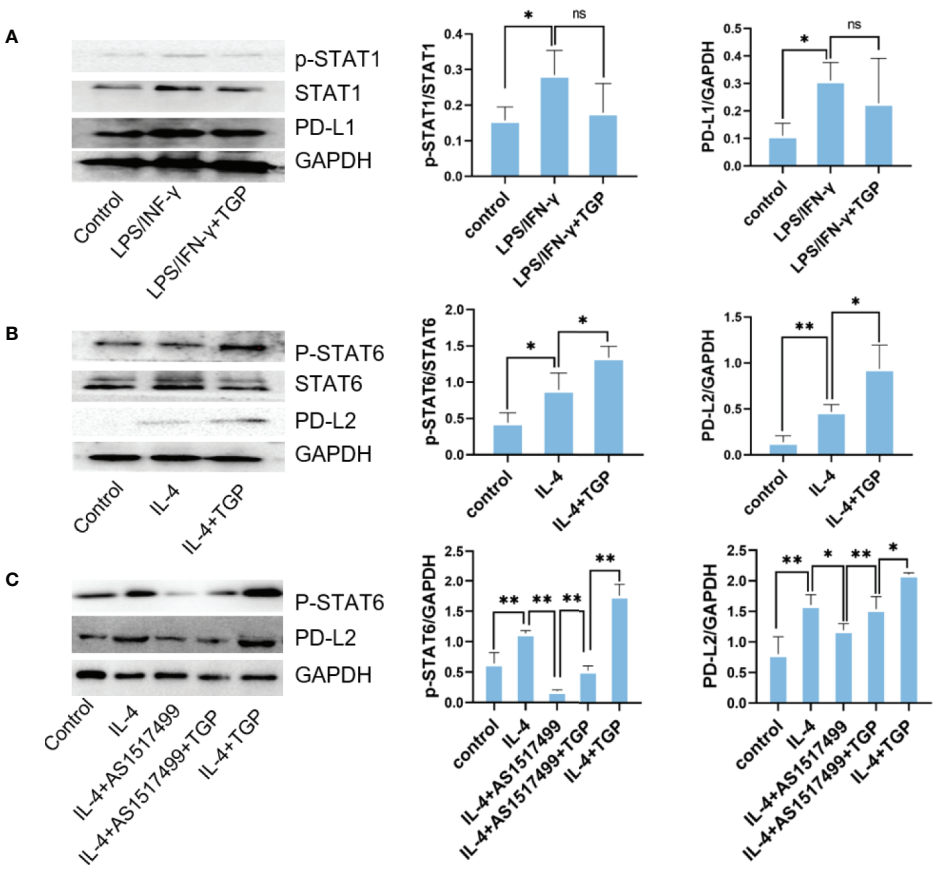


FIGURE 6 | TGP augments PD-L2 expression on macrophages *via* phosphorylating STAT6. **(A)** Raw264.7 cells were pretreated with LPS/IFN-γ for 12 h and treated with TGP for another 48 h, then protein expressions of p-STAT1, STAT1 and PD-L1 were detected *via* western blot analyses. **(B)** Raw264.7 cells were pretreated with IL-4 for 12 h and treated with TGP for another 48 h, the protein expressions of p-STAT6, STAT6 and PD-L2 were then detected *via* western blot analyses. **(C)** To determine if TGP regulates PD-L2 expression *via* STAT6 pathway, Raw264.7 cells were treated with a STAT6 inhibitor, AS1517499, and detected for the expressions of p-STAT6 and PD-L2. Overall, GAPDH was used as internal references. The expressions of p-STAT1, STAT1, PD-L1, p-STAT6, STAT6 and PD-L2 were calculated relatively to GAPDH. Data are presented as means ± SD (n=3, **p<0.01 or *p<0.05, as indicated for direct comparisons, ns, not significant).

studies have shown that TGP treatment attenuates renal inflammation in experimental diabetes (23, 24). In this study, we demonstrated that TGP attenuated proteinuria, decreased serum Scr and anti-dsDNA, and improved renal histology in mice with pristane-induced lupus nephritis. Therefore, TGP treatment could be beneficial to patients with lupus nephritis. Researchers have also shown that TGP was effective in modulating activation of various immune cells, including Treg, Th17, B cells, DCs and macrophages. It was reported that TGP treatment inhibited macrophage proliferation and accumulation in the kidney of diabetic rats (24). In our present study, TGP treatment promoted M2 polarization to $CD206^+PD\text{-}L2^+$ macrophages *via* STAT6 signaling. These results indicate that TGP treatment not only affects the macrophage proliferation, but also alters the polarization of macrophages and their phenotypes.

Macrophages are a main subset of immune cells infiltrating the kidney in lupus nephritis, dominating the renal inflammation and immune responses. Here, using pristane-induced lupus mouse models, we found large infiltrates of $F4/80^+$ macrophages in both renal interstitium and glomeruli, which was consistent with the results from renal histology of patients (25). The functions of macrophages rely on their phenotypes, which are classically defined as M1 and M2 macrophages. Compelling evidence indicates that the M1 macrophage infiltration is strongly correlated with the severity of renal injury in both acute (26) and chronic kidney disease (27, 28). However, M2 macrophages were predominant during the anti-inflammatory or repair process. In the present study, mice treated with pristane exhibited a remarkable decrease in M2 macrophages in the spleen, peritoneal lavage fluid and kidney. In contrast, the M1 macrophage infiltration was increased, but only in the kidney. This discordance between renal tissues and lymphoid organs might be due to the difference in local immune microenvironment and sources of macrophages. TGP treatment for 8 weeks significantly increased the $CD206^+$ frequency in both spleen and peritoneal lavage fluid. In addition, TGP enhanced the kidney infiltration of $F4/80^+Arg1^+$ macrophages and decreased that of $F4/80^+iNOS^+$ macrophages. Our data suggest that TGP

treatment can rebalance the M1/M2 polarization in the kidney of the mice with lupus nephritis.

Besides polarization, the phenotype changes during polarization play an important role in the macrophage function. The programmed death-1 (PD-1) and its ligands (PD-Ls: PD-L1 and PD-L2) are acknowledged as critical immunosuppressive factors in immune responsiveness and autoimmunity (29). Deficiency of PD-Ls is strongly associated with the pathogenesis of many autoimmune diseases, including lupus nephritis, Type 1 diabetes mellitus, RA and so on (29–31). PD-L1 is constitutively and widely expressed on T cells, B cells, macrophages, monocytes, and some nonhemopoietic parenchymal cells. In contrast, PD-L2 expression is limited to activated M2 macrophages and DCs (32). More importantly, at the same ligand concentration, PD-L1 had a delayed interaction with its receptor PD-1 compared with PD-L2 (33). In this study, we demonstrated that PD-L1 was mainly induced by LPS/IFN-γ and expressed on $CD86^+$ macrophages, while PD-L2 was mainly induced by IL-4 and expressed on $CD206^+$ macrophages. Previous studies have shown that the expressions of PD-Ls on monocyte/macrophage contribute to the induction of Tregs and suppression of effector T cells (9, 10). In addition, previous research has also indicated potential associations between PD-Ls expression and polarization, implying that macrophages highly expressing PD-Ls are more prone to M2 polarization (34–36). Taken together, these data suggest that PD-Ls influence both the polarization and immunomodulatory function of macrophages. In this study, we showed that pristane increased PD-L1 expression in splenic and peritoneal macrophages with no effect on PD-L2 expression. However, we found a different expression pattern of PD-Ls in the renal macrophages. Both PD-L1 and PD-L2 expressions in kidney-infiltrating macrophages were actually decreased in pristane-treated mice compared with normal control mice. It was previously reported that in mice with nephrotoxic serum nephritis, PD-L1 and PD-L2 were largely responsible for the protective role of macrophages in attenuating the kidney disease, although an increase in PD-L1 and PD-L2 expressions on renal macrophages was seen (37). We speculate that the differential expression pattern of PD-Ls between nephrotoxic serum nephritis and pristane-induced lupus nephritis may be due to the different timing for establishing models. But, in both models, TGP treatment significantly increased both PD-L1 and PD-L2 expressions in splenic, peritoneal and renal infiltrating macrophages, confirming the actively immunomodulatory roles of PD-Ls on macrophages in inflammatory kidney diseases.

We also studied the effects of TGP on macrophage polarization and the molecular mechanisms underlying its effects on PD-Ls expression. It has been reported the PD-L1 is mainly regulated by Th1 cytokines and STAT1 pathway (38, 39), while PD-L2 is modulated largely by Th2 cytokines and STAT6 pathway (11, 40). In present study, we found that TGP treatment activated the IL-4/STAT6/PD-L2 pathway in M2 macrophages. Unlike its effects on PD-L1 in pristane-induced mice *in vivo*, TGP treatment had no significant effects on STAT1 signaling or PD-L1 expression *in vitro*. The reason for this discrepancy remains to be determined. But it still suggests that TGP does not directly impact STAT1 pathway or PD-L1 expression on M1 macrophages *in vitro*. TGP could alter their PD-L1 expression *in vivo via* indirect effects on other immune cells, which in turn interact with the macrophages.

In conclusion, we demonstrated that TGP treatment not only promoted the macrophage M2 polarization but also increased the PD-L1 and PD-L2 expressions on macrophages, thereby ameliorating the renal inflammation and injury in lupus nephritis. These findings will enhance our understanding of the immunomodulatory effects of TGP on autoimmune diseases. Further in-depth studies on how and why TGP modulates PD-L1 and PD-L2 expressions on the macrophages are warranted, and may help improve the treatment of various autoimmune diseases in the near future.

DATA AVAILABILITY STATEMENT

The original contributions presented in the study are included in the article/supplementary material. Further inquiries can be directed to the corresponding authors.

ETHICS STATEMENT

The animal study was reviewed and approved by The Animal Ethics Committee of Guangdong Provincial Academy of Chinese Medical Sciences.

AUTHOR CONTRIBUTIONS

C-LL performed experiments and wrote the primary draft. HJ, WF, and HL performed some experiments. LH analyzed some data and edited the manuscript. YC, QZ, and FZ analyzed some data. C-JL provided general ideas and crucial reagents. ZD oversaw the study and edited the manuscript. All authors contributed to the article and approved the submitted version.

FUNDING

This work was supported by National Natural Science Foundation of China (81803821), Natural Science Foundation of Guangdong Province (2017A030310127, 2018A030313256, 2018A030310530 and 2019A1515110741), the Specific Research Fund for TCM Science and Technology of Guangdong Provincial Hospital of Chinese Medicine (YN2019MJ03, YN2019QJ07 and YN2019QJ02) and the Specific Fund of State Key Laboratory of Dampness Syndrome of Chinese Medicine (SZ2020ZZ28).

REFERENCES

1. Tektonidou MG, Dasgupta A, Ward MM. Risk of End-Stage Renal Disease in Patients With Lupus Nephritis, 1971-2015: A Systematic Review and Bayesian Meta-Analysis. *Arthritis Rheumatol* (2016) 68(6):1432–41. doi: 10.1002/art.39594
2. Sugiyama M, Kinoshita K, Funauchi M. The Pathogenic Role of Macrophage in Lupus Nephritis. *Nihon Rinsho Meneki Gakkai Kaishi* (2015) 38(3):135–41. doi: 10.2177/jsci.38.135
3. Chalmers SA, Chitu V, Ramanujam M, Putterman C. Therapeutic Targeting of Macrophages in Lupus Nephritis. *Discov Med* (2015) 20(108):43–9.
4. Tang PM, Nikolic-Paterson DJ, Lan HY. Macrophages: Versatile Players in Renal Inflammation and Fibrosis. *Nat Rev Nephrol* (2019) 15(3):144–58. doi: 10.1038/s41581-019-0110-2
5. Zhang X, Zhao Y, Zhu X, Guo Y, Yang Y, Jiang Y, et al. Active Vitamin D Regulates Macrophage M1/M2 Phenotypes Via the STAT-1-TREM-1 Pathway in Diabetic Nephropathy. *J Cell Physiol* (2019) 234(5):6917–26. doi: 10.1002/jcp.27450
6. Bhatia D, Chung KP, Nakahira K, Patino E, Rice MC, Torres LK, et al. Mitophagy-Dependent Macrophage Reprogramming Protects Against Kidney Fibrosis. *JCI Insight* (2019) 4(23):e132826. doi: 10.1172/jci.insight.132826
7. Lu H, Wu L, Liu L, Ruan Q, Zhang X, Hong W, et al. Quercetin Ameliorates Kidney Injury and Fibrosis by Modulating M1/M2 Macrophage Polarization. *Biochem Pharmacol* (2018) 154:203–12. doi: 10.1016/j.bcp.2018.05.007
8. Meng XM, Tang PM, Li J, Lan HY. Macrophage Phenotype in Kidney Injury and Repair. *Kidney Dis (Basel)* (2015) 1(2):138–46. doi: 10.1159/000431214
9. de Freitas ESR, Gálvez RI, Pereira VRA, de Brito MEF, Choy SL, Lotter H, et al. Programmed Cell Death Ligand (PD-L)-1 Contributes to the Regulation of CD4(+) T Effector and Regulatory T Cells in Cutaneous Leishmaniasis. *Front Immunol* (2020) 11:574491. doi: 10.3389/fimmu.2020.574491
10. Shen L, Gao Y, Liu Y, Zhang B, Liu Q, Wu J, et al. PD-1/PD-L Pathway Inhibits M.tb-specific CD4(+) T-Cell Functions and Phagocytosis of Macrophages in Active Tuberculosis. *Sci Rep* (2016) 6:38362. doi: 10.1038/srep38362
11. Huber S, Hoffmann R, Muskens F, Voehringer D. Alternatively Activated Macrophages Inhibit T-Cell Proliferation by Stat6-Dependent Expression of PD-L2. *Blood* (2010) 116(17):3311–20. doi: 10.1182/blood-2010-02-271981
12. Jiang HR, Milovanovic M, Allan D, Niedbala W, Besnard AG, Fukada SY, et al. IL-33 Attenuates EAE by Suppressing IL-17 and IFN-Gamma Production and Inducing Alternatively Activated Macrophages. *Eur J Immunol* (2012) 42(7):1804–14. doi: 10.1002/eji.201141947
13. Zhang L, Yu J, Wang C, Wei W. The Effects of Total Glucosides of Paeony (TGP) and Paeoniflorin (Pae) on Inflammatory-Immune Responses in Rheumatoid Arthritis (RA). *Funct Plant Biol* (2019) 46(2):107–17. doi: 10.1071/fp18080
14. Peng J, Lu X, Xie K, Xu Y, He R, Guo L, et al. Dynamic Alterations in the Gut Microbiota of Collagen-Induced Arthritis Rats Following the Prolonged Administration of Total Glucosides of Paeony. *Front Cell Infect Microbiol* (2019) 9:204. doi: 10.3389/fcimb.2019.00204
15. Yu C, Fan X, Li Z, Liu X, Wang G. Efficacy and Safety of Total Glucosides of Paeony Combined With Acitretin in the Treatment of Moderate-to-Severe Plaque Psoriasis: A Double-Blind, Randomised, Placebo-Controlled Trial. *Eur J Dermatol* (2017) 27(2):150–4. doi: 10.1684/ejd.2016.2946
16. Li B, He S, Liu R, Huang L, Liu G, Wang R, et al. Total Glucosides of Paeony Attenuates Animal Psoriasis Induced Inflammatory Response Through Inhibiting STAT1 and STAT3 Phosphorylation. *J Ethnopharmacol* (2019) 243:112121. doi: 10.1016/j.jep.2019.112121
17. Su J, Zhang P, Zhang JJ, Qi XM, Wu YG, Shen JJ. Effects of Total Glucosides of Paeony on Oxidative Stress in the Kidney From Diabetic Rats. *Phytomedicine* (2010) 17(3-4):254–60. doi: 10.1016/j.phymed.2009.07.005
18. Meng Q, Meng W, Bian H, Zheng F, Gu H, Zuo R, et al. Total Glucosides of Paeony Protects THP-1 Macrophages Against Monosodium Urate-Induced Inflammation Via MALAT1/miR-876-5p/NLRP3 Signaling Cascade in Gouty Arthritis. *BioMed Pharmacother* (2021) 138:111413. doi: 10.1016/j.biopha.2021.111413
19. Chen G, Deng XH, Guo LX, Liu JH. [Effect of Total Glucosides of Paeony on Nuclear Factor-Kappab Activation in Rat Peritoneal Macrophages]. *Zhongguo Zhong Yao Za Zhi* (2008) 33(6):669–71.
20. Chen Y, Wang Y, Xu L, Zhu W, Xu C, Xu M, et al. Influence of Total Glucosides of Paeony on PD-1/PD-L1 Expression in Primary Sjögren's Syndrome. *Int J Rheum Dis* (2019) 22(2):200–6. doi: 10.1111/1756-185x.13391
21. Jiang H, Li J, Wang L, Wang S, Nie X, Chen Y, et al. Total Glucosides of Paeony: A Review of its Phytochemistry, Role in Autoimmune Diseases, and Mechanisms of Action. *J Ethnopharmacol* (2020) 258:112913. doi: 10.1016/j.jep.2020.112913
22. Zhang L, Wei W. Anti-Inflammatory and Immunoregulatory Effects of Paeoniflorin and Total Glucosides of Paeony. *Pharmacol Ther* (2020) 207:107452. doi: 10.1016/j.pharmthera.2019.107452
23. Shao YX, Gong Q, Qi XM, Wang K, Wu YG. Paeoniflorin Ameliorates Macrophage Infiltration and Activation by Inhibiting the TLR4 Signaling Pathway in Diabetic Nephropathy. *Front Pharmacol* (2019) 10:566. doi: 10.3389/fphar.2019.00566
24. Wang K, Wu YG, Su J, Zhang JJ, Zhang P, Qi XM. Total Glucosides of Paeony Regulates JAK2/STAT3 Activation and Macrophage Proliferation in Diabetic Rat Kidneys. *Am J Chin Med* (2012) 40(3):521–36. doi: 10.1142/s0192415x12500401
25. Dias CB, Malafronte P, Lee J, Resende A, Jorge L, Pinheiro CC, et al. Role of Renal Expression of CD68 in the Long-Term Prognosis of Proliferative Lupus Nephritis. *J Nephrol* (2015) 30(2017):87–94. doi: 10.1007/s40620-015-0252-7
26. Liu BC, Tan RZ, Liu J, Zhang YY, Wang HL, Li JC, et al. Curcumin Relieved Cisplatin-Induced Kidney Inflammation Through Inhibiting Mincle-maintained M1 Macrophage Phenotype. *Cell Death Differ* (2019) 52:284–94. doi: 10.1038/s41418-019-0349-y
27. Meshkani R, Vakili S. Tissue Resident Macrophages: Key Players in the Pathogenesis of Type 2 Diabetes and its Complications. *Clin Chim Acta* (2016) 462:77–89. doi: 10.1016/j.cca.2016.08.015
28. Lv LL, Feng Y, Wu M, Wang B, Li ZL, Zhong X, et al. Exosomal miRNA-19b-3p of Tubular Epithelial Cells Promotes M1 Macrophage Activation in Kidney Injury. *Cell Death Differ* (2020) 27(1):210–26. doi: 10.1038/s41418-019-0349-y
29. Zamani MR, Aslani S, Salmaninejad A, Javan MR, Rezaei N. PD-1/PD-L and Autoimmunity: A Growing Relationship. *Cell Immunol* (2016) 310:27–41. doi: 10.1016/j.cellimm.2016.09.009
30. Dai S, Jia R, Zhang X, Fang Q, Huang L. The PD-1/PD-Ls Pathway and Autoimmune Diseases. *Cell Immunol* (2014) 290(1):72–9. doi: 10.1016/j.cellimm.2014.05.006
31. Siwiec A, Majdan M. [The Role of the PD-1 Protein in Pathogenesis of Autoimmune Diseases, With Particular Consideration of Rheumatoid Arthritis and Systemic Lupus Erythematosus]. *Postepy Hig Med Dosw (Online)* (2015) 69:534–42. doi: 10.5604/17322693.1150784
32. Parsa R, Andresen P, Gillett A, Mia S, Zhang XM, Mayans S, et al. Adoptive Transfer of Immunomodulatory M2 Macrophages Prevents Type 1 Diabetes in NOD Mice. *Diabetes* (2012) 61(11):2881–92. doi: 10.2337/db11-1635
33. Ghiotto M, Gauthier L, Serriari N, Pastor S, Truneh A, Nunes JA, et al. PD-L1 and PD-L2 Differ in Their Molecular Mechanisms of Interaction With PD-1. *Int Immunol* (2010) 22(8):651–60. doi: 10.1093/intimm/dxq049
34. Ammons DT, Wheat WH, Dow SW, Zhu Z, Zhang H, Chen B, et al. PD-L1-Mediated Immunosuppression in Glioblastoma is Associated With the Infiltration and M2-Polarization of Tumor-Associated Macrophages. *Cancer Immunol Res* (2020) 11:588552. doi: 10.1158/2326-6066.cir-17-0537
35. Hartley GP, Chow L. Programmed Cell Death Ligand 1 (PD-L1) Signaling Regulates Macrophage Proliferation and Activation. *PloS Biol* (2018) 6(10):1260–73. doi: 10.1371/journal.pbio.3000687
36. Zhang Y, Du W, Chen Z, Xiang C. Upregulation of PD-L1 by SPP1 Mediates Macrophage Polarization and Facilitates Immune Escape in Lung Adenocarcinoma. *Exp Cell Res* (2017) 359(2):449–57. doi: 10.1016/j.yexcr.2017.08.028
37. Menke J, Lucas JA, Zeller GC, Keir ME, Huang XR, Tsuboi N, et al. Programmed Death 1 Ligand (PD-L) 1 and PD-L2 Limit Autoimmune Kidney Disease: Distinct Roles. *J Immunol* (2007) 179(11):7466–77. doi: 10.4049/jimmunol.179.11.7466

38. Moon JW, Kong SK, Kim BS, Kim HJ, Lim H, Noh K, et al. IFNgamma Induces PD-L1 Overexpression by JAK2/STAT1/IRF-1 Signaling in EBV-positive Gastric Carcinoma. *Sci Rep* (2017) 7(1):17810. doi: 10.1038/s41598-017-18132-0
39. Doi T, Ishikawa T, Okayama T, Oka K, Mizushima K, Yasuda T, et al. The JAK/STAT Pathway is Involved in the Upregulation of PD-L1 Expression in Pancreatic Cancer Cell Lines. *Oncol Rep* (2017) 37(3):1545–54. doi: 10.3892/or.2017.5399
40. Loke P, Allison JP. PD-L1 and PD-L2 are Differentially Regulated by Th1 and Th2 Cells. *Proc Natl Acad Sci USA* (2003) 100(9):5336–41. doi: 10.1073/pnas.0931259100

Conflict of Interest: The authors declare that the research was conducted in the absence of any commercial or financial relationships that could be construed as a potential conflict of interest.

Copyright © 2021 Liang, Jiang, Feng, Liu, Han, Chen, Zhang, Zheng, Lu and Dai. This is an open-access article distributed under the terms of the Creative Commons Attribution License (CC BY). The use, distribution or reproduction in other forums is permitted, provided the original author(s) and the copyright owner(s) are credited and that the original publication in this journal is cited, in accordance with accepted academic practice. No use, distribution or reproduction is permitted which does not comply with these terms.

frontiers in Immunology

REVIEW
published: 08 July 2021
doi: 10.3389/fimmu.2021.714340

NLRP3 Inflammasome in Metabolic-Associated Kidney Diseases: An Update

Wei Xiong[1], *Xian-Fang Meng*[2*] *and Chun Zhang*[1*]

[1] Department of Nephrology, Union Hospital, Tongji Medical College, Huazhong University of Science and Technology, Wuhan, China, [2] Department of Neurobiology, School of Basic Medical Sciences, Tongji Medical College, Huazhong University of Science and Technology, Wuhan, China

Metabolic syndrome (MS) is a group of complex metabolic disorders syndrome, which refers to the pathological state of metabolism disorder of protein, fat, carbohydrate and other substances in human body. The kidney is an important organ of metabolism, and various metabolic disorders can lead to the abnormalities in the structure and function of the kidney. The recognition of pathogenesis and treatment measures of renal damage in MS is a very important part for the renal function preserve. Inflammatory response caused by various metabolic factors is a protective mechanism of the body, but persistent inflammation will become a harmful factor and aggravate kidney damage. Inflammasomes are sensors of the innate immune system that play crucial roles in initiating inflammation in response to acute infections and chronic diseases. They are multiprotein complex composed of cytoplasmic sensors (mainly NLR family members), apoptosis-associated speck-like protein (ASC or PYCARD) and pro-caspase-1. After receiving exogenous and endogenous stimuli, the sensors begin to assemble inflammasome and then promote the release of inflammatory cytokines IL-1β and IL-18, resulting in a special way of cell death named pyroptosis. In the kidney, NLRP3 inflammasome can be activated by a variety of pathways, which eventually leads to inflammatory infiltration, renal intrinsic cell damage and renal function decline. This paper reviews the function and specific regulatory mechanism of inflammasome in kidney damage caused by various metabolic disorders, which will provide a new therapeutic perspective and targets for kidney diseases.

Keywords: NLRP3, inflammasome, kidney diseases, metabolic syndrome, innate immunity

OPEN ACCESS

Edited by:
Bin Yang,
University of Leicester,
United Kingdom

Reviewed by:
Xiong Zhong Ruan,
University College London,
United Kingdom
Hui Cai,
Emory University, United States

***Correspondence:**
Chun Zhang
drzhangchun@hust.edu.cn
Xian-Fang Meng
xfmeng@mails.tjmu.edu.cn

Specialty section:
This article was submitted to Molecular Innate Immunity, a section of the journal Frontiers in Immunology

Received: *25 May 2021*
Accepted: *28 June 2021*
Published: *08 July 2021*

Citation:
Xiong W, Meng X-F and Zhang C (2021) NLRP3 Inflammasome in Metabolic-Associated Kidney Diseases: An Update. Front. Immunol. 12:714340. doi: 10.3389/fimmu.2021.714340

INTRODUCTION

Metabolic syndrome (MS) is a group of complex metabolic disorders syndrome, which refers to the pathological state of metabolism disorder of protein, fat, carbohydrate and other substances in human body (1). In the 1990s, the overall prevalence of adult MS in the United States was 22%, and the prevalence increased with age, among which the prevalence rates of 20-29, 60-69 and over 70 years old were 6.7%, 43.5% and 42%, respectively (2). By the 2000's, the prevalence continued to increase to 34.5% (3). The etiology of MS has not been clear, and it is considered to be the result of multi gene and multi environment interaction, which is closely related to genetics and immunity (4).

The disease is affected by many environmental factors, mainly manifested in the high fat, high carbohydrate diet structure, low labor intensity and less exercise (4). MS includes a variety of metabolic disorders, including obesity, hyperglycemia, hypertension, dyslipidemia, high blood viscosity, high uric acid, high fatty liver incidence and hyperinsulinemia (5). At present, it is believed that the common causes of these factors are insulin resistance and hyperinsulinemia caused by obesity, especially central obesity (6). MS is a risk factor for a variety of diseases, such as hypertension, coronary heart disease, stroke, chronic kidney disease (CKD), and even some cancers, including breast cancer, endometrial cancer, prostate cancer related to sex hormone, as well as pancreatic cancer, hepatobiliary cancer, colon cancer in digestive system (6–8).

The kidney is an important organ of metabolism, and various metabolic abnormalities can affect the structure and function of kidney. Among people with MS, the prevalence of CKD exceeds 20%, which is much higher than that of the general population. At the same time, among patients with CKD, the prevalence of MS and subgroup metabolic disorders is much higher than that of non-CKD patients (9). A retrospective analysis of more than 6,000 American adults aged over 20 years found that MS was an independent risk factor for CKD (10). The probability of CKD and microalbuminuria was 2.6 times and 1. 9 times of that of the normal population, and the more abnormal components of MS metabolism, the greater the risk (10). A study of 75,468 Chinese people also supported the above view. The incidence of CKD in MS patients and those without MS was 57% and 28%, respectively (11). The clinical manifestations of MS related renal damage include glomerular hyperfiltration, microalbuminuria, proteinuria, changes in renal tubular function, eGFR < 60ml/(min·1.73m^2), and increase of renal vascular resistance by ultrasonic. Insulin resistance is the central link of MS. Insulin receptors are widely expressed in the kidney, such as podocytes, mesangial cells, endothelial cells and renal tubular epithelial cells (12). Observation of kidney tissue pathology of donor kidneys revealed that chronic pathological changes were more common in kidney tissues of MS patients, manifested as varying degrees of glomerular sclerosis, renal tubular atrophy, renal interstitial fibrosis and arteries hardening (13).

Therefore, exploring the pathogenesis and prevention measures of renal damage in MS is a very important part of the prevention and treatment of CKD. This article summarizes the important role of inflammasome in renal damage caused by different metabolic factors, and provides a new perspective for the treatment of CKD in the future.

GENERAL INTRODUCTION OF NLRP3 INFLAMMASOME

Nod like receptor protein 3 (NLRP3) inflammasome is a macromolecular polyprotein complex with a molecular weight of about 700 kDa, which has the function of regulating chronic inflammatory response. NLRP3 inflammasome consists of nucleotide-binding domain–like receptors (NLRs), apoptosis-associated speck-like protein containing caspase recruitment domain (ASC) and caspase protease. The structure of NLRs mainly includes the middle nucleotide-binding and oligomerization domain (NACHT), the downstream adapter protein pyrindomain (PYD) or caspase recruitment domain (CARD), and leucine-richrepeats (LRRs). Caspase-1 is the activated form of pro-caspase-1, which can cleave cytokine precursors such as interleukin (IL)-1β, IL-18 and other cytokine precursors, transform them into mature form, and participate in the inflammatory reaction (14).

The inflammasome is a complex composed of a variety of proteins in the cytoplasm, which integrates different damage stimulating signals and activates the innate immune defense function (14, 15). The innate immune system recognizes invading microorganisms and danger signals in the body through specific pattern recognition receptors (PRRs). Currently known PRRs are divided into two types, namely toll-like receptors (TLRs) located on the cell membrane and NLRs located in the cytoplasm (16). NLRP3 is the most well-studied and most comprehensive inflammasome in the family of NLRs. After LRRs of NLRP3 recognizes specific signal, it exposes and polymerizes the NACHT domain, and recruits ASC and pro-caspase-1 through PYD-PYD and CARD-CARD. Through the cleavage of pro-caspase-1 to mature caspase-1, cytokine precursors of IL-1β and IL-18 are cleaved into an active form and secreted out of the cell. In addition to promoting the maturation and secretion of IL-1β and IL-18, it can also mediate a special programmed cell death pyroptosis by activating caspase-1, which is characterized by the formation of caspase-1-dependent plasma membrane pore size, a large number of release of inflammatory mediators and DNA damage, and finally leads to osmotic disintegration of cells (17).

Many endogenous and exogenous factors can stimulate the production of NLRP3 inflammasome through different mechanisms. There are clear reports about crystals or particles (cholesterol crystals, asbestos, silica, etc.), bacterial toxins, microorganisms (viruses, bacteria and fungi), and some vaccine adjuvants (18, 19). Given that NLRP3 inflammasome is an intracellular recognition receptor and the diversity of recognition substances, these activators may have a common endogenous signal transduction molecule, however this common endogenous signal transduction molecule is not clear yet (20). At present, there are mainly three different modes to illustrate the activation mechanism of NLRP3 inflammasome. These three modes include potassium channel open and outflow, cathepsin-B secretion caused by lysosomal damage and rupture, and the production of reactive oxygen species (ROS) (21). Various microbial toxins, enzymes and extracellular ATP can activate ATP-P2X7 receptors, make potassium ions outflow, and activate NLRP3 inflammasome (22). Crystalline substances such as silicon dioxide, antibiotics and antifungal drugs activate inflammasome through ROS and cathepsin-B (23, 24).

Renal inflammatory response is the immune response of the kidney to infectious or non-infective activators. The specific

expression of NLRP3 inflammasome components in kidney tissues has not yet been fully clarified. Renal mononuclear phagocytes, such as dendrites and macrophages, can express the components of NLRP3 inflammasome and may induce cell death by activating caspase-1 (25). At the same time, some studies have confirmed that renal tubular epithelial cells and podocytes also activate the NLRP3-ASC-caspase-1 axis, express and release mature IL-1β and IL-18 (26–28). As an intracellular pattern recognition receptor, NLRP3 inflammasome plays an important role in stimulating and regulating immune inflammation. The activation of NLRP3 inflammasome is involved in the acute and chronic inflammation of the kidneys by inducing the secretion of IL-1β and IL-18, leading to the automatic defense and inflammatory response (26, 29). NLRP3 inflammasome also participates in the occurrence and development of a variety of metabolic diseases as an important member (30). Therefore, the in-depth study on the mechanism of NLRP3 inflammasome associated with metabolic disorders and kidney injury will provide new ideas and directions for the treatment of metabolic related kidney diseases. The specific formation and activation of NLRP3 Inflammasome was shown in **Figure 1**.

NLRP3 INFLAMMASOME IN METABOLIC-ASSOCIATED KIDNEY DISEASES

Diabetic Nephropathy

Diabetes mellitus (DM) is a group of metabolic diseases characterized by hyperglycemia. When DM continues to progress, it often causes chronic damage to the eyes, kidneys, blood vessels, and feet. Among them, diabetic nephropathy (DN) is the most harmful inflammatory complication. It is also the main microvascular of DM and the main cause of end-stage renal disease (ESRD). Inflammatory response is the key factor for the sustainable development of DN. The activation of various inflammatory factors, such as C-reactive protein (CRP), monocyte chemoattractant protein-1 (MCP-1) and inflammasomes, promote macrophage infiltration, renal tubular fibrosis, and eventually accelerate glomerulosclerosis (31).

The activation of NLRP3 inflammasome was detected in DN patients and diabetic mice (32). MCC950 was a selective and potent inhibitor of NLRP3 inflammasome, the use of which improved renal function, podocyte injury and renal fibrosis in db/db mice (33). Homozygous and hemizygous caspase-1 deficiency had protective effect on db/db mice, while caspase-3

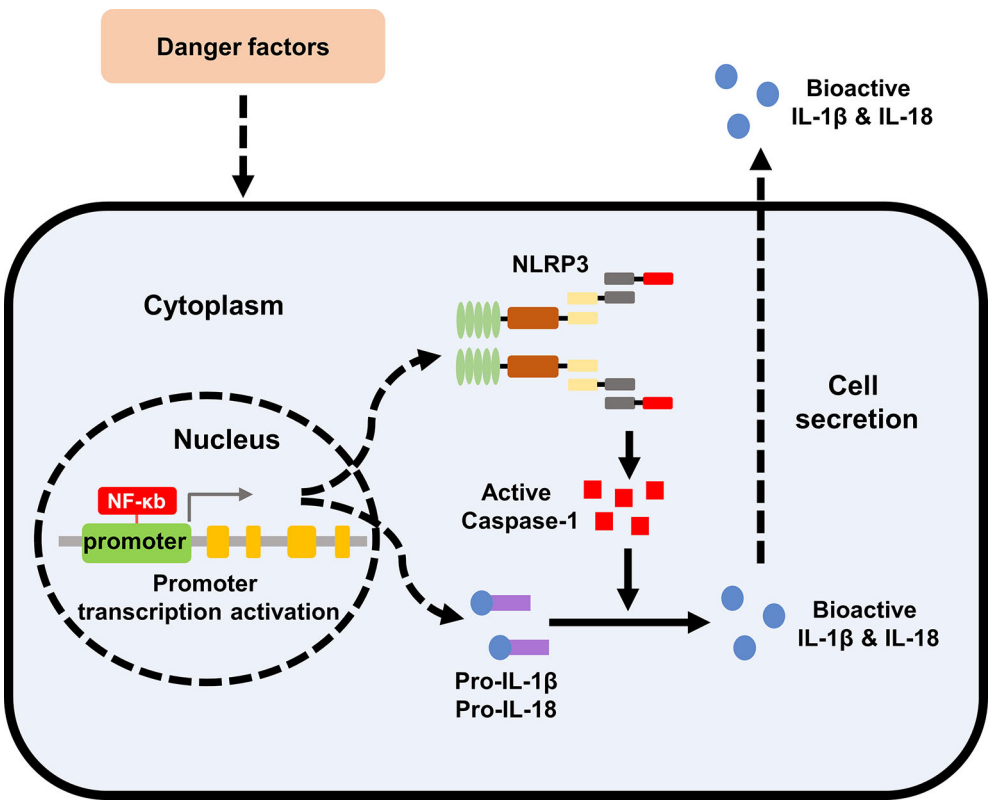


FIGURE 1 | Formation and activation of NLRP3 inflammasome. The effect of extracellular stimulating factors activates the intracellular NF-κB pathway. The activation of NF-κB pathway promotes the expression of inflammasome NLRP3, IL-1β, and IL-18. The activation of the inflammasome NLRP3 promotes the activation of caspase-1, and the activated caspase-1 promotes the maturation of IL-1β and IL-18, which are then secreted into the extracellular to exert biological effects. NLRP3, nod like receptor protein 3; IL, interleukin.

deficiency had not, suggesting that caspase-3-dependent cell death had no significant effect on the formation of DN, while caspase-1-dependent inflammatory activation played an important role (34). Moreover, the use of a novel monoclonal antibody of IL-1β in diabetic mice reduced renal damage markers, ameliorated fibrosis, and preserved the number of podocytes (35). Thioredoxin-interacting protein (TXNIP) was a mediator of oxidative stress and has been reported to interact with NLRP3 inflammasome, leading to its activation (36). The expression of TXNIP and NLRP3 was both significantly increased in diabetic rats (36). Polyphenols, natural antioxidants, have been proved to reduce pyroptosis in DN, probably due to the inhibition of TXNIP/NLRP3 pathway (37). Other drugs with antioxidant function have also been confirmed to improve DN by targeting NLRP3 inflammasome, suggesting that NLRP3 inflammasome plays a crucial role in the pathogenesis of DN (38–40).

Podocytes, namely glomerular visceral epithelial cells, participate in stabilizing glomerular capillaries, maintaining the function of glomerular filtration barrier, regulating ultrafiltration coefficient K/f and maintaining the normal morphology of glomerular basement membrane (GBM) (41). Studies have shown that podocyte injury plays a key role in the pathogenesis of DN (41). High glucose (HG) activated the NLRP3 inflammasome in mouse podocytes, which was manifested by increased protein levels of NLRP3, ASC and caspase-1, and the activity of caspase-1 was also significantly elevated (42). After the podocytes were transfected with NLRP3-small interfering RNA (siRNA), the expression of caspase-1 and IL-1β was reduced, while the expression of the podocyte functional protein nephrin was significantly increased (43). The mechanism of NLRP3 inflammasome on podocytes has not been fully elucidated. It has been found that activation of NLRP3 inflammasome aggravated podocyte autophagy and reduced nephrin expression, while NLRP3 silencing effectively restored podocyte autophagy and alleviated podocyte injury induced by HG, suggesting that autophagy might participate in the regulation of NLRP3 inflammasome on podocytes (44).

Glomerular mesangial cells play an important role in the process of glomerular injury and repair. Early DN mainly manifested in the proliferation of mesangial cells, which then synthesize and secrete of a large number of mesangial matrixes, gradually occlude the capillaries and lead to glomerulosclerosis. It was found that the activation of NLRP3 also existed in glomerular mesangial cells stimulated by HG (45). Some extracts of traditional Chinese medicine have been found to target NLRP3 to alleviate HG induced mesangial cell proliferation (46, 47).

Renal tubular injury is one of the important determinants of progressive renal failure in DN. *In vitro*, the expression of NLRP3 and the release of IL-1β, IL-18 and ATP were significantly increased in HK-2 cells stimulated by HG (48). Knockdown of NLRP3 resisted HG induced tubular EMT by inhibiting ROS production and the phosphorylation of Smad3, p38MAPK and ERK1/2 (49). The overproduction of mitochondrial ROS (mtROS) plays a key role in inflammation. Treating HK-2 cells with the mtROS antioxidant MitoQ inhibited the dissociation of thioredoxin (TRX) from TXNIP, and then blocked the interaction between TXNIP and NLRP3, resulting in the inactivation of NLRP3 inflammasome and the inhibition of IL-1β maturation (50). Another study confirmed that ATP-P2X4 signaling mediated the activation of HG-induced NLRP3 inflammasome, regulated the secretion of IL-1β, and caused the development of tubulointerstitial inflammation in DN (48). IRE1α was endoplasmic reticulum stress (ERS)-related factor. Using IRE1α RNase specific inhibitor (STF-083010) in HG-induced NRK-52E cells inhibited the TXINP/NLRP3 pathway-mediated pyroptosis and renal damage, suggesting that ERS might also leading to the activation of NLRP3 inflammasome (51).

In general, HG stimulation can activate NLRP3 inflammasome through a variety of pathways, which will lead to the abnormalities of intrinsic cells in kidney (**Figure 2**). Current studies have proved that NLRP3 activation was widespread in DN, and targeted therapy of NLRP3 played an important role in the improvement of DN.

Hypertension-Related Nephropathy

Hypertension-related nephropathy is the damage of renal structure and function caused by primary hypertension. The kidney can excrete excess water and sodium salt through urine, and prevent protein and blood cells from leaking out of blood vessels. High blood pressure increases the blood pressure in the blood vessels, leading to the leakage of protein into the urine, causing damage to the renal filter system. Long term poor control of hypertension will cause irreversible damage to the kidney. Clinical hypertension is related to kidney inflammation and increased circulating levels of IL-1β and IL-18, indicating that inflammasome activity may be involve in the blood pressure fluctuation and kidney injury (52).

In mice with deoxycorticosterone acetate and saline (1K/DOCA/salt)-induced hypertension, the mRNA levels of NLRP3, ASC, pro-caspase-1 and pro-IL-1β were evaluated, as well as the protein expression of active caspase-1 and mature IL-1β (53). ASC−/− mice exhibited a sluggish pressor response and the treatment of NLRP3 inflammasome inhibitor MCC950 reversed the hypertension in 1K/DOCA/salt treated mice (53). Nitric oxide (NO) inhibition and salt overload lead to hypertension, albuminuria, glomerulosclerosis, glomerular ischemia and interstitial fibrosis. In this model, allopurinol (ALLO), an NLRP3 inhibitor, significantly improved hypertension, proteinuria and interstitial inflammation and fibrosis (54). In a CKD model of 5/6 nephrectomy (5/6 Nx), the degree of tubulointerstitial fibrosis and proteinuria was decreased in NLRP3−/− mice, meanwhile, the mitochondrial morphology and CKD-related hypertension were also ameliorated (55). So far, some literatures have confirmed the important role of NLRP3 activation in hypertension-related nephropathy, but the specific regulatory mechanism still needs to be further explored.

Obesity-Related Nephropathy

In 1974, Weisinger et al. firstly reported that severe obesity can lead to a large amount of proteinuria, and named this disease as

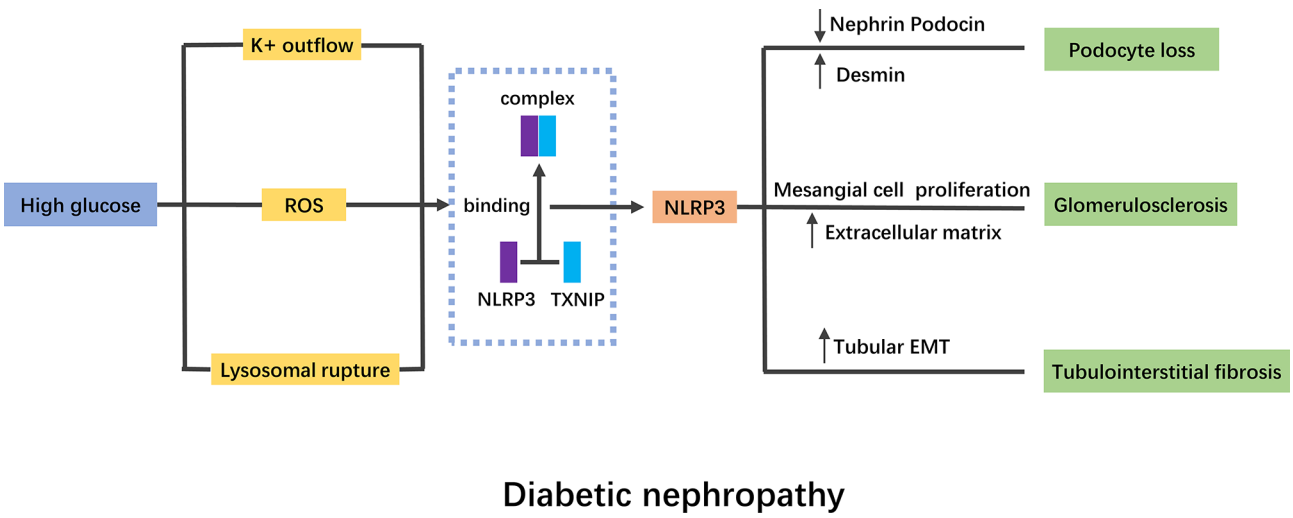


FIGURE 2 | Mechanism of NLRP3 inflammasome in diabetic nephropathy. High glucose stimulation activates NLRP3 inflammasome mainly through K+ outflow, ROS and lysosomal rupture. TNXIP binding to NLRP3 is a pivotal mechanism of NLRP3 inflammasome activation. The activation of NLRP3 inflammasome will lead to podocyte lose, glomerulosclerosis and tubulointerstitial fibrosis. NLRP3, nod like receptor protein 3; ROS, reactive oxygen species; EMT, epithelial mesenchymal transition.

obesity-related nephropathy (ORG) (56). Since then, clinical studies and animal experimental models have confirmed that obesity has a significant effect on the structure and function of the kidney (57). In recent years, although there are many studies on ORG, its specific pathogenesis is not fully understood. It is generally believed to be related to glucagon and insulin resistance, the role of adipocytokines, inappropriate activation of renin-angiotensin-aldosterone system (RAAS), release of inflammatory factors, lipid metabolism disorder and structural changes of kidney caused by obesity itself (58).

It was found that the mRNA levels and protein expressions of NLRP3, ASC and caspase-1 in renal cortex of ORG mice were significantly up-regulated (59). Also accompanied a significant increase by P2X7R, an activation molecule of NLRP3. The treatment of P2X7R antagonist (KN−62 or A438079) reversed the changes of NLRP3 inflammasome components as well as attenuated podocytes injury treated by leptin (59). The expression of IL-1β and IL-18 levels also gradually increased in the kidney of high-fat diet (HFD) fed mice detected by immunohistochemistry (60). Knockdown of caspase-1 expression with siRNA inhibited palmitate-induced death and apoptosis of HK-2 cells (60). Some natural substances and traditional Chinese medicine components have been shown to affect ORG by regulating the activation of NLRP3 inflammasome. Fisetin (FIS) is a natural flavonoid, which significantly attenuated HFD-induced histological changes in renal tissue samples, reduced the expression of kidney injury molecule-1 (KIM-1) and altered the expression of nephrin and podocin, thus improving renal insufficiency (61). In this process, the expression of NLRP3 inflammasome components was also decreased, suggesting that its mechanism might be related to inflammasome (61). Coptidis Rhizoma, a classical traditional Chinese herb, reduced dyslipidemia and improved urinary albumin to creatinine ratio and creatinine clearance rate in obesity-prone (OP) rats with high protein and high fat diet (62). The expression of NLRP3 inflammasome was also downregulated under Coptidis Rhizoma treatment (62).

At present, the research on the pathogenesis and treatment of ORG is relatively lacking, and the activation of NLRP3 may be an important link. Therefore, more extensive and in-depth research will give us a deeper understanding of ORG.

Hyperuricemia

Uric acid is a kind of anionic organic acid which is slightly soluble in water. It is the end product of purine metabolism by xanthine oxidase. About 70% of uric acid in normal human body is excreted through kidney, and the remaining 30% is excreted through bile duct and intestine (63). The generation and excretion of uric acid in healthy human body is in dynamic balance. Once this balance is broken, the generation or excretion of uric acid increase or decrease, resulting in the accumulation of uric acid in the body, which will lead to hyperuricemia. Fasting serum uric acid level > 420 mmol · L^{-1} (male) and > 360 mmol · L^{-1} (female) is usually used as the diagnostic criteria of hyperuricemia.

Hyperuricemia can easily lead to renal hemodynamics, histology and function changes, causing serious consequences such as renal tubulointerstitial inflammation, kidney stones, renal fibrosis and polycystic kidney disease (64). The study of 266 patients with hyperuricemia found that the incidence of nephropathy was 15.11%, while the incidence of nephropathy was only 2.19% in the population with normal serum uric acid level (65). Another study among 190 patients with chronic gout found that the incidence rate of renal damage was 86.13%, significantly higher than 7.14% in the control group, suggesting that hyperuricemia was closely related to the incidence of renal damage and was another risk factor for kidney diseases (66).

At present, it is believed that hyperuricemia induced kidney injury is mainly related to hyperuricemia induced RAAS hyperfunction, inflammatory reaction, renal microvascular injury and so on, but the exact mechanism remains unclear. Affiliated Bao'an Hospital of Shenzhen conducted a cohort study among control, hyperuricemia and gouty nephropathy patients. The results showed that the expression of the NLRP3 inflammasome in peripheral blood mononuclear cells, and the levels of IL-1β and IL-18 in the plasma were upregulated in the gouty nephropathy group compared with the control and hyperuricemia groups (67). In rats with hyperuricemia and dyslipidemia induced by fructose, NLRP3 inflammasome in kidney tissues was activated, which manifested by overexpression of NLRP3, ASC and caspase-1, resulting in excessive production of IL-1β, IL-18, IL-6 (68). Using the CRISPR/Cas9 system to functionally disrupt expression of urate oxidase (UOX) in Wistar rats spontaneously and persistently increased serum uric acid level compared with wild-type rats. UOX-KO rats established increased interstitial fibrosis, macrophage infiltration, increased expression of NLRP3 and IL-1β, and activation signaling pathways associated with autophagy, indicating that autophagy and NLRP3-dependent inflammation played crucial role in the development of hyperuricemia induced kidney injury (69). The activation of NLRP3 inflammasome has been proved to be a target of hyperuricemia induced renal injury. A large number of natural extracts have been found to improve renal function by inhibiting the activity of NLRP3 inflammasome in hyperuricemia (70–73).

Although there are a lot of epidemiological and experimental research reports on the relationship between uric acid and kidney injury, the underlying pathological mechanism still needs further research. The mechanism of hyperuricemia-induced renal injury has a wide range of cross-talks. The activation of NLRP3 inflammasome plays a complex and important role in promoting the occurrence and development of renal disease. The mechanism of its interaction with other factors still needs to be further explored.

Hyperhomocysteinemia

Hyperhomocysteinemia (hHcys) is a disease characterized by elevated homocysteine in the blood, which has been recognized as one of the important risk factors of kidney disease. HHcys can cause anabolism of cholesterol and triglycerides, impaired endothelial function, thrombosis, and monocyte activation (74). Hyperhomocysteinemia is present in 85% of patients with chronic renal failure, and persists after the initiation of dialysis or kidney transplantation (75).

In 2012, Zhang et al. firstly discovered that all the components of NLRP3 inflammasome were existed in podocytes and were significantly evaluated by the treatment with L-homocysteine (L-Hcys) (76). Silencing the ASC gene or inhibiting caspase-1 activity could alleviate podocyte injury and improve glomerulosclerosis in mice with hHcys (76). Podocin, nephrin and desmin are critical markers of podocyte injury. Another study demonstrated that in folate free (FF) diet induced hHcys mice, NLRP3−/− mice showed increased protein level of podocin and nephrin but decreased expression of desmin compared to wild-type mice, indicating the potential pathogenic effects of NLRP3 inflammasome activation (77). The production of ROS plays an important role in the activation of NLRP3 inflammasome in hHcys-induced kidney injury. Nicotinamide adenine dinucleotide phosphate (NADPH) oxidase is considered to be the main source of superoxide in the kidney. NADPH oxidase inhibition (NOX) reversed the upregulated protein levels of NLRP3, ASC and caspase-1 stimulated by Hcys in mouse podocytes (78). *In vivo*, NOX inhibition also protected glomeruli and podocytes from hHcys-induced damage, which was manifested by reduced proteinuria and glomerular sclerosis (78). TEMPOL is a recognized antioxidant. In hHcys mice, the treatment of TEMPOL reduced colocalization of NLRP3 with ASC, caspase-1 activation and as well as IL-1β production, suggesting the treatment inhibited the activation of NLRP3 inflammasome (79). Meanwhile, the glomerular injury induced by hHcys has also been improved (79). As in other metabolic-associated kidney diseases mentioned above, the binding of TXNIP to NLRP3 is a key signaling mechanism in hHcys-induced kidney injury as well. Inhibition of TXNIP by verapamil or TXNIP shRNA transfection broke the binding and disrupted the formation of glomerular inflammasome (80).

As a crucial role in the pathogenic process of hHcys-induced kidney injury, NLRP3 inflammasome has been regarded as a novel target for the treatment of glomerular injury in hHcys. Many compounds with anti-inflammatory properties, such as anandamide, DHA metabolites-resolvins, resolvin D1 (RvD1) and 17S-hydroxy DHA (17SHDHA), blocked podocyte injury and glomerular sclerosis during hHcys *via* the suppression of NLRP3 inflammasome activity (81–83).

CONCLUSION

MS is a group of clinical syndromes of chronic inflammation and metabolic disorders caused by insulin resistance. With the improvement of the economic level and the spread of unhealthy lifestyles, the prevalence of MS is on the rise globally, especially in developing countries and regions. Recent studies have found that MS is an independent risk factor for CKD. The pathogenesis of kidney damage caused by MS is related to poor primary disease control, insulin resistance, chronic inflammation, and endothelial function damage. NLRP3 inflammasome is the sensor of the innate immune system that initiates inflammatory response to stimulations, and participates in the occurrence and development of various metabolic diseases and kidney injury (**Table 1**). As we mentioned above, a variety of metabolic disorders leads to the activation of NLRP3 inflammasome in the kidney. The activation of NLRP3 inflammasome aggravates renal inflammatory infiltration and tissue damage through many pathways including autophagy, inflammatory factor release and EMT. At the same time, factors related to tissue damage, such as ROS, autophagy related molecules continue to stimulate the activation of NLRP3 inflammasome and impair renal function. Therefore, the activation of inflammasome and kidney injury are mutually reinforcing.

TABLE 1 | The role of NLRP3 inflammasome in the kidney under different metabolic disorders.

Metabolic factor	NLRP3 state	Function
Hyperglycemia	activate	podocyte lose, glomerulosclerosis and tubulointerstitial fibrosis
Hypertension	activate	hypertension, proteinuria, interstitial inflammation and fibrosis
Obesity	activate	dyslipidemia, podocyte injury, cell death and apoptosis
Hyperuricemia	activate	interstitial fibrosis and macrophage infiltration
Hyperhomocysteinemia	activate	proteinuria and glomerular sclerosis

Because inflammasomes are intracellular recognition receptors, scientists believe that there may be common factors for their activation. In the kidney damage caused by different metabolic factors, there are currently three recognized activation pathways, namely the outflow of potassium ions, the release of ROS, and the rupture of lysosomes. But for each metabolic factor, specific activators are also found. For example, in DN, NLRP3 inflammasome can also be activated by endoplasmic reticulum stress and autophagy.

Accordingly, to explore the specific mechanism and important role of NLRP3 in kidney injury induced by metabolic disorders will provide new ideas and directions for the prevention and treatment of metabolic-associated kidney diseases.

AUTHOR CONTRIBUTIONS

CZ and X-FM conceived and designed the manuscript. WX did literature searching, drafted the manuscript, and drew the figures. CZ and X-FM reviewed and revised the article. All authors contributed to the article and approved the submitted version.

FUNDING

This work was supported by Grants from the National Natural Science Foundation of China (81961138007, 81974096, 81770711), and program for HUST Academic Frontier Youth Team (2017QYTD20).

REFERENCES

1. Schlaich M, Straznicky N, Lambert E, Lambert G. Metabolic Syndrome: A Sympathetic Disease? *Lancet Diabetes Endocrinol* (2015) 3:148–57. doi: 10.1016/S2213-8587(14)70033-6
2. Ford ES, Giles WH, Dietz WH. Prevalence of the Metabolic Syndrome Among US Adults: Findings From the Third National Health and Nutrition Examination Survey. *JAMA* (2002) 287:356–9. doi: 10.1001/jama.287.3.356
3. Ford ES, Giles WH, Mokdad AH. Increasing Prevalence of the Metabolic Syndrome Among U.S. Adults. *Diabetes Care* (2004) 27:2444–9. doi: 10.2337/diacare.27.10.2444
4. Grundy SM. Metabolic Syndrome: Connecting and Reconciling Cardiovascular and Diabetes Worlds. *J Am Coll Cardiol* (2006) 47:1093–100. doi: 10.1016/j.jacc.2005.11.046
5. Eckel RH, Grundy SM, Zimmet PZ. The Metabolic Syndrome. *Lancet* (2005) 365:1415–28. doi: 10.1016/S0140-6736(05)66378-7
6. Grundy SM. Pre-Diabetes, Metabolic Syndrome, and Cardiovascular Risk. *J Am Coll Cardiol* (2012) 59:635–43. doi: 10.1016/j.jacc.2011.08.080
7. Agrawal V, Shah A, Rice C, Franklin BA, McCullough PA. Impact of Treating the Metabolic Syndrome on Chronic Kidney Disease. *Nat Rev Nephrol* (2009) 5:520–8. doi: 10.1038/nrneph.2009.114
8. Bishehsari F, Voigt RM, Keshavarzian A. Circadian Rhythms and the Gut Microbiota: From the Metabolic Syndrome to Cancer. *Nat Rev Endocrinol* (2020) 16:731–9. doi: 10.1038/s41574-020-00427-4
9. Zhang X, Lerman LO. The Metabolic Syndrome and Chronic Kidney Disease. *Transl Res* (2017) 183:14–25. doi: 10.1016/j.trsl.2016.12.004
10. Chen J, Muntner P, Hamm LL, Jones DW, Batuman V, Fonseca V, et al. The Metabolic Syndrome and Chronic Kidney Disease in U.S. Adults. *Ann Intern Med* (2004) 140:167–74. doi: 10.7326/0003-4819-140-3-200402030-00007
11. Song H, Wang X, Cai Q, Ding W, Huang S, Zhuo L. Association of Metabolic Syndrome With Decreased Glomerular Filtration Rate Among 75,468 Chinese Adults: A Cross-Sectional Study. *PloS One* (2014) 9:e113450. doi: 10.1371/journal.pone.0113450
12. Hale LJ, Coward RJ. The Insulin Receptor and the Kidney. *Curr Opin Nephrol Hypertens* (2013) 22:100–6. doi: 10.1097/MNH.0b013e32835abb52
13. Ohashi Y, Thomas G, Nurko S, Stephany B, Fatica R, Chiesa A, et al. Association of Metabolic Syndrome With Kidney Function and Histology in Living Kidney Donors. *Am J Transplant* (2013) 13:2342–51. doi: 10.1111/ajt.12369
14. Schroder K, Tschopp J. The Inflammasomes. *Cell* (2010) 140:821–32. doi: 10.1016/j.cell.2010.01.040
15. Lamkanfi M, Dixit VM. Inflammasomes and Their Roles in Health and Disease. *Annu Rev Cell Dev Biol* (2012) 28:137–61. doi: 10.1146/annurev-cellbio-101011-155745
16. Hoffman HM, Wanderer AA. Inflammasome and IL-1beta-Mediated Disorders. *Curr Allergy Asthma Rep* (2010) 10:229–35. doi: 10.1007/s11882-010-0109-z
17. Sharma D, Kanneganti TD. The Cell Biology of Inflammasomes: Mechanisms of Inflammasome Activation and Regulation. *J Cell Biol* (2016) 213:617–29. doi: 10.1083/jcb.201602089
18. Duewell P, Kono H, Rayner KJ, Sirois CM, Vladimer G, Bauernfeind FG, et al. NLRP3 Inflammasomes are Required for Atherogenesis and Activated by Cholesterol Crystals. *Nature* (2010) 464:1357–61. doi: 10.1038/nature08938
19. Wen H, Miao EA, Ting JP. Mechanisms of NOD-Like Receptor-Associated Inflammasome Activation. *Immunity* (2013) 39:432–41. doi: 10.1016/j.immuni.2013.08.037
20. Mangan MSJ, Olhava EJ, Roush WR, Seidel HM, Glick GD, Latz E. Targeting the NLRP3 Inflammasome in Inflammatory Diseases. *Nat Rev Drug Discov* (2018) 17:588–606. doi: 10.1038/nrd.2018.97
21. Jin C, Flavell RA. Molecular Mechanism of NLRP3 Inflammasome Activation. *J Clin Immunol* (2010) 30:628–31. doi: 10.1007/s10875-010-9440-3
22. Petrilli V, Papin S, Dostert C, Mayor A, Martinon F, Tschopp J. Activation of the NALP3 Inflammasome Is Triggered by Low Intracellular Potassium Concentration. *Cell Death Differ* (2007) 14:1583–9. doi: 10.1038/sj.cdd.4402195
23. Zhou R, Tardivel A, Thorens B, Choi I, Tschopp J. Thioredoxin-Interacting Protein Links Oxidative Stress to Inflammasome Activation. *Nat Immunol* (2010) 11:136–40. doi: 10.1038/ni.1831
24. Campden RI, Zhang Y. The Role of Lysosomal Cysteine Cathepsins in NLRP3 Inflammasome Activation. *Arch Biochem Biophys* (2019) 670:32–42. doi: 10.1016/j.abb.2019.02.015
25. Lichtnekert J, Kulkarni OP, Mulay SR, Rupanagudi KV, Ryu M, Allam R, et al. Anti-GBM Glomerulonephritis Involves IL-1 But Is Independent of NLRP3/ASC Inflammasome-Mediated Activation of Caspase-1. *PloS One* (2011) 6:e26778. doi: 10.1371/journal.pone.0026778

26. Komada T, Muruve DA. The Role of Inflammasomes in Kidney Disease. *Nat Rev Nephrol* (2019) 15:501–20. doi: 10.1038/s41581-019-0158-z
27. Xiong W, Meng XF, Zhang C. Inflammasome Activation in Podocytes: A New Mechanism of Glomerular Diseases. *Inflamm Res* (2020) 69:731–43. doi: 10.1007/s00011-020-01354-w
28. Lau A, Chung H, Komada T, Platnich JM, Sandall CF, Choudhury SR, et al. Renal Immune Surveillance and Dipeptidase-1 Contribute to Contrast-Induced Acute Kidney Injury. *J Clin Invest* (2018) 128:2894–913. doi: 10.1172/JCI96640
29. Chang A, Ko K, Clark MR. The Emerging Role of the Inflammasome in Kidney Diseases. *Curr Opin Nephrol Hypertens* (2014) 23:204–10. doi: 10.1097/01.mnh.0000444814.49755.90
30. Sharma BR, Kanneganti TD. NLRP3 Inflammasome in Cancer and Metabolic Diseases. *Nat Immunol* (2021) 22:550–9. doi: 10.1038/s41590-021-00886-5
31. Duran-Salgado MB, Rubio-Guerra AF. Diabetic Nephropathy and Inflammation. *World J Diabetes* (2014) 5:393–8. doi: 10.4239/wjd.v5.i3.393
32. Shahzad K, Bock F, Dong W, Wang H, Kopf S, Kohli S, et al. Nlrp3-Inflammasome Activation in Non-Myeloid-Derived Cells Aggravates Diabetic Nephropathy. *Kidney Int* (2015) 87:74–84. doi: 10.1038/ki.2014.271
33. Zhang C, Zhu X, Li L, Ma T, Shi M, Yang Y, et al. A Small Molecule Inhibitor MCC950 Ameliorates Kidney Injury in Diabetic Nephropathy by Inhibiting NLRP3 Inflammasome Activation. *Diabetes Metab Syndr Obes* (2019) 12:1297–309. doi: 10.2147/DMSO.S199802
34. Shahzad K, Bock F, Al-Dabet MM, Gadi I, Kohli S, Nazir S, et al. Caspase-1, But Not Caspase-3, Promotes Diabetic Nephropathy. *J Am Soc Nephrol* (2016) 27:2270–5. doi: 10.1681/ASN.2015060676
35. Lei Y, Devarapu SK, Motrapu M, Cohen CD, Lindenmeyer MT, Moll S, et al. Interleukin-1beta Inhibition for Chronic Kidney Disease in Obese Mice With Type 2 Diabetes. *Front Immunol* (2019) 10:1223. doi: 10.3389/fimmu.2019.01223
36. Samra YA, Said HS, Elsherbiny NM, Liou GI, El-Shishtawy MM, Eissa LA. Cepharanthine and Piperine Ameliorate Diabetic Nephropathy in Rats: Role of NF-kappaB and NLRP3 Inflammasome. *Life Sci* (2016) 157:187–99. doi: 10.1016/j.lfs.2016.06.002
37. An X, Zhang Y, Cao Y, Chen J, Qin H, Yang L. Punicalagin Protects Diabetic Nephropathy by Inhibiting Pyroptosis Based on TXNIP/NLRP3 Pathway. *Nutrients* (2020) 12(5):1516. doi: 10.3390/nu12051516
38. Liu YW, Hao YC, Chen YJ, Yin SY, Zhang MY, Kong L, et al. Protective Effects of Sarsasapogenin Against Early Stage of Diabetic Nephropathy in Rats. *Phytother Res* (2018) 32:1574–82. doi: 10.1002/ptr.6088
39. Lu M, Yin N, Liu W, Cui X, Chen S, Wang E. Curcumin Ameliorates Diabetic Nephropathy by Suppressing NLRP3 Inflammasome Signaling. *BioMed Res Int* (2017) 2017:1516985. doi: 10.1155/2017/1516985
40. Sun Z, Ma Y, Chen F, Wang S, Chen B, Shi J. Artesunate Ameliorates High Glucose-Induced Rat Glomerular Mesangial Cell Injury by Suppressing the TLR4/NF-κB/NLRP3 Inflammasome Pathway. *Chem Biol Interact* (2018) 293:11–9. doi: 10.1016/j.cbi.2018.07.011
41. Mathieson PW. The Podocyte as a Target for Therapies–New and Old. *Nat Rev Nephrol* (2011) 8:52–6. doi: 10.1038/nrneph.2011.171
42. Liu Y, Xu Z, Ma F, Jia Y, Wang G. Knockdown of TLR4 Attenuates High Glucose-Induced Podocyte Injury *Via* the NALP3/ASC/Caspase-1 Signaling Pathway. *BioMed Pharmacother* (2018) 107:1393–401. doi: 10.1016/j.biopha.2018.08.134
43. Li J, Wang B, Zhou G, Yan X, Zhang Y. Tetrahydroxy Stilbene Glucoside Alleviates High Glucose-Induced MPC5 Podocytes Injury Through Suppression of NLRP3 Inflammasome. *Am J Med Sci* (2018) 355:588–96. doi: 10.1016/j.amjms.2018.03.005
44. Hou Y, Lin S, Qiu J, Sun W, Dong M, Xiang Y, et al. NLRP3 Inflammasome Negatively Regulates Podocyte Autophagy in Diabetic Nephropathy. *Biochem Biophys Res Commun* (2020) 521:791–8. doi: 10.1016/j.bbrc.2019.10.194
45. Feng H, Gu J, Gou F, Huang W, Gao C, Chen G, et al. High Glucose and Lipopolysaccharide Prime NLRP3 Inflammasome *Via* ROS/TXNIP Pathway in Mesangial Cells. *J Diabetes Res* (2016) 2016:6973175. doi: 10.1155/2016/6973175
46. Wang S, Zhao X, Yang S, Chen B, Shi J. Salidroside Alleviates High Glucose-Induced Oxidative Stress and Extracellular Matrix Accumulation in Rat Glomerular Mesangial Cells by the TXNIP-NLRP3 Inflammasome Pathway. *Chem Biol Interact* (2017) 278:48–53. doi: 10.1016/j.cbi.2017.10.012
47. Chen F, Wei G, Xu J, Ma X, Wang Q. Naringin Ameliorates the High Glucose-Induced Rat Mesangial Cell Inflammatory Reaction by Modulating the NLRP3 Inflammasome. *BMC Complement Altern Med* (2018) 18:192. doi: 10.1186/s12906-018-2257-y
48. Chen K, Zhang J, Zhang W, Zhang J, Yang J, Li K, et al. ATP-P2X4 Signaling Mediates NLRP3 Inflammasome Activation: A Novel Pathway of Diabetic Nephropathy. *Int J Biochem Cell Biol* (2013) 45:932–43. doi: 10.1016/j.biocel.2013.02.009
49. Song S, Qiu D, Luo F, Wei J, Wu M, Wu H, et al. Knockdown of NLRP3 Alleviates High Glucose or TGFB1-Induced EMT in Human Renal Tubular Cells. *J Mol Endocrinol* (2018) 61:101–13. doi: 10.1530/JME-18-0069
50. Han Y, Xu X, Tang C, Gao P, Chen X, Xiong X, et al. Reactive Oxygen Species Promote Tubular Injury in Diabetic Nephropathy: The Role of the Mitochondrial Ros-Txnip-Nlrp3 Biological Axis. *Redox Biol* (2018) 16:32–46. doi: 10.1016/j.redox.2018.02.013
51. Ke R, Wang Y, Hong S, Xiao L. Endoplasmic Reticulum Stress Related Factor IRE1alpha Regulates TXNIP/NLRP3-Mediated Pyroptosis in Diabetic Nephropathy. *Exp Cell Res* (2020) 396:112293. doi: 10.1016/j.yexcr.2020.112293
52. Krishnan SM, Sobey CG, Latz E, Mansell A, Drummond GR. IL-1beta and IL-18: Inflammatory Markers or Mediators of Hypertension? *Br J Pharmacol* (2014) 171:5589–602. doi: 10.1111/bph.12876
53. Krishnan SM, Dowling JK, Ling YH, Diep H, Chan CT, Ferens D, et al. Inflammasome Activity Is Essential for One Kidney/Deoxycorticosterone Acetate/Salt-Induced Hypertension in Mice. *Br J Pharmacol* (2016) 173:752–65. doi: 10.1111/bph.13230
54. Zambom FFF, Oliveira KC, Foresto-Neto O, Faustino VD, Avila VF, Albino AH, et al. Pathogenic Role of Innate Immunity in a Model of Chronic NO Inhibition Associated With Salt Overload. *Am J Physiol Renal Physiol* (2019) 317:F1058–67. doi: 10.1152/ajprenal.00251.2019
55. Gong W, Mao S, Yu J, Song J, Jia Z, Huang S, et al. NLRP3 Deletion Protects Against Renal Fibrosis and Attenuates Mitochondrial Abnormality in Mouse With 5/6 Nephrectomy. *Am J Physiol Renal Physiol* (2016) 310:F1081–8. doi: 10.1152/ajprenal.00534.2015
56. Weisinger JR, Kempson RL, Eldridge FL, Swenson RS. The Nephrotic Syndrome: A Complication of Massive Obesity. *Ann Intern Med* (1974) 81:440–7. doi: 10.7326/0003-4819-81-4-440
57. Camara NO, Iseki K, Kramer H, Liu ZH, Sharma K. Kidney Disease and Obesity: Epidemiology, Mechanisms and Treatment. *Nat Rev Nephrol* (2017) 13:181–90. doi: 10.1038/nrneph.2016.191
58. Wahba IM, Mak RH. Obesity and Obesity-Initiated Metabolic Syndrome: Mechanistic Links to Chronic Kidney Disease. *Clin J Am Soc Nephrol* (2007) 2:550–62. doi: 10.2215/CJN.04071206
59. Hou XX, Dong HR, Sun LJ, Yang M, Cheng H, Chen YP. Purinergic 2x7 Receptor Is Involved in the Podocyte Damage of Obesity-Related Glomerulopathy *Via* Activating Nucleotide-Binding and Oligomerization Domain-Like Receptor Protein 3 Inflammasome. *Chin Med J (Engl)* (2018) 131:2713–25. doi: 10.4103/0366-6999.245270
60. Li LC, Yang JL, Lee WC, Chen JB, Lee CT, Wang PW, et al. Palmitate Aggravates Proteinuria-Induced Cell Death and Inflammation *Via* CD36-Inflammasome Axis in the Proximal Tubular Cells of Obese Mice. *Am J Physiol Renal Physiol* (2018) 315:F1720–31. doi: 10.1152/ajprenal.00536.2017
61. Ge C, Xu M, Qin Y, Gu T, Lou D, Li Q, et al. Fisetin Supplementation Prevents High Fat Diet-Induced Diabetic Nephropathy by Repressing Insulin Resistance and RIP3-Regulated Inflammation. *Food Funct* (2019) 10:2970–85. doi: 10.1039/c8fo01653d
62. Ren Y, Wang D, Lu F, Zou X, Xu L, Wang K, et al. Coptidis Rhizoma Inhibits NLRP3 Inflammasome Activation and Alleviates Renal Damage in Early Obesity-Related Glomerulopathy. *Phytomedicine* (2018) 49:52–65. doi: 10.1016/j.phymed.2018.05.019
63. Mandal AK, Mount DB. The Molecular Physiology of Uric Acid Homeostasis. *Annu Rev Physiol* (2015) 77:323–45. doi: 10.1146/annurev-physiol-021113-170343
64. Braga TT, Foresto-Neto O, Camara NOS. The Role of Uric Acid in Inflammasome-Mediated Kidney Injury. *Curr Opin Nephrol Hypertens* (2020) 29:423–31. doi: 10.1097/MNH.0000000000000619
65. Toprak O, Cirit M, Esi E, Postaci N, Yesil M, Bayata S. Hyperuricemia as a Risk Factor for Contrast-Induced Nephropathy in Patients With Chronic

Kidney Disease. *Catheter Cardiovasc Interv* (2006) 67:227–35. doi: 10.1002/ccd.20598
66. Padang C, Muirden KD, Schumacher HR, Darmawan J, Nasution AR. Characteristics of Chronic Gout in Northern Sulawesi, Indonesia. *J Rheumatol* (2006) 33:1813–7.
67. Zhang YZ, Sui XL, Xu YP, Gu FJ, Zhang AS, Chen JH. NLRP3 Inflammasome and Lipid Metabolism Analysis Based on UPLC-Q-TOF-MS in Gouty Nephropathy. *Int J Mol Med* (2019) 44:172–84. doi: 10.3892/ijmm.2019.4176
68. Hu QH, Zhang X, Pan Y, Li YC, Kong LD. Allopurinol, Quercetin and Rutin Ameliorate Renal NLRP3 Inflammasome Activation and Lipid Accumulation in Fructose-Fed Rats. *Biochem Pharmacol* (2012) 84:113–25. doi: 10.1016/j.bcp.2012.03.005
69. Wu M, Ma Y, Chen X, Liang N, Qu S, Chen H. Hyperuricemia Causes Kidney Damage by Promoting Autophagy and NLRP3-Mediated Inflammation in Rats With Urate Oxidase Deficiency. *Dis Model Mech* (2021) 14(3): dmm048041. doi: 10.1242/dmm.048041
70. Cui D, Liu S, Tang M, Lu Y, Zhao M, Mao R, et al. Phloretin Ameliorates Hyperuricemia-Induced Chronic Renal Dysfunction Through Inhibiting NLRP3 Inflammasome and Uric Acid Reabsorption. *Phytomedicine* (2020) 66:153111. doi: 10.1016/j.phymed.2019.153111
71. Hu J, Wu H, Wang D, Yang Z, Zhuang L, Yang N, et al. Weicao Capsule Ameliorates Renal Injury Through Increasing Autophagy and NLRP3 Degradation in UAN Rats. *Int J Biochem Cell Biol* (2018) 96:1–8. doi: 10.1016/j.biocel.2018.01.001
72. Li G, Guan C, Xu L, Wang L, Yang C, Zhao L, et al. Scutellarin Ameliorates Renal Injury *Via* Increasing CCN1 Expression and Suppressing NLRP3 Inflammasome Activation in Hyperuricemic Mice. *Front Pharmacol* (2020) 11:584942. doi: 10.3389/fphar.2020.584942
73. Wang M, Zhao J, Zhang N, Chen J. Astilbin Improves Potassium Oxonate-Induced Hyperuricemia and Kidney Injury Through Regulating Oxidative Stress and Inflammation Response in Mice. *BioMed Pharmacother* (2016) 83:975–88. doi: 10.1016/j.biopha.2016.07.025
74. Russo C, Morabito F, Luise F, Piromalli A, Battaglia L, Vinci A, et al. Hyperhomocysteinemia Is Associated With Cognitive Impairment in Multiple Sclerosis. *J Neurol* (2008) 255:64–9. doi: 10.1007/s00415-007-0668-7
75. Ferechide D, Radulescu D. Hyperhomocysteinemia in Renal Diseases. *J Med Life* (2009) 2:53–9.
76. Zhang C, Boini KM, Xia M, Abais JM, Li X, Liu Q, et al. Activation of Nod-Like Receptor Protein 3 Inflammasomes Turns on Podocyte Injury and Glomerular Sclerosis in Hyperhomocysteinemia. *Hypertension* (2012) 60:154–62. doi: 10.1161/HYPERTENSIONAHA.111.189688
77. Xia M, Conley SM, Li G, Li PL, Boini KM. Inhibition of Hyperhomocysteinemia-Induced Inflammasome Activation and Glomerular Sclerosis by NLRP3 Gene Deletion. *Cell Physiol Biochem* (2014) 34:829–41. doi: 10.1159/000363046
78. Abais JM, Zhang C, Xia M, Liu Q, Gehr TW, Boini KM, et al. NADPH Oxidase-Mediated Triggering of Inflammasome Activation in Mouse Podocytes and Glomeruli During Hyperhomocysteinemia. *Antioxid Redox Signal* (2013) 18:1537–48. doi: 10.1089/ars.2012.4666
79. Abais JM, Xia M, Li G, Gehr TW, Boini KM, Li PL. Contribution of Endogenously Produced Reactive Oxygen Species to the Activation of Podocyte NLRP3 Inflammasomes in Hyperhomocysteinemia. *Free Radic Biol Med* (2014) 67:211–20. doi: 10.1016/j.freeradbiomed.2013.10.009
80. Abais JM, Xia M, Li G, Chen Y, Conley SM, Gehr TW, et al. Nod-Like Receptor Protein 3 (NLRP3) Inflammasome Activation and Podocyte Injury *Via* Thioredoxin-Interacting Protein (TXNIP) During Hyperhomocysteinemia. *J Biol Chem* (2014) 289:27159–68. doi: 10.1074/jbc.M114.567537
81. Li G, Xia M, Abais JM, Boini K, Li PL, Ritter JK. Protective Action of Anandamide and Its COX-2 Metabolite Against L-Homocysteine-Induced NLRP3 Inflammasome Activation and Injury in Podocytes. *J Pharmacol Exp Ther* (2016) 358:61–70. doi: 10.1124/jpet.116.233239
82. Zhang Q, Conley SM, Li G, Yuan X, Li PL. Rac1 GTPase Inhibition Blocked Podocyte Injury and Glomerular Sclerosis During Hyperhomocysteinemia *Via* Suppression of Nucleotide-Binding Oligomerization Domain-Like Receptor Containing Pyrin Domain 3 Inflammasome Activation. *Kidney Blood Press Res* (2019) 44:513–32. doi: 10.1159/000500457
83. Li G, Chen Z, Bhat OM, Zhang Q, Abais-Battad JM, Conley SM, et al. NLRP3 Inflammasome as a Novel Target for Docosahexaenoic Acid Metabolites to Abrogate Glomerular Injury. *J Lipid Res* (2017) 58:1080–90. doi: 10.1194/jlr.M072587

Conflict of Interest: The authors declare that the research was conducted in the absence of any commercial or financial relationships that could be construed as a potential conflict of interest.

Copyright © 2021 Xiong, Meng and Zhang. This is an open-access article distributed under the terms of the Creative Commons Attribution License (CC BY). The use, distribution or reproduction in other forums is permitted, provided the original author(s) and the copyright owner(s) are credited and that the original publication in this journal is cited, in accordance with accepted academic practice. No use, distribution or reproduction is permitted which does not comply with these terms.

frontiers in Immunology

ORIGINAL RESEARCH
published: 26 July 2021
doi: 10.3389/fimmu.2021.697751

Long-Term Protection of CHBP Against Combinational Renal Injury Induced by Both Ischemia–Reperfusion and Cyclosporine A in Mice

*Yufang Zhang[1], Yuanyuan Wu[1,2], Wei Wang[2], Feng Liu[2], Yiwen Zhang[2], Cheng Yang[3], Aifen Liu[1], Jing Wu[2], Tongyu Zhu[3], Michael L. Nicholson[4,5], Yaping Fan[2] and Bin Yang[1,2,4]**

[1] Renal Group, Basic Medical Research Centre, Medical College of Nantong University, Nantong, China, [2] Nantong-Leicester Joint Institute of Kidney Science, Department of Nephrology, Affiliated Hospital of Nantong University, Nantong, China, [3] Department of Urology, Zhongshan Hospital, Shanghai Key Laboratory of Organ Transplantation, Fudan University, Shanghai, China, [4] Department of Cardiovascular Sciences, University of Leicester, University Hospitals of Leicester, Leicester, United Kingdom, [5] Department of Surgery, Addenbrooke's Hospital, University of Cambridge, Cambridge, United Kingdom

OPEN ACCESS

Edited by:
Asha Varghese,
Feinstein Institute for Medical Research, United States

Reviewed by:
Zhenhua Dai,
Guangdong Provincial Academy of Chinese Medical Sciences, China
Huiling Wu,
Royal Prince Alfred Hospital, Australia

***Correspondence:**
Bin Yang
by5@le.ac.uk;
dryangbin@hotmail.com

Specialty section:
This article was submitted to Molecular Innate Immunity, a section of the journal Frontiers in Immunology

Received: 20 April 2021
Accepted: 25 June 2021
Published: 26 July 2021

Citation:
Zhang Y, Wu Y, Wang W, Liu F, Zhang Y, Yang C, Liu A, Wu J, Zhu T, Nicholson ML, Fan Y and Yang B (2021) Long-Term Protection of CHBP Against Combinational Renal Injury Induced by Both Ischemia–Reperfusion and Cyclosporine A in Mice. Front. Immunol. 12:697751. doi: 10.3389/fimmu.2021.697751

Renal ischemia–reperfusion (IR) injury and cyclosporine A (CsA) nephrotoxicity affect allograft function and survival. The prolonged effects and underlying mechanisms of erythropoietin derived cyclic helix B peptide (CHBP) and/or caspase-3 small interfering RNA (CASP-3siRNA) were investigated in mouse kidneys, as well as kidney epithelial cells (TCMK-1), subjected to transplant-related injuries. Bilateral renal pedicles were clamped for 30 min followed by reperfusion for 2 and 8 weeks, with/without 35 mg/kg CsA gavage daily and/or 24 nmol/kg CHBP intraperitoneal injection every 3 days. The ratio of urinary albumin to creatinine was raised by IR injury, further increased by CsA and lowered by CHBP at 2, 4, 6 and 8 weeks, whereas the level of SCr was not significantly affected. Similar change trends were revealed in tubulointerstitial damage and fibrosis, HMGB1 and active CASP-3 protein. Increased apoptotic cells in IR kidneys were decreased by CsA and CHBP at 2 and/or 8 weeks. p70 S6 kinase and mTOR were reduced by CsA with/without CHBP at 2 weeks, so were S6 ribosomal protein and GSK-3β at 8 weeks, with reduced CASP-3 at both time points. CASP-3 was further decreased by CHBP in IR or IR + CsA kidneys at 2 or 8 weeks. Furthermore, in TCMK-1 cells CsA induced apoptosis was decreased by CHBP and/or CASP-3siRNA treatment. Taken together, CHBP predominantly protects kidneys against IR injury at 2 weeks and/or CsA nephrotoxicity at 8 weeks, with different underlying mechanisms. Urinary albumin/creatinine is a good biomarker in monitoring the progression of transplant-related injuries. CsA divergently affects apoptosis in kidneys and cultured kidney epithelial cells, in which CHBP and/or CASP-3siRNA reduces inflammation and apoptosis.

Keywords: apoptosis, CASP-3, cyclic helix B peptide, cyclosporine A, ischemia–reperfusion injury

INTRODUCTION

Kidney transplantation is the life-changing treatment for patients with end-stage renal disease, whereas chronic allograft dysfunction (CAD) and donor shortage are still major obstacles (1). Ischemia–reperfusion (IR) injury, unavoidable in organ transplantation, is associated with delayed graft function, acute rejection, and subsequent CAD (2). IR injury initiates immune responses, oxidative damage, inflammation and cell death, in which tubular epithelial cells (TECs) are most vulnerable (3–5). Survived TECs participate in alleviating injury and promoting repair (6) *via* dedifferentiating and entering cell cycle within a few hours post injury (7). Cyclosporine A (CsA) as an immunosuppressant was used after kidney transplantation to reduce acute rejection and early graft losses (8). However, CsA has not improved long-term graft survival due to its nephrotoxicity (9), characterized by tubulointerstitial fibrosis and afferent arteriolar hyalinosis (10).

Erythropoietin (EPO) protected solid organs including kidneys against IR injury through a heterodimer EPO receptor and β-common receptor (EPOR/βcR), also named as innate repair receptor. EPOR/βcR is pharmacologically distinct from the homodimer receptor of $(EPOR)_2$, a mediator of erythropoiesis (11–13). We showed that EPO protected kidneys against IR injury by decreasing tubular cell apoptosis, but promoting inflammatory cell apoptosis (4, 14, 15). However, the renoprotection of EPO required a large dosage that often causes hypertension and thrombosis (16). Helix B surface peptide (HBSP) was then developed from the 3D structure of EPO, composed of 11 amino acids. HBSP only interacts with EPOR/βcR, without stimulating $(EPOR)_2$, but with a short serum half-life only few minutes (17). A novel metabolic stable cyclic HBSP (CHBP) was further produced by Chinese scientists, with prolonged half-life and potent renoprotection (17–20).

Caspase-3 (CASP-3) is a crucial player in CAD, which executes apoptosis and inflammation in transplant-related renal injuries (21, 22). In addition, HMGB1, a damage-associated molecule, is rapidly released from nuclei to extracellular domains upon injury, mediating apoptosis and inflammation (23), and subsequent fibrosis (24, 25). Our previous study showed that CASP-3 and HMGB1 were associated with the degree of renal IR injury and fibrosis (22, 26), while CHBP and CASP-3 siRNA (CASP-3siRNA) reduced CASP-3 and HMGB1 and improved renal injury (18, 22). CHBP improved endoplasmic reticulum stress at 12 h, inhibited inflammation and apoptosis at 5 and 7 days in mouse IR kidneys (18, 26), and also effectively restored kidney function and structure in isolated porcine IR kidneys and kidney grafts with acute rejection (19, 27, 28). In addition, the continuous administration of HBSP mitigated CASP-3, apoptosis, inflammation and fibrosis in 2-week IR ± CsA kidneys, while CHBP administered at the onset of injury reduced renal fibrosis after 12-week IR (19, 20). CHBP protected aristolochic acid induced acute kidney injury and unilateral ureter obstruction induced tubulointerstitial fibrosis (29, 30). CHBP also ameliorated acute myocardial infarction and acute lung injury by inhibiting apoptosis and inflammatory responses (31, 32).

Prolonged effects of CHBP and underling mechanisms are worth exploring. In this study, therefore, the effect of CHBP on IR and/or CsA-induced combinational injuries in mouse kidneys at 2 and 8 weeks (to avoid prolonged time increasing mortality) and kidney epithelial cells, were further investigated. We demonstrated that CHBP protected kidneys against transplant-related injuries, which might be attributed to different mechanistic signaling pathways at two time points, but both with reduced CASP-3. CHBP and CsA may share comparable immune regulations with the reduction of apoptosis in IR kidneys, whereas CHBP and/or CASP-3siRNA protected kidney epithelial cells against CsA-induced apoptosis.

MATERIALS AND METHODS

Renal IR Injury Model

Male BALB/c mice 25–30 g were randomly divided into five groups: Control, IR, IR + CsA, IR + CHBP, and IR + CsA + CHBP, with 5–8 mice in each group using power calculation according to the key parameters of our previous studies (19–21). All animal procedures were performed according to the guidelines from the Animal Care and Use Committee of Nantong University and the Animal Care Ethics Committee of Jiangsu Province. Mice were anesthetized by 1% pentobarbital (0.01 ml/g), and bilateral renal pedicles were clamped for 30 min and reperfused for 2 or 8 weeks. The color changing of kidneys was confirmed for the efficacy of occlusion and reperfusion. For the sham control, abdominal cavity and renal pedicels were exposed without occlusion. CsA (Novartis Pharma GmbH, Eberbach, Germany) was dissolved in olive oil, gavage daily, 35 mg/kg body weight (BW). CHBP (Shanghai Institute of Materia Medica, Chinese Academy of Sciences) was dissolved in 0.9% saline, intraperitoneally injected after reperfusion every 3 days, 24 nmol/kg BW (19, 27). Urine samples were collected every 2 weeks using metabolic cages and used all 2-week urine samples including end time point collection at 2 weeks end time points for analysis. At 2 and 8 weeks, the blood was drawn, animals were sacrificed and harvested kidneys were fixed with 10% (w/v) neutral buffered formalin or snap frozen in liquid nitrogen (**Figure 1A**). However, not all mice survived to the end point, but at least n ≥3 were used for the each group in all detections. Urinary albumin/creatinine and serum creatinine (SCr) were measured using an automatic biochemistry analyzer (Siemens, Berlin, Germany).

TCMK-1 Cell Model

TCMK-1 cells (a mouse kidney epithelial cell line, CCL139™, American Type Culture Collection, Manassas, USA) (18) were incubated in DMEM/F12 medium supplemented with 10% (v/v) of fetal bovine serum (FBS, Gibco Technologies, Logan, USA), 100 unit/ml penicillin G (Gibco), and 100 μg/ml streptomycin (Gibco) at 37°C in 5% CO_2 atmosphere. The cells grown to about 80% confluent in monolayer in 6-well plates were treated by CsA (2.5, 5, 10, 20 and 40 μg/ml) with/without CHBP (2.5, 5, 10, 20 and 40 ng/ml) for 24 h. TCMK-1 cells were transfected with CASP-3siRNA (10, 20, 30 and 40 nM) by Lipofectamine® RNAiMAX 4–6 h before above treatments (18, 26). The sequences of CASP-3siRNA are: 5'-GCUUCUUCAGAGG CGACUAtt-3' and 5'-UAGUCGCCUCUGAAGAAGCta-3', with the negative control siRNA not targeting any known

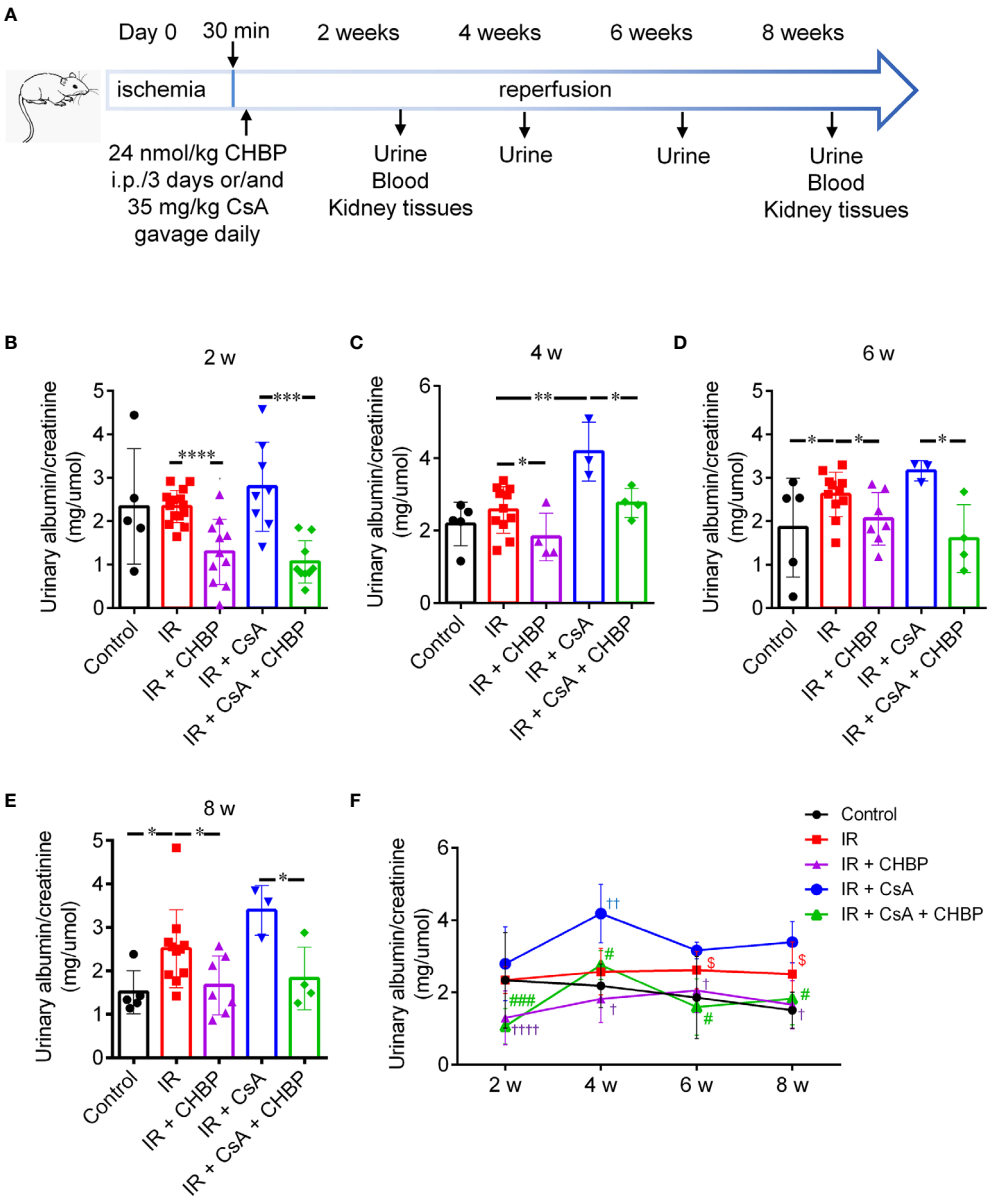


FIGURE 1 | Schematic picture of *in vivo* study design and urinary albumin/creatinine. **(A)** Bilateral renal pedicles were clamped for 30 min followed by reperfusion for 2 and 8 weeks. Approximately 35 mg/kg CsA gavage daily, and/or 24 nmol/kg CHBP intraperitoneal injection every 3 days. Urine samples were collected every 2 weeks, blood samples were drawn and animals were sacrificed at 2 and 8 weeks. **(B–E)** The ratio of urinary albumin/creatinine was shown in the IR group with/without CsA treatment at 2, 4, 6 and 8 weeks. $^{*}P \leq 0.05$, $^{**}P \leq 0.01$, $^{***}P \leq 0.001$, $^{****}P \leq 0.0001$. **(F)** The dynamic profile of urinary albumin/creatinine at all-time points. $^{\dagger}P < 0.05$, $^{\dagger\dagger}P \leq 0.01$, $^{\dagger\dagger\dagger\dagger}P \leq 0.0001$ versus IR; $^{\#}P < 0.05$, $^{\#\#\#}P \leq 0.0005$ versus IR + CsA and $^{\$}P < 0.05$ versus the control. Data were expressed as the mean ± SD of each group (n ≥ 3).

mammalian genes (Thermo Fisher Scientific, Waltham, USA). Obtained data were from three independent experiments at least (**Figure 7A**).

Histological Assessment

Approximately 4 μm paraffin sections were stained by hematoxylin and eosin (H&E). The tubulointerstitial damage (TID) include tubular dilation and vacuolation, interstitial expansion (edema or fibrosis), inflammatory cell infiltration, protein or cell casts in tubular lumina was semi-quantitatively evaluated using 0–4 scales: <5% score 0; 5–25% score 1; 25–50% score 2; 50–75% score 3; and exceeding 75% score 4. Approximately 12 cortical fields of each section at 200× magnification were scored by two examiners blinded to experimental groups (19, 22, 27).

Tubulointerstitial fibrosis was evaluated by Masson's trichrome staining of collagen deposition (19). Twenty fields of

cortical areas were quantified at 400× magnification using the Image-Pro Plus software (Media Cybernetics, Rockville, USA).

Detection of Apoptotic Cells

Fragmented DNAs in paraffin sections were *in situ* end labeled (ISEL) using an ApopTag peroxidase kit (S7100, Appligene Oncor, Illkirch, France) and 3'-amino-9-ethylcarbazole (SK-4200, AEC, Vector, Burlingame, USA) as substrate. Apoptotic cells were counted in tubular, tubular luminal and interstitial areas in 20 fields at 400× magnification (19, 22).

TCMK-1 cells were tripsinized, re-suspended in binding buffer and incubated with FITC-conjugated annexin-V and propidium iodide (PI) for 15 min. Approximately 10,000 cells were analyzed by BD FACS Calibur flow cytometry (BD Biosciences, Franklin Lakes, USA). Living cells (Annexin-V −/PI−), early apoptosis (Annexin-V+/PI−), later apoptosis (Annexin-V+/PI+) or necrosis (Annexin-V−/PI+) were shown as quadrant dot plots and the percentage of the gated cells (18, 26).

Immunohistochemistry

Immunohistochemistry staining of F4/80, a marker of macrophages, was performed on 4 μm paraffin sections treated by 40 μg/ml proteinase K (Sigma, Dorset, UK) at 37°C, 30 min for antigen retrieving. F4/80 (1:50, ab11101, Abcam, Cambridge, UK) was incubated at 4°C overnight. DAKO EnVision™ + Dual Link System-HRP was used as the secondary antibody (DAKO, Glostrup, Denmark). The antibody binding was revealed by 3,3'-diaminobenzidine (SK-4100, DAB, Vector, Burlingame, USA) with hematoxylin counterstaining. The number of macrophages in the tubular, interstitial, and tubular lumen areas were semi-quantitatively analysed in 20 fields at 400× magnification.

Western Blotting Analysis

Kidney proteins (25 μg) were separated by electrophoresis using 12–15% polyacrylamide gels and blotted onto 0.4 μm polyvinylidene difluoride membranes (Roche Diagnostics GmbH, Mannheim, Germany). Membranes were blocked with 5% milk before incubated with full-length CASP-3 (1:200, sc-7148, Santa Cruz Biochemicals, Santa Cruz, USA), HMGB1 (1:1,000, #3935, Cell Signaling Technology, Beverly, USA) or β-actin antibody (1:1,000, ab6276, Abcam, Cambridge, UK). After incubation with peroxidase-conjugated secondary antibody, the binding was revealed by ECL substrate using a Molecular Imager Chemi Doc XRS+ system and semi-quantitatively analyzed by Image Lab Software (Bio-Rad, Berkeley, USA). Optical volume density values of target proteins were expressed as the percentage of average controls after loading correction by β-actin (19, 22).

RT-qPCR

The level of CASP-3 mRNA in kidneys and TCMK-1 cells was detected by reverse transcription (RT) quantitative real-time polymerase chain reaction (qPCR) using a StepOne Plus Real-Time PCR system (Applied Biosystems, Foster City, USA). Approximately 1 μg of total extracted RNAs was used for RT of complementary DNA (cDNA). cDNA was amplified in qPCR reaction buffers (15, 18, 21, 22). The probes of CASP-3 and glyceraldehyde-3-phosphate dehydrogenase (GAPDH) were 6-carboxy-fluorescein (FAM) labeled (Thermo Fisher Scientific). The reaction conditions were as follows: 2 min at 95°C, 40 cycles of 95°C for 10s, then 60°C for 10s. CASP-3 mRNA normalized by GAPDH was calculated against control kidneys using a $2^{-\Delta\Delta Ct}$ method.

Antibody Array Analysis

Eighteen well-characterized phosphorylated or cleaved signaling molecules were simultaneously detected using 50 μg kidney proteins by a slide-based PathScan® Intracellular Signaling Array Kit (#7323, Cell Signaling Technology) according to the manufacturer's instructions. Images were acquired by briefly exposing the slide to the Chemi Doc XRS+ system (Bio-Rad), and semi-quantitatively analyzed by scanning volume density using Alpha View Software 3.3 (Cell Biosciences, Santa Clara, USA) (33).

Statistical Analysis

Data were represented as the mean ± standard deviation (SD). One-way analysis of variance (ANOVA) was used to compare more than two groups, while two-tailed Student's *t*-test was used for two groups using GraphPad Prism 6.0 (GraphPad Software, San Diego, USA). $P \leq 0.05$ was considered to be statistically significant.

RESULTS

CHBP Reduced Urinary Albumin/Creatinine

The ratio of urinary albumin to creatinine (mg/μmol) was increased by CsA compared with that produced by IR kidneys at 4 weeks (**Figures 1B, C**), while this ratio was also increased by IR compared with the sham controls at 6 and 8 weeks (**Figures 1D, E**). Most impressively, CHBP significantly decreased urinary albumin/creatinine produced by IR kidneys with/without CsA treatment at all-time points (**Figures 1B–E**).

The dynamic profile of urinary albumin/creatinine was higher in the IR group compared with the control and CHBP treated groups, and further increased by CsA at all-time points over 2–8 weeks (**Figure 1F**). The difference between the control and IR groups was enlarged by prolonged time, and minimized by CHBP treatment with/without CsA. The change trends in two CsA groups were surprisingly similar, peaked at 4 weeks, decreased at 6 weeks and leveled up to 8 weeks.

Nevertheless, there was no significant difference in the level of SCr between all groups at 2 and 8 weeks (**Supplementary Figures 1A, B**).

CHBP Improved Tissue Damage

The semi-quantitative score of TID in H&E sections was significantly increased by IR compared with the control at both time points (**Figures 2A–D**), further increased by CsA with statistical significance at 8 weeks. Most interestingly, TID was improved by CHBP in IR kidneys at 2 weeks only, and in the CsA-treated kidneys at 2 and 8 weeks.

Interstitial fibrosis revealed in Masson's trichrome stained sections was significantly increased by IR compared with the control, but improved by CHBP at both time points (**Figures 3A–D**), while CsA increased interstitial fibrosis was significantly decreased by CHBP at 8 weeks only.

Cellular Apoptosis in Kidneys Reduced by CHBP and CsA

Apoptotic cells detected by ISEL were mainly located in the tubular and interstitial areas (**Figures 4A–J**), some of them had polymorphic nuclei (4B1, C1), with very few seen in glomerular areas. The total number of apoptotic cells, summed up from that in tubular and interstitial areas and tubular lumina, was greatly increased by IR, but decreased by CsA at 2 and 8 weeks, and by CHBP at 8 weeks (**Figures 4K, L**).

Macrophages in Kidneys Affected by CHBP and CsA

F4/80+ macrophages were mainly located in the interstitial areas (**Supplementary Figure 2A**). The number of macrophages in interstitial areas increased by IR was numerically decreased by CsA and CHBP at 2 weeks, but did not reach statistical significance (**Supplementary Figure 2B**). In addition, the increase trend induced by CsA was also seen at 8 weeks, but there was no statistical significance (**Supplementary Figure 2C**).

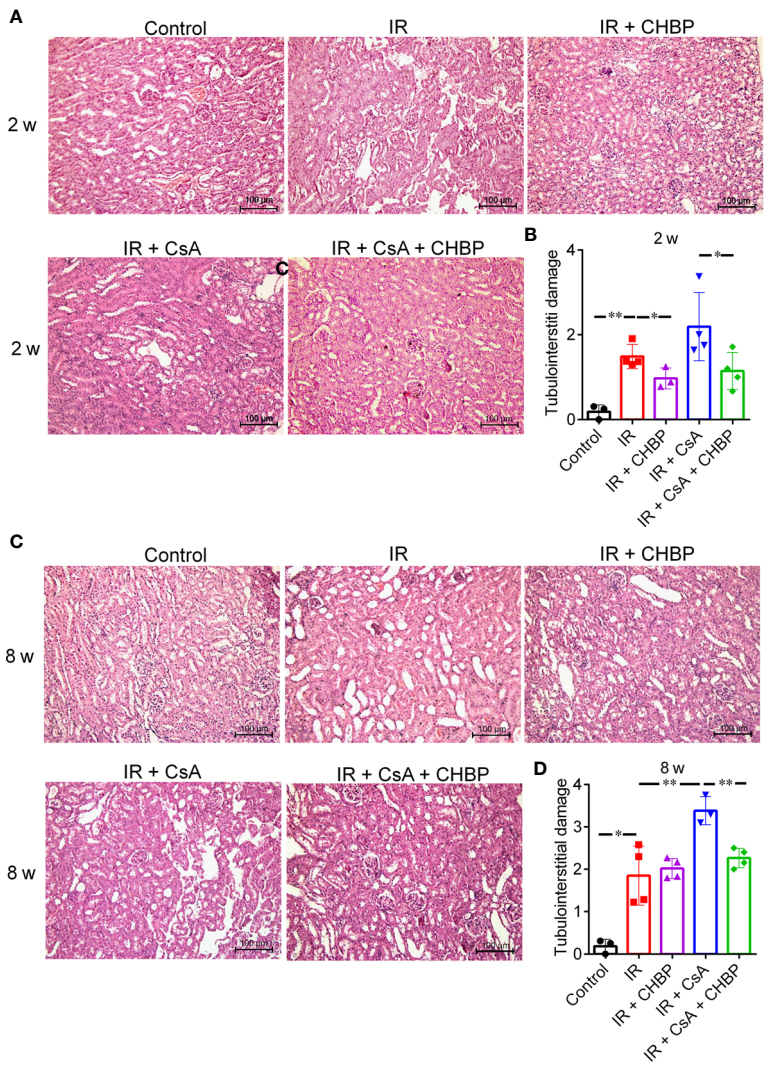


FIGURE 2 | The semi-quantitative score of TID in H&E staining sections. **(A, C)** Tubular dilation, epithelial cell vacuolation, interstitial expansion with edema or inflammation, and cells or cell debris in tubular lumens were mainly seen in IR kidneys. **(B)** CHBP treatment improved the TID compared with IR and IR + CsA groups at 2 weeks. **(D)** The score was further increased in the IR + CsA group but reversed by CHBP at 8 weeks. Data were expressed as the mean ± SD of each group (n ≥ 3). *$P \leq 0.05$; **$P \leq 0.01$.

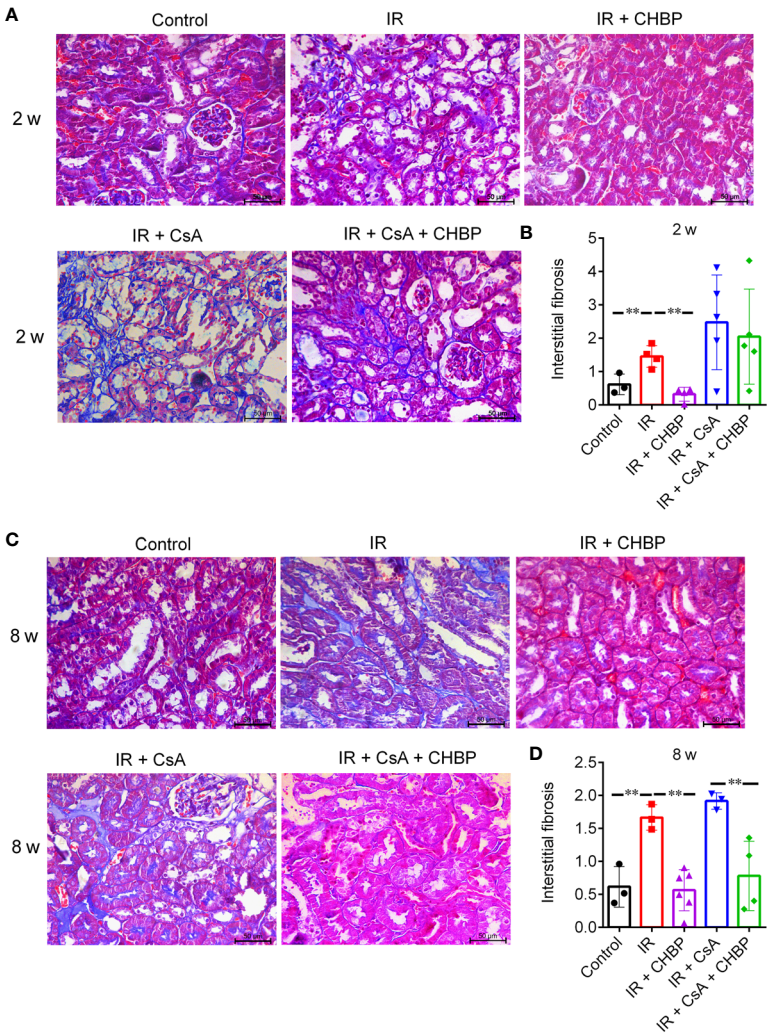


FIGURE 3 | The score of interstitial fibrosis in Masson's trichrome stained sections. **(A, C)** Masson's trichrome staining revealed the interstitial fibrosis. **(B, D)** Interstitial fibrosis was increased by IR compared with the control, but improved by CHBP at both time points. **(D)** The score of fibrosis was significantly decreased by CHBP in the CsA treated group at 8 weeks. Data were expressed as the mean ± SD of each group (n ≥ 3). $^{**}P \leq 0.01$.

CASP-3 mRNA and Its Active Protein Reduced by CHBP

CASP-3 mRNA measured by qPCR was increased by IR at both time points, and further increased by CsA at 2 weeks, but decreased by CHBP in the CsA group at 8 weeks (**Figures 5A, E**).

CASP-3 protein was detected by western blotting, (**Figures 5B, C, F**). Approximately 17 kD active CASP-3 was increased by IR and reversed by CHBP at 2 weeks; further increased by CsA at 8 weeks was also reversed by CHBP (**Figures 5D, G**).

HMGB1 Protein Decreased by CHBP

CHBP decreased the increased HMGB1 protein by IR at 2 weeks (**Figures 5H, I**) and the further increased HMGB1 by CsA compared with IR kidneys at 8 weeks (**Figures 5H, J**), detected by western blotting.

Different Proteins Changed at 2 and 8 Weeks

Eighteen proteins in the kidney were detected at the same time by slide-based antibody array (**Figures 6A, B**). In IR kidneys with/without CHBP treatment, CsA decreased p70 S6 kinase, mTOR and CASP-3 at 2 weeks, and GSK-3β and CASP-3 at 8 weeks (**Figures 6C–E, G, H**). However, S6 ribosomal protein (S6RP) was decreased by CsA in IR kidneys, but reversed by CHBP (**Figure 6F**). CASP-3 was decreased by CHBP in CsA treated IR kidneys at 2 weeks and in IR kidneys at 8 weeks (**Figures 6E–H**).

CHBP Reduced CASP-3 and Apoptosis Increased by CsA in TCMK-1 Cells

CASP-3 mRNA was gradually increased by 2.5–20 μg/ml CsA (**Figure 7B**), so was early apoptotic cells, and reached statistical significance at 10 and 20 μg/ml (**Figure 7C**). However, early

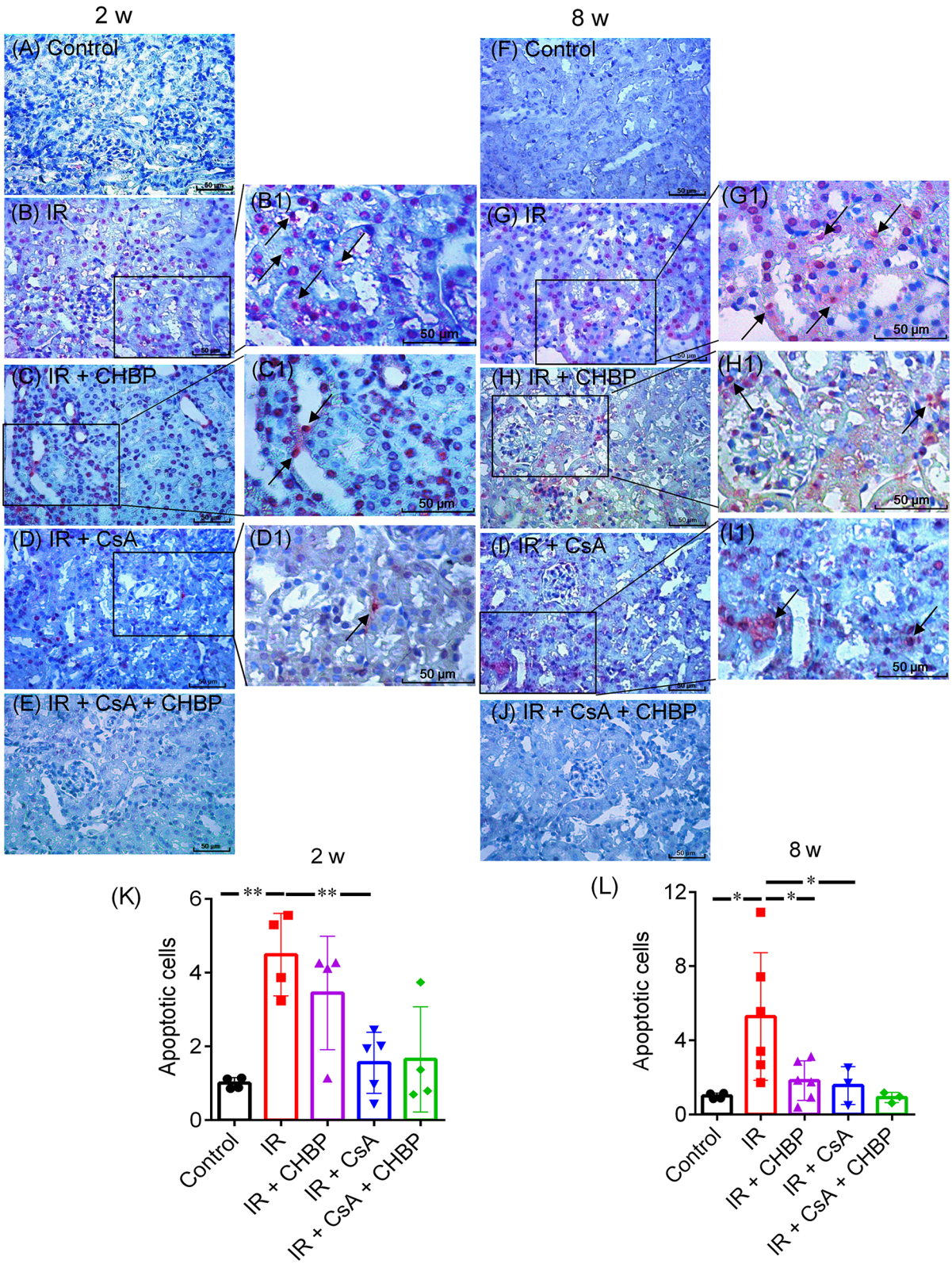


FIGURE 4 | Apoptotic cells detected by labelling fragmented DNAs. **(A–J)** Apoptosis were mainly shown in tubular and interstitial areas. **(B1–D1, G1–I1)** Enlarged pictures were from **(B–D)** and **(G–I)**. **(K, L)** The number of apoptotic cells was greatly increased by IR, but decreased by CsA at 2 and 8 weeks. CHBP treatment decreased apoptotic cells in the IR kidneys at 8 weeks. Data were expressed as the mean ± SD of each group (n ≥ 3). *$P \leq 0.05$; **$P \leq 0.01$.

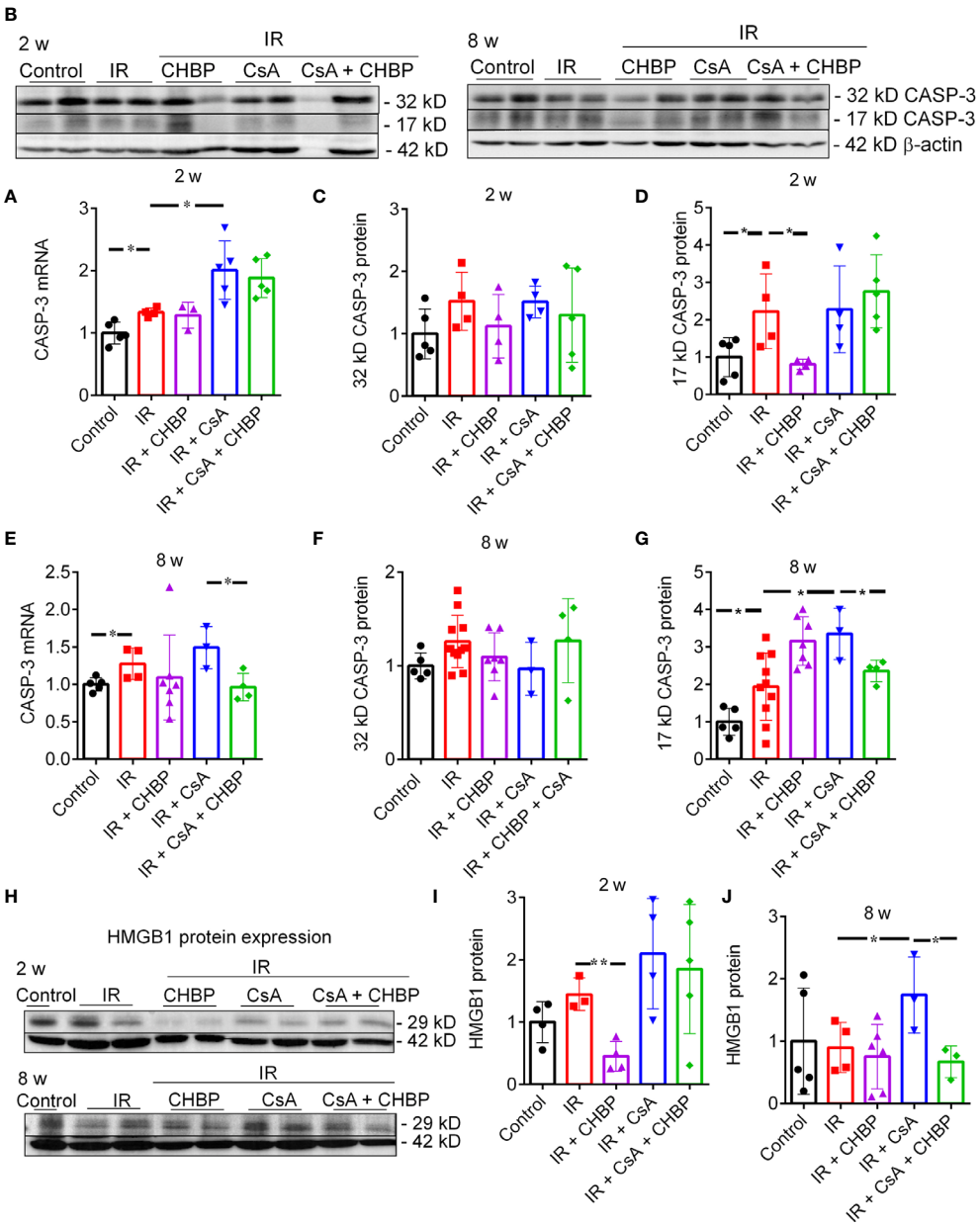


FIGURE 5 | *CASP-3* mRNA and protein, and HMGB1 protein expression. **(A, E)** The relative expression of *caspase 3* mRNA was increased by IR at both time points, and further increased by CsA at 2 weeks, but decreased by CHBP in the CsA group at 8 weeks. **(B–D, F, G)** The level of 17 kD active CASP-3 protein was increased by IR and reversed by CHBP at 2 weeks, and increased by CsA at 8 weeks and also reversed by CHBP. **(H–J)** The expression of HMGB1 protein in 2 and 8 weeks was detected by western blotting. The level of HMGB1 was significantly decreased by CHBP in the IR group at 2 weeks, increased by CsA compared with the IR group and reversed by CHBP at 8 weeks. Data were expressed as the mean ± SD (n ≥ 3). The volume density of western blots was corrected by against 42 kD β-actin as a loading control. $^{*}P \leq 0.05$; $^{**}P \leq 0.01$.

apoptotic cells were gradually reduced by 2.5–40 ng/ml CHBP, and reached statistical significance at 20–40 ng/ml (**Figures 7D, E**).

CASP-3siRNA Decreased CASP-3 mRNA and Apoptosis in TCMK-1 Cells

CASP-3 mRNA was reduced by 10–30 nM/ml CASP-3siRNA compared with the control treated by 20 μg/ml CsA or with NCsiRNA. The suppression was maximized by CASP-3siRNA at 30 nM/ml with 64.85% reduction (**Figure 7F**). CASP-3 mRNA were significantly increased by 20 μg/ml CsA, but reversed by 20 ng/ml CHBP with/without 30 nM CASP-3siRNA (**Figure 7G**).

Early apoptotic cells was also significantly increased by 20 μg/ml CsA, but reversed by CHBP with/without CASP-3siRNA or NCsiRNA (**Figures 7H, I**). Most interestingly, the combined

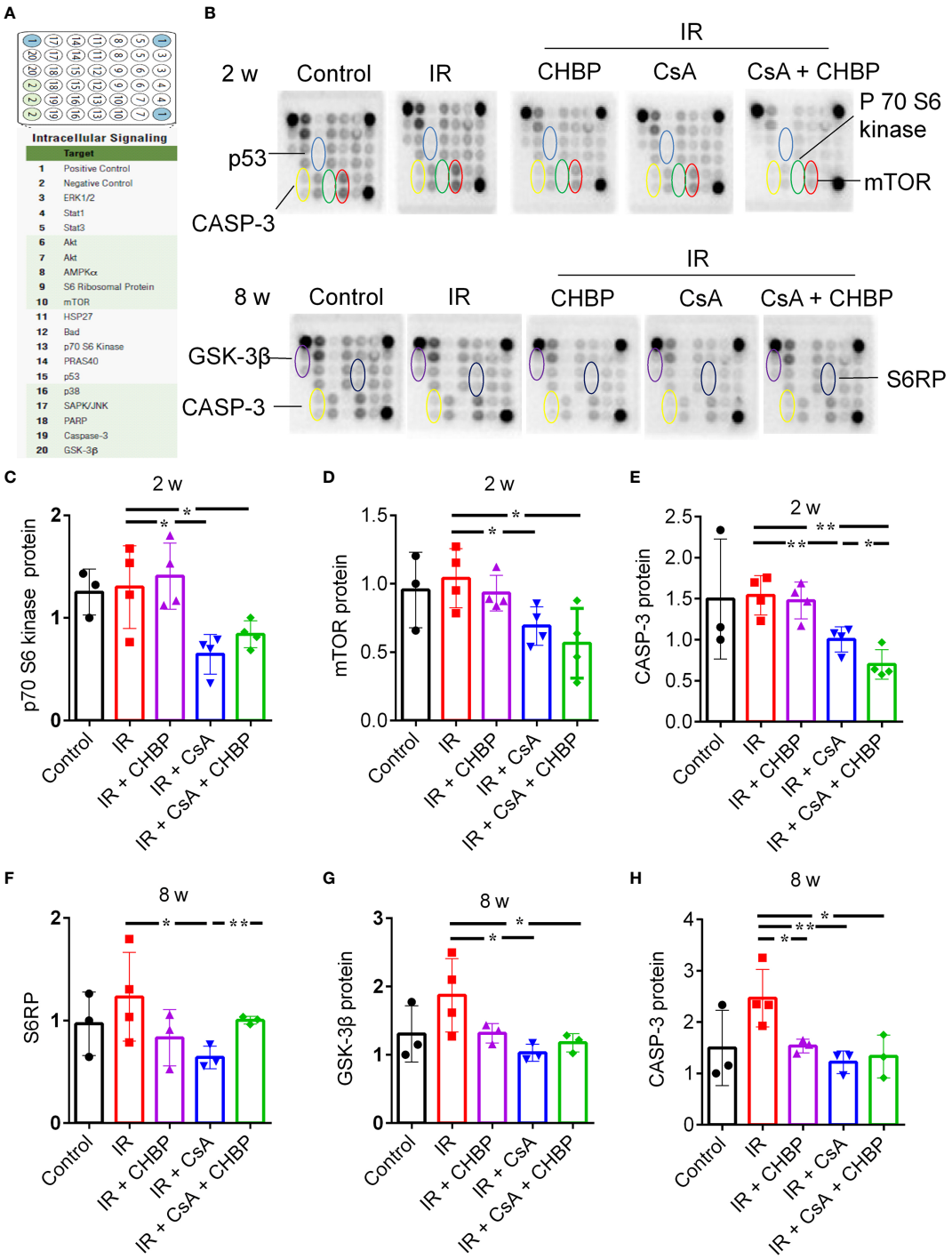


FIGURE 6 | Simultaneous detection of 18 proteins by slide-based antibody array. **(A, B)** The expression of 18 proteins in the kidneys revealed by slide-based antibody array. **(C–E)** CsA decreased p70 S6 kinase, mTOR and caspase-3 at 2 weeks. **(F–H)** S6RP was decreased by CsA in IR kidneys, but reversed by CHBP. CsA decreased GSK-3β and caspase-3 at 8 weeks in IR kidneys with/without CHBP treatment. **(E–H)** Caspase-3 was decreased by CHBP in CsA treated IR kidneys at 2 weeks and in IR kidneys at 8 weeks. Data were expressed as the mean ± SD (n ≥ 3). The volume density was corrected by against the control. $^{*}P \leq 0.05$; $^{**}P \leq 0.01$.

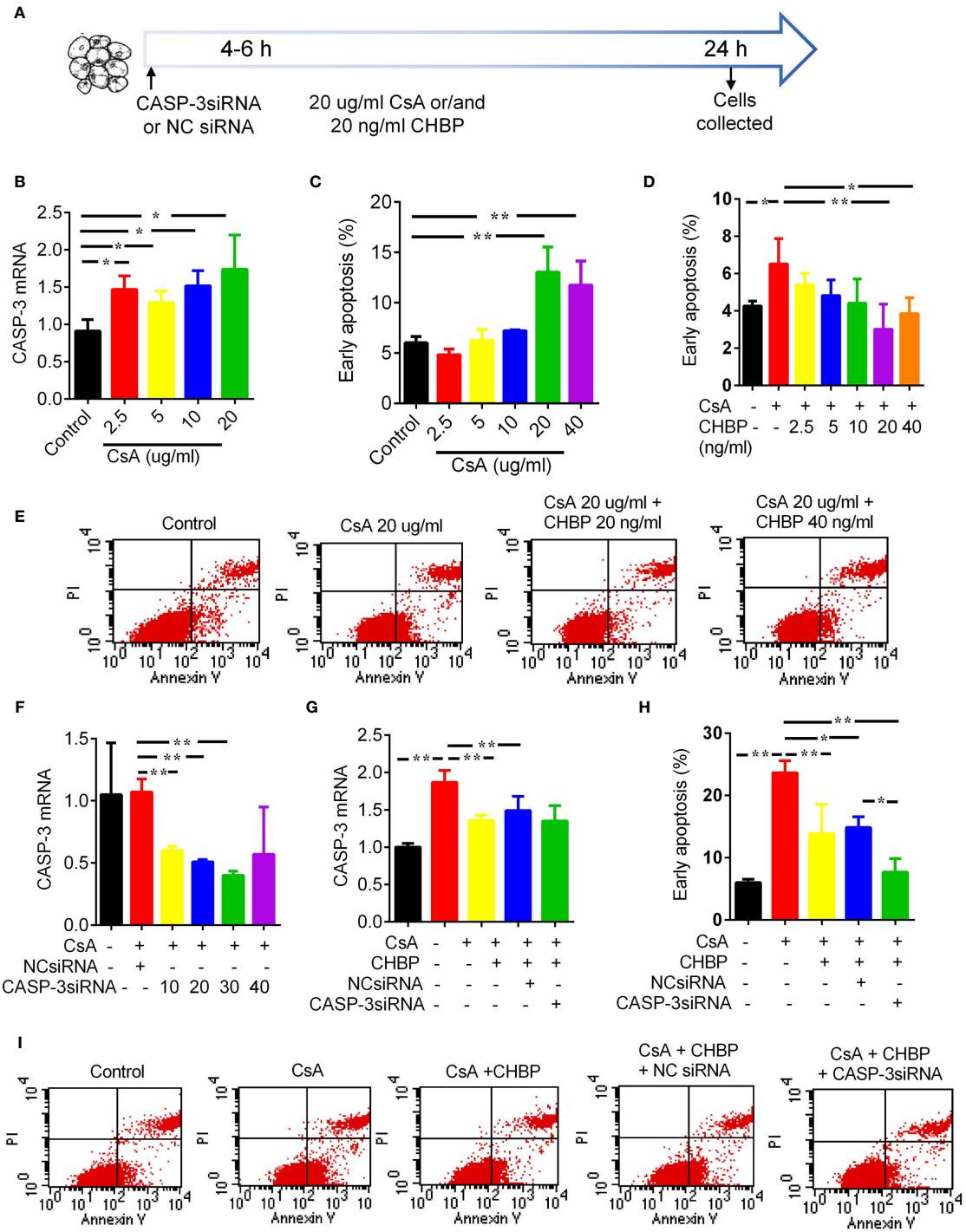


FIGURE 7 | Schematic picture of *in vitro* study design and effects of CsA, CHBP and CASP-3siRNA on TCMK-1 cells. **(A)** TCMK-1 cells were transfected with CASP-3siRNA 4–6 h before treated by CsA with/without CHBP for 24 h. **(B)** The level of CASP-3 mRNA was gradually increased by 2.5–20 μg/ml CsA. **(C)** The percentage of early apoptotic cells was significantly increased by CsA by 20–40 μg/ml and peaked at 20 μg/ml. **(D, E)** Early apoptotic cells was gradually reduced by 2.5–40 ng/ml CHBP, and reached statistical significance at 20–40 ng/ml. **(F)** The expression of CASP-3 mRNA was reduced by 10–30 nM/ml CASP-3siRNA compared with the control treated by 20 μg/ml CsA or with NCsiRNA, but the suppression was maximized at 30 nM/ml with 64.85% reduction. **(G)** CASP-3 mRNA were significantly increased by 20 μg/ml CsA, but reversed by 20 ng/ml CHBP with/without 30 nM CASP-3siRNA. **(H, I)** Early apoptotic cells was significantly increased by 20 μg/ml CsA, but reversed by CHBP with/without CASP-3siRNA or NCsiRNA. Data were expressed as the mean ± SD, (n = 3). $^{*}P < 0.05$, $^{**}P < 0.01$.

treatment of CHBP and CASP-3siRNA further reduced early apoptotic cells compared with the CsA + CHBP + NCsiRNA group.

DISCUSSION

The renoprotection of CHBP against IR injury and HBSP against IR and CsA-induced injury has been shown previously (18, 20, 26, 27). However, there has been no report regarding the long-term effect of CHBP on IR and CsA-induced combinational injury in mouse models. In this study, the renoprotection of CHBP was confirmed not only in renal IR injury but also with CsA nephrotoxicity at 2 and 8 weeks, which better mimicked human kidney transplantation. Urinary albumin/creatinine was more sensitive than SCr in detecting transplant-related injuries, which was supported by changes in apoptosis, inflammation, TID and tubulointerstitial fibrosis. The renoprotective mechanisms of CHBP on IR injury and CsA nephrotoxicity might be different, with decreased mTOR and p70 S6 kinase at 2 weeks, GSK-3β and S6RP at 8 weeks, and CASP-3 protein at both time points. These changes may reflect the dynamic nature of two different injuries, in terms of IR injury gradually eased off in 2 weeks, but CsA nephrotoxicity continuously built up over 8 weeks. In addition, the effect of CsA on apoptosis appeared differently in kidneys having different cell types and kidney epithelial cells *in vitro* (**Supplementary Figure 3**).

CsA is widely used in organ transplantation to prevent rejection, but its nephrotoxicity cannot be ignored (34, 35). Previous long-term studies of kidney IR injury revealed that CsA increased interstitial inflammation and renal fibrosis (19, 21). To explore the pathogenesis of CAD in-depth, the mouse model subjected to renal transplant-related injuries, IR injury and CsA nephrotoxity, was established at 2 and 8 weeks. Urinary albumin/creatinine was increased by IR injury, together with TID, interstitial fibrosis and apoptotic cells in tubular areas. CsA further increased urinary albumin/creatinine from 2 and 4 weeks. However, SCr was not statistically different between groups. Urinary albumin/creatinine, therefore, is a non-invasive and more sensitive biomarker than SCr in monitoring renal transplant-related injuries for middle/long-term.

CsA reduced apoptotic cells in IR kidneys at both time points, which was contradictory to the change in TID, CASP-3, HMGB1, tubulointerstitial fibrosis, and CsA-induced early apoptosis in TCMK-1 cells. Apoptosis is an inevitable phenomenon in transplant-related kidney damage (36), while the apoptosis in different types of cells could lead to inverse outcomes: on one hand excessive TEC apoptosis resulting in tubular atrophy and dysfunction; on the other hand, inflammatory cell apoptosis facilitating the clearance of inflammation, renal structure remodeling and functional recovery (37, 38). Furthermore, the number of macrophages was detected to evaluate the effect of CHBP/CsA on infiltrated inflammatory cells. The results showed that IR increased macrophages mainly located in the interstitial areas were numerously decreased by CsA and further decreased by CHBP at 2 weeks, both of which were reversed at 8 weeks. Because of the large variation between individual animals, there was no any statistically significant difference between groups. Therefore, we concluded that CsA might help renal structure remodeling and functional recovery by decreased apoptosis of TECs at 2 weeks. However, the intensive inflammation at 8 weeks, with decreased apoptosis of inflammatory cells, might aggravate the structural damage of kidneys, impede functional recovery, and lead to tubulointerstitial fibrosis that characterizes CsA-induced long-term nephrotoxicity (21).

The renoprotection of CHBP against IR injury and/or CsA nephrotoxicity was also demonstrated. Given that urinary albumin/creatinine was decreased by CHBP in IR injury and/or CsA groups from 2, 4, 6 to 8 weeks, and TID, active CASP-3 and HMGB1 expression and fibrosis were improved by CHBP in IR kidneys at 2 weeks. IR-induced apoptotic cells were decreased by CHBP at 8 weeks only, which implies the nature of the model in terms of the apoptosis in different types of cells. In addition, CHBP improved interstitial fibrosis, decreased CASP-3 mRNA and 17 kD protein, and HMGB1 in IR kidneys with additional CsA only at 8 weeks, which suggests that the accumulated nephrotoxicity of CsA might further facilitate the renoprotection of CHBP. Therefore, the renoprotection of CHBP was embodied in either improving IR injury, TID and inflammation at 2 weeks, or reducing accumulated CsA nephrotoxicity, apoptosis and interstitial fibrosis at 8 weeks.

To further investigate whether CHBP has comparable immune regulating responses with CsA or what different underlying mechanisms involved in IR injury with/without CsA at 2 and 8 weeks, the expression of multiple mechanistic signaling proteins was analyzed in the same sample by a slide based antibody array. p70 S6 kinase, mTOR, and CASP-3 were decreased by CsA in IR kidneys at 2 weeks, while S6RP, GSK-3β and CASP-3 were reduced at 8 weeks. CHBP also downregulated CASP-3 in IR + CsA treated kidneys at 2 weeks and in IR kidneys at 8 weeks, but upregulated S6RP at 8 weeks in IR kidneys with CsA treatment. It suggests that CHBP protecting IR injury and/or CsA nephrotoxicity might be associated with different mechanistic signaling pathways, with CASP-3 at convergent point. Therefore, CASP3siRNA therapy might be an additional treatment to CHBP for transplant-related renal injury.

Our previous studies have shown the up-regulated CASP-3 in TECs associated with apoptosis and inflammation in different IR-induced acute and chronic kidney injuries (3, 18, 19, 21, 39), and the renoprotection of CASP-3siRNA (22, 40, 41). In order to dissect the effect and mechanism of CHBP and CsA, TCMK-1 cells were stimulated by CsA, and also treated with CHBP and/or CASP-3siRNA. Approximately 20 μg/ml CsA and 20 ng/ml CHBP were most effective at 24 h. CASP-3 mRNA and early apoptotic cells were dose-dependently increased by CsA, but reversed by CHBP with or without CASP-3siRNA, while early apoptotic cells were further decreased by CHBP together with CASP-3siRNA. These results reveal that CHBP combined with CASP-3siRNA had a profound protection against CsA-induced TEC injury by anti-apoptosis. The synergistic effect of both was also revealed in mouse IR kidneys at 48 h in one of our more recent studies (42).

This finding needs to be further validated in animal models at the suitable stage of injury using modified CASP-3siRNA *via* optimized delivery route. The results from this study guide our near future investigations: whether CHBP has comparable immune regulating function with CsA; how different is the underlying mechanism of IR injury and/or CsA nephrotoxity at 2 and 8 weeks; how to combine CHBP with siRNA for therapeutic applications at different stages of injury. The precise mechanism of CHBP and combined effect with CASP-3siRNA are worth further investigating.

In conclusion, the predominant renoprotection of CHBP against IR injury was at 2 weeks, and against CsA nephrotoxicity was at 8 weeks, with urinary albumin/creatinine as a good biomarker in monitoring the progression of transplant-related chronic injuries. The renoprotection of CHBP was associated with different mechanistic signaling proteins such as mTOR at 2 weeks and GSK-3β at 8 weeks, and CASP-3 at both time points. CHBP combined with CASP-3siRNA had a profound protection against CsA-induced injury in TECs, although CsA divergently affected apoptosis in kidneys and TECs.

DATA AVAILABILITY STATEMENT

The raw data supporting the conclusions of this article will be made available by the authors, without undue reservation.

ETHICS STATEMENT

The animal study was reviewed and approved by Animal Care and Use Committee of Nantong University and the Jiangsu Province Animal Care Ethics Committee.

AUTHOR CONTRIBUTIONS

YuZ, FL, and YW contributed equally to this study. BY participated in research design, paper rewriting and funding acquisition. YuZ performed experiments, data analysis and paper preparation. FL, YW, YiZ, AL, and JW participated in the performance of experiments and data analysis. CY performed surgical procedures. TZ, MN, and YF advised research design and performance. All authors contributed to the article and approved the submitted version.

FUNDING

This work was supported by National Natural Science Foundation of China (Grant No. 81170689, 81570677 and 81873622 to BY).

ACKNOWLEDGMENTS

We acknowledge the Basic Medical Research Centre of Nantong University and the Comparative Medicine Institute of Nantong University for providing all facilities. We thank Professor Yaqiu Long (Shanghai Institute of Materia Medica, Chinese Academy of Sciences) for providing CHBP. We also thank Tian Zhao, Zitong Zhao and Long Li (Urology, Zhongshan Hospital, Fudan University) for helping surgically established the animal model.

SUPPLEMENTARY MATERIAL

The Supplementary Material for this article can be found online at: https://www.frontiersin.org/articles/10.3389/fimmu.2021.697751/full#supplementary-material

REFERENCES

1. Papazova DA, Krebber MM, Oosterhuis NR, Gremmels H, van Zuilen AD, Joles JA, et al. Dissecting Recipient From Donor Contribution in Experimental Kidney Transplantation: Focus on Endothelial Proliferation and Inflammation. *Dis Model Mech* (2018) 11:1–13. doi: 10.1242/dmm.035030
2. Zhao H, Alam A, Soo AP, George AJT, Ma D. Ischemia-Reperfusion Injury Reduces Long Term Renal Graft Survival: Mechanism and Beyond. *EBioMedicine* (2018) 28:31–42. doi: 10.1016/j.ebiom.2018.01.025
3. Yang B, Hosgood SA, Da Z, Harper SJ, Waller HL, Kay MD, et al. Biomarkers Assessing Warm Ischemic Injury Using an Isolated Porcine Kidney Hemoreperfusion Model. *Exp Biol Med (Maywood)* (2012) 237:1462–73. doi: 10.1258/ebm.2012.012050
4. Hu L, Yang C, Zhao T, Xu M, Tang Q, Yang B, et al. Erythropoietin Ameliorates Renal Ischemia and Reperfusion Injury *via* inhibiting tubulointerstitial inflammation. *J Surg Res* (2012) 176:260–6. doi: 10.1016/j.jss.2011.06.035S0022-4804(11)00585-3
5. Jansen MP, Emal D, Teske GJ, Dessing MC, Florquin S, Roelofs JJ. Release of Extracellular DNA Influences Renal Ischemia Reperfusion Injury by Platelet Activation and Formation of Neutrophil Extracellular Traps. *Kidney Int* (2017) 91:352–64. doi: 10.1016/j.kint.2016.08.006
6. Liu BC, Tang TT, Lv LL, Lan HY. Renal Tubule Injury: A Driving Force Toward Chronic Kidney Disease. *Kidney Int* (2018) 93:568–79. doi: 10.1016/j.kint.2017.09.033
7. Kusaba T, Lalli M, Kramann R, Kobayashi A, Humphreys BD. Differentiated Kidney Epithelial Cells Repair Injured Proximal Tubule. *Proc Natl Acad Sci U S A* (2014) 111:1527–32. doi: 10.1073/pnas.1310653110
8. Olukman M, Can C, Coskunsever D, Uyanikgil Y, Cavusoglu T, Sozmen E, et al. Urotensin Receptor Antagonist Palosuran Attenuates Cyclosporine-a-Induced Nephrotoxicity in Rats. *Adv Clin Exp Med* (2019) 28:1393–401. doi: 10.17219/acem/104544
9. Koop K, Bakker RC, Eikmans M, Baelde HJ, de Heer E, Paul LC, et al. Differentiation Between Chronic Rejection and Chronic Cyclosporine Toxicity by Analysis of Renal Cortical mRNA. *Kidney Int* (2004) 66:2038–46. doi: 10.1111/j.1523-1755.2004.00976.x
10. Young BA, Burdmann EA, Johnson RJ, Alpers CE, Giachelli CM, Eng E, et al. Cellular Proliferation and Macrophage Influx Precede Interstitial Fibrosis in Cyclosporine Nephrotoxicity. *Kidney Int* (1995) 48:439–48. doi: 10.1038/ki.1995.312
11. Shi M, Flores B, Li P, Gillings N, McMillan KL, Ye J, et al. Effects of Erythropoietin Receptor Activity on Angiogenesis, Tubular Injury, and Fibrosis in Acute Kidney Injury: A "U-shaped" Relationship. *Am J Physiol Renal Physiol* (2018) 314:F501–16. doi: 10.1152/ajprenal.00306.2017
12. Zhang Y, Chen W, Wu Y, Yang B. Renoprotection and Mechanisms of Erythropoietin and Its Derivatives Helix B Surface Peptide in Kidney Injuries. *Curr Protein Pept Sci* (2017) 18:1183–90. doi: 10.2174/1389203717666160909144436
13. Vazquez-Mendez E, Gutierrez-Mercado Y, Mendieta-Condado E, Galvez-Gastelum FJ, Esquivel-Solis H, Sanchez-Toscano Y, et al. Recombinant Erythropoietin Provides Protection Against Renal Fibrosis in Adenine-Induced Chronic Kidney Disease. *Mediators Inflamm* (2020) 2020:8937657. doi: 10.1155/2020/8937657
14. Yang B, Hosgood SA, Bagul A, Waller HL, Nicholson ML. Erythropoietin Regulates Apoptosis, Inflammation and Tissue Remodelling *via* caspase-3 and

IL-1beta in isolated hemoperfused kidneys. *Eur J Pharmacol* (2011) 660:420–30. doi: 10.1016/j.ejphar.2011.03.044S0014-2999(11)00360-8
15. Yang B, Jain S, Ashra SY, Furness PN, Nicholson ML. Apoptosis and Caspase-3 in Long-Term Renal Ischemia/Reperfusion Injury in Rats and Divergent Effects of Immunosuppressants. *Transplantation* (2006) 81:1442–50. doi: 10.1097/01.tp.0000209412.77312.69
16. Palmer SC, Navaneethan SD, Craig JC, Johnson DW, Tonelli M, Garg AX, et al. Meta-Analysis: Erythropoiesis-Stimulating Agents in Patients With Chronic Kidney Disease. *Ann Intern Med* (2010) 153:23–33. doi: 10.7326/0003-4819-153-1-201007060-00252
17. Brines M, Patel NS, Villa P, Brines C, Mennini T, De Paola M, et al. Nonerythropoietic, Tissue-Protective Peptides Derived From the Tertiary Structure of Erythropoietin. *Proc Natl Acad Sci U S A* (2008) 105:10925–30. doi: 10.1073/pnas.0805594105
18. Zhang Y, Wang Q, Liu A, Wu Y, Liu F, Wang H, et al. Erythropoietin Derived Peptide Improved Endoplasmic Reticulum Stress and Ischemia-Reperfusion Related Cellular and Renal Injury. *Front Med (Lausanne)* (2020) 7:5. doi: 10.3389/fmed.2020.00005
19. Wu Y, Zhang J, Liu F, Yang C, Zhang Y, Liu A, et al. Protective Effects of HBSP on Ischemia Reperfusion and Cyclosporine a Induced Renal Injury. *Clin Dev Immunol* (2013) 2013:758159. doi: 10.1155/2013/758159
20. Yang C, Cao Y, Zhang Y, Li L, Xu M, Long Y, et al. Cyclic Helix B Peptide Inhibits Ischemia Reperfusion-Induced Renal Fibrosis *via* the PI3K/Akt/FoxO3a pathway. *J Transl Med* (2015) 13:355. doi: 10.1186/s12967-015-0699-2
21. Yang B, Jain S, Pawluczyk IZ, Imtiaz S, Bowley L, Ashra SY, et al. Inflammation and Caspase Activation in Long-Term Renal Ischemia/Reperfusion Injury and Immunosuppression in Rats. *Kidney Int* (2005) 68:2050–67. doi: 10.1111/j.1523-1755.2005.00662.x
22. Yang C, Zhao T, Zhao Z, Jia Y, Li L, Zhang Y, et al. Serum-Stabilized Naked Caspase-3 siRNA Protects Autotransplant Kidneys in a Porcine Model. *Mol Ther* (2014) 22:1817–28. doi: 10.1038/mt.2014.111
23. Li J, Gong Q, Zhong S, Wang L, Guo H, Xiang Y, et al. Neutralization of the Extracellular HMGB1 Released by Ischaemic Damaged Renal Cells Protects Against Renal Ischaemia-Reperfusion Injury. *Nephrol Dial Transplant* (2011) 26:469–78. doi: 10.1093/ndt/gfq466
24. Lynch J, Nolan S, Slattery C, Feighery R, Ryan MP, McMorrow T. High-Mobility Group Box Protein 1: A Novel Mediator of Inflammatory-Induced Renal Epithelial-Mesenchymal Transition. *Am J Nephrol* (2010) 32:590–602. doi: 10.1159/000320485
25. Cheng M, Liu H, Zhang D, Liu Y, Wang C, Liu F, et al. HMGB1 Enhances the AGE-Induced Expression of CTGF and TGF-Beta *via* RAGE-Dependent Signaling in Renal Tubular Epithelial Cells. *Am J Nephrol* (2015) 41:257–66. doi: 10.1159/000381464
26. Liu A, Wu J, Yang C, Wu Y, Zhang Y, Zhao F, et al. TRPM7 in CHBP-Induced Renoprotection Upon Ischemia Reperfusion-Related Injury. *Sci Rep* (2018) 8:5510. doi: 10.1038/s41598-018-22852-2
27. Yang C, Zhang Y, Wang J, Li L, Wang L, Hu M, et al. A Novel Cyclic Helix B Peptide Inhibits Dendritic Cell Maturation During Amelioration of Acute Kidney Graft Rejection Through Jak-2/STAT3/SOCS1. *Cell Death Dis* (2015) 6:e1993. doi: 10.1038/cddis.2015.338
28. Yang C, Hosgood SA, Meeta P, Long Y, Zhu T, Nicholson ML, et al. Cyclic Helix B Peptide in Preservation Solution and Autologous Blood Perfusate Ameliorates Ischemia-Reperfusion Injury in Isolated Porcine Kidneys. *Transplant Direct* (2015) 1:e6. doi: 10.1097/TXD.0000000000000515
29. Qi RC, Zhang WT, Zheng L, Xu M, Rong RM, Zhu TY, et al. Cyclic Helix B Peptide Ameliorates Renal Tubulointerstitial Fibrosis Induced by Unilateral Ureter Obstruction *via* inhibiting NLRP3 pathway. *Ann Trans Med* (2020) 8:167. doi: 10.21037/atm.2020.02.12
30. Zeng YG, Zheng L, Yang ZR, Yang C, Zhang Y, Li JW, et al. Protective Effects of Cyclic Helix B Peptide on Aristolochic Acid Induced Acute Kidney Injury. *Biomed Pharmacotherapy* (2017) 94:1167–75. doi: 10.1016/j.biopha.2017.07.131
31. Yang C, Zhang C, Jia JG, Wang LY, Zhang WT, Li JW, et al. Cyclic Helix B Peptide Ameliorates Acute Myocardial Infarction in Mice by Inhibiting Apoptosis and Inflammatory Responses. *Cell Death Discov* (2019) 5:78. doi: 10.1038/s41420-019-0161-y
32. Zhang XP, Zhang WT, Qiu Y, Ju MJ, Yang C, Tu GW, et al. Cyclic Helix B Peptide Alleviates Sepsis-Induced Acute Lung Injury by Downregulating NLRP3 Inflammasome Activation in Alveolar Macrophages. *Int Immunopharmacol* (2020) 88:106849. doi: 10.1016/j.intimp.2020.106849
33. Liu W, Zhang L, Xuan K, Hu C, Li L, Zhang Y, et al. Alkaline Phosphatase Controls Lineage Switching of Mesenchymal Stem Cells by Regulating the LRP6/GSK3beta Complex in Hypophosphatasia. *Theranostics* (2018) 8:5575–92. doi: 10.7150/thno.27372
34. Aigner A. Applications of RNA Interference: Current State and Prospects for siRNA-Based Strategies *In Vivo*. *Appl Microbiol Biotechnol* (2007) 76:9–21. doi: 10.1007/s00253-007-0984-y
35. Bhavsar D, Subramanian K, Sethuraman S, Krishnan UM. Translational siRNA Therapeutics Using Liposomal Carriers: Prospects & Challenges. *Curr Gene Ther* (2012) 12:315–32. doi: 10.2174/156652312802083611
36. Hu C, Li L, Ding P, Li L, Ge X, Zheng L, et al. Complement Inhibitor CRIg/FH Ameliorates Renal Ischemia Reperfusion Injury *via* Activation of PI3K/AKT Signaling. *J Immunol* (2018) 201:3717–30. doi: 10.4049/jimmunol.1800987
37. Hesketh EE, Kluth DC, Hughes J. Apoptotic Cell Administration Is Detrimental in Murine Renal Ischaemia Reperfusion Injury. *J Inflamm (Lond)* (2014) 11:31. doi: 10.1186/s12950-014-0031-6
38. Fogarty CE, Bergmann A. The Sound of Silence: Signaling by Apoptotic Cells. *Curr Top Dev Biol* (2015) 114:241–65. doi: 10.1016/bs.ctdb.2015.07.013
39. Yang B, El Nahas AM, Thomas GL, Haylor JL, Watson PF, Wagner B, et al. Caspase-3 and Apoptosis in Experimental Chronic Renal Scarring. *Kidney Int* (2001) 60:1765–76. doi: 10.1046/j.1523-1755.2001.00013.x
40. Yang C, Zhang C, Zhao Z, Zhu T, Yang B. Fighting Against Kidney Diseases With Small Interfering RNA: Opportunities and Challenges. *J Transl Med* (2015) 13:39. doi: 10.1186/s12967-015-0387-2
41. Yang C, Li L, Xue Y, Zhao Z, Zhao T, Jia Y, et al. Innate Immunity Activation Involved in Unprotected Porcine Auto-Transplant Kidneys Preserved by Naked Caspase-3 siRNA. *J Transl Med* (2013) 11:210. doi: 10.1186/1479-5876-11-210
42. Wu Y, Chen W, Zhang Y, Liu A, Yang C, Wang H, et al. Potent Therapy and Transcriptional Profile of Combined Erythropoietin-Derived Peptide Cyclic Helix B Surface Peptide and Caspase-3 siRNA Against Kidney Ischemia/Reperfusion Injury in Mice. *J Pharmacol Exp Ther* (2020) 375:92–103. doi: 10.1124/jpet.120.000092

Conflict of Interest: The authors declare that the research was conducted in the absence of any commercial or financial relationships that could be construed as a potential conflict of interest.

Publisher's Note: All claims expressed in this article are solely those of the authors and do not necessarily represent those of their affiliated organizations, or those of the publisher, the editors and the reviewers. Any product that may be evaluated in this article, or claim that may be made by its manufacturer, is not guaranteed or endorsed by the publisher.

Copyright © 2021 Zhang, Wu, Wang, Liu, Zhang, Yang, Liu, Wu, Zhu, Nicholson, Fan and Yang. This is an open-access article distributed under the terms of the Creative Commons Attribution License (CC BY). The use, distribution or reproduction in other forums is permitted, provided the original author(s) and the copyright owner(s) are credited and that the original publication in this journal is cited, in accordance with accepted academic practice. No use, distribution or reproduction is permitted which does not comply with these terms.

frontiers in Immunology

ORIGINAL RESEARCH
published: 06 September 2021
doi: 10.3389/fimmu.2021.697760

Properdin Deficiency Impairs Phagocytosis and Enhances Injury at Kidney Repair Phase Post Ischemia–Reperfusion

Yuanyuan Wu[1,2†], Zinah D. Zwaini[3†], Nigel J. Brunskill[1,4], Xinyue Zhang[1], Hui Wang[4], Ravinder Chana[3], Cordula M. Stover[3] and Bin Yang[1,4]*

[1] Department of Cardiovascular Sciences, College of Life Sciences, University of Leicester, University Hospitals of Leicester NHS Trust, Leicester, United Kingdom, [2] Basic Medical Research Centre, Medical School of Nantong University, Nantong, China, [3] Department of Respiratory Sciences, College of Life Sciences, University of Leicester, Leicester, United Kingdom, [4] Nantong-Leicester Joint Institute of Kidney Science, Department of Nephrology, Affiliated Hospital of Nantong University, Nantong, China

OPEN ACCESS

Edited by:
Cees Van Kooten, Leiden University, Netherlands

Reviewed by:
Conrad Anthony Farrar, King's College London, United Kingdom
Kushagra Bansal, Harvard Medical School, United States

***Correspondence:**
Bin Yang
by5@le.ac.uk

†These authors have contributed equally to this work and share first authorship

Specialty section:
This article was submitted to Molecular Innate Immunity, a section of the journal Frontiers in Immunology

Received: *20 April 2021*
Accepted: *05 August 2021*
Published: *06 September 2021*

Citation:
Wu Y, Zwaini ZD, Brunskill NJ, Zhang X, Wang H, Chana R, Stover CM and Yang B (2021) Properdin Deficiency Impairs Phagocytosis and Enhances Injury at Kidney Repair Phase Post Ischemia–Reperfusion. Front. Immunol. 12:697760. doi: 10.3389/fimmu.2021.697760

Properdin, a positive regulator of complement alternative pathway, participates in renal ischemia–reperfusion (IR) injury and also acts as a pattern-recognition molecule affecting apoptotic T-cell clearance. However, the role of properdin in tubular epithelial cells (TECs) at the repair phase post IR injury is not well defined. This study revealed that properdin knockout (P^{KO}) mice exhibited greater injury in renal function and histology than wild-type (WT) mice post 72-h IR, with more apoptotic cells and macrophages in tubular lumina, increased active caspase-3 and HMGB1, but better histological structure at 24 h. Raised erythropoietin receptor by IR was furthered by P^{KO} and positively correlated with injury and repair markers. Properdin in WT kidneys was also upregulated by IR, while H_2O_2-increased properdin in TECs was reduced by its small-interfering RNA (siRNA), with raised HMGB1 and apoptosis. Moreover, the phagocytic ability of WT TECs, analyzed by pHrodo *Escherichia coli* bioparticles, was promoted by H_2O_2 but inhibited by P^{KO}. These results were confirmed by counting phagocytosed H_2O_2-induced apoptotic TECs by *in situ* end labeling fragmented DNAs but not affected by additional serum with/without properdin. Taken together, P^{KO} results in impaired phagocytosis at the repair phase post renal IR injury. Properdin locally produced by TECs plays crucial roles in optimizing damaged cells and regulating phagocytic ability of TECs to effectively clear apoptotic cells and reduce inflammation.

Keywords: apoptosis, inflammation, ischemia–reperfusion injury, phagocytosis, properdin, repair

INTRODUCTION

Acute kidney injury (AKI) has high morbidity and mortality and also has a potential of developing chronic kidney disease (CKD) (1–3). Renal ischemia–reperfusion (IR) injury, a major cause of AKI, is characterized by circulatory disturbance, complement activation, tubular injury, interstitial inflammation, and eventual fibrosis (4, 5). Tubular epithelial cells (TECs) are most vulnerable to IR injury but also actively participate in repair through dedifferentiation, proliferation, and clearing

injured cells by phagocytosis (6–8). However, these functions may be maladaptive in severe and repeated mild injury, resulting in persistent complement activation, inflammation, and fibrosis (9, 10).

Complement activation *via* the alternative pathway (AP) is key to induce renal IR injury in rodent models. The suppression of the AP promotor, complement factor B, using monoclonal antibodies (mAb) or genetic modification significantly preserved renal function and morphology in mice subject to IR injury (11, 12). Conversely, the depletion of the AP inhibitors, decay-accelerating factor (DAF) and CD59, also exacerbates renal IR injury (13).

Properdin, the only known positive regulator of the AP, mainly produced by inflammatory cells (14–17), stabilizes complement 3 (C3) convertase (C3bBb), thereby providing a C3b amplification loop, and then stabilizes C5 convertase (18, 19). Inhibiting properdin by either antimouse mAb or gene deletion in DAF and CD59 double-knockout ($DAF^{-/-}CD59^{-/-}$) mice ameliorated early renal IR injury at 24 h (20).

Properdin also functions as a pattern-recognition molecule (PRM) by binding to targets such as damaged cells or bacteria, independent of its main ligand C3b (21–24). Properdin may also bind to the luminal membrane of proximal TECs in the proteinuric kidneys to mediate complement activation (25). However, the precise role of properdin in renal IR injury and repair and its potential function as a PRM in kidneys and TECs are incompletely defined. We hypothesized that properdin may have different roles at different stages of IR injury, either detrimental in the early injury stage by activating AP or beneficial at the late repair stage by facilitating phagocytic clearance of damaged cells.

In this study, properdin knockout (P^{KO}) mice and counterpart wild-type (WT) mice were subject to 30 min of bilateral renal ischemia followed by 72 h reperfusion. TCMK-1 cells (mouse kidney cell line) and TECs isolated from P^{KO} and WT mice, respectively, were exposed to hydrogen peroxidase (H_2O_2) to mimic the oxidative stress of IR injury. The role of properdin as a PRM and beyond was explored at the repair stage of kidneys post IR and in TECs subjected to IR-related injury, focusing on phagocytosis, apoptosis, and inflammation.

MATERIALS AND METHODS

Animal Model

Properdin-deficient mice were generated by site-specific targeting and maintained at University of Leicester (17). Male C57BL/6 WT and P^{KO} mice aged 8–12 weeks were used in this study. All procedures were performed in accordance with the institutional guidelines reviewed by the Animal Welfare and Ethical Review Body and under the license approved by the UK Home Office (Project License, 70/8169 and Personal License, IA536CDE7). Mice were randomly divided into four groups: (I) WT sham (n = 4), (II) P^{KO} sham (n = 5), (III) WT IR (n = 9), and (IV) P^{KO} IR (n = 7). The animals were anesthetized by inhalation of 2.5% isoflurane in oxygen, and experimental procedures were optimized and refined based upon published protocols (26). The body temperature of animals during surgery was maintained at 36.5°C–37°C. Bilateral renal pedicles were exposed in the lateral position, dissected and clamped with a non-traumatic vascular clip for 30 min. After application of clips, the kidney was observed until patchy blanching developed and then replaced into the abdominal cavity. After removal of clips, gradual appearance of a normal pink color indicated kidney reperfusion.

After 72 h, the animals were bled by cardiac puncture and then sacrificed. The kidneys were harvested and snap frozen in liquid nitrogen or fixed in 4% (w/v) formaldehyde in 10% normal saline for further analysis. The animal experimental design is shown in **Figure 1A**.

Renal Function

Serum creatinine (SCr) and blood urine nitrogen (BUN) were determined using the QuantiChrom™ Creatinine or Urea Assay Kit (BioAssay System, Hayward, USA). All procedures were performed according to the manufacturer's instructions.

Histology

Paraffin-embedded kidney tissues were sectioned at 4 μm and stained by hematoxylin and eosin (H&E). The scoring of tubulointerstitial damage (TID) and counting of mitotic figures in the cortex was performed blindly to experimental groups by two independent researchers. The criteria of TID scoring included the loss of tubular epithelia, tubular cell vacuolation, tubular dilatation, luminal cast formation, and interstitial expansion (27). A histological score was assigned based on the percentage of affected areas in observed regions: 0, no damage <1%; 1, 1%–25%; 2, 26%–50%; 3, 51%–75%; and 4, >75%. In addition, mitotic figures were counted as condensed chromosomes aligned in metaphase in dividing cells (28). TID and mitotic figures were evaluated in 12 or 20 non-overlapping cortical fields at 200× or 400× magnification, respectively.

In Situ End Labeling of Apoptotic Cells

Apoptotic cells in kidneys were identified by *in situ* end labeling (ISEL) of fragmented DNA using terminal deoxynucleotidyl transferase-mediated uridine triphosphate provided in ApopTag® Peroxidase Kit (Merck Millipore, Darmstadt, Germany) (27). The ISEL+ cells were counted respectively in the tubular areas, tubular lumens, and interstitial areas of the renal cortex of 20 non-overlapping fields at 400× magnification.

Immunoblotting

Twenty-five micrograms of protein was separated by the electrophoresis of polyacrylamide denaturing gels and transferred onto polyvinylidene fluoride membrane. The primary antibodies, rabbit–antimouse caspase-3 (1:400, 9662, CST, Danvers, USA), rabbit–antimouse high-mobility group box-1 protein (HMGB1, 1:1,000, 3935, CST), mouse–antimouse proliferating cell nuclear antigen (PCNA, 1:1,000, M0879, DAKO, Glostrup, Denmark), rabbit–antimouse erythropoietin receptor (EPOR, 1:1,000, PAB18350, Abnova, Taiwan), rabbit–antimouse properdin (1:1,000, AB186834, Abcam, Cambridge, USA) and

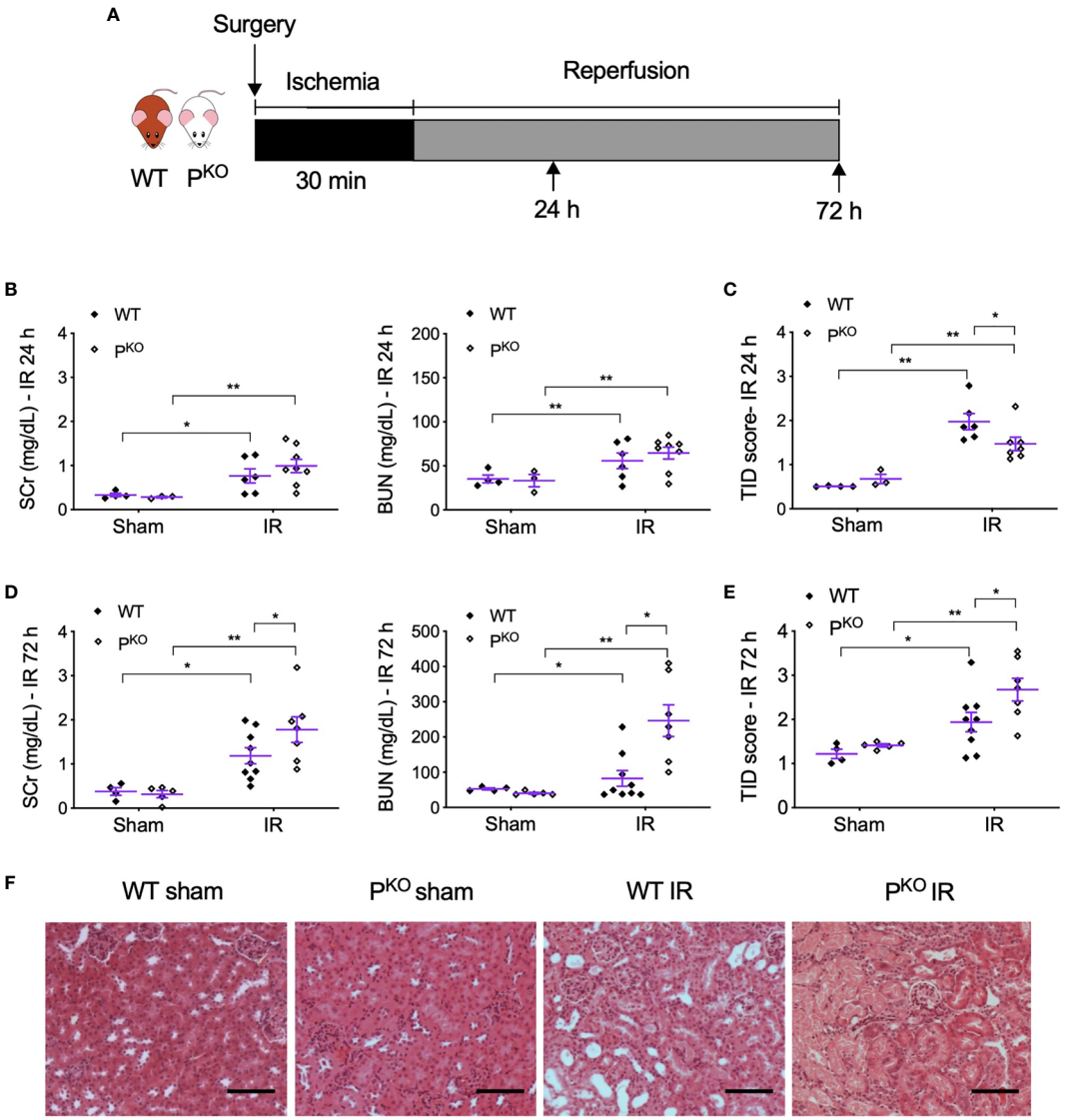


FIGURE 1 | P^{KO} alleviated kidney structural damage at 24 h but aggravated renal functional and structural injury at 72 h post IR. **(A)** Schematic illustration of mouse experimental design. Bilateral kidney ischemia for 30 min and reperfusion for 24 h or 72 h were performed in male WT and P^{KO} C57BL/6 mice. **(B, C)** SCr, BUN, and semiquantitative score of TID in both WT and P^{KO} mice at 24 h were increased by IR, but only TID was improved by P^{KO} (sham: n = 3–4; IR: n = 6–8). **(D, E)** At 72 h, SCr, BUN, and TID score in both WT and P^{KO} mice were also elevated by IR, but all parameters were further increased by P^{KO} (sham: n = 4–5; IR: n = 7–9). Data were shown as means ± SEMs, and analyzed by one-way ANOVA and LSD test. $^{*}p < 0.05$; $^{**}p < 0.01$. **(F)** Representative H&E stained images showing the cortex structure of the kidney at 72 h post IR. Scale bar: 100 μm.

mouse–antimouse β-actin (1:5,000, A5441, Sigma, Dorset, UK), were applied to the membranes overnight at 4°C, followed by the incubation of horseradish peroxidase-labeled secondary antibody (goat–antirabbit/mouse, K4063, DAKO) and developed by enhanced chemiluminescence (Thermo Fisher Scientific, Rockford, USA). The ratio of target protein to β-actin in volume density, as an endogenous loading control, was calculated for each detection, and then, the fold change of detected protein in the experimental group against the WT sham control was obtained as final results (27).

Immunohistochemistry

Antigen retrieval was performed using 20–40 μg/ml proteinase K (Sigma) digestion at 37°C for 15 min. The sections were then blocked with 10% goat serum and 0.5% bovine serum albumin (BSA) in 3% milk for 1 h at room temperature, followed by primary antibody labeling, mouse–antimouse F4/80 (1:100, ab100790, Abcam) or rabbit–antimouse erythropoietin receptor (EPOR, 1:800, PAB18350, Abnova) at 4°C overnight. The next day, DAKO secondary (K4063) was applied to the sections for 30 min. The antibody binding was then revealed by

3,3′-diaminobenzidine (DAB, Vector, Burlingame, USA) and hematoxylin counterstaining.

For double labeling of properdin and F4/80 in the kidneys of WT mice, proteinase K at 40 μg/ml was used for antigen retrieval at 37°C for 30 min. After the staining of F4/80 was obtained, the sections were then incubated with primary antibody rabbit–antimouse properdin (1:200, ABF185, Merck Millipore) at 4°C overnight. Afterwards, biotinylated secondary goat–antirabbit immunoglobulin G (IgG) was applied to the slides for 30 min at 37°C (1:300, BA-1000, Vector), followed by alkaline phosphatase streptavidin (1:200, SA-5100, Vector) for 30 min at 37°C, and then developed by Fast Red (Sigma) for 8 min.

Real-Time Quantitative PCR

Total RNA was extracted using Trizol reagent (Thermo Fisher Scientific). Three micrograms of total RNA was used for reverse transcription (Thermo Fisher Scientific). One microliter of complementary DNA (cDNA) product was amplified with SYBR Green reaction system (Bioline, London, UK) containing 250 nM forward and reverse primers (Sigma, **Table 1**) at 95°C for 10 min followed by 40 cycles of 95°C for 20 s, 60°C for 30 s, and 72°C for 20 s. The level of glyceraldehyde 3-phosphate dehydrogenase (GAPDH) messenger RNA (mRNA) was detected as an endogenous control.

Double Labeling of Apoptotic TCMK-1 Cells With Properdin

TCMK-1 cells (American Type Culture Collection, Manassas, USA), mouse kidney epithelial cell line, were grown in Dulbecco's modified Eagle's medium (DMEM)/F-12 medium (Gibco, Carlsbad, USA) with 10% (v/v) fetal calf serum (Gibco), 2 mM L-glutamine (Gibco), 100 U/ml penicillin G, and 100 mg/ml streptomycin (Sigma, Dorset, UK) at 37°C in a 5% CO_2 humidified atmosphere.

TCMK-1 cells were cultured in serum-free DMEM/F-12 medium (Gibco, Carlsbad, USA) and stimulated with 200 μM H_2O_2 for 24 h. The cells were then fixed and subjected to ISEL and developed with 3,3′-diaminobenzidine (DAB) chromogen (Vector). Antiproperdin antibody (ab186834, Abcam) diluted 1:100 was applied followed by biotinylated goat–antirabbit IgG (1:300, BA-1000, Vector) and alkaline phosphatase streptavidin (1:200, SA-5100, Vector). Binding was detected by Fast Red (Sigma) and hematoxylin counterstaining. For the negative control, the primary antibody was substituted with normal rabbit IgG of same species (Merck Millipore) at same protein concentration.

TCMK-1 Cells Treated by Properdin siRNA

Cells were seeded onto six-well plates at 2×10^5 density. When 50% confluence was reached, the cells were transfected with small interfering RNA (siRNA) targeting properdin (siP, Thermo Fisher Scientific) or negative control siRNA (siNC, does not target any known mammalian genes) at 16 nM, assisted with Lipofectamine™ RNAiMAX (Invitrogen, Carlsbad, USA). After 6 h transfection, the cells were treated with 200 μM H_2O_2 and then lysed at 18 h to extract whole protein for detecting properdin and HMGB1 by Western blotting. In addition, the number of apoptotic cells was evaluated by Annexin V/PI staining (Roche, Mannheim, Germany) according to the manufacturer's instruction and then detected by a flow cytometer (BD, Bergen, USA). Briefly, TCMK-1 cells were tripsinized, resuspended in binding buffer, and incubated with fluorescein isothiocyanate (FITC)-conjugated Annexin-V and propidium iodide (PI) for 15 min. Cells (10,000) were analyzed by BD FACS Calibur flow cytometry (BD Biosciences, Franklin Lakes, USA). Living cells (Annexin-V−/PI−, lower left quadrant), early apoptosis (Annexin-V+/PI−, lower right quadrant), late apoptosis (Annexin-V+/PI+, upper right quadrant), or necrosis (Annexin-V−/PI+, upper left quadrant) were shown as quadrant dot plots and the percentage of the gated cells (29). In each experiment, two replicates per group were used, while the individual experiment was repeated at least three times.

TABLE 1 | The sequence of primers for real-time quantitative PCR.

Genes	Primers (5′–3′)
Properdin	Forward: TTCACCCAGTATGAGGAGT
	Reverse: GCTGACCATTGTGGAGACCT
GAPDH	Forward: CCTGGAGAAACCTGCCAAGTATG
	Reverse: AGAGTGGGAGTTGCTGTTGAAGTC

Primary Isolated TECs From WT and P^{KO} Mice

The TECs were primary isolated from the kidneys of both WT and P^{KO} C57BL/6 male mice aged 8–12 weeks using a well-established method that led to the functional characterization of TECs in the group (30). Briefly, small cortical pieces from the kidney were pulverized and passed through a serial set of sieves with the size from 250, 125, 75, and 45 μm. The primary isolates were maintained in DMEM/F-12 medium containing 10% heat-inactivated fetal bovine serum (FBS, Sigma) and other basic additives as the same for TCMK-1 cells, but with additional recombinant human epithelial growth factor (0.1 μg/ml), insulin (5 μg/ml), transferrin (5 μg/ml), sodium selenite (5 ng/ml), triiodothyronine (4 pg/ml), and hydrocortisone (36 ng/ml). At confluence, TECs (passage 0) were split using trypsin/ethylenediaminetetraacetic acid (EDTA) (Invitrogen), and cells at passages 2–3 were used for experiments. The characterization of isolated TECs was previously validated by the positive staining of cytokeratin and γ-glutamyl transpeptidase and the negative staining of factor VIII and α-smooth muscle actin that are the markers of endothelial cells and mesangial cells, respectively (30). In addition, the morphological characteristics of newly isolated and cultured TECs that formed domes are illustrated in **Supplementary Figure 1** (31).

Assessing Phagocytosis of WT and P^{KO} TECs

Escherichia coli (E. coli) bioparticles (FITC-labeled pHrodo *E. coli* Bioparticles® Conjugate P35366, Thermo Fisher Scientific) were used to assess the phagocytic ability of WT and P^{KO} TECs by flow cytometry. Primary isolates of WT and P^{KO} TECs at passage 2 or 3 were seeded into a 24-well plate at 1.8×10^5 and cultured in the complete medium containing 10% heat-inactivated FBS. Following attachment, the cells were then exposed to 200 μM H_2O_2 for 24 h and followed by incubation

with 500 μl of *E. coli* bioparticles (0.5 mg/ml, suspended in DMEM/F12 medium) for 2 h. Non-phagocytosed *E. coli* bioparticles were removed, and the cells were trypsinized and resuspended. On a fluorescence-activated cell sorting (FACS) system (BD), a total of 10,000 gated cells were analyzed for the fluorescent intensity of FITC. Due to the different level of auto fluorescence in WT TECs and P^{KO} TECs, a different threshold was set up for each phenotype. To make two phenotypes comparable, the fold change of positive cells or FITC fluorescent intensity of total cells was calculated against that of the control—*E. coli* group for each phenotype.

The primary cultured WT TECs and P^{KO} TECs at passage 2 or 3 were also seeded onto glass coverslips precoated with poly-D-lysine (0.1 mg/ml; Sigma) and cultured in the above-described culture medium, either without serum or with 2% serum from WT or P^{KO} mice without heat inactivation for 24 h. The cells were stimulated with 200 μM H_2O_2 for another 24 h. The TECs were fixed by 1% paraformaldehyde for 10 min and then by an ice-cold mixture of ethanol and acetic acid (2:1) at −20°C for 5 min, followed by ISEL staining. The number of ISEL+ cells, phagocytosed ISEL+ cells (normal TEC overlapping with ISEL+ cells), and total cells were counted in 20 random fields at 400× magnification.

Statistical Analysis

Data are expressed as mean ± standard error of the mean (SEM). One-way ANOVA was used to check the homogeneity of variance, followed by *post-hoc* least significant difference (LSD) test for multiple comparisons or unpaired Student's t-tests for comparison between two groups, using SPSS Statistics Standard V26.0 software (IBM, New York, USA). $p < 0.05$ was considered statistically significant.

RESULTS

P^{KO} Preserved Kidney Structure at Early Stagy but Aggravated Kidney Damage at Late Phase Post IR

To differentiate whether properdin has different roles at the different stages of IR injury, we established bilateral renal IR model in mice with 30 min ischemia followed by reperfusion for 24 h as an early predominate injury stage and 72 h for a late kidney repair stage. The experimental design was shown in **Figure 1A**. Compared to sham controls, SCr, BUN, and TID score in H&E-stained sections were elevated by IR in both WT and P^{KO} mice at 24 h (**Figures 1B, C**), with significantly lower TID score in IR P^{KO} kidneys than WT controls. At 72 h, SCr, BUN, and TID score were also elevated by IR in both WT and P^{KO} mice, while, notably, all these parameters were significantly higher in P^{KO} mice than WT controls (**Figures 1D–F**).

P^{KO} Increased Apoptotic Cells in Tubular Luminal Areas Post 72-h IR

As properdin has potential PRM function of labeling apoptotic cells for their recognition by phagocytes, absence of properdin could result in delayed phagocytosis of apoptotic cells and the accumulation of these cells in injured kidneys. Thus, the level of renal apoptosis was assessed by *in situ* labeling of apoptotic cells in IR kidneys of both WT and P^{KO} mice. Apoptotic cells with typical morphologic features, detected by ISEL-fragmented DNAs, mainly distributed in tubulointerstitial areas (**Figure 2A**), were dramatically increased by IR in both WT and P^{KO} kidneys, but were scant in sham kidneys (**Figure 2B**). In the tubular lumen, apoptotic cells were significantly greater in IR P^{KO} kidneys compared with WT kidneys. Similarly, apoptotic cells in tubules and interstitial areas were increased by IR in WT and P^{KO} kidneys, without significant differences between phenotypes.

P^{KO} Increased Inflammation and Its Mediators in Kidneys Post 72-h IR

P^{KO}-associated more severe IR kidney damage at 72 h was further examined closely by assessing infiltrated inflammatory cells in kidneys by the immunostaining of F4/80, a marker of macrophages, and examining injury markers including 17 kDa active caspase-3 and HMGB1 in kidney homogenates using Western blot. F4/80+ macrophages in tubular lumina and tubulointerstitial areas were remarkably increased by IR compared to sham groups, and further elevated by P^{KO} (**Figures 3A, B**). The expression of 17 kDa active caspase-3, an executer of apoptosis (32) and inflammation (33, 34), was increased by IR compared to sham controls of WT and P^{KO} mice, and further raised in IR kidneys by P^{KO} compared to WT (**Figure 3C**). The same change pattern was also revealed in HMGB1 protein (**Figure 3D**), a recruiter of inflammatory cells and activator of complement (35–38).

IR Raised Mitosis and PCNA With P^{KO} Increased EPOR Post 72-h IR

As repair was initiated at 72 h post IR, the compensatory response under the absence of properdin was assessed by mitotic cells and the proliferative marker PCNA. Mitotic cells in H&E-stained sections, reflected kidney repair, were increased by IR in WT and P^{KO} kidneys compared to the phenotype sham (**Figure 4A**), while a similar change was seen in PCNA protein detected by Western blot, without significant differences between P^{KO} and WT (**Figure 4B**).

To further understand the role of P^{KO} in the repair phase post IR, the expression and localization of EPOR, a part of innate repair receptor (39) EPOR/βcR and essential for the phagocytic function of macrophages (40), were evaluated by Western blot and immunostaining. EPOR was increased by IR in WT and P^{KO} kidneys compared to respective sham controls, further elevated by P^{KO} compared to WT (**Figure 4C**). The weak staining of EPOR was evenly distributed in the cytoplasm of TECs in the cortical areas of sham kidneys, greatly enhanced by IR, mainly localized around severely damaged tubules, in WT and P^{KO} mice (**Figure 4D**). The level of EPOR was positively correlated with mitotic figures and PCNA (**Figure 4E**).

Elevated Properdin in IR Kidneys Was Localized in TECs and Macrophages

To observe the involvement of properdin in IR injury and whether properdin tags apoptotic inflammatory cells, the

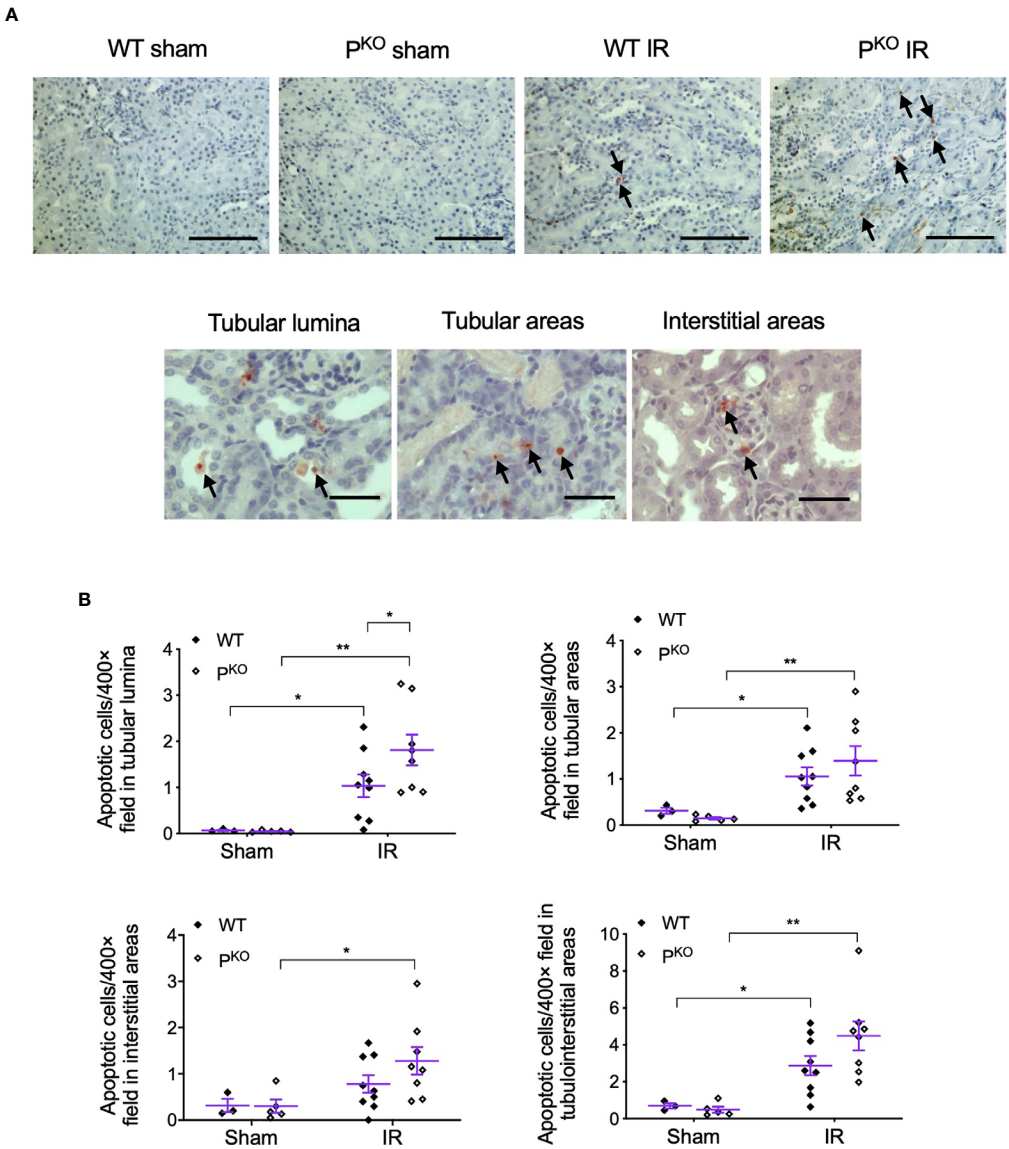


FIGURE 2 | P^{KO} increased the number of apoptotic cells in tubular lumina post IR at 72 h. **(A)** Representative photomicrographs showed apoptotic cells in the indicated groups and tubular lumina, tubular and interstitial areas, revealed by ISEL with AEC (3-amino-9-ethylcarbazole). All images were taken from the renal cortex. Scale bar: 100 μm (upper row) and 50 μm (lower row). **(B)** The number of ISEL+ cells in tubular lumina was increased by IR and furthered by P^{KO}, whereas in the area of tubule, interstitium and tubulointerstitium P^{KO} caused a slightly higher level of apoptosis than the WT control but did not reach statistical significance. Data were shown as means ± SEMs and analyzed by one-way ANOVA and LSD test. *$p < 0.05$; **$p < 0.01$.

expression of properdin mRNA and protein in IR kidneys was first examined and then followed by its double immunostaining with F4/80 proteins. Exons 3–7 of properdin DNA was absent in P^{KO} mice (17), so properdin mRNA was detected by quantitative PCR (qPCR) using primers recognizing properdin inside the exons 3–7. The level of properdin mRNA was raised by IR compared to sham controls in WT kidneys (**Figure 5A**), in which properdin protein was also elevated, but absent in P^{KO} kidneys (**Figure 5B**).

The immunostaining of properdin was mainly localized on the apical surface of TECs and raised by IR in WT kidneys (**Figure 5C**). Properdin and F4/80 double-stained cells with typical apoptotic morphological features were observed in tubular areas, interstitial areas, and tubular lumina in IR WT kidneys (**Figure 5D**).

Properdin Tagged Apoptotic Cells Phagocytosed by Healthy Cells

To further examine the effect of properdin as a PRM on apoptotic renal parenchymal cells, the double staining of properdin and ISEL was performed in H_2O_2-treated TCMK-1

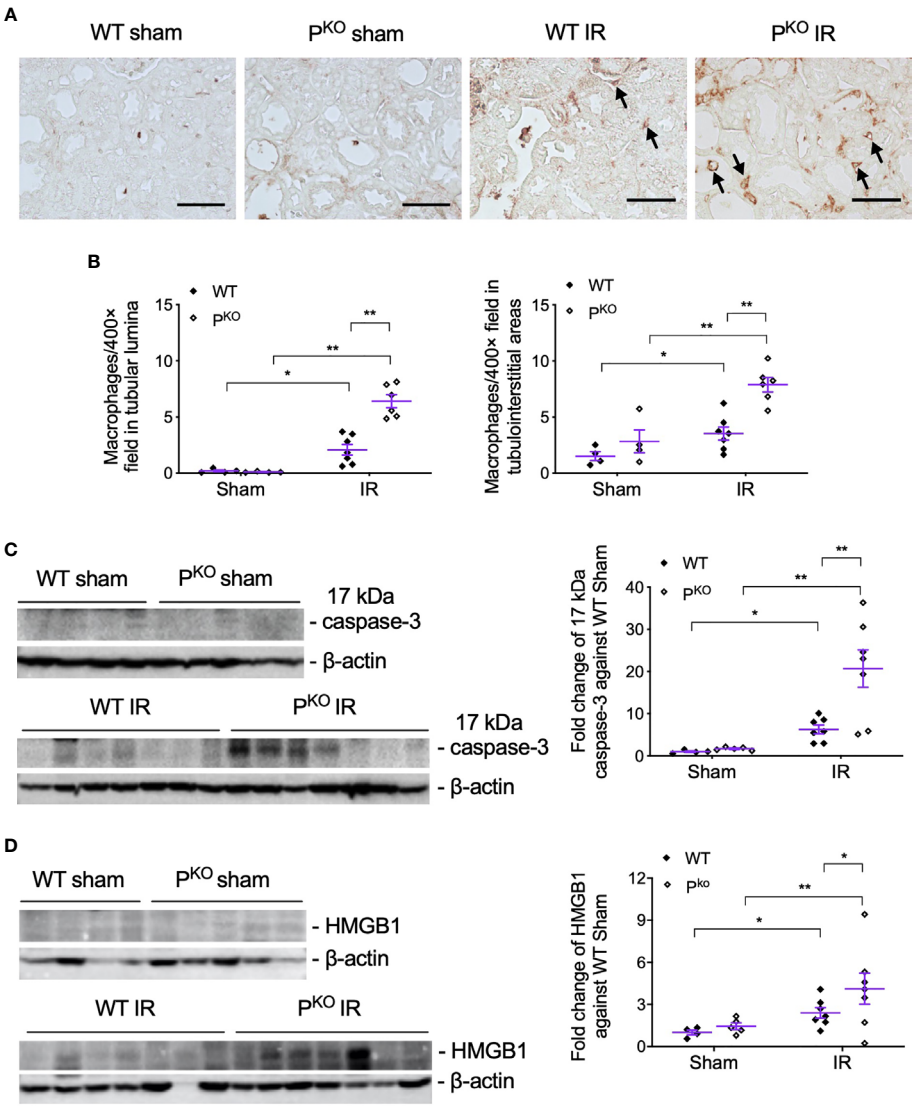


FIGURE 3 | P^{KO} increased the infiltration of inflammatory cells and the expression of injury markers post IR at 72 h. **(A, B)** Representative images of F4/80 immunostaining in the indicated groups, and the semiquantitative analysis, showed more F4/80+ cells in the interstitium and tubulointerstitium of P^{KO} kidneys than WT controls (sham: n = 4; IR: n = 6–7). The images were taken from the cortical area of the kidney. Scale bar: 50 μm. **(C, D)** Seventeen kilodaltons active caspase-3 and HMGB1 protein in the kidney determined by Western blot was increased by IR and furthered by P^{KO} (sham: n = 4-5; IR: n = 7–9). Data were shown as means ± SEMs and analyzed by one-way ANOVA and LSD test. $^{*}p < 0.05$; $^{**}p < 0.01$.

cells *in vitro*. Patchy properdin staining was observed mainly in the cytoplasm of cells, without any staining in negative control cells incubated with normal rabbit IgG (**Figure 6A**). Some properdin+ cells having typical apoptotic features, shrunken nuclei with halos and condensed cytoplasm, or properdin and ISEL double+ cells, and ISEL+ cells were adjacent to or phagocytosed by healthy cells.

The effect of properdin on TECs was further verified by siP in H_2O_2-treated TCMK-1 cells, in which siP downregulated properdin expression but further increased HMGB1 (**Figure 6B**) and the number of early and late apoptotic cells in contrast to the negative control (siNC, **Figure 6C**).

Phagocytic Ability of TECs Reduced by P^{KO}

Lastly, whether properdin affects the phagocytic ability of TECs was assessed by flow cytometry using pHrodo *E. coli* bioparticles. The threshold of fluorescent intensity for WT TECs was set lower than that for P^{KO} TECs, as P^{KO} had higher auto fluorescent intensity (Control - *E. coli*, **Figure 7A**), which was not changed by H_2O_2 treatment (H_2O_2 - *E. coli*). The fold change of FITC fluorescent intensity in all gated cells was increased by H_2O_2 only in WT TECs compared to the controls but decreased by P^{KO} (**Figure 7A**, i), which were also seen in the fold change of positive cells (**Figure 7A**, ii). Moreover, compared to WT TECs, P^{KO} decreased the fold change

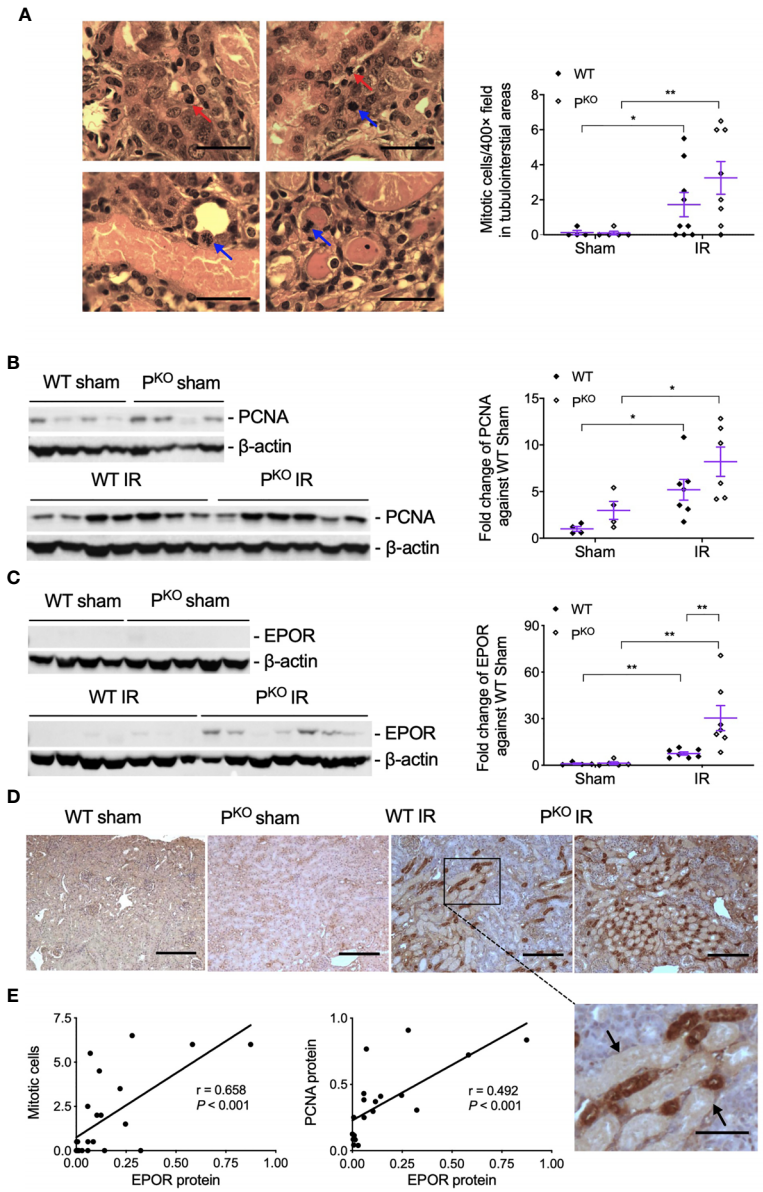


FIGURE 4 | Kidney repair parameters in P^{KO} kidneys post IR at 72 h. **(A)** Mitotic cells with typical morphological features in tubular and interstitial areas were pointed by blue and red arrows (upper panels, WT IR kidneys; lower panels, P^{KO} IR kidneys). The number of mitotic cells was increased by IR in both WT and P^{KO} mice assessed by semiquantitative analysis. Scale bar: 20 μm. **(B)** The expression of PCNA protein in the kidney determined by Western blot was increased by IR in both WT and P^{KO} mice. **(C)** The expression of EPOR protein was also increased in the IR kidneys of both genotypes with a further elevation by P^{KO} compared to WT controls. Data were shown as means ± SEMs and analyzed by one-way ANOVA and LSD test. *$p < 0.05$; **$p < 0.01$. **(D)** Representative images of EPOR immunostaining in the cortex of kidneys, and the area from a dashed box was enlarged and necrotic tubules were pointed by arrows. Scale bar: 100 and 50 μm (the enlarged image). **(E)** The linear correlation showed EPOR protein positively correlated to mitosis and PCNA, respectively.

of FITC fluorescent intensity treated by H_2O_2 and also decreased the fold change of positive cells without H_2O_2.

Apoptotic TECs were approached, engulfed, and phagocytosed by adjacent healthy-appearing TECs (**Figures 7B, C**). The percentage of apoptotic cells against the number of total cells were increased by P^{KO} compared with WT TECs, regardless of serum conditions (**Figure 7D**). However, the percentage of phagocytosed apoptotic cells against the number of apoptotic cells in the P^{KO} TECs was lower than that in WT TECs under all serum conditions.

DISCUSSION

Properdin has diverse and disease-dependent effects that may be modified by the genetic background of animal models (20, 41).

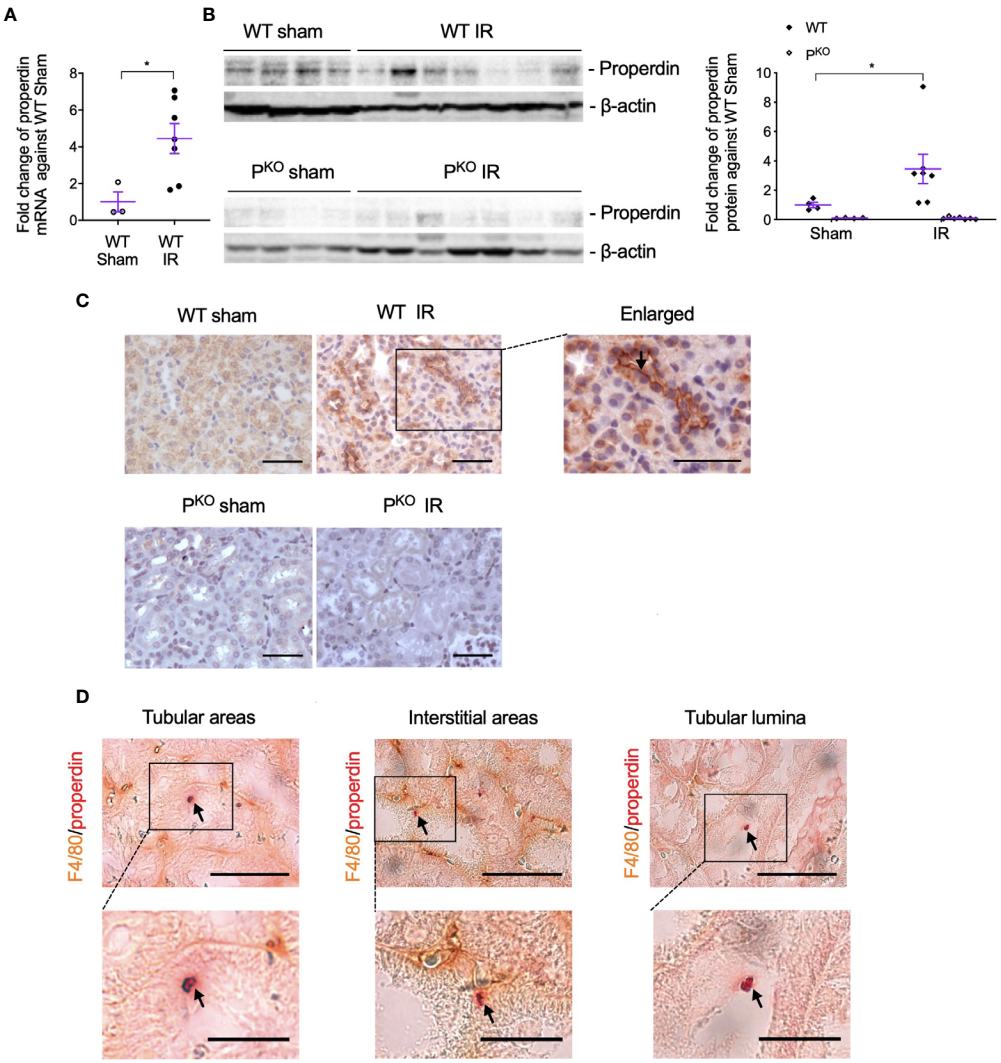


FIGURE 5 | Properdin expression and localization in kidneys post IR at 72 h, as well as its co localization with F4/80+ macrophages. **(A)** The expression of properdin mRNA in kidneys analyzed by qPCR was raised by IR in contrast to the sham control in WT mice. **(B)** The expression of properdin protein in kidney homogenates detected by Western blot was increased by IR in WT mice but was not seen in P^{KO} mice (sham: n = 3–4; IR: n = 7). Data were shown as means ± SEMs. Significance was assessed by unpaired *t*-test for qPCR result and one-way ANOVA and LSD test for Western blots. *$p < 0.05$. **(C)** Representative images of properdin immunostaining in the cortex of WT sham and IR kidneys, with the boxed area enlarged and properdin staining on the apical surface of tubular cells was pointed by an arrow. All scale bar represent 50 μm. **(D)** Properdin and F4/80 double-stained cells were visualized in tubular areas, interstitial areas, and tubular lumina (pointed by arrows), with the boxed area enlarged. Most of double staining positive cells had typical apoptotic features including reduced cell volume, and the cellular membrane becoming ruffling and blebbing were also shown. Scale bar: 50 μm (upper row) and 20 μm (lower row).

In 24-h post renal IR mice, depleting negative regulators of the AP increased properdin and AP activation and TEC injury, whereas inhibiting properdin ameliorated renal IR injury (20, 42). Conversely, P^{KO} aggravates C3 glomerulopathy in mice (43, 44). In addition, emerging evidence indicates that properdin tagging apoptotic/necrotic T cells leads to their uptake by phagocytes *via* C3b opsonization or independent of C3b (22). The present study using sole P^{KO} mice demonstrates that properdin has beneficial effects at 72-h kidney repair stage post IR injury, which was attributed to properdin regulating the phagocytic activity of TECs apart from as a PRM optimizing damaged cells (**Figure 8**).

More severe damage in the P^{KO} IR kidneys at 72 h was associated with increased apoptotic cells in tubular luminal areas, and elevated active caspase-3 and HMGB1. Caspase-3 executes apoptosis and activates inflammatory mediators, while HMGB1 activates the Toll-like receptor 4 (TLR4)/nuclear factor kappa B (NF-κB) signaling pathway (45) and cytokine/chemokine production (35–38). P^{KO} resulted in persistent apoptosis and inflammation in the IR kidneys due to absence of properdin-assisted phagocytic clearance of apoptotic cells (22, 46, 47). The accumulation of apoptotic cells in the tubular lumen of P^{KO} IR kidneys may represent an adaptive mechanism of direct

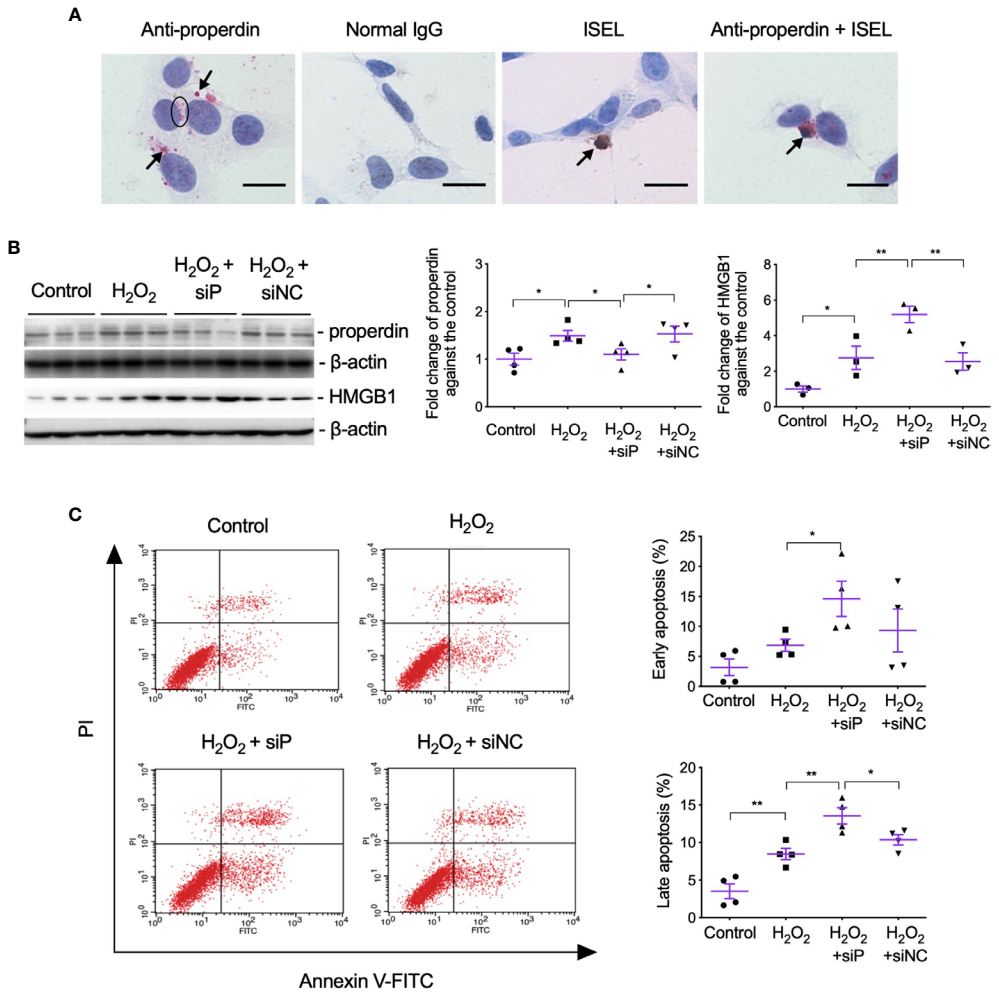


FIGURE 6 | Properdin tagged apoptotic TCMK-1 cells and inhibiting properdin increased apoptotic cells and HMGB1 expression in H_2O_2-treated TCMK-1 cells. **(A)** Properdin protein was visualized in TCMK-1 cells after H_2O_2 treatment for 24 h (indicated by a circle and two arrows nearby), in which the staining of properdin was negatively controlled by normal rabbit IgG. ISEL+ apoptotic TCMK-1 cells and its colocalization with properdin protein were also seen (pointed by another two arrows, n = 3). Scale bar: 5 μm. **(B)** The expression of properdin and HMGB1 detected by Western blot was increased by H_2O_2 treatment for 24 h, whereas siP reduced properdin expression but increased HMGB1 (n = 3). **(C)** The early and late apoptotic TCMK-1 cells detected by flow cytometry analysis were both increased by H_2O_2 treatment for 24 h and furthered by siP (n = 3). FITC fluorescein was tagged to Annexin V, thus can reveal the binding of Annexin V to the cellular surface of apoptotic cells that exposed phosphatidylserine (PS). Propidium iodide (PI) passed leaky necrotic cells to stain the DNA. Data were shown as means ± SEMs and analyzed by one-way ANOVA and LSD test. siP, siRNA targeting properdin; siNC, negative control siRNA. $^*p < 0.05$; $^{**}p < 0.01$.

elimination, while recruited macrophages may phagocytose apoptotic cells and also penetrate through tubular epithelia into the lumen. Properdin-labeled apoptotic macrophages were shown in the different compartment of IR kidneys of WT mice in this study, thus rendering them susceptible to phagocytes *in vivo*.

EPOR is expressed on TECs, where it forms heterodimers with βcR (EPOR/βcR), an innate repair receptor (39), and ameliorates renal damage and promotes tissue self-repair following IR (27, 48). Distributed mainly around damaged tubules (49), EPOR maintains tissue homeostasis by inhibiting the proinflammatory function of macrophages and enhancing their phagocytic function (40, 50). Increased EPOR, therefore, may also represent the compensatory response of repair in P^{KO} IR kidneys at 72 h.

TECs serve as major local semiprofessional phagocytes (8) and express various complement components, with C3 and factors H, B, I, and D being the most predominant (42, 51). Here, properdin was expressed in renal TECs being protective in terms of limiting HMGB1 and apoptosis under oxidative stress. Properdin, released from TECs, binds to the glycosaminoglycan chains of cell surface proteoglycans in apoptotic TECs to facilitate healthy TECs uptake these cells (22). Effectively clearing apoptotic cells by phagocytosis is crucial to limit renal injury and at the same time promote repair/remodeling post IR (8, 52, 53), in which the process of opsonizing damaged cells was absent in P^{KO} kidney resulting in higher level of apoptosis and severer damage.

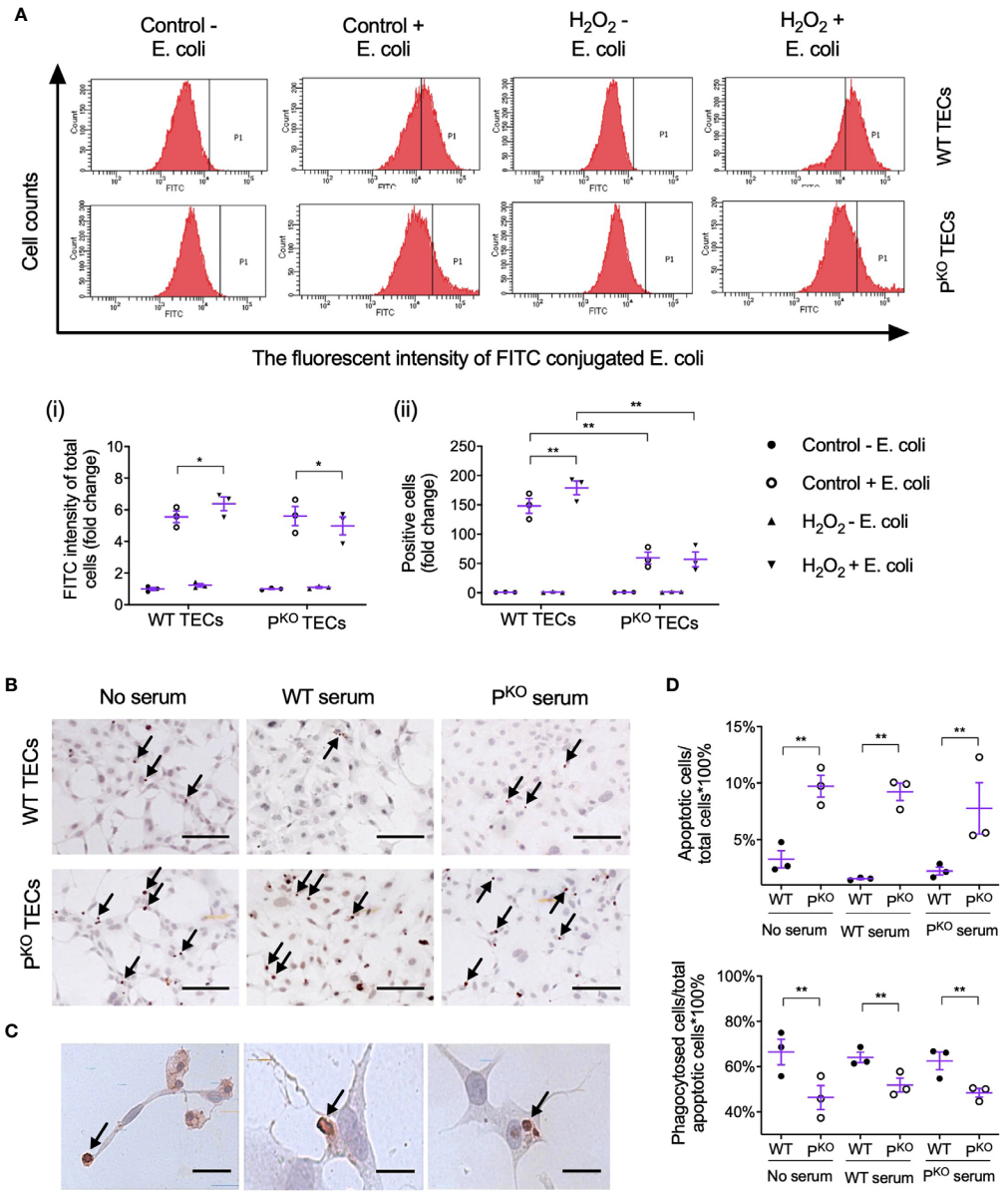


FIGURE 7 | Properdin contributes to the phagocytic efficacy of primary isolated TECs. **(A)** Flow cytometry analysis of phagocytosed FITC-labeled *E. coli* by primary isolated WT and P^{KO} TECs with or without H_2O_2 treatment for 24 h (n = 3). The fluorescent intensity of FITC conjugated *E. coli* reflected the phagocytic function of TECs. (i) The fold change of the average intensity of FITC fluorescence among total cells, calculated against the control (–*E. coli*) group, was increased in WT TECs but decreased in P^{KO} TECs by H_2O_2. (ii) The fold change of *E. coli* positive cell counts (P1 area) in each group against the control (–*E. coli*) group was increased in WT TECs by H_2O_2 but stayed low in P^{KO} TECs of either the control or H_2O_2 groups compared to corresponding WT groups. **(B)** Representative images of apoptotic WT and P^{KO} TECs detected by ISEL (ISEL+ cells indicated by arrows, n = 3). Scale bar: 50 μm. **(C)** Healthy WT TECs approaching, partially engulfing, and phagocytosing adjacent ISEL+ cells were demonstrated and indicated by arrows. Scale bar: 5 μm. **(D)** Semiquantitative analysis showed that the percentage of ISEL+ cells against the total number of cells was increased by P^{KO} regardless of serum conditions, while the percentage of phagocytosed ISEL+ cells against the total number of ISEL+ cells was decreased by P^{KO} after H_2O_2 treatment for 24 h (n = 3). Data were shown as means ± SEMs and analyzed by one-way ANOVA and LSD test. $^*p < 0.05$; $^{**}p < 0.01$.

Additionally, the effect of properdin on the phagocytic ability of TECs was detected by the uptake of fluorescence labeled *E. coli* particles, and oxidative-stress-induced apoptotic cells. Under unstressed and oxidative-stressed condition, P^{KO} significantly reduced the number of phagocytic cells, which indicates that properdin might affect the transformation of TECs to phagocytes. Moreover, P^{KO} significantly decreased the fluorescence intensity of gated P^{KO} TECs under oxidative stress, which was increased in WT TECs, indicating that properdin is essential for upregulating the phagocytic ability of TECs under stress.

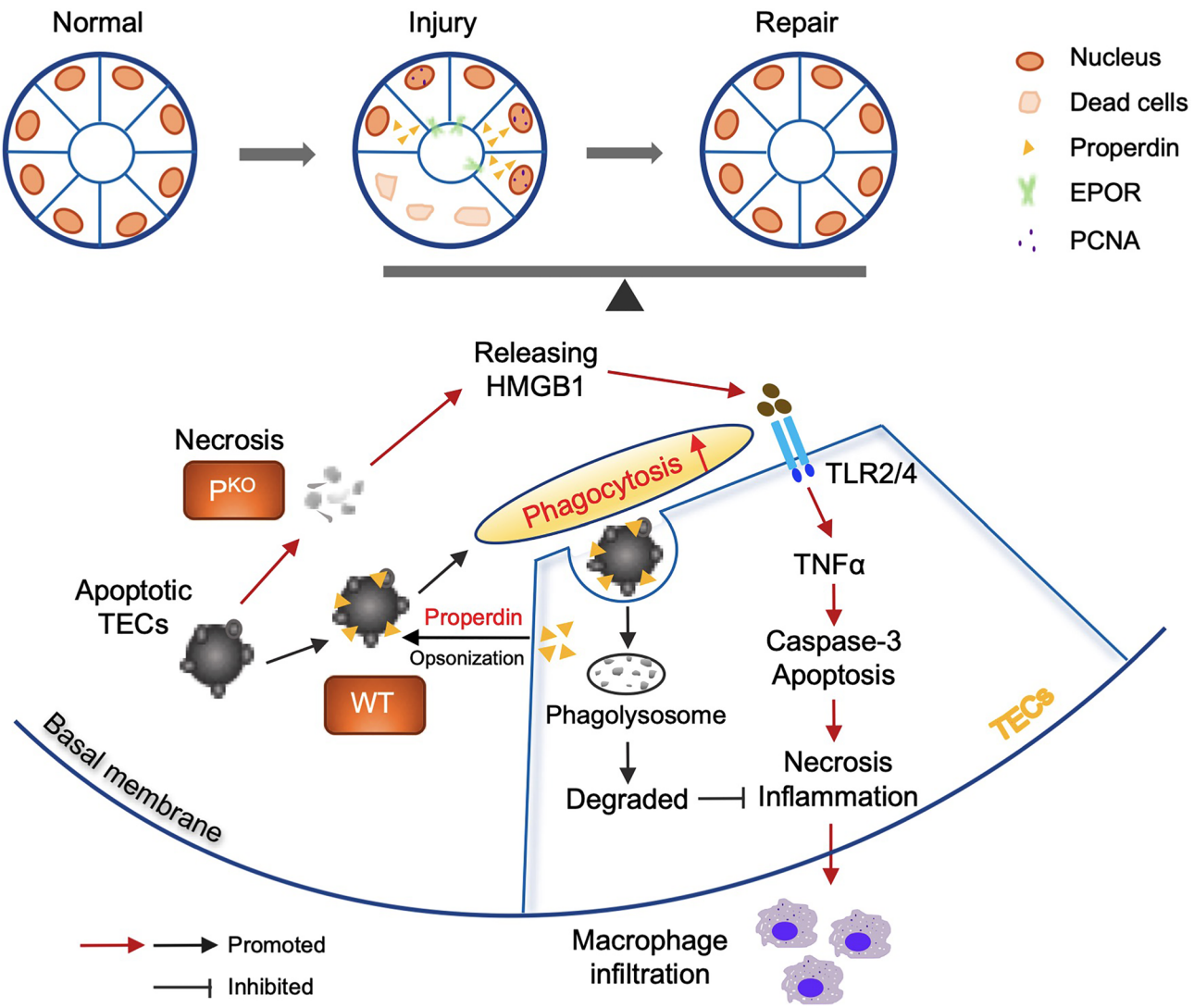


FIGURE 8 | Properdin mediated and enhanced phagocytosis of TECs. Schematic illustration of the role of properdin in the phagocytosis of living TECs from WT and P^{KO} mice. Properdin produced by living TECs tags adjacent apoptotic TECs to facilitate their uptake by neighbor living TECs, promoting damage reduction and inflammatory clearance. Lack of properdin impaired TECs phagocytosing damaged cells and resulted in more severe inflammation and tissue damage and compromised repair activities. Thus, properdin associated phagocytic function of TECs facilitates the balance between injury and repair of the kidney.

P^{KO} may affect the expression of PRM including properdin per se and pattern-recognition receptors (PRRs) on TECs. Apart from certain "eat me" signals expressed on damaged cells, the PRM further facilitates their recognition by phagocytes. Properdin might also be a constitutive "eat me" marker as it was expressed on the plasma membrane of TECs. For instance, the molecule of kidney injury molecule 1 (KIM-1) is one of the PRRs, expressed on TECs (as semiphagocytes) subjected to injury. KIM-1 as a receptor binds to its ligand, phosphatidylserine, as an "eat me" marker exposed on damaged cells (8). The evidence of reduced phagocytosis in P^{KO} TECs indicates that properdin might not only tag apoptotic cells mediating phagocytosis but also directly affect the phagocytic ability of TECs. In addition, the phagocytic feature of WT and P^{KO} TECs was not affected by additional serum with or with properdin, indicating that only locally produced properdin was essential for phagocytosis. Taken together, this study demonstrates for the first time that properdin has a key direct role in the phagocytic ability of TECs.

There are certain limitations in this study. First, the interaction and mechanism of properdin, KIM-1 and EPOR on the phagocytosis of TECs, and macrophages in renal injury and repair are worthy of further investigation. Second, a time-course model of renal IR in P^{KO} mice will be useful to disclose the dynamic change and the precise role of properdin in injury, recovery, or chronic progression.

In conclusion, this study showed that lack of properdin had harmful effects on kidneys at the repair stage post IR injury, which was attributed to properdin not only opsonizing damaged cells but also affecting the phagocytic ability of TECs to effectively clear apoptotic cells and subsequent inflammation. Therefore, a novel mechanism in IR injury and repair was found, in which properdin is crucial for phagocytosis in the repair stage after IR-induced injury.

DATA AVAILABILITY STATEMENT

The original contributions presented in the study are included in the article/**Supplementary Material**. Further inquiries can be directed to the corresponding author.

ETHICS STATEMENT

All animal procedures were subject to institutional review by the Animal Welfare and Ethical Review Body and approved under UK Home Office Project License PPL 70/8169.

AUTHOR CONTRIBUTIONS

BY and CS designed and supervised the study. YW, ZZ, XZ, and HW carried out experiments. YW, ZZ, CS and BY analyzed the data and constructed the figures. RC supervised cell culture work. YW, BY, CS and NB wrote and revised the paper. All authors contributed to the article and approved the submitted version.

FUNDING

This study was supported by the Leicester Kidney Care Appeal, the University Hospitals of Leicester NHS Trust Research and Innovation Department, the University of Leicester; project grants (81570677 and 81873622) from the National Natural Foundation of China; and also a project grant (JC2020036) from Nantong Science and Technology Foundation.

ACKNOWLEDGMENTS

The authors acknowledge the Division of Biomedical Services, Preclinical Research Facility, University of Leicester, for technical support and the care of experimental animals.

SUPPLEMENTARY MATERIAL

The Supplementary Material for this article can be found online at: https://www.frontiersin.org/articles/10.3389/fimmu.2021.697760/full#supplementary-material

REFERENCES

1. Mehta RL, Cerda J, Burdmann EA, Tonelli M, Garcia-Garcia G, Jha V, et al. International Society of Nephrology's 0by25 Initiative for Acute Kidney Injury (Zero Preventable Deaths by 2025): A Human Rights Case for Nephrology. *Lancet* (2015) 385(9987):2616–43. doi: 10.1016/S0140-6736(15)60126-X
2. Zhao Y, Yang L. Perspectives on Acute Kidney Injury Strategy in China. *Nephrol (Carlton)* (2018) 23(Suppl 4):100–3. doi: 10.1111/nep.13458
3. Yang L, Xing G, Wang L, Wu Y, Li S, Xu G, et al. Acute Kidney Injury in China: A Cross-Sectional Survey. *Lancet* (2015) 386(10002):1465–71. doi: 10.1016/S0140-6736(15)00344-X
4. Mehta RL, Burdmann EA, Cerda J, Feehally J, Finkelstein F, Garcia-Garcia G, et al. Recognition and Management of Acute Kidney Injury in the International Society of Nephrology 0by25 Global Snapshot: A Multinational Cross-Sectional Study. *Lancet* (2016) 387(10032):2017–25. doi: 10.1016/S0140-6736(16)30240-9
5. Bellomo R, Kellum JA, Ronco C. Acute Kidney Injury. *Lancet* (2012) 380 (9843):756–66. doi: 10.1016/S0140-6736(11)61454-2
6. Kumar S. Cellular and Molecular Pathways of Renal Repair After Acute Kidney Injury. *Kidney Int* (2018) 93(1):27–40. doi: 10.1016/j.kint.2017.07.030
7. Rosen S, Heyman S. Concerning Cellular and Molecular Pathways of Renal Repair After Acute Kidney Injury. *Kidney Int* (2018) 94(1):218. doi: 10.1016/j.kint.2018.04.001
8. Yang L, Brooks CR, Xiao S, Sabbisetti V, Yeung MY, Hsiao LL, et al. KIM-1-Mediated Phagocytosis Reduces Acute Injury to the Kidney. *J Clin Invest* (2015) 125(4):1620–36. doi: 10.1172/JCI75417
9. Takaori K, Nakamura J, Yamamoto S, Nakata H, Sato Y, Takase M, et al. Severity and Frequency of Proximal Tubule Injury Determines Renal Prognosis. *J Am Soc Nephrol* (2016) 27(8):2393–406. doi: 10.1681/ASN.2015060647
10. Yang L, Besschetnova TY, Brooks CR, Shah JV, Bonventre JV. Epithelial Cell Cycle Arrest in G2/M Mediates Kidney Fibrosis After Injury. *Nat Med* (2010) 16(5):535–43. doi: 10.1038/nm.2144
11. Thurman JM, Ljubanovic D, Edelstein CL, Gilkeson GS, Holers VM. Lack of a Functional Alternative Complement Pathway Ameliorates Ischemic Acute Renal Failure in Mice. *J Immunol* (2003) 170(3):1517–23. doi: 10.4049/jimmunol.170.3.1517
12. Thurman JM, Royer PA, Ljubanovic D, Dursun B, Lenderink AM, Edelstein CL, et al. Treatment With an Inhibitory Monoclonal Antibody to Mouse Factor B Protects Mice From Induction of Apoptosis and Renal Ischemia/Reperfusion Injury. *J Am Soc Nephrol* (2006) 17(3):707–15. doi: 10.1681/ASN.2005070698
13. Yamada K, Miwa T, Liu J, Nangaku M, Song WC. Critical Protection From Renal Ischemia Reperfusion Injury by CD55 and CD59. *J Immunol* (2004) 172 (6):3869–75. doi: 10.4049/jimmunol.172.6.3869
14. Schwaeble W, Huemer HP, Most J, Dierich MP, Strobel M, Claus C, et al. Expression of Properdin in Human Monocytes. *Eur J Biochem* (1994) 219 (3):759–64. doi: 10.1111/j.1432-1033.1994.tb18555.x
15. Schwaeble W, Dippold WG, Schafer MK, Pohla H, Jonas D, Luttig B, et al. Properdin, A Positive Regulator of Complement Activation, Is Expressed in Human T Cell Lines and Peripheral Blood T Cells. *J Immunol* (1993) 151 (5):2521–8.
16. Schwaeble WJ, Reid KB. Does Properdin Crosslink the Cellular and the Humoral Immune Response? *Immunol Today* (1999) 20(1):17–21. doi: 10.1016/s0167-5699(98)01376-0
17. Stover CM, Luckett JC, Echtenacher B, Dupont A, Figgitt SE, Brown J, et al. Properdin Plays a Protective Role in Polymicrobial Septic Peritonitis. *J Immunol* (2008) 180(5):3313–8. doi: 10.4049/jimmunol.180.5.3313
18. Fearon DT, Austen KF. Properdin: Binding to C3b and Stabilization of the C3b-Dependent C3 Convertase. *J Exp Med* (1975) 142(4):856–63. doi: 10.1084/jem.142.4.856
19. Harboe M, Mollnes TE. The Alternative Complement Pathway Revisited. *J Cell Mol Med* (2008) 12(4):1074–84. doi: 10.1111/j.1582-4934.2008.00350.x
20. Miwa T, Sato S, Gullipalli D, Nangaku M, Song WC. Blocking Properdin, the Alternative Pathway, and Anaphylatoxin Receptors Ameliorates Renal Ischemia-Reperfusion Injury in Decay-Accelerating Factor and CD59 Double-Knockout Mice. *J Immunol* (2013) 190(7):3552–9. doi: 10.4049/jimmunol.1202275

21. Spitzer D, Mitchell LM, Atkinson JP, Hourcade DK. Properdin Can Initiate Complement Activation by Binding Specific Target Surfaces and Providing a Platform for *De Novo* Convertase Assembly. *J Immunol* (2007) 179(4):2600–8. doi: 10.4049/jimmunol.179.4.2600
22. Kemper C, Mitchell LM, Zhang L, Hourcade DE. The Complement Protein Properdin Binds Apoptotic T Cells and Promotes Complement Activation and Phagocytosis. *Proc Natl Acad Sci USA* (2008) 105(26):9023–8. doi: 10.1073/pnas.0801015105
23. Kemper C, Atkinson JP, Hourcade DE. Properdin: Emerging Roles of a Pattern-Recognition Molecule. *Annu Rev Immunol* (2010) 28:131–55. doi: 10.1146/annurev-immunol-030409-101250
24. O'Flynn J, Kotimaa J, Faber-Krol R, Koekkoek K, Klar-Mohamad N, Koudijs A, et al. Properdin Binds Independent of Complement Activation in an *In Vivo* Model of Anti-Glomerular Basement Membrane Disease. *Kidney Int* (2018) 94(6):1141–50. doi: 10.1016/j.kint.2018.06.030
25. Gaarkeuken H, Siezenga MA, Zuidwijk K, van Kooten C, Rabelink TJ, Daha MR, et al. Complement Activation by Tubular Cells Is Mediated by Properdin Binding. *Am J Physiol Renal Physiol* (2008) 295(5):F1397–403. doi: 10.1152/ajprenal.90313.2008
26. Wei Q, Dong Z. Mouse Model of Ischemic Acute Kidney Injury: Technical Notes and Tricks. *Am J Physiol Renal Physiol* (2012) 303(11):F1487–94. doi: 10.1152/ajprenal.00352.2012
27. Wu Y, Zhang J, Liu F, Yang C, Zhang Y, Liu A, et al. Protective Effects of HBSP on Ischemia Reperfusion and Cyclosporine a Induced Renal Injury. *Clin Dev Immunol* (2013) 2013:758159. doi: 10.1155/2013/758159
28. Lauren Brasile NH. Giuseppe Orlando, Bart Stubenitsky. Potentiating Renal Regeneration Using Mesenchymal Stem Cells. *Transplantation* (2019) 103 (2):307–13. doi: 10.1097/TP.0000000000002455
29. Zhang Y, Wang Q, Liu A, Wu Y, Liu F, Wang H, et al. Erythropoietin Derived Peptide Improved Endoplasmic Reticulum Stress and Ischemia-Reperfusion Related Cellular and Renal Injury. *Front Med (Lausanne)* (2020) 7:5. doi: 10.3389/fmed.2020.00005
30. Chana RS, Sidaway JE, Brunskill NJ. Statins But Not Thiazolidinediones Attenuate Albumin-Mediated Chemokine Production by Proximal Tubular Cells Independently of Endocytosis. *Am J Nephrol* (2008) 28(5):823–30. doi: 10.1159/000137682
31. Detrisac CJ, Sens MA, Garvin AJ, Spicer SS, Sens DA. Tissue Culture of Human Kidney Epithelial Cells of Proximal Tubule Origin. *Kidney Int* (1984) 25(2):383–90. doi: 10.1038/ki.1984.28
32. Yang B, Hosgood SA, Nicholson ML. Naked Small Interfering RNA of Caspase-3 in Preservation Solution and Autologous Blood Perfusate Protects Isolated Ischemic Porcine Kidneys. *Transplantation* (2011) 91(5):501–7. doi: 10.1097/TP.0b013e318207949f
33. Yang B, Jain S, Ashra SY, Furness PN, Nicholson ML. Apoptosis and Caspase-3 in Long-Term Renal Ischemia/Reperfusion Injury in Rats and Divergent Effects of Immunosuppressants. *Transplantation* (2006) 81(10):1442–50. doi: 10.1097/01.tp.0000209412.77312.69
34. Yang B, Elias JE, Bloxham M, Nicholson ML. Synthetic Small Interfering RNA Down-Regulates Caspase-3 and Affects Apoptosis, IL-1 Beta, and Viability of Porcine Proximal Tubular Cells. *J Cell Biochem* (2011) 112(5):1337–47. doi: 10.1002/jcb.23050
35. Ricklin D, Hajishengallis G, Yang K, Lambris JD. Complement: A Key System for Immune Surveillance and Homeostasis. *Nat Immunol* (2010) 11(9):785–97. doi: 10.1038/ni.1923
36. Kinsey GR, Li L, Okusa MD. Inflammation in Acute Kidney Injury. *Nephron Exp Nephrol* (2008) 109(4):e102–107. doi: 10.1159/000142934
37. Schiller M, Heyder P, Ziegler S, Niessen A, Classen L, Lauffer A, et al. During Apoptosis HMGB1 Is Translocated Into Apoptotic Cell-Derived Membranous Vesicles. *Autoimmunity* (2013) 46(5):342–6. doi: 10.3109/08916934.2012.750302
38. Nauser CL, Farrar CA, Sacks SH. Complement Recognition Pathways in Renal Transplantation. *J Am Soc Nephrol* (2017) 28(9):2571–8. doi: 10.1681/ASN.2017010079
39. Brines M, Grasso G, Fiordaliso F, Sfacteria A, Ghezzi P, Fratelli M, et al. Erythropoietin Mediates Tissue Protection Through an Erythropoietin and Common Beta-Subunit Heteroreceptor. *Proc Natl Acad Sci USA* (2004) 101 (41):14907–12. doi: 10.1073/pnas.0406491101
40. Luo B, Gan W, Liu Z, Shen Z, Wang J, Shi R, et al. Erythropoeitin Signaling in Macrophages Promotes Dying Cell Clearance and Immune Tolerance. *Immunity* (2016) 44(2):287–302. doi: 10.1016/j.immuni.2016.01.002
41. van Essen MF, Ruben JM, de Vries APJ, van Kooten C, consortium C. Role of Properdin in Complement-Mediated Kidney Diseases. *Nephrol Dial Transplant* (2019) 34(5):742–50. doi: 10.1093/ndt/gfy233
42. Miao J, Lesher AM, Miwa T, Sato S, Gullipalli D, Song WC. Tissue-Specific Deletion of Crry From Mouse Proximal Tubular Epithelial Cells Increases Susceptibility to Renal Ischemia-Reperfusion Injury. *Kidney Int* (2014) 86 (4):726–37. doi: 10.1038/ki.2014.103
43. Ruseva MM, Vernon KA, Lesher AM, Schwaeble WJ, Ali YM, Botto M, et al. Loss of Properdin Exacerbates C3 Glomerulopathy Resulting From Factor H Deficiency. *J Am Soc Nephrol* (2013) 24(1):43–52. doi: 10.1681/ASN.2012060571
44. Lesher AM, Zhou L, Kimura Y, Sato S, Gullipalli D, Herbert AP, et al. Combination of Factor H Mutation and Properdin Deficiency Causes Severe C3 Glomerulonephritis. *J Am Soc Nephrol* (2013) 24(1):53–65. doi: 10.1681/ASN.2012060570
45. Chen CB, Liu LS, Zhou J, Wang XP, Han M, Jiao XY, et al. Up-Regulation of HMGB1 Exacerbates Renal Ischemia-Reperfusion Injury by Stimulating Inflammatory and Immune Responses Through the TLR4 Signaling Pathway in Mice. *Cell Physiol Biochem* (2017) 41(6):2447–60. doi: 10.1159/000475914
46. Zwaini Z, Dai H, Stover C, Yang B. Role of Complement Properdin in Renal Ischemia-Reperfusion Injury. *Curr Gene Ther* (2017) 17(6):411–23. doi: 10.2174/1566523218666180214093043
47. Morelli AE, Larregina AT, Shufesky WJ, Zahorchak AF, Logar AJ, Papworth GD, et al. Internalization of Circulating Apoptotic Cells by Splenic Marginal Zone Dendritic Cells: Dependence on Complement Receptors and Effect on Cytokine Production. *Blood* (2003) 101(2):611–20. doi: 10.1182/blood-2002-06-1769
48. Yang C, Hosgood SA, Meeta P, Long Y, Zhu T, Nicholson ML, et al. Cyclic Helix B Peptide in Preservation Solution and Autologous Blood Perfusate Ameliorates Ischemia-Reperfusion Injury in Isolated Porcine Kidneys. *Transplant Direct* (2015) 1(2):e6. doi: 10.1097/TXD.0000000000000515
49. Humphreys BD, Valerius MT, Kobayashi A, Mugford JW, Soeung S, Duffield JS, et al. Intrinsic Epithelial Cells Repair the Kidney After Injury. *Cell Stem Cell* (2008) 2(3):284–91. doi: 10.1016/j.stem.2008.01.014
50. Bohr S, Patel SJ, Vasko R, Shen K, Iracheta-Vellve A, Lee J, et al. Modulation of Cellular Stress Response *via* the Erythropoietin/CD131 Heteroreceptor Complex in Mouse Mesenchymal-Derived Cells. *J Mol Med* (2015) 93(2):199–210. doi: 10.1007/s00109-014-1218-2
51. Delpech PO, Thuillier R, SaintYves T, Danion J, Le Pape S, van Amersfoort ES, et al. Inhibition of Complement Improves Graft Outcome in a Pig Model of Kidney Autotransplantation. *J Trans Med* (2016) 14(1):277. doi: 10.1186/s12967-016-1013-7
52. Ferenbach DA, Sheldrake TA, Dhaliwal K, Kipari TM, Marson LP, Kluth DC, et al. Macrophage/monocyte Depletion by Clodronate, But Not Diphtheria Toxin, Improves Renal Ischemia/Reperfusion Injury in Mice. *Kidney Int* (2012) 82(8):928–33. doi: 10.1038/ki.2012.207
53. Li L, Huang L, Sung SS, Vergis AL, Rosin DL, Rose CE Jr., et al. The Chemokine Receptors CCR2 and CX3CR1 Mediate Monocyte/Macrophage Trafficking in Kidney Ischemia-Reperfusion Injury. *Kidney Int* (2008) 74 (12):1526–37. doi: 10.1038/ki.2008.500

Conflict of Interest: The authors declare that the research was conducted in the absence of any commercial or financial relationships that could be construed as a potential conflict of interest.

Publisher's Note: All claims expressed in this article are solely those of the authors and do not necessarily represent those of their affiliated organizations, or those of the publisher, the editors and the reviewers. Any product that may be evaluated in this article, or claim that may be made by its manufacturer, is not guaranteed or endorsed by the publisher.

Copyright © 2021 Wu, Zwaini, Brunskill, Zhang, Wang, Chana, Stover and Yang. This is an open-access article distributed under the terms of the Creative Commons Attribution License (CC BY). The use, distribution or reproduction in other forums is permitted, provided the original author(s) and the copyright owner(s) are credited and that the original publication in this journal is cited, in accordance with accepted academic practice. No use, distribution or reproduction is permitted which does not comply with these terms.

frontiers in Immunology

ORIGINAL RESEARCH
published: 10 September 2021
doi: 10.3389/fimmu.2021.698894

Myeloid-Derived Suppressor Cells Alleviate Renal Fibrosis Progression *via* Regulation of CCL5-CCR5 Axis

Yue Qiu[1,2†], Yirui Cao[3,4†], Guowei Tu[1†], Jiawei Li[3,4], Ying Su[1], Fang Fang[2], Xuepeng Zhang[1,2], Jing Cang[2], Ruiming Rong[3,4*] and Zhe Luo[1,5*]*

[1] Department of Critical Care Medicine, Zhongshan Hospital, Fudan University, Shanghai, China, [2] Department of Anesthesiology, Zhongshan Hospital, Fudan University, Shanghai, China, [3] Department of Urology, Zhongshan Hospital, Fudan University, Shanghai, China, [4] Shanghai Key Laboratory of Organ Transplantation, Shanghai, China, [5] Department of Critical Care Medicine, Xiamen Branch, Zhongshan Hospital, Fudan University, Xiamen, China

OPEN ACCESS

Edited by:
Bin Yang,
University of Leicester,
United Kingdom

Reviewed by:
Qingrong Huang,
Cornell University, United States
Yang Zhao,
Institute of Zoology (CAS), China

***Correspondence:**
Jing Cang
cang.jing@zs-hospital.sh.cn
Ruiming Rong
rong.ruiming@zs-hospital.sh.cn
Zhe Luo
luo.zhe@zs-hospital.sh.cn

†These authors have contributed equally to this work and share first authorship

Specialty section:
This article was submitted to Molecular Innate Immunity, a section of the journal Frontiers in Immunology

Received: 22 April 2021
Accepted: 23 August 2021
Published: 10 September 2021

Citation:
Qiu Y, Cao Y, Tu G, Li J, Su Y, Fang F, Zhang X, Cang J, Rong R and Luo Z (2021) Myeloid-Derived Suppressor Cells Alleviate Renal Fibrosis Progression via Regulation of CCL5-CCR5 Axis. Front. Immunol. 12:698894. doi: 10.3389/fimmu.2021.698894

Background: Renal fibrosis is inevitable in all progressive chronic kidney diseases (CKDs) and represents a serious public health problem. Immune factors contribute to the progression of renal fibrosis. Thus, it is very possible that immunosuppression cells, such as myeloid-derived suppressor cells (MDSCs), could bring benefits to renal fibrosis. Herein, this study investigated the antifibrotic and reno-protective effect of MDSCs and the possible mechanisms.

Methods: Murine and cell models of unilateral ureter obstruction (UUO) renal fibrosis were used. Bone marrow-induced MDSCs and granulocyte–macrophage colony-stimulating factor (GM-CSF) were pretreated before surgery. Kidney weight, pathological injury, extracellular matrix deposition, and epithelial–mesenchymal transition progression were examined. Transforming growth factor (TGF)-β1)/Smad/Snail signaling pathway involvement was investigated through Western blotting and quantitative PCR (qPCR). Accumulation of MDSC, CD4+ T cell, regulatory T (Treg), and T helper 1 (T_H1) cell accumulation, and CCL5 and CCR5 expression level in MDSCs and non-MDSCs were evaluated using flow cytometry.

Results: *In vitro*- and *in vivo*-induced MDSCs significantly ameliorated UUO-induced tubulointerstitial fibrosis, inhibited the TGF-β1/Smad/Snail signaling pathway, and enhanced MDSC and Treg infiltration in the kidney while downregulating the T_H1 cells. Both *in vitro* and *in vivo* experiments confirmed CCL5 elevation in the two MDSC-treated groups.

Conclusion: *In vitro*- and *in vivo*-induced MDSCs alleviated renal fibrosis similarly through promoting the CCL5–CCR5 axis interaction and TGF-β1/Smad/Snail signaling pathway inhibition. Our results indicate an alternative treatment for renal fibrosis.

Keywords: renal fibrosis, CCL5, CCR5, migration, myeloid-derived suppressor cells

INTRODUCTION

Renal fibrosis is the common outcome of all progressive chronic kidney diseases (CKDs), which brings a great burden to public health (1). Excessive extracellular matrix (ECM) deposition and epithelial–mesenchymal transition (EMT) play essential roles during disease deterioration. Moreover, ameliorating or reversing renal fibrosis progression is difficult. Hence, it is of great urgency to explore feasible treatments to address this challenge.

Several immune factors are reported to contribute to the progression of renal fibrosis (2–4), including immune cells, inflammatory cytokines, chemokine receptors, and their ligands (5–7). Targeted mainly on T cells, myeloid-derived suppressor cells (MDSCs) are a distinctive myeloid cells population with strong immunosuppressive capacity. In mice, MDSCs are characterized by CD11b (integrin α-M) and myeloid differentiation antigen Gr-1 expression (8). Adoptive transference of MDSCs have an excellent performance in autoimmune disease treatment and allograft protection (9–11). Recently, their treating effects have also been confirmed in acute renal injury and chronic renal fibrosis (12). However, the mechanism through which MDSCs ameliorate renal fibrosis remains unclear.

Granulocyte colony-stimulating factor (G-CSF) and granulocyte–macrophage colony stimulating factor (GM-CSF) are capable of inducing *in vitro* and *in vivo* MDSCs expansion (9, 13). Recent studies have indicated that G-CSF pretreatment attenuates acute ischemia–reperfusion injury and subsequent renal fibrosis by increasing MDSC infiltration into the kidney (12). GM-CSF also stimulates neutrophils to MDSCs conversion in early human pregnancy (14). Since there is also an evidence that bone marrow (BM)-induced MDSCs exhibit more potent suppressive function than mice-isolated MDSCs (13), here raises new questions: is there a difference in the function of MDSCs induced *in vitro* or *in vivo*? Is there another mechanism that mediates the enhanced infiltration of MDSCs into renal injury?

Interactions between chemokines and chemokine receptors are involved in MDSC recruitment (15), such as C–X–C motif chemokine ligand (CXCL) 8 and its receptor (16), CXCL1-CXCR2 (17), and C–C chemokine receptor (CCR) 5 and its ligands (18, 19). The C–C motif chemokine ligand (CCL) 5–CCR5 axis, a potential therapeutic target for cancer (19) and human immunodeficiency virus (HIV) (20) infection, is highly involved in MDSC-mediated immunosuppression (21). A previous study has showed that interleukin (IL)-6 and GM-CSF upregulate CCR5 expression during *in vitro* MDSC induction (18). However, in renal fibrosis, whether the CCL5–CCR5 axis plays a role in MDSC recruitment and if there is a difference in the expression level of this axis between *in vivo*- and *in vitro*-induced MDSCs remain unknown.

The transforming growth factor (TGF)-β1/Smad signaling pathway is one of the canonical fibrogenic growth signaling pathways and considered one of the most important renal fibrosis regulators (22–24). The Smad complex is formed and transferred to the nucleus to modulate the expression of target genes after TGF-β1-triggered Smad2 and Smad3 phosphorylation. Among these target genes, Snail is a ubiquitous zinc-finger transcription factor that suppresses E-cadherin expression and accelerates EMT (25) and fibrosis (26, 27). However, it is unclear whether the TGF-β1/Smad/Snail signaling pathway is involved in the renoprotective effect of MDSCs.

In this study, BM and GM-CSF were used to induce MDSCs *in vitro* and *in vivo*, respectively, and their efficacy on renal fibrosis progression was evaluated. To further elucidate the potential mechanisms, the TGF-β1/Smad/Snail signaling pathway and the interaction between CCL5–CCR5 axis were examined. Our results indicate an alternative method for renal protection during CKD.

MATERIALS AND METHODS

Animals and Unilateral Ureter Obstruction-Induced Renal Fibrosis Model

Male 6- to 8-week-old C57BL/6J mice weighing 20–25 g were obtained from the Shanghai SLAC Laboratory Animal Co., Ltd., and bred in a specific pathogen-free (SPF)-grade animal room. All animal procedures were approved by the Animal Ethical Committee of Zhongshan Hospital, Fudan University. Mice were allocated randomly into four groups (n = 6): (1) sham group, (2) unilateral ureter obstruction (UUO) group, (3) UUO + MDSC group (MDSC), and (4) UUO + GM-CSF group (GM-CSF). The UUO-induced renal fibrosis model was established as previously described (28). Briefly, the mice were anesthetized with 100 mg/kg pentobarbital intraperitoneally. After the midline incision, the left kidney was exposed. The left ureter was isolated and ligated at two points with non-absorbable 4–0 silk sutures and then cut between the ligatures. Sterile saline (1 mL) was administered intraperitoneally before the abdominal closure. In the sham group, the left ureter was isolated but not ligated. In the MDSC group, mice were pretreated with 1×10^5 BM-induced MDSCs *via* the tail vein just before the surgery. In the GM-CSF group, 10 μg GM-CSF (PeproTech; RH, USA) was administered intraperitoneally for seven consecutive days prior to UUO. The animals were sacrificed 10 days after the operation.

Cell Culture and Treatment

Mouse renal tubular epithelial cells (mTECs) were purchased from the American Type Culture Collection (ATCC) and cultured in Dulbecco's modified Eagle's medium (DMEM) supplemented with 10% fetal bovine serum (FBS) at 37°C and 5% CO_2 for 24 h. They were divided into four groups for different treatments and seeded into 24-well plates (1×10^5 cells/well): (1) control, (2) TGF-β1, (3) TGF-β1 + 1×10^4 MDSCs (MDSC-L), and (4) TGF-β1 + 1×10^5 MDSCs (MDSC-H). Each group was administered with 10 ng/ml TGF-β1, except the control, which was administered with the same amount of sterile phosphate-buffered saline (PBS). All cells were further cultured for 24 h before being harvested and processed for Western blot and flow cytometry analyses.

In Vitro Induction, Isolation, and Adoptive Transference of MDSC

BM cells collected from 6- to 8-week-old C57BL/6 mice tibia and femur were flushed with PBS. Red blood cell (RBC) lysis buffer (BD Biosciences; CA, USA) was used to lyse red blood cells. Cells (2×10^6) were cultured at 37°C and 5% CO_2 for 7 days in 6 cm dishes

containing 3 ml Roswell Park Memorial Institute (RPMI)-1640 with 10% FBS, 1% streptomycin and penicillin, 1% MEM nonessential amino acids (NEAA) solution, 1% sodium pyruvate (Gibco, NY, USA), 2 μl 2-mercaptoethanol (Sigma-Aldrich, St. Louis, USA), 50 ng/ml GM-CSF (PeproTech), and 40 ng/ml interleukin (IL)-6 (PeproTech). The cells were harvested for testing or sorting by FACS Aria III (BD Biosciences, CA, USA) using CD11b-fluorescein isothiocyanate (FITC) (eBioscience, CA, USA) and Gr-1-PerCP Cy5.5 (eBioscience). Flow cytometry verified that all isolated MDSCs yielded >90% pure population. The purified MDSCs were then adoptively transferred to mice *via* the tail vein just before UUO. For cell tracing, some UUO mice were injected with MDSCs and stained with CFSE (Invitrogen).

Single-Cell Suspension Preparation

One-fourth kidney from the damaged side was dissected and finely minced with a gentleMACS Dissociator (Miltenyi Biotec, CA, USA) in Hank's buffer without Ca^{2+} (Gibco) containing 10% type IV collagenase (Gibco) and 0.002% DNase I (Invitrogen). The spleen was ground and filtered through a 70-μm cell mesh and resuspended in PBS. BM cells were flushed with PBS. Red blood cells were lysed for all the single-cell suspensions. The cells were then filtered and resuspended in PBS + 10% FBS for further experiments.

Cell Staining and Flow Cytometry

The cells were divided into several groups and then stained with fluorophore-conjugated antibodies, including CD11b-FITC or BV421 (eBioscience), Gr-1-PerCP Cy5.5 or APC (eBioscience), CCR5-APC or PE (BioLegend, CA, USA), CD45-AmCyan (BioLegend), CD4-PE (eBioscience), and CD25-FITC (eBioscience) for 30 min at 4°C in staining buffer (PBS with 10% FBS). CCL5-PE/Cyanine7 (BioLegend), Foxp3-APC (eBioscience), and interferon-gamma (IFN-γ)-FITC (eBioscience) were used for intracellular staining after culturing with fixation/permeabilization medium (eBioscience). Data were acquired through FACS AriaIII (BD Biosciences) and analyzed with FlowJo X (BD Biosciences).

Pathological Assessment

Paraffin-embedded one-fourth injured kidney was cut into 5-mm sections from the maximum side and subsequently deparaffinized and rehydrated. Hematoxylin and eosin (H&E) staining, Masson trichrome, and Sirius red staining were performed as previously described. Ten fields of each specimen were randomly chosen for observation at 200× magnification. For H&E staining, the severity of histological injury was evaluated randomly and independently by two renal pathologists according to the grading system described by Lin et al. Semiquantitative assessment of Sirius red and Masson trichrome was performed using ImageJ bundled with Java 1.8.0_172 (Media Cybernetics, MD, USA) to evaluate ECM deposition in the renal interstitium.

Immunofluorescence Staining

α-Smooth muscle actin (SMA) and E-cadherin were detected after staining using a rabbit anti-SMA primary antibody (Abcam, Cambridge, UK) with Alexa Fluor 594-donkey antirabbit secondary antibody (1:1,000; Invitrogen, MA, USA) and a mouse anti-E-cadherin primary antibody (1:200; Cell Signaling Technology, Boston, MA, USA) with Alexa Fluor 488-donkey antimouse antibody (1:200, Invitrogen). Finally, 4′,6-diamidino-2-phenylindole (DAPI) was used for counter-staining.

Western Blot Analysis

Western blot analysis was performed as described previously (29). Briefly, the total protein was extracted from kidney tissue samples or cultured cells (15 μg each) and separated using electrophoresis. After transferring on a polyvinylidene difluoride (PVDF) membrane, the membrane was incubated with 1:1,000 diluted primary antibodies, including anti-α-SMA, anticollagen-I, antifibronectin (all from Abcam), anti-E-cadherin, anti-p-Smad3, anti- Smad2/3, glyceraldehyde 3-phosphate dehydrogenase (GAPDH) (all from Cell Signaling Technology), anti-p-Smad2, anti-Snail (all from Beyotime; SH, China), and anti-CCL5 (ABclonal; WH, China). Goat antirabbit secondary antibody (Abcam) was added and visualized using an enhanced chemiluminescence system (Thermo Fisher Scientific, IL, USA). Band intensity was analyzed using ImageJ software and normalized to the value of GAPDH.

Quantitative Real-Time PCR

Total RNA was extracted from kidney tissue using TRIzol reagent (Invitrogen, Carlsbad, CA, USA). Then, 1 μg RNA was reverse transcribed into complementary DNA (cDNA) using HiScript II Q RT SuperMix for qPCR (Vazyme, NJ, China) in accordance with the manufacturer's instructions. Real-time PCR was performed as described in our previous report using a Mastercycle reprealplex system (Eppendorf, Hamburg, Germany). Target gene expression levels were evaluated by reference to the value of GAPDH using the $2^{-\Delta\Delta Ct}$ method. The PCR primers (including those for fibronectin, collagen I, E-cadherin, α-SMA, TGF-β1, Snail, and GAPDH) were synthesized according to sequences provided by PrimerBank (**Table 1**).

Enzyme-Linked Immunosorbent Assay for Serum TGF-β1

TGF-β1 levels in the serum samples were measured using a commercially available ELISA kit (MLBio, Shanghai, China) according to the manufacturer's instructions.

TABLE 1 | Primers sequences used for RT-PCR.

Gene	Primers
Fibronectin	F: 5′-TGGAGAGACAGGAGGAAATAGC-3′
	R: 5′-CAGTGACAGCATACAGGGTGAT-3′
Collagen I	F: 5′-GAGAGAGCATGACCGATGGA-3′
	R: 5′-CGTGCTGTAGGTGAATCGAC-3′
E-cadherin	F: 5′-CAGGTCTCCTCATGGCTTTGC-3′
	R: 5′-CTTCCGAAAAGAAGGCTGTCC-3′
α-SMA	F: 5′-GTCCCAGACATCAGGGAGTAA-3′
	R: 5′-TCGGATACTTCAGCGTCAGGA-3′
TGF-β1	F: 5′-CTCCCGTGGCTTCTAGTGC-3′
	R: 5′-GCCTTAGTTTGGACAGGATCTG-3′
Snail	F: 5′-CACACGCTGCCTTGTGTCT-3′
	R: 5′-GGTCAGCAAAAGCACGGTT-3′
GAPDH	F: 5′-TCACCATCTTCCAGGAGCGAGAC-3′
	R:5′-TGAGCCCTTCCACAATGCCAAAG-3′

Statistical Analysis

Data are presented as means ± standard deviation (SD). GraphPad Prism 9 (GraphPad Software Inc., CA, USA) was used for the statistical analyses. Two-tailed independent Student's *t*-test was applied for comparison between two groups and one-way analysis of variance (ANOVA) followed by Bonferroni's correction for more groups. Statistical significance was set at $p < 0.05$.

RESULTS

BM-Induced MDSCs and GM-CSF Alleviate Renal Fibrosis

Mice kidney were harvested 10 days after surgery (**Figure 1A**). The kidney weight significantly decreased on the ligation side, and the pelvis and calices were severely dilated with atrophied renal parenchyma in the UUO group (**Figure 1B**). H&E staining showed severe tubular dilation, interstitial expansion, and inflammatory cell infiltration (**Figure 1C**). However, kidney weight increased in the MDSC or GM-CSF groups (**Figure 1B**), and renal fibrosis injury was significantly alleviated (**Figure 1C**). There were no significant differences between the two groups.

Collagen deposition was detected using Sirius red and Masson staining (**Figures 1D, E**, respectively). Compared with that in the sham group, collagen accumulation in the renal interstitium increased significantly in UUO groups, while MDSC transplantation and GM-CSF pretreatment decreased interstitial collagen deposition, although these results were not comparable with those of the sham group. This evidence indicates a definite and similar renoprotective effect of MDSC transplantation and GM-CSF pretreatment.

BM-Induced MDSCs and GM-CSF Reduce ECM Deposition and EMT

The mRNA and protein levels of fibronectin and collagen I were examined to evaluate ECM deposition (**Figures 2A, B**, respectively).

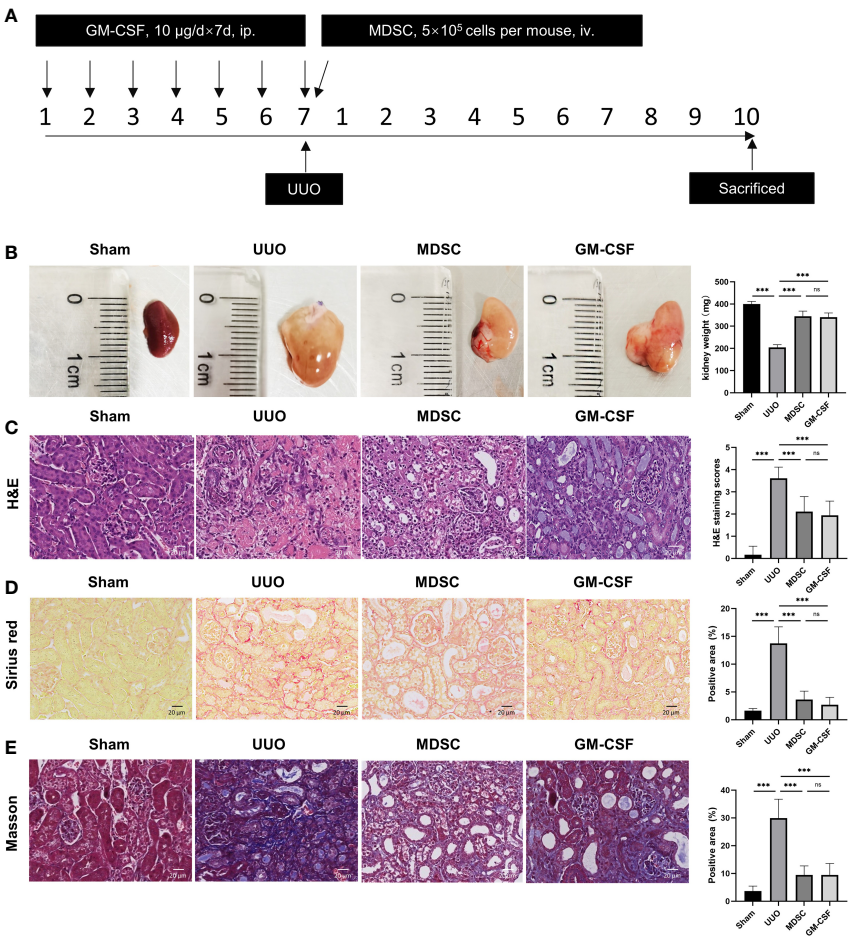


FIGURE 1 | BM-induced MDSCs and GM-CSF alleviate renal fibrosis induced by UUO. **(A)** Flow chart of the *in vivo* study. **(B)** Kidney size and weight at 10 days after UUO. **(C)** Representative micrographs of H&E staining of kidney sections (scale bar, 20 μm) and semiquantitative data of tubule injury score. **(D)** Representative micrographs of Sirius red staining and semiquantitative data of fibrosis area. **(E)** Representative micrographs of Masson staining and semiquantitative data of fibrosis area. Data are presented as the mean ± SD (n = 6). ***$p < 0.001$. ns^P > 0.05.

ECM deposition increased in the UUO group but was similarly downregulated in MDSC or GM-CSF groups. This indicated that MDSC transplantation or GM-CSF pretreatment could both inhibit ECM deposition.

We then examined the epithelial marker E-cadherin and the mesenchymal marker α-SMA to evaluate EMT. qPCR and Western blot analysis revealed high E-cadherin expression and low α-SMA expression in the sham group (**Figures 2C, D**, respectively); however, the result was reversed 10 days after UUO, indicating EMT occurrence. However, α-SMA expression decreased and E-cadherin expression increased significantly in the MDSC and GM-CSF groups than those in the UUO group, which were verified using immunofluorescence (**Figure 2E**). These results further confirmed the similar protective role of the two treatments in renal fibrosis.

To further verify the antifibrotic role of BM-induced MDSCs, we conducted an *in vitro* experiment using mTECs. Corresponding to the results of the *in vivo* experiments, Western blot analysis also

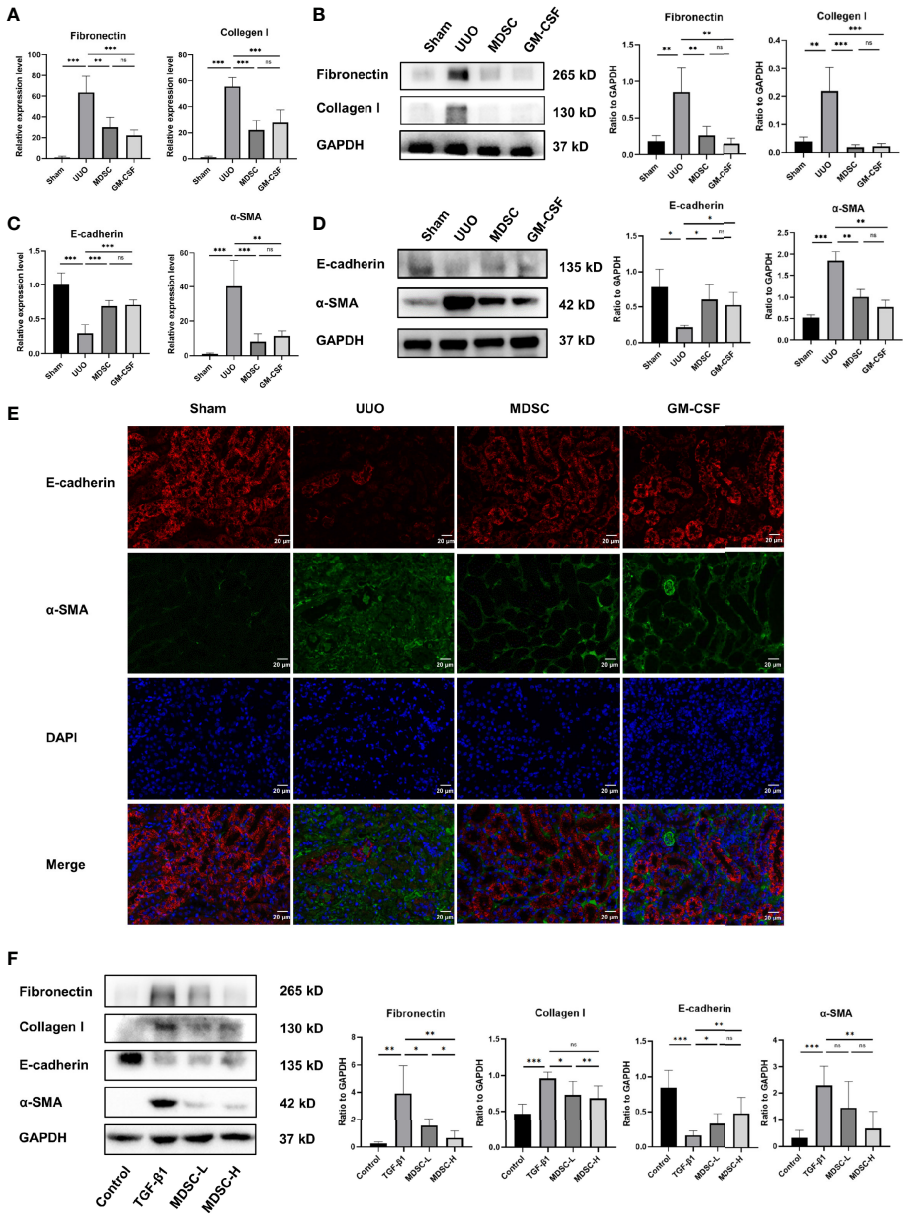


FIGURE 2 | BM-induced MDSCs and GM-CSF reduce ECM deposition and EMT. **(A)** Relative mRNA levels of fibronectin and collagen I in renal tissue. **(B)** Western blot analysis of fibronectin and collagen I in renal tissue and their relative expression level to GAPDH. **(C)** Relative mRNA levels of E-cadherin and α-SMA in renal tissue. **(D)** Western blot analysis of E-cadherin and α-SMA in renal tissue and their relative expression level to GAPDH. **(E)** Representative immunofluorescence staining images of E-cadherin (red), α-SMA (green), and DAPI (blue). **(F)** Western blot analysis of fibronectin, collagen I, E-cadherin, and α-SMA in *in vitro* experiment and their relative expression level to GAPDH. Data are presented as the mean ± SD (n = 6). $^{*}p < 0.05$, $^{**}p < 0.01$, $^{***}p < 0.001$. ns^P > 0.05.

showed a dose-dependent decrease in ECM and EMT markers after treatment with different MDSC concentrations (**Figure 2F**). Thus, BM-induced MDSCs directly influenced TECs.

BM-Induced MDSCs and GM-CSF Play Their Renoprotective Role by Inhibiting TGF-β1 Signaling Pathway

To explore the mechanism by which MDSCs alleviate renal fibrosis, TGF-β1 expression in serum and kidney tissue were examined using ELISA, qPCR, and Western blotting (**Figures 3A–C**, respectively). TGF-β1 was upregulated significantly in the UUO group, whereas treatments downregulated its expression. We further investigated whether the TGF-β1 signaling pathway was involved in the renoprotective effect of BM-induced MDSCs or GM-CSF. As shown in **Figures 3B, C**, Smad2 and Smad3 phosphorylation was significantly elevated in the UUO group, while both BM-induced MDSCs or GM-CSF significantly ameliorated them. The target gene of the Smad complex, Snail, was also upregulated in the UUO group and downregulated in the two treatment groups. Later, in the *in vitro* experiment, TGF-β1, phosphorylated Smad2 and Smad3, and Snail expression levels in mTEC cells were also upregulated in the TGF-β1 group but

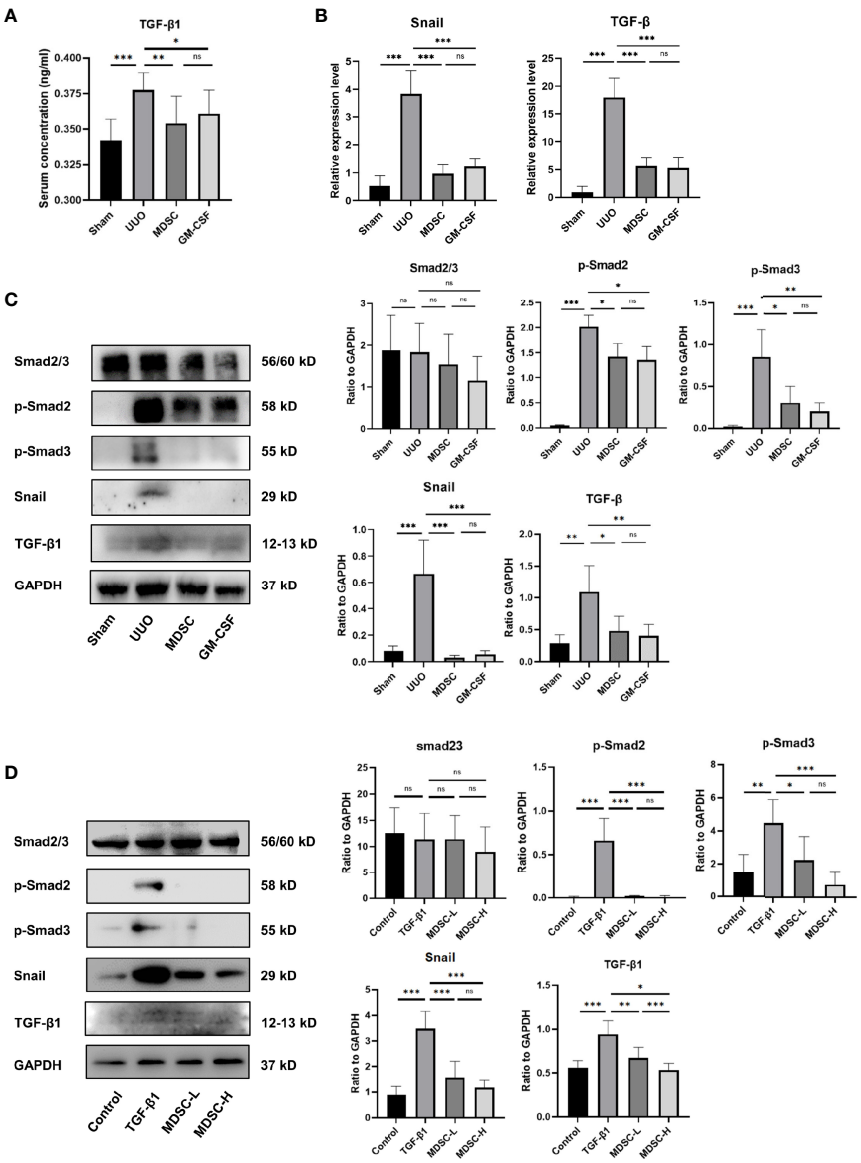


FIGURE 3 | BM-induced MDSCs and GM-CSF play their reno-protective role by inhibiting TGF-β1 signaling pathway. **(A)** Serum concentration of TGF-β1 in all groups. **(B)** Relative mRNA levels of TGF-β1 and Snail in renal tissue. **(C)** Western blot analysis of TGF-β1, Smad2/3, p-Smad2, p-Smad3, and Snail in renal tissues and their relative expression level to GAPDH. **(D)** Western blot analysis of TGF-β1, Smad2/3, p-Smad2, p-Smad3, and Snail in *in vitro* experiment and their relative expression level to GAPDH. Data are expressed as the mean ± SD (n = 6). *$p < 0.05$, **$p < 0.01$, ***$p < 0.001$. ns^P > 0.05.

downregulated in the MDSC-L group and strongly downregulated in the MDSC-H group (**Figure 3D**). These results suggested that BM-induced MDSCs or GM-CSF alleviates UUO by intervening in the TGF-β1/Smad/Snail signaling pathway. The number of MDSCs may affect their antifibrotic effects.

Enhanced MDSC Recruitment Is an Important Mechanism for *In Vivo* or *In Vitro* Induced MDSCs to Alleviate Renal Fibrosis

We then evaluated MDSC accumulation in the kidney after UUO. Compared with that in the sham group, a small number of MDSCs were recruited to the kidneys in the UUO group, while more MDSCs were recruited to the kidneys in both treatment groups (**Figure 4A**). There were no significant differences in the number of MDSCs in the kidneys between the two treatment groups. In addition, among all MDSCs recruited to injury site in the MDSC group, 44.95 ± 0.21% MDSCs were CFSE labeled (incubated with MDSCs before adoptive transference; **Figure 4B**). These results suggest that artificially induced MDSCs (*in vivo* or *in vitro*) have stronger recruitment ability than natural MDSCs, and the recruitment ability of *in vitro*- and *in vivo*-induced MDSCs were comparable.

Observing the MDSC downstream effector cells showed that $CD4^+$ T, regulatory T (Treg), and T helper (T_H) 1 cell recruitment to the kidney increased after UUO (**Figures 4C–E**, respectively). However, the number of T_H1 cells in the kidney decreased significantly after treatment, while the number of Treg cells increased. These results indicated that MDSCs also alleviate renal fibrosis indirectly by affecting the balance between T_H1 and Tregs. This effect was related to their elevated recruitment to the injury site.

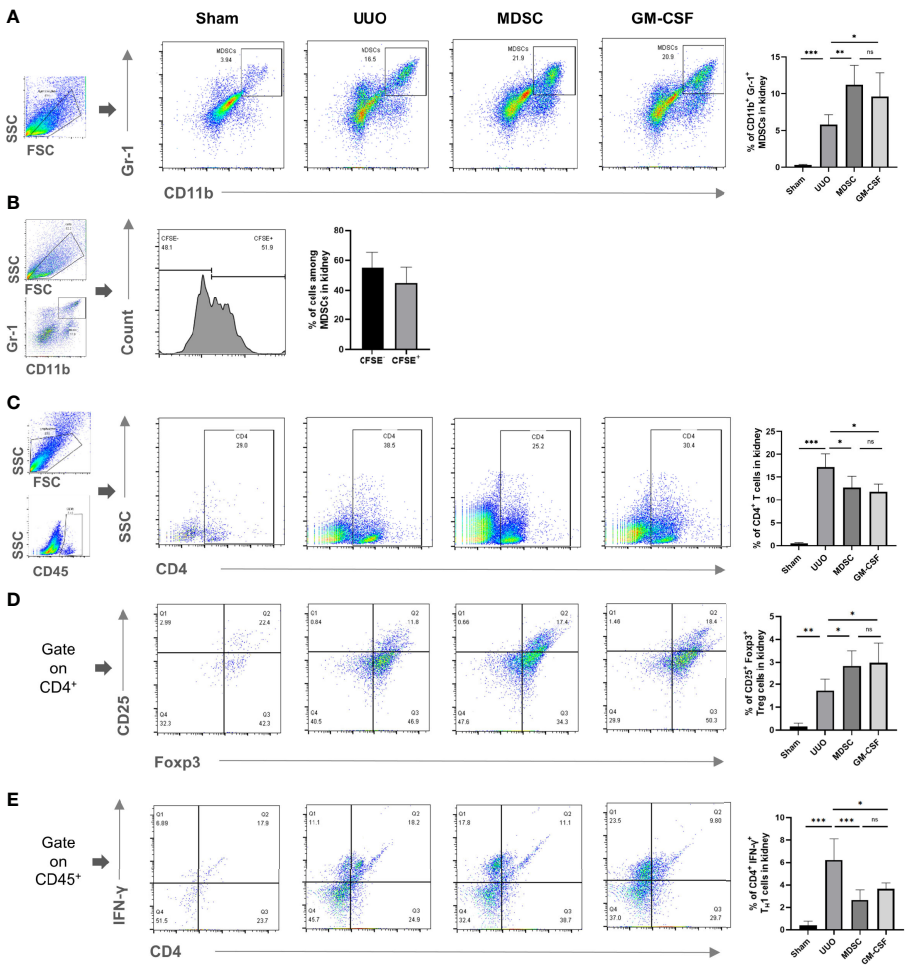


FIGURE 4 | Enhanced MDSC recruitment is an important mechanism for *in vivo* or *in vitro* induced MDSCs to alleviate renal fibrosis. Flow cytometry detected the percentage of **(A)** $CD11b^+$ $Gr\text{-}1^+$ MDSCs in kidney, **(B)** BM-induced MDSCs (CFSE labeled) among all MDSCs in kidney, **(C)** $CD4^+$ T cells in kidney, **(D)** $CD4^+CD25^+Foxp^+$ Tregs in kidney, **(E)** $CD4^+IFN\gamma^+$ T_H1 in kidney. Data are expressed as the mean ± SD (n = 6). $^*p < 0.05$, $^{**}p < 0.01$, $^{***}p < 0.001$. ns^P > 0.05.

Increased CCL5 Expression in *In Vitro*- or *In Vivo*-Induced MDSCs Mediate the Enhanced MDSC Accumulation

To explain the mechanism of enhanced recruitment ability of *in vitro*- or *in vivo*-induced MDSCs, the CCL5 and CCR5 expression levels in MDSCs and non-MDSCs of different tissues (kidney, spleen, and BM) were measured. CCL5 expression increased in the MDSCs located in all tissues in the UUO group than that in the sham group and further increased in the two treatment groups (**Figures 5A, E, F**). However, although CCR5 expression also increased in non-MDSCs located in the kidneys after UUO, they did not differ between UUO and the two treatment groups (**Figure 5D**). Moreover, CCR5 expression level in MDSCs and CCL5 expression in in non-MDSCs were also comparable between UUO and the two treatment groups (**Figures 5B, C**, respectively). *In vitro* experiments further confirmed that the CCL5 and CCR5 expression levels in non-MDSCs (mainly mTEC cells) were not altered (**Figures 6A, B**).

Finally, we tracked CCL5 expression in *in vitro*- and *in vivo*-induced MDSCs. *In vitro*-induced MDSCs were harvested and examined 1, 3, and 7 days after induction. *In vivo*-induced MDSCs were separated from the BM of mice 1, 3, and 7 days

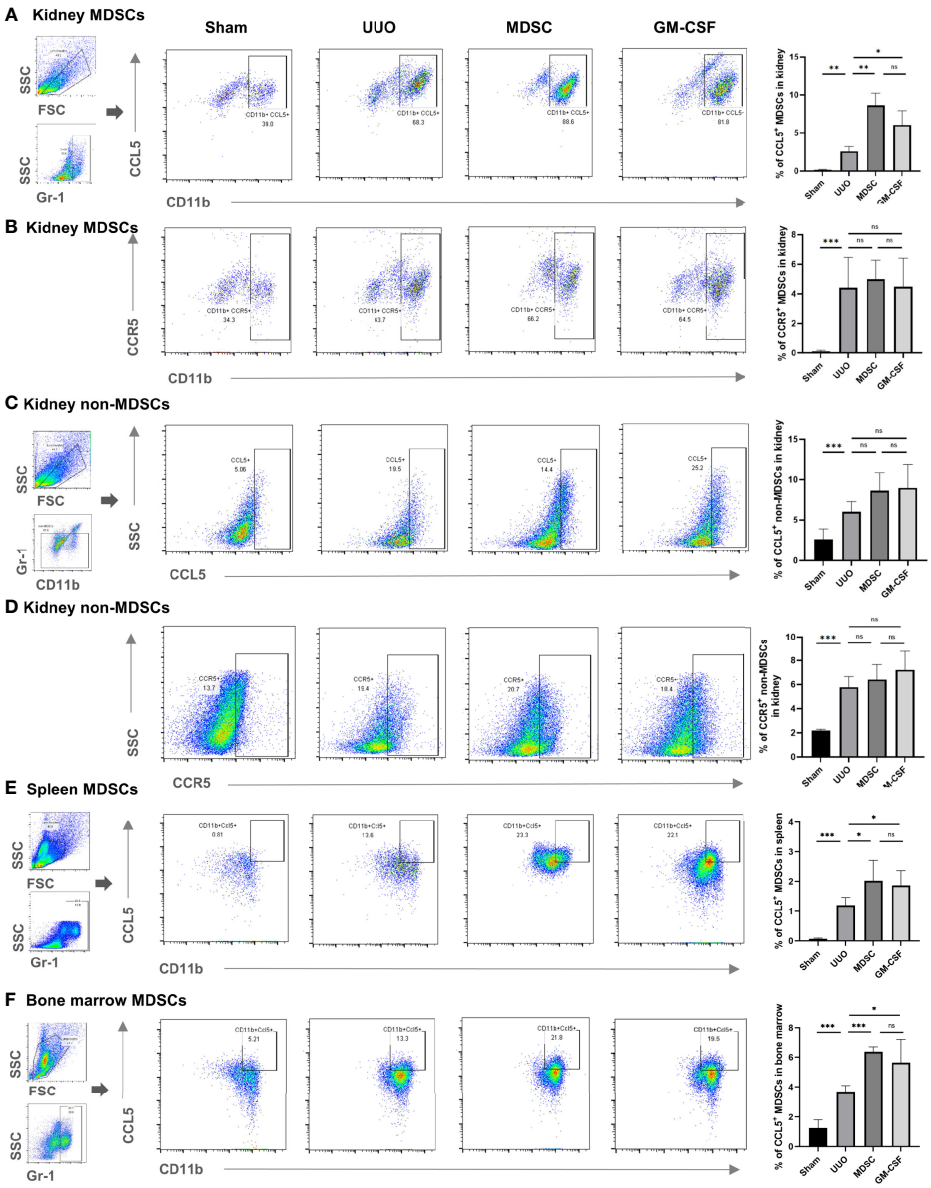


FIGURE 5 | Expression level of CCL5 and CCR5 in MDSCs and non-MDSCs in mice. Flow cytometry detected the percentage of **(A)** $CCL5^+$ MDSCs in kidneys, **(B)** $CCR5^+$ MDSCs in kidney, **(C)** $CCL5^+$ non-MDSCs in kidney, **(D)** $CCR5^+$ non-MDSCs in kidney, **(E)** $CCL5^+$ MDSCs in spleen, and **(F)** $CCL5^+$ MDSCs in bone marrow. Data are expressed as the mean ± SD (n = 6). $^*p < 0.05$, $^{**}p < 0.01$, $^{***}p < 0.001$. ns^P > 0.05.

after GM-CSF treatment. We found that CCL5 increased gradually for 7 days after *in vitro* induction (**Figure 6C**), and the expression level in *in vivo*-induced MDSCs were similar (**Figure 6D**). Thus, *in vitro* and *in vivo* MDSC induction stimulate CCL5 expression. This may also explain the comparable ability of MDSCs to recruit and alleviate renal fibrosis in both regimens.

DISCUSSION

In this study, we found that BM-induced MDSCs or GM-CSF pretreatment increased MDSC infiltration and significantly ameliorated UUO-induced tubulointerstitial fibrosis. TGF-β1 inhibition and its downstream signaling pathway were involved in this renoprotective process. We further elucidated that induced MDSCs, both *in vitro* and *in vivo*, enhanced CCL5 secretion, which promoted their recruitment to kidneys to play immunosuppressive and anti-fibrotic roles (**Figure 7**).

Overexpression of ECM components, such as fibronectin and collagen I, causes ECM deposition (30), thereby destroying the kidney parenchyma and deteriorating renal function, resulting in renal fibrosis progression. In our study, Masson and Sirius red staining showed increased ECM deposition in UUO group, while adoptive transference of MDSCs or GM-CSF pretreatment attenuated it. Western blotting and qPCR showed that fibronectin and collagen I expression also changed similarly. These results demonstrated that adoptive transference of MDSCs or GM-CSF pretreatment effectively ameliorate ECM deposition and eventually delay renal fibrosis progression.

EMT is a process that depicts the transition from epithelial cells to mesenchymal cells, which contributes a lot to the progression of renal fibrosis. TECs acquiring a mesenchymal phenotype have been deemed as the main source of activated myofibroblasts in the injured kidney (31), and they secrete a wide range of proinflammatory cytokines, which further aggravate renal fibrosis. In our study, EMT activation was also observed through immunofluorescence in the UUO group. Western blot and qPCR also confirmed the reduced E-cadherin and elevated α-SMA expression. However, adoptive transference of MDSCs or GM-CSF pretreatment reversed this trend and caused weight gain in the kidneys. These findings further confirmed the renoprotective role of MDSCs and GM-CSF.

TGF-β1 belongs to the TGF-β superfamily and is considered to be an essential mediator of renal fibrosis (22, 23). It promotes ECM production and EMT (32) by regulating inflammatory

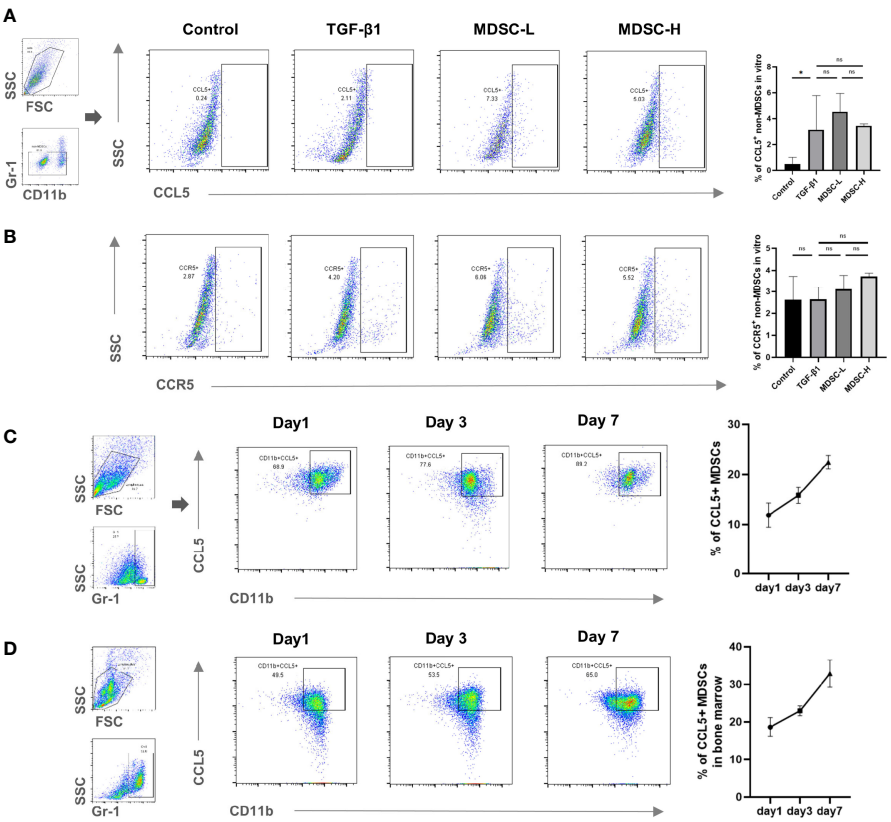


FIGURE 6 | CCL5 expression in *in vitro*- and *in vivo*-induced MDSCs. Flow cytometry detected the percentage of **(A)** $CCL5^+$ non-MDSCs in *in vitro* experiment, **(B)** $CCR5^+$ non-MDSCs in *in vitro* experiment, **(C)** $CCL5^+$ MDSCs in *in vitro*-induced cells, and **(D)** $CCL5^+$ MDSCs in bone marrow of mice pretreated with GM-CSF. Data are expressed as the mean ± SD (n = 6). *$p < 0.05$. ns^P > 0.05.

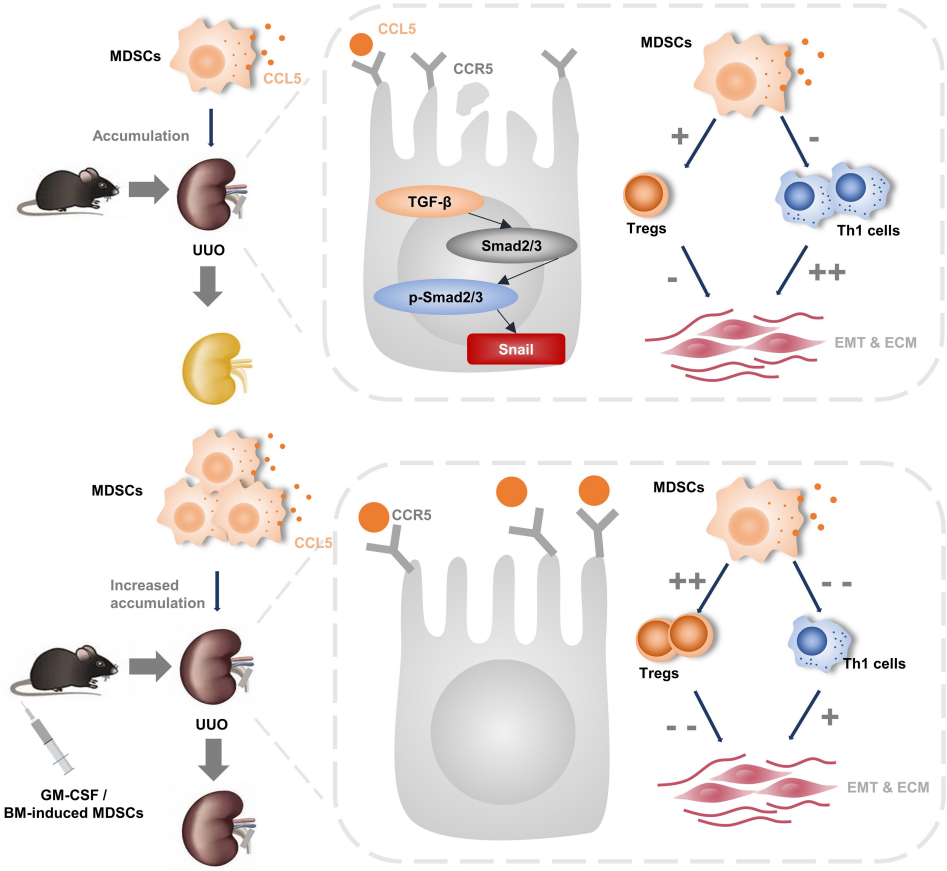


FIGURE 7 | The pictorial summary of induced MDSCs on renal fibrosis. *In vitro*- and *in vivo*-induced MDSCs increased their infiltration to injury by promoting CCL5-CCR5 interaction. In addition, they alleviate renal fibrosis to a similar extend by inhibiting TGF-β1/Smad/Snail signaling pathway and rebalance Th1/Treg.

cells, including T cells and macrophages (23, 24). The TGF-β1/Smad signaling pathway is one of the canonical fibrogenic growth signaling pathways. Once TGF-β1 binds to its receptor, Smad2 and Smad3 phosphorylation is triggered, and the Smad complex is formed by the combination with Smad4. The Smad complex is then transferred to the nucleus to drive the expression of target genes, including Snail, which also contributes to EMT (25) and fibrosis (26, 27). In this study, we detected significant TGF-β1/Smad/Snail signaling pathway activation in the UUO group, which was inhibited by adoptive transference of MDSCs or GM-CSF pretreatment. These phenomena indicate that MDSCs or GM-CSF play a renoprotective role partly by counteracting the TGF-β1/Smad/Snail signaling pathway.

Immune factors, including immune cells, inflammatory cytokines, chemokine receptors, and their ligands, may contribute to renal fibrosis progression (2–7). Recently, researchers have focused on the effect of MDSCs in renal fibrosis (12, 33). MDSCs develop in various chronic inflammatory conditions, such as infection, tumors, autoimmune diseases, and graft-*versus*-host disease (GVHD). It suppresses T helper (T_H) cell accumulation and induces Tregs through signal transducer and transcription activator (9). Tregs further inhibit $CD4^+$ T_H cell proliferation and function by secreting cytokines such as IL-10 and inhibiting IL-2 availability for $CD4^+$ T_H cells (34, 35). The balance between T_H1 and Treg cells has drawn great attention in cancer (36), various inflammatory diseases (37, 38), and autoimmunity diseases (39). Treg accumulation and T_H1 cell downregulation are also necessary for the convalescence of crescentic glomerulonephritis (40). In our study, both *in vitro*- or *in vivo*-induced MDSCs promoted MDSC and Treg infiltration in the kidney and downregulated the total $CD4^+$ T and T_H1 cell infiltration in the kidney. These results suggest that Tregs might partially contribute to MDSC/GM-CSF-induced renal fibrosis remission, which may be mediated by MDSC-induced immunosuppression.

Although natural MDSCs increase their number in inflammation, their immunosuppressive activity might be limited in a highly inflammatory environment due to myeloid differentiation, inflammatory mediator production, and cell-intrinsic inflammasome upregulation (41). Nevertheless, researchers have found that *in vitro*-induced MDSCs after culturing BM cells with G-CSF and GM-CSF obtained a phenotype similar to that of natural MDSCs with a protective effect in various primary target organs and inhibited GVHD-correlated death by 80% (42, 43). This indicated the potent

treatment efficiency of adoptive transference of MDSC-enriched populations after *in vitro* expansion. However, the mechanism underlying the maintenance of the immunosuppressive phenotype by *in vitro*-induced MDSCs remains unclear. In our study, approximately half of the MDSCs accumulated to the injury site were BM induced, which further inhibited T_H1 and promoted Treg expansion. In addition, *in vitro* experiments showed that a high MDSC dose had a strong ability to inhibit ECM and EMT. These results suggest that the number of MDSCs accumulated may have an effect on the maintenance of the immunosuppressive phenotype.

The clinical application of GM-CSF is more convenient than MDSC-adoptive therapy. However, whether they can achieve similar efficacy in renal fibrosis remains unclear. A recent study has reported that enhanced G-CSF and GM-CSF expression promotes MDSC generation and migration (12, 44), indicating that G-CSF and GM-CSF are both efficient for inducing MDSC expansion. However, although G-CSF is more commonly used in clinical settings, GM-CSF is well accepted for *in vitro* MDSC induction because it can induce both MDSC phenotypes ($CD11b^+Ly6G^{int}Ly6C^{low}$ and $CD11b^+Ly6G^{int}Ly6C^{low}$ populations) in a balanced manner. However, their ability to induce MDSCs or immunosuppression *in vivo* remains controversial (45, 46). Thus, we selected GM-CSF for simple and effective MDSC induction. In accordance with our expectations, GM-CSF pretreatment promotes the MDSC infiltration and significantly ameliorates renal fibrosis. The adoptive transference of BM-induced MDSCs showed a similar efficacy. Thus, our results proved the equivalent efficacy of GM-CSF and BM-induced MDSCs and provided an alternative and convenient method for treating renal fibrosis.

The CCL5–CCR5 axis is involved in MDSC recruitment and its immunosuppressive role (19, 47). A previous study has also showed that IL-6 and GM-CSF upregulate CCR5 expression during *in vitro* MDSC induction (18). However, we did not find an increase in CCR5 expression in kidney MDSCs or non-MDSCs or *in vitro* experiments in the treatment groups. In contrast, we found that CCL5 was significantly elevated in MDSCs located in the kidney, spleen, and BM in the two treatment groups. We also found that CCL5 expression gradually increased with time. These results indicated that GM-CSF could increase CCL5 expression in both *in vitro*- or *in vivo*-induced MDSCs. Enhanced CCL5 expression further promotes MDSC recruitment to injuries to exert their immunosuppressive function. A recent case–control study has provided evidence for this hypothesis. Researchers found that decreased serum CCL5 and TGF-β concentrations were highly correlated with reduced blood MDSCs and Tregs in patients with recurrent implantation failure (RIF) (48). Previous research also found that MDSCs from CCL5-knockout mice with breast tumors expressed less NOS_2 and S100A8/9 and showed an immune-stimulatory phenotype (21). All these studies indicated that CCL5 plays an important role in the immunosuppressive function of MDSCs.

This study had some limitations. Although UUO is a well-accepted renal fibrosis animal model, it rarely causes renal fibrosis or progressive kidney failure in clinical settings. Thus, whether GM-CSF or MDSC treatment could have similar therapeutic effects in other obstruction-induced renal fibrosis diseases remains to be explored. Second, considering the higher metabolic rate in mice than that in humans, the effective GM-CSF dose used for *in vivo* induction is much higher than that for clinical use. Therefore, further studies should determine the optimal GM-CSF dose for inducing human MDSCs. Third, GM-CSF affects several cell types, including macrophages and granulocytes. Future studies should explore its role in influencing renal fibrosis. Finally, CCL5 and CCR5 are not unique ligand receptors, and they are not the only chemokine or receptor expressed in MDSCs. Future studies should focus on ruling out the involvement of other receptors or ligands.

In conclusion, our study demonstrated that *in vitro*- and *in vivo*-induced MDSCs alleviate renal fibrosis similarly, both by promoting the CCL5–CCR5 axis interaction and TGF-β1/Smad/Snail signaling pathway inhibition. Our results indicate an alternative treatment for renal fibrosis.

DATA AVAILABILITY STATEMENT

The raw data supporting the conclusions of this article will be made available by the authors, without undue reservation.

ETHICS STATEMENT

The animal study was reviewed and approved by Animal Ethical Committee of Zhongshan Hospital, Fudan University.

AUTHOR CONTRIBUTIONS

ZL, RR, and JC: conceived the project, designed the project, and approved the final manuscript. YQ, GT, and YC: drafted the manuscript, conducted the experiments, and extracted and analyzed data. JL, FF, YS, and XZ: conducted the experiments and extracted and analyzed data. All authors contributed to the article and approved the submitted version.

FUNDING

This work was supported by the National Key R&D Program of China (2018YFA0107501), National Natural Science Foundation of China (81770747, 81970646, and 82070085), construction program of key but weak disciplines of Shanghai Health Commission (2019ZB0105), Natural Science Foundation of Shanghai (20ZR1411100), Program of Shanghai Academic/Technology Research Leader (20XD1421000), Clinical Research Funds of Zhongshan Hospital (2020ZSLC38 and 2020ZSLC27), and Smart Medical Care of Zhongshan Hospital (2020ZHZS01).

REFERENCES

1. Webster AC, Nagler EV, Morton RL, Masson P. Chronic Kidney Disease. *Lancet* (2017) 389(10075):1238–52. doi: 10.1016/S0140-6736(16)32064-5
2. Guiteras R, Sola A, Flaquer M, Hotter G, Torras J, Grinyo JM, et al. Macrophage Overexpressing NGAL Ameliorated Kidney Fibrosis in the UUO Mice Model. *Cell Physiol Biochem* (2017) 42(5):1945–60. doi: 10.1159/000479835
3. Wang H, Gao M, Li J, Sun J, Wu R, Han D, et al. MMP-9-Positive Neutrophils Are Essential for Establishing Profibrotic Microenvironment in the Obstructed Kidney of UUO Mice. *Acta Physiol (Oxf)* (2019) 227(2):e13317. doi: 10.1111/apha.13317
4. Yang L, Besschetnova TY, Brooks CR, Shah JV, Bonventre JV. Epithelial Cell Cycle Arrest in G2/M Mediates Kidney Fibrosis After Injury. *Nat Med* (2010) 16(5):535–43, 1p following 143. doi: 10.1038/nm.2144
5. Zhu Z, Han C, Xian S, Zhuang F, Ding F, Zhang W, et al. Placental Mesenchymal Stromal Cells (PMSCs) and PMSC-Derived Extracellular Vesicles (PMSC-EVs) Attenuated Renal Fibrosis in Rats With Unilateral Ureteral Obstruction (UUO) by Regulating CD4(+) T Cell Polarization. *Stem Cells Int* (2020) 2020:2685820. doi: 10.1155/2020/2685820
6. Hopfer H, Holzer J, Hunemorder S, Paust HJ, Sachs M, Meyer-Schwesinger C, et al. Characterization of the Renal CD4+ T-Cell Response in Experimental Autoimmune Glomerulonephritis. *Kidney Int* (2012) 82(1):60–71. doi: 10.1038/ki.2012.73
7. Paust HJ, Ostmann A, Erhardt A, Turner JE, Velden J, Mittrucker HW, et al. Regulatory T Cells Control the Th1 Immune Response in Murine Crescentic Glomerulonephritis. *Kidney Int* (2011) 80(2):154–64. doi: 10.1038/ki.2011.108
8. Bronte V, Brandau S, Chen SH, Colombo MP, Frey AB, Greten TF, et al. Recommendations for Myeloid-Derived Suppressor Cell Nomenclature and Characterization Standards. *Nat Commun* (2016) 7:12150. doi: 10.1038/ncomms12150
9. Gabrilovich DI, Nagaraj S. Myeloid-Derived Suppressor Cells as Regulators of the Immune System. *Nat Rev Immunol* (2009) 9(3):162–74. doi: 10.1038/nri2506
10. Wu T, Zhao Y, Zhao Y. The Roles of Myeloid-Derived Suppressor Cells in Transplantation. *Expert Rev Clin Immunol* (2014) 10(10):1385–94. doi: 10.1586/1744666X.2014.948424
11. Zhang C, Wang S, Yang C, Rong R. The Crosstalk Between Myeloid Derived Suppressor Cells and Immune Cells: To Establish Immune Tolerance in Transplantation. *J Immunol Res* (2016) 2016:4986797. doi: 10.1155/2016/4986797
12. Yan JJ, Ryu JH, Piao H, Hwang JH, Han D, Lee SK, et al. Granulocyte Colony-Stimulating Factor Attenuates Renal Ischemia-Reperfusion Injury by Inducing Myeloid-Derived Suppressor Cells. *J Am Soc Nephrol* (2020) 31(4):731–46. doi: 10.1681/ASN.2019060601
13. Adeegbe D, Serafini P, Bronte V, Zoso A, Ricordi C, Inverardi L. *In Vivo* Induction of Myeloid Suppressor Cells and CD4(+)Foxp3(+) T Regulatory Cells Prolongs Skin Allograft Survival in Mice. *Cell Transplant* (2011) 20(6):941–54. doi: 10.3727/096368910X540621
14. Li C, Chen C, Kang X, Zhang X, Sun S, Guo F, et al. Decidua-Derived Granulocyte Macrophage Colony-Stimulating Factor Induces Polymorphonuclear Myeloid-Derived Suppressor Cells From Circulating CD15+ Neutrophils. *Hum Reprod* (2020) 35(12):2677–91. doi: 10.1093/humrep/deaa217
15. Li BH, Garstka MA, Li ZF. Chemokines and Their Receptors Promoting the Recruitment of Myeloid-Derived Suppressor Cells Into the Tumor. *Mol Immunol* (2020) 117:201–15. doi: 10.1016/j.molimm.2019.11.014
16. Yue D, Liu S, Zhang T, Wang Y, Qin G, Chen X, et al. NEDD9 Promotes Cancer Stemness by Recruiting Myeloid-Derived Suppressor Cells via CXCL8 in Esophageal Squamous Cell Carcinoma. *Cancer Biol Med* (2021) 18(3):705–20. doi: 10.20892/j.issn.2095-3941.2020.0290
17. Groth C, Arpinati L, Shaul ME, Winkler N, Diester K, Gengenbacher N, et al. Blocking Migration of Polymorphonuclear Myeloid-Derived Suppressor Cells Inhibits Mouse Melanoma Progression. *Cancers (Basel)* (2021) 13(4):726. doi: 10.3390/cancers13040726
18. Weber R, Riester Z, Huser L, Sticht C, Siebenmorgen A, Groth C, et al. IL-6 Regulates CCR5 Expression and Immunosuppressive Capacity of MDSC in Murine Melanoma. *J Immunother Cancer* (2020) 8(2):e000949. doi: 10.1136/jitc-2020-000949
19. Hemmatazad H, Berger MD. CCR5 Is a Potential Therapeutic Target for Cancer. *Expert Opin Ther Targets* (2021) 25(4):311–27. doi: 10.1080/14728222.2021.1902505
20. Lin D, Scheller SH, Robinson MM, Izadpanah R, Alt EU, Braun SE. Increased Efficiency for Biallelic Mutations of the CCR5 Gene by CRISPR-Cas9 Using Multiple Guide RNAs As a Novel Therapeutic Option for Human Immunodeficiency Virus. *CRISPR J* (2021) 4(1):92–103. doi: 10.1089/crispr.2020.0019
21. Ban Y, Mai J, Li X, Mitchell-Flack M, Zhang T, Zhang L, et al. Targeting Autocrine CCL5-CCR5 Axis Reprograms Immunosuppressive Myeloid Cells and Reinvigorates Antitumor Immunity. *Cancer Res* (2017) 77(11):2857–68. doi: 10.1158/0008-5472.CAN-16-2913
22. Massague J, Wotton D. Transcriptional Control by the TGF-Beta/Smad Signaling System. *EMBO J* (2000) 19(8):1745–54. doi: 10.1093/emboj/19.8.1745
23. Gu YY, Liu XS, Huang XR, Yu XQ, Lan HY. TGF-Beta in Renal Fibrosis: Triumphs and Challenges. *Future Med Chem* (2020) 12(9):853–66. doi: 10.4155/fmc-2020-0005
24. Lan HY. Diverse Roles of TGF-Beta/Smads in Renal Fibrosis and Inflammation. *Int J Biol Sci* (2011) 7(7):1056–67. doi: 10.7150/ijbs.7.1056
25. Lamouille S, Xu J, Derynck R. Molecular Mechanisms of Epithelial-Mesenchymal Transition. *Nat Rev Mol Cell Biol* (2014) 15(3):178–96. doi: 10.1038/nrm3758
26. Wang Y, Li S, Zhao J, Li Q, Xu C, Wu H, et al. Snail-Mediated Partial Epithelial Mesenchymal Transition Augments the Differentiation of Local Lung Myofibroblast. *Chemosphere* (2021) 267:128870. doi: 10.1016/j.chemosphere.2020.128870
27. Grande MT, Sanchez-Laorden B, Lopez-Blau C, De Frutos CA, Boutet A, Arevalo M, et al. Snail1-Induced Partial Epithelial-to-Mesenchymal Transition Drives Renal Fibrosis in Mice and Can Be Targeted to Reverse Established Disease. *Nat Med* (2015) 21(9):989–97. doi: 10.1038/nm.3901
28. Gong W, Mao S, Yu J, Song J, Jia Z, Huang S, et al. NLRP3 Deletion Protects Against Renal Fibrosis and Attenuates Mitochondrial Abnormality in Mouse With 5/6 Nephrectomy. *Am J Physiol Renal Physiol* (2016) 310(10):F1081–1088. doi: 10.1152/ajprenal.00534.2015
29. Zheng L, Li L, Qi G, Hu M, Hu C, Wang S, et al. Transplantation of Telocytes Attenuates Unilateral Ureter Obstruction-Induced Renal Fibrosis in Rats. *Cell Physiol Biochem* (2018) 46(5):2056–71. doi: 10.1159/000489445
30. Shen Y, Miao N, Xu J, Gan X, Xu D, Zhou L, et al. Metformin Prevents Renal Fibrosis in Mice With Unilateral Ureteral Obstruction and Inhibits Ang II-Induced ECM Production in Renal Fibroblasts. *Int J Mol Sci* (2016) 17(2):146. doi: 10.3390/ijms17020146
31. Grande MT, Lopez-Novoa JM. Fibroblast Activation and Myofibroblast Generation in Obstructive Nephropathy. *Nat Rev Nephrol* (2009) 5(6):319–28. doi: 10.1038/nrneph.2009.74
32. Lan HY. Tubular Epithelial-Myofibroblast Transdifferentiation Mechanisms in Proximal Tubule Cells. *Curr Opin Nephrol Hypertens* (2003) 12(1):25–9. doi: 10.1097/00041552-200301000-00005
33. Hsieh CC, Lin CL, He JT, Chiang M, Wang Y, Tsai YC, et al. Administration of Cytokine-Induced Myeloid-Derived Suppressor Cells Ameliorates Renal Fibrosis in Diabetic Mice. *Stem Cell Res Ther* (2018) 9(1):183. doi: 10.1186/s13287-018-0915-0
34. Pandiyan P, Zheng L, Ishihara S, Reed J, Lenardo MJ. CD4+CD25+Foxp3+ Regulatory T Cells Induce Cytokine Deprivation-Mediated Apoptosis of Effector CD4+ T Cells. *Nat Immunol* (2007) 8(12):1353–62. doi: 10.1038/ni1536
35. Basu A, Ramamoorthi G, Albert G, Gallen C, Beyer A, Snyder C, et al. Differentiation and Regulation of TH Cells: A Balancing Act for Cancer Immunotherapy. *Front Immunol* (2021) 12:669474. doi: 10.3389/fimmu.2021.669474
36. Pang N, Alimu X, Chen R, Muhashi M, Ma J, Chen G, et al. Activated Galectin-9/Tim3 Promotes Treg and Suppresses Th1 Effector Function in Chronic Lymphocytic Leukemia. *FASEB J* (2021) 35(7):e21556. doi: 10.1096/fj.202100013R
37. Gonzalez MM, Bamidele AO, Svingen PA, Sagstetter MR, Smyrk TC, Gaballa JM, et al. BMI1 Maintains the Treg Epigenomic Landscape to Prevent Inflammatory Bowel Disease. *J Clin Invest* (2021) 131(12):e140755. doi: 10.1172/JCI140755

38. Hou H, Sun Y, Miao J, Gao M, Guo L, Song X. Ponesimod Modulates the Th1/Th17/Treg Cell Balance and Ameliorates Disease in Experimental Autoimmune Encephalomyelitis. *J Neuroimmunol* (2021) 356:577583. doi: 10.1016/j.jneuroim.2021.577583
39. Han P, Hou Y, Zhao Y, Liu Y, Sun Y, Wang H, et al. Low-Dose Decitabine Modulates T Cell Homeostasis and Restores Immune Tolerance in Immune Thrombocytopenia. *Blood* (2021) 138(8):674–88. doi: 10.1182/blood.2020008477
40. Sakai R, Ito M, Komai K, Iizuka-Koga M, Matsuo K, Nakayama T, et al. Kidney GATA3(+) Regulatory T Cells Play Roles in the Convalescence Stage After Antibody-Mediated Renal Injury. *Cell Mol Immunol* (2021) 18(5):1249–61. doi: 10.1038/s41423-020-00547-x
41. Koehn BH, Apostolova P, Haverkamp JM, Miller JS, McCullar V, Tolar J, et al. GVHD-Associated, Inflammasome-Mediated Loss of Function in Adoptively Transferred Myeloid-Derived Suppressor Cells. *Blood* (2015) 126(13):1621–8. doi: 10.1182/blood-2015-03-634691
42. Messmann JJ, Reisser T, Leithauser F, Lutz MB, Debatin KM, Strauss G. In Vitro-Generated MDSCs Prevent Murine GVHD by Inducing Type 2 T Cells Without Disabling Antitumor Cytotoxicity. *Blood* (2015) 126(9):1138–48. doi: 10.1182/blood-2015-01-624163
43. Park MJ, Baek JA, Kim SY, Jung KA, Choi JW, Park SH, et al. Myeloid-Derived Suppressor Cells Therapy Enhance Immunoregulatory Properties in Acute Graft *Versus* Host Disease With Combination of Regulatory T Cells. *J Transl Med* (2020) 18(1):483. doi: 10.1186/s12967-020-02657-6
44. Sun HW, Wu WC, Chen HT, Xu YT, Yang YY, Chen J, et al. Glutamine Deprivation Promotes the Generation and Mobilization of MDSCs by Enhancing Expression of G-CSF and GM-CSF. *Front Immunol* (2020) 11:616367. doi: 10.3389/fimmu.2020.616367
45. Iwasaki M, Adachi Y, Minamino K, Suzuki Y, Zhang Y, Okigaki M, et al. Mobilization of Bone Marrow Cells by G-CSF Rescues Mice From Cisplatin-Induced Renal Failure, and M-CSF Enhances the Effects of G-CSF. *J Am Soc Nephrol* (2005) 16(3):658–66. doi: 10.1681/ASN.2004010067
46. Lendemans S, Kreuzfelder E, Waydhas C, Schade FU, Flohe S. Differential Immunostimulating Effect of Granulocyte-Macrophage Colony-Stimulating Factor (GM-CSF), Granulocyte Colony-Stimulating Factor (G-CSF) and Interferon Gamma (IFNgamma) After Severe Trauma. *Inflammation Res* (2007) 56(1):38–44. doi: 10.1007/s00011-007-6069-7
47. Korbecki J, Grochans S, Gutowska I, Barczak K, Baranowska-Bosiacka I. CC Chemokines in a Tumor: A Review of Pro-Cancer and Anti-Cancer Properties of Receptors CCR5, CCR6, CCR7, CCR8, CCR9, and CCR10 Ligands. *Int J Mol Sci* (2020) 21(20):7619. doi: 10.3390/ijms21207619
48. Jiang H, Zhu M, Guo P, Bi K, Lu Z, Li C, et al. Impaired Myeloid-Derived Suppressor Cells Are Associated With Recurrent Implantation Failure: A Case-Control Study. *J Reprod Immunol* (2021) 145:103316. doi: 10.1016/j.jri.2021.103316

Conflict of Interest: The authors declare that the research was conducted in the absence of any commercial or financial relationships that could be construed as a potential conflict of interest.

Publisher's Note: All claims expressed in this article are solely those of the authors and do not necessarily represent those of their affiliated organizations, or those of the publisher, the editors and the reviewers. Any product that may be evaluated in this article, or claim that may be made by its manufacturer, is not guaranteed or endorsed by the publisher.

Copyright © 2021 Qiu, Cao, Tu, Li, Su, Fang, Zhang, Cang, Rong and Luo. This is an open-access article distributed under the terms of the Creative Commons Attribution License (CC BY). The use, distribution or reproduction in other forums is permitted, provided the original author(s) and the copyright owner(s) are credited and that the original publication in this journal is cited, in accordance with accepted academic practice. No use, distribution or reproduction is permitted which does not comply with these terms.

frontiers in Immunology

ORIGINAL RESEARCH
published: 29 October 2021
doi: 10.3389/fimmu.2021.699192

Comprehensive Molecular and Cellular Characterization of Acute Kidney Injury Progression to Renal Fibrosis

Renyan Wu[1,2†], Jiawei Li[1,3,4†], Guowei Tu[1†], Ying Su[1], Xuepeng Zhang[1], Zhe Luo[1], Ruiming Rong[3,4*] and Yi Zhang[3,4,5*]*

[1] Department of Critical Care Medicine, Zhongshan Hospital, Fudan University, Shanghai, China, [2] Shanghai Institute of Immunology, Department of Immunology and Microbiology, Shanghai Jiao Tong University School of Medicine, Shanghai, China, [3] Department of Urology, Zhongshan Hospital, Fudan University, Shanghai, China, [4] Shanghai Key Laboratory of Organ Transplantation, Shanghai, China, [5] Biomedical Research Center, Institute for Clinical Sciences, Zhongshan Hospital, Fudan University, Shanghai, China

OPEN ACCESS

Edited by:
Bin Yang,
University of Leicester,
United Kingdom

Reviewed by:
Zhichao Fan,
UCONN Health, United States
Tian Hongling,
Tongji University, China

***Correspondence:**
Yi Zhang
yzhang_med@fudan.edu.cn
Ruiming Rong
rong.ruiming@zs-hospital.sh.cn
Zhe Luo
luo.zhe@zs-hospital.sh.cn

[†]These authors have contributed equally to this work

Specialty section:
This article was submitted to Molecular Innate Immunity, a section of the journal Frontiers in Immunology

Received: *23 April 2021*
Accepted: *01 October 2021*
Published: *29 October 2021*

Citation:
Wu R, Li J, Tu G, Su Y, Zhang X, Luo Z, Rong R and Zhang Y (2021) Comprehensive Molecular and Cellular Characterization of Acute Kidney Injury Progression to Renal Fibrosis. Front. Immunol. 12:699192. doi: 10.3389/fimmu.2021.699192

Acute kidney injury (AKI) and chronic kidney disease (CKD) represent different stages of renal failure; thus, CKD can be regarded as a result of AKI deterioration. Previous studies have demonstrated that immune cell infiltration, oxidative stress, and metabolic mentalism can support renal fibrosis progression in AKI cases. However, the most important triggers and cell types involved in this pathological progression remain unclear. This study was conducted to shed light into the underlying cellular and molecular features of renal fibrosis progression through the analysis of three mouse whole kidney and one human single-cell RNA-sequencing datasets publicly available. According to the different causes of AKI (ischemia reperfusion injury [IRI] or cisplatin), the mouse samples were divided into the CIU [control-IRI-unilateral ureteral obstruction (UUO)] and CCU (control-cisplatin-UUO) groups. Comparisons between groups revealed eight different modules of differentially expressed genes (DEGs). A total of 1,214 genes showed the same expression pattern in both CIU and CCU groups; however, 1,816 and 1,308 genes were expressed specifically in the CCU and CIU groups, respectively. Further assessment of the DEGs according to the Kyoto Encyclopedia of Genes and Genomes (KEGG) enrichment pathway and Gene Ontology (GO) showed that T-cell activation, fatty acid metabolic process, and arachidonic acid metabolism were involved in the fibrosis progression in CIU and CCU. Single-cell RNA-sequencing data along with the collected DEGs information also revealed that the T-cell activation mainly happened in immune cells, whereas the fatty acid metabolic process and arachidonic acid metabolism occurred in tubule cells. Taken together, these findings suggest that the fibrosis process differed between the CIU and CCU stages, in which immune and tubule cells have different functions. These identified cellular and molecular features of the different stages of fibrosis progression may pave the way for exploring novel potential therapeutic strategies in the clinic.

Keywords: acute kidney injury, cisplatin, genetic landscape, ischemia reperfusion injury, renal fibrosis, T-cell

INTRODUCTION

Kidney diseases can be classified into glomerular, tubulointerstitial, and renal vascular diseases based on anatomic features. They can also be divided into acute kidney injury (AKI) and chronic kidney disease (CKD). Ischemia reperfusion injury (IRI) is a pathophysiological phenomenon triggered by the damage caused by reperfusion of ischemic tissue after reestablishing blood supply (1) and is a common cause of AKI. Administration of cisplatin can also lead to AKI, being characterized by a complex pathophysiological profile that has been associated to cellular uptake and efflux, apoptosis, vascular injury, oxidative and endoplasmic reticulum stress, and inflammation (2). CKD is defined as persistent functional or structural abnormalities of the kidney, in which the excretory function is impaired due to loss of functional nephrons. Overall, AKI and CKD represent kidney failure at different time phases. However, currently, no clinically targeted, highly effective, and with low toxicity drug and/or treatment are available for AKI or CKD. Indeed, clinical treatments are very passive, and the current renal replacement therapies are limited. Therefore, early diagnosis, prevention, and treatment of AKI and CKD are prominent problems in acute and chronic renal injuries. Mechanistic research and enhanced treatment plans for these diseases urgently needed.

The etiology of renal fibrosis progression is complicated; nevertheless, injury is believed to be the main cause. Moreover, the AKI-to-CKD transition is a complex process mainly facilitated by maladaptive repair mechanisms. Several studies have suggested that it is related to inflammation in the kidneys, as many immune cells are recruited to injured organs (3). However, engagement of innate immune receptors provides tubular epithelial cells with the metabolic flexibility necessary for their plasticity during injury and repair, which drives tubule metabolism to also be involved in injury and fibrosis progression (4). Studies have also reported that oxidative stress caused by injury can hamper cell repair and promote tissue fibrosis (5). Despite of these knowledge advances, the underlying reasons for AKI deterioration and renal fibrosis progression remain unclear.

In this study, we found that regardless of whether AKI was caused by IRI or cisplatin, T cell activation was mainly related to renal fibrosis progression. Fatty acid metabolic processes mainly occurred in tubule cells, and most related genes were both involved in IRI and cisplatin-induced AKI, but only few genes were enriched in cisplatin-induced AKI deterioration. However, arachidonic acid metabolism was significantly different in AKI deterioration, in which genes were changed distinctly in different AKI modules. Our findings emphasize the differences in the AKI-to-fibrosis process caused by different factors and connect these functions with the cell types in the kidney, which made a deeper analysis and understanding of fibrosis caused by injury.

MATERIALS AND METHODS

Data Source

Three mouse bulk kidney mRNA-sequencing data (GSE10669, GSE145053, and GSE153625) and one human single-cell kidney RNA-sequencing data (GSE131685) were obtained from the National Center of Biotechnology Information (NCBI) Gene Expression Omnibus database (GEO). All mouse data were based on C57BL/6 mice and comprised eight cisplatin samples, four IRI samples, nine unilateral ureteral obstruction (UUO) samples, and 12 control samples. GSE131685 comprised three healthy kidney samples, including 23,366 cells.

Data Preprocessing

All raw RNA-sequencing data were obtained using the NCBI SRA (Sequence read archive) Toolkit, and all reads were alignted to the GRCm38 reference genome using *hisat2* (version 2.1.0) algorithm. The average overall mapping rate is more than 90%. After the data was sorted using *samtools* (version 1.7), *htseq* (version 0.11.3) algorithm was used to calculated gene counts.

Identification of Differentially Expressed Genes

Several groups were compared as follows: (i) UUO *vs.* AKI (IRI or cisplatin), (ii) AKI (IRI or cisplatin) *vs.* control. The batch effect between each sample was removed by *limma (version 3.42.2): remove batch effct. Deseq2* (version 1.24.0) was used to normalize the count data and identify DEGs, and Benjamini-Hochberg correction was used to adjust P-value obtained from multiple test. Finally, genes with |log2Fold Change| > 2 and adjusted P-value < 0.0001 were considered as DEGs.

Gene Enrichment Analysis

Kyoto Encyclopedia of Genes and Genomes (KEGG) pathway and Gene Ontology (GO) enrichment analyses were performed using *ClusterProfiler* (version 3.14.3) from Bioconductor. An adjusted P-value < 0.05 and false discovery rate < 0.02 were set as the cutoff criteria to identify significantly enriched KEGG pathways and GO terms.

Single-Cell RNA-Sequencing Data Processing and Analysis

The 10X gene matrix data were loaded in Seurat tool and were filtered based on cells with >3,000 features and 50% mitochondria. The remaining cells were reduced in dimension by Principal Component Analysis (PCA) and then clustered using Uniform Manifold Approximation and Projection for Dimension Reduction (UMAP) tool. Cell type classification was performed using markers as previously described. Specific gene sets were packed using the *AddModuleScore* function to calculate the average expression of each gene set per cell type.

AKI and CKD Mouse Models

C57BL/6 mice (male, 6–8 w, 20–25 g) were purchased from Shanghai SLAC Laboratory Animal Co., Ltd and maintained in the animal facility in Zhongshan Hospital, Fudan University. Kidney IRI, Cisplatin, and Unilateral ureteral obstruction (UUO) model were as our previous study (6, 7).

PCR

Total RNA was extracted from mouse kidneys with TRIzol (Invitrogen) reagent according to the manufacturer's

instructions. Total RNA (3–5 μg) was transcribed into cDNA by Superscript II reverse transcriptase and random primer oligonucleotides (Vazyme). The gene-specific forward and reverse primers for mouse RAC2 and CBR1 are presented in **Table 1**. qPCR was carried out using the Hieff qPCR SYBR Green Master Mix (yeason).

RESULTS

Dataset Collection and Analysis Workflow

Three bulk RNA-sequencing datasets (GSE10669, GSE145053, and GSE153625) comprising 12 AKI samples (including eight cisplatin-induced AKI and four IRI-induced AKI models) and nine renal fibrosis samples (induced by UUO) were evaluated and compared to identify the dynamic gene expression patterns during AKI progression and deterioration. The samples were divided according to the AKI cause in two groups that were used to represent the progression from IRI-induced or cisplatin-induced AKI to renal fibrosis (CIU and CCU groups, respectively). Then, function analysis was performed to identify the common and specific pathways involved in the different AKI-to-fibrosis progression, based on the compared gene modules in CIU and CCU groups. Finally, we mapped the renal fibrosis-related genes to human single-cell data to explore the cell types involved in AKI deterioration and progression (**Figure 1**).

Gene Expression Analysis and Module Selection

PCA was used to investigate the distribution of the different datasets. The gene expression profiles were found to be significantly different between AKI and renal fibrosis samples; however, IRI-induced and cisplatin-induced AKI groups showed similar gene expression landscapes (**Figure 2A**). Then, we used AKI as a dividing line to separate the progression of fibrosis into early and latter processes. This pattern during the fibrosis process divided the DEGs into eight different modules, and we used −1, 0, and 1 to show the downregulated, no significantly changed, and upregulated gene sets (**Figure 2B**). During the occurrence and deterioration of AKI, the proportion of genes in the different modules changed. Based on the diverse IRI- and cisplatin-induced pathological effects, the module gene ratios during the occurrence and deterioration of the two different AKIs were compared. Overall, a clear difference in the proportion of different gene modules between cisplatin- and IRI-induced AKI was noticeable (**Figure 2C**).

TABLE 1 | Primers used for qPCR.

Genes	Forward Primer	Reverse Primer
GAPDH	5'-GACTTCAACAGCAACTCC CAC-3'	5'-TCCACCACCCTGTTGCT GTA-3'
RAC2	5'- CAACGCCTTTCCCGGAG AGT -3'	5'- TCCGTCTGTGGATAGGA GAGC -3'
CBR1	5'- CAGAGACCCCTGTGTAC TTG -3'	5'- CAACTCAGGACAAGGTA CAAAATG -3'

Common and Specific Functions in CIU and CCU Pattern

To investigate the commonalities and specificities of the dynamic gene expression patterns during AKI development and deterioration to fibrosis progression, we compared the DEGs identified in the CIU and CCU groups. A total of 1,214 genes were found to have similar expression patterns in both CIU and CCU groups; however, 1,816 and 1,308 genes were expressed specifically in the CCU and CIU groups, respectively (**Figure 3A**). The whole GO analysis of different modules are presented in **Supplementary Figure 1**. Noteworthy, the genes showing the same expression patterns in the CIU and CCU groups were mainly related to T-cell activation and immune cell regulation, such as regulation of T-cell activation and regulation of leukocyte cell-cell adhesion (**Figure 3B**). Furthermore, GO and KEGG analyses confirmed that T-cell activation was enriched in both CIU and CCU exclusive patterns, and genes involved in module_0_1 and module_1_1. Fatty acid metabolic processes were enriched in both CIU and CCU exclusive patterns in module_−1_0 and module_0_−1; however, some genes involved in fatty acid metabolic processes were specifically enriched in the CCU exclusive pattern with module_−1_0. Arachidonic acid metabolism was shared by CIU and CCU exclusive patterns. Some genes were enriched in the module_1_−1 in the CIU exclusive pattern, whereas others were enriched in the module_−1_0 in the CCU exclusive pattern (**Figure 3C**).

Mapping Common and Specific Genes in Single Cell Data

To investigate which cell types were involved in the progression of AKI to renal fibrosis, three healthy human single-cell RNA-sequencing data were analyzed to explore the cells that expressed the genes related to renal fibrosis progression. Cells were classified into 11 different cell types, including proximal cells, collecting ducts, distal tubules, natural killer (NK) cells, and T-cells (**Figure 4A**). Then, the functions analyzed from the RNA-sequencing data were merged with the cell types in the kidneys. According to the violin plot, T-cell activation was enriched in the module_0_1, which was identified as a common function in both CIU and CCU patterns, and was mainly related with immune cells, especially in NK cells and T-cells. However, T-cell activation in module_1_1 was mainly mapped to the glomerular parietal epithelial cells. Fatty acid metabolic processes, regardless of the common pattern or CCU exclusive pattern, were found to occur in tubule cells, such as the proximal tubule, distal tubule, and collecting duct. However, arachidonic acid metabolism was different in the CIU and CCU patterns. In the CIU pattern, which was in the module_1_−1, the genes were mainly mapped to the distal tubule and collecting duct intercalated cells, whereas the arachidonic acid metabolism was specifically related to the proximal tubules in the CCU pattern (module_−1_0) (**Figure 4B**). According to the cell change prediction, B cells were increased in the CCU pattern, and the counts of monocyte in the IRI model were higher than them in the Cisplatin-induced AKI model. However, counts of NK cells

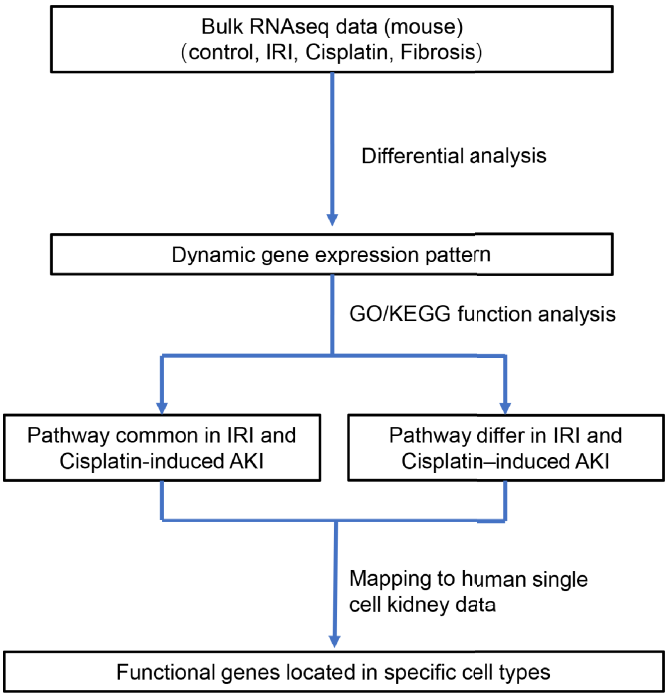


FIGURE 1 | Diagram of the workflow of the study.

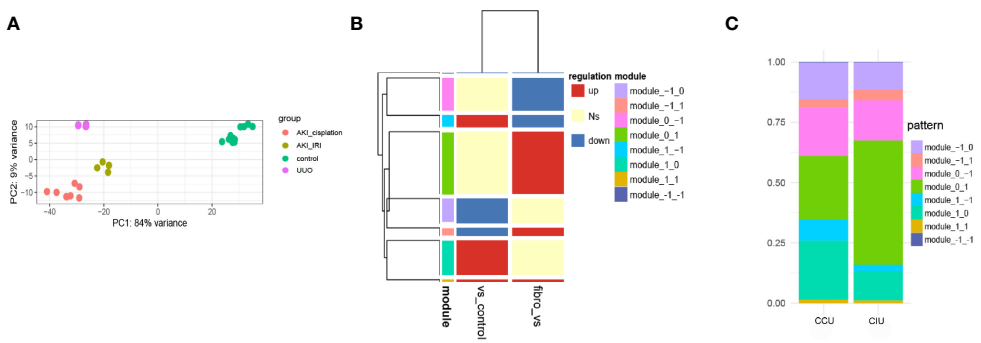


FIGURE 2 | Dynamic gene expression patterns in acute kidney injury (AKI)-to-fibrosis progression. **(A)** Principal component analysis of all datasets. **(B)** Gene expression modules in AKI development and deterioration Fibrosis samples were compared within AKI samples and between AKI and healthy samples. Up shows increased differentially expressed genes (DEGs), down shows decreased DEGs, and Ns shows DEGs that have no significant difference in the comparison. **(C)** The distribution of each module in different AKI progressions. CCU, from healthy to cisplatin-induced AKI to fibrosis; CIU, from healthy to IRI-induced AKI to fibrosis. All data are available at GEO database (GSE10669, GSE145053, GSE153625).

were increased in the Cisplatin-induced AKI, but decreased when AKI transite to CKD (**Figure 4C**).

Function of the Identified DEGs in Different Cell Types

DEGs identified as having different functions were selected and mapped according to single-cell RNA-sequencing data (GSE131685) (**Figure 5A**). *RAC2* was found to be mainly involved in T-cell activation while enriched in both CIU and CCU groups in module_0_1. Noteworthy, it was mainly expressed in immune cell subsets, especially in NK cells and T cells. Interestingly, *CBR1* and *CBR3* were found to be mainly expressed in tubule cells (comprising collecting duct intercalated cells and distal duct), which were also enriched for arachidonic acid metabolism in the CIU group within the module_1_−1. *GGT1* was also found to be involved in the arachidonic acid metabolism but in the CCU group within the module_−1_0, and it was mainly expressed in the proximal convoluted tubule and

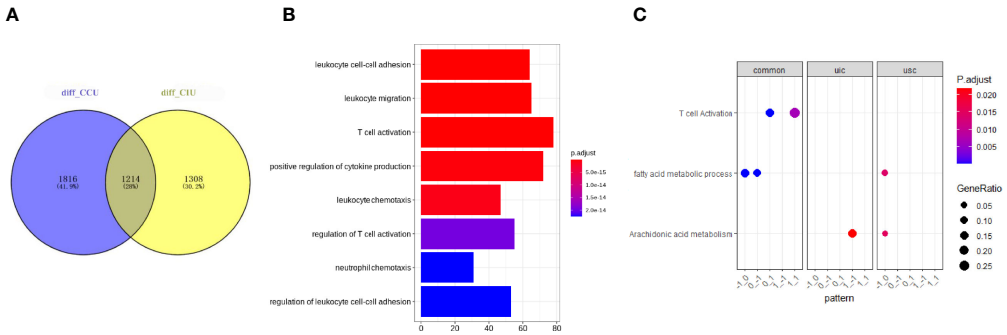


FIGURE 3 | Common and specific functions in CIU and CCU progression patterns. **(A)** Venn plot showing the number of genes in the same or different modules in the CIU and CCU groups. **(B)** Gene ontology enrichment of genes with common expression patterns in CIU and CCU groups. **(C)** Functional analysis of genes in each group. Pattern is referred to as gene modules. CIU (from healthy to IRI-induced AKI to fibrosis) or CCU (from healthy to cisplatin-induced AKI to fibrosis), genes in this pathway are specific to CIU or CCU, respectively; Common, genes in this pathway are shared in the same module of CIU/CCU. The total differential data can be found in **Supplementary CSV File.**

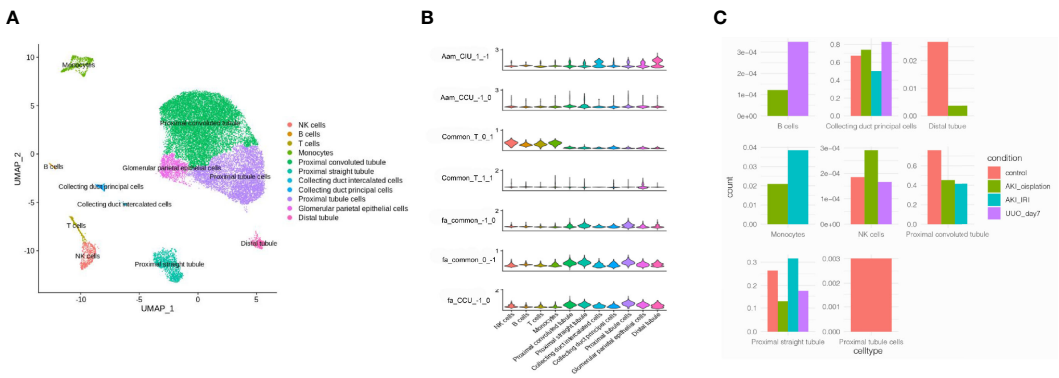


FIGURE 4 | Mapping common and specific genes in single cell data. **(A)** Cell type distribution of human kidney single-cell RNA-sequencing data. **(B)** Enrichment of different pathways in each cell type. Aam, arachidonic acid metabolism; Fa, fatty acid metabolic process; T, T cell activation. CIU (from healthy to IRI-induced AKI to fibrosis) or CCU (from healthy to cisplatin-induced AKI to fibrosis), genes in this pathway are specific to CIU or CCU, respectively; Common, genes in this pathway are shared in the same module of CIU/CCU. 1–1, –10, 01, 11, and 1–1, refer to the gene module. **(C)** Cell counts in different patterns.

proximal straight tubule. *ACAT1* and *PDK2* were identified as being related with the fatty acid metabolic process in the CCU group within the module_–1_0, being expressed in nearly all the tubule cells (**Figure 5B**). Cell-and-cell interactions are presented in **Figure 5C** and protein-and-protein interaction networks of different modules are in **Figure 5D**.

In addition, we established AKI models, RAC2 and CBR1 expression were presented in **Figure 6**.

DISCUSSION

Progression of the long-term consequences of AKI to renal fibrosis has been well recognized in clinical studies and experimental *in vivo* models. The pathophysiology of AKI relies on a complicated network with multidimensional regulation and the contribution of various factors, such as the immune response, metabolic regulation, and signaling transduction, which in turn results in AKI heterogeneity. IRI- and drug-induced AKI are common in the clinic, both of which contribute to the high incidence of renal fibrosis. Therefore, a better understanding of the cellular and molecular patterns of the progression from IRI- and cisplatin-induced AKI to renal fibrosis may offer promising insights into potential therapeutic advances.

Adaptive immunity, especially T-cell activation, plays an essential role in the progression of AKI. In particular, our previous work showed that inhibition of T-cell immunoglobulin mucin-1-mediated T-cell activation by a histone methylation inhibitor greatly ameliorates renal IRI (6). In a cisplatin-induced AKI mouse model, Miyagi et al. also indicated that T cells with high expression of CD69 and CD25 are present in the spleens of AKI mice after cisplatin treatment (8). Taken together, both studies showed a common pattern of T-cell activation during AKI induction.

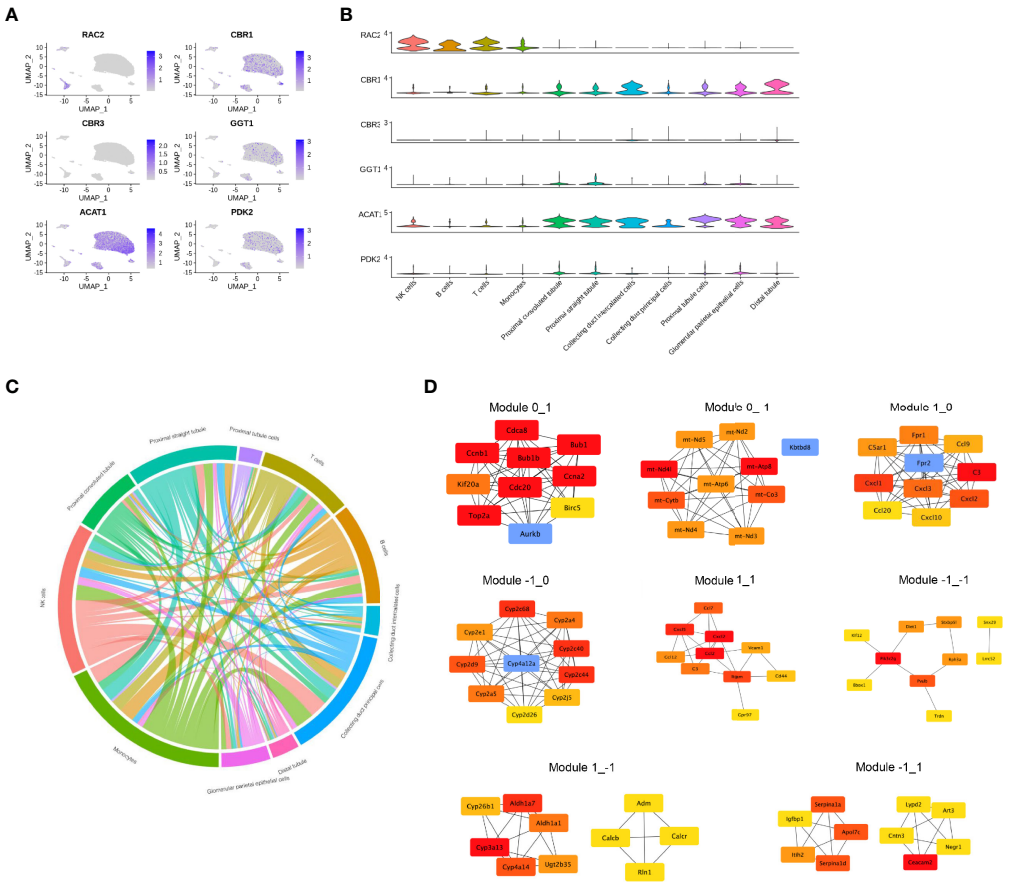


FIGURE 5 | Gene expression profile in each cell type. **(A)** The normalized expression of each gene in the human kidney. **(B)** Violin plot showing the gene expression in each cell type. **(C)** Cell-and-cell interaction between different clusters. **(D)** Protein-and-protein interaction network of different modules.

The independent characteristics of IRI-induced AKI and cisplatin-induced AKI in renal fibrosis remain unclear. Our analysis indicated that, notably, arachidonic acid metabolism showed completely different patterns during the two processes: the metabolism was enhanced in the phase of IRI-induced AKI, but decreased in the subsequent fibrosis phase, whereas it dramatically decreased in the phase of cisplatin-induced AKI, and remained unchanged thereafter. In a murine model of cisplatin-induced AKI, significant fatty acid oxidation dysfunction and extensive lipid deposition in the mice with AKI were found (9). In addition, histone deacetylase activity (HDAC) was inhibited in kidneys of high-fiber fed mice, and dietary manipulation of the gut microbiome could protect against AKI and subsequent CKD, mediated by HDAC inhibition and activation of two G protein-coupled receptors GPR41 and GPR109A by Short-chain fatty acids (10). Arachidonic acid can be converted into prostaglandin E_2 by the cascade catalysis of cyclooxygenase (COX)-1 and -2 and prostaglandin E synthase (PGES). Membrane-associated PGES deletion attenuated cisplatin-induced renal dysfunction and tubular damage, suggesting that decreased metabolism of arachidonic acid plays an important role in cisplatin-induced AKI (11). Moreover, Yamamoto et al. also reported decreased arachidonic acid metabolism with the accumulation of COX-2, PGES, and the PGE receptor EP4 in renal tubules (12). In addition, several studies showed that 20-HETE, another important product of arachidonic acid metabolism, is elevated after IRI (13, 14).

Next, the characteristics of common genes correlated with T-cell activation were evaluated. Among these, *RAC2* has been shown to interact with nitric oxide synthase 2A and correlate with renal fibrosis (15). Another study indicated that *RAC2* is a key control gene in the pathogenesis of chronic glomerulonephritis (16). As for the specific genes enriched in different cell types of IRI-induced renal fibrosis, *CBR1* was mainly expressed in tubule cells and some types of immune cells. *CBR1* was reported to be a therapeutic target for hepatic IRI during liver transplantation, as it may be involved in the inhibition of lipid peroxide formation (17). Although no evidence has proven that *CBR1* may function in the process of kidney IRI, Alshogran et al. demonstrated that the expression of *CBR1* and *CBR3* was correlated with end-stage renal disease (18), which highlighted the potential role of *CBR* in IRI-induced renal fibrosis. Based on the analysis of specific genes expressed in cisplatin-induced renal fibrosis, *ACAT1*, *GGT1*, and *PDK2* were predominantly expressed in tubule cells. Indeed, upregulated expression of *ACAT1* was found during renal fibrosis by

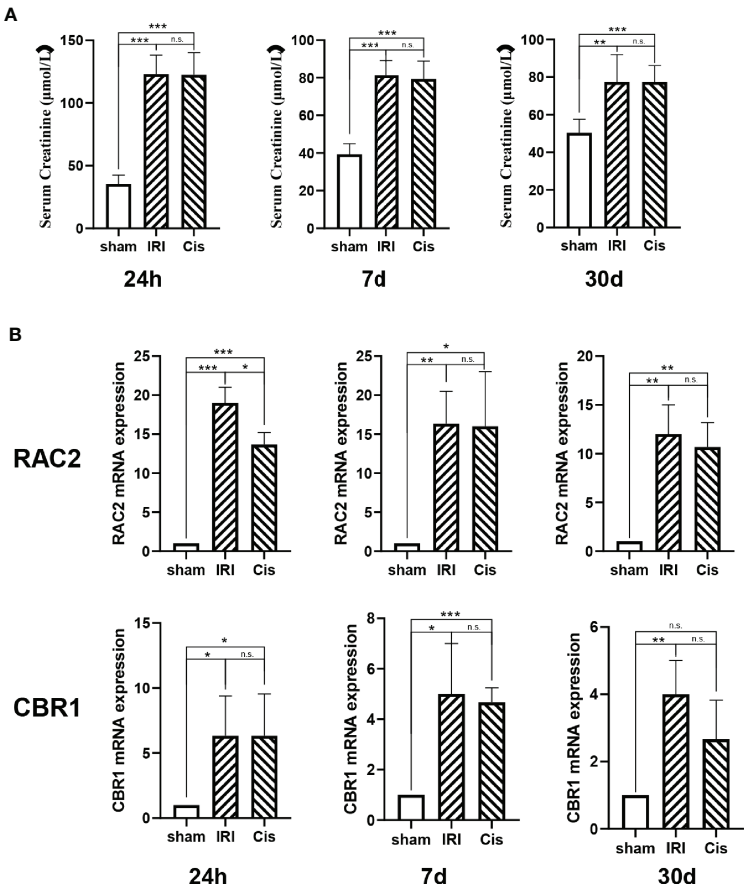


FIGURE 6 | RAC2 and CBR1 mRNA expression in each group. **(A)** Serum Creatinine in sham, IRI, and Cisplatin group after 24 h, 7 d, and 30 d. **(B)** mRNA expression of RAC2 and CBR1 in T cells from kidneys and kidneys. ***P < 0.001, **P < 0.01, *P < 0.05, n.s., no significant differences.

participating in the oxidation of fatty acids (19). Although no correlation between cisplatin and kidney injury has been shown, several studies have indicated that *PDK2* may mediate cisplatin resistance in head and neck cancer and adenocarcinoma (20, 21). In addition, GGT1 may metabolize cisplatin in the proximal tubule cell, suggesting that the expression of *GGT1* is correlated with the accumulation of cisplatin in the kidneys (22). Taken together, these findings of the characteristics of IRI-or cisplatin-induced AKI may provide information for exploring potential clinical therapeutic targets.

DATA AVAILABILITY STATEMENT

The raw data supporting the conclusions of this article will be made available by the authors, without undue reservation.

ETHICS STATEMENT

The animal study was reviewed and approved by Zhongshan Hospital, Fudan University.

AUTHOR CONTRIBUTIONS

RW and JL analyzed the RNA-sequencing data. GT, XZ and YS drafted the manuscript and established mouse models. ZL, RR and YZ conceived the project, designed the projet, and approved the final manuscript. All authors contributed to the article and approved the submitted version.

FUNDING

This study was supported by the National Key R&D Program of China (2018YFA0107501 to RR) and the National Natural Science Foundation of China (81400688 to YZ, and 81770747 and 81970646 to RR).

SUPPLEMENTARY MATERIAL

The Supplementary Material for this article can be found online at: https://www.frontiersin.org/articles/10.3389/fimmu.2021.699192/full#supplementary-material

Supplementary Figure 1 | GO analysis in each pattern.

REFERENCES

1. Hao P. Monitoring of Renal Ischemia Reperfusion Injury in Rabbits by Ultrasonic Contrast and its Relationship With Expression of VEGF in Renal Tissue. *Asian Pac J Trop Med* (2016) 9:188–92. doi: 10.1016/j.apjtm.2016.01.006
2. McSweeney KR, Gadanec LK, Qaradakhi T, Ali BA, Zulli A, Apostolopoulos V. Mechanisms of Cisplatin-Induced Acute Kidney Injury: Pathological Mechanisms, Pharmacological Interventions, and Genetic Mitigations. *Cancers (Basel)* (2021) 13:1572–13. doi: 10.3390/cancers13071572
3. McWilliam SJ, Wright RD, Welsh GI, Tuffin J, Budge KL, Swan L, et al. The Complex Interplay Between Kidney Injury and Inflammation. *Clin Kidney J* (2021) 14:780–8. doi: 10.1093/ckj/sfaa164
4. Tammaro A, Kers J, Scantlebery AML, Florquin S. Metabolic Flexibility and Innate Immunity in Renal Ischemia Reperfusion Injury: The Fine Balance Between Adaptive Repair and Tissue Degeneration. *Front Immunol* (2020) 11:1346. doi: 10.3389/fimmu.2020.01346
5. Rossi M, Korpak K, Doerfler A, Zouaoui Boudjeltia K. Deciphering the Role of Heme Oxygenase-1 (HO-1) Expressing Macrophages in Renal Ischemia-Reperfusion Injury. *Biomedicines* (2021) 9:306–22. doi: 10.3390/biomedicines9030306
6. Li J, Qiu Y, Li L, Wang J, Cheuk YC, Sang R, et al. Histone Methylation Inhibitor DZNep Ameliorated the Renal Ischemia-Reperfusion Injury via Inhibiting TIM-1 Mediated T Cell Activation. *Front Med (Lausanne)* (2020) 7:305. doi: 10.3389/fmed.2020.00305
7. Zheng L, Li L, Qi G, Hu M, Hu C, Wang S, et al. Transplantation of Telocytes Attenuates Unilateral Ureter Obstruction-Induced Renal Fibrosis in Rats. *Cell Physiol Biochem* (2018) 46:2056–71. doi: 10.1159/000489445
8. Miyagi MYS, Latancia MT, Testagrossa LA, Andrade-Oliveira V, Pereira WO, Hiyane MI, et al. Physical Exercise Contributes to Cisplatin-Induced Nephrotoxicity Protection With Decreased CD4+ T Cells Activation. *Mol Immunol* (2018) 101:507–13. doi: 10.1016/j.molimm.2018.08.014
9. Li M, Li CM, Ye ZC, Huang J, Li Y, Lai W, et al. Sirt3 Modulates Fatty Acid Oxidation and Attenuates Cisplatin-Induced AKI in Mice. *J Cell Mol Med* (2020) 24:5109–21. doi: 10.1111/jcmm.15148
10. Liu Y, Li YJ, Loh YW, Singer J, Zhu W, Macia L, et al. Fiber Derived Microbial Metabolites Prevent Acute Kidney Injury Through G-Protein Coupled Receptors and HDAC Inhibition. *Front Cell Dev Biol* (2021) 9:648639. doi: 10.3389/fcell.2021.648639
11. Jia Z, Wang N, Aoyagi T, Wang H, Liu H, Yang T. Amelioration of Cisplatin Nephrotoxicity by Genetic or Pharmacologic Blockade of Prostaglandin Synthesis. *Kidney Int* (2011) 79:77–88. doi: 10.1038/ki.2010.331
12. Yamamoto E, Izawa T, Juniantito V, Kuwamura M, Sugiura K, Takeuchi T, et al. Involvement of Endogenous Prostaglandin E2 in Tubular Epithelial Regeneration Through Inhibition of Apoptosis and Epithelial-Mesenchymal Transition in Cisplatin-Induced Rat Renal Lesions. *Histol Histopathol* (2010) 25:995–1007. doi: 10.14670/HH-25.995
13. Nilakantan V, Maenpaa C, Jia G, Roman RJ, Park F. 20-HETE-Mediated Cytotoxicity and Apoptosis in Ischemic Kidney Epithelial Cells. *Am J Physiol Renal Physiol* (2008) 294:F562–70. doi: 10.1152/ajprenal.00387.2007
14. Fan F, Ge Y, Lv W, Elliott MR, Muroya Y, Hirata T, et al. Molecular Mechanisms and Cell Signaling of 20-Hydroxyeicosatetraenoic Acid in Vascular Pathophysiology. *Front Biosci (Landmark Ed)* (2016) 21:1427–63. doi: 10.2741/4465
15. Li N, Cui Y, Yin M, Liu F. Screening Potential Prognostic Biomarkers of Long non-Coding RNAs for Predicting the Risk of Chronic Kidney Disease. *Braz J Med Biol Res* (2019) 52:e8333. doi: 10.1590/1414-431x20198333
16. Gao JR, Qin XJ, Jiang H, Wang T, Song JM, Xu SZ. Screening and Functional Analysis of Differentially Expressed Genes in Chronic Glomerulonephritis by Whole Genome Microarray. *Gene* (2016) 589:72–80. doi: 10.1016/j.gene.2016.05.031
17. Kwon JH, Lee J, Kim J, Kirchner VA, Jo YH, Miura T, et al. Upregulation of Carbonyl Reductase 1 by Nrf2 as a Potential Therapeutic Intervention for Ischemia/ Reperfusion Injury During Liver Transplantation. *Mol Cells* (2019) 42:672–85. doi: 10.1016/j.hpb.2019.10.2338
18. Alshogran OY, Urquhart BL, Nolin TD. Downregulation of Hepatic Carbonyl Reductase Type 1 in End-Stage Renal Disease. *Drug Metab Lett* (2015) 9:111–8. doi: 10.2174/1872312809666150818111626
19. Chowdhury SS, Lecomte V, Erlich JH, Maloney CA, Morris MJ. Paternal High Fat Diet in Rats Leads to Renal Accumulation of Lipid and Tubular Changes in Adult Offspring. *Nutrients* (2016) 8:521–31. doi: 10.3390/nu8090521
20. Roh JL, Park JY, Kim EH, Jang HJ, Kwon M. Activation of Mitochondrial Oxidation by PDK2 Inhibition Reverses Cisplatin Resistance in Head and Neck Cancer. *Cancer Lett* (2016) 371:20–9. doi: 10.1016/j.canlet.2015.11.023
21. Hu T, Yu S, Li Y, Ren H, Ning Q, Wang J, et al. PDK2 Induces Cisplatin-Resistance in Lung Adenocarcinoma via Transcriptional Regulation of CNNM3. *J Drug Target* (2019) 27:460–5. doi: 10.1080/1061186X.2018.1550648
22. Chang C, Hu Y, Hogan SL, Mercke N, Gomez M, O'Bryant C, et al. Pharmacogenomic Variants May Influence the Urinary Excretion of Novel Kidney Injury Biomarkers in Patients Receiving Cisplatin. *Int J Mol Sci* (2017) 18:1333-49. doi: 10.3390/ijms18071333

Conflict of Interest: The authors declare that the research was conducted in the absence of any commercial or financial relationships that could be construed as a potential conflict of interest.

Publisher's Note: All claims expressed in this article are solely those of the authors and do not necessarily represent those of their affiliated organizations, or those of the publisher, the editors and the reviewers. Any product that may be evaluated in this article, or claim that may be made by its manufacturer, is not guaranteed or endorsed by the publisher.

Copyright © 2021 Wu, Li, Tu, Su, Zhang, Luo, Rong and Zhang. This is an open-access article distributed under the terms of the Creative Commons Attribution License (CC BY). The use, distribution or reproduction in other forums is permitted, provided the original author(s) and the copyright owner(s) are credited and that the original publication in this journal is cited, in accordance with accepted academic practice. No use, distribution or reproduction is permitted which does not comply with these terms.

frontiers in Immunology

ORIGINAL RESEARCH
published: 03 December 2021
doi: 10.3389/fimmu.2021.733808

Hyperoside Suppresses Renal Inflammation by Regulating Macrophage Polarization in Mice With Type 2 Diabetes Mellitus

Jialing Liu[1,2,3†], Yanmei Zhang[1,2†], Hongqin Sheng[1,2†], Chunling Liang[1,4], Huazhen Liu[1,4], Jose Alberto Moran Guerrero[5], Zhaoyu Lu[1,2], Wei Mao[1,2], Zhenhua Dai[1,4,6,7], Xusheng Liu[1,2*] and Lei Zhang[1,2,4,6*]*

[1] State Key Laboratory of Dampness Syndrome of Chinese Medicine, The Second Clinical College of Guangzhou University of Chinese Medicine, Guangzhou, China, [2] Nephrology Department, The Second Affiliated Hospital of Guangzhou University of Chinese Medicine, Guangzhou, China, [3] Department of Biochemistry, School of Medicine, Southern University of Science and Technology, Shenzhen, China, [4] Section of Immunology and Joint Immunology Program, Guangdong Provincial Academy of Chinese Medical Sciences, Guangzhou, China, [5] Monterrey Institute of Technology, Tecnológico, Monterrey, Mexico, [6] Guangdong Provincial Key Laboratory of Clinical Research on Traditional Chinese Medicine Syndrome, Guangzhou, China, [7] Guangdong-Hong Kong-Macau Joint Lab on Chinese Medicine and Immune Diseases, Guangzhou University of Chinese Medicine, Guangzhou, China

OPEN ACCESS

Edited by:
Bin Yang,
University of Leicester,
United Kingdom

Reviewed by:
Dong Zhou,
University of Connecticut,
United States
Gang Huang,
The First Affiliated Hospital of
Sun Yat-sen University, China

***Correspondence:**
Zhenhua Dai
zdai2009@outlook.com
Xusheng Liu
liuxusheng@gzucm.edu.cn
Lei Zhang
zhanglei@gzucm.edu.cn

†These authors have contributed equally to this work

Specialty section:
This article was submitted to Molecular Innate Immunity, a section of the journal Frontiers in Immunology

Received: *30 June 2021*
Accepted: *04 November 2021*
Published: *03 December 2021*

Citation:
Liu J, Zhang Y, Sheng H, Liang C, Liu H, Moran Guerrero JA, Lu Z, Mao W, Dai Z, Liu X and Zhang L (2021) Hyperoside Suppresses Renal Inflammation by Regulating Macrophage Polarization in Mice With Type 2 Diabetes Mellitus. Front. Immunol. 12:733808. doi: 10.3389/fimmu.2021.733808

Accumulating evidence reveals that both inflammation and lymphocyte dysfunction play a vital role in the development of diabetic nephropathy (DN). Hyperoside (HPS) or quercetin-3-O-galactoside is an active flavonoid glycoside mainly found in the Chinese herbal medicine Tu-Si-Zi. Although HPS has a variety of pharmacological effects, including anti-oxidative and anti-apoptotic activities as well as podocyte-protective effects, its underlying anti-inflammatory mechanisms remain unclear. Herein, we investigated the therapeutic effects of HPS on murine DN and the potential mechanisms responsible for its efficacy. We used C57BLKS/6J ^{Lep} *db/db* mice and a high glucose (HG)-induced bone marrow-derived macrophage (BMDM) polarization system to investigate the potentially protective effects of HPS on DN. Our results showed that HPS markedly reduced diabetes-induced albuminuria and glomerular mesangial matrix expansion, accompanied with a significant improvement of fasting blood glucose level, hyperlipidaemia and body weight. Mechanistically, pretreatment with HPS effectively regulated macrophage polarization by shifting proinflammatory M1 macrophages ($F4/80^+CD11b^+CD86^+$) to anti-inflammatory M2 ones ($F4/80^+CD11b^+CD206^+$) *in vivo* and in bone marrow-derived macrophages (BMDMs) *in vitro*, resulting in the inhibition of renal proinflammatory macrophage infiltration and the reduction in expression of monocyte chemoattractant protein-1 (MCP-1), tumor necrosis factor (TNF-α) and inducible nitric oxide synthase (iNOS) while increasing expression of anti-inflammatory cytokine Arg-1 and CD163/CD206 surface molecules. Unexpectedly, pretreatment with HPS suppressed $CD4^+$ T cell proliferation in a coculture model of IL-4-induced M2 macrophages and splenic $CD4^+$ T cells while promoting their differentiation into $CD4^+IL\text{-}4^+$ Th2 and $CD4^+Foxp3^+$ Treg cells.

Taken together, we demonstrate that HPS ameliorates murine DN *via* promoting macrophage polarization from an M1 to M2 phenotype and $CD4^+$ T cell differentiation into Th2 and Treg populations. Our findings may be implicated for the treatment of DN in clinic.

Keywords: diabetic nephropathy, macrophage polarization, hyperoside, renal inflammation, Th1 cell, Treg cell

INTRODUCTION

Diabetic nephropathy (DN) is a serious microvascular complication in patients with diabetes mellitus (DM) and is increasingly regarded as an inflammatory process (1–3). Macrophages are important cells involved in the initiation of inflammatory responses and play a critical role in the pathogenesis of DN by secreting various proinflammatory mediators. They can differentiate into proinflammatory M1 macrophages through the classical activation and anti-inflammatory M2 macrophages *via* the alternative activation (4). In addition, Th1, Th2, Th17 and cytotoxic T cells are also involved in the development and progression of DN (5, 6). Maintaining the M1/M2, Th1/Th2 and Th17/Treg immune balances can reduce the production of proinflammatory cytokines and improve DN (7). Therefore, we hypothesized that the imbalance in both innate (M1/M2) and adaptive immunities (Th1/Th2 and Th17/Treg) could play a crucial role in the pathogenesis of DN, while rebalancing these immune responses might represent a novel approach for the treatment of DN.

As a traditional herbal ingredient, Hyperoside (HPS) is one of the main active components in the Chinese herb Tu-Si-Zi (8) (**Supplementary Figure 1**), which exhibits the anti-inflammatory, anti-oxidant and anti-cancerous properties. Because of its high efficacy and low toxicity, HPS is commonly used in treating a variety of ischemic brain and heart diseases. In recent years, emerging evidence has shown the anti-inflammatory effects of HPS on various diseases, such as non-alcoholic fatty liver disease (9), osteoarthritis (10), DM-induced cognitive dysfunction (11) and pulmonary fibrosis (12) *in vivo*, and on lipopolysaccharide (LPS)-stimulated cell injury in a model of *in vitro* experiments (13–15) by suppressing activation of the NF-κB signaling pathway. Studies have also confirmed that HPS can inhibit the high glucose (HG) induced inflammatory injury *in vitro* and *in vivo*. For example, it can suppress vascular inflammation caused by HG in the human umbilical vein endothelial cells (HUVECs) *in vitro* and in mice (16, 17). And it alleviates HG-induced apoptosis and inflammatory responses of HK-2 cells through the miR-499a-5p/NRIP1 axis (18). However, very few studies have explored the mechanisms underlying the effects of HPS on renal inflammatory injury in diabetic condition. Thus, the effects HPS on DN and its molecular mechanisms of action remain unclear and warrant further investigation.

In the present study, we aimed to investigate the potentially therapeutic effects of HPS on DN and to delineate the mechanisms underlying the therapeutic effects of HPS in a type-2 DN model of *db/db* mice and *in vitro* by focusing on its immunologically regulatory mechanisms responsible for the differentiation and activation of macrophages and $CD4^+$ T cells. We found that HPS indeed attenuated DN in a mouse model of type 2 diabetes mellitus by regulating macrophage polarization.

MATERIALS AND METHODS

Antibodies and Reagents

The micro-albumin assay kit was obtained from Abcam Biotechnology (Abcam, Cambridge, UK). Hyperoside with a purity higher than 98% was purchased from Sigma-Aldrich (St Louis, USA) and was suspended in 0.5% carboxymethyl cellulose sodium salt high viscosity (CMCNa) (MP Biomedicals, LLC, USA) solution for animal experiments or dissolved in 0.1% DMSO for cell culture experiments. Glucose was purchased from Sigma-Aldrich (St Louis, MO, USA) while Trizol reagents were manufactured by Invitrogen (California, USA). cDNA Kit was purchased from Promega (Promega Corporation, Madison, WI). 24-well transwell chamber was bought from Corning (Corning, Shenzhen, China). All flow cytometric antibodies, including F4/80, CD11b, CD86, CD206, CD4, IL4, and Foxp3 were purchased from eBioscience or Biolegend. And details of the antibodies used in this study are listed in the **Table 1**.

A Mouse Model of Diabetic Nephropathy in *db/db* Mice

Male *db/db* mice (C57BL/KsJ) (19) at the age of 8 weeks were used in this study. The *db/db* mice and heterozygote age-matched *db/m* mice were originally obtained from Model Animal Research Center of Nanjing University, Jiangsu, China and were maintained following guideline "Principles of Laboratory Animal Care and Use in Research" (Ministry of Health, Beijing, China). Animals were placed in a controlled environment of humidity (about 60%) and room temperature (about 24 ± 1°C) with an alternating 12h light and dark cycle. The animals were allowed free access to standard laboratory tap water and food. The mice were then randomly divided into four groups and treated without or with HPS intraperitoneally for 12 consecutive weeks, as described below: 1) Control *db/m* mice (n=6) received the same volume of distilling water; 2) Control *db/db* mice (n=6) were given with the same volume of distilling water; 3) *db/db* +HHPS mice (n=7) received Hyperoside at a high dose of 80mg/kg/day; 4) *db/db* +LHPS mice (n=7) were treated with Hyperoside at a low dose of 40mg/kg/day.

Fasting blood glucose levels were measured twice weekly using the Bayer glucose monitor (Bayer, Bergkamen, Germany). Mice were sacrificed 12 weeks after HPS treatment to determine serum concentrations of total cholesterol (TC) and low-density

TABLE 1 | Antibodies used for flow cytometry, IHC and IF.

Antibody name	Source	Catalogue number	Dilution
Antibodies used for flow cytometry			
F4/80	Biolegend	123116	(0.5μg)/test
CD11b	BD Pharmingen	560455	(0.5μg)/test
CD86	Biolegend	105005	(0.5μg)/test
CD206 (MMR)	eBioscience	25-2061-82	(0.5μg)/test
IL-4	BD Pharmingen	554389	(0.5μg)/test
CD4	Biolegend	100516	(0.5μg)/test
Foxp3	Biolegend	126419	(0.5μg)/test
Antibodies used for IHC			
Anti-CD68	Abcam	ab201340	1:400
Anti-MCP1	Abcam	ab7202	1:100
HRP conjugated Goat Anti-Mouse IgG (H+L)	Servicebio	GB23301	1:200
HRP conjugated Goat Anti-Rabbit IgG (H+L)	Servicebio	GB23303	1:200
Antibodies used for IF			
IL-17 antibody	Santa Cruz	374218	1:100
Foxp3 antibody	Santa Cruz	53876	1:100
IFN-γ antibody	R&D	AF-585-NA	1:100
Anti-Mannose Receptor antibody	Abcam	ab64693	1:100
Anti-F4/80 antibody	Abcam	ab16911	1:100
Goat Anti-Rabbit IgG H&L (Alexa Fluor® 488) preadsorbed	Abcam	ab150081	1:1000
Cy3-labeled anti-mouse antibody	Beyotime	A0521	1:200
NL557-labeled anti-Goat antibody	R&D	NL001	1:200

lipoprotein cholesterol (LDL-C). Serum and urinary creatinine levels were measured using the enzymatic colorimetric method *via* an automatic biochemistry analyzer (Toshiba-120FR, Tokyo, Japan). Urinary albumin concentration was measured using the ELISA kit with an anti-mouse albumin antibody (Cusabio, Wuhan, China) and was normalized to the urinary creatinine levels and expressed as urinary mAlb/Cr. UACR was calculated according to the following equation: UACR (mg/g) = urinary albumin(mg)/urinary creatine(g). All animal experiments were approved by the Institutional Animal Care and Use Committee of Guangzhou University of Chinese Medicine.

Renal Pathology

The kidney tissues were fixed in 10% formalin buffer and then embedded in paraffin for light microscopic examination. Serial tissue sections (5μm) were stained with hematoxylin & eosin (HE) and periodic acid-Schiff (PAS). Mesangial matrix expansion was determined by assessing PAS-positive materials in the mesangial region. A percentage of the PAS-positive area was analyzed using Image-Pro Plus (Version 5.1.0.20, Media Cybernetics, Silver Spring, MD, USA) and Leica Q500MC image analysis software. Semi-quantitative analysis was performed with 20 glomeruli randomly selected for each subject (at least five mice in each group) and evaluations were made in coded slides.

Immunohistochemistry

Immunohistochemical staining was performed on paraffin sections using a microwave-based antigen retrieval technique, which involved heat-induced antigen retrieval (HIAR) with sections incubated in ethylenediaminetetraacetic acid (Tris-EDTA) buffer (pH 9.0). The sections were further incubated with the following primary antibodies at 4°C overnight: anti-CD68 (catalog no. ab201340, Abcam) and anti-MCP-1 (catalog no. ab7202, Abcam), followed by the appropriate secondary antibody. The sections were then developed with 3, 3-diaminobenzidine (DAB) to produce a brown product and were counterstained with hematoxylin.

Immunofluorescence

Frozen renal tissue sections embedded in OCT were fixed in precooled acetone for 15min, blocked with 1%BSA for 30 min and then incubated with IFN-γ (catalog no. AF-585-NA, R&D), IL-17 (catalog no. 374218, Santa Cruz), FoxP3 (catalog no. 53876, Santa Cruz), F4/80 (catalog no. ab16911, abcam), or CD206 (catalog no. ab64693, abcam) at a dilution of 1:100 overnight at 4°C, followed by secondary anti-goat IgG (catalog no. NL001, R&D), Cy3-labeled goat anti-mouse IgG (catalog no. A0521, Beyotime) or goat anti-rabbit IgG Alexa Fluor-488 (catalog no. ab150081, abcam). After staining, the cell nuclei were stained with 4',6-diamidino-2-phenylindole (DAPI), and images were obtained using confocal microscopy(400x).

Isolation of Bone Marrow-Derived Macrophages (BMDMs) and Induction of M2 Macrophages

Bone marrow-derived macrophages were isolated from male C57/BL6 mice, as previously described (20), using F4/80 (macrophage marker) and CD11b (myeloid marker), and double-positive macrophages were confirmed with a high purity (about 94.9% of F4/80-positive and CD11b-positive cells on day 7 of culture *in vitro*) (**Supplementary Figure 2**). Briefly, 6-week-old mice were sacrificed, and femur and tibia bone marrow cells were flushed into phosphate-buffered saline (PBS) that contained 2% heat-inactivated fetal bovine serum (FBS), followed by centrifuging at 500g for 5min and lysis with RBC lysis buffer (BOSTER, Wuhan, China). The cells were then

suspended in 15% L929-conditioned medium (RPMI-1640 medium containing 10% FBS, 1% penicillin/streptomycin, and 15% L929 cell culture supernatant) and left to adhere for 24 hrs at 37°C in an atmosphere of 5% CO2. The adherent cells were re-plated in a six-well plate with 15% L929-conditioned medium at a density of 1x10^6 per well for seven days to obtain BMDMs with the medium being changed every two days. The BMDMs were then exposed to high glucose in the presence or absence of HPS for 48 hrs: (1) Control group (8mM glucose); (2) HG group (35mM glucose); (3) HG+HHPS group (35mM glucose +50uM HPS); (4) HG+MHPS group (35mM glucose +25uM HPS); (5) HG +LHPS group (35mM glucose +12.5uM HPS).

Besides, M2 macrophages were obtained through addition of 20ng/ml of recombinant murine IL-4 (cat no.21414, Peprotech) to the bone marrow cells before incubation at 37°C with 5% CO2 for 36 hrs to induce the differentiation of BMDMs into M2 macrophages.

Real-Time Reverse Transcriptase-Polymerase Chain Reaction (RT-PCR)

Total RNA was isolated from kidney tissues or HG-induced macrophages *in vitro* using Trizol reagent (Qiagen, San Diego, CA, USA) following the manufacturer's instructions. 1ug RNA was reversely transcribed to cDNA using Oligo$(dT)_{15}$ primer and superscript reverse transcriptase (Promega Corporation, Madison, WI). Target gene expression was quantified by real-time PCR using SYBR Green Supermix and the ABI Real-Time PCR Reaction System (Bio-Rad Laboratories). PCR conditions were described as the following: denaturation at 95°C for 3 min, followed by 40 cycles at 95°C for 15 s, 57°C for 30 s, and 72°C for 30 s, with final elongation at 72°C for 10 min. A mouse housekeeping gene β-actin was selected as the internal control. Three independent experiments were performed by calculating the relative mRNA levels using $^{2\text{-}\triangle\triangle Ct}$ methods with values normalized to the reference gene β-actin. The primer sequences (Sangon Biotech, Shanghai, China) that were used are listed in **Table 2**.

Purification of Splenic T Cells

The purification of $CD3^+$ T cells was carried out by nylon wool columns as described previously (21). Briefly, spleens from 6-week male C57/BL6 mice were gently and mechanically disassociated through a 70um cell strainer and lysed with RBC lysis buffer (BOSTER, Wuhan, China) to obtain splenic cells suspension. Autoclaved and sterile nylon fibers (0.5g) were put into a 10mL column, and then the column was equilibrated by 20mL warm RPMI-1640 medium, sealed and incubated at 37°C and 5% CO2 for 1 hour. Spleen cells (1x10^8) were added to the column, sealed and incubated at 37°C and 5% CO2 for 1 hour. Cells subjected to nylon wool purification were resuspended with 2mL warm RPMI-1640 medium, and the column was washed with 2mL warm RPMI-1640 twice. Finally, cells were collected, centrifuged and resuspended for further experiment.

Co-Culture of M2 Macrophages and T Cells

Transwell coculture of mouse M2 macrophages and T cells was performed using a 24-well multi-well chamber and polycarbonate membranes (0.4-um porous). Briefly, T cells were collected and seeded in the upper 24-well transwell plate (5x10^4 cells/well) with 10ng/mL IL-2 (Peprotech, USA) and 1x PMA/ionomycin (Multi-Science Biotechnology, China) in complete RPMI-1640 medium, while M2 macrophages were cultured in the lower 24-well transwell plate (5x10^5 cells/well) with complete RPMI-1640 medium in the absence or presence of different concentrations of HPS for 72 hrs. After co-culture, T cells were collected and centrifuged (400g, 4°C, 5min) for flow cytometric analysis.

Cell Proliferation Assays

T cell proliferation in the coculture was determined using Carboxyfluorescein Diacetate Succinimidyl Ester (CFSE) Cell Proliferation Assay and Tracking Kit (Beyotime, China). For CFSE staining, T cells were isolated, purified and resuspended to 1x10^6 cells/ml in 1x CFSE cell labeling solution at 37°C for 10 min, followed by centrifuging and washing with RPMI-1640 complete medium. After the coculture, CFSE-labeled T cells were collected to perform co-further culture with M2 macrophages for 72 hrs, and finally analyzed using a flow cytometer (Novocyte Quanteon). Data were interpreted as the percentage of proliferated cells.

Flow Cytometric Analysis

Single-cell suspensions from spleens were prepared as the following. Briefly, spleens from the *db/m* and *db/db* mice were

TABLE 2 | The primer sequences used in quantitative real-time PCR.

Gene Primer	Forward Sequence (5'-3')	Reverse Sequence (5'-3')
β-actin	GCTTCTTTGCAGCTCCTTCG	GGCCTCGTCACCCACATAG
iNOS	GACATTACGACCCCTCCCAC	GCACATGCAAGGAAGGGAAC
TNF-α	CACCTGGCCTCTCTACCTTG	CGATTACAGTCACGGCTCCC
MCP-1	TTGACCCGTAAATCTGAAGCTAAT	TCACAGTCCGAGTCACACTAGTTCAC
Arg-1	ACATTGGCTTGCGAGACGTA	ATCACCTTGCCAATCCCCAG
IFN-γ	CACGGCACAGTCATTGAAAG	CATCCTTTTGCCAGTTCCTC
IL-10	CCAAGCCTTATCGGAAATGA	TCCTGAGGGTCTTCAGCTTC
IL-17	GTCCAAACACTGAGGCCAAG	ACGTGGAACGGTTGAGGTAG

iNOS, inducible nitric oxide synthase; TNF-α, tumor necrosis factor α; MCP-1, monocyte chemoattractant protein-1; Arg-1, arginase-1; IFN-γ, interferon gamma; IL-10, interleukin 10; IL-17, interleukin 17.

minced and filtered through 40μm nylon meshes, and then the splenic cells were suspended in PBS and lysed with red blood cell-lysis buffer, followed by centrifuging (400g, 4°C) for 5min. As for the bone marrow-derived macrophages (BMDMs), they were first isolated and cultured as described above. Then the splenic T cells and BMDMs were incubated with fluorochrome-conjugated Abs against various surface makers at room temperature for 30 min, including APC-conjugated anti-mouse F4/80 (catalog no. 123116, Biolegend), V450- Rat anti-mouse CD11b (catalog no. 560455, BD), FITC-conjugated anti-mouse CD86 (catalog no. 105005, Biolegend) and PE-Cyanine7-conjugated anti-mouse CD206 (MMR) (catalog no. 25-2061-82, eBioscience). To observe the effects of HPS on the generation of Th2 and Treg cells in a co-culture model of M2 and T cells, T cells were cultured in medium containing 1x BFA/Moensin (Multi-Science Biotechnology, China) for 8 hrs before cells were collected. The T cells were centrifuged, washed and incubated with APC anti-mouse CD4 Ab (catalog no. 100516, Biolegend). For intracellular staining, the cells were permeabilized using FoxP3/Transcription Factor Fixation/Permeabilization Concentrate and Diluent Kit (eBioscience, USA) and then stained with brilliant Violet 421-anti-mouse FoxP3(catalog no. 126419, Biolegend) and PE anti-mouse IL-4 Abs (catalog no.554389, BD). For cell proliferation assays, T cells were first labeled with CFSE before coculture. After 48 hrs of the coculture, T cells were collected, centrifuged, resuspended, and incubated with APC anti-mouse CD4 Ab (catalog no. 100516, Biolegend). Cells finally were analyzed *via* a flow cytometer (Novocyte Quanteon).

Statistical Analysis

All data were expressed as mean ± standard deviation (SD) and analyzed using Graphpad Prism 8.0 software (San Diego, CA, USA). One-way ANOVA with a one-tailed Student's t-test was used to identify significant differences in multiple comparisons. The *post hoc* comparisons using the Student-Newman-Keuls tests were performed for inter-group comparisons of multiple variables. A probability of $P < 0.05$ was considered to be statistically significant.

RESULTS

Hyperoside (HPS) Reduces Albuminuria and Improves Glycolipid Metabolism Dysfunction in *db/db* Mice

We first determined the effects of HPS on proteinuria as well as glycolipid metabolism in *db/db* mice. Compared with control *db/m* mice, the levels of urine albumin-creatine ratio (UACR), body weight (BW), fasting blood glucose (FBG), total cholesterol (TC), and low-density lipoprotein-cholesterol (LDL-C) were significantly higher in *db/db* mice (**Figure 1**). Administration of HPS (either 40 or 80mg/kg/day) for 12 weeks resulted in a significant reduction of these indicators in *db/db* mice (**Figure 1** and **Table 3**).

HPS Improves Renal Morphological Abnormalities in *db/db* Mice

Mesangial matrix expansion and glomerular basement membrane thickening were observed in the kidneys of *db/db* mice and were ameliorated in HPS-treated *db/db* mice (**Figure 2A**). The mesangial expansion index and glomerulosclerosis index, indicating the progression of the mesangial changes in DN, were significantly increased in *db/db* mice compared to *db/m* control mice. However, HPS treatment for 12 weeks significantly decreased both the mesangial expansion index and glomerulosclerosis index, resulting in a reduction of renal mesangial expansion and extracellular matrix accumulation in *db/db* mice (**Figures 2B, C**).

HPS Treatment Reduces Total Macrophages and Chemokine MCP-1 in *db/db* Mice

To determine an impact of HPS on total macrophage numbers in the kidney of *db/db* mice, immunohistochemistry (IHC) staining was performed. We found that compared to control *db/db* mice, administration of HPS remarkedly decreased the number of CD68-positive macrophages in the renal tissue, although they were significantly increased in control *db/db* mice compared to non-diabetic *db/m* control mice (**Figures 3A–E**). On the other hand, IHC staining also showed that HPS significantly reduced MCP-1 expression in the kidney tissue of *db/db* mice (**Figures 3F–J**), indicating that overall, HPS is anti-inflammatory in murine DN.

HPS Alters the Balance of Pro-Inflammatory and Anti-Inflammatory Cytokines in *db/db* Mice

Quantitative real-time PCR analysis was performed to measure the gene expression of the inflammatory cytokines and chemokines in the kidney of *db/db* mice. We found that HPS treatment decreased the gene expression of the pro-inflammatory cytokines/chemokines, including iNOS, MCP-1, IFN-γ, IL-17 and TNF-α, in the renal tissue, whereas it increased the expression of anti-inflammatory cytokines Arg-1 and IL-10 (**Figure 4**). Our results suggest that HPS indeed exerts anti-inflammatory effects in a murine model of DN.

HPS Promotes M2 Macrophage Polarization in the Kidney of *db/db* Mice

Immunofluorescence staining was performed to determine the effects of HPS on M2 macrophage polarization in the kidney of *db/db* mice since M2 macrophages play an important role in controlling renal inflammation. The results showed that expression of F4/80, a marker of total macrophage population, was increased in the kidney of *db/db* mice compared to *db/m* mice while HPS treatment significantly reduced its expression (**Figures 5A, C**). On the other hand, the downregulated expression of M2 macrophage marker CD206 in the kidney of *db/db* mice was markedly increased by HPS (**Figures 5B, D**). The results indicate that HPS reduces renal inflammatory injury in *db/db* mice *via* promoting M2 macrophage polarization.

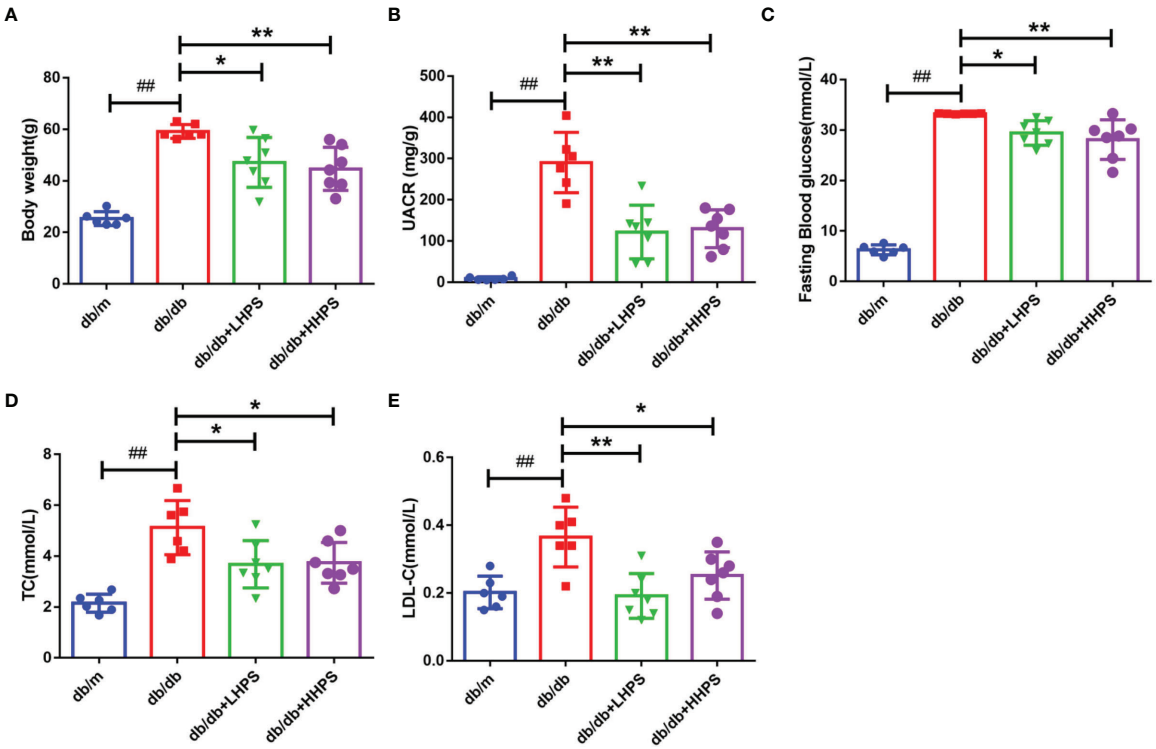


FIGURE 1 | Clinical and metabolic parameters in four groups of mice: *db/m*, *db/db*, *db/db* +LHPS, and *db/db* +HHPS mice. **(A)** Body weight (g), **(B)** Urine albumin-to-creatinine ratio (UACR) (mg/g), **(C)** Fasting blood glucose (FBG) (mmol/L), **(D)** Total cholesterol (TC) (mmol/L), and **(E)** Low density lipoprotein-cholesterol (LDL-C) (mmol/L) were measured after HPS treatment. *db/m*, non-diabetic normal control mice; *db/db*, DN mice treated with distilled water; *db/db*+ LHPS or HHPS, *db/db* mice treated with 40 (LHPS) or 80 mg/kg/day (HHPS) of HPS, respectively. Data are presented as the mean ± SD (n=6-7, with individual donors shown as dots, $^{\#\#}P < 0.01$ *vs db/m*; $^{*}P < 0.05$ and $^{**}P < 0.01$ *vs db/db*).

HPS Promotes Splenic M2 Macrophage Generation in *db/db* Mice

Flow cytometric analysis showed that HPS reduced the total population of splenic MØ macrophages ($F4/80^{+}CD11b^{+}$) in both *db/db* +LHPS and *db/db* +HHPS mice (**Figures 6A, D**). The decreased percentage of $F4/80^{+}CD11b^{+}CD206^{+}$ cells in spleen of *db/db* mice was significantly increased after HHPS treatment (**Figures 6C, F**). We also found a downward trend for the percentage of $F4/80^{+}CD11b^{+}CD86^{+}$ cells in *db/db* mice treated with HHPS. However, there were no statistically

TABLE 3 | The effects of Hyperoside pre-treatment on clinical and metabolic parameters of *db/db* mice.

Index	*db/m*	*db/db*	*db/db* +HHPS	*db/db* +LHPS
BW(g)	25.38 ± 2.68	59.18 ± 2.60$^{\#\#}$	44.66 ± 8.39**	47.14 ± 9.67*
UACR (mg/g)	8.93 ± 4.14	290.33 ± 73.20$^{\#\#}$	129.61 ± 45.85**	121.89 ± 65.09**
FBG (mmol/L)	6.27 ± 0.98	33.22 ± 0.08$^{\#\#}$	28.53 ± 4.31**	29.41 ± 2.42*
TC (mmol/L)	2.15 ± 0.36	5.12 ± 4.22$^{\#\#}$	3.49 ± 3.32*	3.74 ± 3.51*
TG (mmol/L)	1.37 ± 0.95	1.62 ± 0.81	1.97 ± 0.85	1.95 ± 0.74
LDL-C (mmol/L)	0.20 ± 0.05	0.37 ± 0.09$^{\#\#}$	0.25 ± 0.07*	0.19 ± 0.07**
HDL-C(mmol/L)	1.08 ± .0.21	1.99 ± 0.42	1.90 ± 0.39	1.97 ± 0.47
BUN (mmol/L)	9.89 ± 2.21	9.42 ± 1.96	8.51 ± 1.86	8.61 ± 1.85
SCr (μmol/L)	10.00 ± 1.90	8.40 ± 3.36	9.38 ± 2.07	8.50 ± 3.30
UA (μmol/L)	224.30 ± 64.48	317.40 ± 97.57$^{\#}$	352.25 ± 64.67	376.50 ± 75.92
ALB (g/L)	42.12 ± 3.14	46.04 ± 8.51	44.23 ± 8.49	45.18 ± 2.38

db/m: normal mice; db/db: treated with vehicle solution; LHPS and HHPS: db/db mice were treated with 40 or 80 mg/kg/d Hyperoside for 12 weeks after DM establishment respectively. Data are presented as mean ± SD. n=6-7. $^{\#}P < 0.05$ vs db/m mice; $^{\#\#}P < 0.01$ vs db/m mice; $^{*}P < 0.05$ vs db/db mice; $^{**}P < 0.01$ vs db/db mice.

BW, body weight; UACR, urine albumin creatine ratio; FBG, fasting blood glucose; TC, total cholesterol; TG, Triglyceride; LDL-C, low density lipoprotein cholesterol; HDL-C, high density lipoprotein cholesterol; BUN, blood urea nitrogen; SCr, serum creatinine; UA, uric acid; ALB, serum albumin.

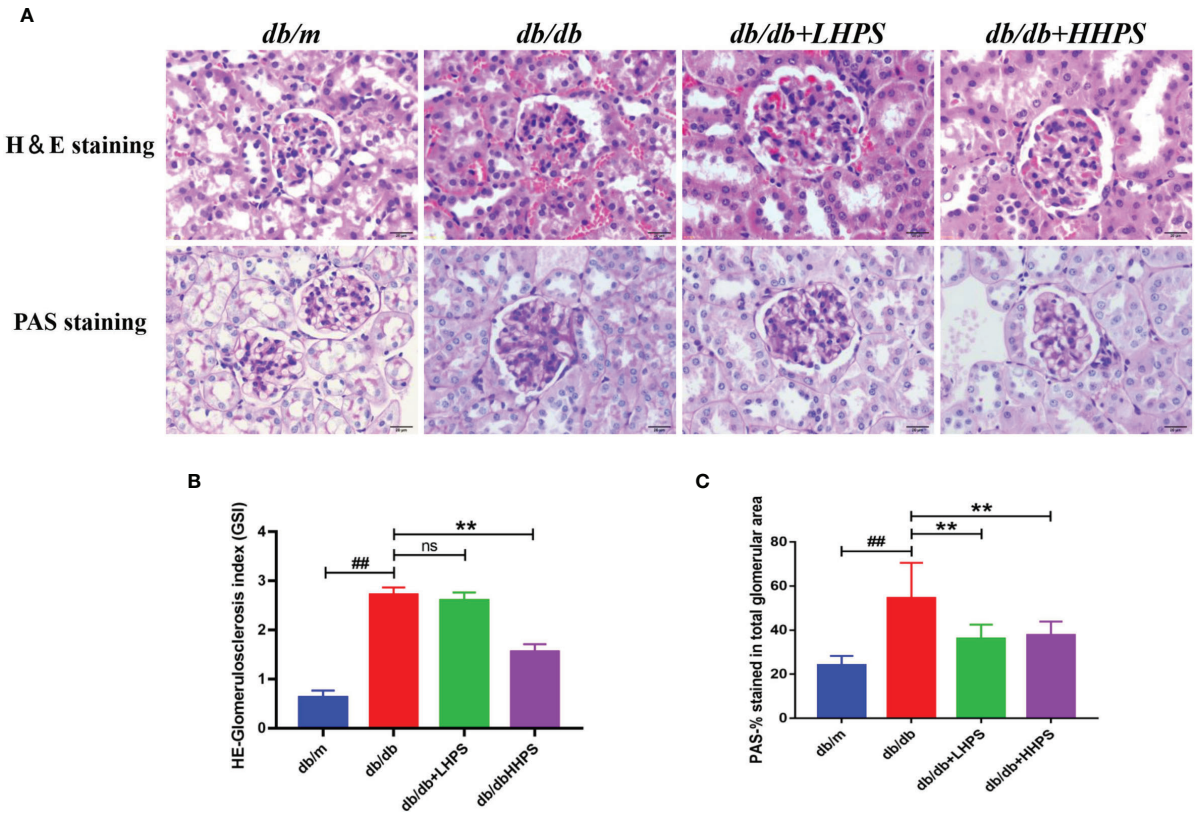


FIGURE 2 | Hyperoside ameliorates mesangial matrix expansion in glomeruli of *db/db* mice. The *db/db* mice were treated with HPS, while control mice receiving vehicle treatment were administered with the same volume of vehicle used to prepare HPS. **(A)** Renal morphology was analyzed by H&E staining on kidney sections while glomerular mesangial matrix fractions and glomerulosclerosis were analyzed using PAS staining in mice at the age of 12 weeks. Figures for representative sections are shown at ×400 magnification. **(B)** Shown is quantification of the glomerulosclerosis index (GSI) for each group. **(C)** The PAS stained areas for each group are also quantified. Values (mean ± SD) were obtained from 3 animals in each group (n=3 per group). Differences between experimental groups were evaluated using ANOVA ($^{\#\#}P < 0.01$ *vs db/m*; $^{**}P < 0.01$ *vs db/db;* ns, not significant). *db/m*, non-diabetic normal mice; *db/db*, diabetic nephropathy mice; *db/db* +LHPS, diabetic nephropathy group mice treated with a low dose of HPS; *db/db*+HHPS, diabetic nephropathy group mice treated with a high dose of HPS; H&E, Hematoxylin and Eosin; PAS, Periodic Acid–Schiff.

significant changes in the percentage of $F4/80^{+}CD11b^{+}CD86^{+}$ cells in control *db/db* mice, compared to *db/m* control mice or HPS treated *db/db* mice (**Figures 6B, E**). These data indicate that HPS promotes splenic M2 macrophage generation in *db/db* mice.

HPS Also Reduces Protein Expression of Proinflammatory Cytokines Associated With CD4+ T-Cells but Increases FoxP3 Expression in the Kidney of *db/db* Mice

To explore whether HPS restores the balance of Th cell subsets or cytokines, we investigated the biological effects of HPS on the protein expression of IFN-γ, IL-17 and FoxP3 in the renal tissue using immunofluorescence (IF) staining. We found that HPS treatment significantly downregulated IFN-γ and IL-17 expressions (**Figures 7A, B**) but upregulated the expression of FoxP3 in the kidney of *db/db* mice compared to that of control *db/db* mice (**Figure 7C**). The same results were confirmed when MFI was analyzed statistically (**Figures 7D–F**), indicating that HPS can alter the balance of Th1/Th17/Treg cells.

HPS Alters the Balance of Pro-Inflammatory and Anti-Inflammatory Cytokines in BMDMs *In Vitro* Under High Glucose Condition

To examining whether HPS could reverse the inflammatory responses *in vitro*, bone marrow-derived macrophages (BMDMs) were incubated and divided into five groups: (1) Control group (8mM glucose); (2) HG group (35mM glucose); (3) HG+HHPS group (35mM glucose +50uM HPS); (4) HG +MHPS group (35mM glucose +25uM HPS); (5) HG+LHPS group (35mM glucose +12.5uM HPS). Compared with the control group (low glucose), upregulation of pro-inflammatory cytokines, including iNOS, TNF-α, IL-17, MCP-1 and IFN-γ (**Figures 8A–E**), and downregulation of anti-inflammatory cytokines Arg-1 and IL-10 (**Figures 8F, G**) were observed in HG group, indicating that HG can trigger an inflammatory response *in vitro*, mimicking a diabetic condition *in vivo*. Compared with the HG group, however, HG plus HPS groups reduced mRNA levels of M1 macrophage-associated

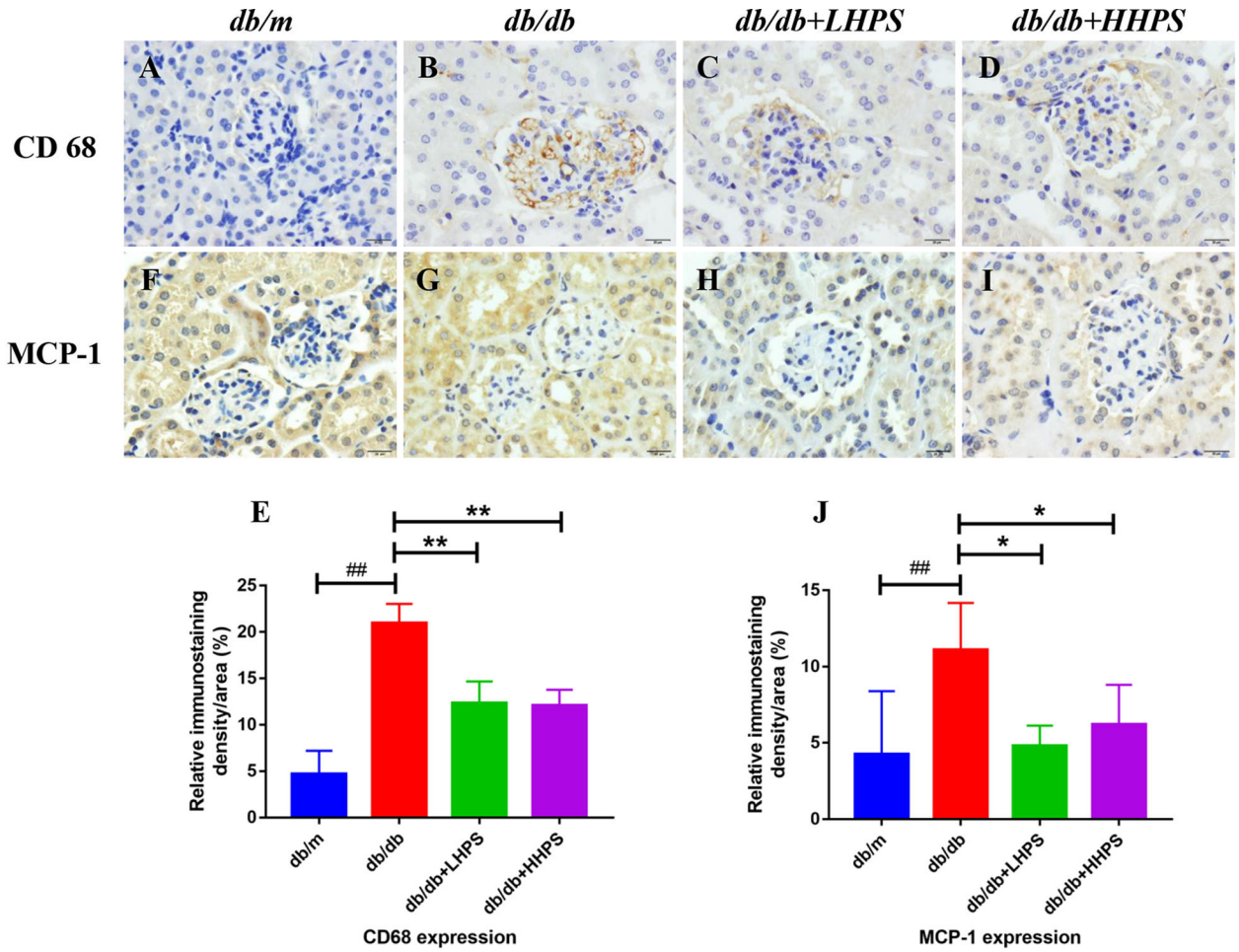


FIGURE 3 | Immunohistochemical staining of CD68 and MCP-1 in glomeruli and interstitial areas (×400, bar=20um) of the kidney in *db/db* mice. Immunohistochemical analysis of CD68-positive **(A–D)** and MCP-1-positive cells **(F–I)** was performed after HPS treatment. The color was developed by incubating with diaminobenzidine and counterstaining with hematoxylin (Magnification x 400). Shown also is quantification of the CD68+ **(E)** or MCP-1+ area **(J)**. The data are presented as the mean ± SD (n = 5 per group, $^{\#\#}P < 0.01$ *vs db/m*; $^{*}P < 0.05$ and $^{**}P < 0.01$ *vs db/db*, with each symbol color representing a particular group).

pro-inflammatory mediators iNOS, TNF-α, IL-17, MCP-1 and IFN-γ (**Figures 8A–E**), while the mRNA levels of anti-inflammatory cytokines Arg-1 and IL-10 (**Figures 8F, G**) were increased in the group with high concentrations of HPS. These data suggest that HPS can diminish pro-inflammatory responses stimulated by HG in BMDMs.

Hyperoside Promotes M2 Macrophage Formation in High Glucose (HG)-Induced BMDMs

We then examined the effects of HPS on macrophage polarization *in vitro*. BMDMs were pretreated with HG to mimic the *in vivo* diabetic condition. M1/M2 macrophage polarization was determined *via* flow cytometry and represented as mean fluorescence intensity (MFI). The percentage of $F4/80^{+}/CD206^{+}$ BMDMs was significantly decreased in the presence of HG, but increased after HPS treatment (**Figures 9B, D**), indicating that HPS promotes M2 macrophage polarization, which otherwise is inhibited by HG. Meanwhile, we found that the proportion of $F4/80^{+}/CD86^{+}$ cells had an upward trend in HG-induced BMDMs and a downward one with a high concentration of HPS treatment (HHPS) (**Figures 9A, C**), yet without a statistical significance. These results indicate that the promotion of M2 macrophage formation may be critical for HPS mediated anti-inflammatory effects in BMDMs in the face of HG.

HPS Inhibits T Cell Proliferation and Drives T Cell Differentiation Towards Th2 and Treg Populations in a Co-Culture Model of T Cells/M2 Macrophages

Given that M2 macrophages affect Treg/Th cell differentiation, we examined the effect of HPS on T cell proliferation and Th2/Treg generation in the coculture of T cells and M2 BMDMs.

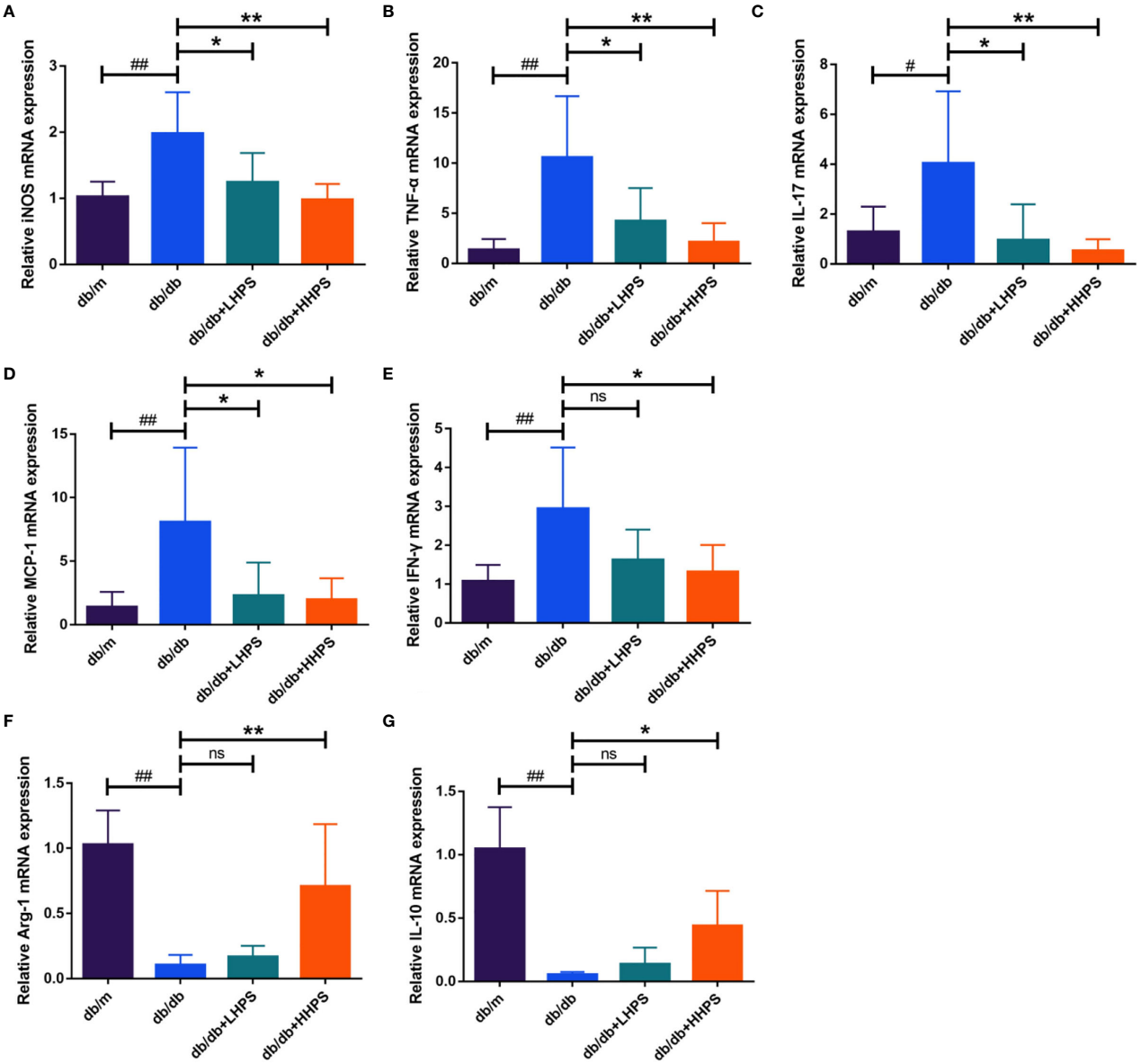


FIGURE 4 | Hyperoside reduces the expression of proinflammatory cytokines while increasing the expression of anti-inflammatory cytokines in the kidney. Quantitative real-time PCR analysis of the proinflammatory cytokines iNOS **(A)**, TNF-α **(B)**, IL-17 **(C)**, MCP-1 **(D)** and IFN-γ **(E)**, and anti-inflammatory cytokines Arg-1 **(F)** and IL-10 **(G)** in the kidney tissue in four groups following HPS treatment: *db/m*, *db/db*, *db/db* +LHPS, and *db/db* +HHPS mice. Relative mRNA expression levels were normalized to β-actin. Data are representatives of three independent experiments and presented as means ± SD (n = 6 per group, $^{\#}P < 0.05$ and $^{\#\#}P < 0.01$ *vs db/m*; $^{*}P < 0.05$ and $^{**}P < 0.01$ *vs db/db;* ns, not significant).

As shown in the **Figure 10**, T-cell proliferation was inhibited by addition of M2 macrophages to the coculture (MT) as compared with T cell culture alone (T) without M2 macrophages (**Figures 10A, D**), while compared with the coculture group of M2 plus T cells (MT), HPS showed more effective inhibition of T cell proliferation (**Figures 10A, D**). Hence, these results indicate that M2 macrophages suppress T cell proliferation and that HPS plus M2 macrophages can further enhance their suppression of T-cell proliferation. Furthermore, we asked whether HPS also affected the differentiation of T cells co-cultured with M2 macrophages. As shown in **Figure 10**, more T cells co-cultured with M2 macrophages expressed Th2 cytokine IL-4 ($CD4^{+}IL4^{+}$) (**Figures 10B, E**) and FoxP3 ($CD4^{+}Foxp3^{+}$) (**Figures 10C, F**) than T cells without M2 macrophages.

Interestingly, compared with the M2 and T cell coculture group (MT) alone, the groups treated with HPS (MT+LHPS or +HHPS) showed further upregulation of the frequency of Th2 ($CD4^{+}IL4^{+}$) (**Figures 10B, E**) and $CD4^{+}Foxp3^{+}$ Treg cells (**Figures 10C, F**).

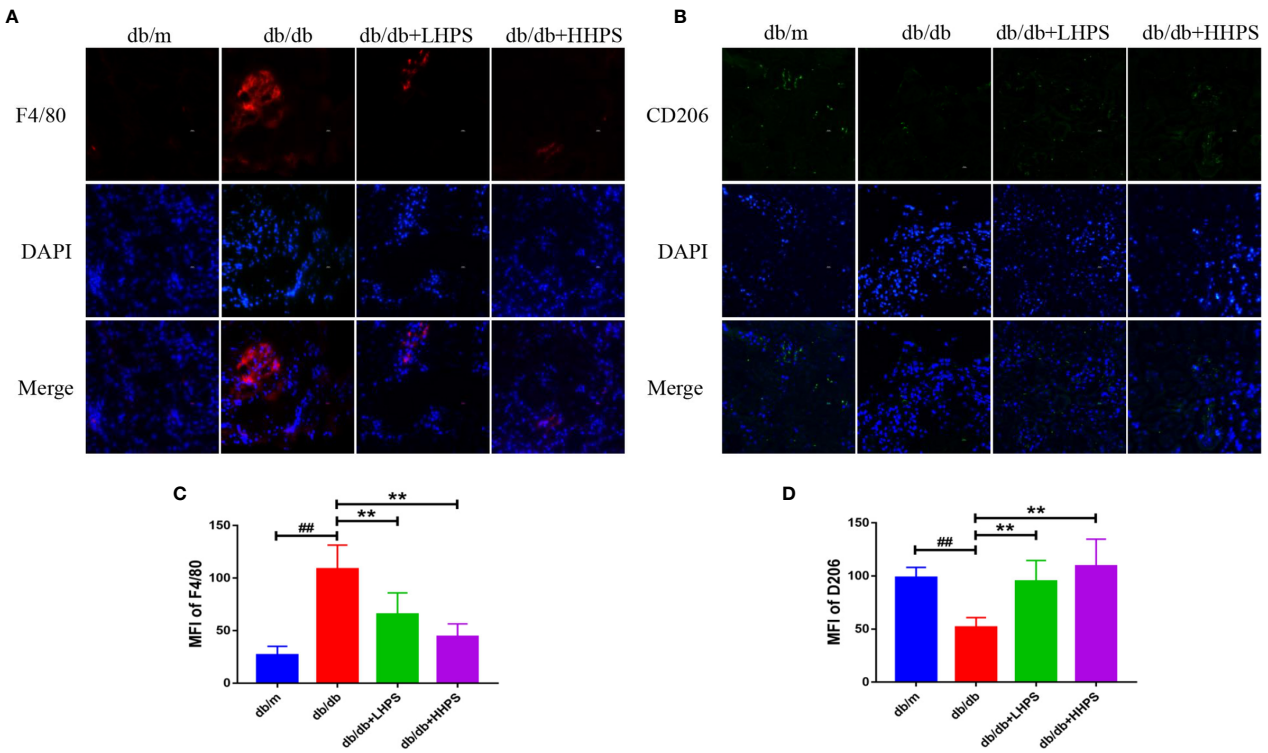


FIGURE 5 | The M2 macrophage polarization in the kidney of *db/db* mice treated with Hyperoside. Immunofluorescence staining showed that Hyperoside promoted the polarization of M2 macrophages and reduced total number of macrophages in the kidney. **(A)** Macrophages were stained for F4/80 (red) in glomeruli of *db/db* mice by immunofluorescence after Hyperoside treatment. **(B)** M2 macrophages were stained for CD206 (green) in glomeruli of *db/db* mice by immunofluorescence. DAPI was used to stain the cellular nucleus. (Original magnification: ×400. Scale bars = 50 μm). Shown is also quantification of F4/80 **(C)** and CD206 expression **(D)**, as presented as MFI. (n=5 per group, $^{\#\#}P < 0.01$ vs *db/m*; $^{**}P < 0.01$ vs *db/db*).

These results indicate that HPS may enhance the ability of M2 macrophages to suppress inflammation by promoting T cell differentiation into Th2/Treg subsets.

DISCUSSION

Proteinuria or albuminuria is a clinical risk of the onset and development of diabetic nephropathy (DN) (22, 23). The results of this present study showed that Hyperoside (HPS) dramatically attenuated albuminuria, which is usually accompanied by dyslipidemia and obesity in *db/db* mice. We also investigated the mechanisms underlying effects of HPS on DN and revealed that HPS regulated inflammation by promoting M2 macrophage polarization in addition to shifting Th cell balance towards Treg and Th2 cells, thus attenuating the pathogenesis of DN. This study provides a rationale for developing HPS as a drug for the treatment of DN.

In this study, a significantly higher urine albumin-to-creatinine ratio (UACR), hyperglycemia, and an increase in body weight, LDL-C and TC in *db/db* mice suggested that the animals developed DN. When compared with *db/db* mice, significant decreases in UACR were observed in HPS-treated *db/db* mice, suggesting that HPS ameliorated proteinuria in diabetic mice. In addition, the levels of fast blood glucose, LDL-C, TC, and body weights were significantly reduced after treatment with HPS, indicating that it exerted an effect on hyperglycemia and hyperlipidemia. However, the parameters of the renal function, such as Scr and BUN, were not significantly improved by HPS. The effects of HPS on hyperglycemia, hyperlipidemia and renal function index is not totally consistent with the report by Zhang J et al (24), which showed that HPS decreased the Scr in DN mice, although it did not affect the glucose and lipid metabolism. This discrepancy may be due to the differences in animal models used in these two studies. The *db/db* mice used in our study have a background of C57BLKS/J strain, which is a widely used mouse model for type 2 diabetes and an approved model of albuminuria associated with DN, and the renal function in these diabetic mice declines at 15-18 weeks without a significant change of serum biochemical indicators, whereas Zhang et al. used low-dose of STZ to induce type 1 diabetes in rats, resulting in obvious deterioration in serum renal function indicators. In the present study, we confirmed the potential protective effects of HPS on glomerulosclerosis in DN. When *db/db* mice were treated with HPS, their histopathology was remarkably improved, which was still

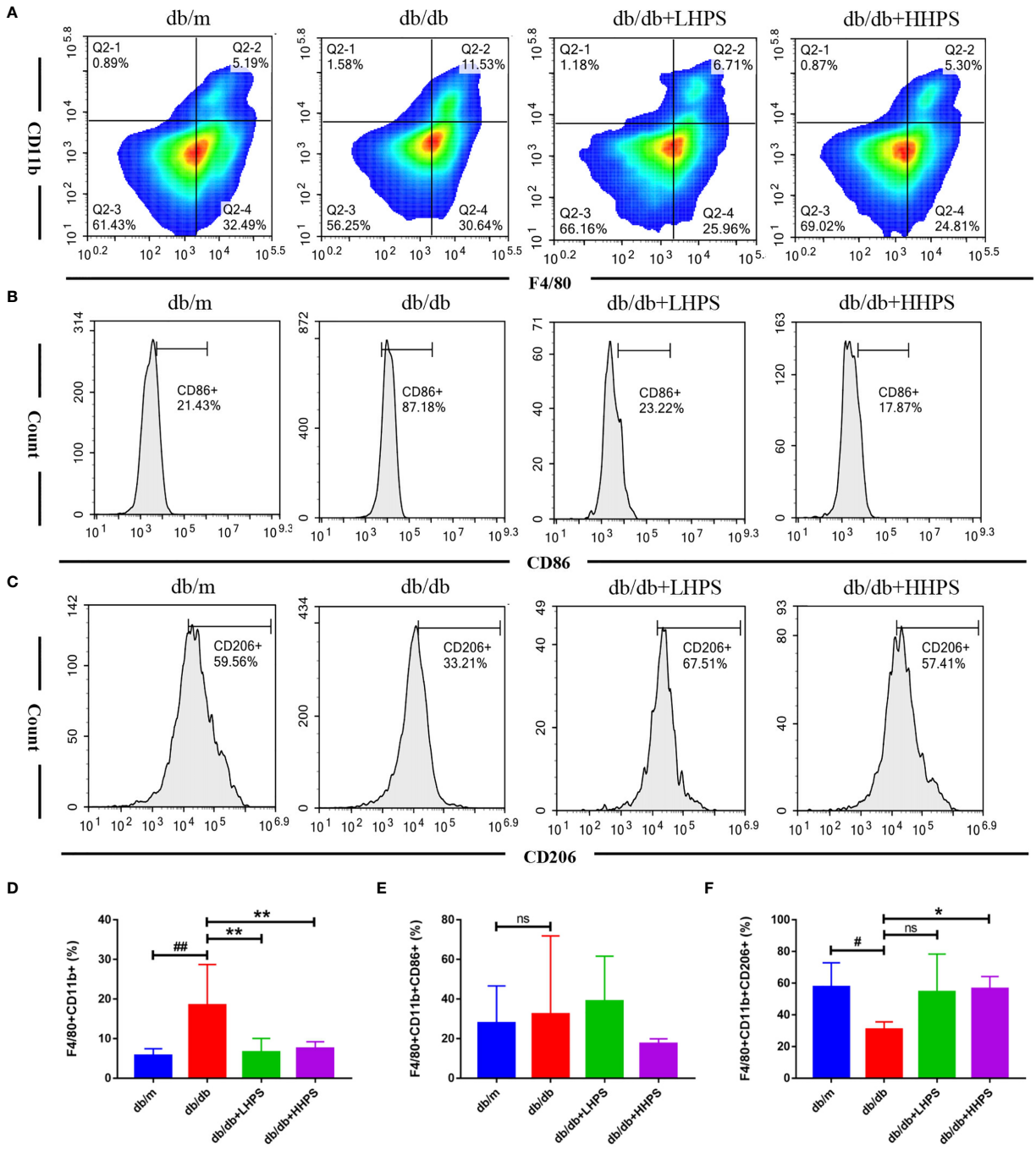


FIGURE 6 | The M2 macrophage polarization in the spleen of *db/db* mice treated with Hyperoside. After HPS treatment, the phenotypes and percentages of MØ ($F4/80^+CD11b^+$) **(A, D)**, M1 ($CD86^+$ gated on $F4/80^+CD11b^+$) **(B, E)** and M2 ($CD206^+$ gated on $F4/80^+CD11b^+$) macrophages **(C, F)** in the spleen of *db/db* mice were determined *via* flow cytometry. Data are presented as mean ± SD (n = 5 per group, $^{\#}P < 0.05$ and $^{\#\#}P < 0.01$ *vs db/m*; $^{*}P < 0.05$ and $^{**}P < 0.01$ *vs db/db*; ns, not significant).

consistent with the findings by Zhang L et al (25) that HPS was involved in the epigenetic regulation of glomerulosclerosis.

Our results demonstrated that HPS exerted an anti-inflammatory effect on DN by regulating macrophage polarization. Macrophages are one of the most abundant innate immune cells in renal tissue of individuals with DN. Activation of macrophages plays a key role in renal inflammatory injury in DN (26). Recently, the role of M1/M2 macrophage

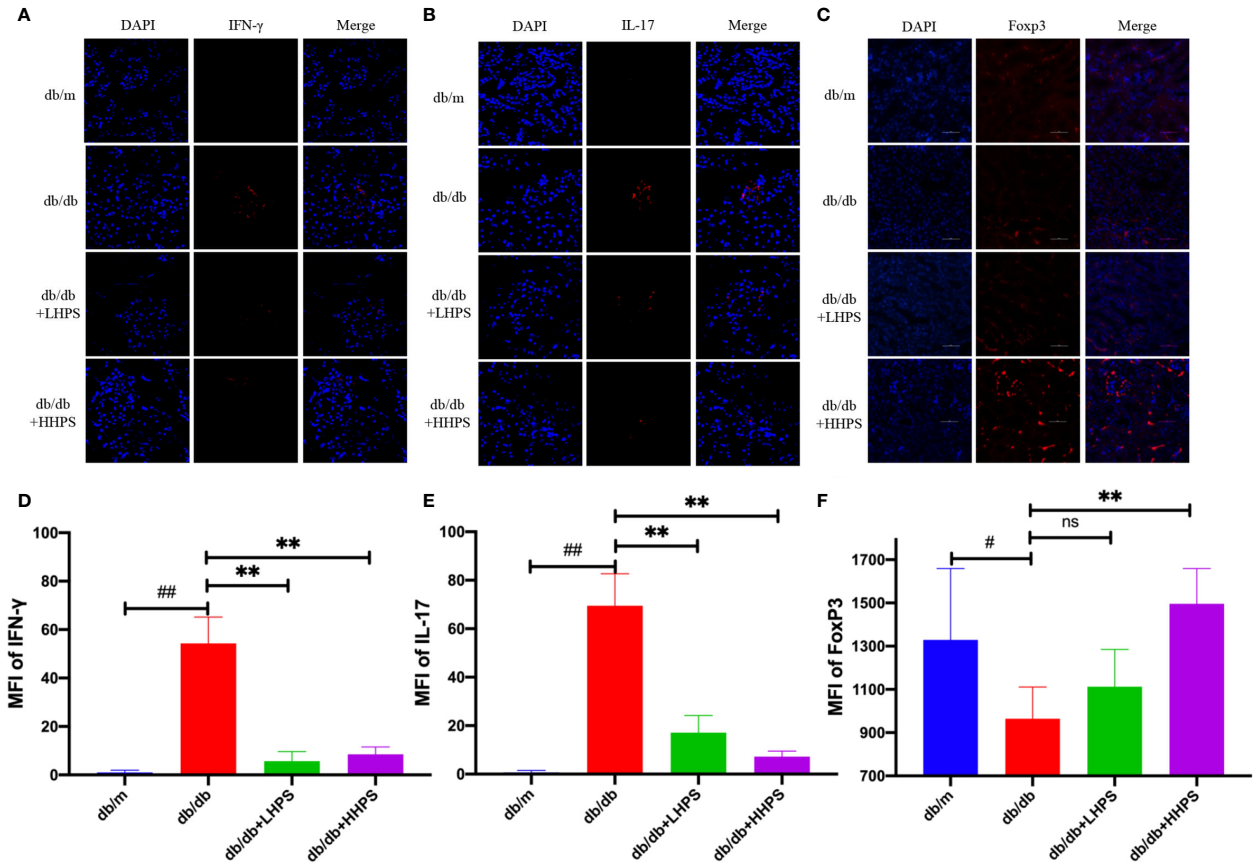


FIGURE 7 | The effects of Hyperoside on the imbalance of T cell differentiation in the kidney. Immunofluorescence staining shows the expressions of CD4+ T-cell associated cytokines, IFN-γ [red, **(A)**], IL-17 [red, **(B)**], and Foxp3 [red, **(C)**] in kidney tissue of *db/db* mice treated with HPS. Quantitative analyses of IFN-γ **(D)**, IL-17 **(E)**, and Foxp3 **(F)** expressions in kidney tissue were also performed (Original magnification: ×400, scale bar = 50 μm). Values are presented as the means ± SD. Differences between experimental groups were evaluated using ANOVA. (n = 5 per group, $^{\#}P < 0.05$ and $^{\#\#}P < 0.01$ *vs db/m*; $^{**}P < 0.01$ *vs db/db*; ns, not significant).

polarization in DN progression has been paid more attention (27, 28). M1 macrophages produce large amounts of pro-inflammatory cytokines iNOS, TNF-α, MCP-1, and other pro-inflammatory mediators that amplify inflammation, resulting in further damages during DN pathogenesis (29, 30). On the other hand, M2 macrophages inhibit renal inflammation and ameliorate injury by secreting anti-inflammatory cytokines, such as IL-10 and Arg-1 (31, 32).

Accumulating evidence has suggested that the levels of proinflammatory factors (proinflammatory cytokines and chemokines) increase with the development of DN and are independently associated with urinary albumin excretion in DN (33, 34). Proinflammatory cytokines that are synthesized and secreted by macrophages in the local microenvironment can directly damage the renal architecture and then trigger the renal fibrosis (35). Therefore, regulation of M1/M2 macrophage phenotypes exhibits anti-proteinuric and renoprotective effects on DN progression (36–38). However, there have been few studies exploring drugs that can regulate macrophage polarization in DN. In this study, we demonstrated that HPS effectively regulated macrophage polarization by shifting proinflammatory M1 macrophages to M2 ones, resulting in the inhibition of proinflammatory macrophage infiltration in the kidney, and thus altered the balance of pro-inflammatory and anti-inflammatory cytokines in *db/db* mice and in BMDMs *in vitro*. Taken together, our results indicated that the anti-inflammatory effects of HPS *via* the regulation of M1/M2 macrophage polarization may be critical for the direct attenuation of proteinuria and improvement of renal tissue damage.

As reported previously, the inflammation and its progression result from not only innate immune responses dominated by macrophage-mediated effects, but also the adaptive immune responsiveness mediated by lymphocytes. Consistently, in addition to the regulation of macrophage polarization, our study showed that HPS also altered the balance of Th1/Th17/Treg cells. Th1 and Th17 cells have been positively associated with renal damages in DN (39). The hallmark of Th1 and Th17 cells is the production of two cytokines interferon γ (IFNγ) and interleukin (IL)-17, which are abundant in diabetic kidneys and

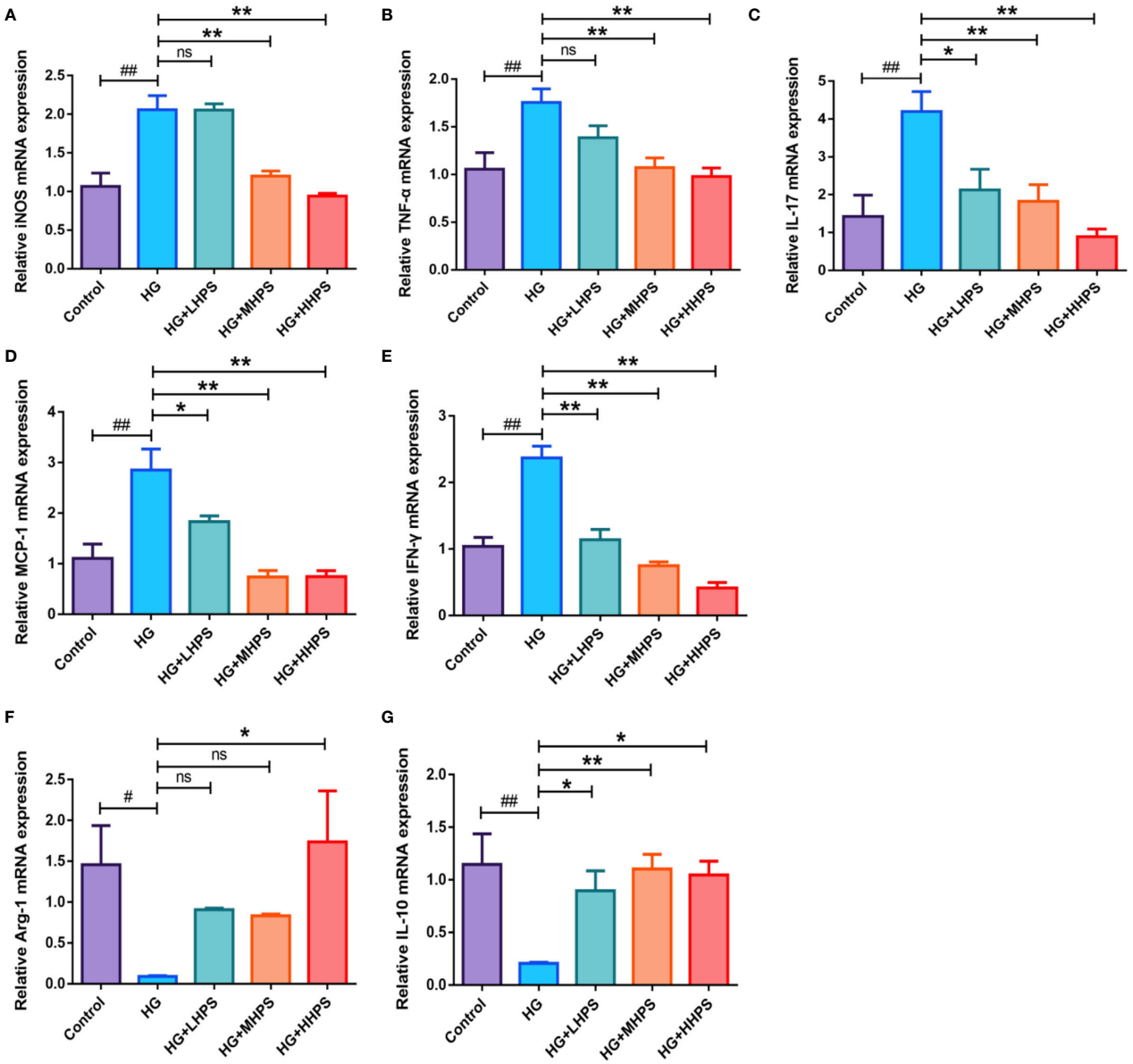


FIGURE 8 | Effects of Hyperoside on the gene expressions of the proinflammatory and anti-inflammatory cytokines in high glucose (HG)-induced BMDMs. BMDMs were treated with high glucose (35mM) for 48 hrs, followed by pretreatment with high-dose HPS (HHPS) (50uM) or low-dose HPS (LHPS) (12.5uM), and then related mRNA expression was determined by qRT-PCR. Relative mRNA expressions of the proinflammatory cytokines iNOS **(A)**, TNF-α **(B)**, IL-17 **(C)**, MCP-1 **(D)** and IFN-γ **(E)**, and anti-inflammatory cytokines Arg-1 **(F)** and IL-10 **(G)** were shown. Values are presented as means ± SD with n = 5 per group. Differences between experimental groups were evaluated using ANOVA ($^{\#}P < 0.05$ and $^{\#\#}P < 0.01$ *vs* Control; $^{*}P < 0.05$ and $^{**}P < 0.01$ *vs* HG; ns, not significant). HG, high glucose treated group; HG+LHPS, high glucose and low dose of HPS treatment group; HG+MHPS, high glucose and middle dose of HPS treatment group; HG+HHPS, high glucose and high dose of HPS treatment group.

play important roles in the development and progression of inflammatory injury in DN (40, 41). Targeting Th17 cells by mycophenolate mofetil or IL-17A neutralizing antibody could attenuate albuminuria and tubulointerstitial fibrosis in mice with DN (6, 42). On the other hand, Treg cells expressing a specific transcription factor forkhead box P3 (FoxP3) have been implicated in the inhibition of DN progression by suppressing the activation of effector T-cells and exerting anti-inflammatory activity (43). Depletion of Tregs exacerbated diabetic-associated renal injury in *db/db* mice, whereas the adoptive transfer of Tregs or induction of Tregs had the opposite effect (44–48). Studies have reported that Th17/Treg imbalance contributed to the development and progression of DN (41, 45, 49), and reversing the imbalance by Dapagliflozin attenuated albuminuria and

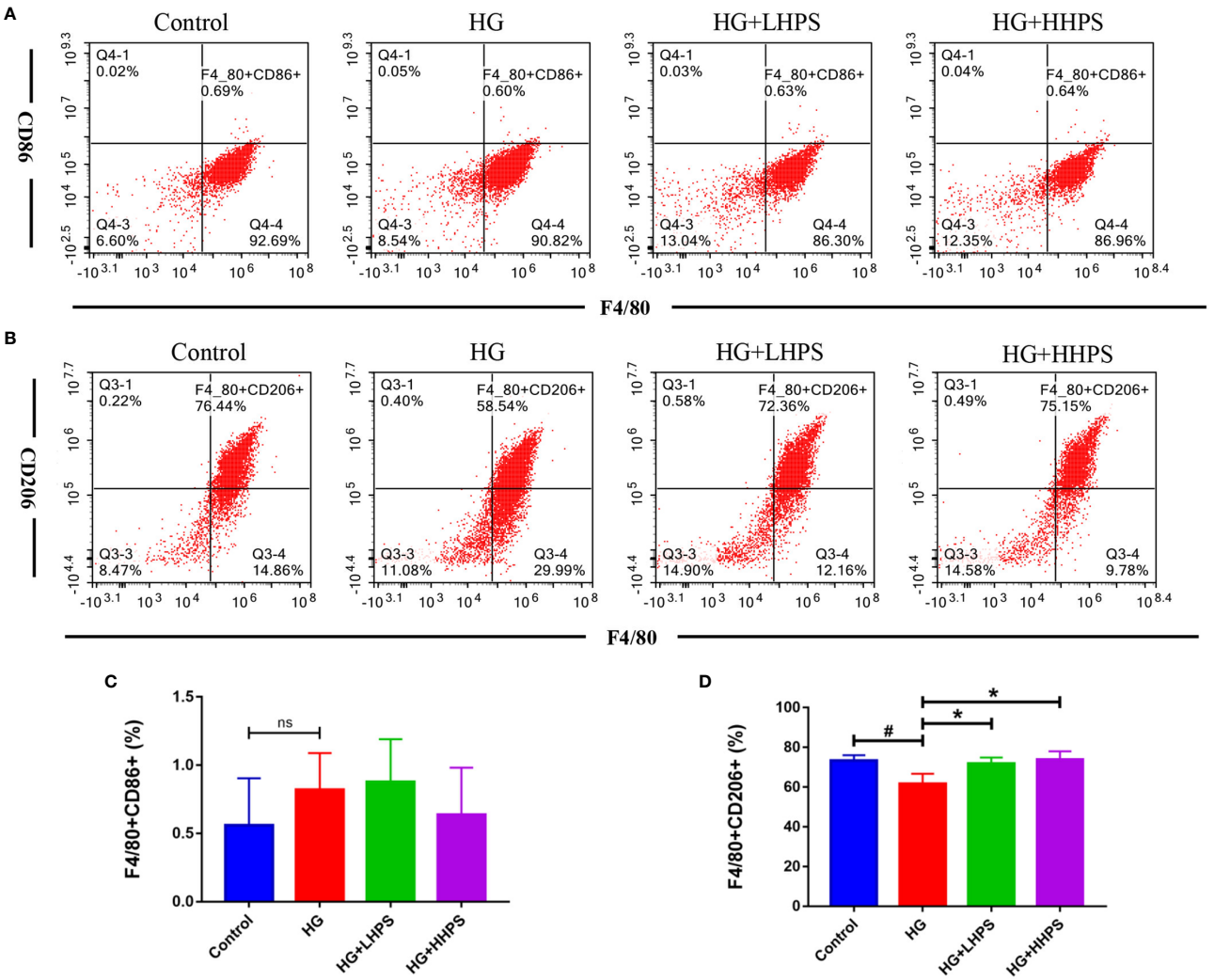


FIGURE 9 | Hyperoside promotes M2 macrophage polarization in high glucose (HG)-induced BMDMs *in vitro*. BMDMs were treated with high glucose (35mM) for 48 hrs, followed by pretreatment with high-dose HPS (HHPS) (50uM) or low-dose HPS (LHPS) (12.5uM), and then collected for flow cytometric analysis. The results showed that there was no significant difference in the proportion of F4/80$^+$/CD86$^+$ macrophages between groups with or without Hyperoside treatment **(A, C)**. However, the proportion of F4/80$^+$/CD206$^+$ macrophages was decreased in BMDMs with high glucose but increased after Hyperoside treatment **(B, D)**. Differences between experimental groups were evaluated using ANOVA ($^{\#}P < 0.05$ *vs* Control; $^{*}P < 0.01$ *vs* HG; ns, not significant). HG, high glucose treated group; HG+LHPS, high glucose and low dose of HPS treatment group; HG+HHPS, high glucose and high dose of HPS treatment group.

tubulointerstitial fibrosis independently of glycemic control in *db/db* mice (50). Therefore, the renoprotective effects of HPS in this study may be also associated with its reversal of Th1/Th17/Treg imbalance.

Interaction of renal tissue macrophages with T cells produces various reactive oxygen species, proinflammatory cytokines, metalloproteinases and growth factors, which in turn enhance the local immune responses and increase inflammation within the kidney in DN (7, 51, 52). Given that HPS remarkedly promoted M2 macrophage polarization in HG-induced BMDMs, we performed co-culture of M2 macrophages and T cells and found that HPS could enhance the ability of M2 macrophages to promote T cell differentiation into Treg and Th2 subsets. Regulation of T-cell proliferation and differentiation by macrophages are well documented in various disease settings, including DN (29, 53, 54). Although the mechanisms of crosstalk between these cells are not clear, it has been reported that M2-polarized macrophages can produce Th2-type and anti-inflammatory cytokines that in turn inhibit T-cell proliferation (55). Therefore, the renoprotective effects of HPS may be attributed to its contribution to the shift of macrophage polarization towards an anti-inflammatory M2 phenotype, which then modulate Th1/Th2 or Th17/Treg balance and thus suppress renal inflammation.

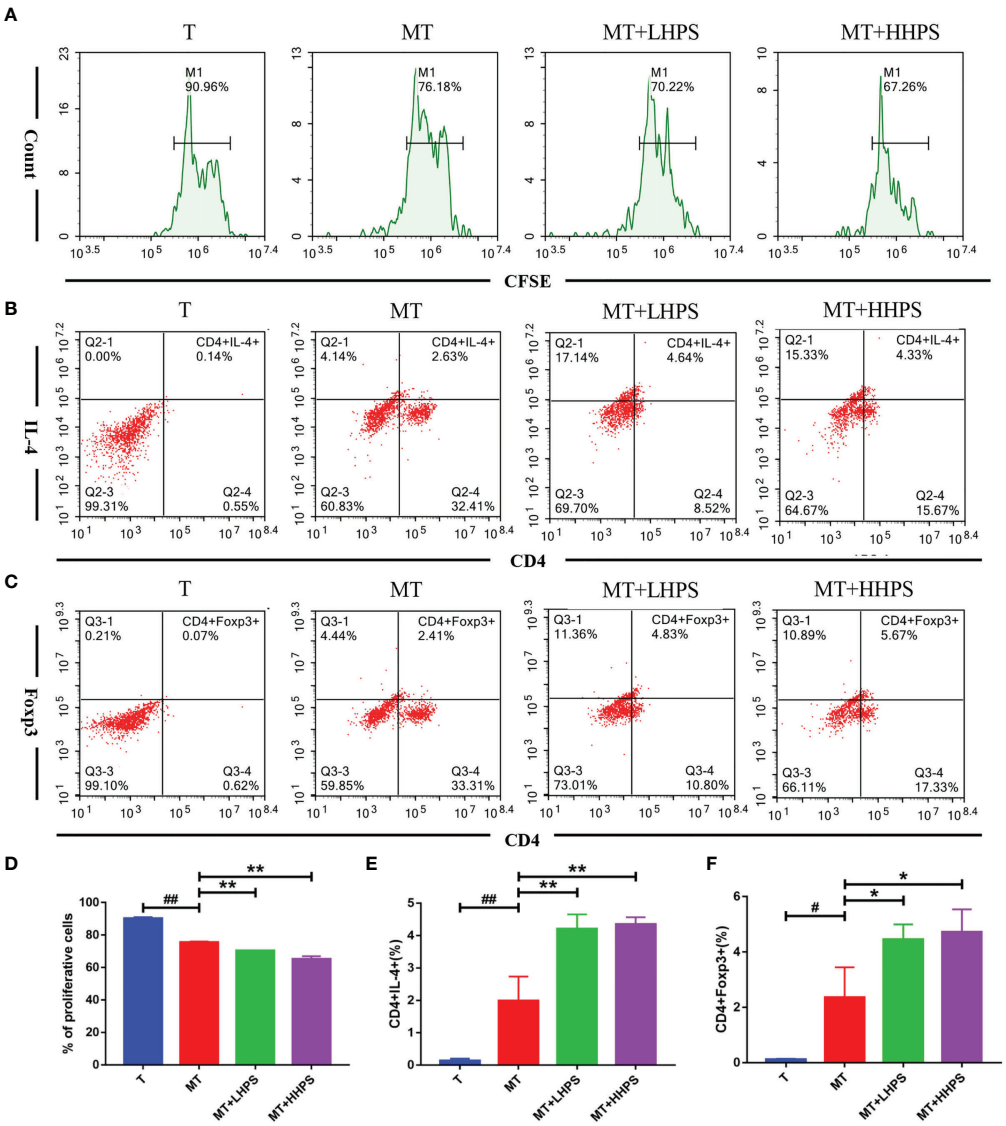


FIGURE 10 | Hyperoside suppresses T cell proliferation while increasing Th2 or Foxp3+ Treg generation in the co-culture with M2 macrophages. T cells cocultured with M2 macrophages at a ratio of 1:10 (T cell/M2 macrophages) were treated with high-dose HPS (HHPS) (50uM) or low-dose HPS (LHPS) (12.5uM) for 72hrs, and then analyzed *via* flow cytometry. **(A, D)** For proliferation assays, T cells were first labeled with CFSE before the co-culture, and the CFSE dilution of CFSE-labeled $CD4^+$T cells was detected by flow cytometry. Flow cytometric analysis showed T-cell proliferation was inhibited by addition of M2 macrophages to the coculture system, and the inhibition was further enhanced by HPS. **(B, E)** The percentage of IL4-expressing $CD4^+$ T cells was increased by HPS treatment compared with a control group (MT). **(C, F)** The percentage of $CD4^+Foxp3^+$ T cell subsets was also increased by HPS treatment compared with a control group (MT). Differences between experimental groups were evaluated using ANOVA ($^{\#}P < 0.05$ and $^{\#\#}P < 0.01$ *vs* T group; $^{*}P < 0.05$ and $^{**}P < 0.01$ *vs* MT group). T, T cells alone; MT, T cells cocultured with M2 macrophages; MT+LHPS, T cells cocultured with M2 macrophages treated with low-dose HPS (12.5 μM); MT+HHPS, T cells cocultured with M2 macrophages treated with high-dose HPS (50 μM).

In conclusion, we demonstrated that HPS ameliorates renal inflammatory injury in DN *via* promoting macrophage polarization from an M1 to M2 phenotype and $CD4^+$ T cell differentiation into Th2 and Treg populations. Moreover, HPS may enhance the ability of M2 macrophages to suppress inflammation by indirectly promoting T cell differentiation into Th2/Treg subsets. Our findings may be implicated for the treatment of DN in clinic. Further studies on how HPS modulates macrophage polarization are warranted.

DATA AVAILABILITY STATEMENT

The raw data supporting the conclusions of this article will be made available by the authors, without undue reservation.

ETHICS STATEMENT

The animal study was reviewed and approved by the Institutional Animal Care and Use Committee of Guangzhou University of Chinese Medicine.

AUTHOR CONTRIBUTIONS

LZ and XL acquired funding for this research. LZ contributed to the conception and design of the experiments, and analysis and interpretation of the data. LZ and JL drafted this manuscript. JL, YZ, and HS contributed to the performance of the experiments and the acquisition and analysis of data. HL and CL contributed to providing specific input relating to the cell experiment. JG contributed to analyzing the renal morphologic results. ZL contributed to the performance of the animal experiments. WM contributed to providing experimental suggestions. ZD and XL contributed to the design of the experiment and edited this manuscript. All authors contributed to the article and approved the submitted version.

FUNDING

This project was supported in part by grants from the State Key Laboratory of Dampness Syndrome of Chinese Medicine (SZ2021ZZ16, SZ2021ZZ43, and SZ2021ZZ18), Guangdong Provincial Key Laboratory of Clinical Research on Traditional Chinese Medicine Syndrome (ZH2020KF02), National Natural Science Foundation of China (81603717, 81873261), Guangzhou University of Chinese Medicine (Grant No: AFD018171Z11099), and Special Fund of Guangdong Provincial Science and Technology Innovation Strategy(Guangdong-Hong Kong-Macau Joint Lab, 2020B1212030006).

SUPPLEMENTARY MATERIAL

The Supplementary Material for this article can be found online at: https://www.frontiersin.org/articles/10.3389/fimmu.2021.733808/full#supplementary-material

REFERENCES

1. Hasegawa G, Nakano K, Sawada M, Uno K, Shibayama Y, Ienaga K, et al. Possible Role of Tumor Necrosis Factor and Interleukin-1 in the Development of Diabetic Nephropathy. *Kidney Int* (1991) 40(6):1007–12. doi: 10.1038/ki.1991.308
2. Hickey FB, Martin F. Role of the Immune System in Diabetic Kidney Disease. *Curr Diabetes Rep* (2018) 18(4):20. doi: 10.1007/s11892-018-0984-6
3. Niewczas MA, Pavkov ME, Skupien J, Smiles A, Md Dom ZI, Wilson JM, et al. A Signature of Circulating Inflammatory Proteins and Development of End-Stage Renal Disease in Diabetes. *Nat Med* (2019) 25(5):805–13. doi: 10.1038/s41591-019-0415-5
4. Martinez FO, Helming L, Gordon S. Alternative Activation of Macrophages: An Immunologic Functional Perspective. *Annu Rev Immunol* (2009) 27:451–83. doi: 10.1146/annurev.immunol.021908.132532
5. Tesch GH. Diabetic Nephropathy - Is This an Immune Disorder? *Clin Sci (Lond)* (2017) 131(16):2183–99. doi: 10.1042/cs20160636
6. Lavoz C, Matus YS, Orejudo M, Carpio JD, Droguett A, Egido J, et al. Interleukin-17A Blockade Reduces Albuminuria and Kidney Injury in an Accelerated Model of Diabetic Nephropathy. *Kidney Int* (2019) 95(6):1418–32. doi: 10.1016/j.kint.2018.12.031
7. Wu CC, Sytwu HK, Lu KC, Lin YF. Role of T Cells in Type 2 Diabetic Nephropathy. *Exp Diabetes Res* (2011) 2011:514738. doi: 10.1155/2011/514738
8. Ye M, Yan Y, Guo DA. Characterization of Phenolic Compounds in the Chinese Herbal Drug Tu-Si-Zi by Liquid Chromatography Coupled to Electrospray Ionization Mass Spectrometry. *Rapid Commun Mass Spectrom* (2005) 19(11):1469–84. doi: 10.1002/rcm.1944
9. Sun B, Zhang R, Liang Z, Fan A, Kang D. Hyperoside Attenuates Non-Alcoholic Fatty Liver Disease Through Targeting Nr4A1 in Macrophages. *Int Immunopharmacol* (2021) 94:107438. doi: 10.1016/j.intimp.2021.107438
10. Sun K, Luo J, Jing X, Xiang W, Guo J, Yao X, et al. Hyperoside Ameliorates the Progression of Osteoarthritis: An *In Vitro* and *In Vivo* Study. *Phytomedicine* (2021) 80:153387. doi: 10.1016/j.phymed.2020.153387
11. Chen X, Famurewa AC, Tang J, Olatunde OO, Olatunji OJ. Hyperoside Attenuates Neuroinflammation, Cognitive Impairment and Oxidative Stress via Suppressing TNF-α/NF-κb/Caspase-3 Signaling in Type 2 Diabetes Rats. *Nutrition Neurosci* (2021) 1-11. doi: 10.1080/1028415x.2021.1901047
12. Huang J, Tong X, Zhang L, Zhang Y, Wang L, Wang D, et al. Hyperoside Attenuates Bleomycin-Induced Pulmonary Fibrosis Development in Mice. *Front Pharmacol* (2020) 11:550955. doi: 10.3389/fphar.2020.550955
13. Kim SJ, Um JY, Lee JY. Anti-Inflammatory Activity of Hyperoside Through the Suppression of Nuclear factor-kappaB Activation in Mouse Peritoneal Macrophages. *Am J Chin Med* (2011) 39(1):171–81. doi: 10.1142/S0192415X11008737
14. Jin XN, Yan EZ, Wang HM, Sui HJ, Liu Z, Gao W, et al. Hyperoside Exerts Anti-Inflammatory and Anti-Arthritic Effects in LPS-Stimulated Human Fibroblast-Like Synoviocytes *In Vitro* and in Mice With Collagen-Induced Arthritis. *Acta Pharmacol Sin* (2016) 37(5):674–86. doi: 10.1038/aps.2016.7
15. Fan HH, Zhu LB, Li T, Zhu H, Wang YN, Ren XL, et al. Hyperoside Inhibits Lipopolysaccharide-Induced Inflammatory Responses in Microglial Cells *via* P38 and NFkappaB Pathways. *Int Immunopharmacol* (2017) 50:14–21. doi: 10.1016/j.intimp.2017.06.004
16. Ku SK, Zhou W, Lee W, Han MS, Na M, Bae JS. Anti-Inflammatory Effects of Hyperoside in Human Endothelial Cells and in Mice. *Inflammation* (2015) 38 (2):784–99. doi: 10.1007/s10753-014-9989-8
17. Ku SK, Kwak S, Kwon OJ, Bae JS. Hyperoside Inhibits High-Glucose-Induced Vascular Inflammation *In Vitro* and *In Vivo*. *Inflammation* (2014) 37 (5):1389–400. doi: 10.1007/s10753-014-9863-8
18. Zhou J, Zhang S, Sun X, Lou Y, Yu J. Hyperoside Protects HK-2 Cells Against High Glucose-Induced Apoptosis and Inflammation *via* the miR-499a-5p/NRIP1 Pathway. *Pathol Oncol Res* (2021) 27:629829. doi: 10.3389/pore.2021.629829
19. Betz B, Conway BR. Recent Advances in Animal Models of Diabetic Nephropathy. *Nephron Exp Nephrol* (2014) 126(4):191–5. doi: 10.1159/000363300
20. Ying W, Cheruku PS, Bazer FW, Safe SH, Zhou B. Investigation of Macrophage Polarization Using Bone Marrow Derived Macrophages. *J Vis Exp* (2013) 76:50323. doi: 10.3791/50323
21. Wohler JE, Barnum SR. Nylon Wool Purification Alters the Activation of T Cells. *Mol Immunol* (2009) 46(5):1007–10. doi: 10.1016/j.molimm.2008.09.017
22. Jefferson JA, Shankland SJ, Pichler RH. Proteinuria in Diabetic Kidney Disease: A Mechanistic Viewpoint. *Kidney Int* (2008) 74(1):22–36. doi: 10.1038/ki.2008.128
23. Sharma K, McCue P, Dunn SR. Diabetic Kidney Disease in the Db/Db Mouse. *Am J Physiol Renal Physiol* (2003) 284(6):F1138–44. doi: 10.1152/ajprenal.00315.2002

24. Zhang J, Fu H, Xu Y, Niu Y, An X. Hyperoside Reduces Albuminuria in Diabetic Nephropathy at the Early Stage Through Ameliorating Renal Damage and Podocyte Injury. *J Nat Med* (2016) 70(4):740–8. doi: 10.1007/s11418-016-1007-z
25. Zhang L, He S, Yang F, Yu H, Xie W, Dai Q, et al. Hyperoside Ameliorates Glomerulosclerosis in Diabetic Nephropathy by Downregulating miR-21. *Can J Physiol Pharmacol* (2016) 94(12):1249–56. doi: 10.1139/cjpp-2016-0066
26. Yang X, Mou S. Role of Immune Cells in Diabetic Kidney Disease. *Curr Gene Ther* (2017) 17(6):424–33. doi: 10.2174/1566523218666180214100351
27. Anders HJ, Ryu M. Renal Microenvironments and Macrophage Phenotypes Determine Progression or Resolution of Renal Inflammation and Fibrosis. *Kidney Int* (2011) 80(9):915–25. doi: 10.1038/ki.2011.217
28. Zhang X, Yang Y, Zhao Y. Macrophage Phenotype and Its Relationship With Renal Function in Human Diabetic Nephropathy. *PloS One* (2019) 14(9):e0221991. doi: 10.1371/journal.pone.0221991
29. Lim AK, Tesch GH. Inflammation in Diabetic Nephropathy. *Mediators Inflammation* (2012) 2012:146154. doi: 10.1155/2012/146154
30. Navarro-Gonzalez JF, Mora-Fernandez C, Muros de Fuentes M, Garcia-Perez J. Inflammatory Molecules and Pathways in the Pathogenesis of Diabetic Nephropathy. *Nat Rev Nephrol* (2011) 7(6):327–40. doi: 10.1038/nrneph.2011.51
31. Cao Q, Harris DC, Wang Y. Macrophages in Kidney Injury, Inflammation, and Fibrosis. *Physiol (Bethesda)* (2015) 30(3):183–94. doi: 10.1152/physiol.00046.2014
32. Chen T, Cao Q, Wang Y, Harris DCH. M2 Macrophages in Kidney Disease: Biology, Therapies, and Perspectives. *Kidney Int* (2019) 95(4):760–73. doi: 10.1016/j.kint.2018.10.041
33. Matoba K, Takeda Y, Nagai Y, Kawanami D, Utsunomiya K, Nishimura R. Unraveling the Role of Inflammation in the Pathogenesis of Diabetic Kidney Disease. *Int J Mol Sci* (2019) 20(14):3393. doi: 10.3390/ijms20143393
34. Donate-Correa J, Ferri CM, Sanchez-Quintana F, Perez-Castro A, Gonzalez-Luis A, Martin-Nunez E, et al. Inflammatory Cytokines in Diabetic Kidney Disease: Pathophysiologic and Therapeutic Implications. *Front Med (Lausanne)* (2020) 7:628289. doi: 10.3389/fmed.2020.628289
35. Samsu N. Diabetic Nephropathy: Challenges in Pathogenesis, Diagnosis, and Treatment. *BioMed Res Int* (2021) 2021:1497449. doi: 10.1155/2021/1497449
36. Ji L, Chen Y, Wang H, Zhang W, He L, Wu J, et al. Overexpression of Sirt6 Promotes M2 Macrophage Transformation, Alleviating Renal Injury in Diabetic Nephropathy. *Int J Oncol* (2019) 55(1):103–15. doi: 10.3892/ijo.2019.4800
37. Yang H, Xie T, Li D, Du X, Wang T, Li C, et al. Tim-3 Aggravates Podocyte Injury in Diabetic Nephropathy by Promoting Macrophage Activation *via* the NF-κb/TNF-α Pathway. *Mol Metab* (2019) 23:24–36. doi: 10.1016/j.molmet.2019.02.007
38. Zhang XL, Guo YF, Song ZX, Zhou M. Vitamin D Prevents Podocyte Injury *via* Regulation of Macrophage M1/M2 Phenotype in Diabetic Nephropathy Rats. *Endocrinology* (2014) 155(12):4939–50. doi: 10.1210/en.2014-1020
39. Nastase MV, Zeng-Brouwers J, Beckmann J, Tredup C, Christen U, Radeke HH, et al. Biglycan, a Novel Trigger of Th1 and Th17 Cell Recruitment Into the Kidney. *Matrix Biol* (2018) 68-69:293–317. doi: 10.1016/j.matbio.2017.12.002
40. Zheng Z, Zheng F. Immune Cells and Inflammation in Diabetic Nephropathy. *J Diabetes Res* (2016) 2016:1841690. doi: 10.1155/2016/1841690
41. Zhang C, Xiao C, Wang P, Xu W, Zhang A, Li Q, et al. The Alteration of Th1/Th2/Th17/Treg Paradigm in Patients With Type 2 Diabetes Mellitus: Relationship With Diabetic Nephropathy. *Hum Immunol* (2014) 75(4):289–96. doi: 10.1016/j.humimm.2014.02.007
42. Kim SM, Lee SH, Lee A, Kim DJ, Kim YG, Kim SY, et al. Targeting T Helper 17 by Mycophenolate Mofetil Attenuates Diabetic Nephropathy Progression. *Transl Res* (2015) 166(4):375–83. doi: 10.1016/j.trsl.2015.04.013
43. Lui PP, Cho I, Ali N. Tissue Regulatory T Cells. *Immunology* (2020) 161(1):4–17. doi: 10.1111/imm.13208
44. Eller K, Kirsch A, Wolf AM, Sopper S, Tagwerker A, Stanzl U, et al. Potential Role of Regulatory T Cells in Reversing Obesity-Linked Insulin Resistance and Diabetic Nephropathy. *Diabetes* (2011) 60(11):2954–62. doi: 10.2337/db11-0358
45. Abouzeid S, Sherif N. Role of Alteration in Treg/Th17 Cells' Balance in Nephropathic Patients With Type 2 Diabetes Mellitus. *Electron Physician* (2015) 7(8):1613–8. doi: 10.19082/1613
46. Herrera M, Soderberg M, Sabirsh A, Valastro B, Molne J, Santamaria B, et al. Inhibition of T-Cell Activation by the CTLA4-Fc Abatacept Is Sufficient to Ameliorate Proteinuric Kidney Disease. *Am J Physiol Renal Physiol* (2017) 312(4):F748–F59. doi: 10.1152/ajprenal.00179.2016
47. Pichler R, Afkarian M, Dieter BP, Tuttle KR. Immunity and Inflammation in Diabetic Kidney Disease: Translating Mechanisms to Biomarkers and Treatment Targets. *Am J Physiol Renal Physiol* (2017) 312(4):F716–F31. doi: 10.1152/ajprenal.00314.2016
48. Sabapathy V, Stremska ME, Mohammad S, Corey RL, Sharma PR, Sharma R. Novel Immunomodulatory Cytokine Regulates Inflammation, Diabetes, and Obesity to Protect From Diabetic Nephropathy. *Front Pharmacol* (2019) 10:572. doi: 10.3389/fphar.2019.00572
49. Zeng C, Shi X, Zhang B, Liu H, Zhang L, Ding W, et al. The Imbalance of Th17/Th1/Tregs in Patients With Type 2 Diabetes: Relationship With Metabolic Factors and Complications. *J Mol Med (Berl)* (2012) 90(2):175–86. doi: 10.1007/s00109-011-0816-5
50. Wang D, Zhang Z, Si Z, Yang Y, Li S, Xue Y. Dapagliflozin Reverses the Imbalance of T Helper 17 and T Regulatory Cells by Inhibiting SGK1 in a Mouse Model of Diabetic Kidney Disease. *FEBS Open Bio* (2021) 11(5):1395–405. doi: 10.1002/2211-5463.13147
51. Rayego-Mateos S, Morgado-Pascual JL, Opazo-Rios L, Guerrero-Hue M, Garcia-Caballero C, Vazquez-Carballo C, et al. Pathogenic Pathways and Therapeutic Approaches Targeting Inflammation in Diabetic Nephropathy. *Int J Mol Sci* (2020) 21(11):3798. doi: 10.3390/ijms21113798
52. Goschl L, Scheinecker C, Bonelli M. Treg Cells in Autoimmunity: From Identification to Treg-Based Therapies. *Semin Immunopathol* (2019) 41(3):301–14. doi: 10.1007/s00281-019-00741-8
53. Cucak H, Nielsen Fink L, Hojgaard Pedersen M, Rosendahl A. Enalapril Treatment Increases T Cell Number and Promotes Polarization Towards M1-Like Macrophages Locally in Diabetic Nephropathy. *Int Immunopharmacol* (2015) 25(1):30–42. doi: 10.1016/j.intimp.2015.01.003
54. Guo H, Pan C, Chang B, Wu X, Guo J, Zhou Y, et al. Triptolide Improves Diabetic Nephropathy by Regulating Th Cell Balance and Macrophage Infiltration in Rat Models of Diabetic Nephropathy. *Exp Clin Endocrinol Diabetes* (2016) 124(6):389–98. doi: 10.1055/s-0042-106083
55. Oishi S, Takano R, Tamura S, Tani S, Iwaizumi M, Hamaya Y, et al. M2 Polarization of Murine Peritoneal Macrophages Induces Regulatory Cytokine Production and Suppresses T-Cell Proliferation. *Immunology* (2016) 149(3):320–8. doi: 10.1111/imm.12647

Conflict of Interest: The authors declare that the research was conducted in the absence of any commercial or financial relationships that could be construed as a potential conflict of interest.

Publisher's Note: All claims expressed in this article are solely those of the authors and do not necessarily represent those of their affiliated organizations, or those of the publisher, the editors and the reviewers. Any product that may be evaluated in this article, or claim that may be made by its manufacturer, is not guaranteed or endorsed by the publisher.

Copyright © 2021 Liu, Zhang, Sheng, Liang, Liu, Moran Guerrero, Lu, Mao, Dai, Liu and Zhang. This is an open-access article distributed under the terms of the Creative Commons Attribution License (CC BY). The use, distribution or reproduction in other forums is permitted, provided the original author(s) and the copyright owner(s) are credited and that the original publication in this journal is cited, in accordance with accepted academic practice. No use, distribution or reproduction is permitted which does not comply with these terms.

frontiers in Immunology

ORIGINAL RESEARCH
published: 27 December 2021
doi: 10.3389/fimmu.2021.768412

Kidney-Draining Lymph Node Fibrosis Following Unilateral Ureteral Obstruction

Xiaofei Li[1,2], Jing Zhao[1], Said Movahedi Naini[1], Gianmarco Sabiu[1], Stefan G. Tullius[1], Su Ryon Shin[3], Jonathan S. Bromberg[4], Paolo Fiorina[1], George C. Tsokos[5], Reza Abdi[1] and Vivek Kasinath[1]**

[1] Transplantation Research Center, Brigham and Women's Hospital, Harvard Medical School, Boston, MA, United States, [2] Key Laboratory of Combinatorial Biosynthesis and Drug Discovery, Ministry of Education, and Wuhan University School of Pharmaceutical Sciences, Wuhan, China, [3] Division of Engineering in Medicine, Department of Medicine, Brigham and Women's Hospital, Harvard Medical School, Cambridge, MA, United States, [4] Departments of Surgery and Microbiology and Immunology, Center for Vascular and Inflammatory Diseases, University of Maryland School of Medicine, Baltimore, MA, United States, [5] Division of Rheumatology and Department of Immunology, Beth Israel Deaconess Medical Center, Boston, MA, United States

OPEN ACCESS

Edited by:
Bin Yang,
University of Leicester,
United Kingdom

Reviewed by:
Veronika Lukacs-Kornek,
University of Bonn, Germany
Paul J. Higgins,
Albany Medical College, United States

***Correspondence:**
Vivek Kasinath
vkasinath@bwh.harvard.edu
Reza Abdi
rabdi@rics.bwh.harvard.edu

Specialty section:
This article was submitted to Molecular Innate Immunity, a section of the journal Frontiers in Immunology

Received: 31 August 2021
Accepted: 01 December 2021
Published: 27 December 2021

Citation:
Li X, Zhao J, Naini SM, Sabiu G, Tullius SG, Shin SR, Bromberg JS, Fiorina P, Tsokos GC, Abdi R and Kasinath V (2021) Kidney-Draining Lymph Node Fibrosis Following Unilateral Ureteral Obstruction. Front. Immunol. 12:768412. doi: 10.3389/fimmu.2021.768412

Although the primary organ has been the subject of intense investigation in the field of organ fibrosis over the past several decades, the presence of lymph node fibrosis due to persistent activation of the immune response in its partner organ remains largely unknown. Previously, we demonstrated that activation of the immune response following ischemia-reperfusion injury (IRI) and crescentic glomerulonephritis (CGN) in the kidney was associated with extracellular matrix (ECM) production by fibroblastic reticular cells (FRCs) of the kidney-draining lymph node (KLN). Here, we sought to determine whether FRCs in the KLN become similarly fibrogenic following unilateral ureteral obstruction (UUO) of the kidney. We subjected 6–8-week-old C57BL/6J mice to UUO for 2, 7, and 14 days. We examined the microarchitecture of the kidney and KLN by immunofluorescence staining at each timepoint, and we quantified immune cell populations in the KLN by flow cytometry. The contralateral kidney unaffected by UUO and its partner KLN were used as controls. We found through immunofluorescence staining that FRCs increased production of ECM fibers and remodeled the microarchitecture of the UUO KLN, contributing to fibrosis that mirrored the changes in the kidney. We also observed by flow cytometry that the populations of $CD11b^+$ antigen-presenting cells, $CD11c^+$ dendritic cells, and activated $CD4^+$ and $CD8^+$ T cells were significantly higher in the UUO KLN than the KLN draining the unaffected contralateral kidney. Expression of the TGFβ/TGFβR signaling pathway was upregulated and colocalized with FRCs in the UUO KLNs, suggesting a possible mechanism behind the fibrosis. Both release of ureteral ligation at 2 days following UUO and depletion of FRCs at

the time of injury onset halted the progression of fibrosis in both the kidney and the KLN. These findings for the first time highlight the association between fibrosis both in the kidney and the KLN during UUO, and they lay the groundwork for future studies that will investigate more deeply the mechanisms behind the connection between FRCs and KLN fibrosis.

Keywords: unilateral ureteral obstruction (UUO), lymph node, fibroblastic reticular cell (FRC), renal immune homeostasis, kidney fibrosis, chronic kidney disease, acute kidney injury

INTRODUCTION

Organ fibrosis has been the subject of intense research over the decades, but the development of fibrosis in draining lymph nodes (DLNs) due to the inflammation and injury responses in the upstream tissues remains unknown.

Lymph nodes (LNs) are the primary sites where the adaptive immune response is determined following injury to the corresponding organ, and increasing evidence indicates that the stromal compartment of DLNs is essential to striking a balance between immunity and tolerance (1). Fibroblastic reticular cells (FRCs) are the major cells that populate the stromal compartment of the T cell zone in the DLN, and they perform several essential functions that maintain the structural and immunological homeostasis of DLNs, including the production of extracellular matrix (ECM) fibers (2). We have demonstrated previously the critical importance of the activity of FRCs in the kidney-draining lymph node (KLN) to the immune response in mouse models of renal ischemia-reperfusion injury (IRI) and crescentic glomerulonephritis (CGN) (3, 4). FRCs inhibit pro-inflammatory properties of T cells through direct contact (1). The loss of the tolerogenic effects of this contact, due to separation of T cells from FRC by the buildup of ECM fibers, may lead to an unchecked local adaptive immune response that results in organ fibrosis. In the IRI study, we found that fibrotic remodeling of the KLN correlated with a higher severity of renal damage following recurrent IRIs (4). However, the importance of FRCs and deposition of ECM in the stromal compartment of the KLN to kidney damage during unilateral ureteral obstruction (UUO) have not been studied before.

UUO is a common preclinical model of chronic kidney disease, and its correlate of obstructive nephropathy in human patients is an important cause of renal damage that occurs commonly following compression of the ureter, often by a malignant intraabdominal or intrapelvic lesion (5). Major advantages to UUO as an *in vivo* model of renal damage include its role as a model of both acute and subacute kidney injury as well as the presence of the contralateral kidney in the animal as a negative control. Numerous previous studies have detailed the molecular pathways that cause fibrosis of the kidney during UUO, and blockade or ablation of these signaling cascades holds major clinical significance for potential prevention of chronic kidney disease (6, 7). Although the presence of a single functional kidney in UUO precludes the usefulness of serological markers, such as blood urea nitrogen (BUN) and serum creatinine (Cr), for assessment of renal damage, the accumulation of fibrosis in the obstructed kidney correlates with its loss of function over time (7). This fibrosis in the obstructed kidney during UUO has been investigated extensively across many years and by a multitude of investigators, but nobody has found whether similar changes occur simultaneously in the stromal compartment of the KLN.

In this study, we performed UUO in mice and examined the correlation between fibrosis in the kidney and ECM deposition by FRCs in the KLNs up to 14 days following ureteral ligation. We found that the density of ECM fibers increased in the UUO KLNs over time, and that FRCs in the KLN produced these fibers. Early release of ureteral ligation 2 days following UUO halted the progression of fibrosis in both the kidneys and KLNs. Ablation of FRCs also resulted in less extensive fibrosis in both the kidney and KLN. These observations reveal new mechanisms of LN fibrosis and set the stage for investigating the utility of entirely innovative therapies targeting FRCs as a novel adjunct treatment for organ fibrosis, for which no therapy exists currently.

MATERIALS AND METHODS

Mice

6-8-week-old C57BL/6J mice (Jackson Laboratory, Bar Harbor, ME) were used in all experiments. UUO was performed by ligation of the left ureter as described (7), and the mice were euthanized 2, 7, or 14 days following the operation. Kidneys and KLNs were harvested at the time of euthanasia and stored at appropriate temperatures for subsequent analysis.

UUO Release

The UUO release (R-UUO) model was achieved as described by Cochrane et al. (8). Ureteral ligation was performed on the left kidney, and the clamp was removed under general anesthesia 2 days or 7 days after the UUO surgery. The UUO release mice were euthanized at 21 days following UUO. Animal studies were approved and conducted according to the Institutional Animal Care and Use Committee of Brigham and Women's Hospital, Boston, MA.

FRC Depletion Using DT

CCL19-Cre (CCL19Cre [Tg (CCL19-cre)489Biat] mice were originally a gift from Shannon Turley (Genentech, South San Francisco, CA). C57BL/6-Gt (ROSA)26Sortm1 (HBEGF)Awai/J (C57BL/6-iDTR) mice were purchased from Jackson

Laboratories. The C57BL/6-iDTR mice were backcrossed with the CCL19-Cre mice to create CCL19-Cre x iDTR mice, a transgenic mouse strain of C57BL/6 background in which FRCs can be depleted significantly following administration of diphtheria toxin (DT) (3, 9). These mice were injected with 100 ng of diphtheria toxin (DT) intraperitoneally (i.p.) daily for 5 days following UUO (Days 0-4) to deplete FRCs. CCL19-Cre x iDTR mice that did not receive DT were used as the control group.

Immunofluorescence Staining

KLNs were frozen and sectioned with a cryomicrotome. After blocking with 3% (vol/vol) bovine serum albumin in phosphate-buffered saline (PBS) for nonspecific antigens, sections were incubated overnight with primary antibodies at 4°C, followed by secondary conjugated antibodies for 1 hour at room temperature. The following antibodies were used: rat anti-MECA79 (Novus Biologicals, 1:200), goat anti-PDPN (R&D Systems, 1:200), rabbit anti-fibronectin (Abcam, 1:300), rabbit anti-collagen I (Abcam,1:300), rabbit anti-LYVE-1 (Abcam, 1:300), fluorescein (FITC)-conjugated rat anti-LYVE-1 (BioLegend, 1:100), and rat anti-TGFβR1 (Santa Cruz, 1:200). The secondary antibodies used were either FITC-anti-rat, Cy3-anti-rabbit/goat, or aminomethylcoumarin acetate (AMCA)-anti-goat (Jackson ImmunoResearch, 1:200). Images were captured using a EvosFL Auto2 fluorescence microscope. Areas of positive staining were assessed semi-quantitatively by ImageJ software (NIH). Statistical analysis was performed using two-tailed Student's t tests by Prism (GraphPad Software, Inc).

Real-Time PCR Experiments

Kidneys and KLNs were stored at -80°C after harvest from the mice. RNA from KLNs was isolated by Direct-zol RNA Miniprep Plus kit (Zymo research, Irvine, CA), as per the manufacturer's protocol. The following primers were used: *Gapdh* forward 5'-AGCCACATCGCTCAGACAC-3' and reverse 5'-GCC CAATACGACCAAATCC-3'; *Tgfb1* forward 5'-CAA CAATTCCTGGCGTTACCTTGG-3' and reverse 5'-GAAA GCCCTGTATTCCGTCTCCTT-3'; *Tgfbr1* forward 5'-TGC CATAACCGCACTGTCA-3' and reverse 5'-AAT GAAAGGGCGATCTAGTGATG-3'; *Tgfbr2* forward 5'- AGCA TCACGGCCATCTGTG-3' and reverse 5'-TGGCAAAC CGTCTCCAGAGT-3'; *Smad7* forward 5'-GGGCTTTCA GATTCCCAACTT-3' and reverse 5'-CACGCGAGT CTTCTCCTCC-3'; *Bmp7* forward 5'-CAAGCAGCGCAGCC AGAATCG-3' and reverse 5'-CAATGATCCAGTCCTGC CAGCCAA-3'.

Flow Cytometry

KLNs were harvested at time of euthanasia, then crushed and filtered through a 70-μm cell strainer. The resulting single-cell suspension was centrifuged at 1,500 rpm for 5 minutes, resuspended in DMEM, then counted manually utilizing 0.4% trypan blue (Thermo Fisher Scientific) to exclude dead cells. The cell suspension was placed in 96-well round-bottom plates for intracellular cytokine staining. The cells were first incubated with phorbol 12-mystirate 13-acetate (100 ng/ml) (Sigma-Aldrich), ionomycin (1 mg/ml) (Sigma-Aldrich), and GolgiStop protein transport inhibitor (BD Biosciences, San Jose, CA) at 37°C for 4 hours. Then the cells were washed and stained according to standard protocols, and flow cytometry was performed *via* BD FACSCanto II flow cytometer (BD Biosciences). Results were analyzed using FlowJo software (FlowJo LLC). All antibodies were purchased from BD (Becton Dickinson Franklin Lakes, NJ).

Electron Microscopy

KLNs were fixed in Karnovsky fixative and processed as previously described (4). Sections were visualized using an FE-SEM (Zeiss Crossbeam 540), using the aSTEM detector.

Statistical Analysis

Data are presented as means ± SEM. Differences between two groups were analyzed for significance by unpaired two-tailed Student's t test, and differences among groups were analyzed for significance by analysis of variance (ANOVA). P values less than 0.05 were considered significant. All statistical analysis was performed using GraphPad Prism.

RESULTS

Podoplanin (PDPN)$^+$ FRCs Produce ECM Fibers More Extensively in UUO KLNs

As the prominent cells of the stromal compartment in DLNs, FRCs are PDPN$^+$ resident stromal cells that support the integrity of the microarchitecture by producing ECM. We have demonstrated previously the importance of ECM deposition and fibrosis in the KLN to the pathogenesis of two other preclinical kidney disease models: renal ischemia-reperfusion injury (4) and glomerulonephritis (3), In those studies, we found that the activity of FRCs is critical to the fibrogenesis in the KLN. However, the contributions of FRCs and ECM deposition in the KLN to the pathogenesis of UUO have not been investigated. Therefore, we examined the KLNs in the UUO model at different time points following ureteral ligation for histological evidence of these changes. To identify the contribution of FRCs in the KLNs after UUO, we investigated whether PDPN colocalized with the ECM markers collagen 1 and fibronectin through immunofluorescence staining. We noticed that the collagen 1 and fibronectin fibers colocalized with PDPN$^+$LYVE-1$^-$ cells, the molecular signature consistent with FRCs, at 2 days, 7 days, and 14 days (Days 2, 7, and 14) following UUO (**Figures 1A, B**). In addition, the density of collagen fibers was significantly higher in the UUO KLN than the KLN draining the unaffected contralateral kidney at all three time points, and the fibronectin fiber density was significantly higher at Days 7 and 14. Moreover, we found through co-staining of PDPN$^+$ cells with αSMA, PDGFRβ, and vimentin that FRCs in the UUO KLNs expressed significantly higher levels of these fibrosis markers than those in the contralateral KLNs (**Figures 1C–E** and **Supplementary Figures 1A–C**). Electron micrographs of the UUO KLN at Day 14 also revealed evidence of extensive ECM deposition within fibrils extending from FRCs (**Supplementary Figure 1D**). This fibrosis was also reflected in a

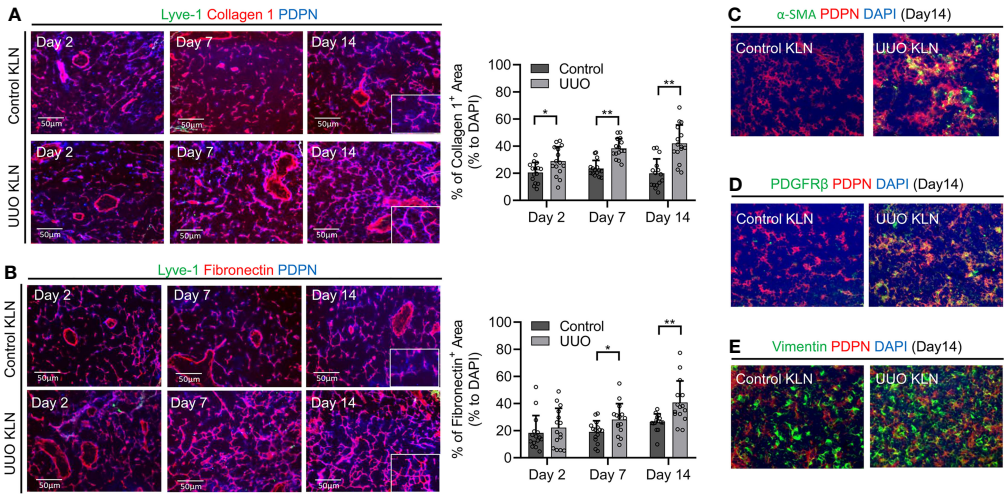


FIGURE 1 | Contribution of FRCs to increase in ECM density in the KLN over time. **(A)** Fluorescence micrographs of Lyve-1$^+$ lymphatic vessels (green), collagen 1 fibers (red), and PDPN$^+$ cells (blue) demonstrate increased density of collagen I fibers and colocalization with Lyve-1$^-$PDPN$^+$ FRCs through Day 14. Semiquantitative analysis and comparison of collagen I$^+$-stained area between the UUO and contralateral (control) KLNs show significantly higher density of collagen 1$^+$ fibers normalized to DAPI-positive area in the UUO KLN at all time points (n=15 random fields of sections from 3 mice). **(B)** Fluorescence micrographs of Lyve-1$^-$PDPN$^+$ FRCs (blue) and fibronectin fibers (red) show increased density of fibronectin fibers and colocalization with FRCs through Day 14. Semi-quantitative analysis and comparison of fibronectin$^+$-stained area shows significantly higher density of fibronectin fibers at Days 7 and 14 in UUO KLN as compared to contralateral (control) KLN (n=15 random microscopic fields of sections from 3 mice). **(C–E)** Fluorescence micrographs of UUO KLN and contralateral (control) KLN sections at Day 14 demonstrate increased expression of **(C)** α-SMA (green), **(D)** PDGFRβ (green), and **(E)** vimentin (green), and increased colocalization (yellow) with PDPN$^+$ FRCs (red) in UUO KLN at Day 14 (DAPI nuclear stain, blue). Data represented by means ± SEM. *$p < 0.05$, **$p < 0.01$.

higher overall density of ECM fibers in the UUO KLNs, as indicated by Masson's trichrome stain (**Supplementary Figure 1E**).

Antigen-Presenting Cells Infiltrate the KLN, and T Cells Are Activated Within the KLN Following UUO

The position of the KLN as the primary secondary lymphoid organ that drains the kidney situates it as the prime site for modulation of adaptive immunity in the kidney, through regulation of the interplay between the innate and adaptive immune responses. Therefore, we sought to investigate this interaction by determining whether macrophage infiltration and T cell activation increase concurrently in the KLN following UUO. We stained the KLNs for CD11b$^+$ antigen-presenting cells by immunofluorescence, and we found that they increased progressively through Day 14 (**Figure 2A**). Semiquantitative analysis indicated that the CD11b$^+$ macrophage population was higher in the UUO KLN than the contralateral KLN; although the comparison did not quite reach significance ($p=0.06$) at Day 7, a significant increase ($p<0.01$) was observed at Day 14 (**Figure 2B**). In addition, the CD11c$^+$ dendritic cell population was significantly higher in the UUO KLN, as quantified by flow cytometry (**Figure 2C**). Moreover, flow cytometric analysis revealed that the TNFα-producing CD4$^+$ and CD8$^+$ T cell populations and IFNγ-producing CD8$^+$ T cell population were significantly higher in the UUO KLN (**Figures 2D–F**). The UUO KLN also contained a higher population of CD4$^+$IFNγ$^+$ cells, although this comparison did not achieve significance (**Figures 2F, G**). Finally, we stained the KLNs for LYVE1$^+$ lymphatics, through which antigen-presenting cells likely traffic from the kidney to the KLN (10, 11), and MECA79$^+$ high endothelial venules, through which naïve T cells enter the KLN from the systemic circulation. We found that the expansion of LYVE1$^+$ lymphatic vessels peaks at Day 14, when the lymphatic vasculature is significantly more extensive than in the contralateral KLN (**Supplementary Figures 2A, B**).

TGFβ/TGFβR1 Pathway Is Activated in the KLN Following UUO

Expression of TGFβ has been linked to fibrosis in secondary lymphoid organs in preclinical HIV models, suggesting a possible signaling pathway that could be responsible for the fibrosis observed in the KLN (12). Hence, we interrogated whether the TGFβ/TGFβR1 pathway is activated in the KLN following UUO. We found through co-staining of PDPN$^+$LYVE-1$^-$ cells with TGFβR1 that FRCs in the UUO KLNs expressed higher amounts of TGFβR1 than those of contralateral KLNs (**Figure 3A**), indicating a possible route for the increase in fibrosis. Gene expression levels of TGFβ, TGFβR1, TGFβR2, the GFβ regulator Smad7, and the TGFβ family member BMP-7 were all significantly higher in the UUO KLNs at Day 7 as compared to the contralateral KLNs (**Figure 3B**). These data suggest that the TGFβ signaling pathway could function as a chief mediator of ECM production by FRCs in the KLN during UUO.

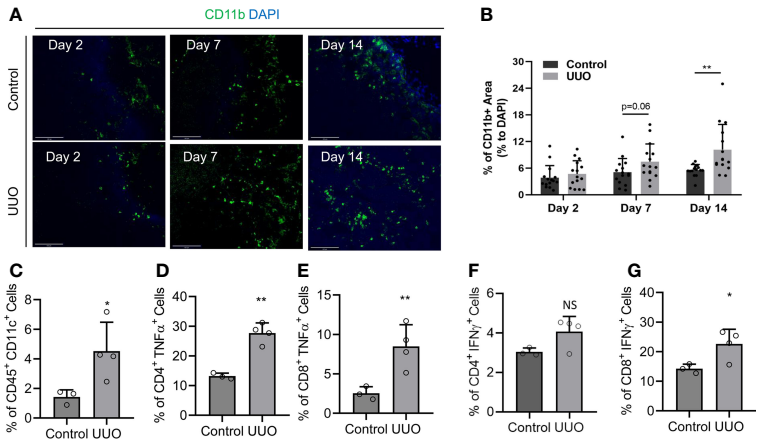


FIGURE 2 | Infiltration of antigen-presenting cells and activation of lymphocytes in the UUO KLN. **(A, B) (A)** Fluorescence micrographs of $CD11b^+$ antigen-presenting cells (green) and **(B)** semiquantitative analysis of $CD11b^+$ staining normalized to $DAPI^+$ area (blue) indicate that the density of $CD11b^+$ antigen-presenting cells increases in the UUO KLN over time, and it is significantly higher than the contralateral (control) KLN at Day 14. **(C–G)** Flow cytometric analysis of KLNs at Day 14 indicate significantly higher percentages of **(C)** $CD45^+CD11c^+$ dendritic cells, **(D)** $CD4^+TNF\alpha^+$ T cells, **(E)** CD8+TNFα+ T cells, **(F)** $CD8^+IFN\gamma^+$ T cells, and higher percentage of **(G)** $CD4^+IFN\gamma^+$ T cells in the UUO KLN than the contralateral (control) KLN at Day 14 (n=3-4 mice). Data represented by means ± SEM. *p < 0.05, **p < 0.01. NS, not significant.

Release of Ligation at 2 Days Following UUO Halts Kidney and KLN Fibrosis but Does Not Alter the Course at 7 Days

A major question within the field of chronic kidney disease is whether the fibrosis associated with impaired kidney function can be reversed. Previous studies of UUO mouse models have sought to answer this question by releasing the ligated ureter at various time points following UUO. These experiments have demonstrated mixed results— the fibrosis that occurs in the kidney following UUO may or may not reverse after the obstruction has resolved (8, 13, 14). However, whether the fibrosis in the KLN resolves following release of ureteral ligation has never been published. Here, we released the ureter from ligation at Day 7 and euthanized the mice at Day 21. Then, we performed immunofluorescence staining to compare the fibrosis in both the kidney and the KLN to the corresponding organs of the mice in which the ureter remained ligated for 21 days. First, we found no significant difference in the extent of fibrosis between the two kidneys, as shown by both collagen I and fibronectin (**Figures 4A, B**). Then, we sought to determine whether this persistence in fibrosis is reflected in the KLN, and we found by immunofluorescence staining that the density of ECM fibers in the KLN was also similar between the UUO and R-UUO groups (**Figure 4C**). Then, we investigated whether releasing the ureteral ligation at an earlier time point could halt progression of fibrosis by releasing the ureters at Day 2 and euthanizing the mice at Day 21. The fibrosis in the R-UUO KLN, as determined by collagen 1 and fibronectin staining, was significantly less dense than the UUO KLN (**Figures 4D, E**). Semiquantitative analysis indicated that the density of collagen I fibers in the R-UUO KLN also was significantly lower, as compared to the UUO KLN (**Figure 4F**).

Depletion of FRCs Is Associated With Less Extensive Fibrosis in the Kidney and KLN Following UUO

As demonstrated here in **Figure 1**, FRCs colocalize closely with the nidus of fibrogenesis that appears in the KLN following

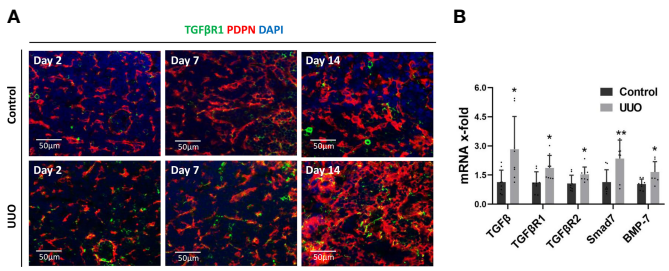


FIGURE 3 | TGFβ/TGFβR signaling pathway is active in the UUO KLN. **(A)** Fluorescence micrographs of UUO and contralateral (control) KLNs demonstrate co-staining (yellow) of TGFβR1 (green) with $PDPN^+$ FRCs (red) through Day 14. **(B)** RT-PCR shows significantly higher expression of TGFβ, TGFβR1, TGFβR2, Smad7, and BMP-7 in UUO KLN than contralateral KLN at Day 7. Each sample was performed in duplication (n=3). Data represented by means ± SEM. *p < 0.05, **p < 0.01.

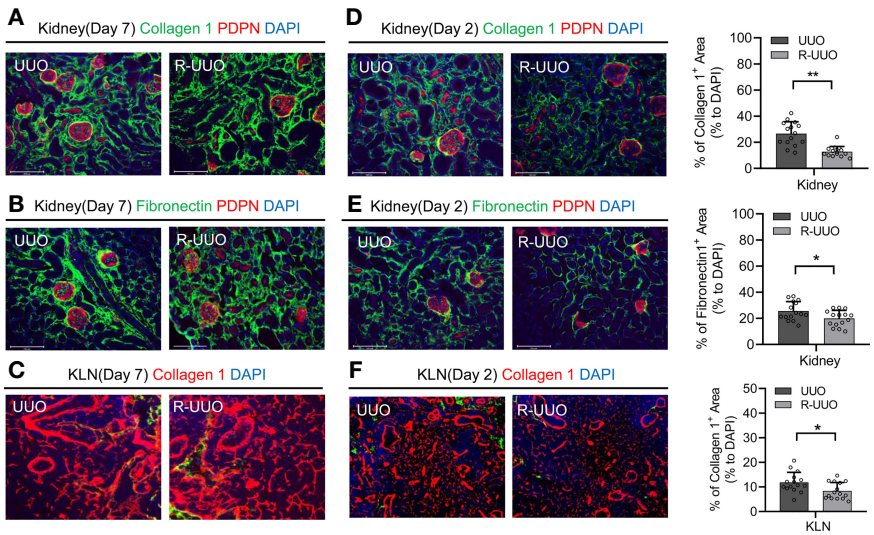


FIGURE 4 | Release of UUO (R-UUO) at Day 2 halts fibrosis in the kidney and KLN but has no effect at Day 7. **(A, B)** Fluorescence micrographs of collagen 1 fibers (green) and fibronectin fibers (green) reveal no difference in fibrosis between the UUO and R-UUO kidneys at Day 21 following release of ureteral ligation at Day 7 (PDPN glomerular stain, red; DAPI nuclear stain, blue). **(C)** Fluorescence micrographs of collagen 1 fibers (red) demonstrate no difference in fibrosis between the UUO and R-UUO KLNs at Day 21 following release of ureteral ligation at Day 7 (DAPI nuclear stain, blue). **(D, E)** Fluorescence micrographs and semiquantitative analysis show significantly higher density of **(D)** collagen 1 fibers (green) and **(E)** fibronectin fibers (green) normalized to DAPI-stained area (blue) in UUO kidneys than R-UUO kidneys at Day 21 following release of ureteral ligation at Day 2 (PDPN glomerular stain, red) (n=15 random microscopic fields of sections from 3 mice). **(F)** Fluorescence micrographs and semiquantitative analysis show significantly higher density of collagen 1 fibers (green) normalized to DAPI-stained area (blue) in UUO KLNs than R-UUO KLNs at Day 21 following release of ureteral ligation at Day 2 (n=15 random microscopic fields of sections from 3 mice). Data represented by means ± SEM. *$p < 0.05$, **$p < 0.01$.

UUO. Therefore, we investigated whether FRCs are the major source of fibrosis in the UUO KLN, through the use of CCL19-Cre x Rosa26-diphtheria toxin receptor (CCL19-Cre x iDTR) mice, a transgenic mouse strain of C57BL/6 background in which FRCs can be depleted significantly following administration of diphtheria toxin (DT) (3, 9). We demonstrated in previous studies of renal IRI and CGN in mouse models that depletion of FRCs was associated with lower kidney damage (3, 4). Here, we sought to determine whether depletion of FRCs would exert similar amelioration of kidney injury following UUO. In this model, we injected C57BL/6 mice with 100 ng of DT daily on 5 days following UUO and euthanized the mice at Day 14. Semiquantitative analysis of immunofluorescence staining of the KLNs revealed significantly lower density of collagen I (**Figure 5A**) and fibronectin fibers (**Figure 5B**) following depletion of FRCs in comparison to the CCL19-Cre x iDTR mice that did not receive DT. Interestingly, this reduction in fibrosis in the KLN was accompanied by a similar significant decrease in fibrosis in the kidneys of the mice that underwent FRC depletion, as reflected by immunofluorescence staining of collagen I and fibronectin (**Figures 5C, D**). $CCL19^+$ cells were non-existent in the control (contralateral) kidney, and they were present in sparse amounts in the UUO kidney. However, these few $CCL19^+$ cells did not co-stain with PDPN (**Supplementary Figure 3**). These observations reflect our earlier findings in models of renal IRI and CGN (3, 4), and they reinforce the concept that the FRCs in the KLN function as prominent arbiters of the direction of the immune response and fibrogenesis observed in the kidney following renal injury.

DISCUSSION

Organ fibrosis is a major subject of investigation, but little is known about fibrosis of the corresponding DLN. Similarly, the importance of LNs to the generation of adaptive immunity is well-established, but the impact on the immune response of massive, continuous changes to the stromal compartment of a DLN during chronic organ dysfunction represents a less explored area of research.

DLNs receive lymphatic drainage from their corresponding organs *via* afferent lymphatic vessels. This anatomical position situates DLNs as prime surveillance sites for the immunological milieu in the organs from which they collect the lymph. Moreover, millions of naive immune cells enter LNs *via* HEVs daily. Therefore, DLNs are dynamic organs wherein antigens are shuttled continuously *via* lymphatics by dendritic cells that present them to T cells that arrive *via* HEVs (15, 16).

FRCs are the prominent cells of the paracortical stroma in DLNs, and they have a well-characterized dual phenotype, typified by both pro-inflammatory and immunoregulatory properties (17). These multifaceted aspects of FRCs are apparent during the immune response to organ injury, as they proliferate and produce ECM during the early phase, expanding the size of the

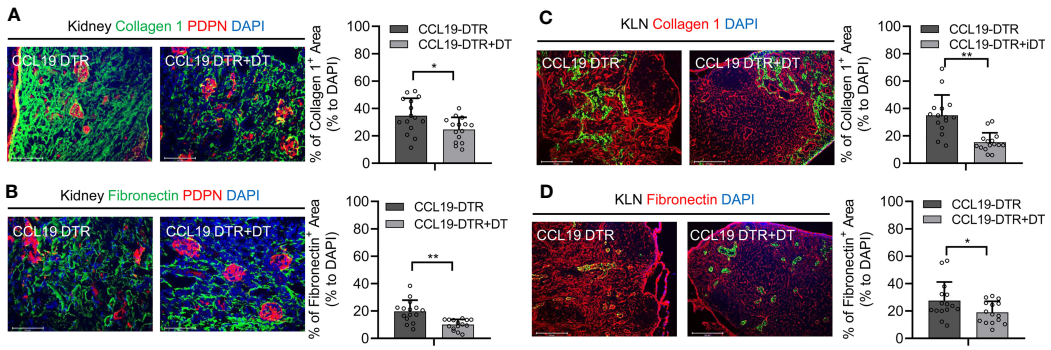


FIGURE 5 | Depletion of FRCs reduces fibrosis in KLNs and kidneys following UUO. **(A, B)** Fluorescence micrographs and semiquantitative analysis reveal significantly lower density of **(A)** collagen 1 fibers (green) and **(B)** fibronectin fibers (green) normalized to DAPI-stained area (blue) in KLNs from CCL19-Cre x iDTR mice following FRC depletion (+DT) at Day 14 (n=5 random microscopic fields of sections from 3 mice). **(C, D)** Fluorescence micrographs and semiquantitative analysis reveal significantly lower density of **(C)** collagen 1 fibers (green) and **(D)** fibronectin fibers (green) normalized to DAPI-stained area (blue) in kidneys from CCL19-Cre x iDTR mice following FRC depletion (+DT) at Day 14 (PDPN glomerular stain, red) (n=15 random microscopic fields of sections from 3 mice). Data represented by means ± SEM. *$p < 0.05$, **$p < 0.01$.

LN and permitting space for the influx of lymphocytes and antigen-presenting cells (18). However, during the late phase, these pro-inflammatory properties of FRCs must resolve, or the FRCs must adopt anti-inflammatory properties to permit the LN to return to its steady state and prevent prolonged inflammation, which can result in fibrosis of the LN (18). Interestingly, Gregory et al. have shown that an expanded FRC network with quiescent gene expression in the LN is associated with the resolution of a viral infection, and this "primes" the LN to respond to future infections (19). On the other hand, dysregulation of the stromal compartment of the LN results in fibrosis, as has been described in studies of patients infected with human immunodeficiency virus (HIV) (20). Therefore, perturbation of this fragile balance in between healing and fibrosis in the LN that leads to hypersecretion of ECM fibers by FRCs is one possible mechanism behind the fibrosis we have observed in the KLN following recurrent or continuous kidney injuries in the IRI and UUO models, respectively.

The interactions of FRCs with T cells are crucial particularly to guiding the direction of adaptive immune responses that contribute to organ damage following an immunogenic or non-immunogenic insult (21). Though we have demonstrated the importance of FRCs in the KLNs to the pathogenesis of a classically cell-mediated disease, such as CGN (3), we have also shown that the activity of FRCs is equally critical to kidney damage in an insult of primarily vascular origin, such as IRI (4). In the latter investigation, we demonstrated that fibrosis within the kidney caused by repetitive IRI was associated with fibrosis and dysregulation of the stromal compartment of the KLN (4). This fibrosis may have interfered with anti-inflammatory effects of FRCs, for which contact with T cells are requisite.

In this study, we sought to determine whether the microarchitecture of the KLN was subject to similar changes as the kidney became fibrotic during UUO, and whether FRCs were implicated in these changes. We found that production of collagen 1 and fibronectin fibers by FRCs led to dramatic remodeling of the KLN stroma during UUO. Interestingly, we found that both fibers increased in the UUO KLN over time, and this increase occurred in parallel to the expansion of the lymphatic vasculature.

LN fibrosis has been described previously in preclinical models of human/simian immunodeficiency virus (HIV/SIV) infection, and pronounced scarring is seen at late stages (12, 22). This scarring has been attributed to sequelae from chronic activation of the immune response (12). However, LN fibrosis has not been studied extensively in other models. Here, we establish for the first time that the KLN undergoes frank fibrosis during UUO. The data from this study in combination with the findings from our previous investigations of renal IRI and CGN suggest that FRC activation in the KLN is a common correlate of the immune activation caused by kidney injury, irrespective of its primary origin—immunogenic or non-immunogenic. Thus, the process of FRC activation and ECM deposition in the KLN appears to be a common pathway following immune-mediated, ischemic, and mechanical sources of kidney injury. However, the specific mechanisms by which fibrosis in the KLN impact immunity and kidney damage remain unclear.

$CD11c^+$ dendritic cells have been found previously to circulate between the kidney and the KLN constitutively in usual states of health (10, 23) and to migrate to the KLN following immune challenge with ovalbumin in mice (11). Here, we demonstrate similarly that the population of $CD11b^+$ and $CD11c^+$ antigen-presenting cells in the KLN increases following UUO. This increase is accompanied by a higher population of activated $CD4^+$ and $CD8^+$ T cells in the UUO KLN, a finding that reflects previous data following ovalbumin administration, IRI, and CGN (3, 4, 11). These expanding T cell subsets could migrate subsequently to the kidney. In future studies, we could investigate whether these $CD4^+$ and $CD8^+$ T cells and their descendants home to the kidney during UUO following adoptive transfer of fluorescently labeled naïve T cells in lymphocyte-deficient RAG-$1^{-/-}$ mice.

Organ fibrosis is thought to be an irreversible condition, during which organ function is lost irretrievably in part due to dysregulation of the stromal compartment. In contrast, the stromal compartment of the LN has the capacity to regenerate following extensive scarring. This capability may arise from the fact that leukocytes vastly outnumber the stromal cells in the LN, which constitute merely ~1% of the cellular population (24). Furthermore, the beneficial effects of preventing the remodeling of the KLN stroma may be suggested by our finding that administering unstimulated FRCs to mice undergoing recurrent renal IRI halted fibrotic changes in the KLN and blunted renal damage (4). Therefore, future investigations could test the efficacy of FRC therapy as a method of prevention for organ fibrosis. Whether administering FRCs will reverse fibrosis in the DLN is another important question that also must be addressed.

The balance between expression of the pro-inflammatory, fibrogenic phenotype and immunoregulatory phenotype in FRCs of the UUO KLN could be crucial to the pathogenesis of kidney injury in this model. TGFβ is known as an important cytokine involved in organ scarring and fibrosis, and our study suggests that activation of the TGFβ-TGFβR signaling pathway should be examined more closely in FRCs of the UUO KLN for its effect on their expression of ECM genes. The source of the TGFβ gene expression in the UUO KLN is unclear, although the antigen-presenting cells that arrive from the kidney are potential culprits. Future research is needed to identify the signaling pathways that govern the important transition of FRCs to an immunoregulatory phenotype, as these pathways are not well understood currently. The lymphotoxin-β receptor (LTβR) signaling pathway is one possible mechanism responsible for control of this phenotypic switch, as previous studies have highlighted its importance in guiding the activity of FRCs during an immune response (1). Thus, blockade of signals that govern formation of the pro-inflammatory phenotype of FRCs and enhancement of those that potentiate anti-inflammatory their properties could serve to reduce kidney damage following UUO.

DATA AVAILABILITY STATEMENT

The raw data supporting the conclusions of this article will be made available by the authors, without undue reservation.

ETHICS STATEMENT

The animal study was reviewed and approved by the Institutional Animal Care and Use Committee (IACUC) of Brigham and Women's Hospital.

AUTHOR CONTRIBUTIONS

Conceptualization: XL, RA, and VK. Formal analysis: XL, RA, and VK. Investigation: XL and JZ. Resources: RA and VK. Writing – original draft: XL, RA, and VK. Writing – review and editing: XL, SN, GS, ST, SS, JB, PF, GT, RA, and VK. Project administration: XL, JZ, RA, and VK. Supervision: RA and VK. Funding acquisition: RA and VK. All authors contributed to the article and approved the submitted version.

FUNDING

This work was supported by the NIH [K08DK124685 (VK), R01AI156084 (RA), and P01AI153003 (RA, JB)] and a grant from Dialysis Clinic, Inc. (VK). The funder was not involved in the study design, collection, analysis, interpretation of data, the writing of this article, or the decision to submit it for publication.

ACKNOWLEDGMENTS

The authors would like to thank Margaret (Peg) Coughlin at the Electron Microscopy Facility at Harvard Medical School (Boston, MA) for capturing electron micrographs of the KLNs, Yarong (Sunny) Lu of InVivoEx (Boston, MA) for cutting and staining KLN sections with Masson's trichrome stain, and Arthur Anderson for assistance in analysis of the electron microscopy images.

SUPPLEMENTARY MATERIAL

The Supplementary Material for this article can be found online at: https://www.frontiersin.org/articles/10.3389/fimmu.2021.768412/full#supplementary-material

REFERENCES

1. Saxena V, Li L, Paluskievicz C, Kasinath V, Bean A, Abdi R, et al. Role of Lymph Node Stroma and Microenvironment in T Cell Tolerance. *Immunol Rev* (2019) 292(1):9–23. doi: 10.1111/imr.12799
2. Katakai T, Hara T, Sugai M, Gonda H, Shimizu A. Lymph Node Fibroblastic Reticular Cells Construct the Stromal Reticulum *via* Contact With Lymphocytes. *J Exp Med* (2004) 200(6):783–95. doi: 10.1084/jem.20040254
3. Kasinath V, Yilmam OA, Uehara M, Jiang L, Ordikhani F, Li X, et al. Activation of Fibroblastic Reticular Cells in Kidney Lymph Node During Crescentic Glomerulonephritis. *Kidney Int* (2019) 95(2):310–20. doi: 10.1016/j.kint.2018.08.040
4. Maarouf OH, Uehara M, Kasinath V, Solhjou Z, Banouni N, Bahmani B, et al. Repetitive Ischemic Injuries to the Kidneys Result in Lymph Node Fibrosis and Impaired Healing. *JCI Insight* (2018) 3(13):1–17. doi: 10.1172/jci.insight.120546
5. Chevalier RL. Obstructive Nephropathy: Towards Biomarker Discovery and Gene Therapy. *Nat Clin Pract Nephrol* (2006) 2(3):157–68. doi: 10.1038/ncpneph0098
6. Ucero AC, Benito-Martin A, Izquierdo MC, Sanchez-Nino MD, Sanz AB, Ramos AM, et al. Unilateral Ureteral Obstruction: Beyond Obstruction. *Int Urol Nephrol* (2014) 46(4):765–76. doi: 10.1007/s11255-013-0520-1
7. Martinez-Klimova E, Aparicio-Trejo OE, Tapia E, Pedraza-Chaverri J. Unilateral Ureteral Obstruction as a Model to Investigate Fibrosis-Attenuating Treatments. *Biomolecules* (2019) 9(4):1–28. doi: 10.3390/biom9040141
8. Cochrane AL, Kett MM, Samuel CS, Campanale NV, Anderson WP, Hume DA, et al. Renal Structural and Functional Repair in a Mouse Model of

Reversal of Ureteral Obstruction. *J Am Soc Nephrol* (2005) 16(12):3623–30. doi: 10.1681/ASN.2004090771
9. Cremasco V, Woodruff MC, Onder L, Cupovic J, Nieves-Bonilla JM, Schildberg FA, et al. B Cell Homeostasis and Follicle Confines Are Governed by Fibroblastic Reticular Cells. *Nat Immunol* (2014) 15(10):973–81. doi: 10.1038/ni.2965
10. Kurts C, Ginhoux F, Panzer U. Kidney Dendritic Cells: Fundamental Biology and Functional Roles in Health and Disease. *Nat Rev Nephrol* (2020) 16 (7):391–407. doi: 10.1038/s41581-020-0272-y
11. Snelgrove SL, Lo C, Hall P, Lo CY, Alikhan MA, Coates PT, et al. Activated Renal Dendritic Cells Cross Present Intrarenal Antigens After Ischemia-Reperfusion Injury. *Transplantation* (2017) 101(5):1013–24. doi: 10.1097/TP.0000000000001427
12. Estes JD. Pathobiology of HIV/SIV-Associated Changes in Secondary Lymphoid Tissues. *Immunol Rev* (2013) 254(1):65–77. doi: 10.1111/imr.12070
13. Song J, Liu J, Luo J, Zhang Q, Xia Y, Shao Q, et al. A Modified Relief of Unilateral Ureteral Obstruction Model. *Ren Fail* (2019) 41(1):497–506. doi: 10.1080/0886022X.2019.1624263
14. Ito K, Chen J, El Chaar M, Stern JM, Seshan SV, Khodadadian JJ, et al. Renal Damage Progresses Despite Improvement of Renal Function After Relief of Unilateral Ureteral Obstruction in Adult Rats. *Am J Physiol Renal Physiol* (2004) 287(6):F1283–93. doi: 10.1152/ajprenal.00441.2003
15. Girard JP, Moussion C, Forster R. Hevs, Lymphatics and Homeostatic Immune Cell Trafficking in Lymph Nodes. *Nat Rev Immunol* (2012) 12 (11):762–73. doi: 10.1038/nri3298
16. Mempel TR, Henrickson SE, Von Andrian UH. T-Cell Priming by Dendritic Cells in Lymph Nodes Occurs in Three Distinct Phases. *Nature* (2004) 427 (6970):154–9. doi: 10.1038/nature02238
17. Perez-Shibayama C, Gil-Cruz C, Ludewig B. Fibroblastic Reticular Cells at the Nexus of Innate and Adaptive Immune Responses. *Immunol Rev* (2019) 289 (1):31–41. doi: 10.1111/imr.12748
18. Lu TT, Browning JL. Role of the Lymphotoxin/LIGHT System in the Development and Maintenance of Reticular Networks and Vasculature in Lymphoid Tissues. *Front Immunol* (2014) 5:47. doi: 10.3389/fimmu.2014.00047
19. Gregory JL, Walter A, Alexandre YO, Hor JL, Liu R, Ma JZ, et al. Infection Programs Sustained Lymphoid Stromal Cell Responses and Shapes Lymph Node Remodeling Upon Secondary Challenge. *Cell Rep* (2017) 18(2):406–18. doi: 10.1016/j.celrep.2016.12.038
20. Schacker TW, Brenchley JM, Beilman GJ, Reilly C, Pambuccian SE, Taylor J, et al. Lymphatic Tissue Fibrosis Is Associated With Reduced Numbers of Naive CD4+ T Cells in Human Immunodeficiency Virus Type 1 Infection. *Clin Vaccine Immunol* (2006) 13(5):556–60. doi: 10.1128/CVI.13.5.556-560.2006
21. Knoblich K, Cruz Migoni S, Siew SM, Jinks E, Kaul B, Jeffery HC, et al. The Human Lymph Node Microenvironment Unilaterally Regulates T-Cell Activation and Differentiation. *PloS Biol* (2018) 16(9):e2005046. doi: 10.1371/journal.pbio.2005046
22. Zeng M, Haase AT, Schacker TW. Lymphoid Tissue Structure and HIV-1 Infection: Life or Death for T Cells. *Trends Immunol* (2012) 33(6):306–14. doi: 10.1016/j.it.2012.04.002
23. Dong X, Swaminathan S, Bachman LA, Croatt AJ, Nath KA, Griffin MD. Antigen Presentation by Dendritic Cells in Renal Lymph Nodes Is Linked to Systemic and Local Injury to the Kidney. *Kidney Int* (2005) 68(3):1096–108. doi: 10.1111/j.1523-1755.2005.00502.x
24. Malhotra D, Fletcher AL, Astarita J, Lukacs-Kornek V, Tayalia P, Gonzalez SF, et al. Transcriptional Profiling of Stroma From Inflamed and Resting Lymph Nodes Defines Immunological Hallmarks. *Nat Immunol* (2012) 13(5):499–510. doi: 10.1038/ni.2262

Conflict of Interest: The authors declare that the research was conducted in the absence of any commercial or financial relationships that could be construed as a potential conflict of interest.

Publisher's Note: All claims expressed in this article are solely those of the authors and do not necessarily represent those of their affiliated organizations, or those of the publisher, the editors and the reviewers. Any product that may be evaluated in this article, or claim that may be made by its manufacturer, is not guaranteed or endorsed by the publisher.

Copyright © 2021 Li, Zhao, Naini, Sabiu, Tullius, Shin, Bromberg, Fiorina, Tsokos, Abdi and Kasinath. This is an open-access article distributed under the terms of the Creative Commons Attribution License (CC BY). The use, distribution or reproduction in other forums is permitted, provided the original author(s) and the copyright owner(s) are credited and that the original publication in this journal is cited, in accordance with accepted academic practice. No use, distribution or reproduction is permitted which does not comply with these terms.

frontiers in Immunology

ORIGINAL RESEARCH
published: 24 January 2022
doi: 10.3389/fimmu.2021.753412

Everolimus Alleviates Renal Allograft Interstitial Fibrosis by Inhibiting Epithelial-to-Mesenchymal Transition Not Only *via* Inducing Autophagy but Also *via* Stabilizing IκB-α

Zeping Gui[1,2†], Chuanjian Suo[2†], Jun Tao[2†], Zijie Wang[2†], Ming Zheng[2], Shuang Fei[2], Hao Chen[2], Li Sun[2], Zhijian Han[2], Xiaobing Ju[2], Hengcheng Zhang[3], Min Gu[1*] and Ruoyun Tan[2*]*

[1] Department of Urology, the Second Affiliated Hospital With Nanjing Medical University, Nanjing, China, [2] Department of Urology, The First Affiliated Hospital With Nanjing Medical University, Nanjing, China, [3] Transplantation Research Center, Brigham and Women's Hospital, Harvard Medical School, Boston, MA, United States

Chronic allograft dysfunction (CAD) is the major cause of late graft loss in long-term renal transplantation. In our previous study, we found that epithelial–mesenchymal transition (EMT) is a significant event in the progression of renal allograft tubulointerstitial fibrosis, and impaired autophagic flux plays a critical role in renal allograft fibrosis. Everolimus (EVR) has been reported to be widely used to prevent the progression of organ fibrosis and graft rejection. However, the pharmacological mechanism of EVR in kidney transplantation remains to be determined. We used CAD rat model and the human kidney 2 (HK2) cell line treated with tumor necrosis factor-α (TNF-α) and EVR to examine the role of EVR on TNF-α-induced EMT and transplanted renal interstitial fibrosis. Here, we found that EVR could attenuate the progression of EMT and renal allograft interstitial fibrosis, and also activate autophagy *in vivo*. To explore the mechanism behind it, we detected the relationship among EVR, autophagy level, and TNF-α-induced EMT in HK2 cells. Our results showed that autophagy was upregulated upon mTOR pathway inhibition by EVR, which could significantly reduce expression of TNF-α-induced EMT. However, the inhibition of EVR on TNF-α-induced EMT was partly reversed following the addition of autophagy inhibitor chloroquine. In addition, we found that TNF-α activated EMT through protein kinase B (Akt) as well as nuclear factor kappa B (NF-κB) pathway according to the RNA sequencing, and EVR's effect on the EMT was only associated with IκB-α stabilization instead of the Akt pathway. Together, our findings suggest that EVR may retard impaired autophagic flux and block NF-κB pathway activation, and thereby prevent progression of TNF-α-induced EMT and renal allograft interstitial fibrosis.

Keywords: chronic renal graft dysfunction, renal allograft interstitial fibrosis, everolimus, autophagy, EMT

OPEN ACCESS

Edited by:
Bin Yang,
University of Leicester,
United Kingdom

Reviewed by:
Giuseppe Fiume,
University of Catanzaro, Italy
Yuanyuan Wu,
Nantong University, China

***Correspondence:**
Ruoyun Tan
tanruoyun112@vip.sina.com
Min Gu
lancetgu@aliyun.com
Hengcheng Zhang
hzhang58@bwh.harvard.edu

These authors have contributed equally to this work

Specialty section:
This article was submitted to Alloimmunity and Transplantation, a section of the journal Frontiers in Immunology

Received: *04 August 2021*
Accepted: *14 December 2021*
Published: *24 January 2022*

Citation:
Gui Z, Suo C, Tao J, Wang Z, Zheng M, Fei S, Chen H, Sun L, Han Z, Ju X, Zhang H, Gu M and Tan R (2022) Everolimus Alleviates Renal Allograft Interstitial Fibrosis by Inhibiting Epithelial-to-Mesenchymal Transition Not Only via Inducing Autophagy but Also via Stabilizing IκB-α. Front. Immunol. 12:753412. doi: 10.3389/fimmu.2021.753412

INTRODUCTION

Renal transplantation has long been regarded as the best therapeutic intervention for patients with end-stage organ failure in recent years (1). While immunosuppression induced by the calcineurin inhibitors tacrolimus (FK506) or cyclosporine A (CsA) has significantly improved short-term graft survival in kidney transplantation, a satisfactory rate of long-term renal allograft survival has not been achieved over the last two decades (2). Chronic allograft dysfunction (CAD), formerly known as chronic allograft nephropathy, is the most prevalent cause of late renal graft loss in kidney transplantation and has a significant impact on the long-term survival of the transplanted kidney (3).

CAD is characterized by glomerulosclerosis, peritubular capillary loss, chronic inflammation and interstitial fibrosis/tubular atrophy (IF/TA) (4). Interstitial fibrosis is an essential factor in determining the outcome of the renal allograft, although the underlying mechanisms are unknown. Several studies, including our previous research, have demonstrated that renal graft interstitial fibrosis is characterized by the accumulation of extracellular matrix (ECM), as a result of increasing fibroblasts and myofibroblasts (5, 6). Myofibroblasts are formed from a variety of distinct cell types, including epithelial cells, endothelial cells, bone marrow-derived fibroblasts, and microvascular pericytes (7, 8). The epithelial–mesenchymal transition (EMT) is the process through which epithelial cells gradually lose their markers, such as E-cadherin, and gain mesenchymal markers such as α-smooth muscle actin (α-SMA) (9). It is divided into several subtypes, with type 2 EMT being involved in tissue regeneration, wound healing, and organ fibrosis (10). EMT occurs as an inherent mechanism to support neovascularization and cardiac healing; this could imply that EMT plays a prosthetic and protective role in pathogenesis following myocardial infarction (11). However, Andugulapati et al. demonstrated that they could inhibit pulmonary fibrosis *in vitro* and *in vivo* by suppressing the transforming growth factor-β (TGF-β)-mediated EMT, myofibroblast differentiation, and collagen deposition. Thus, EMT has been implicated in the development of pulmonary fibrosis by generating collagen-producing myofibroblasts (12). Additionally, it was demonstrated that EMT plays a critical role in renal fibrosis. In the unilateral ureteral obstruction mice model, EMT-related protein Vimentin expression was required for renal fibrosis (13). The characteristics of EMT that are essential for wound healing also link EMT to interstitial fibrosis of the transplanted kidney. Our previous study established that EMT aggravated renal allograft interstitial fibrosis in CAD patients (14).

Organ fibrosis is a complex process involving numerous cytokines and growth factors. Among them, tumor necrosis factor-α (TNF-α) is first synthesized as transmembrane TNF-α, which is then cleaved by the TNF-α converting enzyme to release secretory TNF-α into the bloodstream and exert its effects (15). Several studies have already established a link between TNF-α and renal fibrosis; for example, TNF-α acted as a central mediator of a broad range of biological activities in kidney tubules, including cell proliferation, cell death, differentiation, as well as induction of inflammation and immune modulation, indicating that TNF-α was involved in obstructive kidney disease and diabetic nephropathy fibrosis (16). Our previous research established that TNF-α may activate EMT progression and that process was a critical mediator of renal graft interstitial fibrosis *via* regulation of ECM synthesis (14). Thus, inhibiting TNF-α-induced EMT could improve the survival of renal allografts.

Everolimus (EVR) is a pharmacological agent that was previously used to treat some types of solid tumors. EVR is approved by the Food and Drug Administration (FDA) for the treatment of metastatic renal cell carcinoma, advanced pancreatic neuroendocrine tumors, and advanced hormone receptor-positive breast cancer (17). EVR was recently reported to be used in some foreign clinical trials for anti-rejection therapy following kidney transplantation. According to the clinical study findings, EVR can significantly improve assessed glomerular filtration rate when compared to no change in the CsA group; however, it is associated with several adverse events (18, 19). In addition, a number of other pharmacologic actions of EVR have also been reported in some fibrotic diseases. According to the latest research, it has been reported that EVR attenuates tacrolimus-induced renal interstitial fibrosis in rats through suppressed TGF-β1 production (20). However, one research demonstrated that EVR led to serious pulmonary fibrosis and interstitial pneumonitis after administration in some cancer patients (21). Similarly, EVR also has the double face during the progression of EMT and fibrosis in in hepatic stellate cell and human liver cancer cells (22). Regrettably, the precise anti-fibrosis functional role of EVR in rat kidney transplant CAD model is not fully expounded. Previous studies always focused on the immunosuppression role of EVR. Therefore, a thorough examination of the underlying pharmacological mechanisms of EVR is critical for CAD prevention.

EVR, like Sirolimus and Tamsilorimus, exerts its anti-rejection effect by inhibiting the mammalian target of rapamycin (mTOR), a phosphoinositide 3-kinase-related protein that regulates cell cycle, protein synthesis, angiogenesis, and autophagy (23). Our research group previously revealed that ATG16L-dependent autophagic flux decreased gradually over time following kidney transplantation. In that study, we found that autophagy was downregulated in CAD patients and decreased LC3 predicted poor prognosis in CAD patients (24). Additionally, autophagy and EMT are two critical regulators of organ fibrosis progression and are closely related according to recent evidence (25). Just as autophagy plays a dual role in a variety of diseases, it also has a dichotomous effect in EMT, depending on the cell type and stage of fibrosis progression. Several investigations demonstrated that autophagy promoted EMT by upregulating the expression of an integrin-linked kinase, whereas autophagy enabled epithelial cells to acquire a mesenchymal phenotype (26). On the other hand, other results suggested that autophagy promoted TGF-β2-induced fibrosis by expressing the EMT phenotype during posterior capsular opacification (27). Therefore, the interaction between autophagy and EMT is complex and environment-specific.

In light of these findings, we postulated that EVR contributes to the prevention of interstitial fibrosis through modulating EMT.

In this study, we revealed that EVR alleviated the progression of EMT and improved autophagic flux in kidney-transplanted rats. We then found that TNF-α-induced EMT was inhibited when the autophagy level was altered using EVR. Additionally, we investigated autophagy-independent potential underlying mechanisms of EVR using RNA sequencing. We found that the nuclear factor-κB (NF-κB) pathway was involved in TNF-α-induced EMT and that EVR could reverse this pathway activation by specifically stabilizing IκB-α.

RESULTS

EVR Prevented Allograft Renal Function Impairment and Renal Interstitial Fibrosis in CAD Rat Model

In order to explore the effect of EVR on renal allograft function and renal interstitial fibrosis progression in CAD rat model, we applied EVR (1.5 mg/kg, i.g., qod) to the syngeneic (syn) recipient rats and allogeneic (allo) recipient rats for different times. Masson's trichrome staining and PAS staining assays were chosen to detect the pathological and renal allograft fibrosis level in each group of rats. Masson's trichrome staining results of transplanted kidney samples showed that the Syn group had no renal interstitial fibrosis, while renal interstitial fibrosis was found in the Allo group at 4 weeks, and aggravated after 8 weeks. The results of Masson's trichrome staining also showed that the blue-colored collagen fibers were gradually increased at 8, 14, and 20 weeks after kidney transplantation, compared with the Syn group. PAS staining assays of kidney tissue indicated varying degrees of glomerulosclerosis, tubular atrophy, and interstitial fibrosis in the Allo group at weeks 4, 8, 14, and 20 after kidney transplantation. The tubulointerstitial damage scores represented by PAS staining and the area of renal interstitial fibrosis represented by Masson staining were shown to indicate the development of CAD and renal interstitial fibrosis after renal transplantation in rats. However, treatment with EVR could obviously reduce structural damages and collagen deposition, as shown in PAS staining and Masson's trichrome staining assays of transplanted kidneys (**Figures 1A–D**).

Serum creatinine (Scr), blood urea nitrogen (BUN), and 24-h urine protein are the most commonly used indicators of renal function. In order to test the effect of EVR on renal allograft function, the native right kidney from recipient rats was removed during kidney transplantation. The results showed that the renal allograft function started to be continuously deteriorated in the Allo group after the resection of right kidney compared with the Syn group. However, the increases of serum Cr, BUN, and 24-h urine protein in the Allo group were downregulated and they remained at a relatively low level when rats were treated by EVR at same time (**Figures 1E–G**).

EVR Alleviated the Progression of EMT in CAD Rat Model

In our previous study, we proved the increase of EMT in rat allograft kidney after kidney transplantation (24). Here, we explored the role of EVR in ameliorating the progression of renal allograft EMT after transplantation. EMT is characterized by cells that gradually lose epithelial cell markers, such as E-cadherin, and gain mesenchymal or myofibroblastic phenotype, such as α-smooth muscular actin (α-SMA) and fibronectin (FN). The results of immunohistochemistry (IHC) assays revealed the remarkably high expressions of α-SMA and FN and low expression of E-cadherin in the Allo group compared with the Syn group. However, the positive areas of α-SMA and FN in transplanted kidneys were remarkably decreased and the reduction of E-cadherin was relieved after the treatment of EVR in the Allo group (**Figures 2A, B**). Western blot (WB) analyses results also confirmed the outcomes of IHC assays (**Figures 2C, D**).

EVR Activated Autophagy Flux in CAD Rat Model

The clinical utility of EVR is dependent on its ability to inhibit the mTOR pathway activation, which is frequently involved in protein synthesis, cell cycle and growth, angiogenesis, and autophagy. In our previous study, we discovered that autophagic flux generated by kidney transplantation gradually decreased over time (24). Therefore, we hypothesized that autophagy was involved in the effect of EVR on the progression of EMT and allograft renal interstitial fibrosis. Although IHC assays suggested that autophagy levels increased following kidney transplantation, EVR further up-regulated LC3-II expression (**Figures 3A, B**). Again, WB assay results confirmed the accuracy of IHC assays and demonstrated that EVR could retard the impaired autophagic flux from 8 to 20 weeks (**Figures 3C, D**).

EVR Activated Autophagic Flux Through the mTOR/ULK1 Pathway in HK2 Cells

We hypothesized that EVR might affect autophagy activity in HK2 cells. SQSTM1 is an autophagy substrate; its degradation and increase in MAP1LC3B-II (LC3-II) are markers of increased autophagy activity. WB analysis revealed that EVR increased LC3-II accumulation and decreased SQSTM1 in a dose- and time-dependent manner in HK2 cells. Autophagy level was found to be significantly increased following a 4-h exposure to EVR at a concentration of 10 nM (**Figures 4A–D**). The transmission electron microscope was used to demonstrate the typical organized cytoplasmic structure (autophagosome and autolysosome) formation. The autophagic process is completed when the autophagosome fuses with the lysosome to produce an autolysosome in which the substrates are degraded. As shown in **Figure 4E**, we found that EVR-treated HK2 cells had a greater number of autophagic vacuoles than the control group (**Figures 4E, F**). To further investigate EVR's role in autophagic flux regulation, we then treated HK2 cells with EVR and chloroquine (CQ), simultaneously. CQ, a known inhibitor of autophagosome–lysosome fusion, results in increased autophagosomes, implying that autophagy is inhibited. When CQ inhibits autolysosome breakdown, the sustained increase in LC3 in response to stimulation indicates that the upstream of autophagy is activated. WB analysis revealed that when EVR was combined with CQ,

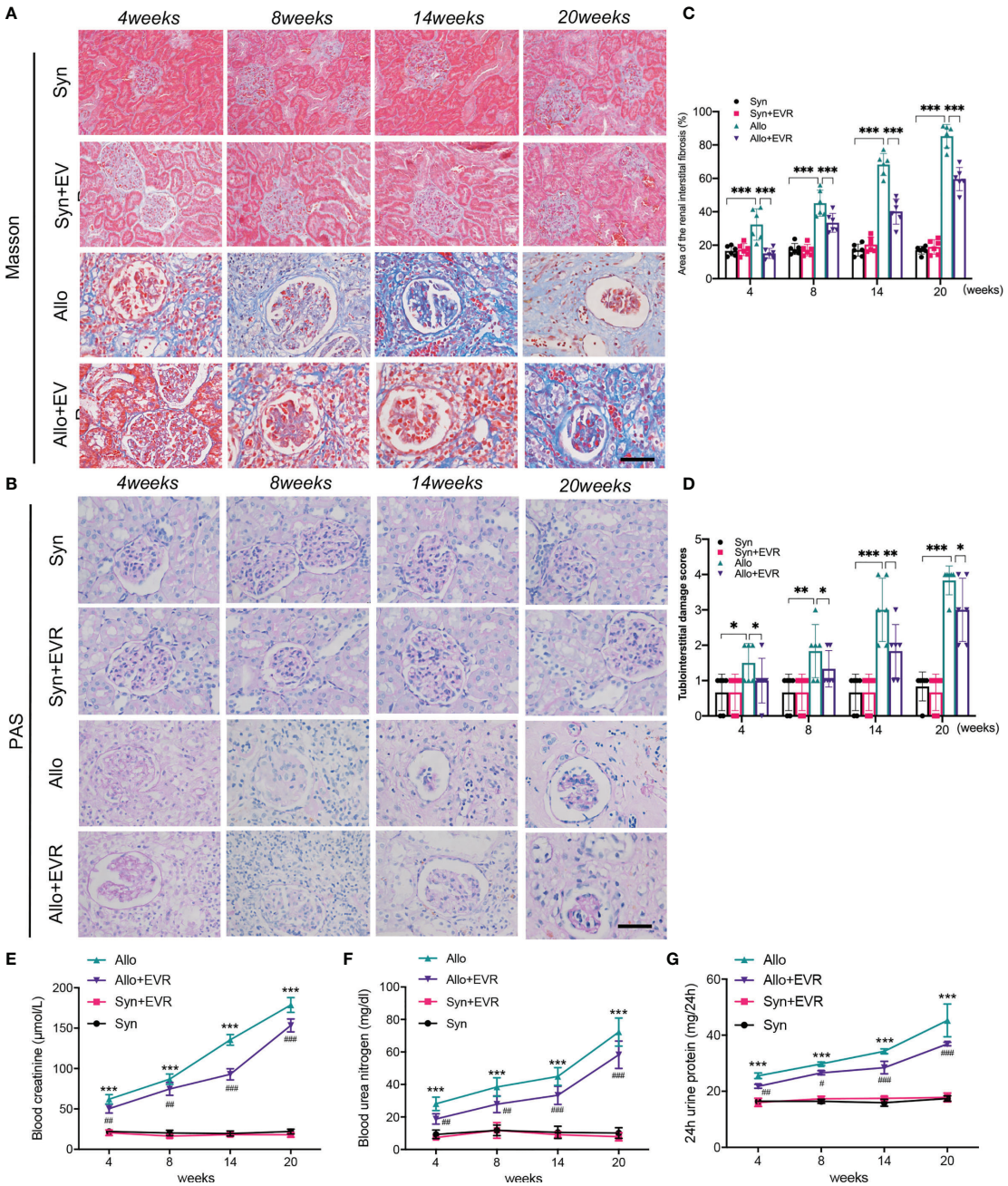


FIGURE 1 | EVR prevented allograft renal function impairment and renal interstitial fibrosis in CAD rat model. **(A, B)** Representative images (n = 6) of Masson's trichrome staining and PAS staining (scale bar: 25 μm) from kidneys of different treatment group rats. **(C)** Semi-quantitative analyses results of Masson's trichrome staining positive area that represented the area of the renal interstitial fibrosis from kidneys of different treatment group rats. Values represented the mean ± SD (n = 6, $^{***}p < 0.001$). **(D)** The statistical analyses of tubulointerstitial damage scores in different treatment group rats. Values represented the mean ± SD (n = 6, $^{*}p < 0.05$, $^{**}p < 0.01$, $^{***}p < 0.001$). **(E–G)** Changes of renal function parameters—serum Cr, BUN, and 24-h urine protein of different treatment group rats. Values represented the mean ± SD (n = 6, $^{***}p < 0.001$ compared with control group, $^{\#}P < 0.05$, $^{\#\#}P < 0.01$, $^{\#\#\#}p < 0.001$ compared with Allo group); EVR, everolimus; PAS, periodic acid–Schiff; Cr, creatinine; BUN, blood urea nitrogen.

the abundance of LC3-II and SQSTM1 was greatly increased in HK2 cells compared to when EVR was administered alone (**Figures 4G, H**). This illustrated that the role of EVR was to induce autophagy upstream.

mTOR signaling is critical for autophagy regulation, with activated mTOR suppressing autophagy, and blocking of mTOR inducing it. Additionally, as shown in **Figure 4E**, we used WB assays to detect total mTOR and mTOR phosphorylation

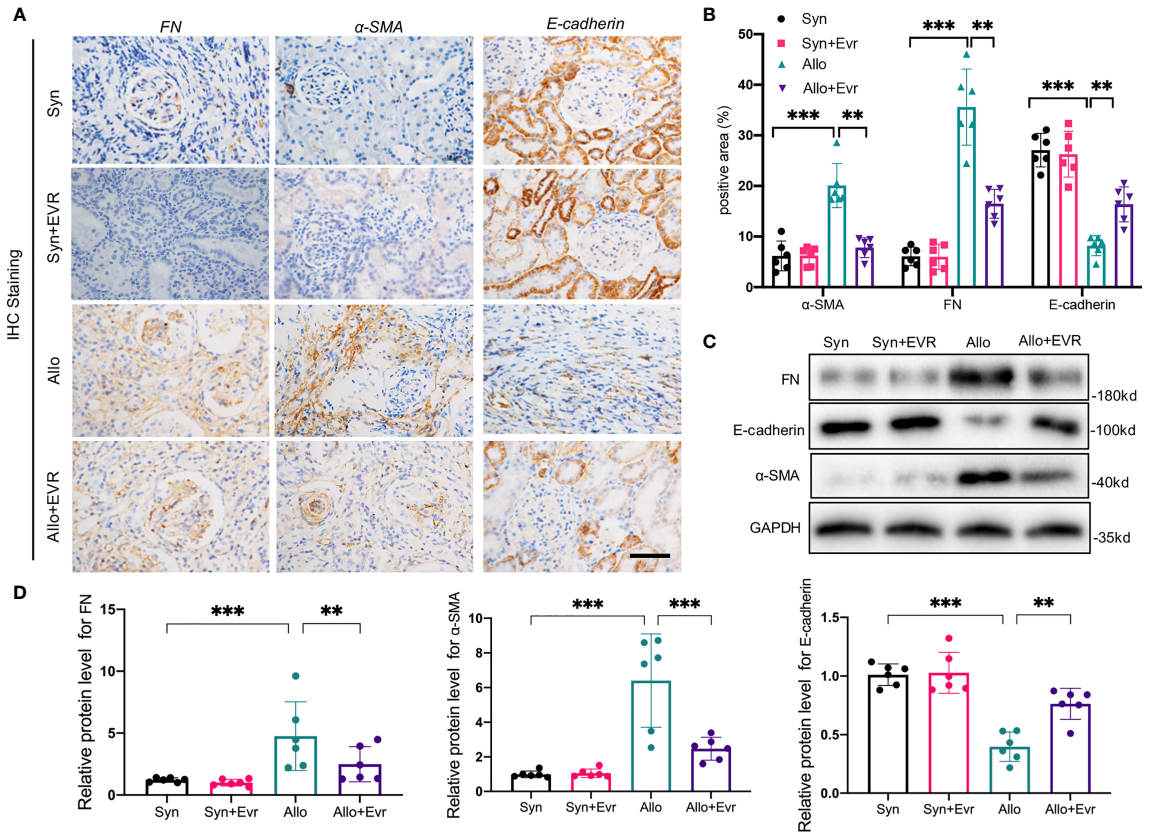


FIGURE 2 | EVR alleviated the progression of renal tubular EMT in CAD rat model. **(A)** Representative IHC images of EMT markers (E-cadherin, α-SMA, and FN) in kidney sections from different treatment group rats (scale bar: 20 μm). **(B)** Semi-quantitative analyses results of IHC positive area in kidney sections from different treatment group rats. Values represented the mean ± SD (n = 6, $^{**}p < 0.01$, $^{***}p < 0.001$). **(C)** Representative Western blotting results of EMT markers (E-cadherin, α-SMA, and FN) in kidney tissues from different treatment group rats. **(D)** Semi-quantitative analyses results of relative protein abundances of E-cadherin, α-SMA, and FN in kidney tissues from different treatment group rats. Values represented the mean ± SD (n = 6, $^{**}p < 0.01$, $^{***}p < 0.001$); IHC, immunohistochemistry; α-SMA, α-smooth muscle actin; EVR, everolimus; EMT, epithelial–mesenchymal transition; FN, fibronectin.

(p-mTOR). As expected, EVR significantly blocked mTOR activity, as did phosphorylation of both 4E-BP1 and p70S6K, which are downstream mediators of mTOR in HK2 cells. Meanwhile, EVR-treated HK2 cells exhibited an increase in ULK1, one of the major downstream targets of the mTOR pathway involved in autophagy regulation. Taken together, these findings indicate that EVR can significantly increase the autophagic flux in HK2 cells *via* the mTOR/ULK1 pathway (**Figures 4I, J**).

EVR Alleviated TNF-α-Mediated EMT, Cell Migration, and Invasion in HK2 Cells

Our previous research established that TNF-α-induced EMT plays an important role in the progression of allograft kidney fibrosis (28). HK2 cells were treated with 50 ng/ml TNF-α with or without EVR to mimic the *in vivo* condition. EVR significantly decreased the protein expressions of α-SMA and FN induced by TNF-α, while partially restoring the expression of E-cadherin (**Figures 5A, B**). Additionally, the results of IF staining for FN and E-cadherin revealed that EVR can inhibit the EMT progression of HK2 cells generated by TNF-α (**Figure 5C**).

Additionally, we assessed changes in cell migration and invasion ability, which are highly associated with EMT. The wound healing test and Transwell assays were used to assess the acquisition of migratory and invasive capacity following treatment with TNF-α and EVR, or in their absence. TNF-α significantly increased the chemokinetic motility of HK2 cells in wound healing experiments, an effect that was reversed by EVR. EVR, similarly, significantly inhibited the TNF-α-induced chemotactic response and migration (**Figures 5D–H**). These findings supported the hypothesis that treating HK-2 cells with EVR could ameliorate TNF-induced EMT.

Blockade of Autophagy Promoted TNF-α-Mediated EMT and Diminished Action of EVR on This Process

To further demonstrate the involvement of autophagy in EVR inhibition of TNF-α-meditated EMT *in vitro*, we first examined the protein expression of α-SMA, E-cadherin, and FN in HK2

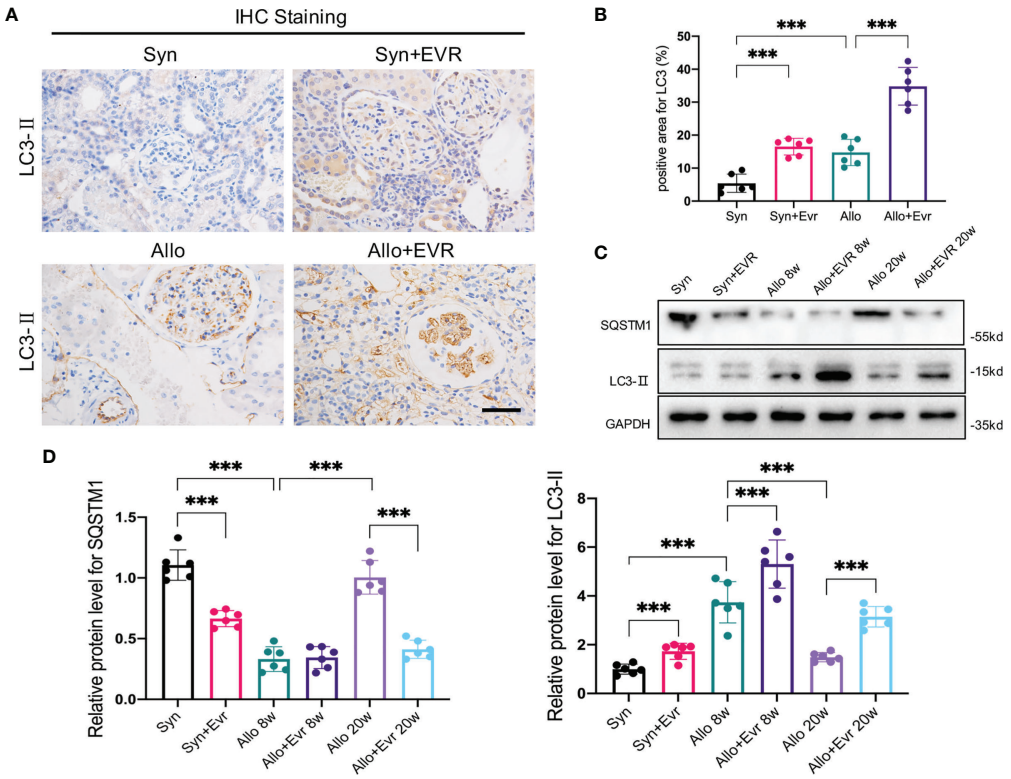


FIGURE 3 | EVR activated autophagy in CAD rat model. **(A)** Representative IHC images of LC3-II in kidney sections from different treatment group rats (scale bar: 15 μm). **(B)** Semi-quantitative analyses results of IHC positive area in kidney sections from different treatment group rats. Values represented the mean ± SD (n = 6, ***p < 0.001). **(C)** Representative Western blotting results of autophagy markers (SQSTM1 and LC3-II) in kidney sections from different treatment group rats at 8 and 20 weeks. **(D)** Semi-quantitative analyses results of relative protein abundances of SQSTM1 and LC3-II in kidney sections from different treatment group rats at 8 and 20 weeks. Values represented the mean ± SD (n = 6, ***p < 0.001). EVR, everolimus.

cells treated with various concentrations of TNF-α and CQ. The WB results demonstrated that CQ at 20 and 40 μM significantly promoted the progression of TNF-α-induced EMT (**Supplementary Figure 1A**). Meanwhile, we found that EVR was capable of decreasing α-SMA and FN expression while increasing E-cadherin expression in the TNF-α+EVR group compared to the TNF-α group. Additionally, the progression of EMT was aggravated in the TNF-α+EVR+CQ group compared to the TNF-α+EVR group, and it was almost recovered with the same level of treatment with TNF-α alone (**Supplementary Figure 1B**). These changes in EMT marker expression were accentuated by co-stimulation with TNF-α and CQ, and the protective effect of EVR against TNF-α-induced EMT could be recovered if CQ was used to block autophagy.

EVR Suppressed TNF-α-Mediated EMT *via* Blocking NF-κB Instead of Akt Signaling Pathway in HK-2 Cells

To further elucidate mechanisms of EVR on TNF-α-induced EMT, besides autophagy, we first performed whole-transcriptome RNA sequencing (RNA-seq) on HK2 cells treated with or without TNF-α. A comparison of the TNF-α group and control groups revealed that 2011 differentially expressed genes were highly expressed while 1332 genes showed decreased expression (**Figure 6A**). The number of downregulated differentially expression gene with log fold change (FC) value lower than minus 2 and p-value less than 0.05 is 531. The number of upregulated differentially expression gene with logFC value higher than 2 and p-value less than 0.05 is 355.

KEGG pathway analysis of the RNA-seq data revealed that a total of 167 pathways were identified, 26 of which were significantly enriched in the TNF-α group compared to the control group. Top pathways identified by KEGG analysis ranked by p-values (**Figure 6B**). In our previous study, we demonstrated that Akt and NF-κB signaling pathway activation was induced by TNF-α in HK2 cells. In our KEGG pathway analysis, the input gene numbers of Akt and the NF-κB signaling pathway are 82 and 28, respectively (p-value < 0.001). To corroborate the RNA-seq data, we used WB analysis to determine whether TNF-α activated the Akt signaling pathway in a time-dependent manner (**Supplementary Figures 2A, B**). To investigate the involvement of the Akt pathway in TNF-α-induced EMT, we suppressed Akt phosphorylation in HK2 cells using MK2206, an Akt pathway-specific inhibitor, and observed that MK2206 significantly decreased FN expression induced by TNF-α (**Supplementary Figures 2C, D**).

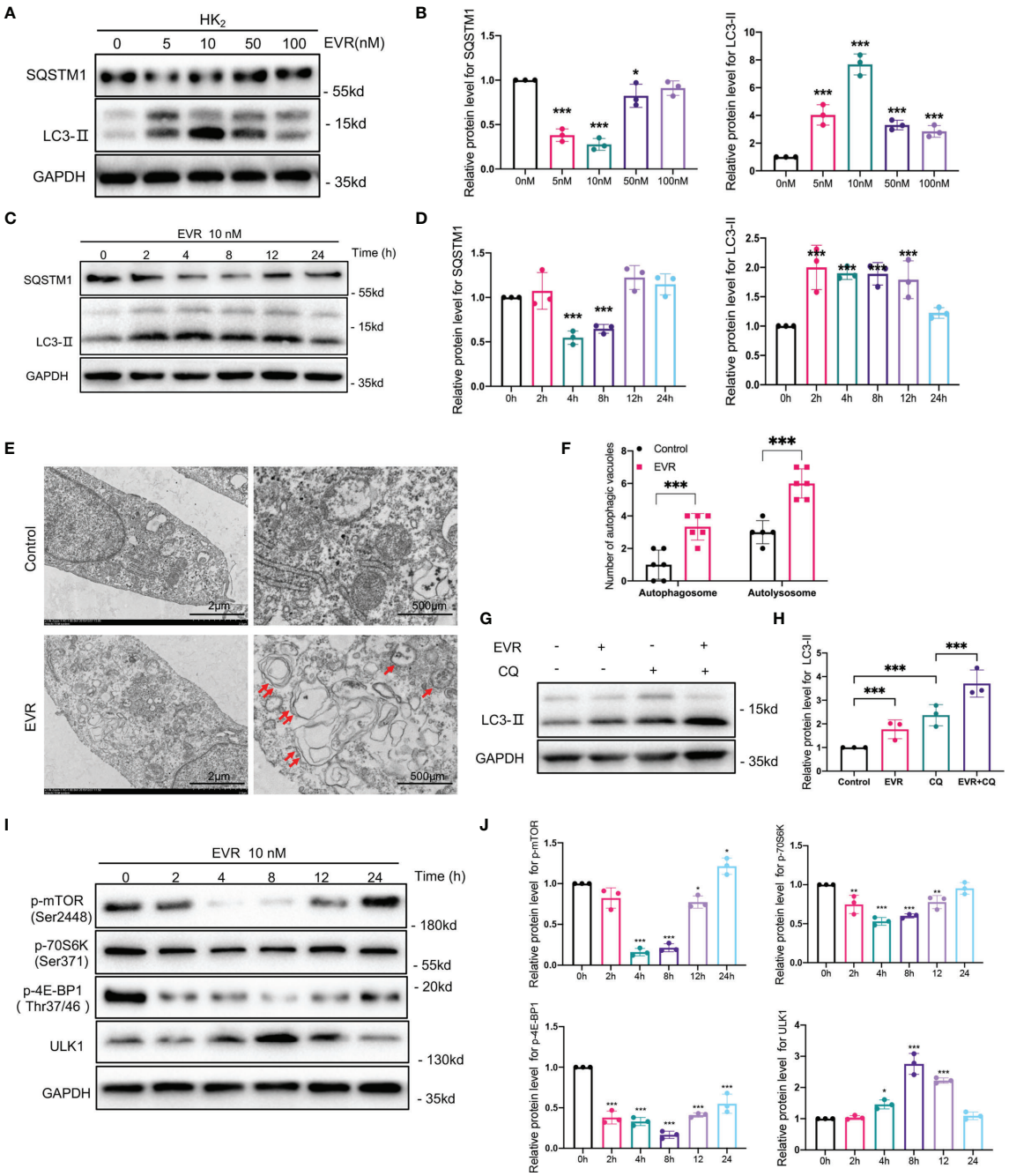


FIGURE 4 | EVR activated autophagic flux through mTOR/ULK1 pathway in HK2 cells. **(A)** Representative Western blotting results of the expressions of SQSTM1 and LC3-II in HK2 cells after EVR treatment for different dosages. **(B)** Semi-quantitative analyses results of relative protein abundances of SQSTM1 and LC3-II in HK2 cells after EVR treatment for different dosage. Values represented the mean ± SD (n = 6, $^{*}p < 0.05$, $^{***}p < 0.001$). **(C)** Representative Western blotting results of the expressions of SQSTM1 and LC3-II in HK2 cells after EVR treatment for different times. **(D)** Semi-quantitative analyses results of relative protein abundances of SQSTM1 and LC3-II in HK2 cells after EVR treatment for different times. Values represented the mean ± SD (n = 6, $^{***}p < 0.001$). **(E)** Representative TEM images of autophagosomes (red double arrow) and autolysosomes (red single arrow) in HK2 cells treated with or without EVR (10 nM) for 24 h (scale bar: 2 and 500 μm). **(F)** Qualitative analyses results of the number of autophagic vacuoles in control and EVR treatment groups under TEM. Values represented the mean ± SD (n = 6, $^{***}p < 0.001$). **(G)** Representative Western blotting results of the expression of LC3-II in HK2 cells treated with EVR (10 nM) and/or CQ (20 μM) for 24 h. **(H)** Semi-quantitative analyses results of relative protein abundance of LC3-II in HK2 cells treated with EVR and/or CQ for 24 h. Values represented the mean ± SD (n = 6, $^{***}p < 0.001$). **(I)** Representative Western blotting results of the expressions of p-mTOR, mTOR, p-70S6K, 70S6K, p-4E-BP1, 4E-BP1, and ULK1 in HK2 cells after EVR treatment for different times. **(J)** Semi-quantitative analyses results of relative protein abundances of p-mTOR, mTOR, p-70S6K, 70S6K, p-4E-BP1, 4E-BP1, and ULK1 in HK2 cells after EVR treatment for different times. Values represented the mean ± SD (n = 6, $^{*}p < 0.05$, $^{**}p < 0.01$, $^{***}p < 0.001$). TEM, transmission electron microscope; IF, immunofluorescence; EVR, everolimus; CQ, chloroquine.

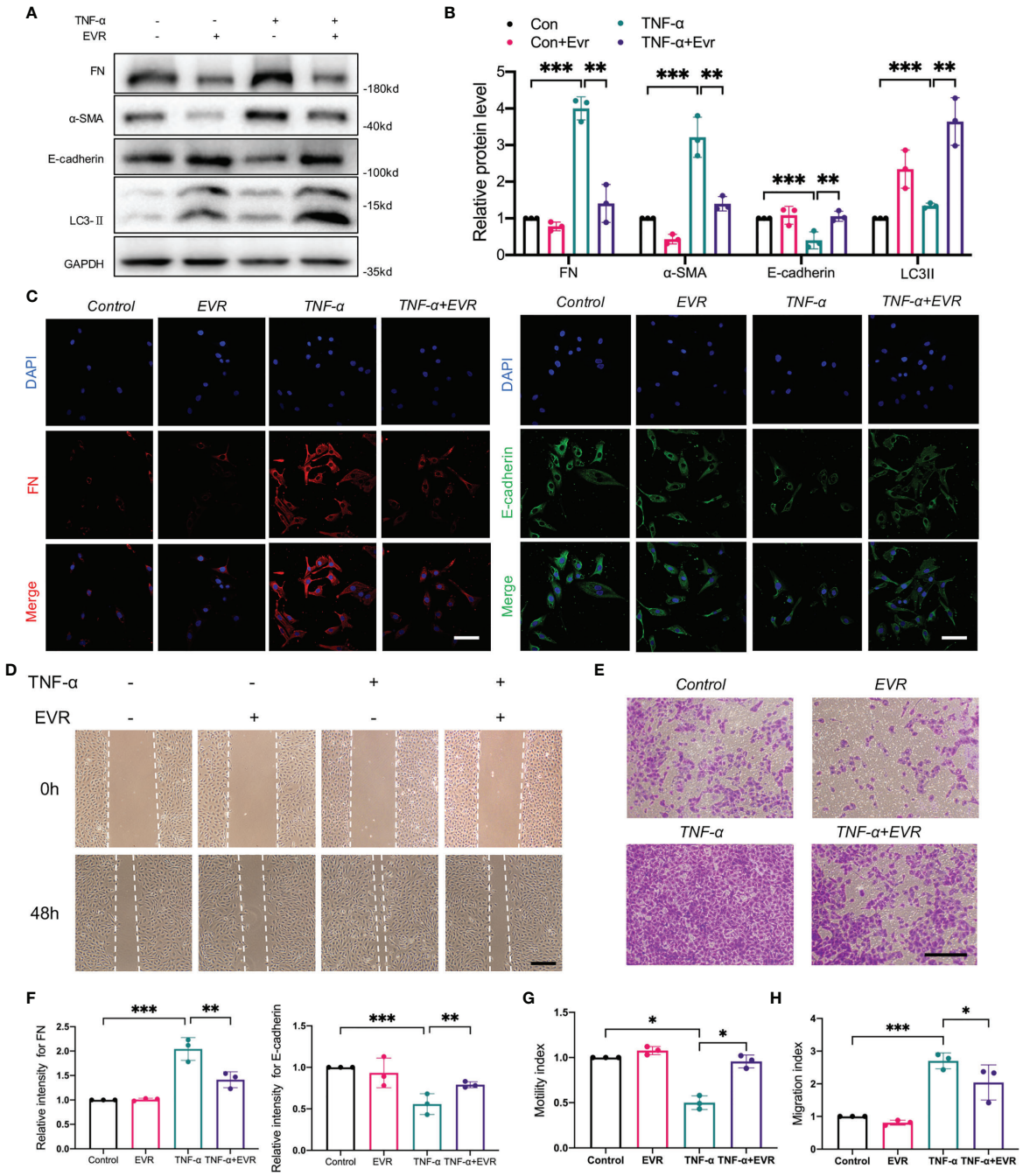


FIGURE 5 | EVR alleviated the TNF-α-mediated EMT, cell migration, and invasion in HK2 cells. **(A)** Representative Western blotting results of EMT markers (E-cadherin, α-SMA, and FN) and LC3-II in HK-2 cells treated with TNF-α (50 ng/ml) and/or EVR (10 nM) for 48 h. **(B)** Semi-quantitative analyses results of relative protein abundances of E-cadherin, α-SMA, FN, and LC3-II in HK-2 cells treated with TNF-α and/or EVR for 48 h. Values represented the mean ± SD ($n = 6$, $^{**}p < 0.01$, $^{***}p < 0.001$). **(C)** Representative IF staining images of E-cadherin and FN in HK-2 cells treated with TNF-α (50 ng/ml) and/or EVR (10 nM) for 24 h (scale bar: 20 μm). **(D)** Representative wound healing test images on HK-2 cells treated with TNF-α (50 ng/ml) and/or EVR (10 nM) for 48 h (scale bar: 20 μm). **(E)** Representative transwell assay images on HK-2 cells treated with TNF-α (50 ng/ml) and/or EVR (10 nM) for 48 h (scale bar: 20 μm). **(F)** Semi-quantitative analyses results of relative IF staining intensity of E-cadherin and FN in HK-2 cells treated with TNF-α (50 ng/ml) and/or EVR (10 nM) for 24 h. Values represented the mean ± SD ($n = 3$, $^{**}p < 0.01$, $^{***}p < 0.001$). **(G)** Quantitative analyses results of the motility index of HK-2 cells treated with TNF-α and/or EVR for 48 h; the motility index has determined by the formula "migration cell number of control group/migration cell number of the other treatment group". Values represented the mean ± SD ($n = 3$, $^{*}p < 0.05$). **(H)** Quantitative analyses results of the migration index of HK-2 cells treated with TNF-α and/or EVR for 48 h; the migration index as determined by the formula "migration cell number of the other treatment group/migration cell number of control group". Values represented the mean ± SD ($n = 3$, $^{*}p < 0.05$, $^{***}p < 0.001$). α-SMA, α-smooth muscle actin; EVR, everolimus; EMT, epithelial–mesenchymal transition; FN, fibronectin; TNF-α, tumor necrosis factor-α.

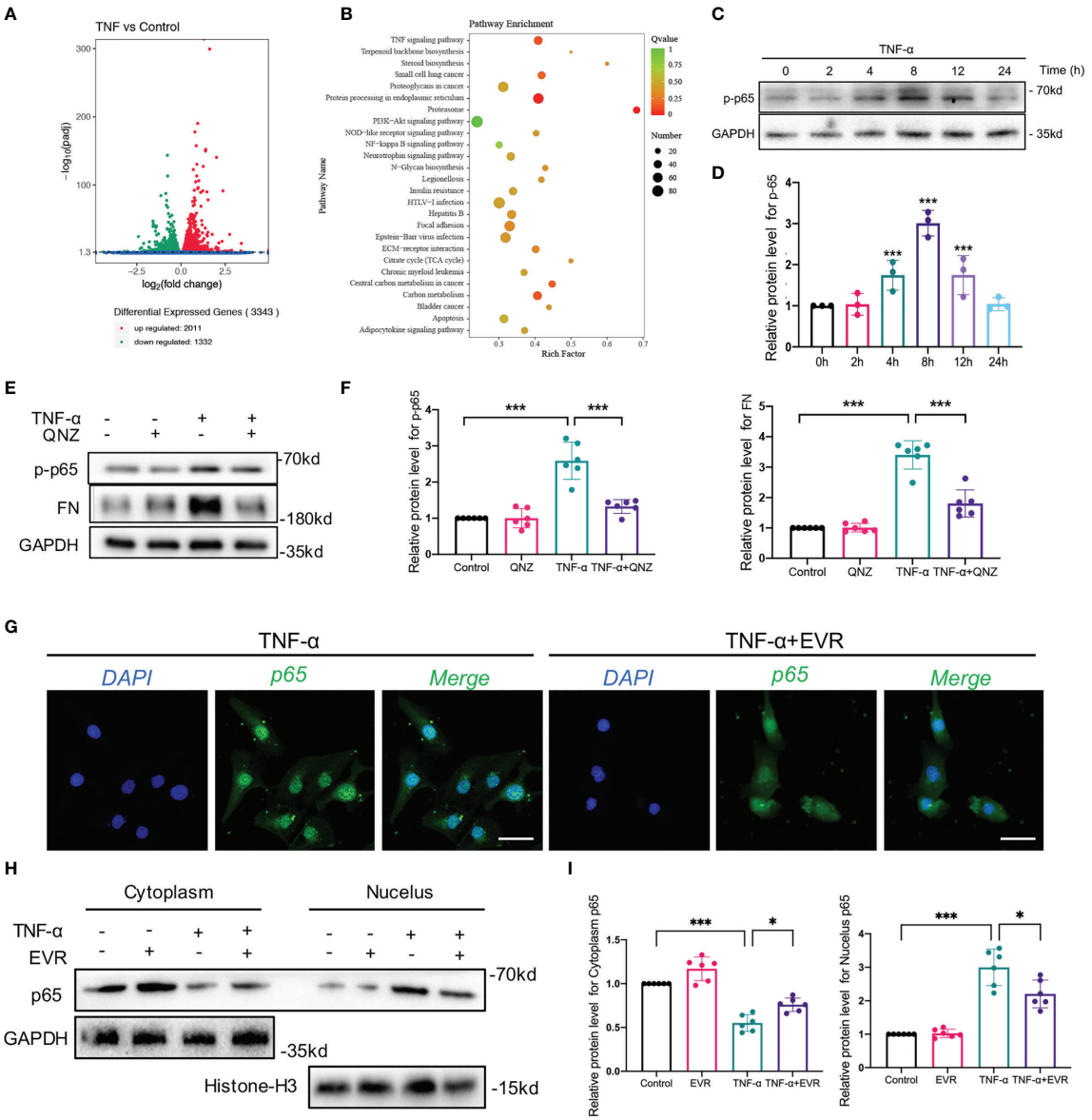


FIGURE 6 | EVR suppressed TNF-α-mediated EMT *via* blocking NF–κB instead of Akt signaling pathway in HK-2 cells. **(A)** The RNA sequencing results of differential genes in HK-2 cells treated with or without TNF-α (50 ng/ml) for 24 h (n = 5). **(B)** KEGG pathway analyses results of the top 20 KEGG enriched gene pathways base on RNA sequencing results. **(C)** Representative Western blotting results of the expression of p-p65 in HK2 cells after TNF-α (50 ng/ml) treatment for different times. **(D)** Semi-quantitative analyses results of relative protein abundance of p-p65 in HK2 cells after TNF-α treatment for different times. Values represented the mean ± SD (n = 6, ***p < 0.001). **(E)** Representative Western blotting results of the expressions of p-p65 and FN in HK2 cells treated with TNF-α (50 ng/ml) and/or QNZ (20 nM) for 24 h. **(F)** Semi-quantitative analyses results of relative protein abundances of p-p65 and FN in HK2 cells treated with TNF-α and/or QNZ for 24 h. Values represented the mean ± SD (n = 6, ***p < 0.001). **(G)** Representative IF staining images of p65 in HK-2 cells treated with TNF-α (50 ng/ml) and/or EVR (10 nM) for 24 h (scale bar: 50 μm). **(H)** Representative Western blotting results of p65 in cytoplasmic and nuclear fractions of HK-2 cells treated with TNF-α (50 ng/ml) and/or EVR (10 nM) for 24 h. **(I)** Semi-quantitative analyses results of relative protein abundance of p65 in HK-2 cells treated with TNF-α and/or EVR for 24 h. Values represented the mean ± SD (n = 6, *p < 0.05, ***p < 0.001). TNF-α, tumor necrosis factor-α; KEGG, Kyoto Encyclopedia of Genes and Genomes; FN, fibronectin; QNZ, NF–κB inhibitor quinazoline; IF, immunofluorescence; EVR, everolimus.

When we investigated the effect of EVR on the TNF-activated-Akt pathway, however, we found that the TNF-activated Akt pathway was not significantly inhibited by EVR intervention (**Supplementary Figures 2E, F**). This phenomenon could be explained by the fact that EVR acts as an inhibitor of mTOR, whereas Akt is the upstream effector of the mTOR pathway.

To investigate a second latent mechanism through which EVR inhibits TNF-α-induced EMT, we identified many important mediators and their phosphorylation levels in the

NF-κB pathway, which was also significantly enriched by the KEGG pathway analysis. The results confirmed our expectations that TNF-α may promote phospho-p65 (p-p65), a marker of the NF-κB pathway activation, in a time-dependent manner (**Figures 6C, D**). TNF-α-induced EMT progression was reversed following treatment with QNZ, a specific inhibitor of the NF-κB pathway that inhibited p-p65 expression (**Figures 6E, F**). Given that p-p65 has been shown to activate the NF-κB pathway by promoting p65 nuclear translocation, we also investigated the effect of EVR on p65 nuclear translocation. The results of IF staining indicated that TNF-α promoted p65 nuclear translocation while increasing cytosolic p65 increased and decreasing nuclear p65 following the addition of EVR in TNF-α-treated HK2 cells (**Figure 6G**). Consistent with the IF staining results, the WB analysis of p65 protein expression in the nucleus and cytoplasm yielded the same results (**Figures 6H, I**).

EVR Inhibited TNF-α-Mediated EMT by Inhibiting Degradation of IκB-α in HK-2 Cells, and Skp2 Played an Essential Role in This Process

Given that phosphorylation/degradation of IκB-α precedes nuclear translocation of NF-κB and that upstream mediator IKK activates phosphorylation/degradation of IκB-α, we investigated IκB-α and IKK phosphorylation to elucidate the inhibitory effect of EVR on the upstream event of NF-κB. Then, using a Western blot assay, we identified several key downstream mediators of the NF-κB pathway in whole-cell lysates (WCL). We found that EVR significantly upregulated IκB-α and downregulated p-p65 protein in the presence of TNF-α stimulation, whereas total p65, IKK-α, and their protein phosphorylation levels remained unchanged compared to the TNF-α-treated group (**Figure 7A**). To ascertain if IκB-α degradation was responsible for NF-κB pathway activation, we also examined the relationship between IκB-α and ubiquitination. We found that IκB-α was coprecipitated with ubiquitin following TNF-α treatment and that this trend could be reversed by EVR (**Figures 7A, B**). Next, we determined whether TNF-α treatment-induced IκB-α downregulation was due to increased degradation or decreased synthesis at the transcriptional level. In contrast to IκB-α protein, NFKBIA mRNA (encoding IκB-α) was increased in TNF-α-treated cells and EVR pretreatment has no effect on this response (**Figure 7C**). This revealed that the EVR-mediated upregulation of IκB-α may be related to increased protein stability rather than increased mRNA expression. Therefore, we identified the roles of two major pathways—autophagy and ubiquitination, which are thought to be responsible for protein degradation on IκB-α protein levels. With TNF-α treatment, the presence of MG132, a ubiquitin–proteasome-mediated degradation inhibitor, significantly increased the stability of IκB-α protein. However, there was no significant variation in IκB-α protein levels when different concentrations of CQ were used (**Figures 7D, E**). The IF co-staining for ubiquitination (red immunofluorescence) and IκB-α (green immunofluorescence) also indicated that the ubiquitin–proteasome pathway was primarily responsible for IκB-α degradation (**Figure 7F**).

To elucidate the mechanism by which EVR inhibited IκB-α ubiquitination and degradation, we predicted the E3 ubiquitin ligase of IκB-α using UbiBrowser, an integrated bioinformatics platform (http://ubibrowser.ncpsb.org) (**Figure 7G**). According to our predicted results, we screened 3 genes (Skp2, Smurf1, and Smurf2) that were upregulated by TNF-α. Among these, EVR significantly decreased the Skp2 protein expression (**Figure 7H**). To further elucidate the function of Skp2 on IκB-α, Skp2 was knocked down using small interfering RNA (siRNA) (**Figures 7I, J**). As demonstrated in our previous study, si-Skp2 functions were similar to EVR. Knockdown of Skp2 expression decreased EMT progression and attenuated the IκB-α decrease in TNF-α-treated HK2 cells (**Figures 7K, L**).

EVR Upregulated IκB-α Protein and Downregulated Skp2 and p-p65 in CAD Rat Model

We used WB and IHC staining assays to confirm that IκB-α protein plays an essential role in the EVR-induced EMT inhibition in rat allograft kidneys. The results of WB demonstrated that the allo group expressed remarkably high levels of Skp2 and p-p65, and low expression of IκB-α, whereas EVR was able to reverse these proteins' expressions (**Figures 8A, B**). Additionally, the IHC staining experiment corroborated the results of the Western blot assay (**Figures 8C, D**). These findings suggested that the mechanism by which EMT progresses in CAD allografts may be related to dysregulation of IκB-α protein degradation and that EVR may play a role in stabilizing IκB-α protein by inhibiting Skp2.

DISCUSSION

In the present study, we demonstrated that EVR inhibited the TNF-α-induced EMT by activating autophagy and stabilizing IκB-α protein degradation, thus attenuating interstitial fibrosis in transplanted kidneys (**Figure 9**). TNF-α promotes EMT in HK2 cells by activating both the Akt and NF-κB pathways. However, it appeared as though EVR had an effect on NF-κB activation rather than the Akt signaling pathway. Although EVR is considered an immunosuppressive agent, it is only used in a few countries in the clinical treatment of rejection reactions. Since EVR can inhibit the mTOR pathway, it is able to regulate autophagy. However, a limited number of studies have been reported that show that EVR influences organ fibrosis through autophagy. Only one reported that EVR reduces postoperative arthrofibrosis inducing autophagy-mediated fibroblast apoptosis (29). To the best of our knowledge, this is the first study to examine the effects and underlying mechanism of EVR on renal interstitial fibrosis in CAD recipients to prevent impaired autophagic flux. Our findings provide new insights into allograft renal interstitial fibrosis treatment and prevention. Additionally, our findings revealed additional novel insights into EVR pharmacological targets that may facilitate CAD modulation. A pharmaceutical intervention that inhibits

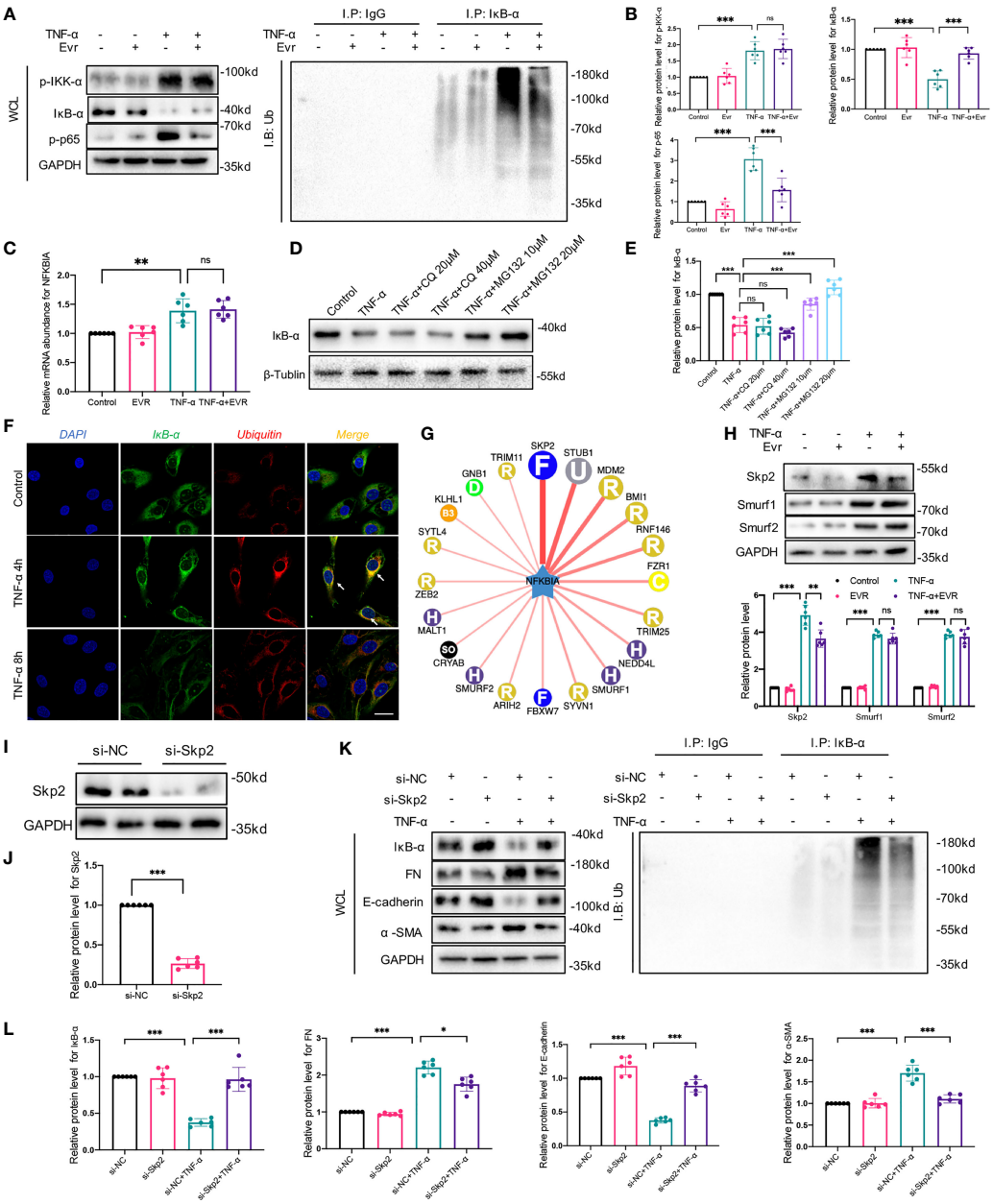


FIGURE 7 | EVR inhibited TNF-α-induced EMT by inhibiting degradation of IκB-α in HK-2 cells, and Skp2 played an essential role in this process. **(A)** Representative Western blotting results f p-IKK-α, IKK-α, IκB-α, p-p65, and p65 in WCL of HK-2 cells treated with TNF-α (50 ng/ml) and/or EVR (10 nM) for 24 h. In addition, immunoprecipitation was performed with a IκB-α antibody, and Western blot assays were used to examine the ubiquitin conjugation among the indicated groups. **(B)** Semi-quantitative analyses results of relative protein abundances of p-IKK-α, IKK-α, IκB-α, p-p65, and p65 in WCL of HK-2 cells treated with TNF-α and/or EVR for 24 h. Values represented the mean ± SD (n = 6, ns, not significant, $^{***}p < 0.001$). **(C)** Relative expression of the NFKBIA in HK-2 cells treated with TNF-α (50 ng/ml) and/or EVR (10 nM) for 24 h. Values represented the mean ± SD (n = 6, ns, not significant, $^{**}p < 0.01$). **(D)** Representative Western blotting results of IκB-α in HK2 cells treated with TNF-α (50 ng/ml) and different concentrations of CQ (20 and 40 μM)/MG132 (10 and 20 μM) for 24 h. **(E)** Semi-quantitative analyses results of relative protein abundance of IκB-α in HK-2 cells treated with TNF-α and CQ/MG132 for 24 h. Values represented the mean ± SD (n = 6, ns, not significant, $^{***}p < 0.001$). **(F)** Representative IF co-localization staining images of IκB-α and ubiquitin in HK-2 cells treated with TNF-α for 4 or 8 h (scale bar: 50 μm). **(G)** The network map of E3 ubiquitin ligase related to IκB-α predicted by UbiBrowser. **(H)** Representative Western blotting results of Skp2, Smurf1, and Smurf2 in HK2 cells treated with TNF-α (50 ng/ml) and/or EVR (10 nM) for 24 h. **(I, J)** Representative Western blotting results of negative control (NC) and small interfering RNA (si-Skp2) transfection efficiency in HK2 cells. **(K, L)** Representative Western blotting results of IκB-α, E-cadherin, α-SMA and FN in WCL of HK-2 cells treated with TNF-α (50 ng/ml) after transfecting si-Skp2 or si-NC. Immunoprecipitation was also performed with an IκB-α antibody, and Western blot assays were used to examine the ubiquitin conjugation among the indicated groups. Values represented the mean ± SD (n = 6, $^{*}p < 0.05$, $^{***}p < 0.001$). WCL, whole-cell lysates; IF, immunofluorescence; EVR, everolimus; CQ, chloroquine; α-SMA, α-smooth muscle actin; FN, fibronectin.

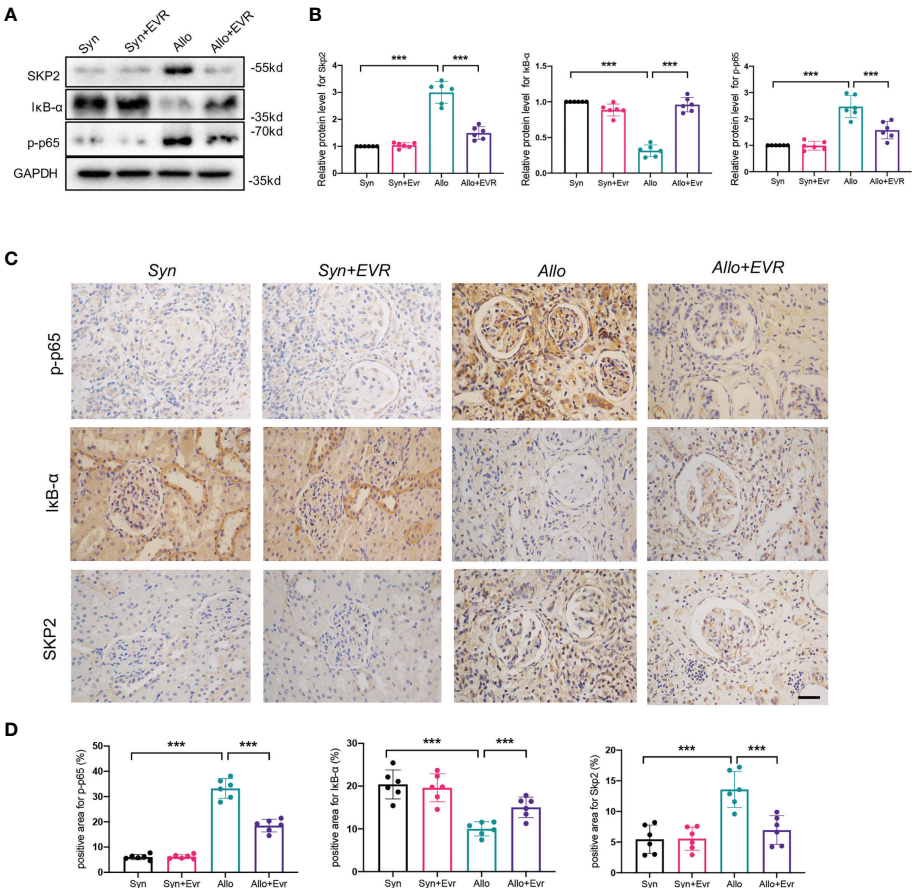


FIGURE 8 | EVR upregulated IκB-α protein and downregulated Skp2 and p-p65 in the CAD rat model. **(A)** Representative Western blotting results of Skp2, IκB-α, and p-p65 in kidney tissues from different treatment group rats. **(B)** Semi-quantitative analyses results of relative protein abundances of Skp2, IκB-α, and p-p65 in kidney tissues from different treatment group rats. Values represented the mean ± SD (n = 6, ***p < 0.001). **(C)** Representative IHC images of Skp2, IκB-α, and p-p65 in kidney sections from different treatment group rats (scale bar: 10 μm). **(D)** Semi-quantitative analyses results of IHC positive staining of Skp2, IκB-α, and p-p65 in kidney sections from different treatment group rats. Values represented the mean ± SD (n = 6, ***p < 0.001).

autophagy, such as EVR, is a promising first-line treatment option for patients who have undergone kidney transplantation.

Although CAD manifests in a variety of ways and causes a variety of different forms of kidney injury, the underlying molecular process remains unknown. EMT is the initial stage of irreversible tubular injury and interstitial fibrosis, which is followed by increasing loss of renal function and eventually results in an annual loss of approximately 5% of allograft function. Unfortunately, while numerous studies demonstrated that EMT was a classic source of myofibroblasts and fibroblasts during renal fibrosis, few effective clinical therapeutic strategies for reversing the course of these modifications were discovered. We previously demonstrated that TNF-α promoted EMT in HK2 cells by activating the Akt pathway, and this process may play a critical role in exacerbating interstitial fibrosis in CAD patients with transplanted kidneys (28). Therefore, in this study, we sought to discover a novel therapeutic agent capable of reversing the course of CAD by inhibiting TNF-α-induced EMT.

Recently, due to its immunosuppressive effect, EVR has garnered much greater attention as a molecular targeting drug (18). Meanwhile, EVR has anti-pulmonary fibrosis, anti-renal fibrosis, anti-arthrofibrosis, and anti-hepatic fibrosis therapeutic potential in addition to its widespread use in traditional anti-cancer therapies (21, 29, 30). However, overall safety data for EVR in CAD patients, obtained from controlled research with the CsA group, revealed that EVR was superior to measured glomerular filtration rate (mGFR), but was associated with more adverse events (19). This study suggested that poor tolerance to EVR was closely related to its dose-limiting toxicity (19). Therefore, we investigated the dose-dependent effect of EVR on HK2 cells treated with different concentrations of EVR, i.e., 5, 10, 50, and 100 nM for 24 h. We discovered that autophagy levels were much lower in the high-dose EVR-treated group than in the control group. Therefore, when we performed other interventions with cells in this study, the concentration of EVR was strictly controlled. The findings were consistent with those from previous studies that high-dose EVR (at least more than

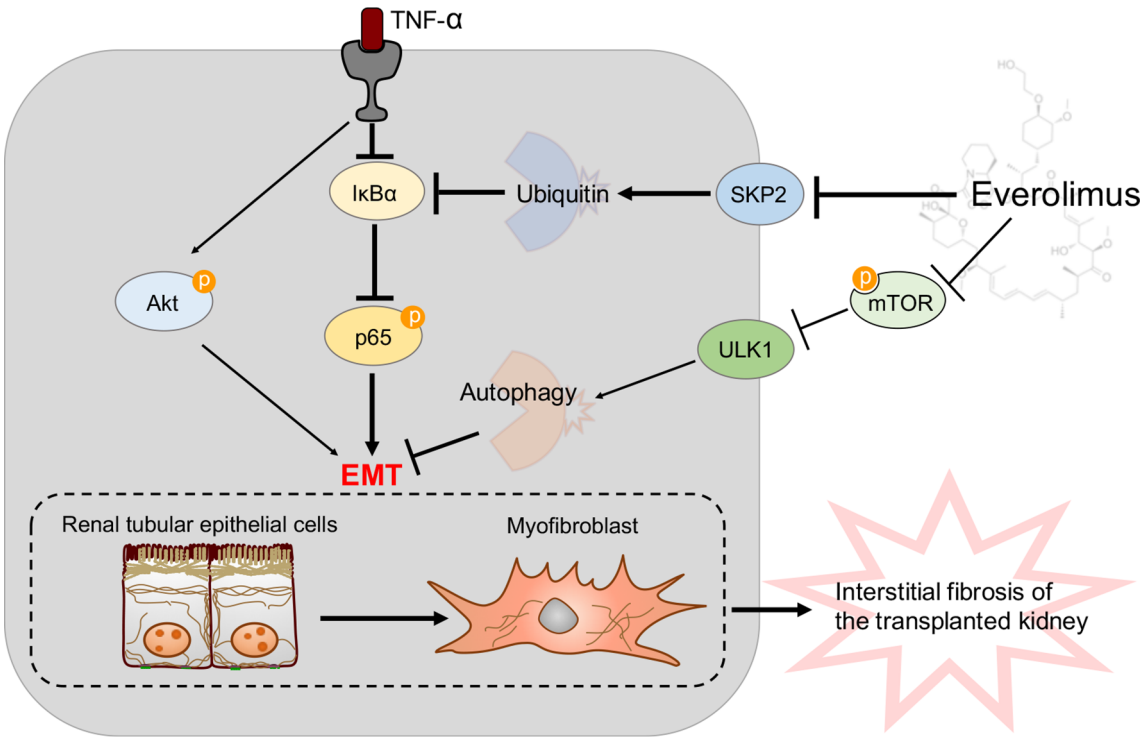


FIGURE 9 | A model is proposed to illustrate the protective mechanisms of EVR on the pathogenesis of transplanted renal tubular EMT and interstitial fibrosis in CAD. TNF-α could induce renal tubular EMT and then promote transplanted renal interstitial fibrosis through Akt and NF-κB signaling pathway activation in CAD recipients. Of these, NF-κB signaling pathway activation was due to IκB-α decrease and p-p65 increase. On the one hand, EVR could inhibit progression of renal tubular EMT *via* blocking the mTOR/ULK1 pathway to activate autophagy flux directly. On the other hand, EVR could also affect Skp2 (a E3 ubiquitin ligase) activity and inhibit IκB-α ubiquitin degradation, and thus restrain progression of renal tubular EMT through impacting NF-κB pathway activation. Red arrows represent the effect of TNF-α and dark blue arrows represent the effect of EVR.

100 nM) could induce EMT in airway epithelial cells and exacerbate pulmonary fibrosis (31). Furthermore, other investigations revealed that the results in intact animals were consistent with the *in vitro* findings that high-dose EVR induced worsening of renal function, but that early treatment with a low dose of EVR was effective in preventing rat kidney injury (32). According to some reports, we assumed that this side effect of EVR was caused by excessive autophagic activation (33, 34).

We previously established that ATG16L and autophagic flux were activated in the early stages of kidney transplantation, but that autophagic flux reduced in a dynamic range at a late stage. mTOR signaling inhibition has been shown to have a positive effect on the cellular autophagy cascade (33, 35). On this basis, we hypothesized that EVR exerted its anti-fibrosis effects through the resistance of impaired autophagic flux following kidney transplantation. To investigate the association between EVR, autophagy, and TNF-α-induced EMT in the transplanted kidneys, EVR was used at an optimum selection concentration in the CAD rat model and HK2 cells. We explored whether EVR could help alleviate renal allograft interstitial fibrosis and the progression of EMT in CAD rats. Meanwhile, autophagy was increased in the Allo+EVR group compared to rats that had only received transplantation, and EVR aided in maintaining a stable state of autophagy flux. These findings were also confirmed in HK2 cells, where EVR restored epithelial cell markers and decreased mesenchymal marker expressions in TNF-α-treated HK2 cells *via* autophagy activation. However, our findings appeared to contradict the findings of Nakagawa et al., that EVR-induced autophagy aggravates tubular dysfunction during kidney injury recovery (34). We hypothesized that the mechanism of action would differ according to the role of autophagy in different pathological environments.

To gain additional insights into the potential mechanisms of EVR on TNF-α-mediated-EMT, total RNA from HK2 cells treated with TNF-α and control cultures were sequenced by RNA-seq. KEGG pathway analysis revealed a significant enrichment of the Akt pathway, which is well known to regulate mTOR upstream. Therefore, we first assumed that EVR had a direct effect on TNF-α-mediated EMT *via* the Akt pathway. Contrary to expectations, we discovered that TNF-α could activate Akt but EVR did not affect Akt phosphorylation. However, other investigations revealed that EVR could reduce arthrofibrosis by downregulating the expression levels of p-PI3K, p-Akt, and p-mTOR (29). Additionally, RNA-seq data revealed a link between EVR and TNF-α-mediated EMT in HK2 cells *via* the NF-κB pathway.

Members of the IκB family include NF-κB1 (p105), NF-κB2 (p100), IκB-α, IκB-β, and IκB-ϵ. Among the IκB family proteins, IκB-α mainly mediates basal inhibition of NF-κB activity. The activated IκB kinase complex phosphorylates IκB-α, which is then followed by the ubiquitination of IκB-α and its subsequent degradation by the proteosome. External stimulatory signals first activate the IκB kinase (IKK), which subsequently phosphorylates IκB-α and decomposes the NF-κB–IκB complex. This process is a prerequisite for NF-κB pathway activation, with p-p65 nuclear translocation being the outcome (36). Therefore, we examined the effect of EVR on the expression of IKK, p-IKK, IκB-α, p65, and p-p65 proteins following TNF-α and/or EVR treatment. In general, p-IKK-mediated IκB-α phosphorylation resulted in its ubiquitination and subsequent degradation (36). Nevertheless, several investigations demonstrated that TNF-α promoted biphasic degradation of IκB-α in intestinal epithelial cells *via* autophagy and the proteasome (37). However, our data indicated that autophagy played a lesser role in the stabilization of IκB-α in epithelial cells of the renal tubules. According to the WB analysis results, EVR had no effect on TNF-α-activated IKK phosphorylation but inhibited IκB-α ubiquitylation degradation. Next, we performed a predictive screening of E3 ubiquitin ligases known to affect IκB-α degradation and found that EVR could decrease IκB-α degradation by inhibiting Skp2 expression. The relationship between rapamycin and Skp2 has been previously described in breast cancer (38). Coincidentally, it has been demonstrated that EVR leads to a suppression of their paracrine and accelerate osteoclast activity by interfering with the NF-κB pathway (39). However, there is no in-depth research to explain how EVR affects this pathway. Our research suggests that derivatives of rapamycin-EVR may also prevent TNF-α-induced EMT by downregulating Skp2 to inhibit IκB-α ubiquitination degradation and NF-κB pathway activation.

Our research has several limitations. The current validation of EVR's effects on TNF-α-induced EMT and renal allograft interstitial fibrosis was conducted in an epithelial cell line and animal model, which may not accurately mimic the complexity of *in vivo* changes occurring during CAD progression. Although we successfully established a rat CAD model to investigate the effects of EVR on the establishment of renal tubular EMT and interstitial fibrosis in allograft kidneys, further confirmation of the role of NF-κB signaling pathway and IκB-α protein on this process may require using knockout mice. Additionally, data from patients treated with EVR after kidney transplantation are also important. At the time of reporting, no therapy with EVR had been attempted in our patients. EVR's safety and long-term effects as an immunosuppressant must still be explored further before it is approved for clinical use.

The findings presented in this paper demonstrate that EVR can attenuate TNF-α-induced EMT and interstitial fibrosis in renal allografts. Our findings further demonstrate that EVR's therapeutic potential is not limited to its ability to induce autophagy, but also to its effect on NF-κB signaling inactivity by inhibiting IκB-α protein ubiquitylation degradation, and Skp2 may serve as a novel target protein between EVR and IκB-α. The findings of this study provide novel insight into the role of EVR in the autophagy-dependent and autophagy-independent pathways. The development of more autophagy-targeting drugs for the treatment and prevention of renal interstitial fibrosis and CAD progression in kidney transplant recipients is expected in the near future. Altogether, the present investigation will contribute to the development of new clinical interventions for CAD patients, and EVR may be recommended as a novel option for the prevention and treatment of renal allograft interstitial fibrosis, in addition to its immunosuppressive effects.

MATERIALS AND METHODS

Rats and Animal Models

First, to minimize alloimmunity, isogeneic transplants were performed between inbred rats. Based on our pervious observations (28) and on the literature (40, 41), a classical rat model of kidney transplantation was established. The stability of the genetic background in inbred rats avoided the fluctuation in the parameters. Thus, adult male Lewis (LEW/Crl; LEW) inbred rats and F344 (F344/DuCrl; CDF) inbred rats (Age 6 to 8 weeks, weight 250 ± 10.3 g) were purchased from Charles River Laboratories (Beijing, China). To observe ethical codes of research, approval of Institutional Animal Care and Use Committee at Nanjing Medical University was obtained (ID: IACUC-2010020). Animal handling was done adhering to the guidelines for animal handling at the Nanjing Medical University and the guidelines published by the US National Institutes of Health. The place for animal experiments was the Laboratory Animal Center of Nanjing Medical University.

Orthotopic left kidney transplantation was performed between F344 and Lewis rats as previously described (28). Right nephrectomy was performed simultaneously. The cold ischemia time was defined as the grafts were stored in cold saline and the warm ischemia time was defined as the period between the cessation of donor blood supply to an organ and the beginning of cold perfusion. Mean cold ischemia time for the kidney transplants was less than 30 min, and for the warm ischemia, it was less than 10 s. A low dose of cyclosporine A (5 mg/kg, qd, ip; Neoral, Novartis, Switzerland) was administered for 10 days after kidney transplantation surgery to prevent acute rejection.

Rats were randomly divided into four groups of 6 rats each before kidney transplantation: Lewis rats used as syngeneic donors were defined as the Syn group (Lewis to Lewis), Lewis rats used as recipients were defined as the Allo group (F344 to Lewis), and the Syn and Allo group rats treated with EVR (1.5 mg/kg body weight, Novartis, Basel, Switzerland) were defined as the Syn+EVR group and the Allo+EVR group. Both groups were treated with EVR or a matched vehicle by oral gavage once per 2 days, continuing for 8 to 20 weeks. Kidneys, serum, and urine samples were collected at 8, 12, 16, and 20 weeks after kidney transplantation. The levels of blood urea nitrogen and serum creatinine were measured to examine renal function by using rat QuantiChromassay kits (Jiancheng, Beijing, China). The 24-h urinary protein concentration was determined by the

commercial kit (Mlbio, Shanghai, China) according to the instructions of the manufacturer.

Renal Histological Pathology Analyses

Histological analyses were performed by using periodic acid–Schiff (PAS) and Masson's trichome staining. PAS and Masson's trichome staining were performed as previously described (28), which was used to evaluate the severity of tubular injury (tubular lumen dilation, cast formation, tubular cell sloughing, atrophy, and basement membrane thickening) and the area of renal interstitial fibrosis separately. Two pathologists double-blindly read the pathological sections and used Image-Pro Plus (Media Cybernetics, Rockville, MD) to quantify the morphometric changes of the transplanted kidneys.

Immunohistochemistry Staining Assay

Kidney samples were fixed in 10% neutral formalin and embedded in paraffin. Three-micrometer-thick sections were used for immunohistochemical staining assay. Simply, paraffin-embedded kidney sections were deparaffinized, hydrated, and antigen-retrieved, and endogenous peroxidase activity was quenched by 3% H_2O_2. Sections were then blocked with 10% normal donkey serum, followed by incubation with anti-FN (Abcam, USA), anti-α-SMA (Abcam, USA), anti-E-cadherin (Abcam, USA), anti-LC3 (CST, USA), anti-p-p65 (CST, USA), and anti-Skp2 (CST, USA) overnight at 4°C. After incubation with secondary antibody for 1 h, sections were incubated with ABC reagents for 1 h at room temperature before being subjected to substrate 3-amino-9-ethylcarbazole or 3,3′diaminobenzidine (Vector Laboratories, Burlingame, CA). The stained slides were photographed using a Nikon Eclipse 80i microscope equipped with a digital camera (DS-Ri1, Nikon, Shanghai, China).

Indirect Immunofluorescence Staining Assay

For tissue indirect immunofluorescence staining, the staining method was the same as in (24). For HK2 cell indirect immunofluorescence staining, a total of 5×10^5 cells were seeded into laser confocal dishes with a preplaced glass slide. Cells were treated by 50 ng/ml TNF-α with or without EVR for 24 h. Then, the cells were fixed with methanol for 15 min at room temperature and washed twice with PBS. After blocking was completed, sections were co-incubated with anti-FN (Abcam, USA), anti-E-cadherin (Abcam, USA), anti-p65 (CST, USA), anti-ubiquitin (Santa Cruz, USA) and anti-IκB-α (CST, USA) overnight at 4°C. Next, the cells were stained with 4,6-diamidino-2-phenylindole (DAPI) to visualize the nuclei and washed twice with PBS. Finally, cells were detected under a Nikon Eclipse 80i microscope (DS-Ri1, Nikon, Shanghai, China).

Wound Healing and Transwell Migration Experiments

HK2 cells that had been treated with TNF-α were seeded into 6-well culture plates. For the wound-healing experiment, a straight scratch was made in the cell monolayer with a 200-μl pipette tip when the cells were 90% confluent. DMEM/F12 with 10% fetal bovine serum (FBS) was changed to serum-free DMEM/F12 (DFSF) for 24 h. The scratch was examined and photographed under a light microscope, and the cell-free area was quantified using the ImageJ software.

For the Transwell migration assay, the cells were seeded into the upper chamber of 24-well Transwell plates with 200 μl of medium. Then, the lower chamber was filled with 600 μl of 10% FBS-supplemented DFSF, and the HK2 cells were cultured for 12 h. Subsequently, the cells on the upper surface of the chamber were removed using a cotton swab. The cells on the bottom surface were fixed in 4% paraformaldehyde (PFA) for 30 min and stained with 0.1% crystal violet for 10 min. The migrated cells were photographed under a microscope, and the images were analyzed using ImageJ software.

Cell Culture and Treatment

The HK2 cells were purchased from KeyGEN BioTECH (Nanjing, China). The cells were cultured in DFSF medium containing 10% FBS (Gibco, Carlsbad, CA, USA) at 37°C with 5% CO_2, supplemented with 1% penicillin-streptomycin. HK2 cells were seeded on six-well culture plates for 24 h in complete medium containing 10% FBS. After starvation with DFSF for 16 h, the cells were modulated with TNF-α (50 ng/ml, Peprotech, Rocky Hill, NJ, USA) and/or EVR (5, 10, 50, and 100 nM, Selleck, Houston, TX, USA) for 48 h. In some experiments, cells were pretreated with CQ (20 μM, Selleck, Houston, TX, USA) or protein kinase B (Akt) inhibitor MK2206 (10 μM, Selleck, Houston, TX, USA) or QNZ (100 nM, Selleck, Houston, TX, USA) for 2 h before the addition of TNF-α and/or EVR. The cells were then collected for different assays. For small interfering RNA (siRNA) transfection assay, HK-2 cells at 80% confluence were transfected with Skp2-specific siRNA by using Lipofectamine 2000 (Invitrogen, Carlsbad, CA, USA) according to the instructions. Then, cells were treated as previously described after transfection for 6 h. The siRNAs were obtained from HanHeng Biotechnology (Shanghai, China). All the experiments were repeated at least three times.

Western Blot and Coimmunoprecipitation Assay

Cells and kidney tissue were lysed by RIPA lysis buffer containing cocktail protease inhibitors for 30 min on ice. To isolate nuclear proteins, HK-2 cells were collected and nuclear were extracted according to the instruction of Nuclear and Cytoplasmic Extraction kit (KeyGEN BioTECH, Nanjing, China). Proteins from HK-2 cells and rat tissues were fractionated by electrophoresis on 8%–12% sodium dodecyl sulfate-polyacrylamide gel electrophoresis, electroblotted to polyvinylidene fluoride filter membranes, and incubated with the primary antibody at 4°C. For the co-IP experiment, briefly, the cell supernatants were pre-treated with protein A/G agarose (Santa Cruz Bio-technology, sc-2003) beads for 1 h at 4°C. Then, 2 μg of the corresponding primary antibody was added to the supernatants overnight at 4°C. Next, 50 μl of protein A/G agarose was added for 4 h. The beads were washed more than three times using ice-cold PBS or cell lysis buffer, and the bound proteins were boiled in loading buffer for further analysis. The primary antibodies were as follows: anti-β-actin (CST, Danvers, MA, USA), anti-Glyceraldehyde 3-phosphate dehydrogenase

(GAPDH) (CST, Danvers, MA, USA), anti-Histone H3 (CST, Danvers, MA, USA), anti-β-tubulin (CST, Danvers, MA, USA), anti-E-cadherin (SAB Biotech, College Park, MD, USA), anti-α-SMA (SAB Biotech, College Park, MD, USA), anti-FN (BD Biosciences, USA), anti-Akt (CST, Danvers, MA, USA), anti-phospho-Akt (CST, Danvers, MA, USA), anti-mammalian target of rapamycin (mTOR) (CST, Danvers, MA, USA), anti-Unc-like kinase 1 (ULK1) (CST, Danvers, MA, USA), anti-phospho-mTOR (CST, Danvers, MA, USA), anti-phospho-P70S6K (CST, Danvers, MA, USA), anti-IκB Kinase α (IKKα) (CST, Danvers, MA, USA), anti-phospho-IKKα (CST, Danvers, MA, USA), anti-IκB-α (CST, Danvers, MA, USA), anti-phospho-IκB-α (CST, Danvers, MA, USA), anti-nuclear factor kappa B (NF-κB) p65 (CST, Danvers, MA, USA), anti-phospho-NF-κB p65 (CST, Danvers, MA, USA), anti-ubiquitin (Santa Cruz, USA), anti-Smurf1 (SAB Biotech, College Park, MD, USA), and anti-Smurf2 (SAB Biotech, College Park, MD, USA). This step was followed by incubation with an anti-rabbit or anti-mouse secondary antibody (1:4,000; ZSGB-BIO, Beijing, China). GAPDH, β-actin, and Histone H3 were used to verify equal loading of proteins. The intensity of the indicated bands were measured by Image Lab software (Bio-Rad, Hercules, CA, USA).

Quantitative Real-Time Polymerase Chain Reaction

Total RNAs were extracted from tissues and cells with the RNA Extraction Kits (TIANGEN, Beijing, China). Detailed steps are described in (24). Gene expressions were measured by real-time PCR assay (Vazyme, Nanjing, China) and a DNA Engine Opticon 2 System (BioRad Laboratories, Hercules, CA, USA). Every experiment was repeated at least three times. The specific primers used were as follows:

NFKBIA: 5′-CTCCGAGACTTTCGAGGAAATAC-3′ (F)
5′-GCCATTGTAGTTGGTAGCCTTCA-3′ (R)

Electron Microscopy

The samples were fixed with ice-cold glutaraldehyde (3% in 0.1 M cacodylate buffer, pH 7.4) and further processed by the Core Facility (Servicebio, Wuhan, China). Observations were performed on a JEOL JEM-2100 transmission electron microscope.

Transcriptome Sequencing

Total RNA was used as input material for the RNA sample preparations. Sequencing libraries were generated using NEBNext® UltraTM RNA Library Prep Kit for Illumina® (NEB, USA) following manufacturer's recommendations and index codes were added to attribute sequences to each sample.

Briefly, mRNA was purified from total RNA using poly-T oligo-attached magnetic beads. Fragmentation was carried out using divalent cations under elevated temperature in NEBNext First Strand Synthesis Reaction Buffer (5×). First strand cDNA was synthesized using random hexamer primer and M-MuLV Reverse Transcriptase (RNase H). Second-strand cDNA synthesis was subsequently performed using DNA Polymerase I and RNase H. Remaining overhangs were converted into blunt ends *via* exonuclease/polymerase activities. After adenylation of 3' ends of DNA fragments, NEBNext Adaptor with hairpin loop structure was ligated to prepare for hybridization. In order to select cDNA fragments of preferentially 250–300 bp in length, the library fragments were purified with AMPure XP system (Beckman Coulter, Beverly, USA). Then 3 μl of USER Enzyme (NEB, USA) was used with size-selected, adaptor-ligated cDNA at 37°C for 15 min followed by 5 min at 95°C before PCR. Then, PCR was performed with Phusion High-Fidelity DNA polymerase, Universal PCR primers, and Index (X) Primer. Last, PCR products were purified (AMPure XP system) and library quality was assessed on the Agilent Bioanalyzer 2100 system.

Statistical Analysis

GraphPad Prism 5.0 (GraphPad Software, Inc., La Jolla, CA, USA) was used for statistical analysis. Data were presented as means ± standard error of the mean (SEM) from at least three independent experiments. Comparison between and within multiple groups was performed using one-way analysis of variance followed by Student-Newman-Keuls test. p-values of <0.05 were considered significant.

DATA AVAILABILITY STATEMENT

The original contributions presented in the study are publicly available. This data can be found here: https://www.ncbi.nlm.nih.gov/PRJNA757419.

ETHICS STATEMENT

The animal study was reviewed and approved by the Institutional Animal Care and Use Committee at Nanjing Medical University. Written informed consent was obtained from the owners for the participation of their animals in this study.

AUTHOR CONTRIBUTIONS

RT and MG supervised and conceived the project. ZG, CS, JT, and ZW designed and carried out most of the experiments. MZ and SF collected the samples of rats. LS, HC, ZH, and XJ analyzed the data. ZG and ZW made the figures. ZG and RT drafted and revised the paper. All authors contributed to the article and approved the submitted version.

FUNDING

This work has been supported by the National Natural Science Foundation of China (grant numbers 82070769, 81870512, 81770751, 81570676, 81470981, and 81100532).

SUPPLEMENTARY MATERIAL

The Supplementary Material for this article can be found online at: https://www.frontiersin.org/articles/10.3389/fimmu.2021.753412/full#supplementary-material

REFERENCES

1. Carney EF. Transplantation: Survival Benefit of Accepting a Diabetic Deceased Donor Kidney. *Nat Rev Nephrol* (2017) 13(8):444. doi: 10.1038/nrneph.2017.88
2. El-Husseini A, Aghil A, Ramirez J, Sawaya B, Rajagopalan N, Baz M, et al. Outcome of Kidney Transplant in Primary, Repeat, and Kidney-After-Nonrenal Solid-Organ Transplantation: 15-Year Analysis of Recent UNOS Database. *Clin Transplant* (2017) 31(11):e13108. doi: 10.1111/ctr.13108
3. Schinstock CA, Stegall M, Cosio F. New Insights Regarding Chronic Antibody-Mediated Rejection and Its Progression to Transplant Glomerulopathy. *Curr Opin Nephrol Hypertens* (2014) 23(6):611–8. doi: 10.1097/MNH.0000000000000070
4. Goldberg RJ, Weng FL, Kandula P. Acute and Chronic Allograft Dysfunction in Kidney Transplant Recipients. *Med Clin North Am* (2016) 100(3):487–503. doi: 10.1016/j.mcna.2016.01.002
5. Wang Z, Han Z, Tao J, Wang J, Liu X, Zhou W, et al. Role of Endothelial-to-Mesenchymal Transition Induced by TGF-Beta1 in Transplant Kidney Interstitial Fibrosis. *J Cell Mol Med* (2017) 21(10):2359–69. doi: 10.1111/jcmm.13157
6. Sutariya B, Jhonsa D, Saraf MN. TGF-Beta: The Connecting Link Between Nephropathy and Fibrosis. *Immunopharmacol Immunotoxicol* (2016) 38 (1):39–49. doi: 10.3109/08923973.2015.1127382
7. An C, Jia L, Wen J, Wang Y. Targeting Bone Marrow-Derived Fibroblasts for Renal Fibrosis. *Adv Exp Med Biol* (2019) 1165:305–22. doi: 10.1007/978-981-13-8871-2_14
8. Cruz-Solbes AS, Youker K. Epithelial to Mesenchymal Transition (EMT) and Endothelial to Mesenchymal Transition (EndMT): Role and Implications in Kidney Fibrosis. *Results Probl Cell Differ* (2017) 60:345–72. doi: 10.1007/978-3-319-51436-9_13
9. Di Gregorio J, Robuffo I, Spalletta S, Giambuzzi G, De Iuliis V, Toniato E, et al. The Epithelial-To-Mesenchymal Transition as a Possible Therapeutic Target in Fibrotic Disorders. *Front Cell Dev Biol* (2020) 8:607483. doi: 10.3389/fcell.2020.607483
10. Yang J, Antin P, Berx G, Blanpain C, Brabletz T, Bronner M, et al. Guidelines and Definitions for Research on Epithelial-Mesenchymal Transition. *Nat Rev Mol Cell Biol* (2020) 21(6):341–52. doi: 10.1038/s41580-020-0237-9
11. Blom JN, Feng Q. Cardiac Repair by Epicardial EMT: Current Targets and a Potential Role for the Primary Cilium. *Pharmacol Ther* (2018) 186:114–29. doi: 10.1016/j.pharmthera.2018.01.002
12. Andugulapati SB, Gourishetti K, Tirunavalli SK, Shaikh TB, Sistla R. Biochanin-A Ameliorates Pulmonary Fibrosis by Suppressing the TGF-Beta Mediated EMT, Myofibroblasts Differentiation and Collagen Deposition in In Vitro and *In Vivo* Systems. *Phytomedicine* (2020) 78:153298. doi: 10.1016/j.phymed.2020.153298
13. Wang Z, Divanyan A, Jourd'heuil FL, Goldman RD, Ridge KM, Jourd'heuil D, et al. Vimentin Expression Is Required for the Development of EMT-Related Renal Fibrosis Following Unilateral Ureteral Obstruction in Mice. *Am J Physiol Renal Physiol* (2018) 315(4):F769–80. doi: 10.1152/ajprenal.00340.2017
14. Zhao C, Xu Z, Wang Z, Suo C, Tao J, Han Z, et al. Role of Tumor Necrosis Factor-Alpha in Epithelial-to-Mesenchymal Transition in Transplanted Kidney Cells in Recipients With Chronic Allograft Dysfunction. *Gene* (2018) 642:483–90. doi: 10.1016/j.gene.2017.11.059
15. Romanowska-Prochnicka K, Felis-Giemza A, Olesinska M, Wojdasiewicz P, Paradowska-Gorycka A, Szukiewicz D. The Role of TNF-Alpha and Anti-TNF-Alpha Agents During Preconception, Pregnancy, and Breastfeeding. *Int J Mol Sci* (2021) 22(6):2922. doi: 10.3390/ijms22062922
16. Al-Lamki RS, Mayadas TN. TNF Receptors: Signaling Pathways and Contribution to Renal Dysfunction. *Kidney Int* (2015) 87(2):281–96. doi: 10.1038/ki.2014.285
17. Fasolo A, Sessa C. Targeting mTOR Pathways in Human Malignancies. *Curr Pharm Des* (2012) 18(19):2766–77. doi: 10.2174/138161212800626210
18. Fischer L, Saliba F, Kaiser GM, De Carlis L, Metselaar HJ, De Simone P, et al. Three-Year Outcomes in *De Novo* Liver Transplant Patients Receiving Everolimus With Reduced Tacrolimus: Follow-Up Results From a Randomized, Multicenter Study. *Transplantation* (2015) 99(7):1455–62. doi: 10.1097/TP.0000000000000555
19. Mjornstedt L, Schwartz Sorensen S, von Zur Muhlen B, Jespersen B, Hansen JM, Bistrup C, et al. Renal Function Three Years After Early Conversion From a Calcineurin Inhibitor to Everolimus: Results From a Randomized Trial in Kidney Transplantation. *Transpl Int* (2015) 28(1):42–51. doi: 10.1111/tri.12437
20. Shigematsu T, Tajima S, Fu R, Zhang M, Itoyama Y, Tsuchimoto A, et al. The mTOR Inhibitor Everolimus Attenuates Tacrolimus-Induced Renal Interstitial Fibrosis in Rats. *Life Sci* (2021) 288:120150. doi: 10.1016/j.lfs.2021.120150
21. Eren MF, Ay Eren A, Sayan M, Yucel B, Elagoz S, Ozguven Y, et al. The Impact of Everolimus and Radiation Therapy on Pulmonary Fibrosis. *Med (Kaunas)* (2020) 56(7):348. doi: 10.3390/medicina56070348
22. Masola V, Carraro A, Zaza G, Bellin G, Montin U, Violi P, et al. Epithelial to Mesenchymal Transition in the Liver Field: The Double Face of Everolimus In Vitro. *BMC Gastroenterol* (2015) 15:118. doi: 10.1186/s12876-015-0347-6
23. Sarbassov DD, Ali SM, Sabatini DM. Growing Roles for the mTOR Pathway. *Curr Opin Cell Biol* (2005) 17(6):596–603. doi: 10.1016/j.ceb.2005.09.009
24. Gui Z, Suo C, Wang Z, Zheng M, Fei S, Chen H, et al. Impaired ATG16L-Dependent Autophagy Promotes Renal Interstitial Fibrosis in Chronic Renal Graft Dysfunction Through Inducing EndMT by NF-kappaB Signal Pathway. *Front Immunol* (2021) 12:650424. doi: 10.3389/fimmu.2021.650424
25. Hill C, Li J, Liu D, Conforti F, Brereton CJ, Yao L, et al. Autophagy Inhibition-Mediated Epithelial-Mesenchymal Transition Augments Local Myofibroblast Differentiation in Pulmonary Fibrosis. *Cell Death Dis* (2019) 10(8):591. doi: 10.1038/s41419-019-1820-x
26. Pang M, Wang H, Rao P, Zhao Y, Xie J, Cao Q, et al. Autophagy Links Beta-Catenin and Smad Signaling to Promote Epithelial-Mesenchymal Transition *via* Upregulation of Integrin Linked Kinase. *Int J Biochem Cell Biol* (2016) 76:123–34. doi: 10.1016/j.biocel.2016.05.010
27. Sun Y, Xiong L, Wang X, Wang L, Chen B, Huang J, et al. Autophagy Inhibition Attenuates TGF-Beta2-Induced Epithelial-Mesenchymal Transition in Lens Epithelial Cells. *Life Sci* (2021) 265:118741. doi: 10.1016/j.lfs.2020.118741
28. Zhou J, Cheng H, Wang Z, Chen H, Suo C, Zhang H, et al. Bortezomib Attenuates Renal Interstitial Fibrosis in Kidney Transplantation *via* Regulating the EMT Induced by TNF-Alpha-Smurf1-Akt-mTOR-P70S6K Pathway. *J Cell Mol Med* (2019) 23(8):5390–402. doi: 10.1111/jcmm.14420
29. Liu Y, Zhang Z, Yan L, Li X, Zhang J, Zhang X, et al. Everolimus Reduces Postoperative Arthrofibrosis in Rabbits by Inducing Autophagy-Mediated Fibroblast Apoptosis by PI3K/Akt/mTOR Signaling Pathway. *Biochem Biophys Res Commun* (2020) 533(1):1–8. doi: 10.1016/j.bbrc.2020.08.039
30. Choi YY, Seok JI, Hwang JI, Kim DS. Co-Administration of Everolimus and N-Acetylcysteine Attenuates Hepatic Stellate Cell Activation and Hepatic Fibrosis. *Am J Transl Res* (2020) 12(6):2627–39.
31. Tomei P, Masola V, Granata S, Bellin G, Carratu P, Ficial M, et al. Everolimus-Induced Epithelial to Mesenchymal Transition (EMT) in Bronchial/Pulmonary Cells: When the Dosage Does Matter in Transplantation. *J Nephrol* (2016) 29(6):881–91. doi: 10.1007/s40620-016-0295-4
32. Ramadan R, Faour D, Awad H, Khateeb E, Cohen R, Yahia A, et al. Early Treatment With Everolimus Exerts Nephroprotective Effect in Rats With Adriamycin-Induced Nephrotic Syndrome. *Nephrol Dial Transplant* (2012) 27(6):2231–41. doi: 10.1093/ndt/gfr581
33. Kurdi A, De Doncker M, Leloup A, Neels H, Timmermans JP, Lemmens K, et al. Continuous Administration of the Mtorc1 Inhibitor Everolimus Induces Tolerance and Decreases Autophagy in Mice. *Br J Pharmacol* (2016) 173 (23):3359–71. doi: 10.1111/bph.13626
34. Nakagawa S, Nishihara K, Inui K, Masuda S. Involvement of Autophagy in the Pharmacological Effects of the mTOR Inhibitor Everolimus in Acute Kidney Injury. *Eur J Pharmacol* (2012) 696(1-3):143–54. doi: 10.1016/j.ejphar.2012.09.010
35. Wang Y, Liu Z, Shu S, Cai J, Tang C, Dong Z. AMPK/mTOR Signaling in Autophagy Regulation During Cisplatin-Induced Acute Kidney Injury. *Front Physiol* (2020) 11:619730. doi: 10.3389/fphys.2020.619730
36. Zhang Q, Lenardo MJ, Baltimore D. 30 Years of NF-Kappab: A Blossoming of Relevance to Human Pathobiology. *Cell* (2017) 168(1-2):37–57. doi: 10.1016/j.cell.2016.12.012
37. Colleran A, Ryan A, O'Gorman A, Mureau C, Liptrot C, Dockery P, et al. Autophagosomal IkappaB Alpha Degradation Plays a Role in the Long Term

Control of Tumor Necrosis Factor-Alpha-Induced Nuclear factor-kappaB (NF-Kappab) Activity. *J Biol Chem* (2011) 286(26):22886–93. doi: 10.1074/jbc.M110.199950

38. Shapira M, Kakiashvili E, Rosenberg T, Hershko DD. The mTOR Inhibitor Rapamycin Down-Regulates the Expression of the Ubiquitin Ligase Subunit Skp2 in Breast Cancer Cells. *Breast Cancer Res* (2006) 8(4):R46. doi: 10.1186/bcr1533
39. Simone V, Ciavarella S, Brunetti O, Savonarola A, Cives M, Tucci M, et al. Everolimus Restrains the Paracrine Pro-Osteoclast Activity of Breast Cancer Cells. *BMC Cancer* (2015) 15:692. doi: 10.1186/s12885-015-1717-8
40. Li J, Basler M, Alvarez G, Brunner T, Kirk CJ, Groettrup M. Immunoproteasome Inhibition Prevents Chronic Antibody-Mediated Allograft Rejection in Renal Transplantation. *Kidney Int* (2018) 93(3):670–80. doi: 10.1016/j.kint.2017.09.023
41. Zhao H, Watts HR, Chong M, Huang H, Tralau-Stewart C, Maxwell PH, et al. Xenon Treatment Protects Against Cold Ischemia Associated Delayed Graft Function and Prolongs Graft Survival in Rats. *Am J Transplant* (2013) 13 (8):2006–18. doi: 10.1111/ajt.12293

Conflict of Interest: The authors declare that the research was conducted in the absence of any commercial or financial relationships that could be construed as a potential conflict of interest.

Publisher's Note: All claims expressed in this article are solely those of the authors and do not necessarily represent those of their affiliated organizations, or those of the publisher, the editors and the reviewers. Any product that may be evaluated in this article, or claim that may be made by its manufacturer, is not guaranteed or endorsed by the publisher.

Copyright © 2022 Gui, Suo, Tao, Wang, Zheng, Fei, Chen, Sun, Han, Ju, Zhang, Gu and Tan. This is an open-access article distributed under the terms of the Creative Commons Attribution License (CC BY). The use, distribution or reproduction in other forums is permitted, provided the original author(s) and the copyright owner(s) are credited and that the original publication in this journal is cited, in accordance with accepted academic practice. No use, distribution or reproduction is permitted which does not comply with these terms.

Advantages of publishing in Frontiers

OPEN ACCESS
Articles are free to read for greatest visibility and readership

FAST PUBLICATION
Around 90 days from submission to decision

HIGH QUALITY PEER-REVIEW
Rigorous, collaborative, and constructive peer-review

TRANSPARENT PEER-REVIEW
Editors and reviewers acknowledged by name on published articles

Frontiers
Avenue du Tribunal-Fédéral 34
1005 Lausanne | Switzerland

Visit us: www.frontiersin.org
Contact us: frontiersin.org/about/contact

REPRODUCIBILITY OF RESEARCH
Support open data and methods to enhance research reproducibility

DIGITAL PUBLISHING
Articles designed for optimal readership across devices

FOLLOW US
@frontiersin

IMPACT METRICS
Advanced article metrics track visibility across digital media

EXTENSIVE PROMOTION
Marketing and promotion of impactful research

LOOP RESEARCH NETWORK
Our network increases your article's readership